

this document downloaded from

vulcanhammer.info

the website about
Vulcan Iron Works
Inc. and the pile
driving equipment it
manufactured

Visit our companion site
<http://www.vulcanhammer.org>

Terms and Conditions of Use:

All of the information, data and computer software ("information") presented on this web site is for general information only. While every effort will be made to insure its accuracy, this information should not be used or relied on for any specific application without independent, competent professional examination and verification of its accuracy, suitability and applicability by a licensed professional. Anyone making use of this information does so at his or her own risk and assumes any and all liability resulting from such use. The entire risk as to quality or usability of the information contained within is with the reader. In no event will this web page or webmaster be held liable, nor does this web page or its webmaster provide insurance against liability, for any damages including lost profits, lost savings or any other incidental or consequential damages arising from the use or inability to use the information contained within.

This site is not an official site of Prentice-Hall, Pile Buck, or Vulcan Foundation Equipment. All references to sources of software, equipment, parts, service or repairs do not constitute an endorsement.



U.S. Department
of Transportation
**Federal Highway
Administration**

Publication No. FHWA HI 97-013
Revised November 1998

NHI Course Nos. 13221 and 13222

Design and Construction of Driven Pile Foundations

Workshop Manual - Volume I



National Highway Institute

NOTICE

This document is disseminated under the sponsorship of the Department of Transportation in the interest of information exchange. The United States Government assumes no liability for its contents or use thereof. The United States Government does not endorse products or manufacturers. Trademarks or manufacturer's names appear herein only because they are considered essential to the object of this document.

Technical Report Documentation Page

1. Report No. FHWA-HI-97-013		2. Government Accession No.		3. Recipient's Catalog No.	
4. Title and Subtitle Design and Construction of Driven Pile Foundations - Volume I		5. Report Date January 1997 - Revised Nov. 1998		6. Performing Organization Code	
		8. Performing Organization Report No.		10. Work Unit No. (TRAIS)	
7. Author(s) Hannigan, P.J., Goble, G.G., Thendean, G., Likins, G.E., and Rausche, F.		9. Performing Organization Name and Address Goble Rausche Likins and Associates, Inc. 4535 Renaissance Parkway Cleveland, Ohio 44128		11. Contract or Grant No. DTFH61-97-D-00025	
12. Sponsoring Agency Name and Address Office of Technology Application Office of Engineering/Bridge Division Federal Highway Administration 400 Seventh Street, S.W., Washington, D.C. 20590		13. Type of Report and Period Covered Final Report - Revision 1		14. Sponsoring Agency Code	
		15. Supplementary Notes FHWA Contracting Officer's Technical Representative: Chien-Tan Chang, HTA-20 FHWA Project Technical Manager: Jerry DiMaggio, HNG-31			
16. Abstract This manual is intended to serve a dual purpose, first as a participant's manual for the FHWA's National Highway Institute courses on driven pile foundations and secondly as FHWA's primary reference of recommended practice for driven pile foundations. The Design and Construction of Driven Pile Foundations manual is directed to geotechnical, structural, and construction engineers involved in the design and construction of pile supported structures. The manual is intended to serve as a practical reference on driven pile foundations. Volume I of the manual addresses design aspects including subsurface exploration, laboratory testing, static analyses, as well as specification and foundation report preparation. Volume II covers construction aspects including dynamic formulas, wave equation analyses, dynamic testing, static load testing, Statnamic testing, the Osterberg cell, as well as pile driving equipment, pile accessories, and pile installation inspection. Step by step procedures, workshop problems and solutions are provided to demonstrate use of the manual material.					
17. Key Words pile foundations, foundation design, static analysis, foundation construction, inspection			18. Distribution Statement No restrictions. This document is available to the public from the National Technical Information Service, Springfield, Virginia 22161		
19. Security Classif. (of this report) Unclassified		20. Security Classif. (of this page) Unclassified		21. No. of Pages 828	22. Price

U.S. - SI Conversion Factors

From English	To SI	Multiply by	Quantity	From SI	To English	Multiply by
ft	m	0.3048	Length	m	ft	3.2808
inch	mm	25.40		mm	inch	0.039
ft ²	m ²	0.0929	Area	m ²	ft ²	10.764
inch ²	mm ²	645.2		mm ²	in ²	0.0015
ft ³	m ³	0.028	Volume	m ³	ft ³	35.714
inch ³	mm ³	16387		mm ³	inch ³	61x10 ⁻⁶
ft ⁴	m ⁴	0.0086	Second	m ⁴	ft ⁴	115.856
inch ⁴	mm ⁴	416231	Moment of Area	mm ⁴	inch ⁴	2x10 ⁻⁶
lbm	kg	0.4536	Mass	kg	lbm	2.2046
lbm/ft ³	kg/m ³	16.02	Mass Density	kg/m ³	lbm/ft ³	0.062
lb	N	4.448	Force	N	lb	0.2248
kip	kN	4.448		kN	kip	0.2248
lbs/ft	N/m	14.59	Force/Unit- Length	N/m	lbs/ft	0.0685
kips/ft	kN/m	14.59		kN/m	kips/ft	0.0685
lbs/in ²	kPa	6.895	Force/Unit- Area; Stress; Pressure; Elastic Mod.	kPa	lbs/in ²	0.145
kips/in ²	MPa	6.895		MPa	kips/in ²	0.145
lbs/ft ²	Pa	47.88		Pa	lbs/ft ²	0.021
kips/ft ²	kPa	47.88		kPa	kips/ft ²	0.021

U.S. - SI Conversion Factors (continued)

From	To	Multiply by	Quantity	From	To	Multiply by
English	SI			SI	English	
lbs/ft ³	N/m ³	157.1	Force/Unit- Volume	N/m ³	lbs/ft ³	0.0064
kips/ft ³	kN/m ³	157.1		kN/m ³	kips/ft ³	0.0064
lb-inch	N-mm	112.98	Moment; or Energy	N-mm	lb-inch	0.0089
kip-inch	kN-mm	112.98		kN-mm	kip-inch	0.0089
lb-ft	N-m	1.356		N-m	lb-ft	0.7375
kip-ft	kN-m	1.356		kN-m	kip-ft	0.7375
ft-lb	Joule	1.356		Joule	ft-lb	0.7375
ft-kip	kJoule	1.356		kJoule	ft-kip	0.7375
s/ft	s/m	3.2808	Damping	s/m	s/ft	0.3048
blows/ft	blows/m	3.2808	Blow count	blows/m	blows/ft	0.3048

PREFACE

Engineers and contractors have been designing and installing pile foundations for many years. During the past three decades this industry has experienced several major improvements including newer and more accurate methods of predicting capacities, highly specialized and sophisticated equipment for pile driving, and improved methods of construction control.

In order to take advantage of these new developments, the FHWA developed a manual in connection with Demonstration Project No. 66, Design and Construction of Driven Pile Foundations. The primary purpose of the Manual was to support educational programs conducted by FHWA for transportation agencies. These programs consisted of (1) a workshop for geotechnical, structural, and construction engineers, and (2) field demonstrations of static and dynamic load testing equipment. Technical assistance on construction projects in areas covered by this Demonstration Project was provided to transportation agencies on request. A second purpose of equal importance was to serve as the FHWA's standard reference for highway projects involving driven pile foundations.

The original Manual was written by Suneel N. Vanikar with review and comment from Messrs. Ronald Chassie, Jerry DiMaggio, and Richard Cheney.

After a decade of use it was necessary that the Manual be updated and modified to include new developments that had taken place in the intervening years and to take advantage of the experience gained in using the Manual in the many workshops that were presented by Demonstration Project 66. The new version of the Manual was prepared by Goble Rausche Likins and Associates, Inc. under contract with the FHWA.

The Manual is presented in two volumes. Volume I addresses design aspects and Volume II presents topics related to driven pile installation, monitoring, and inspection.

The new Manual is intended to serve a dual purpose. First, as a workshop participant's manual for the FHWA's National Highway Institute Courses on Driven Pile Foundations. Similar to the earlier demonstration manual, this document is also intended to serve as FHWA's primary reference of recommended practice for driven pile foundations.

Upon completion of NHI Course 13221, participants will be able to:

1. Describe methods of pile foundation design.
2. Discuss driven pile construction materials and installation equipment.
3. Describe the timing and scope of the involvement of foundation specialists as a project evolves from concept through completion.
4. Perform a foundation economic analysis and determine the need for a driven pile foundation.
5. Recognize the pile type selection process and the advantages and disadvantages of common driven pile types.
6. Compute single and group capacities of driven piles to resist compression, tension and lateral loads.
7. Identify when and how dynamic formulas, wave equation analyses, dynamic pile testing and static load testing should be used on a project.
8. Discuss the components of structural foundation reports and controlling issues of specifications and contracting documents as related to a successful construction project.
9. Describe the concept and project influence of driveability, pile refusal, minimum and estimated pile toe elevations, soil setup and relaxation.

Upon completion of NHI Course 13222, participants will be able to:

1. Describe methods of driven pile construction monitoring and inspection practices and procedures.
2. Discuss pertinent driven pile specification and contract document issues.

3. Describe wave equation, dynamic testing and static testing results in terms of their application and interpretation on construction projects.
4. Identify the basic components and differences between various pile driving systems, associated installation equipment, pile splices and pile toe attachments.
5. Interpret a set of driven pile plan details and specifications.
6. Inspect a drive pile project with knowledge and confidence.

The authors' recognize the efforts of the project technical manager, Mr. Jerry DiMaggio, FHWA Senior Geotechnical Engineer, who provided invaluable guidance and input for the new manual.

The authors' also acknowledge the additional contributions of the following technical review panel members listed in alphabetical order:

Mr. Chien-Tan Chang - FHWA
Mr. Richard Cheney - FHWA
Mr. Tom Cleary - New Hampshire DOT
Mr. Kerry Cook - FHWA
Mr. Chris Dumas - FHWA
Mr. Carl Ealy - FHWA
Mr. Sam Holder - FHWA
Mr. Paul Macklin - Colorado DOT
Mr. Paul Passe - Florida DOT
Mr. Jan Six - Oregon DOT
Mr. Suneel Vanikar - FHWA

The authors' also wish to acknowledge the following individuals of the author's internal peer review team for their technical advice and contributions in preparing the new manual.

Dr. Joseph Caliendo - Utah State University
Dr. D. Michael Holloway - InSituTech
Mr. Robert Lukas - Ground Engineering Consultants

Lastly, the authors' wish to thank the following Goble Rausche Likins and Associates, Inc. employees for their vital contributions and significant effort in preparing this manual: Ms. Barbara Strader, Ms. Beth Richardson, Mr. Scott Webster, Mr. Neil Harnar, Mr. Jay Berger and Mr. Joe Beno.

Design and Construction of Driven Pile Foundations - Volume I

Table of Contents		Page
1.	NEED FOR A PILE MANUAL	1-1
1.1	Scope of Manual	1-2
1.2	Information Sources	1-4
	References	1-5
2.	ECONOMICS OF STRUCTURAL FOUNDATIONS	2-1
2.1	Alternate Foundation Considerations	2-1
2.2	Use of Value Engineering Proposals	2-2
2.3	Design - Build Proposals	2-3
2.4	Examples of Cost Savings by Utilizing Modern Design and Construction Control Practices	2-4
	References	2-13
3.	OVERVIEW OF PILE FOUNDATION DESIGN AND CONSTRUCTION	3-1
3.1	Design of Pile Foundations	3-1
3.2	Construction of Pile Foundations	3-1
3.3	Geotechnical Involvement in Pile Foundation Project Phases	3-2
3.4	Driven Pile Design-Construction Process	3-2
3.5	Communication	3-12
4.	SUBSURFACE EXPLORATIONS	4-1
4.1	Subsurface Exploration Phases	4-1
4.1.1	Planning the Exploration Program (office work)	4-3
4.1.2	Field Reconnaissance Survey	4-3
4.1.3	Detailed Site Exploration	4-6
4.2	Guidelines For Minimum Structure Exploration Programs	4-6
4.3	Methods of Subsurface Exploration	4-8
4.4	Soil and Rock Sampling	4-10
4.4.1	Disturbed Soil Samplers	4-11
4.4.2	Undisturbed Soil Samplers	4-17
4.4.3	Rock Core Samplers	4-17
4.5	Ground Water Monitoring	4-21
4.6	Subsurface Profile Development	4-21
	References	4-23

Table of Contents (continued)

Page

5.	IN-SITU TESTING	5-1
	5.1 Cone Penetration Test (CPT) and (CPTU)	5-1
	5.1.1 Equipment Description and Operation	5-3
	5.1.2 Interpretation of CPT/CPTU Test Results	5-6
	5.1.3 Advantages and Disadvantages of CPT/CPTU Tests	5-6
	5.2 Pressuremeter Test - (PMT)	5-9
	5.3 Dilatometer Test - (DMT)	5-9
	5.4 Vane Shear Test	5-10
	5.5 Dynamic Cone Test	5-10
	References	5-12
6.	LABORATORY TESTING	6-1
	6.1 Types of Tests	6-2
	6.1.1 Classification and Index Tests	6-2
	6.1.2 Shear Strength Tests	6-2
	6.1.3 Consolidation Tests	6-6
	6.1.4 Electro Chemical Classification Tests	6-7
	6.2 Laboratory Testing for Pile Driveability Considerations	6-7
	References	6-9
7.	FOUNDATION DESIGN PROCEDURE	7-1
	7.1 Foundation Design Approach	7-1
	7.2 Consideration of Spread Footing Foundation	7-4
	7.3 Establishment of a Need For a Deep Foundation	7-4
	References	7-8
8.	PILE TYPES AND GUIDELINES FOR SELECTION	8-1
	8.1 Overview of Typical Pile Types	8-1
	8.2 Timber Piles	8-14
	8.3 Steel H-Piles	8-15
	8.4 Steel Pipe Piles	8-17
	8.5 Precast Concrete Piles	8-18
	8.5.1 Prestressed Concrete Piles	8-19
	8.5.2 Reinforced Concrete Piles	8-21
	8.5.3 Concrete Cylinder Piles	8-23
	8.6 Cast In Place Concrete Piles	8-24
	8.6.1 Cased Driven Shell Concrete Piles	8-24
	8.6.2 Uncased Concrete Piles	8-27

Table of Contents (continued)

		Page
8.7	Composite Piles	8-30
8.7.1	Precast Concrete - Steel Piles	8-30
8.7.2	Wood Composite Piles	8-30
8.7.3	Pipe - Corrugated Shell Piles	8-30
8.7.4	Composite Tapered Precast Tip - (TPT)	8-31
8.7.5	Polymer Composite Piles	8-31
8.8	Design Considerations in Aggressive Subsurface Environments	8-31
8.8.1	Corrosion of Steel Piles	8-32
8.8.2	Sulfate and Chloride Attack on Concrete Piles	8-33
8.8.3	Insect and Marine Borer Attack on Timber Piles	8-35
8.8.4	Design Options for Piles Subject to Degradation or Abrasion	8-36
8.9	Selection of Pile Type	8-37
	References	8-41
9.	STATIC ANALYSIS METHODS	9-1
9.1	Basics of Static Analysis	9-2
9.2	Events During and After Pile Driving	9-4
9.2.1	Cohesionless Soils	9-5
9.2.2	Cohesive Soils	9-7
9.3	Load Transfer	9-7
9.4	Effective Overburden Pressure	9-10
9.5	Considerations in Selection of Design Soil Strength Parameters	9-12
9.6	Factors of Safety	9-13
9.7	Design of Single Piles	9-17
9.7.1	Bearing Capacity of Single Piles	9-17
9.7.1.1	Bearing Capacity of Piles in Cohesionless Soils	9-17
9.7.1.1a	Meyerhof Method Based on Standard Penetration Test (SPT) Data	9-17
9.7.1.1b	Nordlund Method	9-22
9.7.1.2	Bearing Capacity of Piles in Cohesive Soils	9-39
9.7.1.2a	Total Stress - α -Method	9-39
9.7.1.3	Effective Stress Method	9-46
9.7.1.4	Bearing Capacity of Piles in Layered Soils	9-52

Table of Contents (continued)		Page
9.7.1.5	Bearing Capacity of Piles Using FHWA Computer Programs	9-52
9.7.1.5a	The SPILE Computer Program	9-52
9.7.1.5b	The DRIVEN Computer Program	9-53
9.7.1.6	Bearing Capacity of Piles on Rock	9-54
9.7.1.7	Methods Based on Cone Penetration Test (CPT) Data	9-55
9.7.1.7a	Nottingham and Schmertmann Method	9-55
9.7.1.7b	Laboratoire des Ponts et Chaussees (LPC)	9-63
9.7.2	Uplift Capacity of Single Piles	9-69
9.7.3	Lateral Capacity of Single Piles	9-70
9.7.3.1	Lateral Capacity Design Methods	9-73
9.7.3.2	Broms' Method	9-74
9.7.3.3	Reese's COM624P Method	9-88
9.8	Design of Pile Groups	9-98
9.8.1	Axial Compression Capacity of Pile Groups	9-100
9.8.1.1	Pile Group Capacity in Cohesionless Soils	9-100
9.8.1.2	Pile Group Capacity in Cohesive Soils	9-102
9.8.1.3	Block Failure of Pile Groups	9-104
9.8.2	Settlement of Pile Groups	9-106
9.8.2.1	Elastic Compression of Piles	9-106
9.8.2.2	Settlements of Pile Groups in Cohesionless Soils	9-107
9.8.2.2a	Method Based on SPT Test Data	9-107
9.8.2.2b	Method Based on CPT Test Data	9-107
9.8.2.3	Settlement of Pile Groups in Cohesive Soils	9-108
9.8.2.4	Settlement of Pile Groups in Layered Soils	9-114
9.8.2.5	Settlement of Pile Groups Using the Janbu Tangent Modulus Approach	9-118
9.8.2.6	Settlement of Pile Groups Using the Neutral Plane Method	9-124
9.8.3	Uplift Capacity of Pile Groups	9-127
9.8.3.1	Group Uplift Capacity by AASHTO Code	9-127
9.8.3.2	Tomlinson Group Uplift Method	9-128
9.8.4	Lateral Capacity of Pile Groups	9-130

Table of Contents (continued)		Page
9.9	Special Design Considerations	9-135
9.9.1	Negative Shaft Resistance or Downdrag	9-135
9.9.1.1	Methods for Determining Negative Shaft Resistance	9-139
9.9.1.1a	Traditional Approach to Negative Shaft Resistance	9-139
9.9.1.2	Methods for Reducing Negative Shaft Resistance Forces	9-143
9.9.2	Vertical Ground Movements from Swelling Soils	9-145
9.9.3	Lateral Squeeze of Foundation Soil	9-145
9.9.3.1	Solutions to Prevent Tilting	9-146
9.9.4	Bearing Capacity of Piles in Soils Subject to Scour	9-146
9.9.5	Soil and Pile Heave	9-149
9.9.6	Seismic Considerations	9-150
9.10	Additional Design and Construction Considerations	9-152
9.10.1	Time Effects on Pile Capacity	9-153
9.10.1.1	Soil Setup	9-153
9.10.1.2	Relaxation	9-154
9.10.1.3	Estimation of Pore Pressures During Driving	9-155
9.10.2	Effects of Predrilling or Jetting on Pile Capacity	9-156
9.10.3	Effects of Site Dewatering on Pile Capacity	9-158
9.10.4	Densification Effects on Pile Capacity and Installation Conditions	9-159
9.10.5	Plugging of Open Pile Sections	9-160
9.10.6	Design Considerations Due to Pile Driving Induced Vibrations	9-162
9.10.7	Pile Driveability	9-165
9.10.7.1	Factors Affecting Driveability	9-166
9.10.7.2	Methods for Determining Pile Driveability	9-167
9.10.7.3	Driveability Versus Pile Type	9-168
References	9-169
Student Exercise #1	- Construct A p_o Diagram	9-179
Student Exercise #2	- Nordlund Capacity Calculation	9-183
Student Exercise #3	- α -Method Pile Capacity Calculation	9-189
Student Exercise #4	- α -Method & Nordlund Method Pile Capacity Calculation in a Layered Soil Profile	9-193

Table of Contents (continued)

Page

	Student Exercise #5 - Effective Stress Pile Capacity Calculation in a Layered Soil Profile	9-199
	Student Exercise #6 - LPC Method Pile Capacity Calculation	9-203
	Student Exercise #7 - Pile Group Settlement in Layered Profile	9-209
	Student Exercise #8 - Broms' Method Lateral Capacity Analysis	9-213
10.	OVERVIEW OF DYNAMIC ANALYSIS METHODS	10-1
	10.1 Need for Modern Dynamic Analysis Methods	10-2
	10.2 Methods of Modern Dynamic Analysis	10-3
	10.3 Driving Resistance Criteria	10-4
	References	10-6
11.	ALLOWABLE PILE STRESSES	11-1
	11.1 Factors Affecting Allowable Design Stresses	11-1
	11.2 Driving Stresses	11-2
	11.3 AASHTO Allowable Design and Driving Stresses	11-3
	11.3.1 Steel H-piles	11-3
	11.3.2 Steel Pipe Piles (unfilled)	11-4
	11.3.3 Steel Pipe Piles (top driven and concrete filled)	11-5
	11.3.4 Precast, Prestressed Concrete Piles	11-6
	11.3.5 Conventionally Reinforced Concrete Piles	11-8
	11.3.6 Timber Piles	11-9
	References	11-10
12.	CONTRACT DOCUMENTS	12-1
	12.1 Overview of Plan and Specification Requirements	12-1
	12.2 Background and Reasons For Specification Improvement	12-4
	12.3 Generic Driven Pile Specification	12-6
	References	12-38
13.	PILE FOUNDATION DESIGN SUMMARY	13-1
	13.1 Introduction	13-1
	13.2 Block 1 - Establish Requirements for Structural Conditions and Site Characterization	13-1
	13.3 Block 2 - Obtain General Site Geology	13-4
	13.4 Block 3 - Collect Foundation Experience from the Area	13-4
	13.5 Block 4 - Develop and Execute Subsurface Exploration Program	13-5

Table of Contents (continued)		Page
13.6	Block 5 - Evaluate Information and Select Foundation System	13-5
13.7	Block 6 - Deep Foundation Type	13-7
13.8	Block 7 and 8 - Select Driven Pile Type	13-7
13.9	Block 9 - Select Pile Length and Calculate Performance Under Specified Loads	13-8
	13.9.1 Single Pile Capacity	13-8
	13.9.2 Pile Group Capacity	13-8
	13.9.3 Group Settlement Calculations	13-13
	13.9.4 Lateral Pile Capacity Analysis	13-14
	13.9.5 Uplift Capacity Calculations	13-15
	13.9.6 Negative Shaft Resistance	13-16
	13.9.7 Lateral Squeeze Evaluation	13-17
	13.9.8 Overall Design Assessment	13-17
13.10	Block 10 - Calculate Driveability	13-17
13.11	Block 11 - Design Satisfactory?	13-18
13.12	Block 12 - Prepare Plans and Specifications, Set Field Capacity Determination Procedure	13-18
13.13	Block 13 - Contractor Selection	13-18
13.14	Block 14 - Perform Wave Equation Analysis of Contractor's Equipment Submission	13-19
13.15	Block 15 - Set Preliminary Driving Criteria	13-19
13.16	Block 16 - Drive Test Pile and Evaluate Capacity	13-19
13.17	Block 17 - Adjust Driving Criteria or Design	13-19
13.18	Block 18 - Construction Control	13-20
14.	FOUNDATION DESIGN REPORT PREPARATION	14-1
	14.1 Guidelines For Foundation Design Report Preparation	14-2
	14.2 Parts of a Foundation Design Report	14-3
	14.3 Information Made Available to Bidders	14-10
	References	14-11

Table of Contents (continued)

Page

List of Appendices

APPENDIX A	List of FHWA Pile Foundation Design and Construction References	A-1
APPENDIX B	List of ASTM Pile Design and Testing Specifications	B-1
APPENDIX C	Information and Data on Various Pile Types	C-1
APPENDIX D	Pile Hammer Information	D-1
APPENDIX E	Subsurface Exploration Results for Peach Freeway Design Problem	E-1
APPENDIX F	Peach Freeway Example Problem Calculations	F-1
APPENDIX G	Student Exercise - Solutions	G-1

	List of Tables	Page
Table 2-1	Cost Saving Recommendations For Pile Foundations	2-5
Table 2-2	Foundation Cost Savings For The Alsea River Bridge	2-7
Table 2-3	Foundation Cost Savings For The Third Lake Washington Bridge	2-9
Table 2-4	Foundation Cost Savings For Oregon Bridges	2-11
Table 4-1	Subsurface Exploration Phases	4-2
Table 4-2	Sources of Subsurface Information and Use	4-4
Table 4-3	Example Field Reconnaissance Report Form	4-5
Table 4-4	Methods of Subsurface Explorations	4-9
Table 4-5	Empirical Values For ϕ , D_r , and Unit Weight of Granular Soils Based on Corrected N' (after Bowles, 1977)	4-18
Table 4-6	Empirical Values For Unconfined Compressive Strength (q_u) and Consistency of Cohesive Soils Based on Uncorrected N (after Bowles, 1977)	4-18
Table 4-7	Undisturbed Soil Samples	4-20
Table 5-1	Summary of In-Situ Test Methods	5-2
Table 5-2	Drill Rig With 45 kN Push Capacity	5-5
Table 5-3	Truck With 180 kN Push Capacity	5-5
Table 6-1	Laboratory Tests on Soils For Foundation Design	6-3
Table 6-2	Typical Values of Sensitivity From Sowers (1979)	6-8
Table 7-1	Foundation Types and Typical Uses	7-3
Table 8-1	Technical Summary of Piles	8-3
Table 8-2	Pile Type Selection Based on Subsurface and Hydraulic Conditions	8-39
Table 8-3	Pile Type Selection Pile Shape Effects	8-40
Table 9-1	Methods of Static Analysis for Piles in Cohesionless Soils	9-18
Table 9-2(a)	Design Table for Evaluating K_s for Piles when $\omega = 0^\circ$ and $V = 0.0093$ to 0.0930 m^3/m	9-34
Table 9-2(b)	Design Table for Evaluating K_s for Piles when $\omega = 0^\circ$ and $V = 0.093$ to 0.930 m^3/m	9-35
Table 9-3	Methods of Static Analysis For Piles in Cohesive Soils	9-40
Table 9-4	Approximate Range of β and N_t Coefficients (Fellenius, 1991)	9-48
Table 9-5	Engineering Classification for In-Situ Rock Quality	9-54
Table 9-6	CPT C_f Values	9-56
Table 9-7	Driven Pile Type Categories for LPC Method	9-64
Table 9-8(a)	Curve Selection Based on Pile Type and Insertion Procedures for Clay and Silt	9-64

List of Tables (continued)

Page

Table 9-8(b)	Curve Selection Based on Pile Type and Insertion Procedures for Sand and Gravel	9-65
Table 9-9	Cone Bearing Capacity Factors for LPC Method	9-65
Table 9-10	Values of Coefficients n_1 and n_2 for Cohesive Soils	9-75
Table 9-11	Values of K_h For Cohesionless Soils	9-75
Table 9-12	Representative Values of ϵ_{50} for Clays	9-96
Table 9-13	Representative k Values for Clays and Sands	9-96
Table 9-14	Typical Modulus and Stress Exponent Values	9-121
Table 9-15	Laterally Loaded Pile Groups Studies	9-133
Table 9-16	Soil Setup Factors (after Rausche <i>et al.</i> , 1996)	9-155
Table 11-1	Maximum Allowable Stresses For Steel H-Piles	11-4
Table 11-2	Maximum Allowable Stresses For Unfilled Steel Pipe Piles	11-5
Table 11-3	Maximum Allowable Stresses For Top Driven, Concrete Filled, Steel Pipe Piles	11-6
Table 11-4	Maximum Allowable Stresses For Precast, Prestressed, Concrete Piles	11-7
Table 11-5	Maximum Allowable Stresses For Conventionally Reinforced Concrete Piles	11-8
Table 11-6	Maximum Allowable Stresses For Timber Piles	11-9
Table 12-1	Alternate Approval Method	12-15
Table 13-1(a)	North Abutment Pile Capacity Summary for 11.5 m Pile Embedment	13-9
Table 13-1(b)	North Abutment Pile Length Summary for a 1,780 kN Ultimate Pile Capacity	13-9
Table 13-2(a)	Pier 2 Pile Capacity Summary for 10.0 m Pile Embedment	13-10
Table 13-2(b)	Pier 2 Pile Length Summary for a 1,780 kN Ultimate Pile	13-10
Table 13-2(c)	Pier 2 Pile Capacity Summary Before and After Channel Degradation Scour Based on Nordlund Method	13-10
Table 13-3(a)	Pier 3 Pile Capacity Summary for 13.0 m Pile Embedment	13-11
Table 13-3(b)	Pier 3 Pile Length Summary for a 1,780 kN Ultimate Pile Capacity	13-11
Table 13-4(a)	South Abutment Pile Capacity Summary for a 17.5 m Pile Embedment	13-12
Table 13-4(b)	South Abutment Pile Length Summary for a 1,780 kN Ultimate Pile Capacity	13-12

List of Figures		Page
Figure 3.1	Driven Pile Design and Construction Process	3-4
Figure 3.2	Design Stage Communication	3-12
Figure 3.3	Construction Stage Communication	3-13
Figure 4.1	Split Barrel Sampler (after FHWA, 1972)	4-12
Figure 4.2	SPT Hammer Types	4-13
Figure 4.3	SPT Test Results for Safety and Automatic Hammers (after Finno, 1989)	4-14
Figure 4.4	Chart for Correction of N-values in Sand for Influence of Effective Overburden Pressure (after Peck, <i>et al.</i> , 1974)	4-16
Figure 4.5	Thin Wall Open Tube (after FHWA, 1972)	4-19
Figure 4.6	Rigid and Swivel Type Double Tube Core Barrels (after FHWA, 1972)	4-19
Figure 5.1	Terminology Regarding the Cone Penetrometer (from Robertson and Campanella, 1989)	5-4
Figure 5.2	Simplified Soil Classification Chart for Standard Electronic Friction Cone (after Robertson <i>et al.</i> , 1986)	5-7
Figure 5.3	Typical CPT Data Presentation	5-8
Figure 5.4	Vane Shear Device (after FHWA, 1972)	5-11
Figure 7.1	Situations in which Deep Foundations may be Needed (modified from Vesic, 1977)	7-6
Figure 8.1	Pile Classification	8-2
Figure 8.2	Typical Prestressed Concrete Piles (after PCI, 1993)	8-20
Figure 8.3	Typical Details of Conventionally Reinforced Concrete Piles (after PCA, 1951)	8-22
Figure 8.4	Concrete Cylinder Pile	8-24
Figure 8.5	Loss of Thickness by Corrosion for Steel Piles in Seawater (after Morley and Bruce, 1983)	8-34
Figure 9.1	Situation Where Two Static Analyses are Necessary - Due to Scour	9-3
Figure 9.2	Situation Where Two Static Analyses are Necessary - Due to Fill Materials	9-3
Figure 9.3	Compaction of Cohesionless Soils During Driving of Piles (Broms 1966)	9-6
Figure 9.4	Disturbance of Cohesive Soils During Driving of Piles (Broms 1966)	9-6
Figure 9.5	Typical Load Transfer Profiles	9-9
Figure 9.6	Effective Overburden Pressure Diagram - Water Table Below Ground Surface	9-11

List of Figures (continued)

	List of Figures (continued)	Page
Figure 9.7	Effective Overburden Pressure Diagram - Water Table Above Ground Surface	9-11
Figure 9.8	Soil Profile for Factor of Safety Discussion	9-15
Figure 9.9	Nordlund's General Equation for Ultimate Pile Capacity	9-24
Figure 9.10	Relation of δ/ϕ and Pile Displacement, V, for Various Types of Piles (after Nordlund, 1979)	9-29
Figure 9.11	Design Curve For Evaluating K_δ For Piles When $\phi = 25^\circ$ (after Nordlund, 1979)	9-30
Figure 9.12	Design Curve For Evaluating K_δ For Piles When $\phi = 30^\circ$ (after Nordlund, 1979)	9-31
Figure 9.13	Design Curve for Evaluating K_δ for Piles when $\phi = 35^\circ$ (after Nordlund, 1979)	9-32
Figure 9.14	Design Curve for Evaluating K_δ for Piles when $\phi = 40^\circ$ (after Nordlund, 1979)	9-33
Figure 9.15	Correction Factor For K_δ When $\delta \neq \phi$ (after Nordlund, 1979)	9-36
Figure 9.16	Chart For Estimating α_t Coefficient and Bearing Capacity Factor N'_q (Chart modified from Bowles, 1977)	9-37
Figure 9.17	Relationship Between Maximum Unit Pile Toe Resistance and Friction Angle for Cohesionless Soils (after Meyerhof, 1976)	9-38
Figure 9.18	Adhesion Values for Piles in Cohesive Soils (after Tomlinson, 1979)	9-43
Figure 9.19	Adhesion Factors for Driven Piles in Clay (after Tomlinson, 1980)	9-44
Figure 9.20	Chart for Estimating β Coefficient versus Soil Type ϕ' Angle (after Fellenius, 1991)	9-48
Figure 9.21	Chart for Estimating N_t Coefficient versus Soil Type ϕ' Angle (after Fellenius, 1991)	9-49
Figure 9.22	Penetrometer Design Curves for Pile Side Friction in Sand (after FHWA Implementation Package, FHWA-TS-78-209)	9-57
Figure 9.23	Design Curve for Pile Side Friction in Clay (after Schmertmann, 1978)	9-59
Figure 9.24	Illustration of Nottingham and Schmertman Procedure for Estimating Pile Toe Capacity (FHWA-TS-78-209)	9-60
Figure 9.25	Maximum Unit Shaft Resistance Curves for LPC Method	9-66
Figure 9.26	Soil Resistance to a Lateral Pile Load (adapted from Smith, 1989)	9-71

List of Figures (continued)

	List of Figures (continued)	Page
Figure 9.27	Ultimate Lateral Load Capacity of Short Piles in Cohesive Soils	9-79
Figure 9.28	Ultimate Lateral Load Capacity of Long Piles in Cohesive Soils	9-80
Figure 9.29	Ultimate Lateral Load Capacity of Short Piles in Cohesionless Soils	9-81
Figure 9.30	Ultimate Lateral Load Capacity of Long Piles in Cohesionless Soils	9-82
Figure 9.31	Load Deflection Relationship Used in Determination of Broms' Maximum Working Load	9-83
Figure 9.32	Lateral Deflection at Ground Surface of Piles in Cohesive Soils	9-85
Figure 9.33	Lateral Deflection at Ground Surface of Piles in Cohesionless Soils	9-86
Figure 9.34	COM624P Pile-Soil Model	9-89
Figure 9.35	Typical p-y Curves for Ductile and Brittle Soil (after Coduto 1994)	9-90
Figure 9.36	Graphical Presentation of COM624 Results (after Reese, 1986)	9-92
Figure 9.37	Comparison of Measured and COM624P Predicted Load-Deflection Behavior versus Depth (after Kyfor <i>et al.</i> 1992)	9-93
Figure 9.38	Stress Zone from Single Pile and Pile Group (after Tomlinson, 1994)	9-99
Figure 9.39	Overlap of Stress Zones for Group of Friction Piles (after Bowles, 1988)	9-101
Figure 9.40	Measured Dissipation of Excess Pore Water Pressure in Soil Surrounding Full Scale Pile Groups (after O'Neill, 1983)	9-103
Figure 9.41	Three Dimensional Pile Group Configuration (after Tomlinson, 1994)	9-105
Figure 9.42	Equivalent Footing Concept	9-109
Figure 9.43	Typical e-log p Curve from Laboratory Consolidation Test	9-110
Figure 9.44	Pressure Distribution Below Equivalent Footing for Pile Group (adapted from Cheney and Chassie, 1993)	9-112
Figure 9.45	Values of the Bearing Capacity Index, C', for Granular Soil (modified after Cheney and Chassie, 1993)	9-115
Figure 9.46	The Non-Linear Relation Between Stress and Strain in Soil (after Fellenius, 1990)	9-118

List of Figures (continued)

Page

Figure 9.47	Neutral Plane (after Goudreal and Fellenius, 1994)	9-125
Figure 9.48	Uplift of Pile Group in Cohesionless Soil (after Tomlinson, 1994)	9-129
Figure 9.49	Uplift of Pile Group in Cohesive Soils (after Tomlinson, 1994)	9-129
Figure 9.50	Illustration of p-multiplier Concept for Lateral Group Analysis	9-131
Figure 9.51	Typical Plots of Load versus Deflection and Bending Moment versus Deflection for Pile Group Analysis (adapted from Brown and Bollman, 1993)	9-136
Figure 9.52(a)	Common Downdrag Situation Due to Fill Weight	9-138
Figure 9.52(b)	Common Downdrag Situation Due to Ground Water Lowering	9-138
Figure 9.53	Pressure Distribution Chart Beneath the End of a Fill (After Cheney and Chassie, 1993)	9-141
Figure 9.54	Examples of Abutment Tilting Due to Lateral Squeeze	9-146
Figure 9.55	Local and Channel Degradation Scour	9-148
Figure 9.56	Balance of Forces on Pile Subject to Heave (after Haggerty and Peck, 1971)	9-151
Figure 9.57	Excess Pore Water Pressure due to Pile Driving (after Poulos and Davis, 1980)	9-157
Figure 9.58	Plugging of Open End Pipe Piles (after Paikowsky and Whitman, 1990)	9-163
Figure 9.59	Plugging of H-Piles (after Tomlinson, 1994)	9-163
Figure 12.1	Pile and Driving Equipment Data Form	12-11
Figure 13.1	Driven Pile Design and Construction Process	13-2
Figure 13.2	Peach Freeway Subsurface Profile	13-6

LIST OF SYMBOLS

- A - Pile cross sectional area.
- A_p - Pile cross section area at pile toe of an unplugged pile section.
- A_s - Pile shaft exterior surface area.
- A_{si} - Pile shaft interior surface area.
- A_t - Pile toe area.
- B - Width of pile group.
- B_d - Projected width of pile group at depth d.
- b - Pile diameter.
- b_f - Distance from midpoint of slope to centerline of embankment fill.
- C - Wave speed of pile material.
- C_f - Conversion factor for cone tip resistance to sleeve friction.
- C_c - Compression index.
- C_{cr} - Recompression index.
- C_d - Pile perimeter at depth d.
- C_F - Correction factor for K_δ when $\delta \neq \phi$.
- C_N - Correction factor for SPT N value.
- C_s - Dimensionless shape factor.
- c - Cohesion.
- c' - Effective cohesion.

LIST OF SYMBOLS (continued)

- c_a - Adhesion or shear stress between the pile and soil at failure.
- c_u - Undrained shear strength or can be determined from $q_u/2$.
- c_{u1} - Average undrained shear strength around pile group.
- c_{u2} - Undrained shear strength below pile toe level.
- D - Pile embedded length.
- D_B - Pile embedded length into bearing stratum.
- D_r - Relative density.
- d - Depth.
- Δd - Length of pile segment.
- E - Modulus of elasticity of pile material.
- E_r - Manufacturers rated hammer energy.
- E_s - Soil modulus.
- e - Void ratio.
- e_c - Eccentricity of applied load for free-headed pile.
- e_0 - Initial void ratio.
- f_s - Cone unit sleeve friction.
- \bar{f}_s - Average cone unit sleeve friction.
- f'_c - Ultimate compression strength for concrete.
- f_n - Negative unit shaft resistance over the shaft surface area.

LIST OF SYMBOLS (continued)

- f_{pe} - Effective prestress after losses.
- f_s - Positive unit shaft resistance over the shaft surface area.
- f_{si} - Interior unit shaft resistance.
- f_{so} - Exterior unit shaft resistance.
- f_y - Yield stress of pile material for steel.
- H - Original thickness of stratum.
- h - Ram stroke.
- h_f - Height of embankment fill.
- I - Moment of inertia.
- I_f - Influence factor for group embedment.
- j - Stress exponent.
- K - Ratio of unit pile shaft resistance to cone unit sleeve friction for cohesionless soils.
- K_c - Cone bearing capacity factor.
- K_h - Coefficient of horizontal subgrade reaction.
- K_o - Coefficient of earth pressure at rest.
- K_p - Rankine passive pressure coefficient.
- K_δ - Coefficient of lateral earth pressure.
- k - Slope of soil modulus.

LIST OF SYMBOLS (continued)

- L - Total pile length.
- ΔL - Length of pile between two measuring points under no load conditions.
- M_y - Resisting moment of the pile.
- m_n - Dimensionless modulus number.
- m_r - Dimensionless recompression modulus number.
- N - Uncorrected field SPT resistance value.
- N' - Corrected SPT resistance value.
- \bar{N}' - Average corrected SPT resistance value.
- N_b - Number of hammer blows per 25 mm.
- N_c - Dimensionless bearing capacity factor.
- N'_q - Dimensionless bearing capacity factor.
- N_t - Toe bearing capacity coefficient.
- n_1 - Empirical coefficient for calculating the coefficient of subgrade reaction.
- n_2 - Empirical coefficient for calculating the coefficient of subgrade reaction.
- P_m - P-multiplier for p-y curve.
- p - Soil resistance per unit pile length.
- Δp - Change in pressure.
- p_c - Preconsolidation pressure.
- p_d - Effective overburden pressure at the center of depth increment d .

LIST OF SYMBOLS (continued)

- p_f - Design foundation pressure.
- p_i - Pressure.
- p_o - Effective overburden pressure.
- \bar{p}_o - Average effective overburden pressure.
- p_t - Total overburden pressure, also effective overburden pressure at the pile toe.
- Q - Load.
- ΔQ - Load increment.
- Q_a - Allowable design load of a pile.
- Q_d - Dead load on a pile.
- Q_l - Live load on a pile.
- Q_m - Maximum allowable lateral working load.
- Q_n - Drag load on a pile.
- Q_u - Ultimate pile capacity.
- Q_{ug} - Ultimate pile group capacity.
- q_c - Cone tip resistance.
- \bar{q}_c - Average cone tip resistance.
- q_L - Limiting unit toe resistance.
- q_t - Unit toe resistance over the pile toe area.
- q_u - Unconfined compressive strength.

LIST OF SYMBOLS (continued)

- R_f - Friction ratio or f_s/q_c .
- R_s - Ultimate pile shaft resistance.
- R_t - Ultimate pile toe resistance.
- R_u - Ultimate soil resistance.
- S - Section modulus about an axis perpendicular to the load plane.
- S_t - Sensitivity of a cohesive soil.
- s - Estimated total settlement.
- s_b - Set per blow.
- s_f - Settlement at failure.
- U - Displacement.
- u - Pore water pressure (neutral pressure).
- V - Volume of soil displaced per unit length of pile.
- W_g - Effective weight of pile/soil block.
- w_p - Weight of soil plug.
- y - Lateral soil (or pile) deflection.
- Z - Length of pile group.
- Z_d - Projected length of pile group at depth d .
- z - Pile spacing.
- α - An empirical adhesion factor.

LIST OF SYMBOLS (continued)

- α' - Ratio of pile unit shaft resistance to cone unit sleeve friction for cohesive soils.
- α_t - Dimensionless factor in Nordlund method (dependent on pile depth-width relationship).
- β - Beta shaft resistance coefficient.
- β_h - Dimensionless length factor for lateral load analysis.
- Δ - Elastic compression.
- Δu_m - Maximum excess pore pressure.
- δ - Friction angle between pile and soil.
- ϵ - Strain.
- ϵ_{50} - Strain at 1/2 maximum principal stress.
- η - Dimensionless length factor for lateral load analysis.
- η_g - Pile group efficiency.
- γ - Total unit weight of soil.
- γ' - Buoyant unit weight of soil.
- γ_D - Dry unit weight of soil.
- γ_f - Unit weight of embankment fill.
- γ_w - Unit weight of water.
- σ - Normal or total overburden stress (pressure).
- σ' - Effective stress or ($\sigma - u$).

LIST OF SYMBOLS (continued)

- σ_a - Maximum allowable stress in compression parallel to the wood grain.
- σ'_p - Preconsolidation pressure or stress.
- σ'_{vc} - Vertical consolidation stress.
- σ'_1 - Effective stress after stress increase.
- σ'_o - Effective stress prior to stress increase.
- σ'_r - Constant reference stress.
- τ - Shear strength of soil.
- ϕ - Angle of internal friction of soil.
- ϕ' - Effective angle of internal friction of soil.
- ω - Angle of pile taper from vertical.

1. NEED FOR A PILE MANUAL

In 1985 the Federal Highway Administration published the first edition of this manual. The goals of that work are unchanged, so it is useful to repeat them here with modest updating.

1. There exists a vast quantity of information on the subject of pile foundations which presently is not compiled in a form which is useful to most practicing engineers. There are proven rational design procedures, information on construction materials, equipment and techniques, and useful case histories. Unfortunately, much of this information is fragmented and scattered. Standard textbooks and other publications on the subject tend to be theoretically oriented; practicing design and construction engineers often find them lacking in practical aspects.
2. Many of the methods currently in practice often lead to unnecessarily conservative designs because they are based solely on experience and tradition with little theoretical background. Newer and more rational design procedures and techniques can be applied to provide more economical pile systems which will safely support the applied structural loads without excessive safety factors.
3. During fiscal year 93, FHWA and the State Transportation departments spent approximately 5.0 billion dollars for constructing, replacing, or rehabilitating bridges. Of that amount approximately 1.5 billion dollars were spent on bridge substructures and of that, at least 750 million dollars were spent on foundations. In addition, city and county governments, whose practices closely follow the State practices, spend large amounts on construction of bridges. There are opportunities for substantial savings in foundation construction costs, specifically in the area of pile foundations.

Cost savings can be achieved by the use of improved methods of design and construction technology. A minimum of fifteen percent of the substructure cost can be easily saved by utilizing such methods and, in most cases, the savings are more significant.

4. A comprehensive manual has been needed for some time to transfer available technology and to upgrade the level of expertise in pile foundations. This manual is intended to fulfill that need as well as to establish minimum design standards.

5. Design criteria for major and unusual bridge structures is becoming more complex and sophisticated. Extreme design events such as scour, debris loading, vessel impact, and seismic events produce great need for foundation performance under lateral and uplift loading, group behavior, and substructure - superstructure interaction. This new series of performance criteria frequently result in foundations which are more costly, more complex to design, and more difficult to construct.

The original manual represented a major advance in that it included the most modern technology for pile design that was available. At the same time, the manual presented this technology so that it was usable to the practicing engineer. The work was very successful helping many transportation departments to modernize their design procedures. Ten years have since elapsed. Changes in pile design, construction, and performance requirements make it necessary to update the manual.

1.1 SCOPE OF MANUAL

Since most piles used for highway structures are driven piles, and to keep this manual to a manageable size, this manual is limited to driven piles. The manual has been divided into two volumes. Volume I covers the design of pile foundations and Volume II covers installation, construction control, and inspection. However, sufficient information is provided in Volume I so that spread footings and drilled/bored piles, *e.g.*, drilled shafts, auger cast piles, *etc.*, can be considered in the foundation type selection process. This manual is intended to serve as a reference to all practical aspects of the design and construction of driven pile foundations.

All aspects of pile foundation design and construction, including subsurface exploration and laboratory testing, design analysis, foundation report preparation, and construction monitoring are covered in a systematic manner. Theoretical discussions have been included only where necessary. Specific recommendations are made wherever appropriate. Workshop exercises are included to provide hands-on knowledge to workshop participants and manual users.

It is important for design and construction engineers and pile construction inspectors to be familiar with pile driving equipment, accessories and inspection procedures. A separate section on this subject is included in this manual to fulfill this need.

During the period that the first edition of this manual was in use, several changes occurred in design requirements. For example, more stringent requirements for scour, vessel impact and seismic events have been implemented in design. The scour requirements make pile driveability analysis more critical. For vessel impact and seismic considerations, both pile uplift and lateral analyses are becoming more important. It has become much more common to consider the effects of soil strength changes with time in the design and construction process. In the past ten years, a better understanding of pile group behavior has been gained and this knowledge is now being put into practice. Finally, Systems International (SI) units are being adopted for highway construction and they will be used throughout the updated manual.

As with the previous document, this edition is still the basis for a course on the design of driven pile foundations. This course will continue the original goal of modernizing transportation department practice in this area. Also, new engineers continue to join transportation department organizations and require updating of their knowledge in the practical aspects of pile design and installation.

The use of Load and Resistance Factor Design (LRFD) for highway bridges has been approved by the Subcommittee for Bridges and Structures of the American Association of State Highway and Transportation Officials (AASHTO). This design philosophy includes foundations and, of course, driven piles. This manual will continue to follow the working stress design philosophy but it is appropriate to include a brief discussion of LRFD here to offer a conceptual introduction to the method.

In the LRFD design approach, the traditional "Safety Factor" is divided into a number of partial safety factors on the loads, Load Factors, as well as factors on the strength, Resistance or " Φ -Factors." The Load Factors have been developed for the various loads and selected load combinations by structural engineers using probabilistic concepts. They have also developed the necessary Φ -Factors for the various structural materials, elements, and failure modes. The results of research studies have been extensively published and discussed in the structural design community. The Φ -Factors for foundation design have also been selected (Barker *et al.* 1991).

The general methods of Load and Resistance Factor Design have been presented in engineering schools for the past 30 years in structural design courses but it is generally a new concept to most foundation specialists.

1.2 INFORMATION SOURCES

The information presented in this manual has been collected from several sources. The information has been condensed, modified and updated as needed. The sources include state-of-the-art technical publications, manufacturers' literature, existing Federal Highway Administration (FHWA) and Transportation Research Board (TRB) publications, standard textbooks, and information provided by State and Federal transportation engineers. Reference lists are provided at the end of each chapter.

REFERENCES

Barker, R.M., Duncan, J.M., Rojiani, K.B., Ooi, P.S.K., Tan, C.K. and Kim, S.G. (1991).
Manuals for the Design of Bridge Foundations. Report 343, National Cooperative
Highway Research Program, Transportation Research Board, National Research
Council, Washington, D.C.

2. ECONOMICS OF STRUCTURAL FOUNDATIONS

Foundation design and construction involve engineering, economic, and constructability considerations pertinent to the particular site in question. The engineering considerations are addressed by determining the foundation loads and performance requirements, development of the foundation design parameters and design analysis. The design analysis coupled with past experience will provide several feasible foundation alternatives.

The next step involves an economics evaluation of potential foundations. Several foundation alternatives may be satisfactory for the subsurface conditions while also meeting superstructure requirements. However, of all the foundation alternatives, generally only one will have the least possible cost.

Last, the constructability of a potential foundation must be considered. A potential foundation solution may appear to be the most economical from purely a design perspective, but may not be most economical when limitations on construction activities are fully considered. Constructability issues such as impact on adjacent structures, equipment, access, methods, work hours, *etc.*, must be considered in design.

2.1 ALTERNATE FOUNDATION CONSIDERATIONS

To determine the most feasible foundation alternatives, both shallow foundations and deep foundations should be considered. Deep foundation alternatives include both piles and drilled shafts. Proprietary deep foundations systems should not be excluded as they may be the most economical alternative in a given condition. This manual covers the design and construction of driven pile foundations. Therefore, design and construction procedures for shallow foundations and drilled shafts will not be covered herein. Additional details on spread footings for highway bridges may be found in FHWA/RD-86/185 Spread Footings for Highway Bridges by Gifford *et al.* (1987). The FHWA/ADSC publication FHWA-HI-88-042 by Reese and O'Neill (1988) summarizes design methods and construction procedures for drilled shafts.

A cost evaluation of all feasible foundation alternatives is essential in the selection of the optimum foundation system. Pile foundation cost data for completed projects can be obtained from statewide average bid prices available from state transportation agencies. Foundation contractors can also provide rough estimates on foundation items.

Cost analyses of all feasible alternatives may lead to the elimination of some foundations qualified under the engineering study. Other factors that must be considered in the final foundation selection are availability of materials and equipment, local contractor and construction force experience, as well as any environmental limitations/considerations on construction access or activities.

For major projects, if the estimated costs of alternatives during the design stage are within 15 percent of each other, then alternate foundation designs should be considered for inclusion in the contract documents. If an alternate design is included in the contract documents, both designs should be adequately detailed. For example, if two pile foundation alternatives are detailed, the bid quantity pile lengths should reflect the estimated pile lengths for each alternative. Otherwise, material costs and not the installed foundation cost will likely determine the low bid. Use of alternate foundation designs will generally provide the most cost effective foundation system.

As noted earlier, proprietary pile types should not be routinely excluded from consideration. In a given soil condition, a proprietary system may be the most economical foundation type. Therefore, a proprietary system should be considered as a viable foundation alternate when design analyses indicate the cost to be within 15% of a conventional design. A conventional design alternate should generally be included with a proprietary design alternate in the final project documents to stimulate competition.

2.2 USE OF VALUE ENGINEERING PROPOSALS

Value engineering is a cost saving technique that can be used either in the pre-bid or post bid stage of a contract. Value engineering consists of a five step logical thought process used to obtain the desired performance for the lowest cost achievable. The five steps may be described as follows:

1. Information gathering.
2. Information analysis to understand the problem.
3. Creative thinking to arrive at alternatives giving the same performance at lower costs.

4. Systematic judging of the results from step 3.

5. Detailing of selected alternatives from step 4.

Value engineering can readily be applied to foundation engineering by allowing the use of value engineering change proposals in design or construction contracts. The obvious benefit of value engineering to the owner is a lower cost foundation. The consultant or contractor reward for an alternative foundation solution is typically a percentage of the cost savings realized by the owner.

For value engineering to be successful, the owner must be assured that the foundation performance criteria remain satisfied. This requires the owner to engage knowledgeable experts to review and comment on submittals as well as to be actively involved in resolution of technical details. In some cases, design verification testing or more sophisticated construction control may be required in order to confirm foundation performance criteria. Lastly, the review of submitted proposals must also be completed in a reasonable time period.

Significant cost savings can result from value engineering. However, the cost savings should not be achieved by acceptance of unproven pile types, splices, etc. Proposed substitutions should be of equivalent quality and have a documented performance record in similar foundation installation conditions.

2.3 DESIGN - BUILD PROPOSALS

Another potential cost saving method is the use of design - build proposals. In this approach, the owner details the general project scope and performance requirements and solicits design - build proposals. New cost effective solutions may emerge from the design - build method since multiple firms are looking at the design and construction issues rather than a single designer. The design - build method also allows contractors to use their knowledge of special equipment or procedures. In design - build projects, it is important for the owner to understand and clearly communicate the project scope, performance requirements, and desired end product as well as method of measurement for payment. Failure to do so may result in a constructed product not meeting the owners expectations or failing to meet the agreed-upon budget.

2.4 EXAMPLES OF COST SAVINGS BY UTILIZING MODERN DESIGN AND CONSTRUCTION CONTROL PRACTICES

There are many factors which enter into the cost of a structure foundation. A failure to understand and consider any one of them will add to the total cost of the work. Use of overly conservative designs and inappropriate construction practices may result in significantly greater foundation costs. These practices are also often associated with increased risk of large change orders or claims.

Use of modern design and construction methods, techniques, and equipment can provide an efficient foundation system without compromising safety or the service life of the structure. Outdated pile foundation practices usually lead either to extremely conservative and inefficient piling systems or unsafe foundations. Opportunities for rational design, construction, and cost savings exist in several areas of pile foundations. These opportunities are summarized in Table 2-1.

Transportation agencies that are taking advantage of modern design and construction control methods have reduced foundation costs while obtaining greater confidence in the safety and the service life of their structures. The following case histories present these facts very clearly:

TABLE 2-1 COST SAVING RECOMMENDATIONS FOR PILE FOUNDATIONS

Factor	Inadequacy of Older Methods	Cost Saving Recommendations	Remarks
A. Design structural load capacity of piles.	1. Allowable pile material stresses may not address site specific considerations.	1. Use realistic allowable stresses for pile materials in conjunction with adequate construction control procedures, <i>i.e.</i> , load testing, dynamic testing and wave equation.	1. Rational consideration of Factors A and B may decrease cost of a foundation by 25 percent or more.
B. Design geotechnical capacity of soil and rock to carry load transferred by piles.	1. Inadequate subsurface explorations and laboratory testing. 2. Rules of thumb and prescription values used in lieu of static design may result in overly conservative designs. 3. High potential for change orders and claims.	1. Perform thorough subsurface exploration including in-situ and laboratory testing to determine design parameters. 2. Use rational and practical methods of design. 3. Perform wave equation driveability analysis. 4. Use design stage pile load testing on large pile driving projects to determine load capacities (load tests during design stage).	1. Reduction of safety factor can be justified because some of the uncertainties about load carrying capacities of piles are reduced. 2. Rational pile design will generally lead to shorter pile lengths and/or smaller number of piles.
C. Alternate foundation design.	1. Alternate foundation designs are rarely used even when possibilities of cost savings exist by allowing alternates in contract documents.	1. For major projects, consider inclusion of alternate foundation designs in the contract documents if estimated costs of feasible foundation alternatives are within 15 percent of each other.	1. Alternative designs often generate more competition which can lead to lower costs.
D. Plans and specifications.	1. Unrealistic specifications. 2. Uncertainties due to inadequate subsurface explorations force the contractors to inflate bid prices.	1. Prepare detailed contract documents based on thorough subsurface explorations, understanding of contractors' difficulties and knowledge of pile techniques and equipment. 2. Provide subsurface information to the contractor.	1. Lower bid prices will result if the contractor is provided with all the available subsurface information. 2. Potential for contract claims is reduced with realistic specifications.
E. Construction determination of pile load capacity during installation.	1. Often used dynamic formulas such as Engineering News are unreliable. Correlations between load capacities determined from Engineering News formula and static load tests indicate safety factors ranging from less than 1 (<i>i.e.</i> failure) to about 20 (<i>i.e.</i> excessive foundation cost).	1. Eliminate use of dynamic formulas for construction control as experience is gained with the wave equation analysis. 2. Use wave equation analysis coupled with dynamic monitoring for construction control and load capacity evaluation. 3. Use pile load tests on projects to substantiate capacity predictions by wave equation and dynamic monitoring.	1. Reduced factor of safety may allow shorter pile lengths and/or smaller number of piles. 2. Pile damage due to excessive driving can be eliminated by using dynamic monitoring equipment. 3. Increased confidence and lower risk results from improved construction control.

1. Oregon Department of Transportation - Alsea River Bridge

The Alsea River Bridge is a 890 meter long concrete arch structure that was completed in 1991 at a cost of about \$35 million. The bridge is supported on 33 to 43 meter long piles driven through thick sand and silt deposits to an underlying siltstone bedrock. The preliminary foundation design was based on a design load of 1335 kN per pile. Approximately 29,850 linear meters of steel pipe piling was anticipated in this foundation design.

Early during the design stage of the Alsea River Bridge project, a pile load test program was conducted as part of FHWA Demonstration Project 66. The static load test frame, dynamic pile testing services, static load testing services and associated technical support were provided as part of the FHWA demonstration project. Both a 508 mm square prestressed concrete pile and a 610 mm diameter steel pipe pile with a wall thickness of 13 mm were driven and load tested.

As a result of this design stage test program, the final foundation design utilized a design load of 2670 kN or twice the design load anticipated in the preliminary design. This resulted in both the number of piles and the pile material quantity being reduced by about one half. As part of the final design, selected production piles were dynamically tested for pile capacity confirmation.

Table 2-2 summarizes the test program costs as well as the foundation savings realized from the design stage test program. The test program cost roughly \$350,000 and resulted in a net foundation cost savings of \$2.1 million or a benefit-cost ratio in excess of 6:1. The foundation cost savings do not consider the cost savings from other items such as smaller footing and cofferdam sizes or reduced construction time making the actual savings even greater. The net foundation cost savings was 6% of the total bridge cost.

TABLE 2-2 FOUNDATION COST SAVINGS FOR THE ALSEA RIVER BRIDGE

Test Program Costs	Static Load Test	\$210,000
	Load Frame and FHWA Technical Services	\$100,000 *
	Dynamic Testing of Production Piles	\$40,000
	Total Cost	\$350,000
Foundation Savings	Elimination of 14,922 Linear Meters of Piling at \$164/m	\$2,447,000
	Smaller Footing and Cofferdam Sizes	Not Quantified
	Decreased Foundation Construction Time from Fewer Piles	Not Quantified
	Total Savings	\$2,447,000
Net Cost Savings		\$2,097,000
Benefit - Cost Ratio		>6:1
Net Savings as Percentage of Total Bridge Cost		6%

* Estimated Cost

2. Washington Department of Transportation - Third Lake Washington Bridge

The Third Lake Washington Bridge is a 2560 meter long bridge that carries I-90 over Lake Washington. The bridge has a total cost of approximately \$96 million with \$64 million for a floating main structure and the remainder for the approach structures that are pile supported. The approach structures were located in water depths of up to 28 meters.

The preliminary foundation design for the approach structures recommended a pile design load of 2670 kN for either 1219 mm diameter steel pipe piles with a wall thickness of 32 mm or 1372 mm diameter prestressed concrete cylinder piles. The soil profile consisted of loose sands and silts over a very dense granular glacial till. It was believed that the pile design load could be increased if pile capacity and driveability into the glacial till could be verified through a testing program. Pile driveability into the glacial till was a critical design requirement for both compression and uplift loading.

A pile load test program was conducted as part of FHWA Demonstration Project 66. The static load test frame, dynamic pile testing services, static load testing services and associated technical support were provided as part of the FHWA demonstration project. For the test program, 1219 mm closed end pipe piles were chosen in order to develop high toe resistances in the glacial till and thereby support large compression loads. Preliminary wave equation analyses indicated that a 19 mm wall thickness could be used instead of the 32 mm wall thickness. To meet uplift requirements, a short non-displacement pile section was spliced below the pipe pile closure plate. Two pipe piles were driven and statically load tested in both compression and tension as part of the test program. One of the two piles was fitted with a 3 m long H-pile section below the pipe pile closure plate and the other with a 3 m long, 1219 mm diameter open pipe section.

As a result of this design stage test program, the final foundation design utilized a design load of 4450 kN, or a 67% increase from the design load anticipated in the preliminary design. Preliminary wave equation analysis results confirmed by test program dynamic and static compression load test results made possible a 40% reduction in the pile wall thickness over the preliminary design pile section. Based on the tension load test results, the H-pile section below the pipe pile closure plate provided the higher uplift capacity and was therefore chosen for final design. The test program reduced the number of foundation piles required and lowered pile material costs.

Table 2-3 summarizes the test program costs as well as the foundation savings realized from the design stage test program. The test program cost roughly \$500,000 and resulted in a net foundation cost savings of \$5 million or a benefit-cost ratio of 10:1. The foundation cost savings includes the cost savings from the increased design load and thus fewer foundation piles, the reduced pile wall thickness, and the smaller pile cap size. The net foundation cost savings was 15% of the pile supported approach structure cost. Additional information on the Third Lake Washington Bridge project may be found in Vanikar and Wilson (1986).

TABLE 2-3 FOUNDATION COST SAVINGS FOR THE THIRD LAKE WASHINGTON BRIDGE		
Test Program Costs	<ul style="list-style-type: none"> • 2-Compression Load Tests • 2-Uplift Load Tests • 2-Reaction Pile and Frame Setups • Dynamic Testing 	\$500,000
Foundation Savings	<ul style="list-style-type: none"> • Fewer Piles through 67% Increase in Pile Design Load • Reduced Material Costs Resulting from 40% Reduction in Pile Wall Thickness • Smaller Pile Cap Size 	\$5,500,000
Net Cost Savings		\$5,000,000
Benefit - Cost Ratio		> 10:1
Net Savings as Percentage of Approach Bridge Cost		15%

3. Oregon Department of Transportation - Construction Stage Load Tests

The Oregon Department of Transportation has conducted static pile load tests during the construction stage of several bridge projects. The purpose for these load tests was to determine the pile lengths needed. Table 2-4 presents a summary of the cost savings achieved on three Oregon DOT projects.

At the Denny Road Interchange Project, two 305 mm square prestressed concrete piles were load tested. The design load was 445 kN with an ultimate pile capacity of 890 kN. Static pile capacity calculations showed that 12 m long piles were needed. A 9 m long load test pile provided an ultimate capacity of approximately 1600 kN. The 9 m long piles (safety factor = 3.6) were used, providing a 3 m reduction in pile length for each of the 542 piles. The reduced pile length resulted in a net cost saving of \$55,000.

At the Allen Boulevard Interchange, static analysis showed that 15 m pile lengths were needed for 305 mm square prestressed concrete piles. The ultimate pile capacity was 1245 kN for piles with a design load of 625 kN. Two piles each at two pier locations were load tested to failure. A 11 m long pile failed at 1174 kN. Another 11 m long pile and two 14 m long piles failed at loads in excess of 1780 kN. Therefore, a 12 m length was selected for production piles with an ultimate pile capacity of 1245 kN. The 3 m reduction in pile length for 516 production piles resulted in a net cost saving of \$60,000.

At the Airport Road Interchange (I-205), static analysis indicated that a pile length of approximately 40 m would be required to obtain an ultimate pile capacity of 1600 kN (design load of 800 kN) with some variations in length depending on the type of pile analyzed. The contract documents allowed the contractor the option to use HP 310x79 H-piles, 324 mm O.D. steel piles (closed ended and concrete filled) or 406 mm octagonal prestressed concrete piles. The project low bidder selected the 324 mm O.D. pipe piles. Two pipe piles were tested at each of two pier locations. At each location 30 m and 33 m long piles were load tested. The ultimate capacities of four load tested piles ranged from 1320 to 2260 kN. The final average length of production piles was 30 m compared to an estimated length of about 40 m. A net cost savings of \$135,000 was achieved on the 409 production piles.

These Oregon DOT projects were not large enough to justify the costs of separate load test programs during the design stage. However, these case histories show cost savings can be achieved from construction stage load tests.

TABLE 2-4 FOUNDATION COST SAVINGS FOR OREGON BRIDGES

Bridge Location	No. of Pile Supported Foundation Units	Pile Size and Type	Reduction in Pile Length	Basis for Reduction in Length	Net Actual Savings	Savings % of Bridge Cost	Savings % of Pile Cost	Remarks
SR 17 Denney Road Interchange, Washington County	14	305 mm square prestressed concrete; 9 m long (combination of toe resistance and shaft resistance in very stiff silty clay).	3 m length reduction in each of 542 piles	Pile load tests with factor of safety of 3.6	\$55,000	3.1%	26.0%	More savings would have resulted from a reduction in factor of safety to 2.0.
SR 217 Allen Boulevard Interchange, Washington County	12	305 mm square prestressed concrete; 12 m long. (combination of toe resistance and shaft resistance in very stiff silty clay).	3 m length reduction in each of 516 piles.	Pile load tests with factor of safety of 2	\$60,000	1.9%	19.7%	
I-205 Airport Road Interchange, Multnomah County	23	324 mm O.D. steel pipe, concrete filled; 30 m long. (combination of toe resistance and shaft resistance in medium to dense sand).	9 m length reduction in each of 409 piles	Pile load tests with factor of safety of 2	\$135,000	4.1%	25.4%	

4. North Carolina Department of Transportation - U.S. 17 Bridges

The North Carolina DOT provided two alternate foundation designs in the contract documents for the dual U.S. 17 Bridges over the Dismal Swamp Canal. Alternate No. 1 was the standard State foundation design and consisted of 559 mm octagonal prestressed concrete piles. Alternate No. 2 consisted of 1372 mm prestressed concrete cylinder piles.

Only one contractor submitted a bid on Alternate No. 1, the standard State pile foundation design. This bid totaled 3.7 million dollars for the foundation items. Five contractors submitted bids for Alternate No. 2. These bids ranged from 2.9 to 4.4 million dollars for the foundation items. The low bid for the bridge contract was for Alternate No. 2 with the 2.9 million dollar bid for the foundation items. Hence, an apparent savings of 0.8 million dollars was achieved over the State's standard pile foundation alternate.

This case history illustrates that alternate designs generate competition and can result in cost savings.

REFERENCES

- Reese, L.C. and O'Neill, M.W. (1988). Drilled Shafts: Construction Procedures and Design Methods. Publication No. FHWA-HI-88-042, U.S. Department of Transportation, Federal Highway Administration, National Highway Institute, McLean, 564.
- Gifford, D.G., Wheeler, J.R., Kraemer, S.R. and McKown, A.F. (1987). Spread Footings for Highway Bridges. FHWA Report No. FHWA/RD-86/185, U.S. Department of Transportation, Federal Highway Administration, Office of Engineering and Highway Operations Research and Development, McLean, 229.
- Vanikar, S.N. and Wilson, L. (1986). State-of-the-Art Pile Load Test Program for the Third Lake Washington Bridge, Public Roads, Vol. 50, No. 1., 21-23.

3. OVERVIEW OF PILE FOUNDATION DESIGN AND CONSTRUCTION

3.1 DESIGN OF PILE FOUNDATIONS

As stated by Professor R. B. Peck, "driving piles for a foundation is a crude and brutal process". The interactions among the piles and the surrounding soil are complex. Insertion of piles generally alters the character of the soil and intense strains are set up locally near the piles. The nonhomogeneity of soils, along with the effects of the pile group and pile shape, add further difficulties to the understanding of soil-pile interaction.

Broad generalizations about pile behavior are unrealistic. An understanding of the significance of several factors involved is required to be successful in the design of pile foundations. Because of the inherent complexities of pile behavior, it is necessary to use practical semi-empirical methods of design, and to focus attention on significant factors rather than minor or peripheral details. The foundation engineer must have a thorough understanding of foundation loads, subsurface conditions including soil/rock properties and behavior, the significance of special design events, foundation performance criteria, and current practices in foundation design and construction in the area where the work is to be done to arrive at the optimum foundation solution.

3.2 CONSTRUCTION OF PILE FOUNDATIONS

Construction of a successful driven pile foundation that meets the design objectives depends on relating the requirements of the static analysis methods presented on the plans to the dynamic methods of field installation and construction control. The tools for obtaining such a foundation must be explicitly incorporated into the plans and specifications as well as included in the contract administration of the project.

It is important that a pile foundation be installed to meet the design requirements for compressive, lateral and uplift capacity. This may dictate driving piles for a required ultimate capacity or to a predetermined length established by the designer. It is equally important to avoid pile damage or foundation cost overruns by excessive driving. These objectives can all be satisfactorily achieved by use of wave equation analysis, dynamic monitoring of pile driving, and static load testing. Commonly used dynamic formulas,

such as Engineering News formula, have proven unreliable as pile capacities increased and more sophisticated pile installation equipment was routinely used by contractors.

Knowledgeable construction supervision and inspection are the keys to proper installation of piles. State-of-the-art designs and detailed plans and specifications must be coupled with good construction supervision to achieve desired results.

Post construction review of pile driving results versus predictions regarding pile driving resistances, pile length, field problems, and load test capacities is essential. These reviews add to the experience of all engineers involved on the project and will enhance their skills.

3.3 GEOTECHNICAL INVOLVEMENT IN PILE FOUNDATION PROJECT PHASES

The input of an experienced geotechnical engineer from the planning stage through project design and construction is essential to produce a successful driven pile foundation. The geotechnical engineer who specializes in foundation design is the most knowledgeable person for selecting the pile type, estimating pile length, and choosing the most appropriate method to determine ultimate pile capacity. Therefore, the geotechnical engineer should be involved throughout the design and construction process. In some project phases, *i.e.* preliminary explorations, preliminary design, and final design, the geotechnical engineer will have significant involvement. In other project phases, such as construction, and post construction review, the geotechnical engineer's involvement may be more of a technical services role. The geotechnical engineer's involvement provides the needed continuity of design personnel in dealing with design issues through the construction stage.

3.4 DRIVEN PILE DESIGN-CONSTRUCTION PROCESS

The driven pile design and construction process has aspects that are unique in all of structural design. Because the driving characteristics are related to pile capacity for most soils, they can be used to improve the accuracy of the pile capacity estimate. In general, the various methods of determining pile capacity from dynamic data such as driving resistance with wave equation analysis and dynamic measurements are considerably more accurate than the static analysis methods based on subsurface

exploration information. Furthermore, pile driveability is a very important aspect of the process and must be considered during the design phase. If the design is completed, a contractor is selected, and then the piles cannot be driven, large costs can be generated. It is absolutely necessary that the design and construction phases be linked in a way that does not exist elsewhere in construction.

The driven pile design-construction process is outlined in the flow chart of Figure 3.1. This flow chart will be discussed block by block using the numbers in the blocks as a reference and it will serve to guide the designer through all of the tasks that must be completed.

Block 1: Establish Requirements for Structural Conditions and Site Characterization

The first step in the entire process is to determine the general structure requirements.

1. Is the project a new bridge, a replacement bridge, a bridge renovation, a retaining wall, a noise wall, or sign or light standard?
2. Will the project be constructed in phases or all at one time?
3. What are the general structure layout and approach grades?
4. What are the surficial site characteristics?
5. Is the structure subjected to any special design events such as seismic, scour, debris, vessel impact, etc.? If there are special design events, the design requirements for the event should be reviewed at this stage so that these considerations can be factored into the site investigation.
6. Are there possible modifications in the structure that may be desirable for the site under consideration?
7. What are the approximate foundation loads? Are there deformation or deflection limitations beyond the usual requirements?

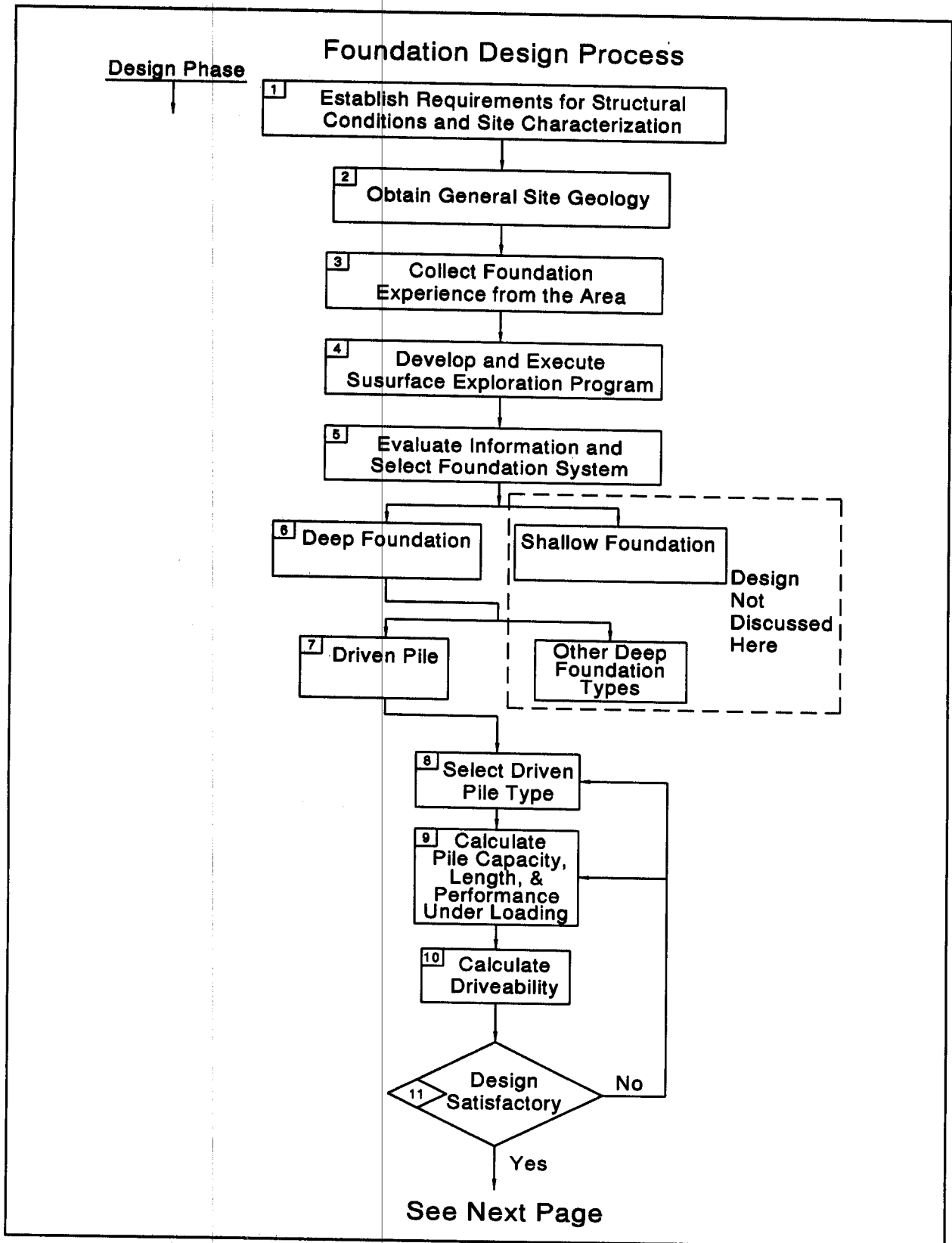


Figure 3.1 Driven Pile Design and Construction Process

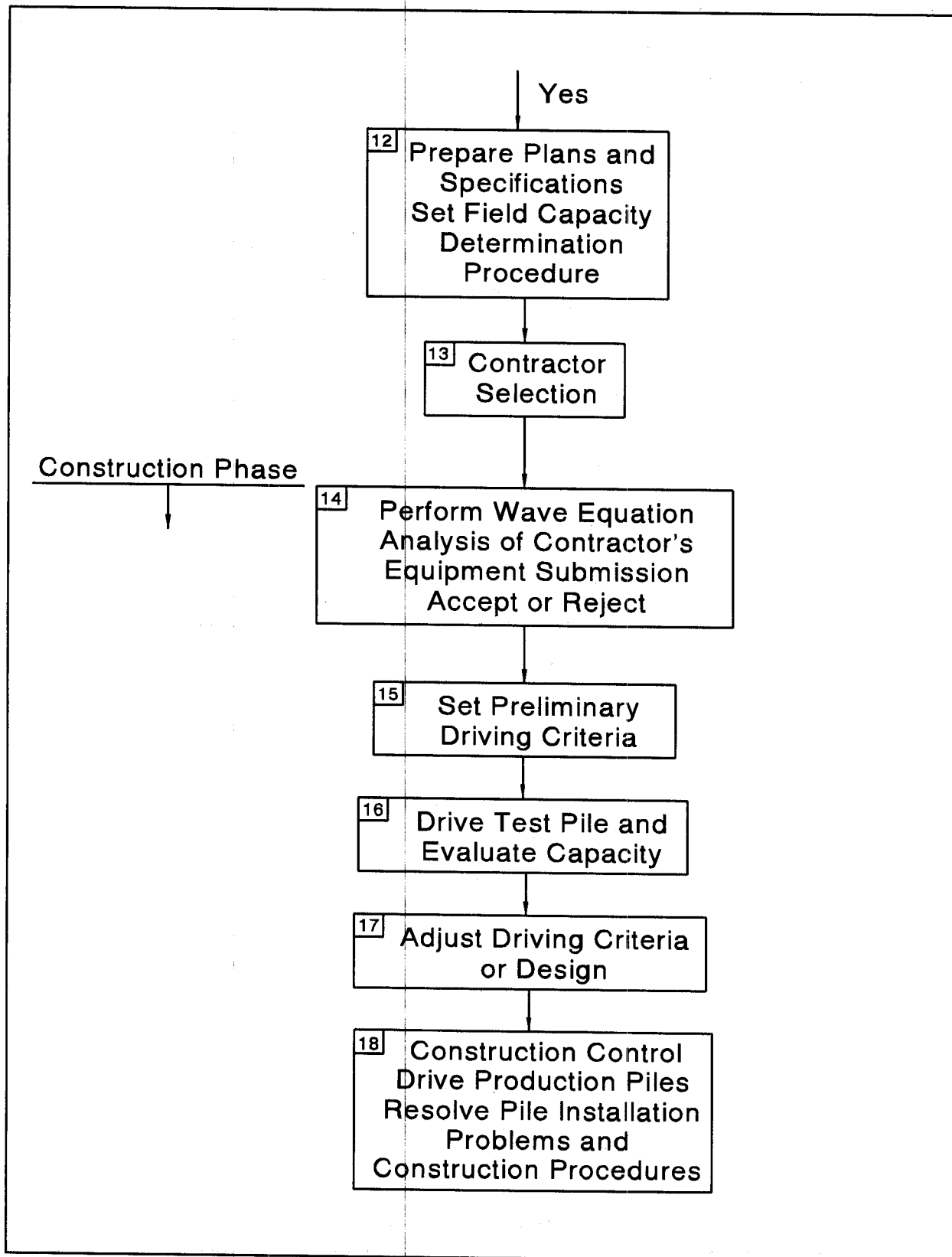


Figure 3.1 Driven Pile Design and Construction Process (continued)

Block 2: Obtain General Site Geology

A great deal can be learned about the foundation requirements with even a very general understanding of the site geology. For small structures, this may involve only a very superficial investigation such as a visit to the site. The foundation design for very large structures may require extensive geologic studies.

Block 3: Collect Foundation Experience from the Area

Frequently there is information available on foundations that have been constructed in the area. This information can be of assistance in avoiding problems. Both subsurface exploration information and foundation construction experience should be sought prior to selecting the foundation type.

Block 4: Develop and Execute Subsurface Exploration Program

Based on the information obtained in Blocks 1-3 it is possible to make decisions regarding the necessary information that must be obtained at the site. The program must meet the needs of the design problem that is to be solved at a cost consistent with the size of the structure. The subsurface exploration program as well as the appropriate laboratory testing must be selected. The results of the subsurface exploration program and the laboratory testing are used to prepare a subsurface profile and identify critical cross sections. These tasks are covered in greater detail in Chapters 4, 5, and 6.

Block 5: Evaluate Information and Select Foundation System

The information collected in Blocks 1-4 must be evaluated and a foundation system selected. The first question to be decided is whether a shallow or a deep foundation is required. This question will be answered based primarily on the strength and compressibility of the site soils, the proposed loading conditions, and the project performance criteria. If settlement is not a problem for the structure, then a shallow foundation will probably be the most economical solution. Ground improvement techniques in conjunction with shallow foundations should be evaluated. Shallow and deep foundation interaction with approach embankments must also be considered. If the performance of a shallow foundation exceeds the structure performance criteria, a deep foundation must be used. The design of shallow foundations and ground improvement techniques are not covered in this manual. The problem of selecting the proper foundation system is discussed in detail in Chapter 7.

Refined foundation loading information and performance criteria should be established at this time. In Block 1, this issue was considered. Probably the result of that effort has matured in the intervening time (which might be quite long for some projects) and better defined foundation loads and performance criteria should now be available. The geotechnical engineer must obtain a completely defined and unambiguous set of foundation loads and performance requirements in order to proceed through the foundation design.

Block 6: Deep Foundation

The decision among deep foundation types is now divided between driven piles and drilled shafts. What is really intended is the difference between driven piles and all other deep foundation systems. These other deep foundation systems have been called a drilled shaft but would also include auger cast piles, micropiles and other drilled-in deep foundation systems. The questions that must be answered in deciding between driven piles and other deep foundation systems will center around the relative costs of available, possible systems. In addition, constructability must be considered. This manual is concerned with driven piles so the other types of deep foundations will not be discussed here. The selection of a deep foundation system is discussed in Chapter 7.

Blocks 7 and 8: Driven Pile - Select Driven Pile Type

At this point on the flow chart, the primary concern is for the design of a driven pile foundation. The pile type must be selected consistent with the applied load per pile. Consider this problem. The general magnitude of the column or pier loads is known from the information obtained in Blocks 1 and 5. However, a large number of combinations of pile capacities and pile types can satisfy the design requirements. Should twenty, 1000 kN capacity piles be used to carry a 20,000 kN load, or would it be better to use ten, 2000 kN capacity piles? This decision should consider both the structural capacity of a pile and the realistic geotechnical capacities of the pile type for the soil conditions at the site, the cost of the available alternative piles, and the capability of available construction contractors to drive the selected pile. Of course, there are many geotechnical factors that must also be considered.

At this stage the loads must be firmly established. In Block 1, approximate loads were determined. At that time the other aspects of the total structural design were probably not sufficiently advanced to establish the final design loads. By the time that Block 5 has been reached the structural engineer should have finalized the various loads. One of the most common inadequacies that is discovered when foundation problems arise is that the design loads were never really accurately defined.

In the former use of the dynamic formula, the pile load specified was a design or working load since a factor of safety was contained in the formula. Modern methods of pile capacity determination **always** use ultimate loads with a factor of safety selected and applied. This should also be made clear in the job specifications so that the contractor has no question regarding the driving requirements.

If there are special design events to be considered, they must be included in the determination of the loads. Vessel impact will be evaluated primarily by the structural engineer and the results of that analysis will give pile design loads for this case. There may be stiffness considerations in dealing with vessel impact since the design requirement is basically a requirement that some vessel impact energy be absorbed.

Scour presents a different requirement. The loads due to the forces from the stream must be determined as specified in the AASHTO Standard Specification for Highway Bridges, Section 3.18 and this should be included in the structural engineer's load determination process. The depth of scour must also be determined as directed in AASHTO Specification, Section 4.3.5. In the design process, it must be assured that after scour the pile will still have adequate capacity.

In many locations in the country, seismic loads will be an important contributor to some of the critical pile load conditions. Since the 1971 San Fernando Earthquake, much more emphasis has been placed on seismic design considerations in the design of highway bridges. The AASHTO Standard Specifications for Highway Bridges has been substantially expanded to improve the determination of the seismic loads. Usually the structural engineer will determine the seismic requirements. Frequently the behavior of the selected pile design will affect the structural response and hence the pile design loads. In this case, there will be another loop in the design process that includes the structural engineer. The geotechnical engineer should review the seismic design requirements in Division I-A of the AASHTO Bridge Design Specification for a general understanding of the design approach.

Pile selection is covered in more detail in Chapter 8.

Block 9: Calculate Pile Length, Capacity, and Performance

For the selected pile type, perform static analyses to determine the length necessary to provide the required compression, uplift and lateral load capacity and to meet performance criteria. The calculation of the geotechnical pile capacity and performance under load is discussed in detail in Chapter 9 and structural pile capacity is discussed in Chapter 11. It may be necessary to change pile type or number of piles at this stage.

Block 10: Calculate Driveability

At this point, the proposed pile type and length have been chosen to meet the foundation loading and performance requirements. However, the design is not complete until it can be verified that the chosen pile can be driven to the required capacity and penetration depth at a reasonable driving resistance without excessive driving stresses. This analysis is performed using the wave equation program. All of the necessary information is available except the hammer selection. Since the hammer to be used on the job will only be known after the contractor is selected, possible hammers must be tried to make sure that the pile is driveable to the capacity and depth required. Pile driveability is introduced in Chapter 9 with additional details on the use of wave equation analysis to check pile driveability described in Chapter 17. Allowable pile driving stresses are presented in Chapter 11.

Block 11: Design Satisfactory

At this point in the process, all aspects of the design should be reviewed and if changes are indicated, the flow chart is re-entered at some earlier point and a new design is developed.

Block 12: Prepare Plans and Specifications, Set Field Capacity Determination Procedure

When the design has been finalized, plans and specifications can be prepared and the procedures that will be used to verify pile capacity can be defined. It is important that all of the quality control procedures are clearly defined for the bidders to avoid claims after construction is underway. Construction specifications are discussed in Chapter 12 and the preparation of the foundation report is covered in Chapter 14.

Block 13: Contractor Selection

After the bidding process is complete, a successful contractor is selected.

Block 14: Perform Wave Equation Analysis of Contractor's Equipment Submission

At this point the engineering effort shifts to the field. The contractor will submit a description of the pile driving equipment that he intends to use on the job for the engineer's evaluation. Wave equation analysis is performed to determine the driving resistance that must be achieved in the field to meet the required capacity and pile penetration depth. Driving stresses are determined and evaluated. If all conditions are satisfactory, the equipment is approved for driving. Some design specifications make this information advisory to the contractor rather than mandatory. Chapters 11, 12, and 17 provide additional information in this area.

On smaller projects, a dynamic formula may be used to evaluate driveability and the Gates Formula should be used. If a dynamic formula is used, then driveability and hammer selection will be based on the driving resistance only, since stresses are not determined. The use of a dynamic formula is covered in more detail in Chapter 16.

Block 15: Set Preliminary Driving Criteria

Based on the results of the wave equation analysis of Block 14 (or the Gates Formula) and any other requirements in the design, the preliminary driving criteria can be set.

Block 16: Drive Test Pile and Evaluate Capacity

The test pile(s) are driven to the preliminary criteria developed in Block 15. Driving requirements may be defined by penetration, driving resistance, dynamic monitoring results or a combination of these conditions. The capacity can be evaluated by driving resistance from wave equation analysis, the results of dynamic monitoring, static load test, the Gates Formula, or a combination of these. Dynamic monitoring is described in Chapter 18. Static load test procedures are discussed in greater detail in Chapter 19 and dynamic formulas are covered in Chapter 16.

Block 17: Adjust Driving Criteria or Design

At this stage the final conditions can be set or, if test results from Block 16 indicate the capacity is inadequate, the driving criteria may have to be changed. In a few cases, it may be necessary to make changes in the design as far back as Block 8. If major changes are required, it will be necessary to repeat Blocks 14, 15, and 16.

In some cases, it is desirable to perform preliminary field testing before final design. When the job is very large and the soil conditions are difficult, it may be possible to achieve substantial cost savings by having results from a design stage test pile program, including actual driving records at the site, as part of the bid package.

Block 18: Construction Control

After the driving criteria is set, the production pile driving begins. Quality control and assurance procedures have been established and are applied. Construction inspection items are discussed in greater detail in Chapter 24. Problems may arise and must be handled as they occur in a timely fashion.

3.5 COMMUNICATION

Good communication between all parties involved in the design and construction of a pile foundation is essential to reach a successful completion of the project. In the design stage, communication and interaction is needed between the structural, geotechnical, geologic, hydraulic, and construction disciplines, as well as with consultants, drill crews and laboratory personnel. In the construction stage, structural, geotechnical and construction disciplines need to communicate for a timely resolution of construction issues as they arise. Figures 3.2 and 3.3 highlight some of the key issues to be communicated in the design and construction stages.

DESIGN STAGE COMMUNICATION						
Subject	Structural	Geotechnical	Hydraulic	Construction	Field Crews	Laboratory
Preliminary Structure Loads and Performance Criteria.	X	X	X			
Determination of Scour Potential.	X	X	X			
Determination of Special Design Event Requirements.	X	X	X			
Review of Past Construction Problems in Project Area.	X	X	X	X		
Implementation of Subsurface Exploration and Testing Programs.	X	X	X		X	X
Determination of Pile Type, Length and Capacity.	X	X				
Effect of Approach Fills on Design.	X	X				
Prepare Plans and Specifications.	X	X	X	X		

Figure 3.2 Design Stage Communication

CONSTRUCTION STAGE COMMUNICATION			
Subject	Structural	Geotechnical	Construction
Establish Appropriate Methods of Construction Control and Quality Assurance.	X	X	X
Perform Wave Equation Analysis of Contractors Driving System to Establish Driving Criteria.	X	X	X
Perform Static Load Test(s) and/or Dynamic Monitoring and Adjust Driving Criteria.	X	X	X
Resolve Pile Installation Problems / Construction Issues.	X	X	X

Figure 3.3 Construction Stage Communication

4. SUBSURFACE EXPLORATIONS

The design of a structure's foundation requires adequate knowledge of the subsurface conditions at the construction site. If the designer has the appropriate information, then an economical foundation system can be designed. The absence of a thorough foundation study or adequate geotechnical data often leads to (1) a foundation system with a large factor of safety which is generally a more expensive foundation and in some cases one that may be difficult to construct, or to (2) an unsafe foundation, or to (3) construction disputes and claims.

A thorough foundation study consists of a subsurface exploration program (which includes borings, sampling, groundwater measurements, and in-situ testing); laboratory testing; geotechnical analysis of all data; a determination of design properties; and design recommendations. This chapter covers the subsurface exploration portion of a foundation design study in a concise manner. A more detailed treatment of this chapter's subject matter may be found in the AASHTO Manual on Subsurface Investigations (1988). Chapter 5 of this manual focuses on in-situ testing which is also considered part of a subsurface exploration, and Chapter 6 discusses laboratory testing. This chapter assumes that a decision with regard to the foundation type, *i.e.*, shallow or deep has not yet been made.

4.1 SUBSURFACE EXPLORATION PHASES

There are three major phases in a subsurface exploration program. These phases are (1) planning the exploration program (office work), (2) completing a field reconnaissance survey, and (3) performing a detailed site exploration program (boring, sampling, and in-situ testing). Each phase should be planned so that a maximum amount of information can be obtained at a minimum cost. Each phase also adds to, or supplements, the information from the previous phase. Table 4-1 lists the purpose of each exploration phase.

TABLE 4-1 SUBSURFACE EXPLORATION PHASES

Phase	Activity	Purpose	Remarks
1.	Planning the exploration (Office Work).	<p>A. Obtain structure information. Determine:</p> <ol style="list-style-type: none"> 1. Type of structure. 2. Preliminary location of piers and abutments. 3. Loading and special design events. 4. Allowable differential settlement and other performance criteria. 5. Any special features and requirements. <p>B. Obtain drilling records for nearby structures and from local well drillers.</p> <p>C. Perform literature reviews including maintenance records, pile driving records, scour history, etc.</p> <p>D. Review FHWA deep foundation load test data base.</p> <p>Obtain overall picture of subsurface conditions in the area.</p>	See Table 4-2 for sources of information.
2.	Field Reconnaissance Survey	<p>Verify information gained from the office phase and plan the detailed subsurface exploration.</p> <p>A. Observe, verify and collect information regarding:</p> <ol style="list-style-type: none"> 1. Topographic and geologic features. 2. New and old construction in the area including utilities. Performance of existing structures. 3. Drilling equipment required, cost, and access for the equipment. <p>B. If appropriate, conduct geophysical testing to obtain preliminary subsurface information.</p>	Field reconnaissance is often conducted by a multi-disciplined team.
3.	Detailed Subsurface Exploration	<p>Develop a preliminary boring plan based on phases 1 and 2. The boring plan should be modified if needed as the borings are performed and detailed subsurface information is obtained.</p> <p>The subsurface exploration should provide the following:</p> <ol style="list-style-type: none"> 1. Depth and thickness of strata (subsurface profile). 2. In-situ field tests to determine soil design parameters. 3. Samples to determine soil and rock design parameters. 4. Groundwater levels including perched, regional, and any artesian conditions. 	For major structures, the pilot boring program is often supplemented with control and verification boring programs.

4.1.1 Planning the Exploration Program (office work)

The purpose of this phase is to obtain information about the proposed structure and general information on the subsurface conditions. The structural information can be obtained from studying the preliminary structure plan prepared by the bridge design office and by meeting with the structural designer. Approach embankment preliminary design and performance requirements can be obtained from the roadway office. General information about the subsurface conditions can be obtained from a variety of sources listed in Table 4-2. **The planning phase prepares the engineer for the field reconnaissance survey, and identifies possible problems and areas to scrutinize.**

4.1.2 Field Reconnaissance Survey

The purpose of this phase is to substantiate the information gained from the office phase and to plan the detailed site exploration program. The field reconnaissance for a structure foundation exploration should include:

- a. Inspection of nearby structures to determine their performance with the particular foundation type used.
- b. Inspection of existing structure footings and stream banks for evidence of scour (for stream crossings) and movement. Large boulders in a stream are often an indication of obstructions which may be encountered in pile installations.
- c. Visual examination of terrain for evidence of landslides.
- d. Recording of the location, type and depth of existing structures which may be affected by the new structure construction.
- e. Relating site conditions to proposed boring operations. This includes recording the locations of both overhead and below ground utilities, site access, private property restrictions, and other obstructions.
- f. Recording of any feature or constraint which may impact the constructability of potential foundation systems.

Table 4-3 contains an example of a field reconnaissance form modified from the AASHTO Foundation Investigation Manual (1978) for recording data pertinent to a site.

TABLE 4-2 SOURCES OF SUBSURFACE INFORMATION AND USE

Source No.	Source	Use
1.	Preliminary structure plans prepared by the bridge design office.	Determine: 1. Type of structure. 2. Preliminary locations of piers and abutments. 3. Footing loads and special design events. 4. Allowable differential settlement and performance criteria. 5. Any special features and requirements.
2.	Construction plans and records for nearby structures.	Foundation type, old boring data, construction information including construction problems.
3.	Topographic maps prepared by the United States Coast and Geodetic Survey (USC and GS), United States Geological Survey (USGS) and State Geology survey.	Existing physical features shown; find landform boundaries and determine access for exploration equipment. Maps from different dates can be used to determine topographic changes over time.
4.	County agricultural soil survey maps and reports prepared by the United States Department of Agriculture (USDA).	Boundaries of landforms shown; appraisal of general shallow subsurface conditions.
5.	Air photos prepared by the United States Geological Survey (USGS) or others.	Detailed physical relief shown; gives indication of major problems such as old landslide scars, fault scarps, buried meander channels, sinkholes, or scour; provides basis for field reconnaissance.
6.	Well drilling record or water supply bulletins from state geology or water resources department.	Old well records or borings with general soils data shown; estimate required depth of explorations and preliminary cost of foundations.
7.	Geologic maps and Geology bulletins.	Type, depth and orientation of rock formations.
8.	FHWA deep foundation load test data base.	Locate prior load test by geologic province, state, city, or geologic coordinates, provides information on soil and pile types.

TABLE 4-3 EXAMPLE FIELD RECONNAISSANCE REPORT FORM

Bridge Foundation Investigation
 Field Reconnaissance Report
 Department of Transportation

Project No: _____ County _____ Sta. No. _____

Reported By: _____ Date _____

1. Staking of Line

_____ Well Staked
 _____ Poorly Staked (We can work)
 _____ Request Division to Restake

2. Bench Marks

In Place: Yes _____ No _____
 Distance from bridge - m _____

3. Property Owners

Granted Permission: Yes _____ No _____
 Remarks on Back _____

4. Utilities

Will Drillers Encounter Underground or
 Overhead Utilities? Yes _____ No _____
 Maybe _____ At Which Holes? _____
 What Type? _____
 Who to See for Definite Location _____

5. Geologic Formation

6. Surface Soils

Sand _____ Clay _____ Sandy Clay _____
 Muck _____ Silt _____ Other _____

7. General Site Description

Topography
 Level _____ Rolling _____ Hillside _____
 Valley _____ Swamp _____ Gullied _____
 Groundcover
 Cleared _____ Farmed _____ Buildings _____
 Heavy Woods _____ Light Woods _____
 Other _____
 Remarks on Back _____

8. Bridge Site

Replacing _____
 Widening _____
 Relocation _____
 Check Appropriate Equipment
 _____ Truck Mounted Drill Rig
 _____ Track Mounted Drill Rig
 _____ Failing 1500
 _____ Truck Mounted Skid Rig
 _____ Skid Rig
 _____ Rock Coring Rig
 _____ Wash Boring Equipment
 _____ Water Wagon
 _____ Pump
 _____ Hose _____ m _____

8. Bridge Site - Continued

Cut Section - m _____
 Fill Section - m _____
 If Stream Crossing:
 Will Pontoons Be Necessary? _____
 Can Pontoons Be Placed in Water Easily? _____

 Can Cable Be Stretched Across Stream?
 _____ How Long? _____
 Is Outboard Motorboat Necessary? _____
 Current:
 Swift _____ Moderate _____ Slow _____
 Describe Streambanks scour.
 If Present Bridge Nearby:
 Type of Foundation _____
 Any Problems Evident in Old Bridge Including
 Scour _____
 (describe on back)
 Is Water Nearby for Wet Drilling - m _____
 Are Abandoned Foundations in Proposed
 Alignment? _____

9. Ground Water Table

Close to Surface - m _____
 nearby Wells - Depth - m _____
 Intermediate Depth - m _____
 Artesian head - m _____

10. Rock

Boulders Over Area? Yes _____ No _____
 Definite Outcrop? Yes _____ No _____
 (show sketch on back)
 What kind? _____

11. Special Equipment Necessary

12. Remarks on Access

(Describe any Problems on Access)

13. Debris and Sanitary Dumps

Stations _____
 Remarks _____

Reference: Modified from 1978 AASHTO Foundation
 Investigation Manual

4.1.3 Detailed Site Exploration

The purpose of any boring program is not just to drill a hole, but to obtain representative information on the subsurface conditions, to recover disturbed and undisturbed soil samples, and to permit in-situ testing. This information provides factual basis upon which all subsequent steps in the pile design and construction process are based. It's quality and completeness are of paramount importance. Each step in the process directly or indirectly relies on this data.

The first step in this phase is to prepare a preliminary boring, sampling, and in-situ testing plan. For major structures, pilot borings are usually performed at a few select locations during the preliminary planning stage. These pilot borings establish a preliminary subsurface profile and thus identify key soil strata for testing and analysis in subsequent design stage borings. During the design stage of major structures, a two phase boring program is recommended. First, control borings are performed at key locations identified in the preliminary subsurface profile to determine what, if any, adjustments are appropriate in the design stage exploration program. Following analysis of the control boring data, verification borings are then performed to fill in the gaps in the design stage exploration program.

4.2 GUIDELINES FOR MINIMUM STRUCTURE EXPLORATION PROGRAMS

The cost of a boring program is comparatively small in relation to the foundation cost. For example, the cost of one 60 mm diameter boring is less than the cost of one 305 mm diameter pile. However, in the absence of adequate boring data, the design engineer must rely on extremely conservative designs with high safety factors. At the same time, the designer assumes enormous risk and uncertainty during the project's construction.

The number of borings required, their spacing, and sampling intervals depend on the uniformity of soil strata and loading conditions. Erratic subsurface conditions require closely spaced borings. Structures sensitive to settlements or subjected to heavy loads require detailed subsurface knowledge. In these cases borings should be closely spaced. Rigid rules for number, spacing, and depth of borings cannot be established. However, the following are general "guidelines" useful in preparing a boring plan.

1. A minimum of one boring with sampling should be performed at each pier or abutment. The boring pattern should be staggered at opposite ends of adjacent footings. Pier and abutment footings over 30 m in length require borings at the extremities of the substructure units.
2. Estimate required boring depths from data gathered in the planning and field reconnaissance phases. Confirmation of boring depth suitability for design purposes should be made by the geotechnical engineer as soon as possible after field crews initiate a boring program. Although less preferred, it may be possible for field crews to adjust boring depths using a resistance criteria such as: "Structure foundation borings shall be terminated when a minimum SPT resistance of 50 blows per 300 mm has been maintained for 7.5 m". (This rule is intended for preliminary guidance to drillers. For heavy structures with high capacity piles, the borings must go deeper. A resistance criteria may also be inappropriate in some geologic conditions such as sites with boulder fields.)
3. All borings should extend through unsuitable strata, such as unconsolidated fill, peat, highly organic materials, soft fine grained soils and loose coarse-grained soils to reach hard or dense materials. Where stiff or dense soils are encountered at shallow depths, one or more borings should be extended through this material to a depth where the presence of underlying weaker strata cannot affect stability or settlement of the structure.
4. Standard Penetration Test (SPT) samples should be obtained at 1.5 m intervals or at changes in material with the test data recorded in accordance with AASHTO T206. Undisturbed tube samples should be obtained in accordance with AASHTO T207 at sites where cohesive soils are encountered. The location and frequency of undisturbed soil sampling should be based on project requirements.
5. When rock is encountered at shallow depths, additional borings or other investigation methods such as probes, test pits, or geophysical tests may be needed to define the rock profile. When feasible, borings should extend a minimum of 3 m into rock having an average core recovery of 50% or greater with an NX-core barrel (54 mm diameter core).

6. Drill crews should maintain a field drilling log of boring operations. The field log should include a summary of drilling procedures including SPT hammer type, sample depth and recovery, strata changes, and visual classification of soil samples. The field log should also include pertinent driller's observations such as location of ground water table, boulders, loss of drilling fluids, artesian pressures, etc. Disturbed and undisturbed soil samples as well as rock cores should be properly labeled, placed in appropriate storage containers (undisturbed tube samples should be sealed in the field), and properly transported to the soils laboratory.
7. The water level reading in a bore hole should be made during drilling, at completion of the bore hole, and a minimum of 24 hours after completion of the bore hole. Long term readings may require installation of an observation well or piezometer in the bore hole. More than one week may be required to obtain representative water level readings in low permeability cohesive soils or in bore holes stabilized with some drilling muds.
8. All bore holes should be properly backfilled and sealed following completion of the subsurface exploration program, data collection, and analysis. Bore hole sealing is particularly important where groundwater migration may adversely effect the existing groundwater conditions (aquifer contamination) or planned construction (integrity of tremie seals in future cofferdams).

These guidelines should result in subsurface exploration data that clearly identify subsurface stratigraphy and any unusual conditions, allow laboratory assessments of soil strength and compressibility, and document the groundwater table conditions. This information permits a technical evaluation of foundation options and probable costs.

4.3 METHODS OF SUBSURFACE EXPLORATION

The most widely used method of subsurface exploration is drilling holes into the ground from which samples are collected for visual classification and laboratory testing. Table 4-4 summarizes the advantages and disadvantages of four commonly used soil boring methods, as well as rock coring, test pits and geophysical methods.

TABLE 4-4 METHODS OF SUBSURFACE EXPLORATIONS*					
Method	Depth	Type of Samples Taken	Advantages	Disadvantages	Remarks
1. Seismic 2. Resistivity	Usually less than 30 m.	No samples are taken.	1. Less expensive than borings. 2. Complements borings. 3. Data obtained very quickly.	1. Indirect method of exploration, no samples are taken. 2. Interpretation of data is critical and requires substantial experience.	Main uses are described in AASHTO (1988). Additional limitations of seismic methods are: 1. Soil layers must increase in seismic velocities with depth. 2. The layer must be thick.
3. Wash Boring	Depends on the equipment. Most equipment can drill to depths of 30 m or more.	Disturbed and undisturbed.	1. Borings of small and large diameter. 2. Equipment is relatively inexpensive. 3. Equipment is light. 4. Washwater provides an indication of change in materials. 5. Method does not interfere with permeability tests.	1. Slow rate of progress. 2. Not suitable for materials containing stones and boulders.	Hole advanced by a combination of the chopping action of a light bit and jetting action of the water coming through the bit.
4. Rotary Drilling	Depends on the equipment. Most equipment can drill to depths of 60 m or more.	Disturbed and undisturbed.	1. Suited for borings 100 to 150 mm in diameter. 2. Most rapid method in most soils and rock. 3. Relatively uniform hole with little disturbance to the soil below the bottom of hole. 4. Experienced driller can detect changes based on rate of progress.	1. Drilling mud if used does not provide an indication of material change as the washwater does. 2. Use of drilling mud hampers the performance of permeability tests.	Hole advanced by rapid rotation of drilling bit and removal of material by water or drilling mud. Rock coring is performed by rotary drilling.
5. Auger Borings	Depends on the equipment. Most equipment can drill to depths of 30 to 60 m.	Disturbed and undisturbed.	1. Boring advanced without water or drilling mud. 2. Hollow stem auger acts as a casing.	1. Difficult to detect change in material. 2. Heavy equipment required. 3. Water level must be maintained in boring equal to or greater than existing water table to prevent sample disturbance.	Hole advanced by rotating and simultaneously pressing an auger into the ground either mechanically or hydraulically.
6. Continuous Sample Method of Advance	Depends on the equipment.	Disturbed and undisturbed.	Almost continuous record of the soil profile can be obtained.	Generally much slower in soils and more expensive than other methods.	Boring advanced by wash method, rotary drilling or auger method and continuous samples are taken.
7. Rock Coring	Rotary drilling equipment is used to drill to depths of 60 m or more.	Continuous rock cores.	Helps differentiate between boulders and bedrock.	Can be slow and fairly expensive.	Several types of core barrels are used including wire line core barrels for deep drilling.
8. Test Pits	Usually less than 6 m.	Disturbed samples and undisturbed block samples.	Least sample disturbance. Valuable in erratic soil deposits such as old fills, landfills, and residual soil deposits.	1. Limited depth. 2. Slower and expensive.	Power equipment used to excavate the pits. Test pits should be located so as not to disturb bearing stratum if footing foundations are feasible.

* Excluding in-situ tests.

4.4 SOIL AND ROCK SAMPLING

One of the main purposes of a subsurface exploration program is to obtain **quality** soil and rock samples. Quality samples are important because soil identification and stratification, strength, and compressibility are all evaluated from samples recovered in the exploration program.

Soil samples are divided into two categories, disturbed and undisturbed. Disturbed samples are those which have experienced large structural disturbance during sampling operations and may be used for identification/classification tests. The primary disturbed sampling method is the split barrel sampler used in the Standard Penetration Test (SPT). The penetration resistance values obtained from the Standard Penetration Test are called N values. These N values provide an indication of soil density or consistency and shear strength. The recommended test procedures outlined in AASHTO T206 should be rigidly followed so that consistent, reliable SPT N values are obtained. SPT N values are commonly used for design of pile foundation design in granular soils. **SPT N values are NOT RECOMMENDED for pile design in cohesive soils.**

Undisturbed samples are those in which structural disturbance is kept to an absolute minimum. Undisturbed samples are used for consolidation tests and strength tests such as direct shear, triaxial shear and unconfined compression as well as for determining unit weight. Strength tests provide shear strength design parameters which are used in static analysis methods for pile foundation design. Consolidation tests provide parameters needed to estimate settlements of embankments, spread footings, or pile groups. Unit weight information is used in determining the effective overburden pressure.

Rock cores obtained from borings allow a qualitative evaluation of rock mass and distinguish between boulders and bedrock. Rock Quality Designation (RQD) values determined from cores indicate rock soundness and characteristics and may thereby be useful in estimating the compressive strength of the rock mass. Unconfined compression tests may also be performed on recovered, high quality core samples.

4.4.1 Disturbed Soil Samplers

The split barrel sampler (Figure 4.1) used in the Standard Penetration Test (SPT) is the primary disturbed soil sampler. The SPT test consists of driving a 51 mm O.D. (35 mm I.D.) split-spoon sampler into the soil with a 64 kg mass dropped 760 mm. The sampler is generally driven 450 mm, and the blow count for each 150 mm increment is recorded. The number of blows required to advance the sampler from a penetration depth of 150 mm to a penetration depth of 450 mm is the SPT resistance value, N .

The SPT hammer type and operational characteristics can have a significant influence on the resulting SPT N values. There are two main hammer types currently in use in the US, the safety hammer and the automatic hammer. A third hammer type, the donut hammer, was used almost exclusively prior to about 1970. However, it is seldom used now due to safety considerations. Figure 4.2 provides illustrations of the three SPT hammer types. The pile design charts and methods provided in Chapter 9 that use SPT N values are based on safety hammer correlations.

Finno (1989), reported on the results of a pile capacity prediction symposium. For this event, two soil borings were drilled less than 10 m apart in a uniform sand soil profile. SPT N values were obtained using a safety hammer in one boring and an automatic hammer in the other boring. Figure 4.3 presents a plot of the SPT N values versus depth from these two borings. The SPT N values from the safety hammer range from 1.9 to 2.7 times the comparable N value from the automatic hammer. **This significant variation in N values clearly indicates that the type of SPT hammer used should be recorded on all drilling logs.**

Cheney and Chassie (1993) list the following common errors that can influence SPT test results:

1. Effect of overburden pressure. Soils of the same density will give smaller SPT N values near the ground surface.
2. Variations in the 760 mm free fall of the drive weight, since this is often done by eye on older equipment using a rope wrapped around a power takeoff (cathead) from the drill motor. Newer automatic hammer equipment does this automatically.
3. Interference with the free fall of the drive weight by the guides or the hoist rope. New equipment eliminates rope interference.

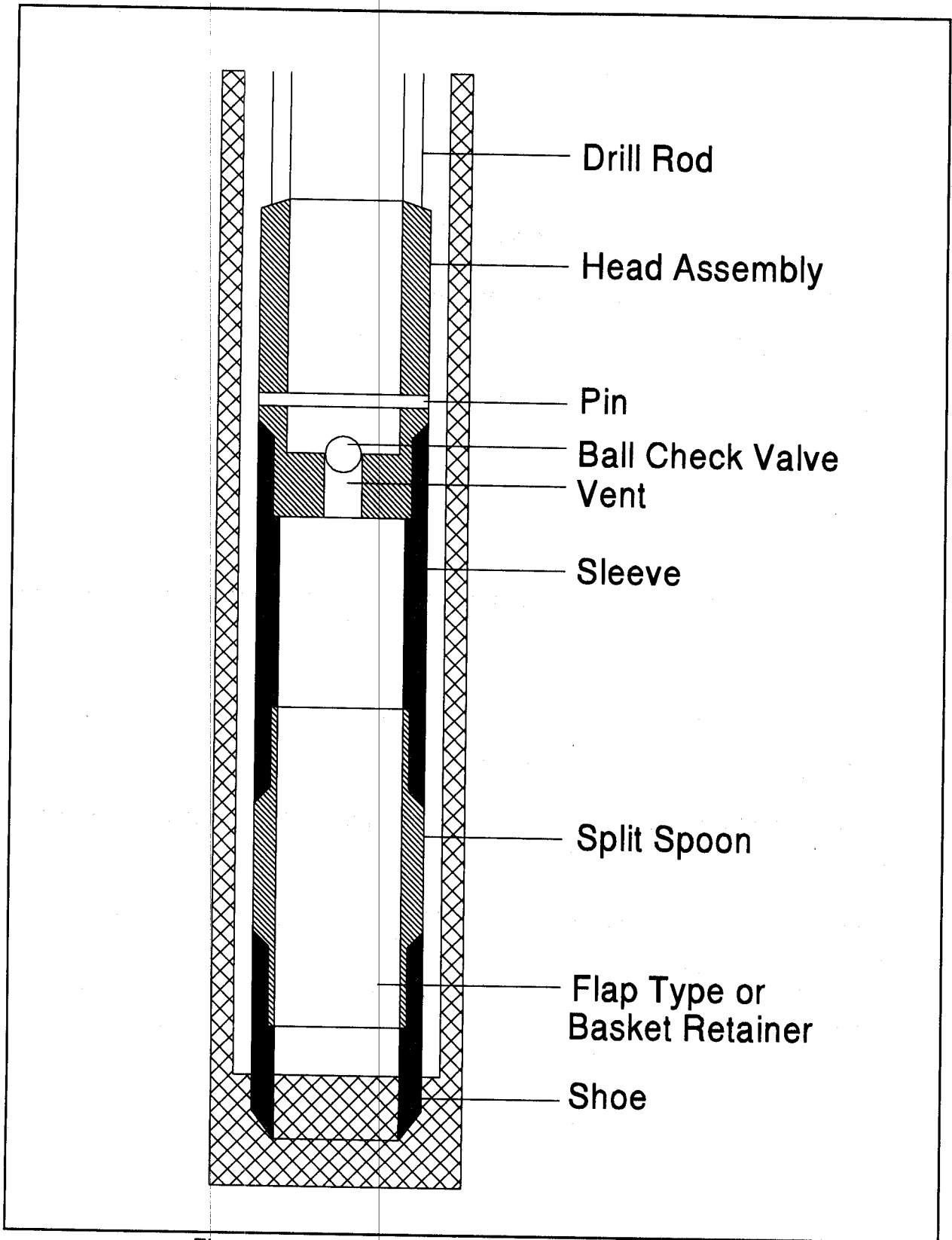


Figure 4.1 Split Barrel Sampler (after FHWA, 1972)

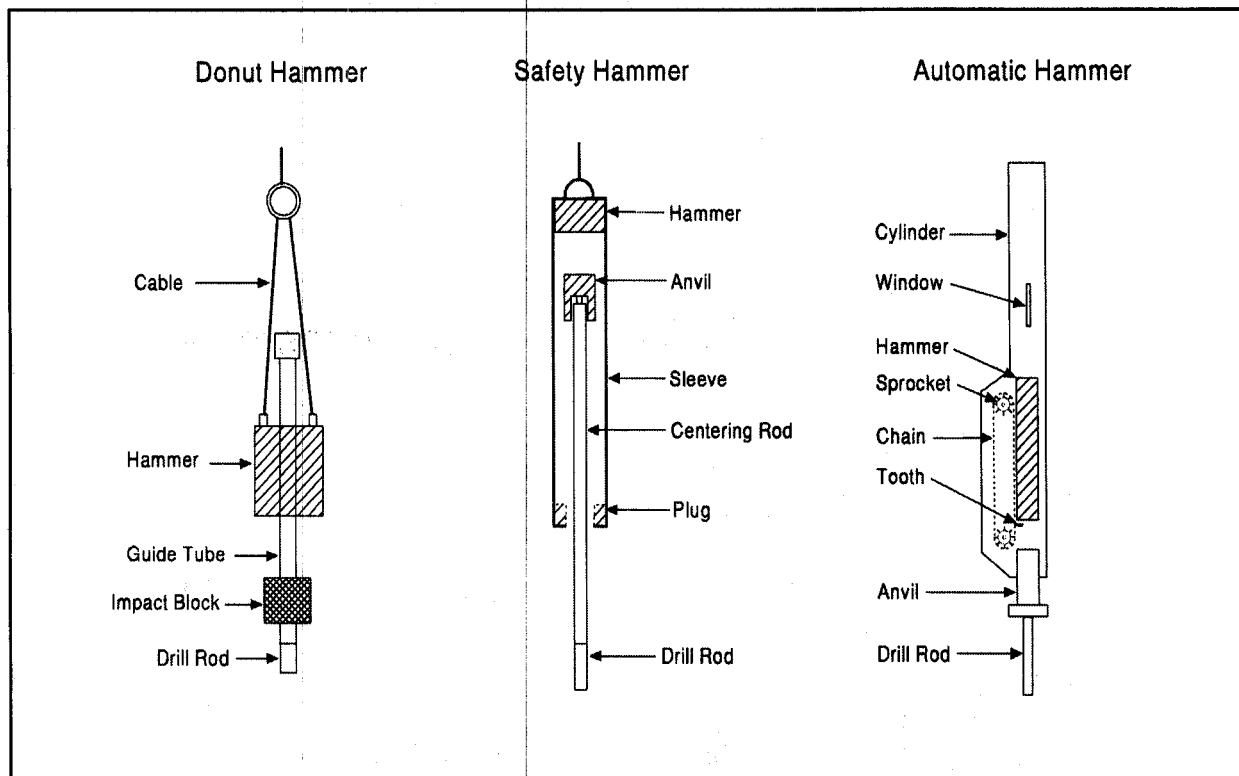


Figure 4.2 SPT Hammer Types

4. Use of a drive shoe that is badly damaged or worn from too many drivings to "refusal" (SPT N values exceeding 100).
5. Failure to properly seat the sampler on undisturbed material in the bottom of the boring.
6. Inadequate cleaning of loosened material from the bottom of the boring.
7. Failure to maintain sufficient hydrostatic pressure in the borehole during drilling or during drill rod extraction. Unbalanced hydrostatic pressures between the borehole drill water and the ground water table can cause the test zone to become "quick". This can happen when using the continuous-flight auger with the end plugged and maintaining a water level in the hollow stem below that in the hole.

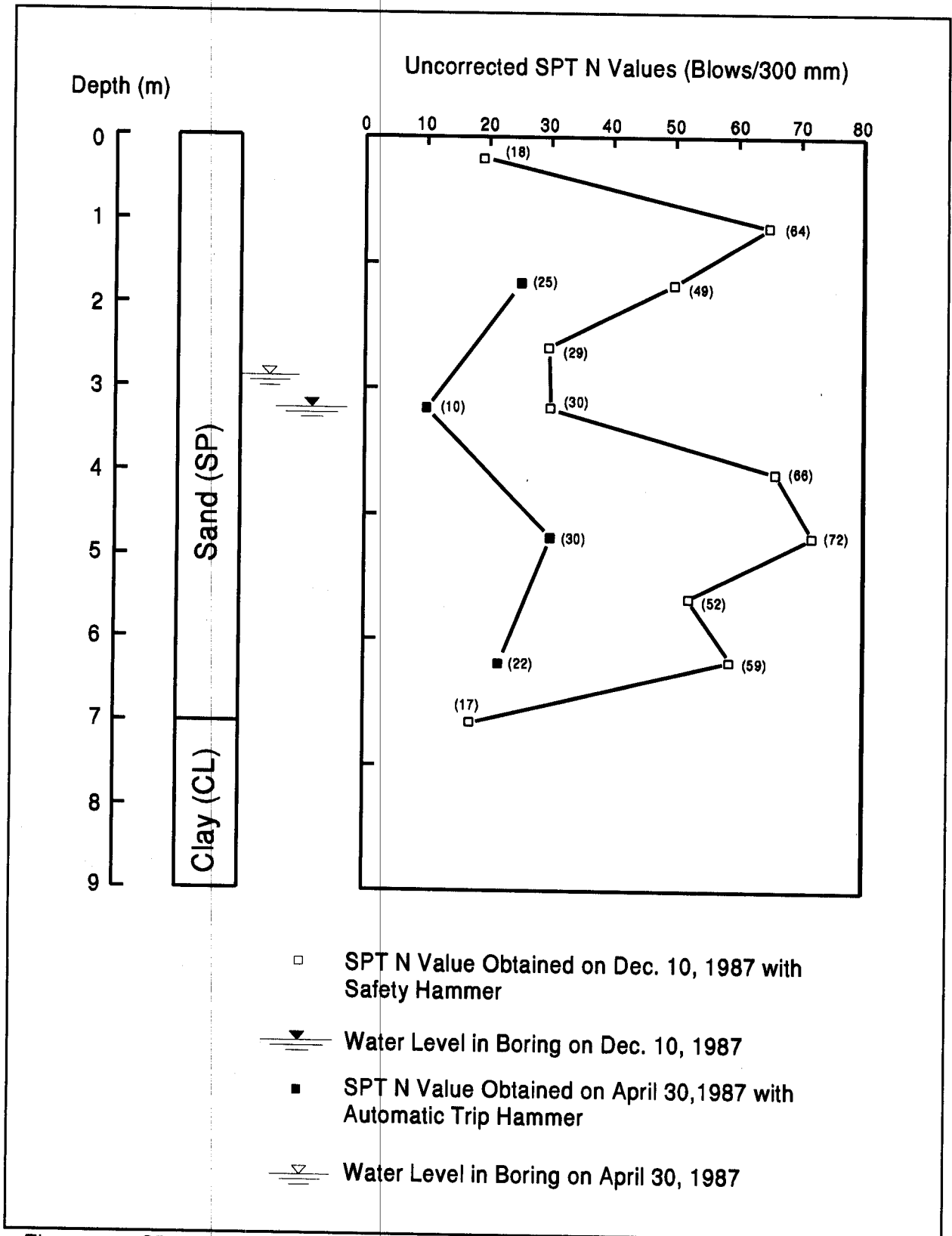


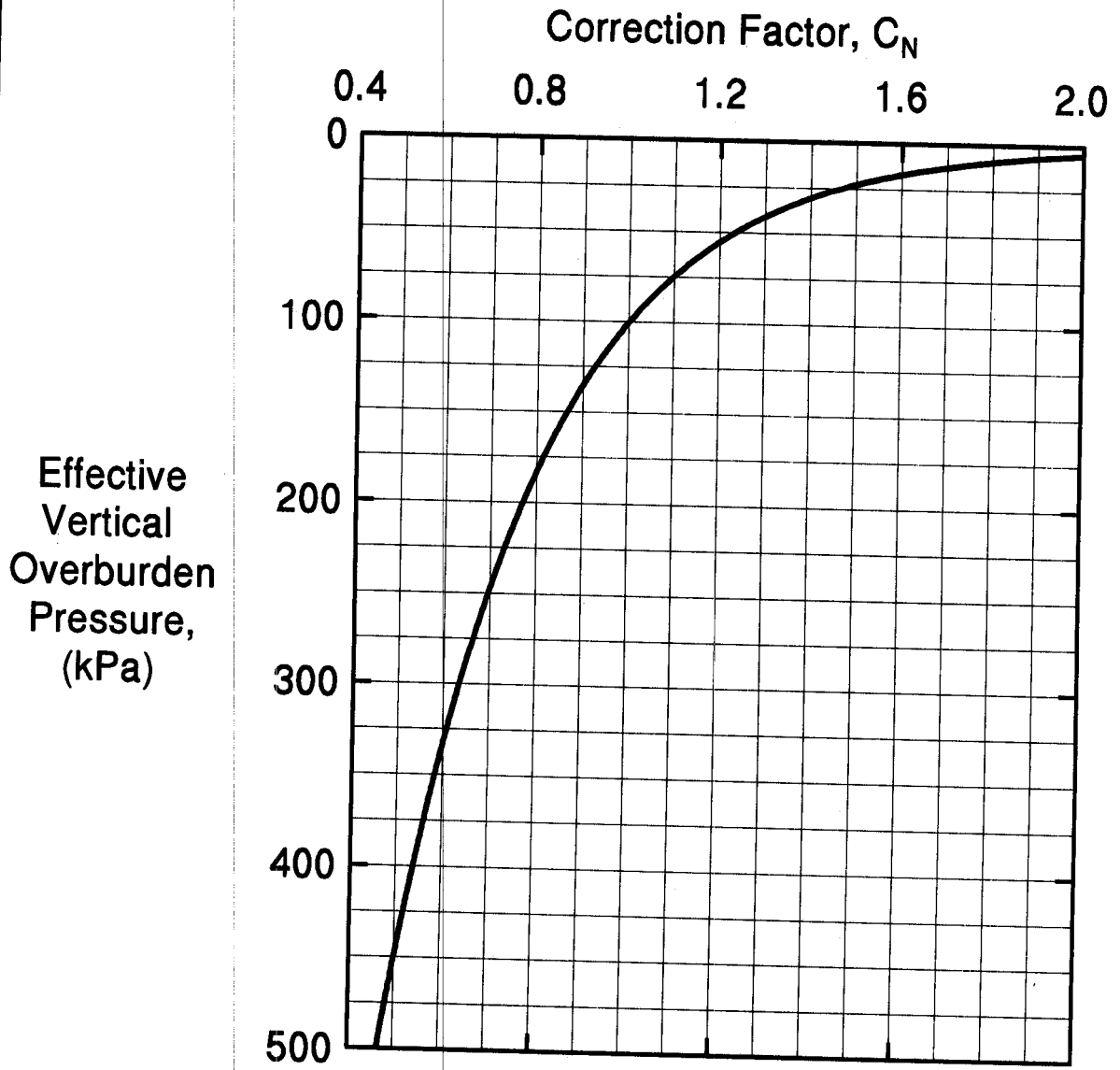
Figure 4.3 SPT Test Results for Safety and Automatic Hammers (after Finno, 1989)

8. SPT results may not be dependable in gravel. Since the split-spoon inside diameter is 35 mm, gravel sizes larger than 35 mm will not enter the spoon. Therefore, soil descriptions may not reflect actual gravel content of the deposit. Also, gravel pieces may jam the end of the spoon which may get plugged and cause the SPT blow count to be erroneously high.
9. Samples retrieved from dilatant soils (fine sands, sandy silts) which exhibit unusually high blow count should be examined in the field to determine if the sampler drive shoe is plugged. Poor sample recovery is a indication of plugging.
10. Careless work on the part of the drill crew.

The use of reliable qualified drillers and adherence to recommended sampling practice cannot be overemphasized. State agencies which maintain their own drilling personnel and equipment achieve much more reliable, consistent results than those who routinely let boring contracts to the low bidder.

A correction of field N values is also necessary to account for the effects of overburden pressures when estimating physical properties in cohesionless soils. The corrected N' value is determined by multiplying the field N value by the correction factor obtained from Figure 4.4. All N' values referred to in this manual are the corrected values. Correlations of cohesive soil physical properties with N values are crude and, therefore, correction of N values in cohesive soils is not necessary.

The corrected N' values and uncorrected N values (blows /300 mm) may be used to estimate the relative density of cohesionless soils and consistency of cohesive soils, respectively. Table 4-5 contains an empirical relationship between N' value, and the relative density, angle of internal friction and unit weight of granular soils. It is emphasized that for soils containing gravel sized particles, this table may yield unreliable results. In those cases, the correlations should be used for rough estimation purposes only. Static analysis procedures to calculate the ultimate capacity of pile foundations in cohesionless soils using SPT N' values are presented in Chapter 9.



$$N' = C_N(N)$$

Where: N' = corrected SPT N value.
 C_N = correction factor for overburden pressure.
 N = uncorrected or field SPT value.

Note: Maximum correction factor is 2.0.

Figure 4.4 Chart for Correction of N-values in Sand for Influence of Effective Overburden Pressure (after Peck et al., 1974)

Table 4-6 contains an empirical relationship between the uncorrected N value and the unconfined compressive strength and saturated unit weight of cohesive soils. The undrained shear strength is one half of the unconfined compressive strength. Correlations of N values to undrained shear strength of clays is crude and unreliable for design. It should be used only for preliminary estimating purposes. Undisturbed cohesive samples should be obtained for laboratory determination of accurate shear strength and unit weight.

4.4.2 Undisturbed Soil Samplers

Several types of undisturbed soil samplers are used in conjunction with boring operations.

- a. Thin wall open tube (Figure 4.5).
- b. Piston sampler.
- c. Hydraulic piston sampler.

Table 4-7 provides a summary of various undisturbed soil samplers, and their advantages and disadvantages.

Great care is necessary in extraction, handling, and in transporting undisturbed samples to avoid disturbing the natural soil structure. Tubes should be pressed and not hammered. Proper storage and transport should be done with the tube upright and encased in an insulated box with cushioning material. Each tube should be physically separated from adjacent tubes.

4.4.3 Rock Core Samplers

Rock Core Samplers (core barrels) are available in various diameters and length. The most widely used types are:

- a. Single tube.
- b. Double tube, rigid type (Figure 4.6).
- c. Double tube, swivel type (Figure 4.6).
- d. Wire line barrels.

TABLE 4-5 EMPIRICAL VALUES FOR ϕ , D_r , AND UNIT WEIGHT OF GRANULAR SOILS BASED ON CORRECTED N' (after Bowles, 1977)

Description	Very Loose	Loose	Medium	Dense	Very Dense
Relative density D_r	0 - 0.15	0.15 - 0.35	0.35 - 0.65	0.65 - 0.85	0.85 - 1.00
Corrected standard penetration no. N'	0 to 4	4 to 10	10 to 30	30 to 50	50+
Approximate angle of internal friction ϕ *	25 - 30°	27 - 32°	30 - 35°	35 - 40°	38 - 43°
Approximate range of moist unit weight (γ) kN/m^3	11.0 - 15.7	14.1 - 18.1	17.3 - 20.4	17.3 - 22.0	20.4 - 23.6

Correlations may be unreliable in soils containing gravel. See discussion in Section 9.5 of Chapter 9.

* Use larger values for granular material with 5% or less fine sand and silt.

TABLE 4-6 EMPIRICAL VALUES FOR UNCONFINED COMPRESSIVE STRENGTH (q_u) AND CONSISTENCY OF COHESIVE SOILS BASED ON UNCORRECTED N (after Bowles, 1977)

Consistency	Very Soft	Soft	Medium	Stiff	Very Stiff	Hard
q_u , kPa	0 - 24	24 - 48	48 - 96	96 - 192	192 - 384	384+
N , Standard penetration resistance	0 - 2	2 - 4	4 - 8	8 - 16	16 - 32	32+
γ (saturated), kN/m^3	15.8 - 18.8	15.8 - 18.8	17.3 - 20.4	18.8 - 22.0	18.8 - 22.0	18.8 - 22.0

The undrained shear strength is $\frac{1}{2}$ of the unconfined compressive strength.

Correlations are unreliable. Use for preliminary estimates only.

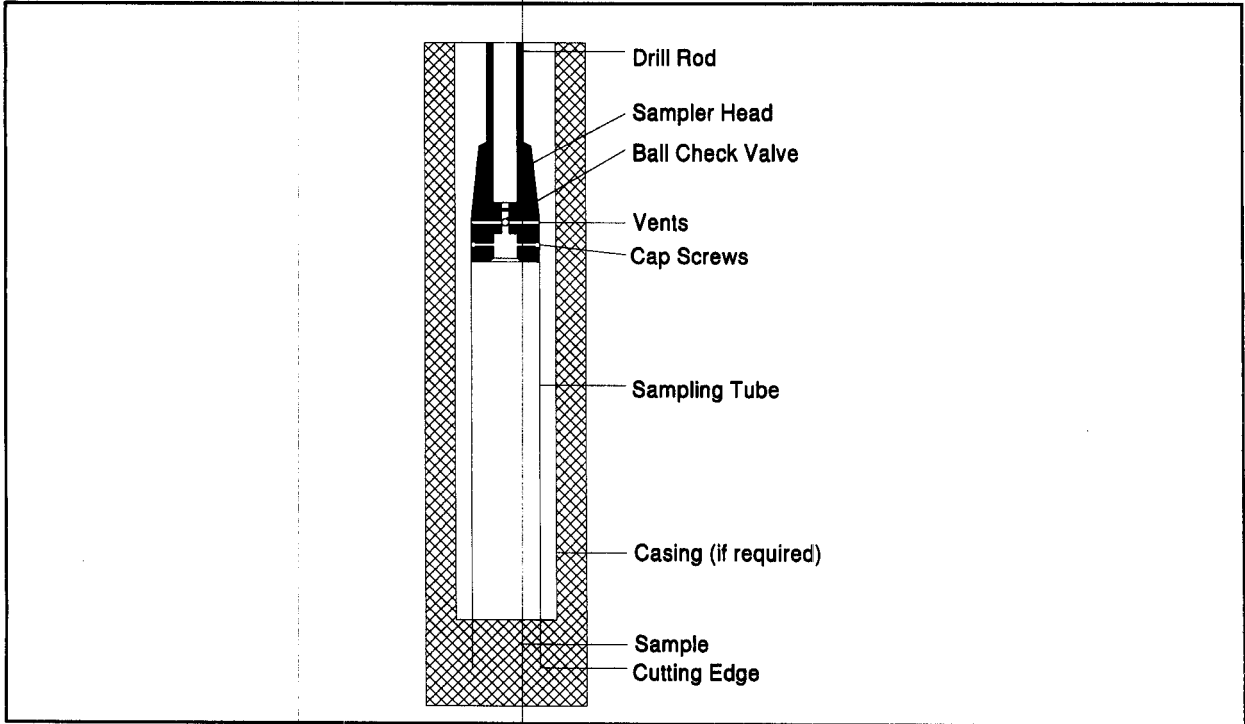


Figure 4.5 Thin Wall Open Tube (after FHWA, 1972)

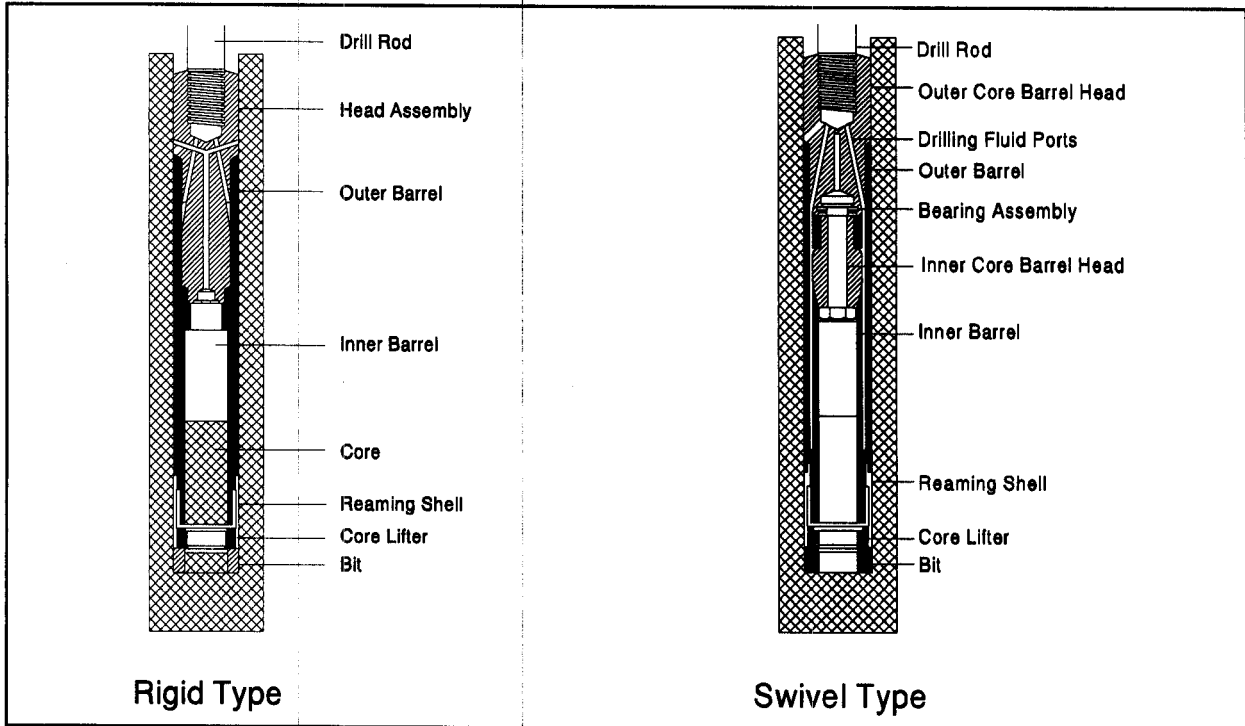


Figure 4.6 Rigid and Swivel Type Double Tube Core Barrels (after FHWA, 1972)

TABLE 4-7 UNDISTURBED SOIL SAMPLES

Sampler	Soil Types Suitable for Sampler	Advantages	Disadvantages	Remarks
Thin wall open tube sampler Figure 4.5.	Soils having some cohesion unless they are too hard or too gravelly for sampler penetration	<ol style="list-style-type: none"> 1. Small area ratio of tube permits obtaining sample with minimum disturbance. 2. Procedure is simple and requires very little time. 	<ol style="list-style-type: none"> 1. Excess or disturbed soil may enter the sampler and cause disturbance. Excess material prevents accurate measurement of recovery length. 2. When using in a bore hole filled with water or drilling fluid, an excess hydrostatic pressure will develop over the sample. 3. Check valve may clog, and may not reduce the hydrostatic pressures. 	Not suited for use in boulders, gravels and coarse soils.
Samplers with stationery pistons.	Soft soils	<ol style="list-style-type: none"> 1. Disturbed soil is prevented from entering the tube which decreases sample disturbance. 2. Atmospheric and hydrostatic pressures over sample area are reduced, which increases recovery ratio. 3. Any downward movement of the sample creates a partial vacuum over the sample and reduces the danger of losing the sample. 4. Much easier to determine recovery ratio since the length of rods can be easily measured. 	<ol style="list-style-type: none"> 1. The apparatus is complicated to use. 2. The insertion, clamping and withdrawal of the rods is time consuming. 	When a piston sampler is needed, the fixed piston sampler is preferable to other types of piston samplers to minimize sample disturbance.
Samplers with free pistons.	Stiff soils	<ol style="list-style-type: none"> 1. Entrance of disturbed and mixed soil is prevented when the sampler is lowered into position. 2. Recovery ratio is easily determined. 3. The piston is more effective than check valve in reducing pressure over the sample. 4. Easier to operate than the fixed piston. 	Additional weight is placed on the soil sample by the weight of the drill rods.	Similar to the fixed piston sampler with the exception that the piston is not fixed when the sample is taken; it is free to ride on top of the sample.
Samplers with retracted pistons.	Stiff soils	<ol style="list-style-type: none"> 1. The sampler is simpler in construction and operation than the stationary or free piston sampler as the piston head is held in place by a screw-type connection. 2. The piston prevents the entrance of disturbed soil into the tube when the tube is being placed into position for sampling. 	<ol style="list-style-type: none"> 1. The retraction of the piston may cause failure in soft soils as the soil may flow into the sampler. 2. The soil displaced during the positioning of the piston sampler may flow into the sampler when the piston is withdrawn. 3. If there is water leakage into the drill rod, excess hydrostatic pressure will develop over the sample. 	Piston is withdrawn just before the beginning of the actual sampling process.
Hydraulic piston sampler.	Soft soils	Eliminates need for center rod required to hold piston on a conventional piston-type sampler. This results in less time required to retrieve a sample.	<ol style="list-style-type: none"> 1. There are no means to determine the amount of penetration of the sampling tube into the soil stratum, since there are no visible signs of movement at the top of the hole. 2. Percent recovery is hard to establish, particularly for short pushes which do not fill the sampler. The weight of water in the drill steel causes the sampler to extend to its full length during retrieval from the hole. 	The sampling technique is the same as for the stationary piston sampler. The activation of the sampling tube is performed by water pressure applied to the sampler through its attached drill steel.

Double tube or wire line core barrels which are capable of recovering rock cores of at least 54 mm in diameter should be used in subsurface exploration for structural projects.

4.5 GROUND WATER MONITORING

Accurate ground water level information is needed for the estimation of soil densities, determination of effective soil pressures and for the preparation of effective soil pressure diagrams. This information is vital for performing foundation design. Water levels will also indicate the construction difficulties which may be encountered in excavations and the level of dewatering effort required.

In most structure foundation explorations, water levels should be monitored during drilling of the boring, upon completion of the boring, and 24 hours after the completion of boring. More than one week may be required to obtain representative water level readings in low permeability cohesive soils or in bore holes stabilized with some drilling muds. In these cases, an observation well or piezometer should be installed in a boring to allow long term ground water monitoring.

4.6 SUBSURFACE PROFILE DEVELOPMENT

A subsurface profile is a visual representation of subsurface conditions interpreted from subsurface explorations and laboratory testing. Uncertainties in the development of a subsurface profile usually indicate that additional explorations and/or laboratory testing are required.

The profile should be developed in stages. First, a rough profile is established from the drillers logs. This helps discover any obvious gaps while the drilling crew is at the site so that additional work can be performed immediately. When borings are completed and laboratory classification and moisture content data is received, the initial soil profile should be revised. Soil stratification and accurate soil descriptions are established at this stage. Overcomplication of a profile by noting minute variations between adjacent soil samples should be avoided. A vertical scale of 10 mm equal to 1 to 3 m and a horizontal scale equal to the vertical scale are recommended.

After the soil layer boundaries and descriptions have been established, a determination of the extent and details of additional laboratory testing, such as consolidation and shear

strength tests, is made. The final soil profile should include the average physical properties of the soil deposits including unit weight, shear strength, etc., as well as a visual description of each deposit. The observed ground water level and the presence of items such as boulders, voids, and artesian pressures should also be noted. A well developed soil profile is necessary to design a cost-effective foundation.

REFERENCES

- American Association of State Highway and Transportation Officials [AASHTO], (1988). Manual on Subsurface Investigations. AASHTO Highway Subcommittee on Bridges and Structures, Washington, D.C., 391.
- American Association of State Highway and Transportation Officials [AASHTO], (1978). Manual on Foundation Investigations. AASHTO Highway Subcommittee on Bridges and Structures, Washington, D.C.
- American Association of State Highway and Transportation Officials [AASHTO], (1995). Standard Methods of Test for Penetration Test and Split-Barrel Sampling of Soils, AASHTO T206.
- American Association of State Highway and Transportation Officials [AASHTO], (1995). Standard Method of Test for Thin-Walled Tube Sampling of Soils, AASHTO T207.
- Bowles, J.E. (1977). Foundation Analysis and Design. Second Edition, McGraw-Hill Book Company, New York, 85-86.
- Canadian Geotechnical Society (1985). Canadian Foundation Engineering Manual. Second Edition, BiTech Publishers, Ltd, Vancouver, 43-68.
- Cheney, R.S. and Chassie, R.G. (1993). Soils and Foundations Workshop Manual. Second Edition, Report No. HI-88-009, U.S. Department of Transportation, Federal Highway Administration, Office of Engineering, Washington, D.C., 395.
- Finno, R.J. (1989). Subsurface Conditions and Pile Installation Data, Predicted and Observed Axial Behavior of Piles. Results of a Pile Prediction Symposium, ASCE Geotechnical Special Publication No. 23, Richard J. Finno, Editor, 1-74.
- Fang, H.Y. (1991). Foundation Engineering Handbook. Second Edition, Van Nostrand Reinhold Company, New York.
- Federal Highway Administration (1972). Soils Exploration and Testing - Demonstration, Project No. 12.
- Peck, R.B., Hanson, W.E., and Thornburn, T.H. (1974). Foundation Engineering. Second Edition, John Wiley & Sons, Inc., New York.

5. IN-SITU TESTING

In-situ testing provides soil parameters for the design of structure foundations especially in conditions where standard drilling and sampling methods cannot be used to obtain high quality undisturbed samples. Undisturbed samples from non-cohesive soils are difficult to obtain, trim, and test in the laboratory. Soft saturated clays, saturated sands and intermixed deposits of soil and gravel are also difficult to sample without disturbance. Therefore, representative strength test data is difficult to obtain on these soils in the laboratory. To overcome these difficulties, test methods have been developed to evaluate soil properties, especially strength and compressibility, in-situ.

Primary in-situ tests that provide data for foundation design are the cone penetration test (CPT), the cone penetration test with pore pressure measurements (CPTU), and the vane shear. Other lesser used in-situ testing devices include the pressuremeter test (PMT), the dilatometer test (DMT), and the dynamic cone penetrometer test. Specific pile design procedures using cone penetration test data are discussed in Chapter 9 of this manual.

The intent of this chapter is to provide a brief summary of in-situ test methods used for deep foundation design. For CPT/CPTU testing a brief summary of the equipment, operation, application, advantages and disadvantages is also provided. The applicability, advantages and disadvantages of all the in-situ testing methods are also briefly summarized in Table 5-1. For a detailed discussion of a particular in-situ testing method, the reader is referred to the publications listed at the end of this chapter.

5.1 CONE PENETRATION TEST (CPT) AND (CPTU)

The cone penetration test (CPT) was first introduced in the U.S. in 1965. By the mid 1970's, the electronic cone began to replace the mechanical cone. In the early 1980's, the piezo-cone or cone penetration test with pore pressure measurements (CPTU) became readily available. Since that time, the CPT/CPTU has developed into one of the most popular in-situ testing devices. Part of this popularity is due to the CPT's ability to provide large quantities of useful data quickly and at an economical cost. Depending upon equipment capability as well as soil conditions, 100 to 350 m of penetration testing may be completed in one day.

TABLE 5-1 SUMMARY OF IN-SITU TEST METHODS

Type of Test	Best Suited for	Not Applicable for	Information that can be Obtained for Pile Foundation Design	Advantages	Disadvantages	Remarks
Cone Penetration Test (CPT)	Sand, silt, and clay	Gravel, very dense deposits, rubble fills, and rock.	Continuous evaluation of subsurface stratigraphy. Correlations for determination of in-situ density and friction angle of sands, undrained shear strength of clays, and liquefaction potential.	<ol style="list-style-type: none"> 1. Cone can be considered as a model pile. 2. Quick and simple test. 3. Can reduce number of borings. 4. Relatively operator independent. 	<ol style="list-style-type: none"> 1. Does not provide soil samples. 2. Should be used in conjunction with soil borings in an exploration program. 3. Local correlations can be important in data interpretation. 	Well suited to the design of axially loaded piles. ASTM D-3441.
Cone Penetration Test with Pore Pressure Measurements (CPTU)	Sand, silt, and clay	Gravel, very dense deposits, and rubble fills.	Finer delineation of continuous subsurface stratigraphy compared to CPT. Correlations for determination of in-situ density and friction angle of sands, undrained shear strength of clays, and liquefaction susceptibility.	<ol style="list-style-type: none"> 1. Same advantages as CPT. 2. Pore pressure measurements can be used to assess soil setup effects. 3. Can help determine if penetration is drained or undrained. 	<ol style="list-style-type: none"> 1. Same disadvantages as CPT. 2. Location and saturation of porous filter can influence pore pressure measurements. 	Probably best in-situ test method for the design of axially loaded piles. ASTM D-3441.
Pressuremeter Test (PMT)	Sand, silt, clay and soft rock.	Organic soils and hard rock.	Bearing capacity from limit pressure and compressibility from pressuremeter deformation modulus.	<ol style="list-style-type: none"> 1. Tests can be performed in and below hard strata that may stop other in-situ testing devices. 2. Tests can be made on non-homogenous soil deposits. 	<ol style="list-style-type: none"> 1. Bore hole preparation very important. 2. Limited number of tests per day. 3. Limited application for axially loaded pile design. 	Good application for laterally loaded pile design. ASTM D-4719.
Dilatometer Test (DMT)	Low to medium strength sand and clay	Dense deposits, gravels and rock.	Correlations for soil type, earth pressure at rest, overconsolidation ratio, undrained shear strength, and dilatometer modulus.	<ol style="list-style-type: none"> 1. Quick, inexpensive test. 2. Relatively operator independent. 	<ol style="list-style-type: none"> 1. Less familiar test method. 2. Intended for soils with particle sizes smaller than fine gravel. 3. Limited application for axially loaded pile design. 	May be potentially useful for laterally loaded pile design. ASTM standard in progress.
Vane Shear Test	Soft clay	Silt, sand, and gravel	Undrained shear strength.	<ol style="list-style-type: none"> 1. Quick and economical. 2. Compares well with unconfined compression test results at shallow depths. 	<ol style="list-style-type: none"> 1. Can be used to depths of only 4 to 6 m without casing bore hole. 	Test should be used with caution in fissured, varved, and highly plastic clays. AASHTO T223.
Dynamic Cone Test	Sand and gravel	Clay	Qualitative evaluation of soil density. Qualitative comparison of stratigraphy.	<ol style="list-style-type: none"> 1. Can be useful in soil conditions where static cone (CPT) reaches refusal. 	<ol style="list-style-type: none"> 1. An unknown fraction of resistance is due to side friction. 2. Overall use is limited. 	Not recommended for final pile design. No AASHTO or ASTM standard.

5.1.1 Equipment Description and Operation

Cone penetration testing can be separated into two main categories:

- a. Electronic cones.
- b. Mechanical cones.

Electronic cones are now the dominant cone type used in cone penetration testing. Hence, mechanical cones will not be discussed further in this chapter. Electronic cones may be further divided into two primary types, the standard friction cone (CPT), and the piezo-cone (CPTU).

In the CPT test, a cone with a 1000 mm² base and a 60° tip attached to a series of rods is continuously pushed into the ground. Typically, a hydraulic ram with 45 to 180 kN of thrust capability is used to continuously advance the cone into the ground at a rate of 20 mm/sec. A friction sleeve with a surface area of 15000 mm² is located behind the conical tip. Built in load cells are used to continuously measure the cone tip resistance, q_c , and the sleeve friction resistance, f_s . The friction ratio, R_f , is the ratio of f_s/q_c and is commonly used in the interpretation of test results.

The piezo-cone (CPTU), is essentially the same as the standard electronic friction cone and continuously measures the cone tip resistance, q_c , and the sleeve friction resistance, f_s , during penetration. In addition to these values, the piezo-cone includes porous filter piezo-elements that may be located at the cone tip, on the cone face, behind the cone tip, or behind the friction sleeve. These porous filter elements are used to measure pore pressure, u , during penetration.

A general schematic of a cone penetrometer is presented in Figure 5.1. Typical penetration depths for a 45 kN and 180 kN thrust capability are presented in Tables 5-2 and 5-3, respectively. Additional information on CPT/CPTU testing and analysis may be found in FHWA-SA-91-043, The Cone Penetrometer Test, by Briaud and Miran (1991). Test procedures may be found in ASTM D-3441, Standard Test Method for Deep Quasi-static, Cone and Friction Cone Penetration Tests of Soil.

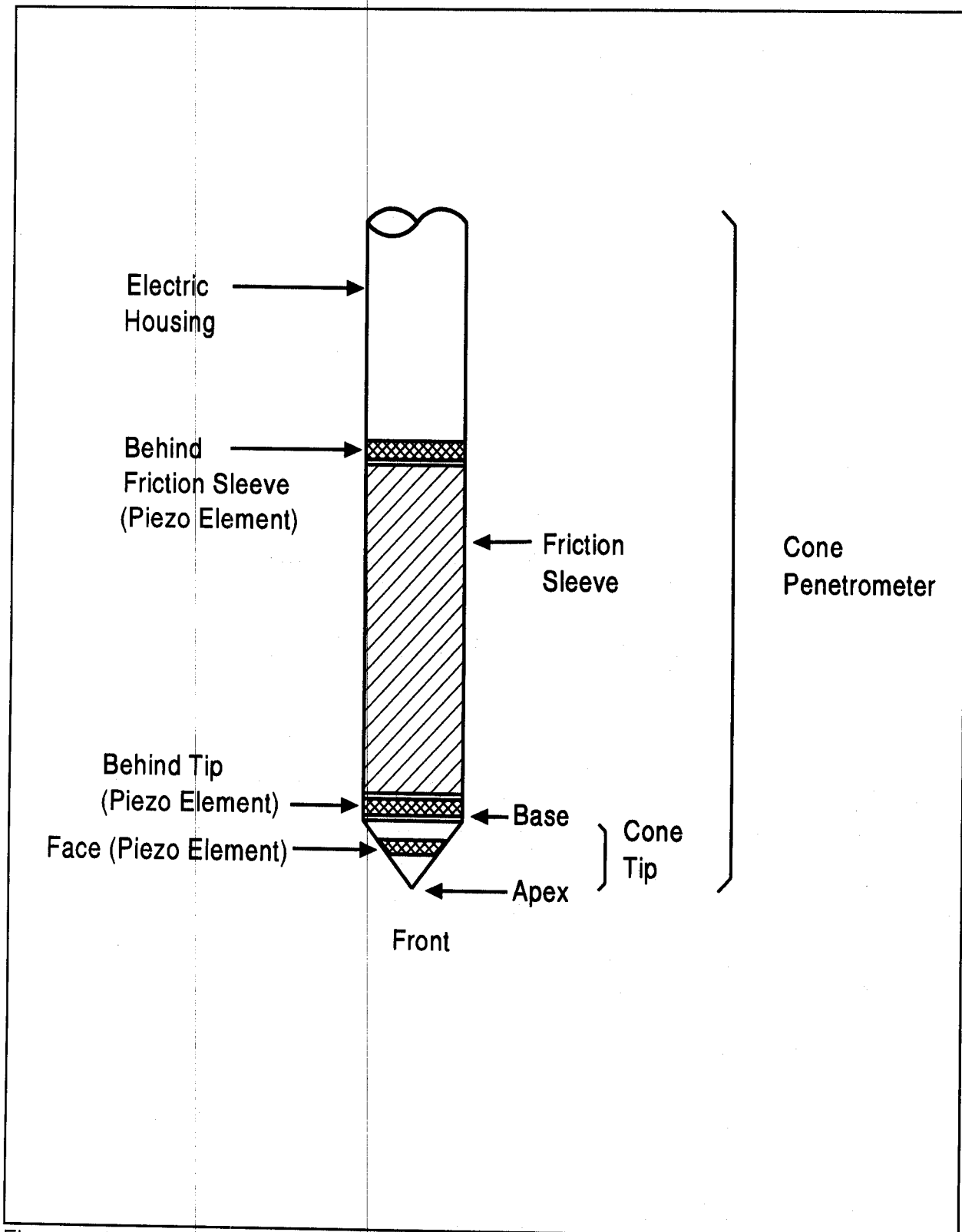


Figure 5.1 Terminology Regarding the Cone Penetrometer (from Robertson and Campanella, 1989)

TABLE 5-2 DRILL RIG WITH 45 kN PUSH CAPACITY						
	Soil					
	Clay			Sand		
Depth m	Soft	Stiff	Hard	Loose	Medium	Dense
1	*	*	*	*	*	
3	*	*		*	*	
4	*	*		*	*	
6	*			*	*	
9	*			*		
12	*			*		
15	*			*		
18	*					
21	*					
24						

TABLE 5-3 TRUCK WITH 180 kN PUSH CAPACITY						
	Soil					
	Clay			Sand		
Depth m	Soft	Stiff	Hard	Loose	Medium	Dense
4	*	*	*	*	*	*
9	*	*	*	*	*	*
18	*	*	*	*	*	*
27	*	*		*	*	
36	*			*		
46	*			*		
61	*					
76	*					
91						

Tables 5-2 and 5-3 (modified from Briaud and Miran, 1991)

5.1.2 Interpretation of CPT/CPTU Test Results

- a. CPT/CPTU data can provide a continuous profile of the subsurface stratigraphy. A simplified soil classification chart for a standard electronic friction cone is presented in Figure 5.2. Typical CPT test results are presented in Figure 5.3.
- b. From correlations with CPT/CPTU data, evaluations of in-situ relative density, D_r , and friction angle, ϕ , of cohesionless soils as well as the undrained shear strength, c_u , of cohesive soils can be made. Correlations for determination of other soil properties, liquefaction susceptibility, and estimates of SPT values may also be determined. The accuracy of these correlations may vary depending upon geologic conditions. Correlation confirmation with local conditions is therefore important.

5.1.3 Advantages and Disadvantages of CPT/CPTU Tests

The primary advantage of CPT/CPTU testing is the ability to rapidly develop a continuous profile of subsurface conditions more economically than any other subsurface exploration or in-situ testing tools. Determination of in-situ soil strength parameters from correlations with CPT/CPTU data is another advantage. The CPT/CPTU test can also reduce the number of conventional borings needed on a project, or focus attention on discrete zones for detailed soil sampling and testing. Lastly, CPT/CPTU results are relatively operator independent.

Limitations of CPT/CPTU testing include the inability to push the cone in dense or coarse soil deposits. To penetrate dense layers, cones are sometimes pushed in bore holes advanced through the dense strata. Another limitation is that soil samples are not recovered for confirmation of cone stratigraphy. Local correlations are also important in data interpretation.

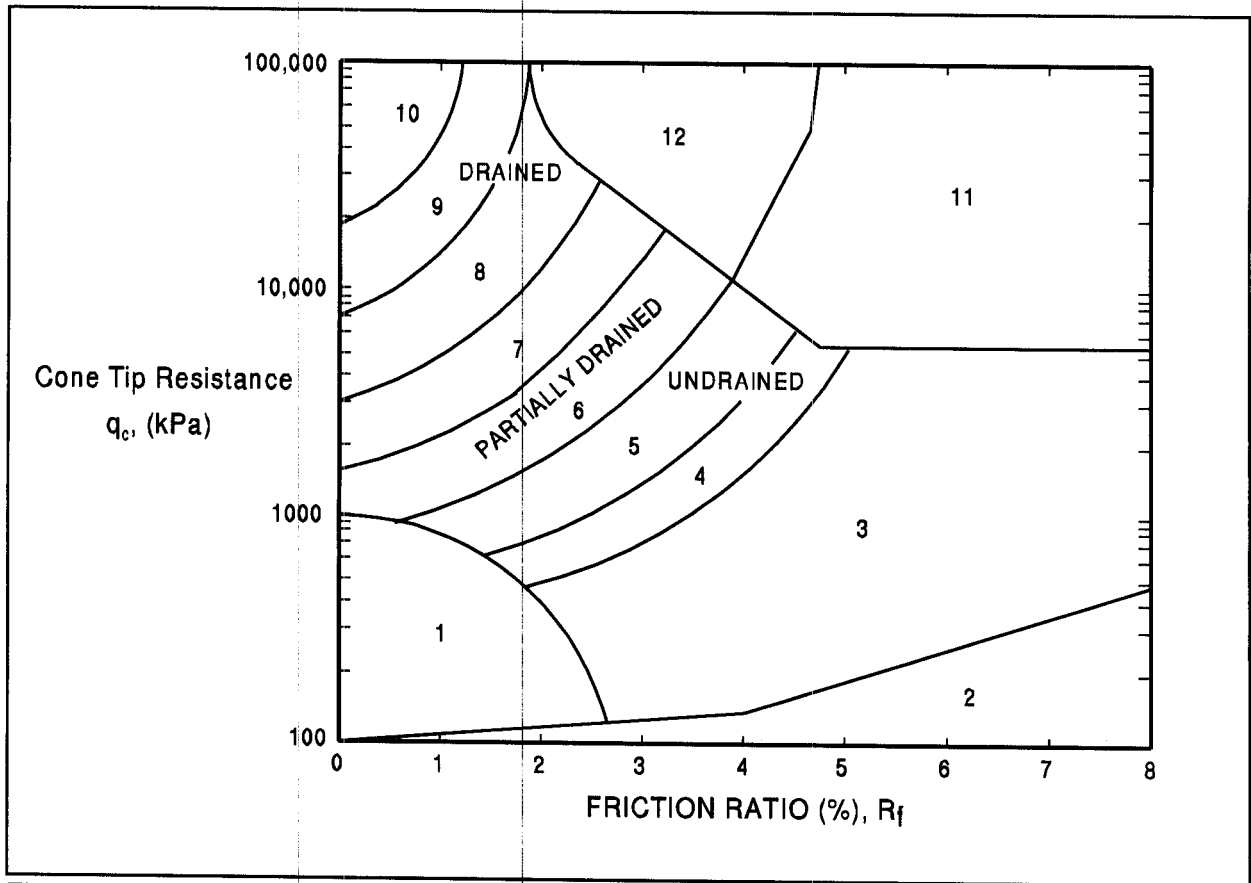


Figure 5.2 Simplified Soil Classification Chart for Standard Electronic Friction Cone (after Robertson *et al.*, 1986)

Zone	q_c/N	Soil Behavior Type
1)	2	sensitive fine grained organic material
2)	1	clay
3)	1	clay
4)	1.5	silty clay to clay
5)	2	clayey silt to silty clay
6)	2.5	sandy silt to clayey silt
7)	3	silty sand to sandy silt
8)	4	sand to silty sand
9)	5	sand
10)	6	gravelly sand to sand
11)	1	very stiff fine grained sand to clayey sand
12)	2	sand to clayey sand

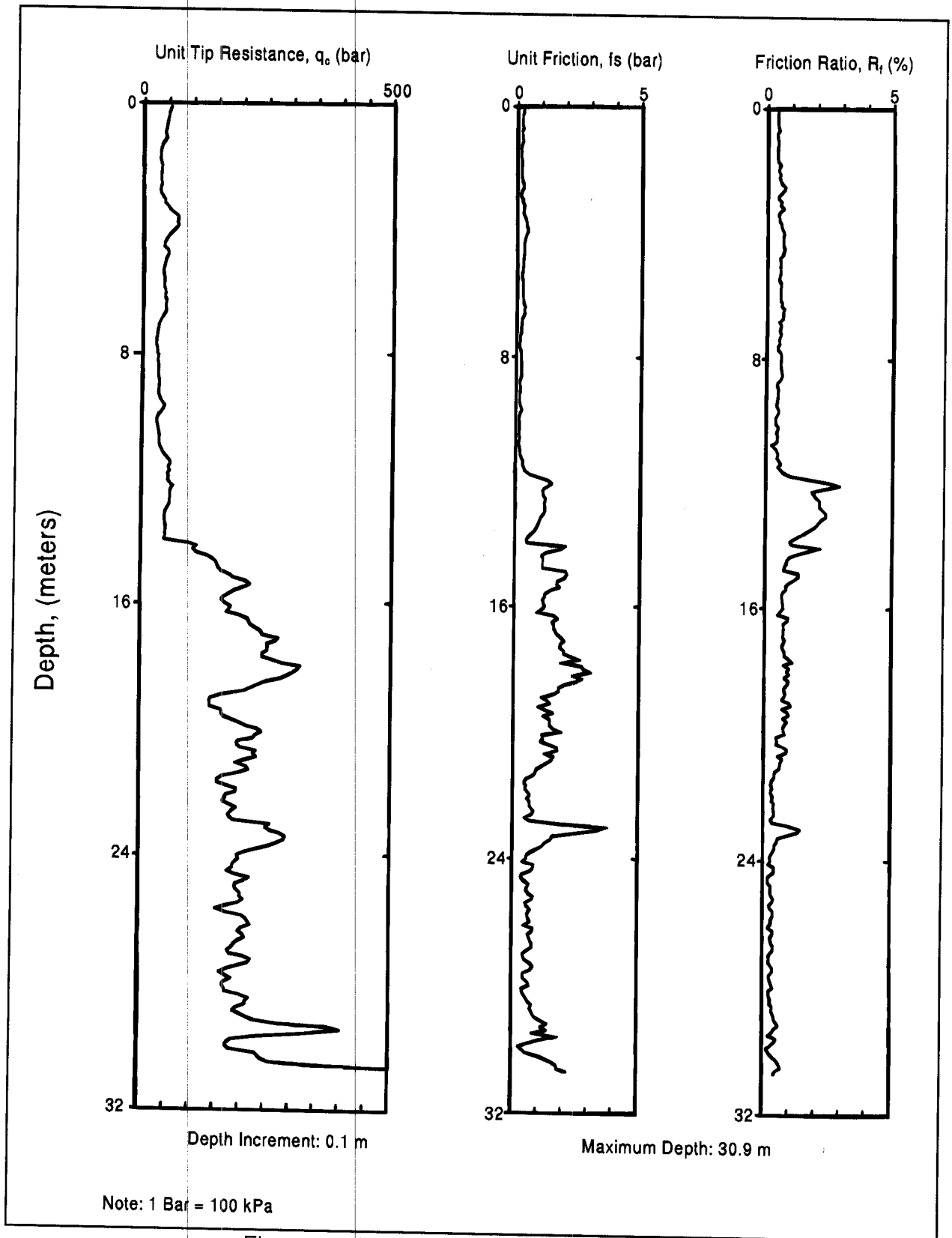


Figure 5.3 Typical CPT Data Presentation

5.2 PRESSUREMETER TEST - (PMT)

The pressuremeter test (PMT) is an in-situ device used to evaluate soil and rock properties. The pressuremeter has been used in Europe for many years and was introduced into the U.S. in the mid 1970's. The pressuremeter imparts lateral pressures to the soil, and the soil shear strength and compressibility are determined by interpretation of a pressure-volume relationship. The test allows a determination of the load-deformation characteristics of soil in axi-symmetric conditions. Deposits such as soft clays, fissured clays, sands, gravels and soft rock can be tested with pressuremeters.

The utilization of test results is based upon semi-empirical correlations from a large number of tests and observations on actual structures. For piles subjected to lateral loads, the pressuremeter test is a useful design tool and is well suited to determination of p-y curves. For design of vertically loaded piles, the pressuremeter test has limited value. Pile design procedures using pressuremeter data have been developed and may be found in FHWA-IP-89-008, The Pressuremeter Test for Highway Applications, by Briaud (1989). Details on test procedures may be found in ASTM D-4719, Standard Test Method for Pressuremeter Testing in Soils.

5.3 DILATOMETER TEST - (DMT)

The dilatometer test is an in-situ testing device that was developed in Italy in the early 1970's and first introduced in the U.S. in 1979. Like the CPT, the DMT is generally hydraulically pushed into the ground although it may also be driven. When the DMT can be pushed into the ground with tests conducted at 200 mm increments, 30 to 40 m of DMT sounding may be completed in a day. The primary utilization of the DMT in pile foundation design is the delineation of subsurface stratigraphy and interpreted soil properties. However, it would appear that the CPT/CPTU is generally better suited to this task than the DMT. The DMT may be a potentially useful test for design of piles subjected to lateral loads. Design methods in this area show promise, but are still in the development stage. For design of axially loaded piles, the dilatometer test has limited direct value.

5.4 VANE SHEAR TEST

The vane shear test is an in-situ test for determining the undrained shear strength of soft to medium clays. Figure 5.4 is a schematic drawing of the essential components. The test consists of forcing a four-bladed vane into undisturbed soil and rotating it until the soil shears. Two shear strengths are usually recorded, the peak shearing strength and the remolded shearing strength. These measurements are used to determine the sensitivity of clay. This allows analysis of the soil resistance to be overcome during pile driving in clays. It is necessary to measure skin friction along the steel connector rods which must be subtracted to determine the actual shear strength. The vane shear test generally provides the most accurate undrained shear strength values for clays with undrained shear strengths less than 50 kPa. The test procedure has been standardized in AASHTO T223-74 and ASTM D-2573.

5.5 DYNAMIC CONE TEST

There are two types of dynamic penetrometers with conical points. The dynamic cone type that is most often used has a shaft diameter that is smaller than the cone diameter. Theoretically, due to the cone being larger than the shaft, the penetrometer measures only point resistance. A lesser used cone type has a shaft and cone of the same diameter. This type of dynamic cone penetrometer records both skin friction and point resistance, but the two components cannot be analyzed independently. Equations have been developed for determining bearing capacity of pile foundations by using the dynamic cone test data, but are not used extensively. The dynamic cone penetrometer is not recommended for final foundation design.

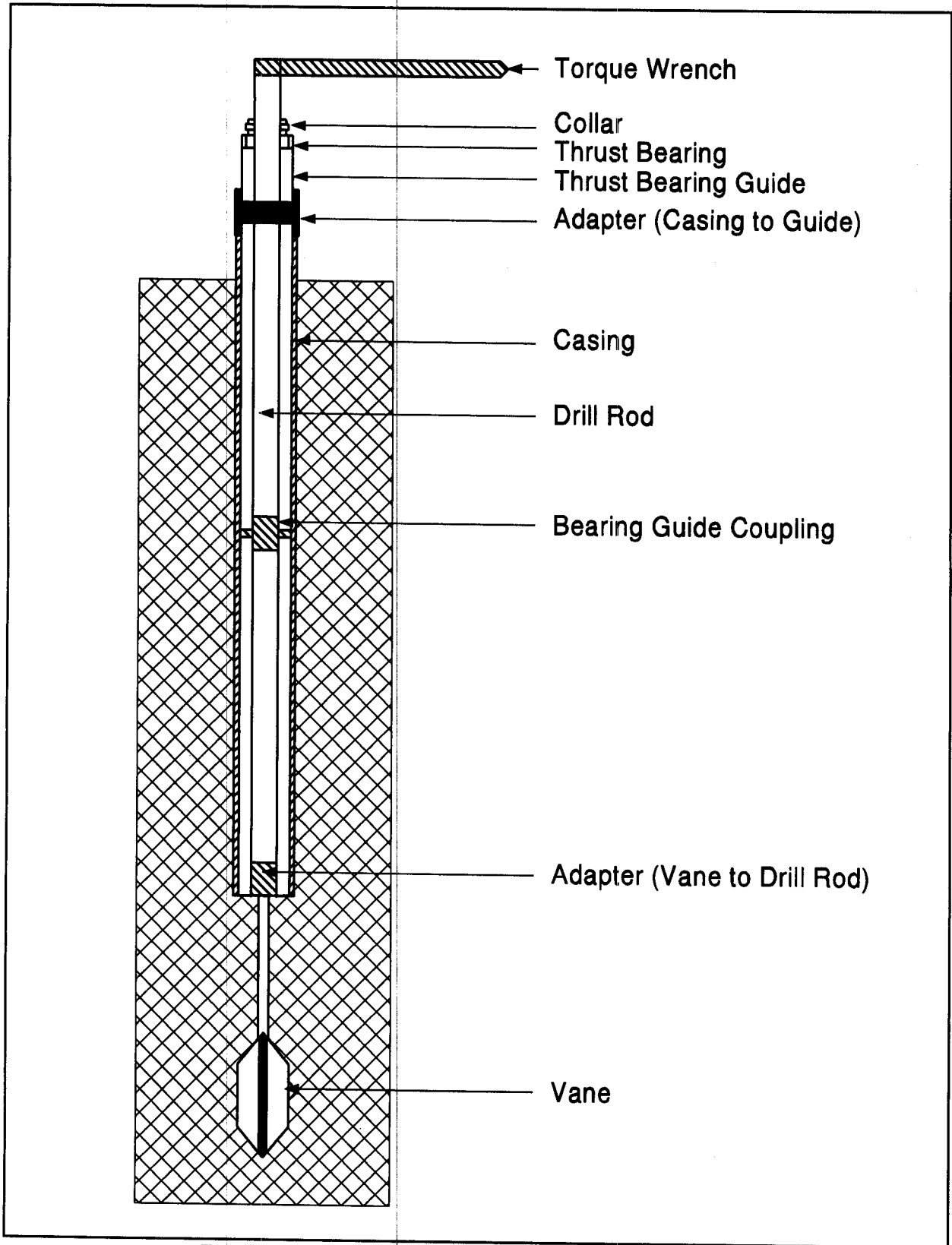


Figure 5.4 Vane Shear Device (after FHWA, 1972)

REFERENCES

- American Association of State Highway and Transportation Officials [AASHTO], (1988). Manual on Subsurface Investigations. AASHTO Highway Subcommittee on Bridges and Structures, Washington, D.C., 391.
- Briaud, J-L. (1989). The Pressuremeter Test for Highway Applications. Report No. FHWA-IP-89-008, U.S. Department of Transportation, Federal Highway Administration, Office of Implementation, McLean, 156.
- Briaud, J-L. and Miran, J. (1991). The Cone Penetrometer Test. Report No. FHWA-SA-91-043, U.S. Department of Transportation, Federal Highway Administration, Office of Technology Applications, Washington, D.C., 161.
- Briaud, J-L. and Miran, J. (1992). The Flat Dilatometer Test. Report No. FHWA-SA-91-044, U.S. Department of Transportation, Federal Highway Administration, Office of Technology Applications, Washington, D.C., 102.
- Canadian Geotechnical Society (1985). Canadian Foundation Engineering Manual. Second Edition, BiTech Publishers Ltd., Vancouver, 45-62.
- Schmertman, J.H. (1988). Guidelines for Using the CPT, CPTU, and Marchetti DMT for Geotechnical Design. Report No. FHWA-PA-022+84-24, U.S. Department of Transportation, Federal Highway Administration, Volumes I-IV, Washington, D.C., 731.
- Robertson P.K., Campanella, R.G., Gillespie, D. and Grieg, J. (1986). Use of Piezometer Cone Data. Proceedings of In-Situ '86, ASCE Specialty Conference, Use of In-Situ Tests in Geotechnical Engineering, Special Publication No. 6, Blacksburg, 1263-1280.
- Robertson P.K. and Campanella, R.G. (1989). Guidelines for Geotechnical Design using the Cone Penetrometer Test and CPT with Pore Pressure Measurement. Fourth Edition, Hogentogler & Company, Inc., Columbia, 193.
- U.S. Department of Transportation (1972). Soil Exploration and Testing. Federal Highway Administration, Demonstration Project No. 12, Arlington.

6. LABORATORY TESTING

The trend to higher capacity piles and greater pile penetration depths required for special design events reinforces the importance of accurately determining soil shear strength and consolidation properties. For cohesionless materials, the SPT and CPT will be the primary tools for strength and compressibility analysis. These tests should be complemented with appropriate laboratory index tests. For cohesive soils, the use of SPT resistance values for estimation and evaluation of soil shear strength and compressibility cannot be recommended as the basis for a final design. **In cohesive soils, traditional laboratory tests on undisturbed samples yield the best results for evaluation of strength and compressibility properties.**

In laboratory testing, the quality of test results is far more important than the quantity of test results. Inaccurate test results may lead to misjudgments in the design stage and/or problems in the construction stage. Owners and designers of structure foundations have a quality assurance responsibility over activities affecting the quality of laboratory test results. Quality control procedures for in-house or consultant laboratories should be in place for:

- Handling and storage of soil samples.
- Sample preparation for testing.
- Establishment of, and adherence to testing procedures.
- Documentation of equipment calibration and maintenance.
- Training and qualification of laboratory personnel.
- Laboratory test result review and checking.
- Reporting of laboratory test results.

The purpose of this chapter is to present a summary of laboratory tests performed to determine basic soil properties as well as soil shear strength and consolidation properties. For detailed information on laboratory testing, additional references are listed at the end of this chapter.

6.1 TYPES OF TESTS

Laboratory tests can be generally categorized as follows:

1. Soil classification and index tests.
2. Shear strength tests.
3. Consolidation tests.
4. Electro chemical classification tests.

The following subsections briefly describe each type of test. Table 6-1 summarizes the advantages, disadvantages and applications of soil classification, strength and compressibility tests.

6.1.1 Classification and Index Tests

For foundation design, soils are usually classified according to the Unified Soil Classification system. The classification of soil determines the type of material, its general characteristics, and whether any further testing for consolidation and strength properties are needed. The following tests are useful in classifying soils:

- a. Moisture content (AASHTO T265).
- b. Particle size analysis (mechanical and hydrometer analysis) AASHTO T88.
- c. Atterberg limits (liquid and plastic limits) AASHTO T89 and T90.
- d. Unit weight (AASHTO T38).

6.1.2 Shear Strength Tests

The shear strength of a soil is a measure of the soil's ability to resist sliding along internal surfaces within the mass.

TABLE 6-1 LABORATORY TESTS ON SOILS FOR FOUNDATION DESIGN

Test Category	Test	Classification or Design Parameters Provided by Test	Advantages	Disadvantages	Direct* Applications	Standard Test Procedure	Soil Types best suited for
Classification and Index Tests (both disturbed and undisturbed samples used unless noted)	Liquid limit	Liquid limit	Assists in correct soil classification.	----	Classification	AASHTO T89-68	Cohesive soils and silts
	Plastic limit	Plastic limit	Assists in correct soil classification.	----	Classification	AASHTO T90-70	Cohesive soils and silts
	Moisture content	Moisture content	Can assist in soil shear strength judgements and water table determination.	----	Classification	AASHTO T265-79	Cohesive soils and silts
	Particle size analysis (mechanical and hydrometer analysis)	Grain size curves	Assists in soil classification.	----	Classification	AASHTO T88-72	Cohesive and cohesionless soils
	Unit weight (Undisturbed samples only)	Dry density	Can assist in soil shear strength judgements.	----	Effective stress computations.	AASHTO T38	Cohesive soils
Shear strength (undisturbed samples used)	Triaxial compression test (UU, CU, or CD tests **)	Cohesion c or c' ; Angle of internal friction ϕ or ϕ' . (In terms of total or effective stresses).	<ol style="list-style-type: none"> 1. Models in-situ conditions better than other two tests. 2. Drainage control 3. Pore water pressure can be measured. 4. More accurate than other two methods. 	<ol style="list-style-type: none"> 1. Expensive. 2. Complicated test procedure. 3. Difficult to use for sands and silts. 	Static capacity calculations for deep foundations.	AASHTO T234-70	Cohesive soils
	Direct shear test	Cohesion, c' ; Angle of internal friction, ϕ' . (In terms of effective stresses).	Simple and quick test.	<ol style="list-style-type: none"> 1. Predetermined failure plane. 2. Poor drainage control. 	Static capacity calculations for deep foundations.	AASHTO T236-72	Cohesionless soils (sands and silts)
	Unconfined compression test	Unconfined compression strength and shear strength.	<ol style="list-style-type: none"> 1. Simple, quick, inexpensive test to measure strength of cohesive soils. 2. More uniform stresses and strains on sample than direct shear test. 3. Failure surface tends to develop at weakest portion of samples unlike the forced shear plane of direct shear test. 	<ol style="list-style-type: none"> 1. No lateral confining pressure during test. 2. Pore water pressures and saturation cannot be controlled. 3. Test results, especially with depth, are conservative and misleading due to release of confining stress when sample is removed from below ground and tested. 	Static capacity calculations for deep foundations.	AASHTO T208-70	Cohesive soils
Consolidation (undisturbed samples used)	Consolidation	Compression index. Recompression index. Coefficient of secondary compression. Coefficient of consolidation. Preconsolidation pressure. Swelling index.	----	----	Computation of foundation settlement and time rate of settlement.	AASHTO T216-74	Cohesive soils

* - All test results permit empirical and engineering judgement guidance with regard to pile installation and construction monitoring.

** - UU = Unconsolidated Undrained, CU = Consolidated Undrained, and CD = Consolidated Drained.

For the design of foundations, a knowledge of the soil shear strength is essential. Shear tests on soil are performed to determine the cohesion, c , and the angle of internal friction, ϕ . Cohesion is the interparticle attraction effect and is independent of the normal stress, σ , but considerably dependent on water content and strain rate. The internal friction angle depends on the interlocking of soil grains and the resistance to sliding between the grains.

Internal friction depends on the roughness of grains and normal stress. The shear strength of a soil is defined as follows:

$$\tau = c + \sigma \tan \phi$$

For pile foundation design, the resistance along the pile shaft and at the pile toe are a function of τ , c and ϕ parameters.

Effective stress, σ' , is defined as the soil grain to soil grain pressure and is equal to the total overburden pressure, σ , minus the pore water pressure (neutral pressure), u . This may be expressed in equation form as:

$$\sigma' = \sigma - u$$

The pore water has no shear strength and is incompressible. Only the intergranular stress (effective stress) is effective in resisting shear or limiting compression of the soil. When pore water drains from soil during consolidation, the decrease in water pressure increases the level of effective stress. Effective stress is important in both laboratory testing and in design, since it correlates directly with soil behavior. An increase in effective stress causes densification and an increase in shear strength.

Three test methods are commonly used to measure shear strength in the laboratory. In order of increasing cost and test sophistication they are as follows:

- a. Unconfined compression test (AASHTO T208).
- b. Direct shear test (AASHTO T236).
- c. Triaxial compression test (AASHTO T234).

The unconfined compression test is the most widely used laboratory test to evaluate soil shear strength. In the unconfined compression test, an axial load is applied on a cylindrical soil sample while maintaining a zero lateral or confining pressure. The axial loading is increased to failure and the shear strength is then considered to be one half the axial stress at failure. Unconfined compression tests are performed only on cohesive soil samples.

Unconfined compression tests on cohesive samples recovered from large depths or samples with a secondary structure, such as sand seams, fissures, or slickensides, can give misleadingly low shear strengths. This is due to the removal of the in-situ confining stress normally present. Triaxial compression tests provide better information on soil shear strength in these cases.

The direct shear test is performed by placing a sample of soil into a shear box which is split into two parts at mid-height. A normal load is then applied to the top of the sample and one half of the shear box is pulled or pushed horizontally past the other half. The shear stress is calculated from the horizontal force divided by the sample area and is plotted versus horizontal deformation. A plot of at least three normal stresses and their corresponding maximum shear stresses provides the shear strength parameters c and ϕ . Bowles (1977) notes that the ϕ values determined from plain strain direct shear tests are approximately 1.1 times the ϕ values determined from triaxial tests. Direct shear tests are primarily performed on recompacted granular soils. Direct shear tests are generally not recommended for cohesive soils due to limitations on drainage control during shear.

The most versatile shear strength test is the triaxial compression test. The triaxial test allows a soil sample to be subjected to three principal stresses under controlled conditions. A cylindrical test specimen is encased in a rubber membrane and is then subjected to a confining pressure. Drainage from the sample is controlled through its two ends. The shearing force is applied axially and increased to failure. A plot of normal stress versus shear stress is developed and parameters c and ϕ are determined. In triaxial tests where full drainage is allowed during shear, or in undrained tests with pore pressure measurements during shear, the effective stress parameters c' and ϕ' can be determined.

In shear testing, the drainage, consolidation, and loading conditions are selected to simulate field conditions. Triaxial compression tests are classified according to the consolidation and drainage conditions allowed during testing. The three test types normally conducted are unconsolidated undrained (UU), consolidated undrained (CU) and consolidated drained (CD). The unconfined compression test may theoretically be considered a UU test performed with no confining pressure. Direct shear tests are usually consolidated under a normal stress then sheared either very slowly to model drained conditions, or rapidly to model undrained conditions.

Total stress and effective stress pile design methods are presented in Chapter 9. The total stress methods use undrained shear strengths. Effective stress design methods use drained shear strength data.

6.1.3 Consolidation Tests

To estimate the amount and rate at which a cohesive soil deposit will consolidate under an applied load of a structure, a one dimensional consolidation test (AASHTO T216) is usually performed. In this test, a saturated soil sample is constrained laterally while being compressed vertically. The vertical compression is measured and related to the void ratio of the soil. Loading the sample results in an increased pore water pressure within the voids of the sample. Over a period of time, as the water is squeezed from the soil, this excess water pressure will dissipate resulting in the soil grains (or skeleton) supporting the load. The amount of water squeezed from the sample is a function of load magnitude and compressibility of soil skeleton. The rate of pressure dissipation is a function of the permeability of the soil.

The results from the test are used to plot void ratio, e , versus pressure, p , on a semi-log scale to determine the preconsolidation pressure, p_c , and compression index, C_c . An illustration of a typical e -log p curve is presented in Figure 9.43. A plot of log time versus sample compression is used to determine coefficient of consolidation. Consolidation test results can be used to estimate magnitude and settlement rate of pile foundations in cohesive soils. A settlement design example using consolidation test data is presented in Chapter 9.

6.1.4 Electro Chemical Classification Tests

The soil and groundwater can contain constituents detrimental to pile materials. Electro chemical classification tests can be used to determine the aggressiveness of the subsurface conditions and the potential for pile deterioration. These electro chemical tests include:

- a. pH (AASHTO T289).
- b. Resistivity (AASHTO T288).
- c. Sulfate ion content (AASHTO T290).
- d. Chloride ion content (AASHTO T291).

Additional discussion of the influence of environmental conditions on pile selection are presented in Section 8.8 of Chapter 8.

6.2 LABORATORY TESTING FOR PILE DRIVEABILITY CONSIDERATIONS

As noted earlier in this chapter, pile foundations are increasingly being driven to greater depths and greater capacities. Laboratory tests to determine the remolded shear strength of cohesive soils and the gradation and fine content of cohesionless soils are important in assessing the pile driveability and the potential soil setup effects (changes in pile capacity with time).

Remolded Shear Strength of Cohesive Soils

Cohesive soils may lose a significant portion of their shear strength when disturbed or remolded, as during the pile driving process. The sensitivity of a cohesive soil, S_t , is defined as:

$$S_t = (q_u \text{ undisturbed}) / (q_u \text{ remolded})$$

Table 6-2 contains typical values of sensitivity as reported by Sowers (1979) which may be useful for preliminary estimates of remolded shear strength. Terzaghi and Peck, (1967) noted that clays with sensitivities less than 16 generally regain a portion to all of their original shear strength with elapsed time. Based upon typical sensitivity values reported by Terzaghi and Peck as well as by Sowers, the remolded shear strength of many cohesive soils during pile driving would be expected to range from about ¼ to ½ the undisturbed shear strength.

Clay of medium plasticity, normally consolidated	2-8
Highly flocculent, marine clays	10-80
Clays of low to medium plasticity, overconsolidated	1-4
Fissured clays, clays with sand seams	0.5-2

To determine site specific soil sensitivity from laboratory data, remolded soil specimens having the same moisture content as the undisturbed specimen should be tested in unconfined compression. However, the best assessment of the remolded shear strength of cohesive soils can be made from the field vane shear test described in Section 5.4.

Gradation of Cohesionless Soils

The gradation and fine content of cohesionless soils are useful information in assessing pile driveability. Soils with a high fine content generally have lower angles of internal friction than soils of similar density with lower fine content. A high fine content can also affect soil drainage and pore pressures during shear, and thus, the effective stresses acting on a pile during driving. Depending upon soil density, cohesionless soils with high fine contents are also more likely to demonstrate soil setup than cohesionless soils with little or no fines. Gradation and angularity of soil grains influence the angle of internal friction.

Routine laboratory grain size analyses (mechanical and hydrometer) can quantify gradation and fine content. With this information, better engineering assessments of pile driveability and soil setup potential in cohesionless soils can be made.

REFERENCES

- American Association of State Highway and Transportation Officials [AASHTO], (1988). Manual on Subsurface Investigations. AASHTO Highway Subcommittee on Bridges and Structures, Washington, D.C., 391.
- Bowles, J.E. (1977). Foundation Analysis and Design. Second Edition, McGraw-Hill Book Company.
- Cheney, R.S. and Chassie, R.G. (1993). Soils and Foundations Workshop Manual. Second Edition, Report No. HI-88-009, U.S. Department of Transportation, Federal Highway Administration, Office of Engineering, Washington, D.C., 395.
- Holtz, R.D. and Kovacs, W.D. (1981). An Introduction to Geotechnical Engineering. Prentice Hall, Inc., Englewood Cliffs, 283-665.
- Sowers, G.F. (1979). Introductory Soil Mechanics and Foundations. Geotechnical Engineering, Fourth Edition, MacMillan Publishing Co. Inc., New York, 217.
- Terzaghi, K. and Peck, R.B. (1967). Soil Mechanics in Engineering Practice. Second Edition, John Wiley & Sons Inc., New York, 51-52.

7. FOUNDATION DESIGN PROCEDURE

A foundation is the interfacing element between the superstructure and the underlying soil or rock. The loads transmitted by the foundation to the underlying soil must not cause soil shear failure or damaging settlement of the superstructure. It is essential to systematically consider various foundation types and to select the optimum alternative based on the superstructure requirements and the subsurface conditions.

7.1 FOUNDATION DESIGN APPROACH

The following design approach is recommended to determine the optimum foundation alternative.

1. Determine the foundation loads to be supported, structure layout, and special requirements such as limits on total and differential settlements, lateral loads, scour, seismic performance, and time constraints on construction. This step is often partially overlooked or vaguely addressed. A complete knowledge of these issues is of paramount importance.
2. Evaluate the subsurface exploration and the laboratory testing data. Ideally, the subsurface exploration and laboratory testing programs were performed with a knowledge of the loads to be transmitted to, and supported by the soil and/or rock materials.
3. Prepare a final soil profile and critical cross sections. Determine soil layers suitable or unsuitable for spread footings, pile foundations, or drilled shafts. Also consider if ground improvement techniques could modify unsuitable layers into suitable support layers.

4. Consider and prepare alternative designs.

Shallow Foundations:
(without ground improvement)

- a. Spread footings.
- b. Mat foundations.

Shallow Foundations:
(with ground improvement)

- a. Spread footings.
- b. Mat foundations.

Deep Foundations:

- a. Pile foundations.
- b. Drilled shafts.

Table 7-1 summarizes shallow and deep foundation types and uses, as well as applicable and non-applicable soil conditions.

5. Prepare cost estimates for feasible alternative foundation designs including all associated substructure costs.

6. Select the optimum foundation alternative. Generally the most economical alternative should be selected and recommended. However, the ability of the local construction force, availability of materials and equipment, as well as environmental considerations/limitations should also be considered.

For major projects, if the estimated costs of feasible foundation alternatives (during the design stage) are within 15 percent of each other, then alternate foundation designs should be considered for inclusion in the contract documents.

TABLE 7-1 FOUNDATION TYPES AND TYPICAL USES*

Foundation Type	Use	Applicable Soil Conditions	Non-suitable or Difficult Soil Conditions
Spread footing, wall footings.	Individual columns, walls, bridge piers.	Any conditions where bearing capacity is adequate for applied load. May use on single stratum; firm layer over soft layer, or weaker layer over firm layer. Check immediate, differential and consolidation settlements.	Any conditions where foundations are supported on soils subject to scour or liquefaction. Bearing layer located below ground water table.
Mat foundation.	Same as spread and wall footings. Very heavy column loads. Usually reduces differential settlements and total settlements.	Generally soil bearing value is less than for spread footings. Over one-half area of structure covered by individual footings. Check settlements.	Same as footings.
Pile foundations (shaft resistance, toe resistance or combination).	In groups to transfer heavy column and bridge loads to suitable soil layers. Also to resist uplift and/or lateral loads.	Poor surface and near surface soils. Soils suitable of load support 5 to 90 m below ground surface. Check settlement of pile groups.	Shallow depth to hard stratum. Sites where pile driving vibrations or heave may adversely impact adjacent facilities. Boulder fields.
Drilled shafts (shaft resistance, toe resistance or combination).	Larger column loads than for piles. Cap sometimes eliminated by using drilled shafts as column extension.	Poor surface and near surface soils. Soils and/or rock of suitable load support located 8 to 90 m below ground surface.	Deep deposits of soft clays and loose water bearing granular soils. Caving formations difficult to stabilize. Artesian conditions. Boulder fields.

* Modified from Bowles (1977).

7.2 CONSIDERATION OF SPREAD FOOTING FOUNDATION

The feasibility of using spread footings for foundation support should be considered in any foundation selection process. Spread footings are generally more economical than deep foundations (piles and drilled shafts); spread footings in conjunction with ground improvement techniques should also be considered. **Deep foundations should not be used indiscriminately for all subsurface conditions and for all structures.** There are subsurface conditions where pile foundations are very difficult and costly to install, and other conditions when they may not be necessary.

7.3 ESTABLISHMENT OF A NEED FOR A DEEP FOUNDATION

The first difficult problem facing the foundation designer is to establish whether or not the site conditions dictate that a deep foundation must be used. Vesic (1977) summarized typical situations in which piles may be needed. These typical situations as well as additional uses of deep foundations are shown in Figure 7.1.

Figure 7.1(a) shows the most common case in which the upper soil strata are too compressible or too weak to support heavy vertical loads. In this case, deep foundations transfer loads to a deeper dense stratum and act as toe bearing foundations. In the absence of a dense stratum within a reasonable depth, the loads must be gradually transferred, mainly through soil resistance along shaft, Figure 7.1(b). An important point to remember is that deep foundations transfer load through unsuitable layers to suitable layers. The foundation designer must define at what depth suitable soil layers begin in the soil profile.

Deep foundations are frequently needed because of the relative inability of shallow footings to resist inclined, lateral, or uplift loads and overturning moments. Deep foundations resist uplift loads by shaft resistance, Figure 7.1(c). Lateral loads are resisted either by vertical deep foundations in bending, Figure 7.1(d), or by groups of vertical and battered foundations, which combine the axial and lateral resistances of all deep foundations in the group, Figure 7.1(e). Lateral loads from overhead highway signs and noise walls may also be resisted by groups of deep foundations, Figure 7.1(f).

Deep foundations are often required when scour around footings could cause loss of bearing capacity at shallow depths, Figure 7.1(g). In this case the deep foundations must extend below the depth of scour and develop the full capacity in the support zone below the level of expected scour. FHWA scour guidelines (1991) require the geotechnical analysis of bridge foundations to be performed on the basis that all stream bed materials in the scour prism have been removed and are not available for bearing or lateral support. Costly damage and the need for future underpinning can be avoided by properly designing for scour conditions.

Soils subject to liquefaction in a seismic event may also dictate that a deep foundation be used, Figure 7.1(h). Seismic events can induce significant lateral loads to deep foundations. During a seismic event, liquefaction susceptible soils offer less lateral resistance as well as reduced shaft resistance to a deep foundation. Liquefaction effects on deep foundation performance must be considered for deep foundations in seismic areas.

Deep foundations are often used as fender systems to protect bridge piers from vessel impact, Figure 7.1(i). Fender system sizes and group configurations vary depending upon the magnitude of vessel impact forces to be resisted. In some cases, vessel impact loads must be resisted by the bridge pier foundation elements. Single deep foundations may also be used to support navigation aids.

In urban areas, deep foundations may occasionally be needed to support structures adjacent to locations where future excavations are planned or could occur, Figure 7.1(j). Use of shallow foundations in these situations could require future underpinning in conjunction with adjacent construction.

Deep foundations are used in areas of expansive or collapsible soils to resist undesirable seasonal movements of the foundations. Deep foundations under such conditions are designed to transfer foundation loads, including uplift or downdrag, to a level unaffected by seasonal moisture movements, Figure 7.1(k).

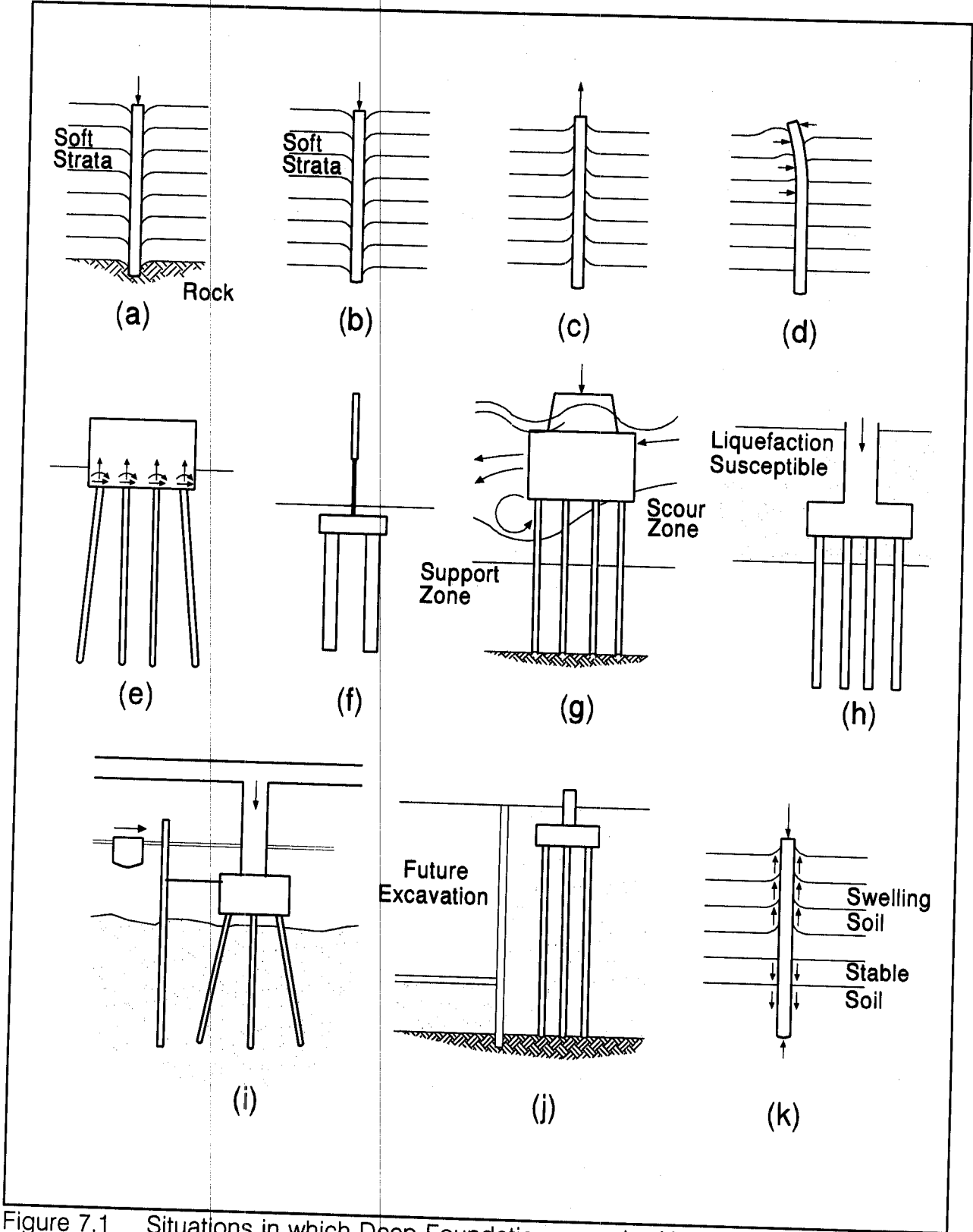


Figure 7.1 Situations in which Deep Foundations may be Needed (modified from Vesic, 1977)

In many instances either a shallow or deep foundation alternative is technically feasible. Under these circumstances, an evaluation of the shallow foundation should include; (1) the dimensions and depth of shallow footings based on allowable bearing capacity, (2) the magnitude and time-rate of settlement under anticipated loads, and (3) detailed cost analysis including such factors as need for cofferdams, overall substructure cost, dewatering and foundation seals, construction time, construction risk and claims potential. A comparative analysis of feasible deep foundation alternatives should also be made. The cost analyses of feasible alternatives should have a significant role in final selection of the foundation type.

Because this manual deals only with driven pile foundations, other types of foundations will not be discussed further.

REFERENCES

- Bowles, J.E. (1977). Foundation Analysis and Design. Third Edition, McGraw-Hill Book Company, New York, 4-5.
- Cheney, R.S. and Chassie, R.G. (1993). Soils and Foundations Workshop Manual. Second Edition, Report No. HI-88-009, U.S. Department of Transportation, Federal Highway Administration, Office of Engineering, Washington, D.C., 395.
- Federal Highway Administration (1991). Technical Advisory No. 5140.23, Evaluating Scour at Bridges. U.S. Department of Transportation, Office of Engineering, Washington, D.C., 6.
- Vesic, A.S. (1977). Design of Pile Foundations. National Cooperative Highway Research Program, Transportation Research Board, National Research Council, Washington, D.C., Synthesis of Highway Practice No. 42.

8. PILE TYPES AND GUIDELINES FOR SELECTION

The selection of a pile foundation type for a structure should be based on the specific soil conditions as well as the foundation loading requirements and final performance criteria. This chapter focuses on the characteristics of driven pile foundation types typically used for highway structures. Design data useful in the selection and design of specific pile types is included in Appendix C. Additional details on pile splices and toe protection devices are presented in Chapter 23.

8.1 OVERVIEW OF TYPICAL PILE TYPES

Piles can be broadly categorized in two main types: foundation piles for support of structural loads and sheet piles for earth retention systems. Discussion of sheet piles is outside the scope of this manual.

There are numerous types of foundation piles. Figure 8.1 shows a pile classification system based on type of material, configuration, installation technique and equipment used for installation. Foundation piles can also be classified on the basis of their method of load transfer from the pile to the surrounding soil mass. Load transfer can be by shaft resistance, toe bearing resistance or a combination of both.

Table 8-1 modified from NAVFAC (1982) summarizes characteristics and uses of common pile types. The table is for preliminary guidance only, and should be confirmed by local practice. In addition the design load should be determined by geotechnical engineering principles, limiting stresses in the pile material, and type and function of structure. Uncased cast in place concrete piles, although outside the scope of this driven pile manual, are included in this chapter because all feasible pile types should be considered in any selection process.

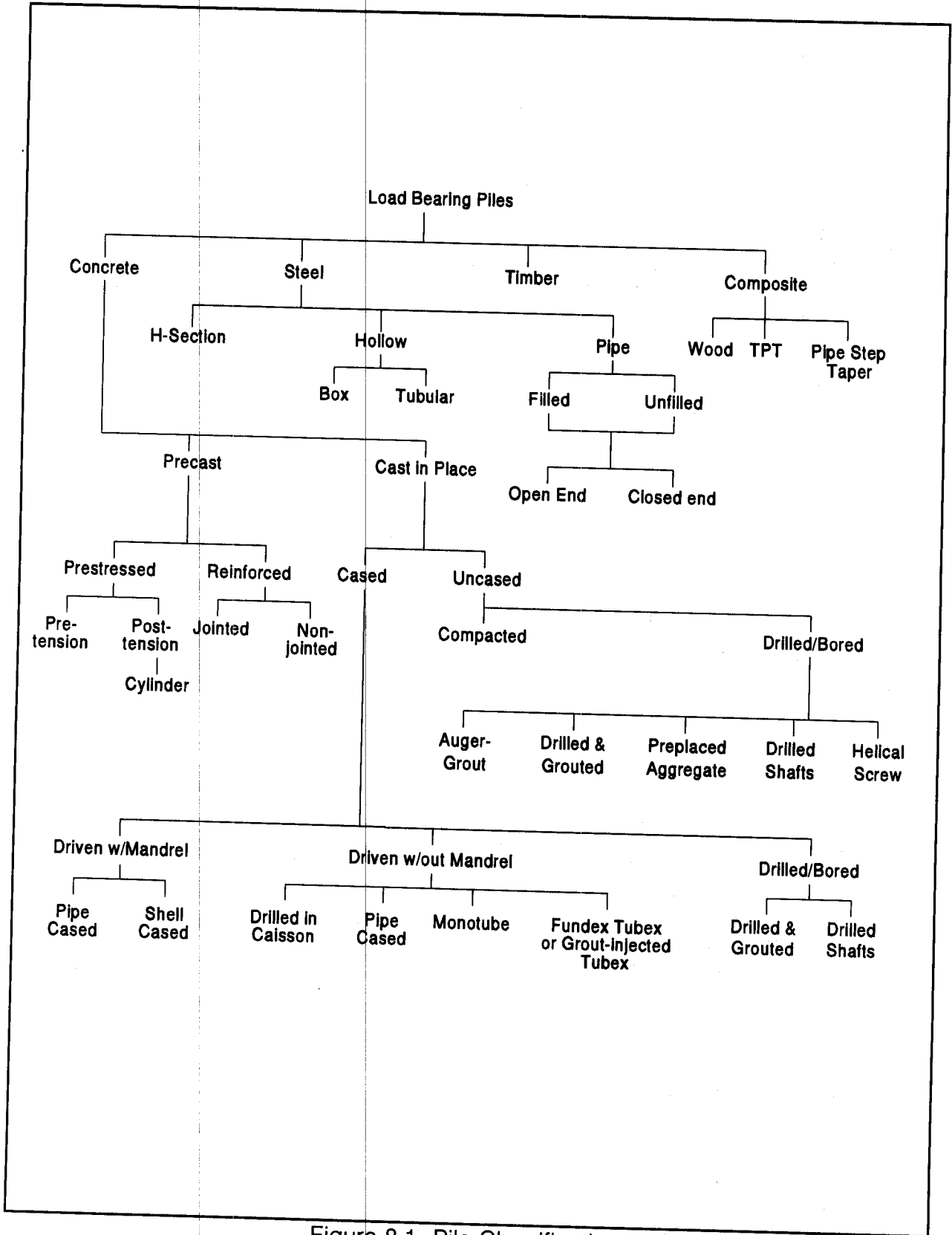
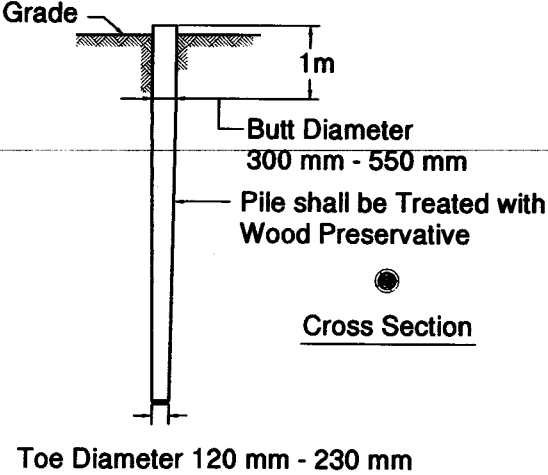


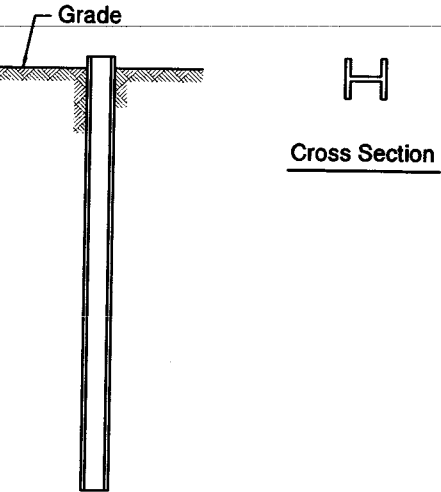
Figure 8.1 Pile Classification

TABLE 8-1 TECHNICAL SUMMARY OF PILES*

PILE TYPE	TIMBER	TYPICAL ILLUSTRATION
TYPICAL LENGTHS	5 m - 20 m	
MATERIAL SPECIFICATIONS	ASTM-D25 AWPA-C3 (if used)	
MAXIMUM STRESSES	See Chapter 11.	
TYPICAL AXIAL DESIGN LOADS	100 kN - 500 kN	
DISADVANTAGES	<ul style="list-style-type: none"> • Difficult to splice. • Vulnerable to damage in hard driving; both pile head and toe may need protection. • Intermittently submerged piles are vulnerable to decay unless treated. 	
ADVANTAGES	<ul style="list-style-type: none"> • Comparatively low in initial cost. • Permanently submerged piles are resistant to decay. • Easy to handle. 	
REMARKS	<ul style="list-style-type: none"> • Best suited for friction piles in granular material. 	

* Table modified and reproduced from NAVFAC DM 7.2 (1982)

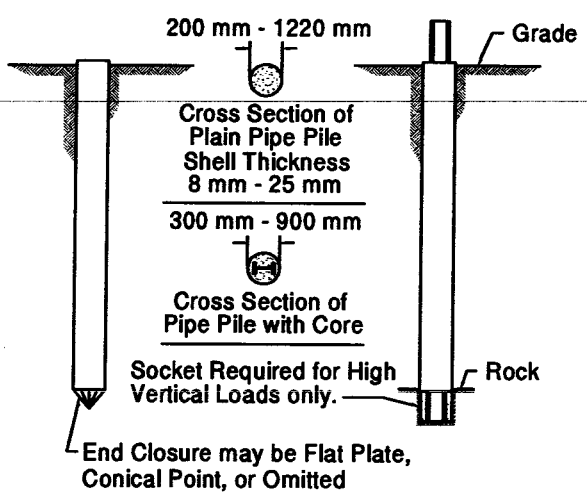
TABLE 8-1 TECHNICAL SUMMARY OF PILES* (CONTINUED)

PILE TYPE	STEEL - H SECTIONS	TYPICAL ILLUSTRATION
TYPICAL LENGTHS	5 m - 30 m	
MATERIAL SPECIFICATIONS	ASTM - A36 or A572, Grade 50	
MAXIMUM STRESSES	See Chapter 11.	
TYPICAL AXIAL DESIGN LOADS	400 kN - 2,000 kN	
DISADVANTAGES	<ul style="list-style-type: none"> • Vulnerable to corrosion where exposed HP section may be damaged or deflected by major obstructions. • Not recommended as a friction pile in granular materials. 	
ADVANTAGES	<ul style="list-style-type: none"> • Easy to splice. • Available in various lengths and sizes. • High capacity. • Small displacement. • Able to penetrate through light obstructions. • Pile toe protection may be needed for penetration through hard obstructions or where soft rock is present. 	
REMARKS	<ul style="list-style-type: none"> • Best suited for toe bearing on rock. • Allowable capacity should be reduced in corrosive locations. 	

8-4

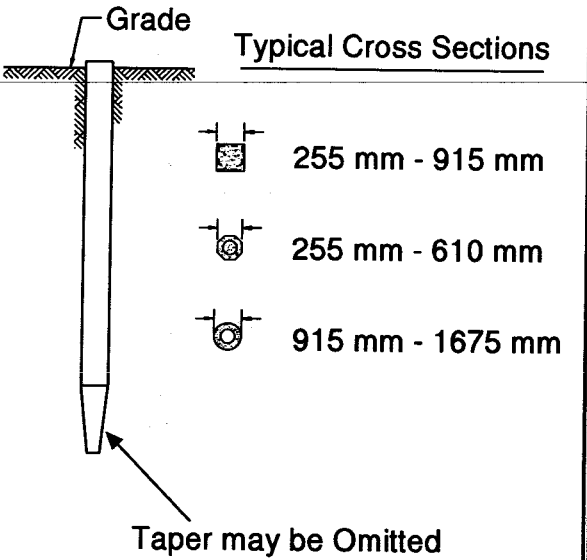
* Table modified and reproduced from NAVFAC DM 7.2 (1982)

TABLE 8-1 TECHNICAL SUMMARY OF PILES* (CONTINUED)

PILE TYPE	STEEL PIPE PILES	TYPICAL ILLUSTRATION
TYPICAL LENGTHS	10 m - 40 m or more.	 <p>The illustration shows two vertical steel pipe piles. The left pile has a conical point at its base. The right pile has a socket at its base, which is shown resting on a rock. Two cross-sections are shown: the top one is for a 'Plain Pipe Pile' with a diameter of 200 mm to 1220 mm and a shell thickness of 8 mm to 25 mm; the bottom one is for a 'Pipe Pile with Core' with a diameter of 300 mm to 900 mm. Labels include 'Grade' at the top, 'Rock' at the base of the right pile, and 'End Closure may be Flat Plate, Conical Point, or Omitted' pointing to the bottom of the left pile.</p>
MATERIAL SPECIFICATIONS	ASTM A252 - for pipe. ACI 318 - for concrete (if filled). ASTM A36 or A572 - for core (if used).	
MAXIMUM STRESSES	See Chapter 11.	
TYPICAL AXIAL DESIGN LOADS	800 kN - 2,500 kN with or without concrete fill and without cores. 5,000 kN - 15,000 kN concrete filled with cores.	
DISADVANTAGES	<ul style="list-style-type: none"> • Displacement for closed end pipe. • Open ended not recommended as a friction pile in granular material. 	
ADVANTAGES	<ul style="list-style-type: none"> • Best control during installation. • Low displacement for open end installation. • Open end pipe is best against obstructions. • Piles can be cleaned out and driven further. • High load capacities. • Easy to splice. 	
REMARKS	<ul style="list-style-type: none"> • Provides high bending resistance where unsupported length is loaded laterally. 	

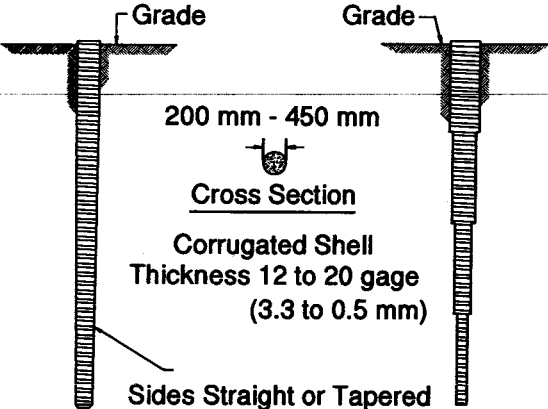
* Table modified and reproduced from NAVFAC DM 7.2 (1982)

TABLE 8-1 TECHNICAL SUMMARY OF PILES* (CONTINUED)

PILE TYPE	PRECAST/PRESTRESSED CONCRETE	TYPICAL ILLUSTRATION
TYPICAL LENGTHS	10 m - 15 m for precast. 15 m - 40 m for prestressed.	 <p data-bbox="1436 579 1750 609">Typical Cross Sections</p> <p data-bbox="1397 669 1750 715">255 mm - 915 mm</p> <p data-bbox="1397 760 1750 805">255 mm - 610 mm</p> <p data-bbox="1397 851 1769 896">915 mm - 1675 mm</p> <p data-bbox="1328 1070 1642 1100">Taper may be Omitted</p> <p data-bbox="1230 1138 1750 1168">Note: Reinforcing may be Prestressed</p>
MATERIAL SPECIFICATIONS	ACI 318 - for concrete. ASTM - A82, A615, A722, and A884 - for reinforcing steel. ASTM - A416, A421, and A882 - for prestressing.	
MAXIMUM STRESSES	See Chapter 11.	
TYPICAL AXIAL DESIGN LOADS	400 kN - 1,000 kN for precast. 400 kN - 4,500 kN for prestressed.	
DISADVANTAGES	<ul style="list-style-type: none"> • Unless prestressed, vulnerable to handling damage. • Relatively high breakage rate, especially when piles are to be spliced. • High initial cost. • Considerable displacement. • Prestressed difficult to splice. 	
ADVANTAGES	<ul style="list-style-type: none"> • High load capacities. • Corrosion resistance obtainable. • Hard driving possible. 	
REMARKS	<ul style="list-style-type: none"> • Cylinder piles are well suited for bending resistance. 	

* Table modified and reproduced from NAVFAC DM 7.2 (1982)

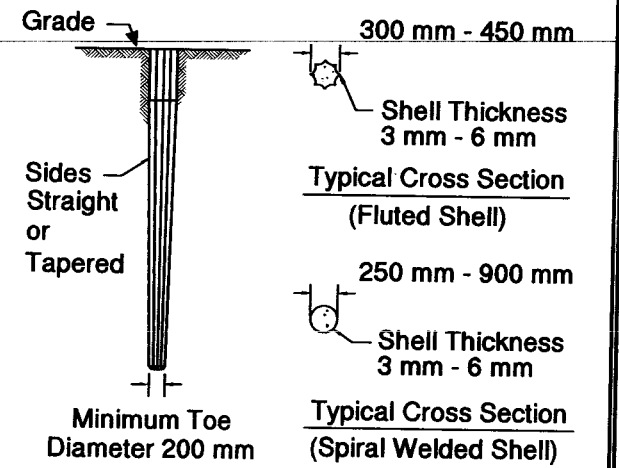
TABLE 8-1 TECHNICAL SUMMARY OF PILES* (CONTINUED)

PILE TYPE	CAST IN PLACE CONCRETE (MANDREL DRIVEN SHELL)	TYPICAL ILLUSTRATION
TYPICAL LENGTHS	3 m - 40 m, but typically in the 15 m - 25 m range.	
MATERIAL SPECIFICATIONS	ACI 318 - for concrete.	
MAXIMUM STRESSES	33% of 28-day strength of concrete, with increase to 40% of 28-day strength provided: <ul style="list-style-type: none"> • Casing is a minimum of 12 gage thickness. • Casing is seamless or with welded seams. • Ratio of steel yield strength to concrete is not less than 6. • Pile diameter not greater than 450 mm. 	
TYPICAL AXIAL DESIGN LOADS	Designed for a wide loading range but generally in the 400-1400 kN range.	
DISADVANTAGES	<ul style="list-style-type: none"> • Difficult to splice after concreting. • Redriving not recommended. • Thin shell vulnerable during driving to excessive earth pressure or impact. • Considerable displacement. 	
ADVANTAGES	<ul style="list-style-type: none"> • Initial economy. • Tapered sections provide higher resistance in granular soil than uniform piles. • Can be inspected after driving. • Relatively less waste of steel. • Can be designed as toe bearing or friction pile. 	
REMARKS	<ul style="list-style-type: none"> • Best suited as friction pile in granular materials. 	

8-7

* Table modified and reproduced from NAVFAC DM 7.2 (1982)

TABLE 8-1 TECHNICAL SUMMARY OF PILES* (CONTINUED)

PILE TYPE	CAST IN PLACE CONCRETE (SHELLS DRIVEN WITHOUT A MANDREL)	TYPICAL ILLUSTRATION
TYPICAL LENGTHS	5 m - 25 m	
MATERIAL SPECIFICATIONS	ACI 318 - for concrete. ASTM A252 - for steel pipe.	
MAXIMUM STRESSES	See Chapter 11.	
TYPICAL AXIAL DESIGN LOADS	500 kN - 1350 kN	
DISADVANTAGES	<ul style="list-style-type: none"> • Difficult to splice after concreting. • Considerable displacement. 	
ADVANTAGES	<ul style="list-style-type: none"> • Can be redriven. • Shell not easily damaged if fluted. 	
REMARKS	<ul style="list-style-type: none"> • Best suited for friction piles of medium length. 	

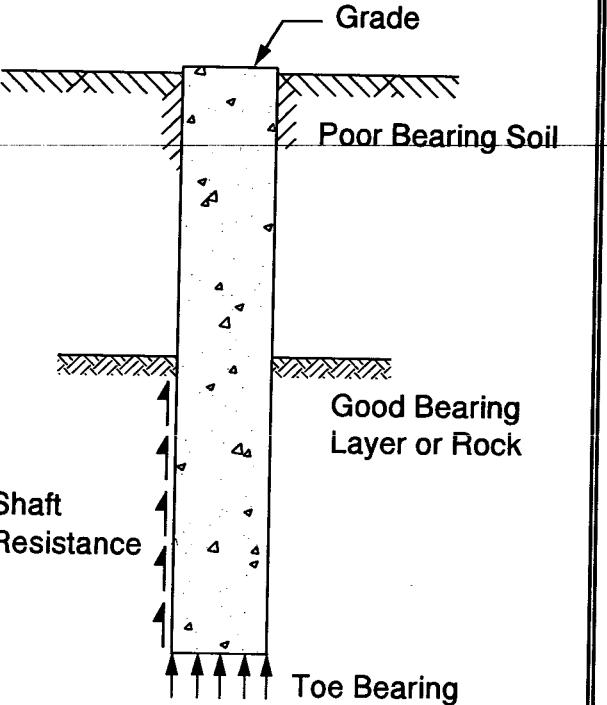
* Table modified and reproduced from NAVFAC DM 7.2 (1982)

TABLE 8-1 TECHNICAL SUMMARY OF PILES* (CONTINUED)

PILE TYPE	COMPOSITE PILES	TYPICAL ILLUSTRATION
TYPICAL LENGTHS	15 m - 65 m	<p style="text-align: center;"><u>Typical Combinations</u></p> <p>The diagram illustrates four typical combinations of composite pile materials. Each combination shows a cross-section of the pile with a horizontal line indicating the ground level (Grade). 1. Precast Concrete (hatched) is shown above an HP Section (solid). 2. Cased or Uncased Concrete (hatched) is shown above a Timber section (solid). 3. Concrete Filled Steel Shell (hatched) is shown above an HP Section (solid). 4. Steel Pipe Concrete Filled (hatched) is shown above an HP Section (solid).</p>
MATERIAL SPECIFICATIONS	ASTM A36 or A572 - for structural section. ASTM A252 - for steel pipe. ASTM D25 - for timber. ACI 318 - for concrete.	
MAXIMUM STRESSES	33% of 28-day strength of concrete. 62 MPa for structural and pipe sections if thickness is greater than 4 mm.	
TYPICAL AXIAL DESIGN LOADS	300 kN - 1,800 kN	
DISADVANTAGES	<ul style="list-style-type: none"> • Difficult to attain good joints between two materials except for pipe composite piles. 	
ADVANTAGES	<ul style="list-style-type: none"> • Considerable length can be provided at comparatively low cost for wood composite piles. • High capacity for pipe and HP composite piles. • Internal inspection for pipe composite piles. 	
REMARKS	<ul style="list-style-type: none"> • The weakest of any material used shall govern allowable stresses and capacity. 	

* Table modified and reproduced from NAVFAC DM 7.2 (1982)

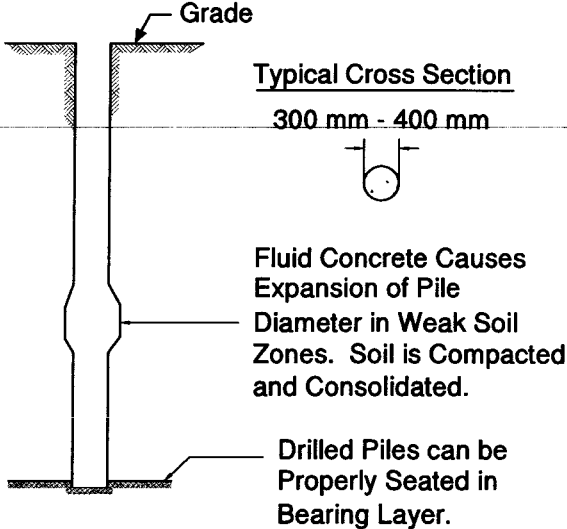
TABLE 8-1 TECHNICAL SUMMARY OF PILES* (CONTINUED)

PILE TYPE	DRILLED SHAFTS	TYPICAL ILLUSTRATION
TYPICAL LENGTHS	Up to 50 m	
MATERIAL SPECIFICATIONS	ACI 318 - for concrete. ASTM A82, A615, A722, and A884 for reinforcing steel.	
MAXIMUM STRESSES	33% of 28-day strength of concrete.	
TYPICAL AXIAL DESIGN LOADS	1,500 kN - 20,000 kN	
DISADVANTAGES	<ul style="list-style-type: none"> • Requires relatively more extensive inspection. • Construction procedures are critical to quality. • Boulders can be a serious problem, especially in small diameter shafts. 	
ADVANTAGES	<ul style="list-style-type: none"> • Length variations easily accommodated. • High bearing capacity and bending resistance. • Availability of several construction methods. • Can be continued above ground as a column. • Can eliminate the need for cofferdam. 	
REMARKS	<ul style="list-style-type: none"> • Not recommended in soft clays and loose sands. 	

8-10

* Table modified and reproduced from NAVFAC DM 7.2 (1982)

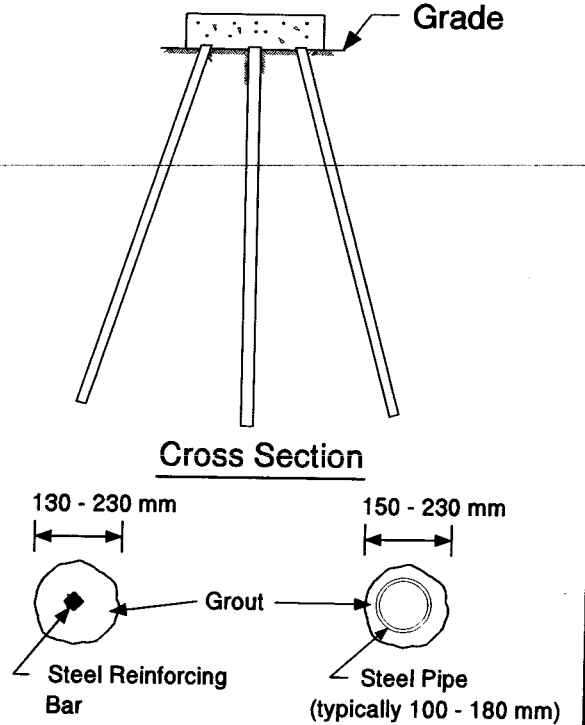
TABLE 8-1 TECHNICAL SUMMARY OF PILES* (CONTINUED)

PILE TYPE	AUGER PLACED, PRESSURE INJECTED CONCRETE PILES (CFA PILES)	TYPICAL ILLUSTRATION
TYPICAL LENGTHS	5 m - 15 m	
MATERIAL SPECIFICATIONS	ACI 318 - for concrete. ASTM A82, A615, A722, & A884 - for reinforcing steel.	
MAXIMUM STRESSES	33% of 28-day strength of concrete.	
TYPICAL AXIAL DESIGN LOADS	350 kN - 700 kN	
DISADVANTAGES	<ul style="list-style-type: none"> • Greater dependence on quality workmanship. • Not suitable through peat or similar highly compressible material. • Requires more extensive subsurface exploration. 	
ADVANTAGES	<ul style="list-style-type: none"> • Economy. • Zero displacement. • Minimal vibration to endanger adjacent structures. • High shaft resistance. • Good contact on rock for end end bearing. • Convenient for low-headroom underpinning work. • Visual inspection of augured material. 	
REMARKS	<ul style="list-style-type: none"> • Best suited as a friction pile in granular material. 	

8-11

* Table modified and reproduced from NAVFAC DM 7.2 (1982)

TABLE 8-1 TECHNICAL SUMMARY OF PILES (CONTINUED)

PILE TYPE	DRILLED AND GROUTED MICROPILES	TYPICAL ILLUSTRATION
TYPICAL LENGTHS	20 m - 30 m	
MATERIAL SPECIFICATIONS	ASTM C150 - for Portland cement. ASTM C595 - for blended hydraulic cement. ASTM A615 - for reinforcing steel.	
TYPICAL AXIAL DESIGN LOADS	300 kN - 1000 kN	
DISADVANTAGES	<ul style="list-style-type: none"> • Cost 	
ADVANTAGES	<ul style="list-style-type: none"> • Low noise and vibrations. • Small amount of spoil. • Applicable for sites with low headroom and restricted access. • Applicability to soil containing rubble and boulders, karstic areas. 	
REMARKS	<ul style="list-style-type: none"> • Can be used for any soil, rock or fill condition. 	

8-12

TABLE 8-1 TECHNICAL SUMMARY OF PILES* (CONTINUED)		
PILE TYPE	PRESSURE INJECTED FOOTINGS	TYPICAL ILLUSTRATION
TYPICAL LENGTHS	3 m - 15 m	<p>430 mm - 660 mm 300 mm - 500 mm</p> <p>Grade</p> <p>Concrete Compacted by Ramming Casing Corrugated Shell or Pipe</p> <p><u>Uncased Shaft</u> <u>Cased Shaft</u></p>
MATERIAL SPECIFICATIONS	ACI 318 - for concrete. ASTM A252 for steel pipe.	
MAXIMUM STRESSES	33% of 28-day strength of concrete. 62 MPa for pipe shell if thickness is greater than 4 mm.	
TYPICAL AXIAL DESIGN LOADS	600 kN - 1,200 kN	
DISADVANTAGES	<ul style="list-style-type: none"> • Base of footing cannot be made in clay or when hard spots (e.g., rock ledges) are present in soil. • When clay layers must be penetrated to reach suitable material, special precautions are required for shafts in groups. 	
ADVANTAGES	<ul style="list-style-type: none"> • Provides means for placing high capacity footings on bearing stratum without necessity for excavation or dewatering. • High blow energy available for overcoming obstructions. • Great uplift resistance if suitably reinforced. 	
REMARKS	<ul style="list-style-type: none"> • Best suited for granular soils where bearing is achieved through compaction around base. • Minimum spacing 1.5 m on center. 	

* Table modified and reproduced from NAVFAC DM 7.2 (1982)

8.2 TIMBER PILES

Timber piles are usually of round, tapered cross section made from tree trunks of Southern Pine or Douglas Fir driven with the small end down. Southern Pine timber piles can be found to lengths up to 23 meters, and some west coast Douglas Fir may be up to 37 meters in length. Oak and other timber types have also been used for piles, but that is infrequent today. ASTM D25, Standard Specification for Round Timber Piles, presents guidelines on minimum timber pile dimensions, straightness, knot sizes, etc. AWPAC3, Piles, Preservative Treatment by Pressure Process, contains penetration and retention values for the various preservatives.

Timber piles are best suited for modest loads when used as friction piles in sands, silts and clays. The taper of timber piles is effective in increasing the shaft resistance, particularly in loose sands. They are not recommended as piles to be driven through dense gravel, boulders, or till, or for toe bearing piles on rock since they are vulnerable to damage at the pile head and toe in hard driving. Overdriving of timber piles can result in the crushing of fibers or brooming at the pile head. This can be controlled by using a helmet with cushion material and/or metal strapping around the head of the pile. In hard driving situations, a metal shoe should be attached to the pile toe.

Timber piles are favored for the construction of bridge fender systems and small jetties due to the good energy absorption properties of wood.

Timber pile splices are difficult and generally undesirable. However, splice details are discussed in Chapter 23.

Durability is generally not a design consideration if a timber pile is below the permanent water table. However, when a timber pile is subjected to alternate wetting and drying cycles or located above the water table, damage and decay by insects may result. Such damage reduces the service life of timber piles significantly unless the pile is treated with a wood preservative. The most common treatments for timber piling are Creosote, Chromated Copper Arsenate (CCA) for Southern Pine, and Ammoniacal Copper Zinc Arsenate (ACZA) for Douglas Fir. Creosote cannot be used alone in southern waters because of attack by *limnoria tripundtata*, but should be used as part of a dual treatment with CCA or ACZA. If cracking of the pile shaft or head occurs and extends below the prescribed pile cut-off level, the initial preservative treatment will not be effective, and the trimmed end of the pile should be treated a second time.

Durability of round timber piling is a function of site-specific conditions:

1. Foundation piles submerged in ground water will last indefinitely.
2. Fully embedded, treated foundation piles partially above the ground water with a concrete cap will last 100 years or longer.
3. Treated trestle piles over land will last as long as utility poles in the area, *i.e.*, about 75 years in northern areas and about 40 years in the southern area of the United States.
4. Treated piles in fresh water will last about five to ten years less than land trestle piles in the same area.
5. For treated piles in brackish water, the longevity should be determined by the experience in the area.
6. Treated marine piles will last about 50 years in northern climates and 25 years in southern climates of the United States, Graham (1995).

8.3 STEEL H-PILES

Steel H-piles consist of rolled wide flange sections that have flange widths approximately equal the section depth. In most H-pile sections, the flange and web thicknesses are the same. They are manufactured in standard sizes ranging from 200 to 360 mm. In some cases, W-sections are also used for piles. A summary of standard H-pile sections including properties needed for design is provided in Appendix C.

Steel H-piles are commonly made to conform with ASTM A36 specifications. Many of the H-piles produced today meet both the requirements of ASTM A36 and A572, Grade 50 steel. Therefore, it may be possible to use the higher strength of the Grade 50 steel if the pile can be installed to sufficient capacity as limited by the soil.

H-piles are suitable for use as toe bearing piles, and as combination shaft resistance and toe bearing piles. Since H-piles generally displace a minimum amount of soil, they can be driven more easily through dense granular layers and very stiff clays than

displacement piles. In addition, the problems associated with soil heave during foundation installation are often reduced by using H-piles. However, sometimes H-piles will "plug". That is, the soil being penetrated will adhere to the web and the inside flange surfaces creating a closed-end, solid section. The pile will then drive as if it were a displacement pile below the depth of plug formation. Plugging can have a substantial effect on both driving resistance and static capacity.

Experience indicates that corrosion is not a practical problem for steel piles driven in natural soil, due primarily to the absence of oxygen in the soil. However, in fill materials at or above the water table, moderate corrosion may occur and protection may be needed. One common protection method requires the application of pile coatings before and after driving. Coal-tar epoxies, fusion bonded epoxies, metallized zinc, metallized aluminum and phenolic mastics are some of the pile coatings available. Encasement by cast in place concrete, precast concrete jackets, or cathodic protection can also provide the necessary protection for piles extending above the water table. Another design option for piles subject to corrosion is to select a heavier section than that required by the design loads, anticipating the loss of material caused by corrosion.

One advantage of H-piles is the ease of extension or reduction in pile length. This makes them suitable for nonhomogeneous soils with layers of hard strata or natural obstructions. Splices are commonly made by full penetration groove welds so that the splice is as strong as the pile in both compression and bending. The welding should always be done by properly qualified welders. Proprietary splices are also used for splicing H-piles. Chapter 23 presents information on typical splices. A steel load transfer cap is not required if the pile head is adequately embedded 305 mm into the concrete pile cap. Pile toe reinforcement using commercially manufactured cast pile shoes is recommended for H-piles driven through or into very dense soil or soil containing boulders or other obstructions. Pile shoes are also used for penetration into sloping rock surfaces. Chapter 23 provides details on available driving shoes.

The disadvantages of H-piles include a tendency to deviate when natural obstructions are encountered. Field capacity verification of H-piles used as friction piles in granular soils based on the driving resistance can also be problematic, and can result in length overruns. Length for length, steel piles tend to be more expensive than concrete piles. On the other hand, steel's high design load for a given weight can reduce pile driving costs.

8.4 STEEL PIPE PILES

Pipe piles consist of seamless, welded or spiral welded steel pipes in diameters ranging from 200 to 1220 mm. Still larger sizes are available, but they are not used commonly in land or nearshore applications. Typical wall thicknesses range from 3 to 25 mm with wall thicknesses of up to 64 mm possible. Pipe piles should be specified by grade with reference to ASTM A-252. In some situations, a contractor may propose to supply used pipe not produced under ASTM standards. Pipe piles not meeting ASTM standards must be evaluated by an engineer for general condition, driveability, and weldability prior to approval. Appendix C includes a table of dimensions and design properties for pipe piles.

Steel pipe piles can be used in friction, toe bearing, a combination of both, or as rock socketed piles. They are commonly used where variable pile lengths are required since splicing is relatively easy. Common offshore or nearshore applications of pipe piles include their use as bridge foundation piles, fender systems, and large diameter mooring dolphins. With the increased ductility requirements for earthquake resistant design, pipe piles are being used extensively in seismic areas.

Pipe piles may be driven either open or closed end. If the capacity from the full pile toe area is required, the pile toe should be closed with a flat plate or a conical tip. Pipe pile shafts may be left open or filled with concrete, and they can also have a structural shape such as an H-section inserted into the concrete. Open end pipe piles can be socketed into bedrock (rock socketed piles). In driving through dense materials, open end piles may form a soil plug. The plug makes the pile act like a closed end pile and can significantly increase the pile toe resistance. The plug should not be removed unless the pile is to be filled with concrete. Most often, pipe piles are driven from the pile head. However, closed end pipe piles can also be bottom driven using a mandrel.

A closed end pipe pile is generally formed by welding a 12 to 25 mm thick flat steel plate or a conical point to the pile toe. When pipe piles are driven to weathered rock or through boulders, a cruciform end plate or a conical point with rounded nose is often used to prevent distortion of the pile toe. Open ended piles can also be reinforced with steel cutting shoes to provide protection against damage.

Typically, pipe piles are spliced using full penetration groove welds. Proprietary splicing sleeves are available and should be used only if the splice can provide full strength in bending (unless the splice will be located at a distance below ground where bending moments are small). Typical pile splices are described in Chapter 23. The discussion presented under H-piles on corrosion is also applicable to steel pipe piles.

The "spin fin pile" is a variation of a pipe pile recently introduced along the west coast. It is a pipe pile with an outside thread made of fins that gradually wind around the lower portion of the pile. During driving the pile rotates, but in response to uplift the pile is prevented from twisting. This results in a plugging effect that increases the pile's uplift capacity.

8.5 PRECAST CONCRETE PILES

This general classification covers both conventionally reinforced concrete and prestressed concrete piles. Both types can be manufactured by various methods and are available in a number of different cross sections. Frequently concrete piles are cast with a hollow core. The hollow core may be used for a jet pipe (if continuous), for placing instrumentation during construction, or for determining pile damage. Precast concrete piles are usually of constant cross section but can also include a tapered section near the pile toe.

Precast concrete piles are suitable for use as friction piles when driven in sand, gravel, or clays. In boulder conditions, a short piece of structural H-section or "stinger" may be cast into or attached to the pile toe for penetrating through the zone of cobbles and boulders. A rock shoe or "Oslo point" cast into the pile toe can assist seating of concrete piles into a rock surface. Precast concrete piles are capable of high capacities when used as toe bearing piles.

Concrete piles are considered resistant to corrosion but can be damaged by direct chemical attack (from organic soil, industrial wastes or organic fills), electrolytic action (chemical or stray direct currents), or oxidation. Concrete can be protected from chemical attack by use of special cements and by special coatings as discussed in Section 8.8.

A necessary consideration when dealing with hollow core precast concrete piles driven in water includes the evaluation of internal pressures within the cylinder which can reach bursting pressures and cause vertical cracks during driving. Another concern for piles driven through water is water jet cracking. If a pile is under high tension stresses during driving, small cracks can open and close during each hammer blow. If the cracks are large enough, water can enter the cracks and subsequently be expelled at high velocities. Water jet pressures will often cause concrete deterioration near the cracks. This process can also be accelerated by the high impact compressive forces induced by driving. A high prestressing force in concrete piles can help reduce this danger by resisting tension stresses during driving and thereby reducing the risk of crack development.

8.5.1 Prestressed Concrete Piles

Prestressed concrete piles consist of a configuration similar to a conventional reinforced concrete pile except that the longitudinal reinforcing steel is replaced by the prestressing steel. The prestressing steel may be in the form of strands or wires which are enclosed in a conventional steel spiral and placed in tension. Prestressing steel must conform to ASTM A416, A421, and A882. Due to the effects of prestressing, these piles can usually be made lighter and longer than reinforced concrete piles of the same size.

Prestressed sections vary from the most common solid square section to a solid octagonal section. In addition, large sections are available but often these sections have internal circular voids. These piles are best suited for friction piles in sands, gravels and clays where a known pile length is required since prestressed piles can be difficult to shorten.

Prestressed piles can either be pretensioned or post-tensioned. Pretensioned piles are usually cast to their full length in permanent casting beds. Post-tensioned piles are usually manufactured in sections and assembled and prestressed to the required pile lengths at the manufacturing plant or on the job site. Figure 8.2 shows typical prestressed concrete piles. Design data for typical prestressed concrete pile sections is presented in Appendix C.

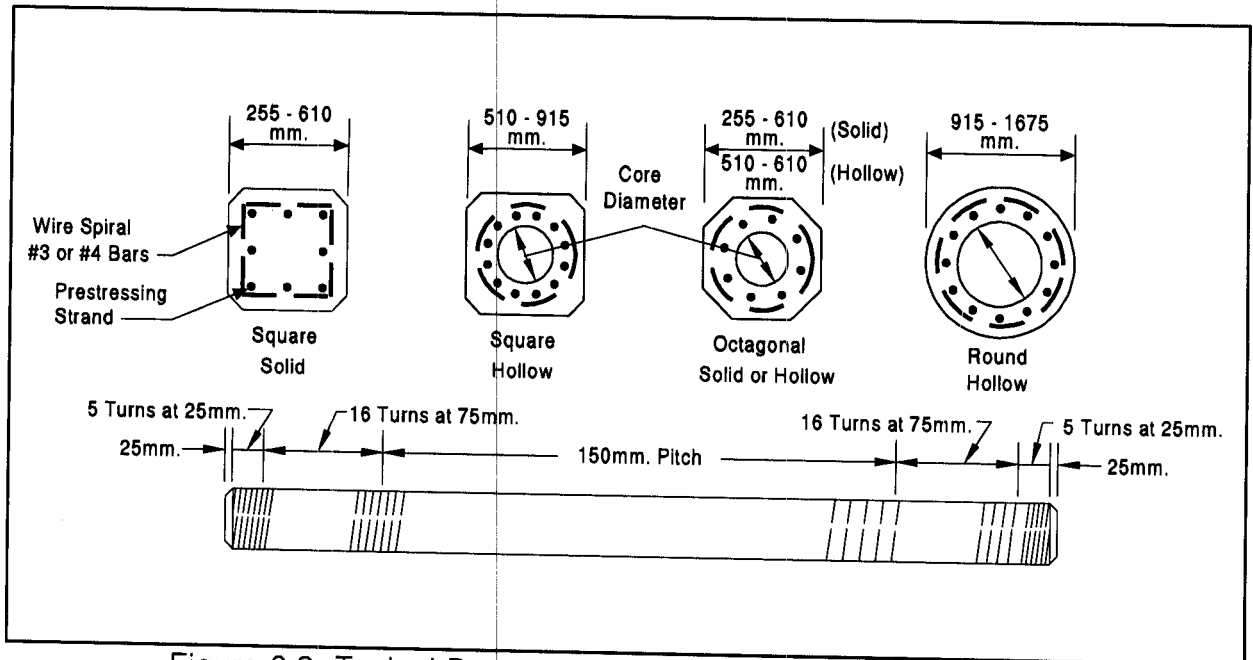


Figure 8.2 Typical Prestressed Concrete Piles (after PCI, 1993)

The primary advantage of prestressed concrete piles compared to conventional reinforced concrete piles is durability. Since the concrete is under continuous compression, hairline cracks are kept tightly closed and thus prestressed piles are usually more resistant to weathering and corrosion than conventionally reinforced piles. This characteristic of prestressed concrete removes the need for special steel coatings since corrosion is not as serious a problem as for reinforced concrete. Another advantage of prestressing is that the tensile stresses which can develop in the concrete under certain driving and handling conditions are less critical.

Prestressed concrete pile are more vulnerable to damage from striking hard layers of soil or obstructions during driving than reinforced concrete piles. This is due to the decrease in axial compression capacity which results from the application of the prestressing force.

Prestressed concrete piles cutoff and splicing problems are considered much more serious by contractors that drive them infrequently than by those that drive only this pile type. Special reinforcement required at the pile head in seismic areas can pose problems if actual lengths vary significantly from the planned length. In these cases, a splice detail must be included so that the seismic reinforcement is extended into the pile cap.

8.5.2 Reinforced Concrete Piles

These piles are manufactured from concrete and have reinforcement consisting of a steel cage made up of several longitudinal bars and lateral or tie steel in the form of individual hoops or a spiral. Steel reinforcing for reinforced concrete piles is governed by ASTM A82, A615, and A884. High yield strength steel reinforcement must conform to ASTM A722 and may be used to resist uplift loads. Figure 8.3 shows a typical reinforced concrete pile.

Reinforced concrete piles as compared to prestressed piles are more susceptible to damage during handling and driving because of tensile stresses. Advantages of reinforced concrete piles include their lower net compressive stresses during driving and under service loads, and a reduced danger of pile head cracking. In addition, these piles are easier to splice than prestressed piles and thus may be used when variable pile lengths are needed. To avoid corrosion of the reinforced concrete joints, splices should be located below the ground surface, or if under water, the mudline. Segmental pile sections can be used to produce piles with varied lengths to accommodate variable soil conditions, and are easily transported to job sites.

The most common type of jointed pile is a square cross section made of high density concrete with each successive unit of shorter length. Typical pile cross sections range from 250 to 400 mm, but sizes above and below this range are produced. Joints between these pile sections can be of the mechanical type, including bayonet fittings or wedges. The joints must be well aligned or energy will be lost during driving and bending stresses may be introduced due to an eccentric connection. These piles are best suited for friction piles in sand, gravel and clay.

Another jointed reinforced concrete pile type utilizes a hexagonal section. The advantages of this cross sectional shape are an improved stress distribution over the pile section and an improved resistance to torsional loading.

Special precautions should be taken when placing piles during cold weather. If piles are driven through ice and water before reaching soil, the air and concrete may be at low temperatures relative to the soil and water. Such temperature gradients can cause concrete to crack due to nonuniform shrinkage and expansion.

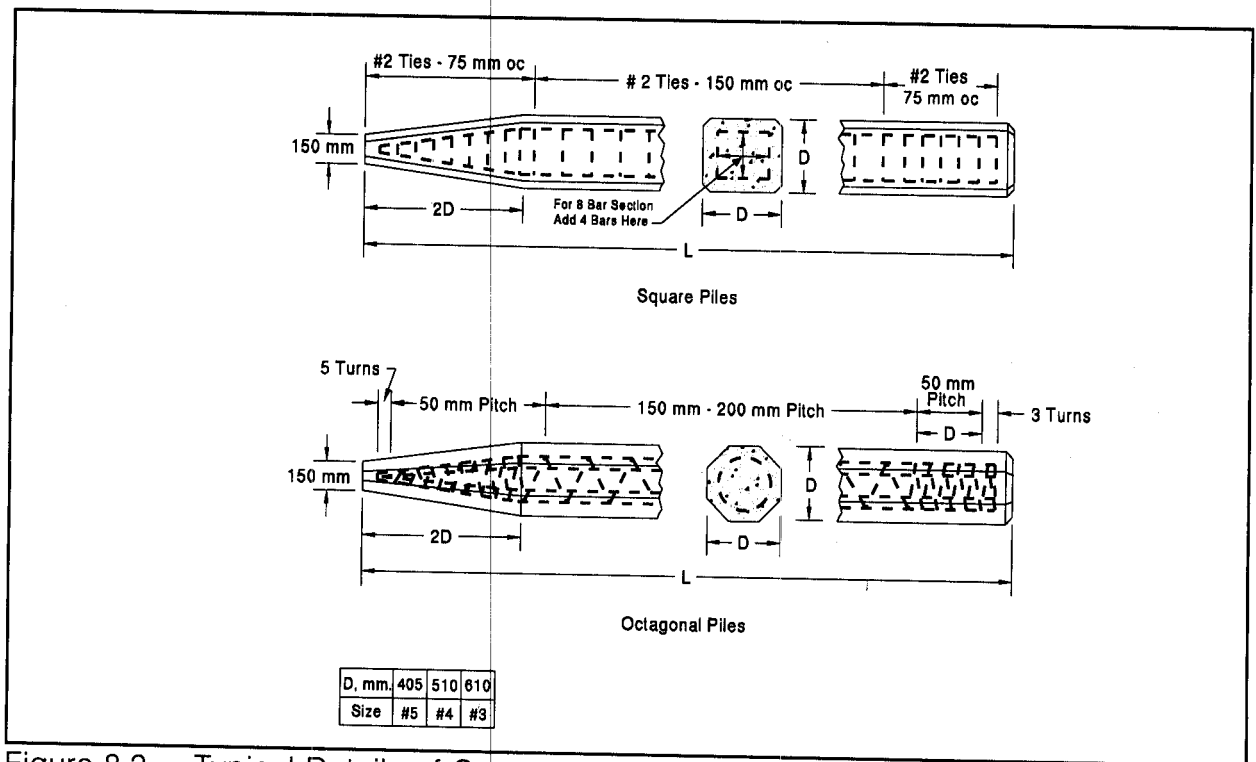


Figure 8.3 Typical Details of Conventionally Reinforced Concrete Piles (after PCA, 1951)

Although most reinforced concrete piles are jointed, there are occasions when non-jointed piles are more economical due to the cost of pile segments. Often for a very large job when thousands of piles will be used, piles can be economically cast on site. Most non-jointed piles have a square cross section and are difficult to change in length. Only a few splicing procedures exist if a situation arises where a reinforced concrete pile must be lengthened. The first method of pile lengthening involves the breakdown of the projecting pile head to provide a suitable lap for reinforcing steel. Concrete is cast to form a joint. A second option is to butt the two piles together within a steel sleeve, and use an epoxy cement to join the two piles. The last lengthening method involves the use of dowel bars to be inserted into drilled holes with epoxy cement to form the joint. If piles are lengthened, the connecting pile sections must be carefully aligned, since excessive bending stresses may result if any eccentricity exists. Splicing problems tend to become less severe or even non-existent when contractors develop experience and techniques. Special reinforcement required at the pile head in seismic areas can pose problems if actual lengths vary significantly from the planned length. In these cases, a splice detail must be included so that the seismic reinforcement is extended into the pile cap.

Reinforced concrete piles are used infrequently in the United States. However, in Europe, Australia, and many Asian countries reinforced concrete piles are used routinely based on economic considerations.

8.5.3 Concrete Cylinder Piles

Concrete cylinder piles are post-tensioned, hollow concrete piles which are cast in sections, bonded with a plastic joint compound, and then post tensioned in lengths containing several segments. Special concrete is cast by a process unique to cylinder piles which achieves high density and low porosity. The pile is virtually impervious to moisture. Results of chloride ion penetration and permeability tests on prestressed cylinder piles indicate that the spun cylinder piles have excellent resistance to chloride intrusion. Figure 8.4 shows the typical configuration of a cylinder pile. Appendix C provides appropriate engineering design data.

Generally cylinder piles are used for marine structures or land trestles and have high resistance to corrosion. In freeze-thaw conditions however, the long term resistance of cylindrical piles is required. The piles typically extend above ground and are designed to resist a combination of axial loads and bending moments. They are available in diameters of 915 to 1675 mm.

Cylinder piles are sometimes quite difficult to drive. However, they usually extend directly to the superstructure support level avoiding the need for a pile cap, which can result in substantial cost savings. Jetting is often used to install cylinder piles to the desired depth. When used, jetting must be controlled to minimize degradation of the lateral soil resistance.

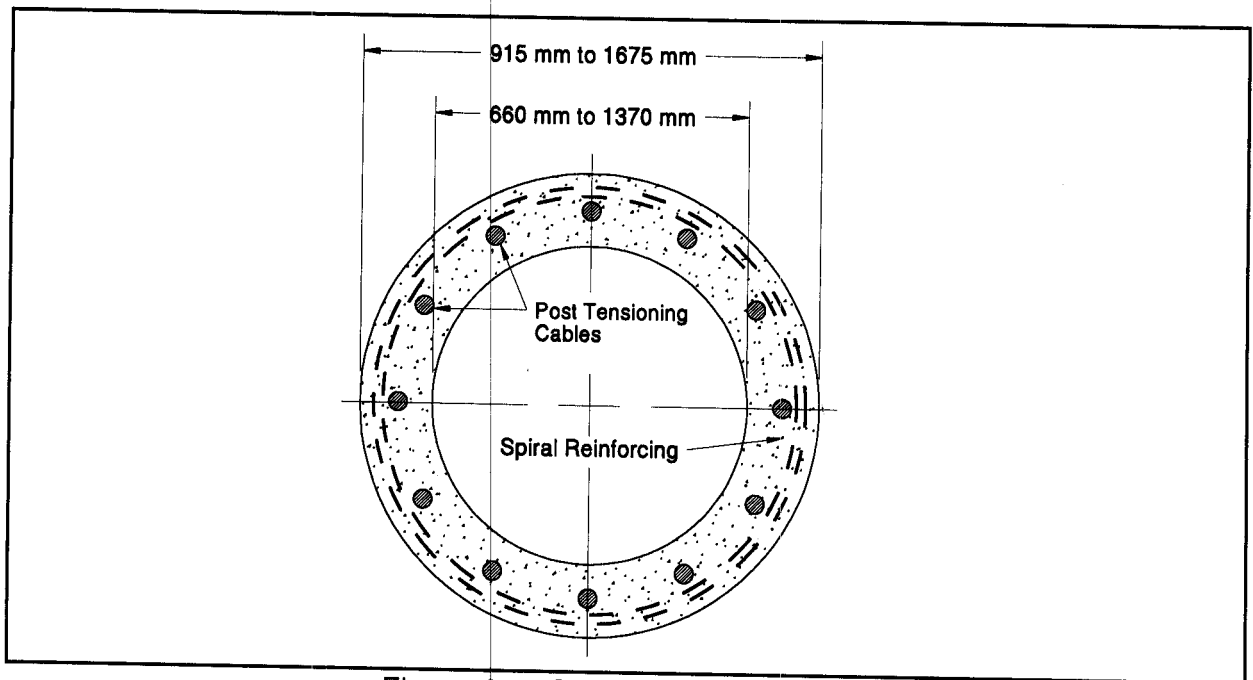


Figure 8.4 Concrete Cylinder Pile

8.6 CAST IN PLACE CONCRETE PILES

Cast in place concrete piles are installed by placing concrete in a steel shell that has been driven or inserted into a bored hole in the ground. The steel shell or casing may be left in place or withdrawn after the concrete is placed. Concrete is also placed in predrilled holes that are uncased. Predetermination of pile lengths is not as critical as for precast concrete piling.

8.6.1 Cased Driven Shell Concrete Piles

The cased driven shell concrete pile is the most widely used type of cast in place concrete pile. There are two principal types of cased piles. One type is driven without a mandrel and the other is driven with a mandrel. A mandrel is usually a heavy tubular steel section inserted into the pile that greatly improves the pile driveability. After driving, the mandrel is removed. Shells driven without mandrels have thicknesses in the range of 3 to 64 mm. Shells driven with mandrels are much thinner, often 10 to 24 gage or 3.3 to 0.5 mm thick. The mandrel driven shells are usually corrugated circumferentially. This results in excellent frictional characteristics and increased collapse strength prior to concrete placement.

After driving, a shell pile is inspected internally along its full length before concrete is placed. Reinforcing steel is required only when the concrete in the pile may be under tension from such conditions as uplift, high lateral loads, or for unsupported pile lengths. Reinforcing steel may also be used to provide additional axial load capacity.

a. Mandrel Driven Shell Concrete Piles

Mandrel driven shells can be used in most soil conditions except where obstacles such as cobbles and boulders are present that could damage the thin shells during driving. In addition, these thin shells are susceptible to collapse under hydrostatic pressure prior to concrete placement. They are best suited for friction piles in granular material.

The pile shells for mandrel driven piles are often produced from sections of corrugated steel and can be of constant diameter, steadily decreasing in diameter from the pile head to the pile toe, or diameter decreasing in discrete steps over the pile length. Typical tapers are on the order of 25 mm per 2.5 meter length. It is also possible to have different lengths for each section. Separate shell sections are usually screw-connected and waterproofed with an O-ring gasket. The Step Taper, Armco Hel-Cor, Republic Corwel and Guild pile are among the piles driven with mandrels.

The properties of the reusable mandrels dictate the driveability of these shell pile sections. This can result in a significant cost advantage for a mandrel driven shell pile since the mandrels result in improved pile driveability and load capacity at low material costs. Construction control of mandrel driven piles should include a wave equation analysis that accounts for the improved pile driveability from the mandrel. A dynamic formula should not be used for construction control of mandrel driven piles. Mandrel driven piles may be costly if it is necessary to drive piles to an unanticipated depth that exceeds the mandrel length available at the job site.

b. Monotube - Cased Concrete Piles

The Monotube pile is a proprietary pile driven without a mandrel. Monotubes are longitudinally fluted and are tapered over the lower pile length. These piles are available in 3 to 9 gage shell thicknesses or roughly 6 mm to 4 mm. The fluted

and tapered design of Monotube piles has several functional advantages. The flutes add stiffness necessary for handling and driving lightweight piles. The flutes also increase the surface area while the tapered section improves the capacity per unit length in compression loading. The flutes are formed by cold working when the pile is manufactured. The cold working increases the yield point of the steel to more than 350 MPa, further improving the pile driveability. Monotube sections are spliced by a frictional connection and a fillet weld between a non-tapered extension and the lower pile section into which it is inserted. The manufacturer's recommended splicing detail should be followed. Additional design data for the Monotube pile is included in Appendix C.

c. Pipe - Cased Concrete Piles

Another variation of the cased, cast in place pile is the concrete filled pipe pile. These pipe piles can be driven either open or closed end. Closed end piles can be driven conventionally from the pile head, can be bottom driven with a mandrel, or by a mandrel engaged at both the pile head and toe. Open end piles are usually driven from the pile head. Piles that are driven open ended, may require internal clean out if the pile will be concrete filled to some distance below grade. Before concrete placement, steel reinforcement and uplift resisting dowels can be added, as necessary. Open end pipe piles are seldom cleaned out full length unless a rock socket is planned or short pile lengths are used.

d. Fundex Tubex or Grout-Injected Tubex Piles

The Fundex pile is a unique form of a pipe-cased, cast in place concrete pile. Instead of the pile being driven into the ground with a hammer, it is screwed into the ground with a special iron drill point which is welded to the end of the first section of pipe. A drill table then forces the pile into the ground utilizing a constant vertical load and torque. When the first pipe section reaches a depth providing sufficient headroom for the attachment of a second pipe section, the second section is welded to the first and drilling is resumed. Depending on the soil conditions, the pipe casing can be installed either grouted or non-grouted. Grouting can be used along the entire pile length or only in the bearing layer of the soil. The grout shell is created by pressure-injecting cement grout throughout the specified pile depth. Once the pile reaches its final design penetration, grouting is stopped and steel reinforcement is placed. The drill

point is left in place at the toe of the pile, providing a waterproof pile toe for concrete filling of the pipe casing.

Some of the advantages of the Fundex Tubex piles include vibrationless and quiet installation, drilling equipment that can be used in confined spaces, and a removable mast that allows installation with only 6 meters of overhead clearance. In addition, the grout-injected Tubex pile can make use of a bentonite-water slurry to lessen frictional drag during installation when grout is not being injected into the soil surrounding the pile wall.

e. Driven and Drilled-In Caisson Piles

The Drilled-In Caisson is a special type of high capacity, cased, cast in place pile used for large engineering structures. The casing of this pile is usually a heavy-walled pipe fitted with a drive shoe which is driven to bedrock and sealed off within the rock. Once the casing reaches bedrock, it is cleaned out and a socket is drilled into the rock with rotary drilling equipment. Next the rock socket is cleaned, and a steel H-shaped core or reinforcing cage is placed before filling the rock socket and cased pipe with concrete.

8.6.2 Uncased Concrete Piles

There are several types of cast in place piles that can be classified as uncased piles. Two principal types of uncased piles are bored piles and compacted concrete piles.

a. Bored Piles

Bored piles are installed by drilling or augering a hole in the ground and filling it with concrete. Bored pile installations should be performed carefully by an experienced contractor and with experienced inspection. Bored piles are susceptible to problems such as necking (smaller pile diameter at some locations along their length), grout contamination by soil, or bore hole collapse. Bored, uncased piles have a high degree of risk for structural integrity. There are several types of bored piles and they do not have the advantage of capacity determination from driving observations.

- (1) Continuous flight auger (CFA) or auger-cast piles are usually installed by turning a continuous-flight hollow-stem auger into the ground to the required depth. As the auger is withdrawn, grout or concrete is pumped under pressure through the hollow stem, filling the hole from the bottom up. Frequently vertical reinforcing steel is pushed down into the grout or concrete shaft before it hardens. Uplift tension reinforcing can be installed by placing a single high strength steel bar through the hollow stem of the auger before grouting. After reinforcing steel is placed, the pile head is cleaned of any lumps of soil which may have fallen from the auger. Then the pile head is formed with a temporary steel sleeve to protect the fresh grout from contamination, or it is formed to the ground surface above the cutoff grade and later trimmed off to the cutoff elevation.
- (2) Drilled shafts are installed by mechanically drilling a hole to the required depth and filling the hole with concrete. Sometimes an enlarged base is formed mechanically to increase the toe bearing area. Drilling slurry or a temporary liner can be used when the sides of the hole are unstable. Reinforcing steel is installed as a cage inserted prior to concrete placement. Drilled shafts are often used where large toe bearing capacities can be achieved, such as on rock or in glacial tills. They are also used where support is primarily developed through shaft resistance in granular and cohesive soils, and rock. Drilled shafts are sometimes designed with a permanent steel casing.
- (3) Drilled and grouted piles (micropiles) are installed by rotating a casing with a cutting edge into the soil or by percussion methods. Soil cuttings are removed with circulating drilling fluid. Reinforcing steel is then inserted and a sand-cement grout is pumped through a tremie. The bored hole is filled from the bottom up while the casing is withdrawn. These piles are principally used for underpinning work, seismic retrofitting and landslide stabilization. Several types of micropiles leave the casing in place for added bending resistance and axial capacity.
- (4) Preplaced aggregate piles are installed by drilling a hole to the required depth, filling the hole with coarse aggregate, pumping grout into the column of aggregate, and filling it from the bottom up.

(5) Helical Screw cast in place piles are formed using the Atlas Piling System. The helical piles are displacement piles formed using a single-start auger head with a short flight. The auger head is carried on a hollow stem which transmits a large torque and compressive force as it is screwed into the ground to the required depth. After reinforcement is placed, concrete is poured through the end of the hollow auger and the auger is slowly unscrewed and removed. This process leaves behind a screw-threaded cast in place pile with large threads which provide increased surface area for improved shaft resistance. In fact, for a given pile size and volume of concrete, pile capacities are greater than for traditionally constructed bored piles. The disadvantage of this pile type is that the restricted diameter of the reinforcement cage limits the bending capacity.

b. Compacted Concrete Pile

The compacted concrete pile is installed by bottom driving a temporary steel casing into the ground using a drop weight driving on a zero slump concrete plug at the bottom of the casing. When the required depth has been reached, the steel casing is restrained from above and the concrete plug is driven out the bottom of the tube. An enlarged base is formed by adding and driving out small batches of zero slump concrete.

Steel reinforcing is then installed prior to adding more concrete to the shaft. It is suggested that widely spaced bars be used to allow the low workability mix to penetrate to the exterior of the piles. After the base is formed and reinforcement is placed, concrete continues to be added and the uncased shaft is formed by compacting the concrete with a drop weight in short lifts as the casing is being withdrawn. Alternatively, if a high workability mix is used to complete the pile, a vibrator can be clamped to the top of the tube and used to compact the concrete into place as the casing is withdrawn.

This type of driven, cast in place pile is often referred to as a Franki pile or pressure injected footing. The best site conditions for these piles are loose to medium dense granular soils.

8.7 COMPOSITE PILES

In general, a composite pile is made up of two or more sections of different materials or different pile types. Depending upon the soil conditions, various composite sections may be used. The upper pile section is often precast concrete, steel pipe, or corrugated shell. The lower pile section may consist of steel H, steel pipe, or timber pile. Composite piles have limited application and are generally used only under special conditions.

8.7.1 Precast Concrete - Steel Piles

One of the more commonly used composite piles consists of a lower section of steel H, or pipe pile embedded in an upper pile section of precast concrete. These composite sections are often used when uplift requirements dictate penetration depths that a displacement pile cannot achieve, or in waterfront construction where surficial soil layers have high corrosion potential.

8.7.2 Wood Composite Piles

Timber-steel or timber-concrete composite sections are sometimes used as foundation piles. It is common to have a timber section below the groundwater level with either a concrete or corrosion protected steel upper section. In the case of the composite timber-concrete pile, an untreated timber pile is first driven below the permanent ground water level, then a corrugated steel shell is connected to the pile head of the timber section with a wedge ring driven into the wood. After driving, the shell is filled with concrete to the cutoff elevation and the pile is complete.

8.7.3 Pipe - Corrugated Shell Piles

This composite pile consists of a pipe pile for the lower section and a corrugated shell for the upper portion of the pile. A variety of pipe and shell diameters can be used to accommodate a range of loading conditions. The pipe-shell pile is mandrel driven. The mandrel provides a guide for alignment of the two pile sections provided it extends to the pipe pile head or partially into the pipe pile. Possible pile joints include; a sleeve joint, a welded joint, and a drive-sleeve joint. Once the pipe and shell are driven and connected, they are filled with concrete to cutoff grade and any excess shell is removed.

8.7.4 Composite Tapered Precast Tip - (TPT)

The most common form of this composite pile consists of a round, tapered, precast concrete tip, attached at the bottom of a pile shaft. The pile shaft may consist of pipe pile or thin corrugated shell. The precast tip is driven to its designed depth with a mandrel, then the pile shaft is socketed into the precast tip and filled with concrete. Enlarged tip piles can be particularly effective if downdrag forces are present. In addition to the reduced shaft resistance created by driving the enlarged tip, the shaft can be coated or wrapped with a material to further resist downdrag. The enlarged tip provides significant toe bearing capacity.

8.7.5 Polymer Composite Piles

The newest type of composite piles are polymer composite piles. These piles are generally tubular sections made from fiber reinforced polymers. Depending upon the manufacturer and intended application, the piles may be driven open ended and left unfilled, driven closed ended and filled with concrete after driving or driven as a composite fiber reinforced polymer tube with a precast concrete core. A steel core has also been used in some composite sections.

Polymer composite piles are resistant to attack from marine borers and are not subject to corrosion. In addition, many of the polymer composite piles have good energy absorption characteristics making them attractive as fender piling. The Federal Highway Administration and the U.S. Army Corps of Engineers Construction Engineering Research Laboratory have on-going research programs that are expected to result in material standards, specifications, and design guidance for these piling systems.

8.8 DESIGN CONSIDERATIONS IN AGGRESSIVE SUBSURFACE ENVIRONMENTS

In every design, consideration should be given to the possible deterioration of the pile over its design life due to the surrounding environment. This section will address design considerations in aggressive subsurface environments where corrosion, chemical attack, abrasion, and other factors can adversely effect pile durability after installation. An assessment of the in-situ soil conditions, fill materials, and groundwater properties is necessary to completely categorize an aggressive subsurface condition.

An aggressive environment can generally be identified by soil resistivity and pH tests. If either the pH or soil resistivity tests indicate the subsurface conditions are aggressive, then the pile selection and foundation design should be based on an aggressive subsurface environment. The design of pile foundations in an aggressive environment is a developing field. Therefore, a corrosion/degradation specialist should be retained for major projects with pile foundations in aggressive environments.

Whenever the pH value is 4.5 or less, the foundation design should be based on an aggressive subsurface environment. Alternatively, if the resistivity is less than 2000 ohms-cm the site should also be treated as aggressive. When the soil resistivity test results are between 2000 and 5000 ohms-cm then chloride ion content and sulfate ion content tests should be performed. If these test results indicate a chloride ion content greater than 100 parts per million (ppm) or a sulfate ion content greater than 200 ppm, then the foundation design should be based on an aggressive subsurface environment. Resistivity values greater than 5000 ohms-cm are considered non-aggressive environments. Electro chemical classification tests for aggressive environments are described in Chapter 6.

Contaminated soil and groundwater can cause significant damage to foundation piles in direct contact with the aggressive chemicals. Acidic groundwater is common at sites with either organic soils or industrial contamination. The subsurface exploration program should indicate if the soil or groundwater is contaminated. If industrial contamination is found, the maximum likely concentrations should be determined as well as an estimate of the lateral and vertical extent of the contamination.

8.8.1 Corrosion of Steel Piles

Steel piles driven through contaminated soil and groundwater conditions may be subject to high corrosion rates and should be designed appropriately. Corrosion of steel or steel reinforced piles may also occur if piles are driven into disturbed ground or fill, if piles are located in a marine environment, or if piles are subject to alternate wetting and drying from tidal action. Corrosion rates are a function of the ambient temperature, pH, access to oxygen, and chemistry of the aqueous environment surrounding the steel member.

For steel piles buried in fill or disturbed natural soils, a conservative estimate of the corrosion rate is 0.08 mm per year. Morley (1979) reported corrosion rates of 0.05 mm

per year for steel piles immersed in fresh water, except at the waterline in canals where the rate was as high as 0.34 mm per year. The high rate at the water line was attributed to debris abrasion and/or cell action between other parts of the structure.

For steel piles in marine environments (salt water), separate zones, each with a different corrosion rate, are present along the length of the pile. Tomlinson (1994) identifies these zones as follows:

1. Atmospheric zone: exposed to the damp atmospheric conditions above the highest water level but subject to airborne spray.
2. Splash zone: above the mean high tide, but exposed to waves, spray, and wash from passing ships.
3. Intertidal zone: between mean high and low tides.
4. Continuous immersion zone: below lowest low tide.
5. Underground zone: below the mudline.

Figure 8.5, after Morley and Bruce (1983), summarizes average and maximum probable marine corrosion rates in these zones as well as in the low water zone.

In corrosive environments, the designer should apply one of the design options for piles in corrosive environments discussed in Section 8.8.4. NCHRP Report 408, by Beavers and Durr (1998) provides a synthesis on the current state of practice in evaluating the predicted corrosion of steel piles in nonmarine applications. In addition, AASHTO provisional standard PP36-97 contains a recommended practice. A followup NCHRP research study on the corrosion of piles is in progress.

8.8.2 Sulfate and Chloride Attack on Concrete Piles

Attack on precast and cast in place concrete occurs in soils with high sulfate or chloride concentrations. Factors influencing the rate of attack of sulfates or chlorides on concrete piles include the pH of the soil, the solubility of the sulfate or chloride, the movement of the groundwater relative to the piles, and the density of the pile concrete.

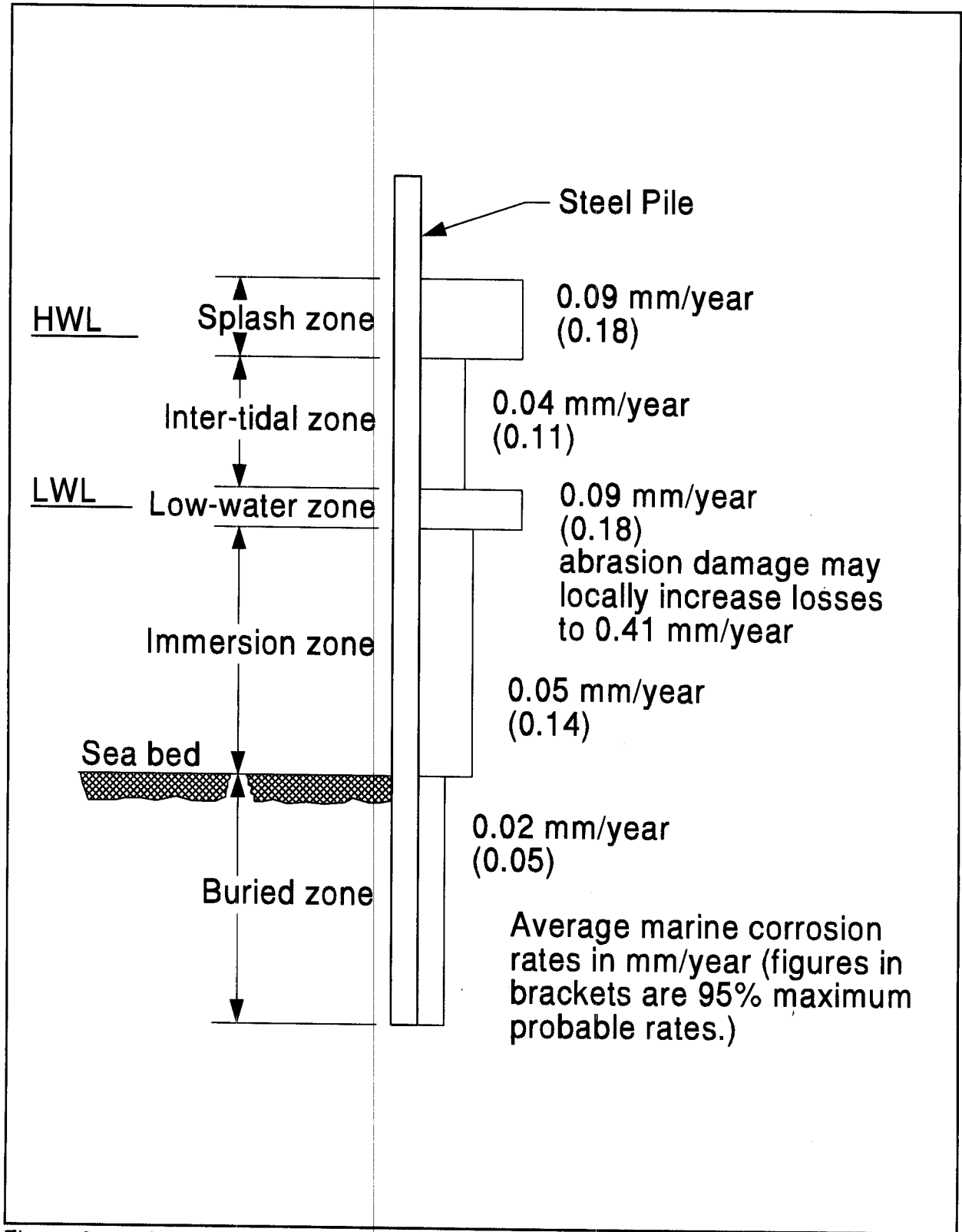


Figure 8.5 Loss of Thickness by Corrosion for Steel Piles in Seawater (after Morley and Bruce, 1983)

The reaction between concrete and sulfate begins with sulfate ions in solution. Once the sulfate ions in the groundwater come in contact with portland cement, an expansive chemical reaction takes place. Expansion of concrete often leads to cracking and spalling which can significantly reduce the available structural capacity of a pile foundation.

One method of reducing sulfate attack is to use a dense concrete which is less permeable to sulfate ions. Other possible deterrents include using sulfate-resisting cement, using cement with 25% pozzolanic material, or creating a physical barrier between the concrete and the groundwater with some sort of pile sleeve.

Chlorides are commonly found in soils, groundwater, or industrial wastes. Instead of attacking concrete, chlorides cause corrosion of reinforcement steel with consequential expansion and bursting of concrete as the products of steel corrosion are formed. Once corrosion begins, it continues at an accelerated rate. This can lead to a loss of bond between steel and concrete and extreme reduction of pile capacity. Protective measures which can reduce corrosion include increased concrete cover around the reinforcing steel, and the use of galvanized, or epoxy coated reinforcement.

8.8.3 Insects and Marine Borers Attack on Timber Piles

Timber piles are subject to insect attack on land by termites and beetles, or in water by marine borers. Incidences of marine borer attack on timber piles have reemerged in some areas as previously polluted water has improved. As mentioned in Section 8.2, arsenate and creosote pressure treatments are the most effective means of protecting timber piles from premature deterioration. In southern waters, creosote must be combined with other preservative treatments because of attack by *limnoria tripundata*. AWPA C3, Piles, Preservative Treatment by Pressure Process, contains penetration and retention values for the various preservatives. Environmental damage from pressure treatments must be a consideration when selecting protection methods.

When designing with timber piles, the wood species is usually not specified unless a specific species of wood is more suitable for design loads and/or environmental conditions. Certain species are not suitable for preservative treatment, while others may provide increased durability. As expected, ASTM standards for timber piles vary with geologic region, as land and fresh water piles have less stringent preservative treatment requirements than piles used in marine environments. Pile specifications are based on

the type of conditioning, heating temperature, duration of heating, and retention of preservative. For example, Southern Pine piles on land or in freshwater are required to have a creosote retention of 1.9 kg/m³ as compared to the retention requirement of 3.1 kg/m³ for use in marine environments.

If timber piles are installed in other aggressive environments such as environments containing chemical wastes, a timber pile specialist should be consulted in determining the appropriate preservative treatment.

8.8.4 Design Options for Piles Subject to Degradation or Abrasion

When a pile must be installed in an aggressive or abrasive environment, several design options can be considered. These design options include:

- a. Use of high-yield steel in a structure designed using mild steel stress limits permits greater loss of metal before stresses become critical.
- b. A heavier steel section than required can be used to provide extra thickness (H and pipe sections). This method is not effective in running water with active bedload to scour the corroded surface.
- c. Cathodic protection of steel piles in soil below the water table or in marine environments. Note that this method of protection tends to be a costly solution and requires periodic anode replacement.
- d. Concrete encasement of steel piles above the mud line. This method may alter the impact absorbing properties of the pile.
- e. Use of copper-bearing steel is effective against atmospheric corrosion but cost is greater than conventional steel.
- f. Sleeving or encapsulating of reinforced, cast in place piles through use of metal casings or polymer or fiberglass jackets isolates contaminants from concrete.
- g. Use of a low water/cement ratio, resistant aggregate, and minimum air content consistent with the environment to improve abrasion resistance of precast concrete piles

- h. Use of a protective metallic or epoxy paint (isocyanate-cured) or fusion bonded epoxy coating on exposed sections of the pile. This method has the same limitations as (b) in running water.
- i. Use of coal-tar epoxies for corrosion protection in marine environments.

Protective coatings cannot be replaced after a pile is driven. Therefore, if a protective coating is used, the coating should be designed to be durable enough to remain undamaged during pile transportation, handling, and placement in the leads for driving as well as resistant to the abrasion resulting from pile driving. The designer should also note that the shaft resistance on a coated pile may be significantly different than on an uncoated pile, depending on the coating.

8.9 SELECTION OF PILE TYPE

The selection of appropriate pile types for any project involves the consideration of several design and installation factors including pile characteristics, subsurface conditions and performance criteria. Pile selection should be based on the factors listed in Tables 8-1, 8-2, and 8-3. Table 8-1 summarizes typical pile characteristics and uses. Table 8-2 provides pile type recommendations for various subsurface conditions. Table 8-3 presents the placement effects of pile shape characteristics.

In addition to the considerations provided in the tables, the problems posed by the specific project location and topography must be considered in any pile selection process. Following are some of the usually encountered problems:

1. Driven piles may cause vibration damage.
2. Remote areas may restrict driving equipment size and, therefore, pile size.
3. Local availability of certain materials and capability of contractors may have decisive effects on pile selection.
4. Waterborne operations may dictate use of shorter pile sections due to pile handling limitations.

5. Steep terrain may make the use of certain pile equipment costly or impossible.

Although one pile type may emerge as the only logical choice for a given set of conditions, more often several different types may meet all the requirements for a particular structure. In such cases, the final choice should be made on the basis of a cost analysis that assesses the over-all cost of alternatives. This would include uncertainties in execution, time delays, cost of load testing programs, as well as differences in the cost of pile caps and other elements of the structure that may differ among alternatives. For major projects, alternate foundation designs should be considered for inclusion in the contract documents if there is a potential for cost savings.

TABLE 8-2* PILE TYPE SELECTION BASED ON SUBSURFACE AND HYDRAULIC CONDITIONS	
TYPICAL PROBLEM	RECOMMENDATIONS
Boulders overlying bearing stratum	Use heavy nondisplacement pile with a point and include contingent predrilling item in contract.
Loose cohesionless soil	Use tapered pile to develop maximum skin friction.
Negative shaft resistance	Use smooth steel pile to minimize drag adhesion; avoid battered piles. Use bitumen coating or plastic wrap (if feasible) or increase design stress.
Deep soft clay	Use rough concrete piles to increase adhesion and rate of pore water dissipation.
Artesian pressure	Caution required for using mandrel driven thin-wall shells, as generated hydrostatic pressure may cause shell collapse; pile heave common to closed-end pile.
Scour	Do not use tapered piles unless a large part of the taper extends well below scour depth; design permanent pile capacity to mobilize soil resistance below scour depth.
Coarse gravel deposits	Use prestressed concrete piles where hard driving is expected. In coarse soils use of H-piles and open end pipe piles often results in excessive pile lengths.

* Table modified and reproduced (Cheney and Chassie, 1993).

TABLE 8-3* PILE TYPE SELECTION PILE SHAPE EFFECTS

SHAPE CHARACTERISTICS	PILE TYPE	PLACEMENT EFFECT
Displacement	Closed end steel pipe	Increase lateral ground stress.
	Precast concrete	Densifies cohesionless soils, remolds and weakens cohesive soils temporarily. Setup time for large pile groups in sensitive clays may be up to six months.
Nondisplacement	Steel H	Minimal disturbance to soil.
	Open end steel pipe	Not suited for friction piles in coarse granular soils. Piles often have low driving resistances in these deposits making field capacity verification difficult thereby often resulting in excessive pile lengths.
Tapered	Timber Monotubes Thin-wall shells	Increased densification of soil, high capacity for short length in granular soils.

* Table modified and reproduced (Cheney and Chassie, 1993).

REFERENCES

- American Concrete Institute (1974). Recommendations for Design, Manufacture and Installation of Concrete Piles. ACI-543.
- Beavers, J.A. and Durr, C.L. (1998). Corrosion of Steel Piling in Non-Marine Applications. NCHRP Report 408, National Cooperative Highway Research Program, Transportation Research Board, Washington, D.C.
- Chellis, R.D. (1961). Pile Foundations. McGraw-Hill Book Company.
- Cheney, R.S. and Chassie, R.G. (1993). Soils and Foundations Workshop Manual. Second Edition, Publication No. FHWA HI-88-009, Federal Highway Administration, National Highway Institute, Washington, D.C.
- Department of the Navy, Naval Facilities Engineering Command, NAVFAC (1982). Foundations and Earth Structures, Design Manual DM 7.2.
- Fleming, W.G.K., Weltman, A.J., Randolph, M.F. Elson, W.K. (1992). Piling Engineering, John Wiley and Sons, Inc., New York.
- Fuller, F.M. (1983). Engineering of Pile Installations. McGraw-Hill, New York. 286.
- Graham, J. (1995). Personal Communication.
- Portland Cement Association [PCA], (1951). Concrete Piles: Design, Manufacture and Driving.
- PCI (1993), Precast/Prestressed Concrete Institute Journal, Volume 38, No. 2, March-April, 1993.
- Prakash, S. and Sharma, H. (1990). Pile Foundations in Engineering Practice. John Wiley and Sons, Inc., New York.
- Morley, J., (1979). The Corrosion and Protection of Steel Piling, British Steel Corporation, Teesside Laboratories.

Morley, J. and Bruce, D.W., (1983). Survey of Steel Piling Performance in Marine Environments, Final Report, Commission of the European Communities, Document EUR 8492 EN.

Rausche, F. (1994). Design, Installation and Testing of Nearshore Piles. Proceedings of the 8th Annual Symposium on Deep Foundations, Vancouver.

Tomlinson, M.J., (1994). Pile Design and Construction Practice, Fourth Edition, E & FN Spon, London 357-372.

Transportation Research Board, (1977). Design of Pile Foundations NCHRP Synthesis of Highway Practice No. 42.

9. STATIC ANALYSIS METHODS

Static analysis methods can be categorized as analytical methods that use soil strength and compressibility properties to determine pile capacity and performance. This chapter will focus on analysis methods for determining compression, uplift, and lateral load capacity of single piles and pile groups. Important design considerations are as follows:

1. Static analysis methods are an integral part of the design process. Static analysis methods are necessary to determine the most cost effective pile type and to estimate the number of piles and the required pile lengths for the design of substructure elements. The foundation designer must have a knowledge of the design loads and the structure performance criteria in order to perform the appropriate static analyses.
2. Many static analysis methods are available. The methods presented in this chapter are relatively simple methods that have proven to provide reasonable agreement with full scale field results. Other more sophisticated analysis methods may be used and in some cases may provide better results.
3. Designers should fully understand the basis for, the limitations of, and the applicability of a chosen method. A selected method should also have a proven agreement with full scale field results.

Construction procedures can have a significant influence on the behavior of pile foundations. The methods described in this chapter lead to successful designs of deep foundations only if adequate construction techniques are used. Construction inspection should be an integral part of the design and construction of any foundation. Static load tests, wave equation analysis or dynamic monitoring for construction control should, whenever possible, be used to confirm the results of a static design method. These items are discussed in greater detail in subsequent chapters.

The first few sections of this chapter will briefly cover background information. Static analysis procedures for piles subject to compression, uplift and lateral loads will be covered, as well as pile group settlement. The influence of special design events on static design will be discussed. Limited guidance on design in liquefaction susceptible soils will be provided. However, seismic design is a special design event beyond the scope of this manual. Last, the chapter will address construction issues pertinent to static design.

9.1 BASICS OF STATIC ANALYSIS

The static capacity of a pile can be defined as the sum of soil/rock resistances along the pile shaft and at the pile toe available to support the imposed loads on the pile. A static analysis is performed to determine the ultimate capacity of an individual pile and of a pile group as well as the deformation response of a pile group to the applied loads. The ultimate capacity of an individual pile and of a pile group is the smaller of: (1) the capacity of surrounding soil/rock medium to support the loads transferred from the pile(s) or, (2) the structural capacity of the pile(s). Static analysis calculations of the deformation response to lateral loads and of pile group settlement are compared to the performance criteria established for the structure. Details of static analysis procedures are presented later in this chapter. Chapter 11 provides a discussion of the allowable stresses in pile materials used for determining structural capacity of piles.

The static pile capacity from the sum of the soil/rock resistances along the pile shaft and at the pile toe can be estimated from geotechnical engineering analysis using:

1. Laboratory determined shear strength parameters of the soil and rock surrounding the pile.
2. Standard Penetration Test data.
3. In-situ test data (*i.e.*, CPT/CPTU).

On many projects, two static analyses are required for a design. First, a static analysis is necessary to determine the number and length of piles necessary to support the structure loads. A second static analysis may be required to determine the total driving resistance the pile will encounter during installation. This second analysis enables the design engineer to determine the necessary capability of the driving equipment. Figures 9.1 and 9.2 illustrate two situations that require two static analyses.

Figure 9.1 shows a situation where piles are to be driven for a bridge pier. In this case, the first static analysis performed should neglect the soil resistance in the soil zone subject to scour, since this resistance may not be available for long term support. The number of piles and pile lengths determined from this analysis will then be representative of the long term conditions in the event of scour. At the time of pile driving however, the scour zone will provide resistance to pile penetration. Therefore, a second static analysis is required

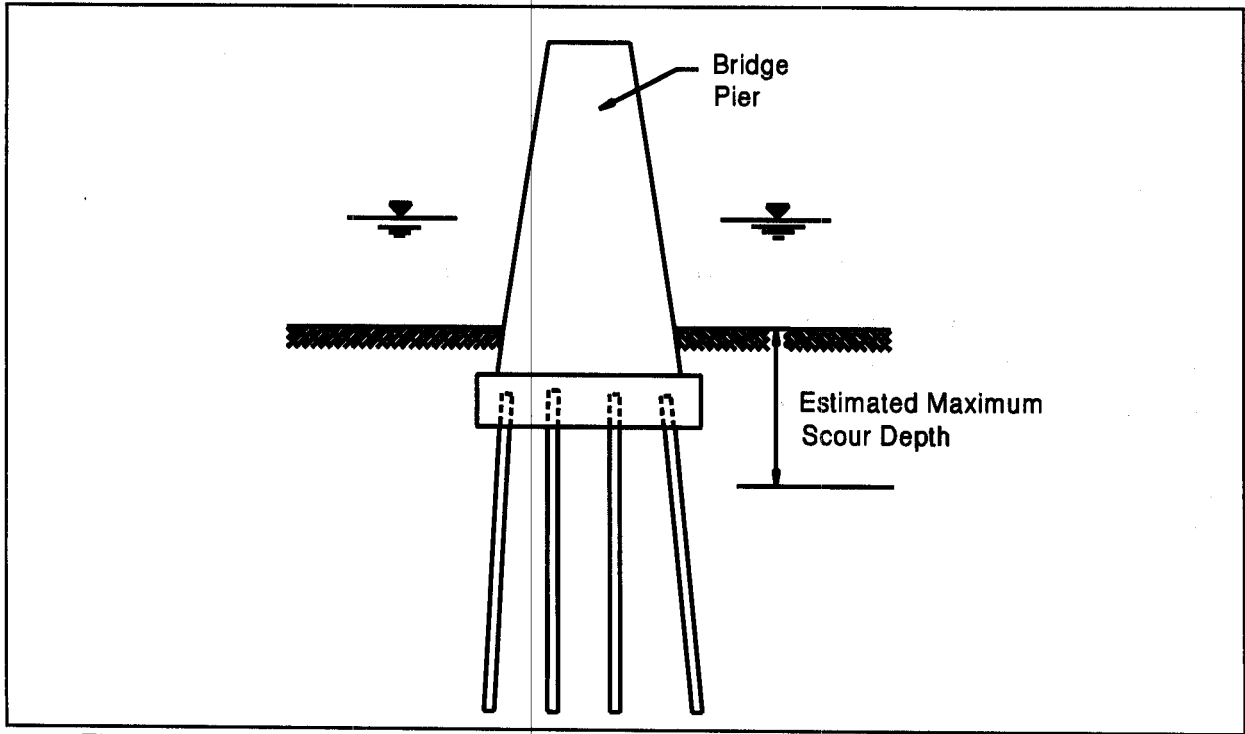


Figure 9.1 Situation Where Two Static Analyses are Necessary - Due to Scour

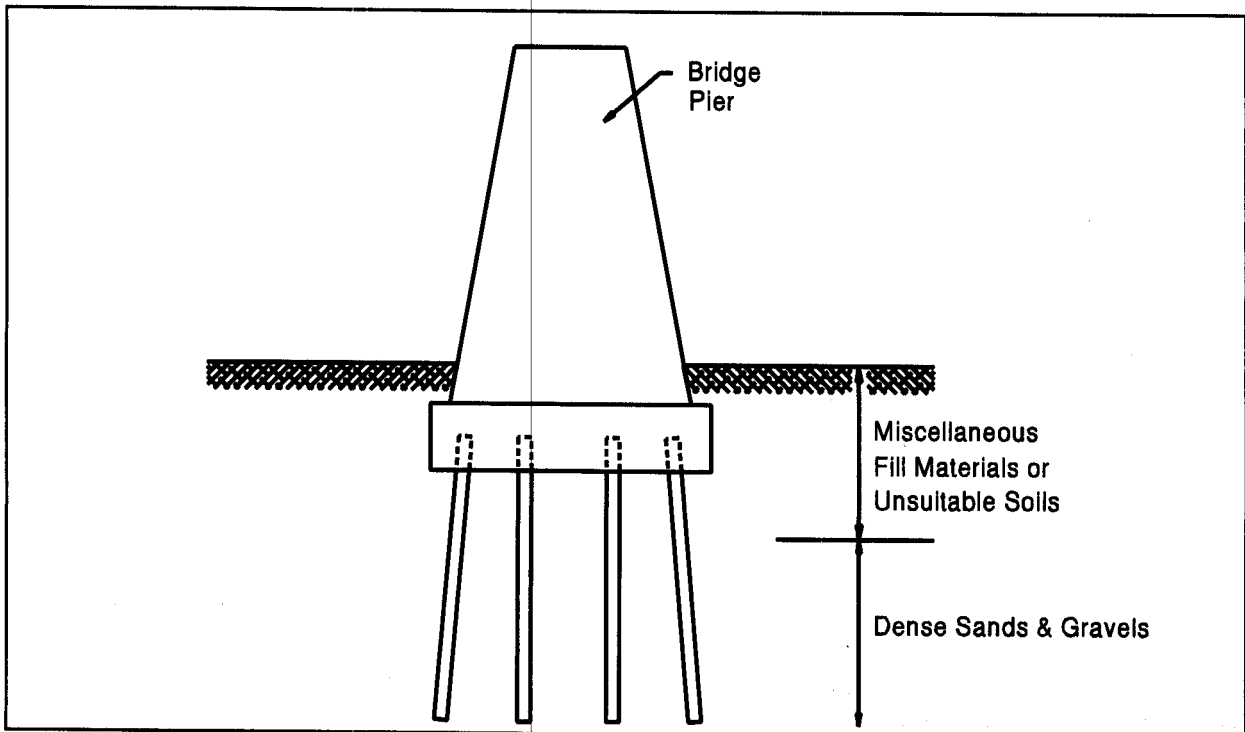


Figure 9.2 Situation Where Two Static Analyses are Necessary - Due to Fill Materials

to estimate the total resistance encountered by the pile during driving to the embedment depth determined in the first analysis. The second static analysis includes the soil resistance in the materials above the scour depth as well as the underlying strata.

Figure 9.2 shows another frequently encountered situation in which piles are driven through loose uncompacted fill material into the natural ground. The loose fill material offers unreliable resistance and is usually neglected in determining the number of piles and the pile lengths required. A second static analysis is then performed to determine total resistance encountered by the pile during driving, which includes the resistance in the fill material. In both examples, the soil resistance to be overcome during driving will be substantially greater than the required ultimate pile capacity.

The results of multiple static analyses should be considered in the development of project plans and specifications. For example, consider a case where scour, uplift loading, or some other special design event dictates that a greater pile penetration depth be achieved than that required for support of the axial compressive loads. The static analyses indicate that 2000 kN of soil resistance must be overcome to obtain the minimum penetration depth for a 1400 kN ultimate capacity pile. This information should be conveyed in the construction documents so that the driving equipment can be properly sized and so that the intent of the design is clearly and correctly interpreted by the contractor and construction personnel. Specifying only a 1400 kN ultimate capacity pile, without including a minimum penetration requirement and the soil resistance to be overcome, can lead to construction claims.

Prior to discussing static design methods for estimating pile capacity in detail, it is desirable to review events that occur in the pile-soil system during and after pile driving as well as basic load-transfer mechanisms.

9.2 EVENTS DURING AND AFTER PILE DRIVING

The soil in which a pile foundation is installed is almost always disturbed. Several factors influence the degree of disturbance. These include the soil type and density, the pile type (displacement, non-displacement), and the method of pile installation (driven, drilled, jetted). **For driven piles, substantial soil disturbance and remolding is unavoidable.**

9.2.1 Cohesionless Soils

The capacity of piles driven into cohesionless soil depends primarily on the relative density of the soil. During driving, the relative density of loose to medium dense cohesionless soil is increased close to the pile due to vibrations and lateral displacement of soil. This effect is most pronounced in the immediate vicinity of displacement piles. Broms (1966) and more recent studies found the zone of densification extends as far as 3 to 5 diameters away from the pile shaft and 3 to 5 diameters below the pile toe as depicted in Figure 9.3.

The increase in relative density increases the capacity of single piles and pile groups. The pile type selection also affects the amount of change in relative density. Piles with large displacement characteristics such as closed-end pipe and precast concrete increase the relative density of cohesionless material more than low displacement open-end pipe or steel H-piles.

The increase in horizontal ground stress, which occurs adjacent to the pile during the driving process, can be lost by relaxation in dense sand and gravels. The relaxation phenomena occurs as the negative pore pressures generated during driving are dissipated. The negative pore pressures occur because of volume change and dilation of dense sand. The phenomena can be explained by considering the following effective stress shear strength equation.

$$\tau = c + (\sigma - u) \tan \phi$$

Where: τ = Shear strength of soil.
 c = Cohesion.
 σ = Vertical (normal) pressure.
 u = Pore water pressure.
 ϕ = Angle of internal friction.

Negative pore pressures temporarily increase the soil shear strength, and therefore pile capacity, by changing the $(\sigma - u) \tan \phi$ component of shear strength to $(\sigma + u) \tan \phi$. As negative pore pressures dissipate, the shear strength and pile capacity decrease.

The pile driving process can also generate high positive pore water pressures in saturated cohesionless silts and loose to medium dense fine sands. Positive pore pressures temporarily reduce the soil shear strength and the pile capacity. This phenomena is

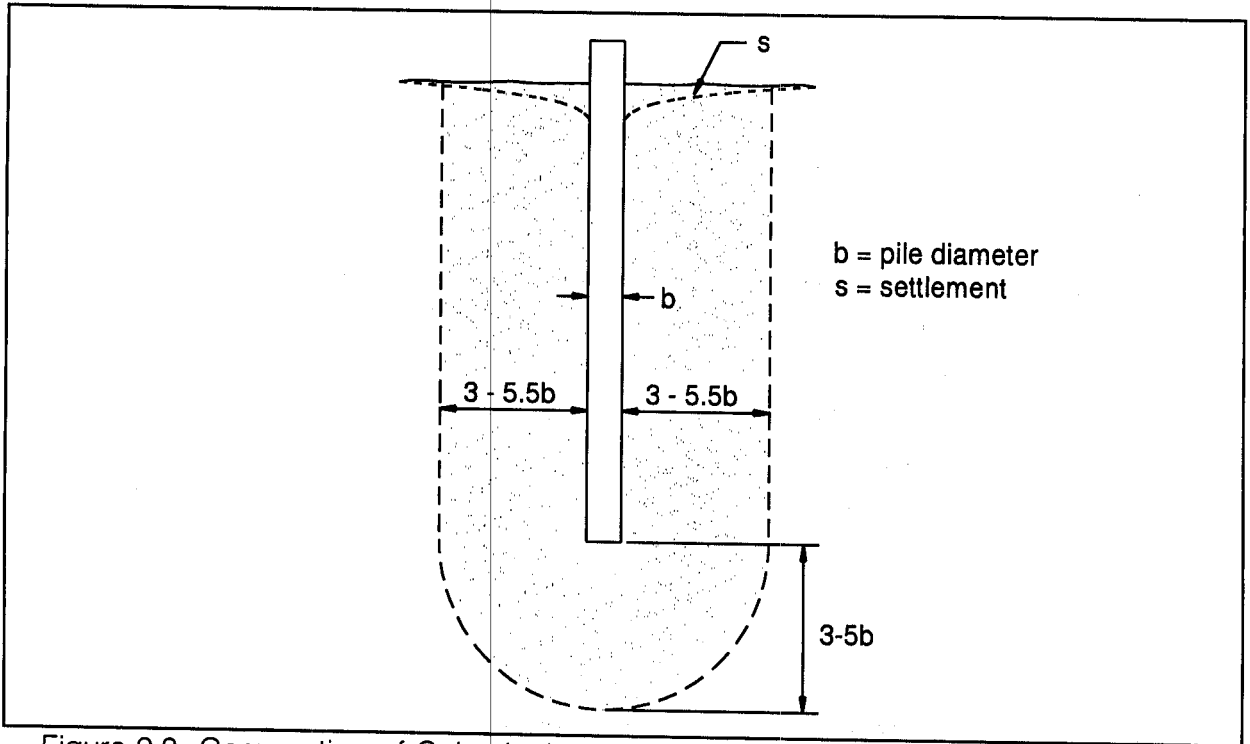


Figure 9.3 Compaction of Cohesionless Soils During Driving of Piles (Broms, 1966)

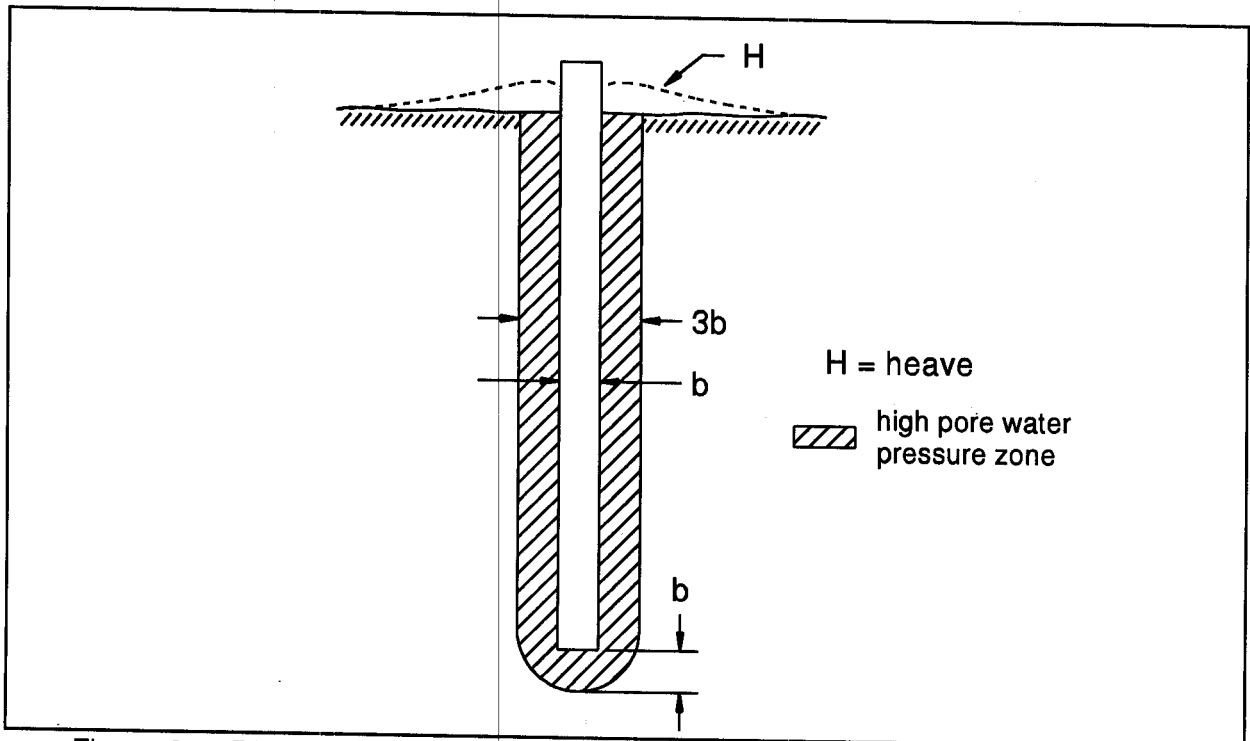


Figure 9.4 Disturbance of Cohesive Soils During Driving of Piles (Broms, 1966)

identical to the one described below for cohesive soils. The gain in capacity with time or soil set-up is generally quicker for sands and silts than for clays because the pore pressures dissipate more rapidly in cohesionless soils than in cohesive soils.

9.2.2 Cohesive Soils

When piles are driven into saturated cohesive materials, the soil near the piles is disturbed and radially compressed. For soft or normally consolidated clays, the zone of disturbance is generally within one pile diameter around the pile. For piles driven into saturated stiff clays, there are also significant changes in secondary soil structure (closing of fissures) with remolding and loss of previous stress history effects in the immediate vicinity of pile. Figure 9.4 illustrates the disturbance zone for piles driven in cohesive soils as observed by Broms (1966). This figure also notes the ground heave that can accompany driving displacement piles in cohesive soils.

The disturbance and radial compression generate high pore pressures (positive pore pressures) which temporarily reduce soil shear strength, and therefore the load capacity of the pile. As reconsolidation of clay around the pile occurs, the high pore pressures are diminished, which leads to an increase in shear strength and pile capacity (setup). This phenomena is opposite to "relaxation" described for cohesionless soils. The zone and magnitude of soil disturbance are dependent on the soil properties of soil sensitivity, driving method, and the pile foundation geometry. Limited data available for partially saturated cohesive soils indicates that pile driving does not generate high pore pressures and hence significant soil setup does not occur.

9.3 LOAD TRANSFER

The ultimate bearing capacity, Q_u , of a pile in homogeneous soil may be expressed by the sum of the shaft resistance R_s and toe resistance R_t , or

$$Q_u = R_s + R_t$$

This may also be expressed in the form

$$Q_u = f_s A_s + q_t A_t$$

where f_s is the unit shaft resistance over the shaft surface area, A_s , and q_t is the unit toe resistance over the pile toe area, A_t . The above equations for pile bearing capacity assume that both the pile toe and the pile shaft have moved sufficiently with respect to the adjacent soil to simultaneously develop the ultimate shaft and toe resistances. Generally, the displacement needed to mobilize the shaft resistance is smaller than that required to mobilize the toe resistance. This simple rational approach has been commonly used for all piles except very large diameter piles.

Figure 9.5 illustrates typical load transfer profiles for a single pile. The load transfer distribution can be obtained from a static load test where strain gages or telltale rods are attached to a pile at different depths along the pile shaft. Figure 9.5 shows the measured axial load, Q_u , in the pile plotted against depth. The shaft resistance transferred to the soil is represented by R_s , and R_t represents the resistance at the pile toe. In Figure 9.5(a), the load transfer distribution for a pile with no shaft resistance is illustrated. In this case the full axial load at the pile head is transferred to the pile toe. In Figure 9.5(b), the axial load versus depth for a uniform shaft resistance distribution typical of a cohesive soil is illustrated. Figure 9.5(c) presents the axial load in the pile versus depth for a triangular shaft resistance distribution typical of cohesionless soils.

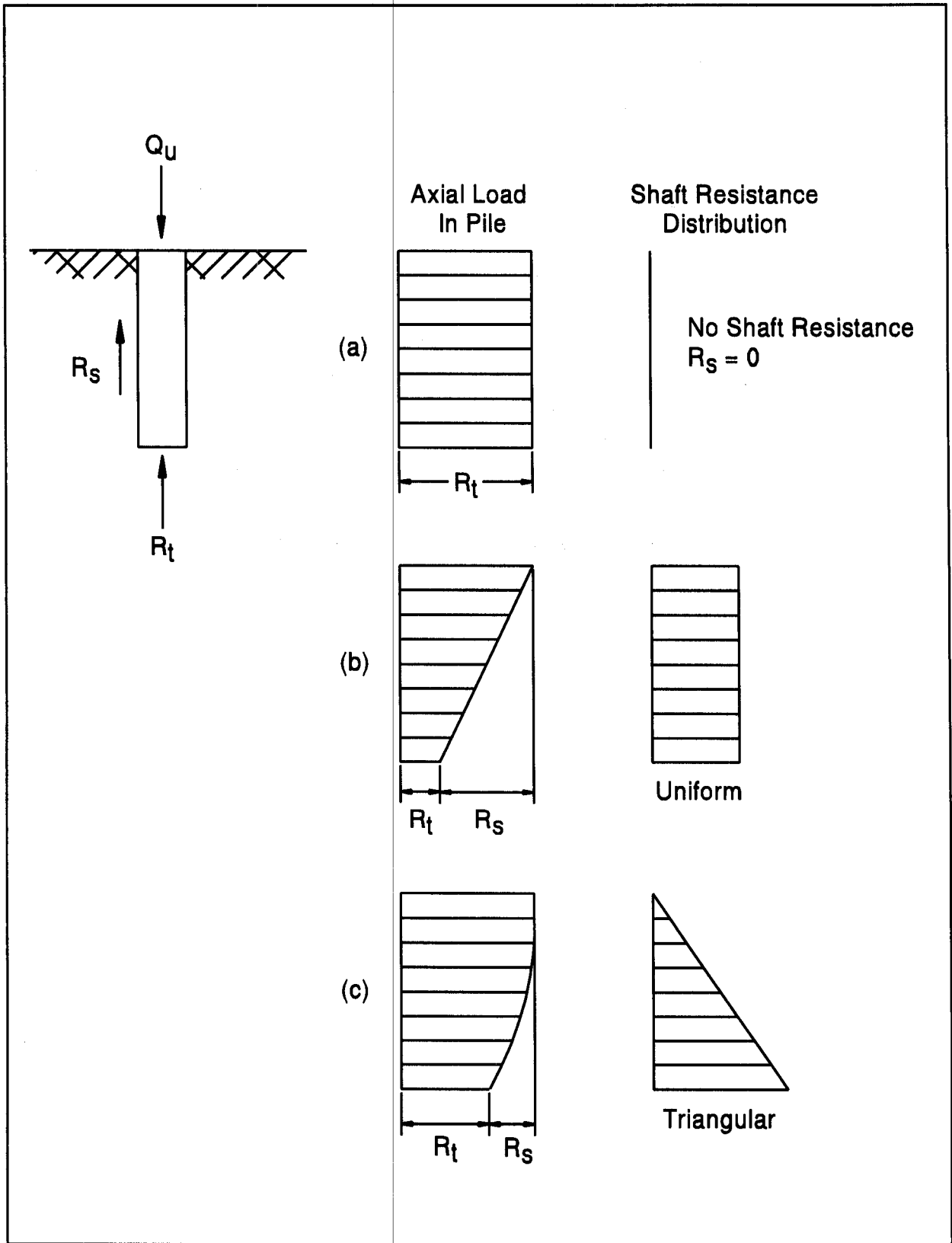


Figure 9.5 Typical Load Transfer Profiles

9.4 EFFECTIVE OVERBURDEN PRESSURE

The effective overburden pressure at a given depth below ground surface is the vertical stress at that depth due to the weight of the overlying soils. A plot of effective overburden pressure versus depth is called a " p_o Diagram" and is used in many static pile capacity and settlement calculations. Therefore, an understanding of how to construct and use a p_o Diagram is important.

Information needed to construct a p_o Diagram includes the total unit weight and thickness of each soil layer as well as the depth of the water table. The soil layer thickness and depth of the water table should be available from the project boring logs. The total unit weight of each soil layer may be obtained from density tests on undisturbed cohesive samples or estimated from Standard Penetration Test (SPT) N values in conjunction with the soil visual classification.

The first step in constructing a p_o Diagram is to calculate the total overburden pressure, p_t , versus depth. This is done by summing the product of the total unit weight times the layer thickness versus depth. Similarly, the pore water pressure, u , is summed versus depth by multiplying the unit weight of water, γ_w , of 9.8 kN/m^3 , times the water height. The effective overburden pressure, p_o , at any depth is then the total overburden pressure minus the pore water pressure at that depth.

The effective overburden pressure at any depth is determined by summing the weights of all layers above that depth as follows:

1. For soil deposits above the static water table:

$$p_o = (\text{total soil unit weight, } \gamma)(\text{thickness of soil layer above the desired depth}).$$

2. For soil deposits below the static water table:

$$p_o = (\text{total soil unit weight, } \gamma)(\text{depth}) - (\text{unit weight of water, } \gamma_w)(\text{height of water}).$$

This may also be expressed as the buoyant or effective unit weight, γ' , ($\gamma' = \gamma - \gamma_w$):

$$p_o = (\text{buoyant unit weight, } \gamma')(\text{depth}).$$

Figures 9.6 and 9.7 present examples of p_o diagrams for cases where the water table is above and below the ground surface level.

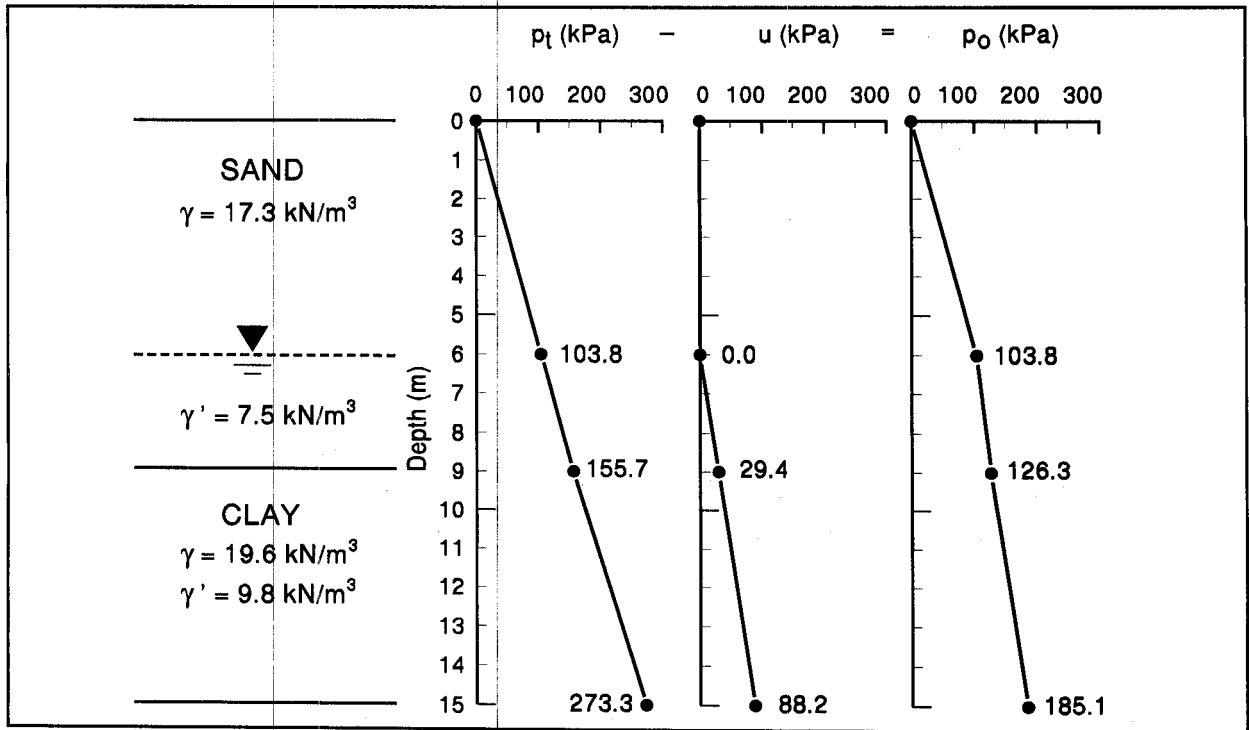


Figure 9.6 Effective Overburden Pressure Diagram - Water Table Below Ground Surface

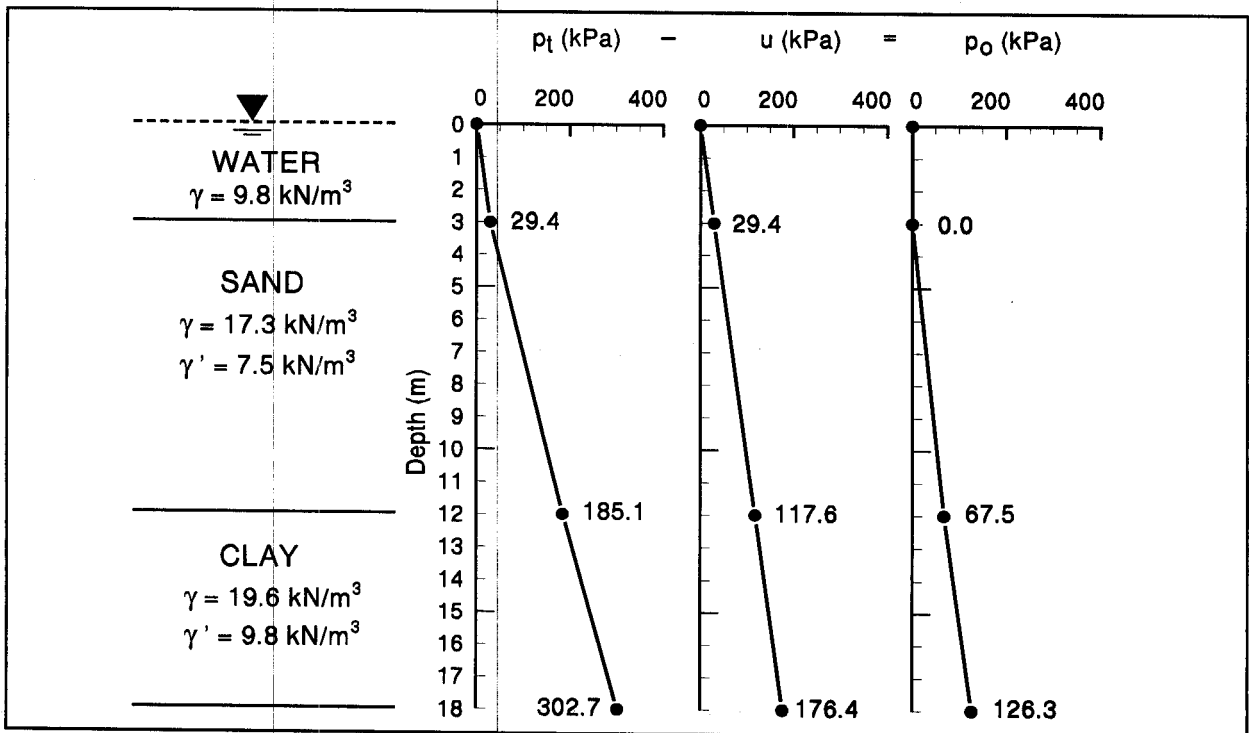


Figure 9.7 Effective Overburden Pressure Diagram - Water Table Above Ground Surface

9.5 CONSIDERATIONS IN SELECTION OF DESIGN SOIL STRENGTH PARAMETERS

Most of the static analysis methods in cohesionless soils directly or indirectly utilize the soil friction angle, ϕ , in calculation of pile capacity. The soil friction angle may be determined from laboratory tests as described in Chapter 6, or may be estimated using corrected Standard Penetration Test (SPT) N values and the empirical values in Table 4-5. The designer should be aware of the many factors that can influence SPT N values discussed in Section 4.4.1 of Chapter 4 when selecting a design friction angle based on SPT values.

In coarse granular deposits, the selection of the design friction angle should be done conservatively. A comparison of ultimate pile capacities from static load test results with static analysis predictions indicates that static analyses often overpredict the shaft resistance in these deposits. This is particularly true for coarse granular deposits comprised of uniform sized or rounded particles. Cheney and Chassie (1993) recommend limiting the shearing resistance by neglecting particle interlock forces. For shaft resistance calculations in gravel deposits, this results in a maximum ϕ angle of 32° for gravels comprised of soft rounded particles, and in a maximum ϕ angle of 36° for hard angular gravel deposits. The ϕ angle used to calculate the toe resistance is determined using normal procedures.

Static analysis methods used for design of pile foundations in cohesive soils require accurate assessment of the soil shear strength and consolidation properties. This information should be obtained from laboratory tests on undisturbed samples as described in Chapter 6 and/or from in-situ testing as described in Chapter 5. Designs based solely on strength and compressibility information estimated from SPT N values from disturbed soil samples should be avoided.

The capacity of a pile when driven in many soil formations is not the same as the long term pile capacity. This is due to the soil disturbance created during installation as described in Section 9.2 of this chapter. For design in cohesive soils, the sensitivity of the cohesive soils should be determined as discussed in Section 6.2 of Chapter 6. Knowledge of the soil sensitivity allows a more accurate static analysis of the driving resistance in cohesive soils. Increases and decreases on pile capacity with time are known as soil setup and relaxation, respectively. These time effects are discussed in greater detail in Section 9.10.1.

For a cost effective foundation design with any static analysis method, it is of paramount importance that the foundation designer logically select the soil strength parameters and include consideration of time dependent soil strength changes.

9.6 FACTORS OF SAFETY

Static analysis results yield an ultimate pile capacity or soil resistance. The allowable pile soil resistance (design load) is selected by dividing the ultimate pile capacity in suitable soil support layers by a factor of safety. In static analysis methods, the design load for a given pile length has typically been calculated by dividing the ultimate capacity in suitable soil support layers by a factor of safety ranging from 2 to 4. The range in the factor of safety has primarily depended upon the reliability of the particular static analysis method with consideration of the following items.

1. The level of confidence in the input parameters. (This is a function of the type and extent of the subsurface exploration and laboratory testing of soil and rock materials.)
2. Variability of the soil and rock.
3. Method of static analysis.
4. Effects of and consistency of the proposed pile installation method.
5. Level of construction monitoring (static load test, dynamic analysis, wave equation analysis, Gates dynamic formula).

A large number of static analysis methods are documented in the literature with specific recommendations on the factor of safety to be used with each method. These recommended factors of safety have routinely disregarded the influence of the construction control method used to complement the static analysis computation. As part of the overall design process, it is important that the foundation designer qualitatively assess the validity of the chosen design analysis method and the reliability of the geotechnical design parameters. These issues have been quantified using Load Resistance Factor Design methods in NCHRP Report 343 by Barker *et al.* (1991). However, their effects are only qualitatively addressed in this manual.

While the range in static analysis factors of safety was from 2 to 4, most of the static analysis methods recommended a factor of safety of 3. As foundation design loads have increased over time, the use of high factors of safety has often resulted in pile installation problems. In addition, experience has shown that construction control methods have a significant influence on pile capacity. Therefore, the factor of safety used in a static analysis

calculation should be based upon the construction control method specified. Provided that the procedures recommended in this manual are used for the subsurface exploration and analysis, the following factors of safety are recommended, based on the specified construction control method. These factors of safety are discussed in greater detail in Chapter 12.

<u>Construction Control Method</u>	<u>Factor of Safety</u>
Static load test with wave equation analysis	2.00
Dynamic testing with wave equation analysis	2.25
Indicator piles with wave equation analysis	2.50
Wave equation analysis	2.75
Gates dynamic formula	3.50

The pile design load should be supported by soil resistance developed only in soil layers that contribute to long term load support. The soil resistance from soils subject to scour, or from soil layers above soft compressible soils should not be considered. An example problem will be used to clarify the use of the factor of safety in static pile capacity calculations for determination of the pile design load as well as for determination of the soil resistance to pile driving.

Consider a pile to be driven through the soil profile described in Figure 9.8. The proposed pile type penetrates through a sand layer subject to scour in the 100 year flood overlying a very soft clay layer unsuitable for long term support and into competent support materials. Hence the soil resistances from the scour susceptible and soft clay layers do not contribute to long term load support and should not be included in the soil resistance for support of the design load. In this example, static load testing with wave equation analysis will be used for construction control. Therefore a factor of safety of 2.0 should be applied to the soil resistance calculated in suitable support layers in the static analysis. It should be noted that this approach is for scour conditions under the 100 year or overtopping flood events and that a different approach would apply for the superflood or 500 year event. Additional discussion on scour considerations is provided in Section 9.9.4 of this chapter.

In the static analysis, a trial pile penetration depth is chosen and an ultimate pile capacity, Q_u , is calculated. This ultimate capacity includes the soil resistance calculated from all soil layers including the shaft resistance in the scour susceptible layer, R_{s1} , the shaft resistance

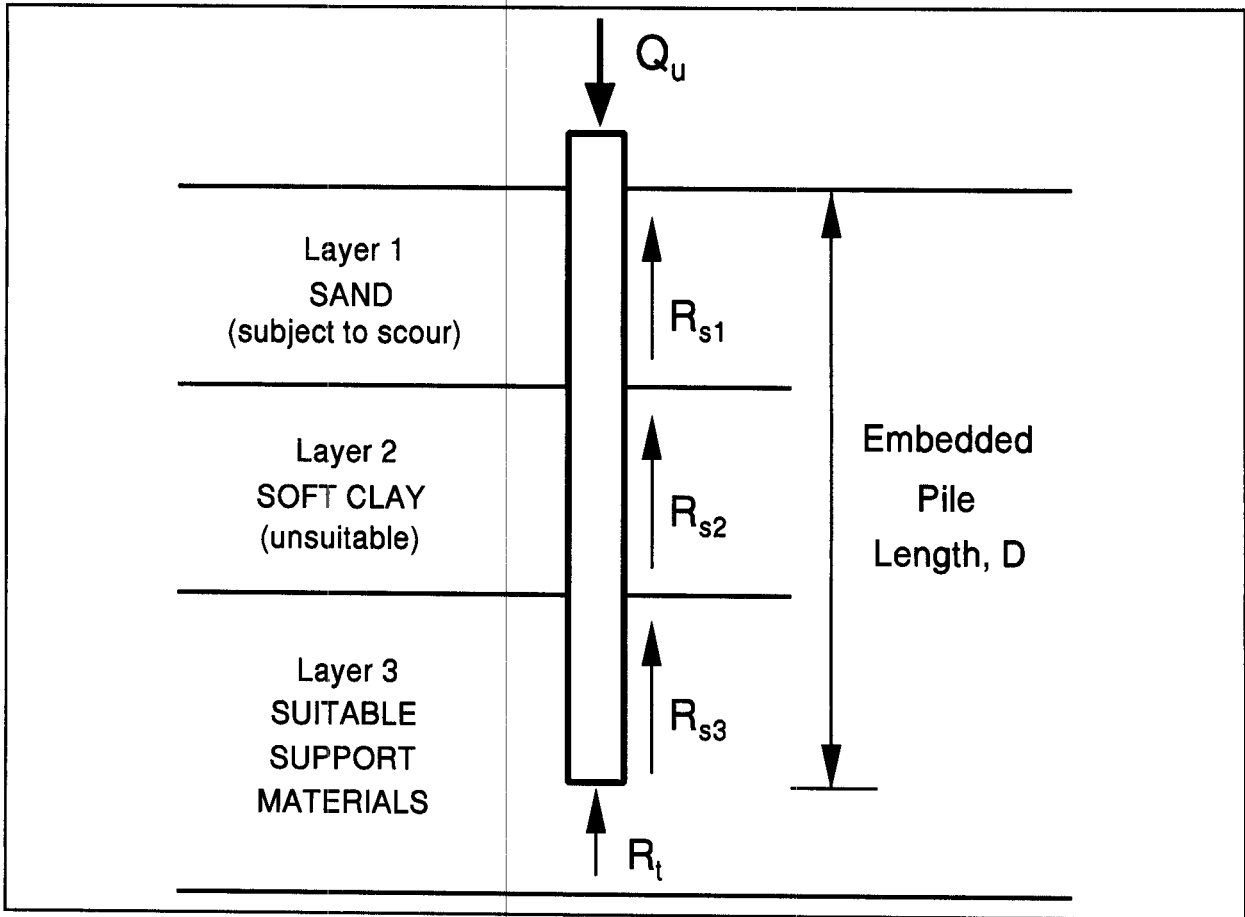


Figure 9.8 Soil Profile for Factor of Safety Discussion

in the unsuitable soft clay layer, R_{s2} as well as the resistance in suitable support materials along the pile shaft, R_{s3} , and at the pile toe resistance, R_t .

$$Q_u = R_{s1} + R_{s2} + R_{s3} + R_t$$

The design load, Q_a , is the sum of the soil resistances from the suitable support materials divided by a factor of safety, FS. As noted earlier, a factor of safety of 2.0 is used in the equation below because of the planned construction control with static load testing.

$$Q_a = (R_{s3} + R_t) / (FS=2)$$

The design load may also be expressed as the sum of the ultimate capacity minus the calculated soil resistances from the scour susceptible and unsuitable layers divided by the factor of safety.

$$Q_a = (Q_u - R_{s1} - R_{s2}) / (FS=2)$$

The result of the static analysis is then the estimated pile penetration depth, D , the design load for that penetration depth, Q_a , and the calculated ultimate capacity, Q_u .

For preparation of construction plans and specifications, the calculated ultimate capacity, Q_u , is specified. Note that if the construction control method changes after the design stage, the required ultimate capacity and the required pile penetration depth for the ultimate capacity will also change. This is apparent when the previous equation for the design load is expressed in terms of the ultimate capacity as follows:

$$Q_u = R_{s1} + R_{s2} + (Q_a)(FS=2)$$

A static analysis should also be used to calculate the soil resistance during driving, or driving resistance, Q_D , that must be overcome to reach the estimated pile penetration depth necessary to develop the ultimate capacity. This information is necessary for the designer to select a pile section with the driveability to overcome the anticipated soil resistance and for the contractor to properly size equipment. Driveability aspects of design are discussed in Section 9.10.7 of this chapter.

In the driving resistance static calculation, a factor of safety is not used. The driving resistance is the sum of the soil resistances from the scour susceptible and unsuitable layers plus the resistance in the suitable support materials to the estimated penetration depth.

$$Q_D = R_{s1} + R_{s2} + R_{s3} + R_t$$

Soil resistances in this calculation should be the resistance at the time of driving. Hence time dependent changes in soil strengths due to soil setup or relaxation should be considered. For the example presented in Figure 9.8, the driving resistance from the unsuitable clay layer would be reduced by the sensitivity of the clay. Therefore, R_{s2} would be $R_{s2} / 2$ for a clay with a sensitivity of 2. The static calculation of the driving resistance at depth D would then be as follows.

$$Q_D = R_{s1} + R_{s2}/2 + R_{s3} + R_t$$

This example problem considers only the driving resistance at the final pile penetration depth. In cases where piles are driven through hard or dense layers above the estimated pile penetration depth, the driving resistance to penetrate these layers should also be calculated. Additional information on the calculation of time dependent soil strength changes is provided in Section 9.10.1 of this chapter.

9.7 DESIGN OF SINGLE PILES

9.7.1 Bearing Capacity of Single Piles

Numerous static analysis methods are available for calculating the bearing capacity of a single pile. The following sections of this chapter will detail analysis methods for piles in cohesionless, cohesive and layered soil profiles using readily available SPT or laboratory test information. Additional methods based on cone penetration test results are also presented.

9.7.1.1 *Bearing Capacity of Piles in Cohesionless Soils*

The ultimate bearing capacity of a single pile in a cohesionless soil is the sum of shaft and toe resistances ($Q_u = R_s + R_t$). The calculation assumes that the shaft resistance and toe bearing resistance can be determined separately and that these two factors do not affect each other. Many analytical and empirical methods have been developed for estimating pile capacity in cohesionless materials. Table 9-1 describes some of the available methods. Each of the methods presented in Table 9-1 is also discussed in subsequent subsections.

9.7.1.1a *Meyerhof Method Based on Standard Penetration Test (SPT) Data*

Existing empirical correlations between Standard Penetration Test (SPT) results and static pile load tests can be used for preliminary estimates of static pile capacity for cohesionless soils. These correlations are based on the analyses of numerous pile load tests in a variety of cohesionless soil deposits. The Meyerhof (1976) method is quick and is easy to use. However, because the method is based on SPT test data which can be influenced by numerous factors, this method should only be used for preliminary estimates and not for final design.

TABLE 9-1 METHODS OF STATIC ANALYSIS FOR PILES IN COHESIONLESS SOILS

Method	Approach	Method of Obtaining Design Parameters	Advantages	Disadvantages	Remarks
Method based on Standard Penetration Test (SPT) data.	Empirical	Results of SPT tests.	Widespread use of SPT test and input data availability. Simple method to use.	Non reproducibility of N values. Not as reliable as the other methods presented in this chapter.	Due to non reproducibility of N values and simplifying assumptions contained in the method, use should be limited to preliminary estimating purposes.
Nordlund Method.	Semi-empirical	Charts provided by Nordlund. Estimate of soil friction angle is needed.	Allows for increased shaft resistance of tapered piles and includes effects of pile-soil friction coefficient for different pile materials.	No limiting value on unit shaft resistance is recommended by Nordlund. Soil friction angle often estimated from SPT data.	Good approach to design that is widely used. Method is based on field observations. Details provided in Section 9.7.1.1b.
Effective Stress Method.	Semi-empirical	Soil classification and estimated friction angle for β and N_t selection.	β value considers pile-soil friction coefficient for different pile materials. Soil resistance related to effective overburden pressure.	Results effected by range in β values and in particular by range in N_t chosen.	Good approach for design. Details provided in Section 9.7.1.3.
Methods based on Cone Penetration Test (CPT) data.	Empirical	Results of CPT tests.	Testing analogy between CPT and pile. Reliable correlations and reproducible test data.	Limitations on pushing cone into dense strata.	Good approach for design. Details provided in Section 9.7.1.7.

Meyerhof (1976) reported that the average unit shaft resistance, f_s , of driven displacement piles, such as closed-end pipe piles and precast concrete piles, in kPa is:

$$f_s = 2\bar{N}' \leq 100 \text{ kPa}$$

The average unit shaft resistance of driven nondisplacement piles, such as H-piles, in kPa is:

$$f_s = \bar{N}' \leq 100 \text{ kPa}$$

where \bar{N}' is the average corrected SPT resistance value, in blows per 300 mm, along the embedded length of pile. Typically, the soil profile is delineated into 3 to 6 meter thick layers, and the average unit shaft resistance is calculated for each soil layer.

Meyerhof (1976) recommended that the unit toe resistance, q_t , in kPa for piles driven into sands and gravels may be approximated by:

$$q_t = 400\bar{N}'_O + \frac{(40\bar{N}'_B - 40\bar{N}'_O)D_B}{b} \leq 400\bar{N}'_B$$

- Where:
- \bar{N}'_O = Average corrected SPT N' value for the stratum overlying the bearing stratum.
 - \bar{N}'_B = Average corrected SPT N' value of the bearing stratum.
 - D_B = Pile embedment depth into the bearing stratum in meters.
 - b = Pile diameter in meters.

The limiting value of $400\bar{N}'_B$ is reached when the embedment depth into the bearing stratum reaches 10 pile diameters. The above equation applies when the pile toe is located near the interface of two strata with a weaker stratum overlying the bearing stratum. For piles driven in a uniform cohesionless stratum, the unit toe resistance can be calculated as follows:

$$q_t = \frac{40\bar{N}'_B D_B}{b} \leq 400\bar{N}'_B$$

It is recommended that the average corrected SPT N' value, \bar{N}'_B , be calculated by averaging N' values within the zone extending 3 diameters below the pile toe. For piles driven into non-plastic silts, Meyerhof recommended the unit toe resistance, q_t , be limited to $300\bar{N}'_B$ instead of the $400\bar{N}'_B$ given in the above equation.

STEP BY STEP PROCEDURE FOR USING METHOD BASED ON SPT DATA

STEP 1 Correct SPT field N values for overburden pressure.

Use correction factors from Figure 4.4 to obtain corrected SPT N' values.

STEP 2 Compute the average corrected SPT N' value, \bar{N}' , for each soil layer.

Along the embedded length of pile, delineate the soil profile into layers based on soil density indicated by N' . The individual soil layers should be selected between 3 and 6 meters thick.

STEP 3 Compute unit shaft resistance, f_s (kPa) for driven, displacement piles from:

$$f_s = 2\bar{N}' \leq 100 \text{ kPa}$$

for driven, non-displacement piles such as H-piles, use:

$$f_s = \bar{N}' \leq 100 \text{ kPa}$$

STEP 4 Compute ultimate shaft resistance, R_s (kN).

$$R_s = f_s A_s$$

Where: A_s = Pile shaft surface area.
= (Perimeter)(embedded length).

For H-piles in cohesionless soils, the "box" area should generally be used for shaft resistance calculations. Additional discussion on the behavior of open pile sections is presented in Section 9.10.5.

STEP 5 Compute average corrected SPT N' values, \bar{N}'_O and \bar{N}'_B , near pile toe.

In cases where the pile toe is situated near the interface of a weaker stratum overlying the bearing stratum, compute the average corrected SPT N' value for the stratum overlying the bearing stratum, \bar{N}'_O , and the average corrected SPT N' value for the bearing stratum, \bar{N}'_B .

In uniform cohesionless soils, compute the average corrected SPT N' value by averaging N' values within the zone extending 3 diameters below the pile toe.

STEP 6 Compute unit toe resistance, q_t (kPa).

For weaker stratum overlying the bearing stratum compute q_t from:

$$q_t = 400\bar{N}'_O + \frac{(40\bar{N}'_B - 40\bar{N}'_O)D_B}{b} \leq 400\bar{N}'_B$$

For piles in a uniform cohesionless deposit compute q_t from:

$$q_t = \frac{40\bar{N}'_B D_B}{b} \leq 400\bar{N}'_B$$

For piles driven into non-plastic silts, the unit toe resistance, q_t , should be limited to $300\bar{N}'_B$ instead of $400\bar{N}'_B$.

STEP 7 Compute ultimate toe resistance, R_t (kN).

$$R_t = q_t A_t$$

Where: A_t = Pile toe area.

For steel H and unfilled open end pipe piles, use only steel cross section area at pile toe unless there is reasonable assurance and previous experience that a soil plug will form at the pile toe. Additional discussion on plug formation in open pile sections is presented in Section 9.10.5. The assumption of a soil plug

would allow the use of a box area at H pile toe and total pipe cross section area for open end pipe pile.

STEP 8 Compute ultimate pile capacity, Q_u (kN).

$$Q_u = R_s + R_t$$

STEP 9 Compute allowable design load, Q_a (kN).

$$Q_a = \frac{Q_u}{\text{Factor of Safety}}$$

Use Factor of Safety based on the construction control method specified as described in Section 9.6.

In using the Meyerhof method, it should be remembered that it is intended to be used only for preliminary capacity and length estimates. Limiting values often apply for the unit shaft and toe resistances and they should be used. It should also be remembered that the Standard Penetration Test is subject to many errors. Thus, judgment must be exercised when performing capacity calculations based on SPT results.

9.7.1.1b Nordlund Method

The Nordlund Method (1963) is based on field observations and considers the shape of pile taper and its soil displacement in calculating the shaft resistance. The method also accounts for the differences in soil-pile coefficient of friction for different pile materials. The method is based on the results of several load test programs in cohesionless soils. Several pile types were used in these test programs including timber, H, closed end pipe, Monotubes and Raymond step taper piles. These piles, which were used to develop the method's design curves, had pile widths generally in the range of 250 to 500 mm. The Nordlund Method tends to overpredict pile capacity for piles with widths larger than 600 mm.

According to the Nordlund Method, the ultimate capacity, Q_u , of a pile in cohesionless soil is the sum of the shaft resistance, R_s and the toe resistance, R_t . Nordlund suggests the shaft resistance is a function of the following variables:

1. The friction angle of the soil.
2. The friction angle on the sliding surface.
3. The taper of the pile.
4. The effective unit weight of the soil.
5. The pile length.
6. The minimum pile perimeter.
7. The volume of soil displaced.

These factors are considered in the Nordlund equation as illustrated in Figure 9.9.

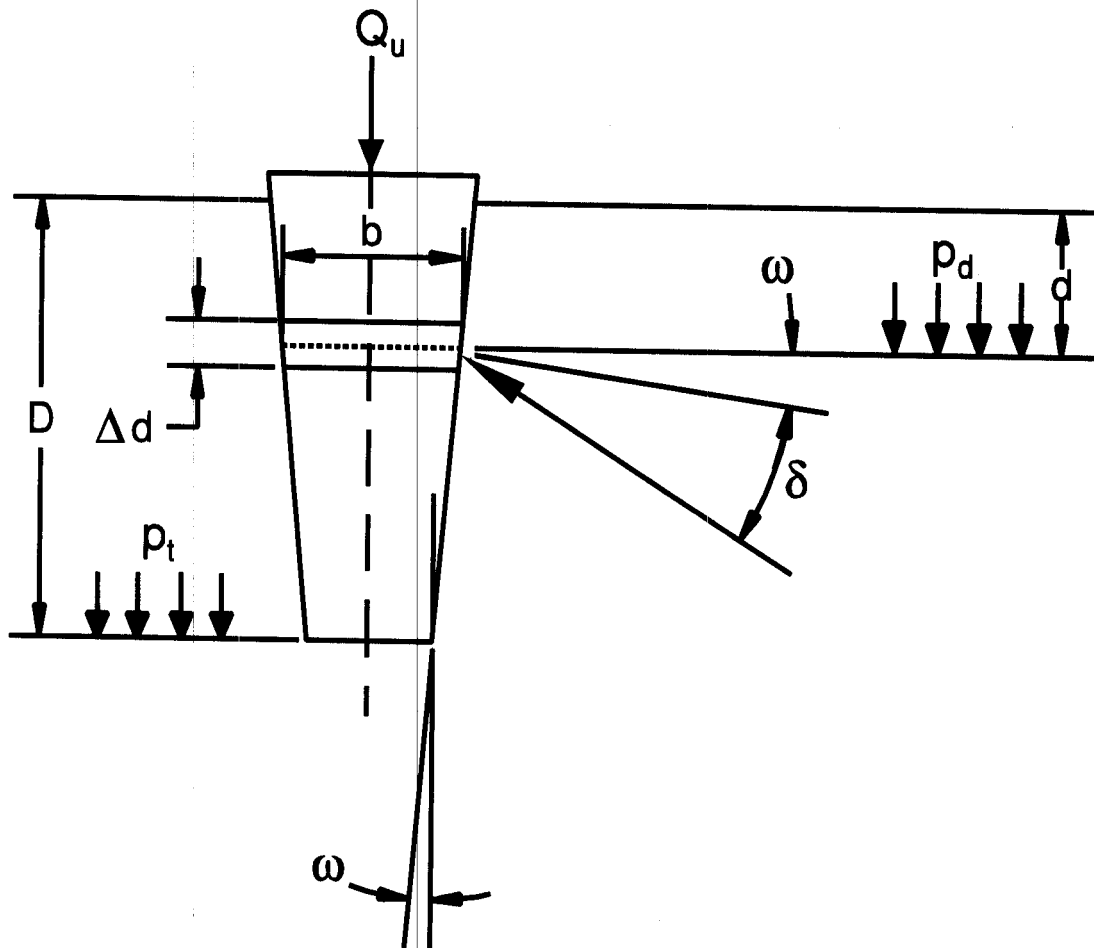
The Nordlund Method equation for computing the ultimate capacity of a pile is as follows:

$$Q_u = \sum_{d=0}^{d=D} K_\delta C_F p_d \frac{\sin(\delta + \omega)}{\cos \omega} C_d \Delta d + \alpha_t N'_q A_t p_t$$

- Where:
- d = Depth.
 - D = Embedded pile length.
 - K_δ = Coefficient of lateral earth pressure at depth d.
 - C_F = Correction factor for K_δ when $\delta \neq \phi$.
 - p_d = Effective overburden pressure at the center of depth increment d.
 - δ = Friction angle between pile and soil.
 - ω = Angle of pile taper from vertical.
 - ϕ = Soil friction angle.
 - C_d = Pile perimeter at depth d.
 - Δd = Length of pile segment.
 - α_t = Dimensionless factor (dependent on pile depth-width relationship).
 - N'_q = Bearing capacity factor.
 - A_t = Pile toe area.
 - p_t = Effective overburden pressure at the pile toe.

For a pile of uniform cross section ($\omega=0$) and embedded length D, driven in soil layers of the same effective unit weight and friction angle, the Nordlund equation becomes:

$$Q_u = (K_\delta C_F p_d \sin \delta C_d D) + (\alpha_t N'_q A_t p_t)$$



$$Q_u = \sum_{d=0}^{d=D} K_{\delta} C_F p_d \frac{\sin(\delta + \omega)}{\cos \omega} C_d \Delta d + \alpha_t N'_q A_t p_t$$

Figure 9.9 Nordlund's General Equation for Ultimate Pile Capacity

The soil friction angle ϕ influences most of the calculations in the Nordlund method. In the absence of laboratory test data, ϕ can be estimated from corrected SPT N' values. Therefore, Figure 4.4 in Chapter 4 should be used for correcting field N values. The corrected SPT N' values may then be used in Table 4-5 of Chapter 4 to estimate ϕ .

Nordlund developed this method in 1963 and updated it in 1979 and has not placed a limiting value on the shaft resistance. However, Nordlund has recommended that the effective overburden pressure, p_v , used for computing the pile toe resistance be limited to 150 kPa.

STEP BY STEP PROCEDURE FOR USING NORDLUND METHOD

Steps 1 through 6 are for computing the shaft resistance and steps 7 through 9 are for computing the pile toe resistance.

- STEP 1 Delineate the soil profile into layers and determine the ϕ angle for each layer.
- Construct p_o diagram using procedure described in Section 9.4.
 - Correct SPT field N values for overburden pressure using Figure 4.4 from Chapter 4 and obtain corrected SPT N' values. Delineate soil profile into layers based on corrected SPT N' values.
 - Determine ϕ angle for each layer from laboratory tests or in-situ data.
 - In the absence of laboratory or in-situ test data, determine the average corrected SPT N' value, \bar{N}' , for each soil layer and estimate ϕ angle from Table 4-5 in Chapter 4.
- STEP 2 Determine δ , the friction angle between pile and soil based on displaced soil volume, V , and the soil friction angle, ϕ .
- Compute volume of soil displaced per unit length of pile, V .
 - Enter Figure 9.10 with V and determine δ/ϕ ratio for pile type.
 - Calculate δ from δ/ϕ ratio.

- STEP 3 Determine the coefficient of lateral earth pressure, K_δ , for each ϕ angle.
- Determine K_δ for ϕ angle based on displaced volume, V , and pile taper angle, ω , using either Figure 9.11, 9.12, 9.13, or 9.14 and the appropriate procedure described in Step 3b, 3c, 3d, or 3e.
 - If the displaced volume is 0.0093, 0.093, or 0.930 m³/m which correspond to one of the curves provided in Figures 9.11 through 9.14 and the ϕ angle is one of those provided, K_δ can be determined directly from the appropriate figure.
 - If the displaced volume is 0.0093, 0.093, or 0.930 m³/m which correspond to one of the curves provided in Figures 9.11 through 9.14 but the ϕ angle is different from those provided, use linear interpolation to determine K_δ for the required ϕ angle. Tables 9-2a and 9-2b also provide interpolated K_δ values at selected displaced volumes versus ϕ angle for uniform piles ($\omega = 0^\circ$).
 - If the displaced volume is other than 0.0093, 0.093, or 0.930 m³/m which correspond to one of the curves provided in Figures 9.11 through 9.14 but the ϕ angle corresponds to one of those provided, use log linear interpolation to determine K_δ for the required displaced volume. An example of this procedure may be found in Appendix F.2.1.2. Tables 9-2a and 9-2b also provide interpolated K_δ values at selected displaced volumes versus ϕ angle for uniform piles ($\omega = 0^\circ$).
 - If the displaced volume is other than 0.0093, 0.093, or 0.930 m³/m which correspond to one of the curves provided in Figures 9.11 through 9.14 and the ϕ angle does not correspond to one of those provided, first use linear interpolation to determine K_δ for the required ϕ angle at the displaced volume curves provided for 0.0093, 0.093, or 0.930 m³/m. Then use log linear interpolation to determine K_δ for the required displaced volume. An example of this procedure may be found in Appendix F.2.1.2. Tables 9-2a and 9-2b also provide interpolated K_δ values at selected displaced volumes versus ϕ angle for uniform piles ($\omega = 0^\circ$).

STEP 4 Determine the correction factor, C_F , to be applied to K_δ if $\delta \neq \phi$.

Use Figure 9.15 to determine the correction factor for each K_δ . Enter figure with ϕ angle and δ/ϕ value to determine C_F .

STEP 5 Compute the average effective overburden pressure at the midpoint of each soil layer, p_d (kPa).

Note: A limiting value is not applied to p_d .

STEP 6 Compute the shaft resistance in each soil layer. Sum the shaft resistance from each soil layer to obtain the ultimate shaft resistance, R_s (kN).

$$R_s = K_\delta C_F p_d \sin \delta C_d D$$

(for uniform pile cross section)

For H-piles in cohesionless soils, the "box" area should generally be used for shaft resistance calculations. Additional discussion on the behavior of open pile sections is presented in Section 9.10.5.

STEP 7 Determine the α_t coefficient and the bearing capacity factor, N'_q , from the ϕ angle near the pile toe.

a. Enter Figure 9.16(a) with ϕ angle near pile toe to determine α_t coefficient based on pile length to diameter ratio.

b. Enter Figure 9.16(b) with ϕ angle near pile toe to determine, N'_q .

c. If ϕ angle is estimated from SPT data, compute the average corrected SPT N' value over the zone from the pile toe to 3 diameters below the pile toe. Use this average corrected SPT N' value to estimate ϕ angle near pile toe from Table 4-5.

STEP 8 Compute the effective overburden pressure at the pile toe, p_t (kPa).

Note: The limiting value of p_t is 150 kPa.

STEP 9 Compute the ultimate toe resistance, R_t (kN).

a. $R_t = \alpha_t N'_q A_t p_t$

b. limiting $R_t = q_L A_t$

q_L value is obtained from:

1. Entering Figure 9.17 with ϕ angle near pile toe determined from laboratory or in-situ test data.
 2. Entering Figure 9.17 with ϕ angle near the pile toe estimated from Table 4-5 and the average corrected SPT N' near toe as described in Step 7.
- c. Use lesser of the two R_t values obtained in steps a and b.

For steel H and unfilled open end pipe piles, use only steel cross section area at pile toe unless there is reasonable assurance and previous experience that a soil plug will form at the pile toe. Additional discussion on plug formation in open pile sections is presented in Section 9.10.5. The assumption of a soil plug would allow the use of a box area at H pile toe and total pipe cross section area for open end pipe pile.

STEP 10 Compute the ultimate pile capacity, Q_u (kN).

$$Q_u = R_s + R_t$$

STEP 11 Compute the allowable design load, Q_a (kN).

$$Q_a = \frac{Q_u}{\text{Factor of Safety}}$$

The factor of safety used in the calculation should be based upon the construction control method to be specified. Recommended factors of safety were described in Section 9.6.

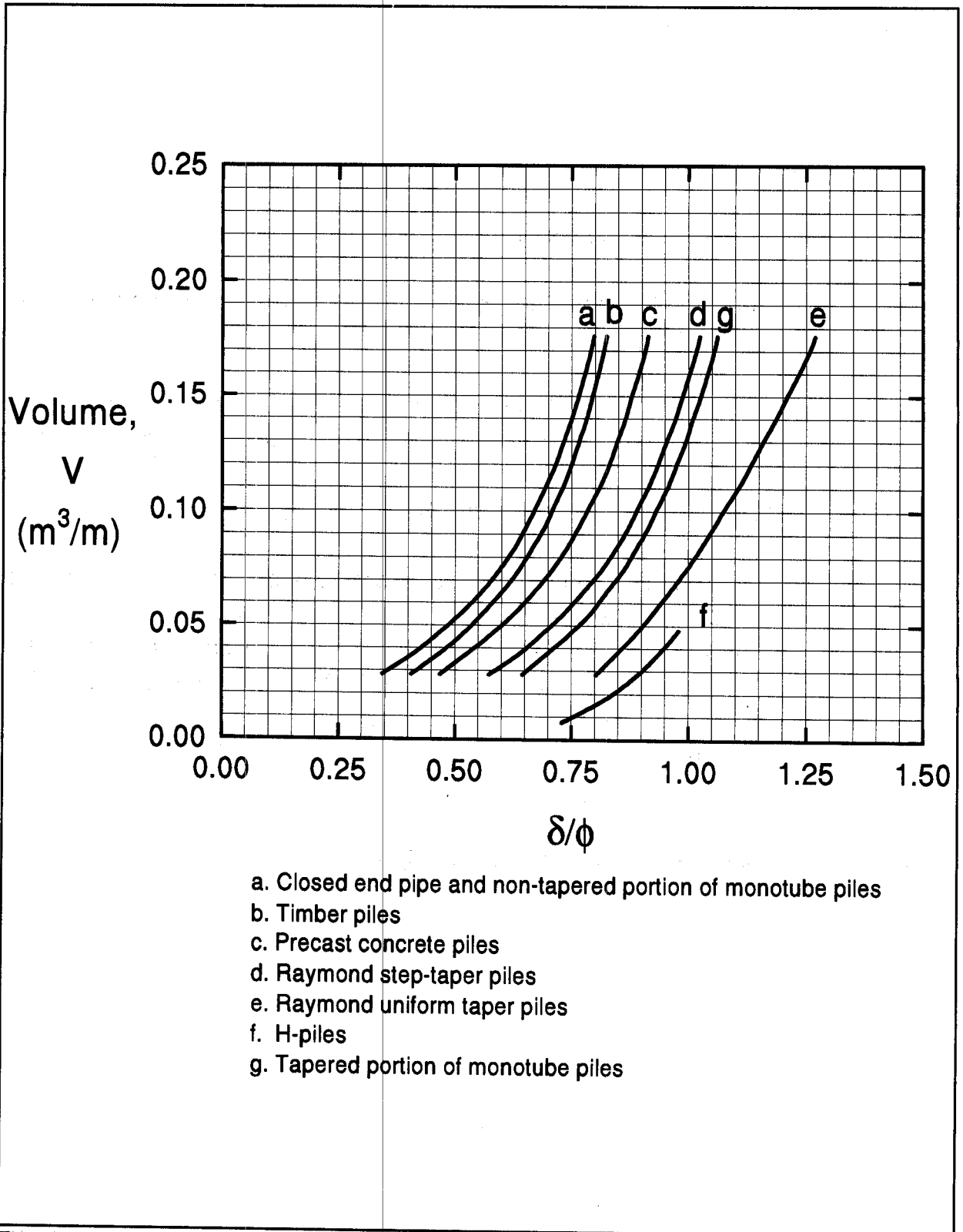


Figure 9.10 Relation of δ/ϕ and Pile Displacement, V , for Various Types of Piles (after Nordlund, 1979)

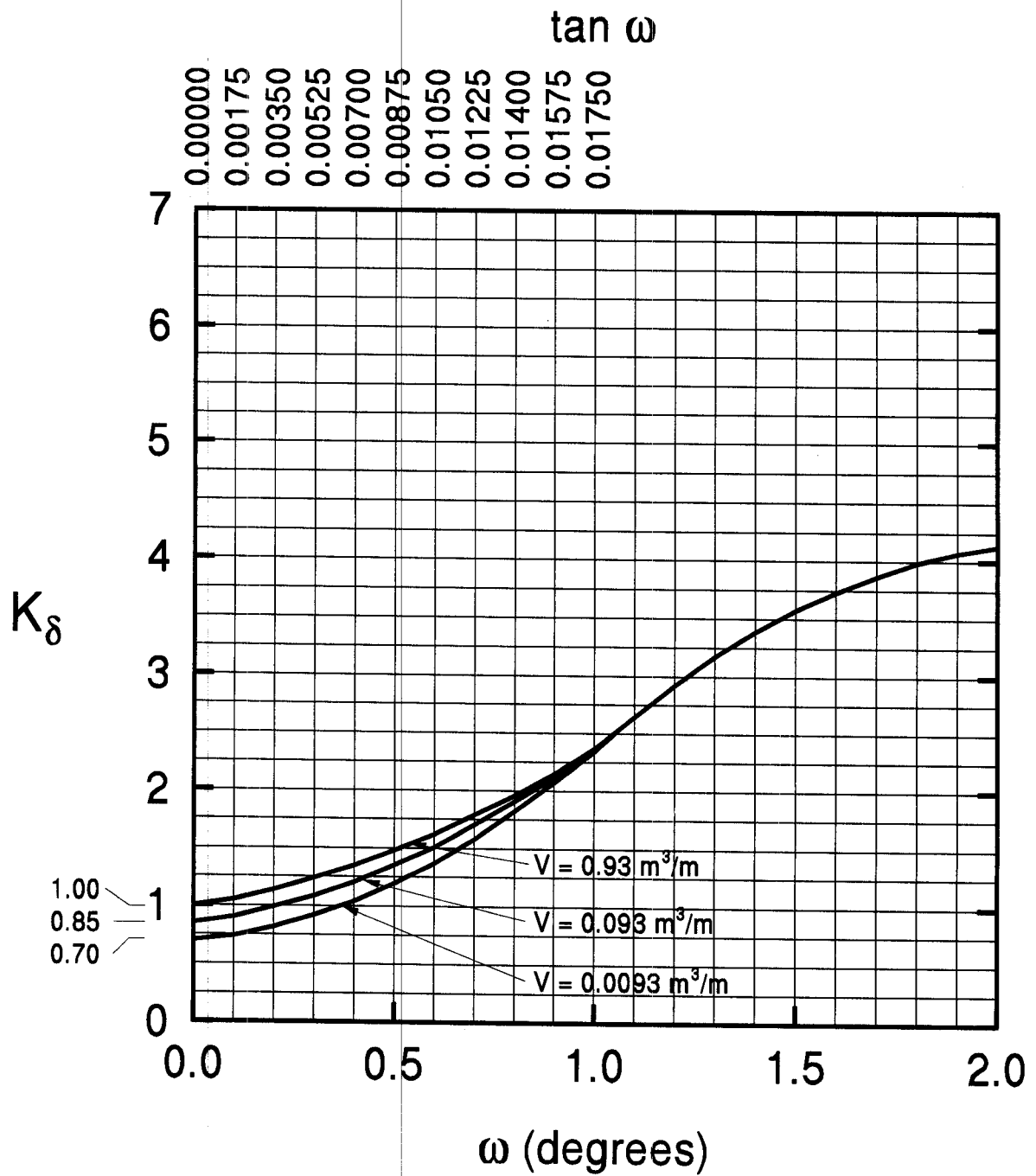


Figure 9.11 Design Curve for Evaluating K_δ for Piles when $\phi = 25^\circ$ (after Nordlund, 1979)

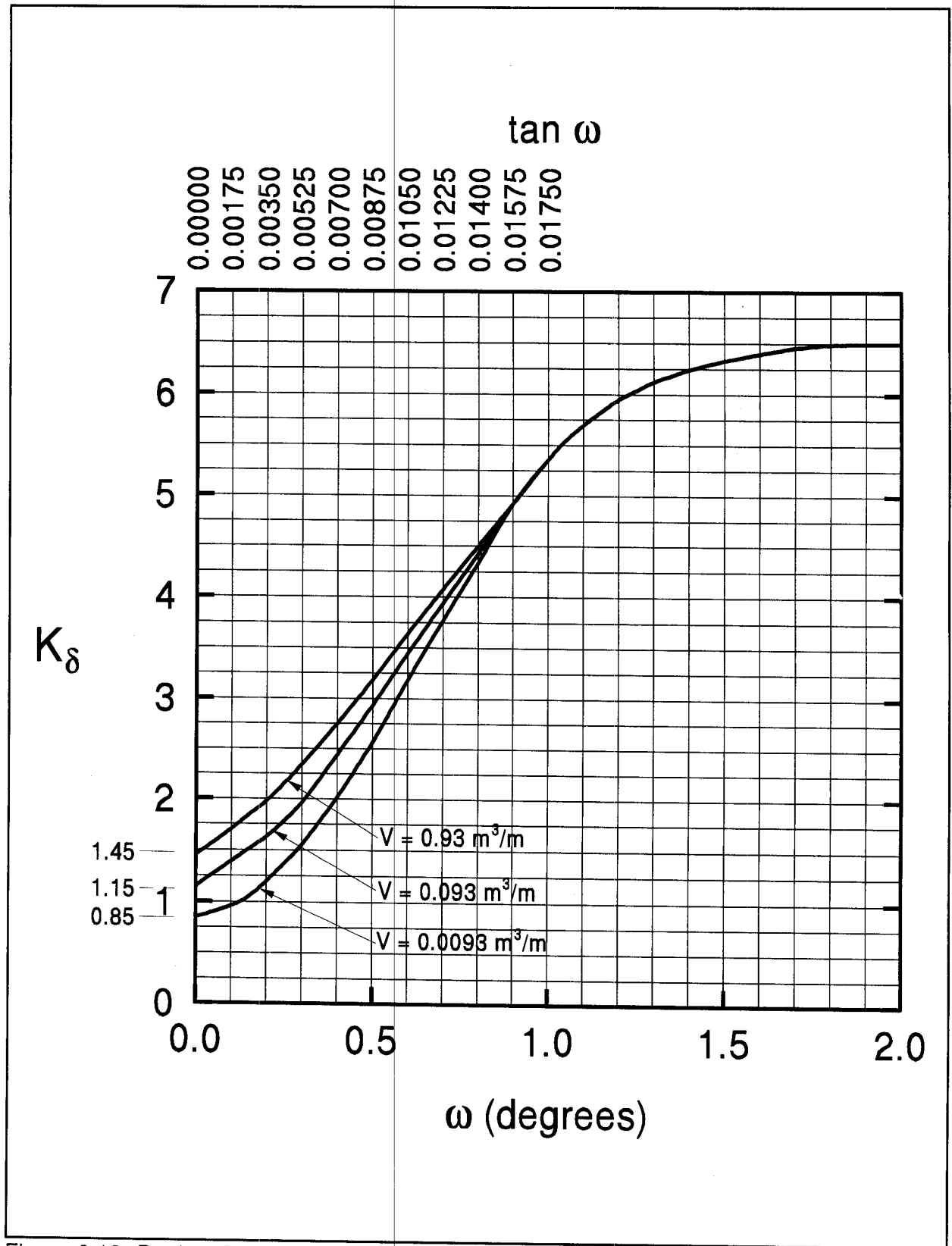


Figure 9.12 Design Curve for Evaluating K_δ for Piles when $\phi = 30^\circ$ (after Nordlund, 1979)

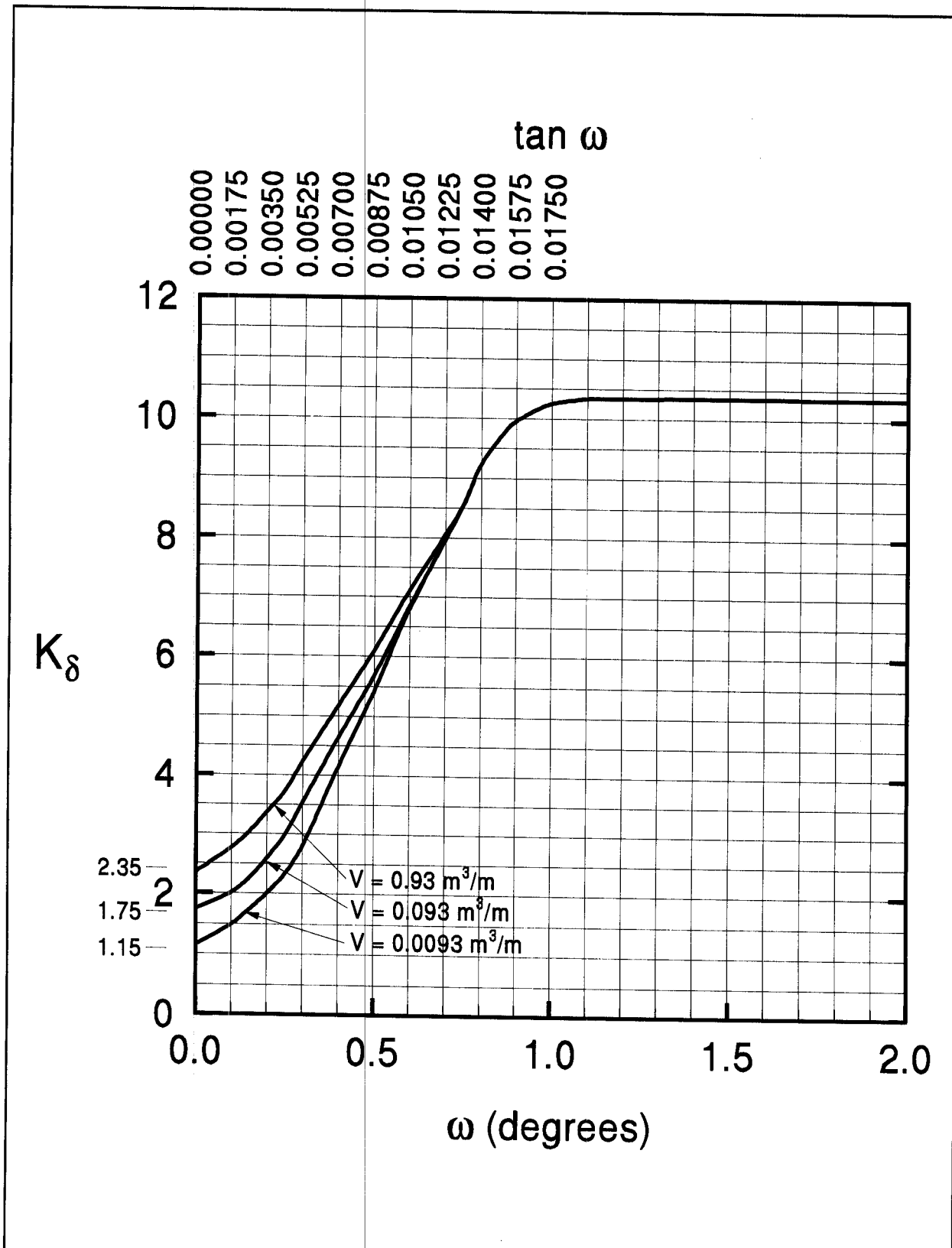


Figure 9.13 Design Curve for Evaluating K_δ for Piles when $\phi = 35^\circ$ (after Nordlund, 1979)

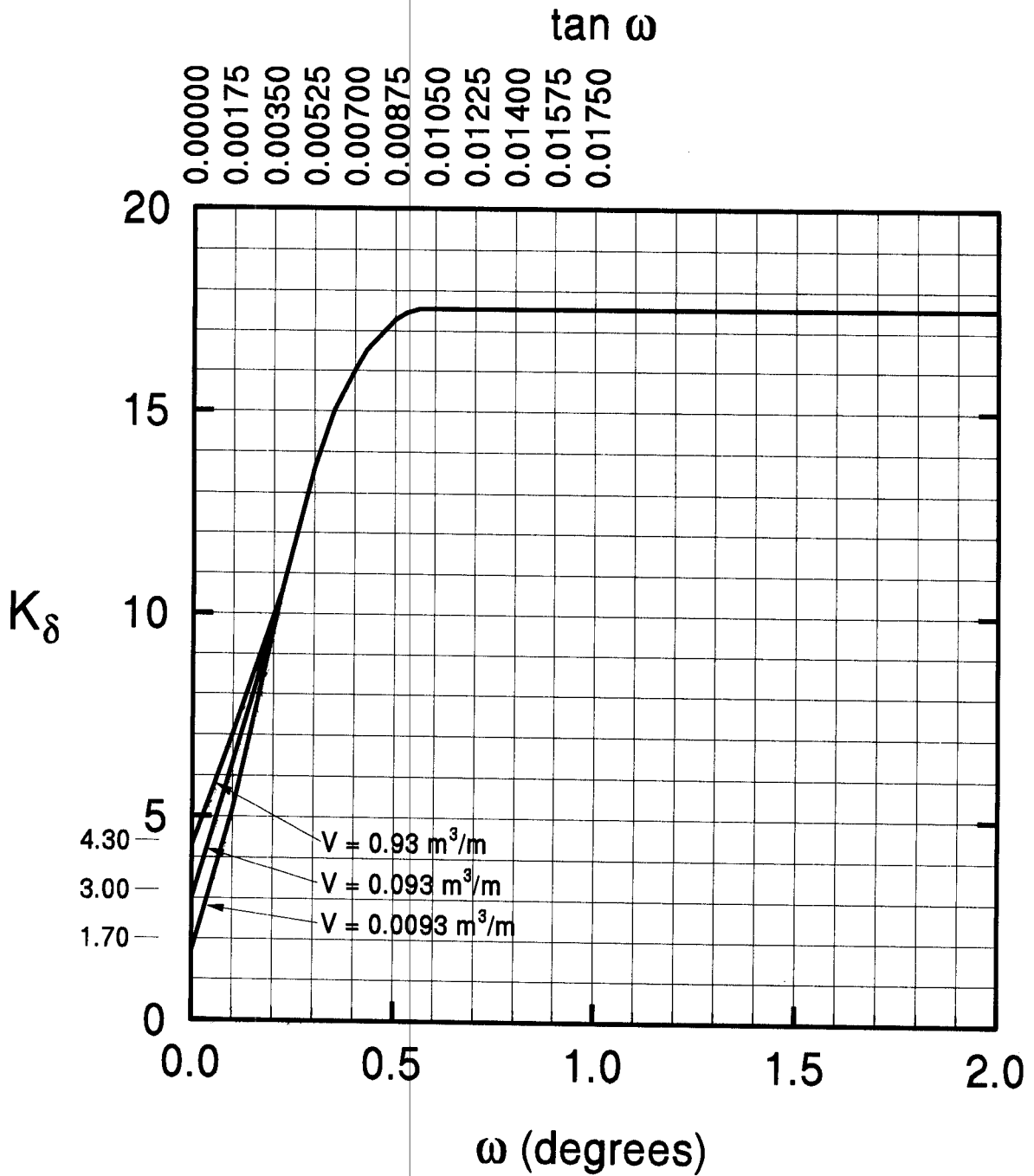


Figure 9.14 Design Curve for Evaluating K_δ for Piles when $\phi = 40^\circ$ (after Nordlund, 1979)

Table 9-2(a) Design Table for Evaluating K_s for Piles when $\omega = 0^\circ$ and $V = 0.0093$ to $0.0930 \text{ m}^3/\text{m}$

ϕ	Displaced Volume (V), m^3/m									
	0.0093	0.0186	0.0279	0.0372	0.0465	0.0558	0.0651	0.0744	0.0837	0.0930
25	0.70	0.75	0.77	0.79	0.80	0.82	0.83	0.84	0.84	0.85
26	0.73	0.78	0.82	0.84	0.86	0.87	0.88	0.89	0.90	0.91
27	0.76	0.82	0.86	0.89	0.91	0.92	0.94	0.95	0.96	0.97
28	0.79	0.86	0.90	0.93	0.96	0.98	0.99	1.01	1.02	1.03
29	0.82	0.90	0.95	0.98	1.01	1.03	1.05	1.06	1.08	1.09
30	0.85	0.94	0.99	1.03	1.06	1.08	1.10	1.12	1.14	1.15
31	0.91	1.02	1.08	1.13	1.16	1.19	1.21	1.24	1.25	1.27
32	0.97	1.10	1.17	1.22	1.26	1.30	1.32	1.35	1.37	1.39
33	1.03	1.17	1.26	1.32	1.37	1.40	1.44	1.46	1.49	1.51
34	1.09	1.25	1.35	1.42	1.47	1.51	1.55	1.58	1.61	1.63
35	1.15	1.33	1.44	1.51	1.57	1.62	1.66	1.69	1.72	1.75
36	1.26	1.48	1.61	1.71	1.78	1.84	1.89	1.93	1.97	2.00
37	1.37	1.63	1.79	1.90	1.99	2.05	2.11	2.16	2.21	2.25
38	1.48	1.79	1.97	2.09	2.19	2.27	2.34	2.40	2.45	2.50
39	1.59	1.94	2.14	2.29	2.40	2.49	2.57	2.64	2.70	2.75
40	1.70	2.09	2.32	2.48	2.61	2.71	2.80	2.87	2.94	3.00

Table 9-2(b) Design Table for Evaluating K_s for Piles when $\omega = 0^\circ$ and $V = 0.093$ to $0.930 \text{ m}^3/\text{m}$

ϕ	Displaced Volume (V), m^3/m									
	0.093	0.186	0.279	0.372	0.465	0.558	0.651	0.744	0.837	0.930
25	0.85	0.90	0.92	0.94	0.95	0.97	0.98	0.99	0.99	1.00
26	0.91	0.96	1.00	1.02	1.04	1.05	1.06	1.07	1.08	1.09
27	0.97	1.03	1.07	1.10	1.12	1.13	1.15	1.16	1.17	1.18
28	1.03	1.10	1.14	1.17	1.20	1.22	1.23	1.25	1.26	1.27
29	1.09	1.17	1.22	1.25	1.28	1.30	1.32	1.33	1.35	1.36
30	1.15	1.24	1.29	1.33	1.36	1.38	1.40	1.42	1.44	1.45
31	1.27	1.38	1.44	1.49	1.52	1.55	1.57	1.60	1.61	1.63
32	1.39	1.52	1.59	1.64	1.68	1.72	1.74	1.77	1.79	1.81
33	1.51	1.65	1.74	1.80	1.85	1.88	1.92	1.94	1.97	1.99
34	1.63	1.79	1.89	1.96	2.01	2.05	2.09	2.12	2.15	2.17
35	1.75	1.93	2.04	2.11	2.17	2.22	2.26	2.29	2.32	2.35
36	2.00	2.22	2.35	2.45	2.52	2.58	2.63	2.67	2.71	2.74
37	2.25	2.51	2.67	2.78	2.87	2.93	2.99	3.04	3.09	3.13
38	2.50	2.81	2.99	3.11	3.21	3.29	3.36	3.42	3.47	3.52
39	2.75	3.10	3.30	3.45	3.56	3.65	3.73	3.80	3.86	3.91
40	3.00	3.39	3.62	3.78	3.91	4.01	4.10	4.17	4.24	4.30

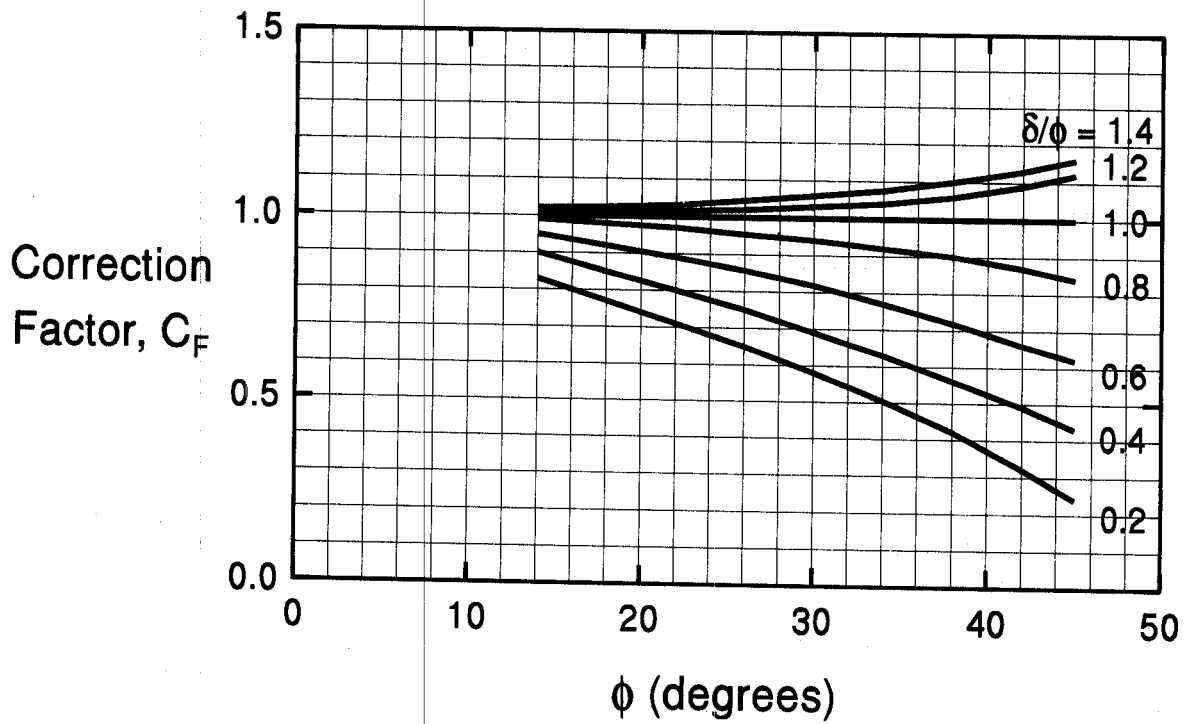


Figure 9.15 Correction Factor for K_s when $\delta \neq \phi$ (after Nordlund, 1979)

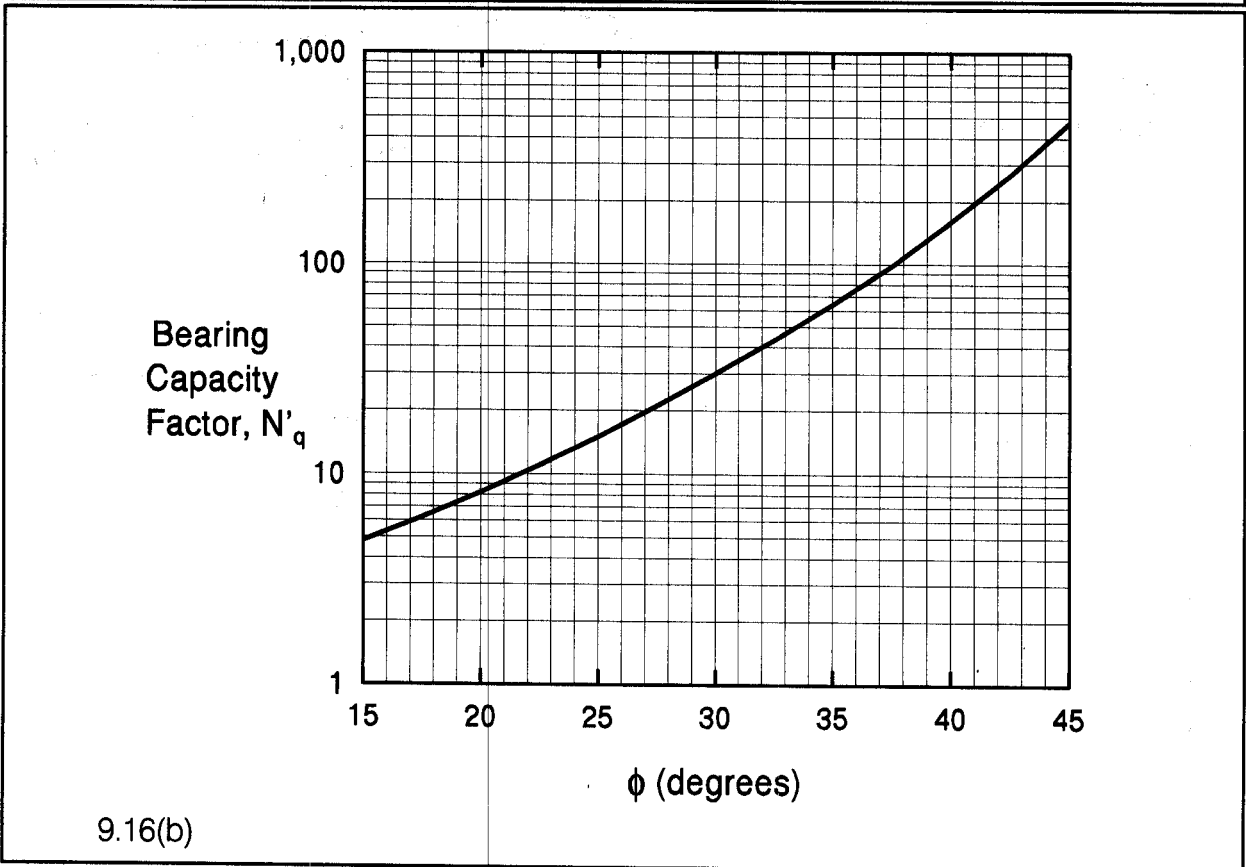
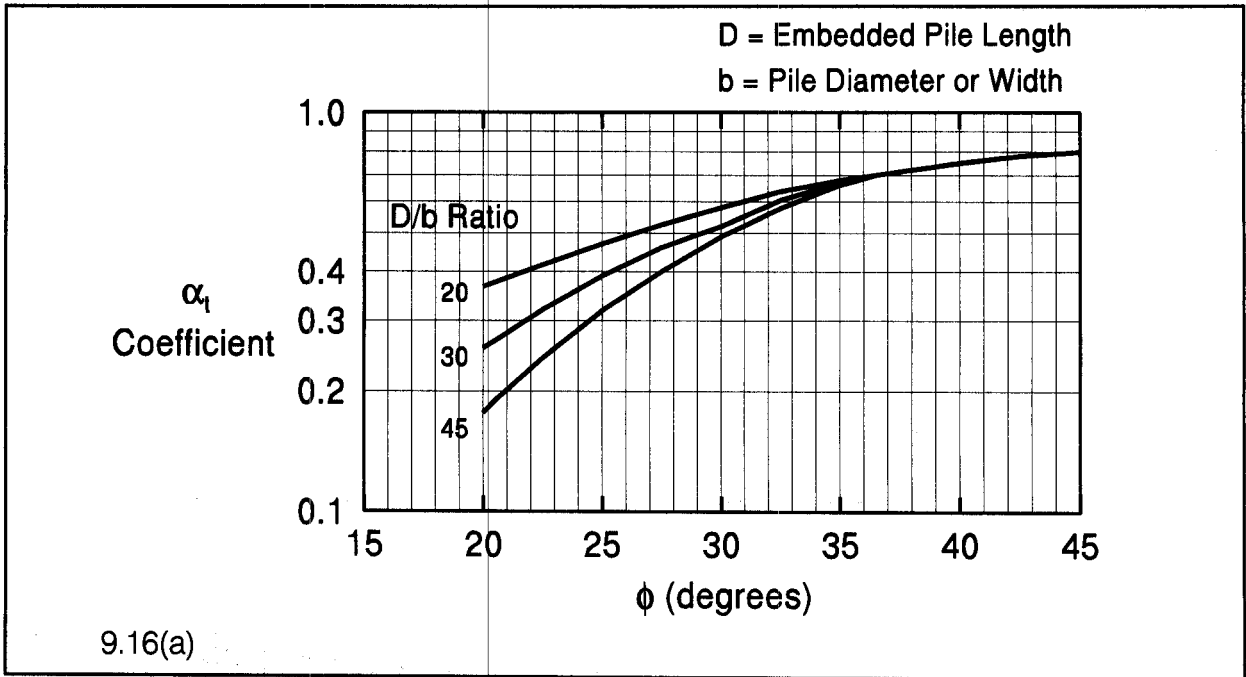


Figure 9.16 Chart for Estimating α_1 Coefficient and Bearing Capacity Factor N'_q (Chart modified from Bowles, 1977)

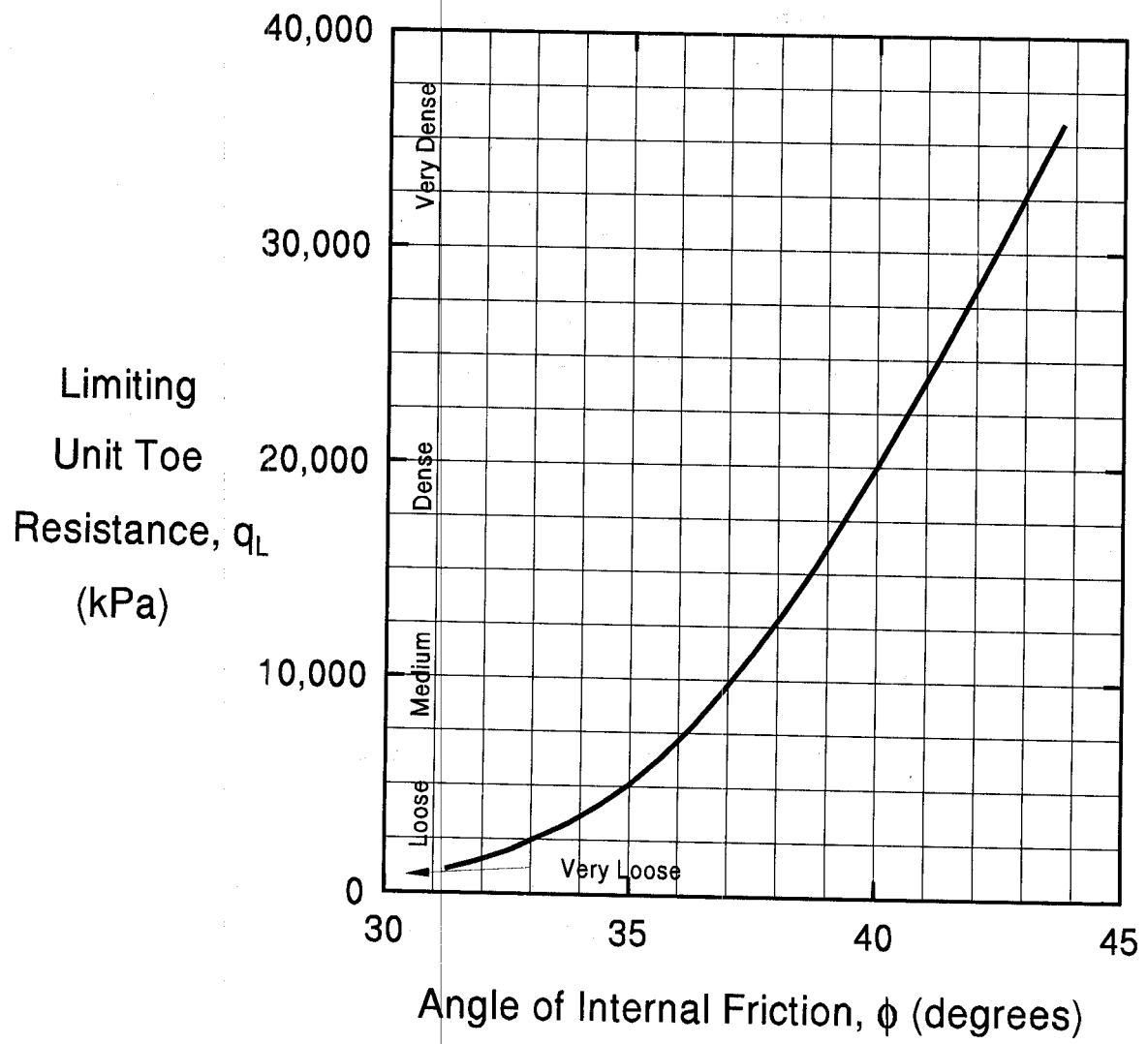


Figure 9.17 Relationship Between Maximum Unit Pile Toe Resistance and Friction Angle for Cohesionless Soils (after Meyerhof, 1976)

9.7.1.2 Bearing Capacity of Piles in Cohesive Soils

The ultimate bearing capacity of a pile in cohesive soil may also be expressed as the sum of the shaft and toe resistances or $Q_u = R_s + R_t$. The shaft and toe resistances can be calculated from static analysis methods using soil boring and laboratory test data in either total stress or effective stress methods. The α -Method is a total stress method that uses undrained soil shear strength parameters for calculating static pile capacity in cohesive soil. The α -Method will be presented in Section 9.7.1.2a. The effective stress method uses drained soil strength parameters for capacity calculations. Since the effective stress method may be used for calculating static pile capacity in cohesive as well as cohesionless soils, this method will be presented in Section 9.7.1.3. Alternatively, in-situ CPT test results can also be used to calculate pile capacity in cohesive soils from cone sleeve friction and cone tip resistance values. CPT based methods are discussed in Section 9.7.1.7. An overview of design methods for cohesive soils is presented in Table 9-3.

The shaft resistance of piles driven into cohesive soils is frequently as much as 80 to 90% of the total bearing capacity. Therefore, it is important that the shaft resistance of piles in cohesive soils be estimated as accurately as possible.

9.7.1.2a Total Stress - α -Method

For piles in clay, a total stress analysis is often used where ultimate capacity is calculated from the undrained shear strength of the soil. This approach assumes that the shaft resistance is independent of the effective overburden pressure and that the unit shaft resistance can be expressed in terms of an empirical adhesion factor times the undrained shear strength.

The unit shaft resistance, f_s , is equal to the adhesion, c_a , which is the shear stress between the pile and soil at failure. This may be expressed in equation form as:

$$f_s = c_a = \alpha c_u$$

in which α is an empirical adhesion factor for reduction of the average undrained shear strength, c_u , of undisturbed clay along the embedded length of the pile. The coefficient α depends on the nature and strength of the clay, pile dimension, method of pile installation, and time effects. The values of α vary within wide limits and decrease rapidly with increasing shear strength.

TABLE 9-3 METHODS OF STATIC ANALYSIS FOR PILES IN COHESIVE SOILS

Method	Approach	Method of Obtaining Design Parameters	Advantages	Disadvantages	Remarks
α -Method (Tomlinson Method).	Empirical, total stress analysis.	Undrained shear strength estimate of soil is needed. Adhesion calculated from Figures 9.18 and 9.19.	Simple calculation from laboratory undrained shear strength values to adhesion.	Wide scatter in adhesion versus undrained shear strengths in literature.	Widely used method described in Section 9.7.1.2a.
Effective Stress Method.	Semi-Empirical, based on effective stress at failure.	β and N_t values are selected from Table 9-4 based on drained soil strength estimates.	Ranges in β and N_t values for most cohesive soils are relatively small.	Range in N_t values for hard cohesive soils such as glacial tills can be large.	Good design approach theoretically better than undrained analysis. Details in Section 9.7.1.3.
Methods based on Cone Penetration Test data.	Empirical.	Results of CPT tests.	Testing analogy between CPT and pile. Reproducible test data.	Cone can be difficult to advance in very hard cohesive soils such as glacial tills.	Good approach for design. Details in Section 9.7.1.7.

It is recommended that Figure 9.18 generally be used for adhesion calculations, unless one of the special soil stratigraphy cases identified in Figure 9.19 is present at a site. In cases where either Figures 9.18 or 9.19 could be used, the inexperienced user should select and use the smaller value obtained from either figure. All users should confirm the applicability of a selected design chart in a given soil condition with local correlations between static capacity calculations and static load tests results.

In Figure 9.18, the adhesion, c_a , is expressed as a function of the undrained shear strength, c_u , with consideration of both the pile type and the embedded pile length, D , to pile diameter, b , ratio. The embedded pile length used in Figure 9.18 should be the minimum value of the length from the ground surface to the bottom of the clay layer, or the length from the ground surface to the pile toe.

Figure 9.19 presents the adhesion factor, α , versus the undrained shear strength as a function of unique soil stratigraphy and pile embedment. The adhesion factor from these soil stratigraphy cases should be used only for determining the adhesion in a stiff clay layer in that specific condition. For a soil profile consisting of clay layers of significantly different consistencies such as soft clays over stiff clays, adhesion factors should be determined for each individual clay layer.

Figure 9.19(a) may be used to select the adhesion factor when piles are driven through a sand or sandy gravel layer and into an underlying stiff clay stratum. This case results in the highest adhesion factors as granular material is dragged into the underlying clays. The greater the pile penetration into the clay stratum, the less the influence of the overlying granular stratum on the adhesion factor. Therefore, for the same undrained shear strength, the adhesion factor decreases with increased pile penetration into the clay stratum.

Figure 9.19(b) should be used to select the adhesion factor when piles are driven through a soft clay layer overlying a stiff clay layer. In this case, the soft clay is dragged into the underlying stiff clay stratum thereby reducing the adhesion factor of the underlying stiff clay soils. The greater the pile penetration into the underlying stiff clay soils, the less the influence the overlying soft clays have on the stiff clay adhesion factor. Therefore, the stiff clay adhesion factor increases with increasing pile penetration into the stiff clay soils.

Last, Figure 9.19(c) may be used to select the adhesion factor for piles driven in stiff clays without any different overlying strata. In stiff clays, a gap often forms between the pile and the soil along the upper portion of the pile shaft. In this case, the shallower the pile penetration into a stiff clay stratum the greater the effect of this gap on the shaft resistance that develops. Hence, the adhesion factor for a given shear strength is reduced at shallow pile penetration depths and increased at deeper pile penetration depths.

In the case of H piles in cohesive soils, the shaft resistance should not be calculated from the surface area of the pile, but rather from the "box" area of the four sides. The shaft resistance for H-piles in cohesive soils consists of the sum of the adhesion, c_a , times the flange surface area along the exterior of the two flanges, plus the undrained shear strength of the soil, c_u , times the area of the two remaining sides of the "box", due to soil-to-soil shear along these faces. This computation can be approximated by determining the adhesion using the appropriate corrugated pile curve in Figure 9.18 and multiplying the adhesion by the H-pile "box" area. Additional information on the behavior of open pile sections is presented in Section 9.10.5.

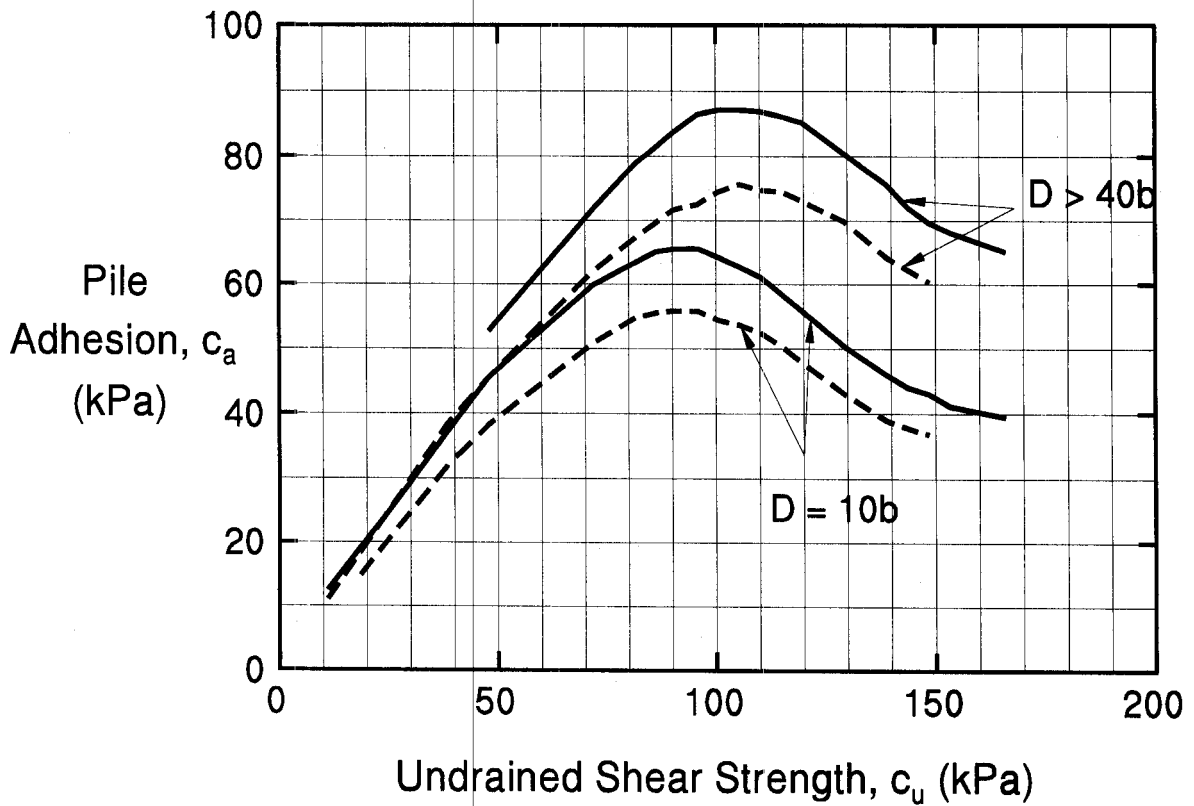
In clays with large shrink-swell potential, static capacity calculations should ignore the shaft resistance from the adhesion in the shrink-swell zone. During dry times, shrinkage will create a gap between the clay and the pile in this zone and therefore the shaft resistance should not be relied upon for long term support.

The unit toe resistance in a total stress analysis for homogeneous cohesive soil can be expressed as:

$$q_t = c_u N_c$$

The term N_c is a dimensionless bearing capacity factor which depends on the pile diameter and the depth of embedment. The bearing capacity factor, N_c , is usually taken as 9 for deep foundations.

It should be remembered that the movement required to mobilize the toe resistance is several times greater than that required to mobilize the shaft resistance. At the movement required to fully mobilize the toe resistance, the shaft resistance may have decreased to a residual value. Therefore, the toe resistance contribution to the ultimate pile capacity in cohesive soils is sometimes ignored except in hard cohesive deposits such as glacial tills.



— Concrete, Timber, Corrugated Steel Piles

- - - Smooth Steel Piles

D = Distance From Ground Surface to Bottom of Clay Layer or
Pile Toe; Whichever is Less

b = Pile Diameter

Figure 9.18 Adhesion Values for Piles in Cohesive Soils (after Tomlinson, 1979)

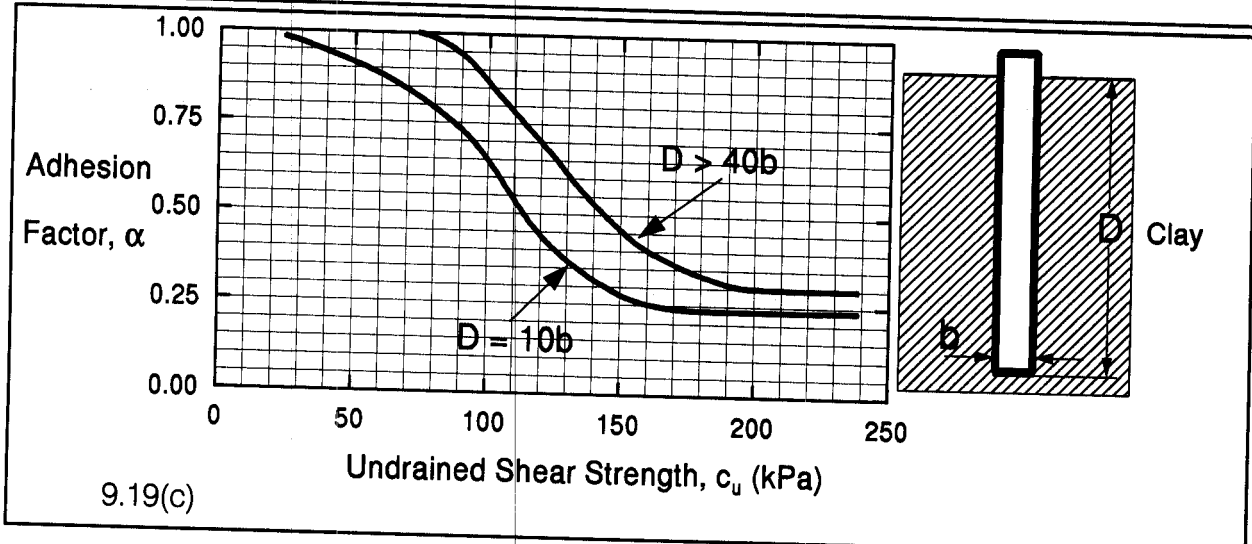
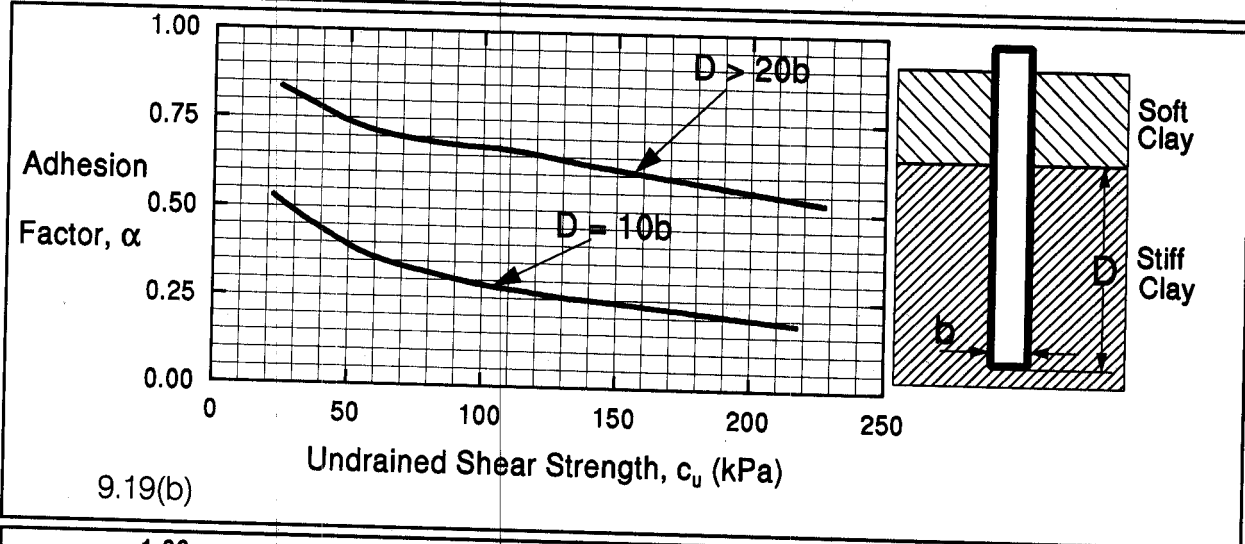
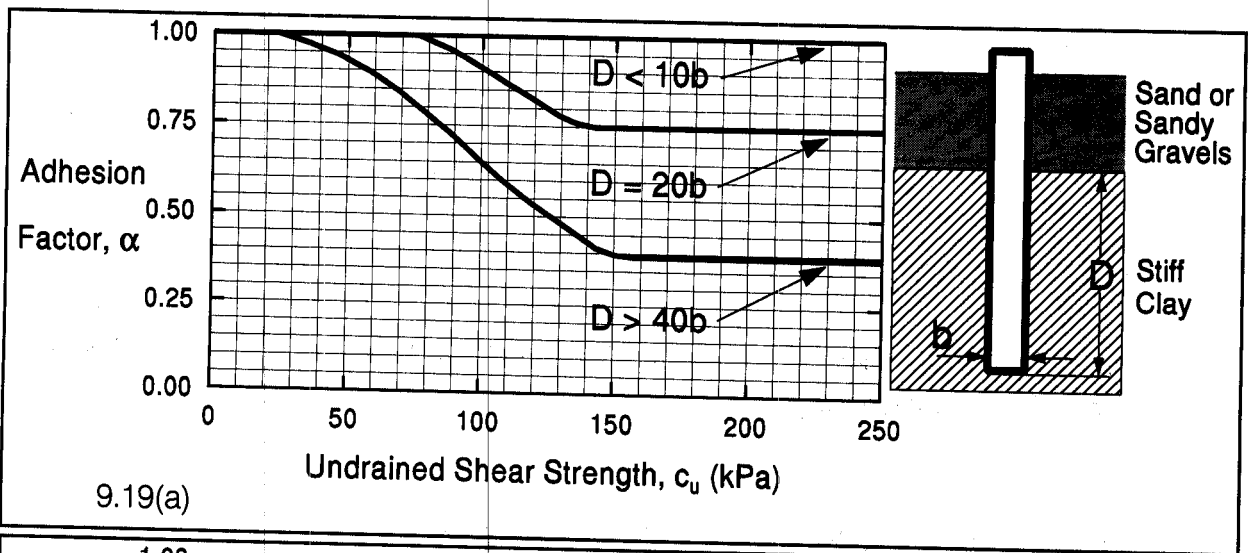


Figure 9.19 Adhesion Factors for Driven Piles in Clay (after Tomlinson, 1980)

STEP BY STEP PROCEDURE FOR - " α -METHOD"

STEP 1 Delineate the soil profile into layers and determine the adhesion, c_a , from Figure 9.18 or adhesion factor, α , from Figure 9.19 for each layer.

Enter appropriate figure with the undrained shear strength of the soil, c_u , and determine adhesion or adhesion factor based on the embedded pile length in clay, D , and pile diameter ratio, b . Use the curve for the appropriate soil and embedment condition.

STEP 2 For each soil layer, compute the unit shaft resistance, f_s (kPa).

$$f_s = c_a = \alpha c_u$$

Where: c_a = Adhesion.

STEP 3 Compute the shaft resistance in each soil layer and the ultimate shaft resistance, R_s (kN), from the sum of the shaft resistance from each layer.

$$R_s = f_s A_s$$

Where: A_s = Pile-soil surface area from pile perimeter and length.

A discussion on the behavior of open pile sections in cohesive soils is presented in Section 9.10.5.

STEP 4 Compute the unit toe resistance, q_t (kPa).

$$q_t = 9 c_u$$

Where: c_u = Undrained shear strength of soil at the pile toe.

STEP 5 Compute the ultimate toe resistance, R_t (kN).

$$R_t = q_t A_t$$

Where: A_t = Area of pile toe.

For open pile sections, refer to the discussion of pile plugging presented in Section 9.10.5.

STEP 6 Compute the ultimate pile capacity, Q_u (kN).

$$Q_u = R_s + R_t$$

STEP 7 Compute the allowable design load, Q_a (kN).

$$Q_a = \frac{Q_u}{\text{Factor of Safety}}$$

The factor of safety in this static calculation should be based on the specified construction control method as described in Section 9.6 of this chapter.

9.7.1.3 Effective Stress Method

Static capacity calculations in cohesionless, cohesive, and layered soils can also be performed using an effective stress based method. Effective stress based methods were developed to model the long term drained shear strength conditions. Therefore, the effective soil friction angle, ϕ' , should be used in parameter selection.

In an effective stress analysis, the unit shaft resistance is calculated from the following expression:

$$f_s = \beta \bar{p}_o$$

Where: β = Bjerrum-Burland beta coefficient = $K_s \tan \delta$.
 \bar{p}_o = Average effective overburden pressure along the pile shaft, (kPa).
 K_s = Earth pressure coefficient.
 δ = Friction angle between pile and soil.

The unit toe resistance is calculated from:

$$q_t = N_t p_t$$

Where: N_t = Toe bearing capacity coefficient.
 p_t = Effective overburden pressure at the pile toe.

Recommended ranges of β and N_t coefficients as a function of soil type and ϕ' angle from Fellenius (1991) are presented in Table 9-4. Fellenius notes that factors affecting the β and N_t coefficients consist of the soil composition including the grain size distribution, angularity and mineralogical origin of the soil grains, the original soil density and density due to the pile installation technique, the soil strength, as well as other factors. Even so, β coefficients are generally within the ranges provided and seldom exceed 1.0.

For sedimentary cohesionless deposits, Fellenius states N_t ranges from about 30 to a high of 120. In very dense non-sedimentary deposits such as glacial tills, N_t can be much higher, but can also approach the lower bound value of 30. In clays, Fellenius notes that the toe resistance calculated using an N_t of 3 is similar to the toe resistance calculated from a traditional analysis using undrained shear strength. Therefore, the use of a relatively low N_t coefficient in clays is recommended unless local correlations suggest higher values are appropriate.

Graphs of the ranges in β and N_t coefficients versus the range in ϕ' angle as suggested by Fellenius are presented in Figure 9.20 and 9.21, respectively. These graphs may be helpful in selection of β or N_t . The inexperienced user should select conservative β and N_t coefficients. As with any design method, the user should also confirm the appropriateness of a selected β or N_t coefficient in a given soil condition with local correlations between static capacity calculations and static load tests results.

It should be noted that the effective stress method places no limiting values on either the shaft or toe resistance.

TABLE 9-4 APPROXIMATE RANGE OF β AND N_t COEFFICIENTS (Fellenius, 1991)			
Soil Type	ϕ'	β	N_t
Clay	25 - 30	0.23 - 0.40	3 - 30
Silt	28 - 34	0.27 - 0.50	20 - 40
Sand	32 - 40	0.30 - 0.60	30 - 150
Gravel	35 - 45	0.35 - 0.80	60 - 300

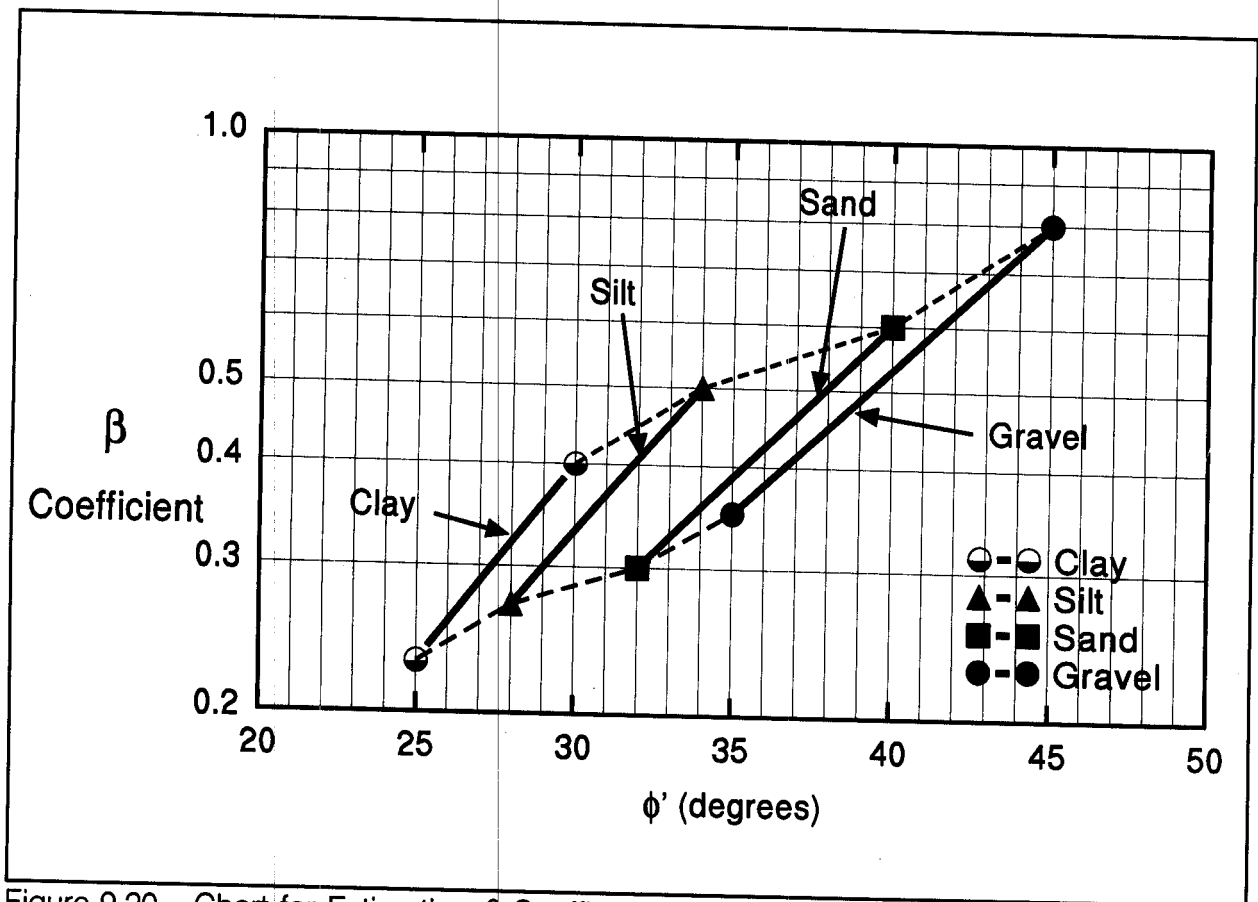


Figure 9.20 Chart for Estimating β Coefficient versus Soil Type ϕ' Angle (after Fellenius, 1991)

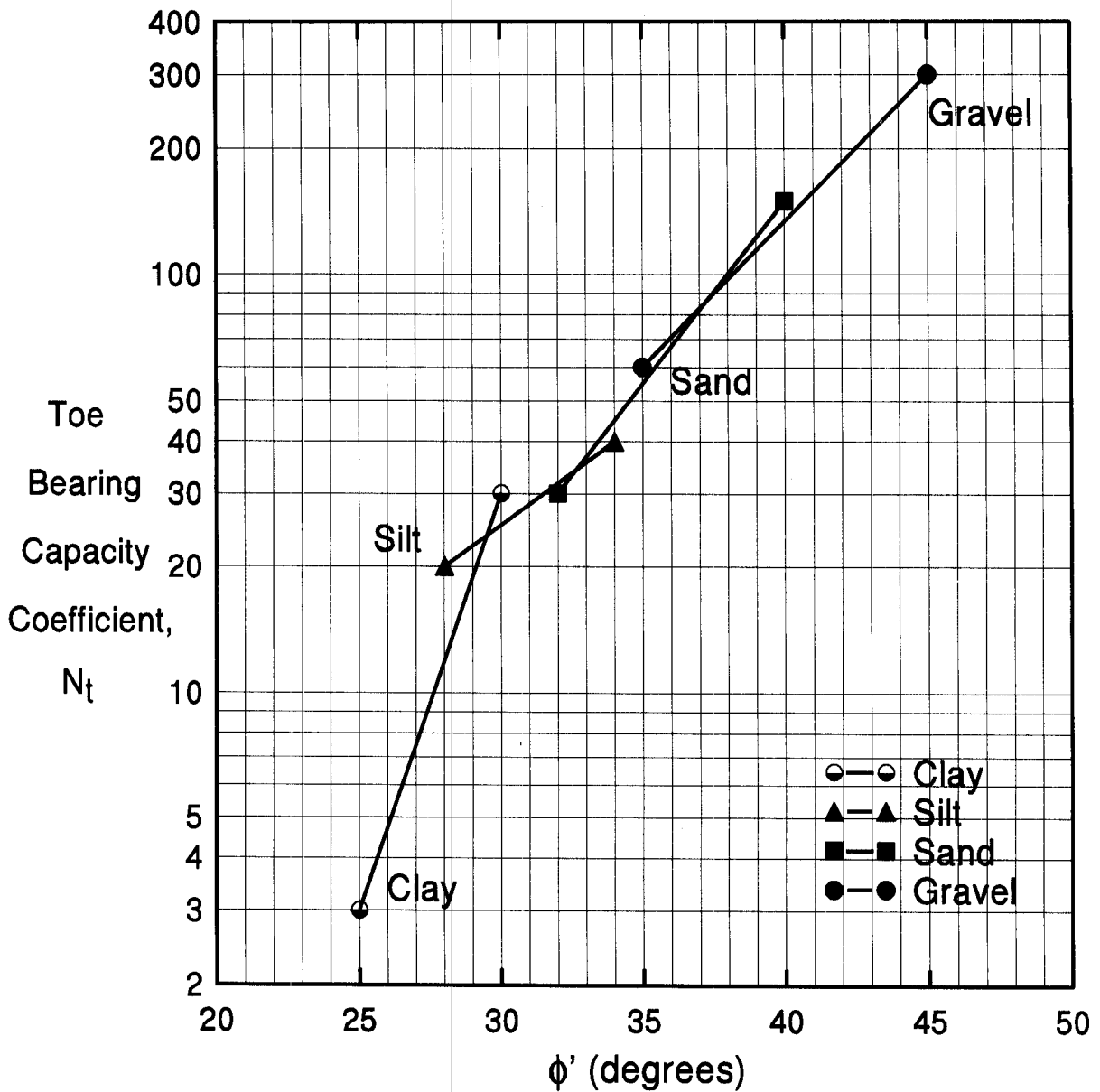


Figure 9.21 Chart for Estimating N_t Coefficients versus Soil Type ϕ' Angle (after Fellenius, 1991)

STEP BY STEP PROCEDURE FOR THE EFFECTIVE STRESS METHOD

- STEP 1 Delineate the soil profile into layers and determine ϕ' angle for each layer.
- Construct p_o diagram using previously described procedure in Section 9.4.
 - Divide soil profile throughout the pile penetration depth into layers and determine the effective overburden pressure, p_o , at the midpoint of each layer.
 - Determine the ϕ' angle for each soil layer from laboratory or in-situ test data.
 - In the absence of laboratory or in-situ data for cohesionless layers, determine the average corrected SPT N' value for each layer and estimate ϕ' angle from Table 4-5 in Chapter 4.

- STEP 2 Select the β coefficient for each soil layer.
- Use local experience to select β coefficient for each layer.
 - In the absence of local experience, use Table 9-4 or Figure 9.20 to estimate β coefficient from ϕ' angle for each layer.

- STEP 3 For each soil layer compute the unit shaft resistance, f_s (kPa).

$$f_s = \beta p_o$$

- STEP 4 Compute the shaft resistance in each soil layer and the ultimate shaft resistance, R_s (kN) from the sum of the shaft resistance from each soil layer.

$$R_s = f_s A_s$$

Where: A_s = Pile-soil surface area from pile perimeter and length.

Refer to Section 9.10.5 for additional information on the behavior of open pile sections.

STEP 5 Compute the unit toe resistance, q_t (kPa).

$$q_t = N_t p_t$$

- a. Use local experience to select N_t coefficient.
- b. In the absence of local experience, estimate N_t from Table 9-4 or Figure 9.21 based on ϕ' angle.
- c. Calculate the effective overburden pressure at the pile toe, p_t .

STEP 6 Compute the ultimate toe resistance, R_t (kN).

$$R_t = q_t A_t$$

Where: A_t = Area of the pile toe.

For open pile sections, refer to the additional information on pile plugging presented in Section 9.10.5.

STEP 7 Compute the ultimate pile capacity, Q_u (kN).

$$Q_u = R_s + R_t$$

STEP 8 Compute the allowable design load, Q_a (kN).

$$Q_a = \frac{Q_u}{\text{Factor of Safety}}$$

The factor of safety in this static calculation should be based on the specified construction control method as described in Section 9.6 of this chapter.

9.7.1.4 *Bearing Capacity of Piles in Layered Soils*

The bearing capacity of piles in layered soils can be calculated by combining the methods previously described for cohesionless and cohesive soils. For example, a hand calculation combining the Nordlund method from Section 9.7.1.1b for cohesionless soil layers with the α -method from Section 9.7.1.2a for cohesive soil layers could be used. The effective stress method as described in Section 9.7.1.3 could also be used for layered soil profiles. Last, the CPT based methods presented in Section 9.7.1.7 could be used in a layered soil profile.

9.7.1.5 *Bearing Capacity of Piles Using FHWA Computer Programs*

9.7.1.5a *The SPILE Computer Program*

The computer program SPILE was developed by the FHWA for calculation of pile capacities using the Nordlund and α -methods previously described in this chapter. The program users manual by Urzua (1993) is entitled SPILE: A Microcomputer Program for Determining Ultimate Vertical Static Pile Capacity and is available as FHWA-SA-92-044.

In the SPILE program the user inputs the soil profile to a planned pile toe depth. For each soil layer, the user selects the way in which the soil friction angle or adhesion is calculated. Variations in pile length and pile type are easily accommodated. The program can be used for closed end pipe, timber piles, circular or square solid concrete piles, H-piles, and Monotube piles. Piles types not handled by the SPILE program include open end pipe piles, concrete cylinder piles, and octagonal concrete piles. Program results include a summary of the pile shaft and toe resistance as well as the ultimate pile capacity. Typical program results are presented in the sample problems included in Appendix F.

Users of the SPILE program may find subtle differences between hand solutions and computer program results. One of the differences is in the selection of the ϕ angle in cohesionless soils. In the SPILE program, the ϕ angle can either be input by the user, using engineering judgment similar to this manual, or automatically calculated by the program using a correlation between corrected SPT N' values and ϕ . In addition to the possible difference between engineering judgment and the correlation used by the program, the SPILE program will also use ϕ angles with two decimal places in the calculation of results rather than a ϕ angle rounded to a degree or half degree that a hand solution would likely employ.

9.7.1.5b *The DRIVEN Computer Program*

The FHWA developed the computer program DRIVEN in 1998 for calculation of static pile capacity. In the DRIVEN program, the user inputs the soil profile consisting of the soil unit weights and strength parameters including the percentage strength loss during driving. For the selected pile type, the program calculates the pile capacity versus depth for the entire soil profile using the Nordlund and α -methods in cohesionless and cohesive layers, respectively. Using the user input soil strength losses, the program calculates the ultimate pile capacity at the time of driving as well as during restrike. The program also generates the soil input file required for a driveability study in the GRLWEAP wave equation program.

The DRIVEN program includes several analysis options that facilitate pile design. These options include:

Soft compressible soils: From a user input depth, the calculated shaft resistance from unsuitable soil layers is subtracted from the ultimate pile capacity calculation.

Scourable soils: Based on a user input depth, the calculated shaft resistance from scourable soils due to local scour is subtracted from the ultimate pile capacity calculation. In the case of channel degradation scour, the reduction in pile capacity from the loss of shaft resistance in the scour zone as well as the influence of the reduced effective overburden pressure from soil removal on the capacity calculated in the underlying layers is considered.

Pile Plugging: DRIVEN handles pile plugging based on the recommendations presented in Section 9.10.5 of this manual.

The DRIVEN program can be used to calculate the capacity of open and closed end pipe piles, H-piles, circular or square solid concrete piles, timber piles, and Monotube piles. The program results can be displayed in both tabular or graphical form. Analyses may be performed in either SI or English units and can be switched between units during analyses. The DRIVEN Program User's Manual by Mathias and Cribbs (1998) is provided in FHWA-SA-98-074.

9.7.1.6 Bearing Capacity of Piles on Rock

Pile foundations on rock are normally designed to carry large loads. For pile foundations which are driven to rock, which include steel H-piles, pipe piles or precast concrete piles, the exact area of contact with rock, the depth of penetration into rock as well as the quality of rock are largely unknown. Therefore, the determination of load capacity of driven piles on rock should be made on the basis of driving observations, local experience and load tests.

Rock Quality Designation (RQD) Values can provide a qualitative assessment of rock mass as shown in Table 9-5. The RQD is only for NX size or larger core samples (double tube core barrel) and is computed by summing the length of all pieces of core equal to or longer than 102 mm and dividing by the total length of the coring run. The result is multiplied by 100 to get RQD in percent. Fresh, irregular breaks should be ignored and the pieces counted as intact lengths.

RQD %	Rock Mass Quality
90-100	Excellent
75-90	Good
50-75	Fair
25-50	Poor
0-25	Very Poor

Except for soft weathered rock, the structural capacity of the pile will generally be lower than the capacity of rock to support loads for toe bearing piles on rock of fair to excellent quality as described in Table 9-5. The structural capacity, which is based on the allowable design stress for the pile material, will therefore govern the pile capacity in many cases. Small

diameter piles supported on fair to excellent quality rock may be loaded to their allowable structural capacity as described in Chapter 11. If H-piles are expected to penetrate to rock through soil deposits without obstructions and pile damage is unlikely, an allowable design stress of 0.33 times the steel yield stress should be used. Piles supported on soft weathered rock, such as shale or other types of very poor or poor quality, should be designed based on the results of pile load tests.

9.7.1.7 Methods Based on Cone Penetration Test (CPT) Data

When subsurface exploration programs include in-situ testing with a static cone penetrometer test (CPT), the CPT data can be used to estimate static capacity of single piles under axial loading. The CPT provides especially useful data as a "model pile" pushed into the strata expected to contribute resistance for a driven pile. The cone penetration resistance often correlates well with that of a driven full-sized pile under static loading conditions.

At sites where the cone soundings satisfactorily penetrate to the depths contemplated for driven piles, the CPT results can provide valuable information for estimating static pile capacities. At locations where a shallow stratum causes "refusal" conditions for the CPT device, it is likely that pile driveability problems could develop in the same stratum.

Two methods of analytical interpretation used to estimate static capacity of single piles under axial loading are the Nottingham and Schmertmann Method and the Laboratoire des Ponts et Chaussees or LPC Method. These CPT methods may be used to calculate pile capacities in cohesionless, cohesive, or layered soil profiles. Both methods are described in the following sections. Additional detailed information on these methods may be found in the FHWA publication FHWA-SA-91-043, "The Cone Penetrometer Test", by Briaud and Miran (1991).

9.7.1.7a Nottingham and Schmertmann Method

One empirical procedure commonly used in U.S. practice was derived from work originally published by Nottingham and Schmertmann (1975), and summarized in publication FHWA-TS-78-209, "Guidelines for Cone Penetration Test, Performance and Design" by Schmertmann (1978).

The ultimate shaft resistance, R_s , in cohesionless soils may be derived from unit sleeve friction of the CPT using the following expression:

$$R_s = K \left[\frac{1}{2} (\bar{f}_s A_s)_{0 \text{ to } 8b} + (\bar{f}_s A_s)_{8b \text{ to } D} \right]$$

- Where:
- K = Ratio of unit pile shaft resistance to unit cone sleeve friction from Figure 9.22 as a function of the full penetration depth, D .
 - \bar{f}_s = Average unit sleeve friction over the depth interval indicated by subscript.
 - A_s = Pile-soil surface area over f_s depth interval.
 - b = Pile width or diameter.
 - D = Embedded pile length.
 - 0 to $8b$ = Range of depths for segment from ground surface to a depth of $8b$.
 - $8b$ to D = Range of depths for segment from a depth equal to $8b$ to the pile toe.

The transfer function K , relating pile shaft resistance to CPT sleeve friction, varies as a function of total pile penetration (depth of embedment/pile diameter), pile material type, and type of cone penetrometer used. No limit was imposed on sleeve friction values in the procedure originally proposed by Nottingham and Schmertmann (1975).

If cone sleeve friction data is not available, R_s can be determined from the cone tip resistance as follows:

$$R_s = C_f \Sigma q_c A_s$$

- Where:
- C_f is obtained from Table 9-6 and
 - q_c = Average cone tip resistance along the pile length.
 - A_s = Pile - soil surface area.

TABLE 9-6 CPT C_f VALUES	
Type of Piles	C_f
Precast Concrete	0.012
Timber	0.018
Steel Displacement	0.012
Open End Steel Pipe	0.008

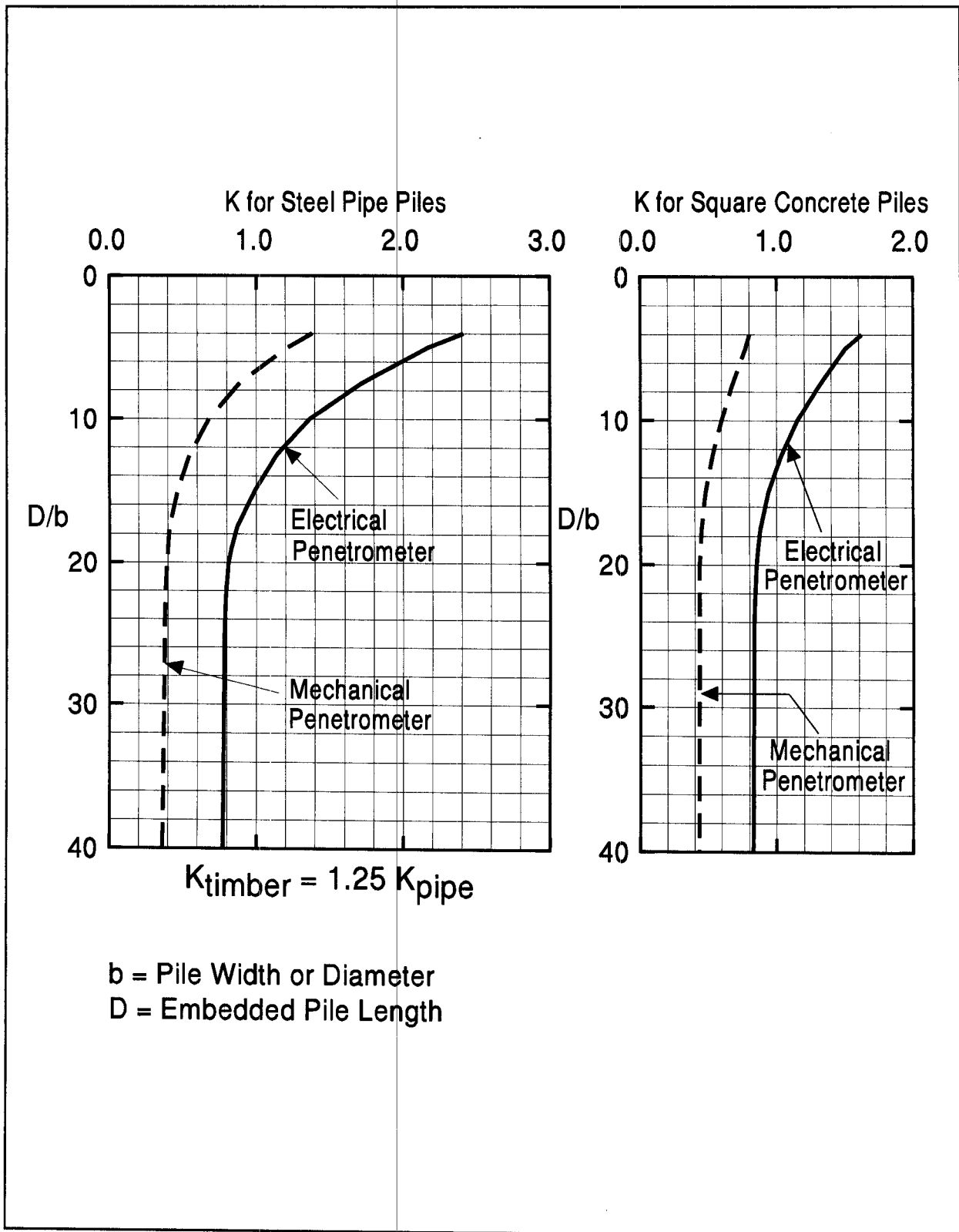


Figure 9.22 Penetrometer Design Curves for Pile Side Friction in Sand (after FHWA Implementation Package, FHWA-TS-78-209)

For shaft resistance in cohesive soils, the ultimate shaft resistance, R_s , is obtained from the sleeve friction values using the following expression:

$$R_s = \alpha' \bar{f}_s A_s$$

Where: α' = Ratio of pile shaft resistance to cone sleeve friction, patterned after Tomlinson's α -method.

The value of α' varies as a function of sleeve friction, f_s , value as shown in Figure 9.23. It is expected that this method of calculating pile shaft resistance is less appropriate in sensitive soils as the friction sleeve of the cone encounters severely disturbed soils behind the cone tip.

The estimation of pile toe ultimate capacity is described in Figure 9.24. In essence an elaborate averaging scheme is used to weight the cone tip resistance values, from 8 pile diameters above the pile toe, to as much as 3.75 pile diameters below the pile toe, favoring the lower cone tip resistance, q_c , values within the depth range. The authors make reference to a "limit" value of q_c between 5000 to 15000 kPa, that should be applied to the ultimate unit pile toe resistance, q_t , unless local experience warrants use of higher values. In the case of mechanical cone soundings in cohesive soils, the q_t value is reduced by 40 percent to account for end bearing effects on the base of the friction sleeve. As discussed in Section 9.10.5, careful consideration of soil plugging phenomena is needed in choosing the cross-sectional area over which q_t is applied for low displacement open ended pipe and H-piles.

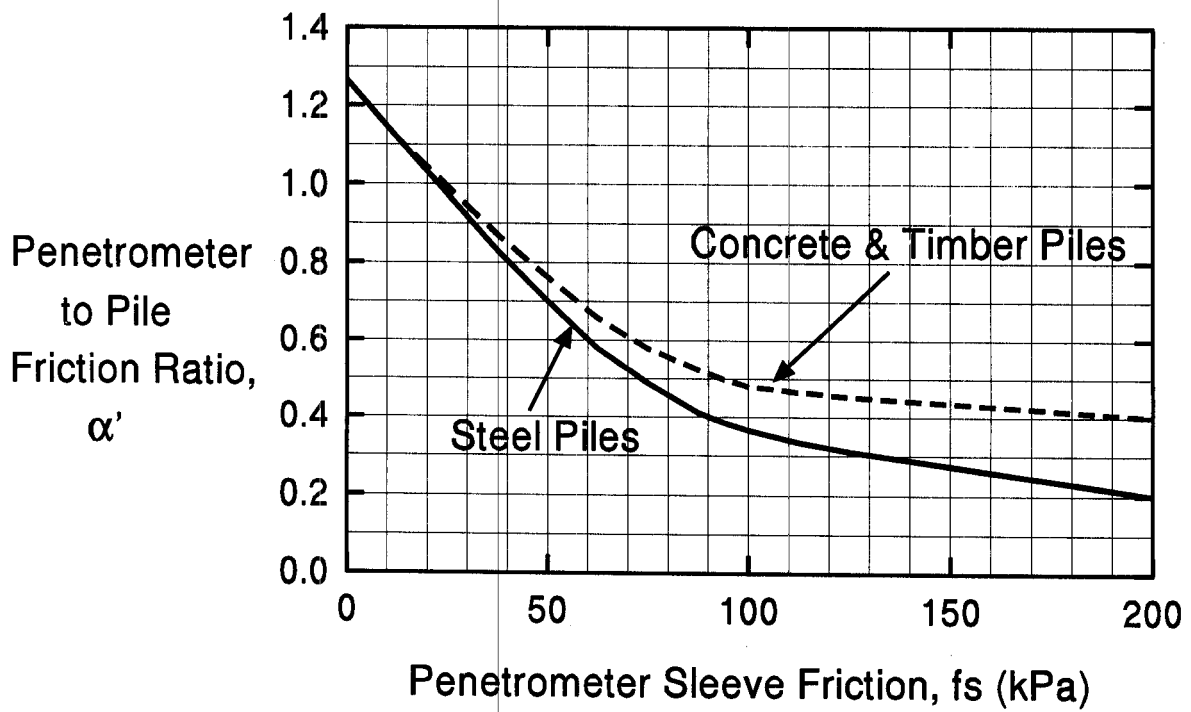


Figure 9.23 Design Curve for Pile Side Friction in Clay (after Schmertmann, 1978)

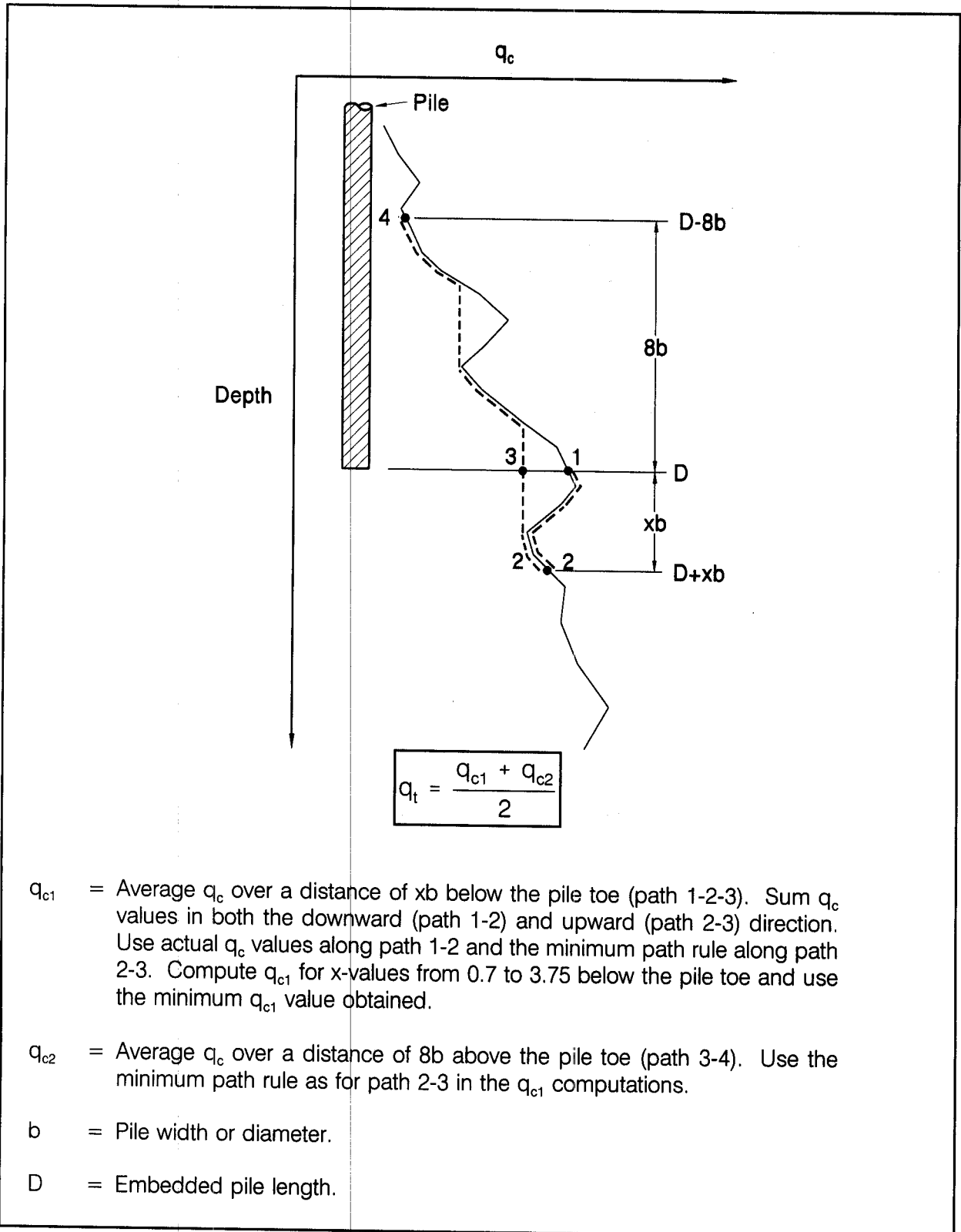


Figure 9.24 Illustration of Nottingham and Schmertman Procedure for Estimating Pile Toe Capacity (FHWA-TS-78-209).

STEP BY STEP PROCEDURE FOR THE NOTTINGHAM AND SCHMERTMANN METHOD

STEP 1 Delineate the soil profile into layers using the cone tip resistance, q_t , and sleeve friction, f_s , values.

STEP 2 Compute the shaft resistance for each soil layer, R_s (kN).

- a. For piles in cohesionless soils, compute ultimate shaft resistance, R_s , using the average sleeve friction value for the layer, \bar{f}_s , and the K value. Note that K should be determined using the full pile penetration depth to diameter ratio from Figure 9.22, and not the penetration depth for the layer. Conversely, the depth d corresponds to the pile toe depth, or the depth to the bottom of the layer, whichever is less. For H-piles in cohesionless soils, the pile-soil surface area A_s , should be the "box" area.

$$R_s = K \left[\frac{1}{2} (\bar{f}_s A_s)_{0 \text{ to } 8b} + (\bar{f}_s A_s)_{8b \text{ to } d} \right]$$

For cohesionless layers below a depth of $8b$, the above equation for shaft resistance in a layer reduces to:

$$R_s = K \bar{f}_s A_s$$

For piles in cohesionless soils without sleeve friction data, compute the ultimate shaft resistance from:

$$R_s = C_f \sum q_c A_s$$

Where: C_f is obtained from Table 9-6 and
 q_c = Average cone tip resistance along the pile length.

- b. For piles in cohesive soils, compute the ultimate shaft resistance using the average sleeve friction value for the layer from:

$$R_s = \alpha' \bar{f}_s A_s$$

Where: α' determined from Figure 9.23.

STEP 3 Calculate the total pile shaft resistance from the sum of the shaft resistances from each soil layer.

STEP 4 Compute the unit pile toe resistance, q_t (kPa).

$$q_t = \frac{q_{c1} + q_{c2}}{2}$$

Where: q_{c1} and q_{c2} = Unit cone tip resistance.

Use procedure shown in Figure 9.24 to determine q_t .

STEP 5 Determine the ultimate toe resistance, R_t (kN).

$$R_t = q_t A_t$$

Where: A_t = Pile toe area.

For steel H and unfilled open ended pipe piles, use only the steel cross section area at the pile toe unless there is reasonable assurance and previous experience that a soil plug would form. For a plugged condition use the "box" area of the H pile and the full cross section area for pipe pile. Additional information on the plugging of open pile sections is presented in Section 9.10.5.

STEP 6 Determine ultimate pile capacity, Q_u (kN).

$$Q_u = R_s + R_t$$

STEP 7 Determine allowable design load, Q_a (kN).

$$Q_a = \frac{Q_u}{\text{Factor of Safety}}$$

The factor of safety in this static calculation should be based on the specified construction control method as described in Section 9.6 of this chapter.

9.7.1.7b *Laboratoire des Ponts et Chaussees (LPC)*

The LPC method was developed and presented by Bustamante and Gianceselli (1983), based on empirical criteria taking into consideration soil type, pile type, and level of cone tip resistance. The approach considers only cone tip resistance, q_c , and factors soil type, pile type, installation method, and q_c , into determination of ultimate shaft resistance along the pile, contributed layer-by-layer, based on a family of prescribed curves. The resistance at the pile toe is calculated as the product of q_c and a cone bearing factor, K_c , that varies by soil type and pile installation method.

In the LPC method, the pile is categorized based on pile type and installation procedure as indicated in Table 9-7. Next Tables 9-8(a) and 9-8(b) are used to determine the shaft resistance design curve in Figures 9.25(a) or 9.25(b) to be used for each soil layer, based on the soil type, pile category and cone tip resistance. In Table 9-8(a), the method provides no guidance on whether to use design curve 1 or 2 when q_c is between 700 and 1200 kPa. Therefore it is recommended to interpolate between curves 1 or 2 when q_c is between 700 and 1200 kPa to determine the unit shaft resistance, f_s .

The unit toe resistance is calculated from the cone bearing capacity factor, K_c , obtained in Table 9-9, times the average cone resistance, q_c , within one pile diameter below the pile toe. This may be expressed in equation from as:

$$q_t = K_c q_c$$

In order to apply the CPT design procedures, it is necessary to characterize the subsurface materials as cohesive or cohesionless. The usual approach is to identify the "soil behavior" type as a function of cone tip resistance, q_c , and friction ratio, R_f . The friction ratio is the cone sleeve friction, f_s , divided by the cone tip resistance, or f_s/q_c . The soil classification chart presented in Figure 5.2 can then be used to characterize the soil as cohesive or cohesionless.

TABLE 9-7 DRIVEN PILE TYPE CATEGORIES FOR LPC METHOD		
Pile Type	Pile Description	Pile Installation Procedure
A	Driven prefabricated concrete piles.	Reinforced or prestressed concrete pile installed by driving or vibro-driving.
B	Driven steel piles.	Pile made of steel only and driven in place: H pile, pipe pile or any shape obtained by welding sheet-pile sections.
C	Driven prestressed concrete tube piles.	Made of hollow cylinder elements of lightly reinforced concrete assembled together by prestressing before driving. Each element is generally 1.5 to 3 m long and 0.7 to 0.9 m in diameter; the thickness is approximately 0.15 m. The piles are driven open-ended.

TABLE 9-8(a) CURVE SELECTION BASED ON PILE TYPE AND INSERTION PROCEDURES FOR CLAY AND SILT			
Curve No.	q_c (kPa)	Pile Type (see Table 9-7)	Comments on Insertion Procedure
1	<700	A, B, C	
2	>1200	A, B, C	For all steel piles, experience shows that, in plastic soils, f_s is often as low as curve 1. Therefore, use curve 1 in plastic soils when no previous load test data is available. For all driven concrete piles use curve 3 in low plasticity soils with sand or sand and gravel layers or containing boulders, and when $q_c > 2500$ kPa.
3	> 1200	A	For all driven concrete piles in low plasticity soils with sand or sand and gravel layers or containing boulders, and when $q_c > 2500$ kPa.

TABLE 9-8(b) CURVE SELECTION BASED ON PILE TYPE AND INSERTION PROCEDURES FOR SAND AND GRAVEL			
Curve No.	q_c (kPa)	Pile Type (see Table 9-7)	Comments on Insertion Procedure
1	<3500	A, B, C	
2	>3500	A, B, C	For fine sands. Since steel piles can lead to very small values of f_s in such soils, use curve 1 unless higher values can be based on load test results. For concrete piles, use curve 2 for fine sands of $q_c > 7500$ kPa.
3	>7500	A, B	For coarse gravelly sand or gravel only. For concrete piles, use curve 4 if it can be justified by a load test.
4	>7500	A	Only for coarse gravelly sand and gravel and, if justified, by load test.

TABLE 9-9 CONE BEARING CAPACITY FACTORS FOR LPC METHOD	
Type of Soil	Cone Bearing Factor, K_c
Clay-silt	0.600
Sand-gravel	0.375

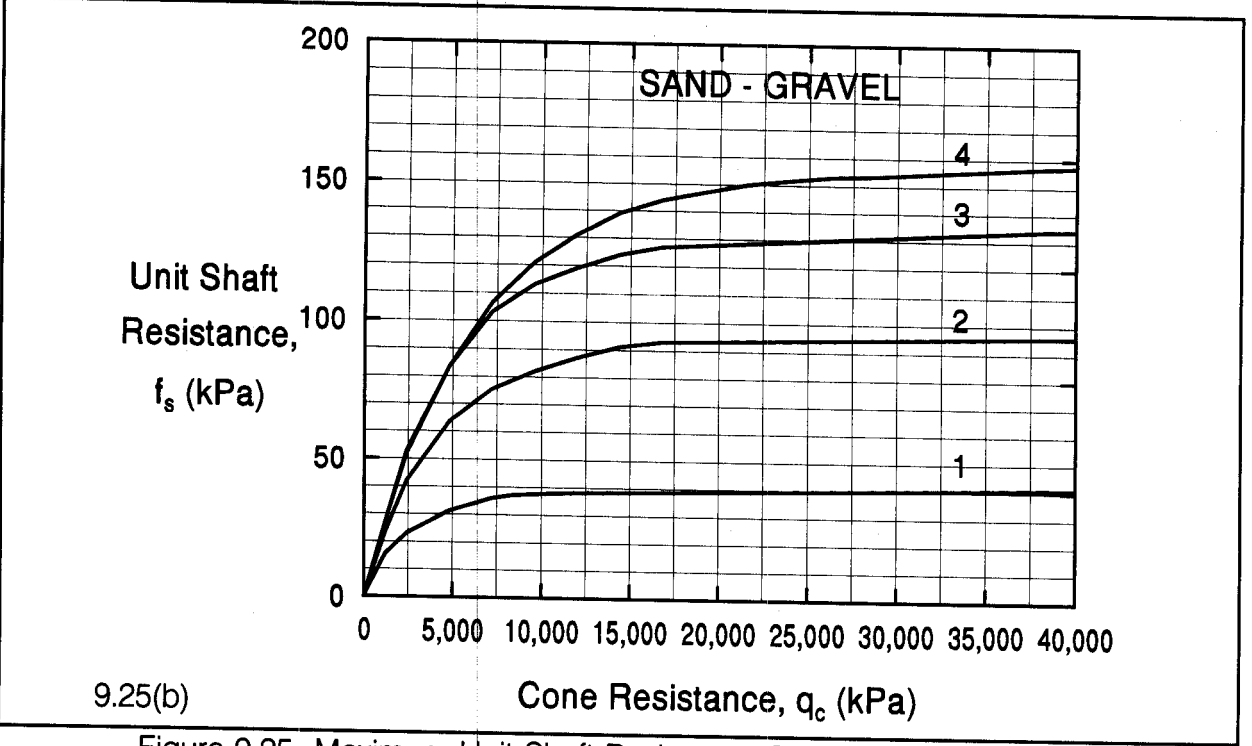
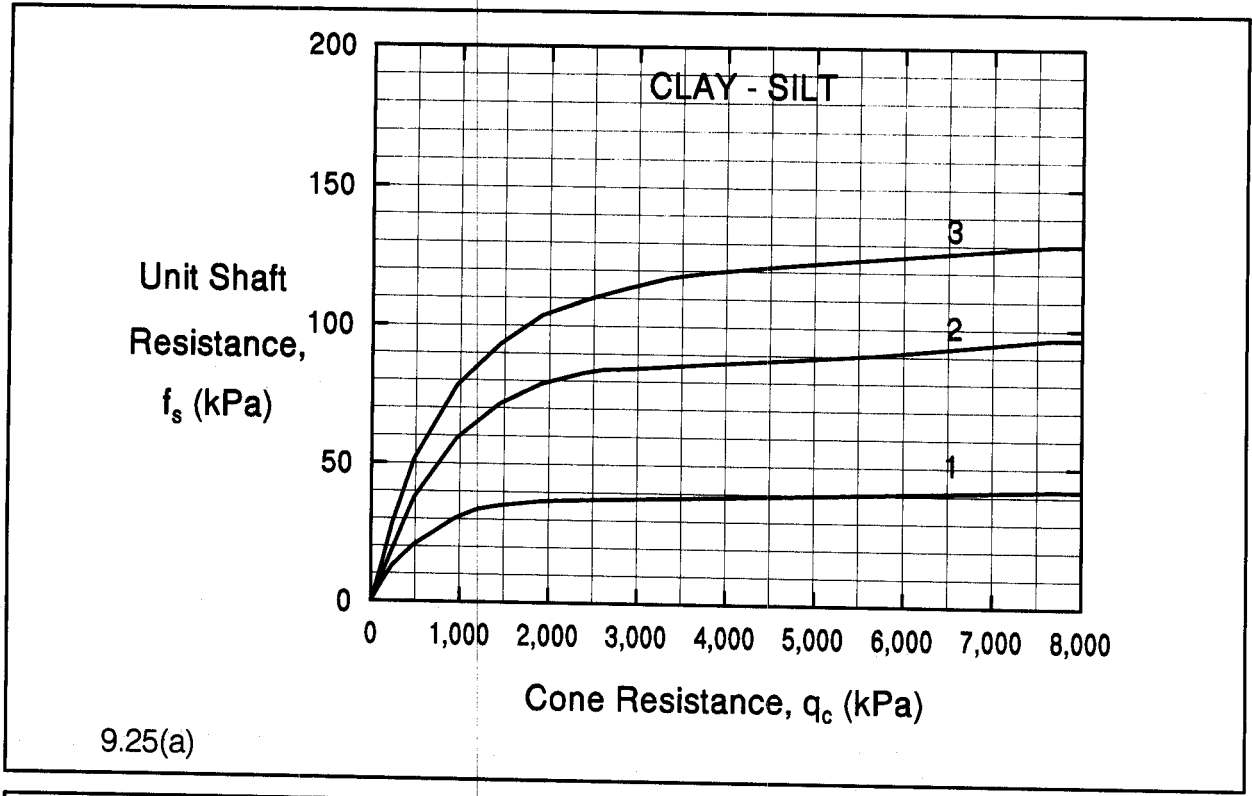


Figure 9.25 Maximum Unit Shaft Resistance Curves for LPC Method

STEP BY STEP PROCEDURE FOR THE LPC METHOD

STEP 1 Delineate the soil profile into layers using the cone tip resistance, q_c , and friction ratio, R_f , values.

Use Figure 5.2 to characterize each layer as cohesive or cohesionless.

STEP 2 Determine unit shaft resistance values for each soil layer, f_s (kPa).

a. Determine the average q_c value for each layer.

b. Use Table 9-8(a) or 9-8(b) to determine appropriate friction design curve in Figure 9.25(a), or Figure 9.25(b) based on pile type from Table 9-7 and soil characterization.

c. Enter Figures 9.25(a) or 9.25(b) with cone tip resistance, q_c , to determine layer unit shaft resistance, f_s (kPa).

STEP 3 Compute the shaft resistance in each soil layer and the ultimate shaft resistance, R_s (kN), from the sum of the shaft resistance from each soil layer.

$$R_s = f_s A_s$$

Where: A_s = Pile-soil surface area from pile perimeter and length.
For H-piles, the "box" area should be used.

STEP 4 Compute the unit pile toe resistance, q_t (kPa).

a. Average q_c value from pile toe to one diameter below pile toe.

b. Obtain cone bearing capacity factor, K_c , from Table 9-9:

c. Compute unit pile toe resistance from following equation.

$$q_t = K_c q_c$$

STEP 5 Compute the ultimate toe resistance, R_t (kN).

$$R_t = q_t A_t$$

Where: A_t = Pile toe area.

Note: For steel H and unfilled open ended pipe piles, use only the steel cross section area at the pile toe unless there is reasonable assurance and previous experience that a soil plug would form. For a plugged condition use the "box" area of the H pile and the full cross section area for pipe pile. Additional discussion on plugging of open pile sections is presented in 9.10.5.

STEP 6 Compute the ultimate pile capacity, Q_u (kN).

$$Q_u = R_s + R_t$$

STEP 7 Determine allowable design load, Q_a (kN).

$$Q_a = \frac{Q_u}{\text{Factor of Safety}}$$

The factor of safety in this static calculation should be based on the specified construction control method as described in Section 9.6 of this chapter.

9.7.2 Uplift Capacity of Single Piles

The design of piles for uplift loading conditions has become increasingly important for structures subject to seismic loading. In some cases, the pile uplift capacity determines the minimum pile penetration requirements. Nicola and Randolph (1993) note that in fine grained cohesive soils, where loading is assumed to occur under undrained conditions, the shaft resistance is generally considered equal in compression and in uplift.

In noncohesive or free draining soils, the uplift capacity of a pile has been more controversial. Nicola and Randolph (1993) state that it has been customary to assume that the shaft resistance in uplift is approximately 70% of the shaft resistance in compression. Based upon a finite difference parametric study, they concluded that a reduction in shaft resistance for uplift in free draining soils should be used, and that piles have lower uplift capacity than their compression shaft resistance. Conversely, the American Petroleum Institute's (1993) recommended design practice considers the pile shaft resistance to be equal in uplift and compression loading. Likewise, Altaee, *et al.*, (1992) presented a case of an instrumented pile in sand where the shaft resistance was approximately equal in compression and uplift when residual stresses were considered.

Tomlinson (1994) notes that the shaft resistance under cyclic loading is influenced by the rate of application of load as well as the degree of degradation of soil particles at the soil-pile interface. Under cyclic or sustained uplift loading in clays, the uplift resistance can decrease from the peak value to a residual value. In sands, particle degradation or reorientation can also result in decrease in uplift capacity under cyclic or sustained uplift loading. Therefore, the designer should consider what effect, if any, sustained or cyclic uplift loading will have on soil strength degradation.

Based on the above issues, the design uplift capacity of a single pile should be taken as $\frac{1}{3}$ of the ultimate shaft resistance calculated from any of the static analysis methods presented in this chapter except for the Meyerhof (SPT) method which should not be used. If a tensile load test is done for design confirmation, the design uplift load may be increased to $\frac{1}{2}$ of the tensile load test failure load as defined in Chapter 19. Selection of the design uplift load should also consider the potential for soil strength degradation due to the duration or frequency of uplift loading, which may not influence the load test results.

The uplift capacity of pile groups is discussed in Section 9.8.3. Tensile load test procedures are described by Kyfor *et al.* (1992) in FHWA-SA-91-042 and in Chapter 19.

9.7.3 Lateral Capacity of Single Piles

In addition to axial compression and uplift loads, piles are routinely subjected to lateral loads. Potential sources of lateral loads on bridge structures include vehicle acceleration and braking forces, wind loads, wave and current forces, debris loading, ice forces, vessel impact loads, earth pressures on the backs of abutment walls, slope movements, and seismic events. These lateral loads can be of the same magnitude as axial compressive loads and therefore warrant careful consideration during design. The foundation deformation under lateral loading must also be within the established performance criterion for the structure.

Historically, designers often used prescription values for the lateral load capacity of vertical piles, or added batter piles to increase a pile group's lateral capacity when it was believed that vertical piles could not provide the needed lateral resistance. However, vertical piles can be designed to withstand significant lateral loads. Modern analysis methods should be employed in the selection of the pile type and pile section.

Coduto (1994) notes that a foundation system consisting of only vertical piles designed to resist both axial and lateral loads is more flexible, and thus more effective at resisting dynamic loads, as well as less expensive to build. Bollmann (1993) reported that the Florida Department of Transportation often uses only vertical piles to resist lateral loads, including ship impact loads because vertical piles are often less expensive than batter piles. In areas where seismic lateral shaking is a serious concern, batter piles can deliver excessively large horizontal forces to the structure during the earthquake event. This phenomena was observed during the Loma Prieta earthquake of 1989 in California and discussed in greater detail by Hadjian *et al.* (1992). In earthquake areas, lateral loads should be resisted by ductile vertical piles, and batter piles should be avoided whenever possible.

Modern analysis methods are now readily available that allow the lateral load-deflection behavior of piles to be rationally evaluated. Lateral loads and moments on a vertical pile are resisted by the flexural stiffness of the pile and mobilization of resistance in the surrounding soil as the pile deflects. The flexural stiffness of a pile is defined by the pile's modulus of elasticity, E , and moment of inertia, I . The soil resistance to an applied lateral load is a combination of soil compression and shear resistance, as shown in Figure 9.26.

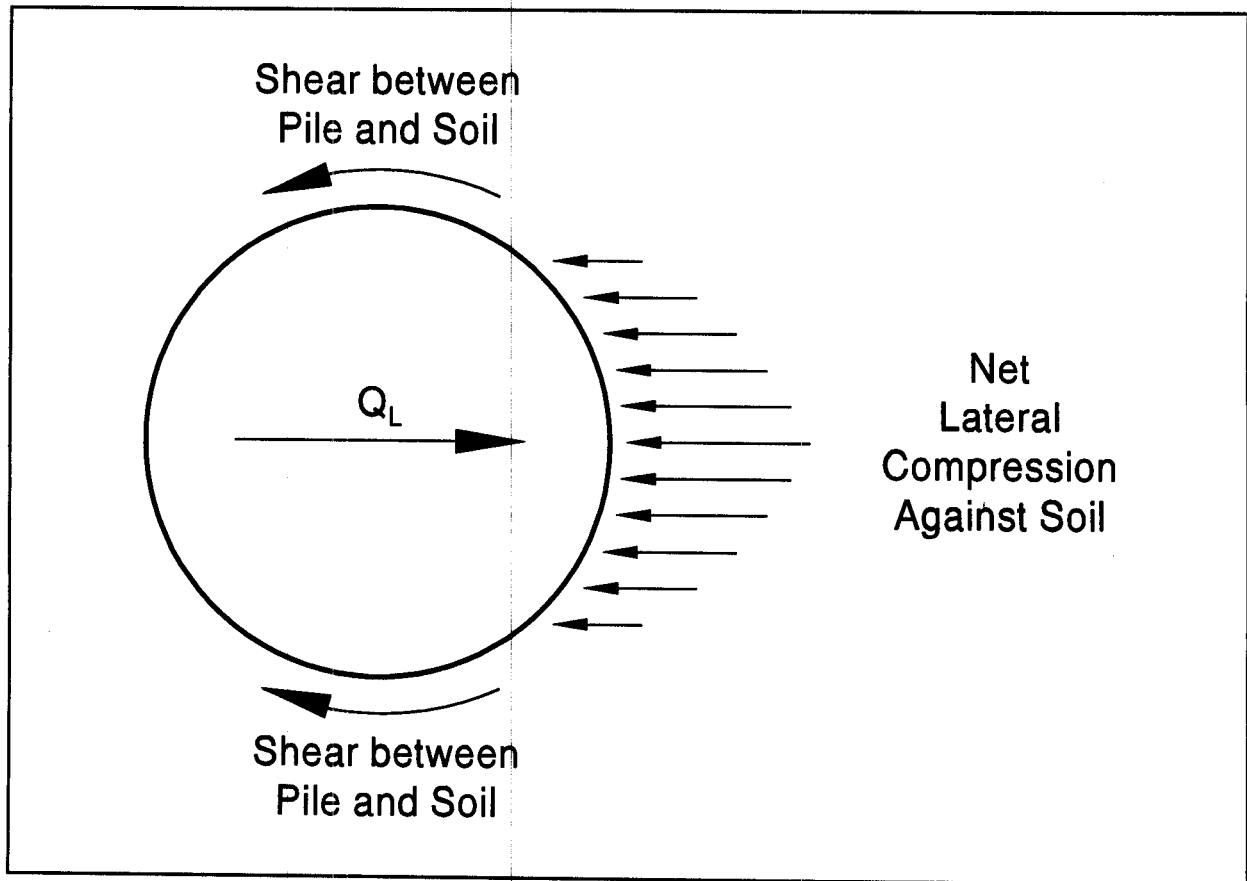


Figure 9.26 Soil Resistance to a Lateral Pile Load (adapted from Smith, 1989).

The design of laterally loaded piles must evaluate both the pile structural response and soil deformation to lateral loads. The factor of safety against both ultimate soil failure and pile structural failure must be determined. In addition, the pile deformation under the design loading conditions must be calculated and compared to foundation performance criteria.

The design of laterally loaded piles requires the combined skills of the geotechnical and structural engineer. It is inappropriate for the geotechnical engineer to analyze a laterally loaded pile without a full understanding of pile-structure interaction. Likewise it is inappropriate for the structural engineer to complete a laterally loaded pile design without a full understanding of how pile section or spacing changes may alter the soil response. Because of the interaction of pile structural and geotechnical considerations, the economical solution of lateral pile loading problems requires communication between the structural and geotechnical engineer.

Soil, pile, and load parameters have significant effects on the lateral load capacity of piles. The factors influencing these parameters are as follows:

1. Soil Parameters

- a. Soil type and physical properties such as shear strength, friction angle, density, groundwater level, and moisture content.
- b. Coefficient of horizontal subgrade reaction (kN/m^3). This coefficient is defined as the ratio between a horizontal pressure per unit area of vertical surface (kN/m^2) and the corresponding horizontal displacement (m). For a given deformation, the greater the coefficient, the greater the lateral load resistance.

2. Pile Parameters

- a. Physical properties such as shape, material, and dimensions.
- b. Pile head conditions (rotational constraint, if any).
- c. Method of pile placement such as driving, jetting, etc.
- d. Group action.

3. Lateral Load Parameters

- a. Static (monotonic or cyclic) or dynamic.
- b. Eccentricity (moment coupled with shear force).

9.7.3.1 *Lateral Capacity Design Methods*

The basic design approaches for lateral pile capacity analysis of vertical piles consist of lateral load tests or analytical methods. Both of these approaches are described in greater detail in the following sections.

1. Lateral Load Tests

Full scale lateral load tests can be conducted at a site during either the design or construction stage. The load-deformation data obtained is used to finalize or confirm the design for the particular site. Factors such as loading rate, cyclic (single or multi-directional) versus monotonic application of design forces, and levels of axial load components should be considered in developing appropriate field testing procedures. These tests may be time-consuming, costly, and cannot be justified on all projects. Chapter 19 provides additional details on lateral load test procedures and interpretation.

2. Analytical Methods

The analytical methods are based on theory and empirical data and permit the rational consideration of various site parameters. Two common approaches are Broms' (1964a, 1964b) hand calculation method and Reese's (1984) computer solution. Both approaches consider the pile to be analogous to a beam on an elastic foundation. FHWA publication FHWA-IP-84-11 by Reese (1984) presents details of both methods.

Broms' method provides a relatively easy hand calculation procedure to determine lateral loads and pile deflections at the ground surface. Broms' method ignores the axial load on the pile. For small projects, Broms' method may be used. However, when there are definitive limits on the allowable pile movements, a more detailed load-deformation analysis may still be required.

Reese's method is a more rigorous computer analysis using the COM624P program. Reese's method permits the inclusion of more complete modeling parameters of a specific problem. The program output provides distributions versus depth of moment, shear, soil and pile moduli, and soil resistance for the entire length of pile, including moments and shears in above ground sections.

For the design of all major pile foundation projects, Reese's more rigorous computer method should be used. The COM624P method is described in more detail in Section 9.7.3.3 Additional information on the COM624P program by Wang and Reese (1993) may be found in FHWA publication FHWA-SA-91-048.

9.7.3.2 Broms' Method

The Broms' method is a straight forward hand calculation method for lateral load analysis of a single pile. The method calculates the ultimate soil resistance to lateral load as well as the maximum moment induced in the pile. Broms' method can be used to evaluate fixed or free head conditions in either purely cohesive or purely cohesionless soil profiles. The method is not conducive to lateral load analyses in mixed cohesive and cohesionless soil profiles. For long fixed head piles in sands, the method can also overpredict lateral load capacities (Long, 1996). Therefore, for mixed profiles and for long fixed head piles in sands, the COM624P program should be used. A step by step procedure developed by the New York State Department of Transportation (1977) on the application of Broms' method is provided below.

STEP BY STEP PROCEDURE FOR BROMS' METHOD

- STEP 1 Determine the general soil type (*i.e.*, cohesive or cohesionless) within the critical depth below the ground surface (about 4 or 5 pile diameters).
- STEP 2 Determine the coefficient of horizontal subgrade reaction, K_h , within the critical depth for cohesive or cohesionless soils.

a. Cohesive Soils:
$$K_h = \frac{n_1 n_2 80 q_u}{b}$$

Where: q_u = Unconfined compressive strength (kPa).

b = Width or diameter of pile (m).

n_1 and n_2 = Empirical coefficients taken from Table 9-10.

b. Cohesionless Soils:

Choose K_h from the Table 9-11. (The values of K_h given in Table 9-11 were determined by Terzaghi.)

TABLE 9-10 VALUES OF COEFFICIENTS n_1 AND n_2 FOR COHESIVE SOILS	
Unconfined Compressive Strength, q_u , (kPa)	n_1
Less than 48 kPa	0.32
48 to 191 kPa	0.36
More than 191 kPa	0.40
Pile Material	n_2
Steel	1.00
Concrete	1.15
Wood	1.30

TABLE 9-11 VALUES OF K_h FOR COHESIONLESS SOILS		
Soil Density	K_h , (kN/m ³)	
	Above Ground Water	Below Ground Water
Loose	1900	1086
Medium	8143	5429
Dense	17644	10857

STEP 3 Adjust K_h for loading and soil conditions.

- a. Cyclic loading (for earthquake loading) in cohesionless soil:
 1. $K_h = \frac{1}{2} K_h$ from Step 2 for medium to dense soil.
 2. $K_h = \frac{1}{4} K_h$ from Step 2 for loose soil.
- b. Static loads resulting in soil creep (cohesive soils):
 1. Soft and very soft normally consolidated clays
 $K_h = (\frac{1}{3} \text{ to } \frac{1}{6}) K_h$ from Step 2.
 2. Stiff to very stiff clays
 $K_h = (\frac{1}{4} \text{ to } \frac{1}{2}) K_h$ from Step 2.

STEP 4 Determine pile parameters.

- a. Modulus of elasticity, E , (MPa).
- b. Moment of inertia, I , (m^4).
- c. Section modulus, S , (m^3) about an axis perpendicular to the load plane.
- d. Yield stress of pile material, f_y , (MPa) for steel or ultimate compression strength, f'_c , (MPa) for concrete.
- e. Embedded pile length, D , (m).
- f. Diameter or width, b , (m).
- g. Eccentricity of applied load e_c for free-headed piles - *i.e.*, vertical distance between ground surface and lateral load (m).
- h. Dimensionless shape factor C_s (for steel piles only):
 1. Use 1.3 for piles with circular cross section.
 2. Use 1.1 for H-section piles when the applied lateral load is in the direction of the pile's maximum resisting moment (normal to the pile flanges).
 3. Use 1.5 for H-section piles when the applied lateral load is in the direction of the pile's minimum resisting moment (parallel to the pile flanges).
- i. M_y , the resisting moment of the pile.
 1. $M_y = C_s f_y S$ (kN-m) (for steel piles).
 2. $M_y = f'_c S$ (kN-m) (for concrete piles).

STEP 5 Determine β_h for cohesive soils or η for cohesionless soils.

a. $\beta_h = \sqrt[4]{K_h b / 4EI}$ for cohesive soil, or

b. $\eta = \sqrt[5]{K_h / EI}$ for cohesionless soil.

STEP 6 Determine the dimensionless length factor.

a. $\beta_h D$ for cohesive soil, or

b. ηD for cohesionless soil.

STEP 7 Determine if the pile is long or short.

a. Cohesive soil:

1. $\beta_h D > 2.25$ (long pile).

2. $\beta_h D < 2.25$ (short pile).

Note: It is suggested that for $\beta_h D$ values between 2.0 and 2.5, both long and short pile criteria should be considered in Step 9, and then the smaller value should be used.

b. Cohesionless soil:

1. $\eta D > 4.0$ (long pile).

2. $\eta D < 2.0$ (short pile).

3. $2.0 < \eta D < 4.0$ (intermediate pile).

STEP 8 Determine other soil parameters over the embedded length of pile.

- a. The Rankine passive pressure coefficient for cohesionless soil, K_p .
 $K_p = \tan^2 (45 + \phi/2)$ where ϕ = angle of internal friction.
- b. The average effective unit weight of soil, γ' (kN/m³).
- c. The cohesion, c_u (kPa).
 $c_u = 1/2$ the unconfined compressive strength, q_u .

STEP 9 Determine the ultimate lateral load for a single pile, Q_u .

- a. Short Free or Fixed-Headed Pile in Cohesive Soil.

Using D/b (and e/b for the free-headed case), enter Figure 9.27, select the corresponding value of $Q_u/c_u b^2$, and solve for Q_u (kN).

- b. Long Free or Fixed-Headed Pile in Cohesive Soil.

Using $M_v/c_u b^3$ (and e/b for the free headed case), enter Figure 9.28, select the corresponding value of $Q_u/c_u b^2$, and solve for Q_u (kN).

- c. Short Free or Fixed-Headed Pile in Cohesionless Soil.

Using D/b (and e/D for the free-headed case), enter Figure 9.29, select the corresponding value of $Q_u/K_p b^3 \gamma$ and solve for Q_u (kN).

- d. Long Free or Fixed-Headed Pile in Cohesionless Soil.

Using $M_v/b^4 \gamma K_p$, (and e/b for the free headed case); enter Figure 9.30, select the corresponding value of $Q_u/K_p b^3 \gamma$ and solve for Q_u (kN).

- e. Intermediate Free or Fixed-Headed Pile in Cohesionless Soil.

Calculate Q_u for both a short pile (Step 9c) and long pile (Step 9d) and use the smaller value.

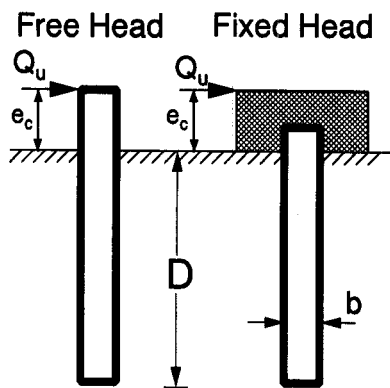
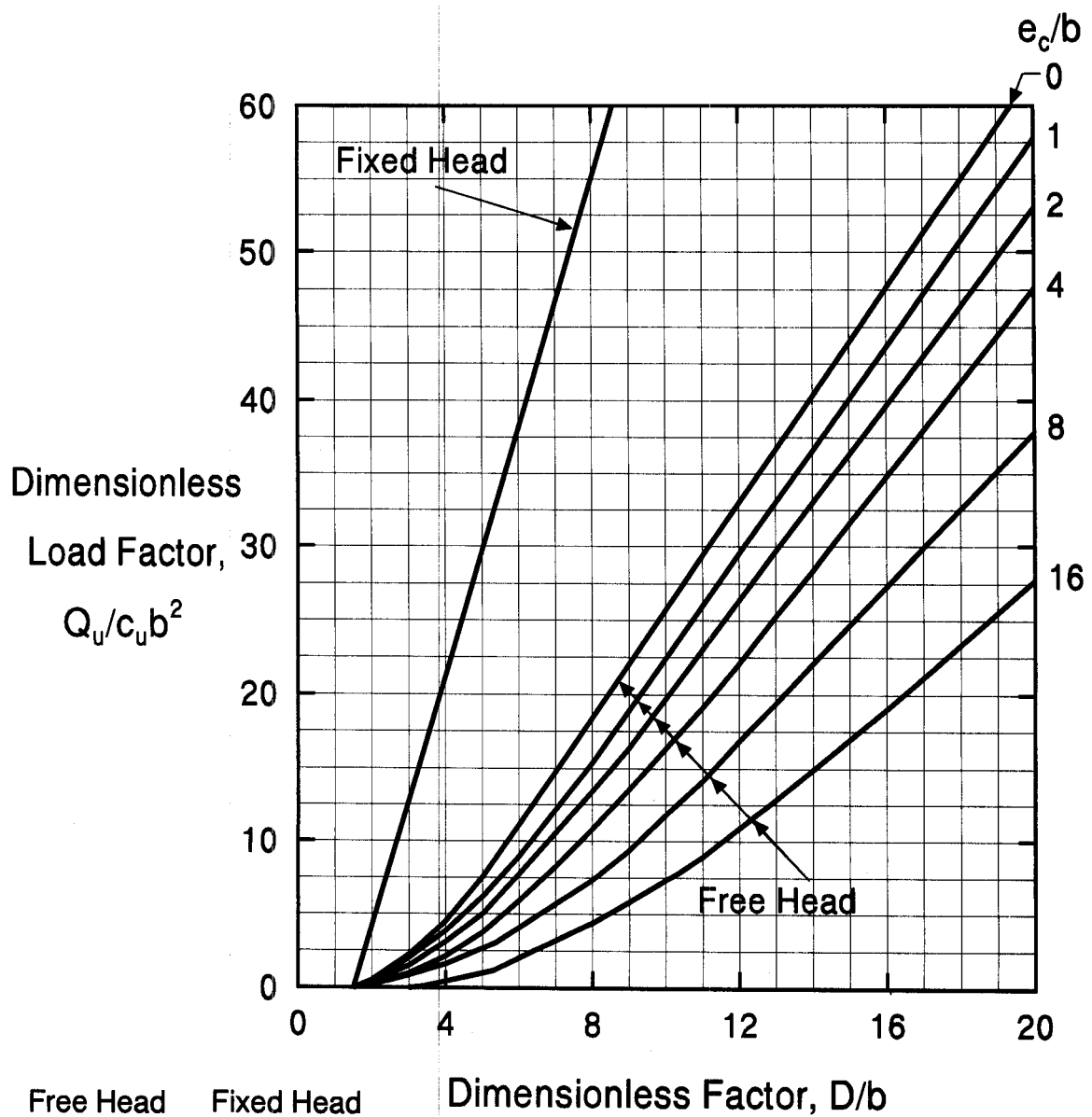


Figure 9.27 Ultimate Lateral Load Capacity of Short Piles in Cohesive Soils

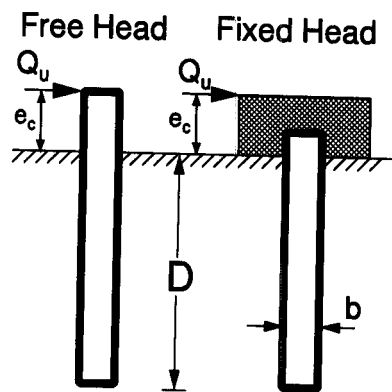
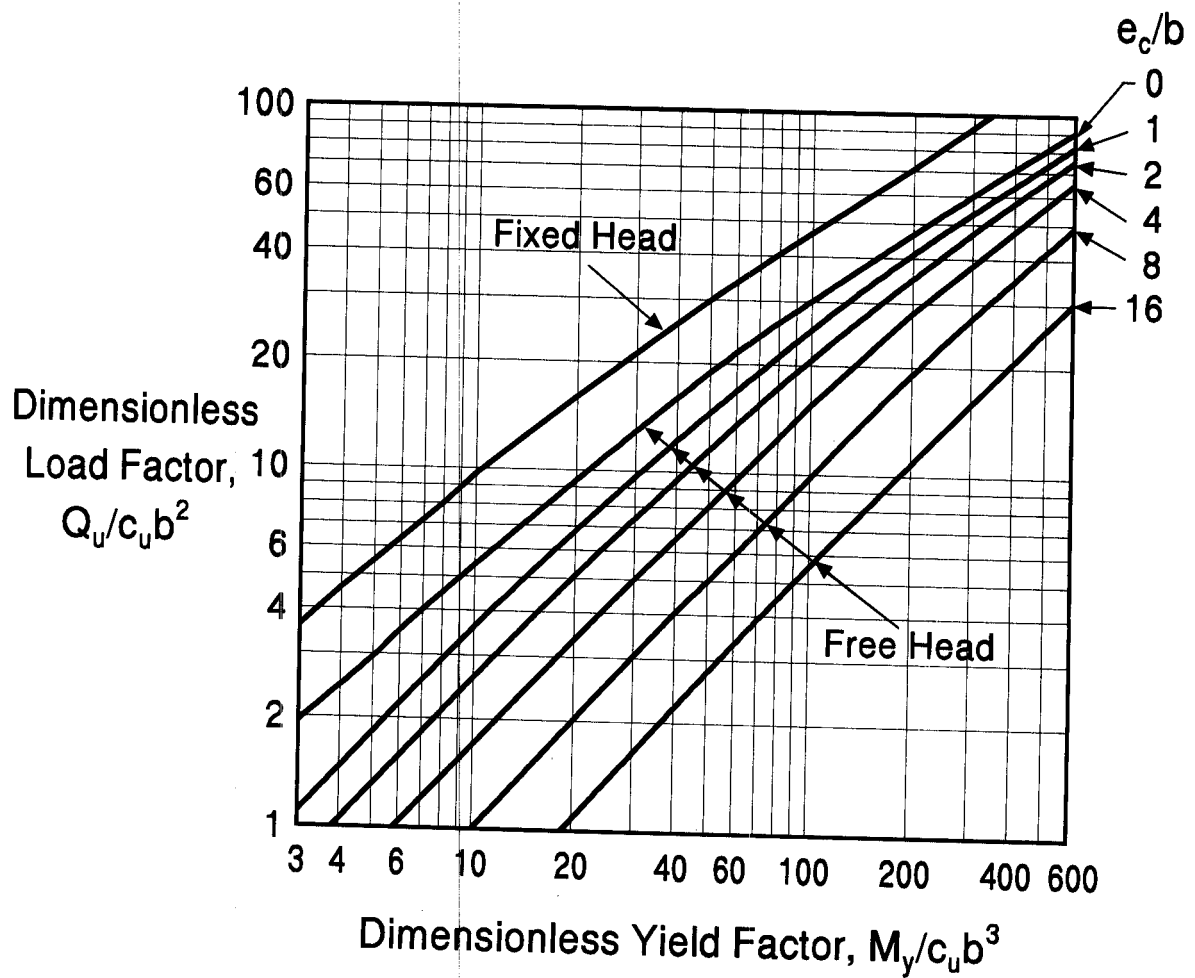


Figure 9.28 Ultimate Lateral Load Capacity of Long Piles in Cohesive Soils

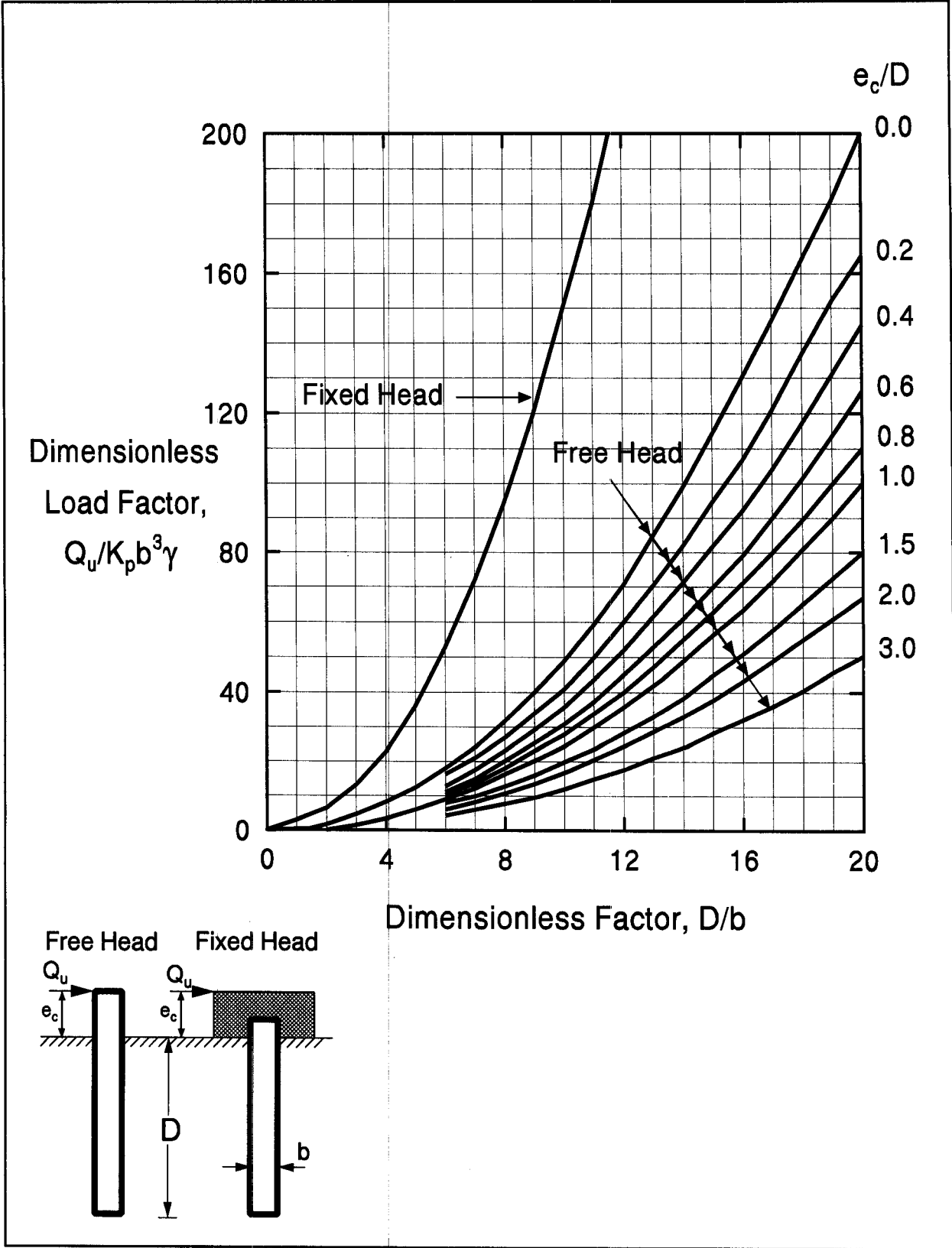


Figure 9.29 Ultimate Lateral Load Capacity of Short Piles in Cohesionless Soils

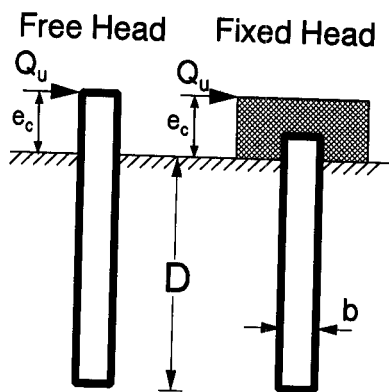
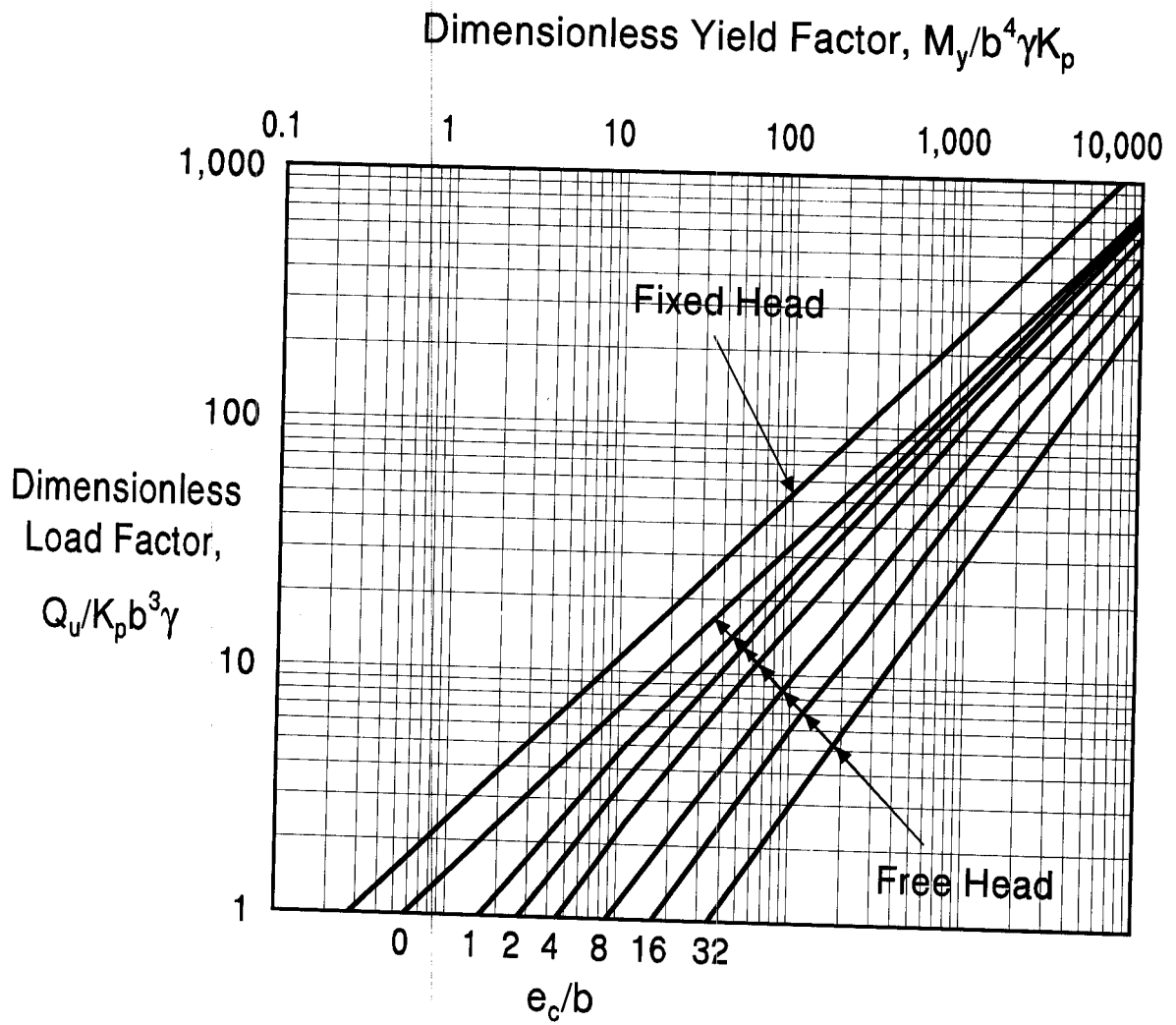


Figure 9.30 Ultimate Lateral Load Capacity of Long Piles in Cohesionless Soils

STEP 10 Calculate the maximum allowable working load for a single pile Q_m .

Calculate Q_m from the ultimate load Q_u determined in Step 9 as shown in Figure 9.31.

$$Q_m = \frac{Q_u}{2.5} \text{ (kN)}$$

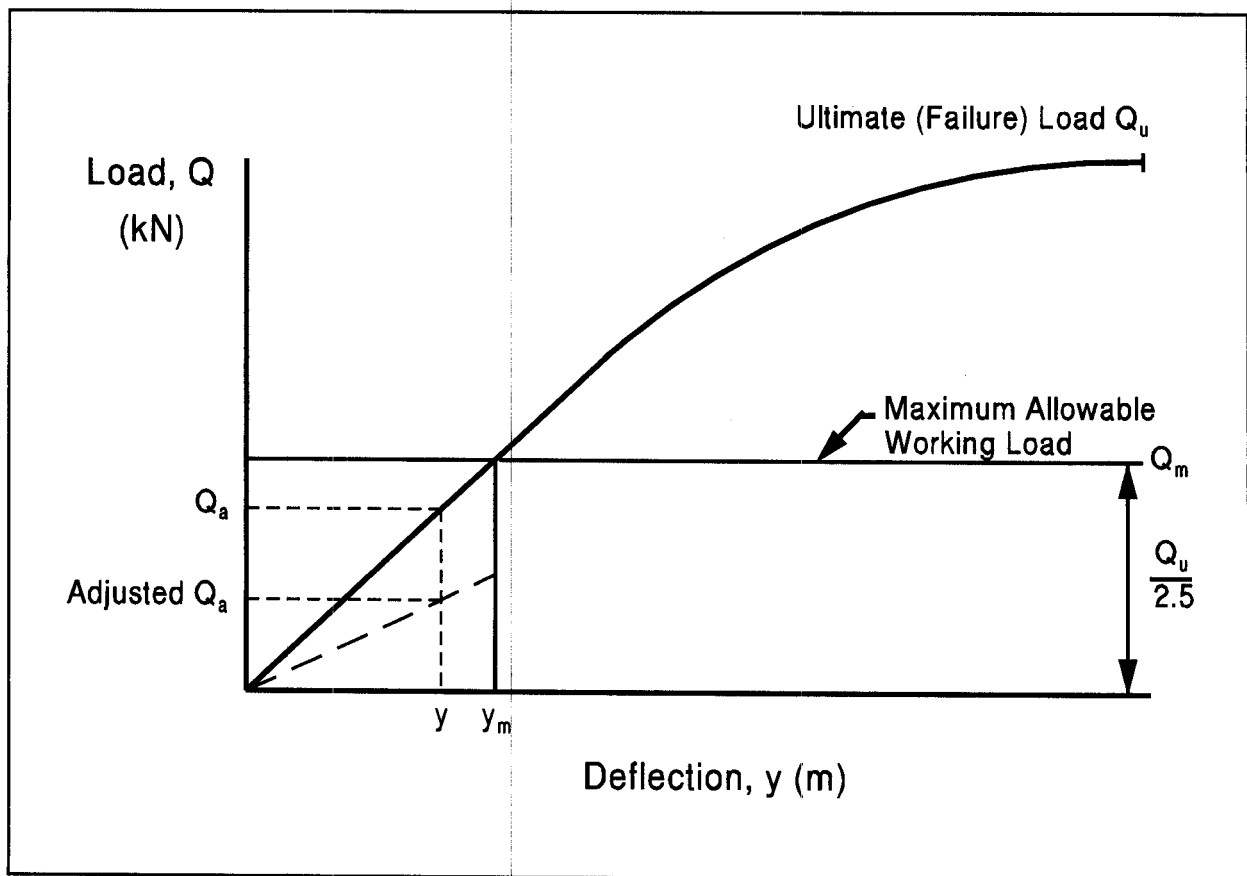


Figure 9.31 Load Deflection Relationship Used in Determination of Broms' Maximum Working Load

STEP 11 Calculate the working load for a single pile, Q_a (kN).

Calculate Q_a corresponding to a given design deflection at the ground surface y , (m) or the deflection corresponding to a given design load. If Q_a and y are not given, substitute the value of Q_m (kN) from Step 10 for Q_a in the following cases and solve for y_m (m):

a. Free or Fixed-Headed Pile in Cohesive Soil.

Using $\beta_n D$ (and e_c/D for the free-headed case), enter Figure 9.32, select the corresponding value of $yK_h bD/Q_a$, and solve for Q_a (kN) or y (m).

b. Free or Fixed-Headed Pile in Cohesionless Soil.

Using ηD (and e_c/D for the free-headed case), enter Figure 9.33, select the corresponding value of $y(EI)^{3/5} K_h^{2/5}/Q_a D$, and solve for Q_a (kN) or y (m).

STEP 12 Compare Q_a to Q_m .

If $Q_a > Q_m$, use Q_m and calculate y_m (Step 11).

If $Q_a < Q_m$ use Q_a and y .

If Q_a and y are not given, use Q_m and y_m .

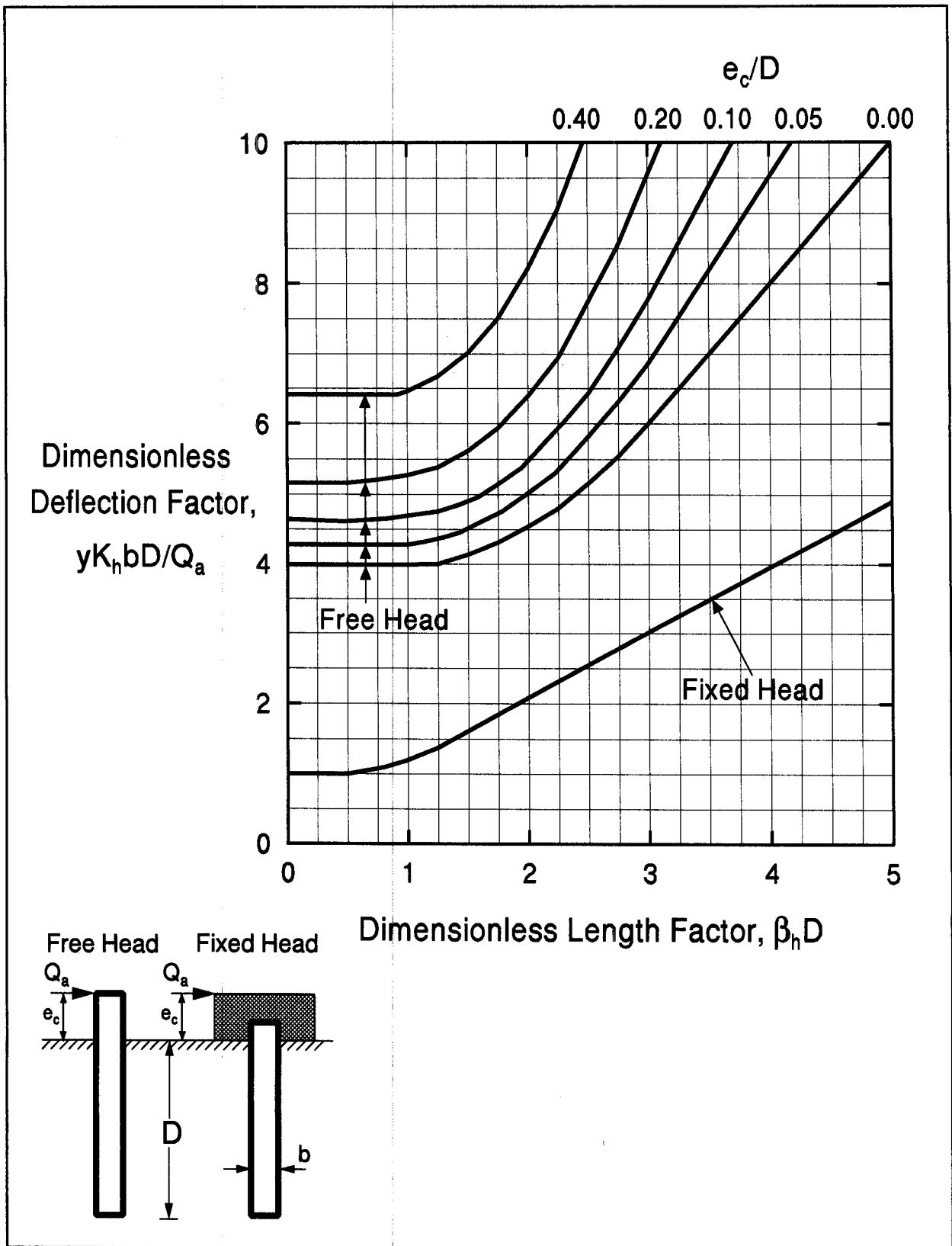


Figure 9.32 Lateral Deflection at Ground Surface of Piles in Cohesive Soils

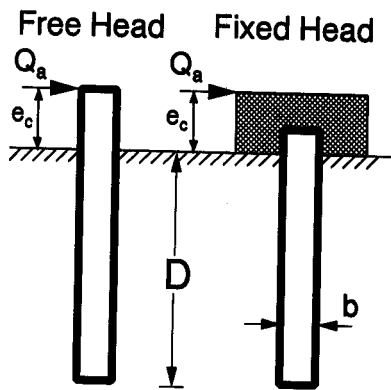
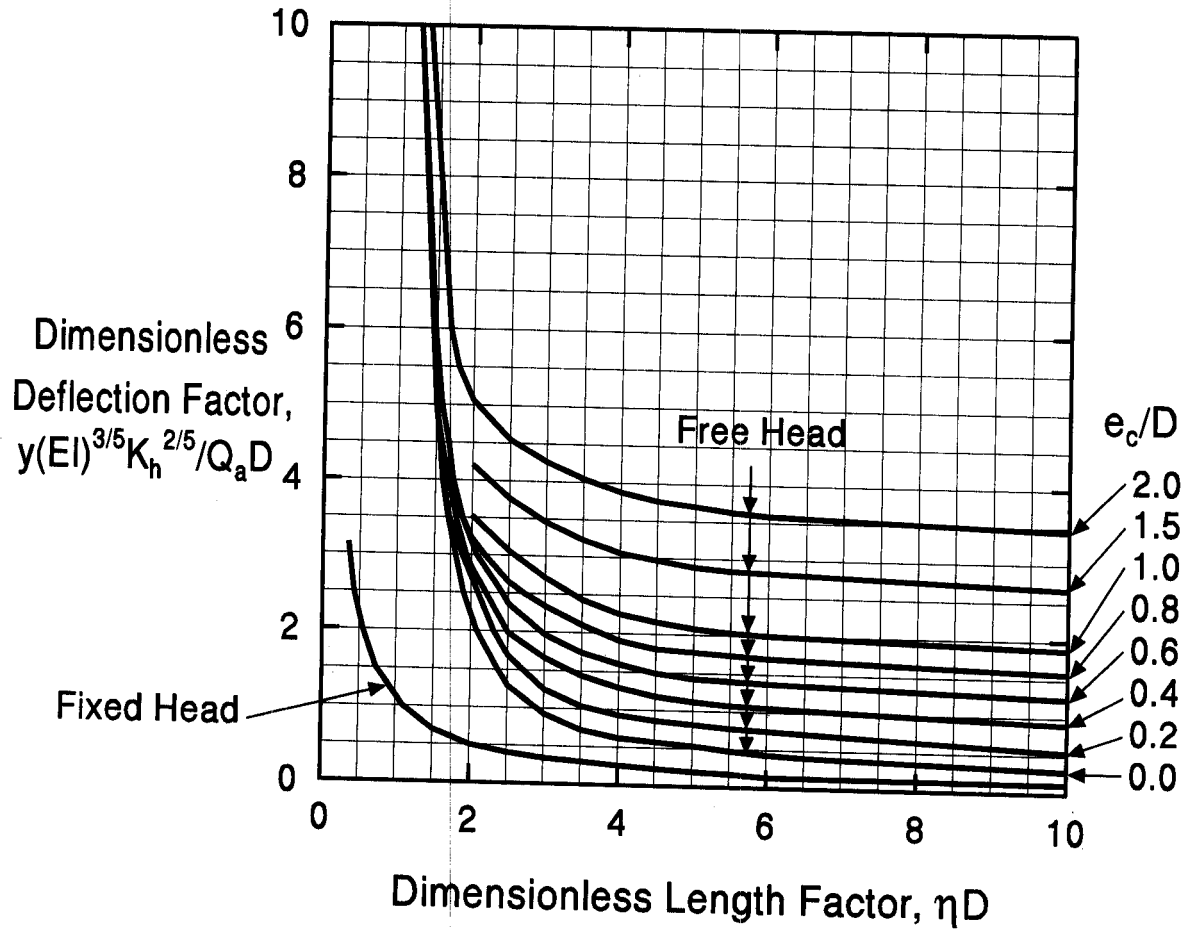
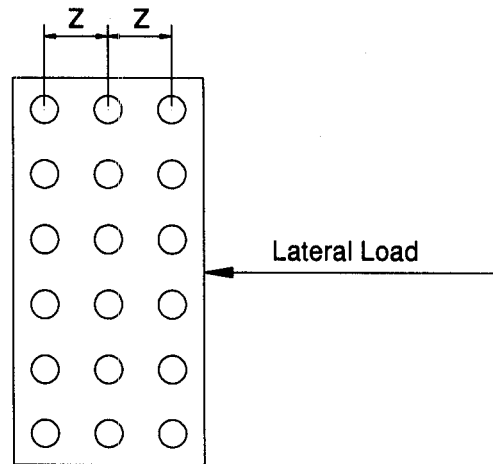


Figure 9.33 Lateral Deflection at Ground Surface of Piles in Cohesionless Soils

STEP 13 Reduce the allowable load from Step 12 for pile group effects and the method of pile installation.

- a. Group reduction factor determined by the center to center pile spacing, z , in the direction of load.

z	Reduction Factor
$8b$	1.0
$6b$	0.8
$4b$	0.5
$3b$	0.4



- b. Method of installation reduction factor.

1. For driven piles use no reduction.
2. For jetted piles use 0.75 of the value from Step 13a.

STEP 14 Determine pile group lateral capacity.

The total lateral load capacity of the pile group equals the adjusted allowable load per pile from Step 13b times the number of piles. The deflection of the pile group is the value selected in Step 12. It should be noted that no provision has been made to include the lateral resistance offered by the soil surrounding an embedded pile cap.

Special Note

Inspection of Figures 9.29 and 9.30 for cohesionless soils indicates that the ultimate load Q_u is directly proportional to γ , the effective soil unit weight. As a result, the ultimate load for short piles in submerged cohesionless soils will be about 50 percent of the value for the same soil in a dry state. For long piles, the reduction in Q_u is somewhat less than 50 percent due to the partially offsetting effect that the reduction in γ has on the dimensionless yield factor. In addition to these considerations, it should be noted that the coefficient of horizontal subgrade reaction K_h is less for the submerged case (Table 9-11) and thus the deflection will be greater than for the dry state.

9.7.3.3 Reese's COM624P Method

The interaction of a pile-soil system subjected to lateral load has long been recognized as a complex function of nonlinear response characteristics. The most widely used nonlinear analysis method is the p-y method, where p is the soil resistance per unit pile length and y is the lateral soil or pile deflection. This method, illustrated in Figure 9.34, models the soil resistance to lateral load as a series of nonlinear springs.

Reese (1984, 1986) has presented procedures for describing the soil response surrounding a laterally loaded pile for various soil conditions by using a family of p-y curves. The procedures for constructing these curves are based on experiments using full-sized, instrumented piles and theories for the behavior of soil under stress.

The soil modulus E_s is defined as follows:

$$E_s = - \frac{p}{y}$$

The negative sign indicates that the soil resistance opposes pile deflection. The soil modulus, E_s , is the secant modulus of the p-y curve and is not constant except over a small range of deflections. Typical p-y curves are shown in Figure 9.35. Ductile p-y curves, such as curve A, are typical of the response of soft clays under static loading and sands. Brittle p-y curves, such as curve B, can be found in some stiff clays under dynamic loading conditions.

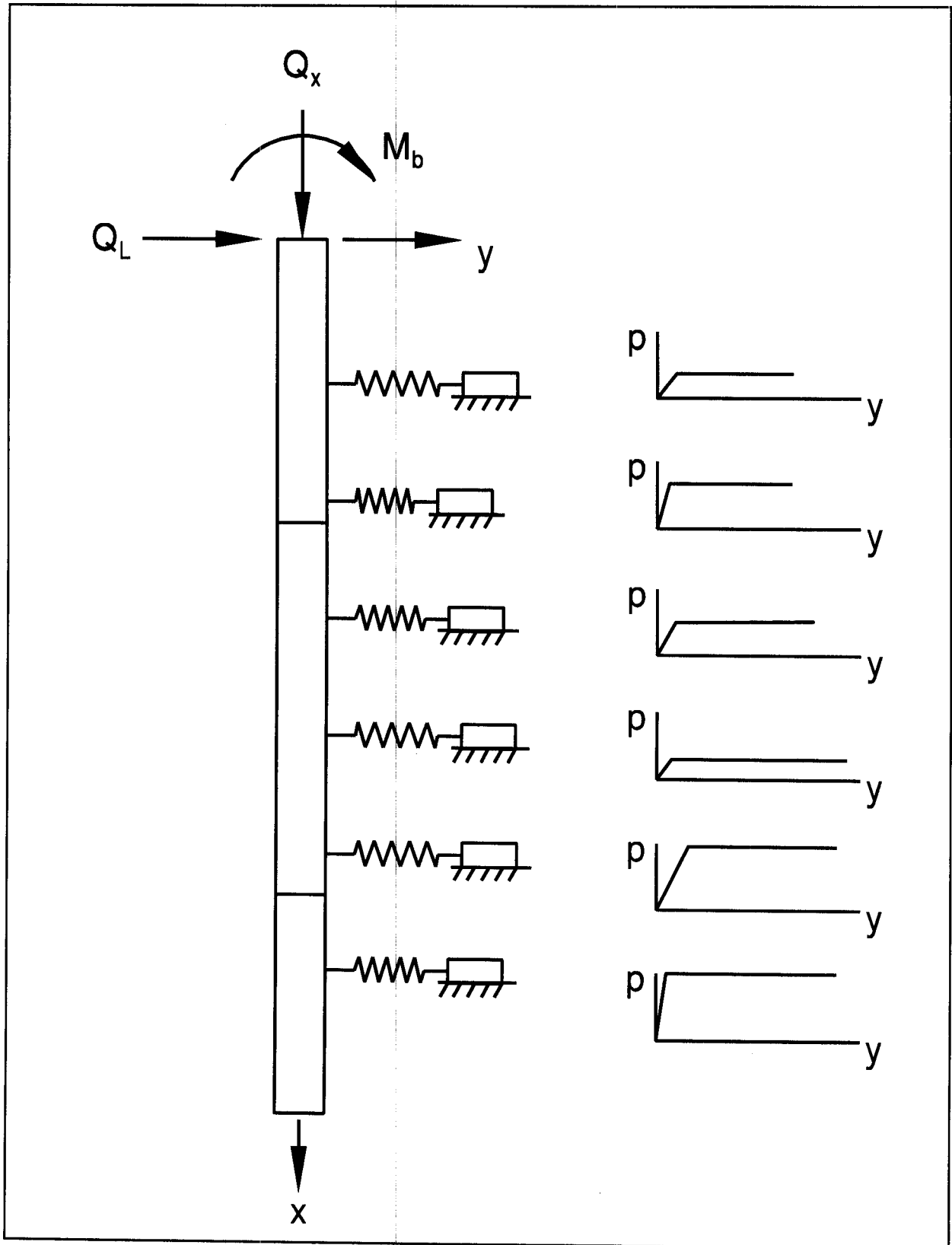


Figure 9.34 COM624P Pile-Soil Model

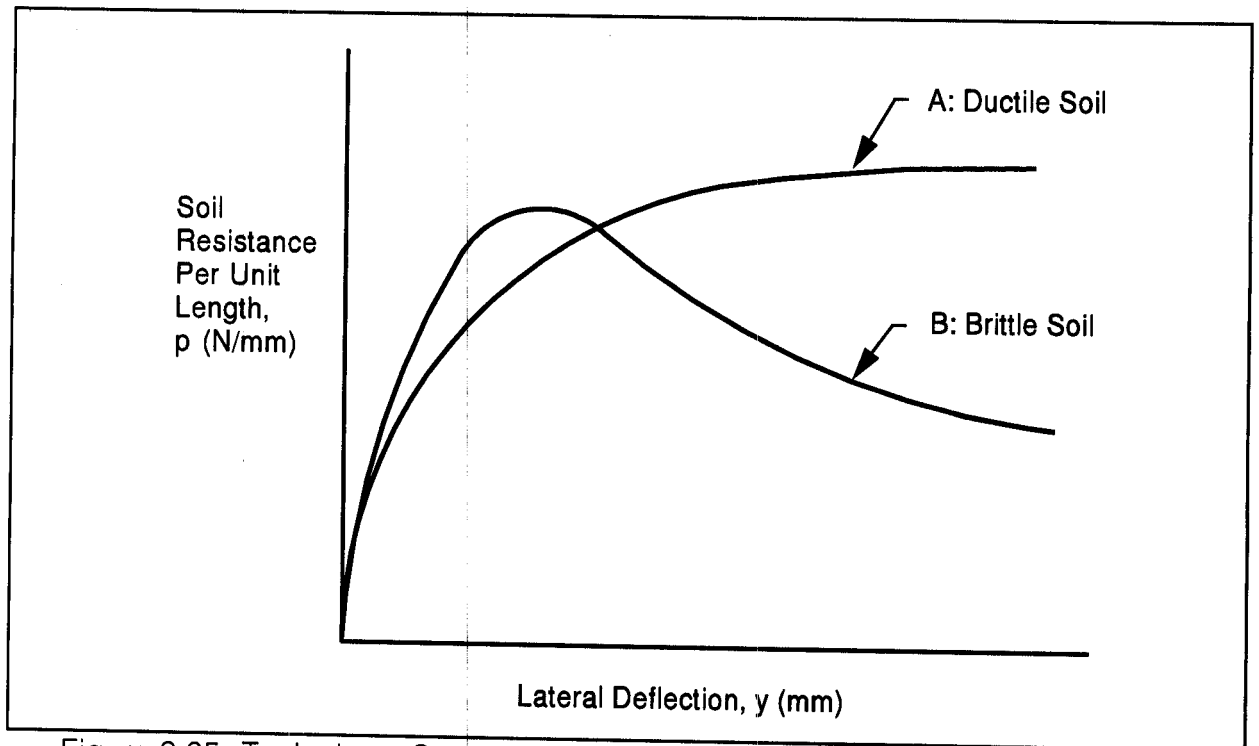


Figure 9.35 Typical p-y Curves for Ductile and Brittle Soil (after Coduto 1994).

The factor most influencing the shape of the p-y curve is the soil properties. However, the p-y curves also depend upon depth, soil stress-strain relationships, pile width, water table location, and loading conditions (static or cyclic). Procedures for constructing p-y curves for various soil and water table conditions as well as static or cyclic loading conditions are provided in the COM624P program documentation by Wang and Reese (1993) FHWA-SA-91-048.

Procedures for p-y curve development cover the following soil and water table conditions:

1. Soft clays below the water table.
2. Stiff clays below the water table.
3. Stiff clays above the water table.
4. Sands above or below the water table.

The COM624P program solves the nonlinear differential equations representing the behavior of the pile-soil system to lateral (shear and moment) loading conditions in a finite difference formulation using Reese's p-y method of analysis. The strongly nonlinear reaction of the surrounding soil to pile-soil deflection is represented by the p-y curve prescribed to act on each discrete element of the embedded pile. For each set of applied boundary (static) loads the program performs an iterative solution which satisfies static equilibrium and achieves an acceptable compatibility between force and deflection (p and y) in every element.

The shape and discrete parameters defining each individual p-y curve may be input by the analyst, but are most often generated by the program. Layered soil systems are characterized by conventional geotechnical data including soil type, shear strength, density, depth, and stiffness parameters, and whether the loading conditions are monotonic or cyclic in nature.

In Version 2.0 of the COM624P, the influence of applied loads (axial, lateral and moment) at each element can be modeled with flexural rigidity varying as a function of applied moment. In this manner, progressive flexural damage such as cracking in a reinforced concrete pile can be treated more rigorously. The COM624P program code includes a subroutine (PMEIX) which calculates the value of flexural rigidity at each element under the boundary conditions and resultant pile-soil interaction conditions.

COM624P problem data is input through a series of menu-driven screens. In most cases help screens are available. Detailed information concerning the software can be found in the FHWA publication FHWA-SA-91-048, COM624P - Laterally Loaded Pile Program for the Microcomputer, Version 2.0, by Wang and Reese (1993). Part I provides a User's Guide, Part II presents the theoretical background on which the program is based, and Part III deals with System Maintenance. The appendices include useful guidelines for integrating COM624P analyses into the overall design process for laterally loaded deep foundations, and a comprehensive case study example implementing the design guidelines.

The COM624P computer printout file summarizes the input information and the analysis results. The input data summarized includes the pile geometry and properties, and soil strength data. Output information includes the generated p-y curves at various depths below the pile head and the computed pile deflections, bending moments, stresses and soil moduli as functions of depth below the pile head. This information allows an

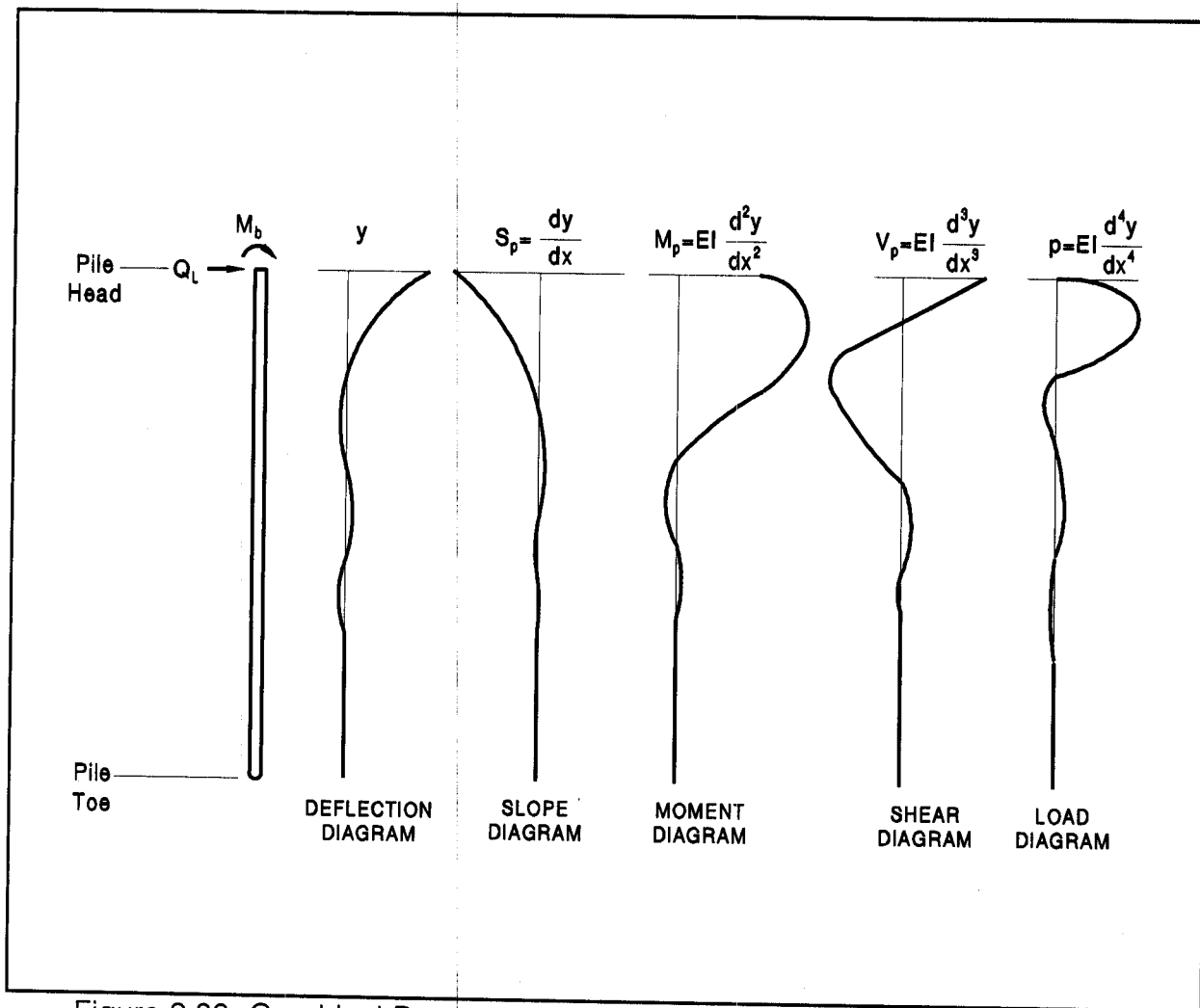


Figure 9.36 Graphical Presentation of COM624 Results (after Reese, 1986).

analysis of the pile's structural capacity. Internally generated (or input) values of flexural rigidity for cracked or damaged pile sections are also output. Graphical presentations versus depth include the computed deflection, slope, moment, and shear in the pile, and soil reaction forces similar to those illustrated in Figure 9.36.

The COM624P analyses characterize the behavior of a single pile under lateral loading conditions. A detailed view is obtained of the load transfer and structural response mechanisms to design conditions. Considerable care is required in extrapolating the results to the behavior of pile groups (pile-soil-pile interaction, etc.), and accounting for the effects of different construction processes such as predrilling or jetting.

In any lateral analysis case, the analyst should verify that the intent of the modeling assumptions, all elastic behavior for example, is borne out in the analysis results. When a lateral load test is performed, the measured load-deflection results versus depth should be plotted and compared with the COM624P predicted behavior so that an evaluation of the validity of the p-y curves used for design can be made, such as that presented in Figure 9.37.

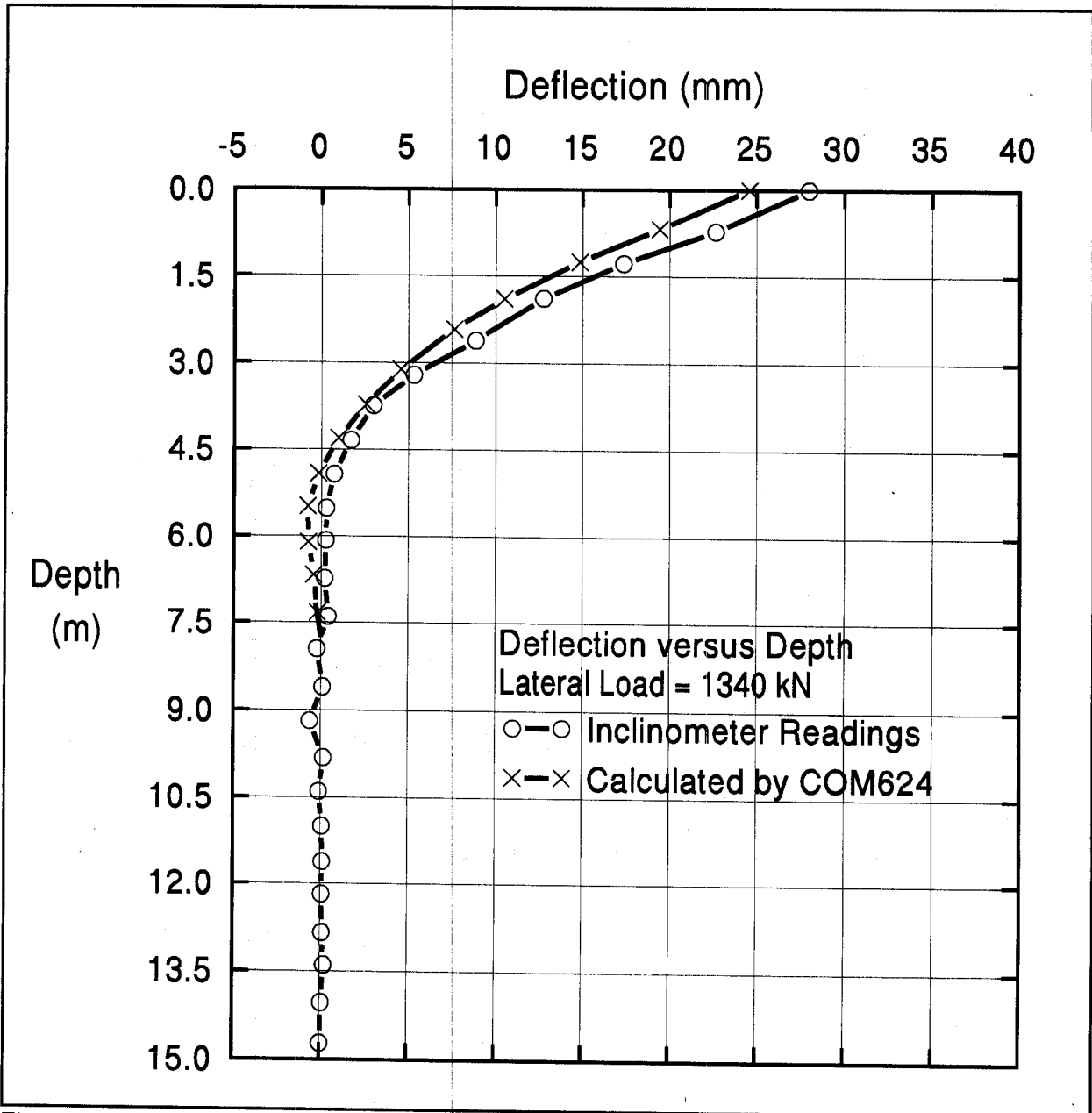


Figure 9.37 Comparison of Measured and COM624P Predicted Load-Deflection Behavior versus Depth (after Kyfor *et al.* 1992).

STEP BY STEP PROCEDURE FOR USING THE COM624P PROGRAM

STEP 1 Determine basic pile input parameters for trial pile.

- a. Pile length (m).
- b. Modulus of elasticity, E (kPa).
- c. Distance from pile head to ground surface (m).
- d. Number of increments for pile model (300 maximum).
- e. Slope of the ground surface, if any. (degrees).

STEP 2 Divide pile into segments with uniform cross sectional properties. For each segment, provide:

- a. X-coordinate at top of segment.
- b. Pile diameter (m).
- c. Moment of inertia, I , (m^4).
- d. Area of pile (m^2).

STEP 3 Delineate the soil profile into layers over the maximum anticipated penetration depth of the trial pile. Soil profile delineation should include:

- a. Location of the ground water table.
- b. Top and bottom depth of each soil layer from the ground surface (m).
- c. Soil layer characterization as cohesive or cohesionless.

STEP 4 Determine the required soil input parameters for each layer.

- a. Soil effective unit weights, γ' (kN/m^3).
- b. Soil strength parameters.
 1. - For cohesive layers:
 - cohesion, c_u (kPa), and
 - ϵ_{50} , the measured strain at $\frac{1}{2}$ maximum principal stress from triaxial tests or an assumed value from Table 9-12.
 2. - For cohesionless layers:
 - ϕ angle from laboratory, in-situ data, or SPT N values.
- c. Slope of soil modulus, k , (kN/m^3) measured from laboratory or in-situ test data or assumed value from Table 9-13.

STEP 5 Develop p-y curves for selected depths. Decide if program or user input p-y curves will be used.

- a. Program p-y curves can be input at user selected depths. Curves are assigned to soil layers using a criteria number.
- b. User p-y curves require input of deflection (m) and soil resistance (kN/m) coordinates for each p-y curve at user selected depths.

Clay Consistency	Average Undrained Shear Strength, c_u (kPa)	ϵ_{50}
Soft Clay	12 - 24	0.02
Medium Clay	24 - 48	0.01
Stiff Clay	48 - 96	0.007
Very Stiff Clay	96 - 192	0.005
Hard Clay	192 - 383	0.004

Soil Type	Average Undrained Shear Strength, c_u (kPa)	Soil Condition	k - Static Loading (kN/m ³)	k - Cyclic Loading (kN/m ³)
Soft Clay	12 - 24	---	8,140	
Medium Clay	24 - 48	---	27,150	
Stiff Clay	48 - 96	---	136,000	54,300
Very Stiff Clay	96 - 192	---	271,000	108,500
Hard Clay	192 - 383	---	543,000	217,000
Loose Sand	---	Submerged	5,430	5,430
Loose Sand	---	Above Water Table	6,790	6,790
Med Dense Sand	---	Submerged	16,300	16,300
Med Dense Sand	---	Above Water Table	24,430	24,430
Dense Sand	---	Submerged	33,900	33,900
Dense Sand	---	Above Water Table	61,000	61,000

- STEP 6 Determine the critical loading combinations and boundary conditions to be analyzed.
- a. For each critical set of loading combination, determine the axial loads, lateral loads, and bending moments to be analyzed. Load information should be supplied by the structural engineer.
 - b. Determine if lateral load is distributed.
 - c. Determine if loading is static or cyclic.
 - d. Determine pile head restraint: free, fixed or partially fixed.
- STEP 7 Determine pile structural acceptability by finding the ultimate lateral load that produces a plastic hinge (ultimate bending moment).
- a. In this step the lateral, axial and bending moments used in the analysis should be ultimate values.
 - b. For concrete piles, the value of I for a cracked section can be determined directly for each loading step by using the subroutine PMEIX, through identification of the properties and configuration of the steel reinforcement. Alternatively, variations in E and I can be entered as a function of depth along the pile.
- STEP 8 Determine pile acceptability based on deflection under service loads.
- a. Use design loading conditions and not ultimate values for lateral and axial loads and bending moments.
 - b. Compare COM624P predicted movement with performance criteria.
- STEP 9 Optimize required pile section and pile penetration depth for lateral loading conditions to meet performance criteria as necessary.

9.8 DESIGN OF PILE GROUPS

The previous sections of this chapter dealt with design procedures for single piles. However piles for almost all highway structures are installed in groups, due to the heavy foundation loads. The next sections of this chapter will address the foundation design procedures for evaluating the axial compression capacity of pile groups as well as the settlement of pile groups under axial compression loads. The axial compression capacity and settlement of pile groups are interrelated and are therefore presented in sequence. Sections covering the design of pile groups for uplift and lateral load capacity will be presented following the axial compression capacity and settlement of pile group sections.

The efficiency of a pile group is defined as the ratio of the ultimate capacity of the group to the sum of the ultimate capacities of the individual piles comprising the group. This may be expressed in equation form as:

$$\eta_g = \frac{Q_{ug}}{n Q_u}$$

Where: η_g = Pile group efficiency.
 Q_{ug} = Ultimate capacity of the pile group.
 n = Number of piles in the pile group.
 Q_u = Ultimate capacity of each individual pile in the pile group.

If piles are driven into compressible cohesive soil or in dense cohesionless material underlain by compressible soil, then the ultimate axial compression capacity of a pile group may be less than that of the sum of the ultimate axial compression capacities of the individual piles. In this case, the pile group has a group efficiency of less than 1. In cohesionless soils, the ultimate axial compression capacity of a pile group is generally greater than the sum of the ultimate axial compression capacities of the individual piles comprising the group. In this case, the pile group has a group efficiency greater than 1.

The settlement of a pile group is likely to be many times greater than the settlement of an individual pile carrying the same load per pile as each pile in the pile group. Figure 9.38(a) illustrates that for a single pile, only a small zone of soil around and below the pile toe is subjected to vertical stress. Figure 9.38(b) illustrates that for a pile group, a considerable depth of soil around and below the pile group is stressed. The settlement of the pile group may be large, depending on the compressibility of the soils within the stressed zone.

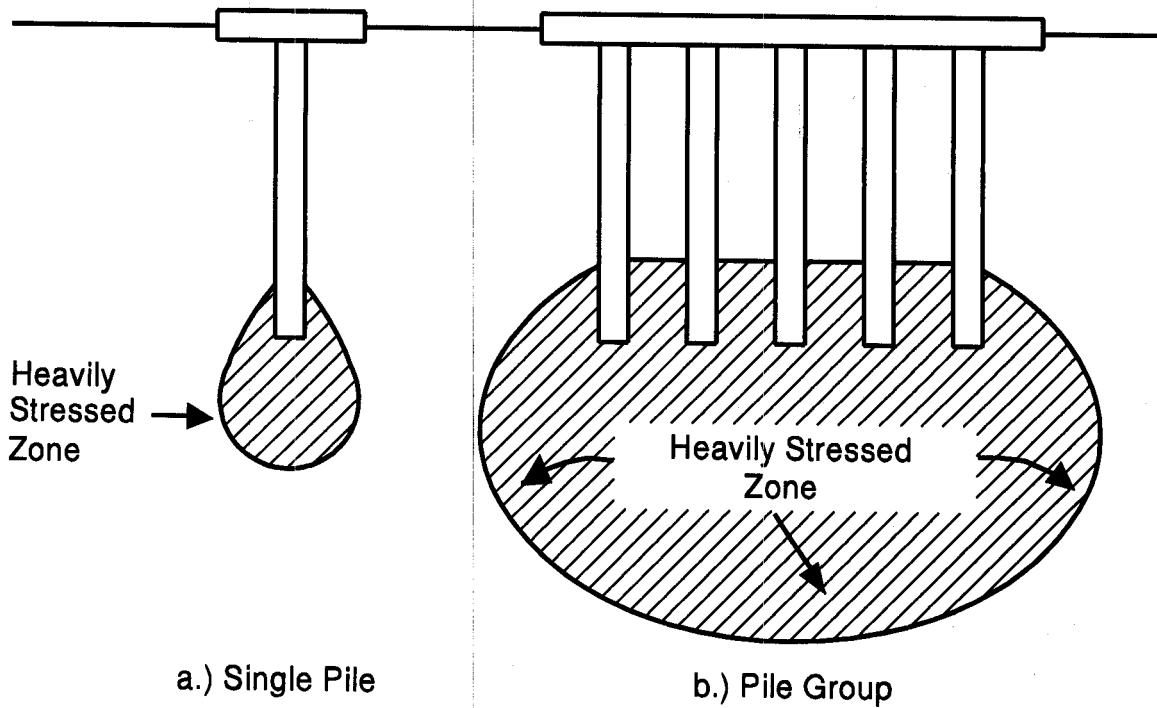


Figure 9.38 Stress Zone from Single Pile and Pile Group (after Tomlinson, 1994)

The soil medium supporting a pile group is also subject to overlapping stress zones from individual piles in the group. The overlapping effect of stress zones for a pile group supported by shaft resistance is illustrated in Figure 9.39.

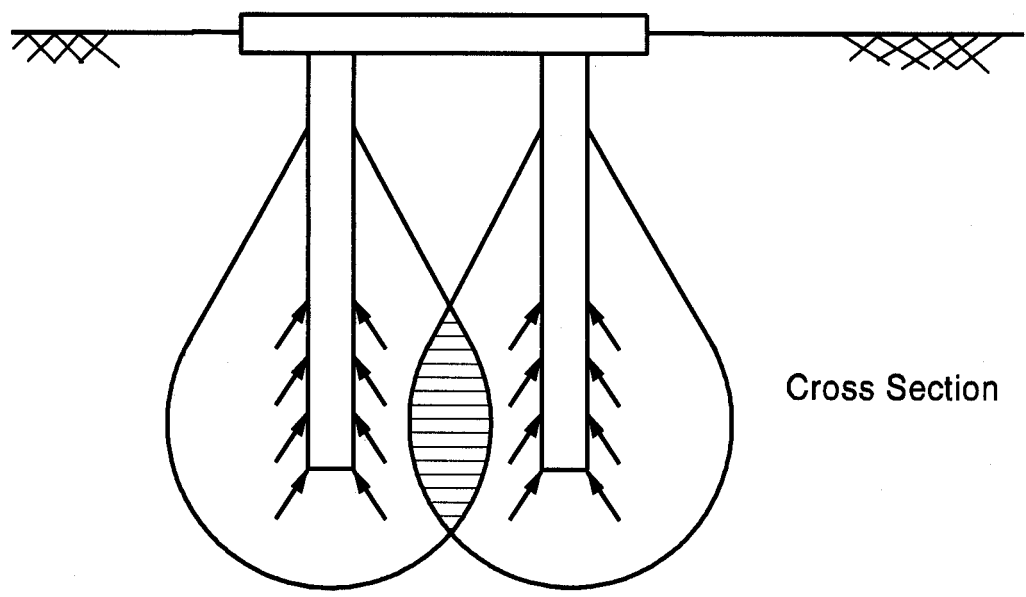
9.8.1 Axial Compression Capacity of Pile Groups

9.8.1.1 Pile Group Capacity in Cohesionless Soils

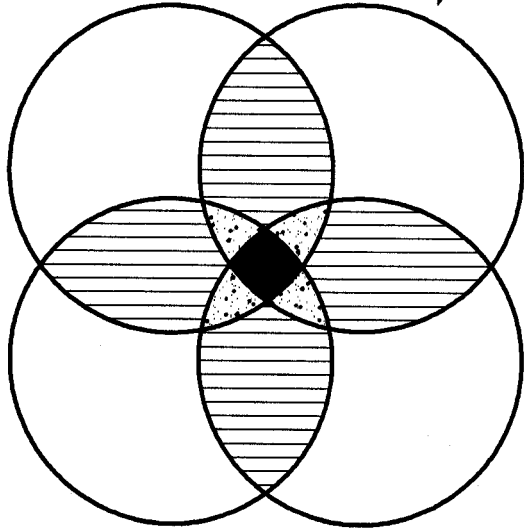
In cohesionless soils, the ultimate group capacity of driven piles with a center to center spacing of less than 3 pile diameters is greater than the sum of the ultimate capacity of the individual piles. The greater group capacity is due to the overlap of individual soil compaction zones near the pile, which increases shaft resistance. Piles in groups at spacings greater than three times the average pile diameter generally act as individual piles.

Design recommendations for estimating group capacity for driven piles in cohesionless soil are as follows:

1. The ultimate group capacity for driven piles in cohesionless soils not underlain by a weak deposit may be taken as the sum of the individual ultimate pile capacities, provided jetting or predrilling was not used in the pile installation process. Jetting or predrilling can result in group efficiencies less than 1. Therefore, jetting or predrilling should be avoided whenever possible and controlled by detailed specifications when necessary.
2. If a pile group founded in a firm bearing stratum of limited thickness is underlain by a weak deposit, then the ultimate group capacity is the smaller value of either the sum of the ultimate capacities of the individual piles, or the group capacity against block failure of an equivalent pier, consisting of the pile group and enclosed soil mass punching through the firm stratum into the underlying weak soil. From a practical standpoint, block failure can only occur when the center to center pile spacing is less than 2 pile diameters, which is less than the minimum center to center spacing of 2.5 diameters allowed by AASHTO code (1994). The method shown for cohesive soils in the Section 9.8.1.3 may be used to evaluate the possibility of a block failure.
3. Piles in groups should not be installed at center to center spacings less than 3 times the average pile diameter. A minimum center to center spacing of 3 diameters is recommended to optimize group capacity and minimize installation problems.



Summing Effects of a Friction Pile Group






-  2 Piles Contributing to Stress
-  3 Piles Contributing to Stress
-  4 Piles Contributing to Stress

Figure 9.39 Overlap of Stress Zones for Group of Friction Piles (after Bowles, 1988)

9.8.1.2 *Pile Group Capacity in Cohesive Soils*

In the absence of negative shaft resistance, the group capacity in cohesive soil is usually governed by the sum of the ultimate capacities of the individual piles, with some reduction due to overlapping zones of shear deformation in the surrounding soil. AASHTO (1993) code states that the group capacity is influenced by whether the pile cap is in firm contact with the ground. If the pile cap is in firm contact with the ground, the soil between the piles and the pile group act as a unit.

The following design recommendations are for estimating ultimate pile group capacity in cohesive soils. The lesser of the ultimate pile group capacity, calculated from Steps 1 to 4, should be used.

1. For pile groups driven in clays with undrained shear strengths of less than 95 kPa and the pile cap not in firm contact with the ground, a group efficiency of 0.7 should be used for center to center pile spacings of 3 times the average pile diameter. If the center to center pile spacing is greater than 6 times the average pile diameter, then a group efficiency of 1.0 may be used. Linear interpolation should be used for intermediate center to center pile spacings.
2. For piles in clays with undrained shear strengths less than 95 kPa, and the pile cap in firm contact with the ground, a group efficiency of 1.0 may be used.
3. For pile groups in clays with undrained shear strength in excess of 95 kPa, a group efficiency of 1.0 may be used regardless of the pile cap - ground contact.
4. Calculate the ultimate pile group capacity against block failure using the procedure described in Section 9.8.1.3.
5. Piles in cohesive soils should not be installed at center to center pile spacings less than 3.0 times the average pile diameter and not less than 1 meter.

It is important to note that the driving of pile groups in cohesive soils can generate large excess pore water pressures. This can result in short term (1 to 2 months after installation) group efficiencies on the order of 0.4 to 0.8. As these excess pore pressures dissipate, the pile group efficiency will increase. Figure 9.40 presents observations on the dissipation of excess pore water pressure versus time for pile groups driven in cohesive soils. Depending

upon the group size, the excess pore pressures typically dissipate within 1 to 2 months after driving. However, in very large groups, full pore pressure dissipation may take up to a year.

If a pile group will experience the full group load shortly after construction, the foundation designer must evaluate the reduced group capacity that may be available for load support. In these cases, piezometers should be installed to monitor pore pressure dissipation with time. Effective stress capacity calculations can then be used to determine if the increase in pile group capacity versus time during construction meets the load support requirements.

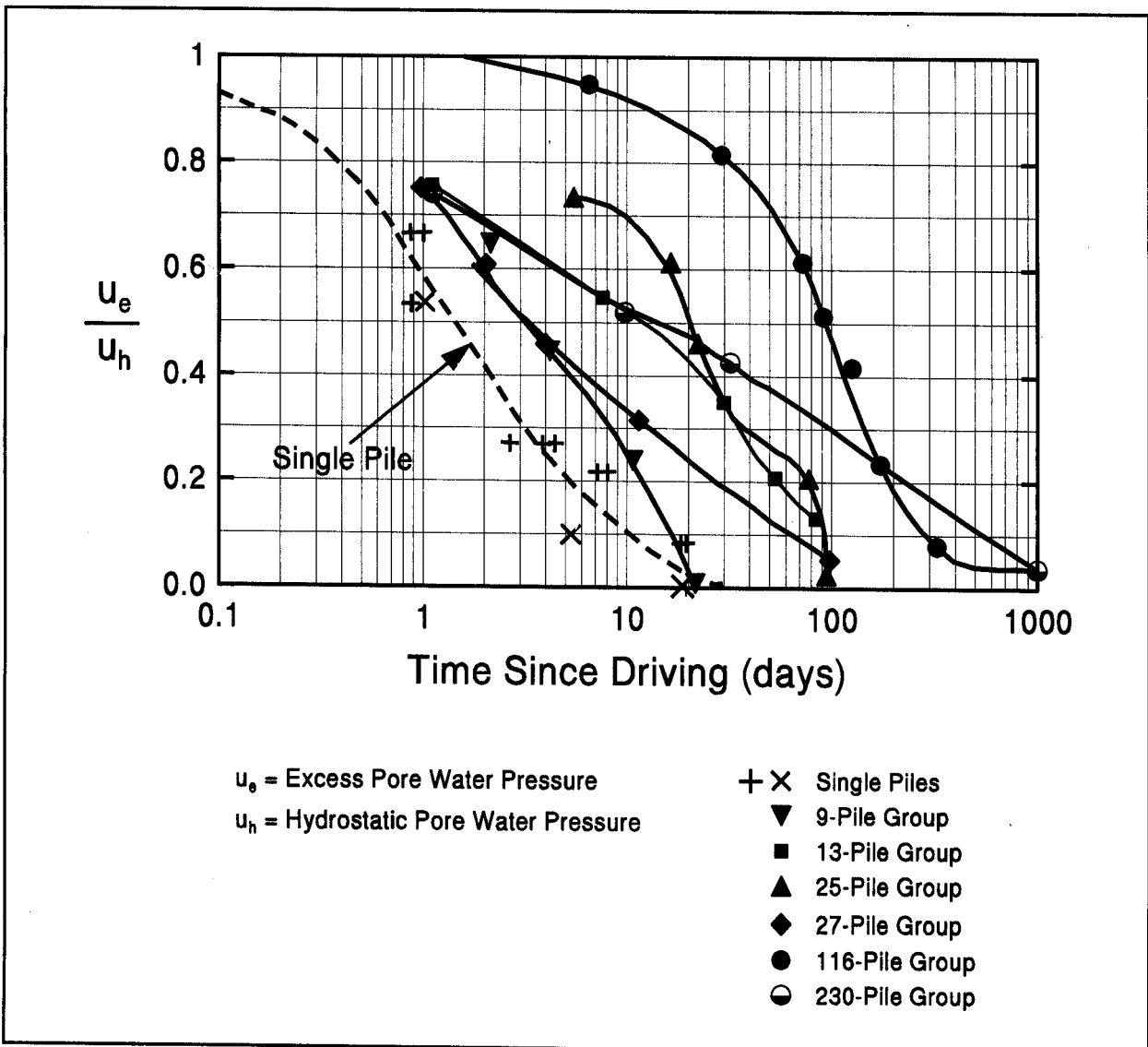


Figure 9.40 Measured Dissipation of Excess Pore Water Pressure in Soil Surrounding Full Scale Pile Groups (after O'Neill, 1983)

9.8.1.3 Block Failure of Pile Groups

Block failure of pile groups is generally only a design consideration for pile groups in soft cohesive soils or in cohesionless soils underlain by a weak cohesive layer. For a pile group in cohesive soil as shown in Figure 9.41, the ultimate capacity of the pile group against a block failure is provided by the following expression:

$$Q_{ug} = 2D (B + Z) c_{u1} + B Z c_{u2} N_c$$

- Where:
- Q_{ug} = Ultimate group capacity against block failure.
 - D = Embedded length of piles.
 - B = Width of pile group.
 - Z = Length of pile group.
 - c_{u1} = Weighted average of the undrained shear strength over the depth of pile embedment for the cohesive soils along the pile group perimeter.
 - c_{u2} = Average undrained shear strength of the cohesive soils at the base of the pile group to a depth of $2B$ below pile toe level.
 - N_c = Bearing capacity factor.

If a pile group will experience the full group load shortly after construction, the ultimate group capacity against block failure should be calculated using the remolded or a reduced shear strength rather than the average undrained shear strength for c_{u1} .

The bearing capacity factor, N_c , for a rectangular pile group is generally 9. However, for pile groups with small pile embedment depths and/or large widths, N_c should be calculated from the following equation.

$$N_c = 5 \left[1 + \frac{D}{5B} \right] \left[1 + \frac{B}{5Z} \right] \leq 9$$

When evaluating possible block failure of pile groups in cohesionless soils underlain by a weak cohesive deposit, the weighted average unit shaft resistance for the cohesionless soils should be substituted for c_{u1} in calculating the ultimate group capacity. The pile group base strength determined from the second part of the ultimate group capacity equation should be calculated using the strength of the underlying weaker layer.

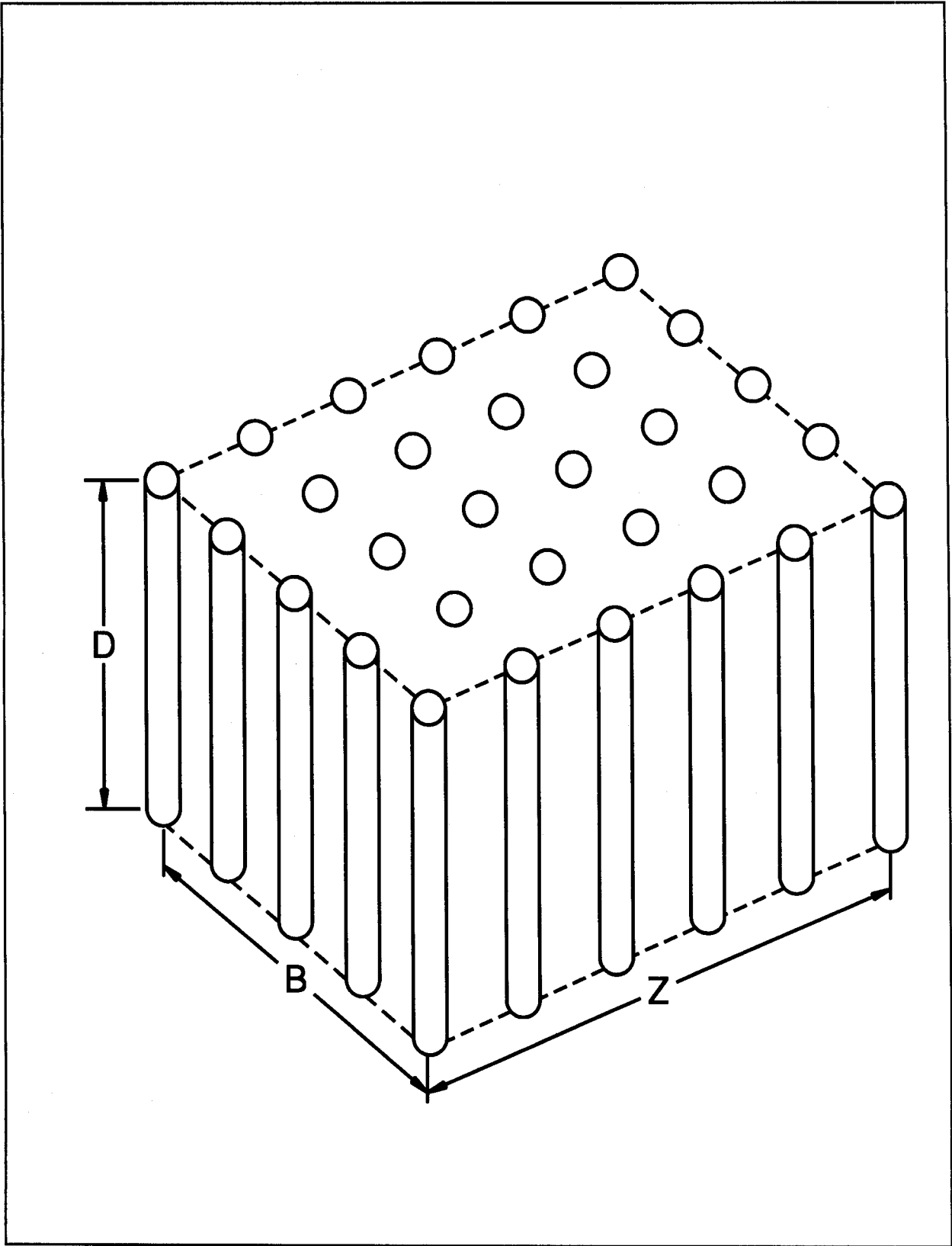


Figure 9.41 Three Dimensional Pile Group Configuration (after Tomlinson, 1994)

9.8.2 Settlement of Pile Groups

Pile groups supported in and underlain by cohesionless soils will produce only immediate settlements. This means the settlements will occur immediately as the pile group is loaded. Pile groups supported in and underlain by cohesive soils may produce both immediate settlements and consolidation settlements that occur over a period of time. In highly over-consolidated clays, the majority of the foundation settlement will occur immediately. Consolidation settlements will generally be the major source of foundation settlement in normally consolidated clays.

Methods for estimating settlement of pile groups are provided in the following sections. Methods for estimating single pile settlements are not provided because piles are usually installed in groups.

9.8.2.1 Elastic Compression of Piles

The pile group settlement methods discussed in the following sections only consider soil settlements and do not include the settlement caused by elastic compression of pile material due to the imposed axial load. Therefore, the elastic compression should also be computed and this settlement added to the group settlement estimates of soil settlement. The elastic compression can be computed by the following expression:

$$\Delta = \frac{Q_a L}{A E}$$

Where:

- Δ = Elastic compression of pile material, (mm).
- Q_a = Design axial load in pile, (kN).
- L = Length of pile (mm).
- A = Pile cross sectional area (m^2).
- E = Modulus of elasticity of pile material, (kPa).

The modulus of elasticity for steel piles is 207,000 MPa. For concrete piles, the modulus of elasticity varies with concrete compressive strength and is generally on the order of 27800 MPa. The elastic compression of short piles is usually quite small and can often be neglected in design.

9.8.2.2 Settlements of Pile Groups in Cohesionless Soils

9.8.2.2a Method Based on SPT Test Data

Meyerhof (1976) recommended that the settlement of a pile group in a homogeneous sand deposit not underlain by a more compressible soil at a greater depth may be conservatively estimated by the following expression:

$$s = \frac{0.96 p_f \sqrt{B} I_f}{\bar{N}'}$$

For silty sand, use:

$$s = \frac{1.92 p_f \sqrt{B} I_f}{\bar{N}'}$$

- Where:
- s = Estimated total settlement (mm).
 - p_f = Design foundation pressure (kPa). Group design load divided by group area.
 - B = Width of pile group (m).
 - \bar{N}' = Average corrected SPT N' value within a depth B below pile toe level.
 - D = Pile embedment depth, (m).
 - I_f = Influence factor for group embedment = $1 - [D / 8B] \geq 0.5$.

For piles in cohesionless soils underlain by cohesive deposits, the method presented in Sections 9.8.2.4 should be used.

9.8.2.2b Method Based on CPT Test Data

Meyerhof (1976) recommended the following relationship to estimate maximum settlements using cone penetration test results for saturated cohesionless soils.

$$s = \frac{42 p_f B I_f}{\bar{q}_c}$$

- Where:
- s, p_f , B, and I_f are as defined in the previous method, and
 - \bar{q}_c = Average static cone tip resistance (kPa) within a depth of B below the pile toe level.

9.8.2.3 Settlement of Pile Groups in Cohesive Soils

Terzaghi and Peck (1967) proposed that pile group settlements could be evaluated using an equivalent footing situated at a depth of $\frac{1}{3} D$ above the pile toe. This concept is illustrated in Figure 9.42. For a pile group consisting of only vertical piles, the equivalent footing has a plan area $(B)(Z)$ that corresponds to the perimeter dimensions of the pile group as shown in Figure 9.41. The pile group load over this plan area is then the bearing pressure transferred to the soil through the equivalent footing. The load is assumed to spread within the frustum of a pyramid of side slopes at 30° and to cause uniform additional vertical pressure at lower levels. The pressure at any level is equal to the load carried by the group divided by the plan area of the base of the frustum at that level. Consolidation settlements are calculated based on the pressure increase in the underlying layers.

Consolidation settlements of cohesive soils are usually computed on the basis of laboratory tests. A typical plot of consolidation test results illustrating the relationships of the compression indices C_c and C_{cr} to void ratio, e , and pressure, p , are shown in Figure 9.43. For pressure increases less than the preconsolidation pressure, p_c , settlement is computed using a value of the compression index representing recompression, C_{cr} . For pressure increases greater than the preconsolidation pressure, settlement is computed using the compression index, C_c .

The following three equations are used to calculate settlements of cohesive soils depending upon the pressure increase and whether the soil is overconsolidated or normally consolidated. The terms used in these equations are as follows:

- s = Total settlement, (mm).
- H = Original thickness of stratum, (mm).
- C_{cr} = Recompression index.
- e_0 = Initial void ratio.
- p_0 = Effective overburden pressure at midpoint of compressible stratum prior to pressure increase, (kPa).
- p_c = Estimated preconsolidation pressure, (kPa).
- C_c = Compression index.
- Δp = Average change in pressure in the compressible stratum, (kPa).

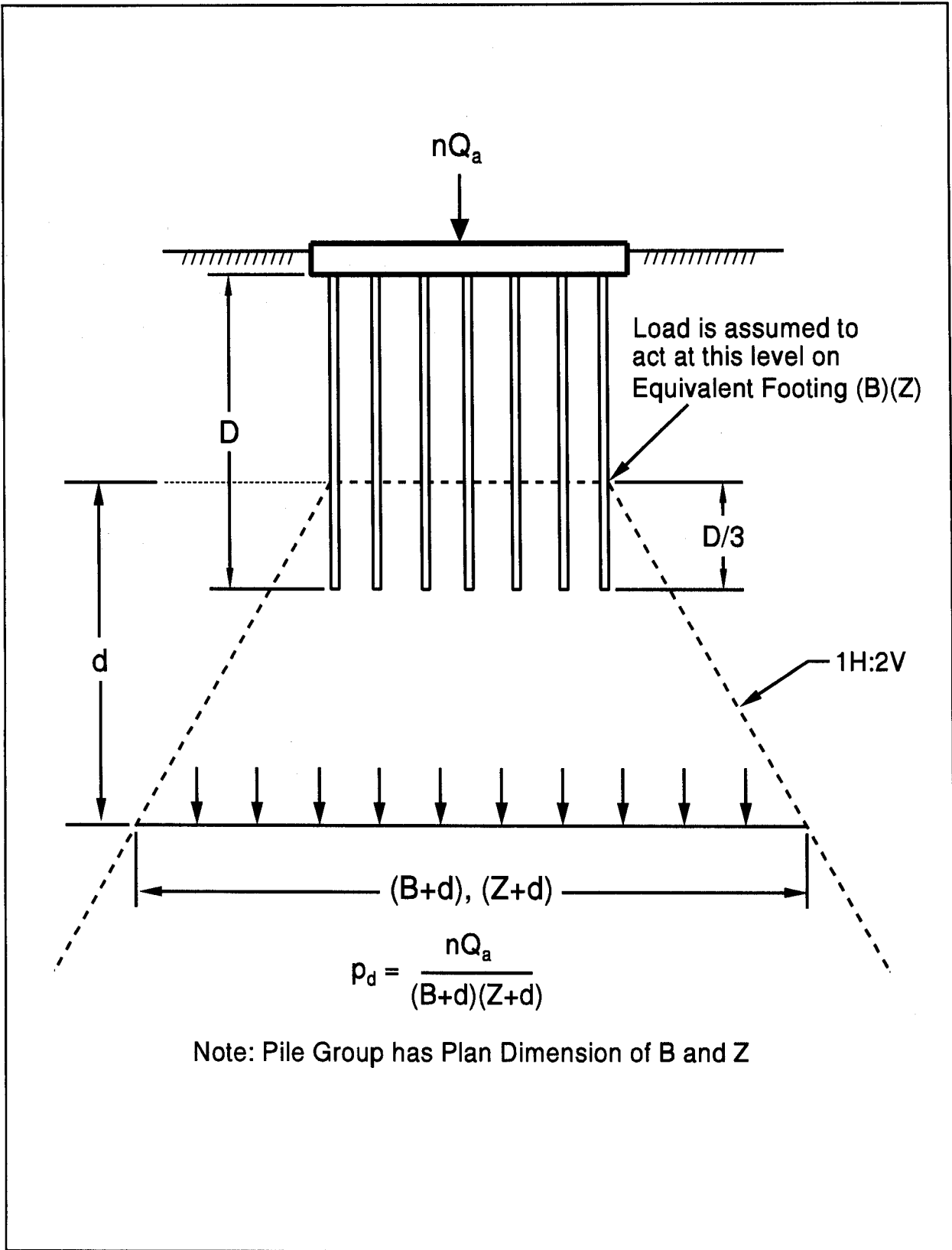


Figure 9.42 Equivalent Footing Concept

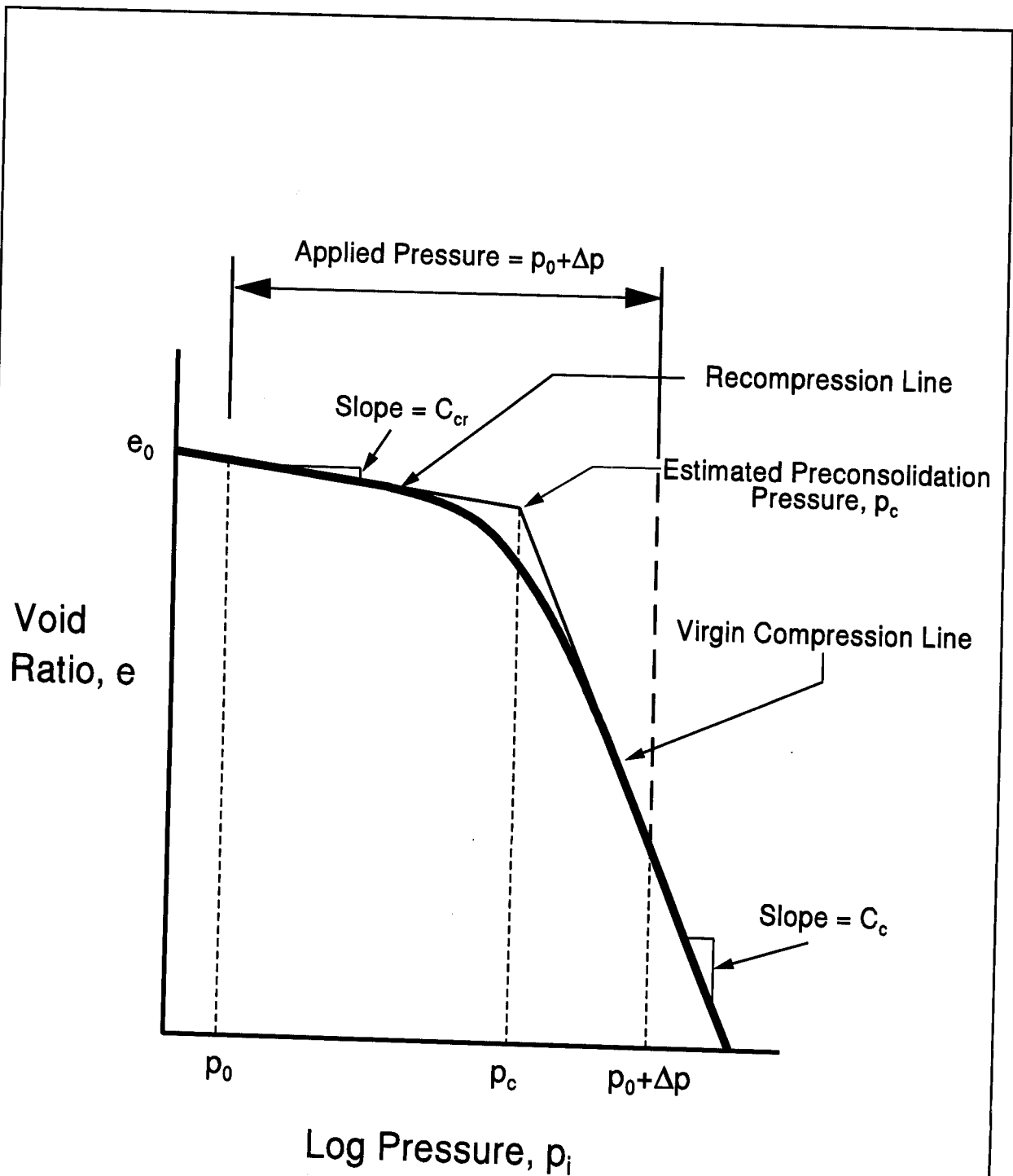


Figure 9.43 Typical e -log p Curve from Laboratory Consolidation Test

For overconsolidated cohesive soils where the pressure after the foundation pressure increase is greater than the soil preconsolidation pressure, settlements may be computed as follows:

$$s = H \left[\frac{C_{cr}}{1+e_0} \log \frac{p_c}{p_o} \right] + H \left[\frac{C_c}{1+e_0} \log \frac{p_o + \Delta p}{p_c} \right]$$

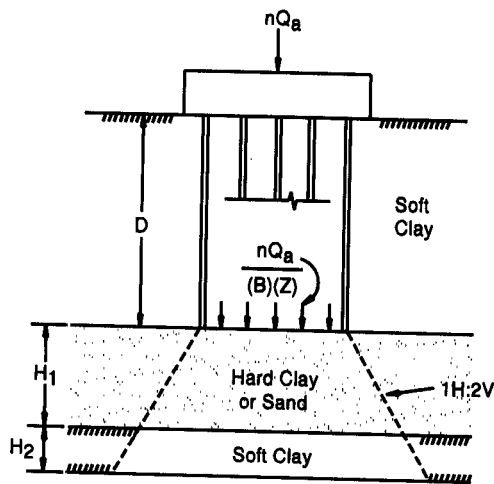
For overconsolidated cohesive soils where the pressure after the foundation pressure increase is less than the soil preconsolidation pressure, settlements should be computed using the following equation:

$$s = H \left[\frac{C_{cr}}{1+e_0} \log \frac{p_o + \Delta p}{p_o} \right]$$

For normally consolidated cohesive soils, settlements should be computed from:

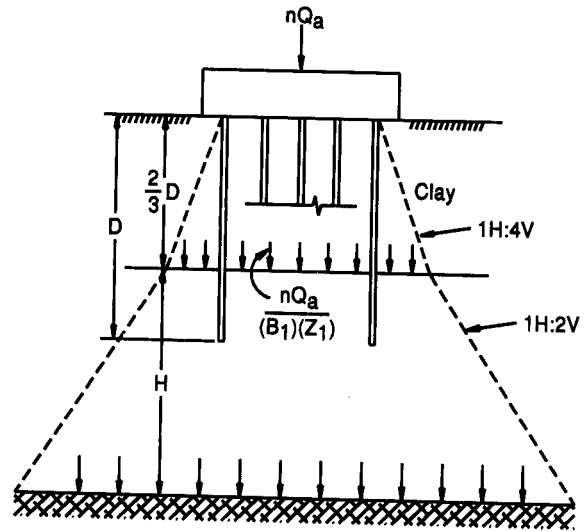
$$s = H \left[\frac{C_c}{1+e_0} \log \frac{p_o + \Delta p}{p_o} \right]$$

Rather than fixing the equivalent footing at a depth of $\frac{1}{3} D$ above the pile toe for all soil conditions, the depth of the equivalent footing should be adjusted based upon soil stratigraphy and load transfer mechanism to the soil. Figure 9.44 presents the recommended location of the equivalent footing for a variety of load transfer and soil resistance conditions.



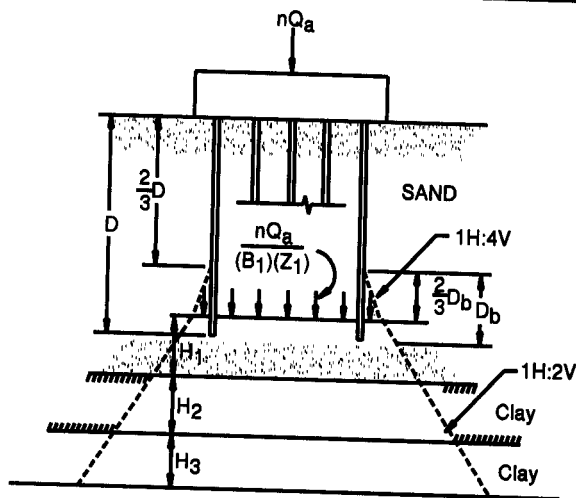
Equivalent Footing at Depth D
Settlement of Pile Group = Compression of Layers H_1 and H_2 Under Pressure Distribution Shown.

a) Toe Bearing Piles in Hard Clay or in Sand Underlain by Soft Clay



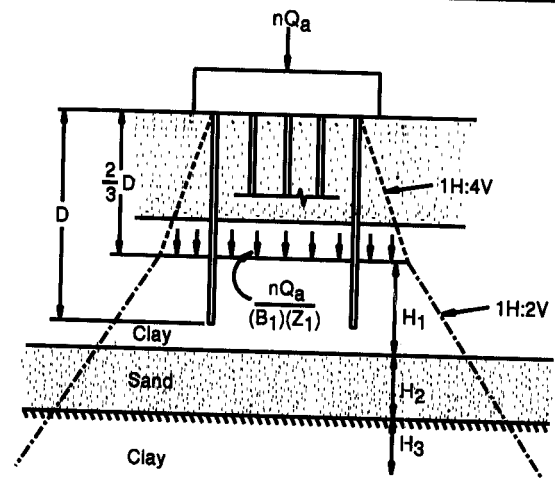
Equivalent Footing at Depth $2/3D$
Settlement of Pile Group = Compression of Layer H Under Pressure Distribution Shown.

b) Piles Supported by Shaft Resistance in Clay



Equivalent Footing at Depth $8/9D$
Settlement of Pile Group = Compression of Layers H_1 , H_2 , and H_3 Under Pressure Distribution Shown.
 nQ_a is Limited by Bearing Capacity of Clay Layers

c) Piles Supported by Shaft Resistance in Sand Underlain by Clay



Equivalent Footing at Depth $2/3D$
Settlement of Pile Group = Compression of Layers H_1 , H_2 , and H_3 Under Pressure Distribution Shown.

d) Piles Supported by Shaft and Toe Resistance in Layered Soil Profile

Notes:

- (1) Plan area of perimeter of pile group = $(B)(Z)$.
- (2) Plan area $(B_1)(Z_1)$ = projection of area $(B)(Z)$ at depth based on shown pressure distribution.
- (3) For relatively rigid pile cap, pressure distribution is assumed to vary with depth as above.
- (4) For flexible slab or group of small separate caps, compute pressures by elastic solutions.

Figure 9.44 Pressure Distribution Below Equivalent Footing for Pile Group (adapted from Cheney and Chassie, 1993)

STEP BY STEP PROCEDURE FOR PILE GROUP SETTLEMENT IN COHESIVE SOILS

STEP 1 Determine the new load imposed on soil by the pile group.

- a. Determine the location of the equivalent footing. For pile groups supported primarily by toe resistance, the equivalent footing is placed at the pile toe as illustrated in Figure 9.44(a). For pile groups supported primarily by shaft resistance, the equivalent footing is placed at a depth of $\frac{2}{3} D$ as shown in Figure 9.44(b).
- b. Determine the dimensions of the equivalent footing. For pile groups consisting only of vertical piles, the equivalent footing (unless modified for load transfer as in Figure 9.44(b)) has the same dimensions as the length and width of the pile group from Figure 9.41. For pile groups supported primarily by shaft resistance that include batter piles, the plan area of the footing should be calculated from the dimensions of the pile group at depth $\frac{2}{3} D$, including the plan area increase due to the pile batter. For toe bearing groups with batter piles, the equivalent footing area should be the dimensions of the pile group at depth D , including the area increase due to pile batter.
- c. Determine the pressure distribution to soil layers below the equivalent footing up to the depth at which the pressure increase from the equivalent footing is less than 10% of existing effective overburden pressure at that depth. Remember that the equivalent footing size may be increased and the footing pressure correspondingly reduced as a result of load transfer above the footing location or in groups with batter piles. The depth at which the pressure increase is less than 10% will provide the total thickness of cohesive soil layer or layers to be used in performing settlement computations. Note that the group design load should be used in determining the pressure distribution for settlement computations, and not the ultimate group load.
- d. Divide the cohesive soil layers in the affected pressure increase zone into several thinner layers of 1.5 to 3 meter thickness. The thickness of each layer is the thickness H for the settlement computation for that layer.
- e. Determine the existing effective overburden pressure, p_o , at midpoint of each layer.

- f. Determine the imposed pressure increase, Δp , at midpoint of each affected soil layer based on the appropriate pressure distribution.

STEP 2 Determine consolidation test parameters.

Plot results of consolidation test(s) as shown in Figure 9.43. Determine p_c , e_o , C_{cr} and C_c values from the consolidation test data.

STEP 3 Compute settlements.

Using the appropriate settlement equation, compute the settlement of each affected soil layer. Sum the settlements of all layers to obtain the total estimated soil settlement from the pile group. Add the elastic compression of the pile under the design load to obtain the total estimated pile group settlement.

9.8.2.4 Settlement of Pile Groups in Layered Soils

Piles are often installed in a layered soil profile consisting of cohesionless and cohesive soils or in soil profiles where an underlying soil stratum of different consistency is affected by the pile group loading. In these cases, group settlement will be influenced by the pressure increase in and compressibility of the affected layers. Figures 9.44(a), 9.44(c) and 9.44(d) may be used to determine the location of the equivalent footing and to evaluate the resulting pressure increase in a soil layer. The settlement of each layer is then calculated using the appropriate settlement equation presented in Section 9.8.2.3 for cohesive layers and from the following equation for cohesionless layers.

$$s = H \left[\frac{1}{C'} \log \frac{p_o + \Delta p}{p_o} \right]$$

- Where:
- s = Total layer settlement, (mm).
 - H = Original thickness of layer, (mm).
 - C' = Dimensionless bearing capacity index from Figure 9.45, determined from average corrected SPT N' value, \bar{N}' , for layer with consideration of SPT hammer type.
 - p_o = Effective overburden pressure at midpoint of layer prior to pressure increase, (kPa).
 - Δp = Average change in pressure in the layer, (kPa).

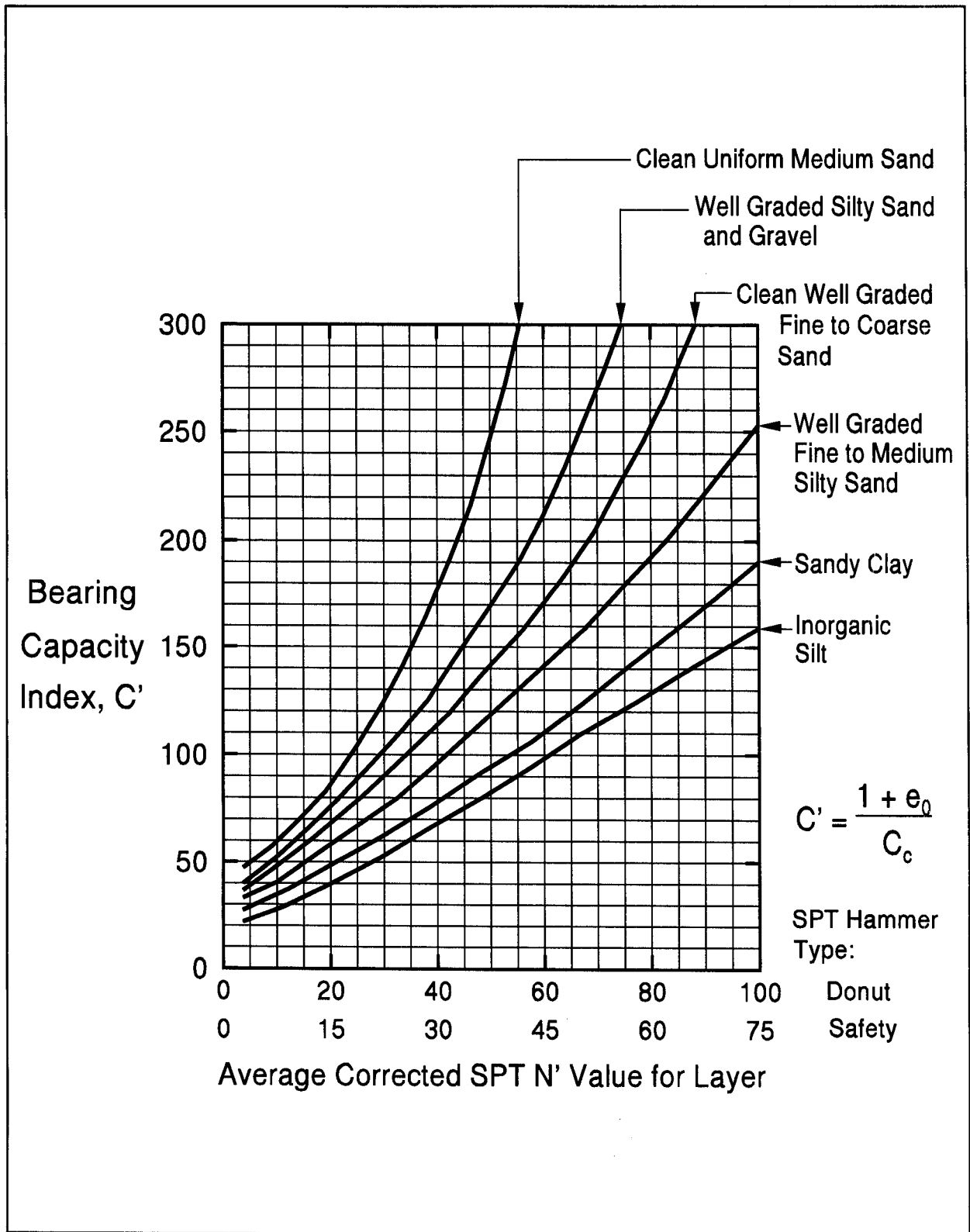


Figure 9.45 Values of the Bearing Capacity Index, C' , for Granular Soil (modified after Cheney and Chassie, 1993).

Cheney and Chassie (1993) report that FHWA experience with this method indicates the method is usually conservative and can overestimate settlements by a factor of 2. This conservatism is attributed to the use of the original bearing capacity index chart from Hough (1959) which was based upon SPT donut hammer data. Based upon average energy variations between SPT donut and safety hammers reported in technical literature, Figure 9.45 now includes a correlation between SPT N values from a safety hammer and bearing capacity index. This modification should improve the accuracy of settlement estimates with this method.

STEP BY STEP PROCEDURE FOR GROUP SETTLEMENT IN LAYERED SOIL PROFILES

- STEP 1 Determine the new load imposed on soil by the pile group.
- a. Determine the location of the equivalent footing. For pile groups supported primarily by toe resistance, the equivalent footing is placed at the pile toe as illustrated in Figure 9.44(a). For pile groups supported primarily by shaft resistance in sands underlain by cohesive soils, the equivalent footing is placed at a depth of $\frac{8}{9} D$ as shown in Figure 9.44(c). For pile groups in layered soils supported by a combination of shaft and toe resistance, the equivalent footing is placed at $\frac{2}{3} D$ as shown in Figure 9.44(d).
 - b. Determine the dimensions of the equivalent footing. For pile groups consisting only of vertical piles, the equivalent footing (unless modified for load transfer as in Figures 9.44(c) and 9.44(d)) has the same dimensions as the length and width of the pile group from Figure 9.41. For pile groups supported primarily by shaft resistance that include batter piles, the plan area of the footing should be calculated from the dimensions of the pile group at the equivalent footing depth that includes the plan area increase due to the pile batter. For toe bearing groups with batter piles, the equivalent footing area should be calculated from the dimensions of the pile group at depth D , including the plan area increase due to the pile batter.
 - c. Determine the pressure distribution to soil layers below the equivalent footing up to the depth at which the pressure increase from the equivalent footing is less than 10% of existing effective overburden pressure at that depth. Remember that the equivalent footing size may be increased and the footing

pressure correspondingly reduced as a result of load transfer above the footing location or in groups with batter piles. The depth at which the pressure increase is less than 10% will provide the total thickness of soil to be evaluated in the settlement computations. Note that the group design load should be used in determining the pressure distribution for settlement computations, and not the ultimate group capacity.

- d. Divide the soil layers in the affected pressure increase zone into several thinner layers of 1.5 to 3 meter thickness. The thickness of each layer is the thickness H for the settlement computation for that layer.
- e. Determine the existing effective overburden pressure, p_o , at midpoint of each soil layer.
- f. Determine the imposed pressure increase, Δp , at midpoint of each affected soil layer based on the appropriate pressure distribution.

STEP 2 Determine consolidation test parameters for each cohesive layer.

Plot results of consolidation test(s) as shown in Figure 9.43. Determine p_c , e_o , C_{cr} and C_c values from the consolidation test data.

STEP 3 Determine bearing capacity index for each cohesionless layer.

Determine the average corrected SPT N' value, \bar{N}' , for each cohesionless layer. Use \bar{N}' for the appropriate SPT hammer type in Figure 9.45 to obtain the bearing capacity index for each layer.

STEP 4 Compute settlements.

Using the appropriate settlement equation, compute the settlement of each affected soil layer. Sum the settlements of all layers to obtain the total estimated soil settlement from the pile group. Add the elastic compression of the pile under the design load to obtain the total estimated pile group settlement.

9.8.2.5 Settlement of Pile Groups Using the Janbu Tangent Modulus Approach

The previous methods of group settlement analyses assume a linear relationship between induced stress and soil strain. However in most soils, a non-linear relationship exists between stress and strain. Figure 9.46 illustrates that a stress increase at a small original stress will result in a larger strain than the same stress increase applied at a greater original stress.

Janbu (1963, 1965) proposed a tangent modulus approach that is referenced in the Canadian Foundation Engineering Manual (1985). In this method, the stress strain relationship of soils is expressed in terms of a dimensionless modulus number, m , and a stress exponent, j . Values of the modulus number can be determined from conventional laboratory triaxial or oedometer tests. The stress exponent, j , can generally be taken as 0.5 for cohesionless soils and 0 for cohesive soils.

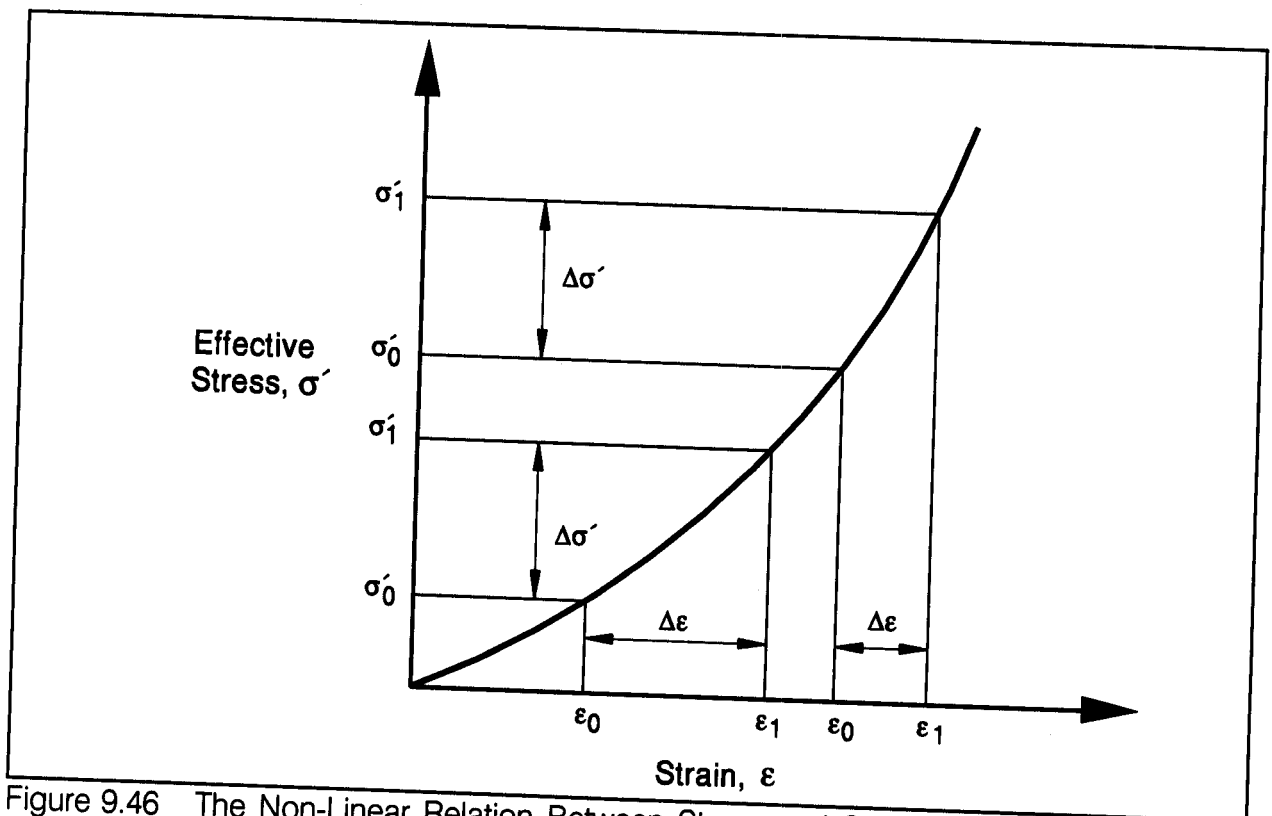


Figure 9.46 The Non-Linear Relation Between Stress and Strain in Soil (after Fellenius, 1990)

The following four equations are used to calculate the strain for normally and over consolidated, cohesionless and cohesive soils. The terms used in these four equations are as follows:

- ϵ = Strain from the increase in effective stress.
- m_n = Dimensionless modulus number.
- m_{nr} = Dimensionless recompression modulus number.
- j = Stress exponent.
- σ'_1 = New effective stress after stress increase, (kPa).
- σ'_o = Original effective stress prior to stress increase, (kPa).
- σ'_p = Preconsolidation stress, (kPa).
- σ_r = Constant reference stress = 100 kPa.

For normally consolidated cohesionless soils, the strain induced by an increase in effective stress may be expressed as follows:

$$\epsilon = \frac{1}{m_n j} \left[\left(\frac{\sigma'_1}{\sigma_r} \right)^j - \left(\frac{\sigma'_o}{\sigma_r} \right)^j \right]$$

For over consolidated cohesionless soils, the following equation should be used to calculate the strain induced by an increase in effective stress:

$$\epsilon = \frac{1}{m_n j} \left[\left(\frac{\sigma'_1}{\sigma_r} \right)^j - \left(\frac{\sigma'_p}{\sigma_r} \right)^j \right] + \frac{1}{m_{nr} j} \left[\left(\frac{\sigma'_p}{\sigma_r} \right)^j - \left(\frac{\sigma'_o}{\sigma_r} \right)^j \right]$$

For cohesive soils, the stress exponent is zero, $j=0$. The strain induced by an increase in effective stress in a normally consolidated cohesive soil is then as follows:

$$\epsilon = \frac{1}{m_n} \ln \left[\left(\frac{\sigma'_1}{\sigma'_o} \right) \right]$$

For over consolidated cohesive soils, the following equation should be used to calculate the strain induced by an increase in effective stress:

$$\epsilon = \frac{1}{m_{nr}} \ln \left[\left(\frac{\sigma'_p}{\sigma'_o} \right) \right] + \frac{1}{m_n} \ln \left[\left(\frac{\sigma'_1}{\sigma'_p} \right) \right]$$

In cohesionless soils, the modulus number can be calculated from the soil modulus of elasticity, E_s (kPa), and the previously described terms using the following equation:

$$m_n = \frac{E_s}{5 \left[\sqrt{\sigma'_1} + \sqrt{\sigma'_o} \right]}$$

In cohesive soils, the modulus number, m_n , or recompression modulus number, m_{nr} , can be calculated from the initial void ratio, e_o , and the compression index, C_c , or recompression index, C_{cr} . The modulus number is calculated from:

$$m_n = 2.30 \left[\frac{1 + e_o}{C_c} \right]$$

The recompression modulus number, m_{nr} , is calculated by substituting the recompression index, C_{cr} , for the compression index, C_c , in the above equation.

The Janbu tangent modulus approach is quite adaptable to calculating pile group settlements in any soil profile. For reference purposes, typical and normally conservative modulus number and stress exponent values from the Canadian Foundation Engineering Manual (1985) are presented in Table 9-14. These values may be useful for preliminary settlement estimates. A step by step procedure for this method follows.

TABLE 9-14 TYPICAL MODULUS AND STRESS EXPONENT VALUES

Soil Type	Consistency	Range in Modulus Number	Stress Exponent
Glacial Till	Very Dense to Dense	1000 - 300	1.0
Gravel	---	400 - 40	0.5
Sand	Dense	400 - 250	0.5
Sand	Medium Dense	250 - 150	0.5
Sand	Loose	150 - 100	0.5
Silt	Dense	200 - 80	0.5
Silt	Medium Dense	80 - 60	0.5
Silt	Loose	60 - 40	0.5
Silty Clay & Clayey Silt	Hard - Stiff	60 - 20	0
Silty Clay & Clayey Silt	Stiff - Firm	20 - 10	0
Silty Clay & Clayey Silt	Soft	10 - 5	0
Marine Clay	Soft	20 - 5	0
Organic Clay	Soft	20 - 5	0
Peat	---	5 - 1	0

STEP BY STEP PROCEDURE FOR PILE GROUP SETTLEMENT BY JANBU METHOD

- STEP 1 Determine the new load imposed on soil by the pile group.
- a. Determine the location of the equivalent footing. For pile groups supported primarily by toe resistance, the equivalent footing is placed at the pile toe as illustrated in Figure 9.44(a). For pile groups supported primarily by shaft resistance in sands underlain by cohesive soils, the equivalent footing is placed at a depth of $\frac{8}{9} D$ as shown in Figure 9.44(c). For pile groups in layered soils supported by a combination of shaft and toe resistance, the equivalent footing is placed at $\frac{2}{3} D$ as shown in Figure 9.44(d).
 - b. Determine the dimensions of the equivalent footing. For pile groups consisting only of vertical piles, the equivalent footing (unless modified for load transfer as in Figures 9.44(c) and 9.44(d) has the same dimensions as the length and width of the pile group from Figure 9.41. For pile groups supported primarily by shaft resistance that include batter piles, the plan area of the footing should be calculated from the dimensions of the pile group at the equivalent footing depth that includes the plan area increase due to the pile batter. For toe bearing groups with batter piles, the equivalent footing area should be calculated from the dimensions of the pile group at depth D , including the plan area increase due to the pile batter.
 - c. Determine the pressure distribution to soil layers below the equivalent footing up to the depth at which the pressure increase from the equivalent footing is less than 10% of existing effective overburden pressure at that depth. Remember that the equivalent footing size may be increased, and the footing pressure correspondingly reduced, as a result of load transfer above the footing location, or in groups with batter piles. The depth at which the pressure increase is less than 10% will provide the total thickness of the soil to be analyzed and the number of soil layers for settlement calculations. Note that the group design load should be used in determining the pressure distribution for settlement computations, and not the ultimate group capacity.
 - d. Divide the soil layers in the affected pressure increase zone into several thinner layers of 1.5 to 3 meter thickness. The thickness of each layer is the thickness H for the settlement computation for that layer.

- e. Determine the existing effective stress, σ'_o , at midpoint of each soil layer.
- f. Determine the preconsolidation stress, σ'_p , at the midpoint of each soil layer and whether the soil layer is overconsolidated or normally consolidated.
- g. Determine the new effective stress, σ'_1 , at midpoint of each affected soil layer based on the equivalent footing pressure distribution.

STEP 2 Determine modulus number and stress exponent for each soil layer.

Use laboratory test data to compute modulus number for each layer. Preliminary settlement estimates can be made by using assumed modulus numbers based on soil type as indicated in Table 9-14.

STEP 3 Select the appropriate strain computation equation for each layer.

Select the strain equation applicable to each layer depending upon whether the soil layer is cohesive or cohesionless, and overconsolidated or normally consolidated.

STEP 4 Compute settlements.

Using the appropriate strain computation equation, compute the settlement, s , of each affected soil layer of thickness, H from: $s = (\epsilon)(H)$. Sum the settlements of all layers to obtain the total estimated soil settlement from the pile group. Add the elastic compression of the pile under the design load to obtain the total estimated pile group settlement.

9.8.2.6 Settlement of Pile Groups Using the Neutral Plane Method

As the previous sections demonstrate, most of the group settlement methods select the depth of the equivalent footing based upon the assumed load transfer behavior. A preferred solution is to determine the depth of the neutral plane, and place the equivalent footing at or below the neutral plane location. The neutral plane occurs at the depth where the group dead load plus the load from negative shaft resistance is equal to the positive shaft resistance plus the toe resistance. The design should aim to locate the neutral plane in competent soils. When this is done, group settlements are usually well within acceptable limits.

The position of the neutral plane and the resulting negative shaft resistance can be determined from a static calculation. As previously stated, the neutral plane is the depth at which the sum of dead load on the pile plus the negative shaft resistance is equal to the positive shaft plus the toe resistance. Above the neutral plane, the settlement of the soil is greater than the settlement of the pile. Any shaft resistance above the neutral plane is negative shaft resistance, since by definition the soil settlement is greater than the pile settlement. Therefore, the soil settlement transfers load to the pile. Below the neutral plane, the settlement of the soil is less than the settlement of the pile and load is transferred from the pile to the soil. Therefore, pile settlement is controlled by the soil compressibility below the neutral plane.

The following step by step procedure adapted from Goudreault and Fellenius (1994) is recommended for determination of the neutral plane.

STEP BY STEP PROCEDURE FOR DETERMINING THE NEUTRAL PLANE DEPTH

- STEP 1 Perform a static capacity calculation.
- a. Determine the ultimate pile capacity, Q_u , from a static capacity calculation.
 - b. Plot the load transfer versus depth by subtracting the shaft resistance at a given depth from the ultimate capacity. This computation is identified as Curve A in Figure 9.47.

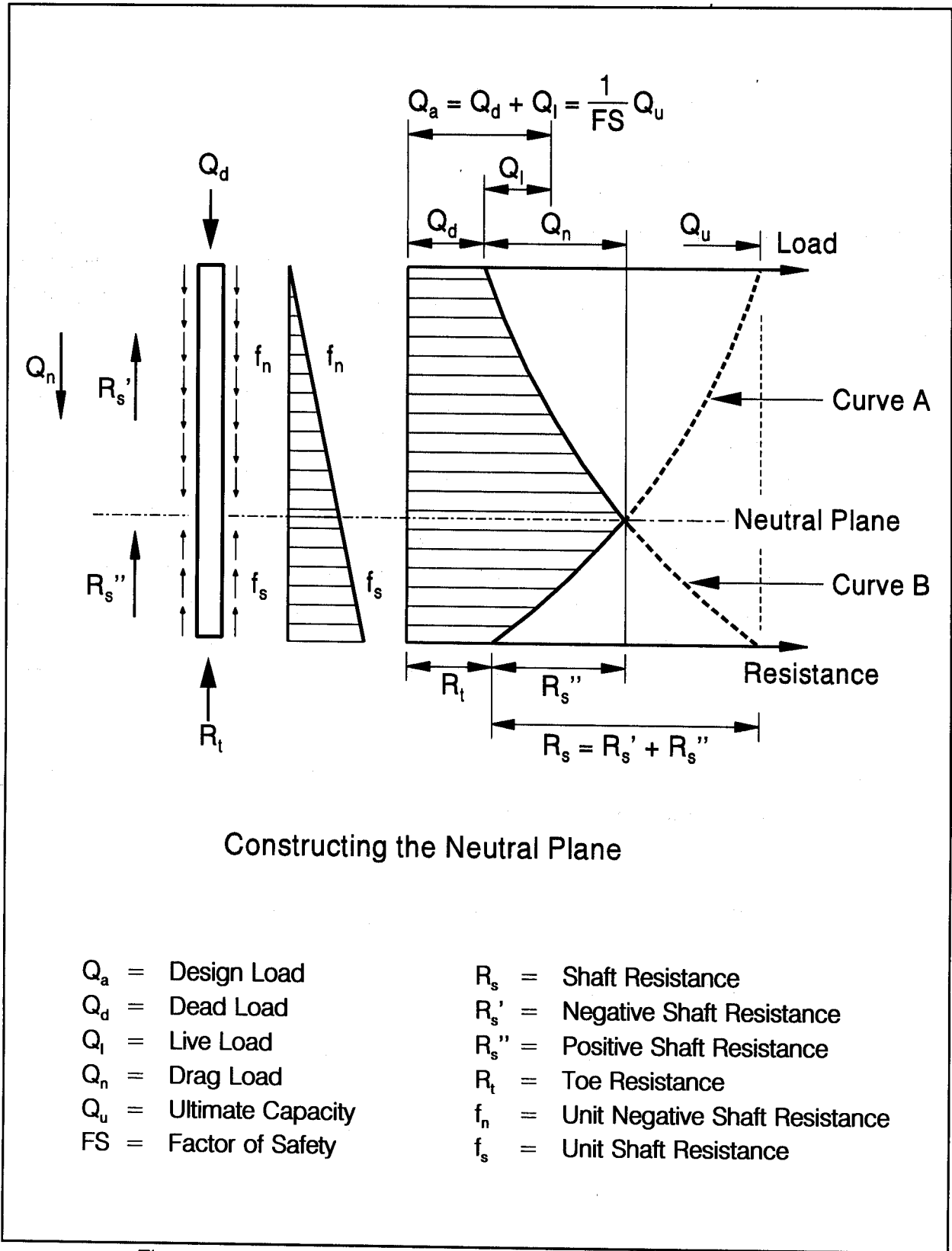


Figure 9.47 Neutral Plane (after Goudrealt and Fellenius, 1994)

STEP 2 Determine the load transfer to the pile above the neutral plane.

- a. Determine the pile dead load, Q_d .
- b. Plot the load transfer to the pile versus depth by adding the shaft resistance at a given depth to the dead load. This computation is labeled as Curve B in Figure 9.47.

STEP 3 Determine the depth of the neutral plane.

- a. The depth where Curves A and B intersect is the depth of the neutral plane.
- b. The location of the neutral plane will move if the dead load is changed or the soil resistance versus depth is altered. Hence, design or construction decisions altering the dead load, or soil resistance versus depth, will require reevaluation of the neutral plane location under the changed conditions. Preaugering, jetting, use of bitumen coatings, *etc.* are but a few of the factors that can change the soil resistance versus depth and thus the neutral plane location.

Goudreault and Fellenius (1994) note that the magnitude of group settlement between the neutral plane and the pile toe level is generally small. This is because the piles below the neutral plane act as reinforcing elements and the compression of the pile-reinforced soil is small. Therefore, for most cases they recommend calculating the pile group settlements based on locating the neutral plane at the pile toe.

The group load is distributed below the neutral plane at a slope of 1H:2V. As in the previous methods, the soil materials below the equivalent footing at the neutral plane and the depth where the pressure increase is less than 10% should be evaluated for settlement. Group settlements are generally calculated based upon the pressure increase and the resulting strain as presented for the Janbu method in Section 9.8.2.5. However, the methods presented for layered soils in Section 9.8.2.4 could also be used.

9.8.3 Uplift Capacity of Pile Groups

The uplift capacity of a pile group is often a significant factor in determining the minimum pile penetration requirements and in some cases can control the foundation design. A few common conditions where group uplift capacity may significantly influence the foundation design include cofferdam seals that create large buoyancy forces, cantilever segmental bridge construction, and seismic, vessel impact, or debris loading. When piles with uplift loads are driven to a relatively shallow bearing stratum, uplift capacity may control the foundation design. Current AASHTO specifications (1994) for the determination of group uplift capacity are presented in Section 9.8.3.1. The AASHTO specifications for group uplift capacity are considered relatively conservative, particularly in cohesionless soils.

In cohesionless soils, Tomlinson's method presented in Section 9.8.3.2 will yield higher group uplift capacities than AASHTO specifications and is recommended for design. Both AASHTO specifications and Tomlinson's method limit the group uplift capacity to the uplift capacity of an individual pile times the number of piles in the group. In the event this limit controls the group uplift capacity, an uplift load test may be cost effective and should be considered. With an uplift load test, a reduced safety factor is used to determine the uplift capacity. This should result in higher individual and group uplift capacities.

In cohesive soils, Tomlinson's method will yield similar results to AASHTO specifications. In the event the uplift capacity of an individual pile times the number of piles in the group limits the group uplift capacity, an uplift load test may again be cost effective and should be considered since an increase in the group uplift capacity would likely result.

9.8.3.1 Group Uplift Capacity by AASHTO Code

AASHTO specifications (1994) for service load design limit the uplift capacity of a pile group to the lesser value determined from any of the following:

1. the design uplift capacity of a single pile times the number of piles in a pile group. The design uplift capacity of a single pile is specified as $\frac{1}{3}$ the ultimate shaft resistance calculated in a static analysis method, or $\frac{1}{2}$ the failure load determined from an uplift load test.
2. $\frac{2}{3}$ the effective weight of the pile group and the soil contained within a block defined by the perimeter of the pile group and the embedded length of the piles.

3. $\frac{1}{2}$ the effective weight of the pile group and the soil contained within a block defined by the perimeter of the pile group and the embedded pile length plus $\frac{1}{2}$ the total soil shear resistance on the peripheral surface of the pile group.

9.8.3.2 Tomlinson Group Uplift Method

Tomlinson (1994) states that the ultimate uplift capacity of a pile group in cohesionless soils may be conservatively taken as the effective weight of the block of soil extending upward from the pile toe level at a slope of 1H:4V, as shown in Figure 9.48. For simplicity in performing the calculation, the weight of the piles within the soil block are considered equal to the weight of the soil. Tomlinson states that a factor of safety of 1 is acceptable in this calculation since the shear resistance around the perimeter of the group is ignored in the calculation. Tomlinson also recommended that the ultimate group uplift capacity determined from this calculation not exceed the sum of the ultimate uplift capacities of the individual piles comprising the pile group divided by an appropriate safety factor. It is recommended that a factor of safety of 2 be used if the ultimate uplift capacity of an individual pile is determined from an uplift load test and a factor of safety of 3 be used if based on the shaft resistance from a static calculation.

For pile groups in cohesive soils as shown in Figure 9.49, Tomlinson recommends the group uplift capacity be calculated based upon the undrained shear resistance of the block of soil enclosed by the group plus the effective weight of the pile cap and pile-soil block. This may be expressed in equation form as:

$$Q_{ug} = 2D (B + Z) c_{u1} + W_g$$

- Where:
- Q_{ug} = Ultimate group capacity against block failure in uplift, (kN).
 - D = Embedded length of piles, (m).
 - B = Width of pile group, (m).
 - Z = Length of pile group, (m).
 - c_{u1} = Weighted average of the undrained shear strength over the depth of pile embedment along the pile group perimeter, (kPa).
 - W_g = Effective weight the pile/soil block including the pile cap weight, (kN).

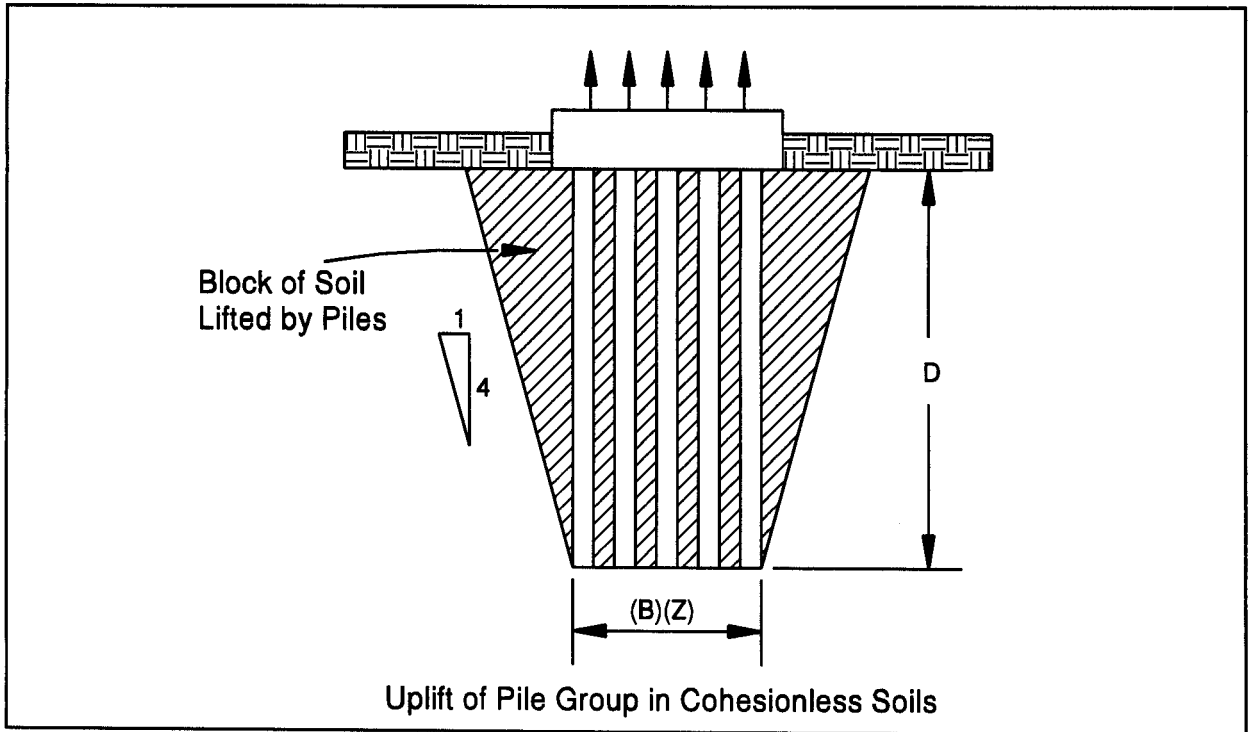


Figure 9.48 Uplift of Pile Group in Cohesionless Soil (after Tomlinson, 1994)

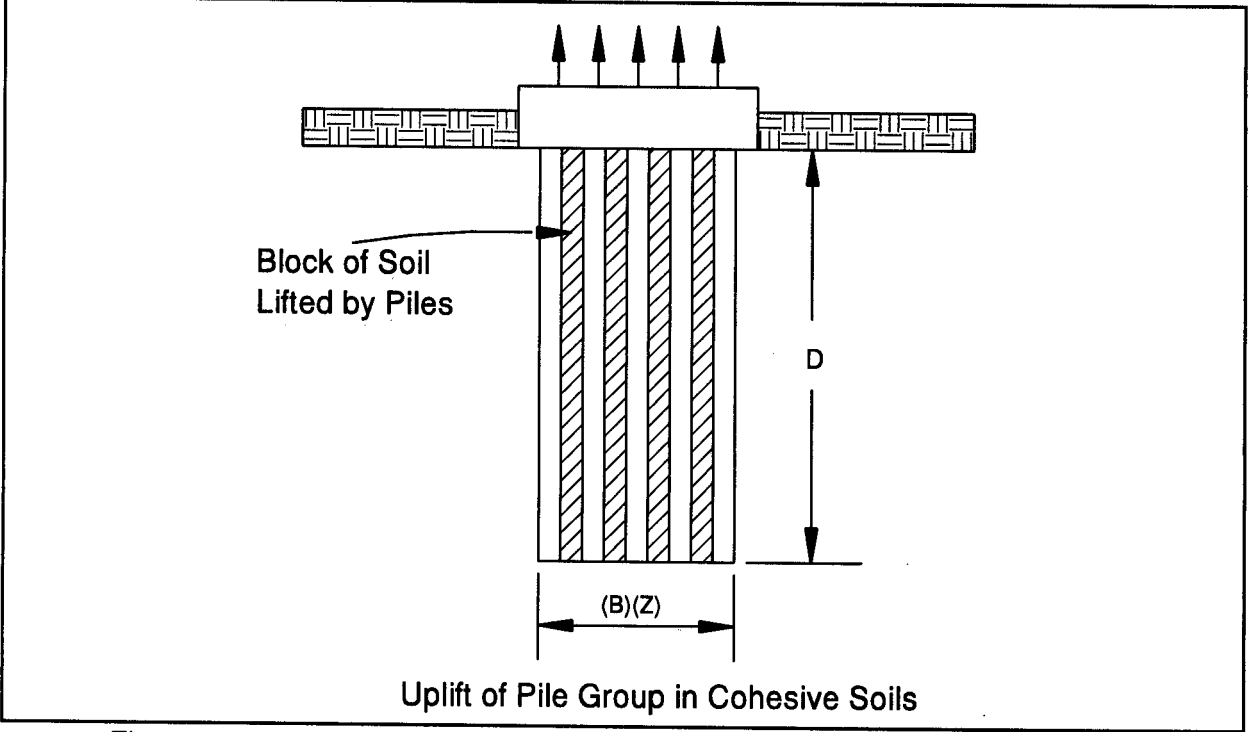


Figure 9.49 Uplift of Pile Group in Cohesive Soils (after Tomlinson, 1994)

Tomlinson states that a factor of safety of 2 should be used with this calculation to allow for possible weakening of the soil around the pile group as a result of the pile group installation. If long term sustained uplift loading is anticipated, a factor of safety of 2.5 to 3 is recommended. Tomlinson also recommends that the ultimate group uplift capacity determined from this calculation not exceed the sum of the ultimate uplift capacities of the individual piles comprising the pile group divided by an appropriate factor of safety. It is recommended that a factor of safety of 2 be used if the ultimate uplift capacity of an individual pile is determined from an uplift load test, and a factor of safety of 3 be used if based on the shaft resistance from a static calculation.

9.8.4 Lateral Capacity of Pile Groups

The ability of a pile group to resist lateral loads from vessel impact, debris, wind, or wave loading, seismic events, and other sources is a significant design issue. The deflection of a pile group under a lateral load is typically 2 to 3 times larger than the deflection of a single pile loaded to the same intensity. Holloway *et al.* (1981), and Brown *et al.* (1988) reported that piles in trailing rows of pile groups have significantly less resistance to a lateral load than piles in the lead row, and therefore exhibit greater deflections. This is due to the pile-soil-pile interaction that takes place in a pile group. The pile-soil-pile interaction results in the lateral capacity of a pile group being less than the sum of the lateral capacities of the individual piles comprising the group. Hence, laterally loaded pile groups have a group efficiency of less than 1.

The lateral capacity of an individual pile in a pile group is a function of its position in the group and the center to center pile spacing. Brown *et al.* (1988) proposed a p-multiplier, P_m , be used to modify the p-y curve of an individual pile based upon the piles row position. An illustration of the p-multiplier concept is presented in Figure 9.50. For piles in a given row, the same P_m value is applied to all p-y curves along the length of the pile. In a lateral load test of a 3 by 3 pile group in very dense sand with a center to center pile spacing of 3b, Brown found the leading row of piles had a P_m of 0.8 times that of an individual pile. The P_m values for the middle and back row of the group were 0.4 and 0.3, respectively.

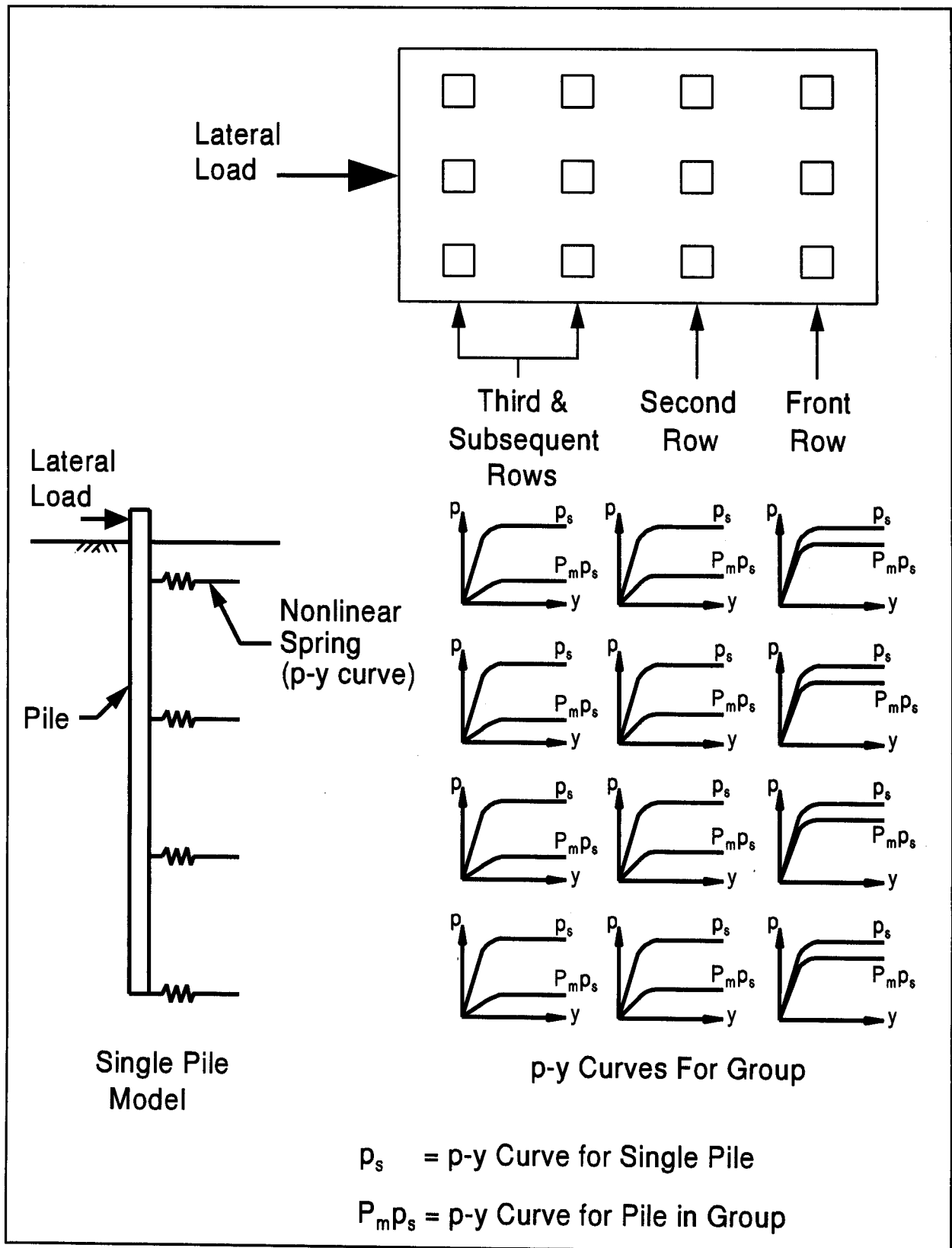


Figure 9.50 Illustration of p-multiplier Concept for Lateral Group Analysis

McVay, *et al.* (1995) performed centrifuge model tests on a 3 by 3 pile group having center to center pile spacings of 3b and 5b. A dense and loose sand condition were simulated in the centrifuge model tests. For the dense sand case at a center to center spacing of 3b, the centrifuge model test results were similar to Brown's field results. However, McVay also found that the P_m values were influenced by soil density and the center to center spacing. The P_m results from McVay's centrifuge tests as well as other recent results for vertical piles in 3 x 3 pile groups are summarized in Table 9-15. McVay's centrifuge tests indicated lateral load group efficiencies in sands on the order of 0.74 for a center to center pile of 3b and 0.93 for a center to center spacing of 5b. Field studies in cohesive soils have also shown that pile-soil-pile interaction occurs. Brown *et al.* (1987) reported P_m values of 0.7, 0.5, and 0.4 for the lead, second, and third row of a laterally loaded pile group in stiff clays.

The most recent work on this topic has included full scale lateral load testing of a 16 pile group in loose sand by Ruesta and Townsend (1997), and a 9 pile group in clayey silt by Rollins *et al.* (1998). A scaled model study of a cyclically laterally loaded pile group in medium clay has also been reported by Moss (1997). The center to center pile spacing, P_m results, and pile head deflections reported in these studies are included in Table 9-15. NCHRP Project 24-09 entitled "Static and Dynamic Lateral Loading of Pile Groups" is also in progress (1998). The objective of this study is to develop and validate an improved design method for pile groups subjected to static and dynamic lateral loads.

Brown and Bollman (1993) proposed a p-multiplier procedure for the design of laterally loaded pile groups. It is recommended that this approach, outlined in the step by step procedure that follows, be used for the design of laterally loaded pile groups. In the future, it is anticipated that the FHWA computer program DEEP FOUNDATIONS currently under development will be the primary design tool for analysis of pile groups under axial and lateral loads. This program, which is a successor of the LPGSTAN program by Hoit and McVay (1994), will use a p-multiplier approach in evaluation of laterally loaded pile groups under axial, lateral, and combined axial and lateral loads. The new program will also be capable of analyzing driven pile and drilled shaft foundation supported sound walls, retaining walls, signs and high mast lighting structures.

TABLE 9-15 LATERALLY LOADED PILE GROUPS STUDIES

Soil Type	Test Type	Center to Center Pile Spacing	Calculated p-Multipliers, P_m For Rows 1, 2, & 3+	Reported Group Efficiency	Deflection (mm)	Reference
Stiff Clay	Field Study	3b	.70, .50, .40	---	51	Brown <i>et al</i> , (1987)
Stiff Clay	Field Study	3b	.70, .60, .50,	---	30	Brown <i>et al</i> , (1987)
Medium Clay	Scale Model-Cyclic Load	3b	.60, .45, .40	---	600 at 50 cycles	Moss (1997)
Clayey Silt	Field Study	3b	.60, .40, .40	---	25-60	Rollins <i>et al</i> , (1998)
V. Dense Sand	Field Study	3b	.80, .40, .30	75%	25	Brown <i>et al</i> , (1988)
M. Dense Sand	Centrifuge Model	3b	.80, .40, .30	74%	76	McVay <i>et al</i> , (1995)
M. Dense Sand	Centrifuge Model	5b	1.0, .85, .70	95%	76	McVay <i>et al</i> , (1995)
Loose M. Sand	Centrifuge Model	3b	.65, .45, .35	73%	76	McVay <i>et al</i> , (1995)
Loose M. Sand	Centrifuge Model	5b	1.0, .85, .70	92%	76	McVay <i>et al</i> , (1995)
Loose F. Sand	Field Study	3b	.80, .70, .30	80%	25-75	Ruesta <i>et al</i> , (1997)

STEP BY STEP DESIGN PROCEDURE FOR LATERALLY LOADED PILE GROUPS

STEP 1 Develop p-y curves for single pile.

- a. Obtain site specific single pile p-y curves from instrumented lateral pile load test at site.
- b. Use p-y curves based on published correlations with soil properties.

- c. Develop site specific p-y curves based on in-situ test data such as pressuremeter.

STEP 2 Perform COM624P analyses.

- a. Perform COM624P analyses using the P_m value for each row position to develop load-deflection and load-moment data.

- b. Based on current data, it is suggested that P_m values of 0.8 be used for the lead row, 0.4 for the second row, and 0.3 for the third and subsequent rows. These recommendations are considered reasonable for center to center pile spacing of $3b$ and pile deflections at the ground surface of $.10$ to $.15b$. For larger center to center spacings or smaller deflections, these P_m values should be conservative.

- c. Determine shear load versus deflection behavior for piles in each row. Plot load versus pile head deflection results similar to as shown in Figure 9.51(a).

STEP 3 Estimate group deflection under lateral load.

- a. Average the load for a given deflection from all piles in the group to determine the average group response to a lateral load as shown in Figure 9.51(a).

- b. Divide the lateral load to be resisted by the pile group by the number of piles in the group to determine the average lateral load resisted per pile. Enter load-deflection graph similar to Figure 9.51(a) with the average load per pile to estimate group deflection using the group average load deflection curve.

STEP 4 Evaluate pile structural acceptability.

- a. Plot the maximum bending moment determined from COM624P analyses versus deflection for each row of piles as illustrated in Figure 9.51(b).
- b. Check the pile structural adequacy for each row of piles. Use the estimated group deflection under the lateral load per pile to determine the maximum bending moment for an individual pile in each row.
- c. Determine maximum pile stress from COM624P output associated with the maximum bending moment.
- d. Compare maximum pile stress with pile yield stress.

STEP 5 Perform refined pile group evaluation that considers superstructure-substructure interaction.

9.9 SPECIAL DESIGN CONSIDERATIONS

In certain situations, additional design problems exist that must be analyzed. These special design considerations include negative shaft resistance, vertical ground movements from swelling soils, lateral squeeze of foundation soils, scour effects on pile capacity, pile heave, and seismic considerations.

9.9.1 Negative Shaft Resistance or Downdrag

When piles are installed through a soil deposit undergoing consolidation, the resulting relative downward movement of the soil around piles induces "downdrag" forces on the piles. These "downdrag" forces are also called negative shaft resistance. Negative shaft resistance is the reverse of the usual positive shaft resistance developed along the pile surface. The downdrag force increases the axial load on the pile and can be especially significant on long piles driven through compressible soils. Therefore, the potential for negative shaft resistance must be considered in pile design. Batter piles should be avoided in soil conditions where large soil settlements are expected because of the additional bending forces imposed on the piles, which can result in pile deformation and damage.

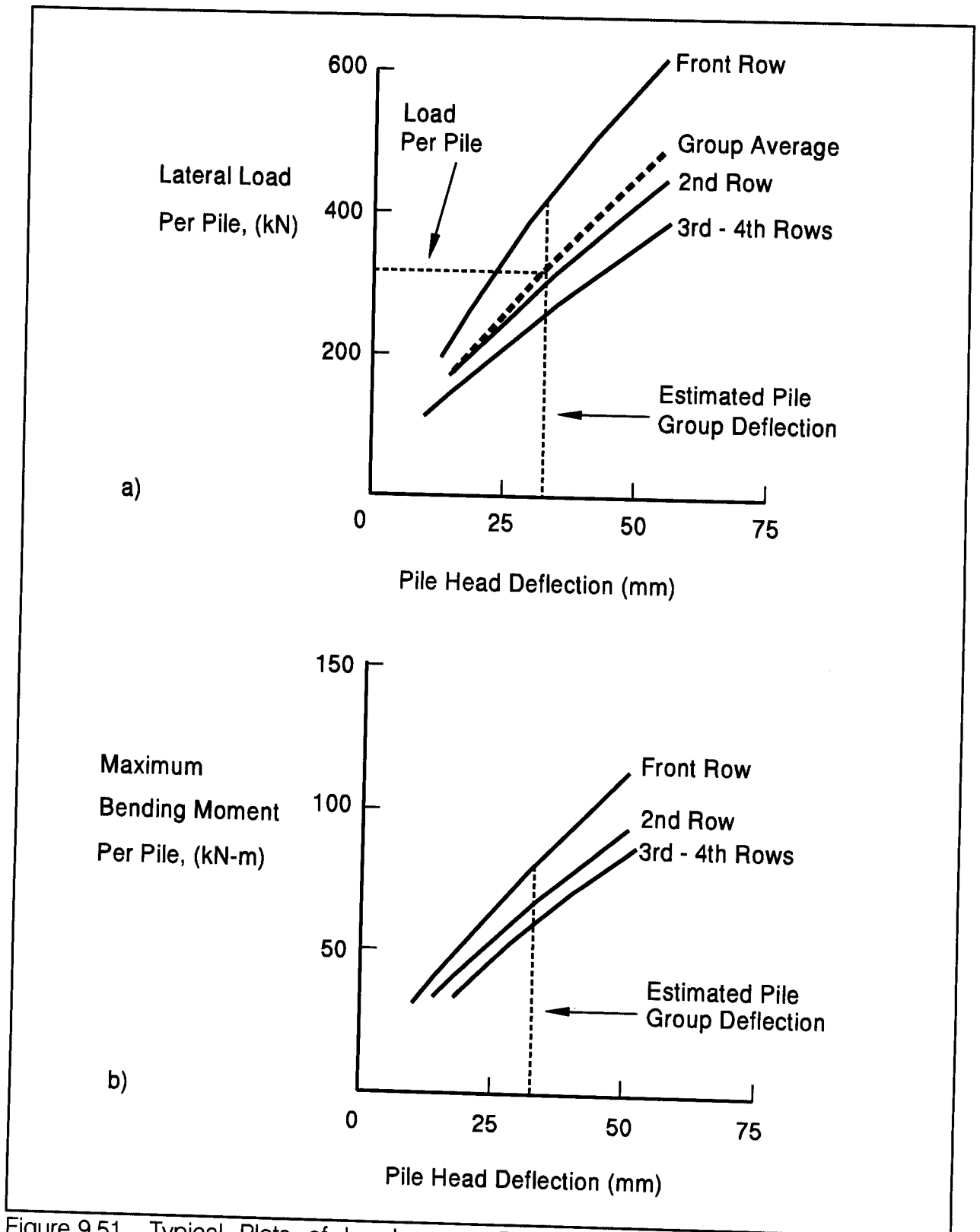


Figure 9.51 Typical Plots of Load versus Deflection and Bending Moment versus Deflection for Pile Group Analysis (adapted from Brown and Bollman, 1993)

Settlement computations should be performed to determine the amount of settlement the soil surrounding the piles is expected to undergo after the piles are installed. The amount of relative settlement between soil and pile that is necessary to mobilize negative shaft resistance is about 10 to 12 mm. At that movement, the maximum value of negative shaft resistance is equal to the soil-pile adhesion. The negative shaft resistance can not exceed this value because slip of the soil along the pile shaft occurs at this value. It is particularly important in the design of friction piles to determine the depth at which the pile will be unaffected by negative shaft resistance. Only below that depth can positive shaft resistance forces provide support to resist vertical loads.

The most common situation where large negative shaft resistance develops occurs when fill is placed over a compressible layer immediately prior to, or after piles are driven. This condition is shown in Figure 9.52(a). Negative shaft resistance can also develop whenever the effective overburden pressure is increased on a compressible layer through which a pile is driven; due to lowering of the ground water table as illustrated in Figure 9.52(b), for example.

Briaud and Tucker (1993) presented the following criteria for identifying when negative shaft resistance may occur. If any one of these criteria is met, negative shaft resistance should be considered in the design. The criteria are:

1. The total settlement of the ground surface will be larger than 100 mm.
2. The settlement of the ground surface after the piles are driven will be larger than 10 mm.
3. The height of the embankment to be placed on the ground surface exceeds 2 m.
4. The thickness of the soft compressible layer is larger than 10 m.
5. The water table will be lowered by more than 4 m.
6. The piles will be longer than 25 m.

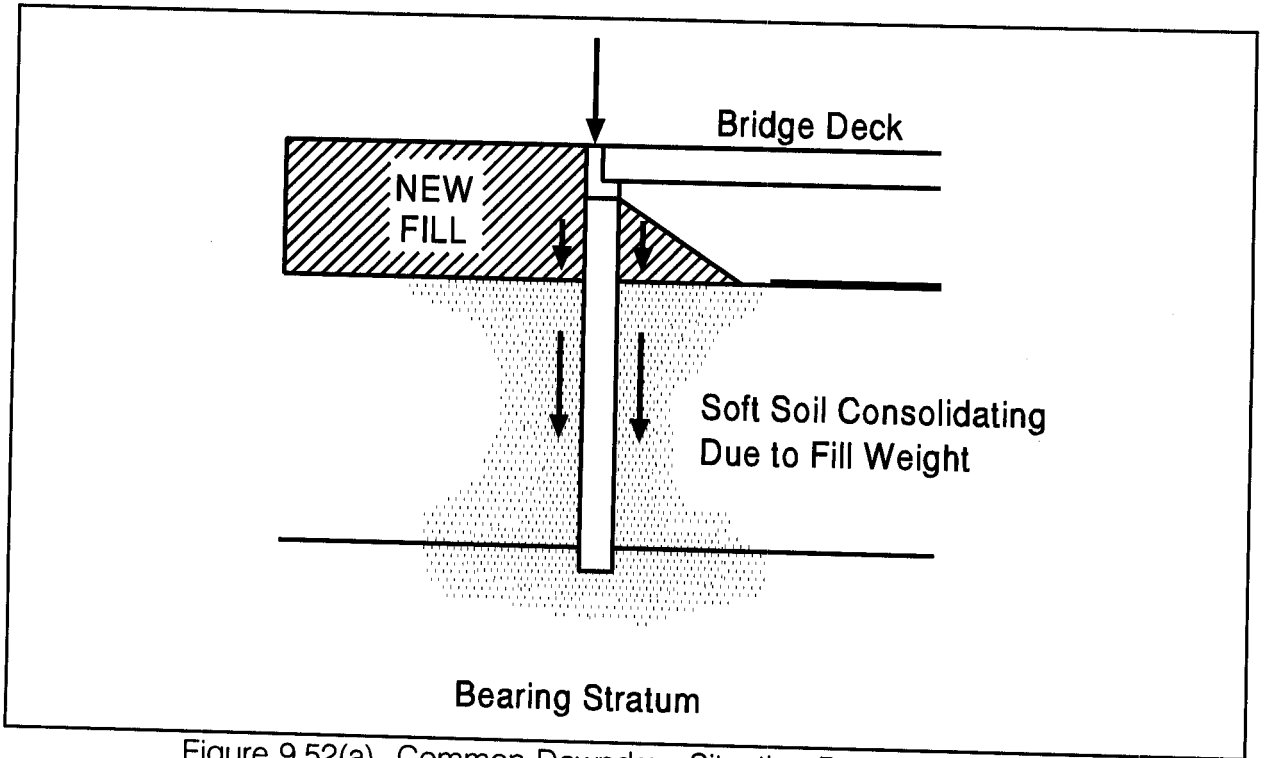


Figure 9.52(a) Common Downdrag Situation Due to Fill Weight

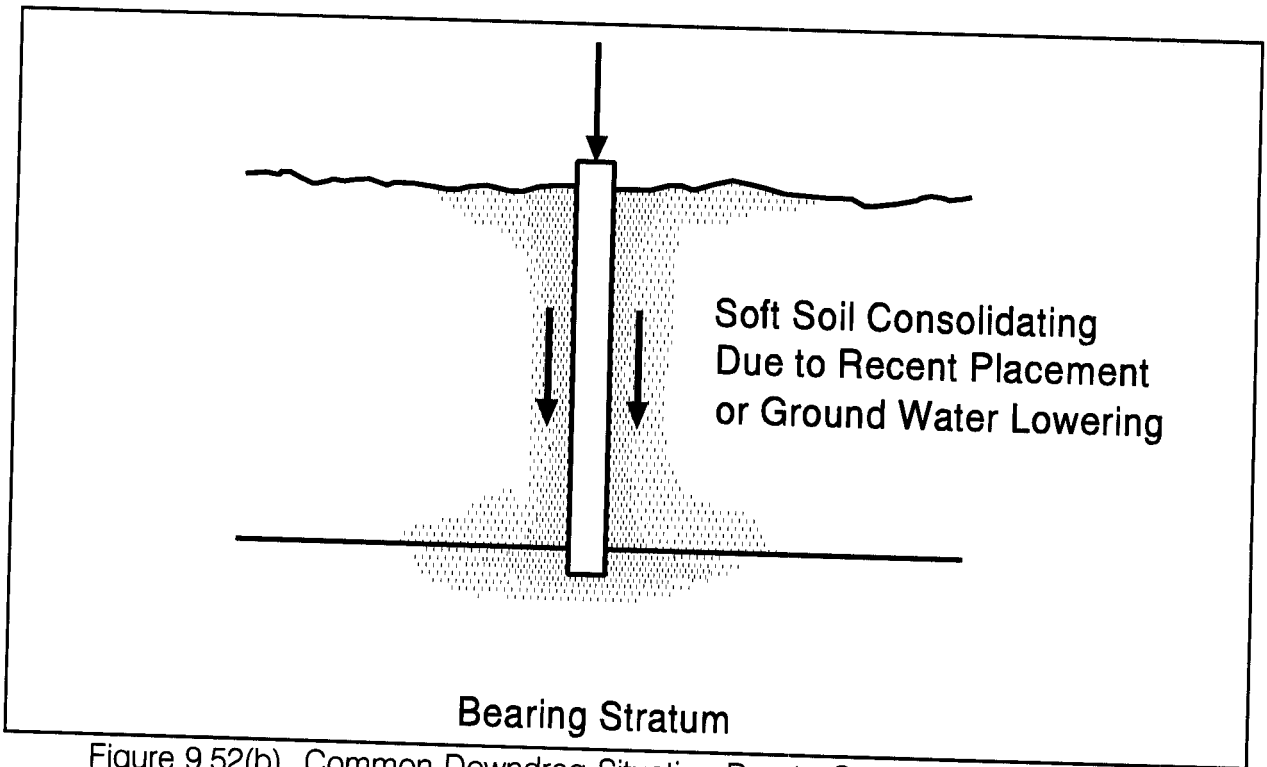


Figure 9.52(b) Common Downdrag Situation Due to Ground Water Lowering

9.9.1.1 *Methods for Determining Negative Shaft Resistance*

Negative shaft resistance is similar to positive shaft resistance, except the direction of force is opposite. Two design approaches have been used for the design of pile foundations subject to negative shaft resistance. The traditional method has been to calculate the shaft resistance from the soil layers above the zone of consolidating soils, and add this resistance as a load the pile supports. In this approach, any of the previously discussed methods for computing positive pile shaft resistance in cohesive and cohesionless soils can be used. Newer methods of determining negative shaft resistance loads are based on the interrelationship between pile movement and the developed negative shaft resistance load, such as used in the NCHRP study entitled "Downdrag on Bitumen-Coated Piles" by Briaud and Tucker (1993).

9.9.1.1a *Traditional Approach to Negative Shaft Resistance*

The total stress α -method presented in Section 9.7.1.3 is often used for computing the negative shaft resistance or drag load in cohesive soils. In this approach, the adhesion calculated from the undrained shear strength of the soil times the pile perimeter is equated to the drag load from the consolidating soil layers. Similarly, the drag load from cohesionless layers above a consolidating soil layer is calculated from the shaft resistance in the cohesionless layers.

When selecting the undrained shear strength for calculation of the negative shaft resistance adhesion in the α -method, it is important to remember that the consolidating cohesive soil will have a higher undrained shear strength with time. The adhesion should be calculated using either the higher adhesion value, determined from the undrained shear strength at the time of the soil borings, or the estimated undrained shear strength of the soil after consolidation. Drag loads equal to 100% of the undrained shear strength of a soft clay, ie $\alpha = 1$, have been reported by Johansesen and Bjerrum (1965) for toe bearing piles driven to a relatively unyielding bearing layer. Engineering judgement should be exercised in determining drag loads so that the drag load is not grossly overestimated, resulting in an expensive foundation design, nor underestimated, resulting in a overloaded foundation.

STEP BY STEP DESIGN PROCEDURE FOR ANALYSIS OF DOWNDRAG LOADING

- STEP 1 Establish the simplified soil profile and soil properties for computing settlement.
- STEP 2 Determine the overburden pressure increase, Δp , versus depth due to the approach embankment fill.

The overburden pressure increase, Δp , is equal to the pressure coefficient, K_r , determined from the pressure distribution chart presented in Figure 9.53, multiplied by the height of fill, h_f , and the unit weight of fill, γ_f .

The pressure distribution chart provides the pressure coefficient, K_r , at various depths below the bottom of the fill (x/b_f), and also at various distances from the centerline of the fill. The depth below the bottom of the fill is given as a multiple of " b_f ", where b_f is the distance from the centerline of the fill to the midpoint of the fill side slope, as shown in Figure 9.53.

For downdrag loading settlement calculations, the overburden pressure increase, Δp , at various depths beneath the centerline of the fill needs to be calculated over the embedded pile length.

- STEP 3 Perform settlement computations for the soil layers along the embedded pile length.
- Determine consolidation test parameters for each soil layer from laboratory consolidation test results.
 - Compute settlement of each soil layer using the appropriate settlement equation provided in Section 9.8.2.3 for cohesive layers or Section 9.8.2.4 for cohesionless layers.
 - Compute the total settlement over the embedded pile length which is equal to the sum of the settlement from each soil layer. Do not include soil settlements below the pile toe level in this computation.

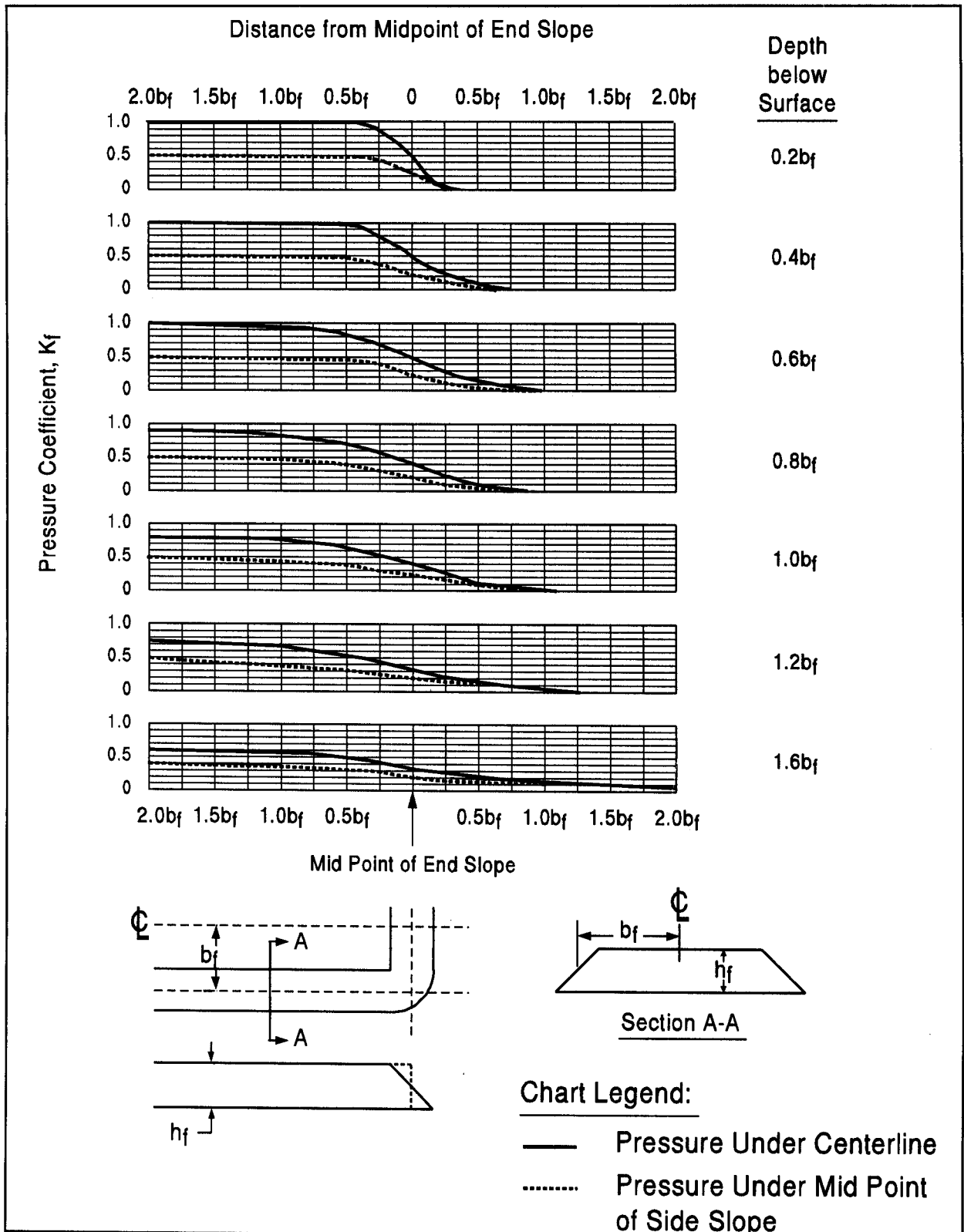


Figure 9.53 Pressure Distribution Chart Beneath the End of a Fill (After Cheney and Chassie, 1993)

STEP 4 Determine the pile length that will experience negative shaft resistance.

Negative shaft resistance occurs due to the settlement between soil and pile. The amount of settlement between soil and pile necessary to mobilize the negative shaft resistance is about 10 mm. Therefore, negative shaft resistance will occur on the pile shaft in each soil layer or portion of a soil layer with a settlement greater than 10 mm.

STEP 5 Determine magnitude of negative shaft resistance, Q_s^- .

The method used to calculate the ultimate negative shaft resistance over the pile length determined in Step 4 should be the same method used to calculate the ultimate positive shaft resistance, except that it will act in the opposite direction.

STEP 6 Calculate the ultimate pile capacity provided by the positive shaft resistance and the toe resistance, Q_u^+ .

Positive shaft and toe resistances will develop below the depth where the relative pile-soil movements are less than 10 mm. The positive soil resistances can be calculated on the pile length remaining below the negative shaft resistance depth from Step 4 using an appropriate static analysis method for the soil type as described in this chapter.

STEP 7 Calculate the net ultimate pile capacity, Q_u^{NET} , available to resist imposed loads.

$$Q_u^{NET} = Q_u^+ - Q_s^-$$

STEP 8 Consider alternatives to obtain higher net ultimate pile capacity.

Alternatives are described in Section 9.9.1.2 and include use of preloading or wick drains to reduce settlements prior to pile installation, use of lightweight fills to reduce settlements that cause downdrag loads, use of friction reducers to reduce downdrag loads, use of higher allowable material stress, and isolation of pile from consolidating soil.

An example calculation using this step by step procedure is included in Appendix F.6.

9.9.1.2 Methods for Reducing Negative Shaft Resistance Forces

In situations where the negative shaft resistance on piles is large and a reduction in the pile design load is impractical, negative shaft resistance forces can be handled or reduced by using one or more of the following techniques:

a. Reduce soil settlement

Preconsolidation of compressible soils can be achieved by preloading and consolidating the soils **prior** to pile installation. This approach is often used for bridge foundations in fill sections. Wick drains are often used in conjunction with preloading in order to shorten the time required for consolidation. Additional information on wick drains is available in "Prefabricated Vertical Drains", FHWA RD 86/168 by Rixner *et al.* (1986) and in "Ground Improvement Technology Manual" for FHWA Demonstration Project 116, Elias *et al.* (1996).

b. Use lightweight fill material

Construct structural fills using lightweight fill material to reduce the downdrag loads. Lightweight fill materials often used, depending upon regional availability, include geofam, foamed concrete, wood chips, blast furnace slag, and expanded shales. Additional information on lightweight fills is available through FHWA Demonstration Project 116, Elias *et al.* (1996).

c. Use a friction reducer

Bitumen coating and plastic wrap are two methods commonly used to reduce the friction at the pile-soil interface. Bitumen coatings should only be applied to the portion of the pile which will be embedded in the negative shaft resistance zone. Case histories on bitumen coatings have reported reductions in negative shaft resistance from as little as 47% to as much as 90%. Goudreault and Fellenius (1994) suggest that the reduction effect of bitumen may be analyzed by using an upper limit of 10 kPa as the pile-soil shear resistance or adhesion in the bitumen coated zone.

One of the major problems with bitumen coatings is protecting the coating during pile installation, especially when driving through coarse soils. An inexpensive solution to this problem is to weld an over-sized collar around the pile where the bitumen ends. The collar opens an adequate size hole to permit passage of the bitumen for moderate pile lengths in fine grained soils. Bitumen coatings can present additional construction problems associated with field coating and handling. The use of bitumen coatings can be quite successful provided proper construction control methods are followed. Bitumen coatings should not be casually specified as the solution to downdrag loading.

The proper bitumen must have relatively low viscosity to permit slippage during soil consolidation, yet high enough viscosity and adherence to insure the coating will stick to the pile surface during storage and driving, and sufficient ductility to prevent cracking and spalling of the bitumen during handling and driving. Therefore, the climate at the time of pile installation should be considered in selection of the proper bitumen coating. Example specifications for bitumen coatings applied to concrete and steel piles are provided in Appendix C. Note that these are generic specifications that should be modified to meet the specific needs of each project.

Plastic wrap has proven to be an economically attractive friction reducer, particularly for abutment piles driven behind and before construction of MSE walls. Tawfig (1994) performed laboratory tests on 0.15 mm thick polyethylene sheets used as a friction reducer. The laboratory test results indicated plastic wraps reduced the pile-soil shear resistance from between 78% for a one wrap layer to 98% for a two layer wrap with mineral oil lubricant of the pile-soil shear resistance. The laboratory test data indicated the pile-soil shear resistance of a one wrap layer was about 10 kPa and only 1 kPa for the lubricated two wrap system.

d. Increase allowable-pile stress

In piles where the allowable pile material strength has not been fully utilized, the pile design stress can be increased to offset the negative shaft resistance load. Increased structural capacity can also be obtained by using higher strength pile materials, or in the case of pipe piles, by using an increased wall thickness. Foundation settlement at the increased loading should be computed and checked against the foundation performance criteria.

e. Prevent direct contact between soil and pile

Pile sleeves are sometimes used to eliminate direct contact between pile and soil. Bentonite slurry has been used in the past to achieve the same purpose. These methods are generally more expensive.

9.9.2 Vertical Ground Movements from Swelling Soils

Detrimental vertical ground movements can also occur in swelling soils subject to seasonal moisture changes, such as expansive clays. In this case, the swell pressures can induce uplift forces on the pile. For piles driven in swelling soils, bitumen coatings on the pile shaft through the swelling soil zone is effective in reducing the uplift forces.

9.9.3 Lateral Squeeze of Foundation Soil

Bridge abutments supported on piles driven through soft compressible cohesive soils may tilt forward or backward depending on the geometry of the backfill and the abutment. This problem is illustrated in Figure 9.54. Large horizontal movements may cause damage to the structure. The unbalanced fill loads shown in Figure 9.54 displace the soil laterally. This lateral displacement may bend the piles, causing the abutment to tilt toward or away from the fill.

The following rules of thumb are recommended for determining whether tilting will occur, as well as estimating the magnitude of horizontal movement.

1. Lateral squeeze and abutment tilting can occur if:

$$[\gamma \text{ fill (kN/m}^3\text{)}] [\text{fill height (m)}] > 3 [\text{undrained shear strength of soft soil (kPa)}]$$

2. If abutment tilting can occur, the magnitude of the horizontal movement can be estimated by the following formula:

$$\text{Horizontal Abutment Movement (mm)} = 0.25 \text{ Vertical Fill Settlement (mm)}$$

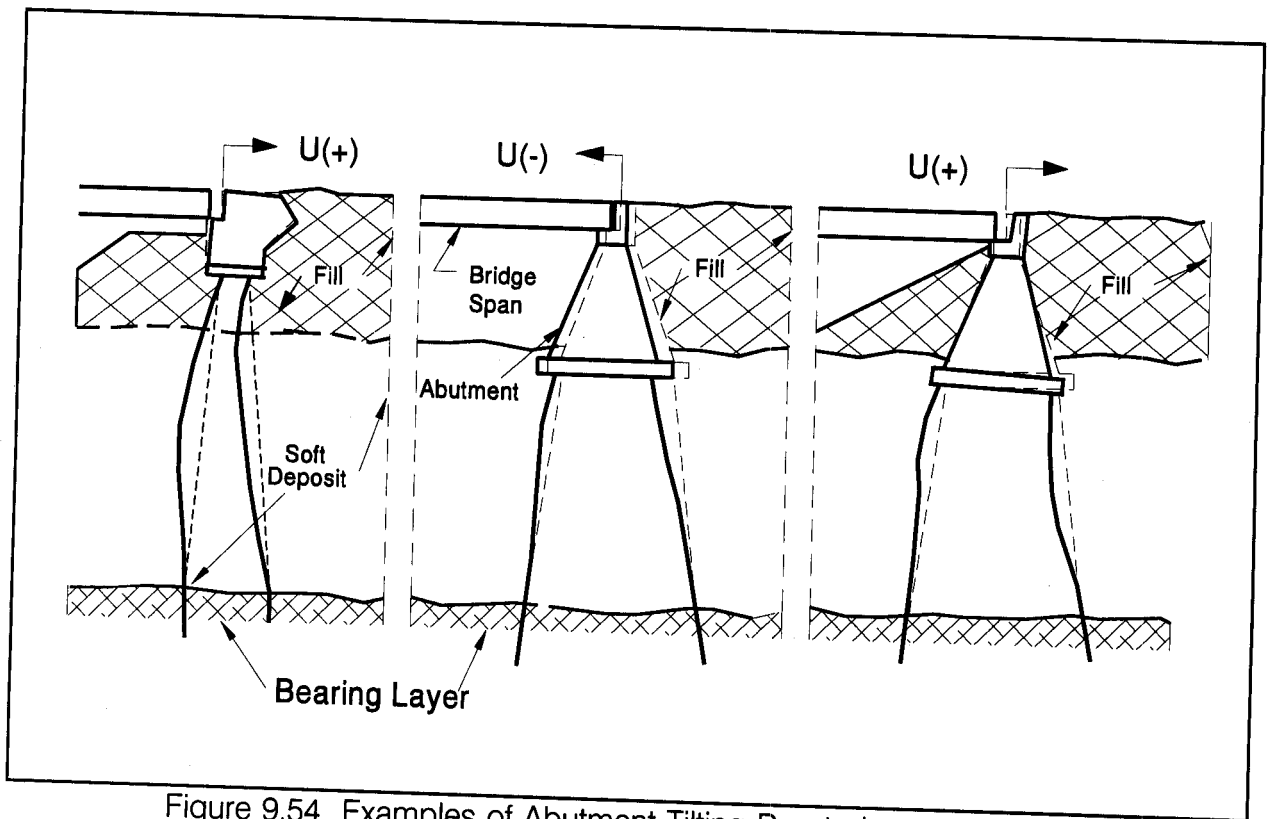


Figure 9.54 Examples of Abutment Tilting Due to Lateral Squeeze

9.9.3.1 Solutions to Prevent Tilting

- Delay installation of abutment piling until after fill settlement has stabilized (best solution).
- Provide expansion shoes large enough to accommodate the movement.
- Use steel H-piles to provide high tensile strength in flexure.
- Use lightweight fill to reduce driving forces.

9.9.4 Bearing Capacity of Piles in Soils Subject to Scour

Scour occurs as a result of flowing water eroding away soil materials from the stream bed and/or stream banks. Scour can be classified as local scour, which effect soils only in the immediate vicinity of a substructure unit, or can be classified as channel degradation scour, where stream bed materials are removed over a large area. In a flood event, loose granular

soils can be eroded away in a few hours. The time required for cohesive or cemented soils to erode is typically longer, but the scour depth of eroded soil materials can be as deep as in cohesionless deposits. As noted earlier in this chapter, the capacity of a driven pile is due to soil resistance along the pile shaft and at the pile toe. Therefore, the erosion of the soil materials providing pile support can have significant detrimental effects on pile bearing capacity and must clearly be evaluated during the design stage.

The ultimate bearing capacity of a pile in a soil deposit subject to local or channel degradation scour requires multiple static analyses. In the case of local scour, the soil resistance in the scour zone provides resistance at the time of driving that cannot be counted on for long term support. Hence, for design purposes the shaft resistance in the scour zone is ignored, but for driveability considerations it is not. For pile capacity calculations in local scour cases, only the reduction in soils resistance in the scour zone is considered, and the effective overburden pressure is unchanged.

The effects of channel degradation scour on pile capacity are more severe. In channel degradation scour, the soil resistance in the scour zone once again provides resistance at the time of driving that cannot be counted on for long term support. Therefore, the shaft resistance in the scour zone is ignored for long term pile support considerations, but not for driveability considerations. More important, pile capacity calculations in channel degradation scour cases must also include the reduction in the effective overburden pressure due to removal of the stream bed materials. This reduction in effective stresses can have a significant effect on the calculated shaft and toe resistances. Figure 9.55 provides an illustration of local and channel degradation scour.

The FHWA publication FHWA-IP-90-017, "Evaluating Scour at Bridges" by Richardson and Davis (1995), more commonly known as HEC-18, recommends the following pile design issues also be considered at bridge sites subject to scour.

1. A reduced number of longer (higher capacity) piles should be used rather than a larger number of shorter (lower capacity) piles. This results in a greater factor of safety against failure due to scour.
2. Pile caps should be situated at or below the maximum anticipated scour depth. This will limit obstruction to flood flows which can cause local scour. It may be desirable to set the pile caps at an even lower depth if the piles can be damaged by erosion or corrosion and degradation from river currents. However in deep water situations, it may be more

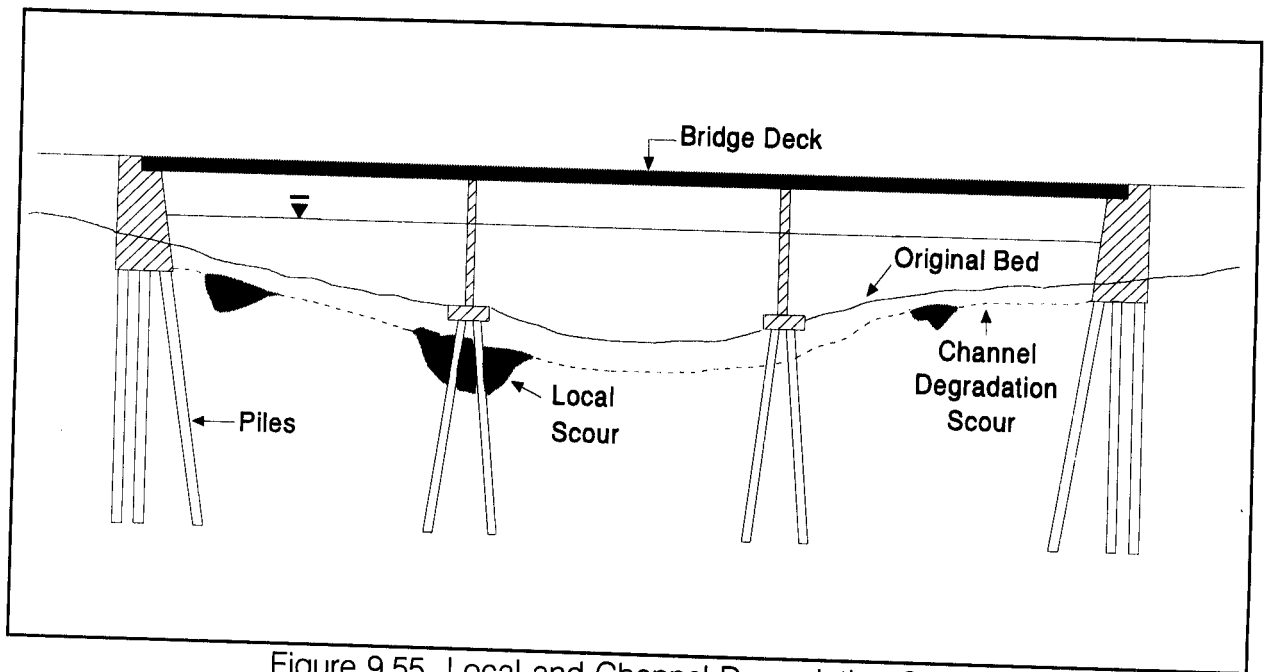


Figure 9.55 Local and Channel Degradation Scour

cost effective to situate the pile cap above the mudline and design the foundation accordingly.

3. Piles should be designed for additional lateral restraint and column action because of the increase in the unsupported pile length after scour. The unsupported pile length is discussed in Chapter 11.
4. Stub abutments founded on piles in the approach embankments should be driven below the elevation of the thalweg, which is the lowest elevation of the river bed in the river channel. In this way, structural integrity is maintained if the thalweg shifts and the approach embankment material is scoured to the thalweg elevation provided that the piles are designed for the unsupported length.

The recommended design procedure for scour is dependent on the design event. For scour depths associated with either the 100 year flood event or the overtopping flood, the procedure illustrated in Section 9.6 should be followed where the factor of safety is linked to the construction control. For the superflood, or 500 year event, HEC-18 states a minimum factor of safety of 1.0 is acceptable. This minimum factor of safety is determined by dividing the maximum pile load by the sum of the shaft and toe resistances available below the scour depth. The shaft and toe resistances should be determined from an appropriate static analysis calculation as detailed earlier in this chapter.

9.9.5 Soil and Pile Heave

As noted by Haggerty and Peck (1971), whenever piles are driven, soil is displaced. This can result in both upward movement (pile heave) and lateral movements of previously driven piles. These soil movements can be detrimental to the capacity of previously driven piles as well as to adjacent facilities. Obviously, the greater the volume of soil displaced by pile driving, the greater the potential for undesirable movements of previously driven piles, or damage to adjacent structures. Heave of toe bearing piles is particularly troublesome since the pile may be lifted from the bearing stratum, thereby greatly reducing the pile capacity and increasing the foundation settlement when loaded. Haggerty and Peck noted that saturated, insensitive clays behave incompressibly during pile driving and have the greatest heave potential.

When piles are to be installed in cohesive soils, it is recommended that the potential magnitude of vertical and lateral soil movements be considered in the design stage. If calculations indicate that movements may be significant, use of an alternate low displacement pile, or specifying a modified installation procedure (such as predrilling to reduce the volume of displaced soil) should be evaluated. A step by step procedure adapted from Haggerty and Peck for estimating soil and pile heave in a saturated insensitive clay follows. The procedure assumes a regular pile driving sequence and a level foundation surface. The paper by Haggerty and Peck should be consulted for modifications to the recommended procedure for conditions other than those stated.

STEP BY STEP PROCEDURE FOR ESTIMATING SOIL AND PILE HEAVE

- STEP 1 Calculate the estimated soil heave at the ground surface.
- a. Divide the volume of inserted piles by the volume of soil enclosed by the pile foundation to obtain the volumetric displacement ratio.
 - b. Estimate the normalized soil heave (soil heave / pile length) from $\frac{1}{2}$ the volumetric displacement ratio calculated in Step 1a.
 - c. Calculate the soil heave at the ground surface by multiplying the normalized soil heave in Step 1b by the average length of piles.

STEP 2 Determine the depth of no pile-soil movement.

- a. Figure 9.56 illustrates a depth, d , exists where the potential upward pushing and downward resisting forces on the pile shaft are equal.
- b. Calculate the pile-soil adhesion along the entire pile shaft using α -method described in Section 9.7.1.2a.
- c. Through multiple iterations determine the depth, d , where the adhesion from the upward pushing force equals the adhesion from the downward resisting force. Remember that only shaft resistance is considered in calculating the downward resisting force.

STEP 3 Calculate the estimated pile heave.

- a. Calculate the percentage of pile length subject to heave from $(D-d) / D$ where D is the embedded pile length, and d is the equilibrium depth from Step 2c.
- b. Calculate the estimated pile heave by multiplying the estimated soil heave from Step 1c by the percentage of pile length subject to heave from Step 3a.

9.9.6 Seismic Considerations

The design issues associated with pile foundation design for seismic events are significant and are beyond the scope of this manual. Other publications such as FHWA RD-86/102, Seismic Design of Highway Bridge Foundations by Lam and Martin (1986), and Division 1A - Seismic Design of AASHTO Standard Specification (1992) should be consulted for design guidance in seismically active areas. The FHWA is currently (1996) developing a geotechnical engineering circular on geotechnical earthquake engineering. This document is scheduled for publication in 1997. Pile foundation design issues in seismic events include liquefaction effects on pile capacity, ground movements, seismic induced foundation loads, and seismic induced drag loads. This manual will therefore only briefly address the identification of liquefiable soils and the consequences of liquefaction on pile foundation design.

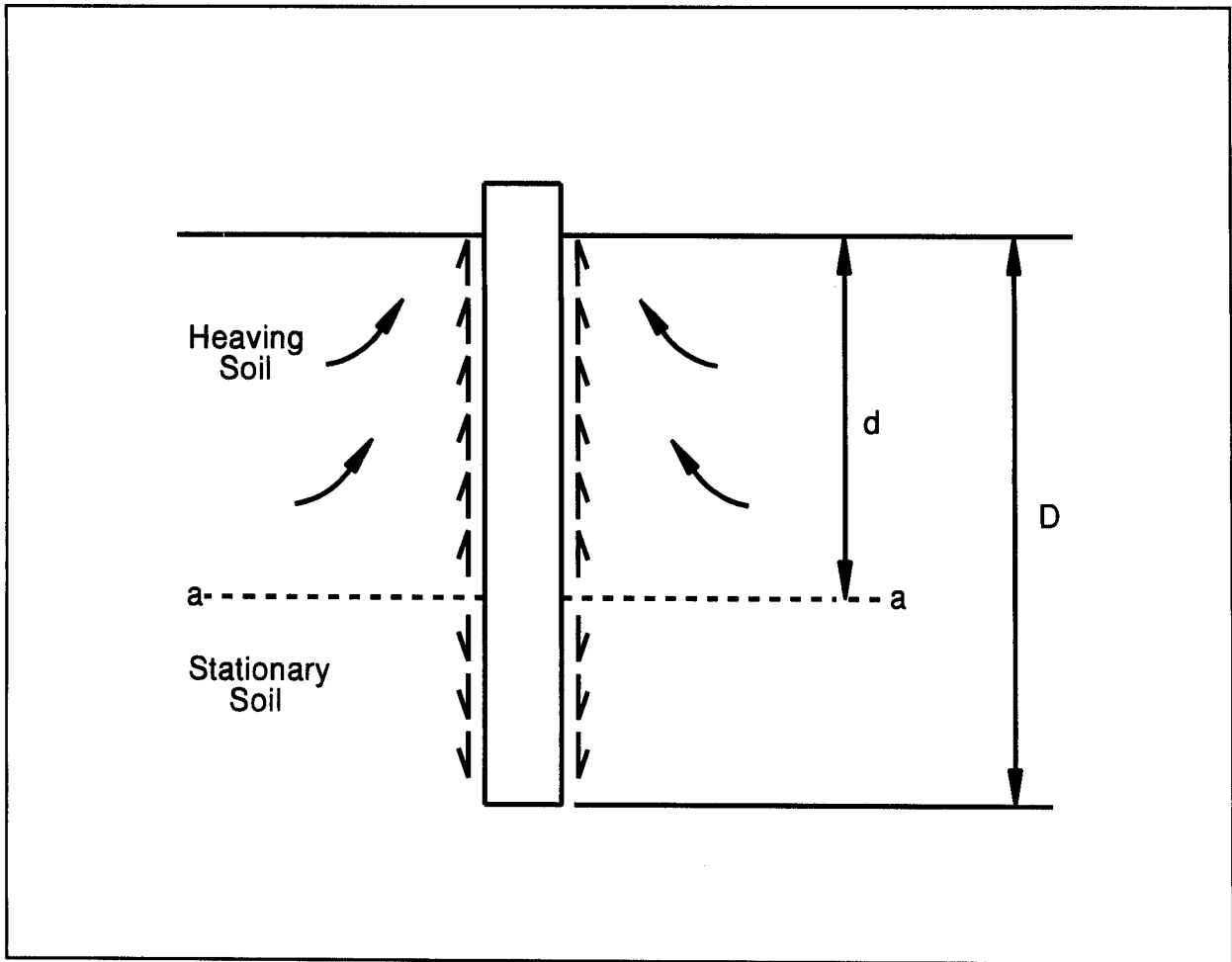


Figure 9.56 Balance of Forces on Pile Subject to Heave (after Haggerty and Peck, 1971)

Soil types most susceptible to liquefaction can be described as saturated, very loose to medium dense, fine to medium grained sands and non-plastic silts. However, liquefaction has also occurred in saturated, very loose to medium dense gravels and certain clayey soils.

In seismically active areas where peak earthquake acceleration will be greater than 0.1g, the soil susceptibility to liquefaction should be evaluated. A commonly used procedure for identification of liquefaction susceptible soils was proposed by Seed *et al.* (1983). This liquefaction evaluation approach is detailed in the Commentary for Section 6, Division 1A of the AASHTO Standard Specifications (1992) as well as Lam and Martin (1986). If the soils are found to liquefy during the design event, the pile foundation must be designed to accommodate the loss of frictional resistance, seismic induced loads, as well as the

anticipated vertical and horizontal displacements. Alternatively, the liquefaction potential may be mitigated through ground improvement techniques.

Pile foundations in liquefiable soils must penetrate through the zone of liquefaction and develop adequate capacity in the underlying soils. Evaluation of compression and uplift capacities during the seismic event can be made by assigning residual strength properties to the liquefiable layers. Residual strengths of sands and silty sands can be approximated from SPT resistance values using a correlation proposed by Seed (1987) and updated by Seed and Harder (1990).

Following a seismic event that induces soil liquefaction, the liquefied layer will consolidate. The soil resistance in and above the liquified layer will then become additional drag load that the pile must support. The pile foundation must be structurally capable of supporting this drag load and the foundation settlement resulting from the drag load must be within the structure's performance criteria.

Liquefaction induced lateral spread can impose significant bending moments in piles driven through liquefiable soils. Therefore, piles in liquefiable soils should be flexible and ductile in order to accommodate lateral loads. The maximum bending moment of piles in liquefiable soils is often evaluated in a COM624P analysis by assigning Reese's soft clay p-y curve with low residual shear strengths and high ϵ_{50} values to the liquefiable layer.

9.10 ADDITIONAL DESIGN AND CONSTRUCTION CONSIDERATIONS

The previous sections of this chapter addressed routine and special event static analysis procedures for pile foundation design. However, the designer should be aware of additional design and construction considerations that can influence the reliability of static analysis procedures in estimating pile capacity. These issues include the influence of time, predrilling or jetting, construction dewatering, soil densification, and the plugging of open pile sections on pile capacity. Pile driving induced vibrations can also influence the final design and static calculation results if potential vibration levels dictate changes in pile type or installation procedures. The closing section of this chapter focuses on pile driveability. Evaluation of pile driveability is a fitting final topic of this design chapter since all the previously described analyses are meaningless if the pile cannot be driven to the required depth and capacity without damage.

9.10.1 Time Effects on Pile Capacity

As noted in Section 9.2, the soil is greatly disturbed when a pile is driven into the soil. As the soil surrounding the pile recovers from the installation disturbance, a time dependent change in pile capacity often occurs. Frequently piles driven in saturated clays, and loose to medium dense silts or fine sands gain capacity after driving has been completed. This phenomenon is called soil setup. Occasionally piles driven into dense saturated fine sands, dense silts, or weak laminated rocks such as shale, will exhibit a decrease in capacity after the driving has been completed. This phenomenon is called relaxation. Case history discussions on soil setup and relaxation may be found in Fellenius *et al.* (1989), and Thompson and Thompson (1985), respectively.

9.10.1.1 Soil Setup

When saturated cohesive soils are compressed and disturbed due to pile driving, large excess pore pressures develop. These excess pore pressures are generated partly from the shearing and remolding of the soil and partly from radial compression as the pile displaces the soil. The excess pore pressures cause a reduction in the effective stresses acting on the pile, and thus a reduction in the soil shear strength. This results in a reduced pile capacity during, and for a period of time after, driving.

After driving, the excess pore pressures will dissipate primarily through radial flow of the pore water away from the pile. With the dissipation of pore pressures, the soil reconsolidates and increases in shear strength. This increase in soil shear strength results in an increase in the static pile capacity and is called soil setup. A similar decrease in resistance to pile penetration with subsequent soil setup may occur in loose to medium dense, saturated, fine grained sands or silts. The magnitude of the gain in capacity depends on soil characteristics, pile material and pile dimensions.

Because the pile capacity may increase after the end of driving, pile capacity assessments should be made from static load testing or retapping performed **after** equilibrium conditions in the soil have been re-established. The time for the return of equilibrium conditions is highly variable and depends on soil type and degree of soil disturbance. Piezometers installed within three diameters of the pile can be used to monitor pore pressure dissipation with time. Effective stress static pile capacity calculation methods can be used to evaluate the increase in capacity with time once pore pressures are quantified.

Static load testing or restrike testing of piles in fine grained soils should not be conducted until after pore pressures dissipate and return to equilibrium. In the absence of site specific pore pressure data from piezometers, it is suggested that static load testing or retapping of piles in clays and other predominantly fine grained soils be delayed for at least two weeks after driving and preferably for a longer period. In sandy silts and fine sands, pore pressures generally dissipate more rapidly. In these more granular deposits, five days to a week is often a sufficient time delay.

Rausche, *et al.* (1996) calculated general soil setup factors based on the predominant soil type along the pile shaft. The soil setup factor was defined as the static load test failure load divided by the end-of-drive wave equation capacity. These results are presented in Table 9-16. The data base for this study was comprised of 99 test piles from 46 sites. The number of sites and the percentage of the data base in a given soil condition is included in the table. While these soil set-up factors may be useful for preliminary estimates, soil setup is better estimated based on site specific data gathered from pile retapping, dynamic measurements, static load testing, and local experience.

9.10.1.2 Relaxation

The ultimate capacity of driven piles can also decrease with time following driving. This is known as relaxation and it has been observed in dense, saturated, fine grained soils such as non-cohesive silts and fine sands, as well as in some shales. In these cases, the driving process is believed to cause the dense soil near the pile toe to dilate (tendency for volume increase), thereby generating negative pore pressures (suction). The negative pore pressures temporarily increase the effective stresses acting on the pile, resulting in a temporarily higher soil strength and driving resistance. When these pore pressures dissipate, the effective stresses acting on the pile decrease, as does the pile capacity. Relaxation in weak laminated rocks has been attributed to a release of locked in horizontal stresses, Thompson and Thompson (1985).

Because the pile capacity may decrease (relaxation) after the end of driving, pile capacity assessments from static load testing or retapping should be made after equilibrium conditions in the soil have been re-established. In the absence of site specific pore pressure data from piezometers, it is suggested that static load testing or retapping of piles in dense silts and fine sands be delayed for five days to a week after driving, or longer if possible. In relaxation prone shales, it is suggested that static load testing or restrike testing be delayed a minimum of two weeks after driving.

TABLE 9-16 SOIL SETUP FACTORS
(after Rausche *et al.*, 1996)

Predominant Soil Type Along Pile Shaft	Range in Soil Set-up Factor	Recommended Soil Set-up Factors*	Number of Sites and (Percentage of Data Base)
Clay	1.2 - 5.5	2.0	7 (15%)
Silt - Clay	1.0 - 2.0	1.0	10 (22%)
Silt	1.5 - 5.0	1.5	2 (4%)
Sand - Clay	1.0 - 6.0	1.5	13 (28%)
Sand - Silt	1.2 - 2.0	1.2	8 (18%)
Fine Sand	1.2 - 2.0	1.2	2 (4%)
Sand	0.8 - 2.0	1.0	3 (7%)
Sand - Gravel	1.2 - 2.0	1.0	1 (2%)

* Confirmation with Local Experience Recommended

Published cases of the relaxation magnitude of various soil types is quite limited. However, data from Thompson and Thompson (1985) as well as Hussein *et al.* (1993) suggest relaxation factors for piles founded in some shales can range from 0.5 to 0.9. The relaxation factor is defined as the pile capacity at the end of initial driving divided by the static load test failure load. Relaxation factors of 0.5 and 0.8 have also been observed in two cases where piles were founded in dense sands and extremely dense silts, respectively. The importance of evaluating time dependent decreases in pile capacity for piles founded in these materials cannot be over emphasized.

9.10.1.3 Estimation of Pore Pressures During Driving

According to Lo and Stermac (1965), the maximum pore pressure induced from pile driving may be estimated from the following equation.

$$\Delta u_m = \left[(1-K_0) + \left(\frac{\Delta u}{p} \right)_m \right] p_i$$

- Where:
- Δu_m = Maximum excess pore pressure (kPa).
 - K_0 = Coefficient of earth pressure at-rest.
 - $(\Delta u/p)_m$ = Maximum value of the pore pressure ratio, $\Delta u/p$, measured in a CU triaxial test with pore pressure measurements.
 - p_i = Initial effective overburden pressure prior to pile driving (kPa).

Ismael and Klym (1979) presented a case history where the above procedure was used. They reported good agreement between measured excess pore pressures with estimates from the Lo and Stermac procedure.

Poulos and Davis (1980) summarized measurements of excess pore pressures due to pile driving from several case histories. In this compilation, the reported excess pore pressure measurements divided by the effective overburden pressure were plotted versus the radial distance from the pile surface divided by the pile radius. These results are presented in Figure 9.57 and indicate that the excess pore pressure at the pile-soil interface can approach 1.4 to 1.9 times the effective overburden pressure, depending upon the clay sensitivity.

The foundation designer should evaluate the potential change in pile capacity with time. Once pore pressures are measured or estimated, effective stress static pile capacity calculation methods can be used to quantify the probable change in pile capacity with time.

9.10.2 Effects of Predrilling, Jetting and Vibratory Installation on Pile Capacity

Piles are sometimes predrilled or jetted to a prescribed depth in order to attain the pile penetration depths required, as well as to reduce other foundation installation concerns, such as ground vibrations. Jetting is usually performed in cohesionless soils that can be freely eroded by water jets. Jetting, which can be very effective in sands, is usually ineffective in cohesive soils. For clays, and other drillable materials, such as thin layers of rock, predrilling the pile locations is more effective. The predrilled hole can be slightly smaller, equal to, or slightly larger than the pile diameter.

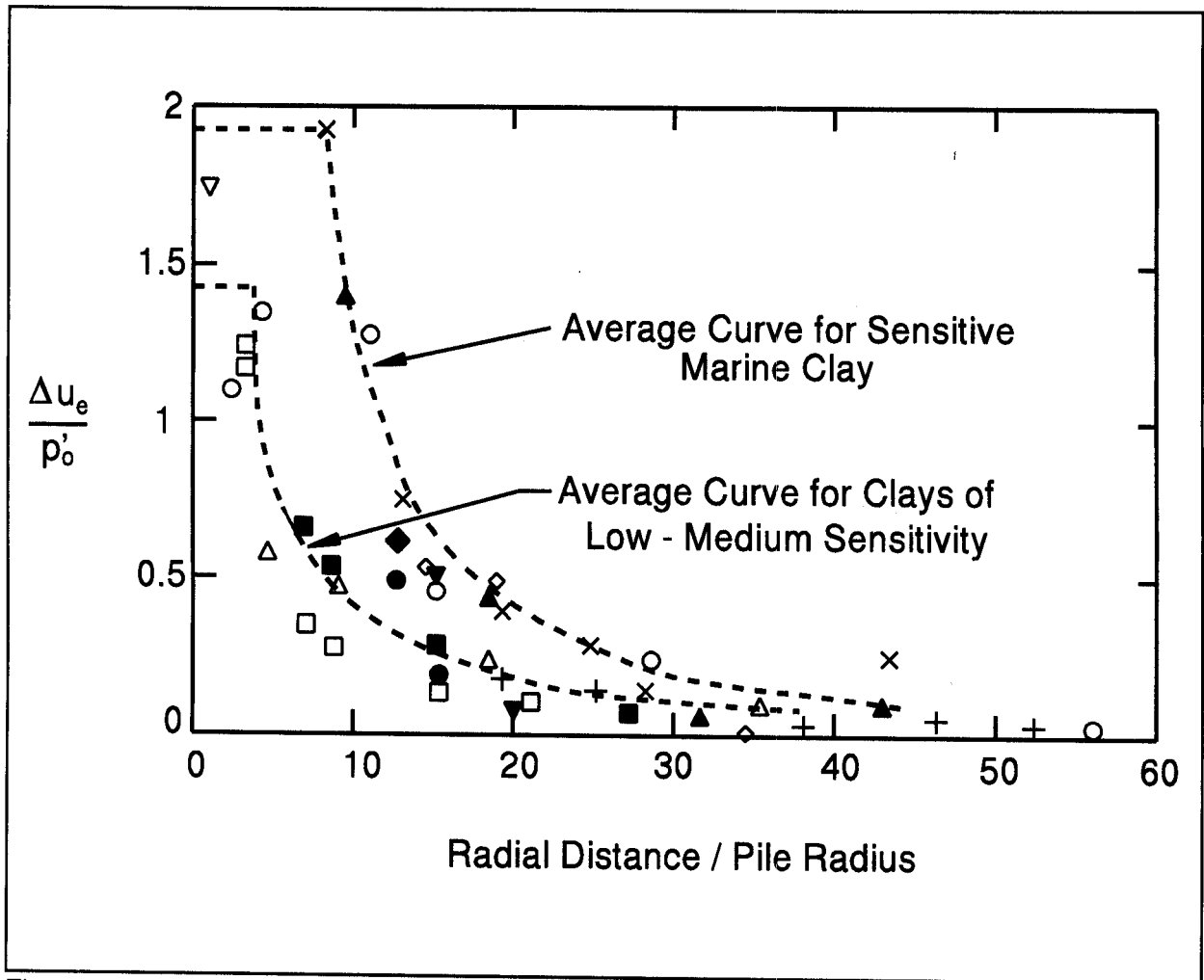


Figure 9.57 Excess Pore Water Pressure due to Pile Driving (after Poulos and Davis, 1980)

The use of predrilling or jetting will result in greater soil disturbance than considered in standard static pile capacity calculations. Therefore, when predrilling or jetting is contemplated, the effect of either of these construction procedures on calculated compression, uplift, and lateral pile capacity should be considered. Poulos and Davis (1980) report that the ultimate shaft resistance should be reduced by 50% of the originally calculated capacity in the jetted zone if the pile is jetted and then driven to the final penetration. McClelland *et al.* (1969) reported that a decrease in shaft resistance over a predrilled depth can range from 50 to 85% of that calculated without predrilling, depending upon the size of the predrilled hole. Hence, the probable reduction in compression, uplift, and lateral capacity from jetting or predrilling should be evaluated whenever predrilling or jetting is being considered.

Agencies are often requested to allow pile installation with a vibratory pile hammer instead of an impact hammer. Mosher (1987) summarized the results from five sites where piles were installed by both impact and vibratory hammers. This study concluded that for a significant majority of the cases, piles installed in sand with a vibratory hammer had a lower ultimate capacity than impact driven piles at the same site. Mosher also concluded that time dependent soil strength changes occurred equally for both installation methods. Hence, the capacity of the vibratory installed piles did not increase to the capacity of the impact driven piles with time. However, it was also observed that impact driving a vibratory installed pile would increase the capacity of the vibratory installed pile to that of an impact driven pile.

O'Neill and Vipulanandan (1989) performed a laboratory evaluation of piles installed with vibratory hammers. This laboratory study found impact driven piles had a 25% greater unit shaft resistance and a 15 to 20% higher unit toe resistance than vibratory installed piles in medium dense to dense, uniform, fine sand. However, in very dense, uniform, fine sand, the impact driven pile had a 20 to 30% lower unit shaft resistance and approximately a 30% lower unit toe resistance than the vibratory installed pile.

These two studies indicate use of vibratory pile installation rather than impact driving will affect the ultimate pile capacity that can be achieved at a given pile penetration depth. Therefore, communication between design and construction personnel should occur, and the influence of vibratory pile installation be evaluated when it is proposed. Impact driving a specified final depth of vibratory installed piles may provide a foundation that meets the engineer's performance requirements at reduced installation cost.

9.10.3 Effects of Site Dewatering on Pile Capacity

When a site is dewatered during construction, a temporary increase in effective stresses will occur. This causes a corresponding temporary increase in soil shear strength that will result in piles driven in a dewatered site to develop a greater capacity at a shallower pile penetration depth as compared to the non-dewatered condition. The soil resistance to be overcome to reach a specified penetration depth will also be greater than in the non-dewatered condition. If not considered in the design stage, the selected pile type may not be driveable to the required penetration depth in the dewatered construction condition. When dewatering is terminated, the effective stresses acting on the pile will decrease as the water table rises. This will result in a decrease in the soil shear strength and a decrease

in long term pile capacity. Hence piles driven to the ultimate capacity in the dewatered condition would have less than the required ultimate capacity once dewatering was terminated.

For projects where significant dewatering is required, the effects of the dewatering on pile capacity and pile driveability should be evaluated. In these cases, multiple static analyses should be performed to determine the pile capacity and driveability requirements under the short term dewatered condition, as well as the long term pile capacity after dewatering has been terminated.

9.10.4 Densification Effects on Pile Capacity and Installation Conditions

As illustrated in Figure 9.3, driving a pile in cohesionless soil influences the surrounding soils to a distance of about 3 to 5 pile diameters away from the pile. The soil displacement and vibrations resulting from driving pile groups in cohesionless soils can further densify cohesionless materials. The use of displacement piles also intensify group densification effects in cohesionless soils.

Densification can result in the pile capacity as well as the resistance to pile penetration being significantly higher than that calculated for a single pile in the static capacity calculations. The added confinement provided by cofferdams or the sequence of pile installation can further aggravate a group densification problem. Piles should be installed from the center of the group outward in order to reduce group densification effects due to installation sequence. Densification can cause significant construction problems if scour, seismic, or other considerations require pile penetration depths that cannot be achieved.

Potential densification effects should be considered in the design stage. Studies by Meyerhof (1959) and Kishida (1967) indicate that an increase in the soil friction angle of up to 4 degrees would not be uncommon for piles in loose to medium dense sands. It is expected that the increase in soil friction angle would be less for dense sands or cohesionless soils with a significant fine content. Densification affects the soil resistance to be overcome during driving and should be evaluated through static analyses performed using higher soil strength parameters than used for design. Results from these static analyses may indicate that a low displacement pile should be used, the pile spacing should be increased, or that a pile installation aid should be specified in order to obtain the required pile penetration depth.

9.10.5 Plugging of Open Pile Sections

Open pile sections include open end pipe piles and H-piles. The use of open pile sections has increased, particularly where special design events dictate large pile penetration depths. When open pile sections are driven, they may behave as low displacement piles and "cookie cut" through the soil, or act as displacement piles if a soil plug forms near the pile toe. It is generally desired that open sections remain unplugged during driving and plugged under static loading conditions.

Stevens (1988) reported that plugging of pipe piles in clays does not occur during driving if pile accelerations (along the plug zone) are greater than 22g's. Holloway and Beddard (1995) reported that hammer blow size (impact force and energy) influenced the dynamic response of the soil plug. With a large hammer blow, the plug "slipped" under the dynamic event whereas under a lesser hammer blow the pile encountered toe resistance typically of a plugged condition. From a design perspective, these cases indicate that pile penetration of open sections can be facilitated if the pile section is designed to accommodate a large pile hammer.

Static pile capacity calculations must determine whether an open pile section will exhibit plugged or unplugged behavior. Studies by O'Neill and Raines (1991), Raines *et al.* (1992), as well as Paikowsky and Whitman (1990) suggest that plugging of open pipe piles in medium dense to dense sands generally begins at a pile penetration to pile diameter ratio of 20, but can be as high as 35. For pipe piles in soft to stiff clays, Paikowsky and Whitman (1990) reported plugging occurs at penetration-to-pile diameter ratios of 10 to 20.

The above studies suggest that plugging in any soil material is probable under static loading conditions once the penetration to pile diameter ratio exceeds 20 in dense sands and clays, or 20 to 30 in medium sands. An illustration of the difference in the soil resistance mechanism that develops on a pipe pile with an open and plugged toe condition is presented in Figure 9.58. Paikowsky and Whitman (1990) recommend that the static capacity of an open end pipe pile be calculated from the lesser of the following equations:

Plugged Condition:

$$Q_u = f_{so} A_s + q_t A_t$$

Unplugged Condition:

$$Q_u = f_{so} A_s + f_{si} A_{si} + q_t A_p - w_p$$

Where:

- Q_u = Ultimate pile capacity, (kN).
- f_{so} = Exterior unit shaft resistance, (kPa).
- A_s = Pile exterior surface area, (m²).
- f_{si} = Interior unit shaft resistance, (kPa).
- A_{si} = Pile interior surface area, (m²).
- q_t = Unit toe resistance (kPa).
- A_t = Toe area of a plugged pile (m²).
- A_p = Pile cross sectional area of an unplugged pile (m²).
- w_p = Weight of the plug, (kN).

The soil stresses and displacements induced by driving an open pile section and a displacement pile section are not the same. Hence, a lower unit toe resistance, q_t , should be used for calculating the toe capacity of open end pipe piles compared to a typical closed end condition. The value of the interior unit shaft resistance in an open end pipe pile is typically on the order of 1/3 to 1/2 the exterior unit shaft resistance, and is influenced by soil type, pile diameter, and pile shoe configuration. These factors will also influence the length of soil plug that may develop.

For open end pipe piles in cohesionless soils, Tomlinson (1994) recommends that the static pile capacity be calculated using a limiting value of 5000 kPa for the unit toe resistance, regardless of the pile size or soil density. Tomlinson states that higher unit toe resistances do not develop, because yielding of the soil plug rather than bearing capacity failure of the soil below the plug governs the capacity.

For open end pipe piles driven in stiff clays, Tomlinson (1994) recommends that the static pile capacity be calculated as follows when field measurements confirm a plug is formed and carried down with the pile:

$$Q_u = 0.8 c_a A_s + 4.5 c_u A_t$$

Where:

- Q_u = Ultimate pile capacity, (kN).
- c_a = Pile adhesion from Figure 9.18 (kPa).
- A_s = Pile-soil surface area, (m²).
- c_u = Average undrained shear strength at the pile toe (kPa).
- A_t = Toe area of a plugged pile (m²).

Static pile capacity calculations for open end pipe piles in cohesionless soils should be performed using the Paikowsky and Whitman equations. Toe resistance should be calculated using the Tomlinson limiting unit toe resistance of 5000 kPa, once Meyerhof's limiting unit toe resistance, determined from Figure 9.17, exceeds 5000 kPa. For open end pipe piles in predominantly cohesive soils, the Tomlinson equation should be used.

The plugging phenomenon in H-piles can be equally difficult to analyze. However, the distance between flanges of an H-pile is smaller than the inside diameter of most open end pipe piles. Therefore, it can usually be assumed that an H-pile will be plugged under static loading conditions and the "box" area of the pile toe can be used for static calculation of the toe capacity in cohesionless and cohesive soils. The toe capacity for H-piles driven to rock is usually governed by the pile structural strength, calculated based on the steel cross sectional area, and should not include the area of a soil plug, if any.

For H-piles in cohesionless soils, arching between the flanges can usually be assumed, and the "box" perimeter can be used for shaft resistance calculations. In most cohesive soils, the shaft resistance is calculated from the sum of the adhesion, c_a , along the exterior of the two flanges plus the undrained shear strength of the soil, c_u , times the surface area of the two remaining sides of the "box" due to soil-to-soil shear along these two faces. Figure 9.59 illustrates that calculation of H-piles in stiff clays can still be problematic. Sheared clay lumps can develop above the plug zone, in which case the shaft resistance may only develop along the flanges in the sheared lump zone.

The above discussions highlight the point that a higher degree of uncertainty often exists for static pile capacity calculations of open pile sections than for displacement piles. Soil plug formation and plug response is often different under static and dynamic loading. This can complicate pile capacity evaluations of open pile sections with all dynamic methods (wave equation, dynamic testing, and dynamic formulas). Therefore, for large diameter open end pipe piles (greater than 450 mm), or for H-piles designed to carry their load primarily in shaft resistance, a static load test is recommended for capacity verification.

9.10.6 Design Considerations Due to Pile Driving Induced Vibrations

Since piles are driven by impact or vibratory hammers, ground vibrations of some magnitude are almost always induced into the surrounding soils during pile installation. Damage to nearby structures can result from vibration induced soil settlements or from the

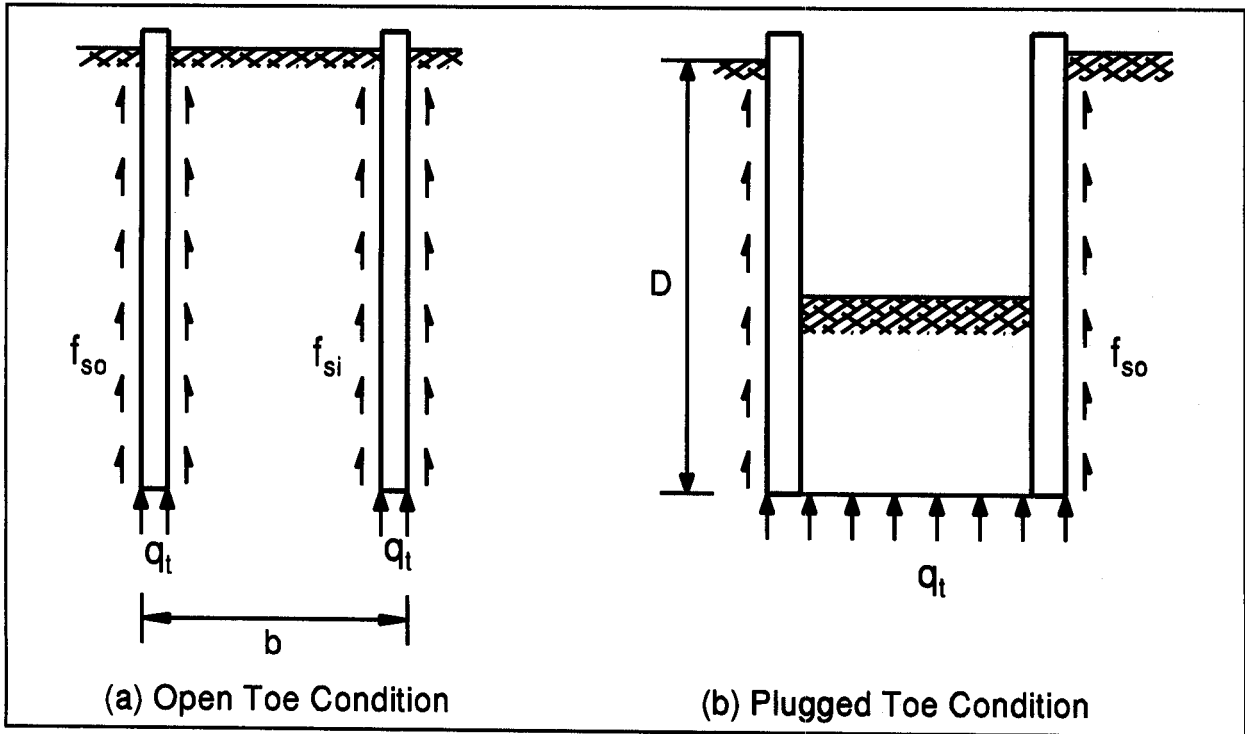


Figure 9.58 Plugging of Open End Pipe Piles (after Paikowsky and Whitman, 1990)

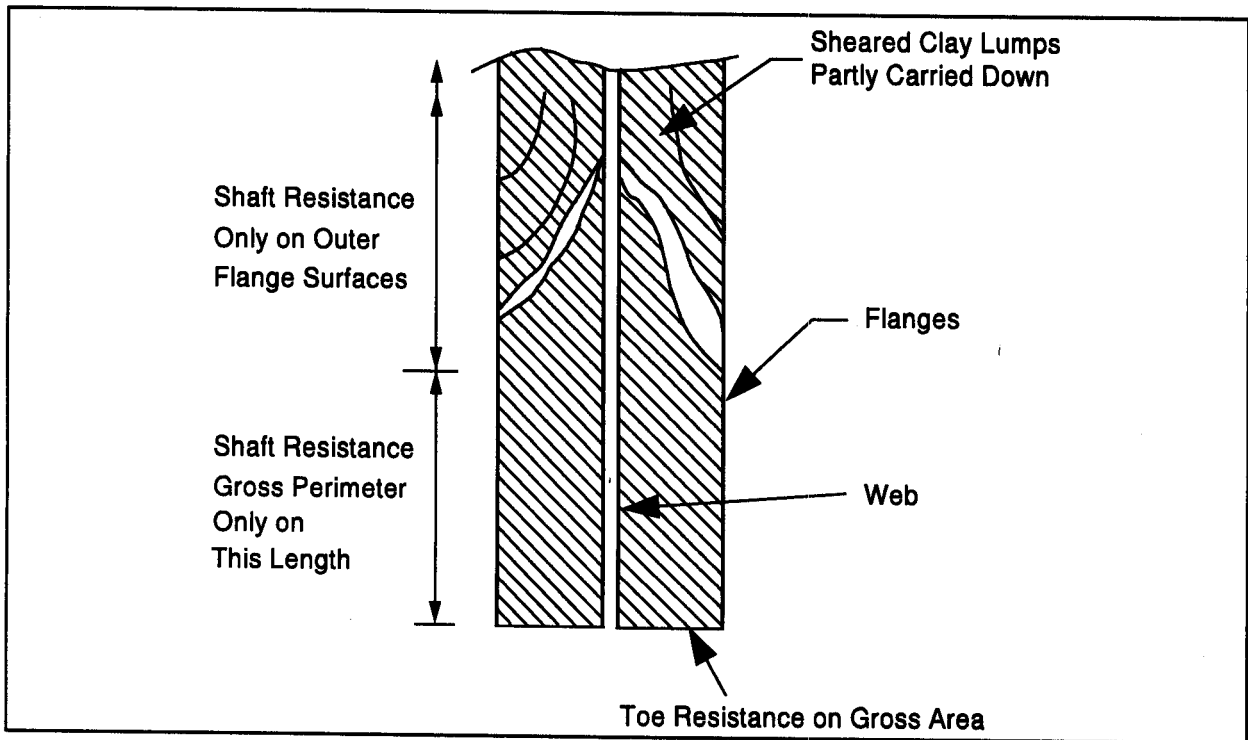


Figure 9.59 Plugging of H-Piles (after Tomlinson, 1994)

effects of vibrations on the structure itself. If a sensitive existing structure is located within approximately 150 meters of the pile driving location, vibrations or vibration induced soil densification may result in settlement damage to the existing structure. In many highway projects, vibrations are of limited concern, as surrounding structures are often greater than 150 meters from the location of pile driving.

For projects in urban areas, and for widening of existing bridges, the proximity of existing structures is often within the zone of potential damage. Careful evaluation of the pile driving procedures and/or monitoring of ground vibrations during pile installations should be performed for these projects. Wiss (1980), reported "safe" levels of ground vibration have typically been recommended between 12 and 100 mm per second. Lacy and Gould (1985) found that vibration induced soil densification settlements and structural damage can occur at peak particle velocities much less than 50 mm per second and that soil gradation is an important factor in this phenomenon. For a specific project, the ground vibration level where structural damage may occur will be dependent upon the type of soils, pile type(s), pile hammer, pile installation techniques, as well as the condition and type of existing structure.

If the potential for damaging ground vibrations is high, pile installation techniques should be specified to reduce vibration levels. Specifications could require predrilling or jetting as well as use of a different pile type or use of a specific type of pile hammer. Since predrilling and jetting influence compression, uplift, and lateral pile capacities, a determination of probable vibration levels and remediation measures should be evaluated in the design stage. A case history illustrating how a change in pile installation procedures reduced vibration induced densification and off-site settlement damage was reported by Lukas and Gill (1990).

NCHRP Project 20-5, Dynamic Effects of Pile Installations on Adjacent Structures, by Woods (1997), provides a synthesis of pile driving induced vibrations and typical mitigation practices. This synthesis noted that vibration problem management is the key to minimizing vibration damage, delays and claims. Two important elements in vibration management are a vibration specification with limits on the maximum peak particle velocity and a predriving survey of surrounding structures. An example vibration specification that details the requirements of a preconstruction survey as well as particle velocity controls is included in the NCHRP synthesis. The predriving survey needs to document conditions within the potential effected area. Woods reported that vibration damage a distance greater than one pile length away from driving is relatively uncommon but settlement damage in loose clean sands can occur up to 400 meters away. Woods also concluded that piles with low

impedances, EA/C, tend to transmit the hammer energy to the soils along the pile shaft and thus increase ground vibrations, whereas piles with higher impedances tend to more effectively transmit the hammer energy to the pile toe resulting in lower ground vibration levels. Hence, selection of a stiffer pile section at sites where vibrations are a concern may reduce vibration problems.

9.10.7 Pile Driveability

Greater pile penetration depths are increasingly being required to satisfy performance criteria in special design events such as scour, vessel impact, ice and debris loading, and seismic events. Therefore, the ability of a pile to be driven to the required penetration depth has become increasingly more important and must be evaluated in the design stage. Pile driveability refers to the ability of a pile to be driven to a desired penetration depth and/or capacity. All of the previously described static analysis methods are meaningless if the pile cannot be driven to the required design depth and ultimate capacity without sustaining damage. The limit of pile driveability is the maximum soil resistance a pile can be driven against without sustaining damage or a refusal driving resistance with a properly sized driving system.

Primary factors controlling the ultimate geotechnical capacity of a pile are the pile type and length, the soil conditions, and the method of installation. Since the pile type, length and method of installation can be specified, it is often erroneously assumed that the pile can be installed as designed to the estimated penetration depth. However, the pile must have sufficient driveability to overcome the soil resistance encountered during driving to reach the estimated or specified pile penetration depth. If a pile section does not have a driveability limit in excess of the soil resistance to be overcome during driving, it will not be driveable to the desired pile penetration depth. The failure to adequately evaluate pile driveability is one of the most common deficiencies in driven pile design practice.

In evaluating the driveability of a pile, the soil disturbance during installation and the time dependent soil strength changes should be considered. Both soil setup and relaxation have been described earlier in this chapter. For economical pile design, the foundation designer must match the soil resistance to be overcome at the time of driving with the pile impedance, the pile material strength, and the pile driving equipment.

9.10.7.1 Factors Affecting Driveability

A pile must satisfy two aspects of driveability. First, the pile must have sufficient stiffness to transmit driving forces large enough to overcome soil resistance. Second, the pile must have sufficient structural strength to withstand the driving forces without damage.

The primary controlling factor on pile driveability is the pile impedance, EA/C . Once the pile material is selected, and thus the pile modulus of elasticity, E , and the pile wave speed, C , only increasing the pile cross sectional area, A , will improve the pile driveability. For steel H-piles, the designer can improve pile driveability by increasing the H-pile section without increasing the H-pile size. The driveability of steel pipe piles can be improved by increasing the pipe wall thickness. For open ended pipe piles, an inside-fitting cutting shoe can improve driveability by delaying the formation of a soil plug and thereby reducing the soil resistance to be overcome. Most concrete piles are solid cross sections. Therefore, increasing the pile area to improve driveability is usually accompanied by an increase in the soil resistance to driving.

A lesser factor influencing pile driveability is the pile material strength. The influence of pile material strength on driveability is limited, since strength does not alter the pile impedance. However, a pile with a higher pile material strength can tolerate higher driving stresses that may allow a larger pile hammer to be used. This may allow a slightly higher capacity to be obtained before refusal driving conditions or pile damage occur.

Other factors that may affect pile driveability include the driving system characteristics such as ram weight, stroke, and speed, as well as the actual system performance in the field. The dynamic soil response can also affect pile driveability. Soils may have higher damping characteristics or elasticity than assumed, both of which can reduce pile driveability. Dynamic soil response is discussed in greater detail in Chapters 17 and 18.

Even if the pile structural capacity and geotechnical capacity both indicate a high pile capacity could be used, a high pile capacity may still not be obtainable because driving stresses may exceed allowable driving stress limits. A pile cannot be driven to an ultimate static capacity that is as high as the structural capacity of the pile because of the additional dynamic resistance or damping forces generated during pile driving. The allowable static design stresses in pile materials by various codes generally represent the static stress levels (pile capacity) which can be consistently developed with normal driving equipment and methods. Maximum allowable design and driving stresses are discussed in Chapter 11.

9.10.7.2 Methods for Determining Pile Driveability

There are three available methods for predicting and/or checking pile driveability. As design tools, all of the methods have advantages and disadvantages and are therefore presented in order of increasing cost and reliability.

1. Wave Equation Analysis

This method, Goble and Rausche (1986), accounts for pile impedance and predicts driving stresses as well as the relationship of pile driving resistance versus ultimate pile capacity. Wave equation analyses performed in the design stage require assumptions on the hammer type and performance level, the drive system components, as well as the soil response during driving. These shortcomings are reflected in variations between predicted and actual field behavior. Even with these shortcomings, the wave equation is a powerful design tool that can and should be used to check driveability in the design stage, to design an appropriate pile section, or to specify driving equipment characteristics. Additional information on the wave equation, including its use as a construction control tool, is presented in Chapter 17.

2. Dynamic Testing and Analysis

Dynamic measurements can be made during pile installation to calculate driving stresses and to estimate static pile capacity at the time of driving. Time dependent changes in pile capacity can be evaluated if measurements are made during restrike tests. Additional signal matching analysis can also provide soil parameters for refined wave equation analysis. A shortcoming of this method as a design tool is that it must be performed during pile driving. Therefore, in order to use dynamic testing information to confirm driveability or to refine a design, a test program is required during the design stage. Additional details on dynamic testing and analysis, including its use as a construction control tool, is presented in Chapter 18.

3. Static Load Tests

Static load tests, Kyfor *et al.* (1992), are useful for checking driveability and confirming pile capacity prior to production pile driving. Test piles are normally driven to estimated lengths and load tested. The confirmation of pile driveability through static load testing is the most accurate method of confirming driveability and pile capacity since a pile is

actually driven and load tested. However, this advantage also illustrates one of its shortcomings as a design tool, in that a test program is required during the design stage. Other shortcomings associated with static load tests for determining driveability include:

- a. cost and time delay that limit their suitability to certain projects.
- b. assessment of driving stresses and extent of pile damage, if any, sustained by the pile is not provided by the test.
- c. can be misleading on projects where soil conditions are highly variable.

Additional details on static load testing, including its use as a construction control tool, is presented in Chapter 19.

As design and construction control tools, methods 1 and 2 offer additional information and complement static load tests. Used properly, methods 1 and 2 can yield significant savings in material costs or reduction of construction delays. These methods can be used to reduce the number of static load tests and also allow evaluation of increases in the maximum allowable design stresses. A determination of the increase (soil setup) or decrease (relaxation) in pile capacity with time can also be made if piles are retapped after initial driving.

9.10.7.3 Driveability Versus Pile Type

Driveability should be checked during the design stage of all driven piles. It is particularly important for closed end steel pipe piles where the impedance of the steel casing may limit pile driveability. Although the designer may attempt to specify a thin-wall pipe in order to save material cost, a thin wall pile may lack the driveability to develop the required ultimate capacity or to achieve the necessary pile penetration depth. Wave equation analyses should be performed in the design stage to select the pile section and wall thickness.

Steel H-piles and open pipe piles, prestressed concrete piles, and timber piles are also subject to driveability limitations. This is particularly true as allowable design stresses increase and as special design events require increased pile penetration depths. The driveability of long prestressed concrete piles can be limited by the pile's tensile strength.

REFERENCES

- Altaee, A., Evgin, E. and Fellenius, B.H. (1992). Axial Load Transfer for Piles in Sand, I: Tests on an Instrumented Precast Pile. *Canadian Geotechnical Journal*, Vol. 29, No. 1, 11-20.
- American Association of State Highway and Transportation Officials [AASHTO], (1992). *Standard Specifications for Highway Bridges. Division 1 and 2*, Washington, D.C.
- Barker, R.M., Duncan, J.M., Rojiani, K.B., Ooi, P.S.K., Tan, C.K. and Kim, S.G. (1991). *Manuals for the Design of Bridge Foundations*. Transportation Research Board, National Research Council, Washington, D.C.
- Bollman, H.T. (1993). Notes on Designing Deep Foundations for Lateral Loads. *Proceedings of Design of Highway Bridges for Extreme Events*, Crystal City, Virginia, 175-199.
- Bowles, J.E. (1977). *Foundation Analysis and Design*. Second Edition, McGraw-Hill Book Company.
- Bowles, J.E. (1988). *Foundation Analysis and Design*. Fourth Edition, McGraw-Hill Book Company, 1004.
- Briaud J-L. and Miran, J. (1992). The Cone Penetration Test. Report No. FHWA-SA-91-043, U.S. Department of Transportation, Federal Highway Administration, Office of Technology Applications, Washington, D.C., 161.
- Briaud, J-L. and Tucker, L.M. (1993). Downdrag on Bitumen-Coated Piles. Preliminary Draft Final Report, National Cooperative Highway Research Program NCHRP 24-5, Washington, D.C., 245.
- Briaud, J-L. and Tucker, L.M. (1986). *User's Manual for PILECPT*. Civil Engineering Department, Texas A&M University.
- Broms, B.B. (1964a). Lateral Resistance of Piles in Cohesive Soils. *American Society of Civil Engineers, Journal for Soil Mechanics and Foundation Engineering*, Vol. 90, SM2, 27-63.

- Broms, B.B. (1964b). Lateral Resistance of Piles in Cohesionless Soils. American Society of Civil Engineers, Journal for Soil Mechanics and Foundation Engineering, Vol. 90, SM3, 123-156.
- Broms, B.B. (1966). Methods of Calculating the Ultimate Bearing Capacity of Piles - A Summary. Sols-Sols No. 18-19, 21-32.
- Brown, D.A., Reese, L.C. and O'Neill, M.W. (1987). Cyclic Lateral Loading of a Large-Scale Pile Group in Sand. American Society of Civil Engineers, Journal of Geotechnical Engineering, Vol. 113, No. 11, 1326-1343.
- Brown, D.A., Morrison, C. and Reese, L.C. (1988). Lateral Load Behavior of Pile Group in Sand. American Society of Civil Engineers, Journal of Geotechnical Engineering, Vol. 114, No. 11, 1261-1276.
- Brown, D.A. and Bollman, H.T. (1993). Pile-Supported Bridge Foundations Designed for Impact Loading. Appended Document to the Proceedings of Design of Highway Bridges for Extreme Events, Crystal City, Virginia, 265-281.
- Bustamante, M. and Gianceselli, L. (1982). Pile Bearing Capacity Prediction by Means of Static Penetrometer CPT. Proceedings of the Second European Symposium on Penetration Testing, Amsterdam, 493-500.
- Canadian Foundation Engineering Manual (1985). Second Edition, Canadian Geotechnical Society, Technical Committee on Foundations, 456.
- Cheney, R.S. and Chassie, R.G. (1993). Soils and Foundation Workshop Manual. Second Edition, Report No. HI-88-009, U.S. Department of Transportation, Federal Highway Administration, Office of Engineering, Washington, D.C., 395.
- Coduto, D.P. (1994). Foundation Design: Principles and Practice. Prentice-Hall, Inc., Englewood Cliffs, 796.
- Elias, V., Welsh, J.P., Warren, J., and Lukas, R.G. (1996). Ground Improvement Technology Manual, Draft Report. U.S. Department of Transportation, Federal Highway Administration, Office of Technology Applications, Washington D.C.

- Fellenius, B.H., Riker, R.E., O'Brien, A.J. and Tracy, G.R. (1989). Dynamic and Static Testing in a Soil Exhibiting Set-up. American Society of Civil Engineers, Journal of Geotechnical Engineering, Vol. 115, No. 7, 984-1001.
- Fellenius, B.H. (1991). Chapter 13 - Pile Foundations, Foundation Engineering Handbook. Second Edition. H.S. Fang, Editor, Van Nostrand Reinhold Publisher, New York, 511-536.
- Goble, G.G. and Rausche, F. (1986). Wave Equation Analysis of Pile Driving - WEAP86 Program. U.S. Department of Transportation, Federal Highway Administration, Implementation Division, McLean, Volumes I-IV.
- Goudereault, P. and Fellenius, B.H. (1990). UNIPILE Program for Unified Analysis of Piles and Pile Groups Considering Capacity, Negative Skin Friction, and Settlement, Users Manual. Bengt Fellenius Consultants, Inc., Ottawa.
- Goudereault, P. and Fellenius, B.H. (1994). UNIPILE Program Background and Manual. Unisoft, Ltd., Ottawa.
- Hadjian, A.H., Fallgren, R.B. and Tufenkjian, M.R. (1992). Dynamic Soil-Pile-Structure Interaction, The State-of-Practice. Geotechnical Special Publication No. 34, Piles Under Dynamic Loads, S. Prakash Editor, American Society of Civil Engineers, ASCE, 1-26.
- Hagerty, D.J. and Peck, R.B. (1971). Heave and Lateral Movements Due to Pile Driving. American Society of Civil Engineers, ASCE, Journal of the Soil Mechanics and Foundations Division, SM11, November, 1513-1531.
- Hoit, M.I. and McVay, M. (1994). LPGSTAN User's Manual. University of Florida, Gainesville.
- Holloway, D.M. and Beddard, D.L. (1995). Dynamic Testing Results Indicator Pile Test Program - I-880. Proceedings of the 20th Annual Members Conference of the Deep Foundations Institute.
- Holloway, D.M., Moriwaki, Y., Stevens, J.B. and Perez, J-Y (1981). Response of a Pile Group to Combined Axial and Lateral Loading. Proceedings of the 10th International Conference on Soil Mechanics and Foundation Engineering, Boulimia Publishers, Stockholm, Vol. 2, 731-734.

- Hough, B.K. (1959). Compressibility as the Basis for Soil Bearing Value. American Society of Civil Engineers, Journal for Soil Mechanics and Foundation Engineering, Vol. 85, SM4, 11-39.
- Hussein, M.H., Likins, G.E. and Hannigan, P.J. (1993). Pile Evaluation by Dynamic Testing During Restrike. Eleventh Southeast Asian Geotechnical Conference, Singapore.
- Ismael, N.F. and Klym, T.W. (1979). Pore-Water Pressures Induced by Pile Driving. American Society of Civil Engineers, Journal of Geotechnical Engineering, Vol. 105, GT11, 1349-1354.
- Kishida, H. (1967). Ultimate Bearing Capacity of Piles Driven in Loose Sands, Soils and Foundations. Japanese Society of Soil Mechanics and Foundation Engineering, Vol. 7, No. 3, 20-29.
- Kyfor, Z.G., Schnore, A.R., Carlo, T.A. and Bailey, P.F. (1992). Static Testing of Deep Foundations. Report No. FHWA-SA-91-042, U.S. Department of Transportation, Federal Highway Administration, Office of Technology Applications, Washington, D.C., 174.
- Lacy H.S. and Gould, J.P. (1985). Settlement from Pile Driving in Sands, Vibration Problems in Geotechnical Engineering. American Society of Civil Engineers, ASCE Special Technical Publication, New York, 152-173.
- Lam, I.P. and Martin, G.R. (1986). Seismic Design of Highway Bridge Foundations. Volume II - Design Procedures and Guidelines, Report No. FHWA/RD-86/102, U.S. Department of Transportation, Federal Highway Administration, Office of Engineering and Highway Operations, McLean, 181.
- Lo, K.Y. and Stermac, A.G. (1965). Induced Pore Pressures During Pile Driving Operations. Proceedings of the 6th International Conference on Soil Mechanics and Foundation Engineering, Vol. 2, Montreal, 285-289.
- Long, J.H. (1996). Personal Communication.
- Lukas, R.G. and Gill, S.A. (1992). Ground Movement from Piling Vibrations. Piling-European Practice and Worldwide Trends, The Institute of Civil Engineers, Thomas Telford House, London, 163-169.

Mathias, D. and Cribbs, M. (1998). DRIVEN 1.0: A Microsoft Windows™ Based Program for Determining Ultimate Vertical Static Pile Capacity. Report No. FHWA-SA-98-074, U.S. Department of Transportation, Federal Highway Administration, Office of Technology Applications, Washington D.C. 112.

McClelland, B., Focht, J.A. and Emrich, W.J. (1969). Problems in Design and Installation of Offshore Piles. American Society of Civil Engineers, ASCE, Journal of the Soil Mechanics and Foundations Division, SM6, 1491-1514.

McVay, M., Casper, R. and Shang, T-I. (1995). Lateral Response of Three-Row Groups in Loose to Dense Sands at 3D and 5D Pile Spacing. American Society of Civil Engineers, Journal of Geotechnical Engineering, Vol. 121, No. 5, 436-441.

Meyerhof, G.G. (1959). Compaction of Sands and Bearing Capacity of Piles. American Society of Civil Engineers, ASCE, Journal of the Soil Mechanics and Foundations Division, Vol. 85, SM6, December, 1-29.

Meyerhof, G.G. (1976). Bearing Capacity and Settlement of Pile Foundations. American Society of Civil Engineers, ASCE, Journal of the Geotechnical Engineering Division, 195-228.

Mosher, R.L. (1987). Comparison of Axial Capacity of Vibratory Driven Piles to Impact Driven Piles. USAEWES Technical Report ITL-877, 36.

Moss, R.E.S. (1997). Cyclic Lateral Loading of Model Pile Groups in Clay Soil, Phase 2B. Master Thesis Research, Utah State University.

New York State Department of Transportation, Engineering Research and Development Bureau (1977). Lateral Load Capacity of Vertical Pile Groups. Report NYSDOT-ERD-77-RR47.

Nordlund, R.L. (1963). Bearing Capacity of Piles in Cohesionless Soils. American Society of Civil Engineers, ASCE, Journal of the Soil Mechanics and Foundations Division, SM3, 1-35.

Nordlund, R.L. (1979). Point Bearing and Shaft Friction of Piles in Sand. Missouri-Rolla 5th Annual Short Course on the Fundamentals of Deep Foundation Design.

- Nottingham, L.C. (1975). Use of Quasi-Static Friction Cone Penetrometer to Predict Load Capacity of Displacement Piles. Ph.D. dissertation to the Department of Civil Engineering, University of Florida, 552.
- O'Neill, M.W. (1983). Group Action in Offshore Piles. Proceedings of the Conference on Geotechnical Practice in Offshore Engineering, S.G. Wright Editor, American Society of Civil Engineers, ASCE, New York, 25-64.
- O'Neill, M.W. and Vipulanandan, C. (1989). Laboratory Evaluation of Piles Installed with Vibratory Drivers. NCHRP Report 316, National Cooperative Highway Research Program, Transportation Research Board, Washington, D.C.
- O'Neill, M.W. and Raines, R.D. (1991). Load Transfer for Pipe Piles in Highly Pressured Dense Sand. American Society of Civil Engineers, Journal of Geotechnical Engineering, Vol. 117, No. 8, 1208-1226.
- Paikowsky, S.G. and Whitman, R.V. (1990). The effects of Plugging on Pile Performance and Design. Canadian Geotechnical Journal, Vol. 27, No. 4, 429-440.
- Peck, R.B., Hanson, W.E. and Thornburn, T. (1974). Foundation Engineering. Second Edition, John Wiley & Sons, New York, 215.
- Poulos, H.G. and Davis, E.H. (1980). Pile Foundation Analysis and Design. John Wiley and Sons, New York, 18-51.
- Raines, R.D., Ugaz, O.G. and O'Neill, M.W. (1992). Driving Characteristics of Open-Toe Piles in Dense Sand. American Society of Civil Engineers, Journal of Geotechnical Engineering, Vol. 118, No. 1, 72-88.
- Rausche, F., Thendean, G., Abou-matar, H., Likins, G. and Goble, G. (1996). Determination of Pile Driveability and Capacity from Penetration Tests. FHWA Contract No. DTFH61-91-C-00047, Final Report, U.S. Department of Transportation, Federal Highway Administration.
- Reese, L.C. (1984). Handbook on Design of Piles and Drilled Shafts Under Lateral Load. Report No. FHWA-IP-84-11, U.S. Department of Transportation, Federal Highway Administration, Office of Implementation, Washington, D.C., 386.

- Reese, L.C. (1986). Behavior of Piles and Pile Groups Under Lateral Load. Report No. FHWA/RD-85/106, U.S. Department of Transportation, Federal Highway Administration, Office of Engineering and Highway Operations Research and Development, Washington, D.C., 311.
- Richardson, E.V. and Davis, S.R. (1995). Evaluating Scour at Bridges, HEC-18. Office of Technology Applications, Federal Highway Administration, Washington, D.C.
- Rixner, J.J., Kraemer, S.R. and Smith, A.D. (1986). Prefabricated Vertical Drains Volume I, Engineering Guidelines. Report No. FHWA/RD-86/168, U.S. Department of Transportation, Federal Highway Administration, Office of Engineering and Highway Operations Research and Development, McLean, 117.
- Rollins, K.M., Peterson, K.T., and Weaver, T.J. (1998). Lateral Load Behavior of Full-Scale Pile Group in Clay. American Society of Civil Engineers, Journal of Geotechnical and Geoenvironmental Engineering, Vol. 124, No. 6, 468-478.
- Ruesta, P.F. and Townsend, F.C. (1997). Evaluation of Laterally Loaded Pile Group at Roosevelt Bridge. American Society of Civil Engineers, Journal of Geotechnical and Geoenvironmental Engineering, Vol. 123, No. 12, 1153-1161.
- Schmertman, J.H. (1978). Guidelines For Cone Penetration Test, Performance, and Design. Report No. FHWA-TS-78-209, U.S. Department of Transportation, Federal Highway Administration, Washington, D.C., 145.
- Seed, H.B., Idriss, I.M. and Arango, I. (1983). Evaluation of Liquefaction Potential Using Field Performance Data. American Society of Civil Engineers, Journal of Geotechnical Engineering, Vol. 109, No. 3, 458-482.
- Seed, H.B. (1987). Design Problems in Soil Liquefaction. American Society of Civil Engineers, Journal of Geotechnical Engineering, Vol. 113, No. 8, 827-845.
- Seed, R.B. and Harder, L.F., Jr. (1990). SPT-Based Analysis of Cyclic Pore Pressure Generation and Undrained Residual Strength. Proceedings, H.B. Bolton Seed Memorial Symposium, J.M. Duncan Editor, BiTech Publishers, Vol. 2, 351-376.

- Smith, T.D. (1989). Fact or Friction: A Review of Soil Response to a Laterally Moving Pile. Foundation Engineering: Current Principles and Practices, F.H. Kulhawy Editor, American Society of Civil Engineers, ASCE, New York, Vol. 1, 588-598.
- Stevens, R.F. (1988). The Effect of a Soil Plug on Pile Driveability in Clay. Proceedings of the Third International Conference on the Application of Stress Wave Theory to Piles, B.H. Fellenius, Editor, BiTech Publishers, Vancouver, 861-868.
- Tawfig, K.S. (1994). Polyethylene Coating for Downdrag Mitigation on Abutment Piles. Proceedings of the International Conference on Design and Construction of Deep Foundations, Vol. 2, 685-698.
- Terzaghi, K. and Peck, R.B. (1967). Soil Mechanics in Engineering Practice. John Wiley and Sons, New York.
- Tomlinson, M.J. (1980). Foundation Design and Construction. Fourth Edition, Pitman Advanced Publishing Program.
- Tomlinson, M.J. (1994). Pile Design and Construction Practice. Fourth Edition, E & FN Spon, London, 411.
- Thompson, C.D. and Thompson, D.E. (1985). Real and Apparent Relaxation of Driven Piles. American Society of Civil Engineers, Journal of Geotechnical Engineering, Vol. 111, No. 2, 225-237.
- Thurman, A.G. (1964). Discussion of Bearing Capacity of Piles in Cohesionless Soils. American Society of Civil Engineers, ASCE, Journal of the Soil Mechanics and Foundations Division, SM1, 127-129.
- Urzua, A. (1992). SPILE A Microcomputer Program for Determining Ultimate Vertical Static Pile Capacity. Users Manual, Report No. FHWA-SA-92-044, U.S. Department of Transportation, Federal Highway Administration, Office of Engineering and Office of Technology Applications, Washington, D.C., 58.

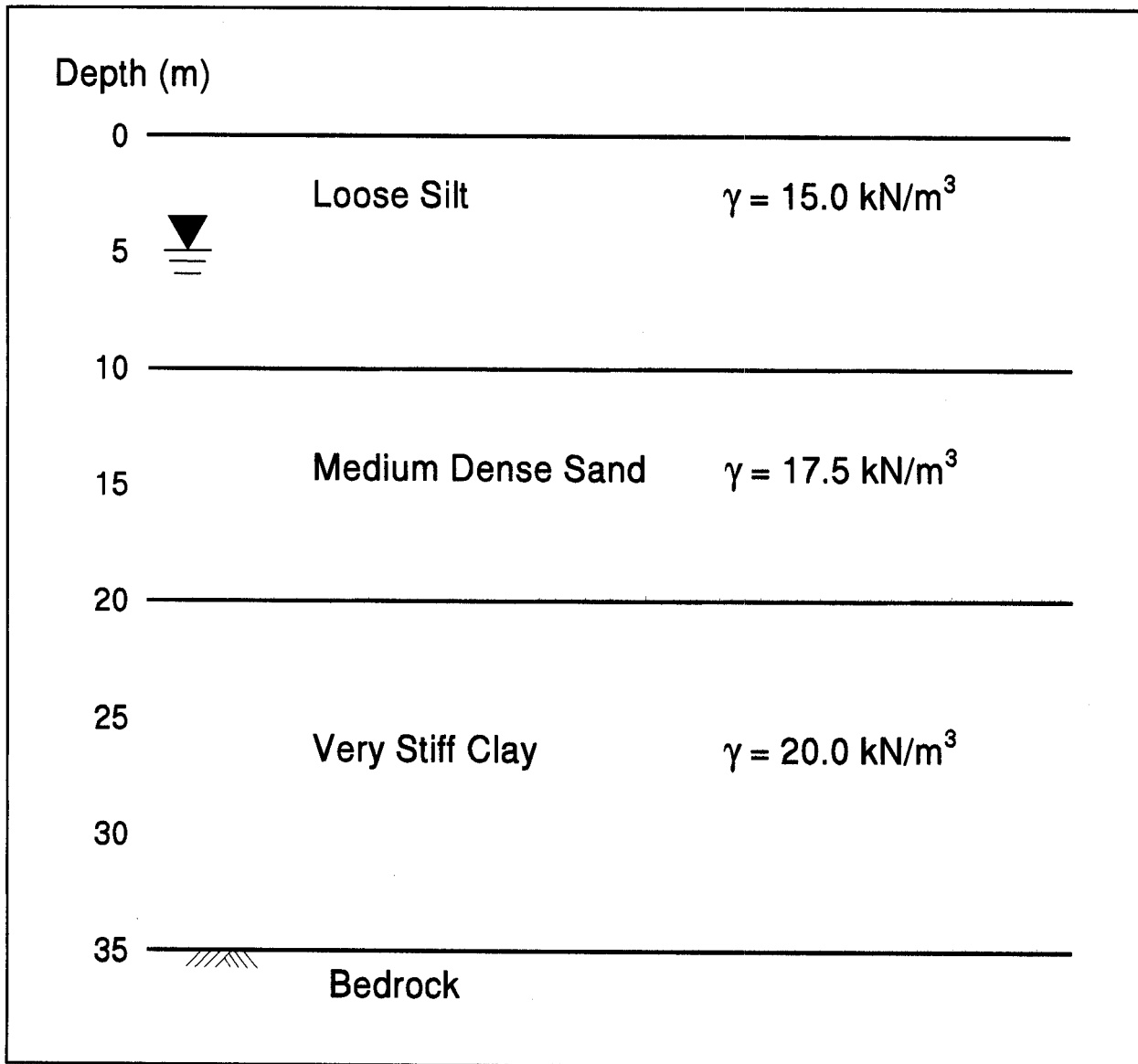
Wang, S-T and Reese, L.C. (1993). COM624P - Laterally Loaded Pile Analysis Program for the Microcomputer. Version 2.0, Report No. FHWA-SA-91-048, U.S. Department of Transportation, Federal Highway Administration, Office of Technology Applications, Washington, D.C., 504.

Woods, R.D. (1997). Dynamic Effects of Pile Installations on Adjacent Structures. NCHRP Synthesis 253, National Cooperative Highway Research Program, Transportation Research Board, Washington, D.C.

Wiss, J.F. (1981). Construction Vibrations: State-of-the-Art. American Society of Civil Engineers, ASCE, Journal of the Geotechnical Engineering Division, February, 167-181.

STUDENT EXERCISE #1 - CONSTRUCT A p_o DIAGRAM

For the soil profile given below, construct the total and effective overburden pressure diagrams. The water table is 5 meters below the ground surface. The unit weight of water is 9.80 kN/m^3 . Construction of a p_o diagram is described in Section 9.4 of Chapter 9. The solution to this problem is presented in Appendix G.

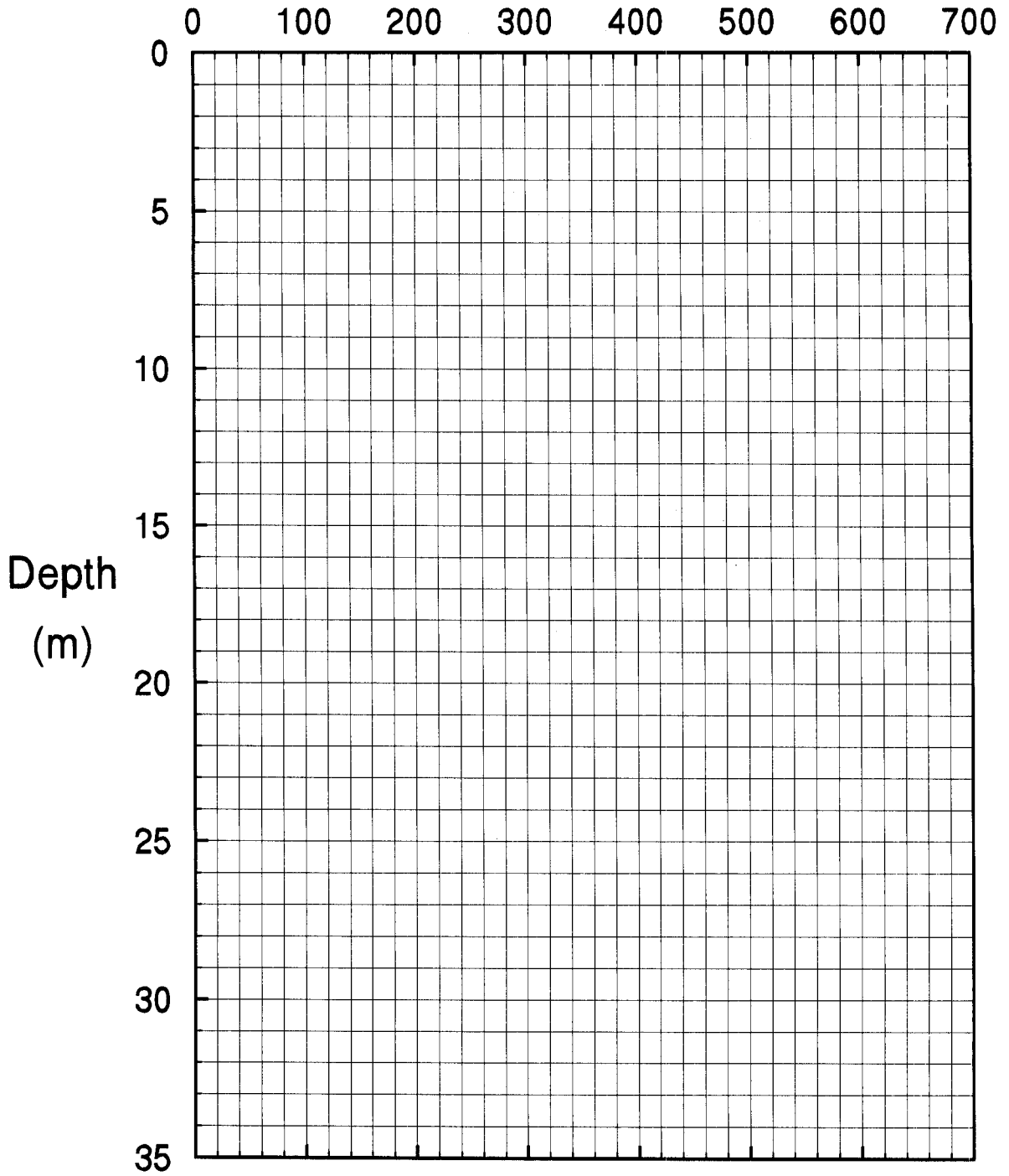


STUDENT EXERCISE #1 - CONSTRUCT A p_o DIAGRAM - STEP BY STEP

The suggested step by step procedure is as follows:

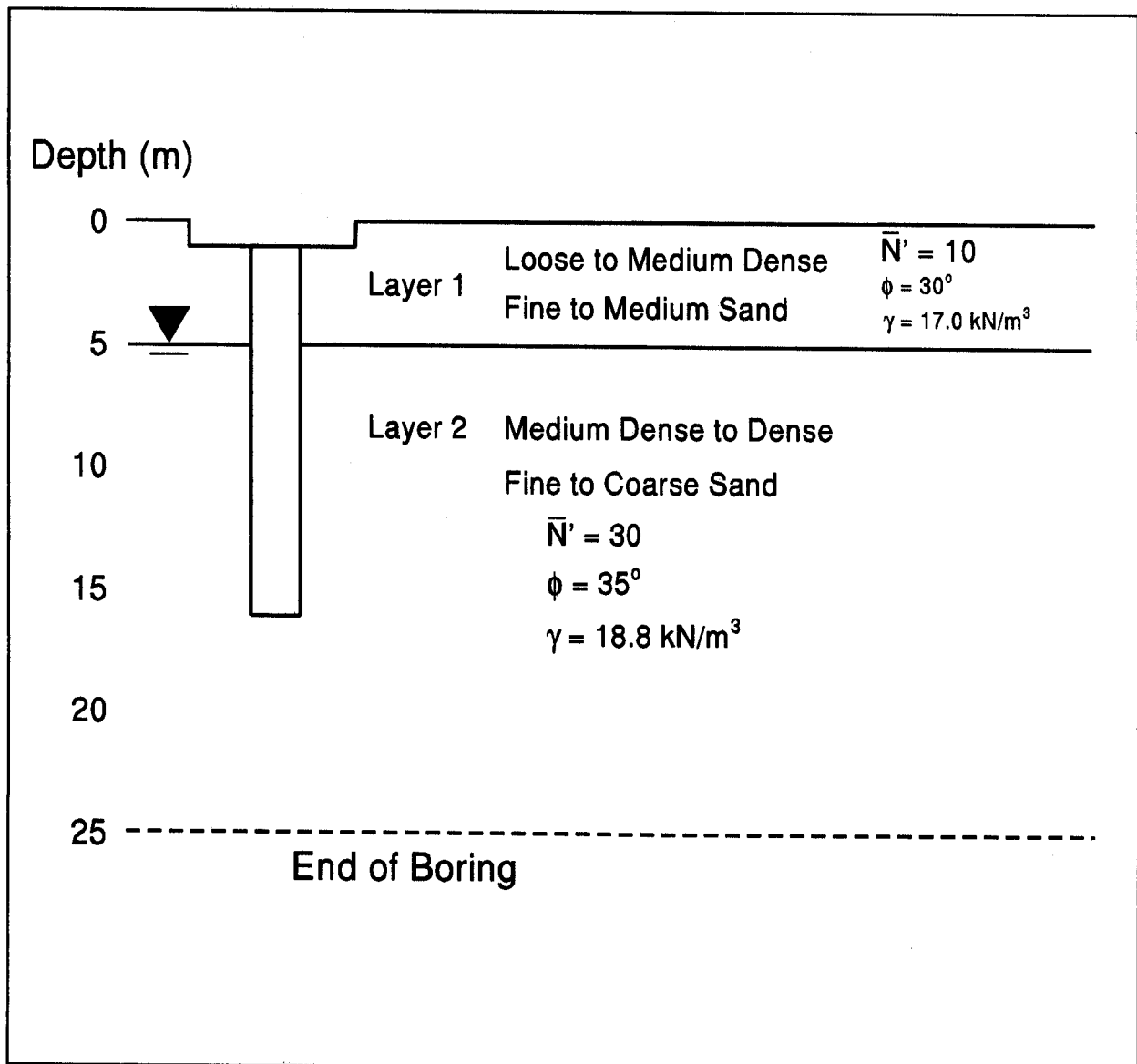
1. Calculate the total overburden pressure, p_t , at the depth of each strata change and at the static water table.
2. Calculate the pore water pressure, u , at each depth.
3. Calculate the effective overburden pressure at each depth from $p_t - u$.
4. Plot p_t and p_o versus depth on the following page.

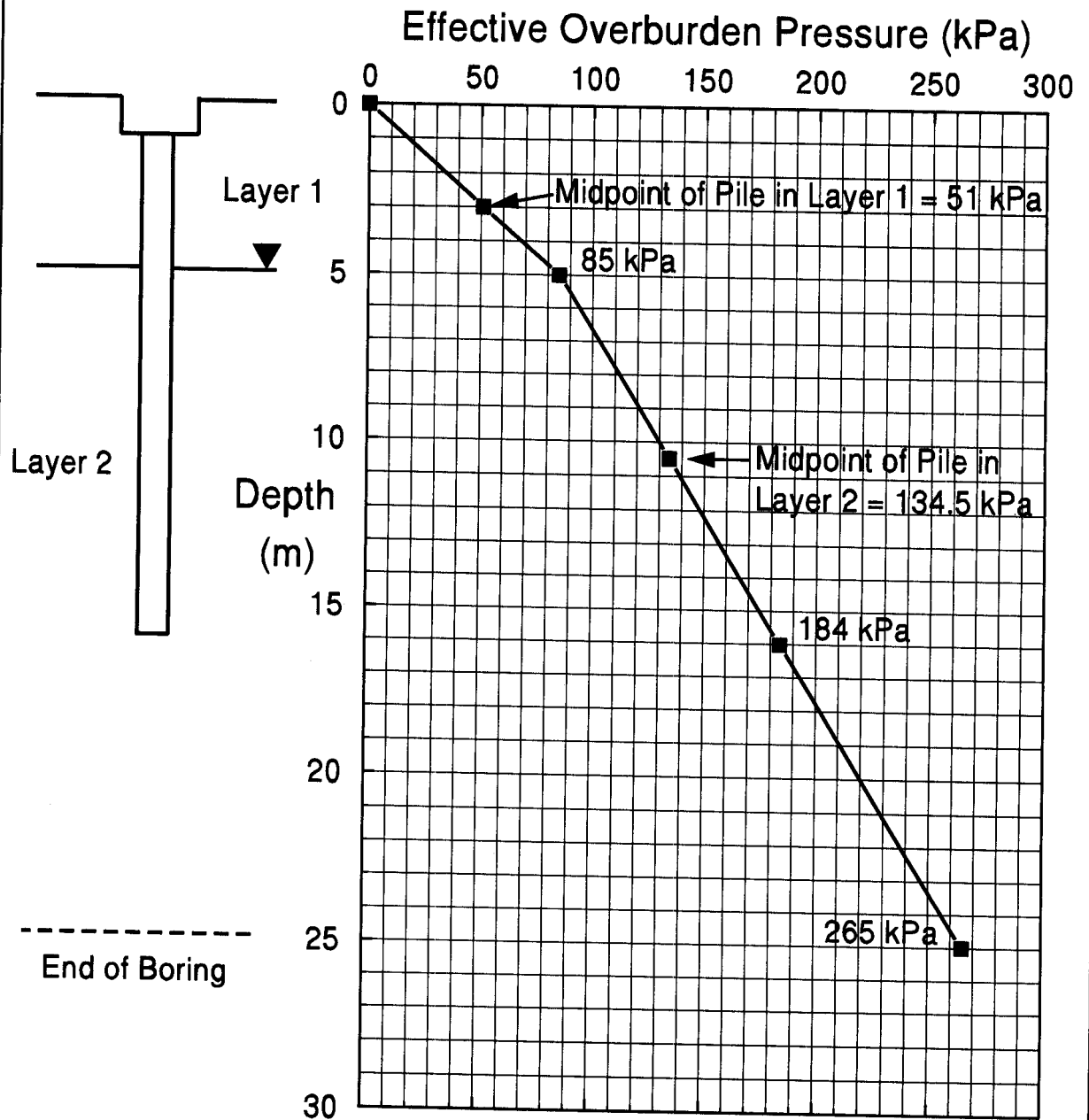
Overburden Pressure (kPa)



STUDENT EXERCISE #2 - NORDLUND CAPACITY CALCULATION

Use the Nordlund method and the step by step procedures described in Section 9.7.1.1b to calculate the ultimate capacity and the allowable design load for a 305 mm square prestressed concrete pile driven into the soil profile described below. A trial pile length of 15 meters below the bottom of the pile cap 1 meter below grade should be used. Begin the calculation with Step 2 of the step by step procedure since the data required from Step 1 has been provided in the problem. The overburden pressure diagram for this problem is included on the next page. The problem solution is presented in Appendix G.





STUDENT EXERCISE #2 - NORDLUND METHOD - STEP BY STEP

STEP 1 The p_o diagram, soil layer determination, and the soil friction angle, ϕ , for each soil layer were presented in the problem introduction. Layer 1 has an ϕ angle of 30° and layer 2 has an ϕ angle of 35° .

STEP 2 Determine δ .

a. Compute volume of soil displaced per unit length of pile, V .

$$V = (0.305 \text{ m})(0.305 \text{ m})(1.0 \text{ m/m}) = 0.093 \text{ m}^3/\text{m}$$

b. Determine δ/ϕ from Figure 9.10.

$$V = 0.093 \text{ m}^3/\text{m} \rightarrow \delta/\phi =$$

c. Calculate δ for each soil layer.

$$\text{Layer 1: } \delta_1 =$$

$$\text{Layer 2: } \delta_2 =$$

STEP 3 Determine K_δ for each soil layer based on displaced volume, V , and pile taper angle, ω .

$$\text{Layer 1: For } \phi = 30^\circ, \quad V = 0.093 \text{ m}^3/\text{m} \text{ and } \omega = 0^\circ$$

$$\text{From Figure 9.12: } K_\delta =$$

$$\text{Layer 2: For } \phi = 35^\circ, \quad V = 0.093 \text{ m}^3/\text{m} \text{ and } \omega = 0^\circ$$

$$\text{From Figure 9.13: } K_\delta =$$

STEP 4 Determine correction factor, C_F , to be applied to K_δ when $\delta \neq \phi$ (Figure 9.15.)

$$\text{Layer 1: } \phi = 30^\circ \text{ and } \delta/\phi = \quad \rightarrow \quad C_F =$$

$$\text{Layer 2: } \phi = 35^\circ \text{ and } \delta/\phi = \quad \rightarrow \quad C_F =$$

STEP 5 Compute effective overburden pressure at midpoint of each soil layer, p_d .

From p_o diagram, p_d for layer 1 is 51 kPa, and

p_d for layer 2 is 134.5 kPa.

STEP 6 Compute the shaft resistance for each soil layer.

$$R_s = K_\delta C_F p_d \sin \delta C_d D$$

$$C_d = \text{pile perimeter} =$$

$$D = \text{embedded length in layer}$$

$$\text{Layer 1: } R_{s1} =$$

$$\text{Layer 2: } R_{s2} =$$

Compute the ultimate shaft resistance, R_s .

$$R_s = R_{s1} + R_{s2} =$$

STEP 7 Determine α_t coefficient and bearing capacity factor N'_q from ϕ angle of 35° at pile toe and Figures 9.16(a) and 9.16(b).

From Figure 9.16(a) $\rightarrow \alpha_t =$

From Figure 9.16(b) $\rightarrow N'_q =$

STEP 8 Compute effective overburden pressure at pile toe.

From effective overburden pressure diagram, p_t at 16 meters is 184 kPa. Therefore, limiting overburden pressure at pile toe of 150 kPa applies.

STEP 9 Compute the ultimate toe resistance, R_t .

a. $R_t = \alpha_t N'_q A_t p_t$

=

b. $R_t = q_L A_t$ determine q_L from Figure 9.17, for $\phi=35^\circ$.

=

c. Use lesser value of R_t from Step 9a and 9b. Therefore, $R_t =$

STEP 10 Compute the ultimate pile capacity, Q_u .

$$Q_u = R_s + R_t =$$

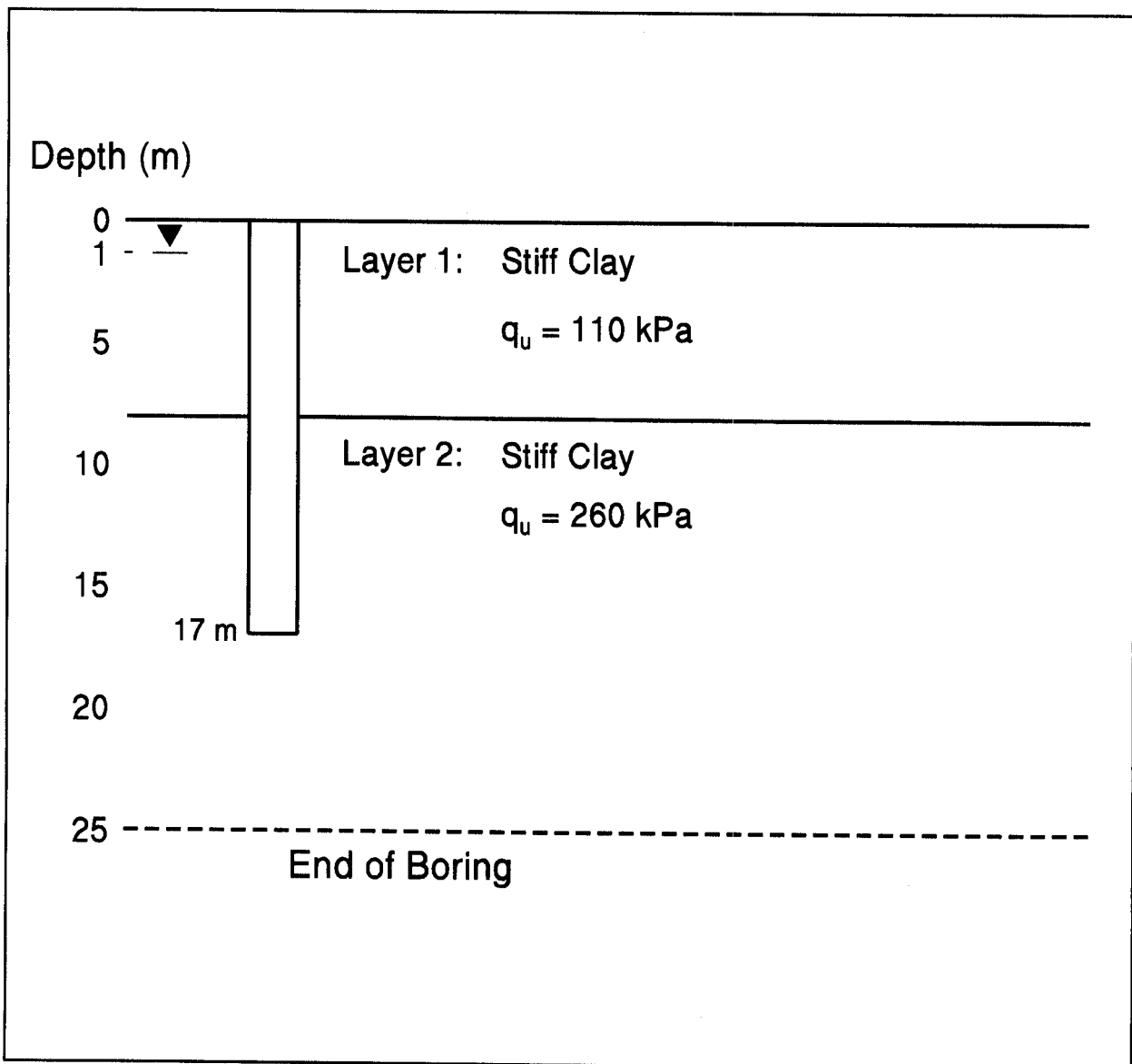
STEP 11 Compute the allowable design load, Q_a based on construction control as described in Section 9.6.

Based on construction control with static load testing $Q_a =$

Based on construction control with the Gates Formula $Q_a =$

STUDENT EXERCISE #3 - α -METHOD PILE CAPACITY CALCULATION

Use the α -Method and step by step procedure described in Section 9.7.1.2a to calculate the ultimate pile capacity and the allowable design load for a 356 mm square, prestressed concrete pile driven into the soil profile described below. The trial pile length for the calculation is 17 meters. The prestressed concrete pile has a pile-soil surface area of $1.42 \text{ m}^2/\text{m}$ and a pile toe area of 0.127 m^2 . Based on the soil profile, Figure 9.18 or 9.19(c) should be used to calculate pile capacity. The problem solution is presented in Appendix G. Note: the soil strengths provided are unconfined compression test results ($c_u = q_u/2$).



STUDENT EXERCISE #3 - α -METHOD - STEP BY STEP

STEP 1 Delineate the soil profile and determine the pile adhesion from Figure 9.18 or the adhesion factor from Figure 9.19(c).

The soil profile was delineated in the problem statement. The bottom of Layer 1 is at 9 meters. Therefore calculations for Layer 1 should be based on an embedded pile length to diameter ratio, D/b , of (9 m) / (.356 m) or 25. The bottom of Layer 2 is at 17 meters. Calculations for Layer 2 should then be based on an embedded pile length to diameter ratio, D/b , of (17 m) / (.356 m) or 48.

Using Figure 9.18, calculate the pile adhesion, c_a , for each layer:

Layer 1: $c_{a1} =$

Layer 2: $c_{a2} =$

or using Figure 9.19(c), calculate the adhesion on factor, α , for each layer:

Layer 1: $\alpha_1 =$

Layer 2: $\alpha_2 =$

STEP 2 Compute the unit shaft resistance, f_s , for each soil layer.

$f_s = c_a$ or $\alpha (c_u)$

Layer 1: $f_{s1} =$

Layer 2: $f_{s2} =$

STEP 3 Compute the shaft resistance per layer and the ultimate shaft resistance.

The embedded pile length is 9 meters in Layer 1 and 8 meters in Layer 2. The pile-soil surface area was defined as $1.42 \text{ m}^2/\text{m}$ in the problem statement.

$$\text{Layer 1: } R_{s1} = (f_{s1}) (A_s) (D_1) =$$

$$\text{Layer 2: } R_{s2} = (f_{s2}) (A_s) (D_2) =$$

The ultimate shaft resistance, R_s , is the sum of the shaft resistance from each individual layer.

$$R_s = R_{s1} + R_{s2} =$$

STEP 4 Compute the unit toe resistance, q_t from $9 c_u$.

$$q_t =$$

STEP 5 Compute the ultimate toe resistance, R_t .

$$R_t = q_t A_t =$$

STEP 6 Compute the ultimate pile capacity, Q_u .

$$Q_u = R_s + R_t$$

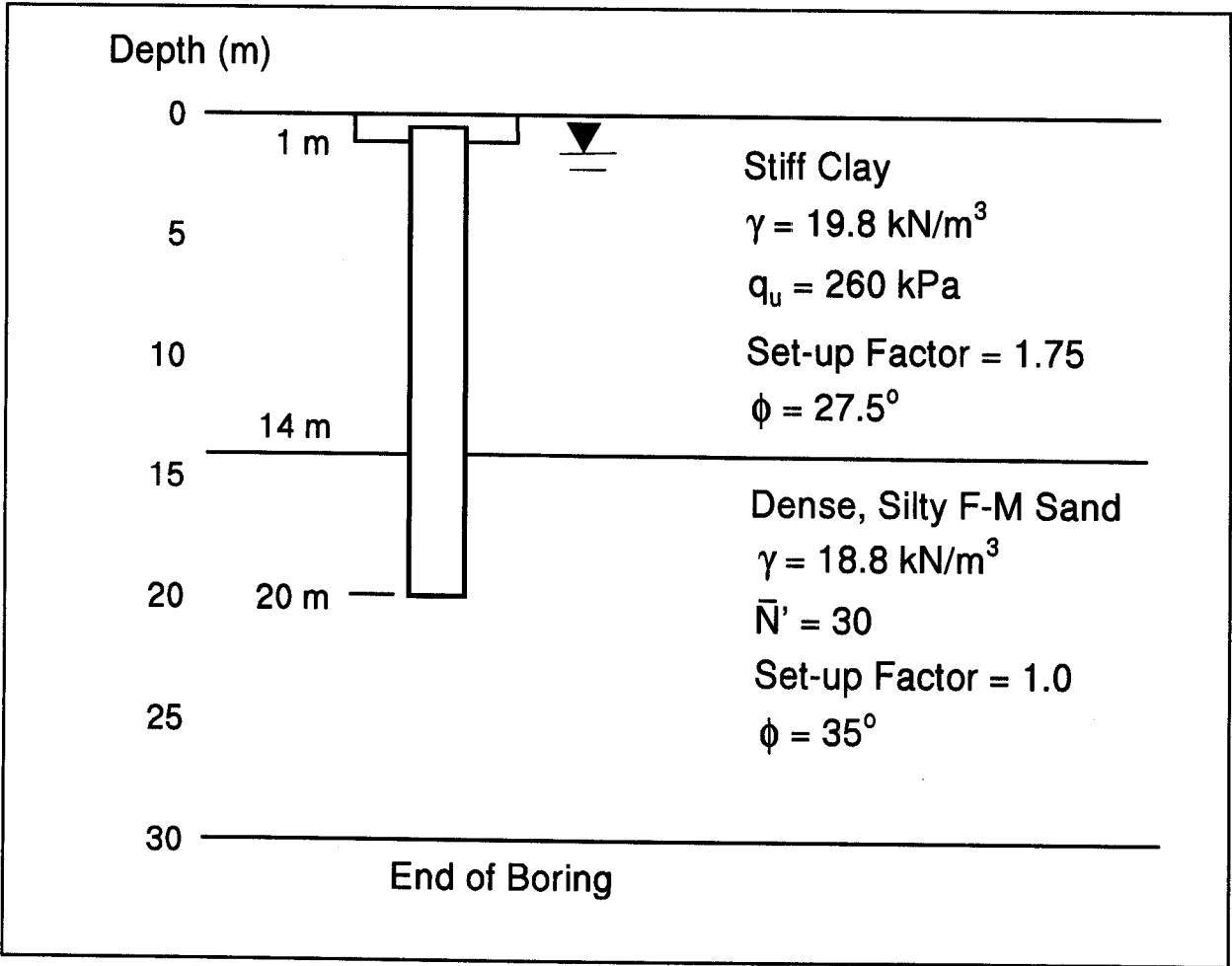
STEP 7 Determine the allowable design load, Q_a based on construction control method as described in Section 9.6.

Based on construction control with static load testing, $Q_a =$

Based on construction control with the Gates Formula, $Q_a =$

STUDENT EXERCISE #4 - α -METHOD & NORDLUND METHOD PILE CAPACITY CALCULATION IN A LAYERED SOIL PROFILE

Use the α -Method described in Section 9.7.1.2a and the Nordlund Method described in Section 9.7.1.1b to calculate the ultimate pile capacity, the resistance to driving, and the allowable design load for a 324 mm O.D. closed end pipe pile driven into the soil profile described below. The trial pile length for the calculation is 19 meters below the pile cutoff elevation 1 meter below grade. The pipe pile has a pile-soil surface area of 1.02 m²/m and a pile toe area of 0.082 m². Use Figure 9.18 to calculate the shaft resistance in the clay layer. The pile volume is 0.082 m³/m. The effective overburden at 17 m, the midpoint of the pile shaft in the sand layer is 177 kPa, and the effective overburden pressure at the pile toe is 204 kPa. The problem solution is presented in Appendix G. Note: the soil strengths provided are unconfined compression test results ($c_u = q_u / 2$).



STUDENT EXERCISE #4 - α -METHOD & NORDLUND METHOD - STEP BY STEP

Calculate the Shaft Resistance in the Clay Layer Using α -Method

STEP 1 Delineate the soil profile and determine the pile adhesion from Figure 9.18.

$$\text{Layer 1: } q_u = 260 \text{ kPa so } c_u =$$

$$D/b =$$

$$\text{Therefore } c_a =$$

STEP 2 Compute the unit shaft resistance, f_s , for each soil layer.

STEP 3 Compute the shaft resistance in the clay layer.

$$\text{Layer 1: } R_{s1} = (f_{s1})(A_s)(D_1) =$$

Calculate the Shaft Resistance in the Sand Layer Using Nordlund Method

STEP 1 The p_o diagram, soil layer determination, and the soil friction angle, ϕ , for each soil layer were presented in the problem introduction.

STEP 2 Determine δ .

a. Compute volume of soil displaced per unit length of pile, V .

$$V = 0.082 \text{ m}^3/\text{m} \text{ (per problem description)}$$

b. Determine δ/ϕ from Figure 9.10.

$$V = 0.082 \text{ m}^3/\text{m} \rightarrow \delta/\phi = \quad \text{or} \quad \delta = \phi$$

c. Calculate δ for each soil layer based on $\delta = \phi$

Layer 2: $\delta_2 =$

STEP 3 Determine K_δ for each soil layer based on displaced volume, V , and pile taper angle, ω .

Layer 2: For $\phi = 35^\circ$, $V = 0.082 \text{ m}^3/\text{m}$ and $\omega = 0^\circ$

d. From Figure 9.13: $K_\delta = 1.15$ for $V = 0.0093 \text{ m}^3/\text{m}$
 $K_\delta = 1.75$ for $V = 0.093 \text{ m}^3/\text{m}$

Using log linear interpolation $K_\delta = 1.72$ for $V = 0.082 \text{ m}^3/\text{m}$

STEP 4 Determine correction factor, C_F , to be applied to K_δ when $\delta \neq \phi$ (Figure 9.15.)

Layer 2: $\phi = 35^\circ$ and $\delta/\phi =$ $\rightarrow C_F =$

STEP 5 Compute effective overburden pressure at midpoint of each soil layer, p_d .

From problem description, p_d for layer 2 is 177 kPa.

STEP 6 Compute the shaft resistance for each soil layer.

$$R_s = K_\delta C_F p_d \sin \delta C_d D$$

$$C_d = \text{pile perimeter} = 1.02 \text{ m}^2/\text{m} \text{ (given)}$$

$$D = \text{embedded length in layer}$$

$$\text{Layer 2: } R_{s2} =$$

Compute the Ultimate Shaft Resistance, R_s

$$R_s = R_{s1} + R_{s2} =$$

Compute the Ultimate Toe Resistance, R_t

STEP 7 Determine α_t coefficient and bearing capacity factor N'_q from ϕ angle of 35° at pile toe and Figures 9.16(a) and 9.16(b)

At pile toe depth $\rightarrow D/b =$

From Figure 9.16(a) $\rightarrow \alpha_t =$

From Figure 9.16(b) $\rightarrow N'_q =$

STEP 8 Compute effective overburden pressure at pile toe.

$p_t =$

STEP 9 Compute the ultimate toe resistance, R_t .

a. $R_t = \alpha_t N'_q A_t p_t$

b. $R_t = q_L A_t$ (q_L determined from Figure 9.17)

c. Use lesser value of R_t from Step 9a and 9b. Therefore, $R_t =$

STEP 10 Compute the ultimate pile capacity, Q_u .

$$Q_u = R_s + R_t =$$

STEP 11 Compute the allowable design load, Q_a , based on construction control methods as described in Section 9.6.

Based on construction control with a static test, $Q_a =$

Based on construction control using the Gates Formula, $Q_a =$

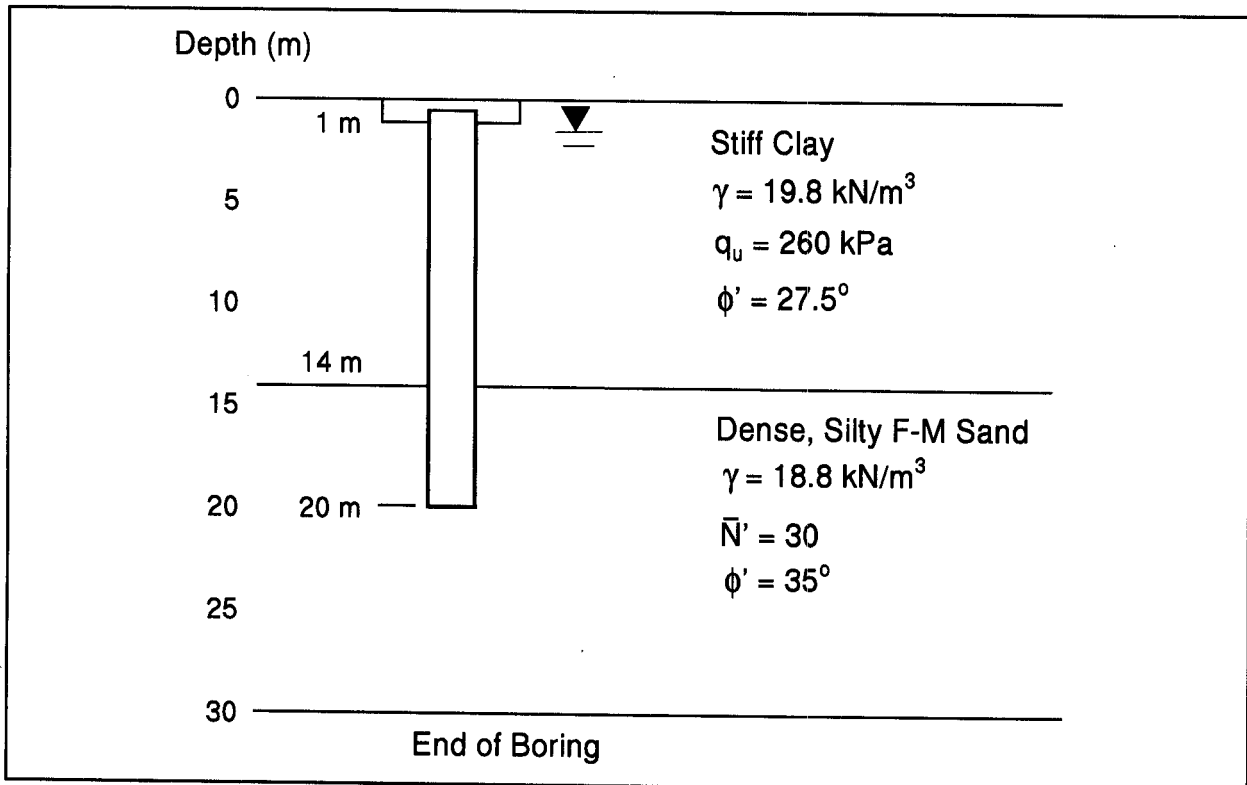
Calculation of the Resistance to Driving

The clay layer has a set-up factor of 1.75 and the sand layer has a set-up factor of 1.0.

STUDENT EXERCISE #5 - EFFECTIVE STRESS PILE CAPACITY CALCULATION IN A LAYERED SOIL PROFILE

Use the Effective Stress Method described in Section 9.7.1.3 to calculate the ultimate pile capacity, the resistance to driving, and the allowable design load for a 324 mm O.D. closed end pipe pile driven into the soil profile described below. The trial pile length for the calculation is 19 meters below the pile cutoff elevation 1 meter below grade. The pipe pile has a pile-soil surface area of $1.02 \text{ m}^2/\text{m}$ and a pile toe area of 0.082 m^2 . Use Table 9-4 or Figure 9.20 to determine β values for calculation of the shaft resistance and Table 9-4 or Figure 9.21 for calculation of N_c . The effective overburden at the midpoint of the pile shaft in the clay layer is 85 kPa and 177 kPa at the midpoint of the sand layer. The effective overburden pressure at the pile toe is 204 kPa.

During driving, the excess pore pressure generated in the clay layer at the pile-soil interface is expected to be 1.4 times the effective overburden pressure based on Figure 9.56. Therefore, use an average effective overburden pressure of 29.5 kPa at the midpoint of the pile shaft in the clay layer to calculate the shaft resistance in the clay layer during driving.



STUDENT EXERCISE #5 - EFFECTIVE STRESS METHOD - STEP BY STEP

STEP 1 Delineate the soil profile and determine the ϕ' angle for each layer.

The soil profile and ϕ' angle were given in the problem description.

STEP 2 Select the β coefficient for each soil layer.

$$\text{Layer 1: } \phi' = 27.5^\circ \rightarrow \beta_1 =$$

$$\text{Layer 2: } \phi' = 35^\circ \rightarrow \beta_2 =$$

STEP 3 Compute the unit shaft resistance, f_s , in each layer.

$$\text{Layer 1: } f_{s1} = \beta_1 (p_o) =$$

$$\text{Layer 2: } f_{s2} = \beta_2 (p_o) =$$

STEP 4 Compute the shaft resistance for each layer and the ultimate shaft resistance.

The shaft resistance for each layer is as follows:

$$\text{Layer 1: } R_{s1} = (f_{s1})(A_s)(D_1) =$$

$$\text{Layer 2: } R_{s2} = (f_{s2})(A_s)(D_2) =$$

The ultimate shaft resistance, R_s is as follows:

$$R_s = R_{s1} + R_{s2} =$$

STEP 5 Compute the unit toe resistance, q_t , using Figure 9.21 and ϕ' at pile toe.

STEP 6 Compute the ultimate toe resistance, R_t .

$$R_t = q_t A_t =$$

STEP 7 Compute the ultimate pile capacity, Q_u .

$$Q_u = R_s + R_t =$$

STEP 8 Compute the allowable design load, Q_a , based on construction control method as described in Section 9.6.

Based on construction control with static load testing, $Q_a =$

Based on construction control with the Gates Formula, $Q_a =$

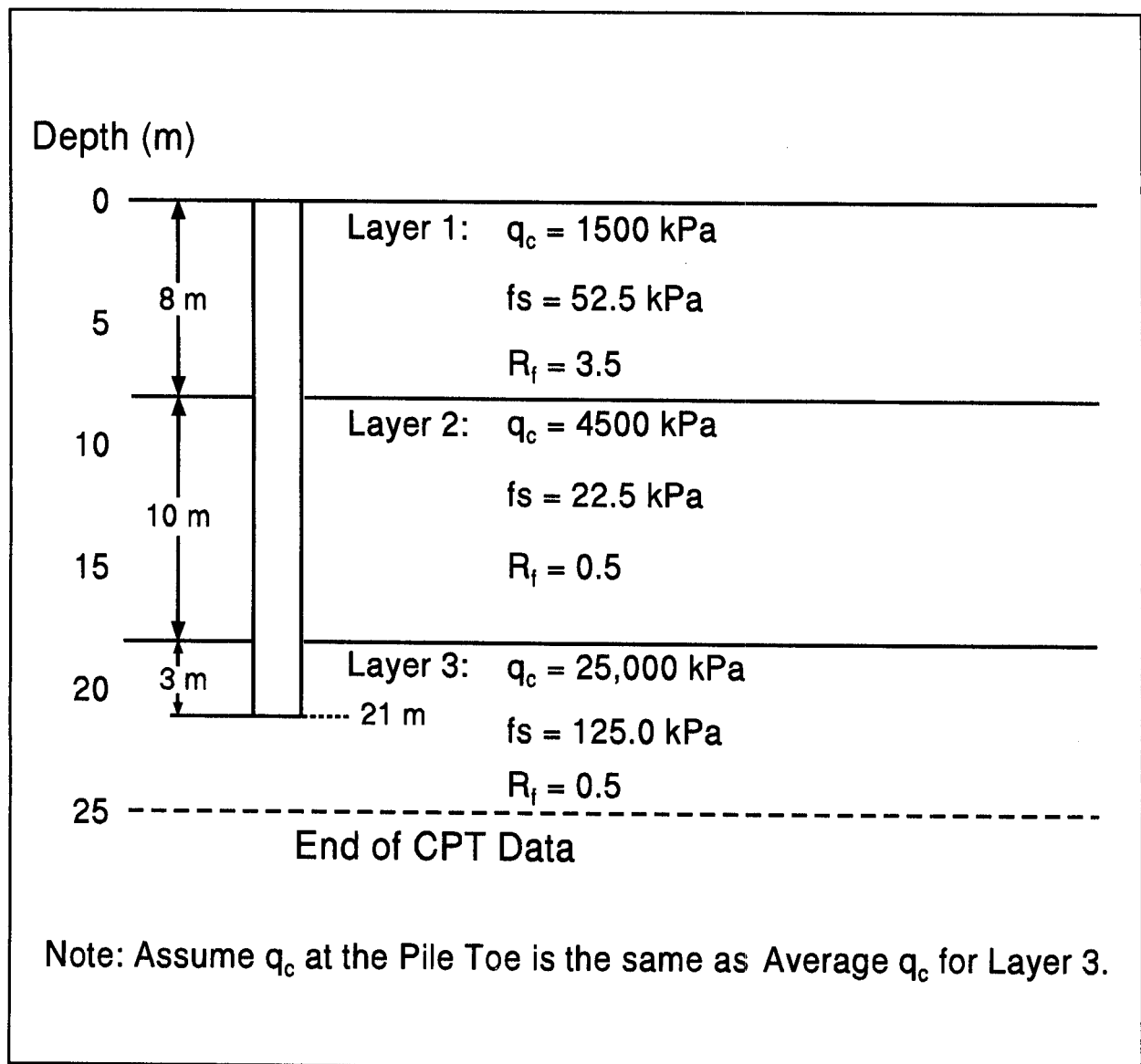
Calculation of the Resistance to Driving

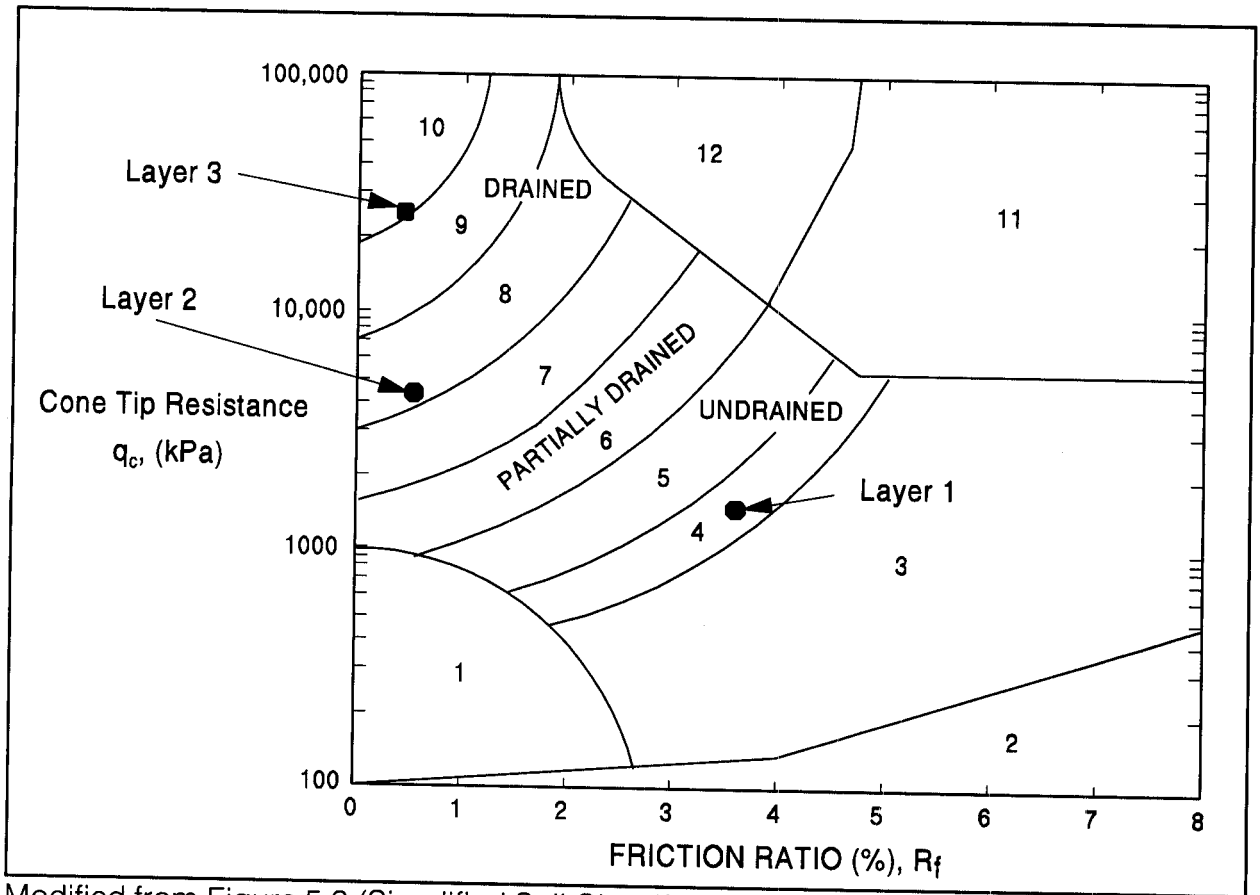
The average effective overburden pressure in the clay layer during driving is estimated to be 29.5 kPa. Therefore, the average unit shaft resistance in the clay layer at the time of driving should be calculated using this effective overburden pressure. The shaft and toe resistance from the sand layer are unchanged. The resistance at the time of driving, Q_D , is:

$$Q_D =$$

STUDENT EXERCISE #6 - LPC METHOD PILE CAPACITY CALCULATION

Cone Penetration Test (CPT) data for a site identified three soil layers having the average CPT results presented below. Use the LPC Method described in Section 9.7.1.7b to calculate the ultimate pile capacity and the allowable design load for a 324 mm diameter closed end pipe pile. Use a trial pile length of 21 meters. The pipe pile has a pile-soil surface area of $1.02 \text{ m}^2/\text{m}$ and a pile toe area of 0.083 m^2 . Previous load test data is not available in the project vicinity. Use Figure 5.2 to characterize the subsurface conditions. The problem solution is presented in Appendix G.





Modified from Figure 5.2 (Simplified Soil Classified Chart for Standard Electronic Friction Cone after Robertson *et al.*, 1986)

Zone	q_c/N	Soil Behavior Type
1)	2	sensitive fine grained
2)	1	organic material
3)	1	clay
4)	1.5	silty clay to clay
5)	2	clayey silt to silty clay
6)	2.5	sandy silt to clayey silt
7)	3	silty sand to sandy silt
8)	4	sand to silty sand
9)	5	sand
10)	6	gravelly sand to sand
11)	1	very stiff fine grained
12)	2	sand to clayey sand

STUDENT EXERCISE #6 - LPC METHOD - STEP BY STEP

STEP 1 Delineate the soil profile. Using the cone tip resistance, q_c , and the friction ratio, R_f , values in Figure 5.2, the soil profile can be characterized as follows:

Layer 1: $q_c = 1500$ kPa and $R_f = 3.5$, the soil type is:

Layer 2: $q_c = 4500$ kPa and $R_f = 0.5$, the soil type is:

Layer 3: $q_c = 25000$ kPa and $R_f = 0.5$, the soil type is:

STEP 2 Determine the unit shaft resistance for each soil layer.

From Table 9-7, the pile type is:

The unit shaft resistance for each layer can be determined from Tables 9-8(a) and 9-8(b) along with Figures 9.25(a) and 9.25(b).

Layer 1: $f_{s1} =$

Layer 2: $f_{s2} =$

Layer 3: $f_{s3} =$

STEP 3 Compute the shaft resistance per layer and the ultimate shaft resistance.

Layer 1: The unit shaft resistance, $f_{s1} =$

The shaft resistance in this layer can be calculated from:

$$R_{s1} = (f_{s1})(A_s)(D_1) =$$

Layer 2: The unit shaft resistance, $f_{s2} =$

The shaft resistance in this layer can be calculated from:

$$R_{s2} = (f_{s2})(A_s)(D_2) =$$

Layer 3: The unit shaft resistance, $f_{s3} =$

The shaft resistance in this layer can be calculated from:

$$R_{s3} = (f_{s3})(A_s)(D_3) =$$

The ultimate shaft resistance, R_s , is the sum of the shaft resistance from each individual layer.

$$R_s = R_{s1} + R_{s2} + R_{s3} =$$

STEP 4 Compute the unit pile toe resistance, q_t .

- a. The average cone tip resistance is 25000 kPa.
- b. From Table 9-9, the cone bearing capacity factor, $K_c =$
- c. The unit pile toe resistance is then:

$$q_t = K_c q_c =$$

STEP 5 Compute the ultimate toe resistance, R_t .

$$R_t = q_t A_t =$$

STEP 6 Compute the ultimate pile capacity, Q_u .

$$Q_u = R_s + R_t =$$

STEP 7 Determine the allowable design load, Q_a , based on construction control method as described in Section 9.6.

Based on construction control using a static test, $Q_a =$

Based on construction control using the Gates Formula, $Q_a =$

STUDENT EXERCISE #7 - PILE GROUP SETTLEMENT IN LAYERED PROFILE

A pile group is to be installed in a fine to medium silty sand deposit that is underlain by a stiff clay layer and then a very dense fine to coarse sand layer. The pile group has a total **design** load of 16,000 kN. The pile group has a plan area of 3 m by 10 m. Use the pile group settlement method for layered soils described in Section 9.8.2.4 to calculate the settlement of the pile group depicted on the following page. For ease of calculation, compute the settlements for each soil layer below the equivalent footing depth using the layer thickness rather than breaking the profile into 1.5 to 3 m thick layers as described in Section 9.8.2.4. Also do not calculate the elastic pile deformation for this problem. Based on your calculation, is the pile group settlement acceptable?

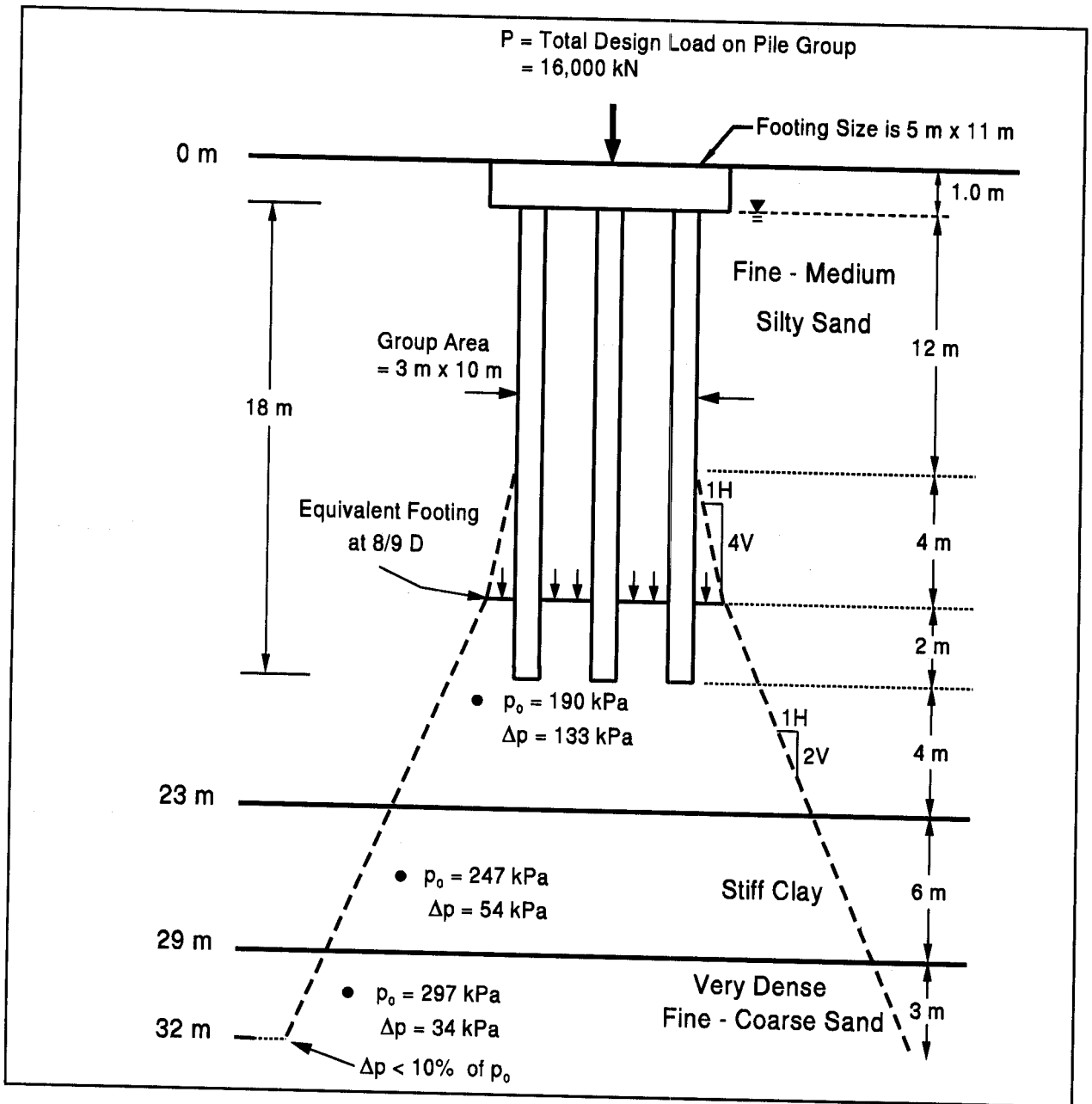
The soil layers have the following properties:

In the zone below the equivalent footing location, the fine to medium sand has an average corrected SPT resistance value of 30 as determined using a SPT safety hammer. The existing overburden pressure at the midpoint of the sand layer below the equivalent footing location is 190 kPa and the corresponding pressure increase at this point is 133 kPa.

The stiff clay layer has an initial void ratio e_o of 0.80, a preconsolidation pressure, p_c , of 247 kPa, a compression index, C_c of 0.30 and recompression index C_{cr} , of 0.03. The existing overburden pressure at the midpoint of the clay layer is 247 kPa and the corresponding pressure increase at this depth is 54 kPa.

The underlying very dense fine to coarse sand layer has an average corrected SPT resistance value of 60 determined by a SPT safety hammer. The pressure increase is less than 10% of the effective overburden pressure at a depth of 32 meters. At the midpoint of the affected portion of the lower sand layer (30.5 m), the effective overburden pressure is 297 kPa and the pressure increase is 34 kPa.

To solve this problem you will need to calculate the sand layer settlement from the equation on page 9-114 and Figure 9.45 on page 9-115. The clay layer settlement should be calculated using the properties described above and the appropriate equation on page 9-111. (Note the terms for these equations are on page 9-108).



Remember settlement computations are based on the design load rather than ultimate loads.

STUDENT EXERCISE #7 - PILE GROUP SETTLEMENT - STEP BY STEP

STEP 1 Calculate the settlement of the fine to medium silty sand layer using the following equation after determining the bearing capacity index for the layer from Figure 9.45.

$$\text{Layer 1: } s_1 = H \left[\frac{1}{C'} \log \frac{p_0 + \Delta p}{p_0} \right] =$$

STEP 2 Calculate settlement in clay layer after determining appropriate settlement equation from page 9-111.

$$\text{Layer 2: } s_2 =$$

STEP 3 Calculate the settlement of the very dense, fine to coarse sand layer after determining the index value from Figure 9.45.

$$\text{Layer 3: } s_3 = H \left[\frac{1}{C'} \log \frac{p_0 + \Delta p}{p_0} \right] =$$

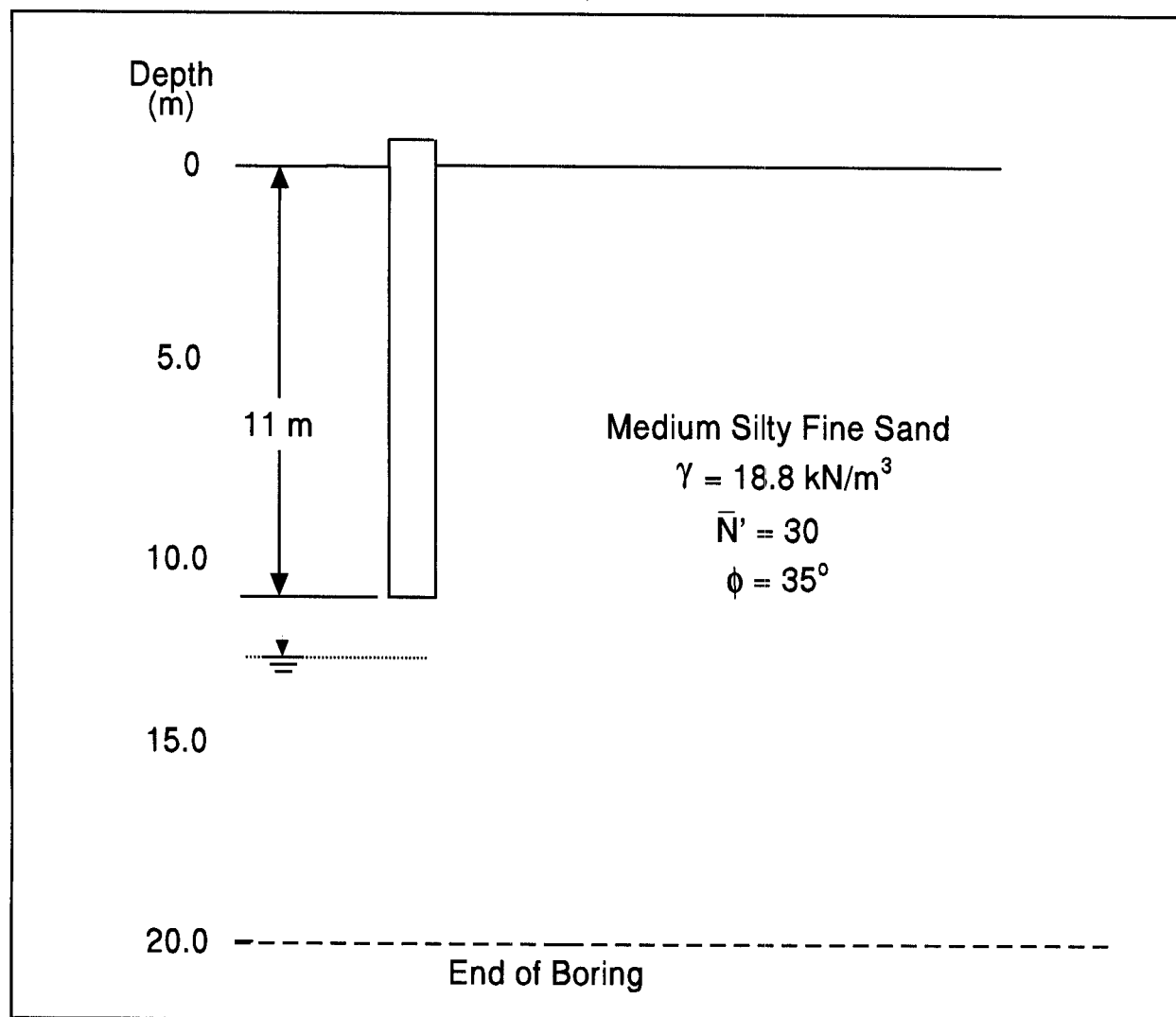
STEP 4 Compute total settlement:

$$s = s_1 + s_2 + s_3 =$$

Is the pile group settlement acceptable?

STUDENT EXERCISE #8 - BROMS' METHOD LATERAL CAPACITY ANALYSIS

Perform a lateral capacity analysis using the Broms' method by following the step by step procedure outlined in Section 9.7.3.2. The pile is a 356-mm square prestressed concrete, which has been driven to a total penetration of 11 meters below grade. The subsurface conditions are presented below. Calculate the maximum allowable lateral load of the pile, and the corresponding deflection at this maximum allowable load. Evaluate the total lateral load capacity of the pile group consisting of 24 piles at 1.5 meters center to center spacing. Assume the pile is to be used in group under a pile cap (fixed head $e_c=0$) with the possibility of cyclic loading during service life. The following pile properties are given: $E = 27,800$ MPa; $f'_c = 34.5$ MPa; $I = 1.32 \times 10^{-3} \text{m}^4$; and $S = 7.46 \times 10^{-3} \text{m}^3$. The problem solution is presented in Appendix G.



EXERCISE #8 - BROMS' METHOD - STEP BY STEP

STEP 1 Determine the general soil type within the critical depth below ground surface (about 4 or 5 pile diameters).

STEP 2 Determine the coefficient of horizontal subgrade reaction, K_h , within the critical depth based on cohesive or cohesionless soils.

STEP 3 Adjust K_h for loading and soil conditions.

$$K_h =$$

STEP 4 Determine pile parameters.

- a. Modulus of elasticity, $E = 27,800 \text{ MPa}$
- b. Moment of inertia, $I = 1.32 \times 10^{-3} \text{ m}^4$
- c. Section modulus, $S = 7.46 \times 10^{-3} \text{ m}^3$
- d. Ultimate compressive strength, $f'_c = 34.5 \text{ MPa}$
- e. Embedded pile length, $D = 11 \text{ m}$
- f. Pile width, $b = 0.356 \text{ m}$
- g. Eccentricity of applied load, $e_c = 0$ for fixed-headed pile
- h. Dimensionless shape factor, C_s , applied only to steel piles.
- i. Resisting moment of pile, $M_y = f'_c S$ for concrete piles

$$M_y =$$

STEP 5 Determine η for cohesionless soils.

$$\eta = \sqrt[5]{K_r/EI} =$$

STEP 6 Determine the dimensionless length factor for cohesionless soil.

$$\eta D =$$

STEP 7 Determine if pile is long or short according to the cohesionless soil criteria.

STEP 8 Determine other soil parameters.

a. Rankine passive pressure coefficient for cohesionless soil, K_p , is:

$$K_p = \tan^2 (45 + \phi/2) =$$

b. Average effective soil unit weight over embedded pile length, γ (kN/m³).

$$\gamma =$$

STEP 9 Determine the ultimate (failure) load, Q_u , for a single pile.

a. Calculate $\frac{M_y}{b^4 \gamma K_p} =$

b. With solution from Step 9a, enter Figure 9.30 and determine $Q_u/(K_p b^3 \gamma)$ from fixed head curve.

c. From Step 9b, $Q_u/(K_p b^3 \gamma) =$ Solve for Q_u

STEP 10 Calculate the maximum allowable working load for a single pile, Q_m , from the ultimate load, Q_u , determined in Step 9, as shown in Figure 9.31.

$$Q_m = \frac{Q_u}{2.5} =$$

STEP 11 Calculate the deflection, y , corresponding to the working load, Q_a .

(Since neither the working load, Q_a , nor the design deflection at the ground surface, y , are given, use Q_m to calculate y_m .)

STEP 12 Compare the design load Q_a , and design deflection, y , (if available) with the maximum allowable working load, Q_m , and deflection, y_m .

STEP 13 Reduce the allowable load selected to account for group effects and method of installation based on Table on page 9-87.

a. Group effects.

b. Method of installation.

STEP 14 Compute the total lateral load capacity of the pile group.

10. OVERVIEW OF DYNAMIC ANALYSIS METHODS

Dynamic analysis methods can be defined as analytical techniques for evaluating the soil resistance against which the pile is driven. A pile foundation designed to meet compression, uplift, and lateral load performance requirements using the static design methods presented in Chapter 9 is of little use if it cannot be installed as designed and without damage. The ability of a selected pile section to be driven within allowable driving stress limits to the required ultimate capacity and to the minimum pile penetration depth should be evaluated by the foundation designer during the design stage through modern dynamic analysis methods.

The soil resistance acting against the pile during driving consists of both static and dynamic resistance components. Of primary interest is the static resistance component because this is the only resistance available to support the applied loads. At the time of driving, the static resistance component is in most cases only a portion of the ultimate pile capacity. The dynamic soil resistance, or damping force, is the temporary viscous resistance on the pile during driving. Therefore, the dynamic resistance component provides resistance to pile penetration during driving but does not provide long term support under static loading conditions.

Traditional dynamic analysis techniques have been dynamic formulas such as the Engineering News formula. Depending upon the formula used, an estimate of the allowable or ultimate pile capacity relative to the pile driving resistance at the time of driving is obtained. Unfortunately, dynamic formulas have fundamental weaknesses in that they do not adequately model the dynamics of the hammer-pile impact, the influence of axial pile stiffness, or the soil response. Dynamic formulas have also proven unreliable in determining pile capacity in many circumstances. Their continued use is not recommended on significant projects.

Wave equation analysis, Goble and Rausche (1986), is the most readily available modern dynamic analysis tool available to the foundation designer during the design stage. A detailed discussion of the wave equation method is presented in Chapter 17. Dynamic testing and analysis, Goble and Hussein (1994), Hannigan (1990) is an additional modern dynamic analysis tool that can be used if a design stage test program is planned. Additional details on dynamic testing and analysis methods are presented in Chapter 18.

These modern dynamic analysis methods not only provide an estimate of the ultimate pile capacity relative to pile driving resistance, but also include an evaluation of pile driving stresses. The proper application of modern dynamic analysis methods is to match the hammer size and pile section to the static and dynamic soil resistance to be overcome to achieve the ultimate pile capacity or to reach the specified pile penetration depth.

10.1 NEED FOR MODERN DYNAMIC ANALYSIS METHODS

Piles are forced into the ground by dynamic means such as impact or vibration. A successful pile foundation which meets the design objectives depends largely on relating the static analysis results presented on the plans to the dynamic methods of field installation and control. During the design and construction stage, the following site specific questions often arise:

1. Can the design pile section be driven to the required penetration depth and capacity with readily available pile hammers (design stage) or a proposed hammer (construction stage)?
2. What soil resistance must be overcome? With the anticipated or proposed hammer, what will be the maximum driving resistance required to overcome this soil resistance and what will be the maximum stresses experienced by the design pile section during driving?
3. If a specific hammer cannot drive the design pile section to the required depth and/or capacity within allowable driving stresses, what hammer characteristics could be specified (design stage) or obtained (construction stage) to drive the pile?

To answer these and other questions that may arise with a specific pile foundation, rational analysis of the hammer-cushion-pile-soil system through modern dynamic analysis methods is invaluable. Experience alone, however important, is not sufficient to answer the above questions.

As noted earlier, the traditional method for field verification of pile capacity has been dynamic formulas, which are discussed in greater detail in Chapter 16. Unfortunately, dynamic formulas have fundamental weaknesses and cannot reliably answer any of the above questions. Dynamic formulas do not provide pile driving stresses and, in many circumstances, have proven unreliable in determining pile capacity. Therefore, their continued use is not recommended on significant projects.

Modern dynamic analysis methods should be used in both the design and construction stages of a project. In a design stage evaluation, wave equation analyses may indicate that the contemplated pile section cannot be driven to the required pile penetration depth and/or ultimate capacity within the allowable driving stresses or within a reasonable driving resistance. A design change should then be considered. The wave equation can then be used to evaluate what changes can be made in pile size, pile type, pile material properties, hammer size, or what installation techniques can be specified to achieve the desired foundation. If a test pile program is performed during the design stage, then information from dynamic testing and analysis of test piles in conjunction with wave equation analyses can be used to evaluate design change alternatives.

If a project is designed without modern dynamic analysis methods, and then problems are detected when these methods are implemented during the construction stage, problem solutions may not be quite as easy. In this case, equipment and materials may already be on-site, thereby limiting potential solutions. For example, few cost effective options exist once a thin walled pipe pile lacking the required driveability arrives on site. In this example, it may be necessary to reduce the ultimate capacity per pile and increase the number of piles, use a pile installation aid such as predrilling, or order new piling having the necessary driveability, assuming that the hammer and crane are still suitably sized. While a construction stage problem is more complicated, modern dynamic analysis methods still offer the most rational way of determining the most cost effective solution.

10.2 METHODS OF MODERN DYNAMIC ANALYSIS

There are two methods of modern dynamic analysis. These include:

- a. Wave equation analysis.
- b. Dynamic testing and analysis.

The wave equation is a computer simulation of the pile driving process that models wave propagation through the hammer-pile-soil system. This computer analysis can be readily used in either the design or construction stage to rationally evaluate pile driveability, size driving equipment, calculate driving stresses, and assess ultimate pile capacity versus pile penetration resistance. These analyses are a significant improvement over the use of dynamic formulas. Two limitations of wave equation analysis involve assumptions that must be made on drive system performance and on the soil model, (*i.e.*, the soil resistance distribution, and the soil quake and damping parameters).

Dynamic testing and analysis consists of measuring strain and acceleration near the pile head during driving, or restriking using a Pile Driving Analyzer or similar data processing device conforming to ASTM D-4945 (1989). The strain and acceleration signals are used to calculate quantities such as energy transfer, pile driving stresses, and estimates of ultimate pile capacity. Further analysis of dynamic testing data using signal matching methods can also characterize the soil model. The information from dynamic testing on drive system performance and the soil model can be used to improve the accuracy of wave equation results. Dynamic testing and analysis offers a significantly better evaluation method and construction control as compared to dynamic formulas.

10.3 DRIVING RESISTANCE CRITERIA

The foundation designer should specify the dynamic analysis method to be used for determination of the driving resistance criteria. The driving resistance criteria usually consists of a specified penetration resistance at a given hammer stroke and, in some cases, a minimum pile penetration depth.

In the past, dynamic formulas were the primary means of establishing the driving resistance criteria. As discussed elsewhere in this manual, dynamic formulas do not provide information on pile driving stresses and, in many circumstances, have proven unreliable in determining pile capacity. Therefore, their continued use is not recommended on significant projects.

The wave equation analysis offers a rational means of establishing a relationship between the static pile capacity of a driven pile with the number of blows per 0.25 meter required by a particular hammer to drive a selected pile to an ultimate capacity in a given soil situation. The driving criteria established from wave equation analysis should be substantiated by static load tests whenever possible.

Dynamic testing and analysis of indicator or test piles allows an assessment of the static pile capacity during driving. This is also an appropriate means of establishing a driving criteria. Again, the driving criteria established by dynamic testing and analysis should be substantiated by static load tests whenever possible.

A driving criteria should also consider time dependent changes in pile capacity. Hence, lower driving resistances than required may be acceptable in soils where soil setup is expected, as are higher driving resistances in cases where relaxation is anticipated. Once again the driving criteria should be substantiated by static load tests whenever possible. In cases where time dependent soil strength changes are anticipated, load tests should be delayed an appropriate waiting period until the anticipated soil strength changes have occurred. Approximate waiting periods for various soil types were discussed in Sections 9.10.1.1 and 9.10.1.2 of Chapter 9.

REFERENCES

- American Society for Testing and Materials [ASTM], (1989). Standard Test Method for High Strain Dynamic Testing of Piles, D-4945, 1-6.
- Goble, G.G. and Hussein, M. (1994). Dynamic Pile Testing in Practice. XII International Conf. on Soil Mechanics and Foundation Engineering, New Delhi, India, January 5-10.
- Goble, G.G. and Rausche, F. (1986). Wave Equation Analysis of Pile Driving - WEAP86 Program. U.S. Department of Transportation, Federal Highway Administration, Implementation Division, McLean, Volumes I-IV.
- Hannigan, P.J. (1990). Dynamic Monitoring and Analysis of Pile Foundation Installations. Deep Foundations Institute Short Course Text, First Edition, 69.

11. ALLOWABLE PILE STRESSES

This chapter deals with the static and dynamic structural pile capacity in terms of allowable stresses for pile materials. Any driven pile has to remain structurally intact and not be stressed to its structural limit during its service life under static loading conditions as well as under dynamic driving induced loads. Therefore, material stress limits are placed on:

1. The maximum allowable design stress during the service life.
2. The maximum allowable driving stresses.

Additional material stress limits, beyond the design and driving stress limits presented in this chapter, may apply to prevent buckling of piles when a portion of the pile is in air, water, or soil not capable of adequate lateral support. In these cases, the structural design of the pile should also be in accordance with the requirements of Sections 8, 9, 10, and 13 of AASHTO code (1994) for compression members.

11.1 FACTORS AFFECTING ALLOWABLE DESIGN STRESSES

Traditionally, the allowable design stress was determined by dividing the ultimate stress of the pile material by a gross factor of safety. The gross factor of safety was based on past experience and includes consideration of load and structural resistance variations. The allowable design stresses in this chapter are in conformance with AASHTO (1994) specifications.

Allowable design stresses for piles are a function of the following variables:

1. Average section strength from an acceptance test such as:
 - a. f_y (yield strength) for steel piles.
 - b. f'_c (unit ultimate strength from 28-day cylinder test for concrete).
 - c. Wood crushing strengths.

2. Reduction for defects such as knots in timber.
3. Reduction for section treatment such as preservation treatment of wood.
4. ϕ - factor which allows for variations in materials, construction dimensions, and calculation approximations. These items are partially under the engineer's control.
5. Load factor to account for the possibility that design service loads may be exceeded.
 - a. Among other causes, increase in load may occur due to overloads permitted on a bridge, pile mislocation, differential settlement and unaccounted negative shaft resistance or downdrag load.
 - b. Decrease in resistance offered by the pile may occur due to variability in pile material properties, corrosion, heave, or undetected driving induced damage.

11.2 DRIVING STRESSES

In almost all cases, the highest stress levels occur in a pile during driving. High driving stresses are necessary to cause pile penetration. The pile must be stressed to overcome the ultimate soil resistance, plus any dynamic resistance forces, in order to be driven to the required penetration depth to support the pile design load. The high strain rate and temporary nature of the loading during pile driving allow a substantially higher driving stress limitation than for the static design case. Wave equation analyses can be used for predicting driving stresses prior to installation. During installation, dynamic testing can be used to calculate driving stresses.

11.3 AASHTO ALLOWABLE DESIGN AND DRIVING STRESSES

The limitations on maximum allowable static design stresses for driven piles in various codes generally represent the static load capacity which can be consistently developed with traditional driving equipment and methods.

The pile material ultimate strength must be greater than the ultimate pile-soil resistance. The recommended AASHTO limits for maximum pile design stresses will generally keep the driving stresses within recommended limits.

11.3.1 Steel H-piles

a. Design Stresses

Table 11-1 contains the AASHTO recommended design and driving stresses for axially loaded steel H-piles in terms of the steel yield stress, f_y . AASHTO limits the maximum allowable design stress to $0.25 f_y$. For A-36 steel with a yield stress of 248 MPa, this results in a maximum design stress of 62 MPa. AASHTO allows the design stress to be increased to a maximum of $0.33 f_y$ in conditions where pile damage is unlikely. However, static and/or dynamic load tests confirming satisfactory results should be performed for design at this stress level. For A-36 steel, a design stress of $0.33 f_y$ corresponds to a design stress of 82 MPa.

b. Driving Stresses

AASHTO specifications limit the maximum compression and tension driving stresses to $0.9 f_y$. For A-36 steel, this results in a maximum driving stress of 223 MPa.

TABLE 11-1 MAXIMUM ALLOWABLE STRESSES FOR STEEL H-PILES	
	AASHTO (1994) Recommendations
Design Stresses	<p>0.25 f_y</p> <p>>0.25 f_y If damage is unlikely and load tests are performed. Evaluation of load test results by the engineer confirms satisfactory results.</p> <p>0.33 f_y If damage is unlikely, and confirming load tests are performed and evaluated by engineer.</p>
Driving Stresses	<p>0.9 f_y</p> <p>223 MPa for ASTM A-36 ($f_y = 248$ MPa)</p> <p>310 MPa for ASTM A-572 or A-690, GR50 ($f_y = 345$ MPa)*</p>

* FHWA experience with allowable driving stresses of 0.9 f_y for high strength steel is limited. The designer should adequately detail splice requirements for high driving stress levels.

11.3.2 Steel Pipe Piles (unfilled)

a. Design Stresses

Table 11-2 summarizes the AASHTO recommended design and driving stresses for axially loaded unfilled steel pipe piles in terms of the steel yield stress, f_y . The maximum AASHTO allowable design stress is limited to 0.25 f_y . For ASTM A-252, Grade 2 steel with a yield stress of 241 MPa, this results in a maximum design stress of 60 MPa. AASHTO allows the design stress to be increased to a maximum of 0.33 f_y in conditions where pile damage is unlikely. However, static and/or dynamic load tests confirming satisfactory results should be performed for design at this stress level. For ASTM A-252, Grade 2 steel, a design stress of 0.33 f_y corresponds to a design stress of 79 MPa.

b. Driving Stresses

AASHTO specifications limit the maximum driving stresses to $0.9 f_y$. For A-252 Grade 2 steel, this results in a maximum driving stress of 217 MPa.

TABLE 11-2 MAXIMUM ALLOWABLE STRESSES FOR UNFILLED STEEL PIPE PILES	
AASHTO (1994) Recommendations	
Design Stresses	$0.25 f_y$ $>0.25 f_y$ If damage is unlikely and load tests are performed. Evaluation of load test results by the engineer confirms satisfactory results. $0.33 f_y$ If damage is unlikely, and confirming load tests are performed and evaluated by engineer.
Driving Stresses	$0.9 f_y$ 186 MPa for ASTM A-252, Grade 1 ($f_y = 207$ MPa) 217 MPa for ASTM A-252, Grade 2 ($f_y = 241$ MPa) 279 MPa for ASTM A-252, Grade 3 ($f_y = 310$ MPa)*

* FHWA experience with allowable driving stresses of $0.9 f_y$ for high strength steel is limited. The designer should adequately detail splice requirements for high driving stress levels.

11.3.3 Steel Pipe Piles (top driven and concrete filled)

a. Design Stresses

Table 11-3 summarizes the AASHTO (1994) recommended design and driving stresses for axially loaded, top driven and concrete filled pipe piles in terms of the steel yield stress, f_y , and the concrete compressive strength, f'_c . These requirements are also applicable to Monotube piles. AASHTO limits the maximum allowable design stress to the sum of $0.25 f_y$ on the steel cross sectional area plus $0.40 f'_c$ on the concrete cross sectional area.

b. Driving Stresses

Concrete filled pipe piles are generally unfilled when driven. Hence, the AASHTO recommended driving stress for unfilled steel pipe piles apply.

TABLE 11-3 MAXIMUM ALLOWABLE STRESSES FOR TOP DRIVEN, CONCRETE FILLED, STEEL PIPE PILES	
AASHTO (1994) Recommendations	
Design Stresses	0.25 f_y (on steel area) <i>plus</i> 0.40 f'_c (on concrete area)
Driving Stresses	0.9 f_y 186 MPa for ASTM A-252, Grade 1 ($f_y = 207$ MPa) 217 MPa for ASTM A-252, Grade 2 ($f_y = 241$ MPa) 279 MPa for ASTM A-252, Grade 3 ($f_y = 310$ MPa)*

* FHWA experience with allowable driving stresses of 0.9 f_y for high strength steel is limited. The designer should adequately detail splice requirements for high driving stress levels.

11.3.4 Precast, Prestressed Concrete Piles

a. Design Stresses

Table 11-4 summarizes the AASHTO recommended design and driving stresses for axially loaded prestressed concrete piles in terms of the concrete compression strength, f'_c , and the effective prestress after losses, f_{pe} . Both f'_c and f_{pe} must be in MPa. Prestressed concrete piles fully embedded in soils providing lateral support are limited to a maximum design stress of $0.33 f'_c - 0.27 f_{pe}$ on the gross cross sectional area of the concrete. The concrete must have a minimum 28 day compression strength of 34.5 MPa.

b. Driving Stresses

AASHTO specifications limit the maximum allowable compression driving stress to 0.85 times the concrete compressive strength, f'_c , minus the effective prestress after losses, f_{pe} . Tension driving stresses are limited to 0.25 times the square root of the concrete compressive strength plus the effective prestress after losses in normal environments, or to the effective prestress after losses in severe corrosive environments. The compression and tension driving stress limits are on the gross concrete area.

Control of driving stresses is particularly important when driving prestressed concrete piles at high driving stress levels while penetrating through dense soil layers into underlying weaker soils.

TABLE 11-4 MAXIMUM ALLOWABLE STRESSES FOR PRECAST, PRESTRESSED, CONCRETE PILES	
	AASHTO (1994) Recommendations
Design Stresses	$0.33 f'_c - 0.27 f_{pe}$ (on gross concrete area) f'_c minimum of 34.5 MPa f_{pe} generally > 5 MPa
Driving Stresses	Compression Limit $< 0.85 f'_c - f_{pe}$ (on gross concrete area) Tension Limit (1) $< 0.25 \sqrt{f'_c} + f_{pe}$ (on gross concrete area) Tension Limit (2) $< f_{pe}$ (on gross concrete area) (1) - Normal Environments (2) - Severe Corrosive Environments Note: f'_c and f_{pe} must be in MPa.

11.3.5 Conventionally Reinforced Concrete Piles

a. Design Stresses

Table 11-5 summarizes the AASHTO recommended design and driving stresses for axially loaded reinforced concrete piles in terms of the concrete compression strength, f'_c , and the yield strength of the reinforcing steel, f_y . The recommended maximum allowable design stress is limited to $0.33 f'_c$ on the gross cross sectional area of the concrete. The concrete must have a minimum 28 day compression strength of 34.5 MPa.

b. Driving Stresses

AASHTO specifications limit the maximum allowable compression driving stress to $0.85 f'_c$ and the maximum tension driving stress to $0.70 f_y$.

Control of driving stresses is particularly important when driving reinforced concrete piles at high driving stress levels while penetrating through dense soil layers into underlying weaker soils.

TABLE 11-5 MAXIMUM ALLOWABLE STRESSES FOR CONVENTIONALLY REINFORCED CONCRETE PILES	
AASHTO (1994) Recommendations	
Design Stresses	$0.33 f'_c$ (on gross concrete area) f'_c minimum of 34.5 MPa
Driving Stresses	Compression Limit $< 0.85 f'_c$ Tension Limit $< 0.70 f_y$ (of steel reinforcement)

11.3.6 Timber Piles

a. Design Stresses

Table 11-6 summarizes AASHTO recommended design and driving stresses for axially loaded timber piles in terms of the maximum allowable design stress in compression parallel to the grain, σ_a . This value varies depending upon the timber species, and for the common species listed in the table below ranges from about 5.5 MPa to 8.3 MPa. The resulting maximum design load is based upon the allowable design stress times the pile toe area.

The engineer can specify species of timber piles but can seldom specify subspecies which have a wide range of strengths. There is a large natural variability of clear wood strength and natural growth imperfections which can also significantly affect wood strength. Therefore, while a high design stress may be allowed, engineering judgement must also be used, taking into account the above factors as well as the installation conditions.

b. Driving Stresses

AASHTO specifications limit maximum allowable compression and tension driving stresses to 3 times the allowable design stress from Table 11-6.

TABLE 11-6 MAXIMUM ALLOWABLE STRESSES FOR TIMBER PILES	
	AASHTO (1994) Recommendations
Design Stresses	5.5 to 8.3 MPa (for pile toe area depending upon species) Southern Pine $\sigma_a = 8.3$ MPa Douglas Fir $\sigma_a = 8.3$ MPa Red Oak $\sigma_a = 7.6$ MPa Eastern Hemlock $\sigma_a = 5.5$ MPa
Driving Stresses	Compression Limit $< 3 \sigma_a$ Tension Limit $< 3 \sigma_a$ σ_a - AASHTO allowable working stress

REFERENCES

American Association of State Highway and Transportation Officials [AASHTO], (1994).
Standard Specifications for Highway Bridges. Fifteenth Edition, Washington, D.C.

12. CONTRACT DOCUMENTS

12.1 OVERVIEW OF PLAN AND SPECIFICATION REQUIREMENTS

Pile foundations generally cannot be inspected after installation. Therefore, construction specifications and control are of prime importance for a successful pile foundation. Preparation of the contract plan details and construction specifications related to piling issues are the responsibility of the foundation designer in cooperation with materials and construction personnel. Project plans should include:

- Location of piles.
- Designation to identify piles.
- Pile cut off elevation.
- Estimated pile toe elevation.
- Minimum pile toe elevation.
- Required pile batter and direction.
- Orientation of H-piles.
- Ultimate pile capacity.
- Location of soil borings.
- Results of subsurface exploration.

It is the designer's responsibility to confirm that plans and specifications have been prepared using compatible language. This is particularly true in defining the required pile capacity, which is an important component of any driven pile specification. Problems can arise when modern dynamic methods, which use ultimate pile capacity, are mixed with specifications written for a dynamic formula that uses allowable pile capacity. For example, plans stating "piles shall be driven to a safe bearing of 1000 kN" may have been suitably worded when construction control was performed with the Engineering News formula, which uses the allowable design load. However, this type of wording with modern dynamic methods creates confusion and could result in piles being driven to only the design load, or to a claim for overdriving. Construction plans should therefore indicate the ultimate pile capacity. This ultimate capacity should include an appropriate factor of safety on the design load as well as the resistances from any unsuitable support layers.

This chapter includes a generic pile specification that was developed with input from State and Federal bridge and geotechnical engineers. The generic specification, originally released in 1985 as FHWA Geotechnical Guideline 13, has been slightly modified and updated as necessary. AASHTO (1994) contains similar specifications without commentary.

The intent of the attached generic specification is to provide designers and highway agencies with a comprehensive driven pile specification. Commentary sections are included where appropriate to explain the reasons behind development of particular sections of the specification and the relationship of the specification requirements to necessary pile design or construction activities. Note that only driven piles are covered by the specification. Other deep foundation types such as drilled shafts require completely different construction controls and should not be included in a driven pile specification.

A good driven pile specification should include the following basic components:

1. Pile Material Details
 - Material type and section.
 - Material grade and strength.
 - Splice details.
 - Toe protection requirement.
 - Coating details.
 - Transportation and handling.

2. Driving System Requirements
 - Hammer.
 - Hammer and pile cushions.
 - Helmet
 - Pile leads.

3. Installation Issues
 - Driving sequence.
 - Pile location tolerances.
 - Pile alignment tolerances.
 - Pile cutoff.
 - Use of followers.
 - Use of jetting.
 - Use of spudding.
 - Predrilling.
 - Pile heave.
 - Pile cap connection.
 - Pile rejection criteria.

4. Capacity Verification
 - Static load testing.
 - Dynamic testing.
 - Wave equation analysis.
 - Dynamic formulas.

5. Basis of Payment
 - Method of measurement.
 - Payment items.

12.2 BACKGROUND AND REASONS FOR SPECIFICATION IMPROVEMENT

Older pile specifications placed the major responsibilities for pile capacity determination on the field staff. Little analysis was done in the design stage to provide accurate estimates of the required pile length to safely support the design load. Nor did many design analyses account for the actual soil resistance which had to be overcome to drive the pile to the estimated length, or the stresses generated in the pile during driving. Older specifications frequently placed the responsibility for determining what pile length to order on the contractor. Delays for reordering additional lengths or splices to reach final penetration requirements were considered incidental to the price bid for the item. This resulted in higher bid prices due to the unknown risks associated with the pile item.

Procedures, equipment, and analysis methods now exist to permit the designer to accurately establish pile section and length for any driving condition. Basic foundation design procedures are routinely followed by nearly all public agencies. Much of this design information is neither reflected in the pile specification of the agency nor utilized by the agencies construction staff. Many agencies perform detailed static analyses to determine pile length, but control the pile length actually installed in the field with the unreliable Engineering News formula. Changes are required in pile specifications to permit the cost effective use of modern construction control methods. The five areas of major change are briefly explained below as well as in commentary sections of the attached driven pile specification.

1. **Ordered Length Replaces Estimated Length:** Public highway agencies should assume responsibility for determining and placing in the contract documents the pile length necessary to safely support the design load. Costs associated with overruns or underruns due to inaccurate length determination should not be borne by the contractor. The attached specification is based on the highway agency performing an adequate subsurface exploration and design analyses to rationally establish pile lengths during the design phase.
2. **Ultimate Pile Capacity Replaces Design Load:** Installation of piling to a predetermined length involves overcoming the design soil resistance, multiplied by the safety factor in suitable pile supporting layers, plus the resistance in any overlying layers unsuitable for long term support. The use of procedures involving design load, such as the Engineering News formula, should be replaced with ultimate load based methods. The ultimate pile load should be based on both the actual resistance to be overcome

to reach the required penetration depth and the confidence in the method of construction control to be used. The attached specification is written in terms of ultimate load.

3. **Increased Emphasis on Approval of Driving Equipment:** The use of properly sized pile driving equipment will practically insure a successful installation of properly designed piles. Conversely, improperly sized pile driving equipment insures a pile project fraught with problems, regardless of how well the pile design was done. Too small a pile hammer results in extremely difficult, time consuming driving. Too large a pile hammer increases the risk of pile damage. The attached specification places great emphasis on a formal approval procedure for the hammer and driving system. This approval procedure is the most significant change to current specifications.
4. **Pile Capacity Control by Modern Methods Instead of Dynamic Formulas:** Good piling practice dictates use of the wave equation and dynamic pile testing to replace the use of dynamic formulas to monitor pile driving on all projects. Continued use of the Engineering News formula can only result in unreliable, costly pile foundations.

Highway agencies need to utilize modern methods in both design and construction control of pile foundations. The wave equation uses ultimate soil resistances, basic soil properties, and calculated pile lengths in conjunction with driving equipment characteristics to determine the necessary pile penetration resistance for the ultimate capacity, as well as the maximum pile stresses during driving. Dynamic pile testing provides a quick, reliable field test supplement and/or alternate to static load testing, as well as a supplement to wave equation analysis. Both methods are detailed in the attached specification, with commentary containing recommended safety factors applied to the pile design load based on the method of construction control selected.

5. **Separation of Payment into Fixed and Variable Cost Items Instead of Lump Sum Costs:** Fair compensation for work performed in pile driving can only be accomplished by recognizing and providing bid items for contract costs which are fixed and contract costs which are variable. The currently popular payment methods used by highway agencies involve lumping fixed and variable costs into a single item. Such lump sum items, with variable contingencies, are recognized as high risk items by contractors who, to avoid a monetary loss, increase the price bid to cover the risk. The attached specification contains a list of bid items which separate the major fixed and variable costs to permit contractors to develop a low risk bid.

12.3 GENERIC DRIVEN PILE SPECIFICATION

<u>SECTION</u>	<u>CONTENTS</u>	<u>PAGE</u>
Section XXX.01	DESCRIPTION	12-7
Section XXX.02	MATERIALS	12-8
Section XXX.03	EQUIPMENT FOR DRIVING PILES	12-8
	A. Pile Hammers	12-8
	B. Approval of Pile Driving Equipment	12-10
	1. Alternate Approval Method	12-15
	C. Drive System Components and Accessories	12-16
	1. Hammer Cushion	12-16
	2. Helmet	12-17
	3. Pile Cushion	12-17
	4. Leads	12-18
	5. Followers	12-18
	6. Jets	12-19
	7. Preboring	12-19
Section XXX.04	CONSTRUCTION METHODS	12-20
	A. Driven Pile Capacity	12-20
	1. Wave Equation	12-20
	2. Dynamic Formula	12-20
	B. Compression Load Tests	12-22
	1. Static Load Tests	12-22
	2. Dynamic Load Tests	12-24
	3. General	12-27
	C. Test Piles (Indicator Piles)	12-28
	D. Ultimate Pile Capacity	12-29
	E. Preparation and Driving	12-30
	1. General	12-30
	2. Preboring	12-30
	3. Location and Alignment Tolerance	12-31
	4. Heaved Piles	12-31
	5. Installation Sequence	12-32
	F. Unsatisfactory Piles	12-32
	G. Splices	12-33
	H. Pile Shoes	12-33
	I. Cutoff Lengths	12-34
Section XXX.05	METHOD OF MEASUREMENT	12-34
	A. Timber, Steel, and Precast Concrete Piles	12-34
	1. Piles Furnished	12-34
	2. Piles Driven	12-34
	B. Cast in Place Pipe or Shell Concrete Piles	12-35
	C. Pile Shoes	12-35
	D. Load Tests	12-35
	E. Splices	12-35
	F. Furnishing Equipment for Driving Piles	12-35
Section XXX.06	BASIS OF PAYMENT	12-36

SECTION XXX.01 DESCRIPTION

This item shall consist of furnishing and driving foundation piles of the type and dimensions designated, including cutting off or building up foundation piles when required. Piling shall conform to and be installed in accordance with these specifications, and at the location, and to the elevation, penetration and/or capacity shown on the plans, or as directed by the Engineer.

The Contractor shall furnish the piles in accordance with an itemized order list which will be furnished by the Engineer, showing the number and length of all piles. When test piles are required, the pile lengths shown on the plans are for estimating purposes only and the actual lengths to be furnished for production piles will be determined by the Engineer after the test piles have been driven. The lengths given in the order list will be based on the lengths which are assumed after cutoff to remain in the completed structure. The Contractor shall, without added compensation, increase the lengths to provide for fresh heading and for such additional length as may be necessary to suit the Contractor's method of operation.

Commentary: *The objective of this specification is to provide criteria by which the Owner can assure that designated piles are properly installed and the Contractor can expect equitable compensation for work performed. The Owner's responsibility is to estimate the pile lengths required to safely support the design load. Pile lengths should be estimated based on subsurface explorations, testing and analysis which are completed during the design phase. Pile contractors who enter contractual agreements to install piles for an owner should not be held accountable or indirectly penalized for inaccuracies in estimated lengths. The Contractor's responsibility is to provide and install designated piles, undamaged, to the lengths specified by the Owner. This work is usually accomplished within an established framework of restrictions necessary to insure a "good" pile foundation. The price bid for this item of work will reflect the Contractor's estimate of both actual cost to perform the work and perceived risk.*

SECTION XXX.02 MATERIALS

Materials shall meet the requirements in the following Subsections of Section XXX - Materials:

- Portland Cement Concrete
- Reinforcing Steel
- Structural Steel
- Castings for Pile Shoes
- Steel Shells for Cast in Place Piles
- Timber Piles
- Paint / Coatings
- Timber Preservative and Treatment

Commentary: *The appropriate sections of each agency's standard specifications should be included under the XXX.02 Materials Section. A generic materials section cannot be provided herein, considering the vast combinations of materials used in piling operations and the varying control methods used by individual highway departments. The above list contains the common material components. Additions or deletions may be required to this list based on the content of individual agency standard specifications and the pile type specified.*

SECTION XXX.03. EQUIPMENT FOR DRIVING PILES

- A. Pile Hammers. Piles may be driven with air, steam, diesel, or hydraulic hammers. Gravity hammers, if specifically permitted in the contract, shall only be used to drive timber piles. When gravity hammers are permitted, the ram shall weigh between 900 and 1600 kg and the height of drop shall not exceed 4 m. In no case shall the weight of gravity hammers be less than the combined weight of helmet and pile. All gravity hammers shall be equipped with hammer guides to insure concentric impact on the helmet.

The plant and equipment furnished for air/steam hammers shall have sufficient capacity to maintain at the hammer, under working conditions, the volume and pressure specified by the manufacturer. The plant and equipment shall be equipped with accurate pressure gauges which are easily accessible to the Engineer. The weight of the striking parts of air and steam hammers shall not be less than $\frac{1}{3}$ the weight of helmet and pile being driven, and in no case shall the striking parts weigh less than 1250 kg.

Open end (single acting) diesel hammers shall be equipped with a device such as rings on the ram to permit the Engineer to visually determine hammer stroke at all times during pile driving operations. Also, the Contractor shall provide the Engineer a chart from the hammer manufacturer equating stroke and blows per minute for the open-end diesel hammer to be used. Closed end (double acting) diesel hammers shall be equipped with a bounce chamber pressure gauge, in good working order, mounted near ground level so as to be easily read by the Engineer. Also, the Contractor shall provide the Engineer a chart, calibrated to actual hammer performance within 90 days of use, equating bounce chamber pressure to either equivalent energy or stroke for the closed-end diesel hammer to be used.

The power plant for hydraulic hammers shall have sufficient capacity to maintain at the hammer, under working conditions, the volume and pressure specified by the manufacturer. The power plant and equipment shall be equipped with accurate pressure gauges which are easily accessible to the Engineer.

Commentary: *Pile inspectors frequently do not possess adequate knowledge or technical information concerning even the most basic details of the Contractor's hammer. Chapters 22 and 24 provide information on driving equipment and inspection. Highway agencies should also provide pile inspectors with basic manuals such as FHWA/RD-86/160 "The Performance of Pile Driving Systems: "Inspections Manual" or "Inspectors Manual for Pile Foundations" and "A Pile Inspectors Guide to Hammers, Second Edition" available from the Deep Foundation Institute, 120 Charlotte Place, Englewood Cliffs, NJ 07632.*

Non-impact hammers, such as vibratory hammers, or driving aids such as jets, followers and prebored holes shall not be used unless either specifically permitted in writing by the Engineer or stated in the contract documents. When permitted, such equipment shall be used for installing production piles only after the pile toe elevation for the ultimate pile capacity is established by load testing and/or test piles driven with an impact hammer. The Contractor shall perform, at his cost, such load tests and/or extra work required to drive test piles as determined by the Engineer as a condition of approval of the non-impact hammers or driving aids. Installation of production piles with vibratory hammers shall be controlled according to power consumption, rate of penetration, specified toe elevation, or other means acceptable to the Engineer which assure the ultimate pile capacity equals or exceeds the ultimate capacity of the test pile. In addition, one of every ten piles driven with a vibratory hammer shall be restruck with an impact hammer of suitable energy to verify the ultimate pile capacity as in XXX.04(D).

Commentary: *At present no formula exists to reliably predict the capacity of piles driven with vibratory hammers. Until reliable procedures are developed for vibratory installation, special precautions must be taken to insure foundation piles installed with vibratory hammers have both adequate capacity and structural integrity. On critical projects, highway agencies should consider the use of dynamic testing during restrike to substantiate pile capacity and integrity.*

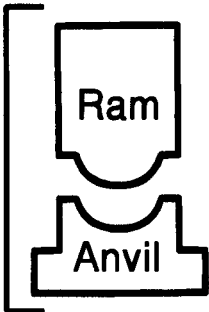
- B. Approval of Pile Driving Equipment. All pile driving equipment furnished by the Contractor shall be subject to the approval of the Engineer. It is the intent of this specification that all pile driving equipment be sized in such a way that the project piles can be driven with reasonable effort to the ordered lengths without damage. Approval of pile driving equipment by the Engineer will be based on wave equation analysis and/or other judgments. In no case shall the driving equipment be transported to the project site until approval of the Engineer is received in writing. Prerequisite to such approval, the Contractor shall submit to the Engineer the necessary pile driving equipment information at least 30 days prior to driving piles. The form which the Contractor shall complete with the above information is shown in Figure 12.1.

Contract No.: _____ Structure Name and/or No.: _____
 Project: _____

 County: _____ Pile Driving Contractor or Subcontractor: _____

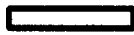
 _____ (Piles driven by)

Hammer Components



Hammer

Manufacturer: _____ Model No.: _____
 Hammer Type: _____ Serial No.: _____
 Manufacturers Maximum Rated Energy: _____ (Joules)
 Stroke at Maximum Rated Energy: _____ (meters)
 Range in Operating Energy: _____ to _____ (Joules)
 Range in Operating Stroke: _____ to _____ (meters)
 Ram Weight: _____ (kg)
 Modifications: _____



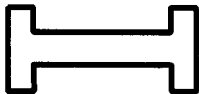
Striker Plate

Weight: _____ (N) Diameter: _____ (mm)
 Thickness: _____ (mm)



Hammer Cushion

Material #1	Material #2 (for Composite Cushion)
Name: _____	Name: _____
Area: _____ (cm ²)	Area: _____ (cm ²)
Thickness/Plate: _____ (mm)	Thickness/Plate: _____ (mm)
No. of Plates: _____	No. of Plates: _____
Total Thickness of Hammer Cushion: _____	



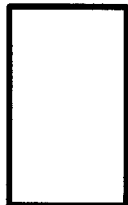
Helmet (Drive Head)

Weight: _____ (kN)



Pile Cushion

Material: _____
 Area: _____ (cm²) Thickness/Sheet: _____ (mm)
 No. of Sheets: _____
 Total Thickness of Pile Cushion: _____ (mm)



Pile

Pile Type: _____
 Wall Thickness: _____ (mm) Taper: _____
 Cross Sectional Area: _____ (cm²) Weight/Meter: _____
 Ordered Length: _____ (m)
 Design Load: _____ (kN)
 Ultimate Pile Capacity: _____ (kN)
 Description of Splice: _____

 Driving Shoe/Closure Plate Description: _____

 Submitted By: _____ Date: _____
 Telephone No.: _____ Fax No.: _____

Figure 12.1 Pile and Driving Equipment Data Form

Commentary: *Use of wave equation analysis for approval of driving equipment can substantially reduce pile driving costs and pile driving claims by checking that the equipment mobilized to the job can drive the pile to the required penetration depth without damage. Public agencies should encourage Contractors to use wave equation analysis to select the optimum hammer for each project. In cases where disputes arise over rejection of pile driving equipment, the Engineer should request the Contractor to submit proof of the adequacy of the pile driving equipment. Such proof should consist of, but not be limited to, a wave equation analysis of the proposed driving equipment performed by a registered professional engineer. All costs of such submissions, if required, shall be the responsibility of the Contractor.*

The pile and driving equipment data form should be submitted for approval even if wave equation analysis will not be used for hammer approval. The approved form should be used by the pile inspector to check the proposed hammer and drive system components are as furnished and are maintained during the driving operation. Few agencies currently supply the pile inspector with any such information on which rational inspection can be based.

The criteria, which the Engineer will use to evaluate the driving equipment from the wave equation results, consists of both the required number of hammer blows per 0.25 meter as well as the pile stresses at the required ultimate pile capacity. The required number of hammer blows indicated by the wave equation at the ultimate pile capacity shall be between 30 and 120 blows per 0.25 meter for the driving equipment to be acceptable.

In addition, for the driving equipment to be acceptable the pile stresses which are indicated by the wave equation to be generated by the driving equipment shall not exceed allowable values. For steel piles, maximum compressive driving stresses shall not exceed 90% of the minimum yield strength of the pile material. For prestressed concrete piles in normal environments, tensile stresses shall not exceed 0.25 multiplied by the square root of the concrete compressive strength, f'_c plus the effective prestress value, f_{pe} , i.e. $(0.25 \sqrt{f'_c} + f_{pe})$. Both f'_c and f_{pe} in this equation must be in MPa. For prestressed concrete piles in severe corrosive environments, tensile stresses shall not exceed f_{pe} . Compressive stresses for

prestressed concrete piles shall not exceed 85% of the compressive strength minus the effective prestress value, *i.e.* $(0.85 f'_c - f_{pe})$. For timber piles, the compressive driving stress shall not exceed three times the allowable static design strength listed on the plans. These criteria will be used in evaluating wave equation results to determine acceptability of the Contractor's proposed driving system.

The Contractor will be notified of the acceptance or rejection of the driving system within 14 calendar days of the Engineer's receipt of the Pile and Driving Equipment Data Form. If the wave equation analyses show that either pile damage or inability to drive the pile with a reasonable driving resistance to the desired ultimate capacity will result from the Contractor's proposed equipment or methods, the Contractor shall modify or replace the proposed methods or equipment at his expense until subsequent wave equation analyses indicate the piles can be reasonably driven to the desired ultimate capacity, without damage. The Engineer will notify the Contractor of the acceptance or rejection of the revised driving system within 7 calendar days of receipt of a revised Pile and Driving Equipment Data Form.

During pile driving operations, the Contractor shall use the approved system. No variations in the driving system will be permitted without the Engineer's written approval. Any change in the driving system will only be considered after the Contractor has submitted the necessary information for a revised wave equation analysis. The Contractor will be notified of the acceptance or rejection of the driving system changes within 7 calendar days of the Engineer's receipt of the requested change. The time required for submission, review, and approval of a revised driving system shall not constitute the basis for a contract time extension to the Contractor.

Commentary: *The ultimate pile capacity during driving is the soil resistance which must be overcome (including resistance from unsuitable layers and scour zone soils) to reach the pile penetration depth where the design load can be obtained with an acceptable safety factor. The safety factor selected will depend on design factors, such as quantity of subsurface information and geotechnical analysis, as well as construction factors such as the use of load tests, wave equation or dynamic formula to determine pile capacity. When proper foundation exploration procedures and static analyses such as those described in this manual are employed, the*

following safety factors on design load may be used, based on the pile construction control procedures specified:

<u>Construction Control Method</u>	<u>Factor of Safety</u>
Static load test with wave equation analysis	2.00
Dynamic testing with wave equation analysis	2.25
Indicator piles with wave equation analysis	2.50
Wave equation analysis	2.75
Gates dynamic formula	3.50

The ultimate pile capacity during driving is affected by:

1. The resistance in unsuitable soil layers overlying suitable support layers,
2. Temporary loss or increase in soil strength due to driving operations.
3. Pile installation methods which alter the in place soil resistance such as jetting, preboring, etc.

The designer must estimate the ultimate pile capacity to be encountered during driving if pile driving resistance is to be used to determine pile capacity. Only on the most routine pile projects will the ultimate pile capacity be equal to the pile design load multiplied by the design safety factor. More typically, piles are used to penetrate upper soil layers which are unsuitable for load support due to either poor soil characteristics, or future loss of load support by scour or erosion. In such cases the resistance in unsuitable layers is not considered in determining the pile penetration necessary to support the design load at the appropriate safety factor. However, the estimated ultimate pile capacity to be encountered during driving must include the resistance to be encountered in penetrating those unsuitable layers, in addition to the design load multiplied by the safety factor. This ultimate pile capacity must be shown on the contract documents to permit the Contractor to properly size the driving equipment and the Engineer to judge the acceptability of the Contractor's driving equipment. Optimum pile installation generally occurs when the ultimate pile capacity is achieved at a driving resistance near the point of maximum curvature (usually

60-100 blows per 0.25 meter) of the wave equation bearing graph. Larger driving resistances result in negligible pile penetration per blow and generally inefficient driving conditions. Excessive driving resistances can also result in damage to the pile or the driving system.

1. **Alternate Approval Method:** An alternate method of driving equipment approval will be used when either the contract documents contain a provision that wave equation analysis will not be used for approval of driving equipment. The alternate approval method requires that the energy of the driving equipment submitted for approval on the Pile and Driving Equipment Data form, be rated by the manufacturer at or above an appropriate minimum energy level for the ultimate pile capacity shown on the plans. The minimum energy requirements are as follows:

TABLE 12-1 ALTERNATE APPROVAL METHOD Minimum Pile Hammer Requirements	
Ultimate Pile Capacity (kN)	Minimum Manufacturers Rated Hammer Energy (Joules)*
800 and under	----
800 to 1350	----
1351 to 1850	----
1851 to 2400	----
2401 to 2650	----
2650 and over	----

* Previously published tables which included specific values were based on assumptions which might not be appropriate for local conditions and were subject to misinterpretation.

Commentary: *A table of the minimum rated hammer energy vs. ultimate pile capacity should be developed using wave equation analyses of commonly available driving systems for the pile types, pile lengths, and pile loads routinely used by the specific agency. These analyses should model the typical soil and pile installation conditions. The wave equation results should be evaluated for driving stress levels and driving resistances to determine which hammer energies are too large (driving stress problems*

or driving resistances at ultimate capacity less than 30 blows per 0.25 meter) and which energies are too small (driving resistances at ultimate capacity greater than 120 blows per 0.25 meter).

Once the specific table of energy values has been developed, it should only be considered for routine projects in uniform soil conditions or when the agency is in the process of phasing the wave equation analysis into standard use. Projects involving long piles or large ultimate pile capacities relative to the design load (such as scour piles or piles to be driven through embankments) should use job specific wave equation analysis to establish minimum driving equipment requirements. Piles to rock should also be evaluated by wave equation analysis to reduce the risk of pile damage from too large a hammer.

During pile driving operations, the Contractor shall use the approved system. If the Engineer determines the Contractor's hammer is unable to transfer sufficient energy to the pile, the hammer shall be removed from service until repaired to the satisfaction of the Engineer. No variations in the driving system will be permitted without the Engineer's written approval. Any changes in the driving system will be considered only after the Contractor has submitted a new Pile and Driving Equipment Data form. The Contractor will be notified of the acceptance or rejection of the proposed change in driving equipment within 7 calendar days of the Engineer's receipt of the form.

C. Drive System Components and Accessories

1. **Hammer Cushion:** Impact pile driving equipment designed to be used with a hammer cushion shall be equipped with a suitable thickness of hammer cushion material to prevent damage to the hammer or pile and to insure uniform driving behavior. Hammer cushions shall be made of durable manufactured materials, provided in accordance with the hammer manufacturer's guidelines. Wood, wire rope, and asbestos hammer cushions are specifically disallowed and shall not be used. A striker plate as recommended by the hammer manufacturer shall be placed on the hammer cushion to insure uniform compression of the cushion material. The hammer cushion shall be removed from the helmet and inspected in the presence of the Engineer when beginning pile driving at each structure or after each 100 hours of pile driving, whichever is less. Any reduction of hammer

cushion thickness exceeding 25% of the original thickness shall be replaced by the Contractor before driving is permitted to continue.

Commentary: *For hammers requiring cushion material, mandatory use of a durable hammer cushion material which will retain uniform properties during driving is necessary to accurately relate driving resistance to pile capacity. Non-durable materials which deteriorate during driving cause erratic estimates of pile capacity and, if allowed to dissolve, result in damage to the pile or driving system.*

- 2. Helmet:** Piles driven with impact hammers require an adequate helmet or drive head to distribute the hammer blow to the pile head. The helmet shall be axially aligned with the hammer and the pile. The helmet shall be guided by the leads and not be free-swinging. The helmet shall fit around the pile head in such a manner as to prevent transfer of torsional forces during driving, while maintaining proper alignment of hammer and pile.

For steel and timber piling, the pile heads shall be cut squarely and a helmet, as recommended by the hammer manufacturer, shall be provided to hold the axis of the pile in line with the axis of the hammer.

For precast concrete and prestressed concrete piles, the pile head shall be plane and perpendicular to the longitudinal axis of the pile to prevent eccentric impacts from the helmet.

For special types of piles, appropriate helmets, mandrels or other devices shall be provided in accordance with the manufacturer's recommendations so that the piles may be driven without damage.

- 3. Pile Cushion:** The heads of concrete piles shall each be protected by a pile cushion. Pile cushions shall be made of plywood, hardwood, or composite plywood and hardwood materials. The minimum pile cushion thickness placed on the pile head prior to driving shall not be less than 100 mm. A new pile cushion shall be provided for each pile. In addition the pile cushion shall be replaced if, during the driving of any pile, the cushion is compressed more than one-half the original thickness or it begins to burn. The pile cushion dimensions shall match the cross sectional area of the pile top. The use of manufactured

pile cushion materials in lieu of a wood pile cushion shall be evaluated on a case by case basis.

Commentary: *A pile cushion is only needed for the protection of concrete piles. If the wave equation analysis of the Contractor's hammer indicates tension stresses exceed specification limits, the pile cushion may need to be substantially thicker than 100 mm. Pile cushion thicknesses up to 460 mm have been used to mitigate tension stresses. Compressive stresses at the pile head can be controlled with a relatively thin pile cushion. However, wood pile cushions may become overly compressed and hard after about 1000 hammer blows. The physical characteristics of manufactured pile cushion materials should be determined by standard test procedures such as the Deep Foundations Institute standard "Testing of Pile Driving Cushion Material".*

4. **Leads:** Piles shall be supported in line and position with leads while being driven. Pile driver leads shall be constructed in a manner that affords freedom of movement of the hammer while maintaining alignment of the hammer and the pile to insure concentric impact for each blow. Leads may be either fixed or swinging type. Swinging leads, when used, shall be fitted with a pile gate at the bottom of the leads and, in the case of batter piles, a horizontal brace may be required between the crane and the leads. The pile section being driven shall not extend above the leads. The leads shall be adequately embedded in the ground or the pile constrained in a structural frame such as a template to maintain alignment. The leads shall be of sufficient length to make the use of a follower unnecessary, and shall be so designed as to permit proper alignment of batter piles.
5. **Followers:** Followers shall only be used when approved in writing by the Engineer, or when specifically stated in the contract documents. In cases where a follower is permitted, the first pile in each bent and every tenth pile driven thereafter shall be driven full length without a follower, to determine that adequate pile penetration is being attained to develop the ultimate pile capacity.

The follower and pile shall be held and maintained in equal and proper alignment during driving. The follower shall be of such material and dimensions to permit the piles to be driven to the penetration depth determined necessary

from the driving of the full length piles. The final position and alignment of the first two piles installed with followers in each substructure unit shall be verified to be in accordance with the location tolerances in Section XXX.04(E) before additional piles are installed.

Commentary: *The use of a follower often causes substantial and erratic reductions in the hammer energy transmitted to the pile due to the follower flexibility, poor connection to the pile head, frequent misalignment, etc. Reliable correlations of driving resistance with ultimate pile capacity are very difficult when followers are used. Severe problems with pile alignment and location frequently occur when driving batter piles with a follower in a cofferdam unless a multi-tier template is used.*

6. **Jets:** Jetting shall only be permitted if approved in writing by the Engineer or when specifically stated in the contract documents. When jetting is not required in the contract documents, but approved after the Contractor's request, the Contractor shall determine the number of jets and the volume and pressure of water at the jet nozzles necessary to freely erode the material adjacent to the pile without affecting the lateral stability of the final in place pile. The Contractor shall be responsible for all damage to the site caused by unapproved or improper jetting operations. When jetting is specifically required in the contract documents, the jetting plant shall have sufficient capacity to deliver at all times a pressure equivalent to at least 700 kPa at two 19 mm jet nozzles. In either case, unless otherwise indicated by the Engineer, jet pipes shall be removed when the pile toe is a minimum of 1.5 m above prescribed toe elevation and the pile shall be driven to the required ultimate pile capacity with an impact hammer. Also, the Contractor shall control, treat if necessary, and dispose of all jet water in a manner satisfactory to the Engineer.
7. **Preboring:** When stated in the contract documents, the Contractor shall prebore holes at pile locations to the depths shown on the plans. Prebored holes shall be of a size smaller than the diameter or diagonal of the pile cross section that is sufficient to allow penetration of the pile to the specified depth. If subsurface obstructions, such as boulders or rock layers, are encountered, the hole diameter may be increased to the least dimension which is adequate for pile installation. Any void space remaining around the pile after completion of driving shall be filled with sand or other approved material. The use of spuds,

a short strong driven member which is removed to make a hole for inserting a pile, shall not be permitted in lieu of preboring.

SECTION XXX.04 CONSTRUCTION METHODS

A. Driven Pile Capacity

1. **Wave Equation:** The ultimate pile capacity shall be determined by the Engineer, based on a wave equation analysis. Piles shall be driven with the approved driving equipment to the ordered length or other lengths necessary to obtain the required ultimate pile capacity. Jetting or other methods to facilitate pile penetration shall not be used unless specifically permitted either in the contract documents or approved by the Engineer after a revised driving resistance is established from the wave equation analysis. Adequate pile penetration shall be considered to be obtained when the specified wave equation resistance criteria is achieved within 1.5 m of the pile toe elevation, based on ordered length. Piles not achieving the specified resistance within these limits shall be driven to penetrations established by the Engineer.
2. **Dynamic Formula:** The ultimate pile capacity will only be determined by dynamic formula if either the contract documents contain a provision that dynamic formula shall be used or the Engineer approves dynamic formula use. In such cases, piles shall be driven to a penetration depth necessary to obtain the ultimate pile capacity according to the following formula:

$$R_u = [7\sqrt{E_r} \log(10N_b)] - 550$$

Where: R_u = the ultimate pile capacity (kN).

E_r = the manufacturer's rated hammer energy (Joules) at the **field observed ram stroke**.

$\log(10N_b)$ = logarithm to the base 10 of the quantity 10 multiplied by N_b , the number of hammer blows per 25 mm at final penetration.

The number of hammer blows per 0.25 meter of pile penetration required to obtain the ultimate pile capacity shall be calculated as follows:

$$N_{qm} = 10(10^x)$$

Where: $x = [(R_u + 550)/(7\sqrt{E_r})] - 1$

Commentary: *Driven pile capacity should be monitored in terms of ultimate pile capacity; not design load. The driving resistance at any penetration depth reflects the total capacity mobilized by the pile. This total capacity may include capacity mobilized temporarily in soil deposits unsuited for bearing, as well as suitable bearing layers. Therefore, the driving resistance should be established for the ultimate pile capacity that must be overcome in order to reach anticipated pile penetration depth. These ultimate capacities are determined by static analysis procedures. In the case of piles to be driven to a specified minimum pile toe elevation, the ultimate pile capacity must be computed by static analysis to include the capacity of all soil layers penetrated by the pile above the minimum pile toe elevation as well as the end bearing resistance at that depth. Also, the ultimate pile capacity is directly related to the maximum pile driving stress during installation. This stress is more critical than the stress caused after installation by the design load.*

Good piling practices dictate use of the wave equation in place of dynamic formulas to monitor driven pile capacity for all projects. The driving resistance and maximum pile stresses should be determined for the ultimate pile capacity. Use of the wave equation will permit the use of lower safety factors on the design load and the minimum permissible pile section to resist the driving force. This will result in significant cost reductions due to savings in pile lengths and use of smaller pile sections. FHWA recommends that all agencies phase in wave equation analysis with an ultimate goal of eliminating use of dynamic formulas on all pile projects. Wave equation analysis is discussed in greater detail in Chapter 17 of this manual.

The Engineering News formula is recognized to be the least accurate and least consistent of all dynamic formula, yet the vast majority of all States continue to use this formula. The Washington State DOT study WA-RD-163.1 "Comparison of Methods for Estimating Pile Capacity" (1988) found that the Hiley, Gates, Janbu, and Pacific Coast Uniform Building code formulas all provide relatively more dependable results than the Engineering News formula. The dynamic formula contained in this specification is the Gates formula which has been revised to reflect the ultimate pile capacity in kilonewtons. The formula in this specification already includes the 80% efficiency factor on the rated energy, E, recommended by Gates.

The Gates formula was also studied by Olson and Flaate (1967) and found to be the most consistent of the dynamic formulas studied. However, all dynamic formulas are not suited for soft cohesive soils. Engineers planning to use dynamic formula should carefully read these references to comprehend the limitations involved with their use. A design safety factor of 3.5 is recommended when using the Gates formula to determine the safe design load, i.e., if a design load of 1000 kN is required in the bearing layer, then an ultimate pile capacity of 3500 kN should be used in the Gates formula to determine the necessary driving resistance. The formula was selected for its relative accuracy, consistency and simplicity of use. However, the top priority for highway agencies should be to change from dynamic formulas to wave equation analysis.

B. Compression Load Tests

1. **Static Load Tests:** Compression load tests shall be performed by procedures set forth in ASTM D-1143 using the quick load test method, except that the test shall be taken to plunging failure or the capacity of the loading system. Testing equipment and measuring systems shall conform to ASTM D-1143, except that the loading system shall be capable of applying 150% of the ultimate pile capacity or 9000 kN, whichever is less, and that a load cell and spherical bearing plate shall be used. The Contractor shall submit to the Engineer for approval detailed plans prepared by a licensed professional engineer of the proposed loading apparatus. The apparatus shall be constructed to allow the

various increments of the load to be placed gradually, without causing vibration to the test pile. When the approved method requires the use of tension (reaction) piles, the tension piles, when feasible, shall be of the same type and diameter as the production piles, and shall be driven in the location of permanent piles except that timber or tapered piles installed in permanent locations shall not be used as tension piles.

The design load shall be defined as 50% of the failure load. The failure load for the pile shall be defined as follows: for piles 610 mm or less in diameter or width, the failure load of a pile tested under axial compressive load is that load which produces a settlement at failure of the pile head equal to:

$$s_f = \Delta + (4.0 + 0.008b)$$

Where: s_f = Settlement at failure in mm.

b = Pile diameter or width in mm.

Δ = Elastic deformation of total pile length in mm.

For piles greater than 610 mm in diameter or width:

$$s_f = \Delta + \frac{b}{30}$$

The top elevation of the test pile shall be determined immediately after driving and again just before load testing to check for heave. Any pile which heaves more than 6 mm shall be redriven or jacked to the original elevation prior to testing. Unless otherwise specified in the contract, a minimum 3-day waiting period shall be observed between the driving of any anchor piles or the load test pile and the commencement of the load test.

Commentary: *The pile capacity may increase (soil setup) or decrease (relaxation) after the end of driving. Therefore, it is essential that static load testing be performed after equilibrium conditions in the soil have re-established. Static load tests performed before equilibrium conditions have re-*

established will underestimate the long term pile capacity in soil setup conditions and overestimate the long term capacity in relaxation cases. For piles in clays, specifications should require at least 2 weeks or longer to elapse between driving and load testing. In sandy silts and sands, 5 days to a week is usually sufficient. Load testing of piles driven into shales should also be delayed for at least 2 weeks after driving. Additional discussion on time dependent changes in pile capacity may be found in Section 9.10.1.

Each static load test pile should be determining the load transferred to the pile toe. Instrumentation commonly consists of strain gages and/or telltale rods mounted at varying depths from the pile toe. Also, a load cell and spherical bearing plate should be mounted between the load frame and the pile head to verify the readings from the hydraulic jack pressure gauge. Due to jack ram friction, loads indicated by a jack pressure gauge are commonly 10% to 20% higher than the actual load imposed on the pile. Last, after completion of a load test on a non production pile, the static test pile should be pulled and checked for damage. The examination of the extracted pile will determine driving damage and its effect on capacity.

When static load tests are used to control production pile driving, the time required to analyze the load test results and establish driving criteria should be specified so that the delay time to the contractor is clearly identified. Static load testing is discussed in greater detail in Chapter 19 of this manual. A more detailed specification for static load testing may be found in FHWA-SA-91-042, Static Testing of Deep Foundations.

- 2. Dynamic Load Tests:** Dynamic measurements following procedures set forth in ASTM D-4945 will be taken by the Engineer during the driving of piles designated as dynamic load test piles.

Commentary: *When static load tests are specified, dynamic load tests are recommended to be performed on at least half the reaction piles prior to driving the static load test pile. The dynamic test results are used both to verify that the desired ultimate pile capacity can be attained at the proposed estimated static load test pile penetration depth and to fine*

tune the dynamic test equipment for site soil conditions. Dynamic monitoring of the load test pile during both initial driving and during restriking after completion of the static load test are also recommended. This allows correlation of static test results with dynamic test results. Signal matching techniques using the dynamic test data can further quantify dynamic soil parameters such as soil quake and damping for the site. When dynamic tests are specified on production piles, the first pile driven in each substructure foundation is recommended to be tested. Where uniform soil conditions exist across a site, the number of dynamic tests may be reduced based on recommendations from the agency's geotechnical engineer.

This section of the specifications applies to the Contractor's activities as they relate to the dynamic testing of piles. If the dynamic tests are to be performed by an independent firm and not transportation department personnel, an additional specification section detailing analysis and reporting requirements must be added. Dynamic tests are discussed in greater detail in Chapter 18 of this manual.

Prior to placement in the leads, the Contractor shall make each designated concrete and/or timber pile available for taking of wave speed measurements and for predrilling the required instrument attachment holes. Predriving wave speed measurements will not be required for steel piles. When wave speed measurements are made, the piling shall be in a horizontal position and not in contact with other piling. The Engineer will furnish the equipment, materials, and labor necessary for drilling holes in the piles for mounting the instruments. The instruments will be attached near the head of the pile with bolts placed in masonry anchors for the concrete piles, or through drilled holes on the steel piles, or with wood screws for timber piles.

The Contractor shall provide the Engineer reasonable means of access to the pile for attaching instruments after the pile is placed in the leads. A platform with minimum size of 1.2 x 1.2 m (1.4 sq. m) designed to be raised to the top of the pile while the pile is located in the leads shall be provided by the Contractor. It is estimated that the Engineer will need approximately 1 hour per pile to install the dynamic test equipment.

The Contractor shall furnish electric power for the dynamic test equipment. The power supply at the outlet shall be 10 amp, 115 volt, 55-60 cycle, A.C. only. Field generators used as the power source shall be equipped with functioning meters for monitoring voltage and frequency levels.

The Contractor shall furnish a shelter to protect the dynamic test equipment from the elements. The shelter shall have a minimum floor size of 2.5 x 2.5 m (6.2 sq. m) and minimum roof height of 2 m. The inside temperature of the shelter shall be maintained above 45 degrees. The shelter shall be located within 15 m of the test location.

With the dynamic testing equipment attached, the Contractor shall drive the pile to the design penetration depth or to a depth determined by the Engineer. The Engineer will use the ultimate pile capacity estimates at the time of driving and/or restriking from dynamic test methods to determine the required pile penetration depth for the ultimate pile capacity. The stresses in the piles will be monitored during driving with the dynamic test equipment to ensure that the values determined do not exceed the values in Section XXX.03(B). If necessary, the Contractor shall reduce the driving energy transmitted to the pile by using additional cushions or reducing the energy output of the hammer in order to maintain stresses below the values in Section XXX.03(B). If non-axial driving is indicated by dynamic test equipment measurements, the Contractor shall immediately realign the driving system.

The Contractor shall wait up to 24 hours (or a longer duration specified in the contract documents) and restrike the dynamic load test pile with the dynamic testing instruments attached. It is estimated that the Engineer will require approximately ½ hour to reattach the instruments. A cold hammer shall not be used for the restrike. The hammer shall be warmed up before restrike begins by applying at least 20 blows to another pile. The maximum amount of penetration required during restrike shall be 150 mm, or the maximum total number of hammer blows required will be 50, whichever occurs first. After restriking, the Engineer will either provide the cutoff elevation or specify additional pile penetration and testing.

Commentary: *For purposes of measurement and payment one dynamic test includes all data collected on one pile during both the initial pile driving and a*

restrike done up to 24 hours after the initial driving. Additional long term restrikes should be paid for as separate tests unless the restrike schedule is specifically stated in the dynamic test specification.

The restrike time and frequency should be clearly stated in the specifications and should be based on the time dependent strength change characteristics of the soil. The following restrike durations are often used:

<u>Soil Type</u>	<u>Time Delay Until Restrike</u>
Clean Sands	1 Day
Silty Sands	2 Days
Sandy Silts	3-5 Days
Silty Clays	7-14 Days*
Shales	10-14 Days*

**Longer times sometimes required.*

The restrike time interval is particularly important when dynamic testing is used for construction control. Specifying too short of a restrike time for friction piles in fine grained deposits may result in pile length overruns. However, it is sometimes difficult for long term restrikes to be accommodated in the construction schedule. In these cases, multiple restrikes are sometimes specified on selected piles with shorter term restrikes at other locations.

The time necessary to analyze the dynamic test results and provide driving criteria to the contractor once restrikes are completed should also be stated in the specifications. This is important when the testing is done by agency personnel or their consultants as well as when the testing firm is retained by the contractor. In cases where the testing is retained by the contractor, the time required for the agency to review the test results and provide driving criteria should be specified relative to the agency's receiving the test results.

- 3. General:** On completion of the load testing, any test or anchor piling not a part of the finished structure shall be removed or cut off at least 300 mm below either

the bottom of footing or the finished ground elevation, if not located within the footing area.

- C. Test Piles (Indicator Piles). Test piles shall be driven when shown on the plans at the locations and to the penetration depths specified by the Engineer. All test piles shall be driven with impact hammers unless specifically stated otherwise in the plans. In general, the specified length of test piles will be greater than the estimated length of production piles in order to provide for variation in soil conditions. The driving equipment used for driving test piles shall be identical to that which the Contractor proposes to use on the production piling. Approval of driving equipment shall conform with the requirements of these Specifications. The Contractor shall excavate the ground at each test pile to the elevation of the bottom of the footing before the pile is driven.

Test piles shall be driven to a driving resistance established by the Engineer at the estimated pile toe elevation. Test piles which do not attain the driving resistance specified above at a depth of 0.25 meter above the estimated pile toe elevation shown on the plans shall be allowed to "set up" for 12 to 24 hours, or as directed by the Engineer, before being redriven. A cold hammer shall not be used for redrive. The hammer shall be warmed up before driving begins by applying at least 20 blows to another pile. If the specified driving resistance is not attained on redriving, the Engineer may direct the Contractor to drive a portion or all of the remaining test pile length and repeat the "set up" redrive procedure. Test piles driven to plan grade and not having the driving resistance required, shall be spliced and driven until the required capacity is obtained.

A record of driving of the test pile will be prepared by the Engineer, including the number of hammer blows per 0.25 meter for the entire driven length, the as-driven length of the test pile, cutoff elevation, penetration in ground, and any other pertinent information. The Contractor shall provide the information listed in Figure 12.1 of Section XXX.03(B) to the Engineer for inclusion in the record. If a redrive is necessary, the Engineer will record the number of hammer blows per 25 mm of pile movement for the first 0.25 meter of redrive. The Contractor shall not order piling to be used in the permanent structure until test pile data has been reviewed and pile order lengths are authorized by the Engineer. The Engineer will provide the pile order list within 7 calendar days after completion of all test pile driving specified in the contract documents.

Commentary: *Test piles are particularly recommended on projects where: 1) large quantities or long length of friction piling are estimated, even if load tests are to be used at adjacent footings; 2) large ultimate soil resistance is expected in relation to the design load and, 3) where concrete piles are used.*

- D. Ultimate Pile Capacity. Piles shall be driven by the Contractor to the penetration depth shown on the plans or to a greater depth if necessary to obtain the ultimate pile capacity. The ultimate pile capacity shall be determined by the Engineer based on one of the methods listed in Section XXX.04(A).

Jetting or other methods shall not be used to facilitate pile penetration unless specifically permitted in the contract plans or in writing by the Engineer. The ultimate pile capacity of jetted piles shall be based on driving resistances recorded during impact driving after the jet pipes have been removed. Jetted piles not attaining the ultimate pile capacity at the ordered length shall be spliced, as required, at the Contractor's cost, and driven with an impact hammer until the ultimate pile capacity is achieved, as indicated by the appropriate criteria in Section XXX.04(A).

The ultimate pile capacity of piles driven with followers shall only be considered acceptable when the follower driven piles attain the same pile toe elevation as the full length piles driven without followers, installed per Section XXX.03(C), which attained the required ultimate pile capacity.

The ultimate pile capacity of piles driven with vibratory hammers shall be based on the driving resistance recorded during impact driving after the vibratory equipment has been removed from the first pile in each group of 10 piles. Vibrated piles not attaining the ultimate pile capacity at the ordered length shall be spliced, as required, at the Contractor's cost, and driven with an impact hammer until the ultimate pile capacity is achieved, as indicated by the appropriate criteria in Section XXX.04(A). When the ultimate pile capacity is attained, the remaining 9 piles shall be installed to similar depths with similar vibratory hammer power consumption and rate of penetration as the first pile.

E. Preparation and Driving

1. **General:** The heads of all piles shall be plane and perpendicular to the longitudinal axis of the pile before the helmet is attached. The heads of all concrete piles shall be protected with a pile cushion as described in Section XXX.03(C).

During pile driving, the pile cushion shall be changed as described in Section XXX.03(C) before excessive compression or damage takes place. Approval of a pile hammer relative to driving stress damage shall not relieve the Contractor of responsibility for piles damaged because of misalignment of the leads, failure of cushion materials, failure of splices, malfunctioning of the pile hammer, or other improper construction methods. Piles damaged for such reasons shall be rejected and replaced at the Contractor's expense when the Engineer determines that the damage impairs the strength of the pile.

2. **Preboring:** Augering, wet-rotary drilling, or other methods of preboring shall be used only when approved by the Engineer or in the same manner as used for any indicator piles or load test piles. When permitted, such procedures shall be carried out in a manner which will not impair the capacity of the piles already in place or the safety of existing adjacent structures.

Except for end bearing piles, preboring shall be stopped at least 1.5 m above the pile toe elevation, determined from the ordered length and the pile shall be driven with an impact hammer to a driving resistance specified by the Engineer. Where piles are to be end-bearing on rock or hardpan, preboring may be carried to the surface of the rock or hardpan, and the piles shall be restruck with an impact hammer to insure proper seating.

If the Engineer determines that preboring has disturbed the capacities of previously installed piles, those piles that have been disturbed shall be restored to conditions meeting the requirements of this specification by re-driving or by other methods acceptable to the Engineer. Re-driving or other remedial measures shall be instituted after the preboring operations in the area have been completed. The Contractor shall be responsible for the costs of any necessary remedial measures, unless the preboring method was specifically included in the contract documents and properly executed by the Contractor.

3. **Location and Alignment Tolerance:** The pile head at cutoff elevation shall be within 50 mm of plan locations for bent caps supported by piles, and shall be within 150 mm of plan locations for all piles capped below final grade. The as-driven centroid of load of any pile group at cutoff elevation shall be within 5% of the plan location of the designed centroid of load. No pile shall be nearer than 100 mm from any edge of the cap. Any increase in size of cap to meet this edge distance requirement shall be at the Contractor's expense.

Piles shall be installed so that the axial alignment of the top 3 m of the pile is within 2% of the specified alignment. For piles that cannot be inspected internally after installation, an alignment check shall be made before installing the last 1.5 m of pile, or after installation is completed provided the exposed portion of the pile is not less than 1.5 m in length. The Engineer may require that driving be stopped in order to check the pile alignment. Pulling laterally on piles to correct misalignment, or splicing a properly aligned section on a misaligned section shall not be permitted.

If the location and/or alignment tolerances specified in the preceding paragraphs are exceeded, the extent of overloading shall be evaluated by the Engineer. If in the judgement of the Engineer, corrective measures are necessary, suitable measures shall be designed and constructed by the Contractor. The Contractor shall bear all costs, including delays, associated with the corrective action.

Commentary: *Conditions exist, such as soft overburden soils directly overlying a sloping bedrock, where final pile location and/or alignment may be beyond the contractor's control. These cases should be identified during the design stage with specifications tailored to meet the site and project requirements.*

4. **Heaved Piles:** Level readings to measure pile heave after driving shall be made by the Engineer at the start of pile driving operations and shall continue until the Engineer determines that such checking is no longer required. Level readings shall be taken immediately after the pile has been driven and again after piles within a radius of 5 m have been driven. If pile heave is observed, accurate level readings referenced to a fixed datum shall be taken by the Engineer on all piles immediately after installation and periodically thereafter as adjacent piles are driven to determine the pile heave range. All piles that have been heaved

more than 6 mm shall be redriven at the Contractor's cost, to the required resistance or penetration. Concrete shall not be placed in pile casings until pile driving has progressed beyond a radius of 5 m from the pile to be concreted. If pile heave is detected for pipe or shell piles which have been filled with concrete, the piles shall be redriven to original position after the concrete has obtained sufficient strength and a proper hammer-pile cushion system, satisfactory to the Engineer, is used.

5. **Installation Sequence:** The order of placing individual piles in pile groups shall be either starting from the center of the group and proceeding outwards in both directions, or starting at the outside row and proceeding progressively across the group.

F. **Unsatisfactory Piles.** The method used in driving piles shall not subject the piles to excessive or undue abuse producing crushing and spalling of concrete, injurious splitting, splintering, and brooming of the wood, or deformation of the steel. Misaligned piles shall not be forced into proper position. Any pile damaged during driving by reason of internal defects, or by improper driving, or driven out of its proper location, or driven below the designated cutoff elevation, shall be corrected by the Contractor, without added compensation, by a method approved by the Engineer.

Commentary: *The following procedures may be used to correct unsatisfactory pile conditions:*

1. *The pile may be withdrawn and replaced by a new and, when necessary, longer pile. In removing piles, jets may be used in conjunction with jacks or other devices for pulling in an effort to remove the whole pile*
2. *A second pile may be driven adjacent to the defective pile.*
3. *The pile may be spliced or built up as otherwise provided herein, or a sufficient portion of the footing extended to properly embed the pile.*
4. *All piles pushed up by the driving of adjacent piles, or by any other cause, shall be redriven.*

Piles which have been bent during installation shall be considered unsatisfactory unless the ultimate capacity is proven by load tests performed at the Contractor's expense. If such tests indicate inadequate capacity, corrective measures as determined by the Engineer shall be taken, such as use of bent piles at reduced capacity, installation of additional piles, strengthening of bent piles, or replacement of bent piles.

A concrete pile will be considered defective if a visible crack, or cracks, appears around the entire periphery of the pile, or if any defect is observed which, as determined by the Engineer, affects the strength or life of the pile.

- G. Splices. Full length piles shall always be used where practical. In no case shall timber piles be spliced. Where splices are unavoidable for steel or concrete piles, their number, locations and details shall be subject to approval of the Engineer. Splices in steel piles and steel pile casings shall be welded in conformance with Section XXX. Splices for cast in place piles shall be watertight. Splices for concrete piles shall be made by the cement dowel method as detailed on the plans unless the Engineer approves alternate splices. Mechanical splices for concrete or steel piles may be approved by the Engineer if the splice can transfer the full pile strength in compression, tension and bending. Shop drawings of any proposed mechanical splice shall be submitted to the Engineer for approval.
- H. Pile Shoes. Pile shoes of the type and dimensions specified shall be provided and installed when shown on the contract plans. Shoes for timber piles shall be metal and shall be fastened securely to the pile. Timber pile toes shall be carefully shaped to secure an even uniform bearing on the pile shoe. Steel pile shoes shall be fabricated from cast steel conforming to ASTM A 27.

Commentary: *H-pile shoes composed of steel plates welded to the flanges and webs are not recommended because this reinforcement provides neither protection nor increased strength at the critical area of the flange to web connection. Only prefabricated pile shoes made of ASTM A 27 cast steel have been proven reliable. The designer should select and detail on the plans the proper pile shoe to suit the application. Additional information on pile shoes is presented in Chapter 23 of this manual.*

- I. Cutoff Lengths. The pile head of all permanent piles and pile casings shall be cutoff at the elevation shown on the plans or as ordered by the Engineer. All cutoff lengths shall become the property of the Contractor, and shall be removed by the Contractor from the site of the work.

Commentary: *Additional structural details for timber, steel, concrete and cast in place piles should be included by each agency in this driven pile specification, either directly or by reference to appropriate sections of the individual agency's standard specification. Typical items include: timber pile butt treatment and preservative treatment; precast concrete pile reinforcement, forming, casting, curing, and handling; steel pile field painting; cast in place pile details for shell, interior reinforcement and concrete.*

SECTION XXX.05. METHOD OF MEASUREMENT

A. Timber, Steel, and Precast Concrete Piles

1. **Piles Furnished:** The unit of measurement for payment for furnishing timber, steel, and precast concrete piles shall be the linear meter. The quantity to be paid for will be the sum of the lengths in meters of the piles, of the types and lengths ordered in writing by the Engineer, furnished in compliance with the material requirements of these specifications, stockpiled in good condition at the site of the work by the Contractor, and accepted by the Engineer. No allowance will be made for that length of piles, including test piles, furnished by the Contractor to replace piles which were previously accepted by the Engineer, but are subsequently damaged prior to completion of the contract.

When extensions of piles are necessary, the extension length ordered in writing by the Engineer will be included in the linear meters of piling furnished.

2. **Piles Driven:** The units of measurement for driving timber, steel, and precast concrete piles shall be per linear meter of piling in place measured below the cutoff elevation. The measured length will be rounded to the nearest meter.

Preboring, jetting or other methods used for facilitating pile driving procedures will not be measured and payment shall be considered included in the unit price bid for the Piles Driven pay item.

- B. Cast in Place Pipe or Shell Concrete Piles. The quantity of cast in place pipe or shell concrete piles to be paid for will be the actual number of linear meters of steel pipe or shell piles driven, cast, and left in place in the completed and accepted work. Measurements will be made from the toe of the steel pipe or shell pile to the bottom of the cap or bottom of the footing, as the case may be.

No separate measurement will be made for reinforcing steel, excavation, drilling, cleaning of drilled holes, drilling fluids, sealing materials, concrete, casing, and or any other items required to complete the work. Preboring, jetting or other methods used for facilitating pile driving procedures will not be measured and payment shall be considered included in the unit price bid for the driven and cast in place pay item.

- C. Pile Shoes. The number of pile shoes measured for payment shall be those shoes actually installed on piles and accepted for payment by the Engineer.
- D. Load Tests. The quantity of load tests to be paid for will be the number of load tests completed and accepted, except that load tests made at the option of the Contractor will not be included in the quantity measured for payment.

Reaction and test piling which are not a part of the permanent structure will be included in the unit price bid for each load test. Reaction and test piling, which are a part of the permanent structure, will be paid for under the appropriate pay item.

- E. Splices. The number of splices measured for payment shall be only those splices actually made as required to drive the piles in excess of the ordered length furnished by the Engineer.
- F. Furnishing Equipment for Driving Piles. Payment will be made at the lump sum price bid for this item as follows: Seventy-five percent (75%) of the amount bid will be paid when the equipment for driving piles is furnished and driving of satisfactory piles has commenced. The remaining 25% will be paid when the work of driving piles is completed. The lump sum price bid shall include the cost of furnishing all

labor, materials and equipment necessary for transporting, erecting, maintaining, replacing any ordered equipment, dismantling and removing of the entire pile driving equipment. The cost of all labor, including the manipulation of the pile driving equipment and materials in connection with driving piles, shall be included in the unit price bid per linear meter for the piles to be driven. The furnishing of equipment for driving sheet piling is not included in this work. Payment for furnishing and using a follower, augers or jetting will be considered as included in the unit price bid for piles.

SECTION XXX.06 BASIS OF PAYMENT

The accepted quantities, determined as provided above, will be paid for at the contract price per unit of measurement, respectively, for each of the particular pay items listed below that is shown in the bid schedule, which prices and payment will be full compensation for the work prescribed in this section. Payment will be made under:

Pay Item	Pay Unit
XXX(1) ___ piles, furnished	Linear meter
XXX(2) ___ piles, driven	Linear meter
XXX(3) ___ piles, driven & cast in place	Linear meter
XXX(4) ___ test piles, furnished	Linear meter
XXX(5) ___ test piles, driven	Linear meter
XXX(6) ___ test piles, driven & cast in place	Linear meter
XXX(7) Pile load test (static)	Each
XXX(8) Pile load test (dynamic)	Each
XXX(9) Splices	Each
XXX(10) Pile Shoes	Each
XXX(11) Furnishing Equipment for Pile Driving	Each

Commentary: *The above pile payment items have been chosen to separate the major fixed costs from the variable costs. Many highway agencies oversimplify pile payment by including all costs associated with the driving operation in the price per meter of pile installed. Contractors bidding such "simple" items need to break down the total cost of the mobilization, splices, shoes, etc., to a price per linear meter based on the total estimated*

quantity. If that quantity underruns, the contractor does not recover the full cost of mobilization, splices, shoes, etc. If that quantity overruns, the highway agency pays an unfair price for the overrun quantity. The use of separate items for operations of major fixed cost such as mobilization can substantially mitigate the inequitable impact of length variations. Similarly, the ordered pile length is the highway agency's responsibility. Separate payment for furnishing piles and driving piles compensates the contractor for actual materials used and installation costs, even when overruns or underruns occur.

REFERENCES

- American Association of State Highway and Transportation Officials [AASHTO], (1994). Standard Specifications for Highway Bridges. Division 2, AASHTO Highway Subcommittee on Bridges and Structures, Washington, D.C.
- American Society for Testing and Materials [ASTM], (1987). Standard Test Method for Piles Under Static Axial Compressive Load, ASTM D-1143.
- The Deep Foundations Institute, Equipment Applications Committee (1995). A Pile Inspector's Guide to Hammers, Second Edition.
- Fragasny, R.J., Higgins, J.D. and Argo, D.E. (1988). Comparison of Methods for Estimating Pile Capacity. Report No. WA-RD 163.1, Washington State Department of Transportation, Olympia, 62.
- Geotechnical Guideline 13 (1985). Geotechnical Engineering Notebook, U.S. Department of Transportation. Federal Highway Administration, Washington, D.C., 37.
- Kylor, Z.G., Schnore, A.R., Carlo, T.A. and Baily, P.F. (1992). Static Testing of Deep Foundations. Report No. FHWA-SA-91-042, U.S. Department of Transportation, Federal Highway Administration, Office of Technology Applications, Washington, D.C., 174.
- Olson, R.E. and Flaate, K.S. (1967). Pile Driving Formula for Friction Piles in Sands. American Society of Civil Engineers, Journal for Soil Mechanics and Foundation Engineering, Vol. 93, SM6, 279-296.
- Rausche, F., Likins, G.E., Goble, G.G. and Hussein, M. (1986). The Performance of Pile Driving Systems. Inspection Manual, Report No. FHWA/RD-86/160, U.S. Department of Transportation, Federal Highway Administration, Office of Research and Development, Washington, D.C., 92.

13. PILE FOUNDATION DESIGN SUMMARY

13.1 INTRODUCTION

In this chapter, the total design process will be reviewed following the procedure outlined in Chapter 3. However, this time the design process will be illustrated through a proposed bridge construction project. The Foundation Design Process flow chart presented in Figure 3.1 is repeated for convenience here as Figure 13.1. The proposed project is a bridge that will carry the imaginary Peach Freeway over Dismal Creek. This is a new freeway that is to be built in a city in the southeastern part of the United States. The alignment of the roadway has been defined and the foundation design now comes into consideration. The design process will be followed using Figure 13.1.

13.2 BLOCK 1 - ESTABLISH REQUIREMENTS FOR STRUCTURAL CONDITIONS AND SITE CHARACTERIZATION

The general structure requirements will now be reviewed following the list from Chapter 3, Section 3.4.

1. The project is a new bridge.
2. The structure will be constructed at one time by a single contract.
3. The structure layout has not been finalized at the time that the foundation engineer first becomes involved. The alignment is quite well defined but the grades have not been established.
4. The foundation engineer has briefly visited the proposed site. Dismal Creek is a flat, shallow stream that, at low water, is more than 30 meters wide in the vicinity of the proposed bridge. At the north end of the structure there is a bank about eight meters high while on the south end the bank slopes up quite slowly. The new bridge will probably be about 80-100 meters long with an approach embankment required for the south approach. Bridge piers will probably be located in Dismal Creek.

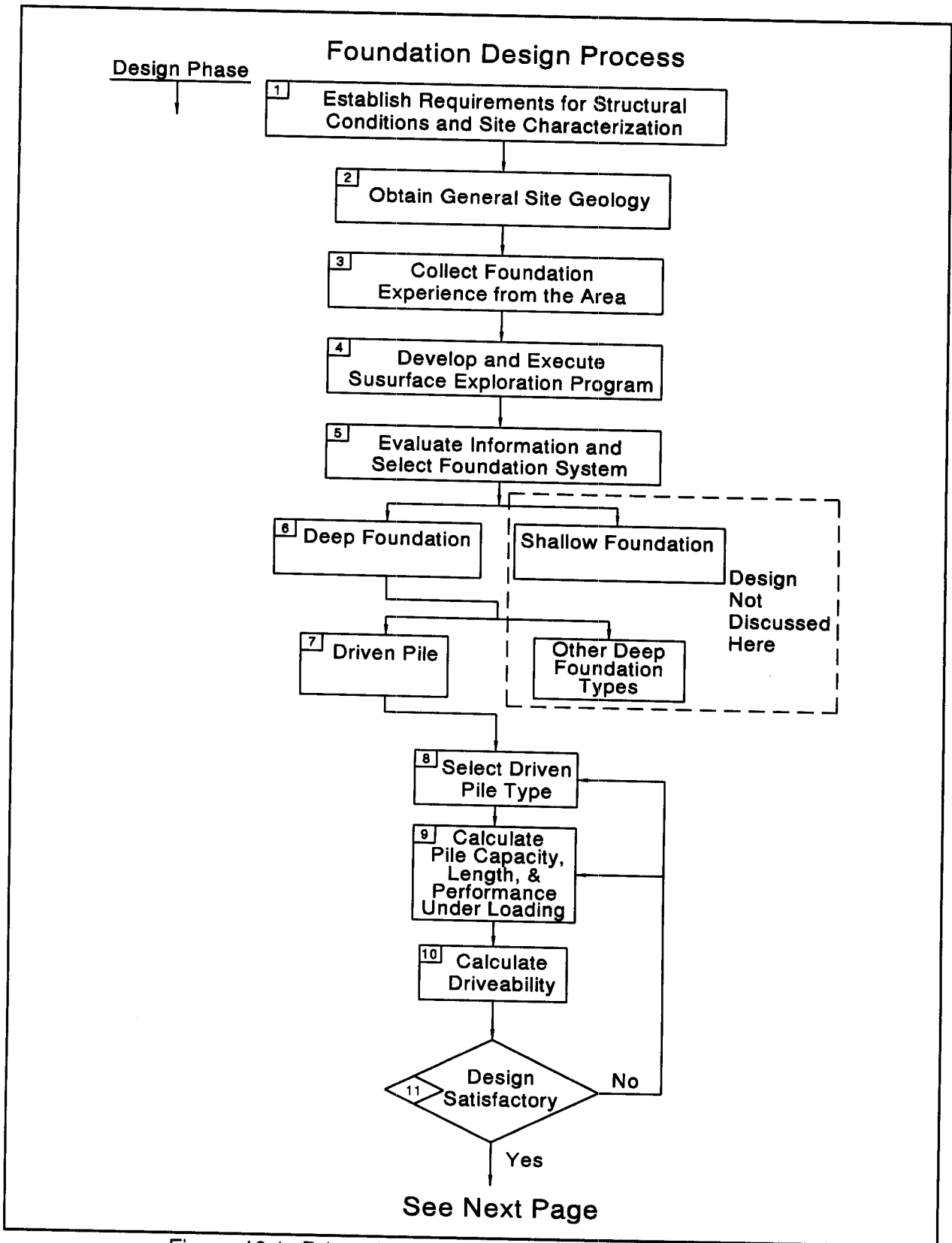


Figure 13.1 Driven Pile Design and Construction Process

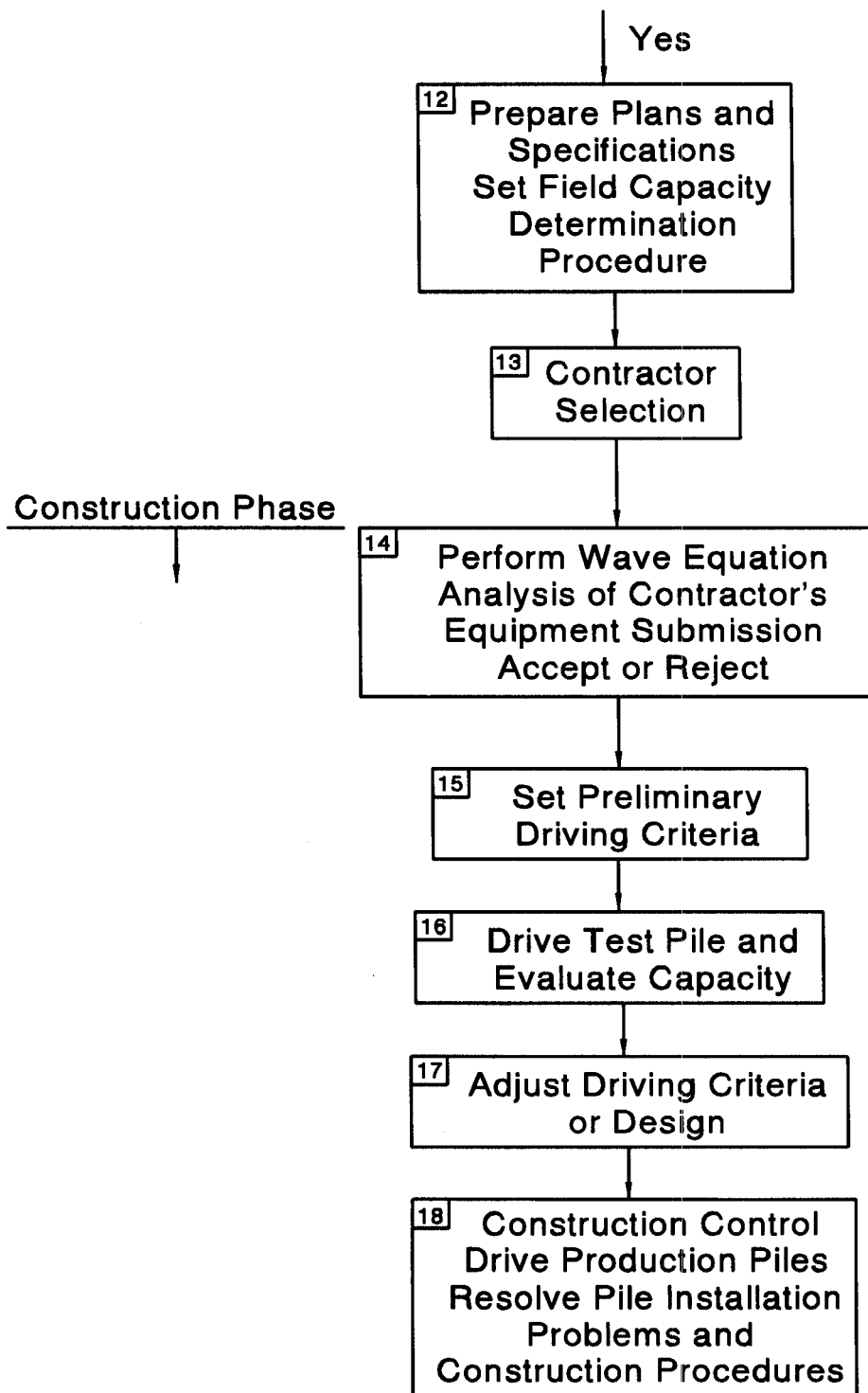


Figure 13.1 Driven Pile Design and Construction Process (continued)

5. Seismic and vessel impact loads are not a design consideration. However, scour and debris loading must be considered for the bridge piers.
6. As yet the structure is not sufficiently defined to consider modifications in the structure due to site considerations.
7. Foundation loads cannot be estimated very accurately at this time. A meeting with the bridge engineer indicates that, based on his experience, compression loads on the order of 10,000 to 15,000 kN per substructure location are likely. Typical deflection and deformation requirements are anticipated.

13.3 BLOCK 2 - OBTAIN GENERAL SITE GEOLOGY

Published data from the sources listed in Table 4-2 has been reviewed in the office planning stage. Geologists have also been contacted to provide information regarding the site geology. At first glance, an extensive subsurface exploration would probably not be required for this modest sized structure. However, a field reconnaissance survey of the area has been made by the foundation engineer and the project bridge engineer. Field observations of the eroded stream banks indicated that the surficial soils on the north side of Dismal Creek consist of silty sands while silty clays were noted in the south stream bank. The granular upland soils on the north approach and the cohesive lowland soils on the south approach further suggest that the subsurface conditions may be quite complex. Therefore, it would be desirable that fairly extensive subsurface exploration be made. The foundation engineer expected the site to be underlain by limestone bedrock at a depth of 30 to 50 meters, based on previous experience.

13.4 BLOCK 3 - COLLECT FOUNDATION EXPERIENCE FROM THE AREA

Agency files have been reviewed to determine if there are any existing soil borings in the area of the proposed bridge site. However, no previous subsurface information has been located. There are also no existing bridges in the vicinity of the planned structure to provide details on subsurface conditions or previous construction information and/or problems.

13.5 BLOCK 4 - DEVELOP AND EXECUTE SUBSURFACE EXPLORATION PROGRAM

Based on the information generated in Blocks 1 to 3, a subsurface exploration program was planned. The foundation engineer requested that the bridge engineer provide additional information on the planned structural configuration. Since some time had elapsed since the initial discussions regarding the proposed structural configuration, it was possible to better define the structure geometry. The proposed bridge will be supported at two abutments and two interior piers. Due to the possibly complex subsurface conditions, both a soil boring and an in-situ cone penetration test will be performed at each substructure location.

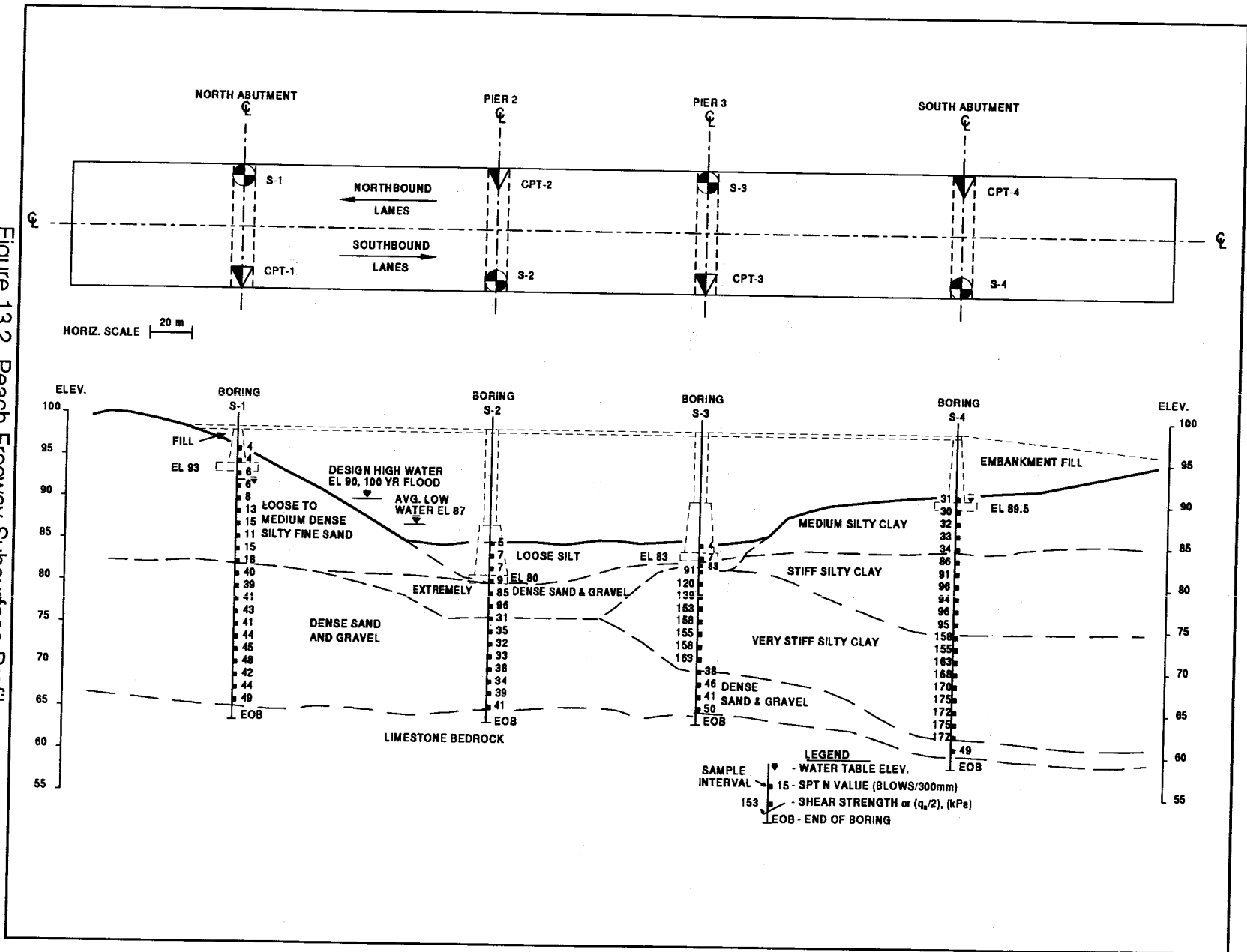
The subsurface program was performed and results of the exploration are included in Appendix E. This data was evaluated and a subsurface profile was prepared and is given in Figure 13.2.

13.6 BLOCK 5 - EVALUATE INFORMATION AND SELECT FOUNDATION SYSTEM

A decision must now be made regarding the foundation system that will be used. First, the foundation engineer met again with the bridge engineer to verify the final design loads and foundation locations. It was determined that the foundations will be located as anticipated at the last meeting. The Peach Freeway Bridge over Dismal Creek will be a three span structure supported at North and South Abutments and interior piers, Pier 2 and Pier 3. At the proposed bridge location, the only extreme event that must be considered is scour. The bridge is not in a region where seismic loads will influence the design and vessel impact is not a design consideration. Lateral loads will be induced by stream debris.

The foundation loads have now been well defined. The total axial compression loads have been established at 12,600 kN per substructure location. Other load conditions that include several combinations of axial and transverse loads result in axial compression, uplift, lateral, and moment loads at each substructure unit. These load combinations are too extensive to be repeated here. However, the lateral loads will range from 600 kN at the interior piers to 900 kN at the abutments, and the maximum uplift load on a pile group will be less than 1800 kN.

Figure 13.2 Peach Freeway Subsurface Profile



The foundation performance requirements have also been established. Maximum pile group settlements less than 25 mm are required under the compression loads with maximum differential settlements between substructure units of 15 mm. Maximum horizontal deflections of up to 10 mm are permissible under lateral loading.

A hydraulics division study indicates that a shallow foundation should not be used under the two piers due to scour. In addition, settlement of a shallow foundation at Pier 3 is expected to be excessive. Therefore, the use of a shallow foundation was ruled out and a deep foundation will be required.

13.7 BLOCK 6 - DEEP FOUNDATION TYPE

A decision must now be made between the use of driven piles and drilled shafts. Both driven piles and drilled shafts are commonly used in the region. However, a cost analysis indicates that a driven pile option will be more economical than drilled shafts because of the complex subsurface conditions. Therefore, a driven pile system is selected.

13.8 BLOCK 7 AND 8 - SELECT DRIVEN PILE TYPE

All of the available information is now used to select a pile type as well as the number of piles and group arrangement. The limitations associated with the various design conditions are used to check the selection by analyzing the response of the pile to the applied loads. Initial design estimates and local availability of materials indicate square, precast, prestressed concrete piles will probably be the most cost effective foundation type. A 356 mm square, prestressed concrete pile is then selected. Pile groups of 24 piles arranged in three rows of eight piles each will be used at each substructure location. The maximum compressive design load is 890 kN, the design uplift load is 100 kN, and the maximum lateral load is 40 kN per pile.

13.9 BLOCK 9 - SELECT PILE LENGTH AND CALCULATE PERFORMANCE UNDER SPECIFIED LOADS

13.9.1 Single Pile Capacity

Several static pile capacity calculations have been performed to determine the estimated pile length at each substructure unit (*i.e.*, North Abutment, Pier 2, Pier 3, and South Abutment) using the procedures presented in Chapter 9. Construction control procedures have been selected that will make a factor of safety of 2.0 appropriate. Therefore, an ultimate axial capacity of 1780 kN is required. At Piers 2 and 3, the effect of scour on the static axial capacity should also be calculated. Static pile capacity calculation details are given in Appendix F (including the scour calculation at Pier 2) and summaries of the calculations are provided in Tables 13-1 to 13-4.

The capacity calculation summaries indicate different static analysis methods will yield different results. Therefore, designers should use a method they fully understand, including the method limitations. Based upon the analyses performed, pile penetration lengths of 11.5 m are selected for the North Abutment, 14 m for Pier 2 (after scour), 13 m for Pier 3 (total stress α -method so scour effect limited) and 21 m for the South Abutment (17.5 m if drag load not considered).

13.9.2 Pile Group Capacity

The North Abutment piles will be driven into a dense cohesionless soil at center to center pile spacings greater than 4 diameters. Therefore, the ultimate pile group capacity for the North Abutment may be taken as the sum of the ultimate capacities of the individual piles in the group as discussed in Section 9.8.1.1. Similarly, the Pier 2 piles will be driven into a dense cohesionless soil at center to center pile spacings greater than 4 diameters. Therefore, the ultimate pile group capacity at Pier 2 may also be taken as the sum of the ultimate capacities of the individual piles in the group.

At Pier 3, the piles will be driven through cohesive soils and into a dense cohesionless layer at center to center pile spacings of 4 diameters. Since the piles will be founded in a dense cohesionless layer, the pile group capacity should be equal to the sum of the ultimate capacities of the individual piles in the group. However, the possibility of block failure should be checked in accordance with the procedures detailed in Section 9.8.1.3 particularly if the dense layer is underlain by a weaker deposit.

TABLE 13-1(a) NORTH ABUTMENT PILE CAPACITY SUMMARY FOR 11.5 m PILE EMBEDMENT			
Method Used for Estimation of Pile Capacity	Calculated Pile Shaft Resistance (kN)	Calculated Pile Toe Resistance (kN)	Calculated Ultimate Pile Capacity (kN)
Meyerhof Method - SPT Data	418	854	1,272
Nordlund Method - SPT Data	898	940	1,838
Effective Stress Method - SPT Data	537	1,294	1,831
SPILE Program - SPT Data	944	1,201	2,145
LPC CPT Program - CPT Data	780	511	1,291
Schmertmann Method - CPT Data	604	1,111	1,715

TABLE 13-1(b) NORTH ABUTMENT PILE LENGTH SUMMARY FOR A 1,780 kN ULTIMATE PILE CAPACITY	
Method Used for Estimation of Pile Capacity	Calculated Pile Length for the 1,780 kN Ultimate Pile Capacity
Meyerhof Method - SPT Data	13.0 meters for 1,840 kN
Nordlund Method - SPT Data	11.5 meters for 1,838 kN
Effective Stress Method	11.5 meters for 1,831 kN
SPILE Program - SPT Data	11.5 meters for 2,145 kN
LPC CPT Program - CPT Data	13.5 meters for 1,815 kN
Schmertmann Method - CPT Data	11.7 meters for 1,939 kN

TABLE 13-2(a) PIER 2 PILE CAPACITY SUMMARY FOR 10.0 m PILE EMBEDMENT			
Method Used for Estimation of Pile Capacity	Calculated Pile Shaft Resistance (kN)	Calculated Pile Toe Resistance (kN)	Calculated Ultimate Pile Capacity (kN)
Meyerhof Method - SPT Data	1,134	1,676	2,810
Nordlund Method - SPT Data	984	854	1,838
Effective Stress Method	451	1,155	1,606
SPILE Program - SPT Data	992	1,106	2,098

TABLE 13-2(b) PIER 2 PILE LENGTH SUMMARY FOR A 1,780 kN ULTIMATE PILE	
Method Used for Estimation of Pile Capacity	Calculated Pile Length for the 1,780 kN Ultimate Pile Capacity
Meyerhof Method - SPT Data	1.0 meters for 2,136 kN
Nordlund Method - SPT Data	10.0 meters for 1,838 kN
Effective Stress Method	12.5 meters for 1,847 kN
SPILE Program - SPT Data	10.0 meters for 2,098 kN

TABLE 13-2(c) PIER 2 PILE CAPACITY SUMMARY BEFORE AND AFTER CHANNEL DEGRADATION SCOUR BASED ON NORDLUND METHOD		
Pile Embedment	Ultimate Pile Capacity	
	Before Scour	After Scour
10 meters	1,838 kN	1,347 kN
14 meters	2,331 kN	1,887 kN

TABLE 13-3(a) PIER 3 PILE CAPACITY SUMMARY FOR 13.0 m PILE EMBEDMENT			
Method Used for Estimation of Pile Capacity	Calculated Pile Shaft Resistance (kN)	Calculated Pile Toe Resistance (kN)	Calculated Ultimate Pile Capacity (kN)
Nordlund and α Method - SPT Data	1,171	635	1,806
Effective Stress Method	525	1,059	1,584
SPILE Program - SPT Data	1,180	1,130	2,310
LPC CPT Program - CPT Data	1,189	841	2030
Schmertmann Method - CPT Data	1,727	1,231	2,958

TABLE 13-3(b) PIER 3 PILE LENGTH SUMMARY FOR A 1,780 kN ULTIMATE PILE CAPACITY	
Method Used for Estimation of Pile Capacity	Calculated Pile Length for the 1,780 kN Ultimate Pile Capacity
Nordlund and α Method - SPT Data	13.0 meters for 1,806 kN
Effective Stress Method	14.0 meters for 1,980 kN
SPILE Program - SPT Data	13.0 meters for 2,310 kN
LPC CPT Program - CPT Data	12.5 meters for 1,826 kN
Schmertmann Method - CPT Data	10.2 meters for 1,808 kN

Note: Strata transitions from very stiff clay to dense sand and gravel at an embedded pile length of 13 m.

TABLE 13-4(a) SOUTH ABUTMENT PILE CAPACITY SUMMARY FOR 17.5 m PILE EMBEDMENT			
Method Used for Estimation of Pile Capacity	Calculated Pile Shaft Resistance (kN)	Calculated Pile Toe Resistance (kN)	Calculated Ultimate Pile Capacity (kN)
α Method	1,648	182	1,830
Effective Stress Method	898	715	1,613
SPILE Program	1,645	182	1,827
LPC CPT Program - CPT Data	1,361	328	1,689
Schmertmann Method - CPT Data	1,717	353	2,070

TABLE 13-4(b) SOUTH ABUTMENT PILE LENGTH SUMMARY FOR A 1,780 kN ULTIMATE PILE CAPACITY	
Method Used for Estimation of Pile Capacity	Calculated Pile Length for the 1,780 kN Ultimate Pile Capacity
α Method	17.5 meters for 1,830 kN
Effective Stress Method	18.7 meters for 1,800 kN
SPILE Program	17.5 meters for 1,827 kN
LPC CPT Program - CPT Data	19.5 meters for 1,807 kN
Schmertmann Method - CPT Data	15.2 meters for 1,828 kN

Note: These analyses do not consider the influence of downdrag loads on pile capacity which are discussed in Section 13.9.6.

At the South Abutment, the ultimate pile group capacity against block failure has been calculated and compared with the ultimate pile group capacity from the sum of the ultimate capacities of the individual piles times the group efficiency. Based on the design recommendations outlined in Section 9.8.1.2, a group efficiency of 1.0 was used. This calculation, included in Section F.2.4.1 of Appendix F, indicates that ultimate capacity against block failure is greater than the ultimate capacity of the group. Therefore, block failure is not a design issue.

At all four substructure locations, the group capacity meets the design requirements.

13.9.3 Group Settlement Calculations

The substructure of the bridge is designed to be supported on a pile group having 3 rows of piles with 8 piles in each row. The piles are arranged at 1.5 m center to center spacing with a total pile group area of 3.36 m by 10.86 m. Piles in a group are combined with a pile cap having a dimension of 4.5 m by 12 m. The maximum pile group settlement should be less than 25 mm under the compression loads with maximum differential settlements of 15 mm between substructure units.

At the North Abutment, group settlement has been calculated using the Meyerhof Method detailed in Section 9.8.2.2. Results of this calculation are given in Appendix F.3.1 and indicate that the total pile group settlement is 12.2 mm due to soil compression and elastic pile compression. This is less than the maximum allowable settlement of 25 mm.

At Pier 2, group settlement has also been calculated using the Meyerhof Method detailed in Section 9.8.2.2. Results of this calculation are given in Appendix F.3.2 and indicate that the total pile group settlement is 13.2 mm due to soil compression and elastic pile compression. This is less than the maximum allowable of 25 mm.

At Pier 3, group settlement has been calculated using the equivalent footing method for layered soils described in Section 9.8.2.4 and the Meyerhof Method detailed in Section 9.8.2.2. Results of these calculations are given in Appendix F.3.3. The calculated settlement using the equivalent footing method is 16.1 mm including soil settlement and elastic pile compression. Most of this calculated settlement (12 mm) is in the clay layer. Since the piles are supported in an underlying dense sand and gravel layer where settlements are calculated to be 3.0 mm, it is unlikely that the calculated settlement in the clay layer could develop due to the lack of strain compatibility between layers. The

Meyerhof Method calculation indicates a group settlement of 9.0 mm including soil settlement and pile compression. In this soil profile, the Meyerhof Method calculation is considered a better indicator of probable foundation performance under load. Therefore the calculated settlement at Pier 3 of 9.0 mm is less than the maximum allowable of 25 mm.

At the South Abutment, group settlement has been calculated using the equivalent footing method described in Section 9.8.2.3. Results of this calculation are provided in Appendix F.3.4 and indicate that the group settlement at the South Abutment is 28 mm including soil and pile compression. This is larger than the maximum allowable pile group settlement of 25 mm. The group settlement will even be larger after the placement of the approach embankment fill materials behind the abutment wall. The settlement from embankment construction alone is calculated to be 500 mm. Therefore, preloading of the South Abutment should be performed prior to pile installation.

With preloading of the South Abutment, group settlements could be kept within the foundation performance criteria. Differential settlements between substructure units have been calculated to be within the 15 mm criterion for differential settlement provided preloading at the South Abutment is performed.

13.9.4 Lateral Pile Capacity Analysis

The bridge division has estimated that the group lateral loads range from 600 kN at the interior pile groups to 900 kN at the abutment pile groups. The maximum lateral load per pile is limited to 40 kN. A horizontal deflection of up to 10 mm is permissible under lateral loading.

A simple Broms' Method lateral pile capacity analysis has been performed for the North Abutment piles. This calculation, included in Appendix F.4.1, indicates that the maximum lateral load per pile is 25 kN in order to meet the 10 mm deflection requirement. This lateral load is less than desired. Therefore, the group capacity of 600 kN (24 piles at 25 kN/pile) is less than the 900 kN required, and more piles would be needed.

A more rigorous COM624P analysis was also performed to evaluate the lateral load capacity of the 356 mm square prestressed concrete pile at the North Abutment. This analysis is included in Appendix F.4.2 and indicates that the pile deflection under the 40 kN design load will be 3.8 mm. The corresponding maximum moment and shear stress are -55.2 m-kN and 14,600 kN/m². The deflection, moment and shear stress under the design load are

acceptable. Hence, the more rigorous COM624P analysis indicates a 40 kN design lateral load could be used whereas the Broms' Method indicated only a 25 kN design load.

A COM624P analysis was also performed to evaluate the lateral load capacity of the 356 mm square prestressed concrete pile at the South Abutment. This analysis is included in Appendix F.4.5 and indicates that the pile deflection under the 40 kN design load will be 2.5 mm. The corresponding maximum moment and shear stress are -46.1 m-kN and 13,400 kN/m². The deflection, moment and shear stress under the design load are acceptable.

Additional COM624P analyses should be performed to evaluate Piers 2 and 3. In addition, the pile group response should be evaluated at all substructure units using the p-multiplier approach described in Section 9.8.4.

13.9.5 Uplift Capacity Calculations

The maximum uplift load on a pile group is estimated to be 1,800 kN with a maximum uplift load per pile of 100 kN. A calculation of the uplift capacity of the North Abutment pile group has been performed following AASHTO Code (1994) for service load design as outlined in Section 9.8.3.1. Following this procedure, the uplift capacity of the North Abutment pile group is 2,475 kN, which is greater than the maximum uplift load of 1,800 kN. Uplift calculation results are included in Appendix F.5.1.

A calculation of the uplift capacity of the Pier 2 pile group has also been performed in Appendix F.5.2. Following this procedure, the uplift capacity of the Pier 2 pile group is 2,616 kN, which is greater than the maximum uplift load of 1,800 kN.

At Pier 3, an uplift capacity calculation in accordance with AASHTO code yielded an uplift capacity of 3,354 kN, which is greater than the maximum uplift load of 1,800 kN. Uplift calculation results for Pier 3 are included in Appendix F.5.3.

A calculation of the uplift capacity of the South Abutment pile group has also been performed. The uplift capacity of the South Abutment pile group is 4,275 kN, which is greater than the maximum uplift load of 1,800 kN. Uplift calculation result for the South Abutment are included in Appendix F.5.4.

13.9.6 Negative Shaft Resistance

Piles at the South Abutment will be subjected to negative shaft resistance or downdrag loading due to soil settlement following the placement of 10 m of approach embankment material behind the abutment after pile installation. This settlement needs to be estimated prior to determining the location of the negative and positive shaft resistances along the pile. The α -method is now used to estimate both the positive and negative shaft resistance components. The step by step procedure for the calculation of downdrag loading is presented in Section 9.9.1.1a.

Following this procedure, a drag load of 259 kN has been calculated. The net ultimate pile capacity for a 17.5 m embedded length available to resist imposed loads is then only 1,312 kN which is smaller than the required ultimate pile capacity. Therefore, alternatives such as preloading to reduce settlement and thereby the drag load, use of bitumen coatings to reduce pile-soil adhesion and thereby the drag load, or use of longer length piles to carry the drag load should be evaluated.

Calculations indicate use of bitumen coating to a depth of 5.5 m pile would reduce the negative shaft resistance to 78 kN. However, the net ultimate pile capacity available to resist imposed loads on a 17.5 m embedded length pile is still only 1,493 kN which is less than the required ultimate pile capacity of 1780 kN.

Calculations indicate the use of a 21 m long pile with a bitumen coating to a depth of 5.5 m would increase the ultimate pile capacity to 1,908 kN. With these 21 m long piles, the net ultimate pile capacity available to resist imposed loads is 1,830 kN. Hence, this alternate provides the required ultimate capacity. However, cost analyses of preloading, bitumen coatings, and longer piles in conjunction with meeting performance criteria requirements should be performed before making the final selection. The negative shaft resistance calculations are given in Appendix F.6.1.

A stub abutment instead of a full height abutment may also be a solution at the South Abutment. The stub abutment could be supported on a spread footing with specified embankment material and density control in the foundation area. A stub abutment with pile foundation is another alternative available for consideration.

This design problem illustrates the difficulties encountered in designing pile foundations in clay where substantial settlements occur and large drag loads are encountered by piles.

13.9.7 Lateral Squeeze Evaluation

The South Abutment should be evaluated for the potential for lateral squeeze following the guidelines presented in Section 9.9.3 of Chapter 9. Following these procedures, calculations presented in Appendix F.7.1 indicate that abutment tilting can occur. If piles are placed before any soil compression occurs, calculations indicate horizontal movement of 124 mm, which is not tolerable. If piles are driven after 90% of vertical settlement has occurred, calculations indicate horizontal movements of 12.4 mm. This is greater than the performance criteria but could be tolerated if provisions were made in the bridge shoe and expansion joint design.

13.9.8 Overall Design Assessment

The selected pile lengths have now been checked for compression, lateral, and uplift loading as well as settlements. With preloading at the South Abutment group capacities and settlements are satisfactory. At this point the design has been found acceptable from a geotechnical perspective to meet the performance requirements.

13.10 BLOCK 10 - CALCULATE DRIVEABILITY

The driveability of the proposed pile section and lengths for the required ultimate pile capacity must now be evaluated using a wave equation program analysis. The soil resistance versus depth has been calculated for each substructure location using the DRIVEN program and then input into the GRLWEAP wave equation program. Details on the DRIVEN program are given in Chapter 9 and the GRLWEAP wave equation program is presented in Chapter 17 of Volume II.

At this stage, driveability analysis results indicate that the proposed 356 mm concrete piles would work well at the abutments. However, at the interior piers, the driveability of these displacement piles through the extremely dense sand and gravel layer may be quite difficult. The driveability results at Pier 2 are presented and discussed in greater detail in Section 17.5.5. These results indicate displacement piles would like encounter refusal driving conditions when penetrating the extremely dense sand and gravel layer. Therefore, a low displacement pile, such as an H-pile, may be necessary at the interior piers to meet pile penetration requirements dictated by scour. Therefore, the design process should return to Block 8 and evaluate an H-pile solution at the interior piers.

13.11 BLOCK 11 - DESIGN SATISFACTORY?

After a driveability review, H-piles are chosen for the pile foundation at the interior pier and precast concrete for the abutments. COM624P analyses for the H-piles at Piers and 3 are then performed and are presented in Appendix F.4.3. and F.4.4, respectively. To satisfy capacity requirements in the event of scour, the H-piles would need to be driven to within 1.5 meters of bedrock. Driveability results for the H-pile solution at Pier 2, presented in Section 17.5.5, indicate H-piles could be driven to bedrock. Therefore, it may also be feasible to increase the pile capacity and use fewer piles. The H-piles at the interior piers were found to meet all the design requirements including driveability. Therefore, all of the design requirements are now satisfied.

13.12 BLOCK 12 - PREPARE PLANS AND SPECIFICATIONS, SET FIELD CAPACITY DETERMINATION PROCEDURE

The foundation design report should now be prepared. This report should summarize the results of the subsurface exploration program, laboratory test data, static analyses, a specific design and construction recommendations. The report should also highlight any special notes which should be incorporated into the plans or specifications which are also prepared at this time. For example, the preloading requirement at the South Abutment to reduce foundation settlements and drag loads should be clearly stated in the project plans and specifications.

Because of the variability of the subsurface site conditions, the foundation report recommended construction control using a static load test. Wave equation analysis is also required for driving system approval. In addition, dynamic testing has been specified during initial driving and restriking of two test piles per each substructure location. These test piles are to be driven in advance of production pile driving. The required ultimate pile capacity, driving stress limits, and testing methods are then incorporated into the plans and specifications.

13.13 BLOCK 13 - CONTRACTOR SELECTION

At this time the bidding process is completed, a successful contractor is selected.

13.14 BLOCK 14 - PERFORM WAVE EQUATION ANALYSIS OF CONTRACTOR'S EQUIPMENT SUBMISSION

The engineering effort now shifts to the field. The contractor has submitted the Pile Driving and Equipment Data form shown in Figure 12.1 for the engineer's evaluation of the proposed driving system. The design stage driveability studies were saved and can now be reanalyzed using the proposed driving system as part of the hammer approval process. Additional wave equation analyses are now performed to determine the driving resistance that must be achieved in the field to meet the required capacity and pile penetration depth. Driving stresses are also determined and checked against specification requirements. All conditions are satisfactory, and the equipment is approved for pile driving.

13.15 BLOCK 15 - SET PRELIMINARY DRIVING CRITERIA

Based on the results of the wave equation analysis of Block 14 along with minimum pile penetration requirements for scour, the preliminary driving criteria is set.

13.16 BLOCK 16 - DRIVE TEST PILE AND EVALUATE CAPACITY

Test piles are now driven using the preliminary driving criteria at each substructure location. Dynamic testing is performed on the test piles during initial driving and during restrike. The ultimate pile capacity is confirmed at each substructure unit by the dynamic test results and the correlating static load test.

13.17 BLOCK 17 - ADJUST DRIVING CRITERIA OR DESIGN

At this stage the final conditions can be set. If test results from Block 16 had indicated the capacity was inadequate, the driving criteria may have to be changed. In a few cases, it may be necessary to make changes in the design as far back as Block 8. If major changes are required, it will be necessary to repeat Blocks 14, 15, and 16.

13.18 BLOCK 18 - CONSTRUCTION CONTROL

After the driving criteria is set, the production pile driving proceeds following established quality control procedures.

14. FOUNDATION DESIGN REPORT PREPARATION

A foundation design report should be prepared to present the results of the subsurface explorations, laboratory test data, analysis, and specific design and construction recommendations for the foundation system of a structure. The foundation report is referred to frequently during the design and construction period as well as in resolving post construction issues such as claims. It is therefore important that the foundation report be clear, concise and accurate. The foundation report is a very important document and should be prepared and reviewed accordingly.

As described in Chapter 13, the foundation design evolves as information is gathered and analyzed. Preliminary design recommendations based on, and/or transmitted with initial subsurface data does not constitute a foundation design report. A foundation design report should be developed with the full knowledge of loads, special design events, performance criteria and any site restrictions. Only with this full knowledge can a foundation design report be prepared with appropriate content and quality. The parts of a foundation design report are described in greater detail in Section 14.2.

The foundation report should be widely distributed to design, construction and maintenance engineers involved in the project. The foundation report should also furnish information regarding anticipated construction problems and solutions. This will provide a basis for the contractor's cost estimates.

The foundation design report should be completed and available to the designer prior to final design. The foundation drawings, special provisions, and foundation design report should all be cross-checked for compliance upon completion of final design documents. Conflicts between any of these documents greatly increases the potential for construction problems.

14.1 GUIDELINES FOR FOUNDATION DESIGN REPORT PREPARATION

1. The geotechnical engineer responsible for the report preparation should have a broad enough background in geotechnical and highway engineering to have knowledge of the foundation requirements and limitations for various types of structures. This includes knowledge in specifications, construction procedures, construction methods, quality control and assurance, and structural components.
2. The geotechnical engineer must have a clear and complete understanding of the compression, uplift and lateral load demands, performance criteria regarding deformations and constraints or restrictions.
3. The report should contain an interpretation and analysis of subsurface and site data. This includes a description of analysis and results in a summarized form.
4. The report should contain specific engineering recommendations for design.
5. Recommendations should be brief, concise, and definitive.
6. Reasons for recommendations and their supporting data should always be included.
7. Extraneous data of little use to the designer or Project Engineer should be omitted.
8. Discussion of soil materials and subsurface conditions which may be encountered during construction should be included.
9. Possible design and/or construction problems should be anticipated and recommendations for their solution should be included in the report.
10. The report should highlight any special notes which need to be placed on the plans or in the specifications.

14.2 PARTS OF A FOUNDATION DESIGN REPORT

A standard format provides uniformity of report writing as well as a checklist, so that major foundation design and construction considerations are not overlooked. The Soil and Foundations Workshop Manual FHWA HI-88-009 by Cheney and Chassie (1993) contains a foundation report outline that has been modified to include information from the AASHTO manual on Subsurface Investigations (1988). This modified outline is presented below and is recommended as a report preparation guide.

- I. Table of Contents
- II. Introduction
 1. Summary of proposed construction, including foundation loading conditions (vertical and horizontal, static and dynamic, various combinations).
 2. Summary of special design events: scour, seismic, vessel impact.
 3. Foundation performance criteria (total and differential settlements, lateral deformation, vibration limits).
- III. Scope of Explorations
 1. Field explorations (summary of dates and methods, appended results).
 2. Laboratory Testing (summary of types of tests, appended results).
- IV. Interpretation of Subsurface Conditions
 1. Description of formations.
 2. Soil types.
 3. Dip and strike of rock.
 - a. Regional.
 - b. Local.

4. Water table data.

- a. Perched.
- b. Regional.
- c. Artesian.

V. Design Soil Parameters

1. Narrative to describe procedure for evaluating all factual data to establish design values.

- a. Shear strength.
- b. Compressibility.

VI. Design Analysis

1. Description of design procedures.

2. Summary of results.

3. Explanation of interpretation.

VII. Geotechnical Conclusions and Recommendations

1. Approach embankment considerations (primarily for fills over soft, weak subsoils).

a. Stability.

1. Excavation and replacement of unsuitable materials.
2. Counter berm.
3. Stage construction, time delay.
4. Other treatment methods: change alignment, lower grade, lightweight fill, etc.
5. Estimated factors of safety with and without treatment: estimated costs for treatment alternates, recommended treatment.

- b. Settlement of subsoils.
 - 1. Estimated settlement amount.
 - 2. Estimated settlement time.
 - 3. Surcharge height.
 - 4. Special foundation treatment: vertical drains, soil densification, soil removal and replacement, *etc.*
 - 5. Waiting periods.
 - 6. Downdrag loads on deep foundations.
 - 7. Lateral squeeze of soft subsoils.

- c. Construction considerations.
 - 1. Select fill material: gradation and compaction requirements.
 - 2. Construction monitoring (instrumentation).

- d. Special notes.

2. Spread footing support.

- a. Elevation of bottom of footing: based on frost depth, scour depth, or depth to competent bearing material.

- b. Allowable bearing pressure: based on settlement or bearing capacity, considering soil or rock type, adjacent foundations, water table, *etc.*

- c. Footing size used in computations.

- d. Estimated settlement of soil supported footings.

- e. Resistance to sliding of soil supported footings.

- f. Excavation, structural fill, and dewatering requirements.

- g. Special notes.

3. Pile foundation support.

- a. Method of pile support: shaft resistance, toe resistance, or both. Delineation of unsuitable support layers due to compressibility, scour, or liquefaction.
- b. Suitable pile types: reasons for choice and/or exclusion of types.
- c. Pile toe elevations.
 - 1. Estimated toe elevation, (average estimated values from static analyses with probable variation potential).
 - 2. Specified toe elevation, (toe elevation required due to underlying soft layers, negative shaft resistance, scour, lateral or uplift loads, piles uneconomically long, etc.).
- d. Estimated pile lengths.
- e. Allowable pile design loads for compression, uplift, and lateral loading.
- f. Estimated pile group settlement; very important for pile groups in cohesive soils and large groups in a cohesionless soil deposit underlain by compressible soils.
- g. Test piles to establish order lengths; specify test locations for maximum utility.
- h. Static pile load tests; specify test locations for maximum utility.
 - 1. Axial compression.
 - 2. Axial tension.
 - 3. Lateral.
- i. Dynamic pile load tests; specify test locations and retap frequency.
- j. Driving criteria; specify use of wave equation analysis or dynamic formula.

- k. Estimated ultimate soil resistance to overcome in order to reach estimated pile length.
 - l. Preboring, pile toe reinforcement, or other requirements to reach pile penetration requirements or handle potential obstructions.
 - m. Pile driving requirements: hammer size, tolerances, etc.
 - n. Cofferdams and seals; seal design should consider potential conflicts between batter piles driven at alignment tolerance limits and depth of sheeting. Group densification inside sheeting for displacement piles in sands, or heave for displacement piles in clays should be considered.
 - o. Corrosion effects or chemical attack; particular concern in marine environments, old dumps, areas with soil or groundwater contaminants.
 - p. Effects of pile driving on adjacent construction; settlements from vibrations and development of excess pore water pressures in soil.
 - q. Special notes.
4. Drilled shaft support.
- a. Method of drilled shaft support: shaft resistance, toe resistance, or both. Delineation of unsuitable support layers.
 - b. Shaft diameter and configuration: straight shafts, belled, rock sockets.
 - c. Anticipated support elevation and resulting shaft length.
 - d. Specified or likely construction method: dry, casing, slurry.
 - e. Allowable shaft load for compression, uplift, and lateral loading with consideration of construction method.
 - f. Estimated settlement.

- g. Load tests; specify test locations for maximum utility.
 - 1. Axial compression (specify static, Osterberg cell, or dynamic).
 - 2. Axial tension.
 - 3. Lateral.
 - h. Integrity tests; specify type, frequency, and access tube material and placement, (if required).
 - 1. Low strain pulse echo tests.
 - 2. Cross hole - sonic logging.
 - 3. Down hole - parallel seismic.
 - 4. High strain dynamic tests.
 - i. Anticipated construction difficulties due to boulders, obstructions, groundwater, artesian conditions, unstable ground, *etc.*
 - j. Special notes.
5. Special design considerations.
- a. Seismic design; design earthquake ground acceleration, liquefaction potential (loose saturated sands and silts).
 - b. Lateral earth pressures against retaining walls and high bridge abutments.

VIII. Construction Considerations

- 1. Water table: fluctuations, control in excavation, pumping, tremie seals, *etc.*
- 2. Excavations: safe slopes for open excavations, need for sheeting shoring, *etc.*
- 3. Adjacent structures: protection against damage from excavation, pile driving vibrations, drilled shaft ground loss, drainage, *etc.*
- 4. Special notes.

VIV. Appendix: Graphic Presentations

1. Map showing project location.
2. Detailed plan of the site showing proposed structure(s) borehole locations and existing structures.
3. Laboratory test data.
4. Finished boring logs and interpreted soil profile.

X. Report Distribution

Copies of the completed Foundation Report should be transmitted to:

1. Bridge design section.
2. Roadway design section.
3. Construction section.
4. Project engineer.
5. Residency or maintenance group.
6. Others, as required by agency policy.

14.3 INFORMATION MADE AVAILABLE TO BIDDERS

The information developed during the foundation design is of value to contractors bidding on the project. Disagreement exists among owners, engineers and lawyers as to what information should be made available to the bidders. It is generally in the interest of the highway agency to release all pertinent information prior to the bid.

The finished boring logs and/or generalized soil profile should be included in the contract plans. Other subsurface information, such as soil and rock samples, results of field and laboratory testing and the foundation design report, should be made available for inspection by bidders.

Disclaimers should be used very carefully. "General" disclaimer clauses should be avoided. "Specific" disclaimer clauses are given more weight by the courts in settling contract disputes. A good example of a "specific" disclaimer is provided in the paragraph below. Refer to Cheney and Chassie (1993) for additional information.

"The observed water levels and/or conditions indicated on the subsurface profiles are as recorded at the time of exploration. These water levels and/or conditions may vary considerably, with time, according to the prevailing climate, rainfall or other factors and are otherwise dependent on the duration of and methods used in the explorations program."

REFERENCES

- American Association of State Highway and Transportation Officials [AASHTO], (1988). Manual on Subsurface Investigations. AASHTO Highway Subcommittee on Bridges and Structures, Washington, D.C., 391.
- Cheney, R.S. and Chassie, R.G. (1993). Soils and Foundations Workshop Manual. Second Edition, Report No. HI-88-009, U.S. Department of Transportation, Federal Highway Administration, Office of Engineering, Washington, D.C., 395.

APPENDIX A

List of FHWA Pile Foundation Design and Construction References

- Briaud, J-L. (1989). The Pressuremeter Test for Highway Applications. Report No. FHWA IP-89-008, U.S. Department of Transportation, Federal Highway Administration, Office of Implementation, McLean, 156.
- Briaud, J-L. and Miran, J. (1991). The Cone Penetrometer Test. Report No. FHWA-SA-91-043, U.S. Department of Transportation, Federal Highway Administration, Office of Technology Applications, Washington, D.C., 161.
- Briaud, J-L. and Miran, J. (1992). The Flat Dilatometer Test. Report No. FHWA-SA-91-44, U.S. Department of Transportation, Federal Highway Administration, Office of Technology Applications, Washington, D.C., 102.
- Briaud, J-L., Tucker, L., Lytton, R.L. and Coyle, H.M. (1985). Behavior of Piles and Pile Groups in Cohesionless Soils. Report No. FHWA/RD-83/038, U.S. Department of Transportation, Federal Highway Administration, Office of Research - Materials Division, Washington, D.C., 233.
- Cheney, R.S. and Chassie, R.G. (1993). Soils and Foundations Workshop Manual. Second Edition, Report No. HI-88-009, U.S. Department of Transportation, Federal Highway Administration, Office of Engineering, Washington, D.C., 395.
- Goble, G.G., and Rausche, F. (1986). Wave Equation Analysis of Pile Driving - WEAP86 Program. U.S. Department of Transportation, Federal Highway Administration, Implementation Division, McLean, Volumes I-IV.
- Kyfor, Z.G., Schnore, A.S., Carlo, T.A. and Bailey, P.F. (1992). Static Testing of Deep Foundations. Report No. FHWA-SA-91-042, U.S. Department of Transportation, Federal Highway Administration, Office of Technology Applications, Washington, D.C., 174.

- Lam, I.P. and Martin, G.R. (1986). Seismic Design of Highway Bridge Foundations. Volume II - Design Procedures and Guidelines, Report No. FHWA/RD-86/102, U.S. Department of Transportation, Federal Highway Administration, Office of Engineering and Highway Operations, McLean, 181.
- Mathias, D. and Cribbs, M. (1998). DRIVEN 1.0: A Microsoft Windows™ Based Program for Determining Ultimate Vertical Static Pile Capacity. Report No. FHWA-SA-98-074, U.S. Department of Transportation, Federal Highway Administration, Office of Technology Applications, Washington D.C. 112.
- Osterberg, J.O. (1995). The Osterberg Cell for Load Testing Drilled Shafts and Driven Piles. Report No. FHWA-SA-94-035, U.S. Department of Transportation, Federal Highway Administration, Office of Technology Applications, Washington, D.C., 92.
- Rausche, F., Likins, G.E., Goble, G.G. and Miner, R. (1985). The Performance of Pile Driving Systems. Main Report, U.S. Department of Transportation, Federal Highway Administration, Office of Research and Development, Washington, D.C., Volumes I-IV.
- Reese, L.C. (1984). Handbook on Design of Piles and Drilled Shafts Under Lateral Load. Report No. FHWA-IP-84 11, U.S. Department of Transportation, Federal Highway Administration, Office of Implementation, McLean, 386.
- Urzua, A. (1992). SPILE A Microcomputer Program for Determining Ultimate Vertical Static Pile Capacity. Users Manual, Report No. FHWA-SA-92-044, U.S. Department of Transportation, Federal Highway Administration, Office of Engineering and Office of Technology Applications, Washington, D.C., 58.
- Wang, S-T, and Reese, L.C. (1993). COM624P - Laterally Loaded Pile Analysis Program for the Microcomputer, Version 2.0. Report No. FHWA-SA-91-048, U.S. Department of Transportation, Federal Highway Administration, Office of Technology Applications, Washington, D.C., 504.

APPENDIX B

List of ASTM Pile Design and Testing Specifications

DESIGN

Standard Specification for Welded and Seamless Steel Pipe Piles.
ASTM Designation: A 252

Standard Specification for Round Timber Piles.
ASTM Designation: D 25

Standard Method for Establishing Design Stresses for Round Timber Piles.
ASTM Designation: D 2899

Standard Methods for Establishing Clear Wood Strength Values.
ASTM Designation: D 2555

TESTING

Standard Method for Testing Piles under Axial Compressive Load.
ASTM Designation: D 1143

Standard Method for Testing Individual Piles under Static Axial Tensile Load.
ASTM Designation: D 3689

Standard Method for Testing Piles under Lateral Load.
ASTM Designation: D 3966

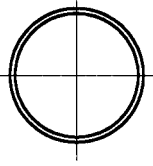
Standard Test Method for High Strain Dynamic Testing of Piles.
ASTM Designation: D 4945

Standard Test Method for Low Strain Dynamic Testing of Piles.
ASTM Designation: D 5882

APPENDIX C

Information and Data on Various Pile Types

	Page
Dimensions and Properties of Pipe Piles	C-3
Data for Steel Monotube Piles	C-17
Typical Prestressed Concrete Pile Sections	C-19
Dimensions and Properties of H-Piles	C-21
Sample Specification for Bitumen Coating on Concrete Piles	C-23
Sample Specification for Bitumen Coating on Steel Piles	C-25



PIPE PILES

Approximate Pile Dimensions and Design Properties

Designation and Outside Diameter	Wall Thickness	Area A	Weight per Meter	Section Properties			Area of Exterior Surface	Inside Cross Sectional Area	Inside Volume	External Collapse Index
				I	S	r				
mm	mm	mm ²	N	mm ⁴ x 10 ⁶	mm ³ x 10 ³	mm	m ² /m	mm ²	m ³ /m	*
PP203	3.58	2,245	173	11.197	110.12	70.61	0.64	30,193	0.0301	266
	4.17	2,607	200	12.903	127.00	70.36	0.64	29,806	0.0298	422
	4.37	2,729	210	13.486	132.74	70.36	0.64	29,677	0.0296	487
	4.55	2,839	218	13.985	137.82	70.36	0.64	29,613	0.0296	548
	4.78	2,974	229	14.651	144.21	70.10	0.64	29,484	0.0293	621
	5.56	3,452	266	16.857	165.51	69.85	0.64	28,968	0.0291	874
PP219	2.77	1,884	145	10.989	100.45	76.45	0.69	35,806	0.0359	97
	3.18	2,155	166	12.570	114.55	76.45	0.69	35,548	0.0356	147
	3.58	2,426	187	14.069	128.47	76.20	0.69	35,290	0.0354	212
	3.96	2,678	206	15.484	141.42	75.95	0.69	35,032	0.0351	288
	4.17	2,813	216	16.233	148.30	75.95	0.69	34,903	0.0349	335
	4.37	2,949	227	16.982	155.02	75.95	0.69	34,774	0.0349	388
	4.55	3,065	236	17.648	160.92	75.95	0.69	34,645	0.0346	438
	4.78	3,213	247	18.481	168.79	75.69	0.69	34,452	0.0344	508
	5.16	3,465	266	19.813	180.26	75.69	0.69	34,258	0.0341	623
	5.56	3,729	287	21.269	195.01	75.44	0.69	33,935	0.0339	744
	6.35	4,245	326	24.017	219.59	75.18	0.69	33,419	0.0334	979
	7.04	4,684	360	26.389	240.89	74.93	0.69	33,032	0.0331	1,180
	7.92	5,258	404	29.344	267.11	74.68	0.69	32,452	0.0324	1,500
	8.18	5,420	417	30.177	275.30	74.68	0.69	32,258	0.0324	1,600
	8.74	5,775	444	31.967	291.69	74.42	0.69	31,935	0.0319	1,820
	9.53	6,271	482	34.506	314.63	74.17	0.69	31,419	0.0314	2,120
	10.31	6,775	520	36.920	337.57	73.91	0.69	30,903	0.0309	2,420
11.13	7,291	559	39.417	358.88	73.66	0.69	30,452	0.0304	2,740	
12.70	8,259	633	44.121	401.48	73.15	0.69	29,484	0.0293	3,340	

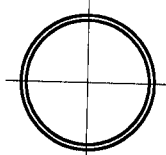
Pile design data converted to SI units from US units published in 1985 version of this manual.

Note: Designer must confirm section properties and local availability of selected pile section.

Material Specifications - ASTM A252

Example of suggested method of designation: PP219 x 2.77

* The External Collapse Index is a non-dimensional function of the diameter to wall thickness ratio and is for general guidance only. The higher the number, the greater is the resistance to collapse.



PIPE PILES

Approximate Pile Dimensions and Design Properties

Designation and Outside Diameter	Wall Thickness	Area A	Weight per Meter	Section Properties			Area of Exterior Surface	Inside Cross Sectional Area	Inside Volume	External Collapse Index
				I	S	r				
mm	mm	mm ²	N	mm ⁴ x 10 ⁶	mm ³ x 10 ³	mm	m ² /m	mm ²	m ³ /m	*
PP254	2.77	2,187	168	17.232	135.68	88.90	0.80	48,516	0.0484	62
	3.05	2,400	185	18.939	148.96	88.65	0.80	48,258	0.0482	83
	3.40	2,678	206	21.020	165.51	88.65	0.80	48,000	0.0479	116
	3.58	2,820	217	22.102	173.70	88.65	0.80	47,871	0.0479	135
	3.81	2,994	230	23.434	185.17	88.39	0.80	47,677	0.0477	163
	4.17	3,271	251	25.515	201.56	88.39	0.80	47,419	0.0474	214
	4.37	3,426	263	26.680	209.75	88.39	0.80	47,226	0.0472	247
	4.55	3,562	274	27.721	217.95	88.14	0.80	47,097	0.0472	279
	4.78	3,742	287	29.053	229.42	88.14	0.80	46,903	0.0469	324
	5.16	4,033	310	31.217	245.81	87.88	0.80	46,645	0.0467	409
	5.56	4,342	334	33.507	263.83	87.88	0.80	46,322	0.0464	515
	5.84	4,555	350	35.088	276.94	87.88	0.80	46,129	0.0462	588
	6.35	4,942	380	37.919	298.24	87.63	0.80	45,742	0.0457	719
PP273	2.77	2,349	181	21.478	157.32	95.50	0.86	56,193	0.0562	50
	3.05	2,587	199	23.559	172.06	95.50	0.86	56,000	0.0559	67
	3.18	2,690	207	24.516	180.26	95.50	0.86	55,871	0.0559	76
	3.40	2,884	222	26.223	191.73	95.25	0.86	55,677	0.0557	93
	3.58	3,032	233	27.513	201.56	95.25	0.86	55,548	0.0554	109
	3.81	3,226	248	29.219	214.67	95.25	0.86	55,355	0.0554	131
	3.96	3,349	258	30.343	222.86	95.25	0.86	55,226	0.0552	148
	4.17	3,516	271	31.800	232.70	95.00	0.86	55,032	0.0549	172
	4.37	3,691	284	33.299	244.17	95.00	0.86	54,839	0.0549	199
	4.55	3,832	295	34.589	254.00	95.00	0.86	54,710	0.0547	224
	4.78	4,026	310	36.212	265.47	94.74	0.86	54,516	0.0544	260
	5.16	4,342	334	38.959	285.13	94.74	0.86	54,193	0.0542	328
	5.56	4,679	359	41.623	306.44	94.49	0.86	53,871	0.0539	414

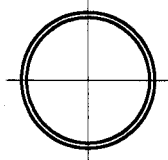
Pile design data converted to SI units from US units published in 1985 version of this manual.

Note: Designer must confirm section properties and local availability of selected pile section.

Material Specifications - ASTM A252

Example of suggested method of designation: PP219 x 2.77

* The External Collapse Index is a non-dimensional function of the diameter to wall thickness ratio and is for general guidance only. The higher the number, the greater is the resistance to collapse.



PIPE PILES

Approximate Pile Dimensions and Design Properties

Designation and Outside Diameter	Wall Thickness	Area A	Weight per Meter	Section Properties			Area of Exterior Surface	Inside Cross Sectional Area	Inside Volume	External Collapse Index
				I	S	r				
mm	mm	mm ²	N	mm ⁴ x 10 ⁸	mm ³ x 10 ³	mm	m ² /m	mm ²	m ³ /m	*
PP273 (cont'd)	5.84	4,904	377	43.704	321.19	94.49	0.86	53,677	0.0537	480
	6.35	5,323	409	47.450	347.41	94.23	0.86	53,226	0.0532	605
	7.09	5,923	455	52.445	383.46	93.98	0.86	52,645	0.0527	781
	7.80	6,517	500	57.024	419.51	93.73	0.86	52,064	0.0522	951
	8.74	7,226	558	63.267	465.39	93.47	0.86	51,290	0.0514	1,180
	9.27	7,678	591	67.013	489.97	93.22	0.86	50,903	0.0509	1,320
	11.13	9,162	704	78.668	576.82	92.71	0.86	49,419	0.0494	1,890
	12.70	10,389	799	88.241	645.65	92.20	0.86	48,193	0.0482	2,380
PP305	3.40	3,226	248	36.587	240.89	106.68	0.96	69,677	0.0697	67
	3.58	3,387	261	38.460	252.36	106.43	0.96	69,677	0.0695	78
	3.81	3,600	277	40.791	267.11	106.43	0.96	69,677	0.0695	94
	4.17	3,936	303	44.537	291.69	106.43	0.96	69,032	0.0690	123
	4.37	4,123	317	46.618	304.80	106.17	0.96	69,032	0.0687	142
	4.55	4,291	330	48.283	317.91	106.17	0.96	68,387	0.0687	161
	4.78	4,503	346	50.780	332.66	106.17	0.96	68,387	0.0685	186
	5.16	4,852	373	54.526	357.24	105.92	0.96	68,387	0.0682	235
	5.56	5,233	402	58.689	383.46	105.92	0.96	67,742	0.0677	296
	5.84	5,484	422	61.186	403.12	105.66	0.96	67,742	0.0675	344
	6.35	5,955	458	66.181	435.90	105.66	0.96	67,097	0.0670	443
	7.14	6,646	513	74.089	485.06	105.16	0.96	66,451	0.0662	616
	7.92	7,420	568	81.581	534.22	104.90	0.96	65,806	0.0655	784
PP324	2.77	2,794	215	36.004	222.86	113.54	1.02	79,355	0.0795	30
	3.18	3,200	246	41.124	254.00	113.28	1.02	79,355	0.0793	45
	3.40	3,426	264	44.121	272.03	113.28	1.02	78,710	0.0790	56
	3.58	3,607	277	46.202	285.13	113.28	1.02	78,710	0.0788	65
	3.81	3,832	295	49.115	303.16	113.29	1.02	78,710	0.0785	78
	3.96	3,981	306	50.780	314.63	113.03	1.02	78,710	0.0785	88
	4.17	4,181	322	53.278	329.38	113.03	1.02	78,064	0.0783	103

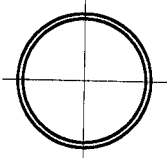
Pile design data converted to SI units from US units published in 1985 version of this manual.

Note: Designer must confirm section properties and local availability of selected pile section.

Material Specifications - ASTM A252

Example of suggested method of designation: PP219 x 2.77

* The External Collapse Index is a non-dimensional function of the diameter to wall thickness ratio and is for general guidance only. The higher the number, the greater is the resistance to collapse.



PIPE PILES

Approximate Pile Dimensions and Design Properties

Designation and Outside Diameter	Wall Thickness	Area A	Weight per Meter	Section Properties			Area of Exterior Surface	Inside Cross Sectional Area	Inside Volume	External Collapse Index
				I	S	r				
mm	mm	mm ²	N	mm ⁴ x 10 ⁶	mm ³ x 10 ³	mm	m ² /m	mm ²	m ³ /m	*
PP324 (cont'd)	4.37	4,387	337	55.775	345.77	113.03	1.02	78,064	0.0780	118
	4.55	4,562	351	58.272	358.88	113.03	1.02	78,064	0.0778	134
	4.78	4,787	368	60.770	376.90	112.78	1.02	77,419	0.0775	155
	5.16	5,162	397	65.765	404.76	112.78	1.02	77,419	0.0773	196
	5.56	5,562	428	70.343	435.90	112.52	1.02	76,774	0.0768	246
	5.84	5,839	449	73.673	455.56	112.52	1.02	76,774	0.0765	286
	6.35	6,336	487	79.916	493.25	112.27	1.02	76,129	0.0760	368
	7.14	7,097	546	89.074	550.61	112.01	1.02	75,484	0.0753	526
	7.92	7,871	605	98.231	606.32	111.76	1.02	74,193	0.0745	684
	8.38	8,323	639	103.225	639.10	111.51	1.02	74,193	0.0740	776
	8.74	8,646	665	107.388	663.68	111.51	1.02	73,548	0.0737	848
	9.53	9,420	723	116.129	717.75	111.25	1.02	72,903	0.0730	1,010
	10.31	10,131	781	124.869	771.83	111.00	1.02	72,258	0.0722	1,170
	11.13	10,905	840	133.610	825.91	110.74	1.02	71,613	0.0715	1,350
12.70	12,389	955	150.676	929.15	109.98	1.02	69,677	0.0700	1,760	
PP356	3.40	3,768	290	58.272	327.74	124.47	1.12	95,484	0.0956	42
	3.58	3,962	305	61.186	345.77	124.47	1.12	95,484	0.0953	49
	3.81	4,213	324	65.348	367.07	124.46	1.12	94,839	0.0951	59
	3.96	4,374	337	67.846	380.18	124.21	1.12	94,839	0.0948	66
	4.17	4,600	354	71.176	399.84	124.21	1.12	94,839	0.0948	77
	4.37	4,820	371	74.505	417.87	124.21	1.12	94,193	0.0946	89
	4.55	5,013	386	77.419	434.26	124.21	1.12	94,193	0.0943	101
	4.78	5,265	405	81.165	455.56	123.95	1.12	94,193	0.0941	117
	5.16	5,678	436	86.992	489.97	123.95	1.12	93,548	0.0936	147
	5.33	5,871	451	89.906	506.36	123.95	1.12	93,548	0.0936	163
	5.56	6,116	470	93.652	527.66	123.70	1.12	92,903	0.0933	815
	5.84	6,420	494	98.231	552.24	123.70	1.12	92,903	0.0928	215
	6.35	6,968	536	106.139	598.13	123.44	1.12	92,258	0.0923	277

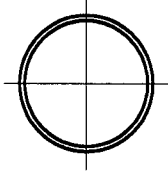
Pile design data converted to SI units from US units published in 1985 version of this manual.

Note: Designer must confirm section properties and local availability of selected pile section.

Material Specifications - ASTM A252

Example of suggested method of designation: PP219 x 2.77

* The External Collapse Index is a non-dimensional function of the diameter to wall thickness ratio and is for general guidance only. The higher the number, the greater is the resistance to collapse.



PIPE PILES

Approximate Pile Dimensions and Design Properties

Designation and Outside Diameter	Wall Thickness	Area A	Weight per Meter	Section Properties			Area of Exterior Surface	Inside Cross Sectional Area	Inside Volume	External Collapse Index
				I	S	r				
mm	mm	mm ²	N	mm ⁴ x 10 ⁶	mm ³ x 10 ³	mm	m ² /m	mm ²	m ³ /m	*
PP356 (cont'd)	7.14	7,807	601	118.626	666.95	123.19	1.12	91,613	0.0916	395
	7.92	8,646	666	130.697	735.78	122.94	1.12	90,968	0.0906	542
	8.74	9,549	732	143.184	806.24	122.68	1.12	89,677	0.0898	691
	9.53	10,389	796	155.254	873.43	122.43	1.12	89,032	0.0890	835
	11.13	12,065	926	178.563	1,006.17	121.92	1.12	87,097	0.0873	1,130
	11.91	12,839	989	190.218	1,070.08	121.67	1.12	86,451	0.0865	1,280
	12.70	13,678	1,052	201.456	1,132.35	121.41	1.12	85,806	0.0855	1,460
PP406	3.40	4,310	331	87.409	430.98	142.49	1.28	125,161	1.2542	28
	3.58	4,529	348	91.987	452.28	142.49	1.28	125,161	0.1252	33
	3.81	4,820	371	97.814	480.14	142.24	1.28	125,161	0.1249	39
	3.96	5,007	385	101.560	499.81	142.24	1.28	124,516	0.1247	44
	4.17	5,265	405	106.555	524.39	142.24	1.28	124,516	0.1244	52
	4.37	5,516	424	111.550	548.97	142.24	1.28	124,516	0.1242	60
	4.55	5,742	441	115.712	570.27	141.99	1.28	123,871	0.1239	67
	4.78	6,026	463	121.540	598.13	141.99	1.28	123,871	0.1237	78
	5.16	6,517	500	130.697	644.01	141.99	1.28	123,226	0.1232	98
	5.56	7,033	539	140.686	693.17	141.73	1.28	122,580	0.1227	124
	5.84	7,355	565	147.346	725.95	141.73	1.28	122,580	0.1224	144
	6.35	8,000	614	159.833	786.58	141.48	1.28	121,935	0.1217	185
	7.14	8,968	688	178.563	878.35	141.22	1.28	120,645	0.1207	264
	7.92	9,936	763	196.877	970.11	140.97	1.28	120,000	0.1199	362
	8.74	10,905	839	216.024	1,061.88	140.72	1.28	118,709	0.1189	487
	9.53	11,873	913	233.922	1,152.01	140.46	1.28	118,064	0.1179	617
	11.13	13,807	1,062	270.134	1,328.99	139.70	1.28	116,129	0.1159	874
11.91	14,775	1,135	287.616	1,414.20	139.45	1.28	114,838	0.1149	1,000	
12.70	15,679	1,208	304.681	1,499.42	139.19	1.28	114,193	0.1141	1,130	

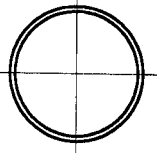
Pile design data converted to SI units from US units published in 1985 version of this manual.

Note: Designer must confirm section properties and local availability of selected pile section.

Material Specifications - ASTM A252

Example of suggested method of designation: PP219 x 2.77

* The External Collapse Index is a non-dimensional function of the diameter to wall thickness ratio and is for general guidance only. The higher the number, the greater is the resistance to collapse.



PIPE PILES

Approximate Pile Dimensions and Design Properties

Designation and Outside Diameter	Wall Thickness	Area A	Weight per Meter	Section Properties			Area of Exterior Surface	Inside Cross Sectional Area	Inside Volume	External Collapse Index
				I	S	r				
mm	mm	mm ²	N	mm ⁴ x 10 ⁶	mm ³ x 10 ³	mm	m ² /m	mm ²	m ³ /m	*
PP457	3.58	5,104	392	131.113	573.55	160.27	1.44	159,355	0.1590	23
	4.37	6,213	478	159,417	696.45	160.02	1.44	158,064	0.1580	42
	4.78	6,775	522	173,569	760.36	160.02	1.44	157,419	0.1573	55
	5.16	7,291	563	186,888	817.71	159.77	1.44	156,774	0.1568	69
	5.56	7,871	607	201,456	879.99	159.77	1.44	156,129	0.1563	87
	5.84	8,259	637	211,029	922.59	159.51	1.44	156,129	0.1558	101
	6.35	8,968	692	228,511	999.61	159.51	1.44	155,484	0.1553	129
	7.14	10,065	776	255,566	1,117.60	159.26	1.44	154,193	0.1540	184
	7.92	11,163	860	282,205	1,235.58	158.75	1.44	152,903	0.1530	253
	8.74	12,323	947	309,676	1,353.57	158.50	1.44	151,613	0.1518	341
	9.53	13,420	1,030	335,899	1,468.28	158.24	1.44	150,967	0.1508	443
	10.31	14,452	1,113	361,705	1,581.35	157.99	1.44	149,677	0.1498	559
	11.13	15,615	1,199	387,928	1,704.25	157.73	1.44	148,387	0.1485	675
	11.91	16,646	1,281	413,318	1,802.58	157.48	1.44	147,742	0.1475	788
12.70	17,743	1,364	437,043	1,917.29	157.23	1.44	146,451	0.1465	900	
PP508	3.58	5,678	436	180,644	711.20	178.31	1.60	196,774	0.1969	17
	4.37	6,904	531	219,354	863.60	178.05	1.60	195,483	0.1957	30
	4.78	7,549	581	238,917	940.62	177.80	1.60	194,838	0.1952	40
	5.16	8,130	626	257,647	1,014.36	177.80	1.60	194,838	0.1947	50
	5.56	8,775	675	277,210	1,091.38	177.55	1.60	194,193	0.1939	63
	6.35	10,002	769	314,671	1,238.86	177.29	1.60	192,903	0.1926	94
	7.14	11,226	864	352,132	1,386.35	177.04	1.60	191,613	0.1914	134
	7.92	12,452	957	389,176	1,532.19	176.78	1.60	190,322	0.1901	184
	8.74	13,678	1,054	428,718	1,687.87	176.53	1.60	189,032	0.1889	247

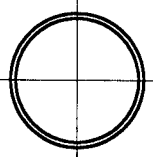
Pile design data converted to SI units from US units published in 1985 version of this manual.

Note: Designer must confirm section properties and local availability of selected pile section.

Material Specifications - ASTM A252

Example of suggested method of designation: PP219 x 2.77

* The External Collapse Index is a non-dimensional function of the diameter to wall thickness ratio and is for general guidance only. The higher the number, the greater is the resistance to collapse.



PIPE PILES

Approximate Pile Dimensions and Design Properties

Designation and Outside Diameter	Wall Thickness	Area A	Weight per Meter	Section Properties			Area of Exterior Surface	Inside Cross Sectional Area	Inside Volume	External Collapse Index
				I	S	r				
mm	mm	mm ²	N	mm ⁴ x 10 ⁶	mm ³ x 10 ³	mm	m ² /m	mm ²	m ³ /m	*
PP508 (cont'd)	9.53	14,904	1,147	462.017	1,818.96	176.28	1.60	187,742	0.1879	321
	10.31	16,130	1,240	499.478	1,966.45	176.02	1.60	186,451	0.1866	409
	11.13	17,357	1,335	536.939	2,113.93	175.77	1.60	185,161	0.1854	515
	11.91	18,583	1,428	570.237	2,245.03	175.51	1.60	183,871	0.1841	618
	12.70	19,743	1,520	607.698	2,392.51	175.26	1.60	183,225	0.1829	719
PP559	4.37	7,613	585	292.611	1,047.13	196.09	1.76	237,419	0.2375	23
	4.78	8,323	639	318.833	1,142.18	195.83	1.76	236,774	0.2370	30
	5.56	9,678	743	370.030	1,324.07	195.58	1.76	235,483	0.2355	47
	6.35	11,034	847	420.394	1,504.33	195.33	1.76	234,193	0.2343	70
	7.14	12,389	951	470.342	1,687.87	195.07	1.76	232,903	0.2328	100
	7.92	13,744	1,055	520.289	1,868.13	194.82	1.76	231,612	0.2315	138
	8.74	15,099	1,161	570.237	2,048.38	194.56	1.76	230,322	0.2303	185
	9.53	16,454	1,264	620.185	2,212.25	194.31	1.76	229,032	0.2288	241
	10.31	17,743	1,366	670.133	2,392.51	194.06	1.76	227,741	0.2275	306
	11.13	19,162	1,472	715.918	2,572.77	193.55	1.76	225,806	0.2260	386
	11.91	20,454	1,574	765.866	2,736.64	193.29	1.76	224,516	0.2248	475
PP610	4.37	8,323	639	380.436	1,248.69	213.87	1.91	283,870	0.2834	18
	4.78	9,097	698	414.983	1,361.77	213.87	1.91	282,580	0.2834	23
	5.56	10,582	812	482.828	1,579.71	213.61	1.91	281,290	0.2809	36
	6.35	12,065	925	549.425	1,802.58	213.36	1.91	279,999	0.2809	54
	7.14	13,486	1,039	611.860	2,015.61	213.11	1.91	278,064	0.2784	77
	7.92	14,970	1,152	678.457	2,228.64	212.85	1.91	276,774	0.2759	106
	8.74	16,517	1,268	745.054	2,441.67	212.34	1.91	275,483	0.2759	142
	9.53	17,937	1,381	807.489	2,654.70	212.09	1.91	274,193	0.2734	185

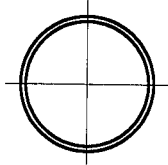
Pile design data converted to SI units from US units published in 1985 version of this manual.

Note: Designer must confirm section properties and local availability of selected pile section.

Material Specifications - ASTM A252

Example of suggested method of designation: PP219 x 2.77

* The External Collapse Index is a non-dimensional function of the diameter to wall thickness ratio and is for general guidance only. The higher the number, the greater is the resistance to collapse.



PIPE PILES

Approximate Pile Dimensions and Design Properties

Designation and Outside Diameter	Wall Thickness	Area A	Weight per Meter	Section Properties			Area of Exterior Surface	Inside Cross Sectional Area	Inside Volume	External Collapse Index
				I	S	r				
mm	mm	mm ²	N	mm ⁴ x 10 ⁶	mm ³ x 10 ³	mm	m ² /m	mm ²	m ³ /m	*
PP610 (cont'd)	10.31	19,421	1,493	869.924	2,867.74	211.84	1.91	272,258	0.2734	235
	11.13	20,904	1,608	936.521	3,080.77	211.58	1.91	270,967	0.2709	296
	11.91	22,388	1,720	998.955	3,277.41	211.33	1.91	269,677	0.2684	364
	12.70	23,809	1,831	1,061.390	3,474.06	211.07	1.91	267,741	0.2684	443
PP660	6.35	13,033	1,003	699.269	2,113.93	231.14	2.08	329,677	0.3286	43
	7.14	14,646	1,126	782.515	2,359.74	230.89	2.08	327,741	0.3286	61
	7.92	16,259	1,249	865.761	2,621.93	230.63	2.08	326,451	0.3261	83
	8.74	17,872	1,376	949.008	2,884.12	230.38	2.08	324,515	0.3236	112
	9.53	19,485	1,498	1,032.254	3,129.93	230.12	2.08	323,225	0.3236	145
	10.31	21,034	1,620	1,111.338	3,375.74	229.87	2.08	321,290	0.3211	184
	11.13	22,711	1,745	1,194.584	3,621.54	229.62	2.08	319,999	0.3211	232
	11.91	24,260	1,866	1,277.830	3,867.35	229.36	2.08	318,064	0.3186	286
	12.70	25,873	1,987	1,356.914	4,113.15	229.11	2.08	316,774	0.3161	347
	14.27	28,969	2,228	1,510.920	4,588.38	228.60	2.08	313,548	0.3135	495
	15.88	32,132	2,472	1,669.088	5,063.60	227.84	2.08	310,322	0.3110	656
	17.48	35,292	2,714	1,823.094	5,522.44	227.33	2.08	307,096	0.3060	814
	19.05	38,389	2,951	1,977.099	5,981.28	226.82	2.08	303,870	0.3035	970
PP711	6.35	14,065	1,081	874.086	2,458.06	249.17	2.23	383,225	0.3838	34
	7.14	15,807	1,214	978.144	2,753.03	248.92	2.23	381,290	0.3813	48
	7.92	17,486	1,346	1,082.202	3,047.99	248.67	2.23	379,999	0.3788	66
	8.74	19,291	1,483	1,190.422	3,342.96	248.41	2.23	378,064	0.3788	89
	9.53	20,969	1,615	1,294.480	3,637.93	248.16	2.23	376,128	0.3763	116
	10.31	22,711	1,746	1,394.375	3,916.51	247.90	2.23	374,838	0.3737	147
	11.13	24,453	1,881	1,498.433	4,211.48	247.65	2.23	372,902	0.3737	185
	11.91	26,195	2,012	1,598.329	4,506.44	247.40	2.23	370,967	0.3712	228

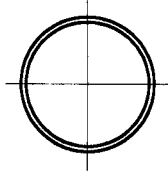
Pile design data converted to SI units from US units published in 1985 version of this manual.

Note: Designer must confirm section properties and local availability of selected pile section.

Material Specifications - ASTM A252

Example of suggested method of designation: PP219 x 2.77

* The External Collapse Index is a non-dimensional function of the diameter to wall thickness ratio and is for general guidance only. The higher the number, the greater is the resistance to collapse.



PIPE PILES

Approximate Pile Dimensions and Design Properties

Designation and Outside Diameter	Wall Thickness	Area A	Weight per Meter	Section Properties			Area of Exterior Surface	Inside Cross Sectional Area	Inside Volume	External Collapse Index
				l	S	r				
mm	mm	mm ²	N	mm ⁴ x 10 ⁶	mm ³ x 10 ³	mm	m ² /m	mm ²	m ³ /m	*
PP711 (cont'd)	12.70	27,874	2,143	1,698.224	4,785.02	246.89	2.23	369,677	0.3687	277
	14.27	31,229	2,403	1,898.015	5,342.18	246.38	2.23	365,806	0.3587	395
	15.88	34,713	2,667	2,097.806	5,899.34	245.87	2.23	362,580	0.3612	544
	17.48	38,068	2,929	2,293.435	6,440.12	245.36	2.23	359,354	0.3587	691
	19.05	41,423	3,185	2,480.739	6,980.89	244.86	2.23	356,128	0.3562	835
PP762	6.35	15,099	1,159	1,078.039	2,818.58	266.70	2.39	440,644	0.4415	28
	7.14	16,904	1,302	1,207.071	3,162.70	266.70	2.39	439,354	0.4390	39
	7.92	18,775	1,444	1,336.103	3,506.83	266.70	2.39	437,418	0.4365	54
	8.74	20,646	1,590	1,465.135	3,850.96	266.70	2.39	435,483	0.4365	72
	9.53	22,517	1,731	1,594.166	4,178.70	266.70	2.39	433,548	0.4340	94
	10.31	24,324	1,873	1,719.036	4,522.83	266.70	2.39	431,612	0.4314	120
	11.13	26,261	2,018	1,848.068	4,850.57	266.70	2.39	429,677	0.4289	150
	11.91	28,066	2,159	1,972.937	5,178.31	264.16	2.39	427,741	0.4289	185
	12.70	29,874	2,299	2,097.806	5,506.05	264.16	2.39	426,451	0.4264	225
	14.27	33,550	2,578	2,343.383	6,145.15	264.16	2.39	422,580	0.4214	321
	15.88	37,228	2,861	2,588.959	6,800.63	264.16	2.39	418,709	0.4189	443
	17.48	40,907	3,143	2,834.536	7,439.73	264.16	2.39	415,483	0.4164	584
19.05	44,454	3,419	3,071.788	8,062.44	261.62	2.39	411,612	0.4114	719	
PP813	6.35	16,065	1,237	1,306.967	3,211.86	284.48	2.55	502,580	0.5017	23
	7.14	18,067	1,389	1,465.135	3,605.15	284.488	2.55	500,644	0.5017	32
	7.92	20,067	1,541	1,623.303	3,998.44	284.48	2.55	498,709	0.4992	44
	8.74	22,067	1,697	1,785.633	4,391.73	284.48	2.55	496,773	0.4967	60
	9.53	24,067	1,848	1,939.638	4,768.64	284.48	2.55	494,838	0.4942	77
	10.31	26,002	1,999	2,093.644	5,145.54	284.48	2.55	492,902	0.4916	98
	11.13	28,003	2,155	2,251.812	5,538.83	284.48	2.55	490,967	0.4916	124
11.91	30,003	2,305	2,401.655	5,915.73	281.94	2.55	489,031	0.4891	152	

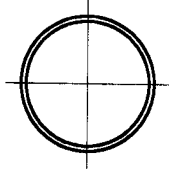
Pile design data converted to SI units from US units published in 1985 version of this manual.

Note: Designer must confirm section properties and local availability of selected pile section.

Material Specifications - ASTM A252

Example of suggested method of designation: PP219 x 2.77

* The External Collapse Index is a non-dimensional function of the diameter to wall thickness ratio and is for general guidance only. The higher the number, the greater is the resistance to collapse.



PIPE PILES

Approximate Pile Dimensions and Design Properties

Designation and Outside Diameter	Wall Thickness	Area A	Weight per Meter	Section Properties			Area of Exterior Surface	Inside Cross Sectional Area	Inside Volume	External Collapse Index
				I	S	r				
mm	mm	mm ²	N	mm ⁴ x 10 ⁶	mm ³ x 10 ³	mm	m ² /m	mm ²	m ³ /m	*
PP813 (cont'd)	12.70	31,937	2,455	2,555.661	6,292.63	281.94	2.55	487,096	0.4866	185
	14.27	35,810	2,754	2,855.348	7,030.05	281.94	2.55	483,225	0.4841	264
	15.88	39,744	3,056	3,155.034	7,767.47	281.94	2.55	479,354	0.4791	364
	17.48	43,680	3,358	3,454.721	8,504.89	281.94	2.55	475,483	0.4741	487
	19.05	47,488	3,653	3,741.921	9,209.53	281.94	2.55	471,612	0.4716	617
PP864	6.35	17,099	1,315	1,569.192	3,637.93	302.26	2.71	568,386	0.5694	19
	7.14	19,228	1,477	1,760.659	4,080.38	302.26	2.71	566,450	0.5669	27
	7.92	21,293	1,638	1,947.963	4,522.83	302.26	2.71	564,515	0.5644	37
	8.74	23,485	1,804	2,143.592	4,965.28	302.26	2.71	562,580	0.5619	50
	9.53	25,551	1,965	2,330.896	5,391.34	302.26	2.71	559,999	0.5594	64
	10.31	27,615	2,126	2,518.200	5,833.79	302.26	2.71	558,063	0.5569	82
	11.13	29,808	2,291	2,705.504	6,276.25	302.26	2.71	556,128	0.5569	103
	11.91	31,873	2,451	2,888.646	6,702.31	302.26	2.71	554,192	0.5544	127
	12.70	33,938	2,611	3,071.788	7,111.99	299.72	2.71	551,612	0.5518	154
	14.27	38,068	2,929	3,433.909	7,964.11	299.72	2.71	547,741	0.5468	219
	15.88	42,262	3,251	3,800.193	8,799.85	299.72	2.71	543,225	0.5443	303
	17.48	46,454	3,572	4,158.152	9,635.59	299.72	2.71	539,354	0.5393	405
	19.05	50,519	3,887	4,495.299	10,438.56	299.72	2.71	535,483	0.5343	527
	22.23	58,779	4,517	5,202.893	12,044.49	297.18	2.71	527,096	0.5268	767
25.40	67,102	5,143	5,868.863	13,617.65	297.18	2.71	518,709	0.5192	1,010	
PP914	6.35	18,130	1,393	1,868.879	4,080.38	320.04	2.87	638,708	0.6396	16
	7.14	20,325	1,564	2,093.644	4,571.99	320.04	2.87	636,128	0.6371	23
	7.92	22,582	1,735	2,318.409	5,063.60	320.04	2.87	634,192	0.6346	31
	8.74	24,840	1,912	2,547.336	5,571.60	320.04	2.87	631,612	0.6321	42

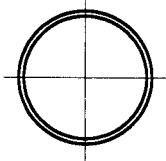
Pile design data converted to SI units from US units published in 1985 version of this manual.

Note: Designer must confirm section properties and local availability of selected pile section.

Material Specifications - ASTM A252

Example of suggested method of designation: PP219 x 2.77

* The External Collapse Index is a non-dimensional function of the diameter to wall thickness ratio and is for general guidance only. The higher the number, the greater is the resistance to collapse.



PIPE PILES

Approximate Pile Dimensions and Design Properties

Designation and Outside Diameter	Wall Thickness	Area A	Weight per Meter	Section Properties			Area of Exterior Surface	Inside Cross Sectional Area	Inside Volume	External Collapse Index
				I	S	r				
mm	mm	mm ²	N	mm ⁴ x 10 ⁸	mm ³ x 10 ³	mm	m ² /m	mm ²	m ³ /m	*
PP914 (cont'd)	9.53	27,098	2,082	2,772.101	6,063.21	320.04	2.87	629,676	0.6296	54
	10.31	29,292	2,252	2,992.704	6,538.44	320.04	2.87	627,096	0.6271	69
	11.13	31,550	2,428	3,221.631	7,046.44	320.04	2.87	625,160	0.6246	87
	11.91	33,808	2,597	3,438.072	7,521.66	320.04	2.87	623,225	0.6221	107
	12.70	36,002	2,766	3,658.674	7,996.89	320.04	2.87	620,644	0.6221	129
	14.27	40,390	3,104	4,087.393	8,947.34	317.50	2.87	616,128	0.6171	184
	15.88	44,841	3,446	4,536.923	9,897.79	317.50	2.87	611,612	0.6120	254
	17.48	49,230	3,786	4,953.154	10,831.85	317.50	2.87	607,741	0.6070	341
	19.05	53,616	4,120	5,369.385	11,749.52	317.50	2.87	603,225	0.6020	443
	22.23	62,326	4,790	6,201.848	13,568.49	314.96	2.87	594,192	0.5945	674
	25.40	70,972	5,455	7,034.311	15,338.29	314.96	2.87	585,805	0.5870	900
31.75	87,747	6,770	8,574.367	18,845.12	312.42	2.87	568,386	0.5694	1,380	
PP965	6.35	19,099	1,471	2,197.702	4,555.60	337.82	3.03	709,676	0.7124	14
	7.14	21,485	1,652	2,464.090	5,112.76	337.82	3.03	709,676	0.7099	19
	7.92	23,809	1,833	2,730.478	5,653.54	337.82	3.03	709,676	0.7074	26
	8.74	26,261	2,019	3,001.029	6,227.08	337.82	3.03	703,224	0.7049	35
	9.53	28,582	2,199	3,263.254	6,767.86	337.82	3.03	703,224	0.7023	46
	10.31	30,971	2,379	3,525.480	7,308.63	337.82	3.03	703,224	0.6998	59
	11.13	33,358	2,564	3,796.031	7,865.79	337.82	3.03	696,773	0.6973	74
	11.91	35,680	2,743	4,054.094	8,406.56	337.82	3.03	696,773	0.6973	90
	12.70	38,002	2,922	4,328.807	8,930.95	337.82	3.03	696,773	0.6923	110
	14.27	42,649	3,279	4,828.285	9,996.11	335.28	3.03	690,321	0.6898	156
	15.88	47,359	3,641	5,327.762	11,061.27	335.28	3.03	683,870	0.6848	216
17.48	52,003	4,001	5,827.240	12,110.04	335.28	3.03	677,418	0.6798	289	

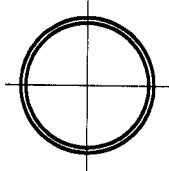
Pile design data converted to SI units from US units published in 1985 version of this manual.

Note: Designer must confirm section properties and local availability of selected pile section.

Material Specifications - ASTM A252

Example of suggested method of designation: PP219 x 2.77

* The External Collapse Index is a non-dimensional function of the diameter to wall thickness ratio and is for general guidance only. The higher the number, the greater is the resistance to collapse.



PIPE PILES

Approximate Pile Dimensions and Design Properties

Designation and Outside Diameter	Wall Thickness	Area A	Weight per Meter	Section Properties			Area of Exterior Surface	Inside Cross Sectional Area	Inside Volume	External Collapse Index
				I	S	r				
mm	mm	mm ²	N	mm ⁴ x 10 ⁶	mm ³ x 10 ³	mm	m ² /m	mm ²	m ³ /m	*
PP965 (cont'd)	19.05	56,649	4,354	6,326.718	13,142.43	335.28	3.03	677,418	0.6748	376
	22.23	65,810	5,063	7,325.673	15,174.42	332.74	3.03	664,515	0.6647	590
	25.40	74,843	5,767	8,283.005	17,206.42	332.74	3.03	658,063	0.6572	805
	31.75	92,909	7,160	10,156.047	20,975.44	330.20	3.03	638,708	0.6396	1,230
	38.10	110,974	8,533	11,945.842	24,744.47	327.66	3.03	620,644	0.6221	1,780
PP1016	7.92	25,098	1,930	3,188.333	6,276.25	355.60	3.20	787,095	0.7851	23
	8.74	27,679	2,126	3,508.831	6,898.95	355.60	3.20	780,644	0.7826	30
	9.53	30,131	2,316	3,812.680	7,505.28	355.60	3.20	780,644	0.7801	39
	10.31	32,583	2,505	4,120.691	8,111.60	355.60	3.20	780,644	0.7776	50
	11.13	35,099	2,701	4,453.676	8,734.31	355.60	3.20	774,192	0.7751	63
	11.91	37,551	2,890	4,745.038	9,324.24	355.60	3.20	774,192	0.7726	77
	12.70	40,002	3,078	5,036.400	9,914.17	355.60	3.20	767,740	0.7701	94
	14.27	44,906	3,454	5,619.124	11,094.04	353.06	3.20	767,740	0.7651	134
	15.88	49,874	3,836	6,243.471	12,273.91	353.06	3.20	761,289	0.7600	185
	17.48	54,842	4,215	6,826.195	13,453.78	353.06	3.20	754,837	0.7550	247
	19.05	59,681	4,588	7,408.919	14,600.87	353.06	3.20	748,386	0.7500	321
	22.23	69,682	5,336	8,574.367	16,878.68	350.52	3.20	741,934	0.7425	514
	25.40	79,360	6,078	9,698.192	19,172.86	350.52	3.20	729,031	0.7324	719
	31.75	98,070	7,549	11,904.219	23,433.50	347.98	3.20	709,676	0.7124	1,130
	38.10	116,781	9,001	14,026.999	27,530.27	345.44	3.20	696,773	0.6923	1,620
44.45	135,492	10,433	16,024.910	31,627.03	342.90	3.20	677,418	0.6748	2,140	
PP1067	7.92	26,389	2,027	3,696.135	6,931.73	373.38	3.35	864,514	0.8679	20
	8.74	29,034	2,233	4,066.581	7,619.98	373.38	3.35	864,514	0.8654	26
	9.53	31,615	2,433	4,412.053	8,291.85	373.38	3.35	864,514	0.8629	34
	10.31	34,260	2,632	4,786.661	8,947.34	373.38	3.35	864,514	0.8604	43

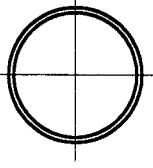
Pile design data converted to SI units from US units published in 1985 version of this manual.

Note: Designer must confirm section properties and local availability of selected pile section.

Material Specifications - ASTM A252

Example of suggested method of designation: PP219 x 2.77

* The External Collapse Index is a non-dimensional function of the diameter to wall thickness ratio and is for general guidance only. The higher the number, the greater is the resistance to collapse.



PIPE PILES

Approximate Pile Dimensions and Design Properties

Designation and Outside Diameter	Wall Thickness	Area A	Weight per Meter	Section Properties			Area of Exterior Surface	Inside Cross Sectional Area	Inside Volume	External Collapse Index
				I	S	r				
mm	mm	mm ²	N	mm ⁴ x 10 ⁶	mm ³ x 10 ³	mm	m ² /m	mm ²	m ³ /m	*
PP1067 (cont'd)	11.13	36,905	2,837	5,161.270	9,635.59	373.38	3.35	858,063	0.8579	54
	11.91	39,486	3,036	5,494.255	10,291.08	373.38	3.35	851,611	0.8554	67
	12.70	42,067	3,234	5,827.240	10,946.56	373.38	3.35	851,611	0.8528	81
	14.27	47,229	3,630	6,534.833	12,257.52	373.38	3.35	845,160	0.8478	116
	15.88	52,390	4,030	7,242.427	13,568.49	370.84	3.35	838,708	0.8403	159
	17.48	57,616	4,430	7,950.020	14,863.07	370.84	3.35	838,708	0.8353	213
	19.05	62,713	4,822	8,615.991	16,141.26	370.84	3.35	832,256	0.8303	277
	22.23	72,908	5,608	9,947.931	18,681.25	368.30	3.35	819,353	0.8202	443
	25.40	83,231	6,390	11,279.872	21,139.31	368.30	3.35	812,902	0.8102	641
	31.75	103,232	7,939	13,818.883	25,891.56	365.76	3.35	793,547	0.7901	1,030
	38.10	123,233	9,468	16,316.272	30,643.81	363.22	3.35	767,740	0.7701	1,460
	44.45	142,589	10,978	18,688.791	35,068.32	360.68	3.35	748,386	0.7500	1,970
50.80	161,945	12,468	20,978.064	39,328.95	360.68	3.35	729,031	0.7324	2,470	
PP1118	8.74	30,453	2,341	4,661.792	8,373.79	391.16	3.51	948,385	0.9507	23
	9.53	33,163	2,550	5,078.023	9,111.21	391.16	3.51	948,385	0.9482	30
	10.31	35,873	2,759	5,494.255	9,832.24	391.16	3.51	941,934	0.9457	38
	11.13	38,647	2,974	5,910.486	10,586.04	391.16	3.51	941,934	0.9432	47
	11.91	41,357	3,182	6,326.718	11,323.46	391.16	3.51	941,934	0.9406	58
	12.70	44,067	3,390	6,742.949	12,044.49	391.16	3.51	935,482	0.9381	70
	15.88	54,971	4,225	8,324.629	14,928.62	388.62	3.51	929,030	0.9256	138
	19.05	65,810	5,056	9,906.308	17,698.03	388.62	3.51	916,127	0.9156	241
	22.23	76,779	5,881	11,487.987	20,483.83	388.62	3.51	903,224	0.9055	384
	25.40	87,102	6,702	12,986.420	23,269.63	386.08	3.51	896,772	0.8930	571

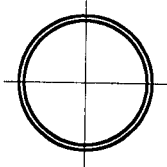
Pile design data converted to SI units from US units published in 1985 version of this manual.

Note: Designer must confirm section properties and local availability of selected pile section.

Material Specifications - ASTM A252

Example of suggested method of designation: PP219 x 2.77

* The External Collapse Index is a non-dimensional function of the diameter to wall thickness ratio and is for general guidance only. The higher the number, the greater is the resistance to collapse.



PIPE PILES

Approximate Pile Dimensions and Design Properties

Designation and Outside Diameter	Wall Thickness	Area A	Weight per Meter	Section Properties			Area of Exterior Surface	Inside Cross Sectional Area	Inside Volume	External Collapse Index
				I	S	r				
mm	mm	mm ²	N	mm ⁴ x 10 ⁶	mm ³ x 10 ³	mm	m ² /m	mm ²	m ³ /m	*
PP1118 (cont'd)	31.75	108,394	8,328	15,983.287	28,513.49	383.54	3.51	870,966	0.8729	941
	38.10	129,040	9,936	18,855.284	33,757.35	381.00	3.51	851,611	0.8528	1,300
	44.45	149,686	11,524	21,602.411	38,673.47	381.00	3.51	832,256	0.8303	1,810
	50.80	170,333	13,092	24,266.292	43,425.72	378.46	3.51	812,902	0.8102	2,290
	57.15	190,334	14,641	26,846.927	48,014.10	375.92	3.51	793,547	0.7901	2,770
PP1219	8.74	33,228	2,555	6,076.979	9,979.72	426.72	3.84	1,135,482	1.1338	18
	9.53	36,196	2,784	6,618.080	10,864.62	426.72	3.84	1,129,030	1.1313	23
	10.31	39,164	3,012	7,159.181	11,733.14	426.72	3.84	1,129,030	1.1288	29
	11.13	42,196	3,247	7,700.281	12,634.43	426.72	3.84	1,122,578	1.1263	36
	11.91	45,164	3,474	8,241.382	13,502.94	426.72	3.84	1,122,578	1.1212	45
	12.70	48,132	3,702	8,740.860	14,371.46	426.72	3.84	1,116,127	1.1187	54
	15.88	60,004	4,615	10,863.640	17,861.90	426.72	3.84	1,109,675	1.1087	106
	19.05	71,617	5,523	12,944.797	21,139.31	424.18	3.84	1,096,772	1.0962	185
	22.23	83,876	6,427	14,984.331	24,580.60	424.18	3.84	1,083,869	1.0836	295
	25.40	95,490	7,325	16,982.242	27,858.01	421.64	3.84	1,070,966	1.0711	443
	31.75	118,717	9,108	20,894.818	34,248.96	419.10	3.84	1,051,611	1.0485	787
	38.10	141,299	10,871	24,682.524	40,476.05	416.56	3.84	1,025,804	1.0259	1,130
	44.45	163,881	12,614	28,345.360	46,539.26	416.56	3.84	1,006,450	1.0034	1,530
	50.80	186,463	14,339	31,883.327	52,274.73	414.02	3.84	980,643	0.9808	1,970
	57.15	208,400	16,043	35,296.425	57,846.34	411.48	3.84	961,288	0.9582	2,410
63.50	230,336	17,729	38,626.276	63,254.07	408.94	3.84	935,482	0.9381	2,850	

Pile design data converted to SI units from US units published in 1985 version of this manual.

Note: Designer must confirm section properties and local availability of selected pile section.

Material Specifications - ASTM A252

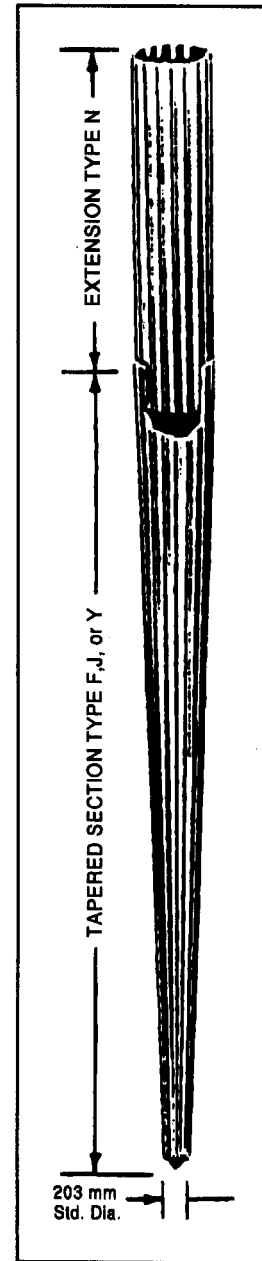
Example of suggested method of designation: PP219 x 2.77

* The External Collapse Index is a non-dimensional function of the diameter to wall thickness ratio and is for general guidance only. The higher the number, the greater is the resistance to collapse.

MONOTUBE PILES

Standard Monotube Weights and Volumes

TYPE	SIZE POINT DIAMETER x BUTT DIAMETER x LENGTH	Weight (N) per m				EST. CONC. VOL. m ³
		9 GA.	7 GA.	5 GA.	3 GA.	
F Taper 3.6 mm per Meter	216 mm x 305 mm x 7.62 m	248	292	350	409	0.329
	203 mm x 305 mm x 9.14 m	233	292	336	394	0.420
	216 mm x 356 mm x 12.19 m	277	321	379	452	0.726
	203 mm x 406 mm x 18.29 m	292	350	409	482	1.284
	203 mm x 457 mm x 22.86 m	-	379	452	511	1.979
J Taper 6.4 mm per Meter	203 mm x 305 mm x 5.18 m	248	292	336	394	0.244
	203 mm x 356 mm x 7.62 m	263	321	379	438	0.443
	203 mm x 406 mm x 10.06 m	292	350	409	467	0.726
	203 mm x 457 mm x 12.19 m	-	379	438	511	1.047
Y Taper 10.2 mm per Meter	203 mm x 305 mm x 3.05 m	248	292	350	409	0.138
	203 mm x 356 mm x 4.57 m	277	321	379	438	0.260
	203 mm x 406 mm x 6.10 m	292	350	409	482	0.428
	203 mm x 457 mm x 7.62 m	-	379	452	511	0.657



Extensions (Overall Length 0.305 m Greater than indicated)

TYPE	DIAMETER + LENGTH	9 GA.	7 GA.	5 GA.	3 GA.	m ³ / m
N 12	305 mm x 305 mm x 6.10 / 12.19 m	292	350	409	482	0.065
N 14	356 mm x 356 mm x 6.10 m / 12.19 m	350	423	496	598	0.088
N 16	406 mm x 406 mm x 6.10 m / 12.19 m	409	482	569	671	0.113
N 18	457 mm x 457 mm x 6.10 m / 12.19 m	-	555	642	759	0.145

Note: Designer must confirm section properties of selected pile section.

Pile design data converted to SI units from US units published in Monotube Pile Corporation Catalog 592.

MONOTUBE PILES

Physical Properties

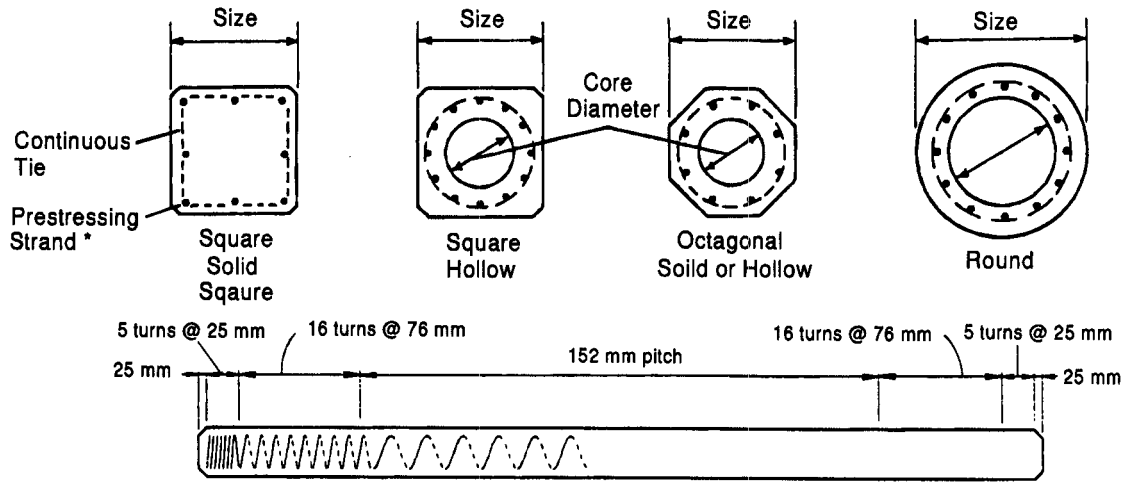
STEEL THICKNESS	POINTS		BUTTS OF PILE SECTIONS							
	203 mm	216 mm	305 mm				356 mm			
	A mm ²	A mm ²	A mm ²	I mm ⁴ x 10 ⁶	S mm ³ x 10 ³	r mm	A mm ²	I mm ⁴ x 10 ⁶	S mm ³ x 10 ³	r mm
9 GAUGE 3.797 mm	2,342	2,535	3,748	42.456	267.109	106	4,355	66.181	360.515	123
7 GAUGE 4.554 mm	2,839	3,077	4,497	50.780	319.548	106	5,252	80.749	437.535	124
5 GAUGE 5.314 mm	3,348	3,619	5,277	60.354	376.902	107	6,129	94.485	507.999	124
3 GAUGE 6.073 mm	3,787	4,245	5,781	61.602	396.567	103	6,839	99.479	550.605	121
CONCRETE AREA mm ²	27,290	30,518	65,161				87,742			

STEEL THICKNESS	POINTS		BUTTS OF PILE SECTIONS							
	203 mm	216 mm	406 mm				457 mm			
	A mm ²	A mm ²	A mm ²	I mm ⁴ x 10 ⁶	S mm ³ x 10 ³	r mm	A mm ²	I mm ⁴ x 10 ⁶	S mm ³ x 10 ³	r mm
9 GAUGE 3.797 mm	2,342	2,535	4,929	96.566	463.754	140	-	-	-	-
7 GAUGE 4.554 mm	2,839	3,077	5,923	115.712	555.521	140	6,710	168.157	712.837	158
5 GAUGE 5.314 mm	3,348	3,619	6,968	136.940	555.521	140	7,871	198.959	839.018	159
3 GAUGE 6.073 mm	3,787	4,245	7,742	144.849	706.282	137	8,774	209.781	907.843	155
CONCRETE AREA mm ²	27,290	30,518	113,548				144,516			

Note: Designer must confirm section properties of selected pile section.

Pile design data converted to SI units from US units published in Monotube Pile Corporation Catalog 592.

PRECAST/PRESTRESSED CONCRETE PILES

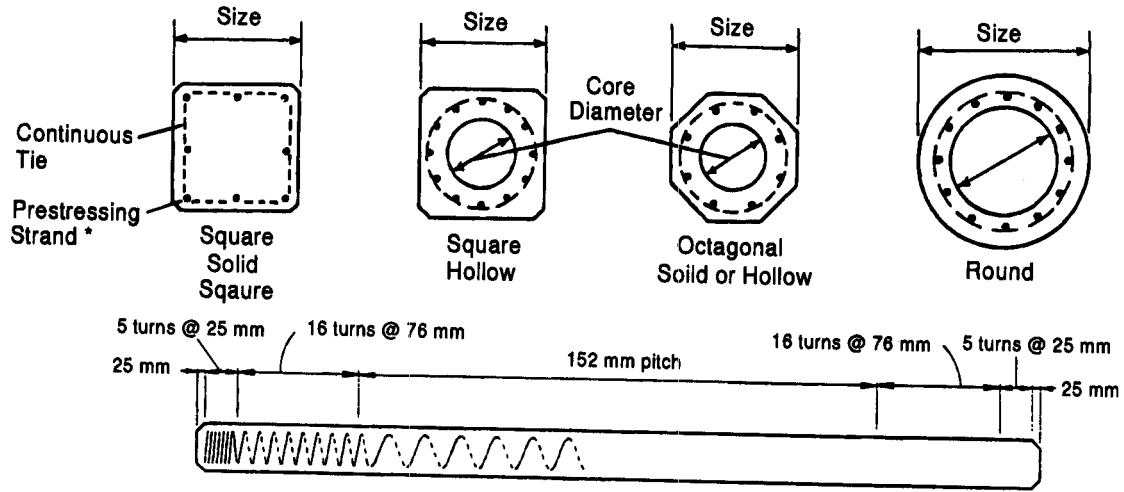


Size mm	Section Properties						
	Core Diameter mm	Area mm ²	Weight N/m	Moment of Inertia mm ⁴ x 10 ⁶	Section Modulus mm ³ x 10 ³	Radius of Gyration mm	Perimeter m
Square Piles							
254	Solid	64,516	1,518	346.721	2,736.640	73.4	1.015
305	Solid	92,903	2,189	719.248	4,719.474	87.9	1.219
356	Solid	126,451	2,977	1,332.357	7,488.888	102.6	1.423
406	Solid	165,161	3,896	2,273.040	11,192.365	117.3	1.625
457	Solid	209,032	4,932	3,641.193	15,928.226	132.1	1.829
508	Solid	258,064	6,085	5,549.614	21,843.956	146.6	2.033
508	279 mm	196,774	4,641	5,250.759	20,680.475	163.3	2.033
610	Solid	371,612	8,756	11,507.966	37,755.795	176.0	2.438
610	305 mm	298,709	7,034	11,084.243	36,362.895	192.5	2.438
610	356 mm	272,258	6,406	10,722.954	35,183.026	198.4	2.438
610	381 mm	257,419	6,056	10,473.631	34,363.673	201.7	2.438
762	457 mm	416,773	9,807	25,950.781	68,121.025	249.4	3.048
914	457 mm	672,257	15,834	56,114.240	122,739.109	289.1	3.658

Note: Designer must confirm section properties for a selected pile. Form dimensions may vary with producers, with corresponding variations in section properties.

Data converted to SI units from US unit properties in PCI (1993), Precast/Prestressed Concrete Institute Journal, Volume 38, No. 2, March-April, 1993.

PRECAST/PRESTRESSED CONCRETE PILES



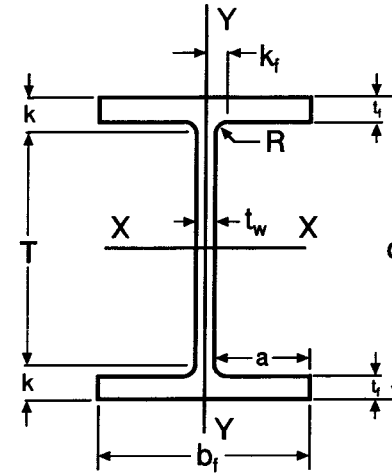
* Strand pattern may be circular or square

Size mm	Core Diameter mm	Section Properties					
		Area mm ²	Weight N/m	Moment of Inertia mm ⁴ x 10 ⁶	Section Modulus mm ³ x 10 ³	Radius of Gyration mm	Perimeter m
Octagonal Piles							
254	Solid	53,548	1,240	231.008	1,818.964	65.8	0.841
305	Solid	76,774	1,824	472.006	3,097.155	78.5	1.009
356	Solid	104,516	2,466	876.167	4,932.506	91.4	1.180
406	Solid	136,774	3,210	1,495.103	7,357.792	104.6	1.347
457	Solid	172,903	4,086	2,374.600	10,471.334	117.1	1.515
508	Solid	213,548	5,035	3,650.350	14,371.455	130.8	1.682
508	279 mm	152,258	3,575	3,350.663	13,191.587	148.3	1.682
559	Solid	258,709	6,129	5,343.163	19,123.704	143.8	1.853
559	330 mm	172,903	4,086	4,761.688	17,042.547	165.9	1.853
610	Solid	307,741	7,224	7,567.087	24,826.402	156.7	2.021
610	381 mm	193,548	4,597	6,533.168	21,434.280	183.6	2.021
Round Piles							
914	660 mm	314,193	7,399	24,976.799	54,634.471	281.9	2.874
1,067	813 mm	374,838	8,829	42,153.005	79,034.810	335.3	3.353
1,219	965 mm	435,483	10,259	65,856.969	108,023.526	388.9	3.831
1,372	1118 mm	496,773	11,704	97,137.176	141,633.394	442.2	4.310
1,676	1372 mm	729,676	17,191	213,954.191	255,261.296	541.5	5.267

Note: Designer must confirm section properties for a selected pile. Form dimensions may vary with producers, with corresponding variations in section properties.

Data converted to SI units from US unit properties in PCI (1993), Precast/Prestressed Concrete Institute Journal, Volume 38, No. 2, March-April, 1993.

H-PILES



C-21

Section Designation	Area A	Depth d	Web Thickness t_w	Flange		Distance					Fillet Radius R	Elastic Properties					
				Width b_f	Thickness t_f	T	k	k_f	a	X-X			Y-Y				
										I		S	r	I	S	r	
mm x kg/m	mm ²	mm	mm	mm	mm	mm	mm	mm	mm	mm	mm ⁴ x 10 ⁶	mm ³ x 10 ³	mm	mm ⁴ x 10 ⁶	mm ³ x 10 ³	mm	
HP360 x 174	22,200	361	20.4	378	20	277	42	30.2	179	20	511	2,830	152	183	968	91	
HP360 x 152	19,400	356	17.9	376	18	277	40	29.0	179	20	442	2,480	151	158	840	90	
HP360 x 132	16,900	351	15.6	373	16	277	37	27.8	179	20	378	2,150	150	135	724	89	
HP360 x 108	13,800	346	12.8	370	13	277	34	26.4	179	20	306	1,770	148	108	584	88	
HP310 x 125	15,800	312	17.4	312	17	244	34	23.7	147	15	270	1,730	131	88	565	75	
HP310 x 110	14,000	308	15.4	310	15	244	32	22.7	147	15	236	1,530	130	77	497	74	
HP310 x 93	11,800	303	13.1	308	13	244	30	21.6	148	15	196	1,290	129	64	414	74	
HP310 x 79	9,970	299	11.0	306	11	244	28	20.5	148	15	162	1,080	127	53	343	73	
HP250 x 85	10,800	254	14.4	260	14	196	29	20.2	123	13	123	969	107	42	325	63	
HP250 x 62	7,980	246	10.5	256	11	96	25	18.3	123	13	88	711	105	30	234	61	
HP200 x 53	6,810	204	11.3	207	11	158	23	15.7	98	10	50	487	86	17	161	50	

Note: Designer must confirm section properties for a selected pile.

Data obtained from FHWA Geotechnical Metrication Guidelines (1995) FHWA-SA-95-035.

BITUMEN COATING FOR CONCRETE PILES

(This is a generic specification that should be modified to meet the specific needs of a given project.)

Description. This work shall consist of furnishing and applying bituminous coating and primer to prestressed concrete pile surfaces as required in the plans and as specified herein.

Materials

- A. Bituminous Coating. Bituminous coating shall be an asphalt type bitumen conforming to ASTM D946, with a minimum penetration grade 50 at the time of pile driving. Bituminous coating shall be applied uniformly over an asphalt primer. Grade 40-50 or lower grades shall not be used.
- B. Primer. Primer shall conform to the requirements of ASTM D41.

Construction Requirements. All surfaces to be coated with bitumen shall be dry and thoroughly cleaned of dust and loose materials. No primer or bitumen shall be applied in wet weather, nor when the temperature is below 18 degrees Celsius.

The primer shall be applied to the surfaces and allowed to completely dry before the bituminous coating is applied. Primer shall be applied uniformly at the quantity of one liter per 2.43 square meters.

Bitumen shall be applied uniformly at a temperature of not less than 149 degrees Celsius, nor more than 177 degrees Celsius, and shall be applied either by mopping, brushing, or spraying at the project site. All holes or depressions in the concrete surface shall be completely filled with bitumen. The bituminous coating shall be applied to a minimum dry thickness of 3.2 mm, but in no case shall the quantity of application be less than 3.29 liters per square meters.

Bitumen coated piles shall be stored before driving and protected from sunlight and heat. Pile coatings shall not be exposed to damage during storage, hauling or handling. The Contractor shall take appropriate measures to preserve and maintain the bitumen coating. At the time of pile driving, the bitumen coating shall have a minimum dry thickness of 3.2 mm and a minimum penetration value of 50. If necessary, the Contractor shall recoat the piles, at his expense, to comply with these requirements.

Method of Measurement. Bitumen coating will be measured by the square meter of coating in place on concrete pile surfaces. No separate payment will be made for primer.

Basis of Payment. The accepted quantities of bitumen coating will be paid for at the contract unit price per square meter, which price shall be full compensation for furnishing all labor, materials, tools, equipment, and incidentals, and for doing all the work involved in applying the bituminous coating and primer, as shown in the plans, and as specified in these specifications, and as directed by the Engineer.

Payment will be made under:

<u>Pay Item</u>	<u>Pay Unit</u>
Bitumen Coating	Square Meters.

BITUMEN COATING FOR STEEL PILES

(This is a generic specification that should be modified to meet the specific needs of a given project.)

Description. This work shall consist of furnishing and applying bituminous coating and primer to steel pile surfaces as required in the plans and as specified herein.

Materials

- A. Bituminous Coating. Canal Liner Bitumen (ASTM D-2521) shall be used for the bitumen coating and shall have a softening point of 88 to 93 degrees Celsius, a penetration of 56 to 61 at 25 degrees Celsius, and a ductility at 25 degrees Celsius, in excess of 35.0 mm.
- B. Primer. Primer shall conform to the requirements of AASHTO M116.

Construction Requirements. All surfaces to be coated with bitumen shall be dry and thoroughly cleaned of dust and loose materials. No primer or bitumen shall be applied in wet weather, nor when the temperature is below 18 degrees Celsius.

Application of the prime coat shall be with a brush or other approved means and in a manner to thoroughly coat the surface of the piling with a continuous film of primer. The purpose of the primer is to provide a suitable bond of the bitumen coating to the pile. The primer shall set thoroughly before the bitumen coating is applied.

The bitumen should be heated to 149 degrees Celsius, and applied at a temperature between 93 and 149 degrees Celsius, by one or more mop coats, or other approved means, to apply an average coating depth of 9.5 mm. Whitewashing of the coating may be required, as deemed necessary by the engineer, to prevent running and sagging of the asphalt coating prior to driving, during hot weather.

Bitumen coated piles shall be stored immediately after the coating is applied for protection from sunlight and heat. Pile coatings shall not be exposed to damage or contamination during storage, hauling, or handling. Once the bitumen coating has been applied, the contractor will not be allowed to drag the piles on the ground or to use cable wraps around the pile during handling. Pad eyes, or other suitable devices, shall be attached to the pile to be used for lifting and handling. If necessary, the contractor shall recoat the piles, at his expense to comply with these requirements.

A nominal length of pile shall be left uncoated where field splices will be required. After completing the field splice, the splice area shall be brush or map coated with at least one coat of bitumen.

Method of Measurement. Bitumen coating will be measured by the linear meter of coating in place on the pile surfaces. No separate payment will be made for primer or coating of the splice areas.

Basis of Payment. The accepted quantities of bitumen coating will be paid for at the contract unit price per linear meter, which price shall be full compensation for furnishing all labor, materials, tools, equipment, and incidentals, and for doing all the work involved in applying the bituminous coating and primer, as shown in the plans, and as specified in these specifications, and as directed by the Engineer.

Payment will be made under:

<u>Pay Item</u>	<u>Pay-Unit</u>
Bitumen Coating	Meter.

APPENDIX D

Pile Hammer Information

	Page
TABLE D-1 DIESEL HAMMER LISTING (sorted by Maximum Energy)	D-3
TABLE D-2 EXTERNAL COMBUSTION HAMMER LISTING (sorted by Maximum Energy)	D-7
TABLE D-3 COMPLETE HAMMER LISTING (sorted by GRLWEAP ID Numbers)	D-13

Note: GRLWEAP hammer ID numbers correspond to those contained in Version 1.996-2 of the GRLWEAP program.

TABLE D-1 DIESEL HAMMER LISTING
(sorted by Maximum Energy)

GRLWEAP ID	Hammer Mfgr	Hammer Name E	Max. Energy kN-m	Ram Weight kN	Eq. Max. Stroke m	Hammer Type T
81	LINKBELT	LB 180	10.98	7.70	1.43	CED
120	ICE	180	11.03	7.70	1.43	CED
1	DELMAG	D 5	11.16	4.89	2.28	OED
36	DELMAG	D 6-32	14.24	5.88	2.42	OED
82	LINKBELT	LB 312	20.37	17.18	1.19	CED
146	MKT	DE 10	20.75	7.57	2.74	OED
147	MKT	DE 20	21.70	8.90	2.44	OED
2	DELMAG	D 8-22	23.87	7.83	3.05	OED
402	BERMINGH	B200	24.41	8.90	2.74	OED
83	LINKBELT	LB 440	24.69	17.80	1.39	CED
122	ICE	440	25.17	17.80	1.41	CED
141	MKT 20	DE333020	27.13	8.90	3.05	OED
151	MKT	DA 35B	28.48	12.46	2.29	CED
148	MKT	DE 30	30.38	12.46	2.44	OED
41	FEC	FEC 1200	30.51	12.24	2.49	OED
127	ICE	30-S	30.52	13.35	2.29	OED
401	BERMINGH	B23	31.18	12.46	2.50	CED
414	BERMINGH	B23 5	31.18	12.46	2.50	CED
121	ICE	422	31.36	17.80	1.76	CED
3	DELMAG	D 12	32.00	12.24	2.62	OED
149	MKT	DA35B SA	32.28	12.46	2.59	OED
150	MKT	DE 30B	32.28	12.46	2.59	OED
61	MITSUB.	M 14	34.24	13.22	2.59	OED
350	HERA	1250	34.38	12.50	2.75	OED
101	KOBE	K 13	34.49	12.77	2.70	OED
84	LINKBELT	LB 520	35.69	22.56	1.58	CED
42	FEC	FEC 1500	36.75	14.68	2.50	OED
201	VULCANI	VUL V12	36.77	12.26	3.00	OED
142	MKT 30	DE333020	37.98	12.46	3.05	OED
62	MITSUB.	MH 15	38.16	14.73	2.59	OED
4	DELMAG	D 15	38.40	14.68	2.62	OED
403	BERMINGH	B225	39.67	13.35	2.97	OED
123	ICE	520	41.19	22.56	1.83	CED
351	HERA	1500	41.25	15.00	2.75	OED
152	MKT	DA 45	41.67	17.80	2.34	CED
37	DELMAG	D 12-32	42.50	12.55	3.39	OED
153	MKT	DE 40	43.40	17.80	2.44	OED
143	MKT 33	DE333020	44.76	14.68	3.05	OED
415	BERMINGH	B250 5	48.02	13.35	3.60	OED
161	MKT	DA 55B	51.81	22.25	2.33	CED
202	VULCAN	VUL V18	52.97	17.66	3.00	OED

TABLE D-1 DIESEL HAMMER LISTING
(sorted by Maximum Energy)

GRLWEAP ID	Hammer Mfgr	Hammer Name E	Max. Energy kN-m	Ram Weight kN	Eq. Max. Stroke m	Hammer Type T
5	DELMAG	D 16-32	53.23	15.66	3.40	OED
128	ICE	40-S	54.25	17.80	3.05	OED
144	MKT 40	DE333020	54.25	17.80	3.05	OED
160	MKT	DA55B SA	54.25	22.25	2.44	OED
404	BERMINGH	B300	54.68	16.69	3.28	OED
410	BERMINGH	B300 M	54.68	16.69	3.28	OED
6	DELMAG	D 22	55.08	21.85	2.52	OED
124	ICE	640	55.10	26.70	2.06	CED
129	ICE	42-S	56.97	18.19	3.13	OED
38	DELMAG	D 19-32	57.51	17.80	3.23	OED
159	MKT	DE 50B	57.65	22.25	2.59	OED
63	MITSUB.	M 23	58.34	22.52	2.59	OED
412	BERMINGH	B400 4.8	58.59	21.36	2.74	OED
413	BERMINGH	B400 5.0	61.04	22.25	2.74	OED
103	KOBE	K22-Est	61.51	21.58	2.85	OED
64	MITSUB.	MH 25	63.53	24.52	2.59	OED
416	BERMINGH	B350 5	64.02	17.80	3.60	OED
7	DELMAG	D 22-02	65.78	21.58	3.05	OED
8	DELMAG	D 22-13	65.78	21.58	3.05	OED
43	FEC	FEC 2500	67.81	24.47	2.77	OED
163	MKT 50	DE70/50B	67.82	22.25	3.05	OED
352	HERA	2500	68.75	25.00	2.75	OED
9	DELMAG	D 22-23	69.53	21.58	3.22	OED
104	KOBE	K 25	69.88	24.52	2.85	OED
125	ICE	660	70.03	33.69	2.08	CED
85	LINKBELT	LB 660	70.03	33.69	2.08	CED
405	BERMINGH	B400	72.90	22.25	3.28	OED
411	BERMINGH	B400 M	72.90	22.25	3.28	OED
44	FEC	FEC 2800	75.95	27.41	2.77	OED
353	HERA	2800	77.00	28.00	2.75	OED
203	VULCAN	VUL V25	78.51	24.53	3.20	OED
417	BERMINGH	B400 5	80.03	22.25	3.60	OED
162	MKT	DE 70B	80.70	31.15	2.59	OED
11	DELMAG	D 30	80.84	29.37	2.75	OED
10	DELMAG	D 25-32	83.40	24.52	3.40	OED
65	MITSUB.	M 33	83.70	32.31	2.59	OED
45	FEC	FEC 3000	85.49	29.37	2.91	OED
66	MITSUB.	MH 35	89.00	34.35	2.59	OED
12	DELMAG	D 30-02	89.52	29.37	3.05	OED
13	DELMAG	D 30-13	89.52	29.37	3.05	OED
131	ICE	70-S	94.95	31.15	3.05	OED

TABLE D-1 DIESEL HAMMER LISTING
(sorted by Maximum Energy)

GRLWEAP ID	Hammer Mfgr	Hammer Name E	Max. Energy kN-m	Ram Weight kN	Eq. Max. Stroke m	Hammer Type T
164	MKT 70	DE70/50B	94.95	31.15	3.05	OED
354	HERA	3500	96.25	35.00	2.75	OED
107	KOBE	K 35	97.90	34.35	2.85	OED
126	ICE	1070	98.47	44.50	2.21	CED
130	ICE	60-S	98.93	31.15	3.18	OED
46	FEC	FEC 3400	99.02	33.29	2.97	OED
14	DELMAG	D 30-23	99.90	29.37	3.40	OED
15	DELMAG	D 30-32	99.90	29.37	3.40	OED
418	BERMINGH	B450 5	105.63	29.37	3.60	OED
67	MITSUB.	M 43	109.06	42.10	2.59	OED
16	DELMAG	D 36	113.69	35.29	3.22	OED
17	DELMAG	D 36-02	113.69	35.29	3.22	OED
18	DELMAG	D 36-13	113.69	35.29	3.22	OED
68	MITSUB.	MH 45	115.87	44.72	2.59	OED
421	BERMINGH	B550 C	119.36	48.95	2.44	OED
19	DELMAG	D 36-23	120.04	35.29	3.40	OED
20	DELMAG	D 36-32	120.04	35.29	3.40	OED
133	ICE	90-S	122.07	40.05	3.05	OED
21	DELMAG	D 44	122.67	42.27	2.90	OED
419	BERMINGH	B500 5	124.84	34.71	3.60	OED
110	KOBE	K 45	125.81	44.14	2.85	OED
24	DELMAG	D 46-13	130.93	45.12	2.90	OED
132	ICE	80-S	134.77	35.60	3.79	OED
136	ICE	200-S	135.64	89.00	1.52	OED
355	HERA	5000	137.50	50.00	2.75	OED
420	BERMINGH	B550 5	144.05	40.05	3.60	OED
22	DELMAG	D 46	145.37	45.12	3.22	OED
23	DELMAG	D 46-02	145.37	45.12	3.22	OED
25	DELMAG	D 46-23	145.37	45.12	3.22	OED
165	MKT 110	DE110150	149.20	48.95	3.05	OED
26	DELMAG	D 46-32	153.49	45.12	3.40	OED
356	HERA	5700	156.75	57.00	2.75	OED
134	ICE	100-S	162.76	44.50	3.66	OED
27	DELMAG	D 55	168.91	52.78	3.20	OED
357	HERA	6200	170.50	62.00	2.75	OED
112	KOBE	KB 60	176.58	58.87	3.00	OED
70	MITSUB.	MH 72B	183.31	70.75	2.59	OED
135	ICE	120-S	202.15	53.40	3.79	OED
71	MITSUB.	MH 80B	202.91	78.32	2.59	OED
166	MKT 150	DE110150	203.45	66.75	3.05	OED
358	HERA	7500	206.25	75.00	2.75	OED

**TABLE D-1 DIESEL HAMMER LISTING
(sorted by Maximum Energy)**

GRLWEAP ID	Hammer Mfgr	Hammer Name E	Max. Energy kN-m	Ram Weight kN	Eq. Max. Stroke m	Hammer Type T
28	DELMAG	D 62-02	206.77	60.79	3.40	OED
29	DELMAG	D 62-12	206.77	60.79	3.40	OED
30	DELMAG	D 62-22	206.77	60.79	3.40	OED
113	KOBE	KB 80	235.43	78.50	3.00	OED
359	HERA	8800	242.00	88.00	2.75	OED
31	DELMAG	D 80-12	252.61	78.41	3.22	OED
32	DELMAG	D 80-23	266.71	78.41	3.40	OED
33	DELMAG	D100-13	333.47	98.03	3.40	OED

**TABLE D-2 EXTERNAL COMBUSTION HAMMER LISTING
(sorted by Maximum Energy)**

GRLWEAP ID	Hammer Mfgr	Hammer Name	Max. Energy kN-m	Ram Weight kN	Eq. Max. Stroke m	Hammer Type
301	MKT	No. 5	1.36	.89	1.52	ECH
302	MKT	No. 6	3.39	1.78	1.90	ECH
303	MKT	No. 7	5.63	3.56	1.58	ECH
205	VULCAN	VUL 02	9.85	13.35	.74	ECH
220	VULCAN	VUL 30C	9.85	13.35	.74	ECH
521	DAWSON	HPH 1200	11.73	10.20	1.15	ECH
304	MKT	9B3	11.87	7.12	1.67	ECH
305	MKT	10B3	17.78	13.35	1.33	ECH
306	MKT	C5-Air	19.26	22.25	.87	ECH
171	CONMACO	C 50	20.35	22.25	.91	ECH
204	VULCAN	VUL 01	20.35	22.25	.91	ECH
251	RAYMOND	R 1	20.35	22.25	.91	ECH
221	VULCAN	VUL 50C	20.48	22.25	.92	ECH
307	MKT	C5-Steam	21.97	22.25	.99	ECH
308	MKT	S-5	22.04	22.25	.99	ECH
522	DAWSON	HPH 2400	23.49	18.64	1.26	ECH
541	BANUT	3 Tonnes	23.53	29.41	.80	ECH
309	MKT	11B3	25.97	22.25	1.17	ECH
222	VULCAN	VUL 65C	26.01	28.92	.90	ECH
172	CONMACO	C 65	26.45	28.92	.91	ECH
206	VULCAN	VUL 06	26.45	28.92	.91	ECH
252	RAYMOND	R 1S	26.45	28.92	.91	ECH
253	RAYMOND	R 65C	26.45	28.92	.91	ECH
254	RAYMOND	R 65CH	26.45	28.92	.91	ECH
223	VULCAN	VUL 65CA	26.54	28.92	.92	ECH
311	MKT	C826 Air	28.75	35.60	.81	ECH
341	IHC Hydh	SC 30	30.02	16.20	1.85	ECH
542	BANUT	4 Tonnes	31.39	39.25	.80	ECH
255	RAYMOND	R 0	33.06	33.38	.99	ECH
310	MKT	C826 Strm	33.10	35.60	.93	ECH
224	VULCAN	VUL 80C	33.20	35.60	.93	ECH
256	RAYMOND	R 80C	33.20	35.60	.93	ECH
257	RAYMOND	R 80CH	33.20	35.60	.93	ECH
449	MENCK	MHF3-3	33.59	31.39	1.07	ECH
515	UDDCOMB	H3H	33.75	29.37	1.15	ECH
173	CONMACO	C 550	33.91	22.25	1.52	ECH
235	VULCAN	VUL 505	33.91	22.25	1.52	ECH
320	IHC Hydh	S 35	35.01	32.35	1.08	ECH
225	VULCAN	VUL 85C	35.25	37.91	.93	ECH
175	CONMACO	C 80	35.27	35.60	.99	ECH
207	VULCAN	VUL 08	35.27	35.60	.99	ECH

TABLE D-2 EXTERNAL COMBUSTION HAMMER LISTING
(sorted by Maximum Energy)

GRLWEAP ID	Hammer Mfgr	Hammer Name	Max. Energy kN-m	Ram Weight kN	Eq. Max. Stroke m	Hammer Type
312	MKT	S-8	35.27	35.60	.99	ECH
381	BSP	HH 3	35.29	29.42	1.20	ECH
481	JUNTTAN	HHK 3	36.01	29.46	1.22	ECH
543	BANUT	5 Tonnes	39.22	49.04	.80	ECH
342	IHC Hydh	SC 40	39.98	24.52	1.63	ECH
321	IHC Hydh	S 40	41.18	24.52	1.68	ECH
313	MKT	MS-350	41.78	34.35	1.22	ECH
450	MENCK	MHF3-4	41.99	39.24	1.07	ECH
174	CONMACO	C 565	44.08	28.92	1.52	ECH
176	CONMACO	C 100	44.08	44.50	.99	ECH
208	VULCAN	VUL 010	44.08	44.50	.99	ECH
236	VULCAN	VUL 506	44.08	28.92	1.52	ECH
258	RAYMOND	R 2/0	44.08	44.50	.99	ECH
314	MKT	S 10	44.08	44.50	.99	ECH
506	HPSI	650	44.08	28.92	1.52	ECH
372	FAIRCHLD	F-32	44.15	48.28	.91	ECH
226	VULCAN	VUL 100C	44.62	44.50	1.00	ECH
516	UDDCOMB	H4H	45.00	39.16	1.15	ECH
544	BANUT	6 Tonnes	47.09	58.87	.80	ECH
482	JUNTTAN	HHK 4	47.97	39.25	1.22	ECH
227	VULCAN	VUL 140C	48.80	62.30	.78	ECH
177	CONMACO	C 115	50.69	51.17	.99	ECH
315	MKT	S 14	50.89	62.30	.82	ECH
551	ICE	110-SH	51.16	51.17	1.00	ECH
552	ICE	115-SH	51.47	51.17	1.01	ECH
441	MENCK	MHF5-5	52.48	49.05	1.07	ECH
451	MENCK	MHF3-5	52.48	49.05	1.07	ECH
209	VULCAN	VUL 012	52.90	53.40	.99	ECH
178	CONMACO	C 80E5	54.25	35.60	1.52	ECH
237	VULCAN	VUL 508	54.25	35.60	1.52	ECH
545	BANUT	7 Tonnes	54.92	68.66	.80	ECH
259	RAYMOND	R 3/0	55.10	55.62	.99	ECH
517	UDDCOMB	H5H	56.25	48.95	1.15	ECH
182	CONMACO	C 140	56.97	62.30	.91	ECH
210	VULCAN	VUL 014	56.97	62.30	.91	ECH
382	BSP	HH 5	58.83	49.04	1.20	ECH
316	MKT	MS 500	59.68	48.95	1.22	ECH
501	HPSI	110	59.68	48.95	1.22	ECH
489	JUNTTAN	HHK 5A	59.79	49.04	1.22	ECH
483	JUNTTAN	HHK 5	59.99	49.08	1.22	ECH
343	IHC Hydh	SC 60	60.00	34.35	1.75	ECH

TABLE D-2 EXTERNAL COMBUSTION HAMMER LISTING
(sorted by Maximum Energy)

GRLWEAP ID	Hammer Mfgr	Hammer Name	Max. Energy kN-m	Ram Weight kN	Eq. Max. Stroke m	Hammer Type
322	IHC Hydh	S 60	60.04	58.86	1.02	ECH
371	FAIRCHLD	F-45	61.04	66.75	.91	ECH
282	MENCK	MRBS 500	61.13	49.04	1.25	ECH
442	MENCK	MHF5-6	62.98	58.86	1.07	ECH
452	MENCK	MHF3-6	62.98	58.86	1.07	ECH
183	CONMACO	C 160	66.12	72.31	.91	ECH
211	VULCAN	VUL 016	66.12	72.31	.91	ECH
260	RAYMOND	R 150C	66.12	66.75	.99	ECH
261	RAYMOND	R 4/0	66.12	66.75	.99	ECH
271	MENCK	MH 68	66.70	34.35	1.94	ECH
518	UDDCOMB	H6H	67.50	58.74	1.15	ECH
179	CONMACO	C 100E5	67.82	44.50	1.52	ECH
507	HPSI	1000	67.82	44.50	1.52	ECH
238	VULCAN	VUL 510	67.82	44.50	1.52	ECH
228	VULCAN	VUL 200C	68.09	89.00	.77	ECH
323	IHC Hydh	S 70	70.05	34.35	2.04	ECH
191	CONMACO	C 160 **	70.23	76.81	.91	ECH
484	JUNTTAN	HHK 6	71.96	58.87	1.22	ECH
443	MENCK	MHF5-7	73.48	68.67	1.07	ECH
453	MENCK	MHF3-7	73.48	68.67	1.07	ECH
262	RAYMOND	R 5/0	77.14	77.88	.99	ECH
180	CONMACO	C 115E5	77.99	51.17	1.52	ECH
344	IHC Hydh	SC 80	79.89	50.02	1.60	ECH
184	CONMACO	C 200	81.38	89.00	.91	ECH
212	VULCAN	VUL 020	81.38	89.00	.91	ECH
231	VULCAN	VUL 320	81.38	89.00	.91	ECH
239	VULCAN	VUL 512	81.38	53.40	1.52	ECH
317	MKT	S 20	81.38	89.00	.91	ECH
502	HPSI	150	81.38	66.75	1.22	ECH
383	BSP	HH 7	82.44	68.65	1.20	ECH
503	HPSI	154	83.55	68.53	1.22	ECH
490	JUNTTAN	HHK 7A	83.71	68.66	1.22	ECH
444	MENCK	MHF5-8	83.97	78.48	1.07	ECH
485	JUNTTAN	HHK 7	83.98	68.71	1.22	ECH
181	CONMACO	C 125E5	84.77	55.62	1.52	ECH
553	ICE	160-SH	86.81	71.20	1.22	ECH
324	IHC Hydh	S 90	90.01	44.14	2.04	ECH
283	MENCK	MRBS 750	91.92	73.56	1.25	ECH
519	UDDCOMB	H8H	94.06	78.32	1.20	ECH
272	MENCK	MH 96	94.17	49.04	1.92	ECH
384	BSP	HH 8	94.27	78.50	1.20	ECH

TABLE D-2 EXTERNAL COMBUSTION HAMMER LISTING
(sorted by Maximum Energy)

GRLWEAP ID	Hammer Mfgr	Hammer Name	Max. Energy kN-m	Ram Weight kN	Eq. Max. Stroke m	Hammer Type
445	MENCK	MHF5-9	94.47	88.29	1.07	ECH
263	RAYMOND	R 30X	101.73	133.50	.76	ECH
446	MENCK	MHF5-10	104.97	98.10	1.07	ECH
345	IHC Hydh	SC 110	105.01	67.68	1.55	ECH
385	BSP	HH 9	106.03	88.29	1.20	ECH
491	JUNTTAN	HHK 9A	107.64	88.29	1.22	ECH
504	HPSI	200	108.51	89.00	1.22	ECH
264	RAYMOND	R 8/0	110.2	111.25	.99	ECH
508	HPSI	1605	112.58	73.87	1.52	ECH
447	MENCK	MHF5-11	115.46	107.91	1.07	ECH
520	UDDCOMB	H10H	117.84	98.12	1.20	ECH
486	JUNTTAN	HHK 10	119.93	98.12	1.22	ECH
185	CONMACO	C 300	122.07	133.50	.91	ECH
213	VULCAN	VUL 030	122.07	133.50	.91	ECH
232	VULCAN	VUL 330	122.07	133.50	.91	ECH
270	9K DROP	9K DROP	122.07	40.05	3.05	ECH
505	HPSI	225	122.07	100.12	1.22	ECH
448	MENCK	MHF5-12	125.96	117.72	1.07	ECH
284	MENCK	MRBS 800	126.53	84.37	1.50	ECH
285	MENCK	MRBS 850	126.53	84.37	1.50	ECH
509	HPSI	2005	128.99	84.64	1.52	ECH
386	BSP	HH 11	129.59	107.91	1.20	ECH
186	CONMACO	C 5200	135.64	89.00	1.52	ECH
240	VULCAN	VUL 520	135.64	89.00	1.52	ECH
265	RAYMOND	R 40X	135.64	178.00	.76	ECH
346	IHC Hydh	SC 150	140.12	107.91	1.30	ECH
273	MENCK	MH 145	142.15	73.56	1.93	ECH
487	JUNTTAN	HHK 12	143.92	117.75	1.22	ECH
229	VULCAN	VUL 400C	154.08	178.00	.87	ECH
454	MENCK	MHF10-15	157.39	147.12	1.07	ECH
214	VULCAN	VUL 040	162.76	178.00	.91	ECH
233	VULCAN	VUL 340	162.76	178.00	.91	ECH
387	BSP	HH 14	164.92	137.33	1.20	ECH
286	MENCK	MRBS1100	167.42	107.91	1.55	ECH
488	JUNTTAN	HHK 14	167.90	137.37	1.22	ECH
287	MENCK	MRBS1502	183.90	147.16	1.25	ECH
388	BSP	HH 16	188.35	156.96	1.20	ECH
274	MENCK	MH 195	191.41	98.12	1.95	ECH
325	IHC Hydh	S 200	199.63	97.90	2.04	ECH
461	MENCK	MHUT 200	199.90	117.75	1.70	ECH
187	CONMACO	C 5300	203.45	133.50	1.52	ECH

TABLE D-2 EXTERNAL COMBUSTION HAMMER LISTING
(sorted by Maximum Energy)

GRLWEAP ID	Hammer Mfgr	Hammer Name	Max. Energy kN-m	Ram Weight kN	Eq. Max. Stroke m	Hammer Type
241	VULCAN	VUL 530	203.45	133.50	1.52	ECH
266	RAYMOND	R 60X	203.45	267.00	.76	ECH
347	IHC Hydh	SC 200	204.81	134.39	1.52	ECH
455	MENCK	MHF10-20	209.81	196.11	1.07	ECH
510	HPSI	3005	209.32	137.35	1.52	ECH
275	MENCK	MHU 220	215.76	111.83	1.93	ECH
389	BSP	HH 20	235.44	196.20	1.20	ECH
390	BSP	HH 20S	235.44	196.20	1.20	ECH
511	HPSI	3505	239.16	156.93	1.52	ECH
348	IHC Hydh	SC 250	240.04	174.62	1.37	ECH
230	VULCAN	VUL 600C	243.01	267.00	.91	ECH
215	VULCAN	VUL 060	244.14	267.00	.91	ECH
234	VULCAN	VUL 360	244.14	267.00	.91	ECH
326	IHC Hydh	S 250	250.44	122.82	2.04	ECH
288	MENCK	MRBS1800	257.46	171.68	1.50	ECH
242	VULCAN	VUL 540	271.27	182.01	1.49	ECH
327	IHC Hydh	S 280	280.11	132.61	2.11	ECH
188	CONMACO	C 5450	305.18	200.25	1.52	ECH
290	MENCK	MRBS2502	306.47	245.24	1.25	ECH
291	MENCK	MRBS2504	306.47	245.24	1.25	ECH
391	BSP	HA 30	353.16	294.30	1.20	ECH
289	MENCK	MRBS2500	355.52	284.49	1.25	ECH
276	MENCK	MHU 400	392.74	225.66	1.74	ECH
328	IHC Hydh	S 400	399.58	197.13	2.03	ECH
462	MENCK	MHUT 400	400.29	234.51	1.71	ECH
243	VULCAN	VUL 560	406.91	278.13	1.46	ECH
245	VULCAN	VUL 3100	406.91	445.00	.91	ECH
292	MENCK	MRBS3000	441.30	294.28	1.50	ECH
392	BSP	HA 40	470.88	392.40	1.20	ECH
189	CONMACO	C 5700	474.73	311.50	1.52	ECH
329	IHC Hydh	S 500	499.54	246.08	2.03	ECH
463	MENCK	MHUT 500	499.89	264.95	1.89	ECH
277	MENCK	MHU 600	588.17	343.36	1.71	ECH
294	MENCK	MRBS4600	676.74	451.27	1.50	ECH
246	VULCAN	VUL 5100	678.18	445.00	1.52	ECH
190	CONMACO	C 6850	691.74	378.25	1.83	ECH
293	MENCK	MRBS3900	696.28	386.53	1.80	ECH
464	MENCK	MHUT700U	700.06	413.09	1.69	ECH
295	MENCK	MRBS5000	735.60	490.52	1.50	ECH
330	IHC Hydh	S 800	800.05	363.00	2.20	ECH
465	MENCK	MHUT700A	839.83	413.09	2.03	ECH

TABLE D-2 EXTERNAL COMBUSTION HAMMER LISTING
 (sorted by Maximum Energy)

GRLWEAP ID	Hammer Mfgr	Hammer Name	Max. Energy kN-m	Ram Weight kN	Eq. Max. Stroke m	Hammer Type
297	MENCK	MRBS7000	856.41	685.30	1.25	ECH
466	MENCK	MHUT1000	999.52	588.73	1.70	ECH
331	IHC Hydh	S 1000	999.99	451.26	2.22	ECH
278	MENCK	MHU 1000	1000.58	565.02	1.77	ECH
247	VULCAN	VUL 5150	1017.27	667.50	1.52	ECH
296	MENCK	MRBS6000	1029.79	588.60	1.75	ECH
298	MENCK	MRBS8000	1176.97	784.85	1.50	ECH
299	MENCK	MRBS8800	1294.69	863.34	1.50	ECH
332	IHC Hydh	S 1600	1597.52	694.20	2.30	ECH
279	MENCK	MHU 1700	1666.80	922.17	1.81	ECH
280	MENCK	MHU 2100	2099.09	1138.31	1.84	ECH
300	MENCK	MBS12500	2145.53	1226.33	1.75	ECH
333	IHC Hydh	S 2300	2298.99	1008.37	2.28	ECH
248	VULCAN	VUL 6300	2441.45	1335.00	1.83	ECH
281	MENCK	MHU 3000	2945.54	1618.73	1.82	ECH
334	IHC Hydh	S 3000	2997.72	1477.40	2.03	ECH

TABLE D-3 COMPLETE HAMMER LISTING
(sorted by GRLWEAP ID Numbers)

GRLWEAP ID	Hammer Mfgr	Hammer Name	Max. Energy kN-m	Ram Weight kN	Eq. Max. Stroke m	Hammer Type
1	DELMAG	D 5	11.16	4.89	2.28	OED
2	DELMAG	D 8-22	23.87	7.83	3.05	OED
3	DELMAG	D 12	32.00	12.24	2.62	OED
4	DELMAG	D 15	38.40	14.68	2.62	OED
5	DELMAG	D 16-32	53.23	15.66	3.40	OED
6	DELMAG	D 22	55.08	21.85	2.52	OED
7	DELMAG	D 22-02	65.78	21.58	3.05	OED
8	DELMAG	D 22-13	65.78	21.58	3.05	OED
9	DELMAG	D 22-23	69.53	21.58	3.22	OED
10	DELMAG	D 25-32	83.40	24.52	3.40	OED
11	DELMAG	D 30	80.84	29.37	2.75	OED
12	DELMAG	D 30-02	89.52	29.37	3.05	OED
13	DELMAG	D 30-13	89.52	29.37	3.05	OED
14	DELMAG	D 30-23	99.90	29.37	3.40	OED
15	DELMAG	D 30-32	99.90	29.37	3.40	OED
16	DELMAG	D 36	113.69	35.29	3.22	OED
17	DELMAG	D 36-02	113.69	35.29	3.22	OED
18	DELMAG	D 36-13	113.69	35.29	3.22	OED
19	DELMAG	D 36-23	120.04	35.29	3.40	OED
20	DELMAG	D 36-32	120.04	35.29	3.40	OED
21	DELMAG	D 44	122.67	42.27	2.90	OED
22	DELMAG	D 46	145.37	45.12	3.22	OED
23	DELMAG	D 46-02	145.37	45.12	3.22	OED
24	DELMAG	D 46-13	130.93	45.12	2.90	OED
25	DELMAG	D 46-23	145.37	45.12	3.22	OED
26	DELMAG	D 46-32	153.49	45.12	3.40	OED
27	DELMAG	D 55	168.91	52.78	3.20	OED
28	DELMAG	D 62-02	206.77	60.79	3.40	OED
29	DELMAG	D 62-12	206.77	60.79	3.40	OED
30	DELMAG	D 62-22	206.77	60.79	3.40	OED
31	DELMAG	D 80-12	252.61	78.41	3.22	OED
32	DELMAG	D 80-23	266.71	78.41	3.40	OED
33	DELMAG	D100-13	333.47	98.03	3.40	OED
36	DELMAG	D 6-32	14.24	5.88	2.42	OED
37	DELMAG	D 12-32	42.50	12.55	3.39	OED
38	DELMAG	D 19-32	57.51	17.80	3.23	OED
41	FEC	FEC 1200	30.51	12.24	2.49	OED
42	FEC	FEC 1500	36.75	14.68	2.50	OED
43	FEC	FEC 2500	67.81	24.47	2.77	OED
44	FEC	FEC 2800	75.95	27.41	2.77	OED
45	FEC	FEC 3000	85.49	29.37	2.91	OED

TABLE D-3 COMPLETE HAMMER LISTING
(sorted by GRLWEAP ID Numbers)

GRLWEAP ID	Hammer Mfgr	Hammer Name	Max. Energy kN-m	Ram Weight kN	Eq. Max. Stroke m	Hammer Type
46	FEC	FEC 3400	99.02	33.29	2.97	OED
61	MITSUB.	M 14	34.24	13.22	2.59	OED
62	MITSUB.	MH 15	38.16	14.73	2.59	OED
63	MITSUB.	M 23	58.34	22.52	2.59	OED
64	MITSUB.	MH 25	63.53	24.52	2.59	OED
65	MITSUB.	M 33	83.70	32.31	2.59	OED
66	MITSUB.	MH 35	89.00	34.35	2.59	OED
67	MITSUB.	M 43	109.06	42.10	2.59	OED
68	MITSUB.	MH 45	115.87	44.72	2.59	OED
70	MITSUB.	MH 72B	183.31	70.75	2.59	OED
71	MITSUB.	MH 80B	202.91	78.32	2.59	OED
81	LINKBELT	LB 180	10.98	7.70	1.43	CED
82	LINKBELT	LB 312	20.37	17.18	1.19	CED
83	LINKBELT	LB 440	24.69	17.80	1.39	CED
84	LINKBELT	LB 520	35.69	22.56	1.58	CED
85	LINKBELT	LB 660	70.03	33.69	2.08	CED
101	KOBE	K 13	34.49	12.77	2.70	OED
103	KOBE	K22-Est	61.51	21.58	2.85	OED
104	KOBE	K 25	69.88	24.52	2.85	OED
107	KOBE	K 35	97.90	34.35	2.85	OED
110	KOBE	K 45	125.81	44.14	2.85	OED
112	KOBE	KB 60	176.58	58.87	3.00	OED
113	KOBE	KB 80	235.43	78.50	3.00	OED
120	ICE	180	11.03	7.70	1.43	CED
121	ICE	422	31.36	17.80	1.76	CED
122	ICE	440	25.17	17.80	1.41	CED
123	ICE	520	41.19	22.56	1.83	CED
124	ICE	640	55.10	26.70	2.06	CED
125	ICE	660	70.03	33.69	2.08	CED
126	ICE	1070	98.47	44.50	2.21	CED
127	ICE	30-S	30.52	13.35	2.29	OED
128	ICE	40-S	54.25	17.80	3.05	OED
129	ICE	42-S	56.97	18.19	3.13	OED
130	ICE	60-S	98.93	31.15	3.18	OED
131	ICE	70-S	94.95	31.15	3.05	OED
132	ICE	80-S	134.77	35.60	3.79	OED
133	ICE	90-S	122.07	40.05	3.05	OED
134	ICE	100-S	162.76	44.50	3.66	OED
135	ICE	120-S	202.15	53.40	3.79	OED
136	ICE	200-S	135.64	89.00	1.52	OED
141	MKT 20	DE333020	27.13	8.90	3.05	OED

TABLE D-3 COMPLETE HAMMER LISTING
(sorted by GRLWEAP ID Numbers)

GRLWEAP ID	Hammer Mfgr	Hammer Name	Max. Energy kN-m	Ram Weight kN	Eq. Max. Stroke m	Hammer Type
142	MKT 30	DE333020	37.98	12.46	3.05	OED
143	MKT 33	DE333020	44.76	14.68	3.05	OED
144	MKT 40	DE333020	54.25	17.80	3.05	OED
146	MKT	DE10	20.75	7.57	2.74	OED
147	MKT	DE 20	21.70	8.90	2.44	OED
148	MKT	DE 30	30.38	12.46	2.44	OED
149	MKT	DA35B SA	32.28	12.46	2.59	OED
150	MKT	DE 30B	32.28	12.46	2.59	OED
151	MKT	DA 35B	28.48	12.46	2.29	CED
152	MKT	DA 45	41.67	17.80	2.34	CED
153	MKT	DE 40	43.40	17.80	2.44	OED
159	MKT	DE 50B	57.65	22.25	2.59	OED
160	MKT	DA55B SA	54.25	22.25	2.44	OED
161	MKT	DA 55B	51.81	22.25	2.33	CED
162	MKT	DE 70B	80.70	31.15	2.59	OED
163	MKT 50	DE70/50B	67.82	22.25	3.05	OED
164	MKT 70	DE70/50B	94.95	31.15	3.05	OED
165	MKT110	DE110150	149.20	48.95	3.05	OED
166	MKT150	DE110150	203.45	66.75	3.05	OED
171	CONMACO	C 50	20.35	22.25	.91	ECH
172	CONMACO	C 65	26.45	28.92	.91	ECH
173	CONMACO	C 550	33.91	22.25	1.52	ECH
174	CONMACO	C 565	44.08	28.92	1.52	ECH
175	CONMACO	C 80	35.27	35.60	.99	ECH
176	CONMACO	C 100	44.08	44.50	.99	ECH
177	CONMACO	C 115	50.69	51.17	.99	ECH
178	CONMACO	C 80E5	54.25	35.60	1.52	ECH
179	CONMACO	C 100E5	67.82	44.50	1.52	ECH
180	CONMACO	C 115E5	77.99	51.17	1.52	ECH
181	CONMACO	C 125E5	84.77	55.62	1.52	ECH
182	CONMACO	C 140	56.97	62.30	.91	ECH
183	CONMACO	C 160	66.12	72.31	.91	ECH
184	CONMACO	C 200	81.38	89.00	.91	ECH
185	CONMACO	C 300	122.07	133.50	.91	ECH
186	CONMACO	C 5200	135.64	89.00	1.52	ECH
187	CONMACO	C 5300	203.45	133.50	1.52	ECH
188	CONMACO	C 5450	305.18	200.25	1.52	ECH
189	CONMACO	C 5700	474.73	311.50	1.52	ECH
190	CONMACO	C 6850	691.74	378.25	1.83	ECH
191	CONMACO	C 160 **	70.23	76.81	.91	ECH
201	VULCAN	VUL V15	36.77	12.26	3.00	OED

TABLE D-3 COMPLETE HAMMER LISTING
(sorted by GRLWEAP ID Numbers)

GRLWEAP ID	Hammer Mfgr	Hammer Name	Max. Energy kN-m	Ram Weight kN	Eq. Max. Stroke m	Hammer Type
202	VULCAN	VUL V18	52.97	17.66	3.00	OED
203	VULCAN	VUL V25	78.51	24.53	3.20	OED
204	VULCAN	VUL 01	20.35	22.25	.91	ECH
205	VULCAN	VUL 02	9.85	13.35	.74	ECH
206	VULCAN	VUL 06	26.45	28.92	.91	ECH
207	VULCAN	VUL 08	35.27	35.60	.99	ECH
208	VULCAN	VUL010	44.08	44.50	.99	ECH
209	VULCAN	VUL012	52.90	53.40	.99	ECH
210	VULCAN	VUL014	56.97	62.30	.91	ECH
211	VULCAN	VUL016	66.12	72.31	.91	ECH
212	VULCAN	VUL020	81.38	89.00	.91	ECH
213	VULCAN	VUL030	122.07	133.50	.91	ECH
214	VULCAN	VUL040	162.76	178.00	.91	ECH
215	VULCAN	VUL060	244.14	267.00	.91	ECH
220	VULCAN	VUL30C	9.85	13.35	.74	ECH
221	VULCAN	VUL50C	20.48	22.25	.92	ECH
222	VULCAN	VUL65C	26.01	28.92	.90	ECH
223	VULCAN	VUL 65CA	26.54	28.92	.92	ECH
224	VULCAN	VUL80C	33.20	35.60	.93	ECH
225	VULCAN	VUL85C	35.25	37.91	.93	ECH
226	VULCAN	VUL 100C	44.62	44.50	1.00	ECH
227	VULCAN	VUL 140C	48.80	62.30	.78	ECH
228	VULCAN	VUL 200C	68.09	89.00	.77	ECH
229	VULCAN	VUL 400C	154.08	178.00	.87	ECH
230	VULCAN	VUL 600C	243.01	267.00	.91	ECH
231	VULCAN	VUL320	81.38	89.00	.91	ECH
232	VULCAN	VUL330	122.07	133.50	.91	ECH
233	VULCAN	VUL340	162.76	178.00	.91	ECH
234	VULCAN	VUL360	244.14	267.00	.91	ECH
235	VULCAN	VUL505	33.91	22.25	1.52	ECH
236	VULCAN	VUL506	44.08	28.92	1.52	ECH
237	VULCAN	VUL508	54.25	35.60	1.52	ECH
238	VULCAN	VUL510	67.82	44.50	1.52	ECH
239	VULCAN	VUL512	81.38	53.40	1.52	ECH
240	VULCAN	VUL520	135.64	89.00	1.52	ECH
241	VULCAN	VUL530	203.45	133.50	1.52	ECH
242	VULCAN	VUL540	271.27	182.01	1.49	ECH
243	VULCAN	VUL560	406.91	278.13	1.46	ECH
245	VULCAN	VUL 3100	406.91	445.00	.91	ECH
246	VULCAN	VUL 5100	678.18	445.00	1.52	ECH
247	VULCAN	VUL 5150	1017.27	667.50	1.52	ECH

TABLE D-3 COMPLETE HAMMER LISTING
(sorted by GRLWEAP ID Numbers)

GRLWEAP ID	Hammer Mfgr	Hammer Name	Max. Energy kN-m	Ram Weight kN	Eq. Max. Stroke m	Hammer Type
248	VULCAN	VUL 6300	2441.45	1335.00	1.83	ECH
251	RAYMOND	R 1	20.35	22.25	.91	ECH
252	RAYMOND	R 1S	26.45	28.92	.91	ECH
253	RAYMOND	R 65C	26.45	28.92	.91	ECH
254	RAYMOND	R 65CH	26.45	28.92	.91	ECH
255	RAYMOND	R 0	33.06	33.38	.99	ECH
256	RAYMOND	R 80C	33.20	35.60	.93	ECH
257	RAYMOND	R 80CH	33.20	35.60	.93	ECH
258	RAYMOND	R 2/0	44.08	44.50	.99	ECH
259	RAYMOND	R 3/0	55.10	55.62	.99	ECH
260	RAYMOND	R 150C	66.12	66.75	.99	ECH
261	RAYMOND	R 4/0	66.12	66.75	.99	ECH
262	RAYMOND	R 5/0	77.14	77.88	.99	ECH
263	RAYMOND	R 30X	101.73	133.50	.76	ECH
264	RAYMOND	R 8/0	110.20	111.25	.99	ECH
265	RAYMOND	R 40X	135.64	178.00	.76	ECH
266	RAYMOND	R 60X	203.45	267.00	.76	ECH
270	9K DROP	9K DROP	122.07	40.05	3.05	ECH
271	MENCK	MH 68	66.70	34.35	1.94	ECH
272	MENCK	MH 96	94.17	49.04	1.92	ECH
273	MENCK	MH 145	142.15	73.56	1.93	ECH
274	MENCK	MH 195	191.41	98.12	1.95	ECH
275	MENCK	MHU 220	215.76	111.83	1.93	ECH
276	MENCK	MHU 400	392.74	225.66	1.74	ECH
277	MENCK	MHU 600	588.17	343.36	1.71	ECH
278	MENCK	MHU 1000	1000.58	565.02	1.77	ECH
279	MENCK	MHU 1700	1666.80	922.17	1.81	ECH
280	MENCK	MHU 2100	2099.09	1138.31	1.84	ECH
281	MENCK	MHU 3000	2945.54	1618.73	1.82	ECH
282	MENCK	MRBS 500	61.13	49.04	1.25	ECH
283	MENCK	MRBS 750	91.92	73.56	1.25	ECH
284	MENCK	MRBS 800	126.53	84.37	1.50	ECH
285	MENCK	MRBS 850	126.53	84.37	1.50	ECH
286	MENCK	MRBS1100	167.42	107.91	1.55	ECH
287	MENCK	MRBS1502	183.90	147.16	1.25	ECH
288	MENCK	MRBS1800	257.46	171.68	1.50	ECH
289	MENCK	MRBS2500	355.52	284.49	1.25	ECH
290	MENCK	MRBS2502	306.47	245.24	1.25	ECH
291	MENCK	MRBS2504	306.47	245.24	1.25	ECH
292	MENCK	MRBS3000	441.30	294.28	1.50	ECH
293	MENCK	MRBS3900	696.28	386.53	1.80	ECH

TABLE D-3 COMPLETE HAMMER LISTING
(sorted by GRLWEAP ID Numbers)

GRLWEAP ID	Hammer Mfgr	Hammer Name	Max. Energy kN-m	Ram Weight kN	Eq. Max. Stroke m	Hammer Type
294	MENCK	MRBS4600	676.74	451.27	1.50	ECH
295	MENCK	MRBS5000	735.60	490.52	1.50	ECH
296	MENCK	MRBS6000	1029.79	588.60	1.75	ECH
297	MENCK	MRBS7000	856.41	685.30	1.25	ECH
298	MENCK	MRBS8000	1176.97	784.85	1.50	ECH
299	MENCK	MRBS8800	1294.69	863.34	1.50	ECH
300	MENCK	MBS12500	2145.53	1226.33	1.75	ECH
301	MKT	No. 5	1.36	.89	1.52	ECH
302	MKT	No. 6	3.39	1.78	1.90	ECH
303	MKT	No. 7	5.63	3.56	1.58	ECH
304	MKT	9B3	11.87	7.12	1.67	ECH
305	MKT	10B3	17.78	13.35	1.33	ECH
306	MKT	C5-Air	19.26	22.25	.87	ECH
307	MKT	C5-Steam	21.97	22.25	.99	ECH
308	MKT	S-5	22.04	22.25	.99	ECH
309	MKT	11B3	25.97	22.25	1.17	ECH
310	MKT	C826 Stm	33.10	35.60	.93	ECH
311	MKT	C826 Air	28.75	35.60	.81	ECH
312	MKT	S-8	35.27	35.60	.99	ECH
313	MKT	MS-350	41.78	34.35	1.22	ECH
314	MKT	S 10	44.08	44.50	.99	ECH
315	MKT	S 14	50.89	62.30	.82	ECH
316	MKT	MS 500	59.68	48.95	1.22	ECH
317	MKT	S 20	81.38	89.00	.91	ECH
320	IHC Hydh	S 35	35.01	32.35	1.08	ECH
321	IHC Hydh	S 40	41.18	24.52	1.68	ECH
322	IHC Hydh	S 60	60.04	58.86	1.02	ECH
323	IHC Hydh	S 70	70.05	34.35	2.04	ECH
324	IHC Hydh	S 90	90.01	44.14	2.04	ECH
325	IHC Hydh	S 200	199.63	97.90	2.04	ECH
326	IHC Hydh	S 250	250.44	122.82	2.04	ECH
327	IHC Hydh	S 280	280.11	132.61	2.11	ECH
328	IHC Hydh	S 400	399.58	197.13	2.03	ECH
329	IHC Hydh	S 500	499.54	246.08	2.03	ECH
330	IHC Hydh	S 800	800.05	363.00	2.20	ECH
331	IHC Hydh	S 1000	999.99	451.26	2.22	ECH
332	IHC Hydh	S 1600	1597.52	694.20	2.30	ECH
333	IHC Hydh	S 2300	2298.99	1008.37	2.28	ECH
334	IHC Hydh	S 3000	2997.72	1477.40	2.03	ECH
341	IHC Hydh	SC 30	30.02	16.20	1.85	ECH
342	IHC Hydh	SC 40	39.98	24.52	1.63	ECH

TABLE D-3 COMPLETE HAMMER LISTING
(sorted by GRLWEAP ID Numbers)

GRLWEAP ID	Hammer Mfgr	Hammer Name	Max. Energy kN-m	Ram Weight kN	Eq. Max. Stroke m	Hammer Type
343	IHC Hydh	SC 60	60.00	34.35	1.75	ECH
344	IHC Hydh	SC 80	79.89	50.02	1.60	ECH
345	IHC Hydh	SC 110	105.01	67.68	1.55	ECH
346	IHC Hydh	SC 150	140.12	107.91	1.30	ECH
347	IHC Hydh	SC 200	204.81	134.39	1.52	ECH
348	IHC Hydh	SC 250	240.04	174.62	1.37	ECH
350	HERA	1250	34.38	12.50	2.75	OED
351	HERA	1500	41.25	15.00	2.75	OED
352	HERA	2500	68.75	25.00	2.75	OED
353	HERA	2800	77.00	28.00	2.75	OED
354	HERA	3500	96.25	35.00	2.75	OED
355	HERA	5000	137.50	50.00	2.75	OED
356	HERA	5700	156.75	57.00	2.75	OED
357	HERA	6200	170.50	62.00	2.75	OED
358	HERA	7500	206.25	75.00	2.75	OED
359	HERA	8800	242.00	88.00	2.75	OED
371	FAIRCHLD	F-45	61.04	66.75	.91	ECH
372	FAIRCHLD	F-32	44.15	48.28	.91	ECH
381	BSP	HH 3	35.29	29.42	1.20	ECH
382	BSP	HH 5	58.83	49.04	1.20	ECH
383	BSP	HH 7	82.44	68.65	1.20	ECH
384	BSP	HH 8	94.27	78.50	1.20	ECH
385	BSP	HH 9	106.03	88.29	1.20	ECH
386	BSP	HH 11	129.59	107.91	1.20	ECH
387	BSP	HH 14	164.92	137.33	1.20	ECH
388	BSP	HH 16	188.35	156.96	1.20	ECH
389	BSP	HH 20	235.44	196.20	1.20	ECH
390	BSP	HH 20S	235.44	196.20	1.20	ECH
391	BSP	HA 30	353.16	294.30	1.20	ECH
392	BSP	HA 40	470.88	392.40	1.20	ECH
401	BERMINGH	B23	31.18	12.46	2.50	CED
402	BERMINGH	B200	24.41	8.90	2.74	OED
403	BERMINGH	B225	39.67	13.35	2.97	OED
404	BERMINGH	B300	54.68	16.69	3.28	OED
405	BERMINGH	B400	72.90	22.25	3.28	OED
410	BERMINGH	B300 M	54.68	16.69	3.28	OED
411	BERMINGH	B400 M	72.90	22.25	3.28	OED
412	BERMINGH	B400 4.8	58.59	21.36	2.74	OED
413	BERMINGH	B400 5.0	61.04	22.25	2.74	OED
414	BERMINGH	B23 5	31.18	12.46	2.50	CED
415	BERMINGH	B250 5	48.02	13.35	3.60	OED

TABLE D-3 COMPLETE HAMMER LISTING
(sorted by GRLWEAP ID Numbers)

GRLWEAP ID	Hammer Mfgr	Hammer Name	Max. Energy kN-m	Ram Weight kN	Eq. Max. Stroke m	Hammer Type
416	BERMINGH	B350 5	64.02	17.80	3.60	OED
417	BERMINGH	B400 5	80.03	22.25	3.60	OED
418	BERMINGH	B450 5	105.63	29.37	3.60	OED
419	BERMINGH	B500 5	124.84	34.71	3.60	OED
420	BERMINGH	B550 5	144.05	40.05	3.60	OED
421	BERMINGH	B550 C	119.36	48.95	2.44	OED
441	MENCK	MHF5-5	52.48	49.05	1.07	ECH
442	MENCK	MHF5-6	62.98	58.86	1.07	ECH
443	MENCK	MHF5-7	73.48	68.67	1.07	ECH
444	MENCK	MHF5-8	83.97	78.48	1.07	ECH
445	MENCK	MHF5-9	94.47	88.29	1.07	ECH
446	MENCK	MHF5-10	104.97	98.10	1.07	ECH
447	MENCK	MHF5-11	115.46	107.91	1.07	ECH
448	MENCK	MHF5-12	125.96	117.72	1.07	ECH
449	MENCK	MHF3-3	33.59	31.39	1.07	ECH
450	MENCK	MHF3-4	41.99	39.24	1.07	ECH
451	MENCK	MHF3-5	52.48	49.05	1.07	ECH
452	MENCK	MHF3-6	62.98	58.86	1.07	ECH
453	MENCK	MHF3-7	73.48	68.67	1.07	ECH
454	MENCK	MHF10-15	157.39	147.12	1.07	ECH
455	MENCK	MHF10-20	209.81	196.11	1.07	ECH
461	MENCK	MHUT 200	199.90	117.75	1.70	ECH
462	MENCK	MHUT 400	400.29	234.51	1.71	ECH
463	MENCK	MHUT 500	499.89	264.95	1.89	ECH
464	MENCK	MHUT700U	700.06	413.09	1.69	ECH
465	MENCK	MHUT700A	839.83	413.09	2.03	ECH
466	MENCK	MHUT1000	999.52	588.73	1.70	ECH
481	JUNTTAN	HHK 3	36.01	29.46	1.22	ECH
482	JUNTTAN	HHK 4	47.97	39.25	1.22	ECH
483	JUNTTAN	HHK 5	59.99	49.08	1.22	ECH
484	JUNTTAN	HHK 6	71.96	58.87	1.22	ECH
485	JUNTTAN	HHK 7	83.98	68.71	1.22	ECH
486	JUNTTAN	HHK 10	119.93	98.12	1.22	ECH
487	JUNTTAN	HHK 12	143.92	117.75	1.22	ECH
488	JUNTTAN	HHK 14	167.90	137.37	1.22	ECH
489	JUNTTAN	HHK 5A	59.79	49.04	1.22	ECH
490	JUNTTAN	HHK 7A	83.71	68.66	1.22	ECH
491	JUNTTAN	HHK 9A	107.64	88.29	1.22	ECH
501	HPSI	110	59.68	48.95	1.22	ECH
502	HPSI	150	81.38	66.75	1.22	ECH
503	HPSI	154	83.55	68.53	1.22	ECH

TABLE D-3 COMPLETE HAMMER LISTING
(sorted by GRLWEAP ID Numbers)

GRLWEAP ID	Hammer Mfgr	Hammer Name	Max. Energy kN-m	Ram Weight kN	Eq. Max. Stroke m	Hammer Type
504	HPSI	200	108.51	89.00	1.22	ECH
505	HPSI	225	122.07	100.12	1.22	ECH
506	HPSI	650	44.08	28.92	1.52	ECH
507	HPSI	1000	67.82	44.50	1.52	ECH
508	HPSI	1605	112.58	73.87	1.52	ECH
509	HPSI	2005	128.99	84.64	1.52	ECH
510	HPSI	3005	209.32	137.35	1.52	ECH
511	HPSI	3505	239.16	156.93	1.52	ECH
515	UDDCOMB	H3H	33.75	29.37	1.15	ECH
516	UDDCOMB	H4H	45.00	39.16	1.15	ECH
517	UDDCOMB	H5H	56.25	48.95	1.15	ECH
518	UDDCOMB	H6H	67.50	58.74	1.15	ECH
519	UDDCOMB	H8H	94.06	78.32	1.20	ECH
520	UDDCOMB	H10H	117.84	98.12	1.20	ECH
521	DAWSON	HPH 1200	11.73	10.20	1.15	ECH
522	DAWSON	HPH 2400	23.49	18.64	1.26	ECH
541	BANUT	3 Tonnes	23.53	29.41	.80	ECH
542	BANUT	4 Tonnes	31.39	39.25	.80	ECH
543	BANUT	5 Tonnes	39.22	49.04	.80	ECH
544	BANUT	6 Tonnes	47.09	58.87	.80	ECH
545	BANUT	7 Tonnes	54.92	68.66	.80	ECH
551	ICE	110-SH	51.16	51.17	1.00	ECH
552	ICE	115-SH	51.47	51.17	1.01	ECH
553	ICE	160-SH	86.81	71.20	1.22	ECH
701	ICE	1412	27.13	4.45	6.10	VIB
702	ICE	815	36.21	4.45	8.14	VIB
703	ICE	812	32.59	4.01	8.14	VIB
704	ICE	416	18.11	2.23	8.14	VIB

APPENDIX E

Subsurface Exploration Results for Peach Freeway Design Problem

	Page
SOIL BORING LOGS	E-3
CONE PENETRATION TEST RESULTS	E-11

SUBSURFACE EXPLORATION LOG BORING NO. S-1 SHEET NO. 1 OF 2

Region <u>6</u>	Hammer Fall-Casing <u>--</u>	Line <u>Baseline</u>
County <u>James</u>	Hammer Fall-Sampler <u>--</u>	Station <u>1223 + 88</u>
Project <u>Peach Freeway</u>	Wt. of Hammer-Casing <u>--</u>	Offset <u>20 m Rt</u>
Structure <u>Dismal River</u>	Wt. of Hammer-Sampler <u>64 kg</u>	Surface Elev. <u>96.0 m</u>
Date Start <u>10-1-1995</u>	SPT Hammer Type <u>Safety Hammer</u>	Water Tbl. Elev. <u>92.0 m</u>
Date Finish <u>10-2-1995</u>	Core Barrel Type <u>Double Tube</u>	Date <u>10-3-1995</u>
Backfill/Sealed <u>10-3-1995</u>	Drill Rig Type <u>Rotary</u>	Time <u>5:00 p.m.</u>
		Depth <u>4.0 m</u>

NO.	BLOWS ON SAMPLER PER 150 mm				DEPTH (m) (ft)	SOIL DESCRIPTION AND REMARKS	q _u (tsf)	γ _D (pcf)	w _c %	
	0-150	150-300	300-450	N						
SS-1	1	1	3	4	0	LOOSE TO MEDIUM DENSE, SILTY FINE SAND				
SS-2	1	2	2	4	1					
SS-3	2	2	4	6	2					
SS-4	2	3	3	6	3					
SS-5	2	3	5	8	4					
SS-6	3	6	7	13	5					
SS-7	4	7	8	15	6					
SS-8	3	5	6	11	7					
SS-9	6	7	8	15	8					
SS-10	7	9	9	18	9					
SS-11	10	19	21	40	10		DENSE SAND AND GRAVEL			
SS-12	15	19	20	39	11					
SS-13	15	20	21	41	12					
SS-14	16	21	22	43	13					

SUBSURFACE EXPLORATION LOG		BORING NO. S-1	SHEET NO. 2 OF 2
Region 6	Hammer Fall-Casing --	Line Baseline	
County James	Hammer Fall-Sampler --	Station 1223 + 88	
Project Peach Freeway	Wt. of Hammer-Casing ..	Offset 20 m Rt	
Structure Dismal River	Wt. of Hammer-Sampler 64 kg	Surface Elev. 96.0 m	
Date Start 10-1-1995	SPT Hammer Type Safety Hammer	Water Tbl. Elev. 92.0 m	
Date Finish 10-3-1995	Core Barrel Type Double Tube	Date 10-3-1995	
Backfill/Sealed 10-3-1995	Drill Rig Type Rotary	Time 5:00 p.m.	
		Depth 4.0 m	

NO.	BLOWS ON SAMPLER PER 150 mm					DEPTH (m) (ft)	SOIL DESCRIPTION AND REMARKS	Q _u kPa (tsf)	γ _D kN/m ³ (pcf)	W _c %
	0	150	300	450	N					
						20	65			
SS-15	15	19	22	41		21	70			
						22	75			
SS-16	17	21	23	44		23	80			
						24	85			
SS-17	18	20	25	45		25	90			
						26	95			
SS-18	19	23	25	48		27	100			
						28	105			
SS-19	15	21	21	42		29	110			
						30	115			
SS-20	17	21	23	44		31	120			
						32	125			
SS-21	20	23	26	49		33	130			
						34				
RUN 1						35				
						36				
						37				
						38				
						39				
						40				

DENSE SAND AND GRAVEL

LIMESTONE BEDROCK
RUN 1 31.0-32.5m REC=83% RQD=81%

END OF BORING @32.5m

NOTES:
SPT N VALUES FROM SAFETY HAMMER.

SUBSURFACE EXPLORATION LOG				BORING NO. S - 2		SHEET NO. 1 OF 2		
Region	6			Hammer Fall-Casing	--		Line	Baseline
County	James			Hammer Fall-Sampler	--		Station	1225 + 13
Project	Peach Freeway			Wt. of Hammer-Casing	--		Offset	20 m Lt
Structure	Dismal River			Wt. of Hammer-Sampler	64 kg		Surface Elev.	85.0 m
Date Start	10-3-1995			SPT Hammer Type	Safety Hammer		Water Tbl. Elev.	87.0 m
Date Finish	10-3-1995			Core Barrel Type	Double Tube		Date	10-3-1995
Backfill/Sealed	10-3-1995			Drill Rig Type	Rotary		Time	5:00 p.m.
							Depth	Surface

NO.	BLOWS ON SAMPLER PER 150 mm				DEPTH (m) (ft)	SOIL DESCRIPTION AND REMARKS	q _u (kPa) (tsf)	γ _D (kN/m ³) (pcf)	W _c (%)
	0-150	150-300	300-450	N					
SS-1	2	2	3	5	0 - 0				
					1 - 5	LOOSE SILT			
SS-2	2	3	4	7	2 - 5				
					3 - 10				
SS-3	3	3	4	7	4 - 10				
					5 - 15				
SS-4	3	4	5	9	6 - 20	EXTREMELY DENSE SAND AND GRAVEL			
					7 - 25				
SS-5	25	39	46	85	8 - 25				
					9 - 30				
SS-6	33	41	55	96	10 - 30	DENSE SAND AND GRAVEL			
					11 - 35				
SS-7	12	13	18	31	12 - 40				
					13 - 45	NOTE: OCCASIONAL COBBLES 15-15.5m.			
SS-8	15	16	19	35	14 - 45				
					15 - 50				
SS-9	11	16	16	32	16 - 50				
					17 - 55				
SS-10	12	15	18	33	18 - 60				
					19 - 65				
SS-11	15	17	21	38	20 - 65				
SS-12	13	16	18	34					
SS-13	17	19	20	39					
SS-14	16	19	22	41					

SUBSURFACE EXPLORATION LOG		BORING NO. S - 2	SHEET NO. 2 OF 2
Region <u>6</u>	Hammer Fall-Casing <u>--</u>	Line <u>Baseline</u>	
County <u>James</u>	Hammer Fall-Sampler <u>--</u>	Station <u>1225 + 13</u>	
Project <u>Peach Freeway</u>	Wt. of Hammer-Casing <u>--</u>	Offset <u>20 m Lt</u>	
Structure <u>Dismal River</u>	Wt. of Hammer-Sampler <u>64 kg</u>	Surface Elev. <u>85.0 m</u>	
Date Start <u>10-3-1995</u>	SPT Hammer Type <u>Safety Hammer</u>	Water Tbl. Elev. <u>87.0 m</u>	
Date Finish <u>10-3-1995</u>	Core Barrel Type <u>Double Tube</u>	Date <u>10-3-1995</u>	
Backfill/Sealed <u>10-3-1995</u>	Drill Rig Type <u>Rotary</u>	Time <u>5:00 p.m.</u>	
		Depth <u>Surface</u>	

NO.	BLOWS ON SAMPLER PER 150 mm				DEPTH (m) (ft)	SOIL DESCRIPTION AND REMARKS	q _u kPa (tsf)	γ _D kN/m ³ (pcf)	w _c %
	0	150	300	N					
					20 - 65				
RUN 1					21 - 70	LIMESTONE BEDROCK			
					22	RUN 1 20.5-22.0m REC.=98%, RQD=67%			
RUN 2					23 - 75	RUN 2 22.0-23.5m REC.=100%, RQD=85%			
					24 - 80	END OF BORING @20.0m			
					25 - 85	NOTES:			
					26 - 90	SPT N VALUES FROM SAFETY HAMMER.			
					27 - 95				
					28 - 100				
					29 - 105				
					30 - 110				
					31 - 115				
					32 - 120				
					33 - 125				
					34 - 130				

Region <u>6</u>	Hammer Fall-Casing <u>--</u>	Line <u>Baseline</u>
County <u>James</u>	Hammer Fall-Sampler <u>--</u>	Station <u>1226 + 13</u>
Project <u>Peach Freeway</u>	Wt. of Hammer-Casing <u>--</u>	Offset <u>20 m Rt</u>
Structure <u>Dismal River</u>	Wt. of Hammer-Sampler <u>64 kg</u>	Surface Elev. <u>85.0 m</u>
Date Start <u>10-4-1995</u>	SPT Hammer Type <u>Safety Hammer</u>	Water Tbl. Elev. <u>87.0 m</u>
Date Finish <u>10-4-1995</u>	Core Barrel Type <u>Double Tube</u>	Date <u>10-4-1995</u>
Backfill/Sealed <u>10-4-1995</u>	Drill Rig Type <u>Rotary</u>	Time <u>5:00 p.m.</u>
		Depth <u>Surface</u>

NO.	BLOWS ON SAMPLER PER 150 mm				DEPTH (m) (ft)	SOIL DESCRIPTION AND REMARKS	q _u (kPa) (tsf)	γ _D (kN/m ³) (pcf)	w _c (%)
	0-150	150-300	300-450	N					
SS-1	1	2	2	4	0 - 0	LOOSE SILT			
					1 - 5				
SS-2	2	3	4	7	2 - 5	EXTREMELY DENSE SAND AND GRAVEL			
SS-3	38	41	42	83	3 - 10				
UD-1					4 - 10	STIFF TO VERY STIFF SILTY CLAY	182	14.6	33
					5 - 15		(1.90)	(93)	
UD-2					6 - 15		240	15.1	31
					7 - 20		(2.51)	(96)	
UD-3					8 - 20		278	15.7	27
					9 - 25		(2.90)	(100)	
UD-4					10 - 25		307	16.2	24
					11 - 30		(3.21)	(103)	
UD-5					12 - 30		316	16.7	22
					13 - 35		(3.30)	(106)	
UD-6					14 - 35		311	16.3	23
					15 - 40		(3.25)	(104)	
UD-7					16 - 40		316	16.7	22
					17 - 45		(3.30)	(106)	
UD-8					18 - 45		326	17.0	21
					19 - 50	(3.40)	(108)		
SS-4	18	19	19	38	20 - 50	DENSE SAND AND GRAVEL			
					21 - 55				
SS-5	21	22	24	46	22 - 55				
					23 - 60				
SS-6	19	19	22	41	24 - 60				
					25 - 65				
SS-7	21	24	26	50	26 - 65				

SUBSURFACE EXPLORATION LOG

BORING NO. S-3

SHEET NO. 2 OF 2

Region 6
 County James
 Project Peach Freeway
 Structure Dismal River
 Date Start 10-4-1995
 Date Finish 10-4-1995
 Backfill/Sealed 10-4-1995

Hammer Fall-Casing --
 Hammer Fall-Sampler --
 Wt. of Hammer-Casing --
 Wt. of Hammer-Sampler 64 kg
 SPT Hammer Type Safety Hammer
 Core Barrel Type Double Tube
 Drill Rig Type Rotary

Line Baseline
 Station 1226 + 13
 Offset 20 m Rt
 Surface Elev. 85.0 m
 Water Tbl. Elev. 87.0 m
 Date 10-4-1995
 Time 5:00 p.m.
 Depth Surface

NO.	BLOWS ON SAMPLER PER 150 mm		N	DEPTH		SOIL DESCRIPTION AND REMARKS	q _u kPa (tsf)	γ _D kN/m ³ (pcf)	w _c %
	0-150	150-300		300-450	(m)				
RUN 1				20	65	LIMESTONE BEDROCK RUN 1 20-21.5m REC.=90%, RQD=79%			
				21	70				
				22	75	END OF BORING @21.5m NOTES: SPT N VALUES FROM SAFETY HAMMER.			
				23	80				
				24	85				
				25	90				
				26	95				
				27	100				
				28	105				
				29	110				
				30	115				
				31	120				
				32	125				
				33					
				34					
				35					
				36					
				37					
				38					
				39					
				40					

SUBSURFACE EXPLORATION LOG

BORING NO. S - 4

SHEET NO. 1 OF 2

Region <u>6</u>	Hammer Fall-Casing <u>--</u>	Line <u>Baseline</u>
County <u>James</u>	Hammer Fall-Sampler <u>--</u>	Station <u>1227 + 38</u>
Project <u>Peach Freeway</u>	Wt. of Hammer-Casing <u>--</u>	Offset <u>20 m Lt</u>
Structure <u>Dismal River</u>	Wt. of Hammer-Sampler <u>64 kg</u>	Surface Elev. <u>91.0 m</u>
Date Start <u>10-5-1995</u>	SPT Hammer Type <u>Safety Hammer</u>	Water Tbl. Elev. <u>90.5 m</u>
Date Finish <u>10-5-1995</u>	Core Barrel Type <u>Double Tube</u>	Date <u>10-6-1995</u>
Backfill/Sealed <u>10-5-1995</u>	Drill Rig Type <u>Rotary</u>	Time <u>5:00 p.m.</u>
		Depth <u>0.5 m</u>

NO.	BLOWS ON SAMPLER PER 150 mm				N	DEPTH (m) (ft)	SOIL DESCRIPTION AND REMARKS	Q _u (kPa) (tsf)	γ _D (kN/m ³) (pcf)	W _c (%)
	0-150	150-300	300-450	450-600						
UD-1						0				
						1	MEDIUM SILTY CLAY	62 (0.65)	13.9 (89)	35
UD-2						2		60 (0.63)	13.6 (87)	38
						3				
UD-3						4		65 (0.68)	14.1 (90)	34
						5				
UD-4						6		67 (0.70)	14.4 (92)	32
						7				
UD-5						8	STIFF SILTY CLAY	69 (0.72)	14.6 (93)	31
						9				
UD-6						10		172 (1.79)	14.9 (95)	30
						11				
UD-7						12		182 (1.89)	15.7 (100)	27
						13				
UD-8						14		192 (2.00)	16.3 (104)	24
						15				
UD-9						16		188 (1.96)	16.0 (102)	26
						17				
UD-10						18		192 (2.00)	16.3 (104)	24
						19				
UD-11						20		190 (1.98)	16.2 (103)	25
						21				
UD-12						22	VERY STIFF SILTY CLAY	316 (3.30)	16.7 (106)	22
						23				
UD-13						24		310 (3.24)	16.5 (105)	23
						25				
UD-14						26		326 (3.40)	17.0 (108)	21

SUBSURFACE EXPLORATION LOG

BORING NO. S - 4

SHEET NO. 2 OF 2

Region 6
 County James
 Project Peach Freeway
 Structure Dismal River
 Date Start 10-5-1995
 Date Finish 10-5-1995
 Backfill/Sealed 10-6-1995

Hammer Fall-Casing --
 Hammer Fall-Sampler --
 Wt. of Hammer-Casing --
 Wt. of Hammer-Sampler 64 kg
 SPT Hammer Type Safety Hammer
 Core Barrel Type Double Tube
 Drill Rig Type Rotary

Line Baseline
 Station 1227 + 38
 Offset 20 m Lt
 Surface Elev. 91.0 m
 Water Tbl. Elev. 90.5
 Date 10-6-1995
 Time 5:00 p.m.
 Depth 0.5 m

NO.	BLOWS ON SAMPLER PER 150 mm				DEPTH (m) (ft)	SOIL DESCRIPTION AND REMARKS	q _u (kPa) (tsf)	γ _D (kN/m ³) (pcf)	w _c (%)
	0-150	150-300	300-450	N					
					20 - 65	STIFF TO VERY STIFF SILTY CLAY			
UD-15					21 - 70		335 (3.50)	16.8 (107)	21
					22 - 75				
UD-16					23 - 80		340 (3.55)	17.0 (108)	20
					24 - 85				
UD-17					25 - 90		350 (3.65)	17.1 (109)	19
					26 - 95				
UD-18					27 - 100		345 (3.60)	17.0 (108)	20
					28 - 105				
UD-19					29 - 110		350 (3.65)	17.2 (110)	19
					30 - 115				
UD-20					31 - 120	354 (3.70)	17.3 (110)	18	
					32 - 125				
SS-1	20	22	27	49	30 - 130				
RUN 1									

InSituTech

Engineer: DM HOLLOWAY

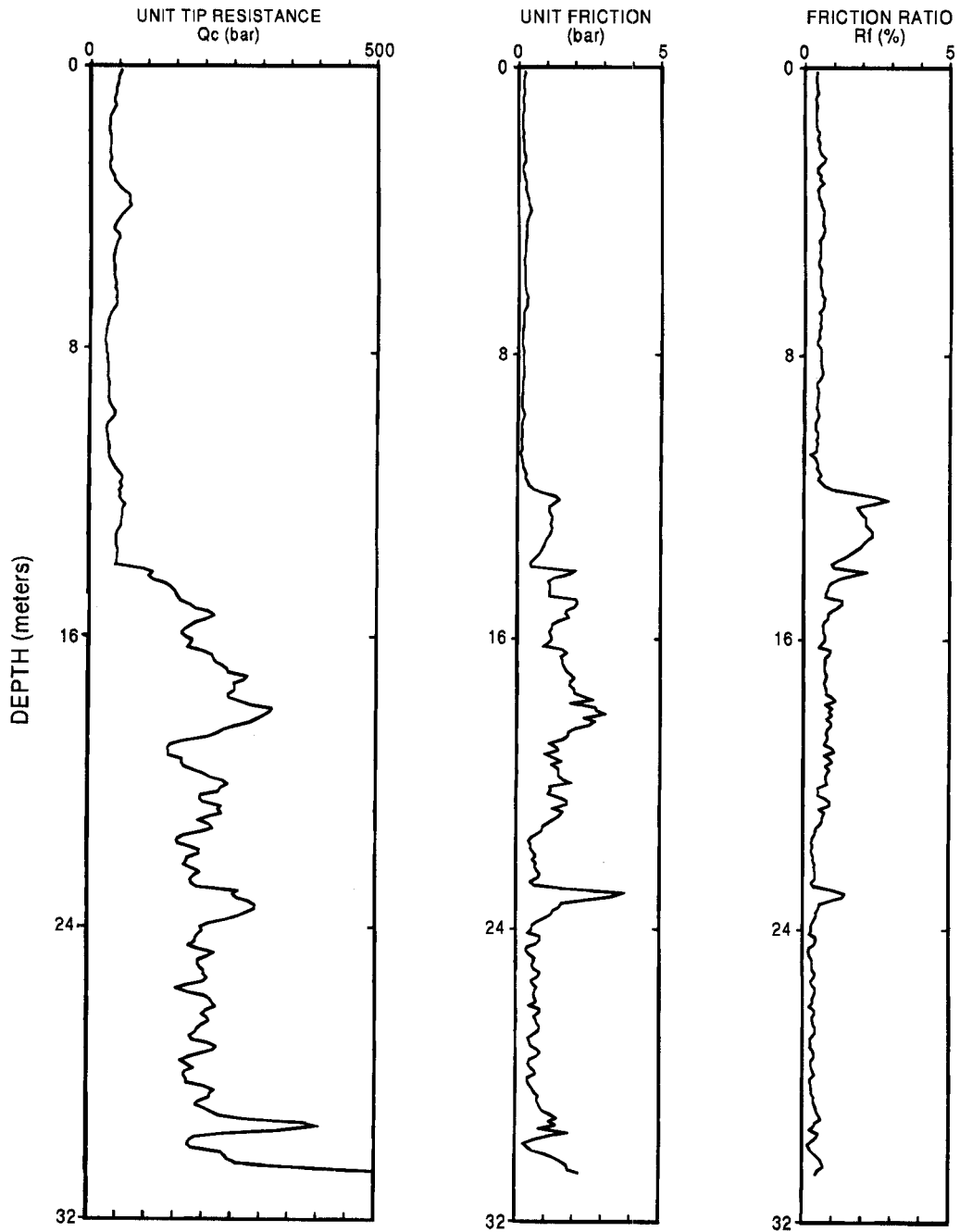
CPT Date: 8/21/89

Page No.: 1 / 1

Location: PEACH FREEWAY, CPT1

Cone Used: 186

Job No.: 93/2/1001



Depth Increment: .1 m

Max Depth: 30.9 m

Licensed to: InSituTech Ltd.
Address: 5 del Valle
City: Orinda, CA 94563, U.S.A.

Interpreter Name: Mike Holloway

File Number: 202
Operator: DM HOLLOWAY
Cone Type: 186

Date: 8/21/89
On Site Location: Peach Freeway CPT-1
Comment: 93/2/1001

SUMMARY SHEET

'a' for calculating Q_t : 0.800
Value for Water Table (in m): 4.000
Valid Zone Classification based on: R_f
Missing unit weight to start depth: 15.720
Method for calculating s_u : Nk
Value of the constant Nk: 15.000
Define Zone 6 for Sand Parameters? Yes
Sand Compressibility for calc D_r : All sands

Soil Behavior Type Zone Numbers for R_f Zone and B_q Zone Classification

Zone #1 = Sensitive fine grained	Zone #7 = Sand with some silt
Zone #2 = Organic material	Zone #8 = Fine sand
Zone #3 = Clay	Zone #9 = Sand
Zone #4 = Silty clay	Zone #10 = Gravelly sand
Zone #5 = Clayey silt	Zone #11 = Very stiff fine grained *
Zone #6 = Silty sand	Zone #12 = Sand to clayey sand *

* Overconsolidated and/or cemented

NOTE: For 8011 classification, R_f values > are assumed to be 8.

NOTE: Since U_2 (pore pressure) has not been defined, Q_t cannot be calculated, therefore, the value of Q_t has been made equal to q_c .

NOTE: ---- means out of range.

PEACH FREEWAY CPT-1											
Depth (meter)	q _c Average (bars)	f _s Average (bars)	R _f (%)	OS Average (bars)	EOS Average (bars)	R _f Zone (zone #)	SPT N (blow/.3 m)	SPT N1 (blow/.3 m)	Dr (%)	s _u (bars)	s _u /EOS (ratio)
0.25	49.900	0.195	0.391	0.054	0.054	8	12	18	89	----	----
0.50	46.867	0.190	0.405	0.103	0.103	8	12	18	78	----	----
0.75	43.900	0.180	0.410	0.152	0.152	8	11	17	71	----	----
1.00	42.633	0.167	0.391	0.201	0.201	8	11	17	66	----	----
1.25	38.650	0.150	0.388	0.251	0.251	8	10	15	60	----	----
1.50	33.600	0.130	0.387	0.299	0.299	7	11	17	54	----	----
1.75	32.450	0.145	0.447	0.346	0.346	7	11	17	51	----	----
2.00	34.700	0.157	0.451	0.393	0.393	7	12	18	51	----	----
2.25	34.250	0.165	0.482	0.440	0.440	7	11	17	49	----	----
2.50	34.400	0.220	0.640	0.487	0.487	7	11	17	47	----	----
2.75	32.150	0.150	0.467	0.534	0.534	7	11	17	44	----	----
3.00	36.633	0.180	0.491	0.582	0.582	7	12	18	47	----	----
3.25	44.200	0.245	0.554	0.630	0.630	8	11	15	51	----	----
3.50	58.667	0.267	0.455	0.679	0.679	8	15	20	58	----	----
3.75	67.250	0.360	0.535	0.728	0.728	8	17	21	61	----	----
4.00	63.733	0.393	0.617	0.777	0.777	8	16	19	58	----	----
4.25	49.750	0.305	0.613	0.826	0.802	8	12	14	51	----	----
4.50	41.733	0.263	0.631	0.874	0.825	7	14	16	45	----	----
4.75	48.500	0.250	0.515	0.922	0.849	8	12	13	49	----	----
5.00	43.733	0.223	0.511	0.972	0.874	8	11	12	46	----	----
5.25	40.200	0.200	0.498	1.020	0.897	7	13	14	43	----	----
5.50	39.667	0.193	0.487	1.067	0.920	7	13	13	42	----	----
5.75	41.350	0.215	0.520	1.115	0.943	8	10	10	43	----	----
6.00	42.400	0.217	0.511	1.164	0.968	8	11	11	43	----	----
6.25	43.950	0.250	0.569	1.213	0.993	8	11	11	44	----	----
6.50	44.600	0.283	0.635	1.261	1.016	7	15	14	44	----	----
6.75	41.550	0.225	0.542	1.309	1.039	7	14	13	42	----	----
7.00	32.767	0.170	0.519	1.356	1.061	7	11	10	35	----	----
7.25	29.100	0.150	0.515	1.403	1.084	7	10	9	31	----	----
7.50	26.567	0.123	0.464	1.450	1.107	7	9	8	28	----	----
7.75	26.350	0.125	0.474	1.497	1.129	7	9	8	28	----	----
8.00	28.900	0.160	0.554	1.544	1.152	7	10	9	30	----	----
8.25	29.950	0.160	0.551	1.591	1.175	7	10	9	31	----	----
8.50	31.033	0.183	0.591	1.639	1.197	7	10	8	31	----	----
8.75	31.400	0.145	0.462	1.686	1.220	7	10	8	31	----	----

PEACH FREEWAY CPT-1

Depth (meter)	q _c Average (bars)	f _s Average (bars)	R _i (%)	OS Average (bars)	EOS Average (bars)	R _i Zone (zone #)	SPT N (blow/.3 m)	SPT N1 (blow/.3 m)	Dr (%)	s _u (bars)	s _u /EOS (ratio)
9.00	32.833	0.147	0.447	1.733	1.242	7	11	9	33	----	----
9.25	32.100	0.140	0.436	1.780	1.265	7	11	9	32	----	----
9.50	36.133	0.150	0.415	1.827	1.288	7	12	10	35	----	----
9.75	42.700	0.195	0.457	1.875	1.311	8	11	9	39	----	----
10.00	32.867	0.123	0.375	1.923	1.335	7	11	9	32	----	----
10.25	29.150	0.130	0.446	1.971	1.358	7	10	8	28	----	----
10.50	31.500	0.133	0.423	2.018	1.380	7	11	8	30	----	----
10.75	33.350	0.105	0.315	2.065	1.403	7	11	8	31	----	----
11.00	35.100	0.143	0.408	2.112	1.425	7	12	9	32	----	----
11.25	42.650	0.195	0.457	2.160	1.449	8	11	8	38	----	----
11.50	54.300	0.290	0.534	2.209	1.474	8	14	10	44	----	----
11.75	53.500	0.445	0.832	2.258	1.498	8	13	9	44	----	----
12.00	51.333	1.207	2.351	2.308	1.523	6	21	15	42	----	----
12.25	58.350	1.215	2.082	2.356	1.546	7	19	13	46	----	----
12.50	56.700	1.140	2.011	2.403	1.569	7	19	13	45	----	----
12.75	55.000	1.165	2.118	2.451	1.593	6	22	15	44	----	----
13.00	50.200	1.163	2.317	2.500	1.617	6	20	13	41	----	----
13.25	46.500	0.990	2.129	2.549	1.642	6	19	13	38	----	----
13.50	47.267	0.843	1.784	2.597	1.665	7	16	10	39	----	----
13.75	47.300	0.590	1.247	2.645	1.688	7	16	10	39	----	----
14.00	62.467	0.973	1.558	2.692	1.711	7	21	13	46	----	----
14.25	106.350	1.525	1.434	2.740	1.734	8	27	17	61	----	----
14.50	127.733	1.110	0.869	2.789	1.759	9	26	16	66	----	----
14.75	149.800	1.110	0.741	2.838	1.784	9	30	19	71	----	----
15.00	162.900	2.047	1.256	2.887	1.808	8	41	25	73	----	----
15.25	196.200	1.715	0.874	2.936	1.833	9	39	24	78	----	----
15.50	203.300	1.477	0.726	2.985	1.857	9	41	25	79	----	----
15.75	170.900	1.155	0.676	3.035	1.882	9	34	20	74	----	----
16.00	168.633	1.153	0.684	3.084	1.907	9	34	20	73	----	----
16.25	173.950	1.240	0.713	3.133	1.931	9	35	20	74	----	----
16.50	208.867	1.610	0.771	3.182	1.956	9	42	24	79	----	----
16.75	224.800	1.605	0.714	3.231	1.980	9	45	26	81	----	----
17.00	252.367	1.877	0.744	3.280	2.005	9	50	28	84	----	----
17.25	260.650	1.840	0.706	3.329	2.030	9	52	29	85	----	----
17.50	249.233	2.083	0.836	3.378	2.054	9	50	28	83	----	----

PEACH FREEWAY CPT-1

Depth (meter)	q _c Average (bars)	f _s Average (bars)	R _f (%)	OS Average (bars)	EOS Average (bars)	R _f Zone (zone #)	SPT N (blow/.3 m)	SPT N1 (blow/.3 m)	Dr (%)	s _u (bars)	s _u /EOS (ratio)
17.75	252.400	2.275	0.901	3.428	2.079	9	50	28	84	----	----
18.00	305.000	2.860	0.938	3.477	2.103	9	61	33	89	----	----
18.25	297.400	2.555	0.859	3.526	2.128	9	59	32	88	----	----
18.50	254.833	2.123	0.833	3.575	2.153	9	51	27	83	----	----
18.75	214.850	1.705	0.794	3.624	2.177	9	43	23	78	----	----
19.00	148.067	1.310	0.885	3.673	2.202	9	30	16	67	----	----
19.25	139.100	1.125	0.809	3.722	2.226	9	28	15	66	----	----
19.50	162.450	1.390	0.856	3.771	2.251	9	32	17	70	----	----
19.75	173.100	1.450	0.838	3.821	2.276	9	35	18	71	----	----
20.00	214.933	1.657	0.771	3.870	2.300	9	43	22	78	----	----
20.25	236.350	1.165	0.493	3.919	2.325	9	47	24	80	----	----
20.50	204.867	1.427	0.696	3.968	2.349	9	41	21	76	----	----
20.75	214.700	1.515	0.706	4.017	2.374	9	43	22	77	----	----
21.00	221.533	1.477	0.667	4.066	2.399	9	44	22	78	----	----
21.25	201.300	1.015	0.504	4.115	2.423	9	40	20	75	----	----
21.50	192.700	0.710	0.368	4.164	2.448	9	39	20	74	----	----
21.75	154.550	0.465	0.301	4.214	2.472	9	31	16	67	----	----
22.00	186.733	0.577	0.309	4.263	2.497	9	37	19	72	----	----
22.25	172.050	0.615	0.357	4.312	2.522	9	34	17	70	----	----
22.50	180.900	0.713	0.394	4.361	2.546	9	36	18	71	----	----
22.75	180.450	0.615	0.341	4.410	2.571	9	36	18	71	----	----
23.00	209.567	2.040	0.973	4.459	2.595	9	42	21	75	----	----
23.25	255.250	2.870	1.124	4.508	2.620	9	51	26	81	----	----
23.50	286.267	1.450	0.507	4.558	2.646	10	48	24	84	----	----
23.75	267.100	1.085	0.406	4.610	2.672	10	45	23	82	----	----
24.00	213.833	0.607	0.284	4.661	2.699	10	36	18	75	----	----
24.25	195.400	0.615	0.315	4.711	2.724	9	39	20	72	----	----
24.50	183.033	0.630	0.344	4.760	2.749	9	37	19	70	----	----
24.75	205.600	0.395	0.192	4.810	2.774	10	34	17	74	----	----
25.00	197.667	0.590	0.298	4.860	2.800	9	40	20	72	----	----
25.25	198.400	0.730	0.368	4.909	2.825	9	40	20	72	----	----
25.50	203.167	0.617	0.304	4.958	2.849	9	41	21	73	----	----
25.75	164.050	0.675	0.411	5.008	2.874	9	33	17	67	----	----
26.00	197.300	0.653	0.331	5.057	2.898	9	39	20	72	----	----
26.25	219.850	0.645	0.293	5.107	2.924	10	37	19	75	----	----

PEACH FREEWAY CPT-1

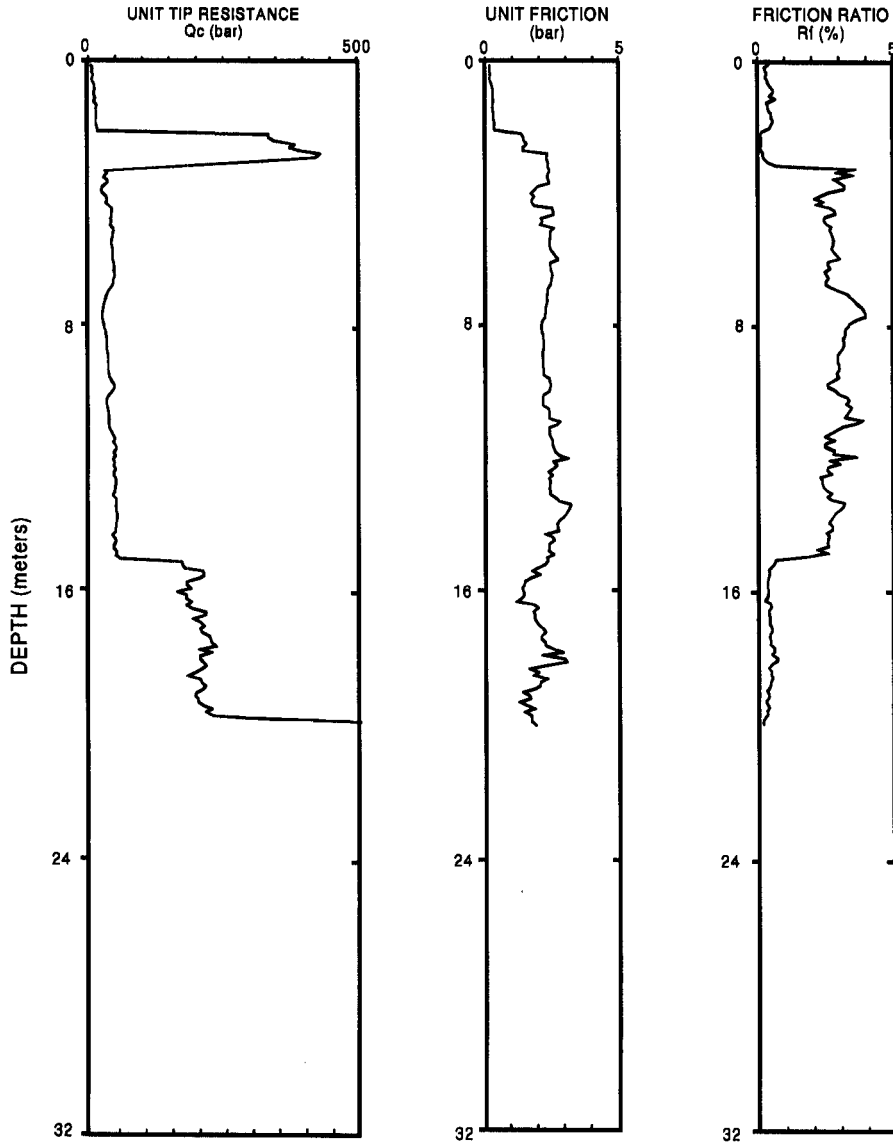
Depth (meter)	q _c Average (bars)	f _s Average (bars)	R _f (%)	OS Average (bars)	EOS Average (bars)	R _f Zone (zone #)	SPT N (blow/.3 m)	SPT N1 (blow/.3 m)	Dr (%)	s _u (bars)	s _u /EOS (ratio)
26.50	204.100	0.700	0.343	5.157	2.950	9	41	21	72	----	----
26.75	205.200	0.770	0.375	5.206	2.974	9	41	21	73	----	----
27.00	185.200	0.600	0.324	5.255	2.999	9	37	19	69	----	----
27.25	196.050	0.480	0.245	5.304	3.023	9	39	20	71	----	----
27.50	211.900	0.753	0.356	5.353	3.048	9	42	21	73	----	----
27.75	167.800	0.440	0.262	5.402	3.073	9	34	17	66	----	----
28.00	175.400	0.593	0.338	5.452	3.097	9	35	18	67	----	----
28.25	169.000	0.400	0.237	5.501	3.122	9	34	17	66	----	----
28.50	198.167	0.560	0.283	5.550	3.146	9	40	20	71	----	----
28.75	213.100	0.755	0.354	5.599	3.171	9	43	22	73	----	----
29.00	194.933	0.837	0.429	5.648	3.196	9	39	20	70	----	----
29.25	222.300	1.285	0.578	5.697	3.220	9	44	22	74	----	----
29.50	351.033	1.137	0.324	5.747	3.246	10	59	30	87	----	----
29.75	282.400	1.410	0.499	5.798	3.272	10	47	24	80	----	----
30.00	179.367	0.430	0.240	5.849	3.298	9	36	18	67	----	----
30.25	207.250	0.805	0.388	5.898	3.323	9	41	21	71	----	----
30.50	248.033	1.580	0.637	5.947	3.347	9	50	25	76	----	----
30.75	425.400	2.005	0.471	5.997	3.373	10	71	36	92	----	----

InSituTech

Engineer: DM HOLLOWAY
Location: PEACH FREEWAY, CPT3

CPT Date: 8/22/89
Cone Used: 186

Page No.: 1 / 1
Job No.: 93/2/1001



Depth Increment: .1 m

Max Depth: 19.9 m

Licensed to: InSituTech Ltd.
Address: 5 del Valle
City: Orinda, CA 94563, U.S.A.

Interpreter Name: Mike Holloway

File Number: 203
Operator: DM HOLLOWAY
Cone Type: 186

Date: 8/22/89
On Site Location: Peach Freeway CPT-3
Comment: 93/2/1001

SUMMARY SHEET

'a' for calculating Q_t : 0.800
Value for Water Table (in m): 0.000
Valid Zone Classification based on: R_f
Missing unit weight to start depth: 15.720
Method for calculating s_u : Nk
Value of the constant Nk: 15.000
Define Zone 6 for Sand Parameters? Yes
Sand Compressibility for calc D_r : All sands

Soil Behavior Type Zone Numbers for R_f Zone and Bq Zone Classification

Zone #1 = Sensitive fine grained	Zone #7 = Sand with some silt
Zone #2 = Organic material	Zone #8 = Fine sand
Zone #3 = Clay	Zone #9 = Sand
Zone #4 = Silty clay	Zone #10 = Gravelly sand
Zone #5 = Clayey silt	Zone #11 = Very stiff fine grained *
Zone #6 = Silty sand	Zone #12 = Sand to clayey sand *

* Overconsolidated and/or cemented

NOTE: For 8011 classification, R_f values > are assumed to be 8.

NOTE: Since U_2 (pore pressure) has not been defined, Q_t cannot be calculated, therefore, the value of Q_t has been made equal to Q_c .

NOTE: ---- means out of range.

PEACH FREEWAY CPT-3											
Depth (Meter)	q _c Average (bars)	f _s Average (bars)	R _f (%)	OS Average (bars)	EOS Average (bars)	R _f Zone (zone #)	SPT N (blow/.3 m)	SPT N1 (blow/.3 m)	D _r (%)	s _u (bars)	s _u /EOS (ratio)
0.25	12.400	0.110	0.887	0.051	0.027	6	5	8	60	----	----
0.50	11.867	0.117	0.983	0.098	0.049	6	5	8	50	----	----
0.75	13.900	0.155	1.115	0.145	0.072	6	6	9	49	----	----
1.00	12.633	0.157	1.240	0.193	0.094	6	5	8	42	----	----
1.25	13.650	0.150	1.099	0.240	0.117	6	5	8	41	----	----
1.50	13.600	0.137	1.005	0.287	0.140	6	5	8	39	----	----
1.75	12.450	0.145	1.165	0.334	0.162	6	5	8	34	----	----
2.00	121.367	0.490	0.404	0.382	0.186	9	24	36	97	----	----
2.25	339.750	1.265	0.372	0.432	0.211	10	57	86	125	----	----
2.50	384.400	1.287	0.335	0.483	0.238	10	64	96	127	----	----
2.75	427.650	2.150	0.503	0.534	0.265	10	71	107	128	----	----
3.00	236.633	2.180	0.921	0.585	0.290	9	47	71	110	----	----
3.25	34.200	2.245	6.564	0.634	0.315	3	34	51	----	2.238	7.108
3.50	35.333	2.267	6.415	0.683	0.339	3	35	53	----	2.311	6.805
3.75	27.250	1.810	6.642	0.732	0.364	3	27	41	----	1.768	4.856
4.00	33.733	1.660	4.921	0.781	0.389	3	34	51	----	2.198	5.653
4.25	34.750	1.655	4.763	0.830	0.413	4	23	35	----	2.262	5.472
4.50	41.733	2.363	5.663	0.879	0.438	3	42	63	----	2.725	6.221
4.75	38.500	1.900	4.935	0.928	0.462	3	39	59	----	2.506	5.416
5.00	40.400	2.133	5.281	0.978	0.487	3	40	60	----	2.629	5.396
5.25	40.200	2.200	5.473	1.027	0.512	3	40	60	----	2.613	5.104
5.50	39.667	2.193	5.529	1.076	0.536	3	40	60	----	2.573	4.798
5.75	41.350	2.365	5.719	1.125	0.561	3	41	62	----	2.682	4.782
6.00	42.400	2.317	5.464	1.174	0.585	3	42	61	----	2.748	4.695
6.25	43.950	2.250	5.119	1.223	0.610	3	44	62	----	2.848	4.669
6.50	44.600	2.283	5.120	1.272	0.635	3	45	62	----	2.889	4.551
6.75	41.550	2.225	5.355	1.321	0.659	3	42	56	----	2.682	4.068
7.00	32.767	2.170	6.623	1.371	0.684	3	33	43	----	2.093	3.061
7.25	29.100	2.150	7.388	1.420	0.708	3	29	37	----	1.845	2.605
7.50	26.567	2.123	7.992	1.469	0.733	3	27	33	----	1.673	2.283

PEACH FREEWAY CPT-3

Depth (Meter)	q _c Average (bars)	f _s Average (bars)	R _f (%)	OS Average (bars)	EOS Average (bars)	R _f Zone (zone #)	SPT N (blow/.3 m)	SPT N1 (blow/.3 m)	D _r (%)	s _u (bars)	s _u /EOS (ratio)
7.75	26.350	2.055	7.799	1.518	0.758	3	26	31	----	1.655	2.185
8.00	28.900	1.960	6.782	1.567	0.782	3	29	34	----	1.822	2.329
8.25	29.950	1.965	6.561	1.616	0.807	3	30	34	----	1.889	2.341
8.50	31.033	1.983	6.391	1.665	0.831	3	31	35	----	1.958	2.355
8.75	31.400	1.945	6.194	1.714	0.856	3	31	34	----	1.979	2.312
9.00	32.833	1.947	5.929	1.764	0.881	3	33	35	----	2.071	2.352
9.25	32.100	1.940	6.044	1.813	0.905	3	32	33	----	2.019	2.231
9.50	36.133	2.083	5.766	1.862	0.930	3	36	37	----	2.285	2.457
9.75	42.700	2.195	5.141	1.911	0.954	3	43	43	----	2.719	2.849
10.00	32.867	1.990	6.055	1.960	0.979	3	33	32	----	2.060	2.105
10.25	29.150	1.930	6.621	2.009	1.004	3	29	28	----	1.809	1.803
10.50	31.500	2.133	6.772	2.058	1.028	3	32	30	----	1.963	1.909
10.75	33.350	2.355	7.061	2.107	1.053	3	33	31	----	2.083	1.978
11.00	35.100	2.243	6.391	2.157	1.077	3	35	32	----	2.196	2.038
11.25	42.650	2.195	5.147	2.206	1.102	3	43	39	----	2.696	2.447
11.50	44.300	2.290	5.169	2.255	1.127	3	44	39	----	2.803	2.488
11.75	43.500	2.445	5.621	2.304	1.151	3	44	38	----	2.746	2.386
12.00	41.333	2.540	6.145	2.353	1.176	3	41	35	----	2.599	2.210
12.25	43.350	2.215	5.110	2.402	1.200	3	43	36	----	2.730	2.274
12.50	45.033	2.207	4.900	2.451	1.225	4	30	25	----	2.839	2.317
12.75	45.000	2.165	4.811	2.500	1.250	4	30	24	----	2.833	2.267
13.00	43.533	2.263	5.199	2.550	1.274	3	44	35	----	2.732	2.144
13.25	46.500	2.740	5.892	2.599	1.299	3	47	37	----	2.927	2.253
13.50	47.267	2.843	6.016	2.648	1.323	3	47	37	----	2.975	2.248
13.75	47.300	2.590	5.476	2.697	1.348	3	47	36	----	2.974	2.206
14.00	45.800	2.473	5.400	2.746	1.373	3	46	35	----	2.870	2.091
14.25	41.350	2.125	5.139	2.795	1.397	3	41	31	----	2.570	1.840
14.50	43.067	2.210	5.132	2.844	1.422	3	43	32	----	2.681	1.886
14.75	46.800	2.210	4.722	2.893	1.446	4	31	23	----	2.927	2.024
15.00	130.900	2.047	1.564	2.943	1.471	8	33	24	70	----	----
15.25	191.200	1.615	0.845	2.992	1.496	9	38	27	80	----	----

PEACH FREEWAY CPT-3											
Depth (Meter)	q _c Average (bars)	f _s Average (bars)	R _f (%)	OS Average (bars)	EOS Average (bars)	R _f Zone (zone #)	SPT N (blow/.3 m)	SPT N1 (blow/.3 m)	D _r (%)	s _u (bars)	s _u /EOS (ratio)
15.50	195.967	1.477	0.754	3.041	1.520	9	39	27	81	----	----
15.75	180.900	1.155	0.638	3.090	1.545	9	36	25	78	----	----
16.00	170.967	1.153	0.675	3.139	1.569	9	34	23	76	----	----
16.25	181.450	1.240	0.683	3.188	1.594	9	36	24	78	----	----
16.50	203.867	1.610	0.790	3.237	1.619	9	41	27	81	----	----
16.75	194.800	1.605	0.824	3.286	1.643	9	39	26	80	----	----
17.00	205.700	1.877	0.912	3.336	1.668	9	41	27	81	----	----
17.25	220.650	1.840	0.834	3.385	1.692	9	44	28	83	----	----
17.50	219.233	2.083	0.950	3.434	1.717	9	44	28	82	----	----
17.75	212.400	2.275	1.071	3.483	1.742	9	42	27	81	----	----
18.00	208.333	2.527	1.213	3.532	1.766	9	42	26	80	----	----
18.25	197.400	1.555	0.788	3.581	1.791	9	39	24	79	----	----
18.50	194.833	1.790	0.919	3.630	1.815	9	39	24	78	----	----
18.75	209.850	1.705	0.812	3.679	1.840	9	42	25	80	----	----
19.00	194.733	1.310	0.673	3.729	1.865	9	39	23	78	----	----
19.25	204.100	1.125	0.551	3.778	1.889	9	41	24	79	----	----
19.50	217.450	1.390	0.639	3.827	1.914	9	43	25	81	----	----
19.75	273.100	1.450	0.531	3.877	1.939	10	46	27	87	----	----
20.00	505.050	1.545	0.306	3.928	1.966	10	84	48	----	----	----

InSituTech

Engineer: DM HOLLOWAY

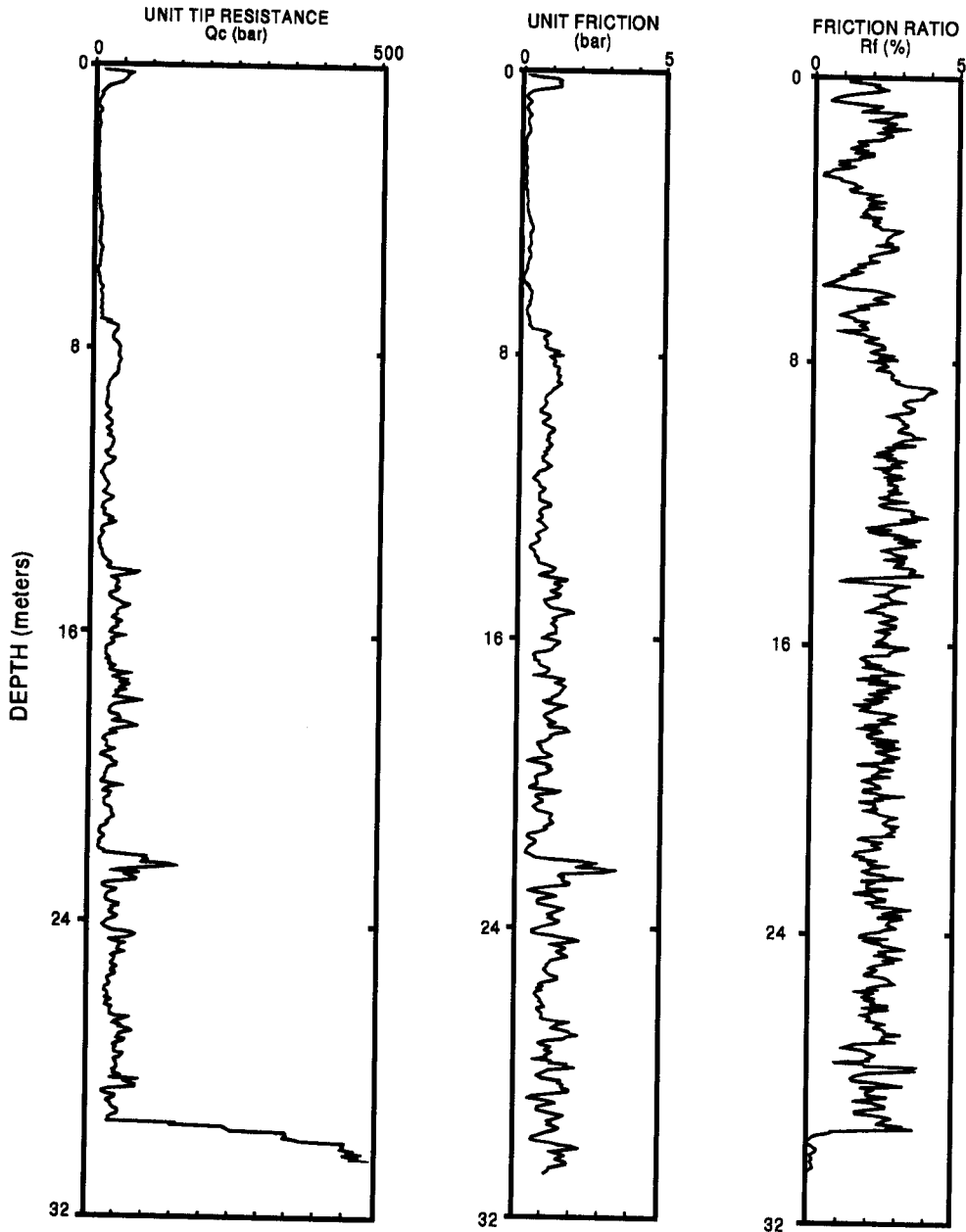
CPT Date: 8/19/89

Page No.: 1 / 1

Location: PEACH FREEWAY, CPT4

Cone Used: 186

Job No.: 93/2/1001



Depth Increment: .05 m

Max Depth: 30.7 m

Licensed to: InSituTech Ltd.
Address: 5 del Valle
City: Orinda, CA 94563, U.S.A.

Interpreter Name: Mike Holloway

File Number: 8 0
Operator: DM HOLLOWAY
Cone Type: 186

Date: 8/19/89
On Site Location: Peach Freeway CPT-4
Comment: 93/2/1001

SUMMARY SHEET

'a' for calculating Q_t : 0.800
Value for Water Table (in m): 1.000
Valid Zone Classification based on: R_f
Missing unit weight to start depth: 15.720
Method for calculating s_u : Nk
Value of the constant Nk: 15.000
Define Zone 6 for Sand Parameters? Yes
Sand Compressibility for calc D_r : All sands

Soil Behavior Type Zone Numbers for R_f Zone and Bq Zone Classification

Zone #1 = Sensitive fine grained	Zone #7 = Sand with some silt
Zone #2 = Organic material	Zone #8 = Fine sand
Zone #3 = Clay	Zone #9 = Sand
Zone #4 = Silty clay	Zone #10 = Gravelly sand
Zone #5 = Clayey silt	Zone #11 = Very stiff fine grained *
Zone #6 = Silty sand	Zone #12 = Sand to clayey sand *

* Overconsolidated and/or cemented

NOTE: For soil classification, R_f values > 8 are assumed to be 8.

NOTE: Since U_2 (pore pressure) has not been defined, Q_t cannot be calculated, therefore, the value of Q_t has been made equal to Q_c .

NOTE: ---- means out of range.

PEACH FREEWAY CPT-4

Depth (Meter)	q _c Average (bars)	f _s Average (bars)	R _f (%)	OS Average (bars)	EOS Average (bars)	R _f Zone (zone #)	SPT N (blow/.3 m)	SPT N1 (blow/.3 m)	D _r (%)	s _u (bars)	s _u /EOS (ratio)
0.25	56.040	2.612	4.661	0.054	0.054	4	37	56	----	3.732	69.071
0.50	29.040	0.964	3.320	0.103	0.103	5	15	23	----	1.929	18.700
0.75	12.560	0.417	3.320	0.151	0.151	4	8	12	----	0.827	5.468
1.00	6.480	0.345	5.327	0.198	0.198	3	6	9	----	0.419	2.110
1.25	8.820	0.463	5.252	0.246	0.221	3	9	14	----	0.572	2.586
1.50	8.240	0.457	5.544	0.293	0.244	3	8	12	----	0.530	1.174
1.75	6.900	0.325	4.713	0.340	0.266	3	7	11	----	0.437	1.642
2.00	5.960	0.208	3.487	0.387	0.289	3	6	9	----	0.372	1.286
2.25	5.160	0.189	3.663	0.434	0.312	3	5	8	----	0.315	1.011
2.50	4.520	0.110	2.442	0.481	0.334	3	5	8	----	0.269	0.806
2.75	5.560	0.085	1.536	0.527	0.355	1	3	5	----	0.336	0.946
3.00	6.720	0.208	3.098	0.572	0.376	3	7	11	----	0.410	1.091
3.25	6.780	0.258	3.808	0.619	0.398	3	7	11	----	0.411	1.032
3.50	7.680	0.336	4.370	0.666	0.421	3	8	12	----	0.468	1.111
3.75	7.900	0.329	4.162	0.713	0.443	3	8	12	----	0.479	1.080
4.00	10.220	0.459	4.495	0.761	0.467	3	10	15	----	0.631	1.350
4.25	12.000	0.648	5.397	0.810	0.492	3	12	18	----	0.746	1.517
4.50	10.800	0.599	5.544	0.860	0.516	3	11	17	----	0.663	1.284
4.75	10.040	0.577	5.745	0.909	0.541	3	10	15	----	0.609	1.126
5.00	11.100	0.495	4.456	0.958	0.565	3	11	17	----	0.676	1.196
5.25	10.840	0.421	3.880	1.007	0.590	3	11	16	----	0.656	1.111
5.50	9.040	0.268	2.962	1.055	0.614	4	6	8	----	0.532	0.867
5.75	6.360	0.108	1.701	1.102	0.636	4	4	5	----	0.351	0.551
6.00	9.740	0.469	4.811	1.149	0.659	3	10	13	----	0.573	0.869
6.25	13.120	0.637	4.852	1.198	0.683	3	13	17	----	0.795	1.165
6.50	13.420	0.448	3.337	1.246	0.706	4	9	11	----	0.812	1.149
6.75	13.160	0.411	3.125	1.293	0.729	4	9	11	----	0.791	1.086
7.00	16.120	0.537	3.330	1.340	0.751	4	11	13	----	0.985	1.311
7.25	35.860	1.482	4.133	1.388	0.775	4	24	28	----	2.298	2.965
7.50	34.820	1.692	4.859	1.437	0.800	3	35	40	----	2.226	2.783

PEACH FREEWAY CPT-4

Depth (Meter)	q _c Average (bars)	f _s Average (bars)	R _i (%)	OS Average (bars)	EOS Average (bars)	R _i Zone (zone #)	SPT N (blow/.3 m)	SPT N1 (blow/.3 m)	D _r (%)	s _v (bars)	s _v /EOS (ratio)
7.75	41.900	2.076	4.955	1.486	0.824	3	42	47	----	2.694	3.269
8.00	44.460	2.370	5.331	1.535	0.849	3	44	48	----	2.862	3.371
8.25	45.780	2.494	5.448	1.585	0.873	3	46	49	----	2.946	3.373
8.50	42.960	2.622	6.103	1.634	0.898	3	43	45	----	2.755	3.068
8.75	31.400	2.582	8.223	----	----	----	----	----	----	----	----
9.00	25.280	1.944	7.690	1.683	0.898	3	25	26	----	1.573	1.752
9.25	24.700	1.738	7.036	1.732	0.923	3	25	26	----	1.531	1.660
9.50	24.920	1.578	6.332	1.781	0.947	3	25	25	----	1.543	1.628
9.75	25.980	1.758	6.767	1.830	0.972	3	26	26	----	1.610	1.657
10.00	31.420	2.184	6.951	1.879	0.996	3	31	30	----	1.969	1.976
10.25	28.120	1.938	6.892	1.928	0.021	3	28	27	----	1.746	1.710
10.50	35.760	2.010	5.621	1.978	0.046	3	36	34	----	2.252	2.154
10.75	28.640	1.676	5.852	2.027	0.070	3	29	27	----	1.774	1.658
11.00	33.540	1.884	5.617	2.076	0.095	3	34	31	----	2.098	1.916
11.25	22.160	1.320	5.957	2.125	0.119	3	22	20	----	1.336	1.193
11.50	19.440	1.182	6.080	2.174	0.144	3	19	17	----	1.151	1.006
11.75	27.160	1.564	5.758	2.223	0.169	3	27	23	----	1.662	1.423
12.00	27.240	1.530	5.617	2.272	0.193	3	27	23	----	1.665	1.395
12.25	25.480	1.788	7.017	2.321	0.218	3	25	21	----	1.544	1.268
12.50	21.400	1.464	6.841	2.371	0.242	3	21	17	----	1.269	1.021
12.75	34.800	1.734	4.983	2.420	0.267	3	35	28	----	2.159	1.704
13.00	19.540	1.338	6.847	2.469	0.292	3	20	16	----	1.138	0.881
13.25	16.000	1.062	6.638	2.518	0.316	3	16	13	----	0.899	0.683
13.50	16.300	1.030	6.319	2.567	1.341	3	16	12	----	0.916	0.683
13.75	21.620	1.442	6.670	2.616	1.365	3	22	17	----	1.267	0.928
14.00	31.480	2.244	7.128	2.665	1.390	3	31	23	----	1.921	1.382
14.25	61.400	2.602	4.238	2.714	1.415	5	31	23	----	3.912	2.766
14.50	45.740	2.640	5.772	2.764	1.439	3	46	34	----	2.865	1.991
14.75	41.460	2.466	5.948	2.813	1.464	3	41	30	----	2.576	1.760
15.00	45.200	2.240	4.956	2.862	1.488	4	30	21	----	2.823	1.896
15.25	54.840	3.188	5.813	2.911	1.513	3	55	39	----	3.462	2.288

PEACH FREEWAY CPT-4

Depth (Meter)	q _c Average (bars)	f _s Average (bars)	R _f (%)	OS Average (bars)	EOS Average (bars)	R _f Zone (zone #)	SPT N (blow/.3 m)	SPT N1 (blow/.3 m)	D _r (%)	s _u (bars)	s _u /EOS (ratio)
15.50	44.960	2.530	5.627	2.960	1.538	3	45	31	----	2.800	1.821
15.75	43.120	2.408	5.584	3.009	1.562	3	43	30	----	2.674	1.712
16.00	42.380	2.494	5.885	3.058	1.587	3	42	28	----	2.621	1.652
16.25	33.980	1.820	5.356	3.107	1.611	3	34	23	----	2.058	1.277
16.50	29.100	1.292	4.440	3.157	1.636	4	19	13	----	1.730	1.057
16.75	34.500	1.968	5.704	3.206	1.661	3	35	23	----	2.086	1.256
17.00	45.820	2.352	5.133	3.255	1.685	3	46	30	----	2.838	1.684
17.25	55.860	3.070	5.496	3.304	1.710	3	56	36	----	3.504	2.049
17.50	53.160	2.690	5.060	3.353	1.734	4	35	22	----	3.320	1.914
17.75	62.300	2.602	4.177	3.402	1.759	5	31	19	----	3.927	2.232
18.00	37.040	2.150	5.805	3.451	1.784	3	37	23	----	2.239	1.255
18.25	46.560	2.264	4.863	3.500	1.808	4	31	19	----	2.871	1.588
18.50	64.020	3.082	4.814	3.550	1.833	4	43	26	----	4.031	2.199
18.75	32.000	1.844	5.763	3.599	1.857	3	32	19	----	1.893	1.019
19.00	30.440	1.768	5.808	3.648	1.882	3	30	18	----	1.786	0.949
19.25	28.940	1.534	5.301	3.697	1.907	3	29	17	----	1.683	0.883
19.50	42.220	2.222	5.263	3.746	1.931	3	42	24	----	2.565	1.328
19.75	30.340	1.482	4.885	3.795	1.956	3	30	17	----	1.770	0.905
20.00	27.260	1.326	4.864	3.844	1.980	3	27	15	----	1.561	0.788
20.25	36.500	1.944	5.326	3.893	2.005	3	37	21	----	2.174	1.084
20.50	30.500	1.482	4.859	3.943	2.030	3	31	17	----	1.770	0.872
20.75	33.600	1.936	5.762	3.992	2.054	3	34	19	----	1.974	0.961
21.00	39.780	2.348	5.902	4.041	2.079	3	40	22	----	2.383	1.146
21.25	27.360	1.592	5.819	4.090	2.103	3	27	15	----	1.551	0.738
21.50	22.380	1.064	4.754	4.139	2.128	3	22	12	----	1.216	0.571
21.75	18.540	0.782	4.218	4.188	2.153	3	19	10	----	0.957	0.444
22.00	46.920	2.124	4.527	4.237	2.177	4	31	16	----	2.846	1.307
22.25	116.780	5.476	4.689	4.288	2.204	11	117	62	----	----	----
22.50	71.180	3.778	5.308	4.341	2.232	11	71	37	----	----	----
22.75	61.100	2.856	4.674	4.393	2.259	4	41	21	----	3.780	1.674
23.00	38.180	1.962	5.139	4.442	2.284	3	38	19	----	2.249	0.985

PEACH FREEWAY CPT-4

Depth (Meter)	q _c Average (bars)	f _s Average (bars)	R _f (%)	OS Average (bars)	EOS Average (bars)	R _f Zone (zone #)	SPT N (blow/.3 m)	SPT N1 (blow/.3 m)	D _r (%)	s _u (bars)	s _u /EOS (ratio)
23.25	33.420	1.898	5.679	4.491	2.308	3	33	17	----	1.929	0.836
23.50	46.080	2.788	6.050	4.540	2.333	3	46	23	----	2.769	1.187
23.75	43.620	2.644	6.061	4.589	2.357	3	44	22	----	2.602	1.104
24.00	46.060	1.416	4.711	4.638	2.382	3	30	15	----	1.695	0.712
24.25	68.280	3.522	5.158	4.689	2.408	11	68	34	----	----	----
24.50	51.380	3.012	5.862	4.740	2.435	3	51	26	----	3.109	1.277
24.75	51.620	3.144	6.091	4.790	2.460	3	52	26	----	3.122	1.269
25.00	39.188	1.978	5.046	4.839	2.484	3	39	20	----	2.290	0.922
25.25	36.660	1.674	4.566	4.888	2.509	4	24	12	----	2.118	0.844
25.50	51.300	2.602	5.072	4.937	2.533	4	34	17	----	3.091	1.220
25.75	54.840	3.222	5.875	4.986	2.558	3	55	28	----	3.324	1.299
26.00	60.740	2.974	4.896	5.035	2.583	4	40	20	----	3.714	1.438
26.25	54.660	2.224	4.069	5.084	2.607	5	27	14	----	3.305	1.268
26.50	52.220	2.088	3.998	5.133	2.632	5	26	13	----	3.139	1.193
26.75	50.380	3.148	6.249	5.183	2.656	3	50	25	----	3.013	1.134
27.00	48.320	1.854	3.837	5.232	2.681	5	24	12	----	2.873	1.071
27.25	----	----	----	----	----	----	----	----	----	----	----
27.50	61.950	3.197	5.161	5.283	2.683	11	62	31	----	----	----
27.75	61.100	2.856	4.674	5.334	2.710	4	41	21	----	3.718	1.372
28.00	0.180	1.962	5.139	5.383	2.734	3	38	19	----	2.186	0.800
28.25	38.420	1.898	4.582	5.432	2.759	4	28	14	----	2.399	0.870
28.50	41.080	2.788	5.799	5.481	2.783	3	48	24	----	2.840	1.020
28.75	121.620	2.644	2.174	5.529	2.807	7	41	21	58	----	----
29.00	306.060	1.416	0.463	5.578	2.832	10	51	26	85	----	----
29.25	394.280	3.522	0.893	5.629	2.857	9	79	40	92	----	----
29.50	457.380	3.012	0.659	5.679	2.883	10	76	38	96	----	----
29.75	495.620	3.144	0.634	5.730	2.909	10	83	42	98	----	----
30.00	699.567	2.203	0.315	5.781	2.936	10	117	59	----	----	----

APPENDIX F

Peach Freeway Example Problem Calculations

	Page
F.1 INTRODUCTION	F-3
F.2 STATIC AXIAL PILE CAPACITY CALCULATIONS	F-7
F.2.1 North Abutment - Soil Boring S-1 (Cohesionless Soil)	F-8
F.2.1.1 Meyerhof SPT Method	F-8
F.2.1.2 Nordlund Method	F-14
F.2.1.3 Effective Stress Method	F-26
F.2.1.4 SPILE Computer Program	F-31
F.2.1.5 LPC CPT Method - Computer Program	F-32
F.2.1.6 Schmertmann Method	F-34
F.2.1.7 Summary of North Abutment Capacity Calculation Results	F-35
F.2.2 Pier 2 - Soil Boring S-2 (Cohesionless Soil)	F-36
F.2.2.1 Meyerhof SPT Method (before scour)	F-36
F.2.2.2 Nordlund Method (before scour at 10 m)	F-42
F.2.2.3 Nordlund Method (after scour at 10 m)	F-48
F.2.2.4 Nordlund Method (before scour at 14 m)	F-56
F.2.2.5 Nordlund Method (after scour at 14 m)	F-62
F.2.2.6 Effective Stress Method (before scour)	F-68
F.2.2.7 SPILE Computer Program (before scour)	F-73
F.2.2.8 Summary of Pier 2 Capacity Calculation Results	F-74
F.2.3 Pier 3 - Soil Boring S-3 (Cohesive and Cohesionless Soil)	F-76
F.2.3.1 Nordlund and α -Methods	F-76
F.2.3.2 Effective Stress Method	F-86
F.2.3.3 SPILE Computer Program	F-91
F.2.3.4 LPC CPT Method - Computer Program	F-92
F.2.3.5 Schmertmann Method	F-94
F.2.3.6 Summary of Pier 3 Capacity Calculation Results	F-95

F.2.4	South Abutment - Soil Boring S-4 (Cohesive Soil)	F-97
F.2.4.1	α -Method	F-97
F.2.4.2	Effective Stress Method	F-104
F.2.4.3	SPILE Computer Program	F-109
F.2.4.3	LPC CPT Method - Computer Program	F-110
F.2.4.4	Schmertmann Method	F-112
F.2.4.5	Summary of South Abutment Capacity Calculation Results	F-114
F.3	GROUP SETTLEMENT CALCULATIONS	F-115
F.3.1	North Abutment - Meyerhof Method based on SPT Test Data	F-115
F.3.2	Pier 2 - Meyerhof Method based on SPT Test Data	F-120
F.3.3	Pier 3 - Equivalent Footing Method for Layered Soils	F-123
F.3.4	South Abutment - Equivalent Footing Method	F-135
F.4	LATERAL PILE CAPACITY ANALYSIS	F-145
F.4.1	Broms' Method - North Abutment	F-145
F.4.2	COM624P - North Abutment	F-152
F.4.3	COM624P - Pier 2 H-pile, X-X Axis and Y-Y Axis	F-164
F.4.4	COM624P - Pier 3 H-pile, X-X Axis and Y-Y Axis	F-183
F.4.5	COM624P - South Abutment	F-202
F.5	UPLIFT LOAD CALCULATIONS	F-213
F.5.1	North Abutment - AASHTO Code (1994)	F-213
F.5.2	Pier 2 - AASHTO Code (1994)	F-217
F.5.3	Pier 3 - AASHTO Code (1994)	F-221
F.5.4	South Abutment - AASHTO Code (1994)	F-225
F.6	NEGATIVE SHAFT RESISTANCE CALCULATIONS	F-229
F.6.1	South Abutment - α -Method	F-229
F.7	LATERAL SQUEEZE CALCULATIONS	F-242
F.7.1	South Abutment - Investigation of Lateral Squeeze	F-242

F.1 INTRODUCTION

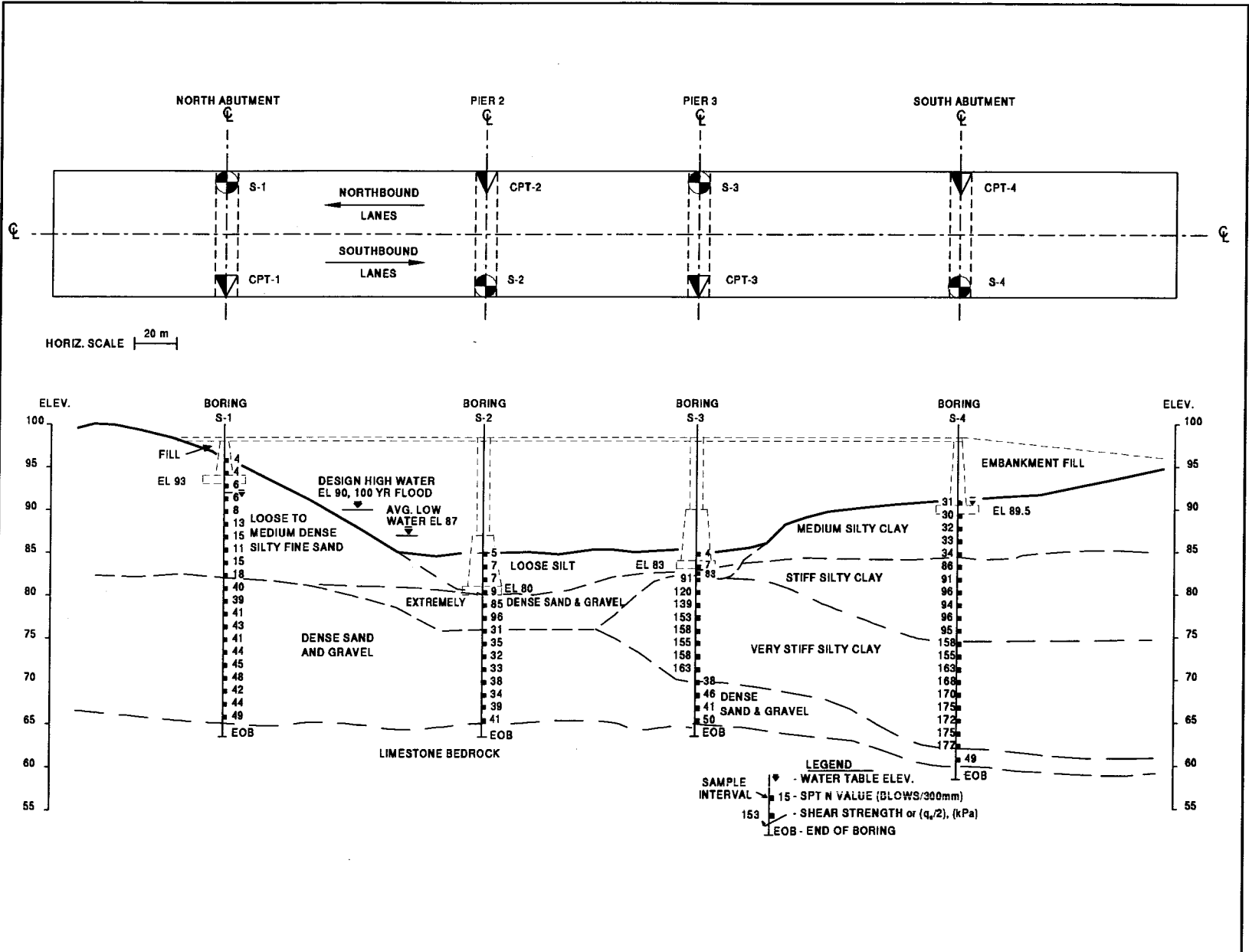
The various design methods presented in Chapter 9 of the manual will be illustrated by applying these methods to foundation design problems for the Peach Freeway Bridge over Dismal Creek. In many real design problems, additional analyses beyond those presented in these example problems would be used to complete the actual foundation design. For example, group lateral load capacity evaluations are not completed at each substructure location in these example problems.

The Peach Freeway Bridge over Dismal Creek will be a three span structure supported at North and South Abutments and interior piers, Pier 2 and Pier 3. One soil boring and one cone penetration test were performed for each substructure location. The subsurface exploration results were included in Appendix E of this manual. The cone penetration test at Pier 2, CPT-2, encountered shallow refusal and therefore, a log of CPT-2 is not included in Appendix E. The subsurface profile developed from the subsurface exploration and laboratory testing program results is presented in Figure F.1.

The "bridge division" has estimated that the maximum compression loads per substructure unit will be 12,600 kN. Each substructure location will be supported on a pile group having three rows of eight piles per row. For abutment pile groups, fewer piles are often required in the middle and rear rows as compared to the front row. The maximum design compression load on any pile will be 890 kN. Lateral loads will range from 600 kN at the interior piers to 900 kN at the abutments with a maximum lateral load per pile of 40 kN. The maximum uplift load on a pile group will be 1,800 kN with a maximum uplift load per pile of 100 kN. Maximum pile group settlements less than 25 mm are required under the compression loads and horizontal deflections of up to 10 mm are permissible under lateral loading. The pile location plan for each substructure location is presented in Figure F.2.

Initial design estimates and local availability of materials indicate square, precast, prestressed concrete piles will probably be the most cost effective foundation type. This pile type should work well at the abutments because they will develop significant load support through both shaft and toe resistance. However, at the interior piers, the driveability of these displacement piles through the extremely dense sand and gravel layer will need to be carefully evaluated. A low displacement pile may be necessary at the interior piers to meet pile penetration requirements.

Figure F.1 Peach Freeway Subsurface Profile



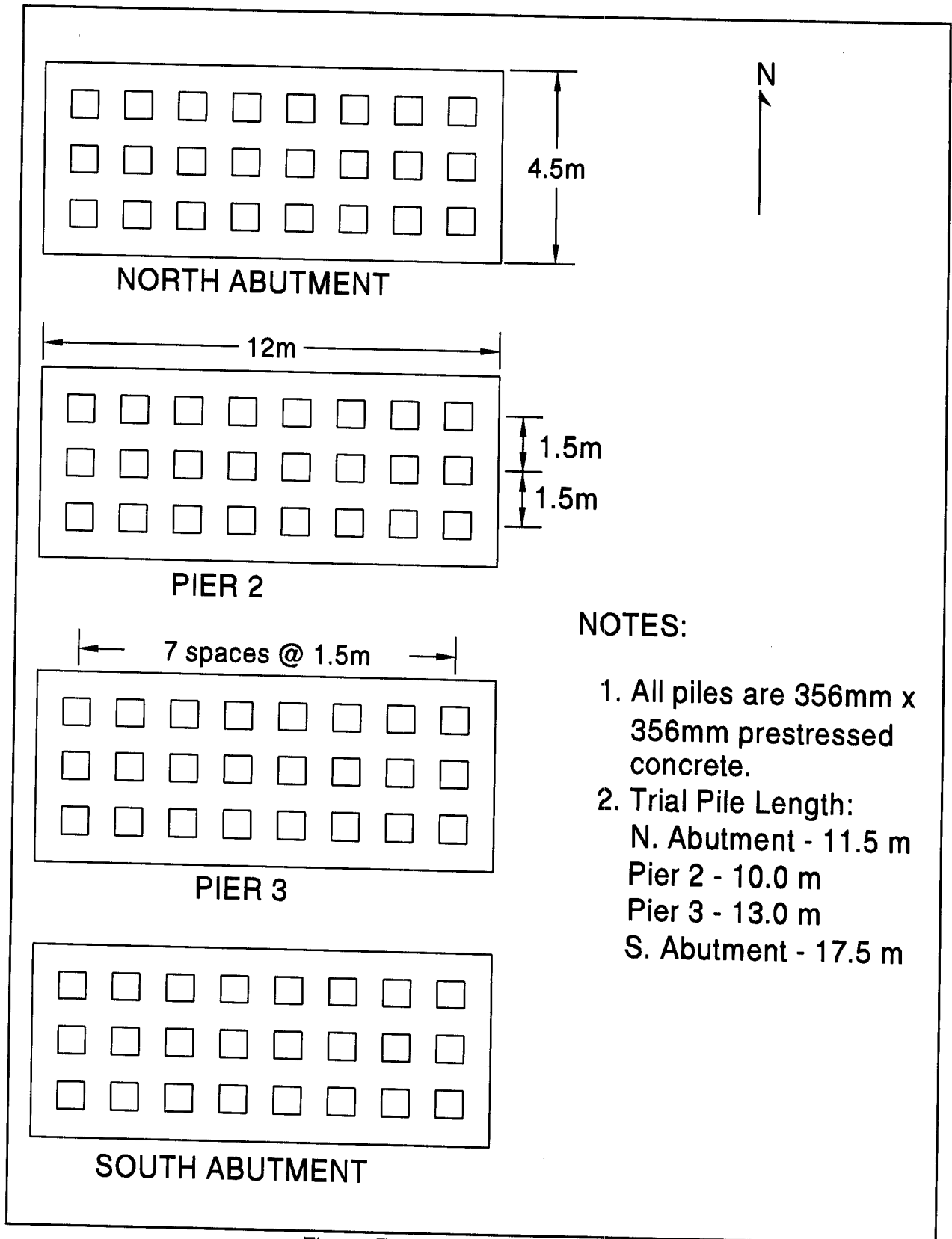


Figure F.2 Pile Foundation Plan

Section F.2 of this Appendix presents static capacity calculations using the applicable methods at each substructure location. Pile group settlement computations for each substructure location are provided in Section F.3. Section F.4 presents lateral pile capacity analyses performed for the North Abutment using both the Brom's Method and the COM624P program. Lateral capacity analysis for Pier 2, Pier 3 and the South Abutment using the COM624P program are also presented. Group uplift computation at each substructure location following AASHTO code are presented in Section F.5. Last, special design considerations of negative shaft resistance and lateral squeeze are presented for the South Abutment in Sections F.6 and F.7, respectively.

F.2 STATIC AXIAL PILE CAPACITY CALCULATIONS

The design load per pile group will be 12,600 kN. The bridge office has determined that the maximum axial design load to be imposed on a single pile will be 890 kN. (At the abutments, the design load on piles in the front row will be 890 kN, whereas the middle and rear rows of piles will have smaller design loads). Construction control will be based on static load test results and a factor of safety of 2.0 will be used on the design load. Therefore, static capacity calculations will be used to evaluate the required pile lengths for a 1780 kN ultimate pile capacity at each substructure location.

Several static axial capacity calculations and computer solutions will be used to determine the required pile length at each substructure unit (*i.e.*, North Abutment, Pier 2, Pier 3, and South Abutment). At Pier 2 location, the effect of scour on the static axial capacity will also be calculated. At all substructure location, pile group capacity will be evaluated. At the South Abutment location, the ultimate pile group capacity against block failure will be calculated and compared with the ultimate pile group capacity from the sum of the ultimate capacities of the individual piles.

The static capacity calculations for each substructure location are presented in the following sections.

F.2.1 North Abutment - Soil Boring S-1 (Cohesionless Soil)

F.2.1.1 Static Axial Pile Capacity Calculations by Meyerhof SPT Method

For the soil profile interpreted from Soil Boring S-1 shown in Figure F.3, perform a Meyerhof method pile capacity calculation for an embedded length of 11.5 meters. The pile top is 3 meters below the existing ground surface. The step-by-step method outlined in Section 9.7.1.1a should be followed.

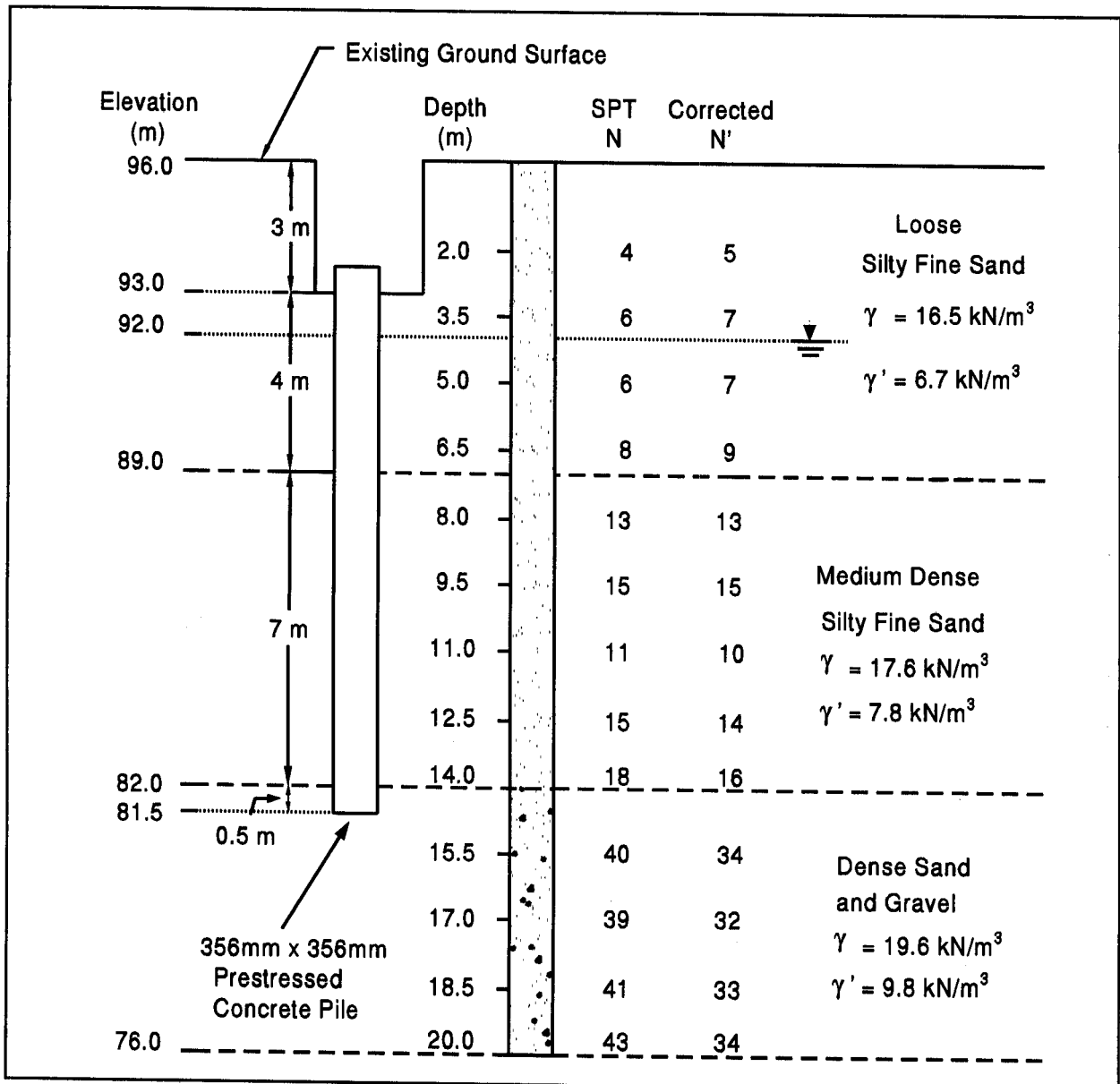


Figure F.3 Interpreted Soil Profile from Soil Boring S-1 at the North Abutment

STEP 1 Correct SPT field N values for overburden pressure.

Effective overburden pressures, p_o , are needed to correct SPT field N values. The method for calculating the effective overburden pressure is explained in Section 9.4. First, the soil profile should be delineated into layers based on soil type and density indicated by the corrected SPT N' value. However, since the corrected SPT N' value has yet to be calculated, the SPT field N' value should be used to estimate soil unit weights. Re-adjust the soil unit weight (if necessary) after the corrected SPT N' value has been obtained. The empirical correlation between soil unit weight and corrected SPT N' value is presented in Table 4-5. The effective overburden pressure diagram is presented below in Figure F.4.

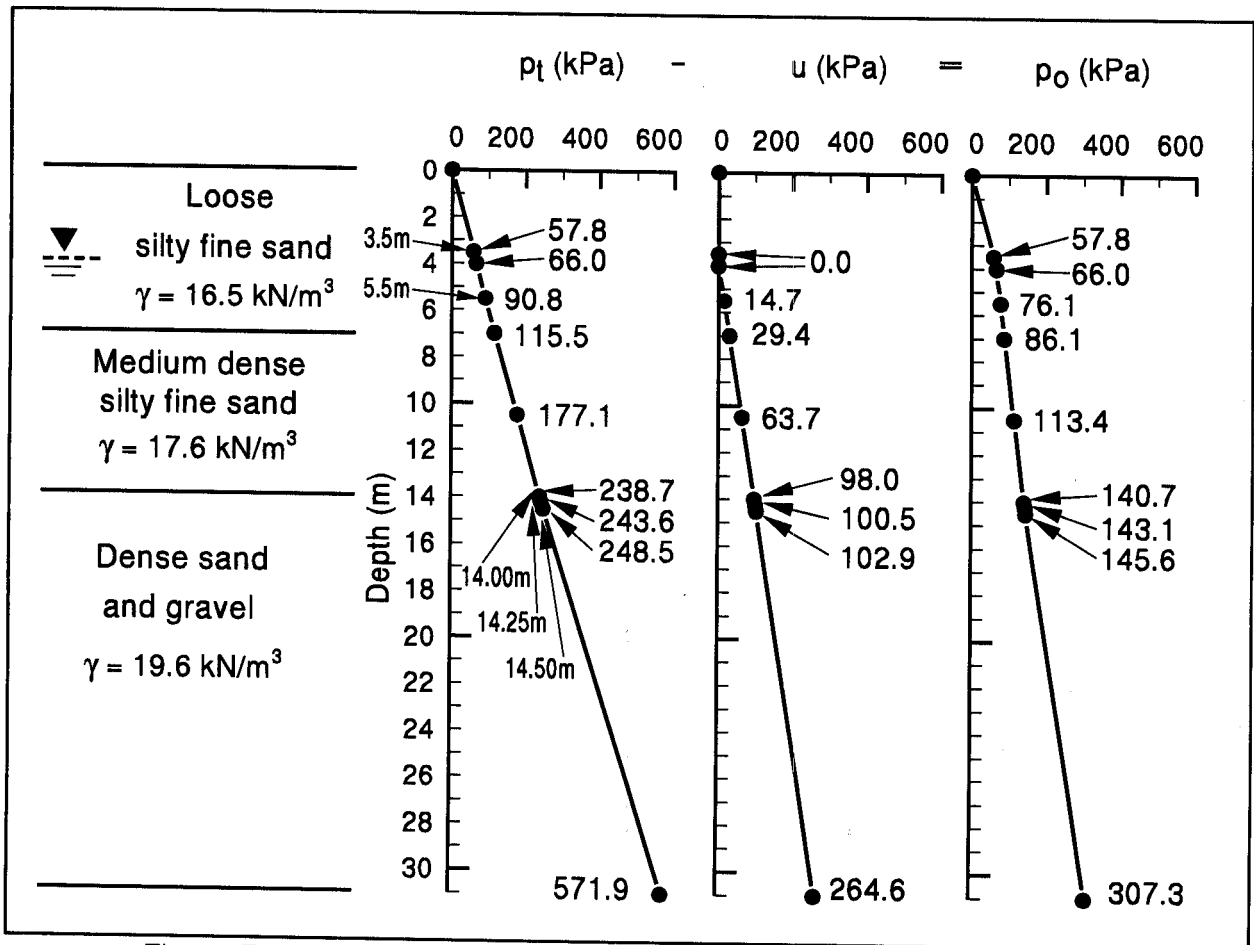


Figure F.4 Effective Overburden Pressure Diagram - North Abutment

STEP 1 (continued)

Use correction factors from Figure 4.4 (Chapter 4) to obtain corrected SPT N' values.

Depth (m)	p_o (kPa)	Field SPT N value	Correction Factor	Corrected SPT N' (Field SPT N x Correction Factor)
0.8	13.2	4	1.65	7
2.0	33.0	4	1.35	5
3.5	57.8	6	1.17	7
5.0	72.7	6	1.12	7
6.5	82.8	8	1.08	9
8.0	93.9	13	1.02	13
9.5	105.6	15	0.98	15
11.0	117.3	11	0.95	10
12.5	129.0	15	0.91	14
14.0	140.7	18	0.87	16
15.5	155.4	40	0.85	34
17.0	170.1	39	0.82	32
18.5	184.8	41	0.80	33
20.0	199.5	43	0.78	34
21.5	214.2	41	0.74	30
23.0	228.9	44	0.72	32
24.5	243.6	45	0.70	32
26.0	258.3	48	0.68	33
27.5	273.0	42	0.67	28
29.0	287.7	44	0.64	28
30.5	302.4	49	0.63	31

STEP 2 Compute the average corrected SPT N' value, \bar{N}' , for each soil layer.

Along the pile embedded length, the soil profile is delineated into three layers. Layer 1 is loose silty fine sand that is 4 meters thick, layer 2 is medium dense silty fine sand that is 7 meters thick, and layer 3 is dense sand and gravel that is 0.5 meter thick.

$$\bar{N}'_1 = \frac{7 + 7 + 9}{3} = 8$$

(Layer 1 - depth 3 to 7 m;
Loose silty fine sand)

$$\bar{N}'_2 = \frac{13 + 15 + 10 + 14 + 16}{5} = 14$$

(Layer 2 - depth 7 to 14 m;
Medium dense silty fine sand)

$$\bar{N}'_3 = 34$$

(Layer 3 - depth 14 to 14.5 m;
Dense sand and gravel)

STEP 3 Compute the unit shaft resistance, f_s (kPa), for each layer using the equation for driven displacement piles:

$$f_s = 2\bar{N}' \leq 100 \text{ kPa}$$

Layer 1: $f_{s-1} = 2 (8) = 16 \text{ kPa}$

Layer 2: $f_{s-2} = 2 (14) = 28 \text{ kPa}$

Layer 3: $f_{s-3} = 2 (34) = 68 \text{ kPa}$

STEP 4 Compute the ultimate shaft resistance, R_s (kN).

$$R_s = f_s A_s$$

$$\text{Layer 1: } R_{s1} = 16 \text{ kPa } (4)(0.356 \text{ m})(4 \text{ m}) = 91 \text{ kN}$$

$$\text{Layer 2: } R_{s2} = 28 \text{ kPa } (4)(0.356 \text{ m})(7 \text{ m}) = 279 \text{ kN}$$

$$\text{Layer 3: } R_{s3} = 68 \text{ kPa } (4)(0.356 \text{ m})(0.5 \text{ m}) = 48 \text{ kN}$$

$$\begin{aligned} \text{Total: } R_s &= R_{s1} + R_{s2} + R_{s3} = 91 \text{ kN} + 279 \text{ kN} + 48 \text{ kN} \\ &= 418 \text{ kN} \end{aligned}$$

STEP 5 Compute the average corrected SPT N' values, \bar{N}'_O and \bar{N}'_B , near pile toe.

The soil near the pile toe is a dense sand and gravel. Since the pile toe is situated near the interface of a weaker stratum overlying the bearing stratum, the average corrected SPT N' value for both the bearing stratum, \bar{N}'_B , and the overlying stratum, \bar{N}'_O , need to be calculated.

Average corrected SPT N' value for the overlying stratum:

$$\bar{N}'_O = \frac{13 + 15 + 10 + 14 + 16}{5} = 14$$

Average corrected SPT N' value for the bearing stratum:

$$\bar{N}'_B = 34$$

STEP 6 Compute the unit toe resistance, q_t (kPa).

Since a weaker stratum overlies the bearing stratum:

$$q_t = 400 \bar{N}'_O + \frac{(40\bar{N}'_B - 40\bar{N}'_O) D_B}{b} \leq 400\bar{N}'_B$$

STEP 6 (continued)

$$\begin{aligned} &= 400 (14) + \frac{ \{ 40 (34) - 40 (14) \} (0.5)}{0.356} \leq 400 (34) \\ &= 6,724 \leq 13,600 \quad \rightarrow \text{so } q_t = 6,724 \text{ kPa} \end{aligned}$$

STEP 7 Compute the ultimate toe resistance, R_t (kN).

$$\begin{aligned} R_t &= q_t A_t = 6,724 \text{ kPa} (0.356 \text{ m}) (0.356 \text{ m}) \\ &= 854 \text{ kN} \end{aligned}$$

STEP 8 Compute the ultimate pile capacity, Q_u (kN).

$$\begin{aligned} Q_u &= R_s + R_t \\ &= 418 \text{ kN} + 854 \text{ kN} \\ &= 1,272 \text{ kN} \end{aligned}$$

Note: The ultimate capacity according to the Meyerhof method is less than the required 1780 kN ultimate capacity. The Meyerhof method would require a pile penetration depth of 13 meters for a 1,780 kN capacity.

STEP 9 Compute allowable design load, Q_a (kN).

$$Q_a = \frac{Q_u}{\text{Factor of Safety}} = \frac{1,272 \text{ kN}}{\text{Factor of Safety}}$$

Note: Factor of Safety should be selected based on the construction control method to be specified. Recommended factors of safety are described in Section 9.6.

F.2.1.2 Static Axial Pile Capacity Calculations by Nordlund Method

For the soil profile interpreted from Soil Boring S-1 as shown in Figure F.3. Perform a Nordlund method pile capacity calculation for an embedded length of 11.5 meters. Use the step-by-step method outlined in Section 9.7.1.1b.

- STEP 1 Delineate the soil profile into layers and determine the ϕ angle for each layer.
- Construct p_o diagram using procedure described in Section 9.4. This is completed in Figure F.4.
 - Correct SPT field N values for overburden pressure using Figure 4.4 from Chapter 4 and obtain corrected SPT N' values. For Soil Boring S-1, this has been done in the previous example (see Section F.2.1.1, Step 1).
 - Determine the ϕ angle for each layer from laboratory tests or in-situ data.

Since the ϕ angle is not provided by either laboratory or in-situ data, it should be determined using the average corrected SPT N' value, \bar{N}' , as calculated below.

- In the absence of laboratory or in-situ test data, determine the average corrected SPT N' value, \bar{N}' , for each soil layer and estimate ϕ angle from Table 4-5 in Chapter 4.

As the example in Section F.2.1.1, the soil profile along the pile embedded length is delineated into three layers of 4.0, 7.0, and 0.5 meters thick. The average corrected SPT N' value for each soil layer is as follow.

Layer 1:	$\bar{N}'_1 = 8$	(Layer 1 - depth 3 to 7 m; Loose silty fine sand)
Layer 2:	$\bar{N}'_2 = 14$	(Layer 2 - depth 7 to 14 m; Medium dense silty fine sand)
Layer 3:	$\bar{N}'_3 = 34$	(Layer 3 - depth 14 to 14.5 m; Dense sand and gravel)

STEP 1 (continued)

Use the average corrected SPT N' value for each soil layer to estimate ϕ angle from Table 4-5 in Chapter 4.

$$\text{Layer 1: } \phi_1 = 29^\circ \quad \text{for } \bar{N}'_1 = 8$$

$$\text{Layer 2: } \phi_2 = 31^\circ \quad \text{for } \bar{N}'_2 = 14$$

$$\text{Layer 3: } \phi_3 = 36^\circ \quad \text{for } \bar{N}'_3 = 34$$

STEP 2 Determine δ , the friction angle between pile and soil based on displaced soil volume, V , and the soil friction angle, ϕ .

- a. Compute the volume of soil displaced per unit length of pile, V .
Since this is a uniform cross section ($\omega = 0^\circ$) pile,

$$V = (0.356 \text{ m}) (0.356 \text{ m}) (1.0 \text{ m/m}) = 0.127 \text{ m}^3/\text{m}$$

For a non-uniform pile cross section ($\omega \neq 0^\circ$), the pile should be divided into sections and the volume for each section should be calculated.

- b. Enter Figure 9.10 with V and determine δ/ϕ ratio for pile type.

For a precast, prestressed concrete pile with $V = 0.127 \text{ m}^3/\text{m}$,

$$\delta/\phi = 0.84$$

- c. Calculate δ from δ/ϕ ratio.

$$\text{Layer 1: } \delta_1 = 0.84 (29^\circ) = 24.4^\circ$$

$$\text{Layer 2: } \delta_2 = 0.84 (31^\circ) = 26.0^\circ$$

$$\text{Layer 3: } \delta_3 = 0.84 (36^\circ) = 30.2^\circ$$

STEP 3 Determine the coefficient of lateral earth pressure, K_s , for each ϕ angle.

- a. Determine K_s for ϕ angle based on displaced volume, V , and pile taper angle, ω , using either Figure 9.11, 9.12, 9.13, or 9.14 and the appropriate procedure described in Step 3b, 3c, 3d, or 3e.

The pile taper angle, ω , = 0° .

For Layer 1:

$\phi_1 = 29^\circ$ and $V = 0.127 \text{ m}^3/\text{m}$, therefore use Step 3e.

First, use linear interpolation to determine K_s for the required ϕ angle of 29° at the given displaced volume curves of 0.093 and $0.93 \text{ m}^3/\text{m}$.

For $V = 0.093 \text{ m}^3/\text{m}$:

$$\phi = 25^\circ \quad K_s = 0.85 \quad (\text{from Figure 9.11})$$

$$\phi = 29^\circ \quad K_s = \quad (\text{using linear interpolation})$$

$$\phi = 30^\circ \quad K_s = 1.15 \quad (\text{from Figure 9.12})$$

Using linear interpolation to determine K_s for $\phi = 29^\circ$:

$$\begin{aligned} K_s &= 0.85 + \frac{(29 - 25)}{(30 - 25)} (1.15 - 0.85) \\ &= 1.09 \end{aligned}$$

For $V = 0.93 \text{ m}^3/\text{m}$:

$$\phi = 25^\circ \quad K_s = 1.00 \quad (\text{from Figure 9.11})$$

$$\phi = 29^\circ \quad K_s = \quad (\text{using linear interpolation})$$

$$\phi = 30^\circ \quad K_s = 1.45 \quad (\text{from Figure 9.12})$$

STEP 3 (continued)

Using linear interpolation to determine K_δ for $\phi = 29^\circ$:

$$\begin{aligned}K_\delta &= 1.0 + \frac{(29 - 25)}{(30 - 25)} (1.45 - 1.0) \\ &= 1.36\end{aligned}$$

Then use log linear interpolation to determine K_δ for $\phi = 29^\circ$ and $V = 0.127 \text{ m}^3/\text{m}$.

$$V = 0.093 \text{ m}^3/\text{m} \quad K_\delta = 1.09$$

$$V = 0.127 \text{ m}^3/\text{m} \quad K_\delta = \quad \text{(using log linear interpolation)}$$

$$V = 0.93 \text{ m}^3/\text{m} \quad K_\delta = 1.36$$

Log linear interpolation for $V = 0.127 \text{ m}^3/\text{m}$:

$$\begin{aligned}K_{\delta 1} &= 1.09 + \frac{\log (0.127) - \log (0.093)}{\log (0.93) - \log (0.093)} (1.36 - 1.09) \\ &= 1.13\end{aligned}$$

Table 9-2b can be used to check the above calculations. From Table 9-2b, for $\phi = 29^\circ$:

$$V = 0.093 \text{ m}^3/\text{m} \quad K_\delta = 1.09 \quad \text{(from Table 9-2b)}$$

$$V = 0.127 \text{ m}^3/\text{m} \quad K_\delta = 1.13 \quad \text{(from log linear interpolation)}$$

$$V = 0.186 \text{ m}^3/\text{m} \quad K_\delta = 1.17 \quad \text{(from Table 9-2b)}$$

STEP 3 (continued)

For Layer 2:

$\phi_2 = 31^\circ$ and $V = 0.127 \text{ m}^3/\text{m}$, therefore use Step 3e.

First, use linear interpolation to determine K_δ for the required ϕ angle of 31° at the given displaced volume curves of 0.093 and $0.93 \text{ m}^3/\text{m}$.

For $V = 0.093 \text{ m}^3/\text{m}$:

$$\phi = 30^\circ \quad K_\delta = 1.15 \quad (\text{from Figure 9.12})$$

$$\phi = 31^\circ \quad K_\delta = \quad (\text{using linear interpolation})$$

$$\phi = 35^\circ \quad K_\delta = 1.75 \quad (\text{from Figure 9.13})$$

Using linear interpolation to determine K_δ for $\phi = 31^\circ$:

$$\begin{aligned} K_\delta &= 1.15 + \frac{(31 - 30)}{(35 - 30)} (1.75 - 1.15) \\ &= 1.27 \end{aligned}$$

For $V = 0.93 \text{ m}^3/\text{m}$:

$$\phi = 30^\circ \quad K_\delta = 1.45 \quad (\text{from Figure 9.12})$$

$$\phi = 31^\circ \quad K_\delta = \quad (\text{using linear interpolation})$$

$$\phi = 35^\circ \quad K_\delta = 2.35 \quad (\text{from Figure 9.13})$$

Using linear interpolation to determine K_δ for $\phi = 31^\circ$:

$$\begin{aligned} K_\delta &= 1.45 + \frac{(31 - 30)}{(35 - 30)} (2.35 - 1.45) \\ &= 1.63 \end{aligned}$$

STEP 3 (continued)

Then use log linear interpolation to determine K_δ for $\phi = 31^\circ$ and $V = 0.127 \text{ m}^3/\text{m}$.

$$V = 0.093 \text{ m}^3/\text{m} \quad K_\delta = 1.27$$

$$V = 0.127 \text{ m}^3/\text{m} \quad K_\delta = \quad \text{(using log linear interpolation)}$$

$$V = 0.93 \text{ m}^3/\text{m} \quad K_\delta = 1.63$$

Log linear interpolation for $V = 0.127 \text{ m}^3/\text{m}$:

$$\begin{aligned} K_{\delta 2} &= 1.27 + \frac{\log(0.127) - \log(0.093)}{\log(0.93) - \log(0.093)} (1.63 - 1.27) \\ &= 1.32 \end{aligned}$$

Table 9-2b can be used to check the above calculations. From Table 9-2b, for $\phi = 31^\circ$:

$$V = 0.093 \text{ m}^3/\text{m} \quad K_\delta = 1.27 \quad \text{(from Table 9-2b)}$$

$$V = 0.127 \text{ m}^3/\text{m} \quad K_\delta = 1.32 \quad \text{(from log linear interpolation)}$$

$$V = 0.186 \text{ m}^3/\text{m} \quad K_\delta = 1.38 \quad \text{(from Table 9-2b)}$$

STEP 3 (continued)

For Layer 3:

$\phi_3 = 36^\circ$ and $V = 0.127 \text{ m}^3/\text{m}$, therefore use Step 3e.

First, use linear interpolation to determine K_δ for the required ϕ angle of 36° at the given displaced volume curves of 0.093 and $0.93 \text{ m}^3/\text{m}$.

For $V = 0.093 \text{ m}^3/\text{m}$:

$$\phi = 35^\circ \quad K_\delta = 1.75 \quad (\text{from Figure 9.13})$$

$$\phi = 36^\circ \quad K_\delta = \quad (\text{using linear interpolation})$$

$$\phi = 40^\circ \quad K_\delta = 3.00 \quad (\text{from Figure 9.14})$$

Using linear interpolation to determine K_δ for $\phi = 36^\circ$:

$$\begin{aligned} K_\delta &= 1.75 + \frac{(36 - 35)}{(40 - 35)} (3.00 - 1.75) \\ &= 2.00 \end{aligned}$$

For $V = 0.93 \text{ m}^3/\text{m}$:

$$\phi = 35^\circ \quad K_\delta = 2.35 \quad (\text{from Figure 9.13})$$

$$\phi = 36^\circ \quad K_\delta = \quad (\text{using linear interpolation})$$

$$\phi = 40^\circ \quad K_\delta = 4.30 \quad (\text{from Figure 9.14})$$

Using linear interpolation to determine K_δ for $\phi = 36^\circ$:

$$\begin{aligned} K_\delta &= 2.35 + \frac{(36 - 35)}{(40 - 35)} (4.30 - 2.35) \\ &= 2.74 \end{aligned}$$

STEP 3 (continued)

Then use log linear interpolation to determine K_δ for $\phi = 36^\circ$ and $V = 0.127 \text{ m}^3/\text{m}$.

$$V = 0.093 \text{ m}^3/\text{m} \quad K_\delta = 2.00$$

$$V = 0.127 \text{ m}^3/\text{m} \quad K_\delta = \quad \text{(using log linear interpolation)}$$

$$V = 0.93 \text{ m}^3/\text{m} \quad K_\delta = 2.74$$

Log linear interpolation for $V = 0.127 \text{ m}^3/\text{m}$:

$$\begin{aligned} K_{\delta 3} &= 2.00 + \frac{\log (0.127) - \log (0.093)}{\log (0.93) - \log (0.093)} (2.74 - 2.00) \\ &= 2.10 \end{aligned}$$

Table 9-2b can be used to check the above calculations. From Table 9-2b, for $\phi = 36^\circ$:

$$V = 0.093 \text{ m}^3/\text{m} \quad K_\delta = 2.00 \quad \text{(from Table 9-2b)}$$

$$V = 0.127 \text{ m}^3/\text{m} \quad K_\delta = 2.10 \quad \text{(from log linear interpolation)}$$

$$V = 0.186 \text{ m}^3/\text{m} \quad K_\delta = 2.22 \quad \text{(from Table 9-2b)}$$

STEP 4 Determine the correction factor, C_F , to be applied to K_δ if $\delta \neq \phi$.

Use Figure 9.15 to determine the correction factor for each K_δ . Enter figure with ϕ angle and $\delta/\phi=0.84$ to determine C_F .

Layer 1: For $\phi_1 = 29^\circ \rightarrow C_{F1} = 0.96$

Layer 2: For $\phi_2 = 31^\circ \rightarrow C_{F2} = 0.94$

Layer 3: For $\phi_3 = 36^\circ \rightarrow C_{F3} = 0.93$

STEP 5 Compute the average effective overburden pressure at the midpoint of each soil layer, p_d (kPa). (Note: a limiting value is not applied to p_d).

The effective overburden pressure at the midpoint of each soil layer is equal to the average effective overburden pressure of that layer. The effective overburden pressure versus depth for the North Abutment has been computed and tabulated in the previous example (see Section F.2.1.1, Step 1). The effective overburden pressure diagram for the North Abutment is presented in Figure F.4. Since the effective overburden pressure is non linear in layer 1, this layer should be split at the water table location into layer 1a and layer 1b. The effective overburden pressure is then calculated at the midpoint of each of these layers.

Layer 1a: $p_{d1a} = 57.8 \text{ kPa}$ (midpoint of layer 1a - at depth of 3.5 m)

Layer 1b: $p_{d1b} = 76.1 \text{ kPa}$ (midpoint of layer 1b - at depth of 5.5 m)

Layer 2: $p_{d2} = 113.4 \text{ kPa}$ (midpoint of layer 2 - at depth of 10.5 m)

Layer 3: $p_{d3} = 143.1 \text{ kPa}$ (midpoint of layer 3 - at depth of 14.25 m)

STEP 6 Compute the shaft resistance in each soil layer. Sum the shaft resistance from each soil layer to obtain the ultimate shaft resistance, R_s (kN).

$$R_s = K_\delta C_F p_d \sin \delta C_d D \quad (\text{for uniform pile cross section})$$

$$\text{where : } C_d = (4)(0.356 \text{ m}) = 1.424 \text{ m}$$

$$\begin{aligned} \text{Layer 1a: } R_{s1a} &= 1.13 (0.96)(57.8 \text{ kPa})(\sin 24.4^\circ)(1.424 \text{ m})(1 \text{ m}) \\ &= 37 \text{ kN} \end{aligned}$$

$$\begin{aligned} \text{Layer 1b: } R_{s1b} &= 1.13 (0.96)(76.1 \text{ kPa})(\sin 24.4^\circ)(1.424 \text{ m})(3 \text{ m}) \\ &= 146 \text{ kN} \end{aligned}$$

$$\begin{aligned} \text{Layer 2: } R_{s2} &= 1.32 (0.94)(113.4 \text{ kPa})(\sin 26.0^\circ)(1.424 \text{ m})(7 \text{ m}) \\ &= 615 \text{ kN} \end{aligned}$$

$$\begin{aligned} \text{Layer 3: } R_{s3} &= 2.10 (0.93)(143.2 \text{ kPa})(\sin 30.2^\circ)(1.424 \text{ m})(0.5 \text{ m}) \\ &= 100 \text{ kN} \end{aligned}$$

$$\begin{aligned} \text{Total: } R_s &= R_{s1a} + R_{s1b} + R_{s2} + R_{s3} \\ &= 37 \text{ kN} + 146 \text{ kN} + 615 \text{ kN} + 100 \text{ kN} \\ &= 898 \text{ kN} \end{aligned}$$

STEP 7 Determine the α_t coefficient and the bearing capacity factor, N'_q , from the ϕ angle near the pile toe.

Since the ϕ angle is not provided by either laboratory tests or in-situ data, the ϕ angle can be estimated from Table 4-5 using the average corrected SPT N' value over the zone from the pile toe to 3 diameter below the pile toe (1.065 meters). The soil near the pile toe is a dense sand and gravel.

$$\bar{N}'_{\text{toe}} = 34 \quad \rightarrow \quad \phi_{\text{toe}} = 36^\circ$$

a. Enter Figure 9.16(a) with ϕ angle near pile toe to determine α_t coefficient based on pile length to diameter ratio.

$$(D/b) = (11.5 \text{ m}) / (0.356 \text{ m}) = 32.3$$

$$\text{For } \phi_{\text{toe}} = 36^\circ \text{ and } (D/b) = 32.3 \quad \rightarrow \quad \alpha_t = 0.68$$

b. Enter Figure 9.16(b) with ϕ angle near pile toe to determine N'_q .

$$\text{For } \phi_{\text{toe}} = 36^\circ \quad \rightarrow \quad N'_q = 75$$

STEP 8 Compute the effective overburden pressure at the pile toe, p_t (kPa).

The effective overburden pressure at the pile toe should be limited to a maximum of 150 kPa.

The effective overburden pressure at the pile toe, p_t , has been computed in the previous example (Section F.2.1.1, Step 1):

$$p_t = 145.6 \text{ kPa} < 150 \text{ kPa} \quad \rightarrow \quad \text{OK}$$

STEP 9 Compute the ultimate toe resistance, R_t (kN).

$$\begin{aligned} \text{a. } R_t &= \alpha_t N'_q A_t p_t \\ &= 0.68 (75) (0.356 \text{ m})(0.356 \text{ m}) (145.6 \text{ kPa}) \\ &= 943 \text{ kN} \end{aligned}$$

$$\text{b. limiting } R_t = q_L A_t$$

Using the estimated $\phi=36^\circ$ and Figure 9.17, the limiting unit toe resistance is:

$$q_L = 7,400 \text{ kPa}$$

Therefore,

$$R_t = 7,400 \text{ kPa} (0.356 \text{ m})(0.356 \text{ m}) = 940 \text{ kN}$$

c. Use lesser of the two R_t values obtained in steps a and b which is:

$$R_t = 940 \text{ kN}$$

STEP 10 Compute the ultimate pile capacity, Q_u (kN).

$$\begin{aligned} Q_u &= R_s + R_t \\ &= 898 \text{ kN} + 940 \text{ kN} = 1,838 \text{ kN} \end{aligned}$$

STEP 11 Compute the allowable design load, Q_a (kN).

$$Q_a = \frac{Q_u}{\text{Factor of Safety}} = \frac{1,838 \text{ kN}}{\text{Factor of Safety}}$$

Note: Factor of Safety should be selected based on the construction control method to be specified. Recommended factors of safety are described in Section 9.6.

F.2.1.3 Static Axial Pile Capacity Calculations by Effective Stress Method

For the soil profile interpreted from Soil Boring S-1 as shown in Figure F.3. Perform an Effective Stress method pile capacity calculation for an embedded length of 11.5 meters. Use the step-by-step method outlined in Section 9.7.1.3.

STEP 1 Delineate the soil profile into layers and determine ϕ' angle for each layer.

a. Use the procedure described in Section 9.4 to construct a p_o diagram.

For Soil Boring S-1, the p_o diagram has been constructed in Section F.2.1.1 - Step 1 and also presented in Figure F.4.

b. Divide the soil profile throughout the pile penetration depth into layers and determine the effective overburden pressure, p_o , at the midpoint of each layer.

As the example in Section F.2.1.1, the soil profile along the pile embedded length is delineated into three layers of 4.0, 7.0, and 0.5 meter thick. Since the effective overburden pressure is non linear in layer 1, this layer should be split at the water table location into layer 1a and 1b. The average effective overburden pressure of each layer is equal to the effective overburden pressure at the midpoint of that layer, as follows.

Layer 1a: $p_{o1a} = 57.8 \text{ kPa}$ (midpoint of layer 1a - at depth of 3.5 m)

Layer 1b: $p_{o1b} = 76.1 \text{ kPa}$ (midpoint of layer 1b - at depth of 5.5 m)

Layer 2: $p_{o2} = 113.4 \text{ kPa}$ (midpoint of layer 2 - at depth of 10.5 m)

Layer 3: $p_{o3} = 143.1 \text{ kPa}$ (midpoint of layer 3 - at depth of 14.25 m)

c. Determine the ϕ' angle for each soil layer from laboratory or in-situ test data.

Since the ϕ' angle is not provided by either laboratory or in-situ test data, the average corrected SPT N' value will be used to estimate the ϕ' angle.

STEP 1 (continued)

- d. In the absence of laboratory or in-situ test data for cohesionless soil layers, determine the average corrected SPT N' value for each soil layer and estimate the ϕ' angle from Table 4-5 in Chapter 4.

As in the previous example (Section F.2.1.1), the average corrected SPT N' value and the soil type for each soil layer is as follows.

Layer 1:	$\bar{N}'_1 = 8$	(Layer 1 - depth 3 to 7 m; Loose silty fine sand)
Layer 2:	$\bar{N}'_2 = 14$	(Layer 2 - depth 7 to 14 m; Medium dense silty fine sand)
Layer 3:	$\bar{N}'_3 = 34$	(Layer 3 - depth 14 to 14.5 m; Dense sand and gravel)

Use the average corrected SPT N' value for each soil layer to estimate ϕ' angle from Table 4-5 in Chapter 4.

Layer 1:	$\phi'_1 = 29^\circ$	for $\bar{N}'_1 = 8$
Layer 2:	$\phi'_2 = 31^\circ$	for $\bar{N}'_2 = 14$
Layer 3:	$\phi'_3 = 36^\circ$	for $\bar{N}'_3 = 34$

STEP 2 Select the β coefficient for each soil layer.

- a. Use local experience to select β coefficient for each layer.

Assume no local experience.

STEP 2 (continued)

- b. In the absence of local experience, use Table 9-4 or Figure 9.20 to estimate β coefficient from ϕ' angle for each layer.

Use the soil type, the estimated ϕ' angle, and Table 9-4 or Figure 9-20 to estimate the β coefficient for each layer.

Layer 1: $\beta_1 = 0.30$ (For loose silty fine sand with $\phi'_1 = 29^\circ$)

Layer 2: $\beta_2 = 0.33$ (For medium dense silty fine sand with $\phi'_2 = 31^\circ$)

Layer 3: $\beta_3 = 0.40$ (For dense sand and gravel with $\phi'_3 = 36^\circ$)

STEP 3 For each soil layer compute the unit shaft resistance, f_s (kPa).

$$f_s = \beta p_o$$

Layer 1a: $f_{s1a} = 0.30 (57.8 \text{ kPa}) = 17.34 \text{ kPa}$

Layer 1b: $f_{s1b} = 0.30 (76.1 \text{ kPa}) = 22.83 \text{ kPa}$

Layer 2: $f_{s2} = 0.33 (113.4 \text{ kPa}) = 37.42 \text{ kPa}$

Layer 3: $f_{s3} = 0.40 (143.1 \text{ kPa}) = 57.24 \text{ kPa}$

STEP 4 Compute the shaft resistance in each soil layer and the ultimate shaft resistance, R_s (kN), from the sum of the shaft resistance from each soil layer.

$$R_s = f_s A_s$$

where A_s = Pile-soil surface area from pile perimeter and length

Layer 1a: $R_{s1a} = 17.34 (4) (0.356 \text{ m}) (1 \text{ m}) = 25 \text{ kN}$

Layer 1b: $R_{s1b} = 22.83 (4) (0.356 \text{ m}) (3 \text{ m}) = 98 \text{ kN}$

STEP 4 (continued)

$$\text{Layer 2: } R_{s2} = 37.42 (4) (0.356 \text{ m}) (7 \text{ m}) = 373 \text{ kN}$$

$$\text{Layer 3: } R_{s3} = 57.24 (4) (0.356 \text{ m}) (0.5 \text{ m}) = 41 \text{ kN}$$

$$\begin{aligned} \text{Total: } R_s &= R_{s1a} + R_{s1b} + R_{s2} + R_{s3} \\ &= 25 \text{ kN} + 98 \text{ kN} + 373 \text{ kN} + 41 \text{ kN} \\ &= 537 \text{ kN} \end{aligned}$$

STEP 5 Compute the unit toe resistance, q_t (kPa).

$$q_t = N_t p_t$$

- a. Use local experience to select N_t coefficient.

Assume no local experience.

- b. In the absence of local experience, estimate N_t coefficient from Table 9-4 or Figure 9.21 based on ϕ' angle.

Table 9-4 or Figure 9.21 are a function of soil type and the ϕ' angle. The soil type for each layer can be obtained from the soil boring. The ϕ' angle for each layer can be obtained from laboratory tests or in-situ data. In the absence of either laboratory or in-situ test data, the ϕ' angle should be estimated from Table 4-5 in Chapter 4 using the average corrected SPT N' value, \bar{N}' , over the zone from the pile toe to 3 diameter below the pile toe (1.065 meters). The soil near the pile toe is a dense sand and gravel.

$$\bar{N}'_{\text{toe}} = 34 \quad \rightarrow \quad \phi'_{\text{toe}} = 36^\circ$$

Use the soil type, the estimated ϕ' angle, and Table 9-4 or Figure 9-21 to estimate the N_t coefficient.

$$N_t = 70 \quad (\text{For dense sand and gravel with } \phi'_{\text{toe}} = 36^\circ)$$

c. Calculate the effective overburden pressure at the pile toe, p_t .

The effective overburden pressure at the pile toe, p_t , has been computed in the previous example (Section F.2.1.1, Step 1):

$$p_t = 145.6 \text{ kPa}$$

The unit toe resistance, q_t is:

$$\begin{aligned} q_t &= N_t p_t \\ &= 70 (145.6 \text{ kPa}) = 10,192 \text{ kPa} \end{aligned}$$

STEP 6 Compute the ultimate toe resistance, R_t (kN).

$$\begin{aligned} R_t &= q_t A_t \\ &= 10,192 (0.356 \text{ m}) (0.356 \text{ m}) \\ &= 1,294 \text{ kN} \end{aligned}$$

STEP 7 Compute the ultimate pile capacity, Q_u (kN).

$$\begin{aligned} Q_u &= R_s + R_t \\ &= 537 \text{ kN} + 1,294 \text{ kN} \\ &= 1,831 \text{ kN} \end{aligned}$$

STEP 8 Compute the allowable design load, Q_a (kN).

$$Q_a = \frac{Q_u}{\text{Factor of Safety}} = \frac{1,831 \text{ kN}}{\text{Factor of Safety}}$$

Note: Factor of Safety should be selected based on the construction control method to be specified. Recommended factors of safety are described in Section 9.6.

F.2.1.4 Static Axial Pile Capacity Calculations by SPILE Computer Program

ULTIMATE STATIC PILE CAPACITY/Federal Highway Administration
Nordlund (1963, 1979) and Tomlinson (1979, 1980) methods

Project Name : BORING S-1 Client : FHWA Manual
 File Name : S1 Project Manager :
 Date : 6/14/95 Computed by : GT
 Depth of Top of Pile = 9.84 ft. Pile length = 37.73 ft.
 Depth to Water Table = 13.10 ft.
 Width of pile = 0.00 in.
 Type of Pile = Precast Concrete Pile

SKIN FRICTION CONTRIBUTION

Layer	Soil Type	Thickness (ft)	Effective Stress (psf)	Internal Friction Angle	N-SPT	Pile Perimeter (ft)
1	Cohesionless	3.28	1205.40	28.82*	6.90*	4.67
2	Cohesionless	9.85	1620.63	28.29*	7.36*	4.67
3	Cohesionless	22.96	2434.32	31.00*	13.33*	4.67
4	Cohesionless	1.64	3055.06	37.31*	34.36*	4.67

Layer	Soil Type	Undrained Shear Strength (psf)	Adhesion	Pile Taper	Sliding Friction Angle	Skin Resistance (Kips)
1	Cohesionless	--	-----	----	24.26	8.07
2	Cohesionless	--	-----	----	24.41	33.09
3	Cohesionless	--	-----	----	26.09	143.46
4	Cohesionless	--	-----	----	31.41	27.58

Total Side Friction : 212.20

POINT RESISTANCE CONTRIBUTION

Effective Stress at pile Tip (psf)	Internal Friction Angle	SPT Value	Pile End Area (ft*ft)	Bearing Capacity Factor Nq	End Bearing Resistance (Kips)
3106.39	36.94*	33.13	1.36	90.37	269.98

Limiting End Bearing Resistance : 275.63

Ultimate Static Pile Capacity : 482.18

In SI Units: Total Side Friction : 944 kN
 End Bearing Resistance : 1,201 kN
 Ultimate Static Pile Capacity : 2,145 kN

F.2.1.5 Static Axial Pile Capacity Calculations by LPC CPT Method - Computer Program

L.P.C. CPT Method

Page 1/2

Peach Freeway CPT-1 at North Abutment -- 356 mm-square PCPS Concrete Pile

Installation Method: 9 - Driven Prefabricated Piles (Concrete)

Depth to Water Table: 4.0 meter

Pile No.	Toe Area (m ²)	Perimeter (m)
1	0.127	1.424

Depth to Bottom of Layer (m)	Soil Type
14.021	5
30.785	7

Depth (m)	Cone Tip Resistance (kPa)
0.0	3,926.20
5.0	3,926.20
10.0	3,399.48
11.5	3,591.00
13.0	5,171.04
14.0	5,075.28
15.0	13,071.24
16.0	15,369.48
17.0	20,588.40
18.0	23,078.16
20.0	19,199.88
23.0	17,188.92
24.0	24,466.68
27.0	18,050.80

Peach Freeway CPT-1 at North Abutment -- 356 mm-square PCPS Concrete Pile

Depth (m)	Unit Friction (kPa)	Toe Bearing (kPa)	Shaft Resistance (kN)	Toe Resistance (kN)	Ultimate Capacity (kN)
0.00	60.66	2,355.70	0.0	298.0	298.0
5.00	36.96	1,474.70	347.4	186.4	533.8
10.00	17.05	1,292.76	539.5	163.7	703.2
11.50	35.96	1,484.28	596.0	187.7	783.7
13.00	40.75	2,312.60	678.3	292.2	970.6
14.00	40.46	3,413.84	735.7	431.5	1,167.2
15.00	62.72	4,677.88	824.7	591.1	1,415.8
16.00	63.58	6,171.73	914.5	780.6	1,695.1
17.00	65.60	7,340.00	1,006.1	928.3	1,934.4
18.00	66.55	7,986.38	1,099.1	1,010.1	2,109.2
20.00	65.07	7,445.34	1,287.7	941.6	2,229.3
23.00	64.30	7,411.82	1,563.5	936.7	2,500.2
24.00	67.08	8,158.75	1,657.3	1,031.5	2,688.8
27.00	64.64	6,846.84	1,938.0	866.0	2,804.0

Note: Depth is referenced from the original ground surface.

F.2.1.6 Static Axial Pile Capacity Calculations by Schmertmann Method

Location: Peach Freeway CPT-1 at North Abutment.

Depth (m)	fs(avg) (bars)	Unit Friction (bars)	Increment Friction (kN)	Shaft Resistance (kN)	q _c (avg) (bars)	q _{c1} (min) (bars)	q _{c2} (bars)	Toe Resistance (kN)	Ultimate Capacity (kN)
12.00	1.21	1.03	35.86	286	51.33				
12.25	1.22	1.03	36.00	322	58.35				
12.50	1.14	0.97	33.78	356	56.70				
12.75	1.17	0.99	34.52	390	55.00				
13.00	1.16	0.99	34.46	425	50.20	47.37	23.63	430	855
13.25	0.99	0.84	29.34	454	46.50				
13.50	0.84	0.72	24.98	479	47.27				
13.75	0.59	0.50	17.48	497	47.30				
14.00	0.97	0.83	28.83	526	62.47				
14.25	1.53	1.30	45.19	571	106.35				
14.50	1.11	0.94	32.89	604	127.73				
14.75	1.11	0.94	32.89	637	149.80				
15.00	2.05	1.74	60.66	697	162.90	173.94	68.33	1,467	2,164
15.25	1.72	1.46	50.82	748	196.20				
15.50	1.48	1.26	43.77	792	203.30				
15.75	1.16	0.98	34.23	826	170.90	169.20	98.38	1,620	2,446
16.00	1.15	0.98	34.17	860	168.63				
16.25	1.24	1.05	36.75	897	173.95				
16.50	1.61	1.37	47.71	945	208.87	216.83	129.36	2,096	3,041
16.75	1.61	1.36	47.56	992	224.80				
17.00	1.88	1.60	55.62	1,048	252.37				
17.25	1.84	1.56	54.53	1,102	260.65	252.40	173.18	2,577	3,679
17.50	2.08	1.77	61.73	1,164	249.23				
17.75	2.28	1.93	67.42	1,231	252.40				
18.00	2.86	2.43	84.75	1,316	305.00				
18.25	2.56	2.17	75.71	1,392	297.40				
18.50	2.12	1.80	62.91	1,455	254.83				
18.75	1.71	1.45	50.52	1,505	214.85				
19.00	1.31	1.11	38.82	1,544	148.70				

Note: Depth is referenced from the original ground surface.

F.2.1.7 Summary of North Abutment Capacity Calculation Results

Summary of Pile Capacity Estimates with an Embedded Pile Length of 11.5 meters

Method Used for Estimation of Pile Capacity	Calculated Pile Shaft Resistance (kN)	Calculated Pile Toe Resistance (kN)	Calculated Ultimate Pile Capacity (kN)
Meyerhof Method - SPT Data	418	854	1,272
Nordlund Method - SPT Data	898	940	1,838
Effective Stress Method - SPT Data	537	1,294	1,831
SPILE Program - SPT Data	944	1,201	2,145
LPC CPT Program - CPT Data	780	511	1,291
Schmertmann Method - CPT Data	604	1,111	1,715

Summary of Pile Length Estimates for the 1,780 kN Ultimate Pile Capacity

Method Used for Estimation of Pile Capacity	Calculated Pile Length for the 1,780 kN Ultimate Pile Capacity
Meyerhof Method - SPT Data	13.0 meters for 1,840 kN
Nordlund Method - SPT Data	11.5 meters for 1,838 kN
Effective Stress Method	11.5 meters for 1,831 kN
SPILE Program - SPT Data	11.5 meters for 2,145 kN
LPC CPT Program - CPT Data	13.5 meters for 1,815 kN
Schmertmann Method - CPT Data	11.7 meters for 1,939 kN

The ultimate pile group capacity at the North Abutment may be taken as the sum of the ultimate capacities of the individual piles in the group as discussed by the design recommendation for estimating group capacity in cohesionless soil presented in Section 9.8.1.1.

F.2.2 Pier 2 - Soil Boring S-2 (Cohesionless Soil)

F.2.2.1 Static Axial Pile Capacity Calculations by Meyerhof SPT Method (before scour)

For the soil profile interpreted from Soil Boring S-2 as shown in Figure F.5. Perform a Meyerhof method pile capacity calculation for an embedded length of 10 meters. Assume that scour has not occurred. Use the step-by-step method outlined in Section 9.7.1.1a.

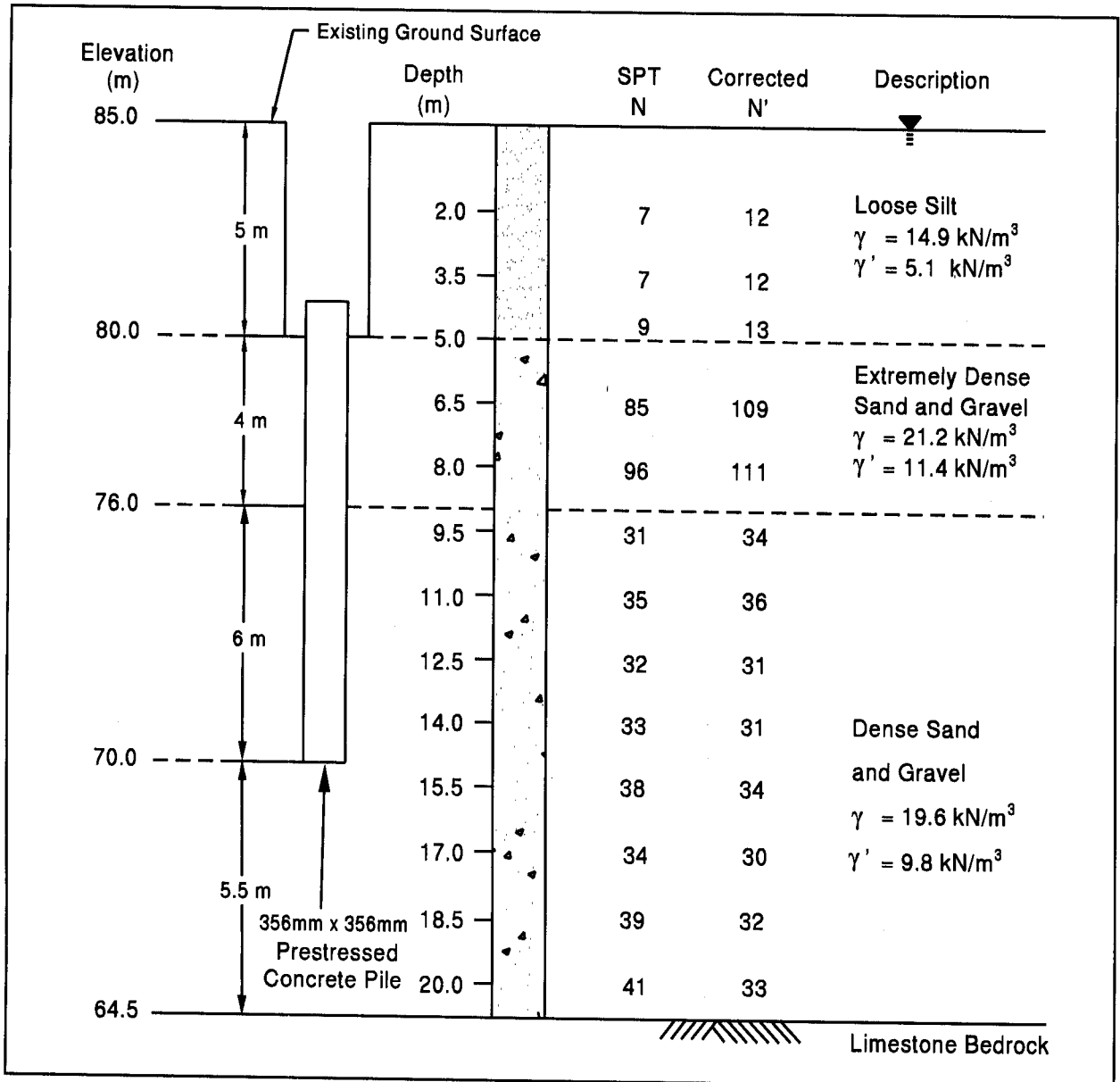


Figure F.5 Interpreted Soil Profile from Soil Boring S-2 at Pier 2

STEP 1 Correct SPT field N values for overburden pressure.

Effective overburden pressures, p_o , are needed to correct SPT field N values. The method for calculating the effective overburden pressure is explained in Section 9.4 and an example was presented earlier in Section F.2.1.1. The effective overburden pressure diagram and the soil layers are presented in Figure F.6 below.

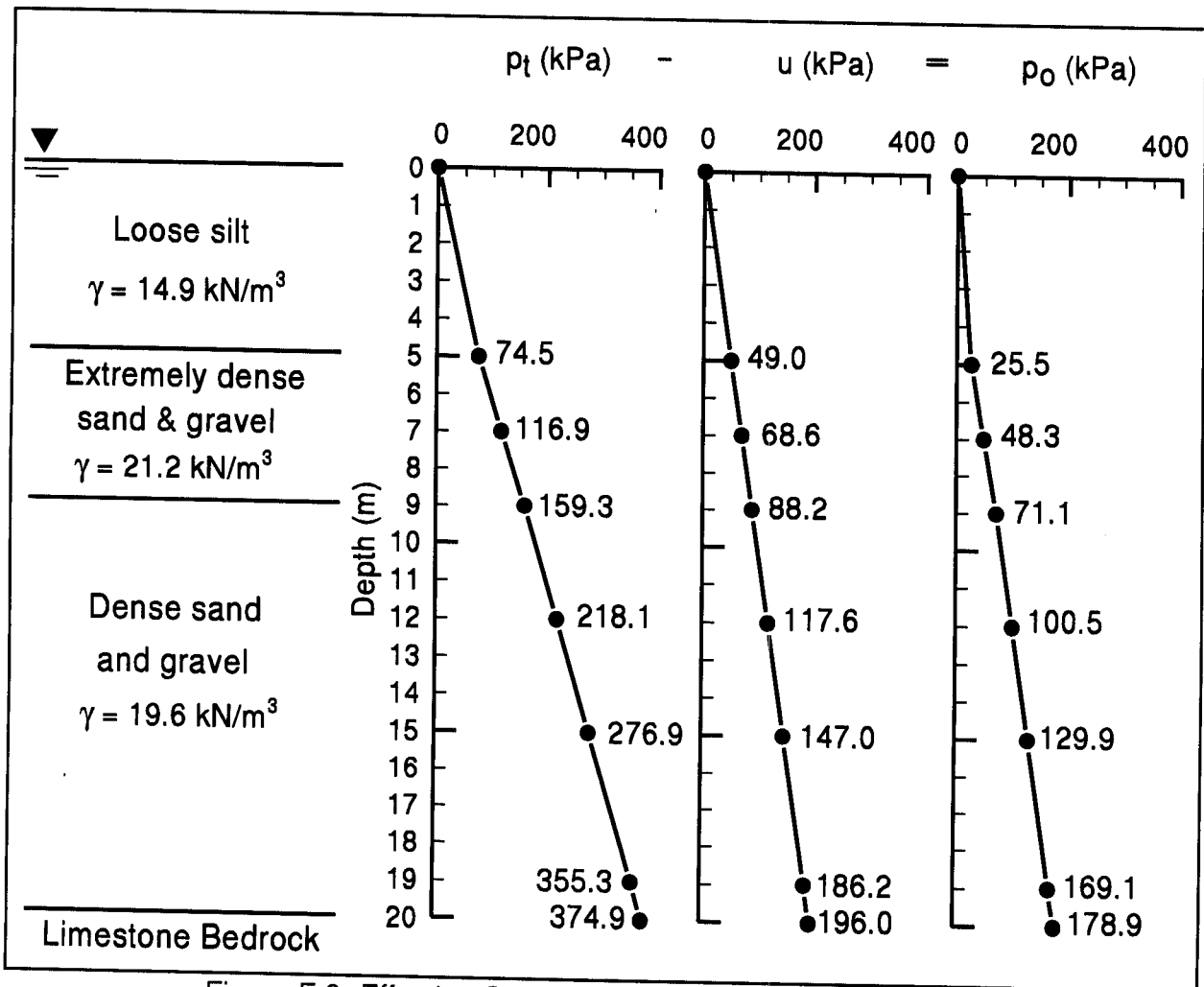


Figure F.6 Effective Overburden Pressure Diagram - Pier 2

STEP 1 (continued)

Use correction factors from Figure 4.4 (Chapter 4) to obtain corrected SPT N' values.

Depth (m)	p_o (kPa)	Field SPT N value	Correction Factor	Corrected SPT N' (Field SPT N x Correction Factor)
2.0	10.2	7	1.75	12
3.5	17.9	7	1.65	12
5.0	25.5	9	1.43	13
6.5	42.6	85	1.28	109
8.0	59.7	96	1.16	111
9.5	76.0	31	1.09	34
11.0	90.7	35	1.04	36
12.5	105.4	32	0.98	31
14.0	120.1	33	0.95	31
15.5	134.8	38	0.90	34
17.0	149.5	34	0.87	30
18.5	164.2	39	0.83	32
20.0	178.9	41	0.81	33

STEP 2 Compute the average corrected SPT N' value, \bar{N}' , for each soil layer.

Along the pile embedded length, the soil profile is delineated into two layers. Layer 1 is extremely dense sand and gravel that is 4 meters thick, and layer 2 is dense sand and gravel that is 6 meters thick.

$$\bar{N}'_1 = \frac{109 + 111}{2} = 110 \quad \text{(Layer 1 - depth 5 to 9 m; Extremely dense sand and gravel)}$$

$$\bar{N}'_2 = \frac{34 + 36 + 31 + 31}{4} = 33 \quad \text{(Layer 2 - depth 9 to 15 m; Dense sand and gravel)}$$

STEP 3 Compute unit shaft resistance, f_s (kPa), using the equation for driven displacement piles:

$$f_s = 2\bar{N}' \leq 100 \text{ kPa}$$

$$\text{Layer 1: } f_{s1} = 2(110) = 220 \text{ kPa, so use } f_{s1} = 100 \text{ kPa}$$

$$\text{Layer 2: } f_{s2} = 2(33) = 66 \text{ kPa}$$

STEP 4 Compute ultimate shaft resistance, R_s (kN).

$$R_s = f_s A_s$$

$$\text{Layer 1: } R_{s1} = 100 \text{ kPa} (4)(0.356 \text{ m})(4 \text{ m}) = 570 \text{ kN}$$

$$\text{Layer 2: } R_{s2} = 66 \text{ kPa} (4)(0.356 \text{ m})(6 \text{ m}) = 564 \text{ kN}$$

$$\begin{aligned} \text{Total: } R_s &= R_{s1} + R_{s2} = 570 \text{ kN} + 564 \text{ kN} \\ &= 1,134 \text{ kN} \end{aligned}$$

STEP 5 Compute average corrected SPT N' value, \bar{N}'_O and \bar{N}'_B near pile toe.

When the pile is embedded to more than 10 pile diameters into the bearing stratum, the effect of overlying stratum becomes irrelevant. The unit toe resistance is governed by the limiting unit toe resistance of the bearing stratum that is $400\bar{N}'_B$.

The average corrected SPT N' value for the bearing stratum should be calculated from the average N' value within the zone extending 3 pile diameters below the pile toe or in this case 1.065 meter. The average corrected SPT N' value for the bearing stratum which consists of dense sand and gravel is:

$$\bar{N}'_B = \frac{34 + 36 + 31 + 31 + 34}{5} = 33$$

STEP 6 Compute unit toe resistance, q_t (kPa).

$$q_t = \frac{40\bar{N}'_B D_B}{b} \leq 400\bar{N}'_B$$
$$= \frac{40\bar{N}'_B (6 \text{ m})}{0.356 \text{ m}} = 674\bar{N}'_B, \text{ so use } q_t = 400\bar{N}'_B$$

$$q_t = 400 (33) = 13,200 \text{ kPa}$$

STEP 7 Compute ultimate toe resistance, R_t (kN).

$$R_t = q_t A_t = 13,200 \text{ kPa } (0.356 \text{ m })(0.356 \text{ m })$$
$$= 1,676 \text{ kN}$$

STEP 8 Compute ultimate pile capacity, Q_u (kN).

$$\begin{aligned} Q_u &= R_s + R_t \\ &= 1,134 \text{ kN} + 1,676 \text{ kN} \\ &= 2,810 \text{ kN} \end{aligned}$$

STEP 9 Compute allowable design load, Q_a (kN).

$$Q_a = \frac{Q_u}{\text{Factor of Safety}} = \frac{2,810 \text{ kN}}{\text{Factor of Safety}}$$

Note: Factor of Safety should be selected based on the construction control method to be specified. Recommended factors of safety are described in Section 9.6.

F.2.2.2 Static Axial Pile Capacity Calculations by Nordlund Method (before scour at 10 m)

For the soil profile interpreted from Soil Boring S-2 as shown in Figure F.5. Perform a Nordlund method pile capacity calculation for an embedded length of 10 meters. Assume that scour has not occurred. Use the step-by-step method outlined in Section 9.7.1.1b.

- STEP 1 Delineate the soil profile into layers and determine the ϕ angle for each layer.
- Construct p_o diagram using the procedure described in Section 9.4. This is completed in Figure F.6.
 - Correct SPT field N values for overburden pressure using Figure 4.4 from Chapter 4 and obtain corrected SPT N' values. For Soil Boring S-2, this has been done in the previous example (see Section F.2.2.1, Step 1).
 - Determine ϕ angle for each layer from laboratory tests or in-situ data.

Since the ϕ angle is not provided by either laboratory or in-situ data, it should be determined using the average corrected SPT N' value, \bar{N}' , as calculated below.

- In the absence of laboratory or in-situ test data, determine the average corrected SPT N' value, \bar{N}' , for each soil layer and estimate ϕ angle from Table 4-5 in Chapter 4.

As the example in Section F.2.2.1, the soil profile along the pile embedded length is delineated into two layers of 4, and 6 meters thick. The average corrected SPT N' value for each soil layer is as follows:

Layer 1: $\bar{N}'_1 = 110$ (Layer 1 - depth 5 to 9 m;
Extremely dense sand and gravel)

Layer 2: $\bar{N}'_2 = 33$ (Layer 2 - depth 9 to 15 m;
Dense sand and gravel)

Use the average corrected SPT N' value for each soil layer to estimate ϕ angle from Table 4-5 in Chapter 4.

STEP 1 (continued)

Based on Table 4-5, the ϕ angle is indicated to be as high as 43° when N' is greater than 50. However, as discussed in Section 9.5, in soil layers with greater than 50% gravel the ϕ angle for shaft resistance calculations should be limited to:

36° for hard angular gravel, and
32° for soft rounded gravel.

A limiting friction angle should be used for layer 1.

Layer 1: $\phi_1 = 36^\circ$ limiting friction angle for hard angular gravel

For layer 2, the friction angle is computed from Table 4-5:

Layer 2: $\phi_2 = 35^\circ$ for $\bar{N}'_2 = 33$

STEP 2 Determine δ , the friction angle between pile and soil based on displaced soil volume, V , and the soil friction angle, ϕ .

- a. Compute volume of soil displaced per unit length of pile, V .
Since this is a uniform cross section ($\omega = 0^\circ$) pile,

$$V = (0.356 \text{ m})(0.356 \text{ m})(1.0 \text{ m/m}) = 0.127 \text{ m}^3/\text{m}$$

For a non-uniform pile cross section ($\omega \neq 0^\circ$), the pile should be divided into sections and the volume for each section should be calculated.

- b. Enter Figure 9.10 with V and determine δ/ϕ ratio for pile type.

For a precast, prestressed concrete pile with $V = 0.127 \text{ m}^3/\text{m}$

$$\delta/\phi = 0.84$$

STEP 2 (continued)

c. Calculate δ from δ/ϕ ratio.

$$\text{Layer 1: } \delta_1 = 0.84 (36^\circ) = 30.2^\circ$$

$$\text{Layer 2: } \delta_2 = 0.84 (35^\circ) = 29.4^\circ$$

STEP 3 Determine the coefficient of lateral earth pressure, K_δ , for each ϕ angle.

a. Determine K_δ for ϕ angle based on displaced volume, V , and pile taper angle, ω , using either Figure 9.11, 9.12, 9.13, or 9.14 and the appropriate procedure described in Step 3b, 3c, 3d, or 3e.

The pile taper angle, ω , = 0° .

For Layer 1:

$$\phi_1 = 36^\circ \quad \text{and} \quad V = 0.127 \text{ m}^3/\text{m}, \text{ therefore use Step 3e.}$$

A step by step procedure for determining K_δ using the linear interpolation and the log linear interpolation is presented in Section F.2.1.2 - Step 3.

For $\phi_1 = 36^\circ$, $\omega = 0^\circ$, and $V = 0.127 \text{ m}^3/\text{m}$:

$$K_{\delta 1} = 2.10$$

For Layer 2:

$$\phi_2 = 35^\circ \quad \text{and} \quad V = 0.127 \text{ m}^3/\text{m}, \text{ therefore use Step 3d.}$$

A step by step procedure for determining K_δ using the log linear interpolation is presented in Section F.2.1.2 - Step 3.

For $\phi_2 = 35^\circ$, $\omega = 0^\circ$, and $V = 0.127 \text{ m}^3/\text{m}$:

$$K_{\delta 2} = 1.83$$

STEP 4 Determine the correction factor, C_F , to be applied to K_δ if $\delta \neq \phi$.

Use Figure 9.15 to determine the correction factor for each K_δ . Enter figure with ϕ angle and $\delta/\phi=0.84$ to determine C_F .

$$\text{Layer 1:} \quad \text{For } \phi_1 = 36^\circ \quad \rightarrow \quad C_{F1} = 0.92$$

$$\text{Layer 2:} \quad \text{For } \phi_2 = 35^\circ \quad \rightarrow \quad C_{F2} = 0.93$$

STEP 5 Compute the average effective overburden pressure at the midpoint of each soil layer, p_d (kPa). (Note: a limiting value is not applied to p_d).

The effective overburden pressure at the midpoint of each soil layer is equal to the average effective overburden pressure of that layer. The effective overburden pressure versus depth for Pier 2 has been computed and tabulated in the previous example (see Section F.2.2.1 - Step 1). The effective overburden pressure diagram for Pier 2 is presented in Figure F.6.

$$\text{Layer 1:} \quad p_{d1} = 48.3 \text{ kPa} \quad (\text{midpoint of layer 1 - at depth of 7.0 m})$$

$$\text{Layer 2:} \quad p_{d2} = 100.5 \text{ kPa} \quad (\text{midpoint of layer 2 - at depth of 12.0 m})$$

STEP 6 Compute the shaft resistance in each soil layer. Sum the shaft resistance from each soil layer to obtain the ultimate shaft resistance, R_s (kN).

$$R_s = K_\delta C_F p_d \sin \delta C_d D \quad (\text{for uniform pile cross section})$$

$$\text{where : } C_d = (4) (0.356 \text{ m}) = 1.424 \text{ m}$$

$$\begin{aligned} \text{Layer 1: } R_{s1} &= 2.10 (0.92) (48.3 \text{ kPa}) (\sin 30.2^\circ) (1.424 \text{ m}) (4 \text{ m}) \\ &= 267 \text{ kN} \end{aligned}$$

$$\begin{aligned} \text{Layer 2: } R_{s2} &= 1.83 (0.93) (100.5 \text{ kPa}) (\sin 29.4^\circ) (1.424 \text{ m}) (6 \text{ m}) \\ &= 717 \text{ kN} \end{aligned}$$

STEP 6 (continued)

$$\begin{aligned}\text{Total: } R_s &= R_{s1} + R_{s2} \\ &= 267 \text{ kN} + 717 \text{ kN} = 984 \text{ kN}\end{aligned}$$

STEP 7 Determine the α_t coefficient and the bearing capacity factor, N'_q , from the ϕ angle near the pile toe.

Since the ϕ angle is not provided by either laboratory tests or in-situ data, the ϕ angle can be estimated from Table 4-5 using the average corrected SPT N' value over the zone from the pile toe to 3 diameter below the pile toe (1.065 meters). The soil near the pile toe is a dense sand and gravel.

$$\bar{N}'_{\text{toe}} = 34 \quad \rightarrow \quad \phi_{\text{toe}} = 36^\circ$$

a. Enter Figure 9.16(a) with ϕ angle near pile toe to determine α_t coefficient based on pile length to diameter ratio.

$$(D/b) = (10.0 \text{ m}) / (0.356 \text{ m}) = 28.1$$

$$\text{For } \phi_{\text{toe}} = 36^\circ \text{ and } (D/b) = 28.1 \quad \rightarrow \quad \alpha_t = 0.69$$

b. Enter Figure 9.16(b) with ϕ angle near pile toe to determine N'_q .

$$\text{For } \phi_{\text{toe}} = 36^\circ \quad \rightarrow \quad N'_q = 75$$

STEP 8 Compute the effective overburden pressure at the pile toe, p_t (kPa).

The effective overburden pressure at the pile toe should be limited to a maximum of 150 kPa.

The effective overburden pressure at the pile toe, p_t , has been computed in the previous example (Section F.2.2.1, Step 1):

$$p_t = 129.9 \text{ kPa} < 150 \text{ kPa} \quad \rightarrow \quad \text{OK}$$

STEP 9 Compute ultimate toe resistance, R_t (kN).

$$\begin{aligned} \text{a. } R_t &= \alpha_t N'_q A_t p_t \\ &= 0.69 (75) (0.356 \text{ m})(0.356 \text{ m}) (129.9 \text{ kPa}) \\ &= 854 \text{ kN} \end{aligned}$$

$$\text{b. limiting } R_t = q_L A_t$$

Using the estimated $\phi=36^\circ$ and Figure 9.17, the limiting unit toe resistance is:

$$q_L = 7,400 \text{ kPa}$$

Therefore,

$$R_t = 7,400 \text{ kPa} (0.356 \text{ m})(0.356 \text{ m}) = 940 \text{ kN}$$

c. Use lesser of the two R_t values obtained in steps a and b which is:

$$R_t = 854 \text{ kN}$$

STEP 10 Compute the ultimate pile capacity, Q_u (kN).

$$\begin{aligned} Q_u &= R_s + R_t \\ &= 984 \text{ kN} + 854 \text{ kN} = 1,838 \text{ kN} \end{aligned}$$

STEP 11 Compute the allowable design load, Q_a (kN).

$$Q_a = \frac{Q_u}{\text{Factor of Safety}} = \frac{1,838 \text{ kN}}{\text{Factor of Safety}}$$

Note: Factor of Safety should be selected based on the construction control method to be specified. Recommended factors of safety are described in Section 9.6.

F.2.2.3 Static Axial Pile Capacity Calculations by Nordlund Method (after scour at 10 m)

For the soil profile interpreted from Soil Boring S-2 after scour as shown in Figure F.7. Perform a Nordlund method pile capacity calculation for an embedded length of 10 meters. Assume that channel degradation scour has removed the 5 meter thick loose silt layer. Use the step-by-step method outlined in Section 9.7.1.1b.

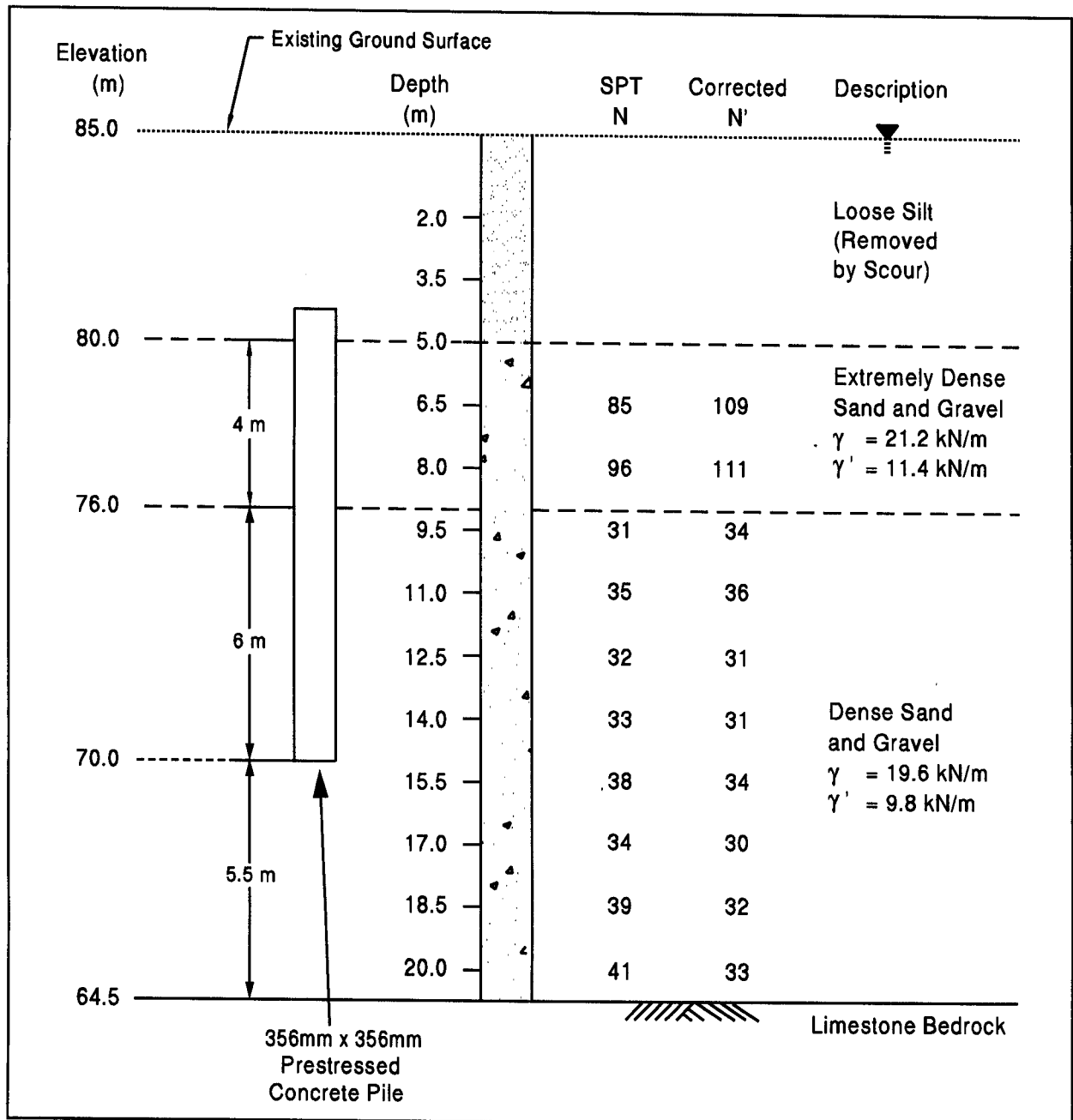


Figure F.7 Interpreted Soil Profile at Pier 2 after Scour

STEP 1 Delineate the soil profile into layers and determine the ϕ angle for each layer.

- a. Construct p_o diagram using procedure described in Section 9.4. This is completed in Figure F.6.
- b. Correct SPT field N values for overburden pressure using Figure 4.4 from Chapter 4 and obtain corrected SPT N' values. For Soil Boring S-2, this was done in the previous example (see Section F.2.2.1, Step 1).

Note: Although scour has eroded the 5 meter thick loose silt layer, the original overburden pressure (with the loose silt layer still in place) should be used when correcting the SPT field N values.

- c. Determine ϕ angle for each layer from laboratory tests or in-situ data.

Since the ϕ angle is not provided by either laboratory or in-situ data, it should be determined using the average corrected SPT N' value, \bar{N}' , as calculated below.

- d. In the absence of laboratory or in-situ test data, determine the average corrected SPT N' value, \bar{N}' , for each soil layer and estimate ϕ angle from Table 4-5 in Chapter 4.

As the example in Section F.2.2.2, the soil profile along the pile embedded length is delineated into two layers of 4, and 6 meters thick. The average corrected SPT N' value for each soil layer is as follow.

Layer 1: $\bar{N}'_1 = 110$ (Layer 1 - depth 5 to 9 m below existing ground surface; Extremely dense sand and gravel)

Layer 2: $\bar{N}'_2 = 33$ (Layer 2 - depth 9 to 15 m below existing ground surface; Dense sand and gravel)

Use the average corrected SPT N' value for each soil layer to estimate ϕ angle from Table 4-5 in Chapter 4.

STEP 1 (continued)

As discussed in Section F.2.2.2 - Step 1, a limiting friction angle should be used for the hard angular gravel of layer 1.

Layer 1: $\phi_1 = 36^\circ$ from limiting friction angle

For layer 2, the friction angle is computed from Table 4-5:

Layer 2: $\phi_2 = 35^\circ$ for $\bar{N}_2' = 33$

STEP 2 Determine δ , the friction angle between pile and soil based on displaced soil volume, V , and the soil friction angle, ϕ .

- a. Compute volume of soil displaced per unit length of pile, V .
Since this is a uniform cross section ($\omega = 0^\circ$) pile,

$$V = (0.356 \text{ m})(0.356 \text{ m})(1.0 \text{ m/m}) = 0.127 \text{ m}^3/\text{m}$$

For a non-uniform pile cross section ($\omega \neq 0^\circ$), the pile should be divided into sections and the volume for each section should be calculated.

- b. Enter Figure 9.10 with V and determine δ/ϕ ratio for pile type.

For a precast, prestressed concrete pile with $V = 0.127 \text{ m}^3/\text{m}$

$$\delta/\phi = 0.84$$

- c. Calculate δ from δ/ϕ ratio.

Layer 1: $\delta_1 = 0.84 (36^\circ) = 30.2^\circ$

Layer 2: $\delta_2 = 0.84 (35^\circ) = 29.4^\circ$

STEP 3 Determine the coefficient of lateral earth pressure, K_δ , for each ϕ angle.

- a. Determine K_δ for ϕ angle based on displaced volume, V , and pile taper angle, ω , using either Figure 9.11, 9.12, 9.13, or 9.14 and the appropriate procedure described in Step 3b, 3c, 3d, or 3e.

The pile taper angle, ω , = 0° .

For Layer 1:

$\phi_1 = 36^\circ$ and $V = 0.127 \text{ m}^3/\text{m}$, therefore use Step 3e.

A step by step procedure for determining K_δ using the linear interpolation and the log linear interpolation is presented in Section F.2.1.2 - Step 3.

For $\phi_1 = 36^\circ$, $\omega = 0^\circ$, and $V = 0.127 \text{ m}^3/\text{m}$:

$$K_{\delta 1} = 2.10$$

For Layer 2:

$\phi_2 = 35^\circ$ and $V = 0.127 \text{ m}^3/\text{m}$, therefore use Step 3d.

A step by step procedure for determining K_δ using the log linear interpolation is presented in Section F.2.1.2 - Step 3.

For $\phi_2 = 35^\circ$, $\omega = 0^\circ$, and $V = 0.127 \text{ m}^3/\text{m}$:

$$K_{\delta 2} = 1.83$$

STEP 4 Determine the correction factor, C_F , to be applied to K_δ if $\delta \neq \phi$.

Use Figure 9.15 to determine the correction factor for each K_δ . Enter figure with ϕ angle and $\delta/\phi=0.84$ to determine C_F .

Layer 1: For $\phi_1 = 36^\circ \rightarrow C_{F1} = 0.92$

Layer 2: For $\phi_2 = 35^\circ \rightarrow C_{F2} = 0.93$

STEP 5 Compute the average effective overburden pressure at the midpoint of each soil layer, p_d (kPa). (Note: a limiting value is not applied to p_d)

The effective overburden pressure at the midpoint of each layer is equal to the average effective overburden pressure of that layer. The effective overburden pressure diagram for Pier 2 after scour is presented in Figure F.8. The purpose of this example is to illustrate how scour reduces the average effective overburden pressures, and hence the pile shaft and toe resistance.

Layer 1: $p_{d1} = 22.8$ kPa (midpoint of layer 1 - at depth of 7.0 m below existing ground surface)

Layer 2: $p_{d2} = 75.0$ kPa (midpoint of layer 2 - at depth of 12.0 m below existing ground surface)

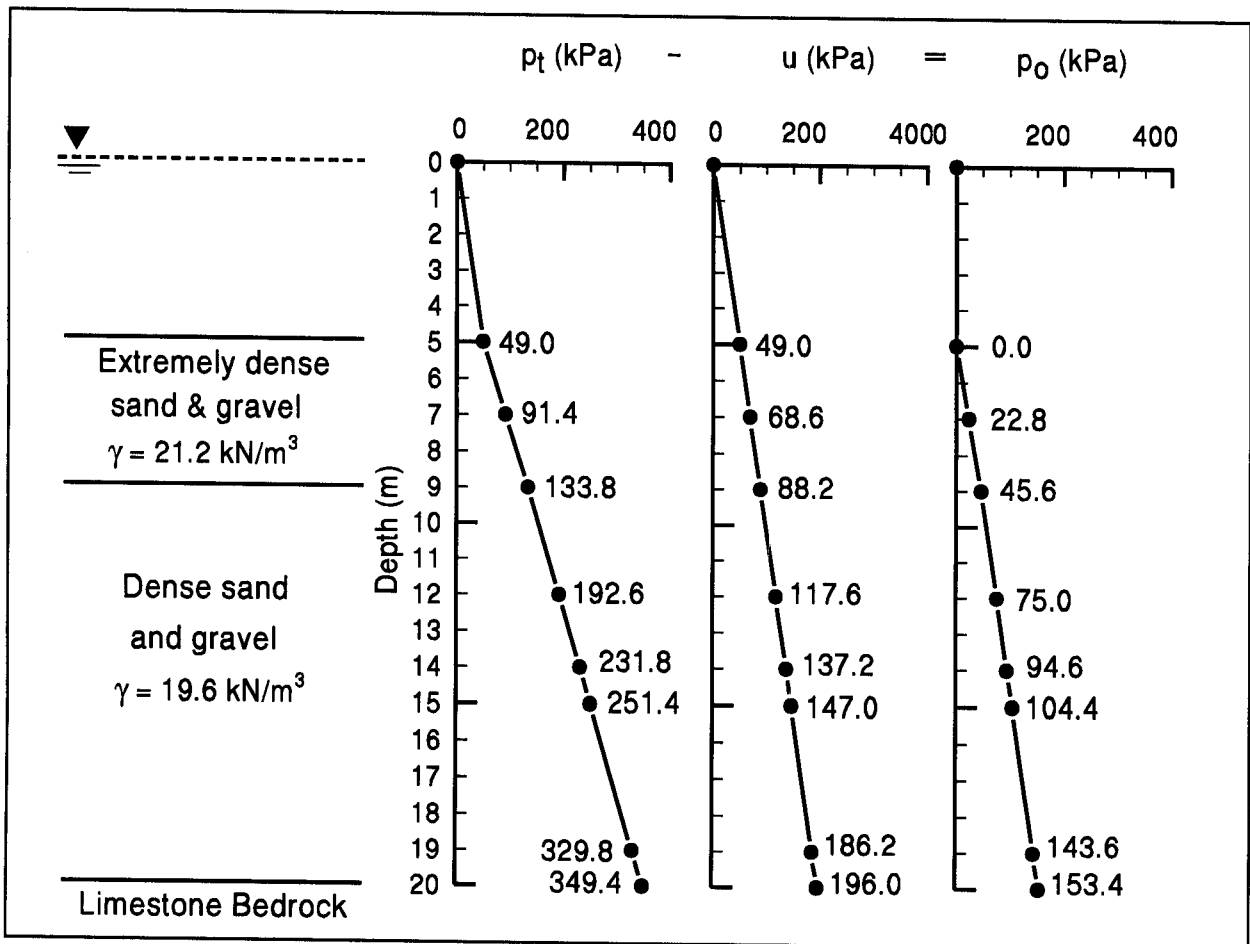


Figure F.8 Effective Overburden Pressure Diagram - Pier 2 after Scour

STEP 6 Compute the shaft resistance in each soil layer. Sum the shaft resistance from each soil layer to obtain the ultimate shaft resistance, R_s (kN).

$$R_s = K_\delta C_F p_d \sin\delta C_d D \quad (\text{for uniform pile cross section})$$

$$\text{where : } C_d = (4) (0.356 \text{ m}) = 1.424 \text{ m}$$

$$\begin{aligned} \text{Layer 1: } R_{s1} &= 2.10 (0.92) (22.8 \text{ kPa}) (\sin 30.2^\circ) (1.424 \text{ m}) (4 \text{ m}) \\ &= 126 \text{ kN} \end{aligned}$$

$$\begin{aligned} \text{Layer 2: } R_{s2} &= 1.83 (0.93) (75.0 \text{ kPa}) (\sin 29.4^\circ) (1.424 \text{ m}) (6 \text{ m}) \\ &= 535 \text{ kN} \end{aligned}$$

$$\begin{aligned} \text{Total: } R_s &= R_{s1} + R_{s2} = 126 \text{ kN} + 535 \text{ kN} \\ &= 661 \text{ kN} \Rightarrow \text{as compared to 984 kN before scour.} \end{aligned}$$

STEP 7 Determine the α_t coefficient and the bearing capacity factor, N'_q , from the ϕ angle near the pile toe.

As in Section F.2.2.2,

$$\bar{N}'_{toe} = 34 \quad \rightarrow \quad \phi_{toe} = 36^\circ$$

a. Enter Figure 9.16(a) with ϕ angle near pile toe to determine α_t coefficient based on pile length to diameter ratio.

$$(D/b) = (10.0 \text{ m}) / (0.356 \text{ m}) = 28.1$$

$$\text{For } \phi_{toe} = 36^\circ \text{ and } (D/b) = 28.1 \quad \rightarrow \quad \alpha_t = 0.69$$

b. Enter Figure 9.16(b) with ϕ angle near pile toe to determine N'_q .

$$\text{For } \phi_{toe} = 36^\circ \quad \rightarrow \quad N'_q = 75$$

STEP 8 Compute the effective overburden pressure at the pile toe, p_t (kPa).

The effective overburden pressure at the pile toe should be limited to a maximum of 150 kPa.

The effective overburden pressure at the pile toe, p_t , after scour has been computed and shown in Figure F.8:

$$p_t = 104.4 \text{ kPa} < 150 \text{ kPa} \rightarrow \text{OK}$$

STEP 9 Compute the ultimate toe resistance, R_t (kN).

a. $R_t = \alpha_t N'_q A_t p_t$

$$= 0.69 (75) (0.356 \text{ m})(0.356 \text{ m})(104.4 \text{ kPa})$$

$$= 686 \text{ kN}$$

b. limiting $R_t = q_L A_t$

Using the estimated $\phi=36^\circ$ and Figure 9.17, the limiting unit toe resistance is:

$$q_L = 7,400 \text{ kPa}$$

Therefore,

$$R_t = 7,400 \text{ kPa} (0.356 \text{ m})(0.356 \text{ m})$$

$$= 940 \text{ kN}$$

c. Use lesser of the two R_t values obtained in steps a and b which is:

$$R_t = 686 \text{ kN} \Rightarrow \text{as compared to } 854 \text{ kN before scour.}$$

STEP 10 Compute the ultimate pile capacity, Q_u (kN).

$$\begin{aligned} Q_u &= R_s + R_t \\ &= 661 \text{ kN} + 686 \text{ kN} \\ &= 1,347 \text{ kN} \Rightarrow \text{as compared to } 1,838 \text{ kN before scour.} \end{aligned}$$

Note: After scour has occurred, the factor of safety is only:

$$\text{Factor of Safety} = \frac{Q_u}{\text{Design Load}} = \frac{1,347 \text{ kN}}{890 \text{ kN}} = 1.51$$

F.2.2.4 Static Axial Pile Capacity Calculations by Nordlund Method (before scour at 14 m)

For the soil profile interpreted from Soil Boring S-2 as shown in Figure F.5. Perform a Nordlund method pile capacity calculation for an embedded length of 14 meters. Assume that scour has not occurred. Use the step-by-step method outlined in Section 9.7.1.1b.

- STEP 1 Delineate the soil profile into layers and determine the ϕ angle for each layer.
- Construct p_o diagram using procedure described in Section 9.4. This is completed in Figure F.6.
 - Correct SPT field N values for overburden pressure using Figure 4.4 from Chapter 4 and obtain corrected SPT N' values. For Soil Boring S-2, this has been done in a previous example (see Section F.2.2.1, Step 1).
 - Determine ϕ angle for each layer from laboratory tests or in-situ data.

Since the ϕ angle is not provided by either laboratory or in-situ data, it should be determined using the average corrected SPT N' value, \bar{N}' , as calculated below.

- In the absence of laboratory or in-situ test data, determine the average corrected SPT N' value, \bar{N}' , for each soil layer and estimate ϕ angle from Table 4-5 in Chapter 4.

The soil profile along the pile embedded length is delineated into two layers of 4, and 10 meters thick. The average corrected SPT N' value for each soil layer is as follow.

$$\bar{N}'_1 = 110 \quad \text{(Layer 1 - depth 5 to 9 m; Extremely dense sand and gravel)}$$

$$\bar{N}'_2 = \frac{34 + 36 + 31 + 31 + 34 + 30 + 32}{7} = 33$$

(Layer 2 - depth 9 to 19 m;
Dense sand and gravel)

STEP 1 (continued)

Use the average corrected SPT N' value for each soil layer to estimate ϕ angle from Table 4-5 in Chapter 4.

As discussed in Section F.2.2.2 - Step 1, a limiting friction angle should be used for the hard angular gravel of layer 1.

Layer 1: $\phi_1 = 36^\circ$ from limiting friction angle

For layer 2, the friction angle is computed from Table 4-5:

Layer 2: $\phi_2 = 35^\circ$ for $\bar{N}'_2 = 33$

STEP 2 Determine δ , the friction angle between pile and soil based on displaced soil volume, V , and the soil friction angle, ϕ .

- a. Compute volume of soil displaced per unit length of pile, V .
Since this is a uniform cross section ($\omega = 0^\circ$) pile,

$$V = (0.356 \text{ m})(0.356 \text{ m})(1.0 \text{ m/m}) = 0.127 \text{ m}^3/\text{m}$$

- b. Enter Figure 9.10 with V and determine δ/ϕ ratio for pile type.

For a precast, prestressed concrete pile with $V = 0.127 \text{ m}^3/\text{m}$

$$\delta/\phi = 0.84$$

- c. Calculate δ from δ/ϕ ratio.

Layer 1: $\delta_1 = 0.84 (36^\circ) = 30.2^\circ$

Layer 2: $\delta_2 = 0.84 (35^\circ) = 29.4^\circ$

STEP 3 Determine the coefficient of lateral earth pressure, K_δ , for each ϕ angle.

- a. Determine K_δ for ϕ angle based on displaced volume, V , and pile taper angle, ω , using either Figure 9.11, 9.12, 9.13, or 9.14 and the appropriate procedure described in Step 3b, 3c, 3d, or 3e.

The pile taper angle, ω , = 0° .

For Layer 1:

$\phi_1 = 36^\circ$ and $V = 0.127 \text{ m}^3/\text{m}$, therefore use Step 3e.

A step by step procedure for determining K_δ using the linear interpolation and the log linear interpolation is presented in Section F.2.1.2 - Step 3.

For $\phi_1 = 36^\circ$, $\omega = 0^\circ$, and $V = 0.127 \text{ m}^3/\text{m}$:

$$K_{\delta 1} = 2.10$$

For Layer 2:

$\phi_2 = 35^\circ$ and $V = 0.127 \text{ m}^3/\text{m}$, therefore use Step 3d.

A step by step procedure for determining K_δ using the log linear interpolation is presented in Section F.2.1.2 - Step 3.

For $\phi_2 = 35^\circ$, $\omega = 0^\circ$, and $V = 0.127 \text{ m}^3/\text{m}$:

$$K_{\delta 2} = 1.83$$

STEP 4 Determine the correction factor, C_F , to be applied to K_δ if $\delta \neq \phi$.

Use Figure 9.15 to determine the correction factor for each K_δ . Enter figure with ϕ angle and $\delta/\phi=0.84$ to determine C_F .

Layer 1: For $\phi_1 = 36^\circ \rightarrow C_{F1} = 0.92$

Layer 2: For $\phi_2 = 35^\circ \rightarrow C_{F2} = 0.93$

STEP 5 Compute the average effective overburden pressure at the midpoint of each soil layer, p_d (kPa). (Note: a limiting value is not applied to p_d).

The effective overburden pressure at the midpoint of each soil layer is equal to the average effective overburden pressure of that layer. The effective overburden pressure versus depth for the Pier 2 has been computed and tabulated in a previous example (see Section F.2.2.1 - Step 1). The effective overburden pressure diagram for Pier 2 is presented in Figure F.6.

$$\text{Layer 1: } p_{d1} = 48.3 \text{ kPa} \quad (\text{midpoint of layer 1 - at depth of 7.0 m})$$

$$\text{Layer 2: } p_{d2} = 120.1 \text{ kPa} \quad (\text{midpoint of layer 2 - at depth of 14.0 m})$$

STEP 6 Compute the shaft resistance in each soil layer. Sum the shaft resistance from each soil layer to obtain the ultimate shaft resistance, R_s (kN).

$$R_s = K_\delta C_F p_d \sin \delta C_d D \quad (\text{for uniform pile cross section})$$

$$\text{where : } C_d = (4) (0.355 \text{ m}) = 1.424 \text{ m}$$

$$\begin{aligned} \text{Layer 1: } R_{s1} &= 2.10 (0.92) (48.3 \text{ kPa}) (\sin 30.2^\circ) (1.424 \text{ m}) (4 \text{ m}) \\ &= 267 \text{ kN} \end{aligned}$$

$$\begin{aligned} \text{Layer 2: } R_{s2} &= 1.83 (0.93) (120.1 \text{ kPa}) (\sin 29.4^\circ) (1.424 \text{ m}) (10 \text{ m}) \\ &= 1,429 \text{ kN} \end{aligned}$$

$$\begin{aligned} \text{Total: } R_s &= 267 \text{ kN} + 1,429 \text{ kN} \\ &= 1,696 \text{ kN} \end{aligned}$$

STEP 7 Determine the α_t coefficient and the bearing capacity factor, N'_q , from the ϕ angle near the pile toe.

Since the ϕ angle is not provided by either laboratory tests or in-situ data, the ϕ angle can be estimated from Table 4-5 using the average corrected SPT N' value over the zone from the pile toe to 3 diameter below the pile toe (1.065 meters). The soil near the pile toe is a dense sand and gravel.

$$\bar{N}'_{\text{toe}} = 33 \quad \rightarrow \quad \phi_{\text{toe}} = 35^\circ$$

a. Enter Figure 9.16(a) with ϕ angle near pile toe to determine α_t coefficient based on pile length to diameter ratio.

$$(D/b) = (14.0 \text{ m}) / (0.356 \text{ m}) = 39.3$$

$$\text{For } \phi_{\text{toe}} = 35^\circ \text{ and } (D/b) = 39.3 \quad \rightarrow \quad \alpha_t = 0.66$$

b. Enter Figure 9.16(b) with ϕ angle near pile toe to determine N'_q .

$$\text{For } \phi_{\text{toe}} = 35^\circ \quad \rightarrow \quad N'_q = 65$$

STEP 8 Compute the effective overburden pressure at the pile toe, p_t (kPa).

The effective overburden pressure at the pile toe should be limited to a maximum of 150 kPa.

The effective overburden pressure at the pile toe, p_t , has been computed in the previous example (Section F.2.2.1, Step 1):

$$p_t = 169.1 \text{ kPa} > 150 \text{ kPa} \quad \rightarrow \quad \text{so use } p_t = 150 \text{ kPa}$$

STEP 9 Compute the ultimate toe resistance, R_t (kN).

$$\begin{aligned} \text{a. } R_t &= \alpha_t N'_q A_t p_t \\ &= 0.66 (65) (0.356 \text{ m})(0.356 \text{ m}) (150.0 \text{ kPa}) \\ &= 817 \text{ kN} \end{aligned}$$

$$\text{b. limiting } R_t = q_L A_t$$

Using the estimated $\phi=35^\circ$ and Figure 9.17, the limiting unit toe resistance is:

$$q_L = 5,000 \text{ kPa}$$

Therefore,

$$R_t = 5,000 \text{ kPa} (0.356 \text{ m})(0.356 \text{ m}) = 635 \text{ kN}$$

c. Use lesser of the two R_t values obtained in steps a and b which is:

$$R_t = 635 \text{ kN}$$

STEP 10 Compute the ultimate pile capacity, Q_u (kN).

$$\begin{aligned} Q_u &= R_s + R_t \\ &= 1,696 \text{ kN} + 635 \text{ kN} = 2,331 \text{ kN} \end{aligned}$$

STEP 11 Compute allowable design load, Q_a (kN).

$$Q_a = \frac{Q_u}{\text{Factor of Safety}} = \frac{2,331 \text{ kN}}{\text{Factor of Safety}}$$

Note: Factor of Safety should be selected based on the construction control method to be specified. Recommended factors of safety are described in Section 9.6.

F.2.2.5 Static Axial Pile Capacity Calculations by Nordlund Method (after scour at 14 m)

For the soil profile interpreted from Soil Boring S-2 after scour as shown in Figure F.7. Perform a Nordlund method pile capacity calculation for an embedded length of 14 meters. Assume that scour has removed the 5 meter thick loose silt layer. Use the step-by-step method outlined in Section 9.7.1.1b.

STEP 1 Delineate the soil profile into layers and determine the ϕ angle for each layer.

- a. Construct p_o diagram using procedure described in Section 9.4. This is completed in Figure F.6.
- b. Correct SPT field N values for overburden pressure using Figure 4.4 from Chapter 4 and obtain corrected SPT N' values. For Soil Boring S-2, this has been done in the previous example (see Chapter F.2.2.1 - Step 1).

Note: Although scour has eroded the 5 meter thick loose silt layer, the original overburden pressure (with the loose silt layer still in place) should be used when correcting the SPT field N values.

- c. Determine ϕ angle for each layer from laboratory tests or in-situ data.

Since the ϕ angle is not provided by either laboratory or in-situ data, it should be determined using the average corrected SPT N' value, \bar{N}' , as calculated below.

- d. In the absence of laboratory or in-situ test data, determine the average corrected SPT N' value, \bar{N}' , for each soil layer and estimate ϕ angle from Table 4-5 in Chapter 4.

The soil profile along the pile embedded length is delineated into two layers of 4, and 10 meters thick. The average corrected SPT N' value for each soil layer is as follow.

$$\bar{N}'_1 = 110$$

(Layer 1 - depth 5 to 9 m;
Extremely dense sand and gravel)

STEP 1 (continued)

$$\bar{N}'_2 = \frac{34 + 36 + 31 + 31 + 34 + 30 + 32}{7} = 33$$

(Layer 2 - depth 9 to 19 m;
Dense sand and gravel)

Use the average corrected SPT N' value for each soil layer to estimate ϕ angle from Table 4-5 in Chapter 4.

As discussed in Section F.2.2.2 - Step 1, a limiting friction angle should be used for the hard angular gravel of layer 1.

Layer 1: $\phi_1 = 36^\circ$ from limiting friction angle

For layer 2, the friction angle is computed from Table 4-5:

Layer 2: $\phi_2 = 35^\circ$ for $\bar{N}'_2 = 33$

STEP 2 Determine δ , the friction angle between pile and soil based on displaced soil volume, V , and the soil friction angle, ϕ .

- a. Compute volume of soil displaced per unit length of pile, V .
Since this is a uniform cross section ($\omega = 0^\circ$) pile,

$$V = (0.356 \text{ m})(0.356 \text{ m})(1.0 \text{ m/m}) = 0.127 \text{ m}^3/\text{m}$$

- b. Enter Figure 9.10 with V and determine δ/ϕ ratio for pile type.

For a precast, prestressed concrete pile with $V = 0.127 \text{ m}^3/\text{m}$

$$\delta/\phi = 0.84$$

- c. Calculate δ from δ/ϕ ratio.

$$\text{Layer 1: } \delta_1 = 0.84 (36^\circ) = 30.2^\circ$$

$$\text{Layer 2: } \delta_2 = 0.84 (35^\circ) = 29.4^\circ$$

STEP 3 Determine the coefficient of lateral earth pressure, K_δ , for each ϕ angle.

- a. Determine K_δ for ϕ angle based on displaced volume, V , and pile taper angle, ω , using either Figure 9.11, 9.12, 9.13, or 9.14 and the appropriate procedure described in Step 3b, 3c, 3d, or 3e.

The pile taper angle, ω , = 0° .

For Layer 1:

$$\phi_1 = 36^\circ \quad \text{and} \quad V = 0.127 \text{ m}^3/\text{m}, \text{ therefore use Step 3e.}$$

A step by step procedure for determining K_δ using the linear interpolation and the log linear interpolation is presented in Section F.2.1.2 - Step 3.

For $\phi_1 = 36^\circ$, $\omega = 0^\circ$, and $V = 0.127 \text{ m}^3/\text{m}$:

$$K_{\delta 1} = 2.10$$

For Layer 2:

$$\phi_2 = 35^\circ \quad \text{and} \quad V = 0.127 \text{ m}^3/\text{m}, \text{ therefore use Step 3d.}$$

A step by step procedure for determining K_δ using the log linear interpolation is presented in Section F.2.1.2 - Step 3.

For $\phi_2 = 35^\circ$, $\omega = 0^\circ$, and $V = 0.127 \text{ m}^3/\text{m}$:

$$K_{\delta 2} = 1.83$$

STEP 4 Determine the correction factor, C_F , to be applied to K_δ if $\delta \neq \phi$.

Use Figure 9.15 to determine the correction factor for each K_δ . Enter figure with ϕ angle and $\delta/\phi=0.84$ to determine C_F .

$$\text{Layer 1:} \quad \text{For } \phi_1 = 36^\circ \quad \rightarrow \quad C_{F1} = 0.92$$

$$\text{Layer 2:} \quad \text{For } \phi_2 = 35^\circ \quad \rightarrow \quad C_{F2} = 0.93$$

STEP 5 Compute the average effective overburden pressure at the midpoint of each soil layer, p_d (kPa). (Note: a limiting value is not applied to p_d).

The effective overburden pressure at the midpoint of each soil layer is equal to the average effective overburden pressure of that layer. The effective overburden pressure diagram for Pier 2 after scour is presented in Figure F.8.

$$\text{Layer 1: } p_{d1} = 22.8 \text{ kPa} \quad (\text{midpoint of layer 1 - at depth of 7.0 m})$$

$$\text{Layer 2: } p_{d2} = 94.6 \text{ kPa} \quad (\text{midpoint of layer 2 - at depth of 14.0 m})$$

STEP 6 Compute the shaft resistance in each soil layer. Sum the shaft resistance from each soil layer to obtain the ultimate shaft resistance, R_s (kN).

$$R_s = K_\delta C_F p_d \sin \delta C_d D \quad (\text{for uniform pile cross section})$$

$$\text{where : } C_d = (4) (0.356 \text{ m}) = 1.424 \text{ m}$$

$$\begin{aligned} \text{Layer 1: } R_{s1} &= 2.10 (0.92) (22.8 \text{ kPa}) (\sin 30.2^\circ) (1.424 \text{ m}) (4 \text{ m}) \\ &= 126 \text{ kN} \end{aligned}$$

$$\begin{aligned} \text{Layer 2: } R_{s2} &= 1.83 (0.93) (94.6 \text{ kPa}) (\sin 29.4^\circ) (1.424 \text{ m}) (10 \text{ m}) \\ &= 1,126 \text{ kN} \end{aligned}$$

$$\begin{aligned} \text{Total: } R_s &= R_{s1} + R_{s2} \\ &= 126 \text{ kN} + 1,126 \text{ kN} \\ &= 1,252 \text{ kN} \end{aligned}$$

STEP 7 Determine the α_t coefficient and the bearing capacity factor, N'_q , from the ϕ angle near the pile toe.

Since the ϕ angle is not provided by either laboratory tests or in-situ data, the ϕ angle can be estimated from Table 4-5 using the average corrected SPT N' value over the zone from the pile toe to 3 diameter below the pile toe (1.065 meters). The soil near the pile toe is a dense sand and gravel.

$$\bar{N}'_{\text{toe}} = 33 \quad \rightarrow \quad \phi_{\text{toe}} = 35^\circ$$

a. Enter Figure 9.16(a) with ϕ angle near pile toe to determine α_t coefficient based on pile length to diameter ratio.

$$\begin{aligned} (D/b) &= (14.0 \text{ m}) / (0.356 \text{ m}) \\ &= 39.3 \end{aligned}$$

$$\text{For } \phi_{\text{toe}} = 35^\circ \text{ and } (D/b) = 39.3 \quad \rightarrow \quad \alpha_t = 0.66$$

b. Enter Figure 9.16(b) with ϕ angle near pile toe to determine N'_q .

$$\text{For } \phi_{\text{toe}} = 35^\circ \quad \rightarrow \quad N'_q = 65$$

STEP 8 Compute the effective overburden pressure at the pile toe, p_t (kPa).

The effective overburden pressure at the pile toe should be limited to a maximum of 150 kPa.

The effective overburden pressure at the pile toe, p_t , after scour has been computed and shown in Figure F.8:

$$p_t = 143.6 \text{ kPa} < 150 \text{ kPa} \quad \rightarrow \quad \text{OK}$$

STEP 9 Compute the ultimate toe resistance, R_t (kN).

$$\begin{aligned} \text{a. } R_t &= \alpha_t N'_q A_t p_t \\ &= 0.66 (65) (0.356 \text{ m})(0.356 \text{ m}) (143.6 \text{ kPa}) \\ &= 782 \text{ kN} \end{aligned}$$

$$\text{b. limiting } R_t = q_L A_t$$

Use the estimated $\phi=35^\circ$ and Figure 9.17, the limiting unit toe resistance is:

$$\begin{aligned} q_L &= 5,000 \text{ kPa} \\ R_t &= 5,000 \text{ kPa} (0.356 \text{ m})(0.356 \text{ m}) \\ &= 635 \text{ kN} \end{aligned}$$

c. Use lesser of the two R_t values obtained in steps a and b which is:

$$R_t = 635 \text{ kN}$$

STEP 10 Compute the ultimate pile capacity, Q_u (kN).

$$\begin{aligned} Q_u &= R_s + R_t \\ &= 1,252 \text{ kN} + 635 \text{ kN} = 1,887 \text{ kN} \end{aligned}$$

STEP 11 Compute allowable design load, Q_a .

$$Q_a = \frac{Q_u}{\text{Factor of Safety}} = \frac{1,887 \text{ kN}}{\text{Factor of Safety}}$$

Note: Factor of Safety should be selected based on the construction control method to be specified. Recommended factors of safety are described in Section 9.6.

F.2.2.6 Static Axial Pile Capacity Calculations by Effective Stress Method (before scour)

For the soil profile interpreted from Soil Boring S-2 as shown in Figure F.5. Perform an Effective Stress method pile capacity calculation for an embedded length of 10 meters. Assuming that scour has not occurred. Use the step-by-step method outlined in Section 9.7.1.3.

STEP 1 Delineate the soil profile into layers and determine ϕ' angle for each layer.

- a. Use the procedure described in Section 9.4 to construct a p_o diagram.

For Soil Boring S-2, the p_o diagram has been constructed in Section F.2.2.1 - Step 1 and also presented in Figure F.6.

- b. Divide the soil profile throughout the pile penetration depth into layers and determine the effective overburden pressure, p_o , at the midpoint of each layer.

As for the example in Section F.2.2.1, the soil profile along the pile embedded length is delineated into two layers of 4 and 6 meters thick. The average effective overburden pressure of each layer is equal to the effective overburden pressure at the midpoint of that layer as follows.

$$\text{Layer 1: } p_{o1} = 48.3 \text{ kPa} \quad (\text{midpoint of layer 1 - at depth of 7.0 m})$$

$$\text{Layer 2: } p_{o2} = 100.5 \text{ kPa} \quad (\text{midpoint of layer 2 - at depth of 12.0 m})$$

- c. Determine the ϕ' angle for each soil layer from laboratory or in-situ test data.

Since the ϕ' angle is not provided by either laboratory or in-situ test data, the average corrected SPT N' value will be used to estimate the ϕ' angle.

- d. In the absence of laboratory or in-situ test data for cohesionless soil layers, determine the average corrected SPT N' value for each soil layer and estimate the ϕ' angle from Table 4-5 in Chapter 4.

STEP 1 (continued)

As in the previous example (Section F.2.2.1), the average corrected SPT N' value and the soil type for each soil layer are as follows.

Layer 1: $\bar{N}'_1 = 110$ (Layer 1 - depth 5 to 9 m;
Extremely dense sand and gravel)

Layer 2: $\bar{N}'_2 = 33$ (Layer 2 - depth 9 to 15 m;
Dense sand and gravel)

Use the average corrected SPT N' value for each soil layer to estimate ϕ' angle from Table 4-5 in Chapter 4.

Layer 1: $\phi'_1 = 36^\circ$ (From limiting friction angle; see discussion in
Section F.2.2.2 - Step 1)

Layer 2: $\phi'_2 = 35^\circ$ for $\bar{N}'_2 = 33$

STEP 2 Select the β coefficient for each soil layer.

- a. Use local experience to select β coefficient for each layer.

Assume no local experience.

- b. In the absence of local experience, use Table 9-4 or Figure 9.20 to estimate β coefficient from ϕ' angle for each layer.

Use the soil type, the estimated ϕ' angle, and Table 9-4 or Figure 9-20 to estimate the β coefficient for each layer.

Layer 1: $\beta_1 = 0.42$ (For extremely dense sand and gravel with
 $\phi'_1 = 36^\circ$)

Layer 2: $\beta_2 = 0.39$ (For dense sand and gravel with $\phi'_2 = 35^\circ$)

STEP 3 For each soil layer compute the unit shaft resistance, f_s (kPa).

$$f_s = \beta p_o$$

$$\text{Layer 1: } f_{s1} = 0.42 (48.3 \text{ kPa}) = 20.29 \text{ kPa}$$

$$\text{Layer 2: } f_{s2} = 0.39 (100.5 \text{ kPa}) = 39.20 \text{ kPa}$$

STEP 4 Compute the shaft resistance in each soil layer and the ultimate shaft resistance, R_s (kN) from the sum of the shaft resistance from each soil layer.

$$R_s = f_s A_s$$

where A_s = Pile-soil surface area from pile perimeter and length

$$\begin{aligned} \text{Layer 1: } R_{s1} &= 20.29 (4) (0.356 \text{ m}) (4 \text{ m}) \\ &= 116 \text{ kN} \end{aligned}$$

$$\begin{aligned} \text{Layer 2: } R_{s2} &= 39.20 (4) (0.356 \text{ m}) (6 \text{ m}) \\ &= 335 \text{ kN} \end{aligned}$$

$$\begin{aligned} \text{Total: } R_s &= R_{s1} + R_{s2} \\ &= 116 \text{ kN} + 335 \text{ kN} \\ &= 451 \text{ kN} \end{aligned}$$

STEP 5 Compute the unit toe resistance, q_t (kPa).

$$q_t = N_t p_t$$

a. Use local experience to select N_t coefficient.

Assume no local experience.

STEP 5 (continued)

- b. In the absence of local experience, estimate N_t coefficient from Table 9-4 or Figure 9.21 based on ϕ' angle.

Table 9-4 or Figure 9.21 are a function of soil type and the ϕ' angle. The soil type for each layer can be obtained from the soil boring. The ϕ' angle for each layer can be obtained from laboratory tests or in-situ data. In the absence of either laboratory or in-situ test data, the ϕ' angle should be estimated from Table 4-5 in Chapter 4 using the average corrected SPT N' value, \bar{N}' , over the zone from the pile toe to 3 diameter below the pile toe (1.065 meters). The soil near the pile toe is a dense sand and gravel.

$$\bar{N}'_{\text{toe}} = 34 \quad \rightarrow \quad \phi'_{\text{toe}} = 36^\circ$$

Use the soil type, the estimated ϕ' angle, and Table 9-4 or Figure 9-21 to estimate the N_t coefficient.

$$N_t = 70 \quad (\text{For dense sand and gravel with } \phi'_{\text{toe}} = 36^\circ)$$

- c. Calculate the effective overburden pressure at the pile toe, p_t .

The effective overburden pressure at the pile toe, p_t , has been computed in the previous example (Section F.2.2.1, Step 1):

$$p_t = 129.9 \text{ kPa}$$

The unit toe resistance, q_t is:

$$\begin{aligned} q_t &= N_t p_t \\ &= 70 (129.9 \text{ kPa}) \\ &= 9,093 \text{ kPa} \end{aligned}$$

STEP 6 Compute the ultimate toe resistance, R_t (kN).

$$\begin{aligned} R_t &= q_t A_t \\ &= 9,093 (0.356 \text{ m}) (0.356 \text{ m}) \\ &= 1,155 \text{ kN} \end{aligned}$$

STEP 7 Compute the ultimate pile capacity, Q_u (kN).

$$\begin{aligned} Q_u &= R_s + R_t \\ &= 451 \text{ kN} + 1,155 \text{ kN} \\ &= 1,606 \text{ kN} \end{aligned}$$

Note: The ultimate capacity according to the Effective Stress method is less than the required 1780 kN ultimate capacity. The Effective Stress method would require a pile penetration depth of 12.5 meters for a 1780 kN capacity.

STEP 8 Compute the allowable design load, Q_a (kN).

$$Q_a = \frac{Q_u}{\text{Factor of Safety}} = \frac{1,606 \text{ kN}}{\text{Factor of Safety}}$$

Note: Factor of Safety should be selected based on the construction control method to be specified. Recommended factors of safety are described in Section 9.6.

F.2.2.7 Static Axial Pile Capacity Calculations by SPILE Computer Program (before scour)

ULTIMATE STATIC PILE CAPACITY/Federal Highway Administration Nordlund (1963, 1979) and Tomlinson (1979, 1980) methods						
Project Name	:	BORING S-2		Client	:	FHWA Manual
File Name	:	S2		Project Manager	:	
Date	:	6/14/95		Computed by	:	GT
Depth of Top of Pile	=	16.39 ft.		Pile length	=	32.81 ft.
Depth to Water Table	=	0.00 ft.				
Width of pile	=	0.00 in.				
Type of Pile	=	Precast Concrete Pile				
SKIN FRICTION CONTRIBUTION						
Layer	Soil Type	Thickness (ft)	Effective Stress (psf)	Internal Friction Angle	N-SPT	Pile Perimeter (ft)
1	Cohesionless	0.01	534.48	30.92*	13.06*	4.67
2	Cohesionless	13.13	1011.26	36.00	--	4.67
3	Cohesionless	19.67	2103.55	35.00	--	4.67
Layer	Soil Type	Undrained Shear Strength (psf)	Adhesion	Pile Taper	Sliding Friction Angle	Skin Resistance (Kips)
1	Cohesionless	--	-----	----	26.03	0.01
2	Cohesionless	--	-----	----	30.30	60.96
3	Cohesionless	--	-----	----	29.46	162.14
Total Side Friction :						223.11
POINT RESISTANCE CONTRIBUTION						
Effective Stress at pile Tip (psf)	Internal Friction Angle (ft*ft)	SPT Value	Pile End Area	Bearing Capacity Factor Nq	End Bearing Resistance (Kips)	
2719.22	37.24*	34.13	1.36	94.44	248.54	
Limiting End Bearing Resistance :						299.21
Ultimate Static Pile Capacity :						471.65

In SI Units:	Total Side Friction	:	992	kN
	End Bearing Resistance	:	1,106	kN
	Ultimate Static Pile Capacity	:	2,098	kN

F.2.2.8 Summary of Pier 2 Capacity Calculation Results

Summary of Pile Capacity Estimates with an Embedded Pile Length of 10.0 meters

Method Used for Estimation of Pile Capacity	Calculated Pile Shaft Resistance (kN)	Calculated Pile Toe Resistance (kN)	Calculated Ultimate Pile Capacity (kN)
Meyerhof Method - SPT Data	1,134	1,676	2,810
Nordlund Method - SPT Data	984	854	1,838
Effective Stress Method	451	1,155	1,606
SPILE Program - SPT Data	992	1,106	2,098

Summary of Pile Length Estimates for the 1,780 kN Ultimate Pile Capacity

Method Used for Estimation of Pile Capacity	Calculated Pile Length for the 1,780 kN Ultimate Pile Capacity
Meyerhof Method - SPT Data	1.0 meters for 2,136 kN
Nordlund Method - SPT Data	10.0 meters for 1,838 kN
Effective Stress Method	12.5 meters for 1,847 kN
SPILE Program - SPT Data	10.0 meters for 2,098 kN

Note: All analyses do not consider scour effects on ultimate capacity.

Summary of Pile Capacity Estimates Before and After Channel Degradation Scour
Based on Nordlund Method

Pile Embedment	Ultimate Pile Capacity	
	Before Scour	After Scour
10 meters	1,838 kN	1,347 kN
14 meters	2,331 kN	1,887 kN

Similar to the North Abutment, the ultimate pile group capacity at Pier 2, may also be taken as the sum of the ultimate capacities of the individual piles in the group. The design recommendation for estimating group capacity in cohesionless soil, presented in Section 9.8.1.1, should be referred to for detail considerations.

F.2.3 Pier 3 - Soil Boring S-3 (Cohesive and Cohesionless Soil)

F.2.3.1 Static Axial Pile Capacity Calculations by Nordlund and α -Method

For the soil profile interpreted from Soil Boring S-3 as shown in Figure F.9. Perform a static pile capacity calculation using the Nordlund and α methods for an embedded length of 13 meters. Use the Nordlund method for the cohesionless soil layer and α -Method for the cohesive soil layer. Use the appropriate portions of the step-by-step methods outlined in Section 9.7.1.1b and 9.7.1.2a.

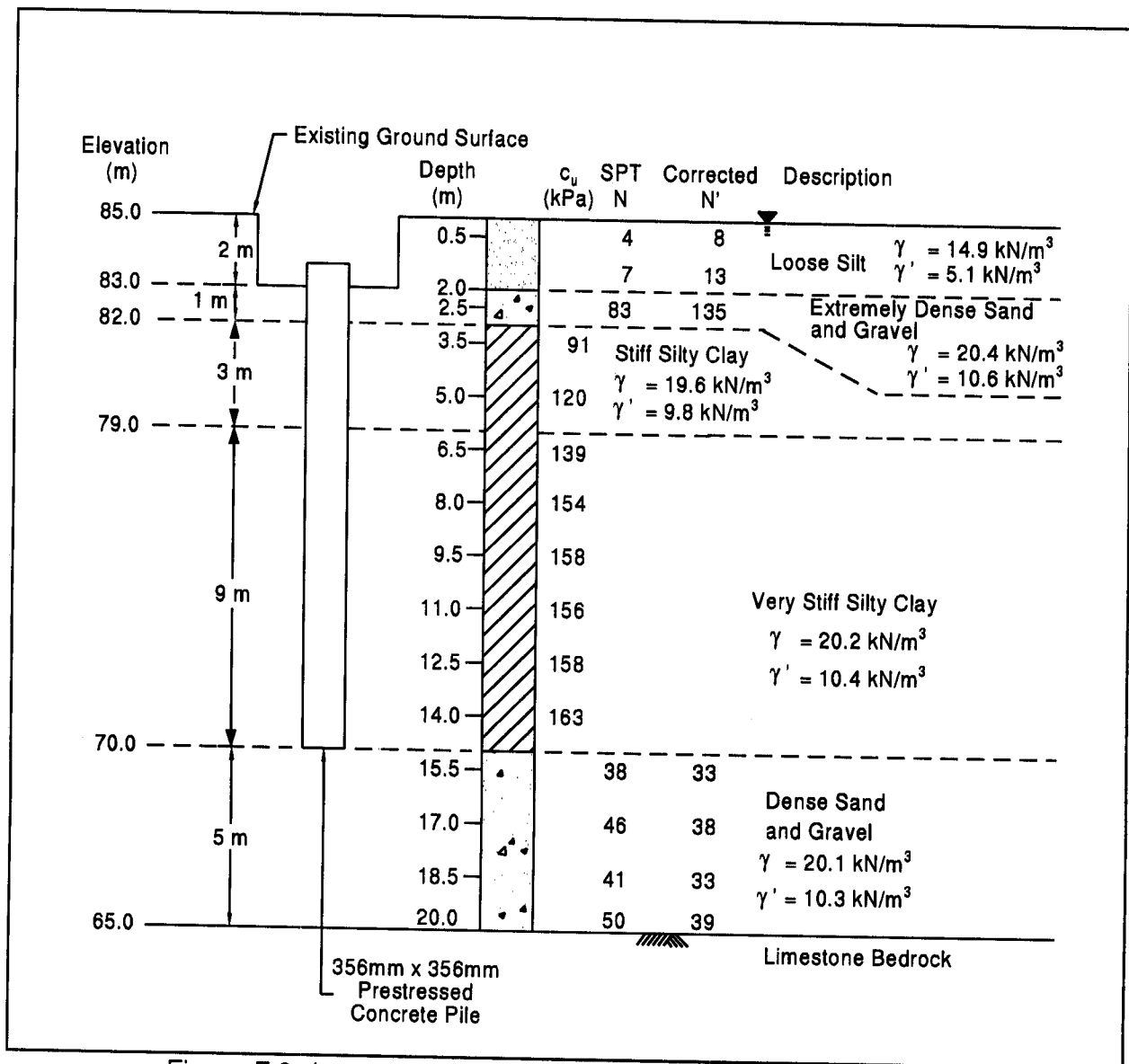


Figure F.9 Interpreted Soil Profile from Soil Boring S-3 at Pier 3

STEP 1 Delineate the soil profile into layers. Determine the ϕ angle for the cohesionless layer, and the undrained shear strength, c_u , for the cohesive layer.

a. Construct p_o diagram using procedure described in Section 9.4.

Effective overburden pressures, p_o , are needed to correct SPT field N values. The method for calculating the effective overburden pressure is explained in Section 9.4. A working example is presented in Section F.2.1.1. The effective overburden pressure diagram and soil layers are presented in Figure F.10.

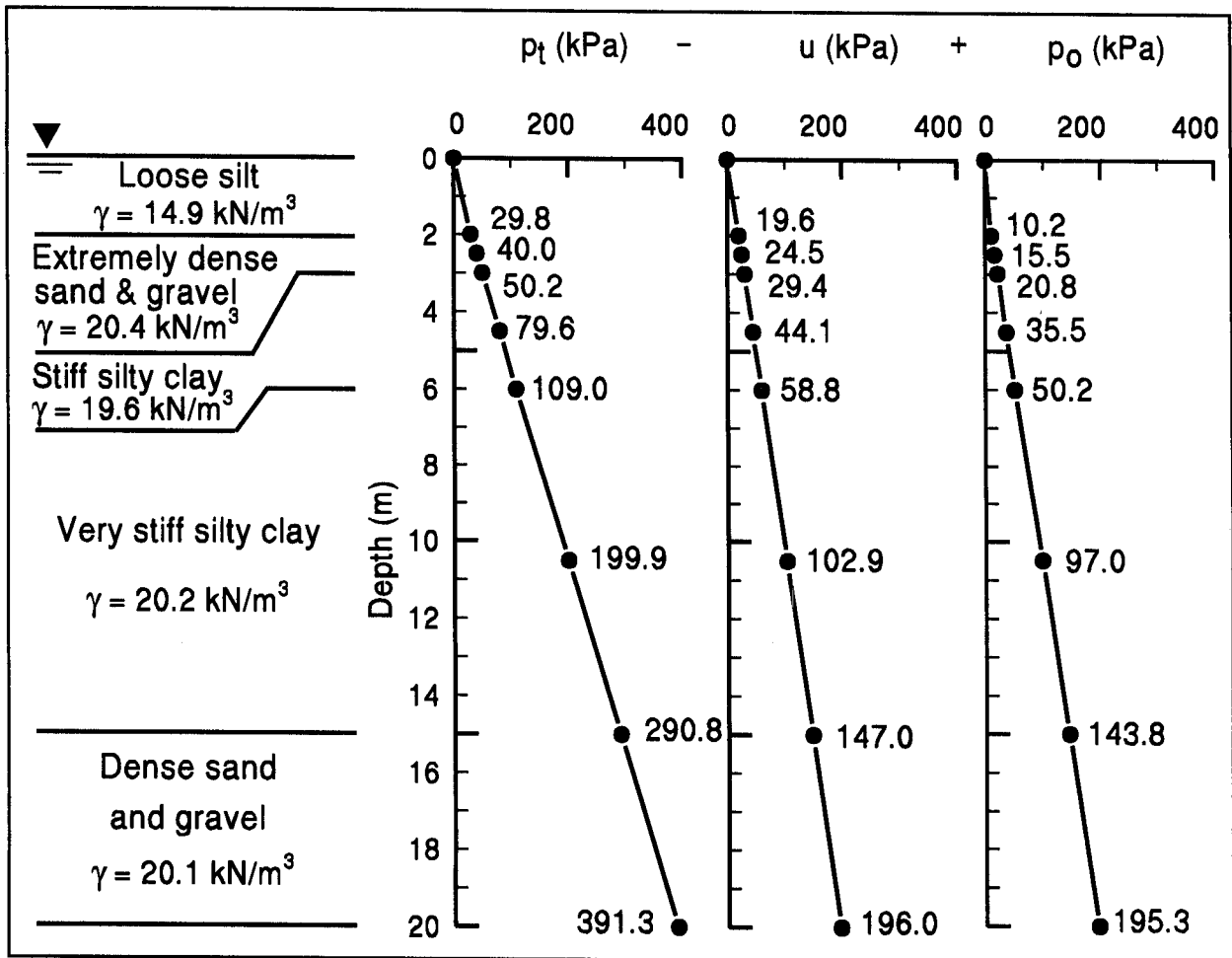


Figure F.10 Effective Overburden Pressure Diagram - Pier 3

STEP 1 (continued)

- b. Correct SPT field N values for overburden pressure using Figure 4.4 from Chapter 4 and obtain corrected SPT N' values.

Depth (m)	p_o (kPa)	Field SPT N value	Correction Factor	Corrected SPT N' (Field SPT N x Correction Factor)
2.0	10.2	7	1.80	13
2.5	15.5	83	1.63	135
15.5	149.0	38	0.87	33
17.0	164.6	46	0.83	38
18.5	180.2	41	0.80	33
20.0	195.3	50	0.77	39

Along the pile embedded length, the soil profile is delineated into three layers. Layer 1 is extremely dense sand and gravel that is 1.0 meter thick (cohesionless), layer 2 is stiff silty clay that is 3.0 meters thick (cohesive), and layer 3 is very stiff silty clay that is 9.0 meters thick (cohesive).

For the cohesionless soil layer, determine the average corrected SPT N' value, \bar{N}' , for the layer and estimate the ϕ angle from Table 4-5 in Chapter 4.

Layer 1: $\bar{N}'_1 = 135$ (Layer 1 - depth 2 to 3 m;
Extremely dense sand and Gravel)

For $N' > 50$, the ϕ angle computed by Table 4-5 can be as high as 43°. However, a limiting friction angle (as discussed in Section F.2.2.2 - Step 1) will govern for soil layer 1 since this layer contains hard angular gravel.

Layer 1: $\phi_1 = 36^\circ$ from limiting friction angle

STEP 1 (continued)

For the cohesive soil layer, determine the average undrained shear strength, c_u , for each soil layer.

$$\text{Layer 2: } c_{u2} = \frac{91 + 120}{2} = 106 \text{ kPa} \quad (\text{Layer 2 - depth 3 to 6 m; Stiff silty clay})$$

$$\text{Layer 3: } c_{u3} = \frac{139 + 154 + 158 + 156 + 158 + 163}{6} = 155 \text{ kPa}$$

(Layer 3 - depth 6 to 15 m;
Very stiff silty clay)

STEP 2 Compute the shaft resistance at soil layer 1 (cohesionless) using Nordlund method.

a. (Nordlund - Step 2): Determine δ , the friction angle between pile and soil based on displaced soil volume, V , and the soil friction angle, ϕ .

(i) Compute volume of soil displaced per unit length of pile, V .

Since this is a uniform cross section ($\omega = 0^\circ$) pile,

$$V = (0.356 \text{ m})(0.356 \text{ m})(1.0 \text{ m/m}) = 0.127 \text{ m}^3/\text{m}$$

(ii) Enter Figure 9.10 with V and determine δ/ϕ ratio for pile type.

For a precast, prestressed concrete pile with $V = 0.127 \text{ m}^3/\text{m}$,

$$\delta/\phi = 0.84$$

(iii) Calculate δ from δ/ϕ ratio.

$$\text{Layer 1: } \delta_1 = 0.84 (36^\circ) = 30.2^\circ$$

STEP 2 (continued)

- b. (Nordlund - Step 3): Determine the coefficient of lateral earth pressure, K_δ , for each ϕ angle.

- (i) Determine K_δ for ϕ angle based on displaced volume, V , and pile taper angle, ω , using either Figure 9.11, 9.12, 9.13, or 9.14 and the appropriate procedure described in Step 3b, 3c, 3d, or 3e.

For $\phi_1 = 36^\circ$ and $V = 0.127 \text{ m}^3/\text{m}$, therefore use Step 3e.

A step by step procedure for determining K_δ using the linear interpolation and the log linear interpolation is presented in Section F.2.1.2 - Step 3.

For $\phi_1 = 36^\circ$, $\omega = 0^\circ$, and $V = 0.127 \text{ m}^3/\text{m}$:

$$K_{\delta 1} = 2.10$$

- c. (Nordlund - Step 4): Determine the correction factor, C_F , to be applied to K_δ if $\delta \neq \phi$.

Use Figure 9.15 to determine the correction factor for each K_δ . Enter figure with ϕ angle and $\delta/\phi=0.84$ to determine C_F .

Layer 1: For $\phi_1 = 36^\circ \rightarrow C_{F1} = 0.92$

- d. (Nordlund - Step 5): Compute the average effective overburden pressure at the midpoint of each soil layer, p_d (kPa). (Note: a limiting value is not applied to p_d).

The effective overburden pressure at the midpoint of the soil layer is equal to the average effective overburden pressure of that layer. The effective overburden pressure diagram for Pier 3 is presented in Figure F.10.

Layer 1: $p_{d1} = 15.5 \text{ kPa}$ (midpoint of layer 1 - at depth of 2.5 m)

STEP 2 (continued)

e. (Nordlund - Step 6): Compute the shaft resistance in soil layer 1.

$$R_s = K_\delta C_F p_d \sin \delta C_d D \quad (\text{for uniform pile cross section})$$

$$\text{where : } C_d = (4) (0.356 \text{ m}) = 1.424 \text{ m}$$

$$\begin{aligned} \text{Layer 1: } R_{s1} &= 2.10 (0.92) (15.5 \text{ kPa}) (\sin 30.2^\circ) (1.424 \text{ m}) (1 \text{ m}) \\ &= 22 \text{ kN} \end{aligned}$$

STEP 3 Compute the shaft resistance at soil layers 2 and 3 (cohesive) using α -method.

a. (α -Method - Steps 1 and 2): Determine the adhesion, c_a , from Figure 9.18 or adhesion factor, α , from Figure 9.19 for the cohesive soil layer.

An extremely dense sand and gravel overlying stiff silty clay of soil layer 2 agrees with the soil stratigraphy shown in Figure 9.19a. The depth to pile diameter ratio is:

$$(D/b) = (3.0 \text{ m}) / (0.356 \text{ m}) = 8.43$$

For $c_{u2} = 106 \text{ kPa}$ and $(D/b) = 8.43$, the adhesion factor interpolated from Figure 9.19a is:

$$\alpha = 1.0$$

The adhesion is:

$$\begin{aligned} c_{a2} &= \alpha c_{u2} \\ &= 1.0 (106 \text{ kPa}) = 106 \text{ kPa} \end{aligned}$$

Therefore, the unit shaft resistance of soil layer 2 is :

$$\text{Layer 2: } f_{s2} = c_{a2} = 106 \text{ kPa}$$

STEP 3 (continued)

For soil layer 3, Figure 9.19 and 9.18 should be used to compute the adhesion of the very stiff silty clay. Depending on the thickness of the extremely dense sand and gravel of soil layer 1 and the thickness of the stiff silty clay of soil layer 2, the soil stratigraphy for soil layer 3 may also agree with that of Figure 9.19a. However, it is reasonable to assume here that the pile would not be able to drag the sand and gravel far enough from soil layer 1 through the stiff silty clay of soil layer 2 to reach soil layer 3. Therefore, soil layer 3 should not be affected by the sand and gravel from soil layer 1 and hence, the adhesion should be determined from Figure 9.19c or 9.18. The depth, D , to pile diameter, b , ratio is:

$$(D/b) = (9.0 \text{ m}) / (0.356 \text{ m}) = 25.28$$

Interpolating the adhesion factor from Figure 9.19c, for $c_{u3} = 155 \text{ kPa}$ and $(D/b) = 25.28$:

$$\alpha = 0.35$$

The adhesion is therefore:

$$\begin{aligned} c_{a3} &= \alpha c_{u3} \\ &= 0.35 (155 \text{ kPa}) \\ &= 54.3 \text{ kPa} \end{aligned}$$

For comparison, using Figure 9.18 for concrete pile with $(D/b) = 25.35$ and $c_{u3} = 155 \text{ kPa}$, the adhesion obtained from the interpolation between curves is:

$$c_{a3} = 54.7 \text{ kPa} \rightarrow \text{similar to Figure 9.19c.}$$

Therefore,

$$\text{Layer 3: } f_{s3} = c_{a3} = 54.3 \text{ kPa}$$

STEP 3 (continued)

- b. (α -Method - Step 3): Compute the ultimate shaft resistance in soil layer 2 and soil layer 3.

$$\begin{aligned}\text{Layer 2: } R_{s2} &= f_{s2} A_s \\ &= 106.0 \text{ kPa } (4)(0.356 \text{ m})(3 \text{ m}) = 453 \text{ kN}\end{aligned}$$

$$\begin{aligned}\text{Layer 3: } R_{s3} &= f_{s3} A_s \\ &= 54.3 \text{ kPa } (4)(0.356 \text{ m})(9 \text{ m}) = 696 \text{ kN}\end{aligned}$$

- STEP 4 Sum the shaft resistance from each soil layer to obtain the ultimate shaft resistance, R_s (kN).

$$\begin{aligned}\text{Total: } R_s &= R_{s1} + R_{s2} + R_{s3} \\ &= 22 \text{ kN} + 453 \text{ kN} + 696 \text{ kN} = 1,171 \text{ kN}\end{aligned}$$

- STEP 5 Compute the ultimate toe resistance using Nordlund method.

Use Nordlund method, since the soil at pile toe is dense sand and gravel (cohesionless).

- (i) (Nordlund - Step 7): Determine the α_t coefficient and the bearing capacity factor, N'_q , from the ϕ angle near the pile toe.

Since the ϕ angle is not provided by either laboratory tests or in-situ data, it can be estimated from Table 4-5 using the average corrected SPT N' value over the zone from the pile toe to 3 diameter below the pile toe (1.065 meters).

$$\bar{N}'_{\text{toe}} = 33 \quad \rightarrow \quad \phi_{\text{toe}} = 35^\circ$$

STEP 5 (continued)

- a. Enter Figure 9.16(a) with ϕ angle near pile toe to determine α_t coefficient based on pile length to diameter ratio.

$$(D/b) = (13.0 \text{ m}) / (0.356 \text{ m}) = 36.52$$

$$\text{For } \phi_{\text{toe}} = 35^\circ \text{ and } (D/b) = 36.52 \rightarrow \alpha_t = 0.67$$

- b. Enter Figure 9.16(b) with ϕ angle near pile toe to determine N'_q .

$$\text{For } \phi_{\text{toe}} = 35^\circ \rightarrow N'_q = 65$$

- (ii) (Nordlund - Step 8): Compute the effective overburden pressure at the pile toe, p_t (kPa).

The effective overburden pressure at the pile toe should be limited to a maximum of 150 kPa.

The effective overburden pressure at the pile toe, p_t , has been computed in Figure F.10:

$$p_t = 143.8 \text{ kPa} < 150 \text{ kPa} \rightarrow \text{OK}$$

- (iii) (Nordlund - Step 9): Compute the ultimate toe resistance, R_t (kN).

$$\text{a. } R_t = \alpha_t N'_q A_t p_t$$

$$= 0.67 (65) (0.356 \text{ m}) (0.356 \text{ m}) (143.8 \text{ kPa}) = 795 \text{ kN}$$

$$\text{b. limiting } R_t = q_L A_t$$

Using the estimated $\phi=35^\circ$ and Figure 9.17, the limiting unit toe resistance is:

$$q_L = 5,000 \text{ kPa}$$

STEP 5 (continued)

Therefore,

$$\begin{aligned} R_t &= 5,000 \text{ kPa } (0.356 \text{ m })(0.356 \text{ m }) \\ &= 635 \text{ kN} \end{aligned}$$

c. Use lesser of the two R_t values obtained in steps a and b which is:

$$R_t = 635 \text{ kN}$$

STEP 6 Compute the ultimate pile capacity, Q_u (kN).

$$\begin{aligned} Q_u &= R_s + R_t \\ &= 1,171 \text{ kN} + 635 \text{ kN} \\ &= 1,806 \text{ kN} \end{aligned}$$

Note: In reality, the pile toe will not stop at the top of the bearing stratum. The pile toe will be driven further into the dense sand and gravel bearing stratum and therefore the ultimate toe resistance of the pile is expected to be higher than 635 kN.

STEP 7 Compute the allowable design load, Q_a (kN).

$$Q_a = \frac{Q_u}{\text{Factor of Safety}} = \frac{1,806 \text{ kN}}{\text{Factor of Safety}}$$

Note: Factor of Safety should be selected based on the construction control method to be specified. Recommended factors of safety are described in Section 9.6.

F.2.3.2 Static Axial Pile Capacity Calculations by Effective Stress Method

For the soil profile interpreted from Soil Boring S-3 as shown in Figure F.9. Perform an Effective Stress method pile capacity calculation for an embedded length of 13 meters. Use the step-by-step method outlined in Section 9.7.1.3.

STEP 1 Delineate the soil profile into layers and determine ϕ' angle for each layer.

- a. Use the procedure described in Section 9.4 to construct a p_o diagram.

For Soil Boring S-3, the p_o diagram has been constructed in Section F.2.3.1 - Step 1 and also presented in Figure F.10.

- b. Divide the soil profile throughout the pile penetration depth into layers and determine the effective overburden pressure, p_o , at the midpoint of each layer.

As the example in Section F.2.3.1, the soil profile along the pile embedded length is delineated into three layers of 1, 3, and 9 meters thick. The average effective overburden pressure of each layer is equal to the effective overburden pressure at the midpoint of that layer as follows.

Layer 1: $p_{o1} = 15.5 \text{ kPa}$ (midpoint of layer 1 - at depth of 2.5 m)

Layer 2: $p_{o2} = 35.5 \text{ kPa}$ (midpoint of layer 2 - at depth of 4.5 m)

Layer 3: $p_{o3} = 97.0 \text{ kPa}$ (midpoint of layer 3 - at depth of 10.5 m)

- c. Determine the ϕ' angle for each soil layer from laboratory or in-situ test data.

Since the ϕ' angle is not provided by either laboratory or in-situ test data, the average corrected SPT N' value will be used to estimate the ϕ' angle.

- d. In the absence of laboratory or in-situ test data for cohesionless soil layers, determine the average corrected SPT N' value for each soil layer and estimate the ϕ' angle from Table 4-5 in Chapter 4.

STEP 1 (continued)

For cohesionless soil layer 1, the average corrected SPT N' value and the soil type for each soil layer is as follows.

Layer 1: $\bar{N}'_1 = 135$ (Layer 1 - depth 2 to 3 m;
Extremely dense sand and gravel)

Use the average corrected SPT N' value for soil layer 1 to estimate the ϕ' angle from Table 4-5 in Chapter 4.

Layer 1: $\phi'_1 = 36^\circ$ (Limiting friction angle is used; See discussion in Section F.2.2.2 - Step 1)

For the cohesive soil layers 2 and 3, the effective friction angle is obtained from from the laboratory triaxial test.

Layer 2: $\phi'_2 = 27^\circ$

Layer 3: $\phi'_3 = 29^\circ$

STEP 2 Select the β coefficient for each soil layer.

- a. Use local experience to select β coefficient for each layer.

Assume no local experience.

- b. In the absence of local experience, use Table 9-4 or Figure 9.20 to estimate β coefficient from ϕ' angle for each layer.

Use the soil type, the estimated ϕ' angle, and Table 9-4 or Figure 9-20 to estimate the β coefficient for each soil layer.

Layer 1: $\beta_1 = 0.40$ (For extremely dense sand and gravel with $\phi'_1 = 36^\circ$)

Layer 2: $\beta_2 = 0.29$ (For stiff silty clay with $\phi'_2 = 27^\circ$)

STEP 2 (continued)

$$\text{Layer 3: } \beta_3 = 0.38 \quad (\text{For stiff silty clay with } \phi'_3 = 29^\circ)$$

STEP 3 For each soil layer compute the unit shaft resistance, f_s (kPa).

$$f_s = \beta p_o$$

$$\text{Layer 1: } f_{s1} = 0.40 (15.5 \text{ kPa}) = 6.20 \text{ kPa}$$

$$\text{Layer 2: } f_{s2} = 0.29 (35.5 \text{ kPa}) = 10.30 \text{ kPa}$$

$$\text{Layer 3: } f_{s3} = 0.38 (97.0 \text{ kPa}) = 36.86 \text{ kPa}$$

STEP 4 Compute the shaft resistance in each soil layer and the ultimate shaft resistance, R_s (kN), from the sum of the shaft resistance from each soil layer.

$$R_s = f_s A_s$$

where A_s = Pile-soil surface area from pile perimeter and length

$$\begin{aligned} \text{Layer 1: } R_{s1} &= 6.20 (4) (0.356 \text{ m}) (1 \text{ m}) \\ &= 9 \text{ kN} \end{aligned}$$

$$\begin{aligned} \text{Layer 2: } R_{s2} &= 10.30 (4) (0.356 \text{ m}) (3 \text{ m}) \\ &= 44 \text{ kN} \end{aligned}$$

$$\begin{aligned} \text{Layer 3: } R_{s3} &= 36.86 (4) (0.356 \text{ m}) (9 \text{ m}) \\ &= 472 \text{ kN} \end{aligned}$$

$$\begin{aligned} \text{Total: } R_s &= R_{s1} + R_{s2} + R_{s3} \\ &= 9 \text{ kN} + 44 \text{ kN} + 472 \text{ kN} \\ &= 525 \text{ kN} \end{aligned}$$

STEP 5 Compute the unit toe resistance, q_t (kPa).

$$q_t = N_t p_t$$

- a. Use local experience to select N_t coefficient.

Assume no local experience.

- b. In the absence of local experience, estimate N_t coefficient from Table 9-4 or Figure 9.21 based on ϕ' angle.

Table 9-4 or Figure 9.21 are a function of soil type and the ϕ' angle. The soil type for each layer can be obtained from the soil boring. The ϕ' angle for each layer can be obtained from laboratory tests or in-situ data. In the absence of either laboratory or in-situ test data, the ϕ' angle should be estimated from Table 4-5 in Chapter 4 using the average corrected SPT N' value, \bar{N}' , over the zone from the pile toe to 3 diameter below the pile toe (1.065 meters). The soil near the pile toe is a dense sand and gravel.

$$\bar{N}'_{\text{toe}} = 33 \quad \rightarrow \quad \phi'_{\text{toe}} = 35^\circ$$

Use the soil type, the estimated ϕ' angle, and Table 9-4 or Figure 9-21 to estimate the N_t coefficient.

$$N_t = 58 \quad (\text{For dense sand and gravel with } \phi'_{\text{toe}} = 35^\circ)$$

- c. Calculate the effective overburden pressure at the pile toe, p_t .

The effective overburden pressure at the pile toe, p_t , has been computed in a previous example (Section F.2.3.1, Step 1):

$$p_t = 143.8 \text{ kPa}$$

STEP 5 (continued)

The unit toe resistance, q_t is:

$$\begin{aligned}q_t &= N_t p_t \\ &= 58 (143.8 \text{ kPa}) = 8,340 \text{ kPa}\end{aligned}$$

STEP 6 Compute the ultimate toe resistance, R_t (kN).

$$\begin{aligned}R_t &= q_t A_t \\ &= 8,340 (0.356 \text{ m}) (0.356 \text{ m}) = 1,059 \text{ kN}\end{aligned}$$

STEP 7 Compute the ultimate pile capacity, Q_u (kN).

$$\begin{aligned}Q_u &= R_s + R_t \\ &= 525 \text{ kN} + 1,059 \text{ kN} = 1,584 \text{ kN}\end{aligned}$$

Note: The ultimate capacity according to the Effective Stress method is less than the required 1780 kN ultimate capacity. As discussed in the Nordlund method, in reality the pile toe will not be stopped at the top of the bearing stratum. The pile toe will be driven further into the dense sand and gravel bearing stratum, and therefore, the ultimate toe resistance of the pile is expected to be higher than 1,059 kN. The Effective Stress method would require a pile penetration depth of 14.0 meters for a 1780 kN capacity.

STEP 8 Compute the allowable design load, Q_a (kN).

$$Q_a = \frac{Q_u}{\text{Factor of Safety}} = \frac{1,584 \text{ kN}}{\text{Factor of Safety}}$$

Note: Factor of Safety should be selected based on the construction control method to be specified. Recommended factors of safety are described in Section 9.6.

F.2.3.3 Static Axial Pile Capacity Calculations by SPILE Computer Program

ULTIMATE STATIC PILE CAPACITY/Federal Highway Administration
Nordlund (1963, 1979) and Tomlinson (1979, 1980) methods

Project Name	: Boring S-3	Client	: FHWA Manual
File Name	: S3	Project Manager	:
Date	: 6/22/95	Computed by	: GT
Depth of Top of Pile	= 6.55 ft.	Pile length	= 42.66 ft.
Depth to Water Table	= 0.00 ft.		
Width of pile	= 0.00 in.		
Type of Pile	= Precast Concrete Pile		

SKIN FRICTION CONTRIBUTION

Layer	Soil Type	Thickness (ft)	Effective Stress (psf)	Internal Friction Angle	N-SPT	Pile Perimeter (ft)
1	Cohesionless	0.02	212.54	30.73*	12.42*	4.67
2	Cohesionless	3.27	323.39	36.00	--	4.67
3	Cohesive	9.85	742.23	---	--	4.67
4	Cohesive	29.52	2033.55	---	--	4.67

Layer	Soil Type	Undrained Shear Strength (psf)	Adhesion	Pile Taper	Sliding Friction Angle	Skin Resistance (Kips)
1	Cohesionless	--	-----	----	25.87	0.01
2	Cohesionless	--	-----	----	30.30	4.85
3	Cohesive	2214.00	2214.00	----	----	101.77
4	Cohesive	3237.00	1151.02	----	----	158.56

Total Side Friction : 265.20

POINT RESISTANCE CONTRIBUTION

Effective Stress at pile Tip (psf)	Internal Friction Angle	SPT Value	Pile End Area (ft*ft)	Bearing Capacity Factor Nq	End Bearing Resistance (Kips)
3016.56	36.76*	32.53	1.36	87.93	254.14

Limiting End Bearing Resistance : 261.52

Ultimate Static Pile Capacity : 519.34

In SI Units:	Total Side Friction	:	1,180	kN
	End Bearing Resistance	:	1,130	kN
	Ultimate Static Pile Capacity	:	2,310	kN

F.2.3.4 Static Axial Pile Capacity Calculations by LPC CPT Method - Computer Program

L.P.C. CPT Method

Page 1/2

Peach Freeway CPT-3 at Pier 3 -- 356 mm-square PCPS Concrete Pile

Installation Method: 9 - Driven Prefabricated Piles (Concrete)

Depth to Water Table: 0.0 meter

Pile No.	Toe Area (m ²)	Perimeter (m)
1	0.127	1.424

Depth to Bottom of Layer (m)	Soil Type
1.9	4
3.0	7
15.0	2
20.0	7

Depth (m)	Cone Tip Resistance (kPa)
0.0	1,244.9
2.0	1,244.9
3.0	33,228.7
7.0	3,715.5
11.0	2,848.9
12.0	4,117.7
13.0	4,237.4
14.0	4,472.0
15.0	4,256.5
16.0	17,715.6
17.0	18,816.8
18.0	20,588.4
19.0	19,056.2
19.5	19,678.7
20.0	23,940.0

Peach Freeway CPT-3 at Pier 3 -- 356 mm-square PCPS Concrete Pile

Depth (m)	Unit Friction (kPa)	Toe Bearing (kPa)	Shaft Resistance (kN)	Toe Resistance (kN)	Ultimate Capacity (kN)
0.00	38.21	746.93	0.0	94.3	94.3
2.00	11.54	2508.91	105.4	317.1	422.6
3.00	70.38	2796.19	163.7	353.6	517.3
7.00	60.14	2231.21	505.7	282.0	787.7
11.00	58.03	1972.66	842.0	249.5	1091.5
12.00	61.14	2236.00	926.5	282.9	1209.4
13.00	61.43	2537.64	1013.7	320.7	1334.4
14.00	62.00	4108.10	1101.3	519.5	1621.3
15.00	61.48	6655.32	1189.4	841.1	2030.5
16.00	64.49	5860.51	1281.0	740.6	2021.6
17.00	64.93	7124.54	1373.1	900.7	2273.8
18.00	65.60	7306.49	1465.6	923.8	2389.5
19.00	65.02	7847.53	1558.6	991.9	2549.6
19.50	65.26	8062.99	1604.8	1019.5	2624.3
20.00	66.84	8259.30	1652.0	1044.4	2696.4

Note: Depth is referenced from the original ground surface.

F.2.3.5 Static Axial Pile Capacity Calculations by Schmertmann Method

Location: Peach Freeway CPT-3 at Pier 3.

Depth (m)	fs(avg) (bars)	Unit Friction (bars)	Increment Friction (kN)	Shaft Resistance (kN)	q _c (avg) (bars)	q _{c1} (min) (bars)	q _{c2} (bars)	Toe Resistance (kN)	Ultimate Capacity (kN)
10.00	1.99	0.80	27.77	1,050	32.87				
10.25	1.93	0.77	26.93	1,077	29.15				
10.50	2.13	0.85	29.76	1,107	31.50				
10.75	2.36	0.94	32.86	1,140	33.35				
11.00	2.24	0.90	31.29	1,171	35.10	38.88	29.68	416	1,587
11.25	2.20	0.88	30.63	1,202	42.65				
11.50	2.29	0.92	31.95	1,234	44.30	42.19	21.49	386	1,620
11.75	2.45	0.98	34.12	1,268	43.50				
12.00	2.54	1.02	35.44	1,303	41.33	42.34	33.71	461	1,764
12.25	2.22	0.89	30.91	1,334	43.35	43.86	34.25	474	1,808
12.50	2.21	0.88	30.79	1,365	45.03	44.03	35.44	482	1,847
12.75	2.17	0.87	30.20	1,395	45.00				
13.00	2.26	0.91	31.58	1,427	43.53	43.32	37.30	489	1,916
13.25	2.74	1.10	38.23	1,465	46.50				
13.50	2.84	1.14	39.67	1,504	47.27	43.39	39.34	502	2,006
13.75	2.59	1.04	36.14	1,541	47.30				
14.00	2.47	0.99	34.51	1,575	45.80	42.46	40.82	505	2,080
14.25	2.13	0.85	29.66	1,605	41.35				
14.50	2.21	0.88	30.84	1,636	43.07	44.93	41.35	523	2,159
14.75	2.21	0.88	30.84	1,666	46.80				
15.00	2.05	1.74	60.69	1,727	130.90	161.05	41.95	1231	2,958
15.25	1.62	1.37	47.88	1,775	191.20				
15.50	1.48	1.26	43.79	1,819	195.97				
15.75	1.16	0.98	34.25	1,853	180.90				
16.00	1.15	0.98	34.19	1,887	170.97				

Note: Depth is referenced from the original ground surface.

F.2.3.6 Summary of Pier 3 Capacity Calculation Results

Summary of Pile Capacity Estimates with an Embedded Pile Length of 13.0 meters

Method Used for Estimation of Pile Capacity	Calculated Pile Shaft Resistance (kN)	Calculated Pile Toe Resistance (kN)	Calculated Ultimate Pile Capacity (kN)
Norlund and α Method - SPT Data	1,171	635	1,806
Effective Stress Method	525	1,059	1,584
SPILE Program - SPT Data	1,180	1,130	2,310
LPC CPT Program - CPT Data	1,189	841	2030
Schmertmann Method - CPT Data	1,727	1,231	2,958

Summary of Pile Length Estimates for the 1,780 kN Ultimate Pile Capacity

Method Used for Estimation of Pile Capacity	Calculated Pile Length for the 1,780 kN Ultimate Pile Capacity
Norlund and α Method - SPT Data	13.0 meters for 1,806 kN
Effective Stress Method	14.0 meters for 1,980 kN
SPILE Program - SPT Data	13.0 meters for 2,310 kN
LPC CPT Program - CPT Data	12.5 meters for 1,826 kN
Schmertmann Method - CPT Data	10.2 meters for 1,808 kN

The ultimate pile group capacity at Pier 3 should be calculated based on Steps 1 to 3 of the design recommendations presented in Section 9.8.1.2, since most of the soil along the pile embedded length is cohesive type. One of the design recommendations for estimating the ultimate pile group capacity in cohesive soil is to calculate the ultimate pile group capacity against block failure using the procedure described in Section 9.8.1.3. The ultimate pile group capacity should be governed by the lesser of the ultimate pile group capacity calculated from steps 1 to 3 of the design recommendations presented in Section 9.8.1.3. An example calculations of the ultimate pile group capacity against block failure for the South Abutment is presented in Section F.2.4.1 - Step 8.

F.2.4 South Abutment - Soil Boring S-4 (Cohesive Soil)

F.2.4.1 Static Axial Pile Capacity Calculations by α -Method

For the soil profile interpreted from Soil Boring S-4 as shown in Figure F.11. Perform the α -method pile capacity calculation for an embedded length of 17.5 meters. Use the step-by-step method outlined in Section 9.7.1.2a.

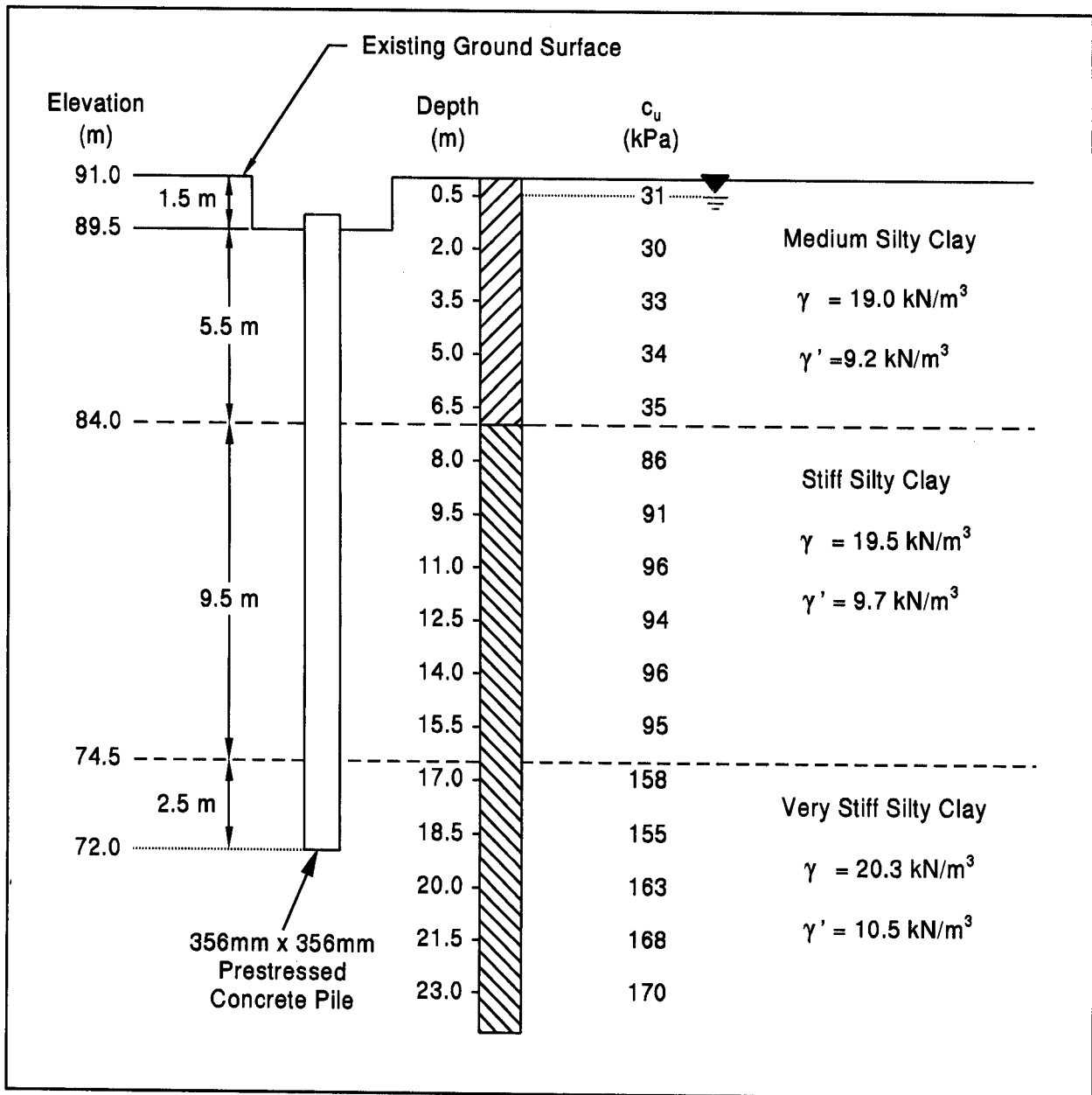


Figure F.11 Interpreted Soil Profile from Soil Boring S-4 at the South Abutment

STEP 1 Delineate the soil profile into layers and determine the adhesion, c_a from Figure 9.18 or adhesion factor, α from Figure 9.19 for each layer.

Enter appropriate figure (based on soil stratigraphy) with the undrained shear strength of the soil, c_u , and determine adhesion or adhesion factor based on the ratio of embedded pile length in clay, D , and pile diameter, b .

Along the pile embedded length, the soil profile is delineated into three layers. Layer 1 is medium silty clay that is 5.5 meters thick, layer 2 is stiff silty clay that is 9.5 meters thick, and layer 3 is very stiff silty clay that is 2.5 meters thick.

Determine the average undrained shear strength, c_u for each soil layer.

$$\text{Layer 1: } c_{u1} = \frac{31 + 30 + 33 + 34 + 35}{5} = 33 \text{ kPa}$$

(Layer 1 - depth 1.5 to 7 m;
Medium silty clay)

$$\text{Layer 2: } c_{u2} = \frac{86 + 91 + 96 + 94 + 96 + 95}{6} = 93 \text{ kPa}$$

(Layer 2 - depth 7 to 16.5 m;
Stiff silty clay)

$$\text{Layer 3: } c_{u3} = \frac{158 + 155}{2} = 157 \text{ kPa}$$

(Layer 3 - depth 16.5 to 19.0 m;
Very stiff silty clay)

The soil stratigraphy of layers 1, 2, and 3 matches that of Figures 9.19c or 9.18. In fact, for concrete piles, the adhesion obtained from Figure 9.18 should be the same as the adhesion factor from Figure 9.19c times the undrained shear strength. Figure 9.18 and the depth to pile diameter ratio, D/b , will be used here to determine the adhesion for soil layers 1, 2, and 3.

STEP 1 (continued)

For soil layer 1:

$$(D/b) = (5.5 \text{ m}) / (0.356 \text{ m}) = 15.45$$

Interpolating from Figure 9.18 for $c_{u1} = 33 \text{ kPa}$ and $(D/b) = 15.45$:

$$c_{a1} = 33 \text{ kPa}$$

For soil layer 2:

$$(D/b) = (15 \text{ m}) / (0.356 \text{ m}) = 42.13$$

Interpolating from Figure 9.18, for $c_{u2} = 93 \text{ kPa}$ and $(D/b) = 42.13$:

$$c_{a2} = 85 \text{ kPa}$$

For soil layer 3:

$$(D/b) = (17.5 \text{ m}) / (0.355 \text{ m}) = 49.16$$

Interpolating from Figure 9.18, for $c_{u3} = 157 \text{ kPa}$ and $(D/b) = 49.16$:

$$c_{a3} = 67 \text{ kPa}$$

STEP 2 For each soil layer, compute the unit shaft resistance, f_s (kPa).

$$f_s = c_a$$

Layer 1: $f_{s1} = c_{a1} = 33 \text{ kPa}$

Layer 2: $f_{s2} = c_{a2} = 85 \text{ kPa}$

Layer 3: $f_{s3} = c_{a3} = 67 \text{ kPa}$

STEP 3 Compute the shaft resistance in each soil layer and the ultimate shaft resistance, R_s (kN) from the sum of the shaft resistance from each layer.

$$R_s = f_s A_s$$

where A_s = Pile-soil surface area from perimeter and length

$$\begin{aligned} \text{Layer 1: } R_{s1} &= 33 \text{ kPa } (4)(0.356 \text{ m})(5.5 \text{ m}) \\ &= 259 \text{ kN} \end{aligned}$$

$$\begin{aligned} \text{Layer 2: } R_{s2} &= 85 \text{ kPa } (4)(0.356 \text{ m})(9.5 \text{ m}) \\ &= 1,150 \text{ kN} \end{aligned}$$

$$\begin{aligned} \text{Layer 3: } R_{s3} &= 67 \text{ kPa } (4)(0.356 \text{ m})(2.5 \text{ m}) \\ &= 239 \text{ kN} \end{aligned}$$

$$\begin{aligned} \text{Total: } R_s &= R_{s1} + R_{s2} + R_{s3} \\ &= 259 \text{ kN} + 1,150 \text{ kN} + 239 \text{ kN} = 1,648 \text{ kN} \end{aligned}$$

STEP 4 Compute the unit toe resistance, q_t (kPa).

$$q_t = 9 c_u$$

Where: c_u = undrained shear strength of soil at the pile toe.

$$\text{At the pile toe } c_u = \frac{155 + 163}{2} = 159 \text{ kPa}$$

STEP 4 (continued)

Therefore, the unit toe resistance is:

$$\begin{aligned}q_t &= 9 (159 \text{ kPa}) \\ &= 1,431 \text{ kPa}\end{aligned}$$

STEP 5 Compute the ultimate toe resistance, R_t (kN).

$$\begin{aligned}R_t &= q_t A_t \\ &= 1,431 \text{ kPa} (0.356 \text{ m})(0.356 \text{ m}) \\ &= 182 \text{ kN}\end{aligned}$$

STEP 6 Compute the ultimate pile capacity, Q_u (kN).

$$\begin{aligned}Q_u &= R_s + R_t \\ &= 1,648 \text{ kN} + 182 \text{ kN} \\ &= 1,830 \text{ kN}\end{aligned}$$

STEP 7 Compute the allowable design load, Q_a (kN).

$$Q_a = \frac{Q_u}{\text{Factor of Safety}} = \frac{1,830 \text{ kN}}{\text{Factor of Safety}}$$

Note: Factor of Safety should be selected based on the construction control method to be specified. Recommended factors of safety are described in Section 9.6.

The group capacity in a cohesive soil should be checked for block failure.

STEP 8 Investigate the possibility of a block failure of pile groups as discussed in Section 9.8.1.3.

Block failure of pile groups should be considered in the design of pile groups in soft cohesive soils or in cohesionless soils underlain by a weak cohesive layer. For a pile group in cohesive soil, the ultimate capacity of the pile group against block failure can be expressed as:

$$Q_{ug} = 2D (B+Z) c_{u1} + B Z c_{u2} N_c$$

Where:

D = embedded lengths of piles = 17.5 m.

B = width of pile group = 3.36 m.

Z = length of pile group = 10.86 m

c_{u1} = the weighted average of the undrained shear strength over the depth of pile embedment for the cohesive soils along the pile group perimeter

Layer 1: $c_{u1-1} = 33$ kPa

Layer 2: $c_{u1-2} = 93$ kPa

Layer 3: $c_{u1-3} = 157$ kPa

c_{u2} = average undrained shear strength of the cohesive soils at the base of the pile group to a depth of 2B below pile toe level

$$= \frac{155 + 162 + 168}{3} = 162 \text{ kPa}$$

N_c = bearing capacity factor = 9

STEP 8 (continued)

The group shaft resistance against block failure is $2D (B+Z) c_{u1}$:

$$\text{Layer 1: } 2 (5.5 \text{ m}) (3.36 \text{ m} + 10.86 \text{ m}) (33 \text{ kPa}) = 5,162 \text{ kN}$$

$$\text{Layer 2: } 2 (9.5 \text{ m}) (3.36 \text{ m} + 10.86 \text{ m}) (93 \text{ kPa}) = 25,127 \text{ kN}$$

$$\text{Layer 3: } 2 (2.5 \text{ m}) (3.36 \text{ m} + 10.86 \text{ m}) (157 \text{ kPa}) = 11,163 \text{ kN}$$

The group toe resistance against block failure is:

$$\begin{aligned} B Z c_{u2} N_c &= 3.36 \text{ m} (10.86 \text{ m}) (162 \text{ kPa}) (9) \\ &= 53,202 \text{ kN} \end{aligned}$$

Therefore,

$$\begin{aligned} Q_{ug} &= 5,162 \text{ kN} + 25,127 \text{ kN} + 11,163 \text{ kN} + 53,202 \text{ kN} \\ &= 94,654 \text{ kN} \end{aligned}$$

The ultimate pile group capacity in cohesive soil should be taken as the lesser of the ultimate pile group capacity calculated from Steps 1 to 4 as described in Section 9.8.1.2. Steps 1 and 2 take into account the pile center to center spacing and the undrained shear strength of the cohesive soil. For the South Abutment soil strength and pile spacing, this results in a group efficiency of 1.0. Therefore, the ultimate pile group capacity is the calculated ultimate pile capacity of 1,830 kN time the 24 piles in the group or 43,920 kN. The ultimate pile group capacity against block failure, Q_{ug} , calculated above is equal to 94,654 kN. Therefore, block failure is not a problem. The ultimate pile group capacity of 43,920 kN is in excess of the required ultimate pile group capacity of 42,720 kN.

F.2.4.2 Static Axial Pile Capacity Calculations by Effective Stress Method

For the soil profile interpreted from Soil Boring S-4 as shown in Figure F.11. Perform an Effective Stress method pile capacity calculation for an embedded length of 17.5 meters. Use the step-by-step method outlined in Section 9.7.1.3.

STEP 1 Delineate the soil profile into layers and determine ϕ' angle for each layer.

- a. Use the procedure described in Section 9.4 to construct a p_o diagram.

For Soil Boring S-4, the p_o diagram is presented below in Figure F.12.

- b. Divide the soil profile throughout the pile penetration depth into layers and determine the effective overburden pressure, p_o , at the midpoint of each layer.

As the example in Section F.2.4.1, the soil profile along the pile embedded length is delineated into three layers of 5.5, 9.5, and 2.5 meter thick. The average effective overburden pressure of each layer is equal to the effective overburden pressure at the midpoint of that layer as follows.

Layer 1: $p_{o1} = 44.0 \text{ kPa}$ (at depth of 4.25 meters)

Layer 2: $p_{o2} = 115.4 \text{ kPa}$ (at depth of 11.75 meters)

Layer 3: $p_{o3} = 174.6 \text{ kPa}$ (at depth of 17.75 meters)

- c. Determine the ϕ' angle for each soil layer from laboratory or in-situ test data.

The effective frictional angle for each layer was obtained from the laboratory triaxial test.

Layer 1: $\phi'_1 = 27^\circ$

Layer 2: $\phi'_2 = 29^\circ$

Layer 3: $\phi'_3 = 30^\circ$

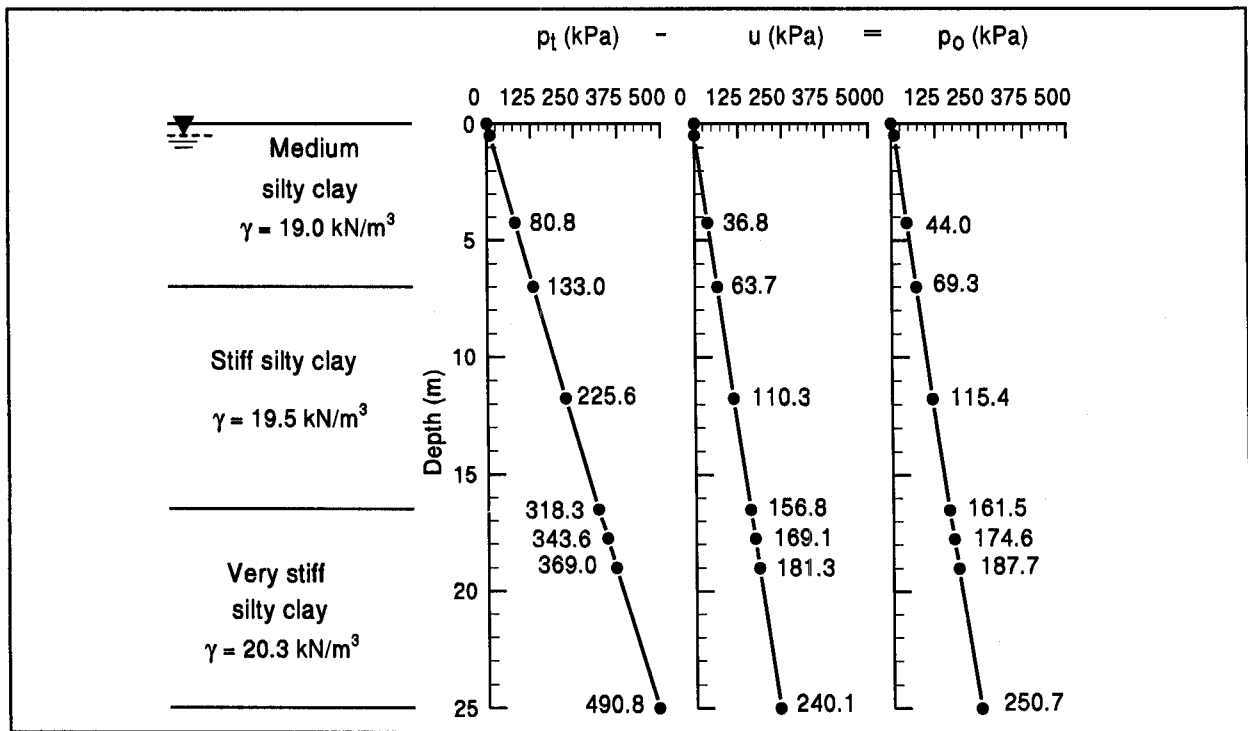


Figure F.12 Effective Overburden Pressure Diagram - South Abutment

STEP 2 Select the β coefficient for each soil layer.

- a. Use local experience to select β coefficient for each layer.

Assume no local experience.

- b. In the absence of local experience, use Table 9-4 or Figure 9.20 to estimate β coefficient from ϕ' angle for each layer.

Use the soil type, the estimated ϕ' angle, and Table 9-4 or Figure 9-20 to estimate the β coefficient for each soil layer.

Layer 1: $\beta_1 = 0.30$ (For medium silty clay with $\phi'_1 = 27^\circ$)

Layer 2: $\beta_2 = 0.35$ (For stiff silty clay with $\phi'_2 = 29^\circ$)

Layer 3: $\beta_3 = 0.40$ (For very stiff silty clay with $\phi'_3 = 30^\circ$)

STEP 3 For each soil layer, compute the unit shaft resistance, f_s (kPa).

$$f_s = \beta p_o$$

Layer 1: $f_{s1} = 0.30 (44.0 \text{ kPa}) = 13.20 \text{ kPa}$

Layer 2: $f_{s2} = 0.35 (115.4 \text{ kPa}) = 40.39 \text{ kPa}$

Layer 3: $f_{s3} = 0.40 (174.6 \text{ kPa}) = 69.84 \text{ kPa}$

STEP 4 Compute the shaft resistance in each soil layer and the ultimate shaft resistance, R_s (kN) from the sum of the shaft resistance from each soil layer.

$$R_s = f_s A_s$$

Layer 1: $R_{s1} = 13.20 (4) (0.356 \text{ m}) (5.5 \text{ m})$
 $= 103 \text{ kN}$

Layer 2: $R_{s2} = 40.39 (4) (0.356 \text{ m}) (9.5 \text{ m})$
 $= 546 \text{ kN}$

Layer 3: $R_{s3} = 69.84 (4) (0.356 \text{ m}) (2.5 \text{ m})$
 $= 249 \text{ kN}$

Total: $R_s = R_{s1} + R_{s2} + R_{s3}$
 $= 103 \text{ kN} + 546 \text{ kN} + 249 \text{ kN}$
 $= 898 \text{ kN}$

STEP 5 Compute the unit toe resistance, q_t (kPa).

$$q_t = N_t p_t$$

- a. Use local experience to select N_t coefficient.

Assume no local experience.

- b. In the absence of local experience, estimate N_t coefficient from Table 9-4 or Figure 9.21 based on ϕ' angle.

Based on the laboratory triaxial test, the undrained frictional angle is:

$$\phi'_{\text{toe}} = 30^\circ$$

Use the soil type, the estimated ϕ' angle, and Table 9-4 or Figure 9-21 to estimate the N_t coefficient.

$$N_t = 30$$

- c. Calculate the effective overburden pressure at the pile toe, p_t .

The effective overburden pressure at the pile toe, p_t , has been computed in Figure F.12:

$$p_t = 187.7 \text{ kPa}$$

The unit toe resistance, q_t is:

$$\begin{aligned} q_t &= N_t p_t \\ &= 30 (187.7 \text{ kPa}) \\ &= 5,631 \text{ kPa} \end{aligned}$$

STEP 6 Compute the ultimate toe resistance, R_t (kN).

$$\begin{aligned} R_t &= q_t A_t \\ &= 5,631 \text{ kPa} (0.356 \text{ m}) (0.356 \text{ m}) \\ &= 715 \text{ kN} \end{aligned}$$

STEP 7 Compute the ultimate pile capacity, Q_u (kN).

$$\begin{aligned} Q_u &= R_s + R_t \\ &= 898 \text{ kN} + 715 \text{ kN} \\ &= 1,613 \text{ kN} \end{aligned}$$

STEP 8 Compute the allowable design load, Q_a (kN).

$$Q_a = \frac{Q_u}{\text{Factor of Safety}} = \frac{1,613 \text{ kN}}{\text{Factor of Safety}}$$

Note: Factor of Safety should be selected based on the construction control method to be specified. Recommended factors of safety are described in Section 9.6.

F.2.1.4 Static Axial Pile Capacity Calculations by SPILE Computer Program

ULTIMATE STATIC PILE CAPACITY/Federal Highway Administration
Nordlund (1963, 1979) and Tomlinson (1979, 1980) methods

Project Name : Boring S-4 Client : FHWA Manual
 File Name : S4 Project Manager :
 Date : 1/11/96 Computed by : GT

Depth of Top of Pile = 4.92 ft. Pile length = 57.41 ft.
 Depth to Water Table = 1.60 ft.
 Width of pile = 0.00 in.
 Type of Pile = Precast Concrete Pile

SKIN FRICTION CONTRIBUTION

Layer	Soil Type	Thickness (ft)	Effective Stress (psf)	Internal Friction Angle	N-SPT	Pile Perimeter (ft)
1	Cohesive	18.04	925.09	---	--	4.67
2	Cohesive	31.17	2431.58	---	--	4.67
3	Cohesive	8.20	3680.83	---	--	4.67

Layer	Soil Type	Undrained Shear Strength (psf)	Adhesion	Pile	Sliding Taper Friction Angle	Skin Resistance (Kips)
1	Cohesive	693.00	679.86	----	----	57.24
2	Cohesive	1953.00	1780.32	----	----	258.97
3	Cohesive	3297.00	1401.21	----	----	53.62

Total Side Friction : 369.82

POINT RESISTANCE CONTRIBUTION

Effective Stress at pile Tip (psf)	Undrained Shear Strength (psf)	SPT Value	Pile End Area (ft*ft)	Bearing Capacity Factor Nq	End Bearing Resistance (Kips)
3957.58	3339.00	----	1.36	----	40.90

Ultimate Static Pile Capacity : 410.72

In SI Units: Total Side Friction : 1,645 kN
 End Bearing Resistance : 182 kN
 Ultimate Static Pile Capacity : 1,827 kN

F.2.4.3 Static Axial Pile Capacity Calculations by LPC CPT Method - Computer Program

L.P.C. CPT Method
 Peach Freeway CPT-4 at South Abutment -- 356 mm-square PCPS Concrete Pile

Installation Method: 9 - Driven Prefabricated Piles (Concrete)
 Depth to Water Table: 1.00 meter

Pile No.	Toe Area (m ²)	Perimeter (m)
1	0.127	1.424

Depth to Bottom of Layer (m)	Soil Type
7.0	1
29.0	2
30.0	8

Depth (m)	Cone Tip Resistance (kPa)
0.0	1,149.1
3.5	1,149.1
7.0	1,053.4
10.0	3,255.8
15.0	2,872.8
16.0	4,438.5
17.0	3,433.0
18.0	4,989.1
19.0	4,141.6
20.0	4,021.9
21.0	3,361.2
22.0	3,064.3
23.0	6,875.6
24.0	5,266.8
26.0	4,979.5
28.0	5,027.4
28.5	4,309.2
29.0	20,492.6
30.0	48,981.2

Depth (m)	Unit Friction (kPa)	Toe Bearing (kPa)	Shaft Resistance (kN)	Toe Resistance (kN)	Ultimate Capacity (kN)
0.00	35.81	689.47	0.0	87.2	87.2
3.50	35.81	689.47	178.4	87.2	265.6
7.00	31.22	1292.76	345.2	163.2	508.4
10.00	59.04	1953.50	596.9	246.9	843.8
15.00	58.08	2025.32	1013.3	256.2	1269.5
16.00	61.91	2164.18	1098.7	273.6	1372.2
17.00	59.47	2542.43	1185.0	321.2	1506.1
18.00	63.25	2513.70	1272.1	318.0	1590.2
19.00	61.19	2590.31	1360.6	327.8	1688.5
20.00	60.90	2312.60	1447.4	292.2	1739.6
21.00	59.28	2168.96	1532.8	274.4	1807.2
22.00	58.56	2666.92	1616.4	337.6	1954.0
23.00	67.85	3011.65	1706.3	380.8	2087.0
24.00	63.92	3385.12	1800.1	427.9	2228.0
26.00	63.20	3026.02	1981.1	382.5	2363.7
28.00	63.35	8637.55	2160.8	1092.4	3253.3
28.50	61.57	9576.00	2205.3	1210.8	3416.1
29.00	101.07	9576.00	2263.1	1210.8	3473.9
30.00	76.37	9576.00	2371.7	1210.8	3582.4

Note: Depth is referenced from the original ground surface.

F.2.4.4 Static Axial Pile Capacity Calculations by Schmertmann Method

Location: Peach Freeway CPT-4 at South Abutment.

Depth (m)	fs(avg) (bars)	Unit Friction (bars)	Increment Friction (kN)	Shaft Resistance (kN)	q _c (avg) (bars)	q _{c1} (min) (bars)	q _{c2} (bars)	Toe Resistance (kN)	Ultimate Capacity (kN)
15.00	2.24	0.90	31.22	1,191	45.20				
15.25	3.19	1.28	44.44	1,235	54.84				
15.50	2.53	1.01	35.27	1,271	44.96	33.90	20.38	329	1,599
15.75	2.41	0.96	33.57	1,304	43.12				
16.00	2.49	1.00	34.76	1,339	42.38	32.13	25.23	347	1,686
16.25	1.82	0.73	25.37	1,364	33.98				
16.50	1.29	0.58	20.26	1,385	29.10	31.80	27.41	358	1,743
16.75	1.97	0.79	27.43	1,412	34.50	40.16	28.48	416	1,828
17.00	2.35	0.94	32.78	1,445	45.82	43.94	29.55	445	1,890
17.25	3.07	1.23	42.80	1,488	55.86				
17.50	2.69	1.08	37.49	1,525	53.16	40.59	29.83	426	1,951
17.75	2.60	1.04	36.27	1,561	62.30				
18.00	2.15	0.86	29.97	1,591	37.04	34.39	28.94	383	1,975
18.25	2.26	0.91	31.56	1,623	46.56				
18.50	3.08	1.23	42.96	1,666	64.02	33.90	28.94	380	2,046
18.75	1.84	0.74	25.71	1,692	32.00				
19.00	1.77	0.72	25.26	1,717	30.44	29.32	28.94	353	2,070
19.25	1.53	0.66	22.99	1,740	28.94				
19.50	2.22	0.89	30.98	1,771	42.22	30.27	28.94	358	2,129
19.75	1.48	0.62	21.69	1,793	30.34				
20.00	1.33	0.60	20.80	1,813	27.26	29.92	27.26	346	2,160
20.25	1.94	0.78	27.10	1,841	36.50				
20.50	1.48	0.62	21.69	1,862	30.50	23.62	18.54	255	2,117
20.75	1.94	0.77	26.99	1,889	33.60				
21.00	2.35	0.94	32.73	1,922	39.78	22.78	18.54	250	2,172
21.25	1.59	0.67	23.30	1,945	27.36				
21.50	1.06	0.52	18.17	1,963	22.38	19.50	18.54	230	2,194
21.75	0.78	0.45	15.53	1,979	18.54				

Note: Depth is referenced from the original ground surface.

Location: Peach Freeway CPT-4 at South Abutment (continued).

Depth (m)	fs(avg) (bars)	Unit Friction (bars)	Increment Friction (kN)	Shaft Resistance (kN)	q _c (avg) (bars)	q _{c1} (min) (bars)	q _{c2} (bars)	Toe Resistance (kN)	Ultimate Capacity (kN)
22.00	2.12	0.85	29.61	2,090	46.92	47.34	18.54	399	2,407
22.25	5.48	4.65	162.21	2,171	116.78				
22.50	3.78	3.21	111.91	2,283	71.18	42.20	22.26	390	2,673
22.75	2.86	1.14	39.81	2,323	61.10				
23.00	1.96	0.78	27.35	2,350	38.18	34.17	22.38	342	2,692
23.25	1.90	0.76	26.46	2,376	33.42				
23.50	2.79	1.12	38.87	2,415	46.08	34.99	24.30	359	2,774

Note: Depth is referenced from the original ground surface.

F.2.4.5 Summary of South Abutment Capacity Calculation Results

Summary of Pile Capacity Estimates with an Embedded Pile Length of 17.5 meters

Method Used for Estimation of Pile Capacity	Calculated Pile Shaft Resistance (kN)	Calculated Pile Toe Resistance (kN)	Calculated Ultimate Pile Capacity (kN)
α Method	1,648	182	1,830
Effective Stress Method	898	715	1,613
SPILE Program - SPT Data	1,645	182	1,827
LPC CPT Program - CPT Data	1,361	328	1,689
Schmertmann Method - CPT Data	1,717	353	2,070

Summary of Pile Length Estimates for the 1,780 kN Ultimate Pile Capacity

Method Used for Estimation of Pile Capacity	Calculated Pile Length for the 1,780 kN Ultimate Pile Capacity
α Method	17.5 meters for 1,830 kN
Effective Stress Method	18.7 meters for 1,800 kN
SPILE Program - SPT Data	17.5 meters for 1,827 kN
LPC CPT Program - CPT Data	19.5 meters for 1,807 kN
Schmertmann Method - CPT Data	15.2 meters for 1,828 kN

The ultimate pile group capacity at the South Abutment should be calculated based on the lesser of the ultimate pile group capacity calculated from Steps 1 to 4 of the design recommendations presented in Section 9.8.1.2. The ultimate pile group capacity based on the design recommendations is equal to 43,920 kN which is in excess of the required ultimate pile group capacity of 42,720 kN.

F.3 GROUP SETTLEMENT CALCULATIONS

The substructure of the bridge is designed to be supported on a pile group having three rows of piles with 8 piles in each row. The piles are arranged at 1.5 m center to center spacing with a total pile group area of 3.36 m by 10.86 m. Piles in a group are combined with a pile cap having a dimension of 4.5 m by 12 m.

The bridge division has estimated that the maximum compression loads per substructure unit are 12,600 kN. The maximum pile group settlement should be less than 25 mm under the compression loads.

Calculations of pile group settlement will be demonstrated for pile groups embedded in both cohesionless, cohesive, and combined layers of cohesionless and cohesive soils. The pile groups at the North Abutment and Pier 2 has a cohesionless soil profile. The pile groups at Pier 3 has a combined layers of cohesionless and cohesive soils, and the pile groups at the South Abutment has a cohesive soil profile.

F.3.1 North Abutment - Meyerhof Method Based on SPT Test Data

The soil profile interpreted from Soil Boring S-1 for the pile group at the North Abutment was shown in Figure F.3. Calculate the immediate settlement of pile group using the Meyerhof method based on SPT test data for an embedded pile length of 11.5 meters. Use the method outlined in Section 9.8.2.2a.

STEP 1 Calculate total pile group settlement due to soil compression.

Meyerhof recommended that the settlement of a pile group in a homogeneous sand deposit not underlain by a more compressible soil at a greater depth may be conservatively estimated by the following expression:

$$s = \frac{0.96 p_f \sqrt{B} l_f}{\bar{N}'}$$

STEP 1 (continued)

Where:

p_f = foundation pressure (kPa). Group load divided by group area.
Notes: settlement should be calculated for the design load to be imposed on the pile group, and not the ultimate or allowable pile group capacities.

$$= \frac{12,600 \text{ kN}}{(3.36 \text{ m})(10.86 \text{ m})} = 345 \text{ kPa}$$

B = the width of pile group = 3.36 m

\bar{N}' = average corrected SPT N' value within a depth B below pile toe level.

$$= \frac{34 + 32 + 33}{3} = 33$$

D = pile embedment depth = 11.5 m

I_f = influence factor for group embedment.

$$= 1 - [D / 8B] \geq 0.5$$

$$= 1 - [(11.5 \text{ m}) / 8(3.36 \text{ m})] = 0.572$$

Therefore,

s = estimated total pile group settlement due to soil compression.

$$= \frac{0.96 (345 \text{ kPa}) \sqrt{3.36} (0.572)}{33} = 10.52 \text{ mm}$$

Note: For silty sand, a different equation should be used as indicated in Section 9.8.2.2a.

STEP 2 Calculate the elastic compression of pile material under design load on each pile as described in Section 9.8.2.1.

The design load on each pile = 890 kN. The elastic compression of each pile can be calculated with the following expression:

$$\Delta = \frac{Q_a L}{A E}$$

Where:

L = Length of pile (mm) = 11,500 mm

A = Pile cross sectional area (m²) = 0.127 m²

E = Modulus of elasticity of pile material (kPa) = 27.8 x 10⁶ kPa

Q_a = Design axial load in pile (kN), as discussed below.

Because of the shaft resistance, the axial load transferred to the pile varies along the pile length. For this reason, the average axial load in each pile segment should be calculated. The pile is divided into four segments according to the number of soil layers used in shaft resistance computations presented in Section F.2.1.2 (Nordlund Method). The first segment is 1 meter length, the second is 3 meters, the third is 7 meters, and the fourth is 0.5 meters. The shaft resistance as calculated using the Nordlund method for the first, second, third, and fourth segment is 37 kN, 146 kN, 615 kN, and 100 kN, respectively. The average axial load transferred to each pile segment is equal to the axial load transferred to the mid length of each pile segment as shown in Figure F.13. The average axial load transferred is used to calculate the elastic compression of the pile segment. The total elastic compression of the pile is equal to the sum of elastic compression from each pile segment.

Pile segment 1a:
$$\Delta_{1a} = \frac{(872 \text{ kN}) (1000 \text{ mm})}{(0.127 \text{ m}^2) (27,800,000 \text{ kPa})} = 0.247 \text{ mm}$$

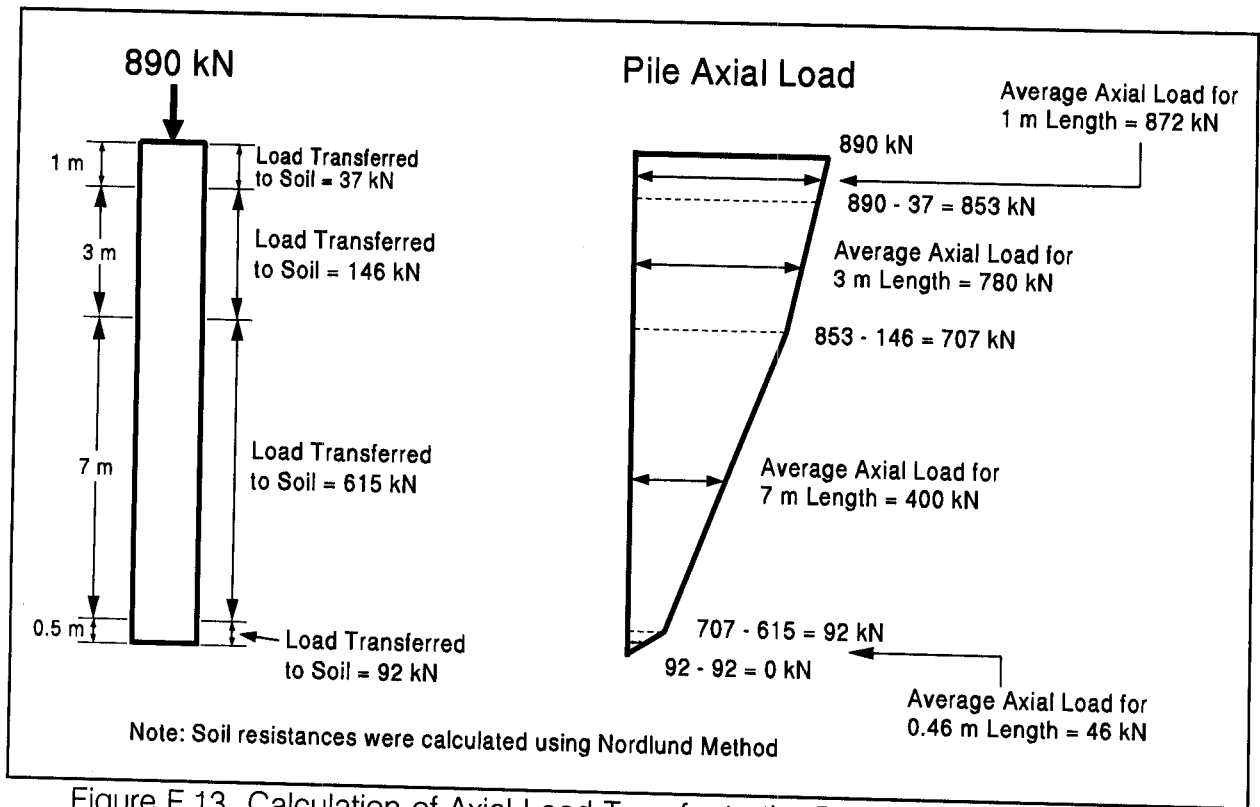


Figure F.13 Calculation of Axial Load Transfer to the Pile at the North Abutment

STEP 2 (continued)

Pile segment 1b:
$$\Delta_{1b} = \frac{(780 \text{ kN})(3000 \text{ mm})}{(0.127 \text{ m}^2)(27,800,000 \text{ kPa})} = 0.663 \text{ mm}$$

Pile segment 2:
$$\Delta_2 = \frac{(400 \text{ kN})(7000 \text{ mm})}{(0.127 \text{ m}^2)(27,800,000 \text{ kPa})} = 0.793 \text{ mm}$$

Pile segment 3:
$$\Delta_3 = \frac{(46 \text{ kN})(460 \text{ mm})}{(0.127 \text{ m}^2)(27,800,000 \text{ kPa})} = 0.006 \text{ mm}$$

Total:
$$\Delta = \Delta_{1a} + \Delta_{1b} + \Delta_2 + \Delta_3$$

$$= 0.247 \text{ mm} + 0.663 \text{ mm} + 0.793 \text{ mm} + 0.006 \text{ mm} = 1.709 \text{ mm}$$

STEP 3 Compute total pile group settlement.

$$\begin{aligned}\Delta(\text{ total }) &= \Delta(\text{ soil compression }) + \Delta(\text{ elastic pile compression }) \\ &= 10.52 \text{ mm} + 1.709 \text{ mm} \\ &= 12.23 \text{ mm} \quad \text{or} \quad 0.012 \text{ m}\end{aligned}$$

Note: Total pile group settlement is less than the maximum allowable settlement of 25 mm.

F.3.2 Pier 2 - Meyerhof Method Based on SPT Test Data

The soil profile interpreted from Soil Boring S-2 for the pile group at Pier 2 was shown in Figure F.5. Calculate the immediate settlement of pile group using the Meyerhof method based on SPT test data for an embedded pile length of 10 meters. Use the method outlined in Section 9.8.2.2a.

STEP 1 Calculate total pile group settlement due to soil compression.

Meyerhof recommended that the settlement of a pile group in a homogeneous sand deposit not underlain by a more compressible soil at a greater depth may be conservatively estimated by the following expression:

$$s = \frac{0.96 p_f \sqrt{B} I_f}{\bar{N}'}$$

Where:

p_f = foundation pressure (kPa). Group load divided by group area.
Notes: settlement should be calculated for the design load to be imposed on the pile group, and not the ultimate or allowable pile group capacities.

$$= \frac{12,600 \text{ kN}}{(3.36 \text{ m})(10.86 \text{ m})} = 345 \text{ kPa}$$

B = the width of pile group = 3.36 m

\bar{N}' = average corrected SPT N' value within a depth B below pile toe level

$$= \frac{34 + 30 + 32}{3} = 32$$

D = pile embedment depth = 10 m

STEP 1 (continued)

$$\begin{aligned} I_f &= \text{influence factor for group embedment} \\ &= 1 - [D / 8B] \geq 0.5 \\ &= 1 - [(10 \text{ m}) / 8 (3.36 \text{ m})] = 0.628 \end{aligned}$$

Therefore,

$$\begin{aligned} s &= \text{estimated total pile group settlement due to soil compression} \\ &= \frac{0.96 (345 \text{ kPa}) \sqrt{3.36} (0.628)}{32} = 11.91 \text{ mm} \end{aligned}$$

Note: For silty sand, a different equation should be used as indicated in Section 9.8.2.2a.

STEP 2 Calculate the elastic compression of pile material under design load on each pile.

The design load on each pile = 890 kN. The elastic compression of each pile can be calculated with the following expression:

$$\Delta = \frac{Q_a L}{A E}$$

Where:

$$L = \text{Length of pile (mm)} = 10,000 \text{ mm}$$

$$A = \text{Pile cross sectional area (m}^2\text{)} = 0.127 \text{ m}^2$$

$$E = \text{Modulus of elasticity of pile material (kPa)} = 27.8 \times 10^6 \text{ kPa}$$

$$Q_a = \text{Design axial load in pile (kN), as discussed below.}$$

Because of the shaft resistance, the axial load transferred to the pile varies along the pile length. For this reason, the average axial load in each pile segment should be calculated. The pile is divided into two segments according to the

STEP 2 (continued)

number of soil layers presented in Figure F.5. The first segment is 4 meters length and the second is 6 meters. The shaft resistance as calculated using the Nordlund method (as presented in Section F.2.2.2) for the first and second segment is 267 kN and 717 kN, respectively. The average axial load transferred to each pile segment is equal to the axial load transferred to the mid length of each pile segment as described earlier in Section F.3.1 and shown in Figure F.14. The average axial load transferred is used to calculate the elastic compression of the pile segment. The total elastic compression of the pile is equal to the sum of elastic compression from each pile segment.

$$\text{Pile segment 1: } \Delta_1 = \frac{(757 \text{ kN})(4000 \text{ mm})}{(0.127 \text{ m}^2)(27,800,000 \text{ kPa})} = 0.858 \text{ mm}$$

$$\text{Pile segment 2: } \Delta_2 = \frac{(312 \text{ kN})(5213 \text{ mm})}{(0.127 \text{ m}^2)(27,800,000 \text{ kPa})} = 0.461 \text{ mm}$$

$$\begin{aligned} \text{Total: } \Delta &= \Delta_1 + \Delta_2 \\ &= 0.858 \text{ mm} + 0.461 \text{ mm} = 1.319 \text{ mm} \end{aligned}$$

STEP 3 Compute total pile group settlement.

$$\begin{aligned} \Delta(\text{ total }) &= \Delta(\text{ soil compression }) + \Delta(\text{ elastic pile compression }) \\ &= 11.91 \text{ mm} + 1.319 \text{ mm} \\ &= 13.23 \text{ mm} \quad \text{or} \quad 0.013 \text{ m} \end{aligned}$$

Note: Total pile group settlement is less than the maximum allowable settlement of 25 mm.

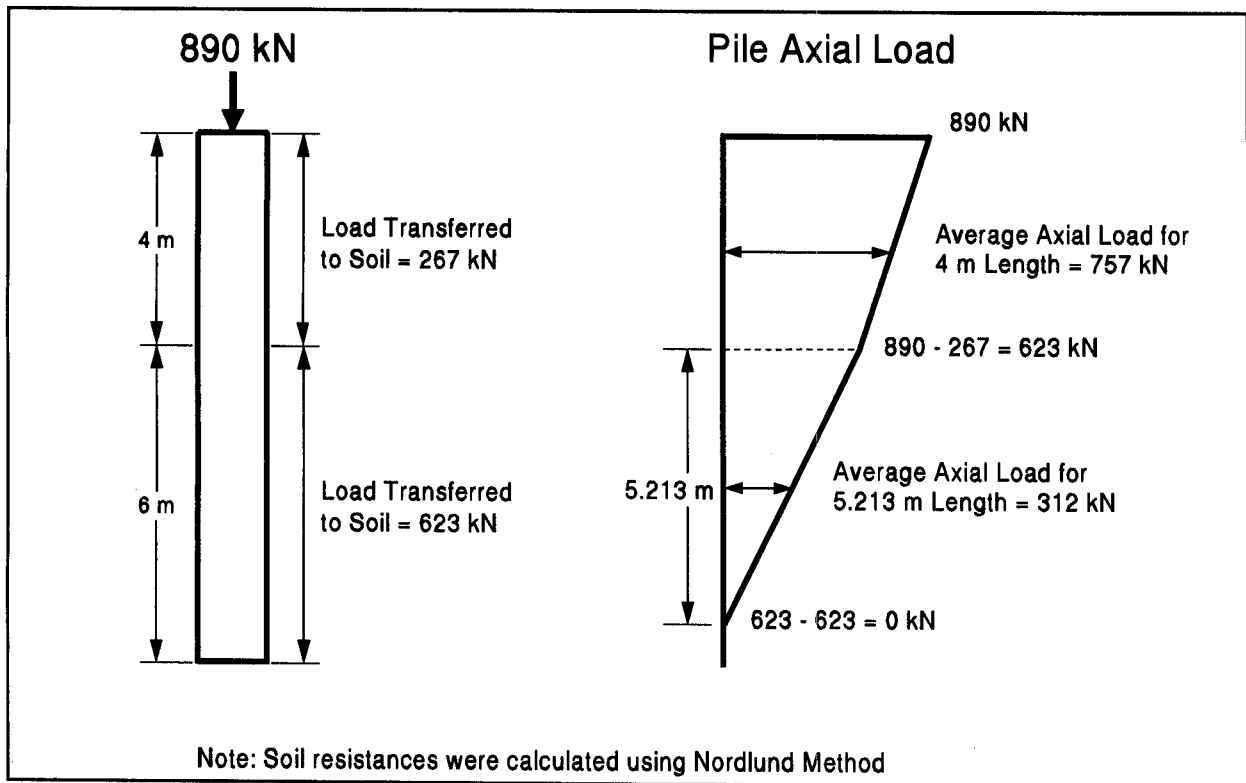


Figure F.14 Calculation of Axial Load Transfer to the Pile at Pier 2

F.3.3 Pier 3 - Equivalent Footing Method for Layered Soils

For the pile group at Pier 3 and the soil profile interpreted from Soil Boring S-3 as shown in Figure F.9. Calculate the immediate settlements of pile groups using the equivalent footing method for layered soils for an embedded pile length of 13 meters. Use the step-by-step method outlined in Section 9.8.2.4.

STEP 1 Determine the new load imposed on soil by the pile group.

- a. Determine the location of the equivalent footing.

The location of the equivalent footing is based on the shaft and toe resistance condition and the soil profile. Figure 9.44 should be used to determine the location of the equivalent footing and the pressure distribution. The soil profile for Soil Boring S-3, and the shaft and toe resistance combination match that in Figure 9.44(d), and therefore the equivalent footing is placed at depth of $\frac{2}{3} D$ from the bottom of the pile cap as shown in the figure.

STEP 1 (continued)

Depth of Equivalent Footing:

- below the pile cap $= \frac{2}{3} (13.0 \text{ m}) = 8.67 \text{ m}$
- or below the existing ground $= 8.67 \text{ m} + 2.0 \text{ m} = 10.67 \text{ m}$

b. Determine the dimensions of the equivalent footing.

All the piles in the pile group are vertical, and the pile group has a dimension of 3.36 meters by 10.86 meters. To account for load transfer, the equivalent footing has a modified dimension that spreads as a pyramid with a side slope of 1H:4V, as shown in Figure 9.44(d). Since the equivalent footing is 8.67 meters below the pile cap, the equivalent footing dimensions are:

$$\begin{aligned} \text{The width of the equivalent footing, } B_1 &= 3.36 \text{ m} + 2 \left(\frac{8.67 \text{ m}}{4} \right) \\ &= 7.70 \text{ m} \end{aligned}$$

$$\begin{aligned} \text{The length of the equivalent footing, } Z_1 &= 10.86 \text{ m} + 2 \left(\frac{8.67 \text{ m}}{4} \right) \\ &= 15.20 \text{ m} \end{aligned}$$

c. Determine the pressure distribution to soil layers below the equivalent footing up to the depth at which the pressure increase from the equivalent footing is less than 10% of existing effective overburden pressure at that depth.

The pressure distribution diagram below the equivalent footing is presented in Figure F.15. Note, the pressure distribution area increases with depth below the equivalent footing which results in a pressure reduction with depth below the equivalent footing. The dimension of the pressure distribution surface also spreads as a pyramid with depth but with a side slope of 1H:2V.

For example, at depth of 0.67 meter below the equivalent footing (or 11.34 meters below the existing ground surface), the pressure distribution surface has the following dimensions:

STEP 1 (continued)

$$\text{Width of pressure distribution surface, } B_2 = 7.70 \text{ m} + 2\left(\frac{0.67 \text{ m}}{2}\right) = 8.37 \text{ m}$$

$$\text{Length of pressure distribution surface, } Z_2 = 15.20 \text{ m} + 2\left(\frac{0.67 \text{ m}}{2}\right) = 15.87 \text{ m}$$

$$\begin{aligned} \text{Area of pressure distribution surface, } A_2 &= (B_2) (Z_2) = (8.37 \text{ m}) (15.87 \text{ m}) \\ &= 132.8 \text{ m}^2 \end{aligned}$$

Therefore, at depth of 0.67 meter below the equivalent footing the pressure increase due to the imposed design load is:

$$\Delta p = \left(\frac{12,600 \text{ kN}}{132.8 \text{ m}^2} \right) = 94.88 \text{ kPa}$$

The pressure increase at other locations below the equivalent footing is summarized in Table F-1. The limestone bedrock was reached before the imposed pressure increase becomes less than 10% of existing effective overburden pressure. Therefore for settlement calculation, the total soil thickness up to the bedrock will be used.

- d. Divide the cohesive soil layers in the affected pressure increase zone into several thinner layers of 1.5 to 3 meter thickness. The thickness of each layer is the thickness H for the settlement computation for that layer.

For this example, the soil is divided into 1.5 meter thick layers as presented in column 3 of Table F-2. The soil layer boundaries are presented in column 2 of Table F-2.

- e. Determine the existing effective overburden pressure, p_o , at the midpoint of each layer.

The midpoint location of each soil layer below the existing ground is presented in column 4 of Table F-2. The effective overburden pressure, p_o , at the midpoint of each layer is presented in column 5 of Table F-2.

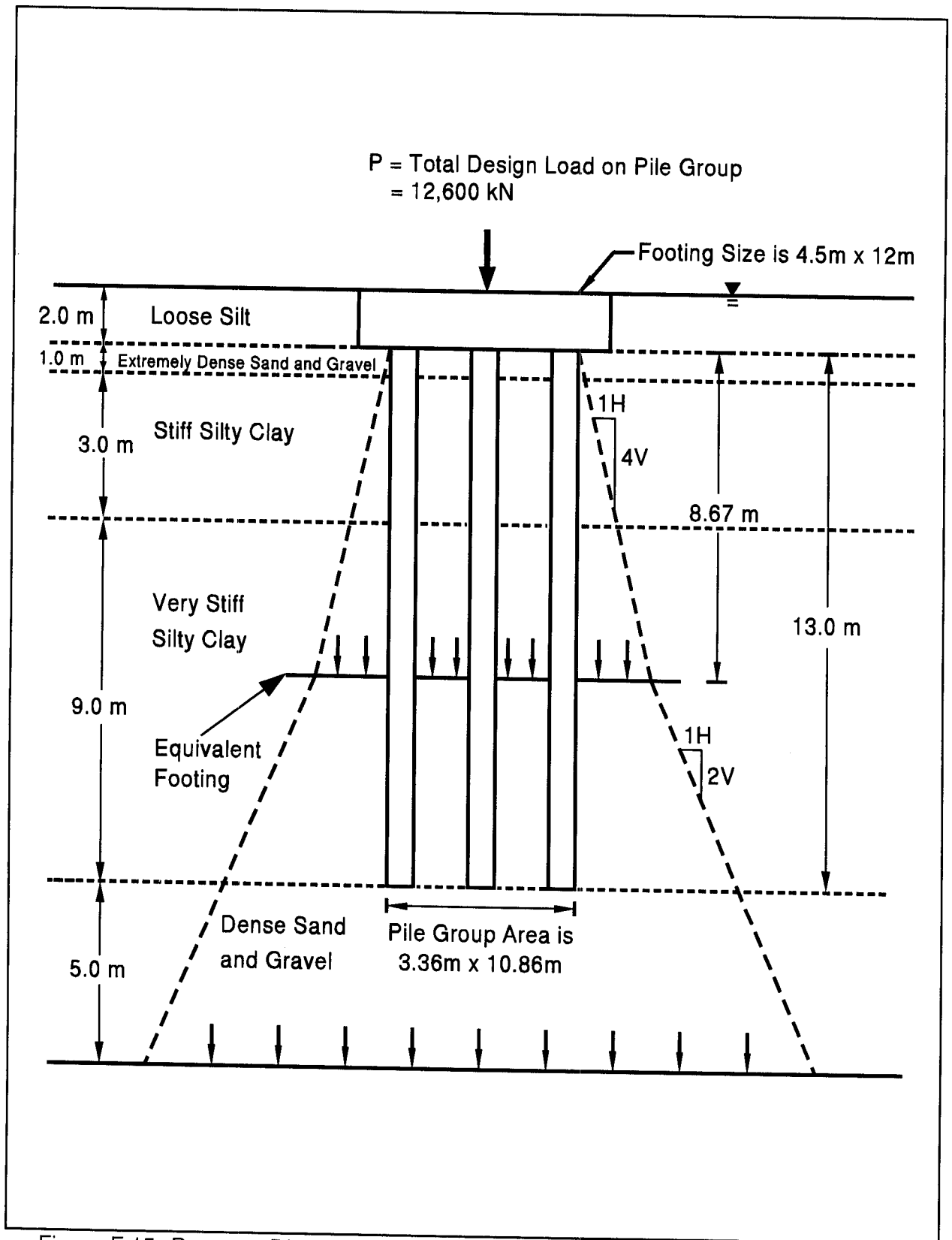


Figure F.15 Pressure Distribution Below Equivalent Footing for Pile Group at Pier 3

Table F-1 Summary of Pressure Distribution Below Equivalent Footing							
Depth Below Existing Ground (m)	Depth Below Equivalent Footing (m)	Load Distribution Surface			Imposed Pressure Increase Δp (kPa)	Effective Overburden Pressure p_o (kPa)	$\left(\frac{\Delta p}{p_o}\right)$ 100% (%)
		Width B_2 (m)	Length Z_2 (m)	Area $(B_2)(Z_2)$ (m ²)			
10.67	0.00	7.70	15.20	117.0	107.66	98.77	109.0
11.34	0.67	8.37	15.87	132.8	94.88	105.74	89.7
12.75	2.08	9.78	17.28	169.0	74.56	120.40	61.9
14.25	3.58	11.28	18.78	211.8	59.48	136.00	43.7
15.75	5.08	12.78	20.28	259.2	48.62	151.53	32.1
17.25	6.58	14.28	21.78	311.0	40.51	166.98	24.3
18.75	8.08	15.78	23.28	367.4	34.30	182.43	18.8
19.75	9.08	16.78	24.28	407.4	30.93	192.73	16.1

Note: Equivalent Footing is at 10.67 meters below existing ground.

STEP 1 (continued)

- f. Determine the imposed pressure increase, Δp , at the midpoint of each affected soil layer based on the appropriate pressure distribution surface.

The imposed pressure increase, Δp , at the midpoint of each affected soil layer is presented in column 6 of Table F-2. Calculations of the imposed pressure increase based on the pressure distribution area were presented earlier in Step 1c.

STEP 2 Determine consolidation test parameters for the cohesive soil layer.

The laboratory consolidation test results on the undisturbed samples of stiff silty clay from layer 2 and very stiff silty clay from layer 3 were plotted on the "log pressure, p versus void ratio, e " (similar to Figure 9.43).

Table F-2 Settlement Calculations

1 Soil Type	2 Soil Layer Below Existing Ground (m)	3 Soil Layer Thickness (m)	4 Depth of Midpoint Below Existing Ground (m)	5 Effective Overburden Pressure at Midpoint p_o (kPa)	6 Imposed Pressure Increase at Midpoint Δp (kPa)	7 $(p_o + \Delta p)$ (kPa)	8 Layer Settlement (m)
Layer 3 $p_c=297$ kPa; $e_o=0.54$ $C_c=0.20$; $C_{cr}=0.020$	10.67 - 12.00	1.33	11.34	105.74	94.88	200.62	0.0048
	12.00 - 13.50	1.50	12.75	120.40	74.56	194.96	0.0041
	13.50 - 15.00	1.50	14.25	136.00	59.48	195.48	0.0031
Layer 4 $\bar{N}'=33$; $C'=146$ $\bar{N}'=38$; $C'=173$ $\bar{N}'=33$; $C'=146$ $\bar{N}'=39$; $C'=180$							
	15.00 - 16.50	1.50	15.75	151.53	48.62	200.15	0.0012
	16.50 - 18.00	1.50	17.25	166.98	40.51	207.49	0.0008
	18.00 - 19.50	1.50	18.75	182.43	34.30	216.73	0.0008
	19.50 - 20.00	0.50	19.75	192.73	30.93	223.66	0.0002
Total Settlement =							0.0150

F-128

STEP 2 (continued)

The following consolidation test parameters were obtained from the plot.

Soil Layer 3 (very stiff silty clay):

Preconsolidation pressure, $p_c = 297$ kPa

Initial void ratio, $e_0 = 0.54$

Compression index, $C_c = 0.20$

Recompression index, $C_{cr} = 0.020$

STEP 3 Determine bearing capacity index for each cohesionless layer.

Determine the average corrected SPT N' value, \bar{N}' , for each cohesionless layer. Use \bar{N}' for the appropriate SPT hammer type in Figure 9.45 to obtain the bearing capacity index for each layer.

Soil Layer 4:

Layer 15.0 - 16.5: $\bar{N}' = 33$ from Safety Hammer; $C' = 146$ from Figure 9.45

Layer 16.5 - 18.0: $\bar{N}' = 38$ from Safety Hammer; $C' = 173$ from Figure 9.45

Layer 18.0 - 19.5: $\bar{N}' = 33$ from Safety Hammer; $C' = 146$ from Figure 9.45

Layer 19.5 - 20.0: $\bar{N}' = 39$ from Safety Hammer; $C' = 180$ from Figure 9.45

STEP 4 Compute settlement due to soil compression.

Compute settlement of each cohesive soil layer using the following equations:

$$s = H \left[\frac{C_{cr}}{1+e_0} \log \frac{p_o + \Delta p}{p_o} \right] \quad \text{when } p_o + \Delta p \leq p_c$$

$$= H \left[\frac{C_{cr}}{1+e_0} \log \frac{p_c}{p_o} \right] + H \left[\frac{C_c}{1+e_0} \log \frac{p_o + \Delta p}{p_c} \right] \quad \text{when } p_o + \Delta p > p_c$$

For example, the soil layer increment 10.67 m to 12.00 m corresponds to:

$$(p_o + \Delta p) = 200.62 \text{ kPa} < p_c = 297 \text{ kPa}$$

STEP 4 (continued)

Therefore, layer settlement as shown in column 8 of settlement calculations table:

$$\begin{aligned} s &= H \left[\frac{C_{cr}}{1+e_0} \log \frac{p_o + \Delta p}{p_o} \right] \\ &= 1.33 \left[\frac{0.020}{(1+0.54)} \log \left(\frac{200.62}{105.74} \right) \right] = 0.0048 \text{ m} \end{aligned}$$

Compute settlement of each cohesionless soil layer using the following equations:

$$s = H \left[\frac{1}{C'} \log \frac{p_o + \Delta p}{p_o} \right]$$

For the soil layer increment 15.0 m to 16.5 m corresponds to soil layer 3:

Therefore, the settlement for the soil layer increment as shown in column 8 of Table F-2 is:

$$s = 1.50 \left[\frac{1}{146} \log \left(\frac{200.15}{151.53} \right) \right] = 0.0012 \text{ m}$$

Following similar procedures, the total estimated pile group settlement due to soil compression is equal to the sum of settlements of all layers, or the sum of column 8 of Table F-2 and is equal to 0.0150 meter or 15.0 mm.

STEP 5 Calculate the elastic compression of pile material under design load on each pile. (See Section 9.8.2.1)

Note, for elastic compression calculations, it is assumed that all piles in the group are loaded with the 890 kN design load. This assumption is conservative because piles in the middle and rear rows have smaller loads. The elastic compression of each pile can be calculated with the following expression:

$$\Delta = \frac{Q_a L}{A E}$$

STEP 5 (continued)

Where:

L = Length of pile (mm) = 13,000 mm

A = Pile cross sectional area (m²) = 0.127 m²

E = Modulus of elasticity of pile material (kPa) = 27.8 x 10⁶ kPa

Q_a = Design axial load in pile (kN), as discussed below.

Because of shaft resistances, the axial load transferred to the pile varies along the length of the pile. Therefore, for elastic compression calculations the pile should be divided into segments with the average axial load in each segment calculated. For this example, the pile is divided into three segments based on the soil layers presented in Figure F.9. The first segment is 1.0 meter length, the second is 3.0 meters, and the third is 9.0 meters. The shaft resistance as calculated using the Nordlund method for the cohesionless soil layer and the α -method for the cohesive soil layer (as presented in Section F.2.3.1) for the first, second, and third segment is 22 kN, 453 kN, and 696 kN, respectively.

The average axial load transferred to each pile segment is equal to the axial load transferred to the mid-length of the segment, as shown in Figure F.16. The average axial load is used to calculate the elastic compression of each pile segment. Figure F.16 also shows that there is 868 kN to be transferred to soil layer 2, and 415 kN to be transferred to soil layer 3 which is capable of supporting up to 696 kN over the 9.0 meter layer thickness. Therefore, the 415 kN load will be fully transferred to the soil at depth of (415 kN / 696 kN) times (9.0 meters), or 5.366 meters below the top of layer 3, or the 890 kN total load will be fully transferred to the soil at depth of 9.366 meters below the pile cap. In other words, the lower 3.634 meters of the pile will not be subjected to any load or elastic compression.

$$\text{Pile segment 1: } \Delta_1 = \frac{(879 \text{ kN}) (1,000 \text{ mm})}{(0.127 \text{ m}^2) (27,800,000 \text{ kPa})} = 0.249 \text{ mm}$$

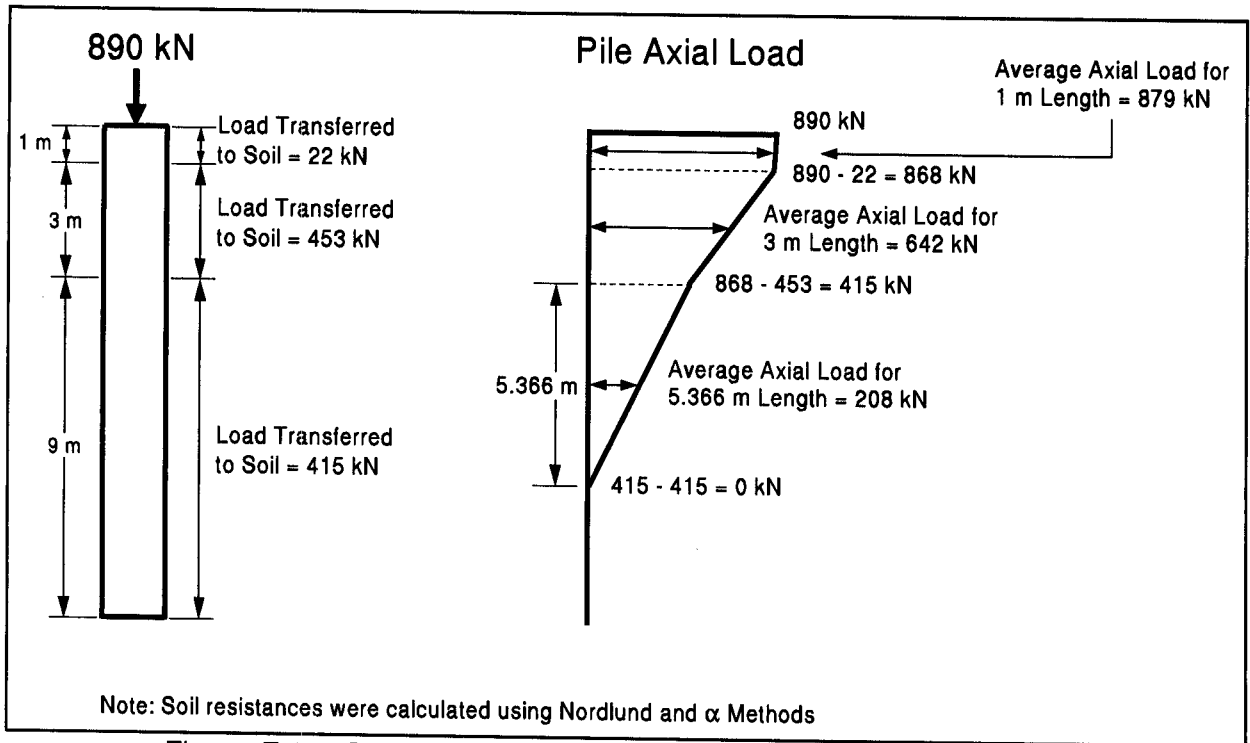


Figure F.16 Calculation of Axial Load Transfer to the Pile at Pier 3

STEP 5 (continued)

$$\text{Pile segment 2: } \Delta_2 = \frac{(642 \text{ kN}) (3,000 \text{ mm})}{(0.127 \text{ m}^2) (27,800,000 \text{ kPa})} = 0.546 \text{ mm}$$

$$\text{Pile segment 3: } \Delta_3 = \frac{(208 \text{ kN}) (5,366 \text{ mm})}{(0.127 \text{ m}^2) (27,800,000 \text{ kPa})} = 0.316 \text{ mm}$$

$$\begin{aligned} \text{Total: } \Delta &= \Delta_1 + \Delta_2 + \Delta_3 \\ &= 0.249 \text{ mm} + 0.546 \text{ mm} + 0.316 = 1.111 \text{ mm} \end{aligned}$$

Note: The elastic pile compression is small relative to the soil compression (15.0 mm), and therefore it is usually ignored.

STEP 6 Compute total pile group settlement.

$$\begin{aligned}\Delta(\text{ total }) &= \Delta(\text{ soil compression }) + \Delta(\text{ elastic pile compression }) \\ &= 15.0 \text{ mm} + 1.111 \text{ mm} = 16.111 \text{ mm or } 0.016 \text{ m}\end{aligned}$$

The total pile group settlement is smaller than the maximum allowable pile group settlement of 25 mm.

The Meyerhof method for settlement calculations based on SPT test data (Section 9.8.2.2a) will be performed on the following to compare with settlement calculated above.

STEP 1 Calculate total pile group settlement due to soil compression.

Meyerhof recommended that the settlement of a pile group in a homogeneous sand deposit not underlain by a more compressible soil at greater depth may be conservatively estimated by the following expression:

$$s = \frac{0.96 p_f \sqrt{B} I_f}{\bar{N}'}$$

Where:

p_f = foundation pressure (kPa). Group load divided by group area. Notes: settlement should be calculated for the design load to be imposed on the pile group, and not the ultimate or allowable pile group capacities.

$$= \frac{12,600 \text{ kN}}{(3.36 \text{ m})(10.86 \text{ m})} = 345 \text{ kPa}$$

B = the width of pile group = 3.36 m

\bar{N}' = average corrected SPT N' value within a depth B below pile toe level

$$= \frac{33 + 38 + 33}{3} = 35$$

STEP 1 (continued)

D = pile embedment depth = 13 m

I_r = influence factor for group embedment

$$= 1 - [D / 8B] \geq 0.5$$

$$= 1 - [(13 \text{ m}) / 8 (3.36 \text{ m})] = 0.516$$

Therefore,

s = estimated total pile group settlement due to soil compression

$$= \frac{0.96 (345 \text{ kPa}) \sqrt{3.36} (0.516)}{35} = 8.95 \text{ mm}$$

The settlement estimated using the Meyerhof method (8.95 mm) is less than the settlement calculated based on the equivalent method (15.2 mm). In this soil profile, the equivalent footing method calculates most of the foundation settlement (12 mm) to occur in the clay layer with minimal settlement of the underlying sand layer in which the piles are founded. It is unlikely that the magnitude of settlement calculated in the clay layer would occur due to the lack of strain compatibility between the layers. Therefore, the Meyerhof method is a better estimate of group settlement in this profile.

F.3.4 South Abutment - Equivalent Footing Method

For the pile group at the South Abutment and the soil profile interpreted from Soil Boring S-4 as shown in Figure F.11. Calculate the immediate settlements of pile groups using the equivalent footing method for an embedded pile length of 17.5 meters. Use the step-by-step method outlined in Section 9.8.2.3.

STEP 1 Determine the new load imposed on soil by the pile group.

- a. Determine the location of the equivalent footing.

The location of the equivalent footing is based on the shaft and toe resistance condition and the soil profile. Figure 9.44 should be used to determine the location of the equivalent footing and the pressure distribution. The soil profile for Soil Boring S-4 matches Figure 9.44(b), and therefore the equivalent footing is placed at depth of $\frac{2}{3} D$ from the bottom of the pile cap as shown in the figure.

Depth of Equivalent Footing:

- below the pile cap $= \frac{2}{3} (17.5 \text{ m}) = 11.67 \text{ m}$
- or below the existing ground $= 11.67 \text{ m} + 1.50 \text{ m} = 13.17 \text{ m}$

- b. Determine the dimensions of the equivalent footing.

All the piles in the pile group are vertical, and the pile group has a dimension of 3.36 meters by 10.86 meters. To account for load transfer, the equivalent footing has a modified dimension that spreads as a pyramid with a side slope of 1H:4V, as shown in Figure 9.44(b). Since the equivalent footing is 11.67 meters below the pile cap, the equivalent footing dimensions are:

$$\begin{aligned} \text{The width of the equivalent footing, } B_1 &= 3.36 \text{ m} + 2 \left(\frac{11.67 \text{ m}}{4} \right) \\ &= 9.20 \text{ m} \end{aligned}$$

STEP 1 (continued)

$$\begin{aligned}\text{The length of the equivalent footing, } Z_1 &= 10.86 \text{ m} + 2 \left(\frac{11.67 \text{ m}}{4} \right) \\ &= 16.70 \text{ m}\end{aligned}$$

- c. Determine the pressure distribution to soil layers below the equivalent footing up to the depth at which the pressure increase from the equivalent footing is less than 10% of existing effective overburden pressure at that depth.

The pressure distribution diagram below the equivalent footing is presented in Figure F.17. Note, the pressure distribution area increases with depth below the equivalent footing which results in a pressure reduction with depth below the equivalent footing. The dimension of the pressure distribution surface also spreads as a pyramid with depth but with a side slope of 1H:2V.

For example, at depth of 0.17 meter below the equivalent footing (or 13.34 meters below the existing ground surface), the pressure distribution surface has the following dimensions:

$$\text{Width of pressure distribution surface, } B_2 = 9.20 \text{ m} + 2 \left(\frac{0.17 \text{ m}}{2} \right) = 9.37 \text{ m}$$

$$\text{Length of pressure distribution surface, } Z_2 = 16.70 \text{ m} + 2 \left(\frac{0.17 \text{ m}}{2} \right) = 16.87 \text{ m}$$

$$\begin{aligned}\text{Area of pressure distribution surface, } A_2 &= (B_2) (Z_2) = (9.37 \text{ m}) (16.87 \text{ m}) \\ &= 158.1 \text{ m}^2\end{aligned}$$

Therefore, at depth of 0.17 meter below the equivalent footing the pressure increase due to the imposed design load is:

$$\Delta p = \left(\frac{12,600 \text{ kN}}{158.1 \text{ m}^2} \right) = 79.71 \text{ kPa}$$

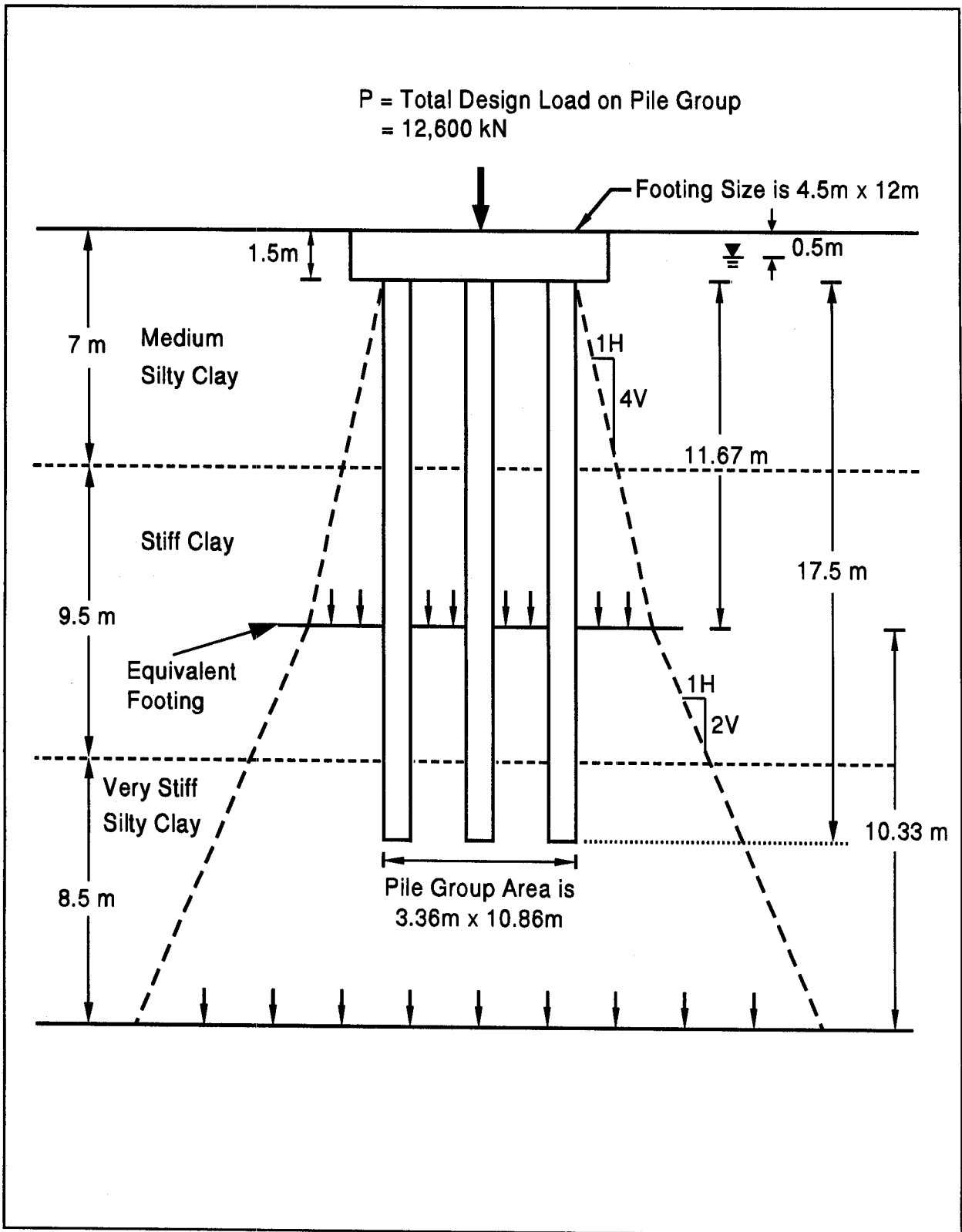


Figure F.17 Pressure Distribution Below Equivalent Footing for Pile Group at the South Abutment

STEP 1 (continued)

The pressure increase at other locations below the equivalent footing is summarized in Table F-3. The imposed pressure increase becomes less than 10% of existing effective overburden pressure at depth of 11.58 meters below the equivalent footing or 24.75 meters below the existing ground.

- d. Divide the cohesive soil layers in the affected pressure increase zone into several thinner layers of 1.5 to 3 meter thickness. The thickness of each layer is the thickness H for the settlement computation for that layer.

For this example, the soil is divided into 1.5 meter thick layers as presented in column 3 of Table F-4. The soil layer boundaries are presented in column 2 of Table F-4.

- e. Determine the existing effective overburden pressure, p_o , at the midpoint of each layer.

The midpoint location of each soil layer below the existing ground is presented in column 4 of Table F-4. The effective overburden pressure, p_o , at the midpoint of each layer is presented in column 5 of Table F-4.

- f. Determine the imposed pressure increase, Δp , at the midpoint of each affected soil layer based on the appropriate pressure distribution surface.

The imposed pressure increase, Δp , at the midpoint of each affected soil layer is presented in column 6 of Table F-4. Calculations of the imposed pressure increase based on the pressure distribution area were presented earlier in Step 1c.

Table F-3 Summary of Pressure Distribution Below Equivalent Footing							
Depth Below Existing Ground (m)	Depth Below Equivalent Footing (m)	Load Distribution Surface			Imposed Pressure Increase Δp (kPa)	Effective Overburden Pressure p_o (kPa)	$\left(\frac{\Delta p}{p_o}\right)$ 100% (%)
		Width B_2 (m)	Length Z_2 (m)	Area $(B_2)(Z_2)$ (m ²)			
13.17	0.00	9.20	16.70	153.5	82.08	129.15	63.6
13.34	0.17	9.37	16.87	158.1	79.71	130.80	60.9
14.25	1.08	10.28	17.78	182.8	68.94	139.63	49.4
15.75	2.58	11.78	19.28	227.1	55.48	154.18	36.0
17.25	4.08	13.28	20.78	276.0	45.66	169.33	27.0
18.75	5.58	14.78	22.28	329.3	38.26	185.08	20.7
20.25	7.08	16.28	23.78	387.1	32.55	200.83	16.2
21.75	8.58	17.78	25.28	449.5	28.03	216.58	12.9
23.25	10.08	19.28	26.78	516.3	24.40	232.33	10.5
24.75	11.58	20.78	28.28	587.7	21.44	248.08	8.6

Note: Equivalent Footing is at 13.17 meters below existing ground.

STEP 2 Determine consolidation test parameters.

The laboratory consolidation test results on the undisturbed samples of stiff silty clay from layer 2 and very stiff silty clay from layer 3 were plotted on the "log pressure, p versus void ratio, e " (similar to Figure 9.43). The following consolidation test parameters were obtained from the plot.

Soil Layer 2:

Preconsolidation pressure, $p_c = 200$ kPa

Initial void ratio, $e_o = 0.80$

Compression index, $C_c = 0.30$

Recompression index, $C_{cr} = 0.030$

Table F-4 Settlement Calculations

1 Soil Type	2 Soil Layer Below Existing Ground (m)	3 Soil Layer Thickness (m)	4 Depth of Midpoint Below Existing Ground (m)	5 Effective Overburden Pressure at Midpoint p_o (kPa)	6 Imposed Pressure Increase at Midpoint Δp (kPa)	7 $(p_o + \Delta p)$ (kPa)	8 Layer Settlement (m)
Layer 2 $p_c=200$ kPa; $e_o=0.80$ $C_c=0.30$; $C_{\alpha}=0.030$	13.17 - 13.50	0.33	13.34	130.80	79.71	210.51	0.0022
	13.50 - 15.00	1.50	14.25	139.63	68.94	208.57	0.0085
	15.00 - 16.50	1.50	15.75	154.18	55.48	209.66	0.0079
Layer 3 $p_c=297$ kPa $e_o=0.54$ $C_c=0.20$ $C_{\alpha}=0.020$	16.50 - 18.00	1.50	17.25	169.33	45.66	214.99	0.0020
	18.00 - 19.50	1.50	18.75	185.08	38.26	223.34	0.0016
	19.50 - 21.00	1.50	20.25	200.83	32.55	233.38	0.0013
	21.00 - 22.50	1.50	21.75	216.58	28.03	244.61	0.0010
	22.50 - 24.00	1.50	23.25	232.33	24.40	256.73	0.0008
	24.00 - 25.50	1.50	24.75	248.08	21.44	269.52	0.0007
Total Settlement =							0.0260

STEP 2 (continued)

Soil Layer 3:

Preconsolidation pressure, $p_c = 297$ kPa

Initial void ratio, $e_0 = 0.54$

Compression index, $C_c = 0.20$

Recompression index, $C_{cr} = 0.020$

STEP 3 Compute settlement due to soil compression.

Compute settlement of each soil layer using the following equations:

$$s = H \left[\frac{C_{cr}}{1+e_0} \log \frac{p_o + \Delta p}{p_o} \right] \quad \text{when } p_o + \Delta p \leq p_c$$

$$= H \left[\frac{C_{cr}}{1+e_0} \log \frac{p_c}{p_o} \right] + H \left[\frac{C_c}{1+e_0} \log \frac{p_o + \Delta p}{p_c} \right] \quad \text{when } p_o + \Delta p > p_c$$

For example, the soil layer increment 13.17 m to 13.50 m corresponds to:

$$(p_o + \Delta p) = 210.51 \text{ kPa} > p_c = 200 \text{ kPa}$$

Therefore, layer settlement as shown in column 8 of settlement calculations table:

$$\begin{aligned} s &= H \left[\frac{C_{cr}}{1+e_0} \log \frac{p_c}{p_o} \right] + H \left[\frac{C_c}{1+e_0} \log \frac{p_o + \Delta p}{p_c} \right] \\ &= 0.33 \left[\frac{0.030}{(1+0.80)} \log \left(\frac{200}{130.80} \right) \right] + 0.33 \left[\frac{0.30}{(1+0.80)} \log \left(\frac{210.51}{200} \right) \right] = 0.0022 \text{ m} \end{aligned}$$

For the soil layer increment 16.50 m to 18.00 m corresponds to soil layer 3:

$$(p_o + \Delta p) = 214.99 \text{ kPa} < p_c = 297 \text{ kPa}$$

STEP 3 (continued)

Therefore, the settlement for the soil layer increment as shown in column 8 of Table F-4 is:

$$s = H \left[\frac{C_{cr}}{1+e_0} \log \frac{p_o + \Delta p}{p_o} \right]$$
$$= 1.5 \left[\frac{0.020}{(1+0.54)} \log \left(\frac{214.99}{169.33} \right) \right] = 0.0020 \text{ m}$$

Following similar procedures, the total estimated pile group settlement due to soil compression is equal to the sum of settlements of all layers, or the sum of column 8 of Table F-4 and is equal to 0.0260 meter or 26.0 mm.

STEP 4 Calculate the elastic compression of pile material under design load on each pile as described in Section 9.8.2.1a.

Note, for elastic compression calculations, it is assumed that all piles in the group are loaded with the 890 kN design load. This assumption is conservative because piles in the middle and rear rows have smaller loads. The elastic compression of each pile can be calculated with the following expression:

$$\Delta = \frac{Q_a L}{A E}$$

Where:

L = Length of pile (mm) = 17,500 mm

A = Pile cross sectional area (m²) = 0.127 m²

E = Modulus of elasticity of pile material (kPa) = 27.8 x 10⁶ kPa

Q_a = Design axial load in pile (kN), as discussed below.

STEP 4 (continued)

Because of shaft resistances, the axial load transferred to the pile varies along the length of the pile. Therefore, for elastic compression calculations the pile should be divided into segments with the average axial load in each segment calculated. For this example, the pile is divided into three segments based on the soil layers presented in Figure F.11. The first segment is 5.5 meters length, the second is 9.5 meters, and the third is 2.5 meters. The shaft resistance as calculated using the α -method (as presented in Section F.2.4.1) for the first, second, and third segment is 259 kN, 1,150 kN, and 239 kN, respectively.

The average axial load transferred to each pile segment is equal to the axial load transferred to the mid-length of the segment, as shown in Figure F.18. The average axial load is used to calculate the elastic compression of each pile segment. Figure F.18 also shows that there is 631 kN to be transferred to soil layer 2 which is capable of supporting up to 1,150 kN over the 9.5 meter layer thickness. Therefore, the 631 kN load will be fully transferred to the soil at depth of $(631 \text{ kN} / 1,150 \text{ kN})$ times (9.5 meters) , or 5.213 meters below the top of layer 2, or the 890 kN total load will be fully transferred to the soil at depth of 10.713 meters below the pile cap. In other words, the lower 6.787 meters of the pile will not be subjected to any load or elastic compression.

$$\text{Pile segment 1: } \Delta_1 = \frac{(761 \text{ kN}) (5,500 \text{ mm})}{(0.127 \text{ m}^2) (27,800,000 \text{ kPa})} = 1.186 \text{ mm}$$

$$\text{Pile segment 2: } \Delta_2 = \frac{(316 \text{ kN}) (5,213 \text{ mm})}{(0.127 \text{ m}^2) (27,800,000 \text{ kPa})} = 0.467 \text{ mm}$$

$$\begin{aligned} \text{Total: } \Delta &= \Delta_1 + \Delta_2 \\ &= 1.186 \text{ mm} + 0.467 \text{ mm} = 1.653 \text{ mm} \end{aligned}$$

Note: The elastic pile compression is small relative to the soil compression (26.0 mm), and therefore it is usually ignored.

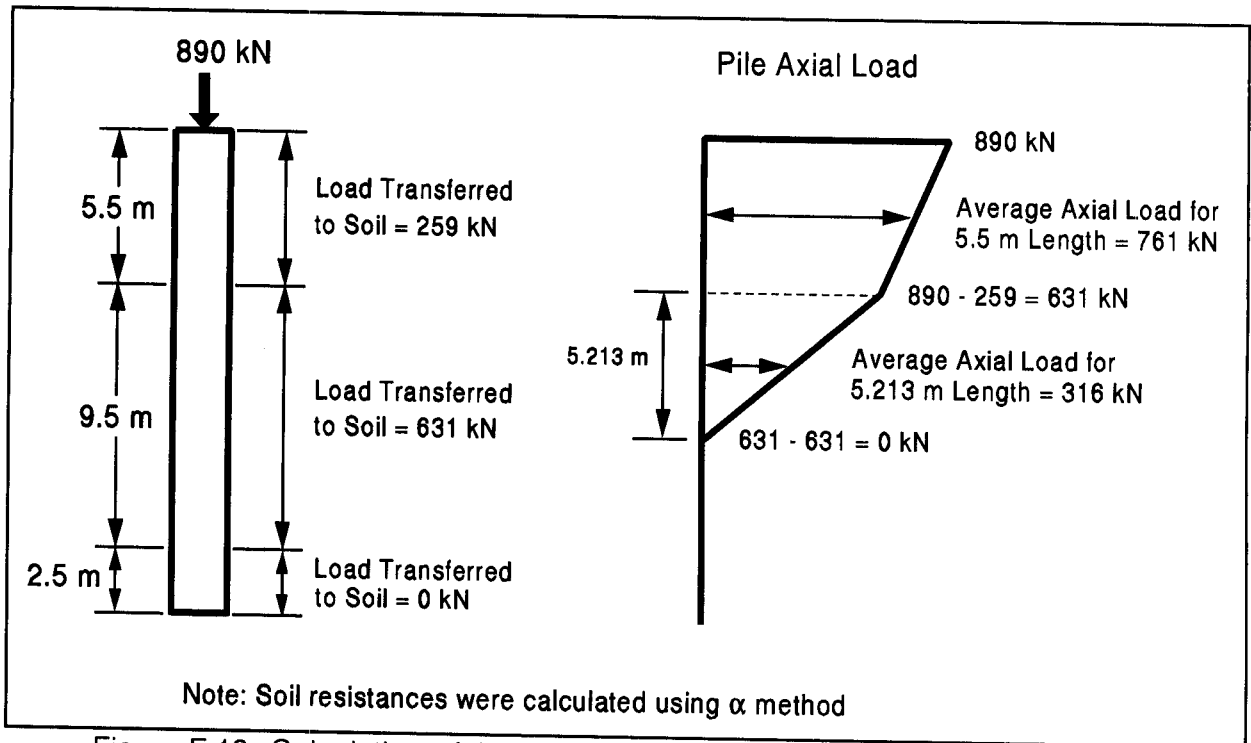


Figure F.18 Calculation of Axial Load Transfer to the Pile at South Abutment

STEP 5 Compute total pile group settlement.

$$\begin{aligned}
 \Delta(\text{total}) &= \Delta(\text{soil compression}) + \Delta(\text{elastic pile compression}) \\
 &= 26.0 \text{ mm} + 1.653 \text{ mm} \\
 &= 27.653 \text{ mm} \quad \text{or} \quad 0.028 \text{ m}
 \end{aligned}$$

The total pile group settlement is larger than the maximum allowable pile group settlement of 25 mm. The total settlement will even be larger after the placement of the approach embankment fill materials behind the abutment wall, as discussed in Section F.6. Therefore, preloading of the South Abutment should be performed prior to pile installation. The interaction of the approach embankment fill with the South Abutment foundation is discussed in greater detail in Section F.6.

F.4 LATERAL PILE CAPACITY ANALYSIS

The bridge division estimated that the group lateral loads range from 600 kN at the interior pile groups to 900 kN at the abutment pile groups. The maximum lateral load per pile is limited to 40 kN. A horizontal deflection of up to 10 mm is permissible under lateral loading.

F.4.1 Broms' Method - North Abutment

Perform a lateral pile capacity analysis for a pile at the North Abutment using Soil Boring S-1 as shown in Figure F.3. Perform the analysis based on an embedded pile length of 11.5 meters. Use the step by step procedure for the Broms' method outlined in Section 9.7.3.2.

STEP 1 Determine the general soil type within the critical depth below ground surface (about 4 or 5 pile diameters).

For pile diameter of 0.356 meter, the critical depth below the ground surface is about 1.42 to 1.78 meters. Based on the soil conditions for the North Abutment shown in Figure F.3, the general soil type within the critical depth below the ground surface is a loose silty fine sand cohesionless soil.

STEP 2 Determine the coefficient of horizontal subgrade reaction, K_h , within the critical depth based on cohesive or cohesionless soils.

For cohesionless soils, choose the K_h from Table 9-11 based on soil density and ground water table. For a loose silty fine sand, K_h is either 1,086 or 1,900 kN/m³ depending on whether the ground water table is below or above the critical depth, respectively. When the ground water table is within the critical depth region, a linear interpolation between these two values should be used to calculate K_h .

Assuming the critical depth is at 1.60 meters depth below the bottom of the excavation. Based on Figure F.3, the ground water table is at 1.0 meter below the bottom of the excavation. Therefore, using a linear interpolation, the coefficient of horizontal subgrade reaction, K_h , is:

STEP 2 (continued)

$$K_h = 1,086 + \frac{1.00}{1.60} (1,900 - 1,086) = 1,595 \text{ kN/m}^3$$

STEP 3 Adjust K_h for loading and soil conditions.

Assuming that a cyclic loading exists at the site. For cyclic loading in loose cohesionless soils:

$$\begin{aligned} K_h &= \frac{1}{4} K_h \\ &= \frac{1}{4} (1,595) = 399 \text{ kN/m}^3 \end{aligned}$$

STEP 4 Determine pile parameters.

- a. Modulus of elasticity, E = 27,800 MPa
- b. Moment of inertia, I = $1.32 \times 10^{-3} \text{ m}^4$
- c. Section modulus, S = $7.46 \times 10^{-3} \text{ m}^3$
- d. Ultimate compressive strength, f'_c = 34.5 MPa
- e. Embedded pile length, D = 11.5 m
- f. Pile width, b = 0.356 m
- g. Eccentricity of applied load, e_c = 0 for fixed-headed pile
- h. Dimensionless shape factor, C_s , applied only to steel piles.
- i. Resisting moment of pile, M_y = $f'_c S$ for concrete piles
= 34.5 MPa ($7.46 \times 10^{-3} \text{ m}^3$)
= 257.4 kN-m

STEP 5 Determine η for cohesionless soils.

$$\eta = \sqrt[5]{K_H/EI} = \sqrt[5]{\frac{399 \text{ kN/m}^3}{(27.8 \times 10^6 \text{ kN/m}^2) (1.32 \times 10^{-3} \text{ m}^4)}} \\ = 0.405 \text{ m}^{-1}$$

STEP 6 Determine the dimensionless length factor for cohesionless soil.

$$\eta D = 0.405 \text{ m}^{-1} (11.5 \text{ m}) = 4.66$$

STEP 7 Determine if pile is long or short according to the cohesionless soil criteria.

Since $\eta D = 4.66$ is greater than 4.0, the pile is long.

STEP 8 Determine other soil parameters.

a. Rankine passive pressure coefficient for cohesionless soil, K_p , is:

$$K_p = \tan^2 (45 + \phi/2)$$

where ϕ is the average soil friction angle along the embedded pile length.

As shown in Figure F.3, the soil profile along the embedded pile length is divided into three layers. As discussed in Section F.2.1.2, the soil friction angle, ϕ , from each layer is calculated using the corrected SPT N' value and Table 4-5.

$$\text{Layer 1 (4 m depth): } \bar{N}'_1 = 8 \quad \rightarrow \quad \phi_1 = 29^\circ$$

$$\text{Layer 2 (7 m depth): } \bar{N}'_2 = 14 \quad \rightarrow \quad \phi_2 = 31^\circ$$

$$\text{Layer 3 (0.5 m depth): } \bar{N}'_3 = 34 \quad \rightarrow \quad \phi_3 = 36^\circ$$

The average ϕ angle is calculated from the weighted ϕ angle based on the thickness of each layer.

STEP 8 (continued)

The average ϕ angle is:

$$\phi = \frac{29^\circ (4 \text{ m}) + 31^\circ (7 \text{ m}) + 36^\circ (0.5 \text{ m})}{11.5 \text{ m}} = 30.5^\circ$$

Therefore, the Rankine passive pressure coefficient, K_p , is:

$$\begin{aligned} K_p &= \tan^2 (45 + \phi/2) \\ &= \tan^2 (45 + 30.5/2) = 3.06 \end{aligned}$$

b. Average effective soil unit weight over embedded length of pile, γ (kN/m^3).

The average effective soil unit weight, γ , will also be calculated from the weighted γ of each layer based on the thickness of each layer.

$$\begin{aligned} \gamma &= \frac{16.5 \text{ kN/m}^3 (1 \text{ m}) + 6.7 \text{ kN/m}^3 (3 \text{ m}) + 7.8 \text{ kN/m}^3 (7 \text{ m}) + 9.8 \text{ kN/m}^3 (0.5 \text{ m})}{11.5 \text{ m}} \\ &= 8.36 \text{ kN/m}^3 \end{aligned}$$

STEP 9 Determine the ultimate (failure) lateral load, Q_u , for a single pile.

The pile will be used in a group under a pile cap, therefore it is considered a fixed headed pile. For a long fixed headed pile in a cohesionless soil, Figure 9.30 should be used to calculate the ultimate load. First $M_y/(b^4 \gamma K_p)$ must be calculated.

$$\frac{M_y}{b^4 \gamma K_p} = \frac{257.4 \text{ kN-m}}{(0.356 \text{ m})^4 (8.36 \text{ kN/m}^3) (3.06)} = 626$$

Enter Figure 9.30 with this value to the fixed head curve to obtain $Q_u/K_p b^3 \gamma = 190$.

STEP 9 (continued)

So,

$$\begin{aligned} Q_u &= 190 K_p b^3 \gamma \\ &= 190 (3.06) (0.356 \text{ m})^3 (8.36 \text{ kN/m}^3) \\ &= 219 \text{ kN} \end{aligned}$$

STEP 10 Calculate the maximum allowable working load for a single pile, Q_m , from the ultimate load, Q_u , determined in Step 9, as shown in Figure 9.31.

$$Q_m = \frac{Q_u}{2.5} = \frac{219 \text{ kN}}{2.5} = 88 \text{ kN}$$

STEP 11 Calculate the deflection, y , corresponding to the desired design load, Q_a of 40 kN.

For fixed headed pile in cohesionless soil, enter Figure 9.33 with $\eta D = 4.66$ to obtain $y(EI)^{3/5} K_h^{2/5} / Q_a D$. This results in

$$y(EI)^{3/5} K_h^{2/5} / Q_a D = 0.21$$

The calculated deflection y is:

$$\begin{aligned} y &= 0.21 Q_a D / (EI)^{3/5} K_h^{2/5} \\ &= 0.21 (40 \text{ kN}) (11.5 \text{ m}) / (27.8 \times 10^6 \text{ kN/m}^2)^{3/5} (1.32 \times 10^{-3} \text{ m}^4)^{3/5} (399 \text{ kN/m}^3)^{2/5} \\ &= 0.016 \text{ m} \quad \text{or} \quad 16 \text{ mm} \end{aligned}$$

Therefore, the desired design load of 40 kN will cause the pile head to deflect 16 mm at the ground surface which exceeds the bridge division's allowable deflection of 10 mm. Therefore, the maximum design load that will not exceed the 10 mm deflection should be determined.

STEP 11 (continued)

$$y = 0.21 Q_a D / (EI)^{3/5} K_h^{2/5}$$

$$.01 = 0.21 (Q_a) (11.5 \text{ m}) / (21 \times 10^6 \text{ kN/m}^2)^{3/5} (1.32 \times 10^{-3} \text{ m}^4)^{3/5} (399 \text{ kN/m}^3)^{2/5}$$

$$Q_a = 0.01 (27.8 \times 10^6 \text{ kN/m}^2)^{3/5} (1.32 \times 10^{-3} \text{ m}^4)^{3/5} (399 \text{ kN/m}^3)^{2/5} / (0.21)(11.5 \text{ m})$$
$$= 24.9 \text{ kN}$$

STEP 12 Compare the design load Q_a , and design deflection, y , with the maximum allowable working load, Q_m , and deflection, y_m .

The maximum design load of 24.9 kN determined from the design deflection is less than the maximum allowable working load of 87 kN.

STEP 13 Reduce the maximum allowable load to account for group effects and method of installation.

a. Group effects.

The center to center pile spacing, z , is designed to be 1.5 meters.

$$(z/b) = (1.5 \text{ m}) / (0.356 \text{ m}) = 4.21$$

Using the reduction factor table and linear interpolation:

$$\text{reduction factor} = 0.532$$

$$\text{So, } Q_m = 0.532 Q_m = 0.532 (88 \text{ kN}) = 47 \text{ kN}$$

b. Method of installation.

No reduction is required for driven piles. So, $Q_m = 47 \text{ kN}$.

STEP 14 Compute the total lateral load capacity of the pile group.

The total lateral load capacity of the pile group is equal to the adjusted allowable load per pile from Step 13b times the number of piles.

$$\text{Total Pile Group Lateral Load Capacity} = 24 (47 \text{ kN}) = 1,128 \text{ kN}$$

However, this group lateral load cannot be achieved at the deflection limit required by the bridge division and therefore a lower group load must be used.

To meet the 10 mm deflection requirements, a design lateral load of 25 kN per pile must be used. This lateral load is less than desired. Therefore, the group capacity of 600 kN (24 piles at 25 kN/pile) is insufficient, and more piles would be required.

F.4.2 COM624P Analysis - North Abutment

A COM624P analysis was performed to evaluate the lateral load capacity of the 356 mm square prestressed concrete pile at the North Abutment. The concrete pile was driven 11.5 m into the dense sand and gravel stratum as depicted in Figure F.3.

The North Abutment concrete pile was analyzed considering full fixity at the base of the pile cap. The geometric and elastic properties of the pile were input along with the relevant soil properties and stratigraphic information. Soil input parameters were obtained from Table 9-12. Moment-dependent flexural rigidity (concrete cracking effects) are included explicitly in the analyses. In order to rigorously evaluate the moment-stiffness relationship (implementing calculations via the PMEIX subroutine), the longitudinal reinforcement (4 No. 8 bars) was also characterized with respect to cross-section geometry and steel properties. The p-y curves were generated by the program assuming cyclic loading conditions were applied. The program calculated internally the flexural rigidity along the pile as a function of bending moment and axial force (assumed full 890 kN compression load) for each applied lateral load level. Ten equal 20 kN increments of load were applied to a maximum of 200 kN. For 40, 80, 120, 160, and 200 kN steps, the full sets of computed values were saved for presentation, while at the intermediate steps only the summary information was retained.

An echo print of the input file is presented on the following page. This is followed by the input and output summary of the PMEIX subroutine results for calculation of the ultimate bending resistance and flexural rigidity of the pile. Last, COM624P generated summaries of the problem input and output are provided. For selected lateral loads, Figures F.19 to F.22 provide graphical presentations of deflection, movement, shear, and soil reaction versus depth.

The COM624P solutions for the North abutment indicate the pile deflection under the 40 kN design load will be 3.8 mm. The corresponding maximum moment and shear stress are -55.6 m-kN and 14,700 kN/m², respectively. The deflection, moment and shear stress under the design load are acceptable. Hence, the more rigorous COM624P analysis indicates a 40 kN design lateral load could be used whereas the Broms' method indicated only a 24.9 kN design load. Additional COM624P analyses should be performed to evaluate group response using the p-multiplier approach described in Section 9.8.4.

FHWA North Abut. - 355 mm-sq PSC Fixed-Head/Cyclic/Crack Modeled

2	3	1			
100	4	1	0		
8	6	0			
11.500		27800000	0.000	0.000	
1	2				
2	1	0	20		
100		0.00000100	1.00000000		
0.0000		0.3550	0.0013	0.1260	
1	4	0.0000	1.0000	6790.0000	
2	4	1.0000	4.0000	5430.0000	
3	4	4.0000	11.0000	16300.0000	
4	4	11.0000	11.5000	33900.0000	
0.0000		16.50000			
1.0000		16.50000			
1.0000		6.70000			
4.0000		6.70000			
4.0000		7.80000			
11.0000		7.80000			
11.0000		9.80000			
11.5000		9.80000			
0.0000		0.0000	29.0000	0.00000	
4.0000		0.0000	29.0000	0.00000	
4.0000		0.0000	30.0000	0.00000	
11.0000		0.0000	30.0000	0.00000	
11.0000		0.0000	36.0000	0.00000	
11.5000		0.0000	36.0000	0.00000	
5					
1.0000					
2.0000					
3.0000					
4.0000					
5.0000					
10					
0	20.0000	0.0000	890.0000		
1	40.0000	0.0000	890.0000		
0	60.0000	0.0000	890.0000		
1	80.0000	0.0000	890.0000		
0	100.0000	0.0000	890.0000		
1	120.0000	0.0000	890.0000		
0	140.0000	0.0000	890.0000		
1	160.0000	0.0000	890.0000		
0	180.0000	0.0000	890.0000		
1	200.0000	0.0000	890.0000		
1	10				
890.00					
890.00					
890.00					
890.00					
890.00					
890.00					
890.00					
890.00					
890.00					
890.00					
41370.00	248220.00	0.00	206850000.00		
0.36	0.36	0.00	0.00	0.00	0.00
8	4	2	0.0762		
0.1020	0.0006				
-0.1020	0.0006				

North Abutment - Echo of Input File

FHWA North Abut. - 355 mm-sq PSC Fixed-Head/Cyclic/Crack Modeled

 ULTIMATE BENDING RESISTANCE AND FLEXURAL RIGIDITY

WIDTH = .36 M DEPTH = .36 M
 CONCRETE COMPRESSIVE STRENGTH = 41370.00 KN/ M**2
 REBAR YIELD STRENGTH = 248220.00 KN/ M**2
 MODULUS OF ELASTICITY OF STEEL = 206850000.00 KN/ M**2
 NUMBER OF REINFORCING BARS = 4
 NUMBER OF ROWS OF REINFORCING BARS = 2
 COVER THICKNESS = .076 M
 SQUASH LOAD CAPACITY = 4812.99 KN

ROW NUMBER	AREA OF REINFORCEMENT M**2	DISTANCE TO CENTROIDAL AXIS M
1	.000600	.1020
2	.000600	-.1020

OUTPUT RESULTS FOR AN AXIAL LOAD = 890.00 KN

MOMENT M- KN	EI KN- M**2	PHI 1/ M	MAX STR M/ M	N AXIS M
.000	.00000	.000001	.00022	224.368
.000	.00000	.000051	.00023	4.579
38.908	37020.	.001051	.00042	.398
74.839	36489.	.002051	.00058	.284
91.417	29963.	.003051	.00072	.237
103.156	25464.	.004051	.00085	.209
112.645	22302.	.005051	.00097	.191
121.010	19998.	.006051	.00108	.178
128.596	18238.	.007051	.00119	.168
135.593	16842.	.008051	.00129	.160
142.083	15698.	.009051	.00140	.154
145.181	14444.	.010051	.00149	.148
147.090	13310.	.011051	.00157	.142
148.618	12332.	.012051	.00165	.137
149.678	11469.	.013051	.00173	.133
150.685	10724.	.014051	.00181	.129
151.842	10088.	.015051	.00189	.126
152.586	9506.3	.016051	.00197	.123
153.714	9015.0	.017051	.00205	.120
154.229	8544.1	.018051	.00212	.118
154.441	8106.7	.019051	.00219	.115
155.064	7733.5	.020051	.00227	.113
155.653	7394.1	.021051	.00235	.112
155.797	7065.3	.022051	.00242	.110
156.165	6774.8	.023051	.00250	.108
156.452	6505.0	.024051	.00258	.107
156.452	6245.4	.025051	.00266	.106
156.591	6010.9	.026051	.00273	.105
156.601	5789.1	.027051	.00281	.104
156.970	5595.9	.028051	.00289	.103
156.970	5403.2	.029051	.00297	.102
156.970	5223.4	.030051	.00306	.102
156.970	5055.2	.031051	.00314	.101
156.970	4897.5	.032051	.00322	.100
156.970	4749.3	.033051	.00329	.100
156.970	4609.8	.034051	.00338	.099
156.970	4478.3	.035051	.00346	.099
156.970	4354.1	.036051	.00354	.098
156.970	4236.6	.037051	.00363	.098
156.970	4125.2	.038051	.00371	.098
156.970	4019.6	.039051	.00380	.097
156.970	3919.2	.040051	.00388	.097

THE ULTIMATE BENDING MOMENT AT A CONCRETE STRAIN OF 0.003 IS : .157E+03 M- KN

FHWA North Abut. - 355 mm-sq PSC Fixed-Head/Cyclic/Crack Modeled

UNITS--METR

 PILE DEFLECTION, BENDING MOMENT, SHEAR & SOIL RESISTANCE

 INPUT INFORMATION

THE LOADING IS CYCLIC

NO. OF CYCLES = .20E+02

PILE GEOMETRY AND PROPERTIES

PILE LENGTH = 11.50 M
 MODULUS OF ELASTICITY OF PILE = .278E+08 KN/ M**2
 1 SECTION(S)

X	DIAMETER	MOMENT OF INERTIA	AREA
M	M	M**4	M**2
.00			
11.50	.355	.130E-02	.126E+00

SOILS INFORMATION

X-COORDINATE AT THE GROUND SURFACE = .00 M
 SLOPE ANGLE AT THE GROUND SURFACE = .00 DEG.

4 LAYER(S) OF SOIL

LAYER 1

THE LAYER IS A SAND

X AT THE TOP OF THE LAYER = .00 M
 X AT THE BOTTOM OF THE LAYER = 1.00 M
 VARIATION OF SOIL MODULUS, k = .679E+04 KN/ M**3

LAYER 2

THE LAYER IS A SAND

X AT THE TOP OF THE LAYER = 1.00 M
 X AT THE BOTTOM OF THE LAYER = 4.00 M
 VARIATION OF SOIL MODULUS, k = .543E+04 KN/ M**3

LAYER 3

THE LAYER IS A SAND

X AT THE TOP OF THE LAYER = 4.00 M
 X AT THE BOTTOM OF THE LAYER = 11.00 M
 VARIATION OF SOIL MODULUS, k = .163E+05 KN/ M**3

LAYER 4

THE LAYER IS A SAND

X AT THE TOP OF THE LAYER = 11.00 M
 X AT THE BOTTOM OF THE LAYER = 11.50 M
 VARIATION OF SOIL MODULUS, k = .339E+05 KN/ M**3

DISTRIBUTION OF EFFECTIVE UNIT WEIGHT WITH DEPTH

X, M	WEIGHT, KN/ M**3
.00	.17E+02
1.00	.17E+02
1.00	.67E+01
4.00	.67E+01
4.00	.78E+01
11.00	.78E+01
11.00	.98E+01
11.50	.98E+01

DISTRIBUTION OF STRENGTH PARAMETERS WITH DEPTH

X, M	C, KN/ M**2	PHI, DEGREES	E50
.00	.000E+00	29.000	-----
4.00	.000E+00	29.000	-----
4.00	.000E+00	30.000	-----
11.00	.000E+00	30.000	-----
11.00	.000E+00	36.000	-----
11.50	.000E+00	36.000	-----

FHWA North Abut. - 355 mm-sq PSC Fixed-Head/Cyclic/Crack Modeled

UNITS--METR

FINITE DIFFERENCE PARAMETERS

NUMBER OF PILE INCREMENTS	=	100	
TOLERANCE ON DETERMINATION OF DEFLECTIONS	=	.100E-05	M
MAXIMUM NUMBER OF ITERATIONS ALLOWED FOR PILE ANALYSIS	=	100	
MAXIMUM ALLOWABLE DEFLECTION	=	.10E+01	M

INPUT CODES

OUTPT	=	1
KCYCL	=	0
KBC	=	2
KPYOP	=	1
INC	=	2

FHWA North Abut. - 355 mm-sq PSC Fixed-Head/Cyclic/Crack Modeled
UNITS--METR

O U T P U T I N F O R M A T I O N

GENERATED P-Y CURVES

THE NUMBER OF CURVE IS = 5
THE NUMBER OF POINTS ON EACH CURVE = 17

DEPTH BELOW GS M	DIAM M	PHI	GAMMA KN/ M**3	A	B
1.00	.36	29.0	.2E+02	.95	.73

Y M	P KN/ M
.000	.000
.000	2.361
.001	4.721
.001	7.082
.002	9.442
.002	11.803
.003	14.164
.003	16.524
.004	18.885
.004	21.246
.005	23.606
.005	25.221
.006	25.781
.013	33.918
.368	33.918
.723	33.918
1.078	33.918

COMPUTED LATERAL FORCE AT PILE HEAD = .19994E+02 KN

**** WARNING ****
THE COMPUTED HORIZONTAL FORCE AT THE PILE HEAD EXCEEDS
TOLERANCE. THE ERROR IS .285E-03
COMPUTED SLOPE AT PILE HEAD = .00000E+00 M/ M

THE OVERALL MOMENT IMBALANCE = .668E-02 M- KN
THE OVERALL LATERAL FORCE IMBALANCE = -.728E-11 KN

**** WARNING ****
THE OVERALL MOMENT IMBALANCE EXCEEDS TOLERANCE

PILE HEAD DEFLECTION = .234E-02 M
MAXIMUM BENDING MOMENT = -.234E+02 M- KN
MAXIMUM TOTAL STRESS = .103E+05 KN/ M**2

NO. OF ITERATIONS = 8
MAXIMUM DEFLECTION ERROR = .997E-06 M

----- *** -----

FHWA North Abut. - 355 mm-sq PSC Fixed-Head/Cyclic/Crack Modeled

UNITS--METR

PILE LOADING CONDITION

LATERAL LOAD AT PILE HEAD = .400E+02 KN
 SLOPE AT PILE HEAD = .000E+00 M/ M
 AXIAL LOAD AT PILE HEAD = .000E+00 KN

X	DEFLECTION	MOMENT	TOTAL STRESS	SHEAR	SOIL RESIST	FLEXURAL RIGIDITY
M	M	M- KN	KN/ M**2	KN	KN/ M	KN- M**2
*****	*****	*****	*****	*****	*****	*****
.00	.382E-02	-.556E+02	.147E+05	.400E+02	.000E+00	.368E+05
.23	.378E-02	-.464E+02	.134E+05	.397E+02	.335E+01	.369E+05
.46	.367E-02	-.373E+02	.122E+05	.382E+02	.982E+01	.355E+05
.69	.351E-02	-.287E+02	.110E+05	.351E+02	.165E+02	.273E+05
.92	.330E-02	-.209E+02	.991E+04	.308E+02	.206E+02	.198E+05
1.15	.304E-02	-.140E+02	.898E+04	.268E+02	.170E+02	.133E+05
1.38	.272E-02	-.803E+01	.816E+04	.227E+02	.187E+02	.951E+04
1.61	.237E-02	-.299E+01	.747E+04	.183E+02	.192E+02	.951E+04
1.84	.200E-02	.105E+01	.721E+04	.140E+02	.187E+02	.951E+04
2.07	.163E-02	.410E+01	.762E+04	.982E+01	.173E+02	.951E+04
2.30	.129E-02	.622E+01	.791E+04	.606E+01	.153E+02	.951E+04
2.53	.982E-03	.750E+01	.809E+04	.282E+01	.129E+02	.951E+04
2.76	.715E-03	.806E+01	.816E+04	.158E+00	.103E+02	.951E+04
2.99	.492E-03	.804E+01	.816E+04	-.190E+01	.768E+01	.951E+04
3.22	.314E-03	.758E+01	.810E+04	-.339E+01	.529E+01	.951E+04
3.45	.178E-03	.679E+01	.799E+04	-.436E+01	.322E+01	.951E+04
3.68	.797E-04	.580E+01	.786E+04	-.491E+01	.154E+01	.951E+04
3.91	.136E-04	.470E+01	.771E+04	-.511E+01	.279E+00	.951E+04
4.14	-.265E-04	.357E+01	.755E+04	-.496E+01	-.171E+01	.951E+04
4.37	-.467E-04	.250E+01	.740E+04	-.438E+01	-.318E+01	.951E+04
4.60	-.529E-04	.159E+01	.728E+04	-.357E+01	-.381E+01	.951E+04
4.83	-.503E-04	.864E+00	.718E+04	-.269E+01	-.380E+01	.951E+04
5.06	-.427E-04	.337E+00	.711E+04	-.186E+01	-.340E+01	.951E+04
5.29	-.333E-04	-.121E-01	.707E+04	-.115E+01	-.277E+01	.951E+04
5.52	-.239E-04	-.215E+00	.709E+04	-.588E+00	-.207E+01	.951E+04
5.75	-.156E-04	-.308E+00	.711E+04	-.188E+00	-.141E+01	.951E+04
5.98	-.898E-05	-.323E+00	.711E+04	.701E-01	-.848E+00	.951E+04
6.21	-.417E-05	-.292E+00	.710E+04	.213E+00	-.409E+00	.951E+04
6.44	-.971E-06	-.237E+00	.710E+04	.270E+00	-.989E-01	.951E+04
6.67	.909E-06	-.176E+00	.709E+04	.268E+00	.961E-01	.951E+04
6.90	.181E-05	-.118E+00	.708E+04	.233E+00	.198E+00	.951E+04
7.13	.205E-05	-.704E-01	.707E+04	.183E+00	.232E+00	.951E+04
7.36	.189E-05	-.343E-01	.707E+04	.131E+00	.221E+00	.951E+04
7.59	.154E-05	-.962E-02	.706E+04	.834E-01	.186E+00	.951E+04
7.82	.113E-05	.530E-02	.706E+04	.457E-01	.141E+00	.951E+04
8.05	.753E-06	.127E-01	.707E+04	.185E-01	.965E-01	.951E+04
8.28	.441E-06	.150E-01	.707E+04	.819E-03	.581E-01	.951E+04
8.51	.211E-06	.140E-01	.707E+04	-.902E-02	.286E-01	.951E+04
8.74	.583E-07	.115E-01	.707E+04	-.131E-01	.812E-02	.951E+04
8.97	-.304E-07	.844E-02	.706E+04	-.134E-01	-.436E-02	.951E+04
9.20	-.722E-07	.554E-02	.706E+04	-.117E-01	-.106E-01	.951E+04
9.43	-.830E-07	.317E-02	.706E+04	-.894E-02	-.125E-01	.951E+04
9.66	-.758E-07	.144E-02	.706E+04	-.613E-02	-.117E-01	.951E+04
9.89	-.605E-07	.311E-03	.706E+04	-.367E-02	-.957E-02	.951E+04
10.12	-.433E-07	-.313E-03	.706E+04	-.177E-02	-.701E-02	.951E+04
10.35	-.277E-07	-.564E-03	.706E+04	-.437E-03	-.458E-02	.951E+04
10.58	-.151E-07	-.569E-03	.706E+04	.377E-03	-.256E-02	.951E+04
10.81	-.564E-08	-.434E-03	.706E+04	.777E-03	-.976E-03	.951E+04
11.04	.142E-08	-.244E-03	.706E+04	.850E-03	.360E-03	.951E+04
11.27	.712E-08	-.733E-04	.706E+04	.594E-03	.185E-02	.951E+04
11.50	.124E-07	.000E+00	.706E+04	.000E+00	.332E-02	.951E+04

COMPUTED LATERAL FORCE AT PILE HEAD = .40000E+02 KN
 COMPUTED SLOPE AT PILE HEAD = -.18856E-17 M/ M
 THE OVERALL MOMENT IMBALANCE = .313E-04 M- KN
 THE OVERALL LATERAL FORCE IMBALANCE = .255E-10 KN

FHWA North Abut. - 355 mm-sq PSC Fixed-Head/Cyclic/Crack Modeled

UNITS--METR

OUTPUT SUMMARY

PILE HEAD DEFLECTION = .382E-02 M
 MAXIMUM BENDING MOMENT = -.556E+02 M- KN
 MAXIMUM TOTAL STRESS = .147E+05 KN/ M**2

NO. OF ITERATIONS = 7
 MAXIMUM DEFLECTION ERROR = .386E-06 M

COMPUTED LATERAL FORCE AT PILE HEAD = .60004E+02 KN
 COMPUTED SLOPE AT PILE HEAD = .00000E+00 M/ M

THE OVERALL MOMENT IMBALANCE = -.623E-02 M- KN
 THE OVERALL LATERAL FORCE IMBALANCE = -.367E-10 KN

PILE HEAD DEFLECTION = .590E-02 M
 MAXIMUM BENDING MOMENT = -.890E+02 M- KN
 MAXIMUM TOTAL STRESS = .192E+05 KN/ M**2

NO. OF ITERATIONS = 6
 MAXIMUM DEFLECTION ERROR = .690E-06 M

----- *** -----

S U M M A R Y T A B L E

LATERAL LOAD (KN)	BOUNDARY CONDITION BC2	AXIAL LOAD (KN)	YT (M)	ST (M/ M)	MAX. MOMENT (M- KN)	MAX. STRESS (KN/ M**2)
.200E+02	.000E+00	.890E+03	.234E-02	.000E+00	-.234E+02	.103E+05
.400E+02	.000E+00	.890E+03	.382E-02	-.189E-17	-.556E+02	.147E+05
.600E+02	.000E+00	.890E+03	.590E-02	.000E+00	-.890E+02	.192E+05
.800E+02	.000E+00	.890E+03	.881E-02	-.754E-17	-.117E+03	.230E+05
.100E+03	.000E+00	.890E+03	.121E-01	.000E+00	-.139E+03	.260E+05
.120E+03	.000E+00	.890E+03	.153E-01	.000E+00	-.168E+03	.300E+05
.140E+03	.000E+00	.890E+03	.212E-01	.000E+00	-.218E+03	.368E+05
.160E+03	.000E+00	.890E+03	.615E-01	.302E-16	-.300E+03	.481E+05
.180E+03	.000E+00	.890E+03	.867E-01	-.603E-16	-.362E+03	.565E+05
.200E+03	.000E+00	.890E+03	.149E+00	.000E+00	-.430E+03	.658E+05

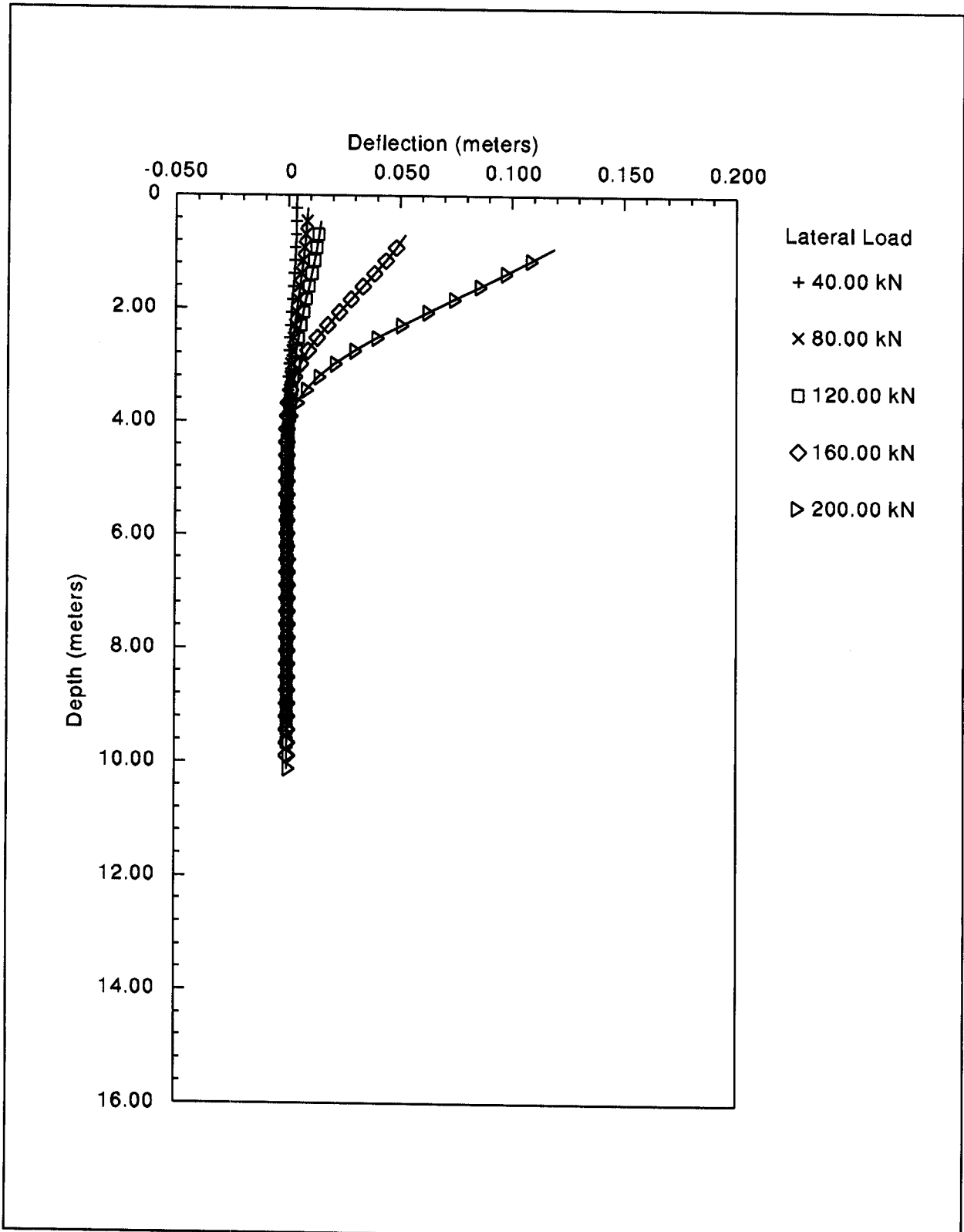


Figure F.19: North Abutment - Plot of Deflection versus Depth as a Function of Lateral Load

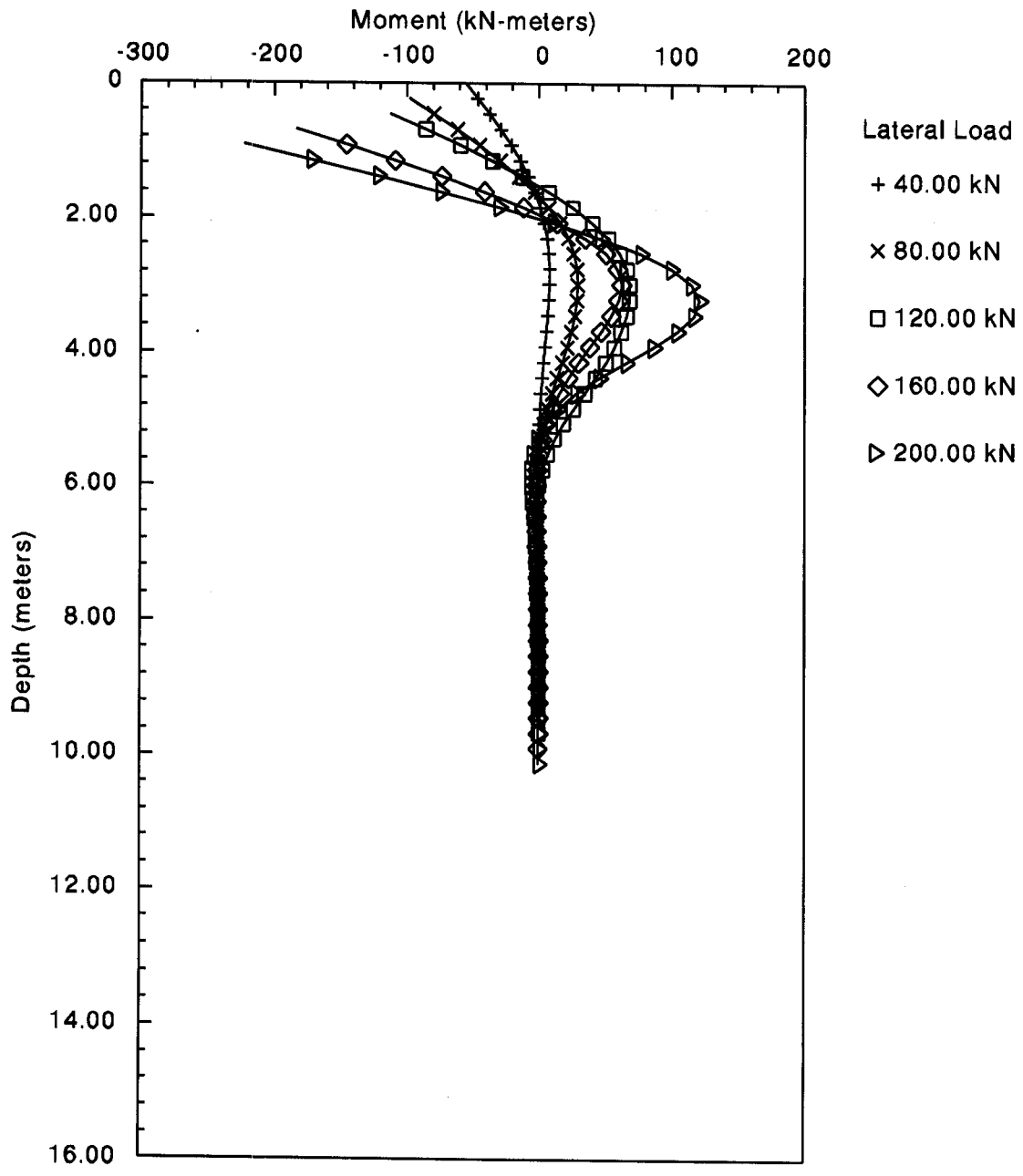


Figure F.20: North Abutment - Plot of Moment versus Depth as a Function of Lateral Load

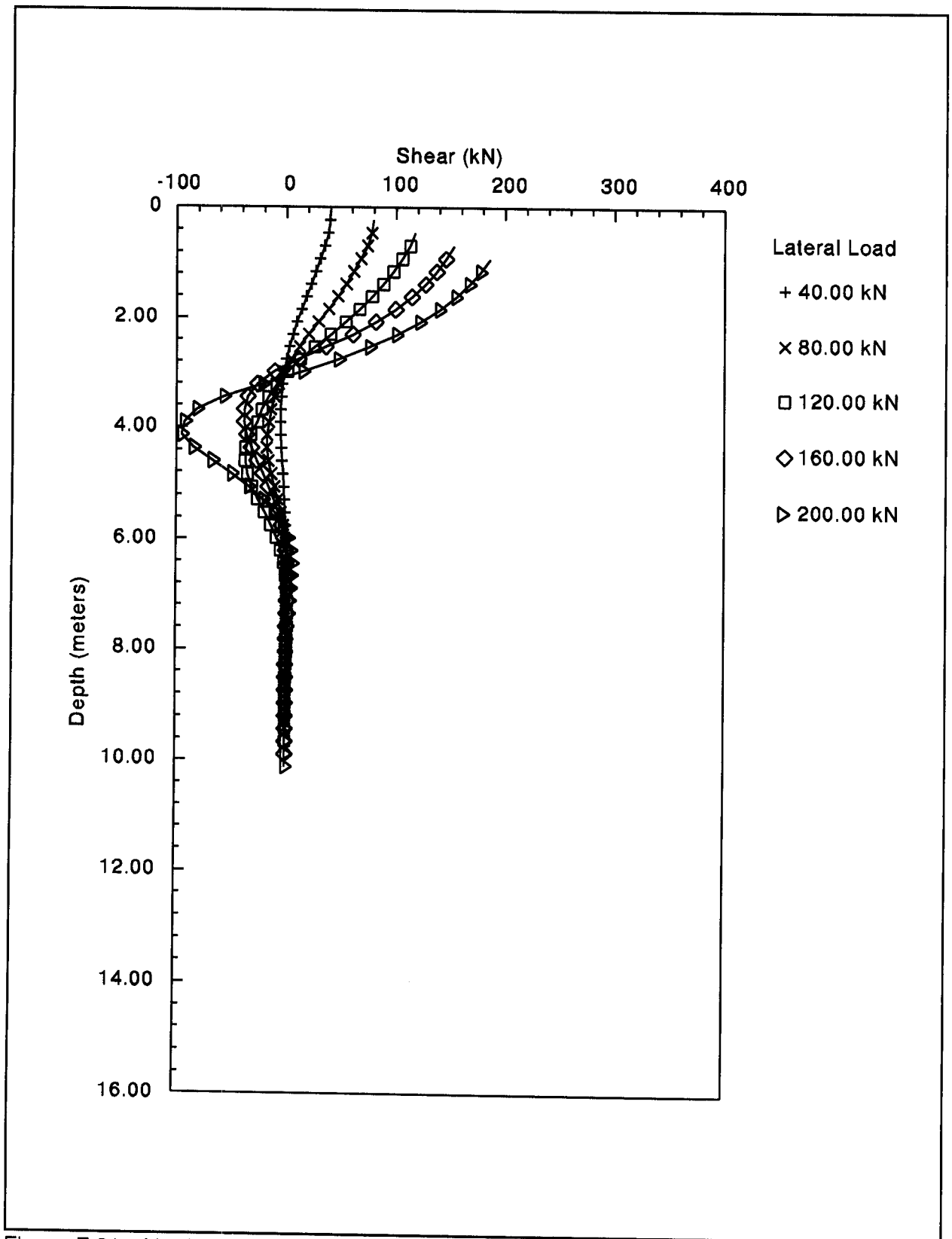


Figure F.21: North Abutment - Plot of Shear versus Depth as a Function of Lateral Load

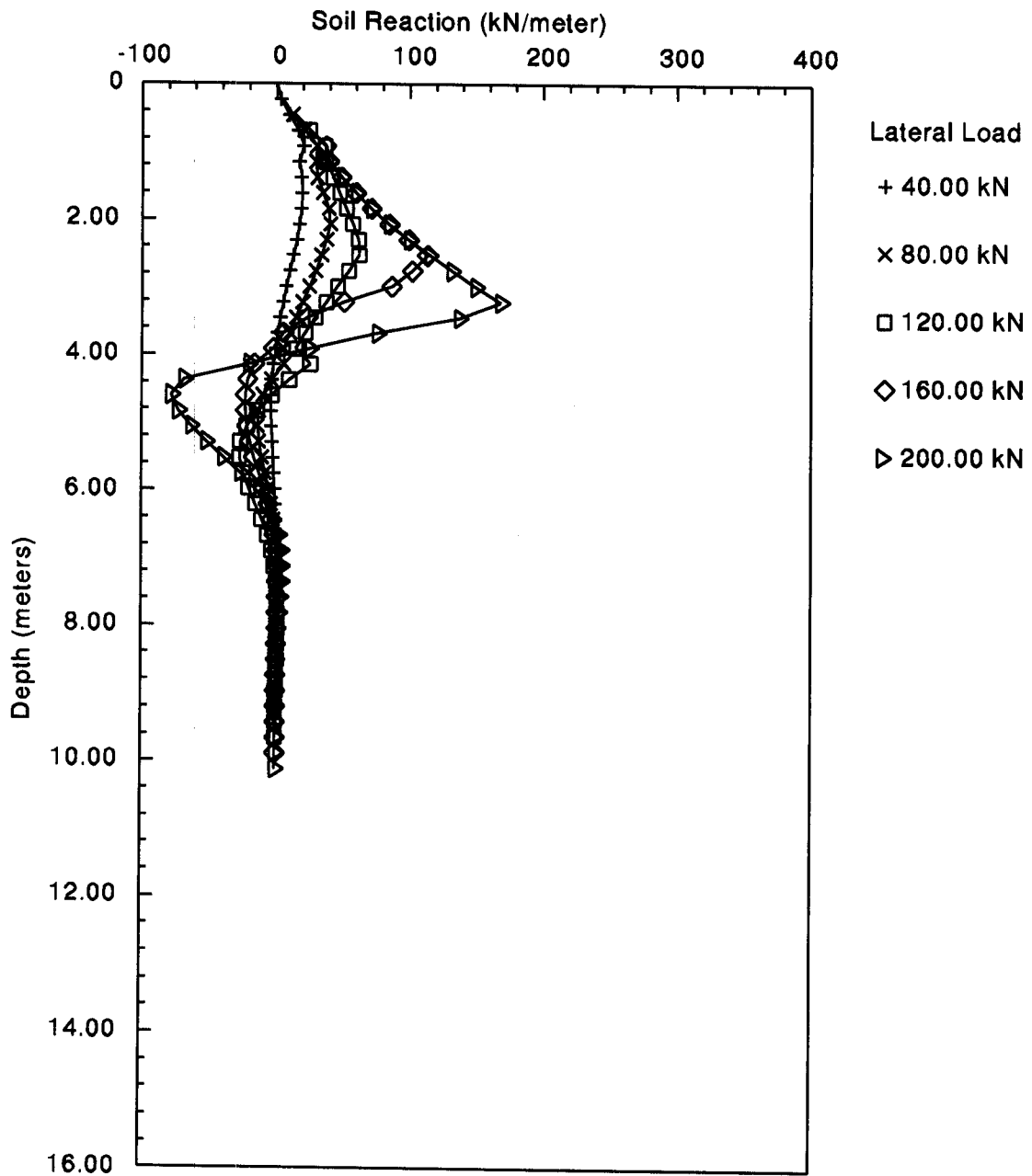


Figure F.22: North Abutment - Plot of Soil Reaction versus Depth as a Function of Lateral Load

F.4.3 COM624P - Pier 2 H-pile, X-X Axis and Y-Y Axis

As discussed in Chapter 13, wave equation driveability analyses at the internal piers indicated a potential driveability problem for 356 mm concrete piles. Therefore, low displacement HP 360x152 H-piles were chosen for the pile foundations at the interior piers.

For the selected H-pile section at Pier 2, COM624P solutions for lateral loading in the major (X-X) and minor (Y-Y) axis directions were obtained. These analyses again assumed full fixity at the base of the pier. At Pier 2, it was assumed that near-surface scour protection prevented removal of materials below the pier base in this case. In the full design process a number of other variables such as partial rotational constraint or extreme scour depth could be evaluated. The presence of the extremely dense sand and gravel stratum in the upper 4 m of the soil profile introduced a considerably stiffer soil response in comparison with that modeled at the North Abutment. Table 9-13 only has dense sand, therefore the slope of soil modulus for this extremely dense sand and gravel was assumed to be $50,000 \text{ kN/m}^3$. As in the previous example, the detailed results were saved only for every other lateral load increment up to the maximum lateral load evaluated of 220 kN.

COM624P analysis of lateral loading in the X-X and Y-Y axis are presented on the following pages. The analysis output includes an echo print of the input file followed by the COM624P generated summaries of the problem input and output. The output includes a summary table of deflection, moment, shear, and soil reaction versus lateral load. For selected lateral loads in the X-X axis, Figures F.23 to F.26 provide graphical presentations of deflection, moment, shear, and soil reaction versus depth. These graphical presentations for loads in the Y-Y axis are presented in Figure F.27 to F.30.

The COM624P analyses indicate the performance of the H-pile is acceptable when laterally loaded in either axis. The maximum deflection under the 40 kN design load is less than 2 mm.

Additional COM624P analyses should be performed to evaluate group response using the p-multiplier approach described in Section 9.8.4.

FHWA PIER2, HP360X152 X-X AXIS/FIXED-HEAD CYCLIC

2	1	0		
100	2	1	0	
4	4	0		
14.000	210000000	0.000	0.000	
1	2			
2	1	0	20	
100	0.00001000	2.00000000		
0.0000	0.3564	0.0004	0.0194	
1	4	0.0000	4.0000	50000.0000
2	4	4.0000	14.0000	33900.0000
0.0000	11.40000			
4.0000	11.40000			
4.0000	9.80000			
14.0000	9.80000			
0.0000	0.0000	36.0000	0.00000	
4.0000	0.0000	36.0000	0.00000	
4.0000	0.0000	35.0000	0.00000	
14.0000	0.0000	35.0000	0.00000	
5				
1.0000				
2.0000				
3.0000				
4.0000				
5.0000				
10				
1	40.0000	0.0000	890.0000	
0	60.0000	0.0000	890.0000	
1	80.0000	0.0000	890.0000	
0	100.0000	0.0000	890.0000	
1	120.0000	0.0000	890.0000	
0	140.0000	0.0000	890.0000	
1	160.0000	0.0000	890.0000	
0	180.0000	0.0000	890.0000	
1	200.0000	0.0000	890.0000	
0	220.0000	0.0000	890.0000	

FHWA PIER2, HP360X152 X-X AXIS/FIXED-HEAD CYCLIC

UNITS - - METR

 PILE DEFLECTION, BENDING MOMENT, SHEAR & SOIL RESISTANCE

 INPUT INFORMATION

THE LOADING IS CYCLIC

NO. OF CYCLES = .20E+02

PILE GEOMETRY AND PROPERTIES

PILE LENGTH = 14.00 M
 MODULUS OF ELASTICITY OF PILE = .210E+09 KN/ M**2
 1 SECTION(S)

X	DIAMETER	MOMENT OF INERTIA	AREA
M	M	M**4	M**2
.00			
14.00	.356	.400E-03	.194E-01

SOILS INFORMATION

X-COORDINATE AT THE GROUND SURFACE = .00 M
 SLOPE ANGLE AT THE GROUND SURFACE = .00 DEG.

2 LAYER(S) OF SOIL

LAYER 1

THE LAYER IS A SAND

X AT THE TOP OF THE LAYER = .00 M

X AT THE BOTTOM OF THE LAYER = 4.00 M

VARIATION OF SOIL MODULUS, k = .500E+05 KN/ M**3

LAYER 2

THE LAYER IS A SAND

X AT THE TOP OF THE LAYER = 4.00 M

X AT THE BOTTOM OF THE LAYER = 14.00 M

VARIATION OF SOIL MODULUS, k = .339E+05 KN/ M**3

DISTRIBUTION OF EFFECTIVE UNIT WEIGHT WITH DEPTH

X, M	WEIGHT, KN/ M**3
.00	.11E+02
4.00	.11E+02
4.00	.98E+01
14.00	.98E+01

DISTRIBUTION OF STRENGTH PARAMETERS WITH DEPTH

X, M	C, KN/ M**2	PHI, DEGREES	E50
.00	.000E+00	36.000	-----
4.00	.000E+00	36.000	-----
4.00	.000E+00	35.000	-----
14.00	.000E+00	35.000	-----

FINITE DIFFERENCE PARAMETERS

NUMBER OF PILE INCREMENTS = 100
 TOLERANCE ON DETERMINATION OF DEFLECTIONS = .100E-04 M
 MAXIMUM NUMBER OF ITERATIONS ALLOWED FOR PILE ANALYSIS = 100
 MAXIMUM ALLOWABLE DEFLECTION = .20E+01 M

INPUT CODES

OUTPT = 1
 KCYCL = 0
 KBC = 2
 KPYOP = 1
 INC = 2

FHWA PIER2, HP360X152 X-X AXIS/FIXED-HEAD CYCLIC
 UNITS--METR

OUTPUT INFORMATION

GENERATED P-Y CURVES

THE NUMBER OF CURVE IS = 5
 THE NUMBER OF POINTS ON EACH CURVE = 17

DEPTH BELOW GS M	DIAM M	PHI	GAMMA KN/ M**3	A	B
1.00	.36	36.0	.1E+02	.96	.73
	Y M		P KN/ M		
	.000		.000		
	.000		20.089		
	.001		23.911		
	.001		26.474		
	.002		28.459		
	.002		30.099		
	.003		31.510		
	.003		32.754		
	.004		33.872		
	.004		34.889		
	.005		35.825		
	.005		36.693		
	.006		37.504		
	.013		49.281		
	.370		49.281		
	.726		49.281		
	1.083		49.281		

----- *** -----

FHWA PIER2, HP360X152 X-X AXIS/FIXED-HEAD CYCLIC

UNITS--METR

PILE LOADING CONDITION

LATERAL LOAD AT PILE HEAD = .400E+02 KN
 SLOPE AT PILE HEAD = .000E+00 M/ M
 AXIAL LOAD AT PILE HEAD = .000E+00 KN

X	DEFLECTION	MOMENT	TOTAL STRESS	SHEAR	SOIL RESIST	FLEXURAL RIGIDITY
M	M	M- KN	KN/ M**2	KN	KN/ M	KN- M**2
*****	*****	*****	*****	*****	*****	*****
.00	.819E-03	-.472E+02	.669E+05	.400E+02	.000E+00	.840E+05
.28	.798E-03	-.360E+02	.619E+05	.396E+02	.344E+01	.840E+05
.56	.744E-03	-.251E+02	.571E+05	.377E+02	.105E+02	.840E+05
.84	.666E-03	-.150E+02	.525E+05	.336E+02	.188E+02	.840E+05
1.12	.574E-03	-.627E+01	.487E+05	.278E+02	.211E+02	.840E+05
1.40	.476E-03	.835E+00	.462E+05	.227E+02	.152E+02	.840E+05
1.68	.379E-03	.666E+01	.488E+05	.181E+02	.185E+02	.840E+05
1.96	.288E-03	.110E+02	.508E+05	.124E+02	.220E+02	.840E+05
2.24	.207E-03	.137E+02	.520E+05	.601E+01	.233E+02	.840E+05
2.52	.139E-03	.146E+02	.524E+05	.300E+00	.176E+02	.840E+05
2.80	.844E-04	.141E+02	.522E+05	-.380E+01	.119E+02	.840E+05
3.08	.429E-04	.127E+02	.515E+05	-.637E+01	.666E+01	.840E+05
3.36	.132E-04	.107E+02	.506E+05	-.759E+01	.224E+01	.840E+05
3.64	-.659E-05	.853E+01	.497E+05	-.771E+01	-.119E+01	.840E+05
3.92	-.184E-04	.645E+01	.487E+05	-.702E+01	-.361E+01	.840E+05
4.20	-.242E-04	.462E+01	.479E+05	-.611E+01	-.344E+01	.840E+05
4.48	-.256E-04	.305E+01	.472E+05	-.508E+01	-.389E+01	.840E+05
4.76	-.242E-04	.178E+01	.467E+05	-.399E+01	-.390E+01	.840E+05
5.04	-.211E-04	.808E+00	.462E+05	-.294E+01	-.360E+01	.840E+05
5.32	-.172E-04	.118E+00	.459E+05	-.200E+01	-.311E+01	.840E+05
5.60	-.132E-04	-.330E+00	.460E+05	-.122E+01	-.251E+01	.840E+05
5.88	-.951E-05	-.582E+00	.461E+05	-.604E+00	-.190E+01	.840E+05
6.16	-.635E-05	-.686E+00	.462E+05	-.155E+00	-.133E+01	.840E+05
6.44	-.382E-05	-.685E+00	.462E+05	.144E+00	-.836E+00	.840E+05
6.72	-.192E-05	-.618E+00	.462E+05	.320E+00	-.440E+00	.840E+05
7.00	-.601E-06	-.515E+00	.461E+05	.399E+00	-.144E+00	.840E+05
7.28	.239E-06	-.401E+00	.461E+05	.409E+00	.585E-01	.840E+05
7.56	.705E-06	-.290E+00	.460E+05	.375E+00	.181E+00	.840E+05
7.84	.899E-06	-.193E+00	.460E+05	.315E+00	.239E+00	.840E+05
8.12	.912E-06	-.115E+00	.459E+05	.246E+00	.251E+00	.840E+05
8.40	.816E-06	-.553E-01	.459E+05	.178E+00	.233E+00	.840E+05
8.68	.668E-06	-.141E-01	.459E+05	.118E+00	.197E+00	.840E+05
8.96	.506E-06	.119E-01	.459E+05	.691E-01	.154E+00	.840E+05
9.24	.354E-06	.258E-01	.459E+05	.322E-01	.111E+00	.840E+05
9.52	.225E-06	.310E-01	.459E+05	.670E-02	.730E-01	.840E+05
9.80	.126E-06	.304E-01	.459E+05	-.916E-02	.419E-01	.840E+05
10.08	.541E-07	.265E-01	.459E+05	-.174E-01	.186E-01	.840E+05
10.36	.716E-08	.211E-01	.459E+05	-.203E-01	.256E-02	.840E+05
10.64	-.201E-07	.155E-01	.459E+05	-.195E-01	-.724E-02	.840E+05
10.92	-.328E-07	.104E-01	.459E+05	-.167E-01	-.122E-01	.840E+05
11.20	-.359E-07	.619E-02	.459E+05	-.131E-01	-.136E-01	.840E+05
11.48	-.330E-07	.306E-02	.459E+05	-.934E-02	-.129E-01	.840E+05
11.76	-.273E-07	.925E-03	.459E+05	-.601E-02	-.109E-01	.840E+05
12.04	-.206E-07	-.362E-03	.459E+05	-.331E-02	-.846E-02	.840E+05
12.32	-.143E-07	-.988E-03	.459E+05	-.130E-02	-.600E-02	.840E+05
12.60	-.885E-08	-.115E-02	.459E+05	.584E-04	-.380E-02	.840E+05
12.88	-.444E-08	-.100E-02	.459E+05	.851E-03	-.195E-02	.840E+05
13.16	-.971E-09	-.708E-03	.459E+05	.118E-02	-.437E-03	.840E+05
13.44	.184E-08	-.377E-03	.459E+05	.112E-02	.841E-03	.840E+05
13.72	.430E-08	-.110E-03	.459E+05	.720E-03	.201E-02	.840E+05
14.00	.665E-08	.000E+00	.459E+05	.000E+00	.317E-02	.840E+05

COMPUTED LATERAL FORCE AT PILE HEAD = .40000E+02 KN
 COMPUTED SLOPE AT PILE HEAD = .38722E-18 M/ M
 THE OVERALL MOMENT IMBALANCE = .360E-11 M- KN
 THE OVERALL LATERAL FORCE IMBALANCE = -.996E-11 KN

FHWA PIER2, HP360X152 X-X AXIS/FIXED-HEAD CYCLIC

UNITS--METR

OUTPUT SUMMARY

PILE HEAD DEFLECTION = .819E-03 M
 MAXIMUM BENDING MOMENT = -.472E+02 M- KN
 MAXIMUM TOTAL STRESS = .669E+05 KN/ M**2

NO. OF ITERATIONS = 5
 MAXIMUM DEFLECTION ERROR = .372E-05 M

COMPUTED LATERAL FORCE AT PILE HEAD = .60000E+02 KN
 COMPUTED SLOPE AT PILE HEAD = .15489E-17 M/ M

THE OVERALL MOMENT IMBALANCE = .102E-10 M- KN
 THE OVERALL LATERAL FORCE IMBALANCE = -.183E-10 KN

PILE HEAD DEFLECTION = .151E-02 M
 MAXIMUM BENDING MOMENT = -.772E+02 M- KN
 MAXIMUM TOTAL STRESS = .803E+05 KN/ M**2

NO. OF ITERATIONS = 6
 MAXIMUM DEFLECTION ERROR = .434E-05 M

----- *** -----

S U M M A R Y T A B L E

LATERAL LOAD (KN)	BOUNDARY CONDITION BC2	AXIAL LOAD (KN)	YT (M)	ST (M/ M)	MAX. MOMENT (M- KN)	MAX. STRESS (KN/ M**2)
.400E+02	.000E+00	.890E+03	.819E-03	.387E-18	-.472E+02	.669E+05
.600E+02	.000E+00	.890E+03	.151E-02	.155E-17	-.772E+02	.803E+05
.800E+02	.000E+00	.890E+03	.231E-02	-.155E-17	-.109E+03	.944E+05
.100E+03	.000E+00	.890E+03	.322E-02	-.310E-17	-.142E+03	.109E+06
.120E+03	.000E+00	.890E+03	.419E-02	.000E+00	-.176E+03	.124E+06
.140E+03	.000E+00	.890E+03	.524E-02	-.310E-17	-.211E+03	.140E+06
.160E+03	.000E+00	.890E+03	.636E-02	.000E+00	-.247E+03	.156E+06
.180E+03	.000E+00	.890E+03	.753E-02	-.310E-17	-.283E+03	.172E+06
.200E+03	.000E+00	.890E+03	.874E-02	.000E+00	-.320E+03	.188E+06
.220E+03	.000E+00	.890E+03	.100E-01	.000E+00	-.357E+03	.205E+06

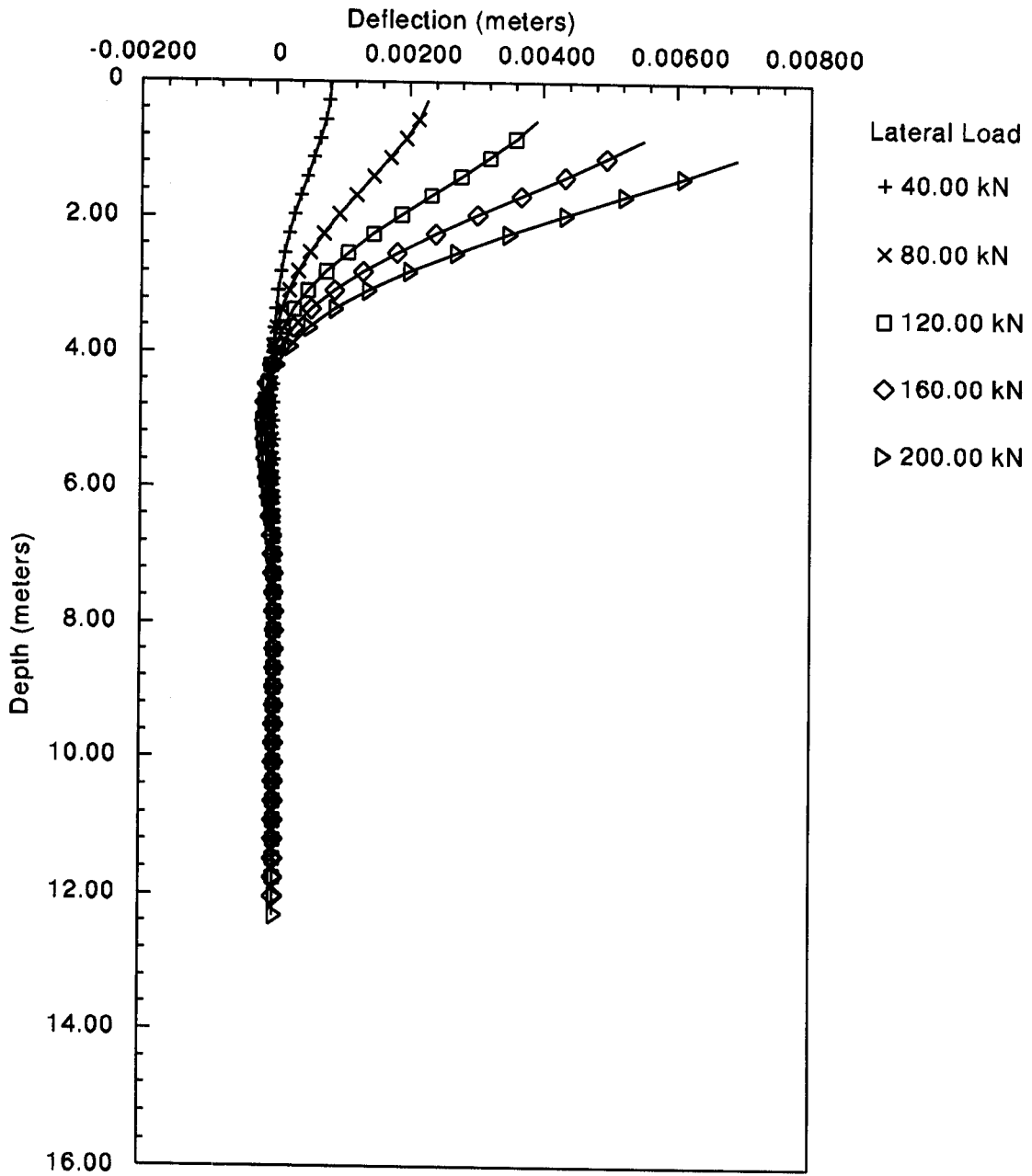


Figure F.23: Pier 2 - Plot of Deflection versus Depth as a Function on Lateral Load on X-X Axis

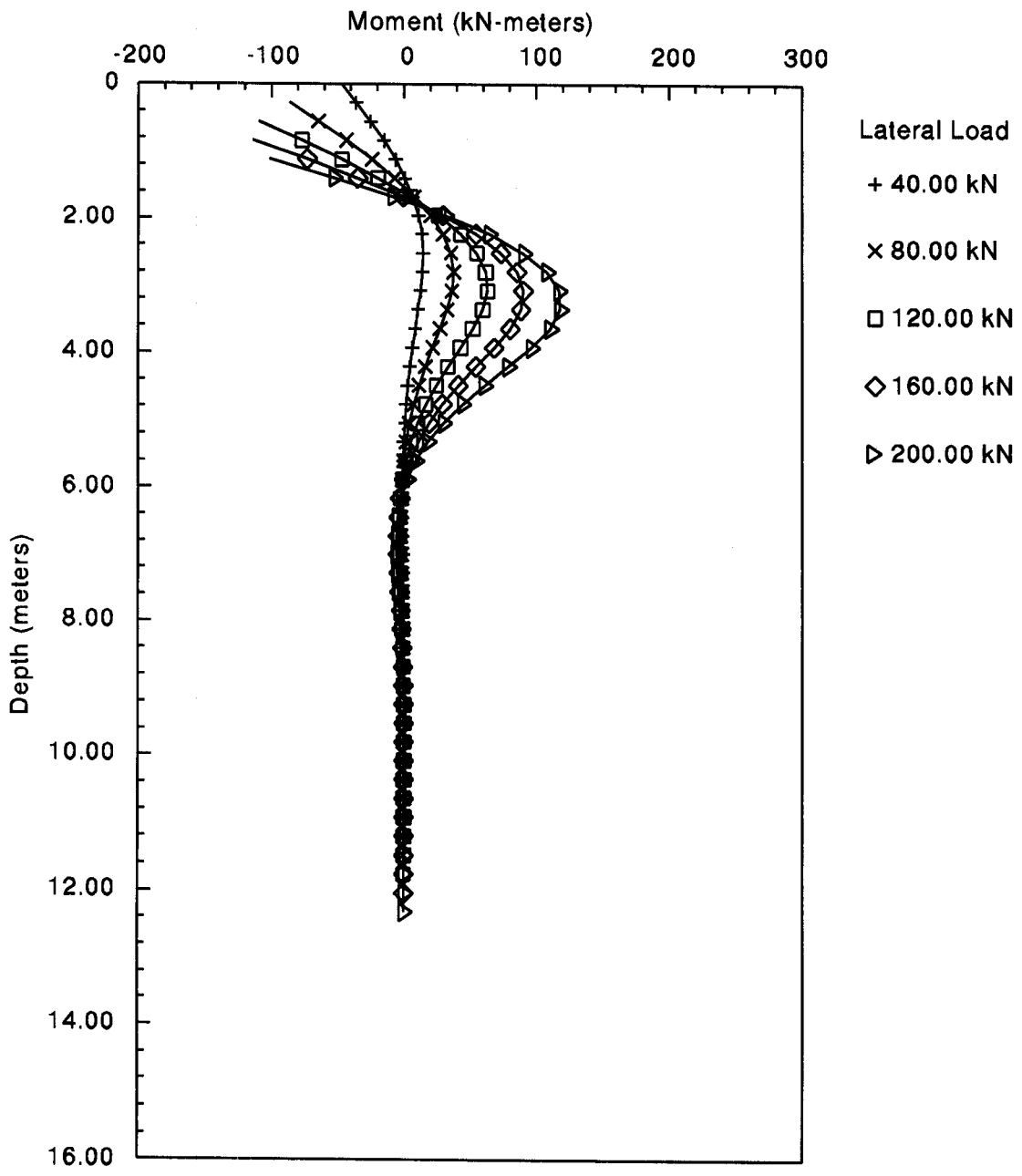


Figure F.24: Pier 2 - Plot of Moment versus Depth as a Function of Lateral Load on X-X Axis

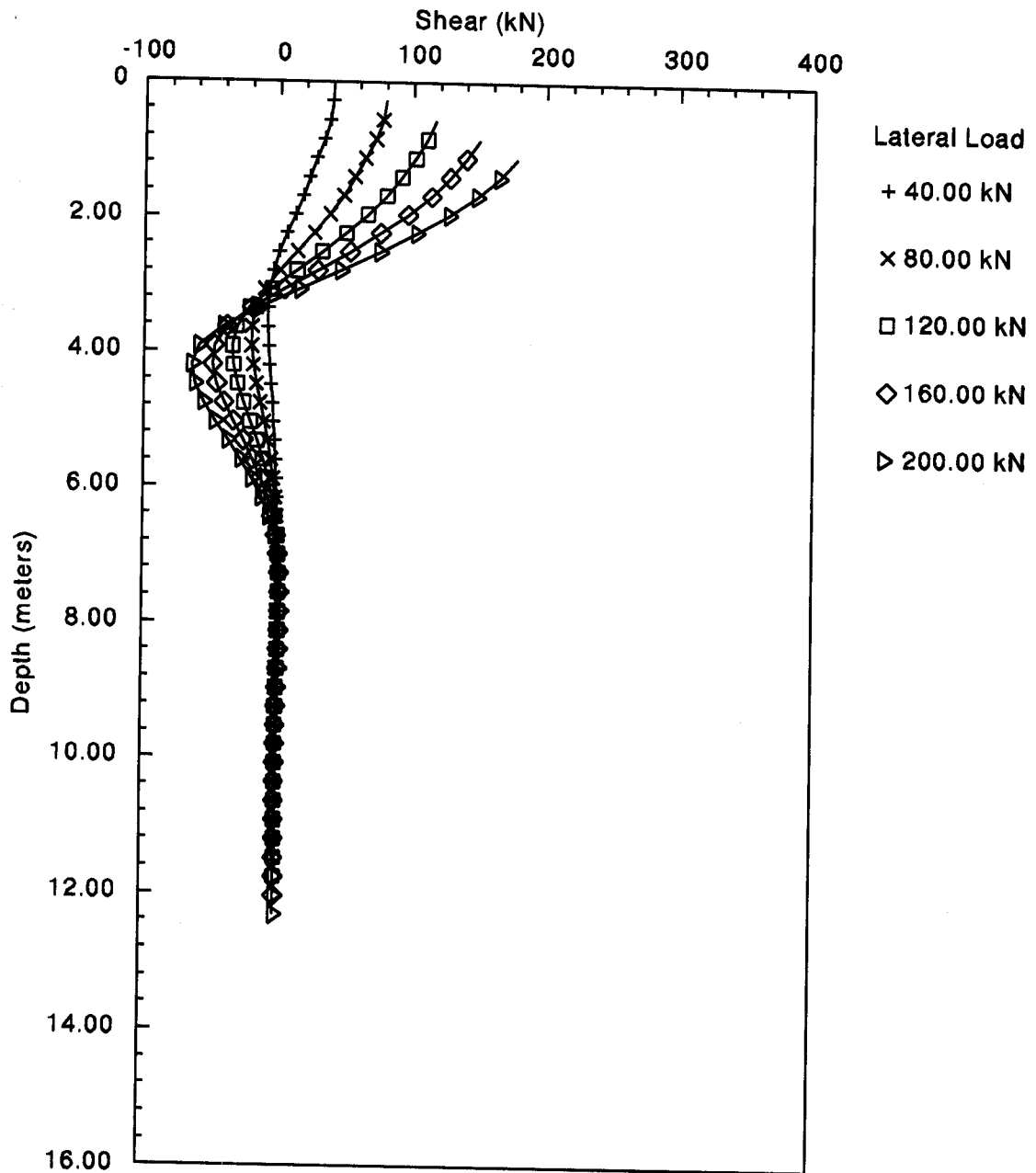


Figure F.25: Pier 2 - Plot of Shear versus Depth as a Function of Lateral Load on X-X Axis

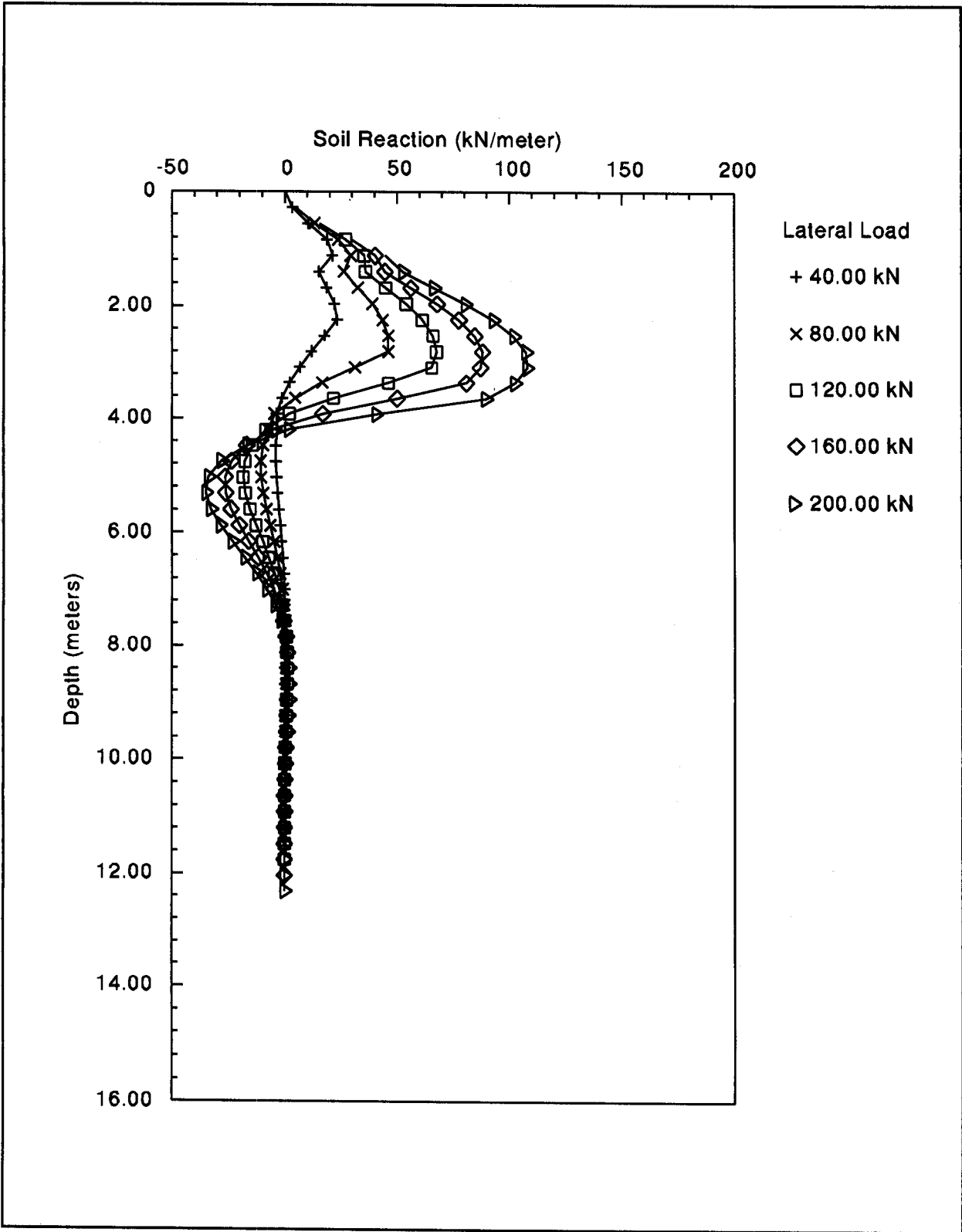


Figure F.26: Pier 2 - Plot of Soil Reaction versus Depth as a Function of Lateral Load on X-X Axis

FHWA PIER2, HP360X152 Y-Y AXIS/FIXED-HEAD CYCLIC

2	1	0		
100	2	1	0	
4	4	0		
14.000		210000000	0.000	0.000
1	2			
2	1	0	20	
100		0.00001000	2.00000000	
0.0000		0.3760	0.0002	0.0194
1	4	0.0000	4.0000	50000.0000
2	4	4.0000	14.0000	33900.0000
0.0000		11.40000		
4.0000		11.40000		
4.0000		9.80000		
14.0000		9.80000		
0.0000		0.0000	36.0000	0.00000
4.0000		0.0000	36.0000	0.00000
4.0000		0.0000	35.0000	0.00000
14.0000		0.0000	35.0000	0.00000
5				
1.0000				
2.0000				
3.0000				
4.0000				
5.0000				
10				
1	40.0000	0.0000	890.0000	
0	60.0000	0.0000	890.0000	
1	80.0000	0.0000	890.0000	
0	100.0000	0.0000	890.0000	
1	120.0000	0.0000	890.0000	
0	140.0000	0.0000	890.0000	
1	160.0000	0.0000	890.0000	
0	180.0000	0.0000	890.0000	
1	200.0000	0.0000	890.0000	
0	220.0000	0.0000	890.0000	

FHWA PIER2, HP360X152 Y-Y AXIS/FIXED-HEAD CYCLIC

UNITS--METR

 PILE DEFLECTION, BENDING MOMENT, SHEAR & SOIL RESISTANCE

 INPUT INFORMATION

THE LOADING IS CYCLIC

NO. OF CYCLES = .20E+02

PILE GEOMETRY AND PROPERTIES

PILE LENGTH = 14.00 M
 MODULUS OF ELASTICITY OF PILE = .210E+09 KN/ M**2
 1 SECTION(S)

X	DIAMETER	MOMENT OF INERTIA	AREA
M	M	M**4	M**2
.00	.376	.200E-03	.194E-01
14.00			

SOILS INFORMATION

X-COORDINATE AT THE GROUND SURFACE = .00 M
 SLOPE ANGLE AT THE GROUND SURFACE = .00 DEG.

2 LAYER(S) OF SOIL

LAYER 1

THE LAYER IS A SAND

X AT THE TOP OF THE LAYER = .00 M

X AT THE BOTTOM OF THE LAYER = 4.00 M

VARIATION OF SOIL MODULUS, k = .500E+05 KN/ M**3

LAYER 2

THE LAYER IS A SAND

X AT THE TOP OF THE LAYER = 4.00 M

X AT THE BOTTOM OF THE LAYER = 14.00 M

VARIATION OF SOIL MODULUS, k = .339E+05 KN/ M**3

DISTRIBUTION OF EFFECTIVE UNIT WEIGHT WITH DEPTH

X, M	WEIGHT, KN/ M**3
.00	.11E+02
4.00	.11E+02
4.00	.98E+01
14.00	.98E+01

DISTRIBUTION OF STRENGTH PARAMETERS WITH DEPTH

X, M	C, KN/ M**2	PHI, DEGREES	E50
.00	.000E+00	36.000	-----
4.00	.000E+00	36.000	-----
4.00	.000E+00	35.000	-----
14.00	.000E+00	35.000	-----

FINITE DIFFERENCE PARAMETERS

NUMBER OF PILE INCREMENTS = 100
 TOLERANCE ON DETERMINATION OF DEFLECTIONS = .100E-04 M
 MAXIMUM NUMBER OF ITERATIONS ALLOWED FOR PILE ANALYSIS = 100
 MAXIMUM ALLOWABLE DEFLECTION = .20E+01 M

INPUT CODES

OUTPUT = 1
 KCYCL = 0
 KBC = 2
 KPYOP = 1
 INC = 2

FHWA PIER2, HP360X152 Y-Y AXIS/FIXED-HEAD CYCLIC
 UNITS--METR

O U T P U T I N F O R M A T I O N

GENERATED P-Y CURVES

THE NUMBER OF CURVE IS = 5
 THE NUMBER OF POINTS ON EACH CURVE = 17

DEPTH BELOW GS	DIAM	PHI	GAMMA	A	B
M	M		KN/ M**3		
1.00	.38	36.0	.1E+02	.97	.75

Y	P
M	KN/ M
.000	.000
.001	21.842
.001	25.705
.002	28.274
.002	30.251
.003	31.880
.003	33.275
.004	34.502
.004	35.602
.005	36.601
.005	37.518
.006	38.367
.006	39.160
.014	50.660
.390	50.660
.766	50.660
1.142	50.660

----- *** -----

FHWA PIER2, HP360X152 Y-Y AXIS/FIXED-HEAD CYCLIC

UNITS--METR

PILE LOADING CONDITION

LATERAL LOAD AT PILE HEAD = .400E+02 KN
 SLOPE AT PILE HEAD = .000E+00 M/ M
 AXIAL LOAD AT PILE HEAD = .000E+00 KN

X	DEFLECTION		MOMENT	TOTAL STRESS	SHEAR	SOIL RESIST	FLEXURAL RIGIDITY
	M	M	M- KN	KN/ M**2	KN	KN/ M	KN- M**2
0.00	.122E-02	-.432E+02	.865E+05	.400E+02	.000E+00	.420E+05	
0.28	.118E-02	-.320E+02	.760E+05	.396E+02	.378E+01	.420E+05	
0.56	.108E-02	-.211E+02	.657E+05	.375E+02	.115E+02	.420E+05	
0.84	.946E-03	-.110E+02	.562E+05	.329E+02	.209E+02	.420E+05	
1.12	.789E-03	-.255E+01	.483E+05	.262E+02	.254E+02	.420E+05	
1.40	.626E-03	.397E+01	.496E+05	.196E+02	.205E+02	.420E+05	
1.68	.470E-03	.885E+01	.542E+05	.143E+02	.198E+02	.420E+05	
1.96	.331E-03	.122E+02	.573E+05	.823E+01	.230E+02	.420E+05	
2.24	.215E-03	.137E+02	.587E+05	.159E+01	.239E+02	.420E+05	
2.52	.123E-03	.133E+02	.584E+05	-.395E+01	.154E+02	.420E+05	
2.80	.567E-04	.117E+02	.569E+05	-.721E+01	.782E+01	.420E+05	
3.08	.119E-04	.951E+01	.548E+05	-.855E+01	.175E+01	.420E+05	
3.36	-.152E-04	.712E+01	.526E+05	-.842E+01	-.260E+01	.420E+05	
3.64	-.289E-04	.490E+01	.505E+05	-.730E+01	-.528E+01	.420E+05	
3.92	-.335E-04	.308E+01	.488E+05	-.563E+01	-.656E+01	.420E+05	
4.20	-.322E-04	.172E+01	.475E+05	-.421E+01	-.455E+01	.420E+05	
4.48	-.277E-04	.718E+00	.466E+05	-.298E+01	-.417E+01	.420E+05	
4.76	-.218E-04	.382E-01	.459E+05	-.189E+01	-.349E+01	.420E+05	
5.04	-.159E-04	-.368E+00	.462E+05	-.103E+01	-.268E+01	.420E+05	
5.32	-.105E-04	-.562E+00	.464E+05	-.384E+00	-.187E+01	.420E+05	
5.60	-.623E-05	-.607E+00	.464E+05	.427E-01	-.117E+01	.420E+05	
5.88	-.305E-05	-.557E+00	.464E+05	.290E+00	-.598E+00	.420E+05	
6.16	-.913E-06	-.459E+00	.463E+05	.398E+00	-.185E+00	.420E+05	
6.44	.371E-06	-.344E+00	.462E+05	.411E+00	.834E-01	.420E+05	
6.72	.101E-05	-.234E+00	.461E+05	.366E+00	.231E+00	.420E+05	
7.00	.122E-05	-.142E+00	.460E+05	.292E+00	.287E+00	.420E+05	
7.28	.115E-05	-.712E-01	.459E+05	.212E+00	.282E+00	.420E+05	
7.56	.949E-06	-.226E-01	.459E+05	.138E+00	.242E+00	.420E+05	
7.84	.704E-06	.719E-02	.459E+05	.774E-01	.186E+00	.420E+05	
8.12	.471E-06	.223E-01	.459E+05	.332E-01	.128E+00	.420E+05	
8.40	.278E-06	.272E-01	.459E+05	.422E-02	.784E-01	.420E+05	
8.68	.136E-06	.259E-01	.459E+05	-.122E-01	.393E-01	.420E+05	
8.96	.410E-07	.213E-01	.459E+05	-.193E-01	.121E-01	.420E+05	
9.24	-.142E-07	.156E-01	.459E+05	-.203E-01	-.458E-02	.420E+05	
9.52	-.402E-07	.102E-01	.459E+05	-.177E-01	-.130E-01	.420E+05	
9.80	-.471E-07	.581E-02	.459E+05	-.136E-01	-.156E-01	.420E+05	
10.08	-.429E-07	.259E-02	.459E+05	-.937E-02	-.146E-01	.420E+05	
10.36	-.338E-07	.511E-03	.459E+05	-.564E-02	-.118E-01	.420E+05	
10.64	-.236E-07	-.647E-03	.459E+05	-.279E-02	-.844E-02	.420E+05	
10.92	-.146E-07	-.114E-02	.459E+05	-.860E-03	-.533E-02	.420E+05	
11.20	-.757E-08	-.120E-02	.459E+05	.281E-03	-.284E-02	.420E+05	
11.48	-.280E-08	-.103E-02	.459E+05	.823E-03	-.107E-02	.420E+05	
11.76	.572E-10	-.773E-03	.459E+05	.961E-03	.323E-04	.420E+05	
12.04	.147E-08	-.513E-03	.459E+05	.866E-03	.603E-03	.420E+05	
12.32	.193E-08	-.297E-03	.459E+05	.664E-03	.802E-03	.420E+05	
12.60	.182E-08	-.142E-03	.459E+05	.441E-03	.773E-03	.420E+05	
12.88	.144E-08	-.475E-04	.459E+05	.243E-03	.624E-03	.420E+05	
13.16	.963E-09	-.171E-05	.459E+05	.949E-04	.426E-03	.420E+05	
13.44	.481E-09	.105E-04	.459E+05	.413E-05	.217E-03	.420E+05	
13.72	.175E-10	.558E-05	.459E+05	-.277E-04	.678E-05	.420E+05	
14.00	-.436E-09	.000E+00	.459E+05	.000E+00	-.207E-03	.420E+05	

COMPUTED LATERAL FORCE AT PILE HEAD = .40000E+02 KN
 COMPUTED SLOPE AT PILE HEAD = -.77443E-18 M/ M
 THE OVERALL MOMENT IMBALANCE = .340E-11 M- KN
 THE OVERALL LATERAL FORCE IMBALANCE = -.582E-11 KN

FHWA PIER2, HP360X152 Y-Y AXIS/FIXED-HEAD CYCLIC

UNITS--METR

OUTPUT SUMMARY

PILE HEAD DEFLECTION = .122E-02 M
 MAXIMUM BENDING MOMENT = -.432E+02 M- KN
 MAXIMUM TOTAL STRESS = .865E+05 KN/ M**2

 NO. OF ITERATIONS = 5
 MAXIMUM DEFLECTION ERROR = .338E-05 M

 COMPUTED LATERAL FORCE AT PILE HEAD = .60000E+02 KN
 COMPUTED SLOPE AT PILE HEAD = .00000E+00 M/ M

 THE OVERALL MOMENT IMBALANCE = -.219E-11 M- KN
 THE OVERALL LATERAL FORCE IMBALANCE = -.107E-10 KN

 PILE HEAD DEFLECTION = .232E-02 M
 MAXIMUM BENDING MOMENT = -.713E+02 M- KN
 MAXIMUM TOTAL STRESS = .113E+06 KN/ M**2

 NO. OF ITERATIONS = 7
 MAXIMUM DEFLECTION ERROR = .465E-05 M

----- *** -----

S U M M A R Y T A B L E

LATERAL LOAD (KN)	BOUNDARY CONDITION BC2	AXIAL LOAD (KN)	YT (M)	ST (M/ M)	MAX. MOMENT (M- KN)	MAX. STRESS (KN/ M**2)
.400E+02	.000E+00	.890E+03	.122E-02	-.774E-18	-.432E+02	.865E+05
.600E+02	.000E+00	.890E+03	.232E-02	.000E+00	-.713E+02	.113E+06
.800E+02	.000E+00	.890E+03	.362E-02	.000E+00	-.101E+03	.141E+06
.100E+03	.000E+00	.890E+03	.509E-02	.310E-17	-.132E+03	.170E+06
.120E+03	.000E+00	.890E+03	.668E-02	.310E-17	-.164E+03	.200E+06
.140E+03	.000E+00	.890E+03	.839E-02	.000E+00	-.197E+03	.231E+06
.160E+03	.000E+00	.890E+03	.102E-01	.000E+00	-.231E+03	.263E+06
.180E+03	.000E+00	.890E+03	.121E-01	.620E-17	-.264E+03	.294E+06
.200E+03	.000E+00	.890E+03	.140E-01	.620E-17	-.298E+03	.326E+06
.220E+03	.000E+00	.890E+03	.160E-01	.000E+00	-.333E+03	.359E+06

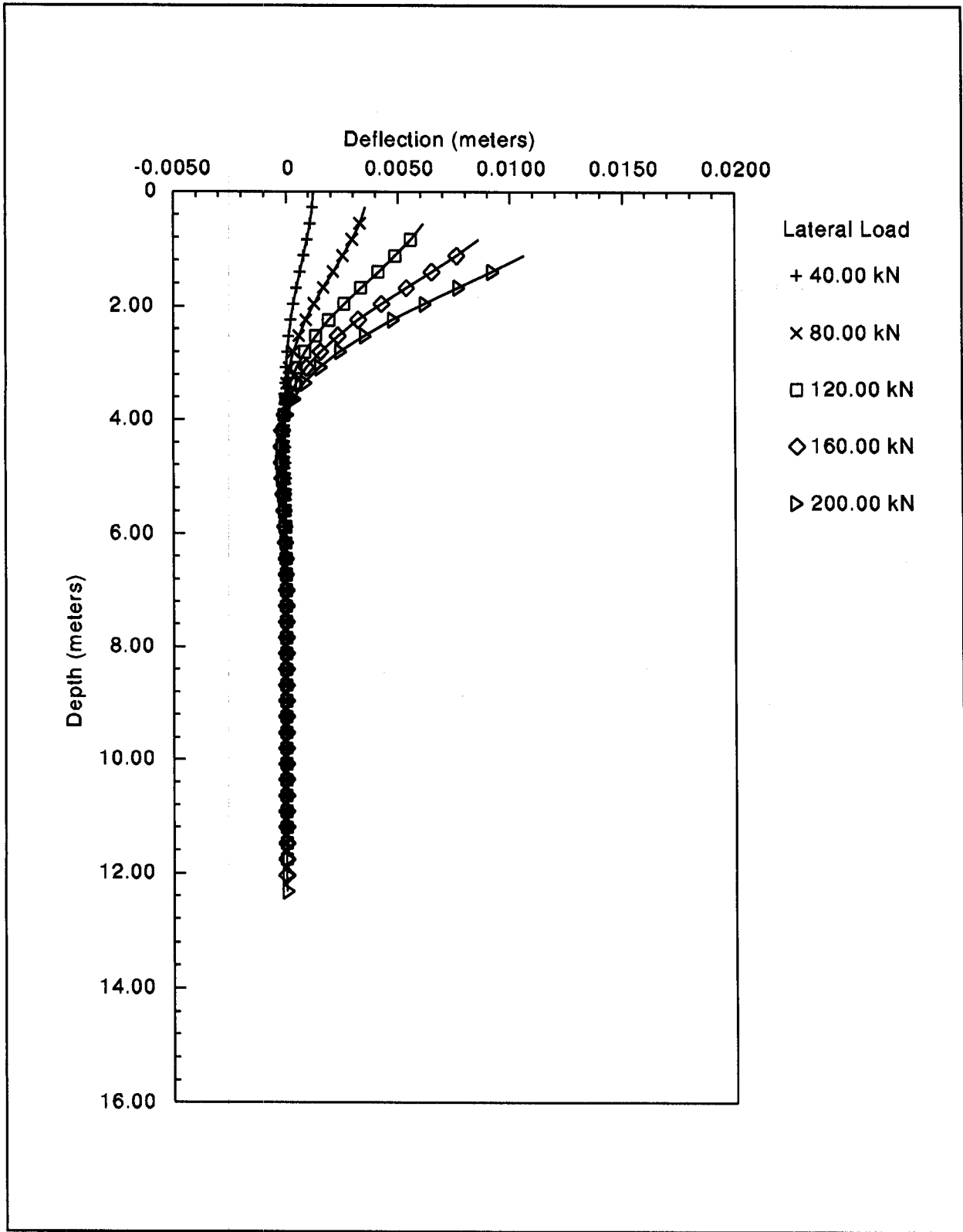


Figure F.27: Pier 2 - Plot of Deflection versus Depth as a Function of Lateral Load on Y-Y Axis

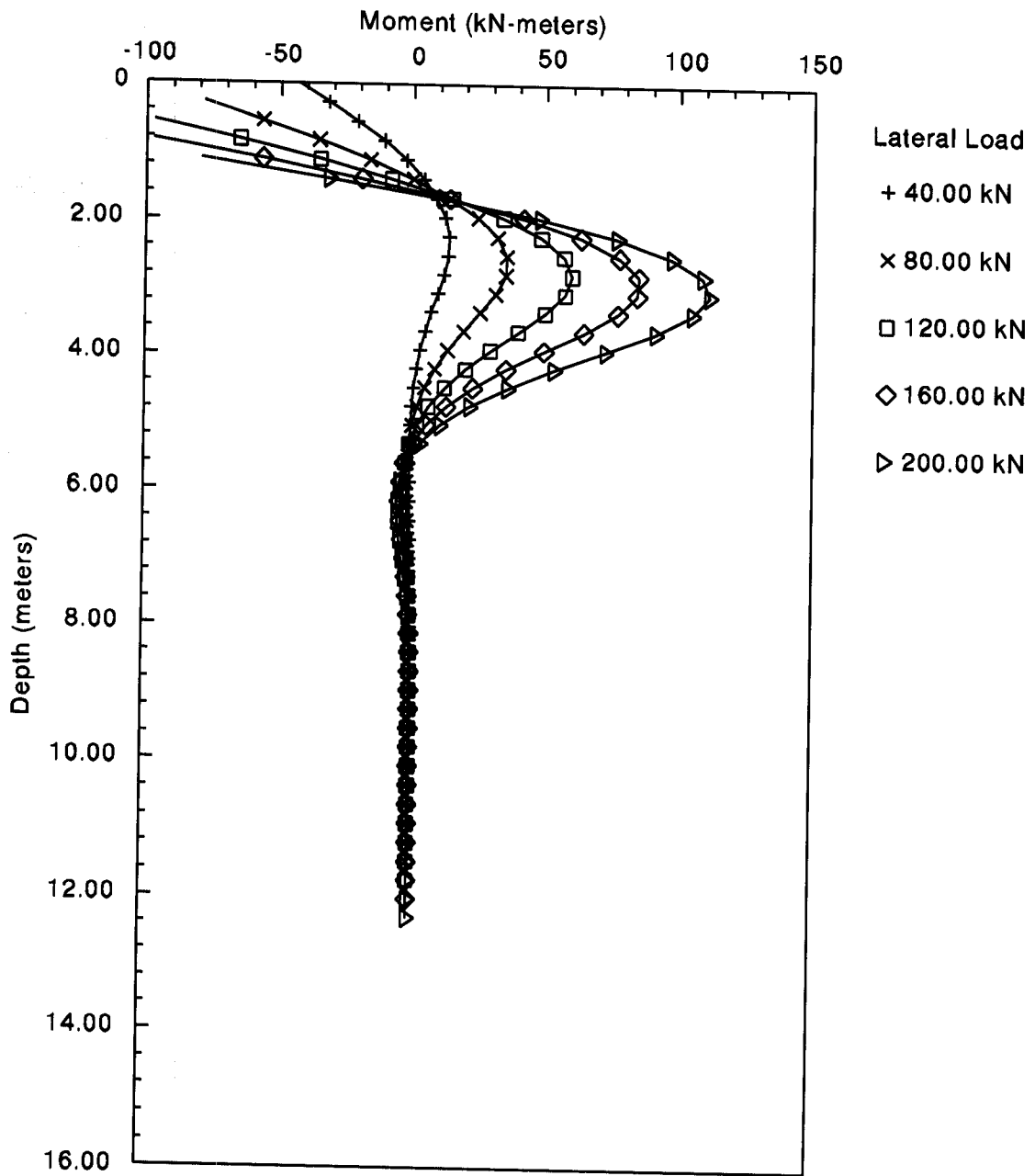


Figure F.28: Pier 2 - Plot of Moment versus Depth as a Function of Lateral Load on Y-Y Axis

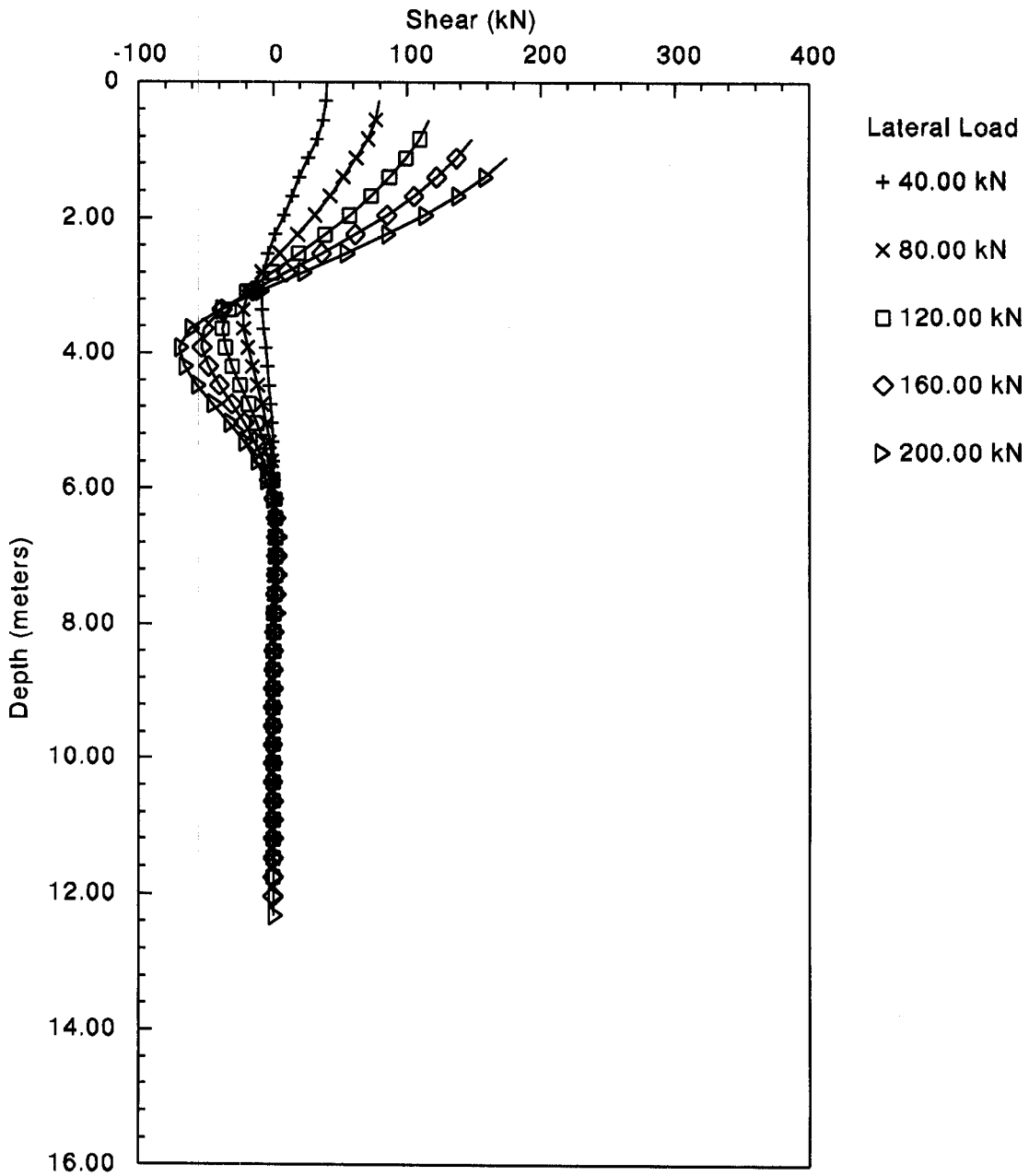


Figure F.29: Pier 2 - Plot of Shear versus Depth as a Function of Lateral Load on Y-Y Axis

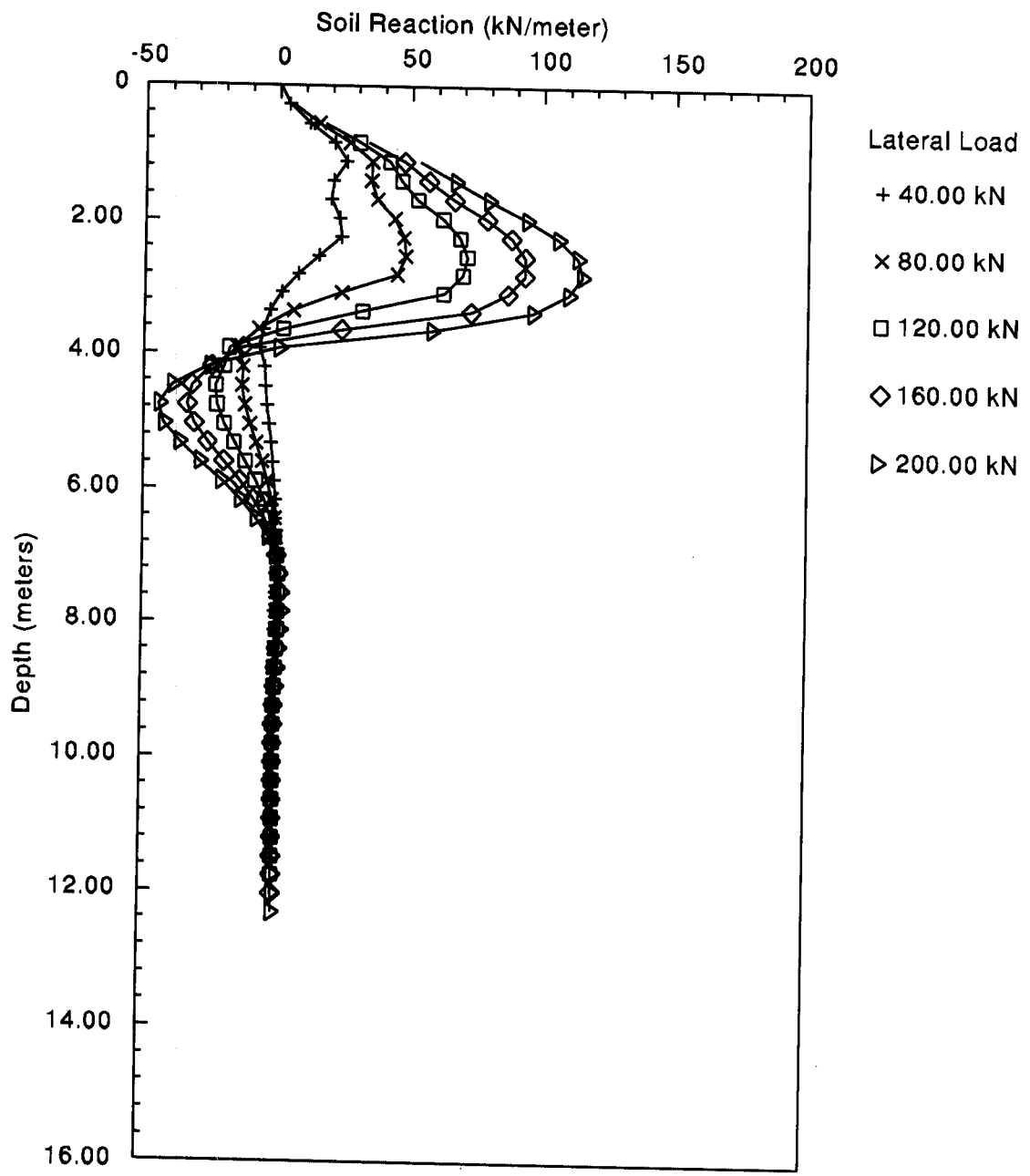


Figure F.30: Pier 2 - Plot of Soil Reaction versus Depth as a Function of Lateral Load on Y-Y Axis

F.4.4 COM624P - Pier 3 H-pile, X-X Axis and Y-Y Axis

As discussed in Chapter 13, wave equation driveability analyses at the internal piers indicated a potential driveability problem for 356 mm concrete piles. Therefore, low displacement HP 360x152 H-piles were chosen for the pile foundations at the interior piers.

COM624P solutions for lateral loading of the selected H-pile section at Pier 3 in both the major (X-X) and minor (Y-Y) axes directions were also obtained. The same assumptions used for Pier 2 also apply to Pier 3. The four meter extremely dense sand and gravel layer at Pier 2 decreases to one meter at Pier 3 location. The same assumed slope soil modulus ($50,000 \text{ kN/m}^3$) was used for the extremely dense sand and gravel layer. Soil parameters for the cohesive soil layers were obtained from Tables 9-12 and 9-13.

COM624P analysis of lateral loading in the X-X and Y-Y axes are presented on the following pages. The analysis output includes an echo print of the input file followed by the COM624P generated summaries of the problem input and output. The output includes a summary table of deflection, moment, shear, and soil reaction versus lateral load. For selected lateral loads in the X-X axis, Figures F.31 to F.34 provide graphical presentations of deflection, moment, shear, and soil reaction versus depth. These graphical presentations for loads in the Y-Y axis are presented in Figure F.35 to F.38. Note, the maximum lateral load analyzed was only 170 kN because a sudden failure occurred at 180 kN.

The COM624P analyses indicate the performance of the H-pile subjected to lateral loading is acceptable in either axis. The maximum deflection under the 40 kN design load is less than 1 mm.

Additional COM624P analyses should be performed to evaluate group response using the p-multiplier approach described in Section 9.8.4.

FHWA PIER3, HP360X152 X-X AXIS/FIXED-HEAD CYCLIC

2	1	0	1	0
100	3	0		
6	6	0		
13.000		210000000	0.000	0.000
1	2			
2	1	0	20	
100		0.00001000	2.00000000	
0.0000		0.3564	0.0004	0.0194
1	4	0.0000	1.0000	50000.0000
2	2	1.0000	4.0000	54300.0000
3	2	4.0000	13.0000	108500.0000
0.0000		10.60000		
1.0000		10.60000		
1.0000		9.80000		
4.0000		9.80000		
4.0000		10.40000		
13.0000		10.40000		
0.0000		0.0000	36.0000	0.00000
1.0000		0.0000	36.0000	0.00000
1.0000		106.0000	0.0000	0.00500
4.0000		106.0000	0.0000	0.00500
4.0000		155.0000	0.0000	0.00500
13.0000		155.0000	0.0000	0.00500
5				
1.0000				
2.0000				
3.0000				
4.0000				
5.0000				
10				
1	40.0000	0.0000	890.0000	
0	60.0000	0.0000	890.0000	
1	80.0000	0.0000	890.0000	
0	100.0000	0.0000	890.0000	
1	120.0000	0.0000	890.0000	
0	130.0000	0.0000	890.0000	
1	140.0000	0.0000	890.0000	
0	150.0000	0.0000	890.0000	
1	160.0000	0.0000	890.0000	
0	170.0000	0.0000	890.0000	

FHWA PIER3, HP360X152 X-X AXIS/FIXED-HEAD CYCLIC

UNITS--METR

 PILE DEFLECTION, BENDING MOMENT, SHEAR & SOIL RESISTANCE

 INPUT INFORMATION

THE LOADING IS CYCLIC

NO. OF CYCLES = .20E+02

PILE GEOMETRY AND PROPERTIES

PILE LENGTH = 13.00 M
 MODULUS OF ELASTICITY OF PILE = .210E+09 KN/ M**2
 1 SECTION(S)

X	DIAMETER	MOMENT OF INERTIA	AREA
M	M	M**4	M**2
.00			
13.00	.356	.400E-03	.194E-01

SOILS INFORMATION

X-COORDINATE AT THE GROUND SURFACE = .00 M
 SLOPE ANGLE AT THE GROUND SURFACE = .00 DEG.
 3 LAYER(S) OF SOIL

LAYER 1

THE LAYER IS A SAND

X AT THE TOP OF THE LAYER = .00 M
 X AT THE BOTTOM OF THE LAYER = 1.00 M
 VARIATION OF SOIL MODULUS, k = .500E+05 KN/ M**3

LAYER 2

THE LAYER IS A STIFF CLAY BELOW THE WATER TABLE

X AT THE TOP OF THE LAYER = 1.00 M
 X AT THE BOTTOM OF THE LAYER = 4.00 M
 VARIATION OF SOIL MODULUS, k = .543E+05 KN/ M**3

LAYER 3

THE LAYER IS A STIFF CLAY BELOW THE WATER TABLE

X AT THE TOP OF THE LAYER = 4.00 M
 X AT THE BOTTOM OF THE LAYER = 13.00 M
 VARIATION OF SOIL MODULUS, k = .109E+06 KN/ M**3

DISTRIBUTION OF EFFECTIVE UNIT WEIGHT WITH DEPTH

6 POINTS

X, M	WEIGHT, KN/ M**3
.00	.11E+02
1.00	.11E+02
1.00	.98E+01
4.00	.98E+01
4.00	.10E+02
13.00	.10E+02

DISTRIBUTION OF STRENGTH PARAMETERS WITH DEPTH

6 POINTS

X, M	C, KN/ M**2	PHI, DEGREES	E50
.00	.000E+00	36.000	-----
1.00	.000E+00	36.000	-----
1.00	.106E+03	.000	.500E-02
4.00	.106E+03	.000	.500E-02
4.00	.155E+03	.000	.500E-02
13.00	.155E+03	.000	.500E-02

FINITE DIFFERENCE PARAMETERS

NUMBER OF PILE INCREMENTS = 100
 TOLERANCE ON DETERMINATION OF DEFLECTIONS = .100E-04 M
 MAXIMUM NUMBER OF ITERATIONS ALLOWED FOR PILE ANALYSIS = 100
 MAXIMUM ALLOWABLE DEFLECTION = .20E+01 M

INPUT CODES

OUTPT = 1
 KCYCL = 0
 KBC = 2
 KPYOP = 1
 INC = 2

FHWA PIER3, HP360X152 X-X AXIS/FIXED-HEAD CYCLIC

UNITS--METR

O U T P U T I N F O R M A T I O N

GENERATED P-Y CURVES

THE NUMBER OF CURVE IS = 5
THE NUMBER OF POINTS ON EACH CURVE = 17

DEPTH BELOW GS DIAM C CAVG GAMMA E50
M M KN/ M**2 KN/ M**2 KN/ M**3
1.00 .356 .1E+03 .1E+03 .1E+02 .500E-02

AS =.58 AC =.30 Y, M P, KN/ M

	.000		.000
	.000		12.473
	.000		24.946
	.001		37.420
	.001		49.893
	.001		62.366
	.001		74.839
	.001		87.312
	.002		99.785
	.002		112.259
	.002		120.585
	.002		118.265
	.003		113.316
	.004		80.576
	.006		47.817
	.008		15.059
	.085		15.059

----- *** -----

FHWA PIER3, HP360X152 X-X AXIS/FIXED-HEAD CYCLIC

UNITS--METR

PILE LOADING CONDITION

LATERAL LOAD AT PILE HEAD = .400E+02 KN
 SLOPE AT PILE HEAD = .000E+00 M/ M
 AXIAL LOAD AT PILE HEAD = .000E+00 KN

X	DEFLECTION	MOMENT	TOTAL STRESS	SHEAR	SOIL RESIST	FLEXURAL RIGIDITY
M	M	M- KN	KN/ M**2	KN	KN/ M	KN- M**2
0.00	.646E-03	-.440E+02	.655E+05	.400E+02	.000E+00	.840E+05
.26	.629E-03	-.336E+02	.608E+05	.397E+02	.268E+01	.840E+05
.52	.586E-03	-.234E+02	.563E+05	.383E+02	.820E+01	.840E+05
.78	.523E-03	-.137E+02	.520E+05	.353E+02	.152E+02	.840E+05
1.04	.450E-03	-.497E+01	.481E+05	.303E+02	.275E+02	.840E+05
1.30	.372E-03	.203E+01	.468E+05	.230E+02	.280E+02	.840E+05
1.56	.296E-03	.716E+01	.491E+05	.160E+02	.265E+02	.840E+05
1.82	.225E-03	.105E+02	.506E+05	.949E+01	.234E+02	.840E+05
2.08	.163E-03	.123E+02	.513E+05	.397E+01	.193E+02	.840E+05
2.34	.111E-03	.127E+02	.516E+05	-.423E+00	.147E+02	.840E+05
2.60	.690E-04	.122E+02	.513E+05	-.362E+01	.101E+02	.840E+05
2.86	.368E-04	.110E+02	.508E+05	-.567E+01	.577E+01	.840E+05
3.12	.133E-04	.938E+01	.501E+05	-.667E+01	.212E+01	.840E+05
3.38	-.253E-05	.761E+01	.493E+05	-.688E+01	-.395E+00	.840E+05
3.64	-.123E-04	.586E+01	.485E+05	-.656E+01	-.194E+01	.840E+05
3.90	-.173E-04	.424E+01	.478E+05	-.594E+01	-.273E+01	.840E+05
4.16	-.189E-04	.281E+01	.471E+05	-.493E+01	-.436E+01	.840E+05
4.42	-.182E-04	.167E+01	.466E+05	-.382E+01	-.421E+01	.840E+05
4.68	-.162E-04	.815E+00	.462E+05	-.279E+01	-.375E+01	.840E+05
4.94	-.135E-04	.209E+00	.460E+05	-.190E+01	-.313E+01	.840E+05
5.20	-.106E-04	-.188E+00	.460E+05	-.118E+01	-.247E+01	.840E+05
5.46	-.791E-05	-.418E+00	.461E+05	-.621E+00	-.184E+01	.840E+05
5.72	-.551E-05	-.525E+00	.461E+05	-.220E+00	-.128E+01	.840E+05
5.98	-.353E-05	-.545E+00	.461E+05	.490E-01	-.820E+00	.840E+05
6.24	-.198E-05	-.510E+00	.461E+05	.213E+00	-.461E+00	.840E+05
6.50	-.840E-06	-.442E+00	.461E+05	.296E+00	-.196E+00	.840E+05
6.76	-.554E-07	-.361E+00	.460E+05	.321E+00	-.135E-01	.840E+05
7.02	.438E-06	-.279E+00	.460E+05	.309E+00	.101E+00	.840E+05
7.28	.707E-06	-.203E+00	.460E+05	.274E+00	.164E+00	.840E+05
7.54	.811E-06	-.138E+00	.459E+05	.228E+00	.188E+00	.840E+05
7.80	.805E-06	-.847E-01	.459E+05	.179E+00	.187E+00	.840E+05
8.06	.730E-06	-.443E-01	.459E+05	.133E+00	.170E+00	.840E+05
8.32	.618E-06	-.152E-01	.459E+05	.921E-01	.144E+00	.840E+05
8.58	.494E-06	.428E-02	.459E+05	.586E-01	.115E+00	.840E+05
8.84	.373E-06	.160E-01	.459E+05	.326E-01	.868E-01	.840E+05
9.10	.264E-06	.219E-01	.459E+05	.136E-01	.615E-01	.840E+05
9.36	.173E-06	.236E-01	.459E+05	.476E-03	.404E-01	.840E+05
9.62	.101E-06	.226E-01	.459E+05	-.770E-02	.236E-01	.840E+05
9.88	.472E-07	.200E-01	.459E+05	-.121E-01	.110E-01	.840E+05
10.14	.917E-08	.166E-01	.459E+05	-.137E-01	.216E-02	.840E+05
10.40	-.155E-07	.130E-01	.459E+05	-.135E-01	-.358E-02	.840E+05
10.66	-.296E-07	.969E-02	.459E+05	-.121E-01	-.688E-02	.840E+05
10.92	-.360E-07	.679E-02	.459E+05	-.101E-01	-.836E-02	.840E+05
11.18	-.368E-07	.445E-02	.459E+05	-.791E-02	-.856E-02	.840E+05
11.44	-.341E-07	.267E-02	.459E+05	-.577E-02	-.792E-02	.840E+05
11.70	-.291E-07	.143E-02	.459E+05	-.386E-02	-.677E-02	.840E+05
11.96	-.230E-07	.633E-03	.459E+05	-.229E-02	-.535E-02	.840E+05
12.22	-.164E-07	.198E-03	.459E+05	-.111E-02	-.381E-02	.840E+05
12.48	-.957E-08	.178E-04	.459E+05	-.329E-03	-.223E-02	.840E+05
12.74	-.274E-08	-.125E-04	.459E+05	.404E-04	-.642E-03	.840E+05
13.00	.408E-08	.000E+00	.459E+05	.000E+00	.944E-03	.840E+05

COMPUTED LATERAL FORCE AT PILE HEAD = .40000E+02 KN
 COMPUTED SLOPE AT PILE HEAD = -.41700E-18 M/ M

THE OVERALL MOMENT IMBALANCE = -.494E-11 M- KN
 THE OVERALL LATERAL FORCE IMBALANCE = .669E-11 KN

FHWA PIER3, HP360X152 X-X AXIS/FIXED-HEAD CYCLIC

UNITS--METR

OUTPUT SUMMARY

PILE HEAD DEFLECTION = .646E-03 M
 MAXIMUM BENDING MOMENT = -.440E+02 M- KN
 MAXIMUM TOTAL STRESS = .655E+05 KN/ M**2

NO. OF ITERATIONS = 5
 MAXIMUM DEFLECTION ERROR = .367E-05 M

COMPUTED LATERAL FORCE AT PILE HEAD = .60000E+02 KN
 COMPUTED SLOPE AT PILE HEAD = .83400E-18 M/ M

THE OVERALL MOMENT IMBALANCE = .104E-10 M- KN
 THE OVERALL LATERAL FORCE IMBALANCE = -.145E-10 KN

PILE HEAD DEFLECTION = .102E-02 M
 MAXIMUM BENDING MOMENT = -.679E+02 M- KN
 MAXIMUM TOTAL STRESS = .761E+05 KN/ M**2

NO. OF ITERATIONS = 3
 MAXIMUM DEFLECTION ERROR = .482E-05 M

 S U M M A R Y T A B L E

LATERAL LOAD (KN)	BOUNDARY CONDITION BC2	AXIAL LOAD (KN)	YT (M)	ST (M/ M)	MAX. MOMENT (M- KN)	MAX. STRESS (KN/ M**2)
.400E+02	.000E+00	.890E+03	.646E-03	-.417E-18	-.440E+02	.655E+05
.600E+02	.000E+00	.890E+03	.102E-02	.834E-18	-.679E+02	.761E+05
.800E+02	.000E+00	.890E+03	.140E-02	.000E+00	-.921E+02	.869E+05
.100E+03	.000E+00	.890E+03	.178E-02	.000E+00	-.116E+03	.977E+05
.120E+03	.000E+00	.890E+03	.216E-02	.000E+00	-.141E+03	.108E+06
.130E+03	.000E+00	.890E+03	.235E-02	.000E+00	-.153E+03	.114E+06
.140E+03	.000E+00	.890E+03	.254E-02	.167E-17	-.165E+03	.119E+06
.150E+03	.000E+00	.890E+03	.273E-02	.000E+00	-.177E+03	.125E+06
.160E+03	.000E+00	.890E+03	.298E-02	.000E+00	-.190E+03	.131E+06
.170E+03	.000E+00	.890E+03	.334E-02	.167E-17	-.206E+03	.138E+06

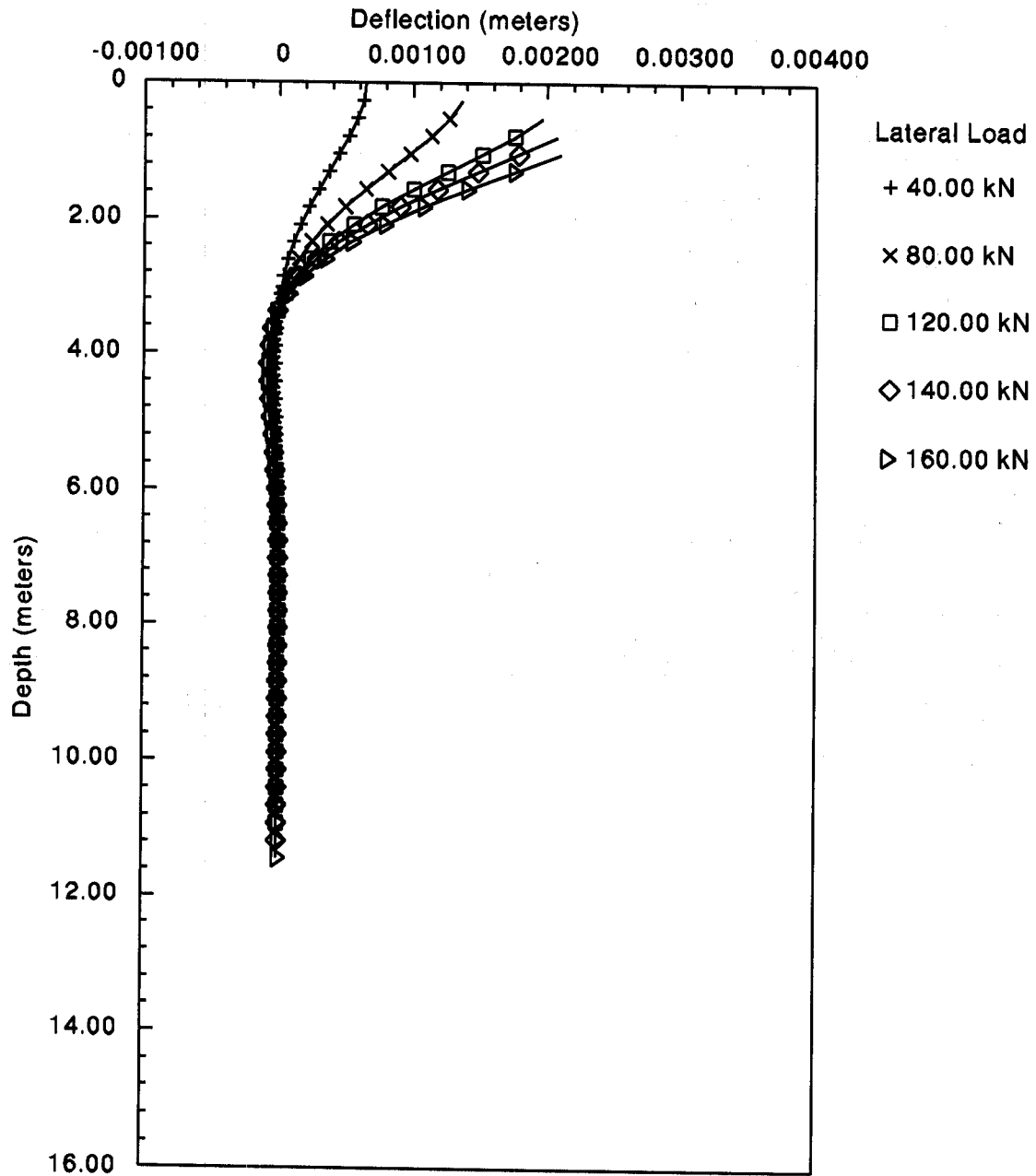


Figure F.31: Pier 3 - Plot of Deflection versus Depth as a Function on Lateral Load on X-X Axis

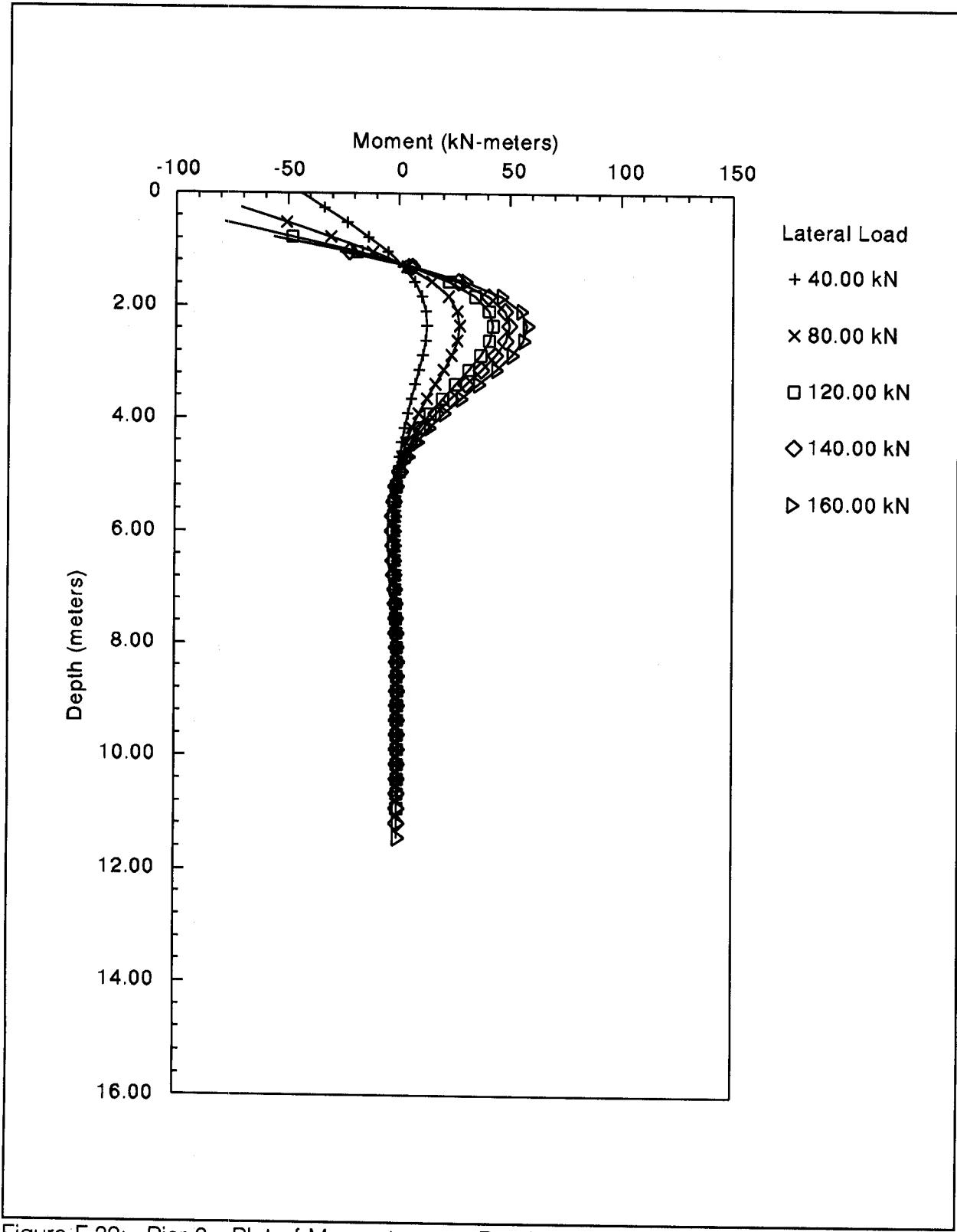


Figure F.32: Pier 3 - Plot of Moment versus Depth as a Function of Lateral Load on X-X Axis

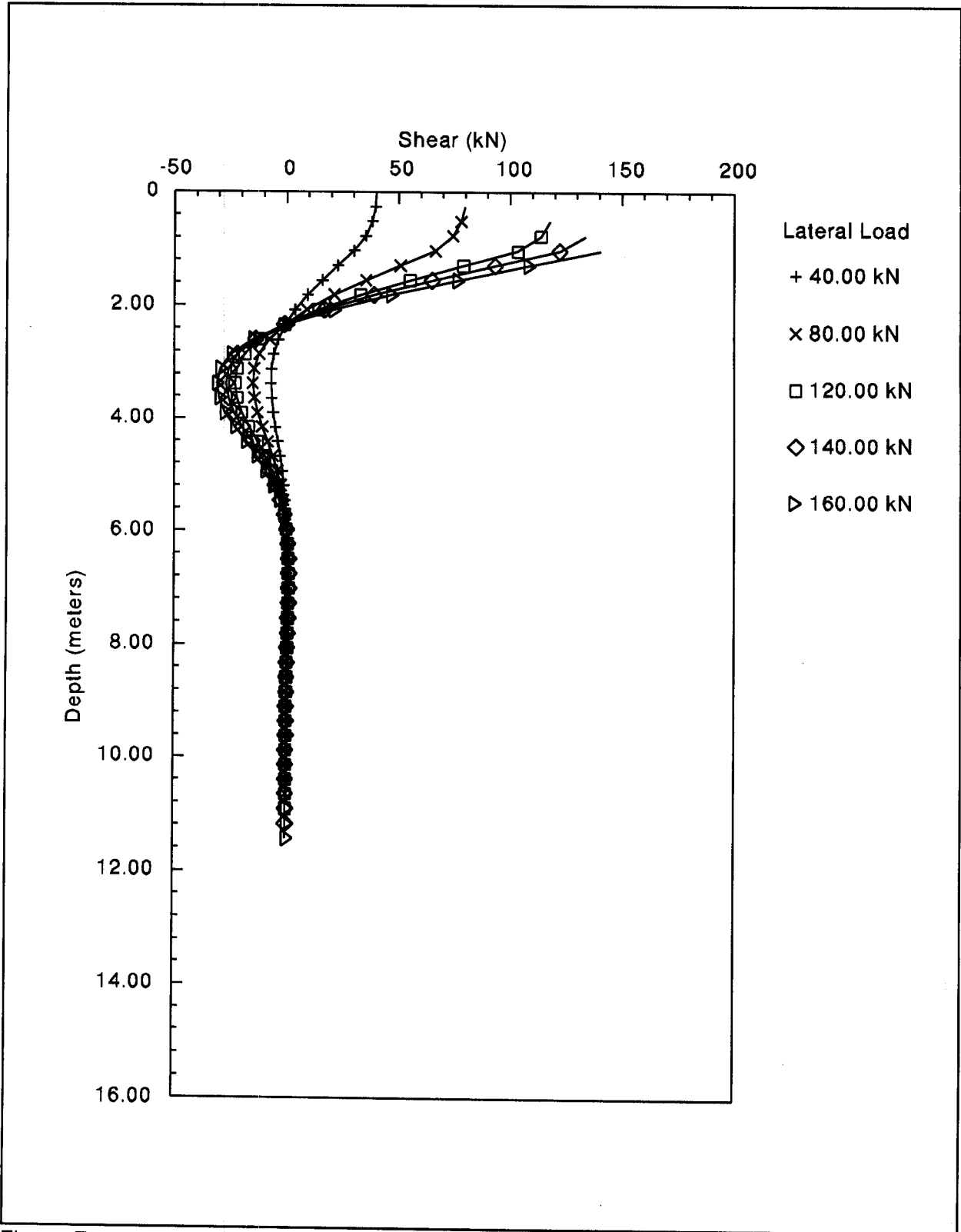


Figure F.33: Pier 3 - Plot of Shear versus Depth as a Function of Lateral Load on X-X Axis

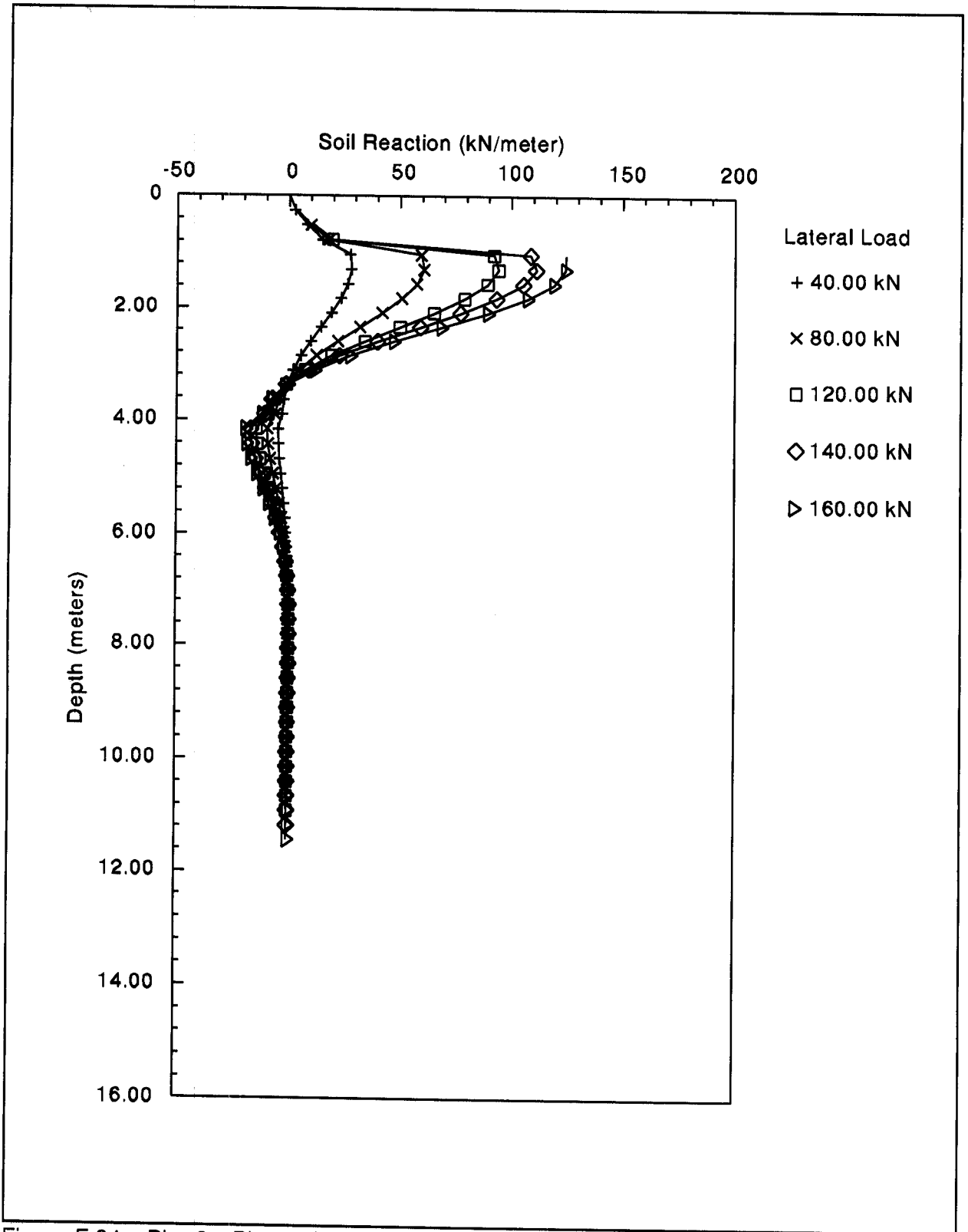


Figure F.34: Pier 3 - Plot of Soil Reaction versus Depth as a Function of Lateral Load on X-X Axis

FHWA PIER3, HP360X152 Y-Y AXIS/FIXED-HEAD CYCLIC

2	1	0		
100	3	1	0	
6	6	0		
1			0.000	0.000
13.000	210000000			
2	1	0		20
100	0.00001000		2.00000000	
0.0000	0.3755		0.0002	0.0194
1	4	0.0000	1.0000	55000.0000
2	2	1.0000	4.0000	54300.0000
3	2	4.0000	13.0000	108500.0000
0.0000	10.60000			
1.0000	10.60000			
1.0000	9.80000			
4.0000	9.80000			
4.0000	10.40000			
13.0000	10.40000			
0.0000	0.0000	36.0000	0.00000	
1.0000	0.0000	36.0000	0.00000	
1.0000	106.0000	0.0000	0.00500	
4.0000	106.0000	0.0000	0.00500	
4.0000	155.0000	0.0000	0.00500	
14.0000	155.0000	0.0000	0.00500	
5				
1.0000				
2.0000				
3.0000				
4.0000				
5.0000				
10				
1	40.0000	0.0000	890.0000	
0	60.0000	0.0000	890.0000	
1	80.0000	0.0000	890.0000	
0	100.0000	0.0000	890.0000	
1	120.0000	0.0000	890.0000	
0	130.0000	0.0000	890.0000	
1	140.0000	0.0000	890.0000	
0	150.0000	0.0000	890.0000	
1	160.0000	0.0000	890.0000	
0	170.0000	0.0000	890.0000	

FHWA PIER3, HP360X152 Y-Y AXIS/FIXED-HEAD CYCLIC

UNITS--METR

 PILE DEFLECTION, BENDING MOMENT, SHEAR & SOIL RESISTANCE

INPUT INFORMATION

THE LOADING IS CYCLIC

NO. OF CYCLES = .20E+02

PILE GEOMETRY AND PROPERTIES

PILE LENGTH = 13.00 M
 MODULUS OF ELASTICITY OF PILE = .210E+09 KN/ M**2
 1 SECTION(S)

X	DIAMETER	MOMENT OF INERTIA	AREA
M	M	M**4	M**2
.00			
13.00	.376	.200E-03	.194E-01

SOILS INFORMATION

X-COORDINATE AT THE GROUND SURFACE = .00 M
 SLOPE ANGLE AT THE GROUND SURFACE = .00 DEG.

3 LAYER(S) OF SOIL

LAYER 1

THE LAYER IS A SAND

X AT THE TOP OF THE LAYER = .00 M
 X AT THE BOTTOM OF THE LAYER = 1.00 M
 VARIATION OF SOIL MODULUS, k = .500E+05 KN/ M**3

LAYER 2

THE LAYER IS A STIFF CLAY BELOW THE WATER TABLE

X AT THE TOP OF THE LAYER = 1.00 M
 X AT THE BOTTOM OF THE LAYER = 4.00 M
 VARIATION OF SOIL MODULUS, k = .543E+05 KN/ M**3

LAYER 3

THE LAYER IS A STIFF CLAY BELOW THE WATER TABLE

X AT THE TOP OF THE LAYER = 4.00 M
 X AT THE BOTTOM OF THE LAYER = 13.00 M
 VARIATION OF SOIL MODULUS, k = .109E+06 KN/ M**3

DISTRIBUTION OF EFFECTIVE UNIT WEIGHT WITH DEPTH

6 POINTS	
X, M	WEIGHT, KN/ M**3
.00	.11E+02
1.00	.11E+02
1.00	.98E+01
4.00	.98E+01
4.00	.10E+02
13.00	.10E+02

DISTRIBUTION OF STRENGTH PARAMETERS WITH DEPTH

6 POINTS			
X, M	C, KN/ M**2	PHI, DEGREES	E50
.00	.000E+00	36.000	-----
1.00	.000E+00	36.000	-----
1.00	.106E+03	.000	.500E-02
4.00	.106E+03	.000	.500E-02
4.00	.155E+03	.000	.500E-02
14.00	.155E+03	.000	.500E-02

FINITE DIFFERENCE PARAMETERS

NUMBER OF PILE INCREMENTS = 100
 TOLERANCE ON DETERMINATION OF DEFLECTIONS = .100E-04 M
 MAXIMUM NUMBER OF ITERATIONS ALLOWED FOR PILE ANALYSIS = 100
 MAXIMUM ALLOWABLE DEFLECTION = .20E+01 M

INPUT CODES

OUTPT = 1
 KCYCL = 0
 KBC = 2
 KPYOP = 1
 INC = 2

FHWA PIER3, HP360X152 Y-Y AXIS/FIXED-HEAD CYCLIC

UNITS--METR

O U T P U T I N F O R M A T I O N

GENERATED P-Y CURVES

THE NUMBER OF CURVE IS = 5
THE NUMBER OF POINTS ON EACH CURVE = 17

DEPTH BELOW GS DIAM C CAVG GAMMA E50
M M KN/ M**2 KN/ M**2 KN/ M**3 .500E-02
1.00 .376 .1E+03 .1E+03 .1E+02

AS = .58 AC = .30 Y, M P, KN/ M
.000 .000
.000 12.697
.000 25.394
.001 38.092
.001 50.789
.001 63.486
.001 76.183
.002 88.881
.002 101.578
.002 114.275
.002 119.482
.002 117.183
.003 112.279
.004 80.157
.006 48.016
.008 15.876
.089 15.876

FHWA PIER3, HP360X152 Y-Y AXIS/FIXED-HEAD CYCLIC

UNITS--METR

PILE LOADING CONDITION

LATERAL LOAD AT PILE HEAD = .400E+02 KN
 SLOPE AT PILE HEAD = .000E+00 M/ M
 AXIAL LOAD AT PILE HEAD = .000E+00 KN

X	DEFLECTION	MOMENT	TOTAL STRESS	SHEAR	SOIL RESIST	FLEXURAL RIGIDITY
M	M	M- KN	KN/ M**2	KN	KN/ M	KN- M**2
.00	.932E-03	-.401E+02	.835E+05	.400E+02	.000E+00	.420E+05
.26	.902E-03	-.297E+02	.738E+05	.397E+02	.294E+01	.420E+05
.52	.824E-03	-.195E+02	.641E+05	.382E+02	.893E+01	.420E+05
.78	.714E-03	-.980E+01	.551E+05	.349E+02	.167E+02	.420E+05
1.04	.589E-03	-.123E+01	.470E+05	.290E+02	.352E+02	.420E+05
1.30	.462E-03	.524E+01	.508E+05	.200E+02	.342E+02	.420E+05
1.56	.342E-03	.942E+01	.547E+05	.116E+02	.302E+02	.420E+05
1.82	.238E-03	.116E+02	.567E+05	.455E+01	.244E+02	.420E+05
2.08	.152E-03	.121E+02	.572E+05	-.889E+00	.178E+02	.420E+05
2.34	.855E-04	.114E+02	.565E+05	-.462E+01	.112E+02	.420E+05
2.60	.372E-04	.987E+01	.551E+05	-.674E+01	.541E+01	.420E+05
2.86	.467E-05	.801E+01	.534E+05	-.752E+01	.757E+00	.420E+05
3.12	-.150E-04	.608E+01	.516E+05	-.728E+01	-.236E+01	.420E+05
3.38	-.248E-04	.429E+01	.499E+05	-.645E+01	-.390E+01	.420E+05
3.64	-.277E-04	.275E+01	.485E+05	-.536E+01	-.436E+01	.420E+05
3.90	-.261E-04	.150E+01	.473E+05	-.426E+01	-.412E+01	.420E+05
4.16	-.221E-04	.553E+00	.464E+05	-.294E+01	-.511E+01	.420E+05
4.42	-.172E-04	-.545E-01	.459E+05	-.177E+01	-.398E+01	.420E+05
4.68	-.123E-04	-.394E+00	.462E+05	-.886E+00	-.286E+01	.420E+05
4.94	-.810E-05	-.541E+00	.464E+05	-.277E+00	-.188E+01	.420E+05
5.20	-.471E-05	-.560E+00	.464E+05	.103E+00	-.110E+01	.420E+05
5.46	-.222E-05	-.504E+00	.463E+05	.308E+00	-.517E+00	.420E+05
5.72	-.533E-06	-.412E+00	.463E+05	.388E+00	-.125E+00	.420E+05
5.98	.491E-06	-.310E+00	.462E+05	.387E+00	.113E+00	.420E+05
6.24	.102E-05	-.215E+00	.461E+05	.340E+00	.236E+00	.420E+05
6.50	.119E-05	-.135E+00	.460E+05	.273E+00	.277E+00	.420E+05
6.76	.115E-05	-.733E-01	.459E+05	.202E+00	.268E+00	.420E+05
7.02	.990E-06	-.294E-01	.459E+05	.137E+00	.230E+00	.420E+05
7.28	.780E-06	-.910E-03	.459E+05	.840E-01	.181E+00	.420E+05
7.54	.566E-06	.154E-01	.459E+05	.436E-01	.132E+00	.420E+05
7.80	.377E-06	.229E-01	.459E+05	.154E-01	.878E-01	.420E+05
8.06	.224E-06	.244E-01	.459E+05	-.251E-02	.522E-01	.420E+05
8.32	.110E-06	.224E-01	.459E+05	-.124E-01	.257E-01	.420E+05
8.58	.322E-07	.185E-01	.459E+05	-.166E-01	.755E-02	.420E+05
8.84	-.161E-07	.141E-01	.459E+05	-.170E-01	-.371E-02	.420E+05
9.10	-.417E-07	.991E-02	.459E+05	-.151E-01	-.969E-02	.420E+05
9.36	-.514E-07	.633E-02	.459E+05	-.123E-01	-.119E-01	.420E+05
9.62	-.507E-07	.353E-02	.459E+05	-.921E-02	-.118E-01	.420E+05
9.88	-.443E-07	.152E-02	.459E+05	-.634E-02	-.103E-01	.420E+05
10.14	-.353E-07	.189E-03	.459E+05	-.395E-02	-.822E-02	.420E+05
10.40	-.260E-07	-.588E-03	.459E+05	-.211E-02	-.606E-02	.420E+05
10.66	-.176E-07	-.957E-03	.459E+05	-.800E-03	-.411E-02	.420E+05
10.92	-.108E-07	-.105E-02	.459E+05	.465E-04	-.251E-02	.420E+05
11.18	-.555E-08	-.967E-03	.459E+05	.530E-03	-.129E-02	.420E+05
11.44	-.189E-08	-.797E-03	.459E+05	.748E-03	-.443E-03	.420E+05
11.70	.489E-09	-.595E-03	.459E+05	.786E-03	.112E-03	.420E+05
11.96	.191E-08	-.399E-03	.459E+05	.711E-03	.443E-03	.420E+05
12.22	.269E-08	-.231E-03	.459E+05	.571E-03	.625E-03	.420E+05
12.48	.309E-08	-.105E-03	.459E+05	.397E-03	.718E-03	.420E+05
12.74	.331E-08	-.268E-04	.459E+05	.204E-03	.771E-03	.420E+05
13.00	.349E-08	.000E+00	.459E+05	.000E+00	.813E-03	.420E+05

COMPUTED LATERAL FORCE AT PILE HEAD = .40000E+02 KN
 COMPUTED SLOPE AT PILE HEAD = .00000E+00 M/ M

THE OVERALL MOMENT IMBALANCE = .332E-11 M- KN
 THE OVERALL LATERAL FORCE IMBALANCE = .155E-11 KN

FHWA PIER3, HP360X152 Y-Y AXIS/FIXED-HEAD CYCLIC

UNITS--METR

OUTPUT SUMMARY

PILE HEAD DEFLECTION = .932E-03 M
 MAXIMUM BENDING MOMENT = -.401E+02 M- KN
 MAXIMUM TOTAL STRESS = .835E+05 KN/ M**2

NO. OF ITERATIONS = 5
 MAXIMUM DEFLECTION ERROR = .573E-05 M

COMPUTED LATERAL FORCE AT PILE HEAD = .60000E+02 KN
 COMPUTED SLOPE AT PILE HEAD = .83400E-18 M/ M

THE OVERALL MOMENT IMBALANCE = -.948E-11 M- KN
 THE OVERALL LATERAL FORCE IMBALANCE = .160E-10 KN

PILE HEAD DEFLECTION = .147E-02 M
 MAXIMUM BENDING MOMENT = -.620E+02 M- KN
 MAXIMUM TOTAL STRESS = .104E+06 KN/ M**2

NO. OF ITERATIONS = 3
 MAXIMUM DEFLECTION ERROR = .783E-05 M

----- *** -----

S U M M A R Y T A B L E

LATERAL LOAD (KN)	BOUNDARY CONDITION BC2	AXIAL LOAD (KN)	YT (M)	ST (M/ M)	MAX. MOMENT (M- KN)	MAX. STRESS (KN/ M**2)
.400E+02	.000E+00	.890E+03	.932E-03	.000E+00	-.401E+02	.835E+05
.600E+02	.000E+00	.890E+03	.147E-02	.834E-18	-.620E+02	.104E+06
.800E+02	.000E+00	.890E+03	.202E-02	-.167E-17	-.840E+02	.125E+06
.100E+03	.000E+00	.890E+03	.258E-02	-.167E-17	-.106E+03	.146E+06
.120E+03	.000E+00	.890E+03	.313E-02	.000E+00	-.128E+03	.166E+06
.130E+03	.000E+00	.890E+03	.343E-02	.000E+00	-.140E+03	.177E+06
.140E+03	.000E+00	.890E+03	.382E-02	.000E+00	-.153E+03	.189E+06
.150E+03	.000E+00	.890E+03	.436E-02	.000E+00	-.167E+03	.203E+06
.160E+03	.000E+00	.890E+03	.514E-02	.334E-17	-.185E+03	.219E+06
.170E+03	.000E+00	.890E+03	.638E-02	-.334E-17	-.207E+03	.240E+06

Pier 3 Y-Y Axis - COM624P Problem Output

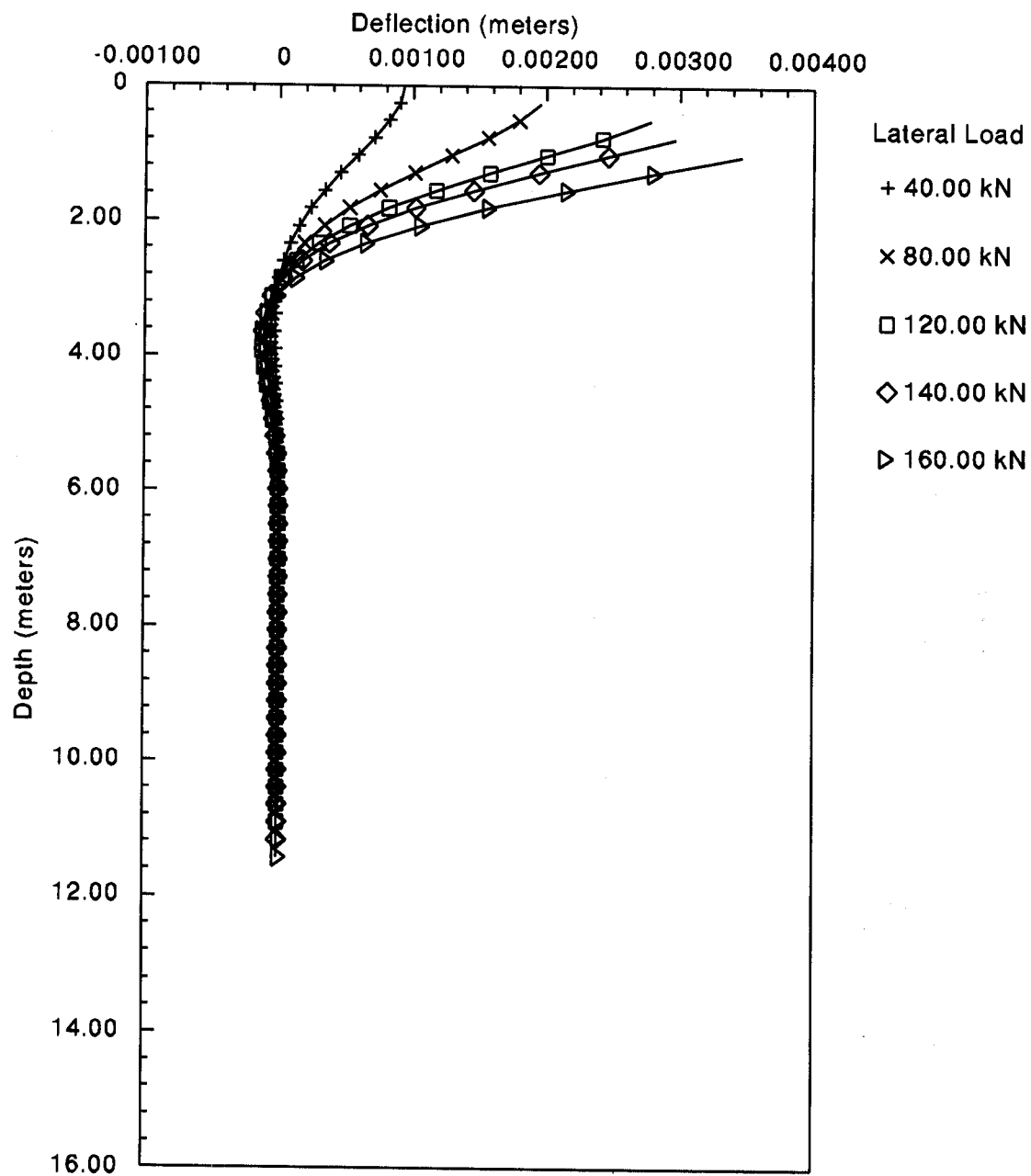


Figure F.35: Pier 3 - Plot of Deflection versus Depth as a Function of Lateral Load on Y-Y Axis

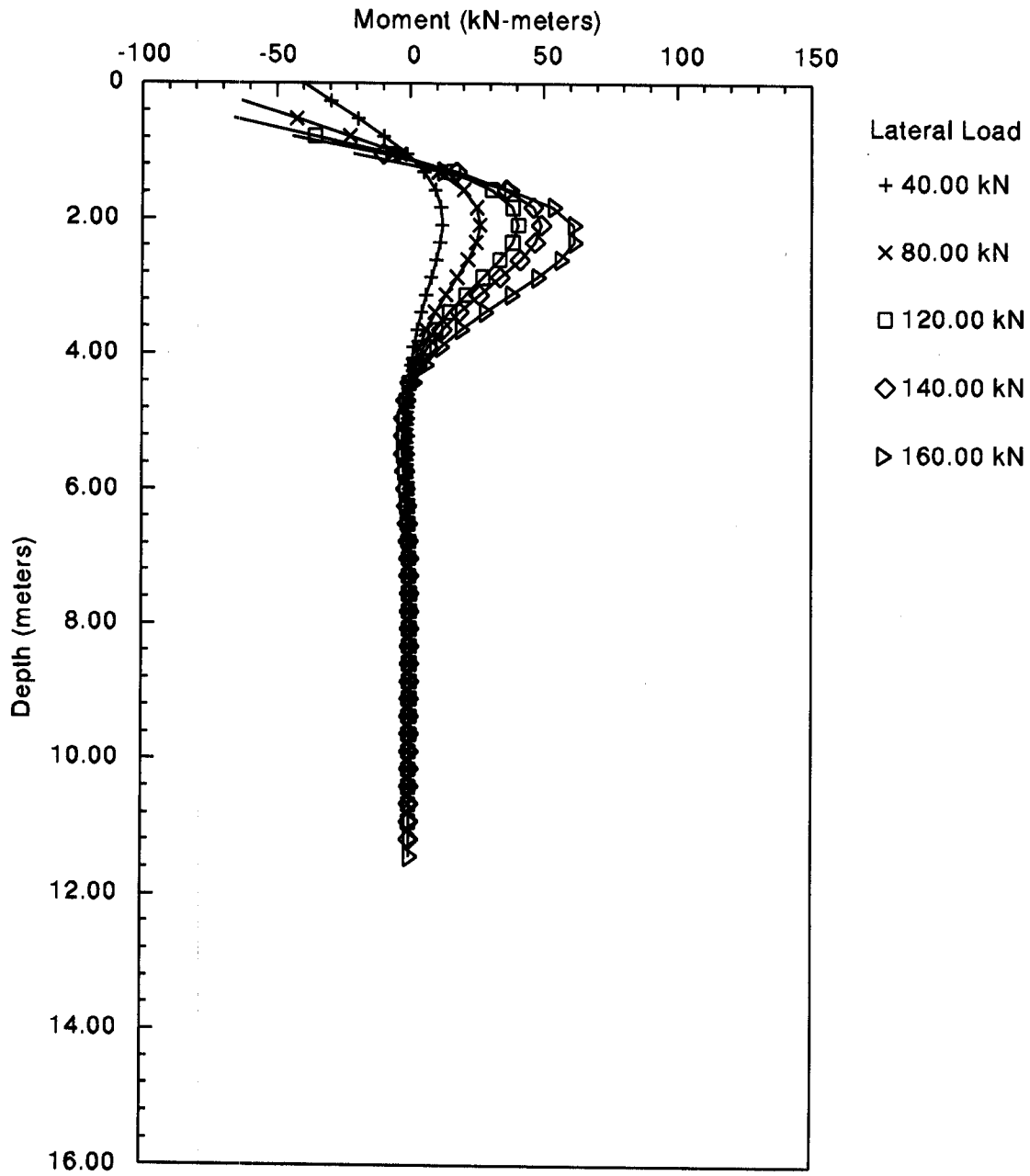


Figure F.36: Pier 3 - Plot of Moment versus Depth as a Function of Lateral Load on Y-Y Axis

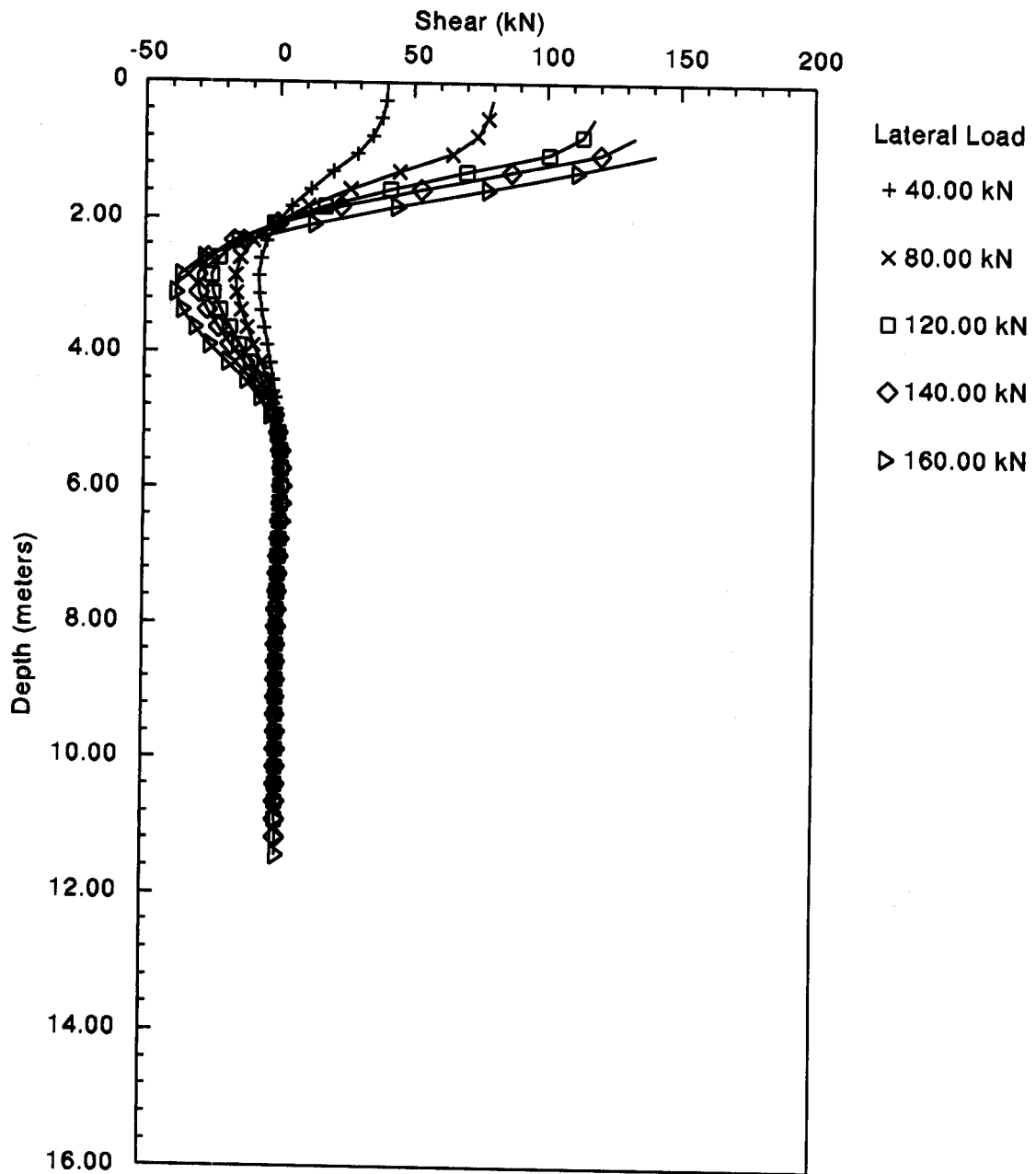


Figure F.37: Pier 3 - Plot of Shear versus Depth as a Function of Lateral Load on Y-Y Axis

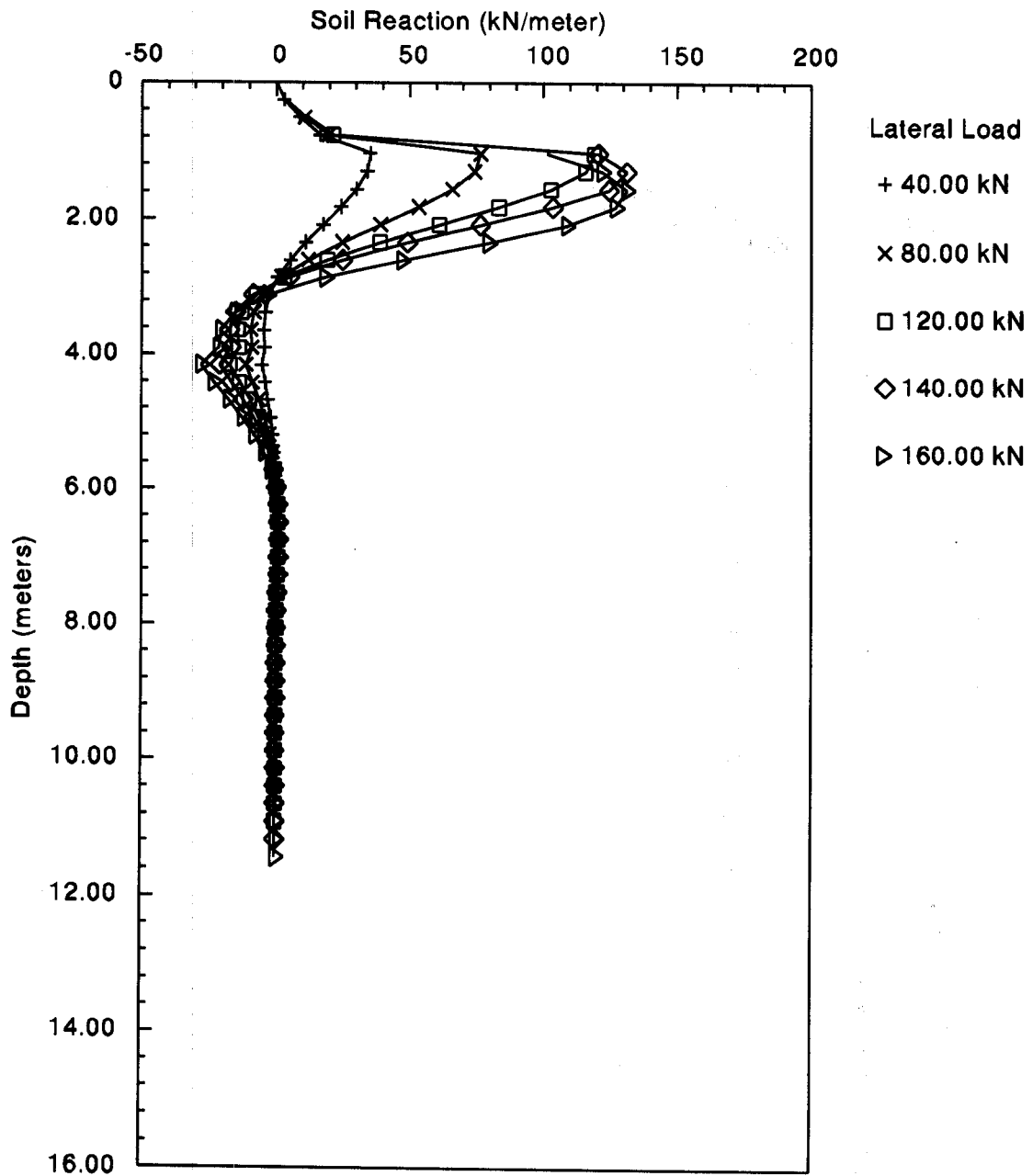


Figure F.38: Pier 3 - Plot of Soil Reaction versus Depth as a Function of Lateral Load on Y-Y Axis

F.4.5 COM624P Analysis - South Abutment

A COM624P analysis was performed to evaluate the performance of the 356 mm square prestressed concrete pile under lateral load at the South abutment. Unlike the North Abutment, the soil at the South abutment consists of only cohesive type. Again, soil parameters were obtained from Tables 9-12 and 9-13.

The same assumptions and analysis options as the North abutment were used. Ten lateral loads were analyzed, as follows: 20, 40, 60, 80, 90, 100, 110, 120, 130, and 140 kN. However, for presentation only the 40, 80, 100, 120, and 140 kN were retained. Note, a sudden failure occurred when the lateral load exceed 140 kN.

An echo print of the input file is presented on the following page. This is followed by the input and output summary of the PMEIX subroutine results for calculation of the ultimate bending resistance and flexural rigidity of the pile. Last, COM624P generated summaries of the problem input and output are provided. For selected lateral loads, Figures F.39 to F.42 provide graphical presentations of deflection, movement, shear, and soil reaction versus depth.

The COM624P solutions for the South abutment indicate the pile deflection under the 40 kN design load will be 2.5 mm. The corresponding maximum moment and shear stress are -46.1 m-kN and 13,400 kN/m², respectively. The deflection, moment and shear stress under the design load are acceptable.

Additional COM624P analyses should be performed to evaluate group response using the p-multiplier approach described in Section 9.8.4.

FHWA South Abut. - 355 mm-sq PSC Fixed-Head/Cyclic/Crack Modeled

2	3	1			
100		1	0		
6	6	0			
21.000		27800000	0.000	0.000	
1	2				
2	1	0	20		
100		0.00000100	1.00000000		
0.0000		0.3550	0.0013	0.1260	
1	1	0.0000	5.5000	27150.0000	
2	2	5.5000	15.0000	54300.0000	
3	2	15.0000	21.0000	108500.0000	
0.0000		9.20000			
5.5000		9.20000			
5.5000		9.70000			
15.0000		9.70000			
15.0000		10.50000			
21.0000		10.50000			
0.0000		33.0000	0.0000	0.01000	
5.5000		33.0000	0.0000	0.01000	
5.5000		93.0000	0.0000	0.00700	
15.0000		93.0000	0.0000	0.00700	
15.0000		161.0000	0.0000	0.00500	
21.0000		161.0000	0.0000	0.00500	
5					
1.0000					
2.0000					
3.0000					
4.0000					
5.0000					
10					
0	20.0000	0.0000	890.0000		
1	40.0000	0.0000	890.0000		
0	60.0000	0.0000	890.0000		
1	80.0000	0.0000	890.0000		
0	90.0000	0.0000	890.0000		
1	100.0000	0.0000	890.0000		
0	110.0000	0.0000	890.0000		
1	120.0000	0.0000	890.0000		
0	130.0000	0.0000	890.0000		
1	140.0000	0.0000	890.0000		
1	10				
890.00					
890.00					
890.00					
890.00					
890.00					
890.00					
890.00					
890.00					
890.00					
890.00					
41370.00	248220.00	0.00	206850000.00		
0.36	0.36	0.00	0.00	0.00	0.00
8	4	2	0.0762		
0.1020	0.0006				
-0.1020	0.0006				

FHWA South Abut. - 355 mm-sq PSC Fixed-Head/Cyclic/Crack Modeled
 UNITS--METR

 ULTIMATE BENDING RESISTANCE AND FLEXURAL RIGIDITY

 WIDTH = .36 M DEPTH = .36 M
 CONCRETE COMPRESSIVE STRENGTH = 41370.00 KN/ M**2
 REBAR YIELD STRENGTH = 248220.00 KN/ M**2
 MODULUS OF ELASTICITY OF STEEL = 206850000.00 KN/ M**2
 NUMBER OF REINFORCING BARS = 4
 NUMBER OF ROWS OF REINFORCING BARS = 2
 COVER THICKNESS = .076 M
 SQUASH LOAD CAPACITY = 4812.99 KN

ROW NUMBER	AREA OF REINFORCEMENT M**2	DISTANCE TO CENTROIDAL AXIS M
1	.000600	.1020
2	.000600	-.1020

OUTPUT RESULTS FOR AN AXIAL LOAD = 890.00 KN

MOMENT M- KN	EI KN- M**2	PHI 1/ M	MAX STR M/ M	N AXIS M
.000	.00000	.000001	.00022	224.368
.000	.00000	.000051	.00023	4.579
38.908	37020.	.001051	.00042	.398
74.839	36489.	.002051	.00058	.284
91.417	29963.	.003051	.00072	.237
103.156	25464.	.004051	.00085	.209
112.645	22302.	.005051	.00097	.191
121.010	19998.	.006051	.00108	.178
128.596	18238.	.007051	.00119	.168
135.593	16842.	.008051	.00129	.160
142.083	15698.	.009051	.00140	.154
145.181	14444.	.010051	.00149	.148
147.090	13310.	.011051	.00157	.142
148.618	12332.	.012051	.00165	.137
149.678	11469.	.013051	.00173	.133
150.685	10724.	.014051	.00181	.129
151.842	10088.	.015051	.00189	.126
152.586	9506.3	.016051	.00197	.123
153.714	9015.0	.017051	.00205	.120
154.229	8544.1	.018051	.00212	.118
154.441	8106.7	.019051	.00219	.115
155.064	7733.5	.020051	.00227	.113
155.653	7394.1	.021051	.00235	.112
155.797	7065.3	.022051	.00242	.110
156.165	6774.8	.023051	.00250	.108
156.452	6505.0	.024051	.00258	.107
156.452	6245.4	.025051	.00266	.106
156.591	6010.9	.026051	.00273	.105
156.601	5789.1	.027051	.00281	.104
156.970	5595.9	.028051	.00289	.103
156.970	5403.2	.029051	.00297	.102
156.970	5223.4	.030051	.00306	.102
156.970	5055.2	.031051	.00314	.101
156.970	4897.5	.032051	.00322	.100
156.970	4749.3	.033051	.00329	.100
156.970	4609.8	.034051	.00338	.099
156.970	4478.3	.035051	.00346	.099
156.970	4354.1	.036051	.00354	.098
156.970	4236.6	.037051	.00363	.098
156.970	4125.2	.038051	.00371	.098
156.970	4019.6	.039051	.00380	.097
156.970	3919.2	.040051	.00388	.097

THE ULTIMATE BENDING MOMENT AT A CONCRETE STRAIN OF 0.003
 IS : .157E+03 M- KN

Input and Output Summary from PMEIX Subroutine

FHWA South Abut. - 355 mm-sq PSC Fixed-Head/Cyclic/Crack Modeled

UNITS--METR

 PILE DEFLECTION, BENDING MOMENT, SHEAR & SOIL RESISTANCE

 INPUT INFORMATION

THE LOADING IS CYCLIC

NO. OF CYCLES = .20E+02

PILE GEOMETRY AND PROPERTIES

PILE LENGTH = 21.00 M
 MODULUS OF ELASTICITY OF PILE = .278E+08 KN/ M**2
 1 SECTION(S)

X	DIAMETER	MOMENT OF INERTIA	AREA
M	M	M**4	M**2
.00	.355	.130E-02	.126E+00
21.00			

SOILS INFORMATION

X-COORDINATE AT THE GROUND SURFACE = .00 M
 SLOPE ANGLE AT THE GROUND SURFACE = .00 DEG.
 3 LAYER(S) OF SOIL

LAYER 1

THE LAYER IS A SOFT CLAY

X AT THE TOP OF THE LAYER = .00 M
 X AT THE BOTTOM OF THE LAYER = 5.50 M
 VARIATION OF SOIL MODULUS, k = .272E+05 KN/ M**3

LAYER 2

THE LAYER IS A STIFF CLAY BELOW THE WATER TABLE

X AT THE TOP OF THE LAYER = 5.50 M
 X AT THE BOTTOM OF THE LAYER = 15.00 M
 VARIATION OF SOIL MODULUS, k = .543E+05 KN/ M**3

LAYER 3

THE LAYER IS A STIFF CLAY BELOW THE WATER TABLE

X AT THE TOP OF THE LAYER = 15.00 M
 X AT THE BOTTOM OF THE LAYER = 21.00 M
 VARIATION OF SOIL MODULUS, k = .109E+06 KN/ M**3

DISTRIBUTION OF EFFECTIVE UNIT WEIGHT WITH DEPTH

6 POINTS

X, M	WEIGHT, KN/ M**3
.00	.92E+01
5.50	.92E+01
5.50	.97E+01
15.00	.97E+01
15.00	.11E+02
21.00	.11E+02

DISTRIBUTION OF STRENGTH PARAMETERS WITH DEPTH

6 POINTS

X, M	C, KN/ M**2	PHI, DEGREES	E50
.00	.330E+02	.000	.100E-01
5.50	.330E+02	.000	.100E-01
5.50	.930E+02	.000	.700E-02
15.00	.930E+02	.000	.700E-02
15.00	.161E+03	.000	.500E-02
21.00	.161E+03	.000	.500E-02

FINITE DIFFERENCE PARAMETERS

NUMBER OF PILE INCREMENTS = 100
 TOLERANCE ON DETERMINATION OF DEFLECTIONS = .100E-05 M
 MAXIMUM NUMBER OF ITERATIONS ALLOWED FOR PILE ANALYSIS = 100
 MAXIMUM ALLOWABLE DEFLECTION = .10E+01 M

INPUT CODES

OUTPT = 1
 KCYCL = 0
 KBC = 2
 KPYOP = 1
 INC = 2

South Abutment - COM624P Problem Input Summary

FHWA South Abut. - 355 mm-sq PSC Fixed-Head/Cyclic/Crack Modeled
 UNITS--METR

O U T P U T I N F O R M A T I O N

GENERATED P-Y CURVES

THE NUMBER OF CURVE IS = 5
 THE NUMBER OF POINTS ON EACH CURVE = 17

DEPTH BELOW GS M	DIAM M	C KN/ M**2	GAMMA KN/ M**3	E50 .100E-01
1.00	.355	.3E+02	.9E+01	
		Y, M	P, KN/ M	
		.000	.000	
		.000	5.491	
		.002	17.296	
		.004	21.791	
		.007	24.945	
		.009	27.456	
		.011	29.576	
		.013	31.429	
		.016	33.086	
		.018	34.592	
		.020	35.977	
		.022	37.263	
		.024	38.466	
		.027	39.598	
		.071	27.695	
		.133	11.118	
		.178	11.118	

COMPUTED LATERAL FORCE AT PILE HEAD = .19997E+02 KN

**** WARNING ****

THE COMPUTED HORIZONTAL FORCE AT THE PILE HEAD EXCEEDS TOLERANCE. THE ERROR IS .154E-03

COMPUTED SLOPE AT PILE HEAD = -.10326E-17 M/ M

THE OVERALL MOMENT IMBALANCE = .243E-02 M- KN
 THE OVERALL LATERAL FORCE IMBALANCE = -.271E-12 KN

**** WARNING ****

THE OVERALL MOMENT IMBALANCE EXCEEDS TOLERANCE

PILE HEAD DEFLECTION = .101E-02 M
 MAXIMUM BENDING MOMENT = -.158E+02 M- KN
 MAXIMUM TOTAL STRESS = .923E+04 KN/ M**2

NO. OF ITERATIONS = 13
 MAXIMUM DEFLECTION ERROR = .688E-06 M

----- *** -----

FHWA South Abut. - 355 mm-sq PSC Fixed-Head/Cyclic/Crack Modeled

UNITS--METR

PILE LOADING CONDITION

LATERAL LOAD AT PILE HEAD = .400E+02 KN
 SLOPE AT PILE HEAD = .000E+00 M/ M
 AXIAL LOAD AT PILE HEAD = .000E+00 KN

X	DEFLECTION	MOMENT	TOTAL STRESS	SHEAR	SOIL RESIST	FLEXURAL RIGIDITY
M	M	M- KN	KN/ M**2	KN	KN/ M	KN- M**2
*****	*****	*****	*****	*****	*****	*****
.00	.254E-02	-.461E+02	.134E+05	.400E+02	.116E+02	.369E+05
.42	.244E-02	-.303E+02	.112E+05	.346E+02	.141E+02	.288E+05
.84	.217E-02	-.168E+02	.935E+04	.282E+02	.162E+02	.160E+05
1.26	.174E-02	-.600E+01	.788E+04	.211E+02	.174E+02	.951E+04
1.68	.121E-02	-.180E+01	.731E+04	.137E+02	.176E+02	.951E+04
2.10	.712E-03	.647E+01	.795E+04	.654E+01	.165E+02	.951E+04
2.52	.332E-03	.814E+01	.818E+04	.443E-01	.142E+02	.951E+04
2.94	.995E-04	.719E+01	.804E+04	-.518E+01	.104E+02	.951E+04
3.36	-.200E-05	.430E+01	.765E+04	-.760E+01	-.318E+01	.951E+04
3.78	-.233E-04	.155E+01	.728E+04	-.511E+01	-.728E+01	.951E+04
4.20	-.143E-04	.267E-01	.707E+04	-.224E+01	-.618E+01	.951E+04
4.62	-.359E-05	-.424E+00	.712E+04	-.100E+00	-.389E+01	.951E+04
5.04	.747E-07	-.186E+00	.709E+04	.733E+00	.111E+01	.951E+04
5.46	.848E-07	.884E-02	.706E+04	.147E+00	.973E+00	.951E+04
5.88	-.436E-07	.528E-02	.706E+04	-.833E-02	-.809E-02	.951E+04
6.30	-.733E-07	.229E-02	.706E+04	-.573E-02	-.101E-01	.951E+04
6.72	-.590E-07	.496E-03	.706E+04	-.292E-02	-.740E-02	.951E+04
7.14	-.344E-07	-.289E-03	.706E+04	-.973E-03	-.400E-02	.951E+04
7.56	-.144E-07	-.463E-03	.706E+04	.216E-04	-.149E-02	.951E+04
7.98	-.272E-08	-.368E-03	.706E+04	.357E-03	-.132E-03	.951E+04
8.40	.222E-08	-.212E-03	.706E+04	.353E-03	.382E-03	.951E+04
8.82	.318E-08	-.879E-04	.706E+04	.234E-03	.431E-03	.951E+04
9.24	.245E-08	-.156E-04	.706E+04	.115E-03	.304E-03	.951E+04
9.66	.138E-08	.145E-04	.706E+04	.353E-04	.159E-03	.951E+04
10.08	.549E-09	.201E-04	.706E+04	-.387E-05	.557E-04	.951E+04
10.50	.799E-10	.153E-04	.706E+04	-.161E-04	.150E-05	.951E+04
10.92	-.109E-09	.851E-05	.706E+04	-.149E-04	-.177E-04	.951E+04
11.34	-.137E-09	.334E-05	.706E+04	-.953E-05	-.184E-04	.951E+04
11.76	-.101E-09	.443E-06	.706E+04	-.449E-05	-.125E-04	.951E+04
12.18	-.550E-10	-.703E-06	.706E+04	-.125E-05	-.627E-05	.951E+04
12.60	-.207E-10	-.863E-06	.706E+04	.280E-06	-.204E-05	.951E+04
13.02	-.197E-11	-.630E-06	.706E+04	.714E-06	.975E-07	.951E+04
13.44	.513E-11	-.340E-06	.706E+04	.626E-06	.801E-06	.951E+04
13.86	.585E-11	-.126E-06	.706E+04	.387E-06	.774E-06	.951E+04
14.28	.410E-11	-.103E-07	.706E+04	.177E-06	.503E-06	.951E+04
14.70	.208E-11	.347E-07	.706E+04	.496E-07	.237E-06	.951E+04
15.12	.656E-12	.422E-07	.706E+04	-.149E-07	.160E-06	.951E+04
15.54	-.151E-13	.271E-07	.706E+04	-.430E-07	-.220E-07	.951E+04
15.96	-.183E-12	.109E-07	.706E+04	-.308E-07	-.594E-07	.951E+04
16.38	-.141E-12	.167E-08	.706E+04	-.139E-07	-.414E-07	.951E+04
16.80	-.603E-13	-.171E-08	.706E+04	-.386E-08	-.167E-07	.951E+04
17.22	-.878E-14	-.243E-08	.706E+04	.181E-08	-.267E-07	.951E+04
17.64	.289E-14	-.625E-09	.706E+04	.327E-08	.104E-07	.951E+04
18.06	.124E-14	.642E-10	.706E+04	.512E-09	.419E-08	.951E+04
18.48	.226E-16	.606E-10	.706E+04	-.152E-09	.142E-10	.951E+04
18.90	-.887E-16	.679E-11	.706E+04	-.687E-10	-.321E-09	.951E+04
19.32	-.184E-16	-.327E-11	.706E+04	-.157E-11	-.624E-10	.951E+04
19.74	.312E-17	-.112E-11	.706E+04	.486E-11	.126E-10	.951E+04
20.16	.192E-17	.354E-13	.706E+04	.100E-11	.704E-11	.951E+04
20.58	.115E-18	.764E-13	.706E+04	-.205E-12	.330E-12	.951E+04
21.00	-.351E-18	.000E+00	.706E+04	.000E+00	-.132E-11	.951E+04

COMPUTED LATERAL FORCE AT PILE HEAD = .40000E+02 KN
 COMPUTED SLOPE AT PILE HEAD = .00000E+00 M/ M
 THE OVERALL MOMENT IMBALANCE = .619E-04 M- KN
 THE OVERALL LATERAL FORCE IMBALANCE = -.366E-11 KN

FHWA South Abut. - 355 mm-sq PSC Fixed-Head/Cyclic/Crack Modeled

UNITS--METR

OUTPUT SUMMARY

PILE HEAD DEFLECTION = .254E-02 M
 MAXIMUM BENDING MOMENT = -.461E+02 M- KN
 MAXIMUM TOTAL STRESS = .134E+05 KN/ M**2

NO. OF ITERATIONS = 14
 MAXIMUM DEFLECTION ERROR = .679E-06 M

COMPUTED LATERAL FORCE AT PILE HEAD = .59997E+02 KN
 COMPUTED SLOPE AT PILE HEAD = .00000E+00 M/ M

THE OVERALL MOMENT IMBALANCE = .380E-02 M- KN
 THE OVERALL LATERAL FORCE IMBALANCE = .222E-11 KN

PILE HEAD DEFLECTION = .490E-02 M
 MAXIMUM BENDING MOMENT = -.809E+02 M- KN
 MAXIMUM TOTAL STRESS = .181E+05 KN/ M**2

NO. OF ITERATIONS = 14
 MAXIMUM DEFLECTION ERROR = .652E-06 M

----- *** -----

S U M M A R Y T A B L E

LATERAL LOAD (KN)	BOUNDARY CONDITION BC2	AXIAL LOAD (KN)	YT (M)	ST (M/ M)	MAX. MOMENT (M- KN)	MAX. STRESS (KN/ M**2)
.200E+02	.000E+00	.890E+03	.101E-02	-.103E-17	-.158E+02	.923E+04
.400E+02	.000E+00	.890E+03	.254E-02	.000E+00	-.461E+02	.134E+05
.600E+02	.000E+00	.890E+03	.490E-02	.000E+00	-.809E+02	.181E+05
.800E+02	.000E+00	.890E+03	.847E-02	.413E-17	-.111E+03	.222E+05
.900E+02	.000E+00	.890E+03	.105E-01	.413E-17	-.122E+03	.238E+05
.100E+03	.000E+00	.890E+03	.131E-01	-.413E-17	-.135E+03	.255E+05
.110E+03	.000E+00	.890E+03	.157E-01	.000E+00	-.149E+03	.274E+05
.120E+03	.000E+00	.890E+03	.177E-01	.000E+00	-.168E+03	.301E+05
.130E+03	.000E+00	.890E+03	.216E-01	.826E-17	-.187E+03	.326E+05
.140E+03	.000E+00	.890E+03	.262E-01	.826E-17	-.215E+03	.364E+05

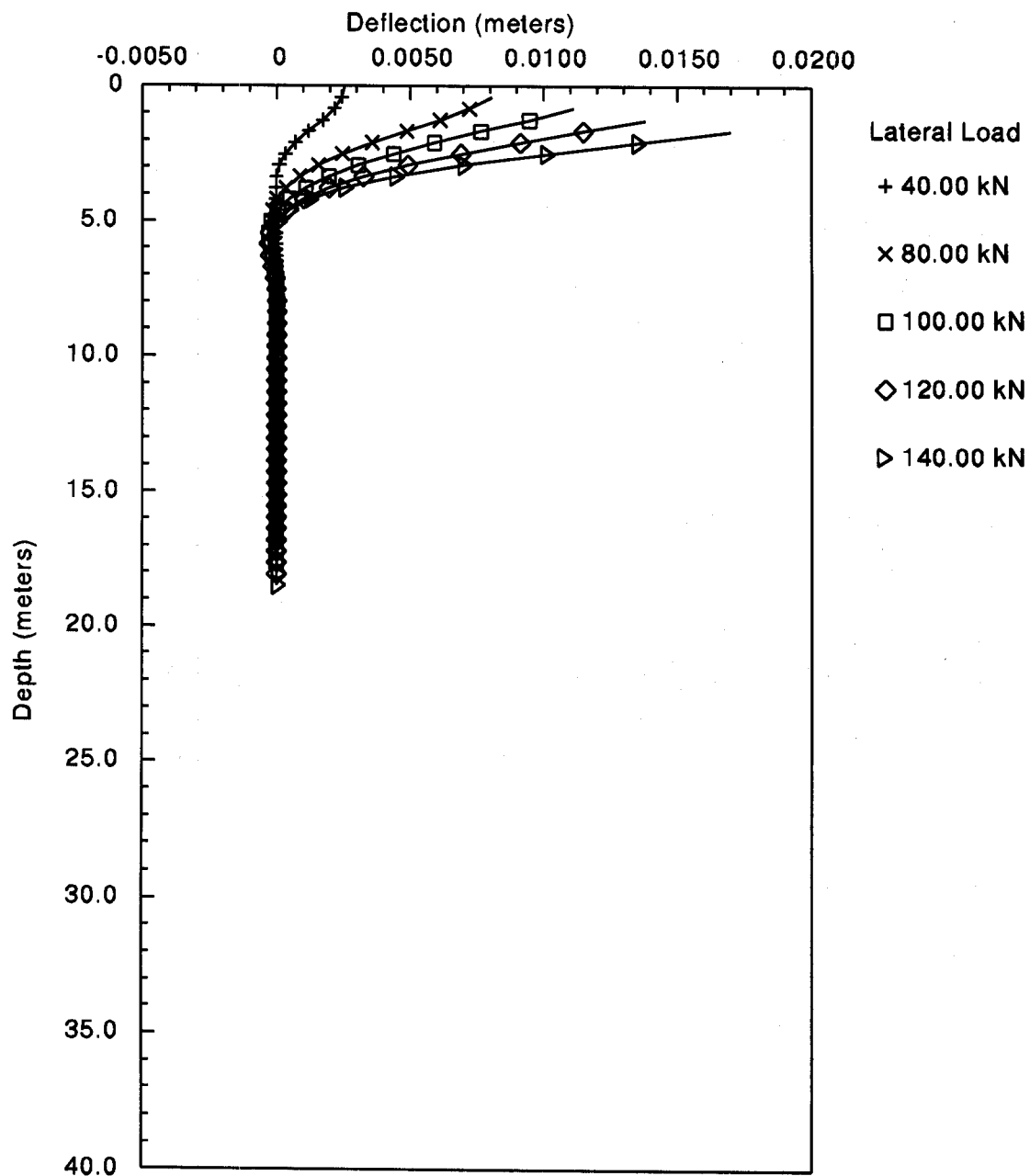


Figure F.39: South Abutment - Plot of Deflection versus Depth as a Function of Lateral Load

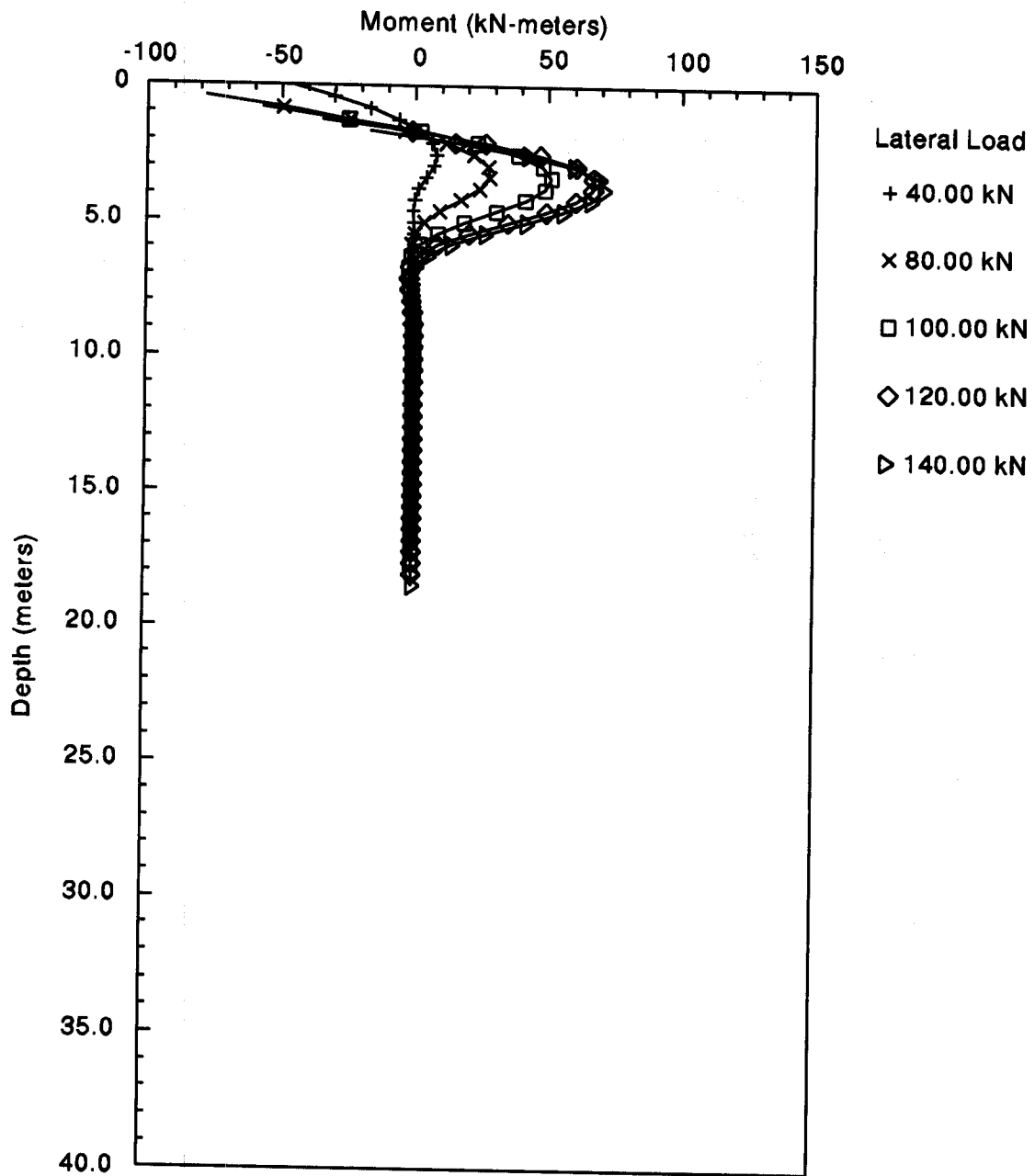


Figure F.40: South Abutment - Plot of Moment versus Depth as a Function of Lateral Load

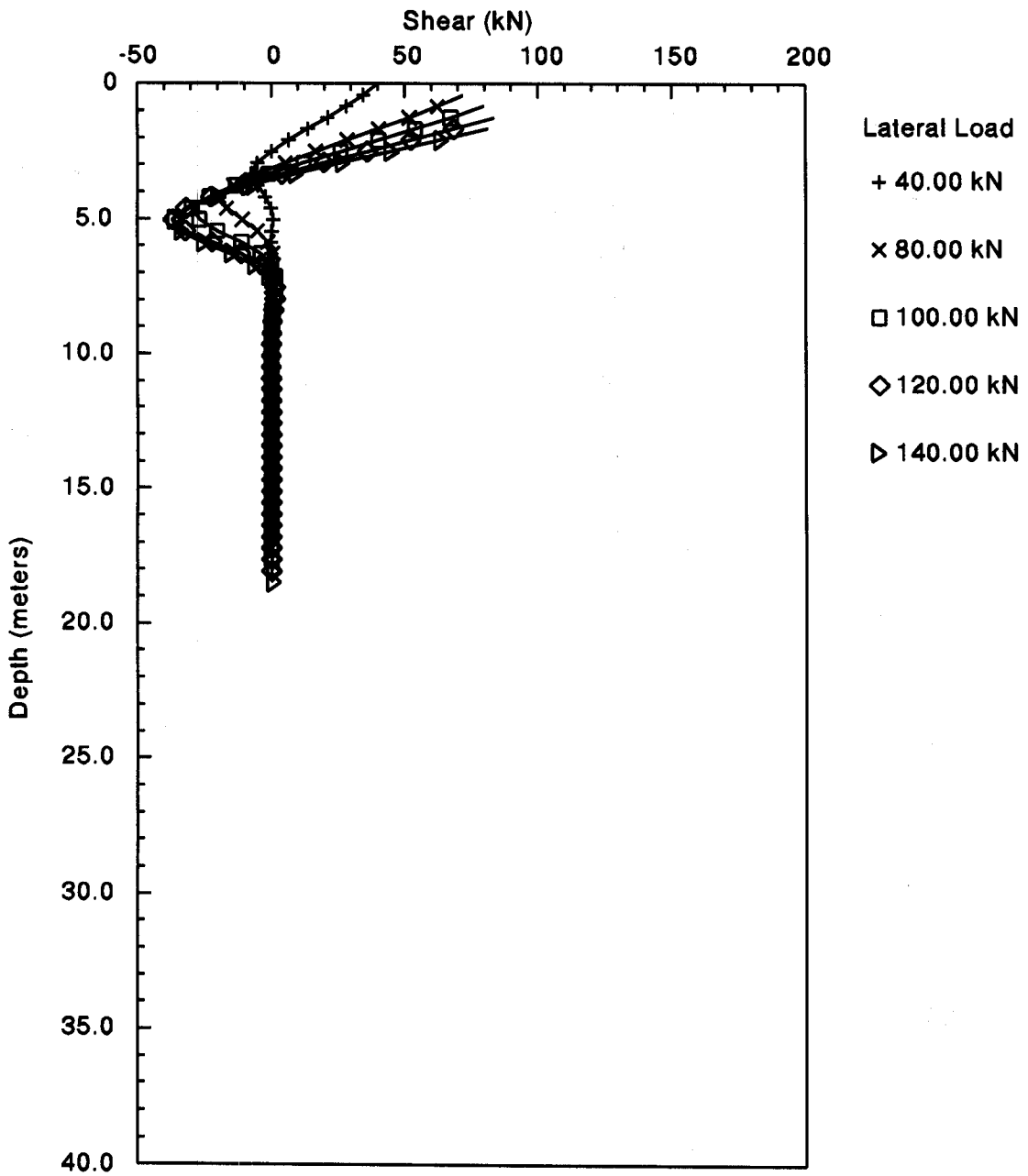


Figure F.41: South Abutment - Plot of Shear versus Depth as a Function of Lateral Load

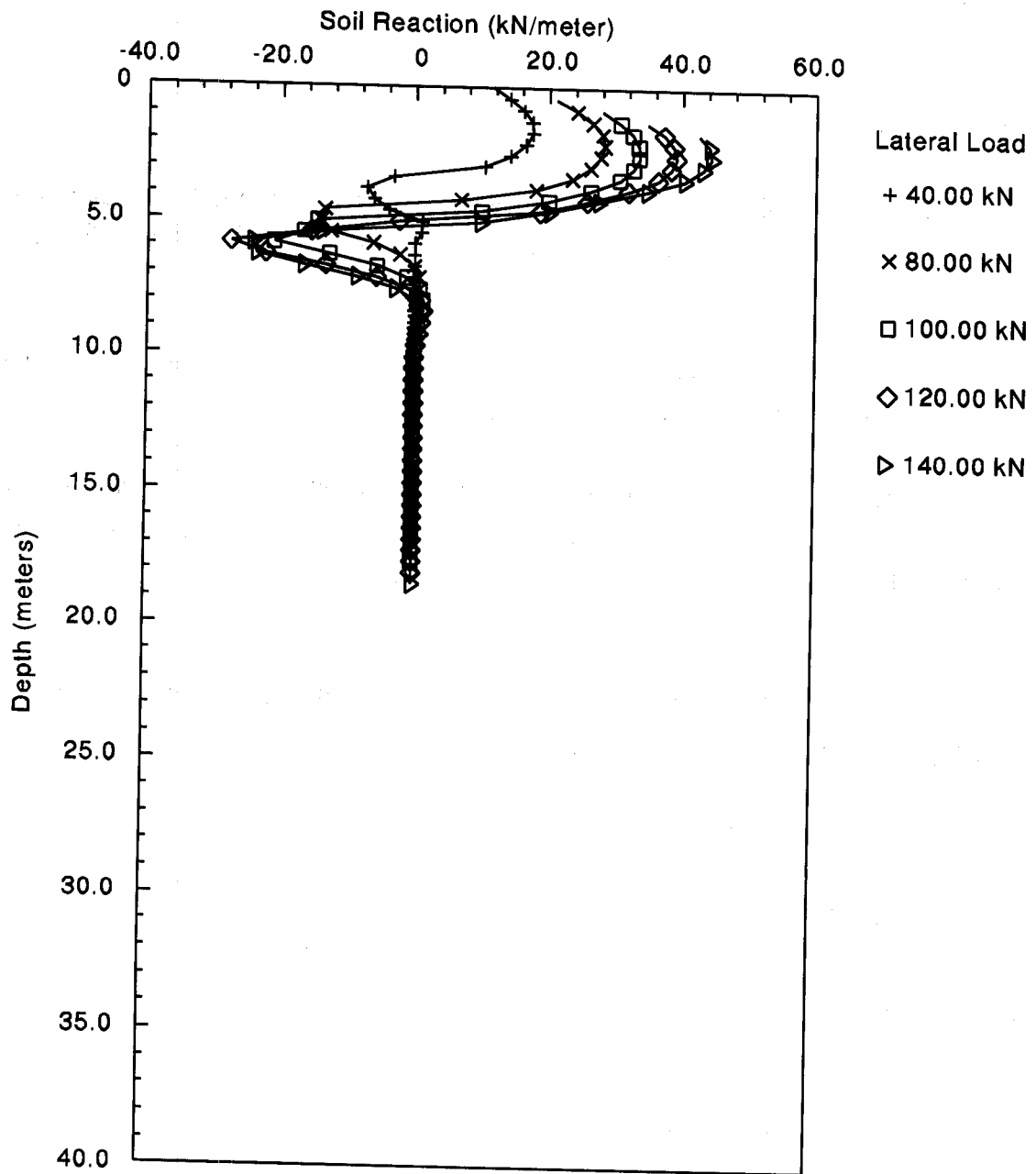


Figure F.42: South Abutment - Plot of Soil Reaction versus Depth as a Function of Lateral Load

F.5 GROUP UPLIFT LOAD CALCULATIONS

The maximum uplift load on a pile group is estimated to be 1,800 kN with a maximum uplift load per pile of 100 kN.

F.5.1 North Abutment - AASHTO Code (1994)

For the pile group at the North Abutment and the soil profile interpreted from Soil Boring S-1 as shown in Figure F.3. Perform an uplift capacity calculations based on the AASHTO Code for service load design. Use the method outlined in Section 9.8.3.1.

According to AASHTO specifications (1994), the uplift capacity of a pile group should be limited to the lesser value determined from any of the following.

1. The design uplift capacity of a single pile times the number of piles in a pile group. The design uplift capacity of a single pile is specified as $\frac{1}{3}$ the ultimate shaft resistance calculated in a static analysis method or $\frac{1}{2}$ the failure load determined from an uplift load test.

The ultimate shaft resistance for a single pile as calculated from a static analysis using the Nordlund method is 898 kN. The design uplift capacity is:

$$= \frac{1}{3} \text{ (ultimate shaft resistance)}$$

$$= \frac{1}{3} \text{ (898 kN)}$$

$$= 299 \text{ kN}$$

The design group uplift capacity based on criterion 1 is:

$$= \text{(uplift capacity of a single pile) (number of piles in a group)}$$

$$= 299 \text{ kN (24)}$$

$$= 7,176 \text{ kN}$$

North Abutment - AASHTO Code (1994) (continued)

2. Two-thirds ($\frac{2}{3}$) of the effective weight of the pile group and the soil contained within a block defined by the perimeter of the pile group and the embedded length of the piles.

$$\text{Bouyant unit weight of concrete} = 24 \text{ kN/m}^3 - 9.8 \text{ kN/m}^3 = 14.2 \text{ kN/m}^3$$

Effective weight of pile group (24 piles):

$$\begin{aligned} &= 24 (0.356 \text{ m}) (0.356 \text{ m}) (11.5 \text{ m}) (24 \text{ kN/m}^3 - 9.8 \text{ kN/m}^3) \\ &= 497 \text{ kN} \end{aligned}$$

Effective weight of soil:

$$\begin{aligned} &= (\text{Layer 1} + \text{Layer 2} + \text{Layer 3}) (\text{Gross Area of Pile Group} - \text{Pile Area}) \\ &= [16.5 \text{ kN/m}^3 (1.0 \text{ m}) + 6.7 \text{ kN/m}^3 (3.0 \text{ m}) + 7.8 \text{ kN/m}^3 (7.0 \text{ m}) + \\ &\quad 9.8 \text{ kN/m}^3 (0.5 \text{ m})] \{ (3.36 \text{ m}) (10.86 \text{ m}) - 24 (0.356 \text{ m}) (0.356 \text{ m}) \} \\ &= [16.5 \text{ kN/m}^2 + 20.1 \text{ kN/m}^2 + 54.6 \text{ kN/m}^2 + 4.9 \text{ kN/m}^2] \{ 36.49 \text{ m}^2 - 3.04 \text{ m}^2 \} \\ &= [96.1 \text{ kN/m}^2] \{ 33.45 \text{ m}^2 \} = 3,215 \text{ kN} \end{aligned}$$

The effective weight of the pile group and the soil contained within a block defined by the perimeter of the pile group and the embedded length of the pile is equal to 497 kN plus 3,215 kN, or 3,712 kN.

The design group uplift capacity based on criterion 2 is:

$$\begin{aligned} &= \frac{2}{3} (3,712 \text{ kN}) \\ &= 2,475 \text{ kN} \end{aligned}$$

North Abutment - AASHTO Code (1994) (continued)

3. One-half ($\frac{1}{2}$) the effective weight of the pile group and the soil contained within a block defined by the perimeter of the pile group and the embedded pile length plus $\frac{1}{2}$ the total soil shear resistance on the peripheral surface of the pile group.

The effective weight of the pile group and the soil contained within a block defined by the perimeter of the pile group, as calculated in criteria 2 above, is equal to 3,712 kN.

The total soil shear resistance on the peripheral surface of the pile group is calculated from the following equation.

$$\text{Unit shear resistance of cohesionless soil} = p_d \tan \phi$$

Where:

p_d is the effective overburden stress at depth d , and

ϕ is the friction angle of the soil.

Note: $p_d \tan \phi$ is used for a soil-to-soil failure.

As calculated in Section F.2.1.2:

Layer 1a: $p_{d1a} = 57.8 \text{ kPa}$ (midpoint of layer 1a - 1 m thick)

$$\phi_{1a} = 29^\circ$$

Layer 1b: $p_{d1b} = 76.1 \text{ kPa}$ (midpoint of layer 1b - 3 m thick)

$$\phi_{1b} = 29^\circ$$

Layer 2: $p_{d2} = 113.4 \text{ kPa}$ (midpoint of layer 2 - 7 m thick)

$$\phi_2 = 31^\circ$$

North Abutment - AASHTO Code (1994) (continued)

$$\text{Layer 3: } p_{d3} = 143.1 \text{ kPa (midpoint of layer 3 - 0.5 m thick)}$$

$$\phi_3 = 36^\circ$$

Thus,

$$\text{Layer 1a: } R_{s1a} = 57.8 \text{ kPa } (\tan 29^\circ) (3.36 \text{ m} + 10.86 \text{ m}) (1 \text{ m}) (2)$$

$$= 911 \text{ kN}$$

$$\text{Layer 1b: } R_{s1a} = 76.1 \text{ kPa } (\tan 29^\circ) (3.36 \text{ m} + 10.86 \text{ m}) (3 \text{ m}) (2)$$

$$= 3,599 \text{ kN}$$

$$\text{Layer 2: } R_{s2} = 113.4 \text{ kPa } (\tan 31^\circ) (3.36 \text{ m} + 10.86 \text{ m}) (7 \text{ m}) (2)$$

$$= 13,565 \text{ kN}$$

$$\text{Layer 3: } R_{s3} = 143.1 \text{ kPa } (\tan 36^\circ) (3.36 \text{ m} + 10.86 \text{ m}) (0.5 \text{ m}) (2)$$

$$= 1,478 \text{ kN}$$

$$\text{Total soil shear resistance} = R_{s1a} + R_{s1b} + R_{s2} + R_{s3}$$

$$= 911 \text{ kN} + 3,599 \text{ kN} + 13,565 \text{ kN} + 1,478 \text{ kN}$$

$$= 19,553 \text{ kN}$$

The design group uplift capacity based on criterion 3 is:

$$= \frac{1}{2} (3,712 \text{ kN}) + \frac{1}{2} (19,553 \text{ kN})$$

$$= 1,856 \text{ kN} + 9,777 \text{ kN} = 11,633 \text{ kN}$$

According to AASHTO specifications (1994), the uplift capacity of this pile group is limited to 2,475 kN. This is greater than the maximum uplift load in the pile group of 1,800 kN.

F.5.2 Pier 2 - AASHTO Code (1994)

For the pile group at Pier 2 and the soil profile interpreted from Soil Boring S-2 as shown in Figure F.5. Perform an uplift capacity calculations based on the AASHTO Code for service load design. Use the method outlined in Section 9.8.3.1.

According to AASHTO specifications (1994), the uplift capacity of a pile group should be limited to the lesser value determined from any of the following.

1. The design uplift capacity of a single pile times the number of piles in a pile group. The design uplift capacity of a single pile is specified as $\frac{1}{3}$ the ultimate shaft resistance calculated in a static analysis method or $\frac{1}{2}$ the failure load determined from an uplift load test.

The ultimate shaft resistance for a single pile as calculated from a static analysis using the Nordlund method is 984 kN. The design uplift capacity is:

$$= \frac{1}{3} (\text{ultimate shaft resistance})$$

$$= \frac{1}{3} (984 \text{ kN})$$

$$= 328 \text{ kN}$$

The design group uplift capacity based on criterion 1 is:

$$= (\text{uplift capacity of a single pile}) (\text{number of piles in a group})$$

$$= 328 \text{ kN} (24)$$

$$= 7,872 \text{ kN}$$

Pier 2 - AASHTO Code (1994) (continued)

2. Two-thirds ($\frac{2}{3}$) of the effective weight of the pile group and the soil contained within a block defined by the perimeter of the pile group and the embedded length of the piles.

Effective weight of pile group (24 piles):

$$\begin{aligned} &= 24 (0.356 \text{ m}) (0.356 \text{ m}) (10.0 \text{ m}) (24 \text{ kN/m}^3 - 9.8 \text{ kN/m}^3) \\ &= 432 \text{ kN} \end{aligned}$$

Effective weight of soil:

$$\begin{aligned} &= (\text{Layer 1} + \text{Layer 2}) (\text{Gross Area of Pile Group} - \text{Pile Area}) \\ &= [11.4 \text{ kN/m}^3 (4.0 \text{ m}) + 9.8 \text{ kN/m}^3 (6.0 \text{ m})] \\ &\quad \{ (3.36 \text{ m}) (10.86 \text{ m}) - 24 (0.356 \text{ m}) (0.356 \text{ m}) \} \\ &= [45.6 \text{ kN/m}^2 + 58.8 \text{ kN/m}^2] \{ 36.49 \text{ m}^2 - 3.04 \text{ m}^2 \} \\ &= [104.4 \text{ kN/m}^2] \{ 33.45 \text{ m}^2 \} \\ &= 3,492 \text{ kN} \end{aligned}$$

The effective weight of the pile group and the soil contained within a block defined by the perimeter of the pile group and the embedded length of the pile is equal to 432 kN plus 3,492 kN, or 3,924 kN.

The design group uplift capacity based on criterion 2 is:

$$\begin{aligned} &= \frac{2}{3} (3,924 \text{ kN}) \\ &= 2,616 \text{ kN} \end{aligned}$$

Pier 2 - AASHTO Code (1994) (continued)

3. One-half ($\frac{1}{2}$) the effective weight of the pile group and the soil contained within a block defined by the perimeter of the pile group and the embedded pile length plus $\frac{1}{2}$ the total soil shear resistance on the peripheral surface of the pile group.

The effective weight of the pile group and the soil contained within a block defined by the perimeter of the pile group, as calculated in criteria 2 above, is equal to 3,924 kN.

The total soil shear resistance on the peripheral surface of the pile group is calculated from the following equation.

$$\text{Unit shear resistance of cohesionless soil} = p_d \tan \phi$$

Where:

p_d is the effective overburden stress at depth d , and

ϕ is the friction angle of the soil.

Note: $p_d \tan \phi$ is used for a soil-to-soil failure.

As calculated in Section F.2.2.2:

Layer 1: $p_{d1} = 48.3 \text{ kPa}$ (midpoint of layer 1 - 4 m thick)

$$\phi_1 = 36^\circ$$

Layer 2: $p_{d2} = 100.5 \text{ kPa}$ (midpoint of layer 2 - 6 m thick)

$$\phi_2 = 35^\circ$$

Pier 2 - AASHTO Code (1994) (continued)

Thus,

$$\begin{aligned} \text{Layer 1: } R_{s1} &= 48.3 \text{ kPa } (\tan 36^\circ) (3.36 \text{ m} + 10.86 \text{ m}) (4 \text{ m}) (2) \\ &= 3,992 \text{ kN} \end{aligned}$$

$$\begin{aligned} \text{Layer 2: } R_{s2} &= 100.5 \text{ kPa } (\tan 35^\circ) (3.36 \text{ m} + 10.86 \text{ m}) (6 \text{ m}) (2) \\ &= 12,008 \text{ kN} \end{aligned}$$

$$\begin{aligned} \text{Total soil shear resistance} &= R_{s1} + R_{s2} \\ &= 3,992 \text{ kN} + 12,008 \text{ kN} \\ &= 16,000 \text{ kN} \end{aligned}$$

The design group uplift capacity based on criterion 3 is:

$$\begin{aligned} &= \frac{1}{2} (3,924 \text{ kN}) + \frac{1}{2} (16,000 \text{ kN}) \\ &= 9,962 \text{ kN} \end{aligned}$$

According to AASHTO specifications (1994), the uplift capacity of this pile group is limited to 2,616 kN. This is greater than the maximum uplift load in the pile group of 1,800 kN.

F.5.3 Pier 3 - AASHTO Code (1994)

For the pile group at Pier 3 and the soil profile interpreted from Soil Boring S-3 as shown in Figure F.9. Perform an uplift capacity calculations based on the AASHTO Code for service load design. Use the method outlined in Section 9.8.3.1.

According to AASHTO specifications (1994), the uplift capacity of a pile group should be limited to the lesser value determined from any of the following.

1. The design uplift capacity of a single pile times the number of piles in a pile group. The design uplift capacity of a single pile is specified as $\frac{1}{3}$ the ultimate shaft resistance calculated in a static analysis method or $\frac{1}{2}$ the failure load determined from an uplift load test.

The ultimate shaft resistance for a single pile as calculated from a static analysis using the Nordlund method and α -Method is 1,171 kN. The design uplift capacity is:

$$= \frac{1}{3} (\text{ultimate shaft resistance})$$

$$= \frac{1}{3} (1,171 \text{ kN})$$

$$= 390 \text{ kN}$$

The design group uplift capacity based on criterion 1 is:

$$= (\text{uplift capacity of a single pile}) (\text{number of piles in a group})$$

$$= 390 \text{ kN} (24)$$

$$= 9,360 \text{ kN}$$

Pier 3 - AASHTO Code (1994) (continued)

2. Two-thirds ($\frac{2}{3}$) of the effective weight of the pile group and the soil contained within a block defined by the perimeter of the pile group and the embedded length of the piles.

Effective weight of pile group (24 piles):

$$\begin{aligned} &= 24 (0.356 \text{ m}) (0.356 \text{ m}) (13.0 \text{ m}) (24 \text{ kN/m}^3 - 9.8 \text{ kN/m}^3) \\ &= 562 \text{ kN} \end{aligned}$$

Effective weight of soil:

$$\begin{aligned} &= (\text{Layer 1} + \text{Layer 2} + \text{Layer 3}) (\text{Gross Area of Pile Group} - \text{Pile Area}) \\ &= [10.6 \text{ kN/m}^3 (1.0 \text{ m}) + 9.8 \text{ kN/m}^3 (3.0 \text{ m}) + 10.4 \text{ kN/m}^3 (9.0 \text{ m})] \\ &\quad \{ (3.36 \text{ m}) (10.86 \text{ m}) - 24 (0.356 \text{ m}) (0.356 \text{ m}) \} \\ &= [10.6 \text{ kN/m}^2 + 29.4 \text{ kN/m}^2 + 93.6 \text{ kN/m}^2] \{ 36.49 \text{ m}^2 - 3.04 \text{ m}^2 \} \\ &= [133.6 \text{ kN/m}^2] \{ 33.45 \text{ m}^2 \} \\ &= 4,469 \text{ kN} \end{aligned}$$

The effective weight of the pile group and the soil contained within a block defined by the perimeter of the pile group and the embedded length of the pile is equal to 562 kN plus 4,469 kN, or 5,031 kN.

The design group uplift capacity based on criterion 2 is:

$$\begin{aligned} &= \frac{2}{3} (5,031 \text{ kN}) \\ &= 3,354 \text{ kN} \end{aligned}$$

Pier 3 - AASHTO Code (1994) (continued)

- 3 One-half ($\frac{1}{2}$) the effective weight of the pile group and the soil contained within a block defined by the perimeter of the pile group and the embedded pile length plus $\frac{1}{2}$ the total soil shear resistance on the peripheral surface of the pile group.

The effective weight of the pile group and the soil contained within a block defined by the perimeter of the pile group, as calculated in criteria 2 above, is equal to 5,031 kN.

The total soil shear resistance on the peripheral surface of the pile group is calculated from the following equation.

$$\text{Unit shear resistance of cohesionless soil} = p_d \tan \phi$$

$$\text{Unit shear resistance of cohesive soil} = c_u$$

Where:

p_d is the effective overburden stress at depth d ,

ϕ is the friction angle of the soil, and

c_u is the average undrained shear strength of the soil.

Note: $p_d \tan \phi$ is used for a soil-to-soil failure.

As calculated in Section F.2.3.1:

$$\text{Layer 1: } p_{d1} = 15.5 \text{ kPa} \quad (\text{midpoint of layer 1 - 1 m thick})$$

$$\phi_1 = 36^\circ$$

$$\text{Layer 2: } c_{u2} = 106 \text{ kPa} \quad (\text{layer 2 - 3 m thick})$$

$$\text{Layer 3: } c_{u3} = 155 \text{ kPa} \quad (\text{layer 3 - 9 m thick})$$

Pier 3 - AASHTO Code (1994) (continued)

Thus,

$$\begin{aligned}\text{Layer 1: } R_{s1} &= 15.5 \text{ kPa } (\tan 36^\circ) (3.36 \text{ m} + 10.86 \text{ m}) (1 \text{ m}) (2) \\ &= 320 \text{ kN}\end{aligned}$$

$$\begin{aligned}\text{Layer 2: } R_{s2} &= 106 \text{ kPa } (3.36 \text{ m}) (10.86 \text{ m}) (3 \text{ m}) (2) \\ &= 9,044 \text{ kN}\end{aligned}$$

$$\begin{aligned}\text{Layer 3: } R_{s3} &= 155 \text{ kPa } (3.36 \text{ m}) (10.86 \text{ m}) (9 \text{ m}) (2) \\ &= 39,674 \text{ kN}\end{aligned}$$

$$\begin{aligned}\text{Total soil shear resistance} &= R_{s1} + R_{s2} + R_{s3} \\ &= 320 \text{ kN} + 9,044 \text{ kN} + 39,674 \text{ kN} \\ &= 49,038 \text{ kN}\end{aligned}$$

The design group uplift capacity based on criterion 3 is:

$$\begin{aligned}&= \frac{1}{2} (5,031 \text{ kN}) + \frac{1}{2} (49,038 \text{ kN}) \\ &= 27,035 \text{ kN}\end{aligned}$$

According to AASHTO specifications (1994), the uplift capacity of this pile group is limited to 3,354 kN. This is greater than the maximum uplift load in the pile group of 1,800 kN.

F.5.4 South Abutment - AASHTO Code (1994)

For the pile group at the South Abutment and the soil profile interpreted from Soil Boring S-4 as shown in Figure F.11. Perform an uplift capacity calculations based on the AASHTO Code for service load design. Use the method outlined in Section 9.8.3.1.

According to AASHTO specifications (1994), the uplift capacity of a pile group should be limited to the lesser value determined from any of the following.

1. The design uplift capacity of a single pile times the number of piles in a pile group. The design uplift capacity of a single pile is specified as $\frac{1}{3}$ the ultimate shaft resistance calculated in a static analysis method or $\frac{1}{2}$ the failure load determined from an uplift load test.

The ultimate shaft resistance for a single pile as calculated from a static analysis using the α -Method is 1,648 kN. The design uplift capacity is:

$$= \frac{1}{3} \text{ (ultimate shaft resistance)}$$

$$= \frac{1}{3} \text{ (1,648 kN)}$$

$$= 549 \text{ kN}$$

The design group uplift capacity based on criterion 1 is:

$$= \text{(uplift capacity of a single pile) (number of piles in a group)}$$

$$= 549 \text{ kN (24)}$$

$$= 13,176 \text{ kN}$$

South Abutment - AASHTO Code (1994) (continued)

2. Two-thirds ($\frac{2}{3}$) of the effective weight of the pile group and the soil contained within a block defined by the perimeter of the pile group and the embedded length of the piles.

Effective weight of pile group (24 piles):

$$\begin{aligned} &= 24 (0.356 \text{ m}) (0.356 \text{ m}) (17.5 \text{ m}) (24 \text{ kN/m}^3 - 9.8 \text{ kN/m}^3) \\ &= 756 \text{ kN} \end{aligned}$$

Effective weight of soil:

$$\begin{aligned} &= (\text{Layer 1} + \text{Layer 2} + \text{Layer 3}) (\text{Gross Area of Pile Group} - \text{Pile Area}) \\ &= [9.2 \text{ kN/m}^3 (5.5 \text{ m}) + 9.7 \text{ kN/m}^3 (9.5 \text{ m}) + 10.5 \text{ kN/m}^3 (2.5 \text{ m})] \\ &\quad \{ (3.36 \text{ m}) (10.86 \text{ m}) - 24 (0.356 \text{ m}) (0.356 \text{ m}) \} \\ &= [50.6 \text{ kN/m}^2 + 92.2 \text{ kN/m}^2 + 26.3 \text{ kN/m}^2] \{ 36.49 \text{ m}^2 - 3.04 \text{ m}^2 \} \\ &= [169.1 \text{ kN/m}^2] \{ 33.45 \text{ m}^2 \} \\ &= 5,656 \text{ kN} \end{aligned}$$

The effective weight of the pile group and the soil contained within a block defined by the perimeter of the pile group and the embedded length of the pile is equal to 756 kN plus 5,656 kN, or 6,412 kN.

The design group uplift capacity based on criterion 2 is:

$$\begin{aligned} &= \frac{2}{3} (6,412 \text{ kN}) \\ &= 4,275 \text{ kN} \end{aligned}$$

South Abutment - AASHTO Code (1994) (continued)

3. One-half ($\frac{1}{2}$) the effective weight of the pile group and the soil contained within a block defined by the perimeter of the pile group and the embedded pile length plus $\frac{1}{2}$ the total soil shear resistance on the peripheral surface of the pile group.

The effective weight of the pile group and the soil contained within a block defined by the perimeter of the pile group, as calculated in criteria 2 above, is equal to 6,412 kN.

The total soil shear resistance on the peripheral surface of the pile group is calculated from the following equation.

$$\text{Unit shear resistance of cohesive soil} = c_u$$

Where: c_u is the average undrained shear strength of the soil.

As calculated in Section F.2.4.1:

$$\text{Layer 1: } c_{u1} = 33 \text{ kPa} \quad (\text{layer 1 - 5.5 m thick})$$

$$\text{Layer 2: } c_{u2} = 93 \text{ kPa} \quad (\text{layer 2 - 9.5 m thick})$$

$$\text{Layer 3: } c_{u3} = 157 \text{ kPa} \quad (\text{layer 3 - 2.5 m thick})$$

Thus,

$$\begin{aligned} \text{Layer 1: } R_{s1} &= 33 \text{ kPa} (3.36 \text{ m} + 10.86 \text{ m}) (5.5 \text{ m}) (2) \\ &= 5,162 \text{ kN} \end{aligned}$$

$$\begin{aligned} \text{Layer 2: } R_{s2} &= 93 \text{ kPa} (3.36 \text{ m} + 10.86 \text{ m}) (9.5 \text{ m}) (2) \\ &= 25,127 \text{ kN} \end{aligned}$$

South Abutment - AASHTO Code (1994) (continued)

$$\begin{aligned}\text{Layer 3: } R_{s3} &= 157 \text{ kPa } (3.36 \text{ m} + 10.86 \text{ m}) (2.5 \text{ m}) (2) \\ &= 11,163 \text{ kN}\end{aligned}$$

$$\begin{aligned}\text{Total soil shear resistance} &= R_{s1} + R_{s2} + R_{s3} \\ &= 5,162 \text{ kN} + 25,127 \text{ kN} + 11,163 \text{ kN} \\ &= 41,452 \text{ kN}\end{aligned}$$

The design group uplift capacity based on criterion 3 is:

$$\begin{aligned}&= \frac{1}{2} (6,412 \text{ kN}) + \frac{1}{2} (41,452 \text{ kN}) \\ &= 23,932 \text{ kN}\end{aligned}$$

According to AASHTO specifications (1994), the uplift capacity of this pile group is limited to 4,275 kN. This is greater than the maximum uplift load in the pile group of 1,800 kN.

F.6 NEGATIVE SHAFT RESISTANCE CALCULATIONS

F.6.1 South Abutment - α -Method

Piles at the South Abutment will be subjected to negative shaft resistance due to soil settlement following the placement of 10 m of approach embankment material behind the abutment after pile installation. This settlement needs to be estimated prior to determining the location of the negative and positive shaft resistances along the pile. The α -method is used to estimate both the positive and negative shaft resistance components. The step-by-step procedure for the analysis of downdrag loading is outlined in Section 9.9.1.1a. The soil profile for the South Abutment interpreted from Soil Boring S-4 is presented in Figure F.11.

STEP 1 Establish the simplified soil profile and soil properties for computing settlement.

Schematic of the South Abutment showing the approach embankment backfill material and the soil profile is presented in Figure F.43.

STEP 2 Determine the overburden pressure increase, Δp , due to the approach embankment fill placed behind the abutment.

The overburden pressure increase, Δp , is calculated using the pressure coefficient, K_f , determined from the pressure distribution chart presented in Figure F.44. The pressure distribution chart calculates the pressure coefficient, K_f , at various depths below the bottom of the fill ($x b_f$), and also at various distances from the centerline of the fill. The depth below the bottom of the fill is given as a multiple of " b_f ", where b_f is the distance from the centerline of the fill to the midpoint of the fill slope, as shown in Figure F.44. Given:

The top width of the fill = 12 m

Side slope of the fill = 2H:1V

The height of the fill, h_f = 10 m

$$\text{Thus, } b_f = \left(\frac{12 \text{ m}}{2} \right) + \left(\frac{10 \text{ m}}{2} \right) 2 = 16 \text{ m}$$

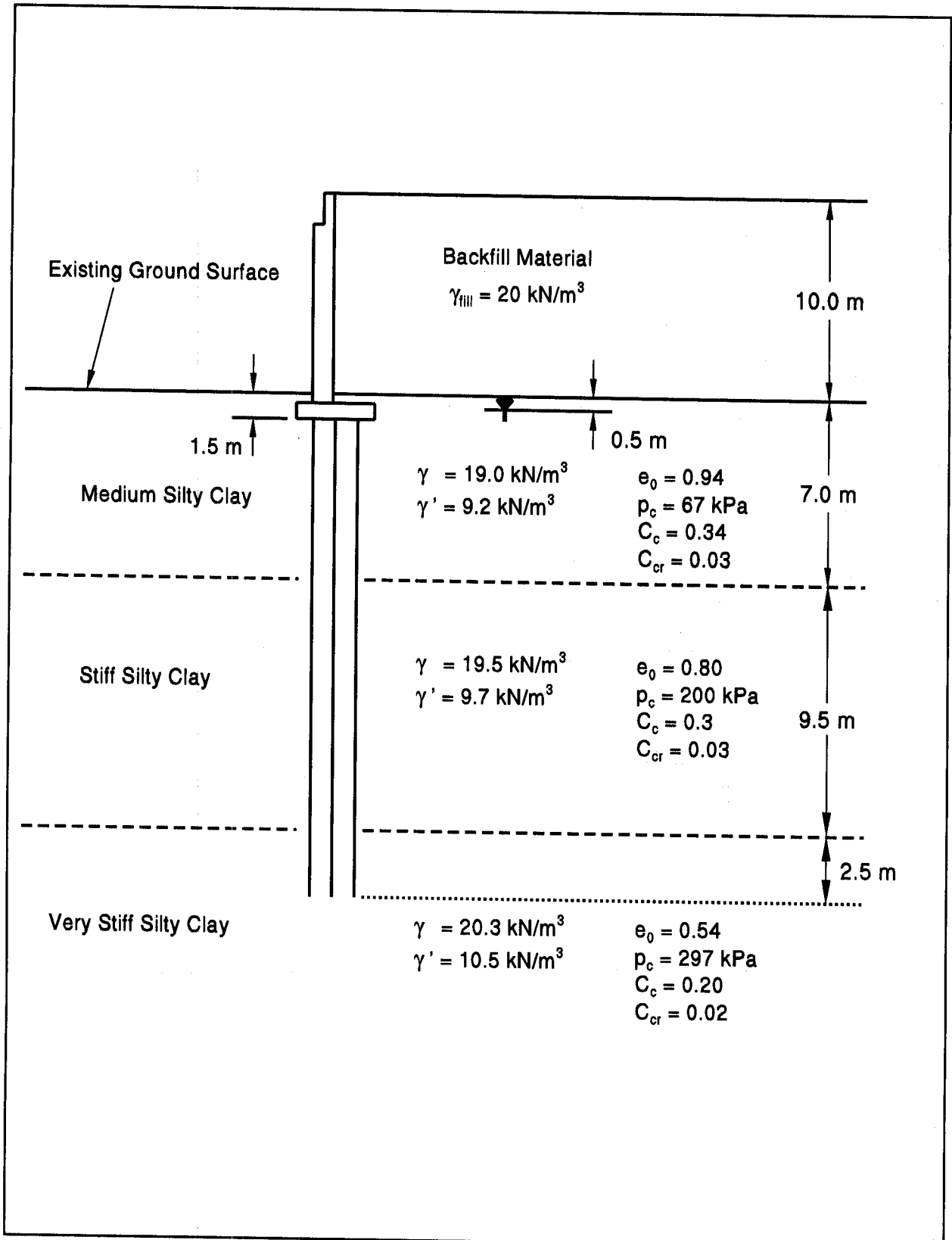


Figure F.43 Schematic of South Abutment Showing the Backfill Material and Soil Profile

Pressure Distribution Chart

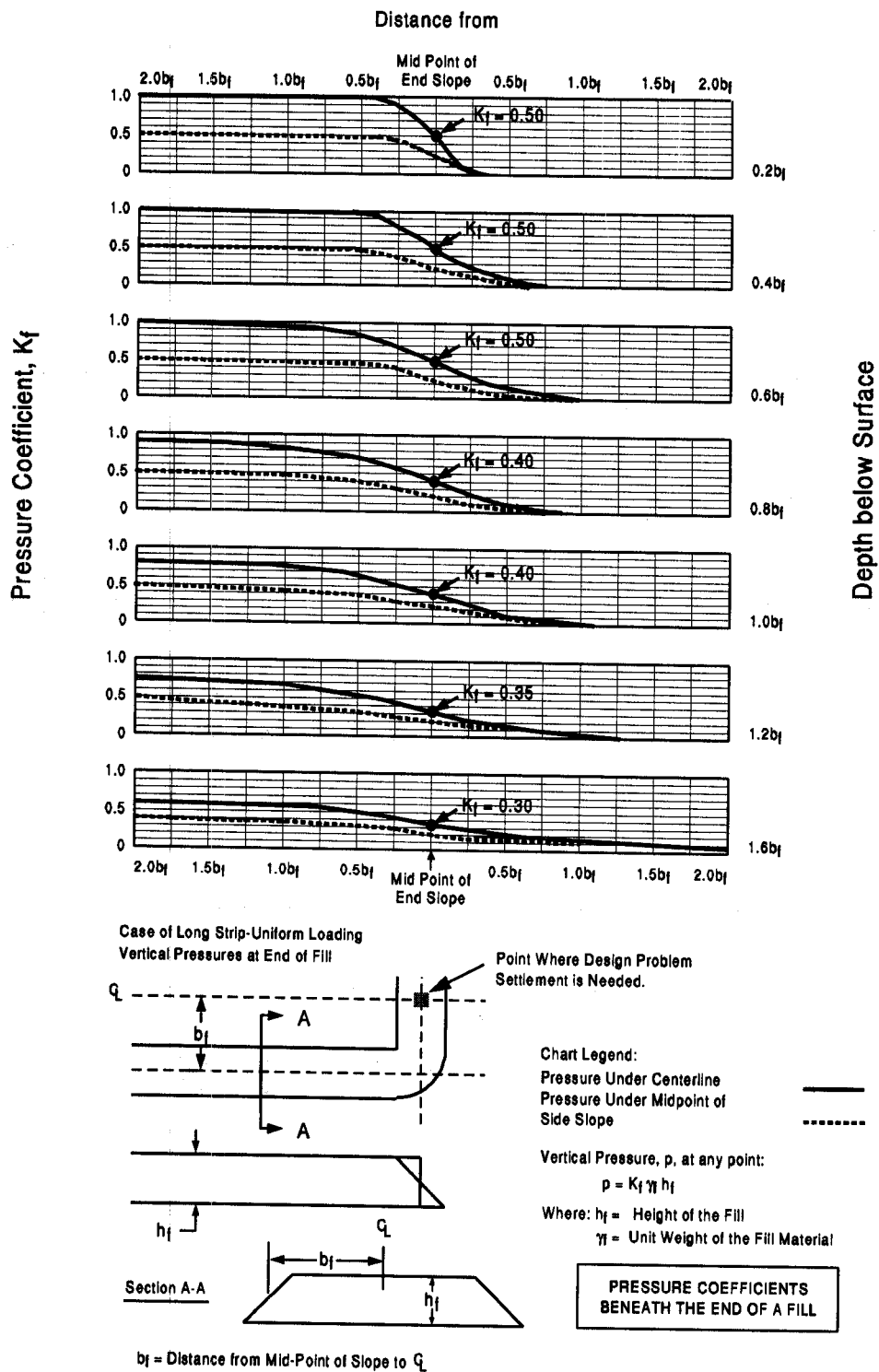


Figure F.44 Pressure Distribution Chart

STEP 2 (continued)

For settlement calculations, the overburden pressure increase, Δp , at various depths beneath the centerline of the fill needs to be calculated. The overburden pressure increase is equal to the pressure coefficient, K_f , multiplied by the unit weight of the fill, γ_f , and the height of the fill, h_f . The unit weight of the fill, γ_f , is 20 kN/m^3 . The height of the fill, h_f , is 10 meters. Table F-5 shows the overburden pressure increase, Δp , at various depths beneath the bottom of the fill. The effective overburden pressure diagram in Figure F.45 shows the effective overburden pressure, p_o , before the backfill is placed, and the effective pressure, $p_o + \Delta p$, after the backfill placement.

For example at depth 3.2 meters below existing ground, the overburden pressure increase, Δp , is equal to:

$$\Delta p = 0.5 (20 \text{ kN/m}^3) (10 \text{ m}) = 100 \text{ kPa}$$

Depth Below Existing Ground (m)	Pressure Coefficient K_f	$\Delta p = K_f \gamma_f h_f$ (kPa)
Existing Ground Surface = 0	0.50	100.0
$0.2b_f = 3.2 \text{ m}$	0.50	100.0
$0.4b_f = 6.4 \text{ m}$	0.50	100.0
$0.6b_f = 9.6 \text{ m}$	0.50	100.0
$0.8b_f = 12.8 \text{ m}$	0.40	80.0
$1.0b_f = 16.0 \text{ m}$	0.40	80.0
$1.2b_f = 19.2 \text{ m}$	0.35	70.0
$1.6b_f = 25.6 \text{ m}$	0.30	60.0

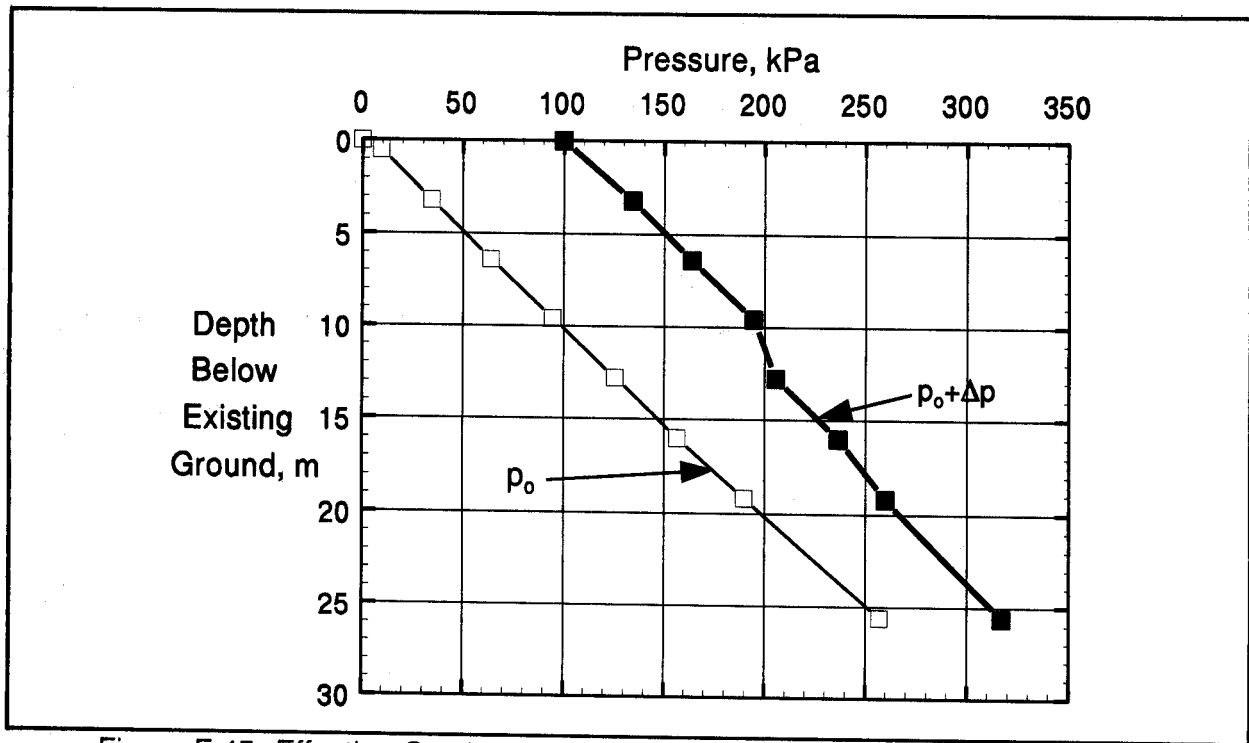


Figure F.45 Effective Overburden Diagram - Original and Original+Increase

STEP 3 Perform settlement computations for the soil layers along the embedded pile length.

- a. Determine consolidation test parameters for each soil layer from laboratory consolidation test results.

The laboratory consolidation test results on the undisturbed samples were plotted on the "log pressure, p versus void ratio, e " (similar to Figure 9.43). The following consolidation test parameters were obtained from the plot.

Soil Layer 1: Preconsolidation pressure, $p_c = 67$ kPa
 Initial void ratio, $e_0 = 0.94$
 Compression index, $C_c = 0.34$
 Recompression index, $C_{cr} = 0.030$

Soil Layer 2: Preconsolidation pressure, $p_c = 200$ kPa
 Initial void ratio, $e_0 = 0.80$
 Compression index, $C_c = 0.30$
 Recompression index, $C_{cr} = 0.030$

STEP 3 (continued)

Soil Layer 3: Preconsolidation pressure, $p_c = 297$ kPa
Initial void ratio, $e_0 = 0.54$
Compression index, $C_c = 0.20$
Recompression index, $C_{cr} = 0.020$

- b. Compute settlement of each soil layer using the appropriate settlement equation provided in Section 9.8.2.3 for cohesive layers or Section 9.8.2.4 for cohesionless layers.

The following equations apply to cohesive layers (see Section 9.8.2.3):

$$s = H \left[\frac{C_{cr}}{1+e_0} \log \frac{p_o + \Delta p}{p_o} \right] \quad \text{when } p_o + \Delta p \leq p_c$$

$$= H \left[\frac{C_{cr}}{1+e_0} \log \frac{p_c}{p_o} \right] + H \left[\frac{C_c}{1+e_0} \log \frac{p_o + \Delta p}{p_c} \right] \quad \text{when } p_o + \Delta p > p_c$$

The settlement of each layer is summarized in the settlement computations in Table F-6. An example of settlement calculation has been presented earlier in Section F.3.

- b. Compute the total settlement over the embedded pile length which is equal to the sum of the settlement from each soil layer.

Based on the settlement calculation table, the calculated settlement is 0.499 meters. Because the total long term settlement of the clay is very high (0.499 m), it is assumed that preloading of soil will be performed by placing additional temporary surcharge for the necessary time period prior to pile installation. It is also assumed that 90% consolidation of clay will be achieved prior to pile installation. Therefore, after installation, the piles will only be subjected to the 10% consolidation settlement left as shown in column 9 of the settlement calculation table, or a total settlement of 0.0499 meter or 49.9 mm.

Table F-6 Settlement Calculations Table - South Abutment

1 Soil Type	2 Soil Layer Below Existing Ground (m)	3 Soil Layer Thick- ness (m)	4 Depth of Midpoint Below Existing Ground (m)	5 Effective Overburden Pressure at Midpoint p_o (kPa)	6 Imposed Pressure Increase at Midpoint Δp (kPa)	7 $(p_o + \Delta p)$ (kPa)	8 Layer Settle- ment (m)	9 10% of Layer Settle- ment (m)	10 Depth Below Existing Ground (m)	11 Relative Soil Movement due to 10% Settlement (m)
Layer 1 $p_c=67\text{kPa}$; $e_0=0.94$ $C_c=0.34$; $C_{cr}=0.030$									0.0	0.0499
	0.0 - 3.0	3.0	1.50	18.7	100.0	118.7	0.156	0.0156	3.0	0.0343
	3.0 - 7.0	4.0	5.00	50.9	100.0	150.9	0.255	0.0255	7.0	0.0088
Layer 2 $p_c=200\text{kPa}$; $e_0=0.80$ $C_c=0.30$; $C_{cr}=0.030$	7.0 - 10.5	3.5	7.75	76.6	100.0	176.6	0.021	0.0021	10.5	0.0067
	10.5 - 13.5	3.0	12.00	117.8	85.0	202.8	0.015	0.0015	13.5	0.0052
	13.5 - 16.5	3.0	15.00	146.9	80.0	226.9	0.034	0.0034	16.5	0.0018
Layer 3 $p_c=297\text{kPa}$; $e_0=0.54$ $C_c=0.20$; $C_{cr}=0.020$	16.5 - 19.5	3.0	18.00	177.2	73.8	251.0	0.006	0.0006	19.5	0.0012
	19.5 - 22.5	3.0	21.00	208.7	67.2	275.9	0.005	0.0005	22.5	0.0007
	22.5 - 25.5	3.0	24.00	240.2	62.5	302.7	0.007	0.0007	25.5	0.0000
Total Settlement =							0.499	0.0499		

STEP 4 Determine the pile length that will experience negative shaft resistance.

Negative shaft resistance occurs due to the settlement between soil and pile. The amount of settlement between soil and pile necessary to mobilize the negative shaft resistance is about 10 mm. Therefore, negative shaft resistance will occur on the pile shaft in each soil layer or portion of a soil layer with a settlement greater than 10 mm.

Column 11 of Table F-6 presents the settlement between soil and pile due to the 10% consolidation settlement at various locations along the pile embedded length. The existing ground surface will experience a total consolidation settlement of 0.0499 meter. At a depth of 3 meters below the existing ground surface, a lesser total settlement will occur which is equal to the total settlement at the existing ground surface minus the consolidation settlement of the top 3 meter soil layer, or 0.0343 meter, as shown in column 11 of the table.

The table also shows that the settlement between soil and pile due the 10% consolidation settlement at 7 meters depth below existing ground is already less than 10 mm which is the minimum required to mobilized the negative shaft resistance. The 7 meter depth also happens to be the end of soil layer 1. Therefore, the pile segment above the 7 meter depth will be subjected to the negative shaft resistances (downdrag) from soil layer 1 while the pile segment below the 7 meter depth will provide the positive shaft resistances (or capacity) to sustain loads from the structure and the negative shaft resistances (downdrag).

STEP 5 Determine magnitude of negative shaft resistance, Q_s^- .

The method used to calculate the ultimate negative shaft resistance over the pile length determined in Step 4 should be the same method used to calculate the ultimate positive shaft resistance, except that it will act in the opposite direction.

As calculated in Step 4 above, the negative shaft resistance will be caused by soil layer 1 which is a medium silty clay. The pile length in soil layer 1 is 5.5 meters. The ultimate positive shaft resistance in soil layer 1 has been calculated with the α -method in Section F.2.4.1 and is equal to:

$$R_{s1} = 259 \text{ kN}$$

STEP 5 (continued)

Therefore, the ultimate negative shaft resistance is equal to:

$$Q_s^- = 259 \text{ kN}$$

STEP 6 Calculate the ultimate pile capacity provided by the positive shaft resistance and the toe resistance, Q_u^+ .

Positive shaft and toe resistances will develop below the depth where the relative pile-soil movements are less than 10 mm. The positive soil resistances can be calculated on the pile length remaining below the negative shaft resistance depth from Step 4 using an appropriate static analysis method for the soil type.

The ultimate pile capacity will be provided by the shaft resistance from soil layers 2 and 3, and the toe resistance, as calculated in Section F.2.4.1. The shaft resistance provided by each of soil layer and the ultimate positive shaft resistance is as follows:

$$\text{Layer 2: } R_{s2}^+ = 1,150 \text{ kN}$$

$$\text{Layer 3: } R_{s3}^+ = 239 \text{ kN}$$

$$\begin{aligned} \text{Total: } R_s^+ &= R_{s2}^+ + R_{s3}^+ \\ &= 1,150 \text{ kN} + 239 \text{ kN} \\ &= 1,389 \text{ kN} \end{aligned}$$

Also as calculated in Section F.2.4.1, the ultimate toe resistance is equal to:

$$R_t = 182 \text{ kN}$$

STEP 6 (continued)

Hence, the ultimate pile capacity is equal to:

$$\begin{aligned} Q_u^+ &= R_s^+ + R_t \\ &= 1,389 \text{ kN} + 182 \text{ kN} = 1,571 \text{ kN} \end{aligned}$$

STEP 7 Calculate the net ultimate pile capacity, Q_u^{NET} , available to resist imposed loads.

$$\begin{aligned} Q_u^{\text{NET}} &= Q_u^+ - Q_s^- \\ &= 1,571 \text{ kN} - 259 \text{ kN} = 1,312 \text{ kN} \end{aligned}$$

The net ultimate pile capacity is smaller than the required ultimate pile capacity of 1780 kN. Therefore, alternatives to obtain higher pile capacities must be considered.

STEP 8 Consider alternatives to obtain higher net ultimate pile capacity.

Alternatives are described in Section 9.9.1.2 and include use of preloading or wick drains to reduce settlements prior to pile installation, use of lightweight fills to reduce settlements that cause downdrag loads, use of friction reducers to reduce downdrag loads, use of higher allowable material stress, and isolation of pile from consolidating soil.

Three alternatives will be further investigated on the following.

Alternate 1: Use bitumen coating on piles to reduce negative shaft resistance.

According to Goudreault and Fellenius (1994), the maximum pile adhesion, c_a , used in the static pile capacity calculation should be limited to 10 kPa when the pile is coated with bitumen.

STEP 8 (continued)

According to the α -method presented in Section F.2.4.1, the pile adhesion from soil layer 1, c_{a1} , is equal to 33 kPa. If the 5.5 m pile length in layer 1 is coated with bitumen, the pile adhesion will become 10 kPa, and therefore the positive or negative shaft resistance is equal to:

$$\begin{aligned} R_{st}^+ &= Q_s^- = 10 \text{ kPa} (4) (0.356 \text{ m}) (5.5 \text{ m}) \\ &= 78 \text{ kN} \end{aligned}$$

The net ultimate pile capacity available to resist imposed loads is equal to:

$$\begin{aligned} Q_u^{\text{NET}} &= Q_u^+ - Q_s^- \\ &= 1,571 \text{ kN} - 78 \text{ kN} = 1,493 \text{ kN} \end{aligned}$$

This is still less than the required ultimate bearing capacity (1780 kN).

- Notes:
1. Bitumen coating should be applied only to the top 5.5 m of the pile.
 2. Batter piles should be avoided if possible.

Alternate 2: Use longer piles driven to a stiffer or denser noncompressible layer.

Try an extra pile embedded length of 3.5 meters or a total pile embedded length of 21.0 meters. This extra pile embedded length will increase the shaft resistance from soil layer 3 and the toe resistance.

The average undrained shear strength of soil layer 3 is equal to:

$$c_{u3} = \frac{158 + 155 + 163 + 168}{4} = 161 \text{ kPa}$$

$$(D/b) = (20.5 \text{ m}) / (0.356 \text{ m}) = 57.58$$

STEP 8 (continued)

Using Figure 9.18 and for $c_{u3} = 161$ kPa and $(D/b) = 57.58$, the pile adhesion is:

$$c_{a3} = 66 \text{ kPa} \quad \text{and therefore } f_{s3} = 66 \text{ kPa}$$

Hence,

$$\begin{aligned} R_{s3} &= 66 \text{ kPa} (4) (0.356 \text{ m}) (6.0 \text{ m}) \\ &= 564 \text{ kN} \end{aligned}$$

The ultimate positive shaft resistance:

$$\begin{aligned} R_s^+ &= R_{s2}^+ + R_{s3}^+ \\ &= 1,150 \text{ kN} + 564 \text{ kN} \\ &= 1,714 \text{ kN} \end{aligned}$$

The average undrained shear strength of soil at the pile toe is equal 170 kPa. The unit toe resistance, q_t , is:

$$\begin{aligned} q_t &= 9 c_u \\ &= 9 (170 \text{ kPa}) = 1,530 \text{ kPa} \end{aligned}$$

The ultimate toe resistance, R_t , is equal to:

$$\begin{aligned} R_t &= 1,530 \text{ kPa} (0.356 \text{ m}) (0.356 \text{ m}) \\ &= 194 \text{ kN} \end{aligned}$$

STEP 8 (continued)

The ultimate pile capacity is equal to:

$$\begin{aligned} Q_u^+ &= R_s^+ + R_t \\ &= 1,714 \text{ kN} + 194 \text{ kN} \\ &= 1,908 \text{ kN} \end{aligned}$$

The net ultimate pile capacity available to resist imposed loads, with an increased pile length to 20.5 meters and a bitumen coating on the top 5.5 meter of the pile:

$$\begin{aligned} Q_u^{\text{NET}} &= Q_u^+ - Q_s^- \\ &= 1,908 \text{ kN} - 78 \text{ kN} \\ &= 1,830 \text{ kN} \end{aligned}$$

This alternate provides the required ultimate capacity, but a cost analysis of alternatives 1 and 2 and a combination of both alternatives should be performed before making the selection.

Alternate 3: A stub abutment instead of a full height abutment may be a better choice for the south abutment. The stub abutment could be supported on a spread footing with specified embankment material and density control in the foundation area. A stub abutment with pile foundation is another alternative available for consideration.

This design problem illustrates the difficulties encountered in designing pile foundations in clay where substantial settlements occur and large downdrag loads are encountered by piles.

F.7 LATERAL SQUEEZE CALCULATIONS

F.7.1 South Abutment - Investigation of Lateral Squeeze

Use the guidelines presented in Section 9.9.3 of Chapter 9.

STEP 1 Determine if abutment tilting can occur.

The backfill material properties:

$$\gamma_f = 20 \text{ kN/m}^3.$$

$$h_f = 10 \text{ meters.}$$

Any tilting which may occur will take place on the top soil layer which is the medium silty clay. The average undrained shear strength, c_u , of the medium silty clay layer is 33 kPa.

Abutment tilting will occur if the following condition govern:

$$\gamma_f h_f > 3 c_u$$

$$20 \text{ kN/m}^3 (10 \text{ m}) > 3 (33 \text{ kPa})$$

$$200 \text{ kPa} > 99 \text{ kPa}$$

Hence, abutment tilting can occur.

STEP 2 Determine the magnitude of horizontal movement.

Two cases will be investigated on the following.

Case 1: If piles are placed before any soil compression occurs.

The computations performed previously for negative shaft resistance indicated the vertical fill settlement is equal to 0.495 meter.

Estimated horizontal movement = $0.25 (0.495 \text{ m}) = 0.124 \text{ m}$

This horizontal movement is not tolerable as it is greater than the 10 mm allowable by the bridge division.

Case 2: If piles are driven after 90% of vertical settlement has occurred.

Estimated vertical fill settlement after 90% settlement has occurred is 0.0495 meter.

Estimated horizontal movement = $0.25 (0.0495 \text{ m}) = 0.0124 \text{ m}$

This movement is also larger than the 10 mm allowed by the bridge division. Because the estimated movement is close, provisions can be made in the bridge shoe and expansion joint design so this movement is tolerable.

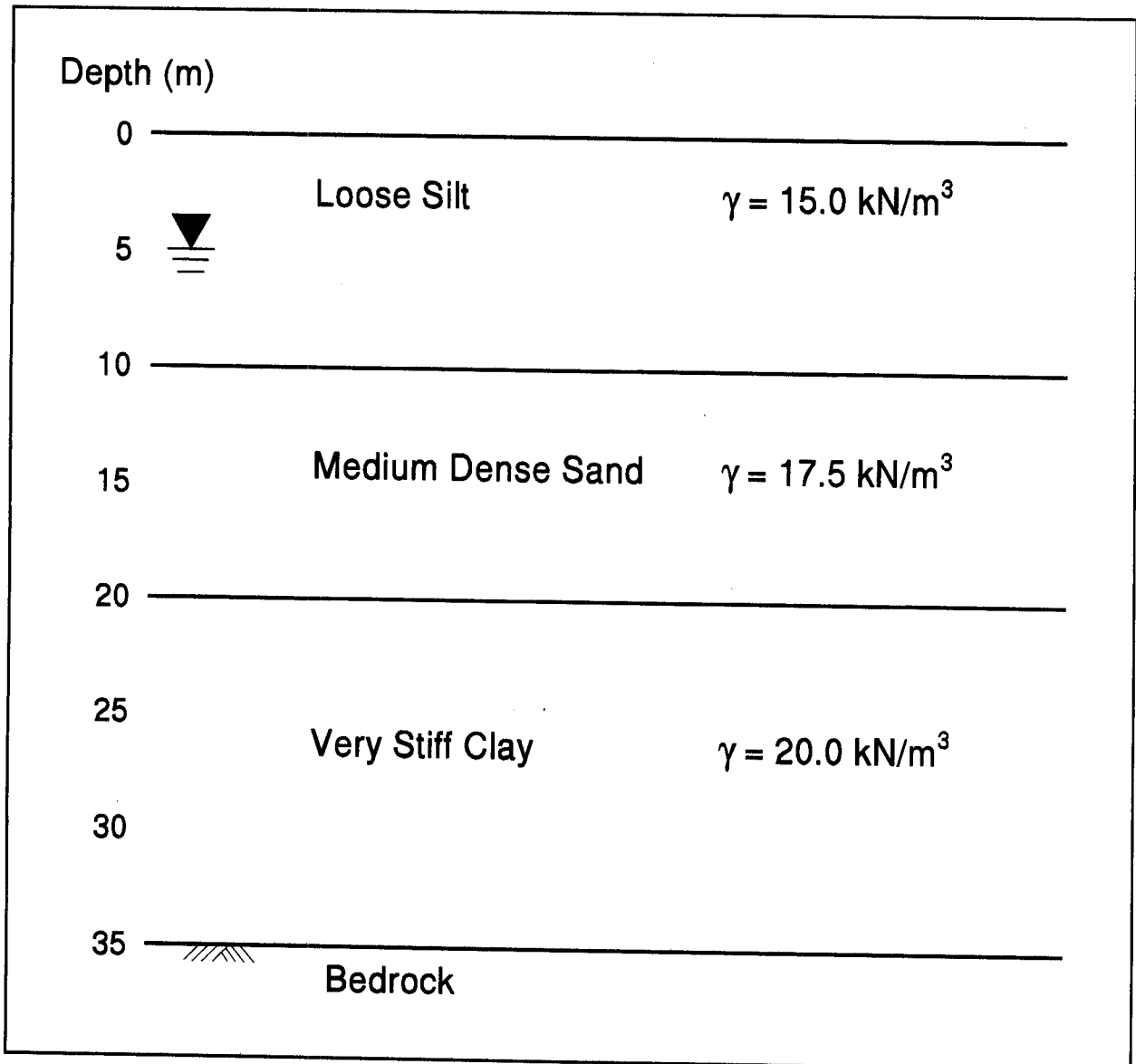
APPENDIX G

Student Exercise - Solutions

	Page
STUDENT EXERCISE #1 - CONSTRUCT A p_o DIAGRAM	G-3
STUDENT EXERCISE #2 - NORDLUND CAPACITY CALCULATION	G-5
STUDENT EXERCISE #3 - α -METHOD PILE CAPACITY CALCULATION	G-11
STUDENT EXERCISE #4 - α -METHOD AND NORDLUND METHOD PILE CAPACITY CALCULATION IN A LAYERED SOIL PROFILE	G-17
STUDENT EXERCISE #5 - EFFECTIVE STRESS PILE CAPACITY CALCULATION IN A LAYERED SOIL PROFILE	G-23
STUDENT EXERCISE #6 - LPC METHOD PILE CAPACITY CALCULATION	G-27
STUDENT EXERCISE #7 - PILE GROUP SETTLEMENT IN LAYERED PROFILE	G-33
STUDENT EXERCISE #8 - BROMS' METHOD LATERAL CAPACITY ANALYSIS	G-37

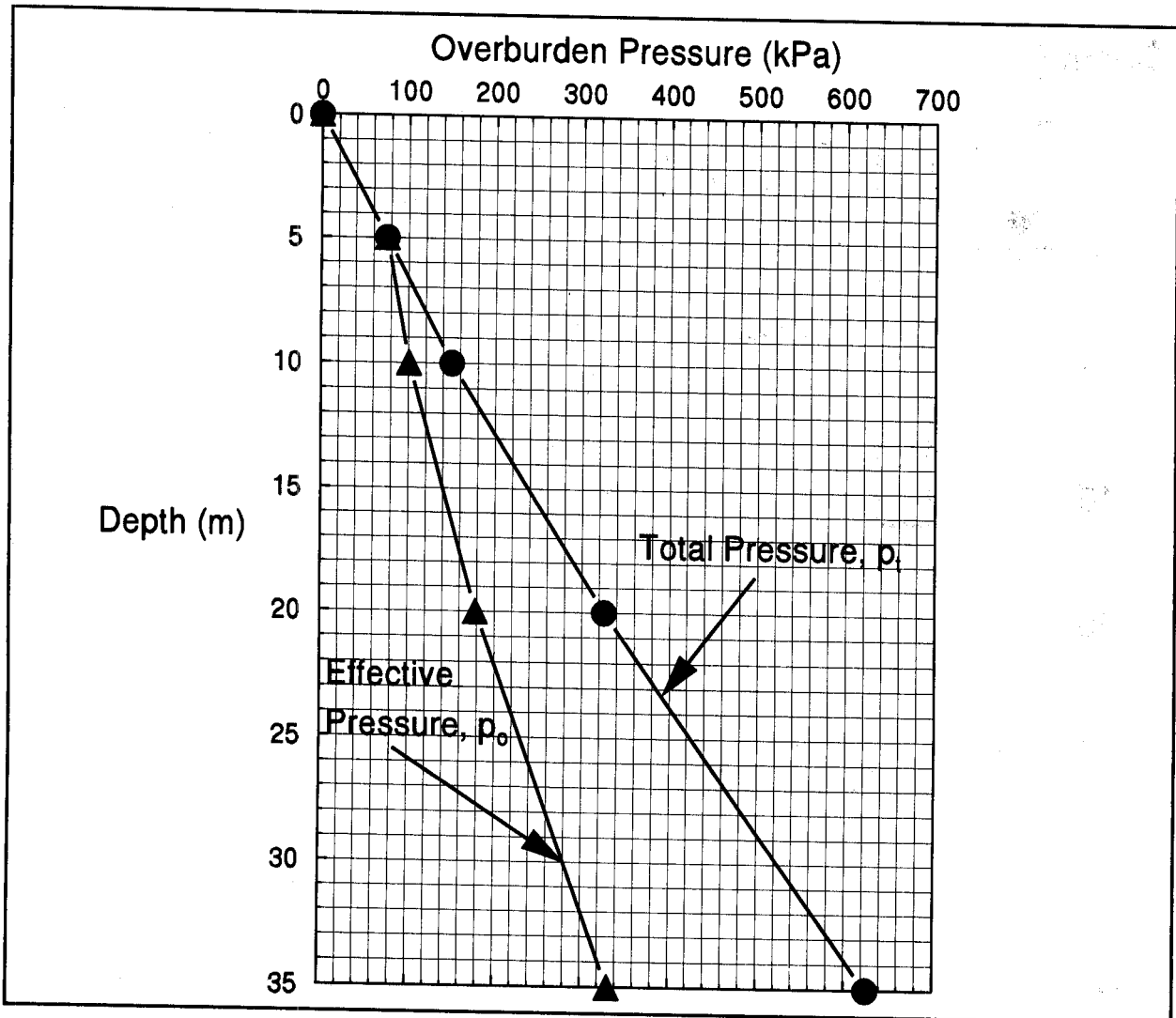
STUDENT EXERCISE #1 - CONSTRUCT A p_o DIAGRAM

For the soil profile given below, construct the total and effective overburden pressure diagrams. The water table is 5 meters below the ground surface. The unit weight of water is 9.80 kN/m^3 . Construction of a p_o diagram is described in Section 9.4 of Chapter 9.



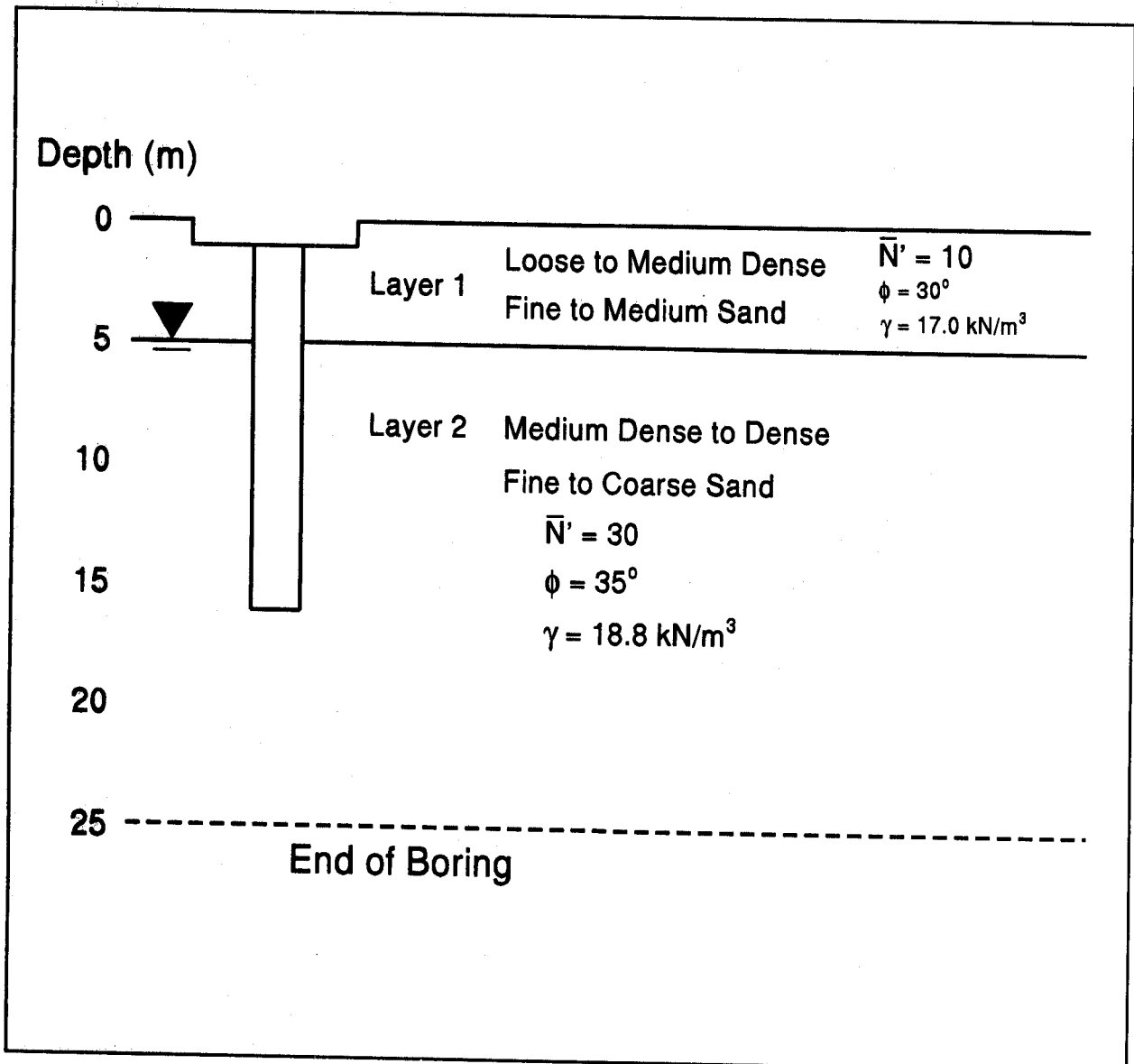
STUDENT EXERCISE #1 - SOLUTION FOR A p_o DIAGRAM

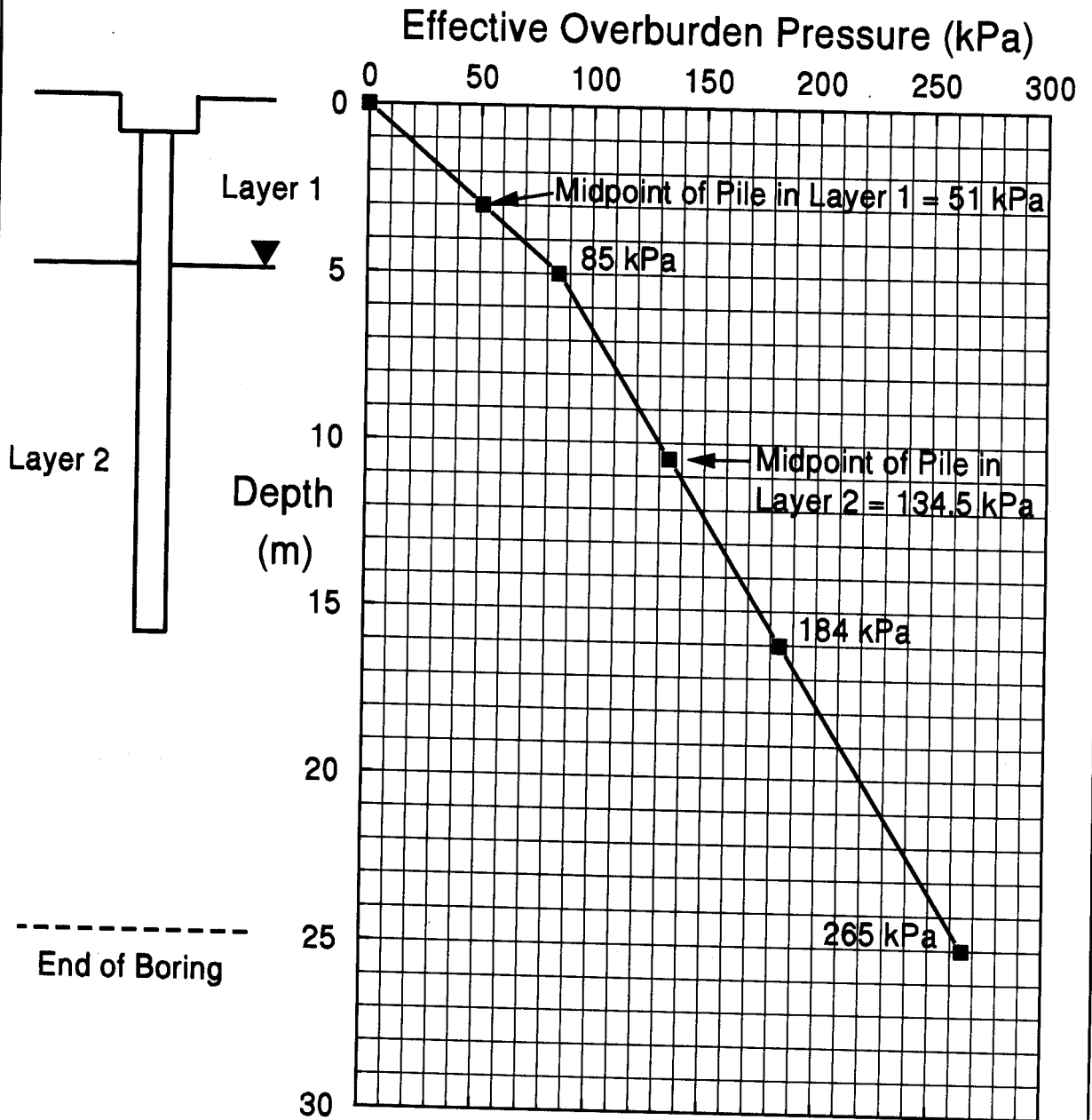
Depth (m)	Layer Thickness t (m)	Unit Weight of Layer Soil γ (kN/m ³)	Overburden Pressure from Layer t(γ) (kPa)	Total Overburden Pressure at Depth $p_t = \sum t(\gamma)$ (kPa)	Unit Weight of Water γ_w (kN/m ³)	Pore Water Pressure from Layer t(γ_w) (kPa)	Total Pore Water Pressure at Depth $u = \sum t(\gamma_w)$ (kPa)	Effective Overburden Pressure $p_o = p_t - u$ (kPa)
0	0	15.0	0	0	--	0	0	0
5	5	15.0	75	75	--	0	0	75
10	5	15.0	75	150	9.8	49	49	101
20	10	17.5	175	325	9.8	98	147	178
35	15	20.0	300	625	9.8	147	294	331



STUDENT EXERCISE #2 - NORDLUND CAPACITY CALCULATION

Use the Nordlund method and the step by step procedures described in Section 9.7.1.1b to calculate the ultimate capacity and the allowable design load for a 305 mm square prestressed concrete pile driven into the soil profile described below. A trial pile length of 15 meters below the bottom of the pile cap 1 meter below grade should be used. Begin the calculation with Step 2 of the step by step procedure since the data required from Step 1 has been provided in the problem. The overburden pressure diagram for this problem is included on the next page.





STUDENT EXERCISE #2 - SOLUTION FOR NORDLUND CAPACITY CALCULATION

STEP 1 The p_o diagram, soil layer determination, and the soil friction angle, ϕ , for each soil layer were presented in the problem introduction.

STEP 2 Determine δ .

a. Compute volume of soil displaced per unit length of pile, V .

$$V = (0.305 \text{ m}) (0.305 \text{ m}) (1.0 \text{ m/m}) = 0.093 \text{ m}^3/\text{m}$$

b. Determine δ/ϕ from Figure 9.10.

$$V = 0.093 \text{ m}^3/\text{m} \rightarrow \delta/\phi = 0.75 \text{ or } \delta = 0.75\phi$$

c. Calculate δ for each soil layer based on $\delta = 0.75\phi$.

$$\text{Layer 1: } \delta_1 = 0.75 (30^\circ) = 22.50$$

$$\text{Layer 2: } \delta_2 = 0.75 (35^\circ) = 26.25$$

STEP 3 Determine K_δ for each soil layer based on displaced volume, V , and pile taper angle, ω .

$$\text{Layer 1: For } \phi = 30^\circ, \quad V = 0.093 \text{ m}^3/\text{m} \text{ and } \omega = 0^\circ$$

$$\text{From Figure 9.12: } K_\delta = 1.15$$

$$\text{Layer 2: For } \phi = 35^\circ, \quad V = 0.093 \text{ m}^3/\text{m} \text{ and } \omega = 0^\circ$$

$$\text{From Figure 9.13: } K_\delta = 1.75$$

STEP 4 Determine correction factor, C_F , to be applied to K_δ when $\delta \neq \phi$ (Figure 9.15.)

$$\text{Layer 1: } \phi = 30^\circ \text{ and } \delta/\phi = 0.75 \rightarrow C_F = 0.90$$

$$\text{Layer 2: } \phi = 35^\circ \text{ and } \delta/\phi = 0.75 \rightarrow C_F = 0.85$$

STEP 5 Compute effective overburden pressure at midpoint of each soil layer, p_d .

From p_o diagram, p_d for layer 1 is 51 kPa, and

p_d for layer 2 is 134.5 kPa.

STEP 6 Compute the shaft resistance for each soil layer.

$$R_s = K_\delta C_F p_d \sin \delta C_d D$$

$$C_d = \text{pile perimeter} = 1.22 \text{ m}^2/\text{m}$$

D = embedded length in layer

$$\begin{aligned} \text{Layer 1: } R_{s1} &= 1.15 (0.90) (51 \text{ kPa}) (\sin 22.5^\circ) (1.22 \text{ m}^2/\text{m}) (4 \text{ m}) \\ &= 99 \text{ kN} \end{aligned}$$

$$\begin{aligned} \text{Layer 2: } R_{s2} &= 1.75 (0.85) (134.5 \text{ kPa}) (\sin 26.25^\circ) (1.22 \text{ m}^2/\text{m}) (11 \text{ m}) \\ &= 1188 \text{ kN} \end{aligned}$$

Compute the ultimate shaft resistance, R_s

$$R_s = R_{s1} + R_{s2} = 99 \text{ kN} + 1188 \text{ kN} = 1287 \text{ kN}$$

STEP 7 Determine α_t coefficient and bearing capacity factor N'_q from ϕ angle of 35° at pile toe and Figures 9.16(a) and 9.16(b).

From Figure 9.16(a) $\rightarrow \alpha_t = 0.67$

From Figure 9.16(b) $\rightarrow N'_q = 65$

STEP 8 Compute effective overburden pressure at pile toe.

From effective overburden pressure diagram, p_t at 16 meters is 184 kPa. Therefore, limiting overburden pressure at pile toe of 150 kPa applies.

STEP 9 Compute the ultimate toe resistance, R_t .

a. $R_t = \alpha_t N'_q A_t p_t$

$$= (0.67) (65) (0.09 \text{ m}^2) (150 \text{ kPa}) = 588 \text{ kN}$$

b. $R_t = q_L A_t$ from Figure 9.17, $q_L = 5000 \text{ kPa}$ for $\phi = 35^\circ$.

$$= (5000 \text{ kPa}) (0.09 \text{ m}^2) = 450 \text{ kN}$$

c. Use lesser value of R_t from Step 9a and 9b. Therefore, $R_t = 450 \text{ kN}$.

STEP 10 Compute the ultimate pile capacity, Q_u .

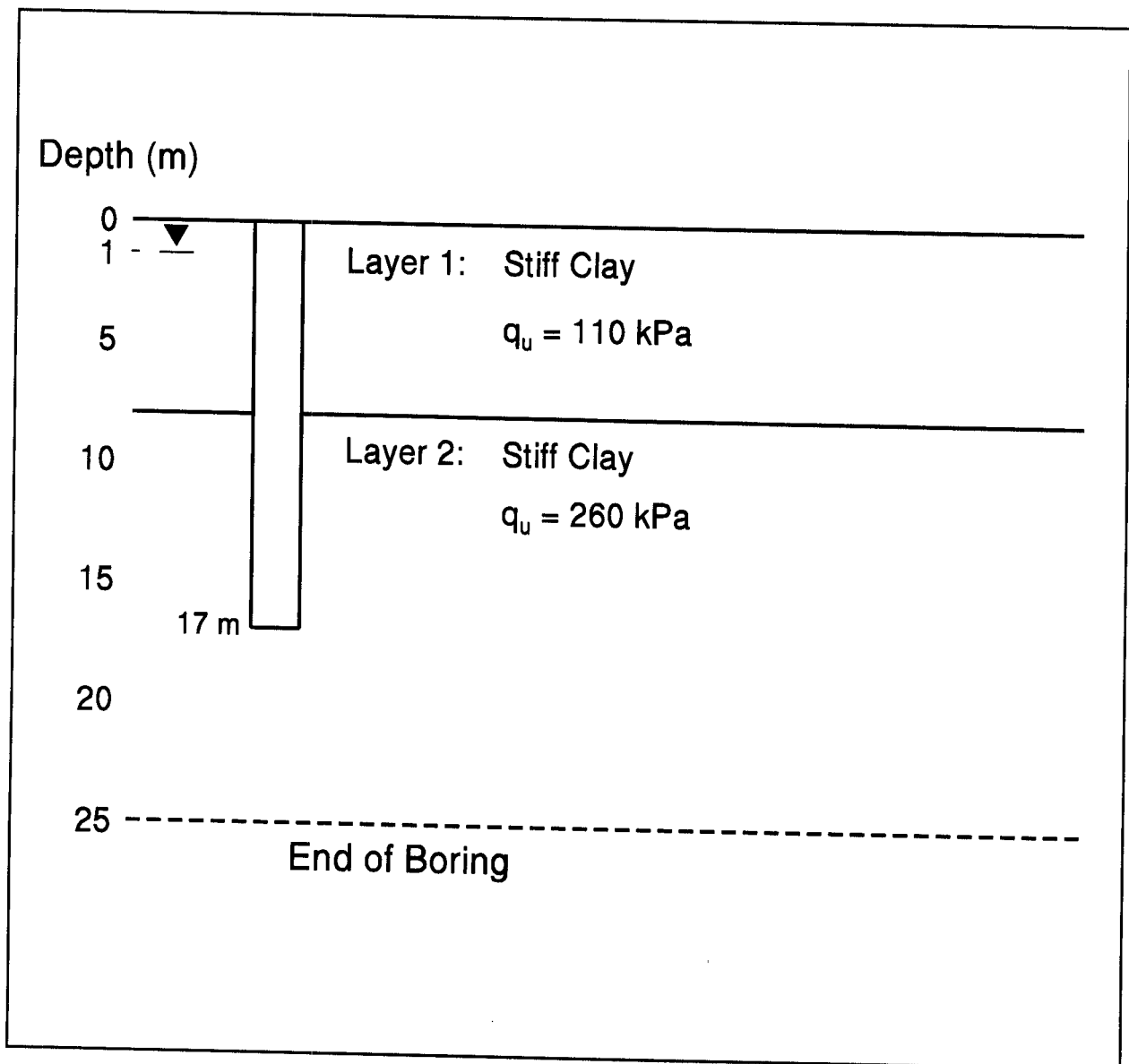
$$Q_u = R_s + R_t = 1287 \text{ kN} + 450 \text{ kN} = 1737 \text{ kN}$$

STEP 11 Compute the allowable design load, Q_a .

The allowable design load is Q_u /Factor of Safety based on construction control method as described in Section 9.6. Therefore, the allowable design load would range from 496 to 868 kN depending upon construction control method specified.

STUDENT EXERCISE #3 - α -METHOD PILE CAPACITY CALCULATION

Use the α -Method and step by step procedure described in Section 9.7.1.2a to calculate the ultimate pile capacity and the allowable design load for a 356 mm square, prestressed concrete pile driven into the soil profile described below. The trial pile length for the calculation is 17 meters. The prestressed concrete pile has a pile-soil surface area of $1.42 \text{ m}^2/\text{m}$ and a pile toe area of 0.127 m^2 . Based on the soil profile, Figure 9.18 or 9.19(c) should be used to calculate pile capacity. Note: the soil strengths provided are unconfined compression test results ($c_u = q_u/2$).



STUDENT EXERCISE #3 - SOLUTION FOR α -METHOD CAPACITY CALCULATION

STEP 1 Delineate the soil profile and determine the pile adhesion from Figure 9.18 or the adhesion factor from Figure 9.19(c).

The soil profile was delineated in the problem statement. The bottom of Layer 1 is at 9 meters. Therefore calculations for Layer 1 should be based on an embedded pile length to diameter ratio, D/b , of $(9 \text{ m}) / (.356 \text{ m})$ or 25. The bottom of Layer 2 is at 17 meters. Calculations for Layer 2 should then be based on an embedded pile length to diameter ratio, D/b , of $(17 \text{ m}) / (.356 \text{ m})$ or 48.

Using Figure 9.18, the pile adhesion for each layer is as follows;

Layer 1: $q_u = 110 \text{ kPa}$ so $c_u = 55 \text{ kPa}$. For a D/b of 25, a pile adhesion of 55 kPa is obtained by interpolating between the two curves for a concrete pile.

Layer 2: $q_u = 260 \text{ kPa}$ so $c_u = 130 \text{ kPa}$. For a D/b of 48, the $D > 40b$ curve for a concrete pile should be used. This results in a pile adhesion of 80 kPa.

Using Figure 9.19(c), the adhesion factor, α , for each layer is as follows;

Layer 1: $q_u = 110 \text{ kPa}$ so $c_u = 55 \text{ kPa}$. For a D/b of 25, a pile adhesion factor of 0.95 is obtained by interpolating between the $D=10b$ and $D > 40b$ curves.

Layer 2: $q_u = 260 \text{ kPa}$ so $c_u = 130 \text{ kPa}$. For a D/b of 48, the $D > 40b$ curve should be used and an adhesion factor of 0.60 is obtained.

STEP 2 Compute the unit shaft resistance, f_s , for each soil layer.

Using Figure 9.18, the unit shaft resistance equals the pile adhesion and is therefore 55 kPa for Layer 1 and 80 kPa for Layer 2.

Using Figure 9.19(c), the unit shaft resistance equals the adhesion factor times the undrained shear strength or $f_s = \alpha (c_u)$. For Layer 1, $\alpha (c_u)$ is 0.95 (55 kPa) which results in a unit shaft resistance of 52 kPa. For Layer 2, $\alpha (c_u)$ is 0.60 (130 kPa) results in a unit shaft resistance of 78 kPa.

STEP 3 Compute the shaft resistance per layer and the ultimate shaft resistance.

The embedded pile length is 9 meters in Layer 1 and 8 meters in Layer 2. The pile-soil surface area was defined as 1.42 m²/m in the problem statement.

Using Figure 9.18, the shaft resistance for each layer is as follows;

Layer 1: The unit shaft resistance, f_{s1} , is 55 kPa. The pile-soil surface area, A_s is 1.42 m²/m and the length of pile in Layer 1, D_1 is 9 meters. Therefore, the shaft resistance in this layer can be calculated from:

$$\begin{aligned} R_{s1} &= (f_{s1}) (A_s) (D_1) \\ &= (55 \text{ kPa}) (1.42 \text{ m}^2/\text{m}) (9 \text{ m}) = 703 \text{ kN} \end{aligned}$$

Layer 2: The unit shaft resistance, f_{s2} , is 80 kPa. The pile-soil surface area, A_s is 1.42 m²/m and the length of pile in Layer 2, D_2 is 8 meters. Therefore, the shaft resistance in this layer can be calculated from:

$$\begin{aligned} R_{s2} &= (f_{s2}) (A_s) (D_2) \\ &= (80 \text{ kPa}) (1.42 \text{ m}^2/\text{m}) (8 \text{ m}) = 909 \text{ kN} \end{aligned}$$

The ultimate shaft resistance, R_s , is the sum of the shaft resistance from each individual layer.

$$\begin{aligned} R_s &= R_{s1} + R_{s2} \\ &= 703 + 909 = 1612 \text{ kN} \end{aligned}$$

Using Figure 9.19(c), the shaft resistance for each layer is as follows;

Layer 1: The unit shaft resistance, f_{s1} , is 52 kPa. The pile-soil surface area, A_s is $1.42 \text{ m}^2/\text{m}$ and the length of pile in Layer 1, D_1 is 9 meters. Therefore, the shaft resistance in this layer can be calculated from:

$$\begin{aligned} R_{s1} &= (f_{s1})(A_s)(D_1) \\ &= (52 \text{ kPa})(1.42 \text{ m}^2/\text{m})(9 \text{ m}) = 665 \text{ kN} \end{aligned}$$

Layer 2: The unit shaft resistance, f_{s2} , is 78 kPa. The pile-soil surface area, A_s is $1.42 \text{ m}^2/\text{m}$ and the length of pile in Layer 2, D_2 is 8 meters. Therefore, the shaft resistance in this layer can be calculated from:

$$\begin{aligned} R_{s2} &= (f_{s2})(A_s)(D_2) \\ &= (78 \text{ kPa})(1.42 \text{ m}^2/\text{m})(8 \text{ m}) = 886 \text{ kN} \end{aligned}$$

The ultimate shaft resistance, R_s , is the sum of the shaft resistance from each individual layer.

$$\begin{aligned} R_s &= R_{s1} + R_{s2} \\ &= 665 + 886 = 1551 \text{ kN} \end{aligned}$$

STEP 4 Compute the unit toe resistance, q_t .

The unit toe resistance is calculated from $q_t = 9 c_u$. Since the undrained shear strength at the pile toe is 130 kPa, the unit pile toe resistance is 9 (130 kPa) or 1170 kPa.

STEP 5 Compute the ultimate toe resistance, R_t .

The ultimate toe resistance is calculated from:

$$\begin{aligned} R_t &= q_t A_t \\ &= (1170 \text{ kPa})(0.127 \text{ m}^2) = 149 \text{ kN} \end{aligned}$$

STEP 6 Compute the ultimate pile capacity, Q_u .

Using Figure 9.18, the ultimate pile capacity is as follows:

$$\begin{aligned} Q_u &= R_s + R_t \\ &= 1612 + 149 = 1761 \text{ kN} \end{aligned}$$

Using Figure 9.19(c), the ultimate pile capacity is as follows:

$$\begin{aligned} Q_u &= R_s + R_t \\ &= 1551 + 149 = 1700 \text{ kN} \end{aligned}$$

The lesser of the two ultimate pile capacities of 1700 kN should be selected.

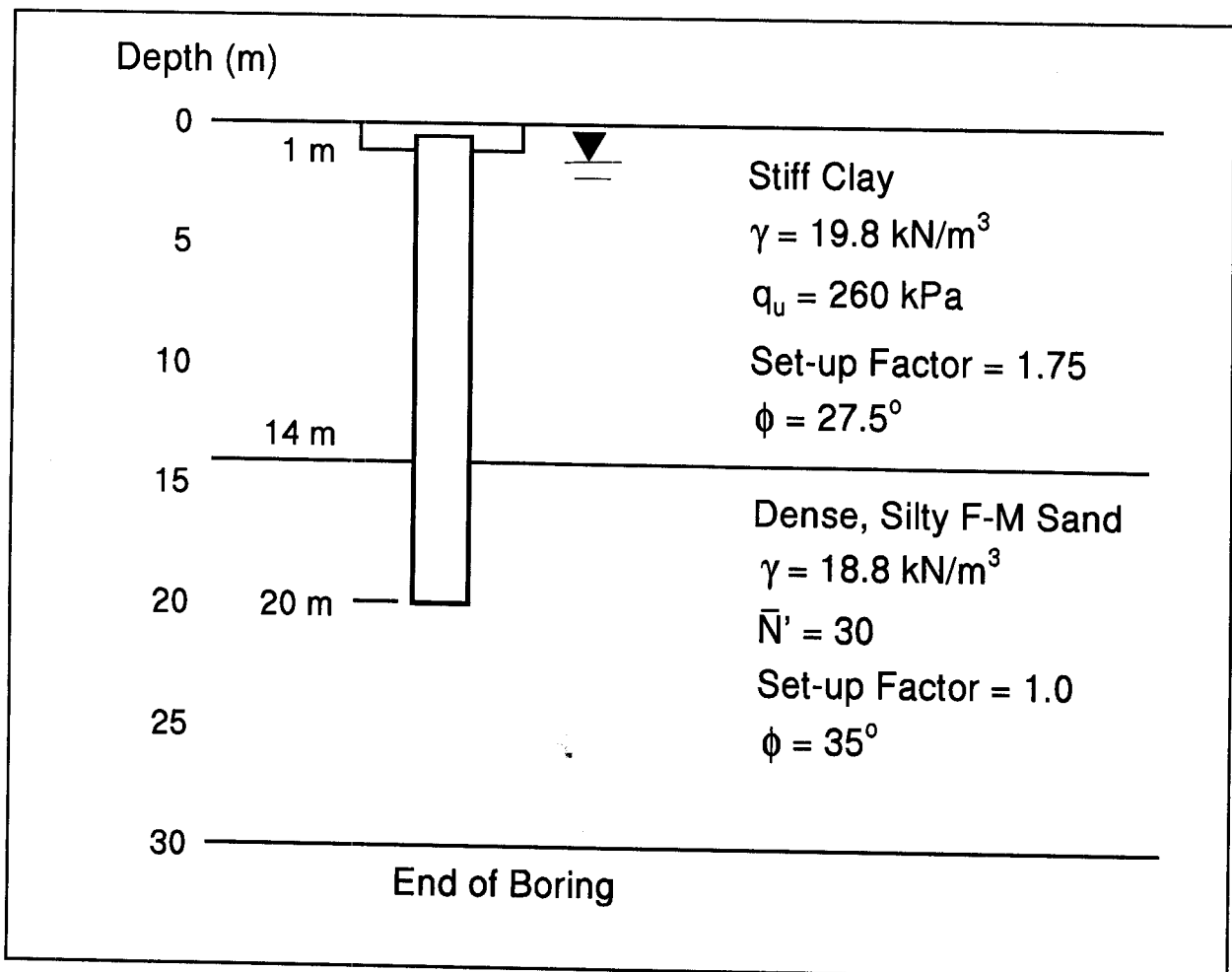
STEP 7 Determine the allowable design load, Q_a .

$$Q_a = Q_u / (\text{Factor of Safety})$$

Based on the construction control method specified, the factor of safety could range from 2.0 to 3.5. Therefore, the allowable design load could range from 486 to 850 kN.

STUDENT EXERCISE #4 - α -METHOD AND NORDLUND METHOD PILE CAPACITY CALCULATION IN A LAYERED SOIL PROFILE

Use the α -Method described in Section 9.7.1.2a and the Nordlund Method described in Section 9.7.1.1b to calculate the ultimate pile capacity, the resistance to driving, and the allowable design load for a 324 mm O.D. closed end pipe pile driven into the soil profile described below. The trial pile length for the calculation is 19 meters below the pile cutoff elevation 1 meter below grade. The pipe pile has a pile-soil surface area of 1.02 m²/m and a pile toe area of 0.082 m². Use Figure 9.18 to calculate the shaft resistance in the clay layer. The pile volume is 0.082 m³/m. The effective overburden at 17 m, the midpoint of the pile shaft in the sand layer is 177 kPa, and the effective overburden pressure at the pile toe is 204 kPa. Note: the soil strengths provided are unconfined compression test results ($c_u = q_u/2$).



STUDENT EXERCISE #4 - SOLUTION FOR α -METHOD AND NORDLUND METHOD CAPACITY CALCULATION IN A LAYERED SOIL PROFILE

Calculate the Shaft Resistance in the Clay Layer Using α -Method

STEP 1 Delineate the soil profile and determine the pile adhesion from Figure 9.18.

The soil profile was delineated in the problem statement. The bottom of Layer 1 is at 14 meters. Therefore calculations for Layer 1 should be based on an embedded pile length to diameter ratio, D/b , of $(14 \text{ m}) / (.324 \text{ m})$ or 43.

Using Figure 9.18, the pile adhesion for each layer is as follows;

Layer 1: $q_u = 260 \text{ kPa}$ so $c_u = 130 \text{ kPa}$. For a D/b of 43, a pile adhesion of 70 kPa is obtained for a smooth steel pile.

STEP 2 Compute the unit shaft resistance, f_s , for each soil layer.

The unit shaft resistance equals the pile adhesion and is therefore 70 kPa for Layer 1.

STEP 3 Compute the shaft resistance in the clay layer.

The embedded pile length is 13 meters in Layer 1. The pile-soil surface area was defined as $1.02 \text{ m}^2/\text{m}$ in the problem statement.

Therefore, the shaft resistance for the clay layer is as follows;

Layer 1: The unit shaft resistance, f_{s1} , is 70 kPa. The pile-soil surface area, A_s is $1.02 \text{ m}^2/\text{m}$ and the length of pile in Layer 1, D_1 is 13 meters. Therefore, the shaft resistance in this layer can be calculated from:

$$\begin{aligned} R_{s1} &= (f_{s1})(A_s)(D_1) \\ &= (70 \text{ kPa})(1.02 \text{ m}^2/\text{m})(13 \text{ m}) = 928 \text{ kN} \end{aligned}$$

Calculate the Shaft Resistance in the Sand Layer Using Nordlund Method

STEP 1 The p_o diagram, soil layer determination, and the soil friction angle, ϕ , for each soil layer were presented in the problem introduction.

STEP 2 Determine δ .

a. Compute volume of soil displaced per unit length of pile, V .

$$V = 0.082 \text{ m}^3/\text{m} \text{ (per problem description)}$$

b. Determine δ/ϕ from Figure 9.10.

$$V = 0.082 \text{ m}^3/\text{m} \rightarrow \delta/\phi = 0.62 \text{ or } \delta = 0.62\phi$$

c. Calculate δ for each soil layer based on $\delta = 0.62\phi$.

$$\text{Layer 2: } \delta_2 = 0.62 (35^\circ) = 21.70$$

STEP 3 Determine K_δ for each soil layer based on displaced volume, V , and pile taper angle, ω .

$$\text{Layer 2: For } \phi = 35^\circ, \quad V = 0.082 \text{ m}^3/\text{m} \text{ and } \omega = 0^\circ$$

d. From Figure 9.13: $K_\delta = 1.15$ for $V = 0.0093 \text{ m}^3/\text{m}$
 $K_\delta = 1.75$ for $V = 0.093 \text{ m}^3/\text{m}$

Using log linear interpolation $K_\delta = 1.72$ for $V = 0.082 \text{ m}^3/\text{m}$

STEP 4 Determine correction factor, C_F , to be applied to K_δ when $\delta \neq \phi$ (Figure 9.15.)

$$\text{Layer 2: } \phi = 35^\circ \text{ and } \delta/\phi = 0.62 \rightarrow C_F = 0.78$$

STEP 5 Compute effective overburden pressure at midpoint of each soil layer, p_d .

From problem description, p_d for layer 2 is 177 kPa.

STEP 6 Compute the shaft resistance for each soil layer.

$$R_s = K_\delta C_F p_d \sin \delta C_d D$$

$$C_d = \text{pile perimeter} = 1.02 \text{ m}^2/\text{m}$$

$$D = \text{embedded length in layer}$$

$$\begin{aligned} \text{Layer 2: } R_{s2} &= 1.72 (0.78) (177 \text{ kPa}) (\sin 21.70^\circ) (1.02 \text{ m}^2/\text{m}) (6 \text{ m}) \\ &= 537 \text{ kN} \end{aligned}$$

Compute the Ultimate Shaft Resistance, R_s

$$R_s = R_{s1} + R_{s2} = 928 \text{ kN} + 537 \text{ kN} = 1465 \text{ kN}$$

Compute the Ultimate Toe Resistance, R_t

STEP 7 Determine α_t coefficient and bearing capacity factor N'_q from ϕ angle of 35° at pile toe and Figures 9.16(a) and 9.16(b) based on D/b of 62.

$$\text{From Figure 9.16(a)} \rightarrow \alpha_t = 0.67$$

$$\text{From Figure 9.16(b)} \rightarrow N'_q = 65$$

STEP 8 Compute effective overburden pressure at pile toe.

The effective overburden pressure at the pile toe was given as 204 kPa in the problem description. Therefore, limiting overburden pressure at pile toe of 150 kPa applies.

STEP 9 Compute the ultimate toe resistance, R_t .

a. $R_t = \alpha_t N'_q A_t p_t$

$$= (0.67) (65) (0.082 \text{ m}^2) (150 \text{ kPa}) = 536 \text{ kN}$$

b. $R_t = q_L A_t$ from Figure 9.17, $q_L=5000 \text{ kPa}$ for $\phi=35^\circ$.

$$= (5000 \text{ kPa}) (0.082 \text{ m}^2) = 410 \text{ kN}$$

c. Use lesser value of R_t from Step 9a and 9b. Therefore, $R_t = 410 \text{ kN}$.

STEP 10 Compute the ultimate pile capacity, Q_u .

$$Q_u = R_s + R_t = 1465 \text{ kN} + 410 \text{ kN} = 1875 \text{ kN}$$

STEP 11 Compute the allowable design load, Q_a .

The allowable design load is Q_u /Factor of Safety based on construction control method as described in Section 9.6. Therefore, the allowable design load would range from 536 to 938 kN depending upon construction control method specified.

Calculation of the Resistance to Driving

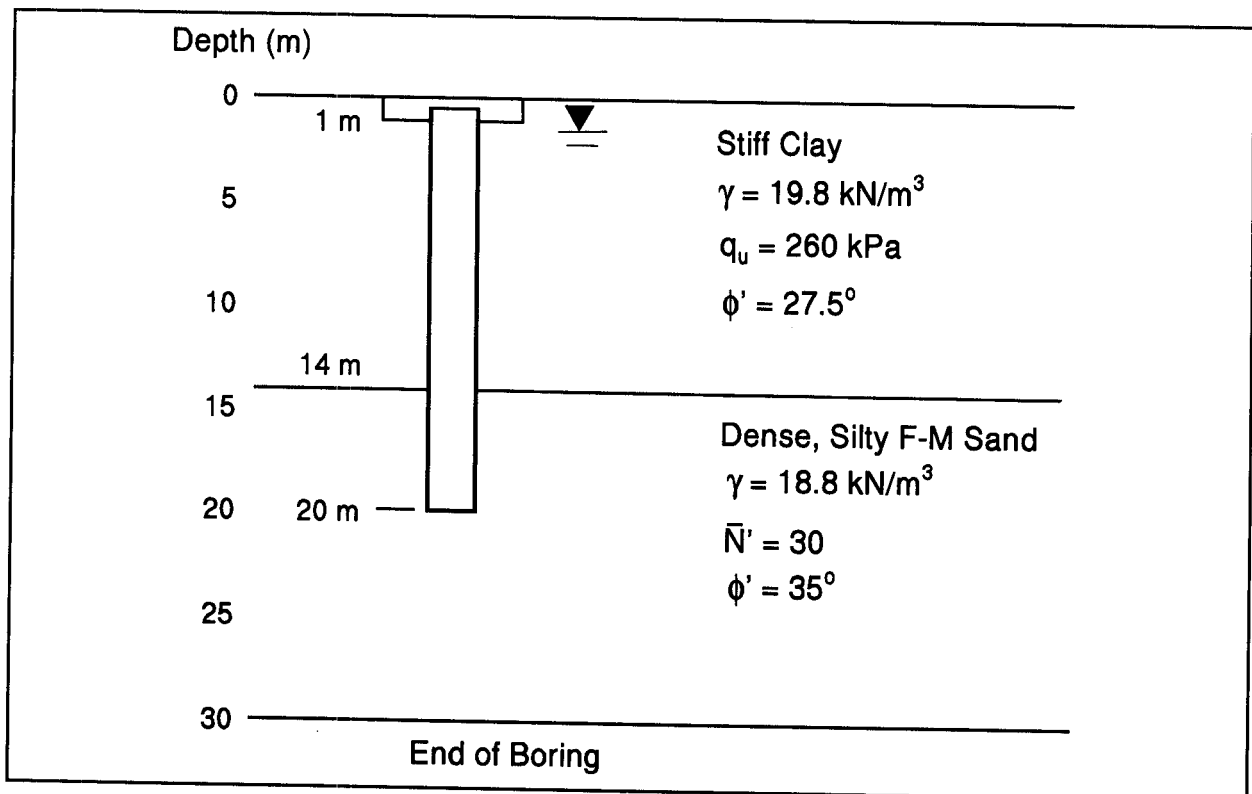
The clay layer has a set-up factor of 1.75. Therefore, the resistance from the clay layer at the time of driving is $(928 \text{ kN}) / (1.75)$ or 530 kN. The shaft and toe resistance from the sand layer are unchanged and are 537 and 410 kN, respectively. Therefore, the resistance at the time of driving, Q_D , is:

$$Q_D = 530 \text{ kN} + 537 \text{ kN} + 410 \text{ kN} = 1477 \text{ kN}.$$

STUDENT EXERCISE #5 - EFFECTIVE STRESS PILE CAPACITY CALCULATION IN A LAYERED SOIL PROFILE

Use the Effective Stress Method described in Section 9.7.1.3 to calculate the ultimate pile capacity, the resistance to driving, and the allowable design load for a 324 mm O.D. closed end pipe pile driven into the soil profile described below. The trial pile length for the calculation is 19 meters below the pile cutoff elevation 1 meter below grade. The pipe pile has a pile-soil surface area of $1.02 \text{ m}^2/\text{m}$ and a pile toe area of 0.082 m^2 . Use Table 9-4 or Figure 9.20 to determine β values for calculation of the shaft resistance and Table 9-4 or Figure 9.21 for calculation of N_t . The effective overburden at the midpoint of the pile shaft in the clay layer is 85 kPa and 177 kPa at the midpoint of the sand layer. The effective overburden pressure at the pile toe is 204 kPa.

During driving, the excess pore pressure generated in the clay layer at the pile-soil interface is expected to be 1.4 times the effective overburden pressure based on Figure 9.56. Therefore, use an average effective overburden pressure of 29.5 kPa at the midpoint of the pile shaft in the clay layer to calculate the shaft resistance in the clay layer during driving.



STUDENT EXERCISE #5 - SOLUTION FOR EFFECTIVE STRESS METHOD PILE CAPACITY CALCULATION IN A LAYERED SOIL PROFILE

STEP 1 Delineate the soil profile and determine the ϕ' angle for each layer.

The soil profile and ϕ' angle were given in the problem description.

STEP 2 Select the β coefficient for each soil layer.

Based on the given ϕ' angles, the clay layer would have a β coefficient of 0.30 and the sand layer would have a β coefficient of 0.40.

STEP 3 Compute the unit shaft resistance, f_s , in each layer.

The unit shaft resistance for each layer is as follows:

$$\text{Layer 1: } f_{s1} = \beta_1 (p_o) = 0.30 (85 \text{ kPa}) = 25.5 \text{ kPa}$$

$$\text{Layer 2: } f_{s2} = \beta_2 (p_o) = 0.40 (177 \text{ kPa}) = 70.8 \text{ kPa}$$

STEP 4 Compute the shaft resistance for each layer and the ultimate shaft resistance.

The shaft resistance for each layer is as follows:

$$\begin{aligned} \text{Layer 1: } R_{s1} &= (f_{s1})(A_s)(D_1) \\ &= (25.5 \text{ kPa})(1.02 \text{ m}^2/\text{m})(13 \text{ m}) = 338 \text{ kN} \end{aligned}$$

$$\begin{aligned} \text{Layer 2: } R_{s2} &= (f_{s2})(A_s)(D_2) \\ &= (70.8 \text{ kPa})(1.02 \text{ m}^2/\text{m})(6 \text{ m}) = 433 \text{ kN} \end{aligned}$$

The ultimate shaft resistance, R_s is as follows:

$$R_s = R_{s1} + R_{s2} = 338 \text{ kN} + 433 \text{ kN} = 771 \text{ kN}$$

STEP 5 Compute the unit toe resistance, q_t .

$$q_t = N_t p_t$$

From Figure 9.21 and a ϕ' angle of 35° , $N_t = 55$. The effective overburden pressure at the pile toe, p_t , was given as 204 kPa.

$$q_t = (55) (204 \text{ kPa}) = 11,220 \text{ kPa}$$

STEP 6 Compute the ultimate toe resistance, R_t .

$$R_t = q_t A_t = (11,220 \text{ kPa})(0.082 \text{ m}^2) = 920 \text{ kN}$$

STEP 7 Compute the ultimate pile capacity, Q_u .

$$Q_u = R_s + R_t = 771 \text{ kN} + 920 \text{ kN} = 1691 \text{ kN}$$

STEP 8 Compute the allowable design load, Q_a .

The allowable design load is Q_u /Factor of Safety based on construction control method as described in Section 9.6. Therefore, the allowable design load would range from 483 to 845 kN depending upon construction control method specified.

Calculation of the Resistance to Driving

The average effective overburden pressure in the clay layer during driving is estimated to be 29.5 kPa. Therefore, the average unit shaft resistance in the clay layer at the time of driving should be calculated using this effective overburden pressure. The shaft and toe resistance from the sand layer are unchanged. The resistance at the time of driving, Q_D , is:

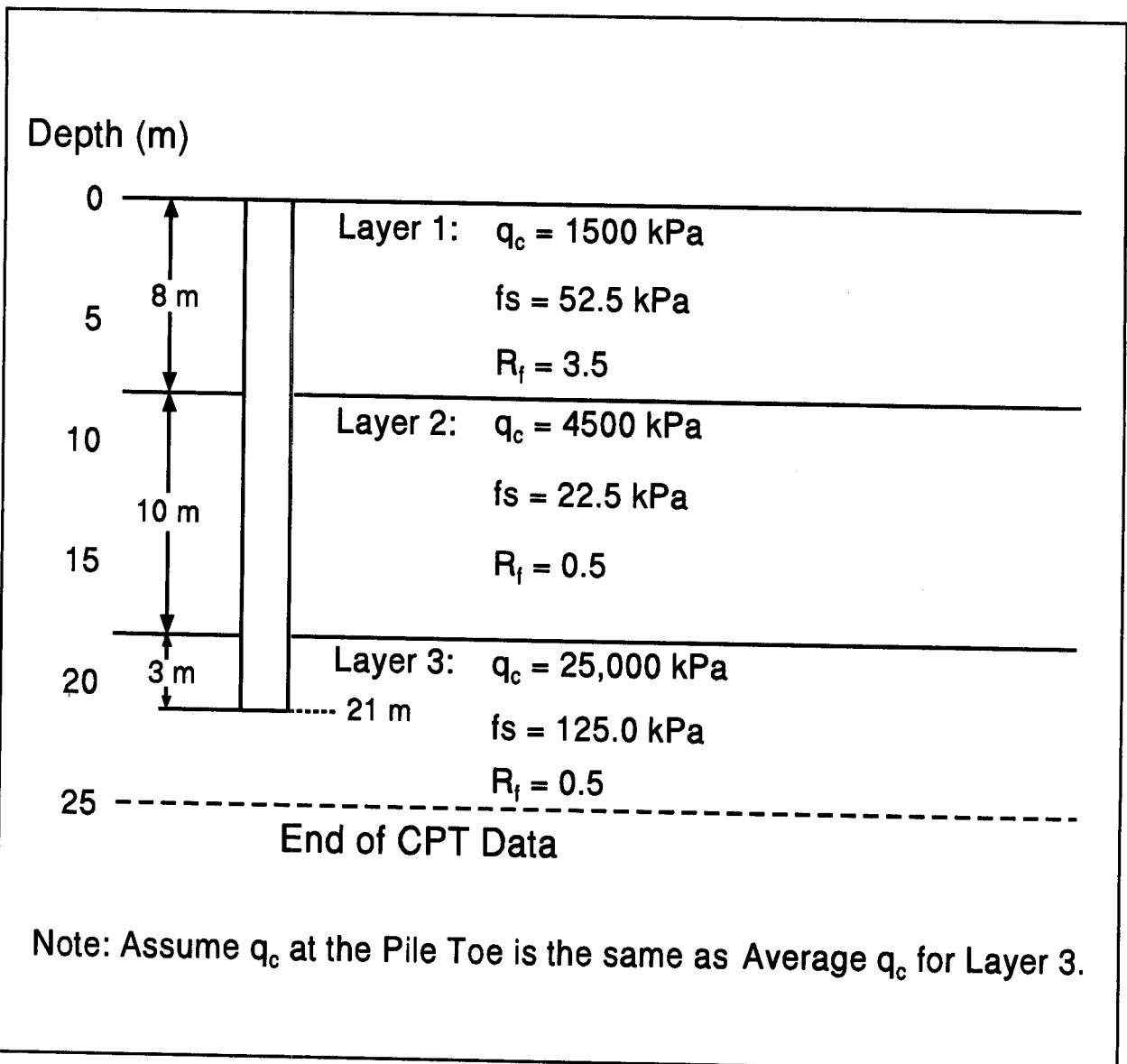
$$f_{s1} = \beta_1 (p_o) = 0.30 (29.5 \text{ kPa}) = 8.85 \text{ kPa}$$

$$R_{s1} = (f_{s1})(A_s)(D_1) = (8.85 \text{ kPa}) (1.02 \text{ m}^2/\text{m})(13 \text{ m}) = 117 \text{ kN}$$

$$Q_D = 117 \text{ kN} + 433 \text{ kN} + 920 \text{ kN} = 1470 \text{ kN}$$

STUDENT EXERCISE #6 - LPC METHOD PILE CAPACITY CALCULATION

Cone Penetration Test (CPT) data for a site identified three soil layers having the average CPT results presented below. Use the LPC Method described in Section 9.7.1.7b to calculate the ultimate pile capacity and the allowable design load for a 324 mm diameter closed end pipe pile. Use a trial pile length of 21 meters. The pipe pile has a pile-soil surface area of $1.02 \text{ m}^2/\text{m}$ and a pile toe area of 0.083 m^2 . Previous load test data is not available in the project vicinity. Use Figure 5.2 to characterize the subsurface conditions.



STUDENT EXERCISE #6 - LPC METHOD SOLUTION

STEP 1 Delineate the soil profile. Using the cone tip resistance, q_c , and the friction ratio, R_f , values in Figure 5.2, the soil profile can be characterized as follows:

Layer 1: $q_c = 1500$ kPa and $R_f = 3.5$. This data plots in Zone 4 of Figure 5.2 which characterizes the soil as a silty clay to clay.

Layer 2: $q_c = 4500$ kPa and $R_f = 0.5$. This data plots in Zone 8 of Figure 5.2 which characterizes the soil as a sand to silty sand.

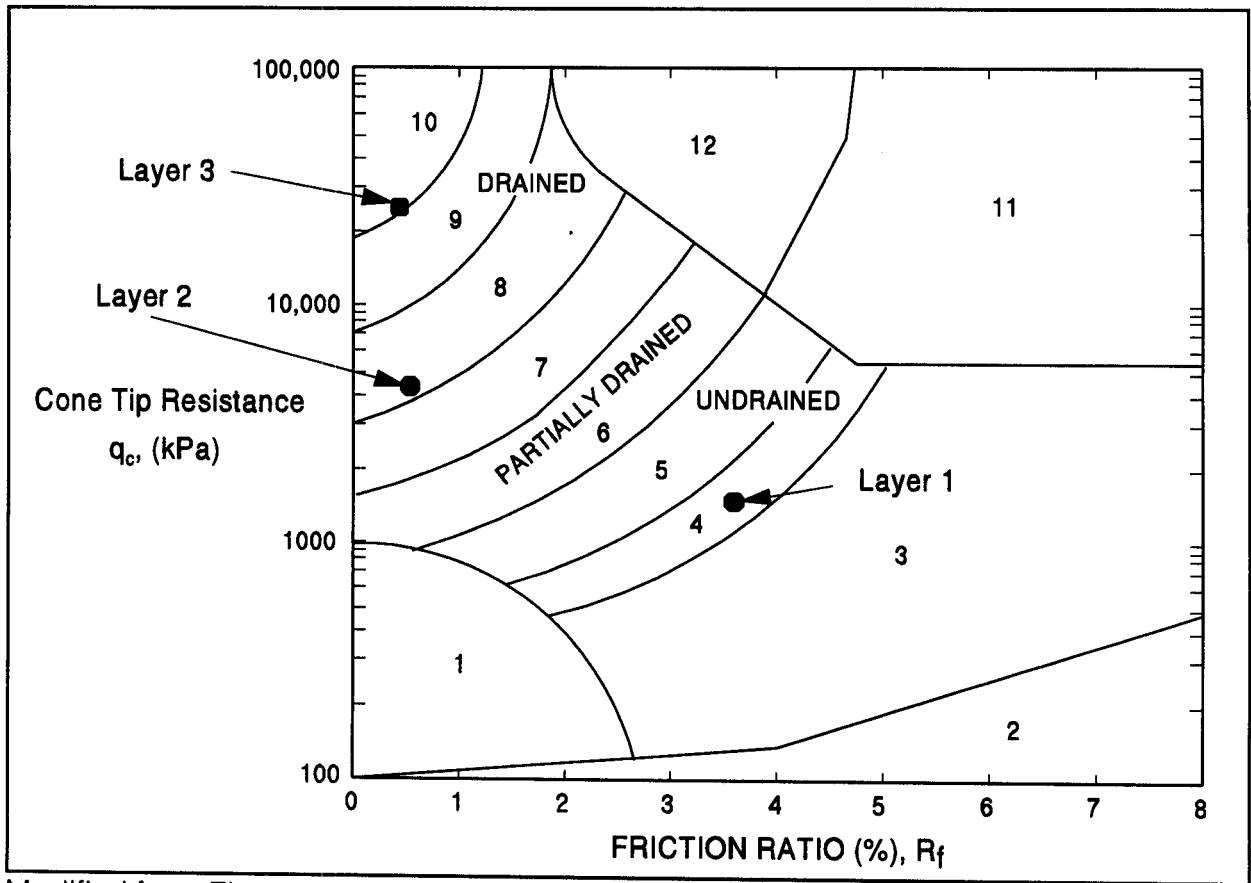
Layer 3: $q_c = 25000$ kPa and $R_f = 0.5$. This data plots on the borderline of Zones 9 and 10 of Figure 5.2 which characterizes the soil as a sand to gravelly sand.

STEP 2 Determine the unit shaft resistance for each soil layer. From Table 9-7, the pile type is type B.

Layer 1: The soil type is clay and q_c is 1500 kPa. Therefore, Table 9-8(a) should be used and indicates Curve 2 based on q_c value. However, the table comments section indicates to use Curve 1 for steel piles when no previous load test data is available. Enter Figure 9.25(a) with a q_c value of 1500 kPa. Curve 1 then indicates a unit shaft resistance of 35 kPa.

Layer 2: The soil type is sand and q_c is 4500 kPa. Therefore, Table 9-8(b) should be used and indicates Curve 2 based on q_c value. However, the table comments section indicates to use Curve 1 for steel piles when no previous load test data is available. Enter Figure 9.25b with a q_c value of 4500 kPa. Curve 1 then indicates a unit shaft resistance of 30 kPa.

Layer 3: The soil type is gravelly sand and q_c is 25000 kPa. Therefore, Table 9-8(b) should be used and indicates Curve 3 based on q_c value. Enter Figure 9.25(b) with a q_c value of 25000 kPa. Curve 3 then indicates a unit shaft resistance of 130 kPa.



Modified from Figure 5.2 (Simplified Soil Classified Chart for Standard Electronic Friction Cone after Robertson *et al.*, 1986)

Zone	q_c/N	Soil Behavior Type
1)	2	sensitive fine grained
2)	1	organic material
3)	1	clay
4)	1.5	silty clay to clay
5)	2	clayey silt to silty clay
6)	2.5	sandy silt to clayey silt
7)	3	silty sand to sandy silt
8)	4	sand to silty sand
9)	5	sand
10)	6	gravelly sand to sand
11)	1	very stiff fine grained
12)	2	sand to clayey sand

STEP 3 Compute the shaft resistance per layer and the ultimate shaft resistance.

Layer 1: The unit shaft resistance, f_{s1} , is 35 kPa. The pile-soil surface area, A_s is $1.02 \text{ m}^2/\text{m}$ and the length of pile in Layer 1, D_1 is 8 meters. Therefore, the shaft resistance in this layer can be calculated from:

$$\begin{aligned} R_{s1} &= (f_{s1})(A_s)(D_1) \\ &= (35 \text{ kPa})(1.02 \text{ m}^2/\text{m})(8 \text{ m}) = 286 \text{ kN} \end{aligned}$$

Layer 2: The unit shaft resistance, f_{s2} , is 30 kPa. The pile-soil surface area, A_s is $1.02 \text{ m}^2/\text{m}$ and the length of pile in Layer 2, D_2 is 10 meters. Therefore, the shaft resistance in this layer can be calculated from:

$$\begin{aligned} R_{s2} &= (f_{s2})(A_s)(D_2) \\ &= (30 \text{ kPa})(1.02 \text{ m}^2/\text{m})(10 \text{ m}) = 306 \text{ kN} \end{aligned}$$

Layer 3: The unit shaft resistance, f_{s3} , is 130 kPa. The pile-soil surface area, A_s is $1.02 \text{ m}^2/\text{m}$ and the length of pile in Layer 3, D_3 is 3 meters. Therefore, the shaft resistance in this layer can be calculated from:

$$\begin{aligned} R_{s3} &= (f_{s3})(A_s)(D_3) \\ &= (130 \text{ kPa})(1.02 \text{ m}^2/\text{m})(3 \text{ m}) = 398 \text{ kN} \end{aligned}$$

The ultimate shaft resistance, R_s , is the sum of the shaft resistance from each individual layer.

$$\begin{aligned} R_s &= R_{s1} + R_{s2} + R_{s3} \\ &= 286 + 306 + 398 = 990 \text{ kN} \end{aligned}$$

STEP 4 Compute the unit pile toe resistance, q_t .

- a. The average cone tip resistance is 25000 kPa.
- b. From Table 9-9, the cone bearing capacity factor, K_c , is 0.375.
- c. The unit pile toe resistance is then:

$$\begin{aligned}q_t &= K_c q_c \\ &= 0.375 (25000 \text{ kPa}) = 9375 \text{ kPa}.\end{aligned}$$

STEP 5 Compute the ultimate toe resistance, R_t .

$$\begin{aligned}R_t &= q_t A_t \\ &= (9375 \text{ kPa})(0.083 \text{ m}^2) = 778 \text{ kN}\end{aligned}$$

STEP 6 Compute the ultimate pile capacity, Q_u .

$$\begin{aligned}Q_u &= R_s + R_t \\ &= 990 + 778 = 1768 \text{ kN}\end{aligned}$$

STEP 7 Determine the allowable design load, Q_a .

$$Q_a = Q_u / (\text{Factor of Safety})$$

Based on the construction control method specified, the factor of safety could range from 2.0 to 3.5. Therefore, the allowable design load could range from 505 to 884 kN.

STUDENT EXERCISE #7 - PILE GROUP SETTLEMENT IN LAYERED PROFILE

A pile group is to be installed in a fine to medium silty sand deposit that is underlain by a stiff clay layer and then a very dense fine to coarse sand layer. The pile group has a total **design** load of 16,000 kN. The pile group has a plan area of 3 m by 10 m. Use the pile group settlement method for layered soils described in Section 9.8.2.4 to calculate the settlement of the pile group depicted on the following page. For ease of calculation, compute the settlements for each soil layer below the equivalent footing depth using the layer thickness rather than breaking the profile into 1.5 to 3 m thick layers as described in Section 9.8.2.4. Also do not calculate the elastic pile deformation for this problem. Based on your calculation, is the pile group settlement acceptable?

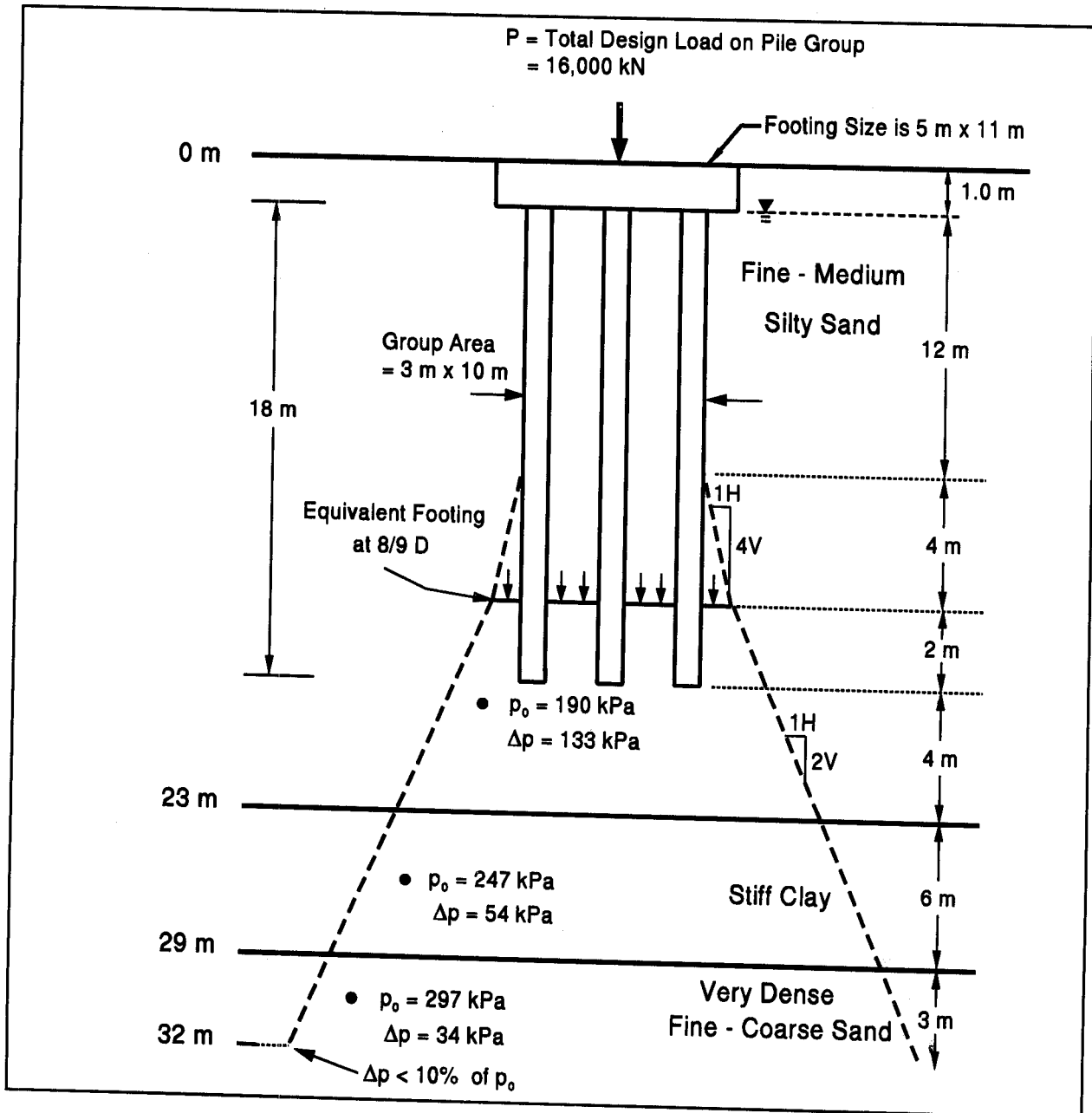
The soil layers have the following properties:

In the zone below the equivalent footing location, the fine to medium sand has an average corrected SPT resistance value of 30 as determined using a SPT safety hammer. The existing overburden pressure at the midpoint of the sand layer below the equivalent footing location is 190 kPa and the corresponding pressure increase at this point is 133 kPa.

The stiff clay layer has an initial void ratio e_o of 0.80, a preconsolidation pressure, p_c , of 247 kPa, a compression index, C_c of 0.30 and recompression index C_{cr} , of 0.03. The existing overburden pressure at the midpoint of the clay layer is 247 kPa and the corresponding pressure increase at this depth is 54 kPa.

The underlying very dense fine to coarse sand layer has an average corrected SPT resistance value of 60 determined by a SPT safety hammer. The pressure increase is less than 10% of the effective overburden pressure at a depth of 32 meters. At the midpoint of the affected portion of the lower sand layer (30.5 m), the effective overburden pressure is 297 kPa and the pressure increase is 34 kPa.

To solve this problem you will need to calculate the sand layer settlement from the equation on page 9-114 and Figure 9.45 on page 9-115. The clay layer settlement should be calculated using the properties described above and the appropriate equation on page 9-111 (Note the terms for these equations are on page 9-108.)



Remember settlement computations are based on the design load rather than ultimate loads.

STUDENT EXERCISE #7 - PILE GROUP SETTLEMENT SOLUTION

STEP 1 Calculate the settlement of the fine to medium silty sand layer using the following equation after determining the bearing capacity index for the layer from Figure 9.45.

Based on Figure 9.45, the fine to medium silty sand layer has a bearing capacity index value of 95 for an average corrected SPT N value of 30 from a SPT safety hammer.

The settlement of the sand layer is then calculated using the following equation:

$$\text{Layer 1: } s_1 = H \left[\frac{1}{C'} \log \frac{p_0 + \Delta p}{p_0} \right]$$

$$s_1 = (6 \text{ m}) \left[\frac{1}{95} \log \frac{190 + 133}{190} \right] = 0.0145 \text{ m} = 14.5 \text{ mm}$$

STEP 2 Calculate settlement in clay layer after determining appropriate settlement equation from page 9-111.

The clay layer is normally consolidated and the pressure increase is greater than the preconsolidation pressure. The settlement of the 6 meter thick layer can then be calculated as follows:

$$\text{Layer 2: } s_2 = H \left[\frac{C_c}{1+e_0} \log \frac{p_0 + \Delta p}{p_0} \right]$$

$$s_2 = (6 \text{ m}) \left[\frac{0.30}{1+0.80} \log \frac{247 + 54}{247} \right] = 0.0858 \text{ m} = 85.8 \text{ mm}$$

STEP 3 Calculate the settlement of the very dense, fine to coarse sand layer after determining the index value from Figure 9.45.

Based on Figure 9.45, the very dense, fine to coarse sand layer has a bearing capacity index value of 250 for an average SPT safety hammer corrected N value of 60.

The settlement of the lower sand layer is then calculated using the following equation:

$$\text{Layer 3: } s_3 = H \left[\frac{1}{C'} \log \frac{p_0 + \Delta p}{p_0} \right]$$

$$s_3 = (3 \text{ m}) \left[\frac{1}{250} \log \frac{297 + 34}{297} \right] = 0.0005 \text{ m} = 0.5 \text{ mm}$$

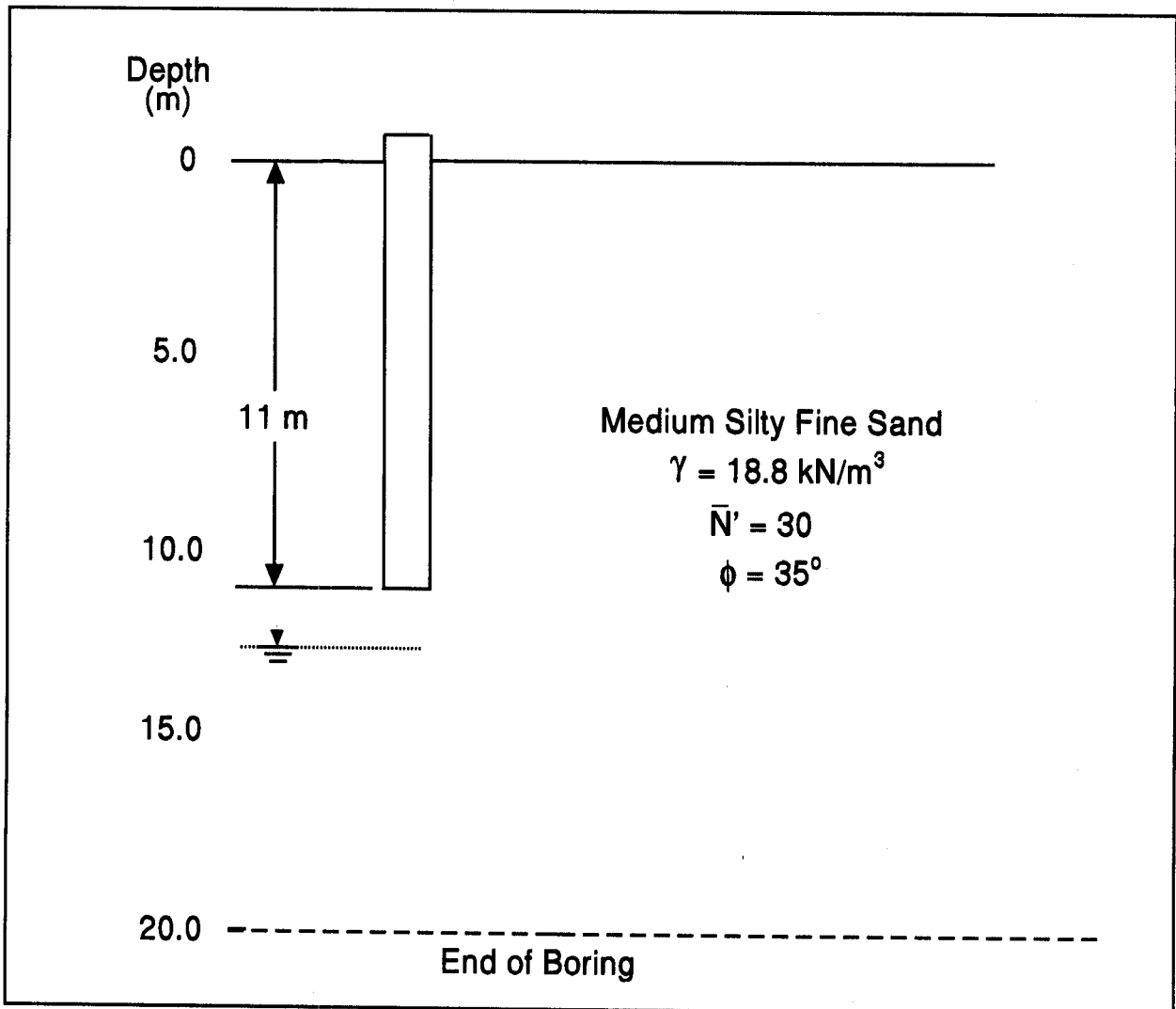
STEP 4 Compute total settlement:

$$s = s_1 + s_2 + s_3 = 14.5 + 85.8 + 0.5 = 100.8 \text{ mm}$$

The total soil settlement of 100.8 mm is excessive.

STUDENT EXERCISE #8 - BROMS' METHOD LATERAL CAPACITY ANALYSIS

Perform a lateral capacity analysis using the Broms' method by following the step by step procedure outlined in Section 9.7.3.2. The pile is a 356-mm square prestressed concrete, which has been driven to a total penetration of 11 meters below grade. The subsurface conditions are presented below. Calculate the maximum allowable lateral load of the pile, and the corresponding deflection at this maximum allowable load. Evaluate the total lateral load capacity of the pile group consisting of 24 piles at 1.5 meters center to center spacing. Assume the pile is to be used in group under a pile cap (fixed head $e_c=0$) with the possibility of cyclic loading during service life. The following pile properties are given: $E = 27,800 \text{ MPa}$; $f'_c = 34.5 \text{ MPa}$; $I = 1.32 \times 10^{-3} \text{ m}^4$; and $S = 7.46 \times 10^{-3} \text{ m}^3$.



EXERCISE #8 - BROMS' METHOD LATERAL CAPACITY ANALYSIS SOLUTION

STEP 1 Determine the general soil type within the critical depth below ground surface (about 4 or 5 pile diameters).

For pile diameter of 0.356 meter, the critical depth below the ground surface is about 1.42 to 1.78 meters (or an average of 1.60 meters). Therefore, the general soil type within the critical depth below the ground surface is cohesionless soil described as medium silty fine sand.

STEP 2 Determine the coefficient of horizontal subgrade reaction, K_h , within the critical depth based on cohesive or cohesionless soils.

For cohesionless soils, choose the K_h from Table 9-11 based on soil density and ground water table. For a medium silty fine sand, K_h is around 8,143 kN/m^3 when the ground water table is below the critical depth.

STEP 3 Adjust K_h for loading and soil conditions.

For cyclic loading in medium dense cohesionless soils:

$$\begin{aligned} K_h' &= \frac{1}{2} K_h \\ &= \frac{1}{2} (8,143) = 4072 \text{ kN/m}^3 \end{aligned}$$

STEP 4 Determine pile parameters.

- a. Modulus of elasticity, $E = 27,800 \text{ MPa}$
- b. Moment of inertia, $I = 1.32 \times 10^{-3} \text{ m}^4$
- c. Section modulus, $S = 7.46 \times 10^{-3} \text{ m}^3$
- d. Ultimate compressive strength, $f'_c = 34.5 \text{ MPa}$

- e. Embedded pile length, $D = 11 \text{ m}$
- f. Pile width, $b = 0.356 \text{ m}$
- g. Eccentricity of applied load, $e_c = 0$ for fixed-headed pile
- h. Dimensionless shape factor, C_s , applied only to steel piles.
- i. Resisting moment of pile, $M_y = f'_c S$ for concrete piles
 - $= 34.5 \text{ MPa } (7.46 \times 10^{-3} \text{ m}^3)$
 - $= 257.4 \text{ kN-m}$

STEP 5 Determine η for cohesionless soils.

$$\eta = \sqrt[5]{K_w/EI} = \sqrt[5]{\frac{4,072 \text{ kN/m}^3}{(27.8 \times 10^6 \text{ kN/m}^2) (1.32 \times 10^{-3} \text{ m}^4)}}$$

$$= 0.644 \text{ m}^{-1}$$

STEP 6 Determine the dimensionless length factor for cohesionless soil.

$$\eta D = 0.644 \text{ m}^{-1} (11 \text{ m}) = 7.09$$

STEP 7 Determine if pile is long or short according to the cohesionless soil criteria.

Since $\eta D = 7.09$ which is greater than 4.0 therefore the pile is long.

STEP 8 Determine other soil parameters.

a. Rankine passive pressure coefficient for cohesionless soil, K_p , is:

$$K_p = \tan^2 (45 + \phi/2)$$

where ϕ is the average soil friction angle along the embedded pile length.

Therefore, the Rankine passive pressure coefficient, K_p , is:

$$\begin{aligned} K_p &= \tan^2 (45 + \phi/2) \\ &= \tan^2 (45 + 35/2) = 3.69 \end{aligned}$$

b. Average effective soil unit weight over embedded length of pile, γ (kN/m^3).

Since the water table is below the bottom of the pile, the average effective soil unit weight, γ , is total weight of 18.8 kN/m^3

STEP 9 Determine the ultimate (failure) load, Q_u , for a single pile.

The pile will be used in group under a pile cap, *i.e.*, fixed headed pile. Figure 9.30 should be used to calculate the ultimate load of a long fixed headed pile.

$$\frac{M_y}{b^4 \gamma K_p} = \frac{257.4 \text{ kN-m}}{(0.355 \text{ m})^4 (18.8 \text{ kN/m}^3) (3.69)} = 234$$

From the fixed head curve in Figure 9.30, $Q_u/K_p b^3 \gamma = 95$. Therefore,

$$Q_u = 95 K_p b^3 \gamma = 95 (3.69) (0.355 \text{ m})^3 (18.8 \text{ kN/m}^3) = 295 \text{ kN}$$

STEP 10 Calculate the maximum allowable working load for a single pile, Q_m , from the ultimate load, Q_u , determined in Step 9, as shown in Figure 9.31.

$$Q_m = \frac{Q_u}{2.5} = \frac{295 \text{ kN}}{2.5} = 118 \text{ kN}$$

STEP 11 Calculate the deflection, y , corresponding to the working load, Q_a .

Since neither the working load, Q_a , nor the design deflection at the ground surface, y , are given, Q_m should be used to calculate y_m . For fixed headed pile in cohesionless soil with $\eta D = 7.09$, and using Figure 9.33 results in

$$y(EI)^{3/5} K_h^{2/5} / Q_a D = 0.13$$

Replace Q_a with Q_m to calculate for y_m :

$$\begin{aligned} y_m &= 0.13 Q_m D / (EI)^{3/5} K_h^{2/5} \\ &= 0.13(118 \text{ kN})(11 \text{ m}) / [(27.8 \times 10^6 \text{ kN/m}^2) (1.32 \times 10^{-3} \text{ m}^4)]^{3/5} (4,072 \text{ kN/m}^3)^{2/5} \\ &= 0.011 \text{ m or } 11.0 \text{ mm} \end{aligned}$$

Therefore, the maximum allowable working load of 118 kN will cause the pile head to deflect 11.0 mm at the ground surface.

STEP 12 Compare the design load Q_a , and design deflection, y , (if available) with the maximum allowable working load, Q_m , and deflection, y_m .

Q_a and y are not known.

STEP 13 Reduce the allowable load selected to account for group effects and method of installation.

a. Group effects.

The center to center pile spacing, z , is designed to be 1.5 meters.

$$(z/b) = (1.5 \text{ m}) / (0.356 \text{ m}) = 4.21$$

Using the reduction factor table and linear interpolation:

$$\text{Reduction factor} = 0.535$$

$$\text{So, } Q_m = 0.535 Q_m = 0.535 (118 \text{ kN}) = 63 \text{ kN}$$

b. Method of installation.

No reduction is required for driven piles. So, $Q_m = 63 \text{ kN}$.

STEP 14 Compute the total lateral load capacity of the pile group.

The total lateral load capacity of the pile group is equal to the adjusted allowable load per pile from Step 13b times the number of piles.

$$\text{Total pile group lateral load capacity} = 24 (63 \text{ kN}) = 1,512 \text{ kN}$$

Pile group deflection as calculated in Step 11 is equal to 11.0 mm.

Note: The lateral resistance from the soil surrounding the embedded pile cap has not been taken into account.



U.S. Department
of Transportation

**Federal Highway
Administration**

Publication No. FHWA HI 97-014
Revised November 1998

NHI Course Nos. 13221 and 13222

Design and Construction of Driven Pile Foundations

Workshop Manual - Volume II



National Highway Institute

NOTICE

This document is disseminated under the sponsorship of the Department of Transportation in the interest of information exchange. The United States Government assumes no liability for its contents or use thereof. The United States Government does not endorse products or manufacturers. Trademarks or manufacturer's names appear herein only because they are considered essential to the object of this document.

Technical Report Documentation Page

1. Report No. FHWA-HI-97-013		2. Government Accession No.		3. Recipient's Catalog No.	
4. Title and Subtitle Design and Construction of Driven Foundations - Volume II				5. Report Date January 1997 - Revised Nov. 1998	
				6. Performing Organization Code	
7. Author(s) Hannigan, P.J., Goble, G.G., Thendean, G., Likins, G.E., and Rausche, F.				8. Performing Organization Report No.	
9. Performing Organization Name and Address Goble Rausche Likins and Associates, Inc. 4535 Renaissance Parkway Cleveland, Ohio 44128				10. Work Unit No. (TRAIS)	
				11. Contract or Grant No. DTFH61-97-D-00025	
12. Sponsoring Agency Name and Address Office of Technology Application Office of Engineering/Bridge Division Federal Highway Administration 400 7th Street, S.W. Washington, D.C. 20590				13. Type of Report and Period Covered Final Report - Revision 1	
				14. Sponsoring Agency Code	
15. Supplementary Notes FHWA Contracting Officer's Technical Representative: Chien-Tan Chang, HTA-20 FHWA Project Technical Manager: Jerry DiMaggio, HNG-31					
16. Abstract This manual is intended to serve a dual purpose, first as a participant's manual for the FHWA's National Highway Institute courses on driven pile foundations and secondly as FHWA's primary reference of recommended practice for driven pile foundations. The Design and Construction of Driven Pile Foundations manual is directed to geotechnical, structural, and construction engineers involved in the design and construction of pile supported structures. The manual is intended to serve as a practical reference on driven pile foundations. Volume I of the manual addresses design aspects including subsurface exploration, laboratory testing, static analyses, as well as specification and foundation report preparation. Volume II covers construction aspects including dynamic formulas, wave equation analyses, dynamic testing, static load testing, Statnamic testing, the Osterberg cell, as well as pile driving equipment, pile accessories, and pile installation inspection. Step by step procedures, workshop problems and solutions are provided to demonstrate use of the manual material.					
17. Key Words pile foundations, foundation design, static analysis, foundation construction, inspection			18. Distribution Statement No restrictions. This document is available to the public from the National Technical Information Service, Springfield, Virginia 22161		
19. Security Classif. (of this report) Unclassified		20. Security Classif. (of this page) Unclassified		21. No. of Pages 448	22. Price

U.S. - SI Conversion Factors

From English	To SI	Multiply by	Quantity	From SI	To English	Multiply by
ft	m	0.3048	Length	m	ft	3.2808
inch	mm	25.40		mm	inch	0.039
ft ²	m ²	0.0929	Area	m ²	ft ²	10.764
inch ²	mm ²	645.2		mm ²	in ²	0.0015
ft ³	m ³	0.028	Volume	m ³	ft ³	35.714
inch ³	mm ³	16387		mm ³	inch ³	61x10 ⁻⁶
ft ⁴	m ⁴	0.0086	Second Moment of Area	m ⁴	ft ⁴	115.856
inch ⁴	mm ⁴	416231		mm ⁴	inch ⁴	2x10 ⁻⁶
lbm	kg	0.4536	Mass	kg	lbm	2.2046
lbm/ft ³	kg/m ³	16.02	Mass Density	kg/m ³	lbm/ft ³	0.062
lb	N	4.448	Force	N	lb	0.2248
kip	kN	4.448		kN	kip	0.2248
lbs/ft	N/m	14.59	Force/Unit- Length	N/m	lbs/ft	0.0685
kips/ft	kN/m	14.59		kN/m	kips/ft	0.0685
lbs/in ²	kPa	6.895	Force/Unit- Area; Stress; Pressure; Elastic Mod.	kPa	lbs/in ²	0.145
kips/in ²	MPa	6.895		MPa	kips/in ²	0.145
lbs/ft ²	Pa	47.88		Pa	lbs/ft ²	0.021
kips/ft ²	kPa	47.88		kPa	kips/ft ²	0.021

U.S. - SI Conversion Factors (continued)

From	To	Multiply by	Quantity	From	To	Multiply by
English	SI			SI	English	
lbs/ft ³	N/m ³	157.1	Force/Unit- Volume	N/m ³	lbs/ft ³	0.0064
kips/ft ³	kN/m ³	157.1		kN/m ³	kips/ft ³	0.0064
lb-inch	N-mm	112.98	Moment; or Energy	N-mm	lb-inch	0.0089
kip-inch	kN-mm	112.98		kN-mm	kip-inch	0.0089
lb-ft	N-m	1.356		N-m	lb-ft	0.7375
kip-ft	kN-m	1.356		kN-m	kip-ft	0.7375
ft-lb	Joule	1.356		Joule	ft-lb	0.7375
ft-kip	kJoule	1.356		kJoule	ft-kip	0.7375
s/ft	s/m	3.2808	Damping	s/m	s/ft	0.3048
blows/ft	blows/m	3.2808	Blow count	blows/m	blows/ft	0.3048

PREFACE

Engineers and contractors have been designing and installing pile foundations for many years. During the past three decades this industry has experienced several major improvements including newer and more accurate methods of predicting capacities, highly specialized and sophisticated equipment for pile driving, and improved methods of construction control.

In order to take advantage of these new developments, the FHWA developed a manual in connection with Demonstration Project No. 66, Design and Construction of Driven Pile Foundations. The primary purpose of the Manual was to support educational programs conducted by FHWA for transportation agencies. These programs consisted of (1) a workshop for geotechnical, structural, and construction engineers, and (2) field demonstrations of static and dynamic load testing equipment. Technical assistance on construction projects in areas covered by this Demonstration Project was provided to transportation agencies on request. A second purpose of equal importance was to serve as the FHWA's standard reference for highway projects involving driven pile foundations.

The original Manual was written by Suneel N. Vanikar with review and comment from Messrs. Ronald Chassie, Jerry DiMaggio, and Richard Cheney.

After a decade of use it was necessary that the Manual be updated and modified to include new developments that had taken place in the intervening years and to take advantage of the experience gained in using the Manual in the many workshops that were presented by Demonstration Project 66. The new version of the Manual was prepared by Goble Rausche Likins and Associates, Inc. under contract with the FHWA.

The Manual is presented in two volumes. Volume I addresses design aspects and Volume II presents topics related to driven pile installation, monitoring, and inspection.

The new Manual is intended to serve a dual purpose. First, as a workshop participant's manual for the FHWA's National Highway Institute Courses on Driven Pile Foundations. Similar to the earlier demonstration manual, this document is also intended to serve as FHWA's primary reference of recommended practice for driven pile foundations.

Upon completion of NHI Course 13221, participants will be able to:

1. Describe methods of pile foundation design.
2. Discuss driven pile construction materials and installation equipment.
3. Describe the timing and scope of the involvement of foundation specialists as a project evolves from concept through completion.
4. Perform a foundation economic analysis and determine the need for a driven pile foundation.
5. Recognize the pile type selection process and the advantages and disadvantages of common driven pile types.
6. Compute single and group capacities of driven piles to resist compression, tension and lateral loads.
7. Identify when and how dynamic formulas, wave equation analyses, dynamic pile testing and static load testing should be used on a project.
8. Discuss the components of structural foundation reports and controlling issues of specifications and contracting documents as related to a successful construction project.
9. Describe the concept and project influence of driveability, pile refusal, minimum and estimated pile toe elevations, soil setup and relaxation.

Upon completion of NHI Course 13222, participants will be able to:

1. Describe methods of driven pile construction monitoring and inspection practices and procedures.
2. Discuss pertinent driven pile specification and contract document issues.

3. Describe wave equation, dynamic testing and static testing results in terms of their application and interpretation on construction projects.
4. Identify the basic components and differences between various pile driving systems, associated installation equipment, pile splices and pile toe attachments.
5. Interpret a set of driven pile plan details and specifications.
6. Inspect a drive pile project with knowledge and confidence.

The authors' recognize the efforts of the project technical manager, Mr. Jerry DiMaggio, FHWA Senior Geotechnical Engineer, who provided invaluable guidance and input for the new manual.

The authors' also acknowledge the additional contributions of the following technical review panel members listed in alphabetical order:

Mr. Chien-Tan Chang - FHWA
Mr. Richard Cheney - FHWA
Mr. Tom Cleary - New Hampshire DOT
Mr. Kerry Cook - FHWA
Mr. Chris Dumas - FHWA
Mr. Carl Ealy - FHWA
Mr. Sam Holder - FHWA
Mr. Paul Macklin - Colorado DOT
Mr. Paul Passe - Florida DOT
Mr. Jan Six - Oregon DOT
Mr. Suneel Vanikar - FHWA

The authors' also wish to acknowledge the following individuals of the author's internal peer review team for their technical advice and contributions in preparing the new manual.

Dr. Joseph Caliendo - Utah State University
Dr. D. Michael Holloway - InSituTech
Mr. Robert Lukas - Ground Engineering Consultants

Lastly, the authors' wish to thank the following Goble Rausche Likins and Associates, Inc. employees for their vital contributions and significant effort in preparing this manual: Ms. Barbara Strader, Ms. Beth Richardson, Mr. Scott Webster, Mr. Neil Harnar, Mr. Jay Berger and Mr. Joe Beno.

Design and Construction of Driven Pile Foundations- Volume II

Table of Contents		Page
15.	INTRODUCTION TO CONSTRUCTION MONITORING	15-1
15.1	The Role of Construction Monitoring	15-1
15.2	Selection of Factor of Safety	15-3
15.3	Communication	15-4
	References	15-5
16.	DYNAMIC FORMULAS FOR STATIC CAPACITY DETERMINATION	16-1
16.1	Accuracy of Dynamic Formulas	16-1
16.2	Problems with Dynamic Formulas	16-5
16.3	Dynamic Formulas	16-6
16.4	Alternatives to Use of Dynamic Formulas	16-7
16.5	Dynamic Formula Case Histories	16-8
16.5.1	Case History 1	16-8
16.5.2	Case History 2	16-9
16.5.3	Case History 3	16-9
	References	16-11
	Student Exercise #9 - Gates Formula Ultimate Capacity	16-13
	Student Exercise #10 - Gates Formula Driving Criterion	16-15
17	DYNAMIC ANALYSIS BY WAVE EQUATION	17-1
17.1	Introduction	17-1
17.2	Wave Propagation	17-2
17.3	Wave Equation Methodology	17-2
17.4	Wave Equation Applications	17-6
17.5	Wave Equation Examples	17-9
17.5.1	Example 1 - General Bearing Graph	17-9
17.5.2	Example 2 - Constant Capacity / Variable Stroke Option	17-12
17.5.3	Example 3 - Tension and Compression Stress Control	17-14
17.5.4	Example 4 - Use of Soil Setup	17-17
17.5.5	Example 5 - Driveability Studies	17-19
17.5.6	Example 6 - Driving System Characteristics	17-24
17.5.7	Example 7 - Assessment of Pile Damage	17-26
17.5.8	Example 8 - Selection of Wall Thickness	17-29

Table of Contents (continued)

		Page
	17.5.9 Example 9 - Evaluation of Vibratory Driving	17-32
17.6	Analysis Decisions for Wave Equation Problems	17-36
	17.6.1 Selecting the Proper Approach	17-36
	17.6.2 Hammer Data Input, External Combustion Hammers . .	17-37
	17.6.3 Hammer Data Input, Diesel Hammers	17-38
	17.6.4 Cushion Input	17-39
	17.6.5 Soil Parameter Selection	17-40
	17.6.6 Comparison With Dynamic Measurements	17-42
17.7	Wave Equation Input Parameters	17-43
	17.7.1 GRLWEAP Input - Page 1	17-45
	17.7.1.1 Hammer Input and Analysis Options	17-45
	17.7.1.2 Pile Input and Analysis Options	17-46
	17.7.1.3 Shaft Resistance Input and Driveability Analysis Options	17-47
	17.7.1.4 Helmet and Hammer Cushion Information . .	17-47
	17.7.2 GRLWEAP Input - Page 2	17-48
	17.7.2.1 Pile Cushion Information	17-48
	17.7.2.2 Pile Information	17-48
	17.7.2.3 Hammer Override Values	17-49
	17.7.2.4 Soil Parameters	17-50
	17.7.3 GRLWEAP Input - Page 3	17-51
	17.7.3.1 Ultimate Capacities	17-51
17.8	GRLWEAP Output	17-52
17.9	Plotting of GRLWEAP Results	17-55
17.10	Suggestions for Problem Solving	17-56
	References	17-61
	Student Exercise #11 - Wave Equation Hammer Approval	17-63
	Student Exercise #12 - Wave Equation Inspectors Chart	17-67
18.	DYNAMIC PILE TESTING AND ANALYSIS	18-1
	18.1 Background	18-1
	18.2 Applications for Dynamic Testing Methods	18-2
	18.2.1 Static Pile Capacity	18-2
	18.2.2 Hammer and Driving System Performance	18-3
	18.2.3 Driving Stresses and Pile Integrity	18-3
	18.3 Dynamic Testing Equipment	18-4
	18.4 Basic Wave Mechanics	18-7
	18.5 Dynamic Testing Methodology	18-15

Table of Contents (continued)

Page

18.5.1	Case Method Capacity	18-15
18.5.2	Energy Transfer	18-19
18.5.3	Driving Stresses and Integrity	18-19
18.5.4	The CAPWAP Method (<u>C</u> Ase <u>P</u> ile <u>W</u> ave <u>A</u> nalysis <u>P</u> rogram)	18-21
18.6	Usage of Dynamic Testing Methods	18-27
18.7	Presentation and Interpretation of Dynamic Testing Results . . .	18-28
18.8	Advantages	18-38
18.9	Disadvantages	18-39
18.10	Case History	18-39
18.11	Low Strain Integrity Testing Methods	18-41
18.11.1	Pulse Echo Method	18-42
18.11.2	Transient Response Method (TRM)	18-44
18.11.3	Low Strain Applications to Unknown Foundations	18-45
18.11.4	Limitations and Conclusions of Low Strain Methods . . .	18-45
References	18-47
19.	STATIC PILE LOAD TESTING	19-1
19.1	Reasons for Load Testing	19-1
19.2	Prerequisites for Load Testing	19-1
19.3	Developing a Load Test Program	19-2
19.4	Advantages of Static Load Testing	19-3
19.5	When to Load Test	19-4
19.6	Effective Use of Load Tests	19-5
19.6.1	Design Stage	19-5
19.6.2	Construction Stage	19-6
19.7	Compression Load Tests	19-6
19.7.1	Compression Test Equipment	19-8
19.7.2	Recommended Compression Test Loading Method . . .	19-10
19.7.3	Presentation and Interpretation of Compression Test Results	19-11
19.7.4	Plotting the Load-Movement Curve	19-13
19.7.5	Determination of the Ultimate Load	19-13
19.7.6	Determination of the Allowable Load	19-14
19.7.7	Load Transfer Evaluations	19-14
19.7.8	Limitations of Compression Load Tests	19-16
19.8	Tensile Load Tests	19-17
19.8.1	Tension Test Equipment	19-17

Table of Contents (continued)

Page

	19.8.2 Tension Test Loading Methods	19-18
	19.8.3 Presentation and Interpretation of Tension Test Results	19-19
19.9	Lateral Load Tests	19-20
	19.9.1 Lateral Load Test Equipment	19-20
	19.9.2 Lateral Test Loading Methods	19-21
	19.9.3 Presentation and Interpretation of Lateral Test Results	19-22
	References	19-24
	Student Exercise #13 - Determination of Load Test Failure Load	19-27
20.	THE OSTERBERG CELL METHOD	20-1
	20.1 Osterberg Cell Background	20-1
	20.2 Test Equipment	20-3
	20.3 Interpretation of Test Results	20-7
	20.4 Applications	20-9
	20.5 Advantages	20-10
	20.6 Disadvantages	20-11
	20.7 Case Histories	20-11
	References	20-17
21.	THE STATNAMIC METHOD	21-1
	21.1 Statnamic Background	21-1
	21.2 Test Equipment	21-2
	21.3 Test Interpretation	21-6
	21.4 Applications	21-9
	21.5 Case Histories	21-10
	21.6 Advantages	21-13
	21.7 Disadvantages	21-13
	References	21-16
22.	PILE DRIVING EQUIPMENT	22-1
	22.1 Leads	22-1
	22.2 Templates	22-8
	22.3 Helmets	22-8
	22.4 Pile Cushions	22-12
	22.5 Hammers	22-13
	22.5.1 Hammer Energy Concepts	22-13

Table of Contents (continued)

Page

22.6	Drop Hammers	22-17
22.7	Single Acting Air/Steam Hammers	22-18
22.8	Double Acting Air/Steam Hammers	22-21
22.9	Differential Acting Air/Steam Hammers	22-23
22.10	Single Acting (Open End) Diesel Hammer	22-25
22.11	Double Acting (Closed End) Diesel Hammer	22-27
22.12	Hydraulic Hammers	22-30
22.13	Vibratory Hammers	22-33
22.14	Hammer Size Selection	22-35
22.15	Followers	22-35
22.16	Jetting	22-37
22.17	Predrilling	22-38
22.18	Spudding	22-39
22.19	Representative List of U.S.A. Hammer Manufacturers and Suppliers	22-40
	References	22-45
	Student Exercise #14 - Equipment Submittal Review	22-47
23.	ACCESSORIES FOR PILE INSTALLATION	23-1
23.1	Timber Piles	23-1
	23.1.1 Pile Toe Attachments	23-1
	23.1.2 Attachment at Pile Head	23-3
	23.1.3 Splices	23-3
23.2	Steel H-Piles	23-5
	23.2.1 Pile Toe Attachments	23-5
	23.2.2 Splices	23-7
23.3	Accessories for Steel Pipe Piles	23-7
	23.3.1 Pile Toe Attachments	23-7
	23.3.2 Splices	23-10
23.4	Precast Concrete Piles	23-10
	23.4.1 Pile Toe Attachments	23-10
	23.4.2 Splices	23-13
23.5	A List of Manufacturers and Suppliers of Pile Accessories	23-17
	References	23-19
24.	INSPECTION OF PILE INSTALLATION	24-1
24.1	Items to be Inspected	24-2
24.2	Review of Project Plans and Specifications	24-2

Table of Contents (continued)		Page
24.3	Inspector's Tools	24-4
24.4	Inspection of Piles Prior To and During Installation	24-4
24.4.1	Timber Piles	24-5
24.4.2	Precast Concrete Piles	24-5
24.4.3	Steel H-Piles	24-7
24.4.4	Steel Pipe Piles	24-8
24.5	Inspection of Driving Equipment	24-8
24.6	Inspection of Driving Equipment During Installation	24-12
24.6.1	Drop Hammers	24-13
24.6.2	Single Acting Air/Steam Hammers	24-14
24.6.3	Double Acting or Differential Air/Steam Hammers	24-17
24.6.4	Single Acting Diesel Hammers	24-20
24.6.5	Double Acting Diesel Hammers	24-27
24.6.6	Hydraulic Hammers	24-30
24.6.7	Vibratory Hammers	24-36
24.7	Inspection of Test or Indicator Piles	24-36
24.8	Inspection of Production Piles	24-39
24.9	Driving Records and Reports	24-48
	References	24-52
	Student Exercise #15 - Hammer Inspection	24-53
	Student Exercise #16 - Determining Pile Toe Elevations	24-59

List of Appendices

APPENDIX A	List of FHWA Pile Foundation Design and Construction References	A-1
APPENDIX B	List of ASTM Pile Design and Testing Specifications	B-1
APPENDIX C	Information and Data on Various Pile Types	C-1
APPENDIX D	Pile Hammer Information	D-1
APPENDIX E	Student Exercise - Solutions	E-1

List of Tables

Page

Table 15-1	Responsibilities of Design and Construction Engineers . . .	15-2
Table 16-1	Mean Values and Coefficients of Variation for Various Methods	16-3
Table 17-1	Suggested Use of the Wave Equation to Solve Field Problems	17-56
Table 17-2	Wave Equation Analysis Problems	17-59
Table 18-1	Summary of Case Damping Factors for RSP Equation . . .	18-17
Table 18-2	Pile Damage Guidelines (Rausche and Goble, 1979)	18-21
Table 18-3	Typical Tabular Presentation of Dynamic Testing Results versus Depth	18-36
Table 22-1	Typical Pile Hammer Characteristics and Uses	22-15
Table 22-2	Approximate Minimum Hammer Energy Requirements . . .	22-35
Table 23-1	Summary of Precast Concrete Pile Splices	23-14
Table 24-1	Common Problems and Problem Indicators for Air/Steam Hammer (from Williams Earth Sciences, 1995)	24-16
Table 24-2	Common Problems and Problem Indicators for Single Acting Diesel Hammers (from Williams Earth Sciences, 1995)	24-25
Table 24-3	Common Problems and Problem Indicators for Double Acting Diesel Hammer (from Williams Earth Sciences, 1995)	24-30
Table 24-4	Common Problems and Problem Indicators for Hydraulic Hammers (from Williams Earth Sciences, 1995)	24-34
Table 24-5	Common Pile Installation Problems & Possible Solutions	24-44

	List of Figures	Page
Figure 16.1	Log Normal Probability Density Function for four Capacity Prediction Methods (after Rausche <i>et al.</i> 1996)	16-3
Figure 17.1	Wave Propagation in a Pile (adapted from Cheney and Chassie, 1993)	17-3
Figure 17.2	Typical Wave Equation Model	17-5
Figure 17.3	Example 1 Problem Profile	17-10
Figure 17.4	Example 1 Typical Bearing Graph	17-11
Figure 17.5	Example 2 Constant Capacity Analysis	17-13
Figure 17.6	Example 3 Problem Profile	17-14
Figure 17.7	Example 3 Bearing Graph Comparison of Two Pile Cushion Thickness	17-16
Figure 17.8	Example 3 Bearing Graph for End of Driving Condition . . .	17-17
Figure 17.9	Example 4 Problem Profile	17-18
Figure 17.10	Example 4 Using of Bearing Graph with Soil Setup	17-19
Figure 17.11	Example 5 Problem Profile	17-20
Figure 17.12	Example 5 Driveability Results for First 356 mm Concrete Pile	17-22
Figure 17.13	Example 5 Driveability Results for Later 356 mm Concrete Piles with Densification	17-23
Figure 17.14	Example 5 Driveability Results for H-Pile	17-23
Figure 17.15	Example 6 Problem Profile	17-25
Figure 17.16	Example 6 Bearing Graph Comparison of Two Hammers with Equivalent Potential Energy	17-25
Figure 17.17	Example 7 Problem Profile	17-27
Figure 17.18	Example 7 Wave Equation Bearing Graph for Proposed Driving System	17-27
Figure 17.19	Example 7 Comparison of Wave Equation Bearing Graphs for Damaged and Undamaged Piles	17-29
Figure 17.20	Example 8 Problem Profile	17-30
Figure 17.21	Example Bearing Graphs for 6.3 and 7.1 mm Wall Pipe Piles	17-31
Figure 17.22	Example 8 Bearing Graph for 7.9 and 9.5 mm Wall Pipe Piles	17-31
Figure 17.23(a)	Example 9 Soil Resistance Information for Vibratory Sheet Pile Driving	17-33
Figure 17.23(b)	Example 9 Vibratory Hammer Model and Hammer Options	17-34
Figure 17.23(c)	Example 9 Pile and Soil Model and Options	17-35

List of Figures (continued)		Page
Figure 17.23(d)	Example 9 Final Summary Table	17-35
Figure 17.24	Pile and Driving Equipment Data Form	17-44
Figure 17.25	Input Page 1: Title, Options, Hammer Cushion	17-45
Figure 17.26	Input Page 2: Pile Cushion, Pile, Hammer Modifications, Soil	17-48
Figure 17.27	Input Page 3: Ultimate Capacities	17-51
Figure 17.28	Hammer Model, Driving System and Hammer Option Output	17-52
Figure 17.29	Pile, Soil Model and Analysis Options	17-53
Figure 17.30	Extrema Table Output	17-54
Figure 17.31	GRLWEAP Final Summary for Bearing Graph Analyses . . .	17-55
Figure 18.1	Pile Preparation for Dynamic Testing	18-5
Figure 18.2	Pile Positioned for Driving and Gage Attachment	18-5
Figure 18.3	Strain Transducer and Accelerometer Bolted to Pipe Pile . .	18-6
Figure 18.4	Pile Driving Analyzer (courtesy of Pile Dynamics, Inc.)	18-6
Figure 18.5	Free End Wave Mechanics	18-8
Figure 18.6	Force and Velocity Measurements versus Time for Free End Condition	18-9
Figure 18.7	Fixed End Wave Mechanics	18-10
Figure 18.8	Force and Velocity Measurements versus Time for Fixed End Condition	18-11
Figure 18.9	Soil Resistance Effects on Force and Velocity Records (after Hannigan, 1990)	18-13
Figure 18.10	Typical Force and Velocity Records for Various Soil Resistance Conditions (after Hannigan, 1990)	18-14
Figure 18.11	Standard, RSP and Maximum, RMX, Case Method Capacity Estimates	18-18
Figure 18.12	Energy Transfer Computation (after Hannigan, 1990)	18-20
Figure 18.13	Schematic of CAPWAP Analysis Method	18-22
Figure 18.14	Factors Most Influencing CAPWAP Force Wave Matching (after Hannigan, 1990)	18-23
Figure 18.15	CAPWAP Iteration Matching Process (after Hannigan, 1990)	18-25
Figure 18.16	CAPWAP Final Results Table	18-26
Figure 18.17	CAPWAP Stress Distribution Profile	18-26
Figure 18.18	Typical Dynamic Test System Screen Display	18-29
Figure 18.19	Transfer Efficiencies for Select Hammer and Pile Combinations	18-31

List of Figures (continued)		Page
Figure 18.20(a)	Histograms of Transfer Efficiency for Diesel Hammers	18-32
Figure 18.20(b)	Histograms of Transfer Efficiency for Single Acting Air/Steam Hammers	18-33
Figure 18.21	Force and Velocity Record for Damaged Pile	18-35
Figure 18.22	Force and Velocity Record for H-pile to Rock	18-35
Figure 18.23	Typical Graphical Presentation of Dynamic Testing Results versus Depth	18-37
Figure 18.24	Pulse Echo Velocity versus Time Record for Undamaged Pile	18-43
Figure 18.25	Pulse Echo Velocity versus Time Record for Damaged Pile	18-43
Figure 18.26	Typical Response Curve from a TRM Test	18-44
Figure 19.1	Basic Mechanism of a Pile Load Test	19-7
Figure 19.2	Typical Arrangement for Applying Load in an Axial Compressive Test (Kyfor <i>et al.</i> 1992)	19-9
Figure 19.3	Typical Compression Load Test Arrangement with Reaction Piles	19-10
Figure 19.4	Typical Compression Load Test Arrangement using a Weighted Platform	19-11
Figure 19.5	Presentation of Typical Static Pile Load-Movement Results	19-12
Figure 19.6	Example of Residual Load Effects on Load Transfer Evaluation	19-16
Figure 19.7	Tension Load Test Arrangement on Batter Pile (courtesy of Florida DOT)	19-18
Figure 19.8	Typical Tension Load Test Load-Movement Curve	19-19
Figure 19.9	Typical Lateral Load Test Arrangement (courtesy of Florida DOT)	19-21
Figure 19.10	Typical Lateral Load Test Pile Head Load-Deflection Curve	19-22
Figure 19.11	Comparison of Measured and COM624P Predicted Load- Deflection Behavior versus Depth (after Kyfor <i>et al.</i> 1992)	19-23
Figure 20.1	Schematic Comparison Between Osterberg Cell and Conventional Tests	20-2
Figure 20.2	Osterberg Cell and Related Equipment Used for Static Pile Tests	20-4
Figure 20.3	Osterberg Cell Ready for Placement in Concrete Pile Form (courtesy of Loadtest, Inc.)	20-5

	List of Figures (continued)	Page
Figure 20.4	Osterberg Test in Progress on a 457 mm Concrete Pile (courtesy of Loadtest, Inc.)	20-6
Figure 20.5	Summary of Subsurface Profile and Test Results at Pines River Bridge, MA	20-13
Figure 20.6	Test Results from Pines River Bridge, MA	20-14
Figure 20.7	Equivalent Pile Head Load-Movement Curve from Pines River Bridge, MA	20-14
Figure 20.8	Summary of Subsurface Profile and Test Results at Aucilla River Bridge, FL	20-15
Figure 20.9	Test Results from Aucilla River Bridge, FL	20-16
Figure 20.10	Equivalent Pile Head Load-Movement Curve from Aucilla River Bridge, FL	20-16
Figure 21.1	Statnamic Concept (courtesy of Berminghammer Foundation Equipment)	21-2
Figure 21.2	Schematic of Statnamic Loading System (after Birmingham and Janes, 1989)	21-3
Figure 21.3	Statnamic Test in Progress	21-4
Figure 21.4	Measured Statnamic Signals (courtesy of Berminghammer Foundation Equipment)	21-5
Figure 21.5	Load versus Displacement (courtesy of Berminghammer Foundation Equipment)	21-5
Figure 21.6	Free Body Diagram of Pile Forces in a Statnamic Test (after Middendorp <i>et al.</i> 1992)	21-7
Figure 21.7	Five Stages of a Statnamic Test (after Middendorp <i>et al.</i> 1992)	21-7
Figure 21.8	Derived Statnamic Load-Displacement Curve With Rate Effects (courtesy of Berminghammer Foundation Equipment)	21-10
Figure 21.9	Lateral Statnamic Test on Nine Group (courtesy of Utah State University)	21-11
Figure 21.10	Static Load Test and Statnamic Comparison from Pittsburgh Site (courtesy of Berminghammer Foundation Equipment)	21-12
Figure 21.11	Static Load Test and Statnamic Comparison from San Francisco Site (courtesy of Berminghammer Foundation Equipment)	21-12
Figure 21.12	Statnamic Hydraulic Catch Mechanism (courtesy of Berminghammer Foundation Equipment)	21-14

List of Figures (continued)		Page
Figure 22.1	Swinging Lead Systems (after D.F.I. Publication, 1981)	22-2
Figure 22.2	Fixed Lead Systems (after D.F.I. Publication, 1981)	22-3
Figure 22.3	Lead Configurations for Batter Piles (after D.F.I. Publication, 1981)	22-4
Figure 22.4	Typical Offshore Lead Configuration	22-5
Figure 22.5	Typical Lead Types (after D.F.I. Publication, 1981)	22-6
Figure 22.6	Typical Template Arrangement	22-9
Figure 22.7	Template Elevation Effects on Batter Piles (after Passe 1994)	22-9
Figure 22.8	Helmet Components (after D.F.I. Publication, 1981)	22-10
Figure 22.9	Helmet on H-pile	22-11
Figure 22.10	Plywood Pile Cushion	22-12
Figure 22.11	Pile Hammer Classification	22-14
Figure 22.12	Typical Drop Hammer	22-18
Figure 22.13	Schematic of Single Acting Air/Steam Hammer	22-19
Figure 22.14	Single Acting Air Hammer	22-20
Figure 22.15	Double Acting Air Hammer	22-20
Figure 22.16	Schematic of Double Acting Air/Steam Hammer	22-22
Figure 22.17	Schematic of Differential Air/Steam Hammer	22-24
Figure 22.18	Schematic of Single Acting Diesel Hammer	22-26
Figure 22.19	Single Acting Diesel Hammer (courtesy of Pileco)	22-28
Figure 22.20	Double Acting Diesel Hammer	22-28
Figure 22.21	Schematic of Double Acting Diesel Hammer	22-29
Figure 22.22	Schematics of Single and Double Acting Hydraulic Hammers	22-31
Figure 22.23	Single Acting Hydraulic Hammer	22-32
Figure 22.24	Double Acting Hydraulic Hammer	22-32
Figure 22.25	Vibratory Hammer	22-34
Figure 22.26	Follower used for Driving H-piles	22-36
Figure 22.27	Dual Jet System Mounted on a Concrete Pile (courtesy of Florida DOT)	22-37
Figure 22.28	Jet/Punch System (courtesy of Florida DOT)	22-38
Figure 22.29	Solid Flight Auger Predrilling System (courtesy of Florida DOT)	22-39
Figure 23.1	Timber Pile Toe Attachments	23-2
Figure 23.2	Banded Timber Pile Head	23-3
Figure 23.3	Splices for Timber Piles	23-4
Figure 23.4	Damaged H-piles without Pile Toe Protection	23-6

List of Figures (continued)

Page

Figure 23.5	Driving Shoes for Protection of H-pile Toes	23-6
Figure 23.6	Typical H-pile Splicer	23-8
Figure 23.7	Pile Toe Attachments For Pipe Piles	23-9
Figure 23.8	Splices For Pipe Piles	23-11
Figure 23.9	Splicer for Pipe Pile	23-11
Figure 23.10	Pile Toe Attachments for Precast Concrete Piles	23-12
Figure 23.11	Steel H-pile Tip for Precast Concrete Pile	23-12
Figure 23.12	Commonly used Prestressed Concrete Pile Splices (after PCI, 1993)	23-15
Figure 23.13	Cement-Dowel Splice (after Bruce and Herbert, 1974)	23-16
Figure 24.1	Pile Inspection Flow Chart	24-3
Figure 24.2	Hammer Cushion Check	24-10
Figure 24.3	Damaged Hammer Cushion	24-10
Figure 24.4	Pile Cushion Replacement	24-10
Figure 24.5	Air Compressor Display Panel	24-15
Figure 24.6	Inspection Form for Single Acting Air/Steam Hammers	24-18
Figure 24.7	Inspection Form for Enclosed Double Acting Air/Steam Hammers	24-21
Figure 24.8	Fixed Four Step Fuel Pump on Delmag Hammer	24-23
Figure 24.9	Variable Fuel Pump on FEC Hammer	24-23
Figure 24.10	Adjustable Pressure Pump for Fuel Setting on ICE Hammer	24-23
Figure 24.11	Inspection Form for Single Acting Diesel Hammers	24-26
Figure 24.12	Typical External Bounce Chamber Pressure Gauge	24-28
Figure 24.13	Inspection Form for Double Acting Diesel Hammers	24-31
Figure 24.14	IHC Hydraulic Hammer Readout Panel (courtesy of L.B. Foster Co.)	24-33
Figure 24.15	Inspection Form for Hydraulic Hammers	24-35
Figure 24.16	Driving Sequence of Displacement Pile Groups (after Passe, 1994)	24-42
Figure 24.17	Pile Driving Log	24-49
Figure 24.18	Daily Inspection Report	24-51

LIST OF SYMBOLS

A	-	Pile cross sectional area.
A_g	-	Pile area at gage location.
A_{np}	-	Net area of piston.
a	-	Acceleration.
a_m	-	Measured acceleration.
b	-	Pile diameter.
C	-	Wave speed of pile material.
C_4	-	Statnamic damping constant.
E	-	Modulus of elasticity of pile material.
E_p	-	Energy transferred to pile.
E_d	-	Dynamic stiffness.
E_r	-	Manufacturers rated hammer energy.
F	-	Force.
F_a	-	Statnamic inertia force.
F_p	-	Statnamic pore water pressure force.
F_u	-	Statnamic static soil resistance force.
F_v	-	Statnamic dynamic soil resistance force.
F_{stn}	-	Statnamic induced force.
$F(t)$	-	Force measured at gage location.

LIST OF SYMBOLS (continued)

- Δf - Dominant frequency.
- h - Hammer stroke.
- J - Soil damping factor.
- J_c - Dimensionless Case damping factor.
- L - Total pile length.
- ΔL - Length of pile between two measuring points under no load conditions.
- L_g - Pile length below gage location.
- m - Mass.
- N_b - The number of hammer blows per 25 mm.
- p_h - Pressure at hammer.
- Q - Load.
- Q_a - Allowable design load of a pile.
- Q_{avg} - Average load in the pile.
- Q_f - Failure load.
- Q_h - Applied pile head load.
- Q_o - Osterberg cell load.
- Q_r - Load from reaction system.
- Q_u - Ultimate bearing capacity of a pile.
- q - Soil quake.

LIST OF SYMBOLS (continued)

R	-	Soil resistance.
R_1	-	Deflection reading at upper of two measuring points.
R_2	-	Deflection reading at lower of two measuring points.
R_s	-	Ultimate pile shaft resistance.
R_t	-	Ultimate pile toe resistance.
R_u	-	Ultimate soil resistance.
s_b	-	Set per blow.
s_f	-	Settlement at failure.
t_1	-	Time of initial impact.
t_2	-	Time of reflection of initial impact from pile toe ($t_1 + 2L/c$).
t_4	-	Time at Statnamic stage 4.
t_{umax}	-	Time of maximum displacement.
U	-	Displacement.
$V(t)$	-	Velocity measured at gage location.
v_i	-	Impact velocity.
W	-	Ram weight.
Δ	-	Elastic compression.
ϵ	-	Strain.
ϕ	-	Angle of internal friction of soil.

15. INTRODUCTION TO CONSTRUCTION MONITORING

Volume II of the Manual on Design and Construction of Driven Pile Foundations focuses on the construction aspects of driven pile foundations. Following this introductory chapter are chapters on pile capacity evaluation using dynamic formulas (Chapter 16), wave equation analysis (Chapter 17), dynamic testing and analysis (Chapter 18), static load testing (Chapter 19), the Osterberg load cell device (Chapter 20) and the Statnamic method (Chapter 21). These chapters on pile testing methods are followed by chapters detailing pile driving equipment (Chapter 22), driven pile accessories (Chapter 23), and pile inspection (Chapter 24).

15.1 THE ROLE OF CONSTRUCTION MONITORING

Proper pile installation is as important as rational pile design in order to obtain a cost effective and safe end product. Driven piles must develop the required capacity without sustaining structural damage during installation. Construction control of driven piles is much more difficult than for spread footings where the footing excavation and footing construction can be visually observed to assure quality. Since piles cannot be seen after their installation, direct quality control of the finished product is impossible. Therefore substantial control must be exercised over peripheral operations leading to the piles' placement within the foundation.

It is essential that any pile installation limitations be considered during the project design stage so that the piles shown on the plans can be installed as designed. For example, consideration should be given to how new construction may affect existing structures and how limitations on construction equipment access, size, or operation area may dictate the pile type that can be most cost effectively installed.

Construction monitoring should be exercised in three areas: pile materials, installation equipment, and the estimation of static load capacity. These areas are interrelated since changes in one affects the others. Table 15-1 highlights the items to be included in the plans and specifications that are the design engineer's responsibility, and the items to be checked for quality assurance that are the construction engineer's responsibility.

TABLE 15-1 RESPONSIBILITIES OF DESIGN AND CONSTRUCTION ENGINEERS

Item	Design Engineer's Responsibilities	Construction Engineer's Responsibilities
Pile Details	Include in plans and specifications: <ol style="list-style-type: none"> a. Material and strength: concrete, steel, or timber. b. Cross section: diameter, tapered or straight, and wall thickness. c. Special coatings for corrosion or downdrag. d. Splices, toe protection, etc. e. Estimated pile length. f. Pile design load and ultimate capacity. g. Allowable driving stresses. 	Quality control testing or certification of materials.
Soils Data	Include in plans and specifications: <ol style="list-style-type: none"> a. Subsurface profile. b. Soil resistance to be overcome to reach estimated length. c. Minimum pile penetration requirements. d. Special notes: boulders, artesian pressure, buried obstructions, time delays for embankment fills, etc. 	Report major discrepancies in soil profile to the designer.
Installation	Include in plans and specifications: <ol style="list-style-type: none"> a. Method of hammer approval. b. Method of determining ultimate pile capacity. c. Compression, tension, and lateral load test requirements (as needed) including specification for tests and the method of interpretation of test results. d. Dynamic testing requirements (as needed). e. Special notes: spudding, predrilling, jetting, set-up period, etc. 	<ol style="list-style-type: none"> a. Confirm that the hammer and driving system components agree with the contractor's approved submittal. b. Confirm that the hammer is maintained in good working order and the hammer and pile cushions are replaced regularly. c. Determination of the final pile length from driving resistance, estimated lengths and subsurface conditions. d. Pile driving stress control. e. Conduct pile load tests. f. Documentation of field operations. g. Ensure quality control of pile splices, coatings, alignment and driving equipment.

15.2 SELECTION OF FACTOR OF SAFETY

In the design stage, a design load is selected for the pile section as a result of static analyses and consideration of the allowable stresses in the pile material. A factor of safety is applied to the design load depending upon the confidence in the static analysis method, the quality of the subsurface exploration program, and the construction control method specified. Static analyses yield the estimated pile length, based on the penetration depth in suitable soils required to develop the design load times the factor of safety. Soil resistance from unsuitable support layers, or layers subject to scour, are not included in determining the required pile penetration depth.

During construction, the ultimate pile capacity to be obtained is the sum of the design load, times a factor of safety, plus the soil resistance from unsuitable layers not counted on for long term support or subject to scour. The plans and specifications should state the ultimate pile capacity to be obtained in conjunction with the construction control method to be used for determination of the ultimate pile capacity.

The factor of safety used should be based on the quality of the subsurface exploration information and the construction control method used for capacity verification. There are several capacity verification methods that can be used for construction control which are described in subsequent chapters. The factor of safety applied to the design load should increase with the increasing unreliability of the method used for determining ultimate pile capacity during construction. The recommended factor of safety on the design load for various construction control methods from Cheney and Chassie (1993) and/or AASHTO (1992) are shown below.

<u>Construction Control Method</u>	<u>Recommended Factor of Safety</u>
Static Load Test	2.00
Dynamic Measurements and Analysis coupled with Wave Equation Analysis	2.25
Indicator Piles coupled with Wave Equation Analysis	2.50
Wave Equation Analysis	2.75
Gates Dynamic Formula	3.50
Engineering News Formula	Not a Recommended Method

For example, consider a pile with a design load of 700 kN. If no unsuitable soil layers exist, and a static load test will be performed for construction control, then an ultimate pile capacity of 1400 kN would be specified. For this same example, an ultimate pile capacity of 1925 kN would be required when construction control is by wave equation analysis.

If unsuitable or scour susceptible layers exist, the resistance from these layers should be added to the required ultimate pile capacity. For a pile with a design load of 700 kN in a soil profile with 250 kN of soil resistance from unsuitable soils, or soils subject to scour, an ultimate pile capacity of 1650 kN would be required for construction control with a static load test. For this case, an ultimate pile capacity of 2175 kN would be specified for construction control by wave equation analysis.

15.3 COMMUNICATION

Proper construction monitoring of pile driving requires good communication between design and construction engineers. Such communication cannot always follow traditional lines and still be effective. Information is needed in a short time to minimize expensive contractor down time or to prevent pile driving from continuing in an unacceptable fashion.

Good communication should begin with a pre-construction meeting of the foundation designer and the construction engineer on all projects with significant piling items. Prior to the meeting, the construction engineer should review the project foundation report and be fully aware of any construction concerns. At the meeting, the designer should briefly explain the design and point out uncertainties and potential problem areas. The primary objective of this meeting is to establish a direct line of communication.

During construction, the construction engineer should initiate communication with the designer if proposed pile installation methods or results differ from the plans and specifications. The designer should advise the construction engineer on the design aspects of the field problems. The construction engineer should provide feedback on construction monitoring data to the design engineer.

The ultimate decision making authority should follow along the traditional lines of communication established by the state transportation agency. However, informal interaction between design offices and the field should be encouraged and will simplify and expedite decisions.

REFERENCES

- American Association of State Highway and Transportation Officials [AASHTO], (1992). Standard Specifications for Highway Bridges. Fifteenth Edition, AASHTO Highway Subcommittee on Bridges and Structures, Washington, D.C., 686.
- Cheney, R.S. and Chassie, R.G. (1993). Soils and Foundations Workshop Manual. Second Edition, Publication No. FHWA-HI-88-009, U.S. Department of Transportation, Federal Highway Administration and the National Highway Institute, Washington, D.C., 395.

16. DYNAMIC FORMULAS FOR STATIC CAPACITY DETERMINATION

Ever since engineers began using piles to support structures, they have attempted to find rational methods for determining the pile's load carrying capacity. Methods for predicting capacities were proposed, using pile penetration observations obtained during driving. The only realistic measurement that could be obtained during driving was the pile set per blow. Thus energy concepts equating the kinetic energy of the hammer to the resistance on the pile as it penetrates the soil were developed to determine pile capacity. In equation form this can be expressed as:

$$Wh = Rs_b$$

Where: W = Ram weight.
h = Ram stroke.
R = Soil resistance.
s_b = Set per blow.

These types of expressions are known as dynamic formulas. Because of their simplicity, dynamic formulas have been widely used for many years. More comprehensive dynamic formulas include consideration of pile weight, energy losses in drive system components, and other factors. Whether simple or more comprehensive dynamic formulas are used, pile capacities determined from dynamic formulas have shown poor correlations and wide scatter when statistically compared with static load test result. Therefore, except where well supported empirical correlations under a given set of physical and geological conditions are available, dynamic formulas should not be used.

16.1 ACCURACY OF DYNAMIC FORMULAS

Wellington proposed the popular Engineering News formula in 1893. It was developed for evaluating the capacity of timber piles driven primarily with drop hammers in sands. Concrete and steel piles were unknown at that time as were many of the pile hammer types and sizes used today. Therefore, it should be of little surprise that the formula performs poorly in predicted capacities of modern pile foundations.

The inadequacies of dynamic formulas have been known for a long time. In 1941, an ASCE committee on pile foundations assembled the results of numerous pile load tests along with the predicted capacities from several dynamic formulas, including the Engineering News, Hiley, and Pacific Coast formulas. The mean failure load of the load test data base was 91 tons. After reviewing the data base, Peck (1942) proposed that a new and simple dynamic formula could be used that stated the capacity of every pile was 91 tons. Peck concluded that the use of this new formula would result in a prediction statistically closer to the actual pile capacity than that obtained by using any of the dynamic formulas contained in the 1941 study.

More recently, Chellis (1961) noted that the actual factor of safety obtained by using the Engineering News formula varied from as low as $\frac{1}{2}$ to as high as 16. Sowers (1979) reported that the safety factor from the Engineering News formula varied from as low as $\frac{2}{3}$ to as high as 20. Fragasny *et al.* (1988) in the Washington State DOT study entitled "Comparison of Methods for Estimating Pile Capacity" found that the Hiley, Gates, Janbu, and Pacific Coast Uniform Building code formulas all provide relatively more dependable results than the Engineering News formula. Unfortunately, many transportation departments continue to use the Engineering News formula, which also remains the dynamic formula contained in current AASHTO Standard Specifications for Highway Bridges (1994).

As part of a recent FHWA research project, Rausche *et al.* (1996) compiled a data base of static load test piles that included pile capacity predictions using the FHWA recommended static analysis methods, preconstruction and refined wave equations, as well as dynamic measurements coupled with CAPWAP analysis. The reliability of the various capacity prediction methods were then compared with the results of the static loading tests. The results of these comparisons are presented in Figure 16.1 in the form of probability density function curves versus the ratio of predicted load over the static load test result. The mean values and coefficients of variation for the methods studied are presented in Table 16-1.

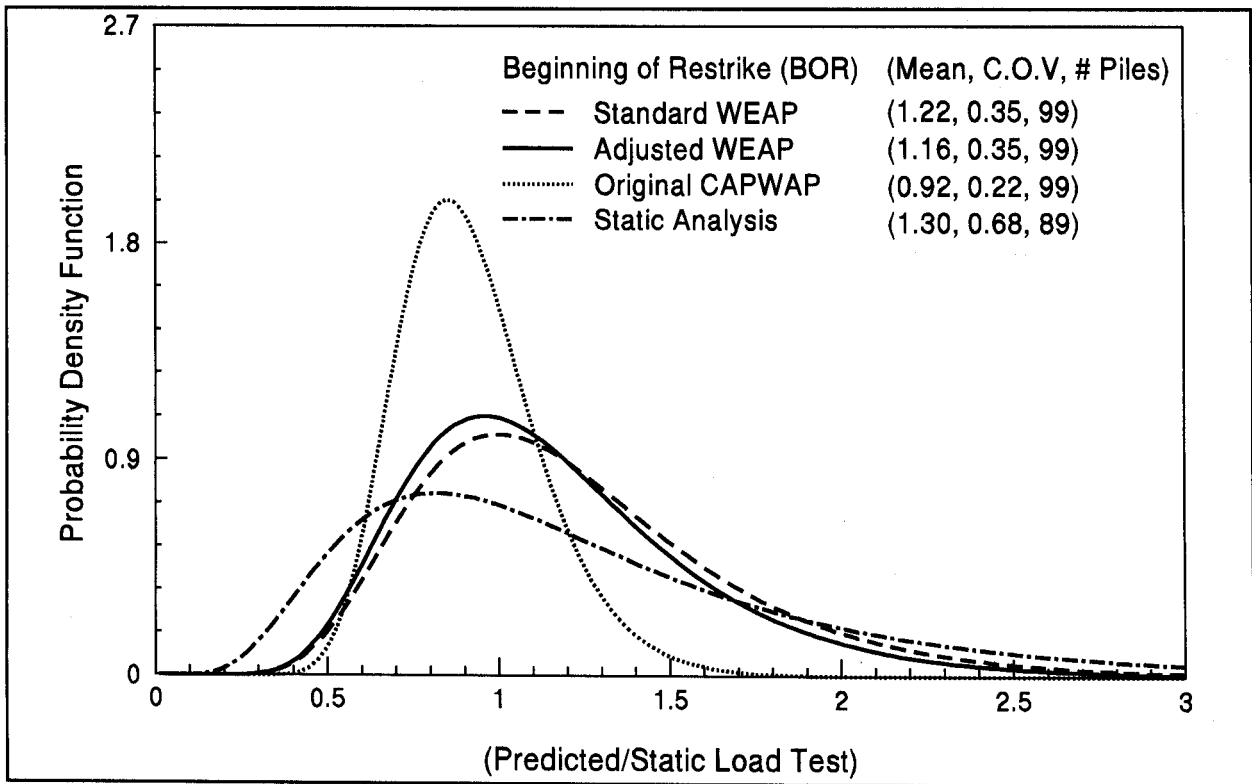


Figure 16.1 Log Normal Probability Density Function for four Capacity Prediction Methods (after Rausche *et al.* 1996)

TABLE 16-1 MEAN VALUES AND COEFFICIENTS OF VARIATION FOR VARIOUS METHODS				
Prediction Method	Status	Mean	C.O.V.	# Piles
Standard WEAP*	BOR	1.22	0.35	99
Hammer Performance Adjusted WEAP*	BOR	1.16	0.35	99
CAPWAP*	BOR	0.92	0.22	99
Static Analysis*	-	1.30	0.68	89
Engineering News Formula	EOD	1.22	0.74	139
Engineering News Formula	BOR	1.89	0.46	122
Gates Formula	EOD	0.96	0.41	139
Gates Formula	BOR	1.33	0.48	122

* From Rausche *et al.* (1996)

EOD = End of Driving, BOR = Beginning of Restrike

The data base compiled by Rausche *et al.* (1996) has been modified to include capacity predictions from the Engineering News and Gates dynamic formulas at both the end of driving and beginning of restrrike. The data base for the dynamic formulas has also been expanded, and includes additional data sets. For evaluation of dynamic formula performance, the allowable load determined using the Engineering News formula was compared to one half of the ultimate capacity determined from the static load test. The ultimate capacity from the Gates formula was compared directly to the ultimate capacity determined from the static load test. The correlation results of the dynamic formulas are included in Table 16-1.

Based on the end of driving data, the Engineering News formula had a mean value of 1.22 and a coefficient of variation of 0.74, while the Gates had a mean value of 0.96 with a coefficient of variation of 0.41. The coefficient of variation is the standard deviation divided by the mean value. Hence, the greater a method's mean value is from 1.0 the lower the accuracy of the method, and the larger the coefficient of variation the less reliable the method. Table 16-1 clearly shows the Engineering News formula has a tendency to overpredict pile capacity. The higher coefficient of variation also suggests that the Engineering News formula is significantly less reliable than the Gates formula.

Table 16-1 illustrates that evaluation of pile capacity, by either Gates or Engineering News dynamic formula from restrrike set and energy observations, has a significant tendency to overpredict pile capacity. The Engineering News formula capacity results, from restrrike observations, had a mean value of 1.89 and a coefficient of variation of 0.46. The Gates formula capacity results, from restrrike observations, had a mean value of 1.33 and a coefficient of variations of 0.48

If the static load test failure loads are divided by the Engineering News allowable design loads, the data base indicates an average factor of safety of 2.3 as compared to the factor of safety of 6.0 theoretically included in the formula. More important, the actual factor of safety from the Engineering News formula ranged from 0.6 to 13.1. This lack of reliability causes the Engineering News formula to be ineffective as a tool for estimating pile capacity. The fact that 12% of the data base has a factor of safety of 1.0 or less is also significant. However, complete failure of a bridge due to inadequate pile capacity determined by Engineering News formula is unusual. The problem usually is indicated by long term damaging settlements which occur after construction when the maximum load is intermittently applied.

16.2 PROBLEMS WITH DYNAMIC FORMULAS

Dynamic formulas are fundamentally incorrect. The problems associated with pile driving formulas can be traced to the modeling of each component within the pile driving process: the driving system, the soil, and the pile. Dynamic formulas offer a poor representation of the driving system and the energy losses of drive system components. Dynamic formulas also assume a rigid pile, thus neglecting pile axial stiffness effects on driveability, and further assume that the soil resistance is constant and instantaneous to the impact force. A more detailed discussion of these problems is presented below.

First, the derivation of most formulas is not based on a realistic treatment of the driving system. Most formulas only consider the kinetic energy of the driving system. The variability of equipment performance is typically not considered. Driving systems include many elements in addition to the ram, such as the anvil for a diesel hammer, the helmet, the hammer cushion, and for a concrete pile, the pile cushion. These components affect the distribution of the hammer energy with time, both at and after impact, which influences the magnitude and duration of peak force. The peak force and its duration determines the ability of the driving system to advance the pile into the soil.

Second, the soil resistance is very crudely treated by assuming that it is a constant force. This assumption neglects even the most obvious characteristics of real soil behavior. The dynamic soil resistance is the resistance of the soil to rapid pile penetration produced by a hammer blow. This resistance is by no means identical with the static soil resistance. However, most dynamic formulas consider the resistance during driving equal to the static resistance or pile capacity. The rapid penetration of the pile into the soil during driving is resisted not only by static friction and cohesion, but also by the soil viscosity, which is comparable to the viscous resistance of liquids against rapid displacement under an applied force. The net effect is that the driving process creates dynamic resistance forces along the pile shaft and at the pile toe, due to the high shear rate. The soil resistance during driving, from the combination of dynamic soil resistance and available static soil resistance, is generally not equal to the static soil resistance or pile capacity under static loads.

Third, the pile is assumed to be rigid and its length is not considered. This assumption completely neglects the pile's flexibility, which affects its ability to penetrate the soil. The energy delivered by the hammer sets up time-dependent stresses and displacements in the helmet, in the pile, and in the surrounding soil. In addition, the pile behaves, not

as a concentrated mass, but as a long elastic rod in which stresses travel longitudinally as waves. Compressive waves which travel to the pile toe are responsible for advancing the pile into the ground.

16.3 DYNAMIC FORMULAS

As noted in Section 16.1, the Engineering News formula is generally recognized to be one of the least accurate and least consistent of dynamic formulas. Due to the overall poor correlations documented between pile capacities determined from this method and static load test results, the use of the Engineering News formula is not recommended.

For small projects where a dynamic formula is used, statistics indicate that the Gates formula is preferable, since it correlates better with static load test results. The Gates formula presented below has been revised to reflect the ultimate pile capacity in kilonewtons and includes the 80 percent efficiency factor on the rated energy, E_r , recommended by Gates.

$$R_u = [7 \sqrt{E_r} \log(10N_b)] - 550$$

Where: R_u = The ultimate pile capacity (kN).

E_r = The manufacturer's rated hammer energy (Joules) at the field observed ram stroke.

$\log(10N_b)$ = Logarithm to the base 10 of the quantity 10 multiplied by N_b , the number of hammer blows per 25 mm at final penetration.

It is sometimes desirable to calculate the number of hammer blows per 0.25 meter (250 mm) of pile penetration, N_{qm} , required to obtain the ultimate pile capacity. For this need, the Gates formula can be written in the following form:

$$N_{qm} = 10(10^x)$$

Where: $x = [(R_u + 550)/(7\sqrt{E_r})] - 1$

Most dynamic formulas are in terms of ultimate pile capacity, rather than allowable or design load. For ultimate pile capacity formulas, the design load should be multiplied by a factor of safety to obtain the ultimate pile capacity that is input into the formula to determine the "set", or amount of pile penetration per blow required. A factor of safety of 3.5 is recommended when using the Gates formula. For example, if a design load of 700 kN is required in the bearing layer, then an ultimate pile capacity of 2450 kN should be used in the Gates formula to determine the necessary driving resistance.

Highway agencies should establish long term correlations between pile capacity prediction from dynamic formulas and static load test results to failure. The Federal Highway Administration has created a national data base of pile load test results that can be accessed by Highway agencies to supplement local test information.

16.4 ALTERNATIVES TO USE OF DYNAMIC FORMULAS

Most shortcomings of dynamic formulas can be overcome by a more realistic analysis of the pile driving process. The one-dimensional wave equation analysis discussed in Chapter 17 is a more realistic method. However as little as ten years ago, wave equation analyses were primarily performed on main frame computers. Therefore, wave equation analysis was often viewed as a tool for special projects and not routine use. With the widespread use of fast personal computers in every day practice, wave equation analysis can now be easily performed in a relatively short amount of time.

As indicated in Table 16-1, ultimate pile capacity estimates from standard wave equation analysis using restrike driving resistance observations had a mean value of 1.22 and a coefficient of variation of 0.35. The performance of the wave equation capacity predictions improved when adjusted for measured drive system performance from dynamic measurements.

Dynamic testing and analysis is another tool which is superior to use of dynamic formulas. This topic will be discussed in greater detail in Chapter 18. Table 16-1 illustrates that dynamic measurements with CAPWAP analysis performed better than either the Engineering News or Gates dynamic formulas. Ultimate pile capacity estimates from restrike dynamic measurements with CAPWAP analysis had a mean value of 0.92 and a coefficient of variation of 0.22.

Modern dynamic methods of wave equation analysis, as well as dynamic testing and analysis, are superior to traditional dynamic formulas. Modern methods should be used in conjunction with static pile load tests whenever possible, and the use of dynamic formulas should be discontinued.

16.5 DYNAMIC FORMULA CASE HISTORIES

To illustrate the variable performance of dynamic formulas compared to modern dynamic methods, three case histories will be briefly discussed. The case histories were selected to include a range of pile types and sizes, hammer types, and soil conditions.

16.5.1 Case History 1

Case History 1 involves a 610 mm square prestressed concrete pile with a 305 mm diameter circular void at the pile center. The concrete pile was driven through loose to medium dense clayey sands to a dense clayey sand layer. A Vulcan 020 single acting air hammer operated at a reduced stroke of 0.9 meters and corresponding rated energy of 81 kJ was used to drive the pile. The pile was driven to a final penetration resistance of 34 blows per 0.25 meter. When restruck 13 days after initial driving, the pile had a penetration resistance of 118 blows per 0.25 meter. This pile was then statically load tested.

Using end of driving set observations, the Engineering News formula predicted an allowable design load of 1360 kN and the Gates formula predicted an ultimate pile capacity of 2476 kN. Modern dynamic methods of the wave equation and dynamic testing with CAPWAP analysis gave restrrike ultimate pile capacities of 4561 and 4111 kN, respectively. The static load test pile had a Davisson failure load of 4223 kN. Hence, the Engineering News and Gates dynamic formulas significantly underpredicted the allowable and ultimate pile capacity, respectively. Dynamic test data indicated the restrrike capacity was 2.5 times the capacity at the end of initial driving. This high setup condition most likely caused the underpredictions by the dynamic formulas.

16.5.2 Case History 2

Case History 2 involves a 356 mm O.D. closed end pipe pile driven into a dense to very dense sand and gravel. The pile had a design load of 620 kN and a required ultimate capacity of 1550 kN, which included an anticipated capacity loss due to scour. An IHC S-70 hydraulic hammer with a maximum rated energy of 69 kJ was used to install the pile. The IHC hydraulic hammers can be operated over a wide energy range and include a readout panel that indicates for each blow the hammer kinetic energy prior to impact. The static load test pile was driven to a final penetration resistance of 26 blows per 0.25 meter at a readout panel energy of 28 kJ. Restrike tests at the site indicated minimal changes in pile capacity with time.

Based on end of driving set observations, the Engineering News formula predicted an allowable design load of 387 kN and the Gates formula predicted an ultimate pile capacity of 1142 kN. The preconstruction wave equation analysis predicted an ultimate pile capacity of 1333 kN. Restrike dynamic testing with CAPWAP analysis predicted an ultimate pile capacity of 1605 kN. The static load test pile had a Davisson failure load of 1627 kN. Hence, both the Engineering News and Gates dynamic formulas significantly underpredicted the allowable and ultimate pile capacity, respectively. In this particular case, the poor performance of the dynamic formulas is most likely attributed to the high energy transfer efficiency of the IHC type hydraulic hammer relative to its kinetic energy rating based on the readout panel.

16.5.3 Case History 3

In Case History 3, a 356 mm O.D. closed end pipe pile was driven through loose to medium dense sands to toe bearing in a very dense sand. The pipe pile had a design load of 980 kN and a required ultimate pile capacity of 1960 kN. An ICE 42-S single acting diesel hammer with a rated energy of 57 kJ was used to drive the load test pile to a final driving resistance of 148 blows per 0.25 meter at a hammer stroke of 3 meters.

Using the end of driving set observations, the Engineering News formula predicted an allowable design load of 2180 kN and the Gates formula predicted an ultimate pile capacity of 2988 kN. Dynamic testing with CAPWAP analysis indicated an ultimate pile capacity of 2037 kN at the end of initial driving, that decreased to an ultimate capacity of 1824 kN during restrike. The static load test pile had a Davisson failure load of 1868 kN. Assuming a safety factor of 2, the allowable pile capacity would be 934 kN. Hence,

the Engineering News formula overpredicted the allowable design load by more than 230% and the Gates formula overpredicted the ultimate pile capacity by 60%.

The magnitude of the overprediction by the dynamic formulas is at least partially attributed to the soil relaxation (capacity at end of driving higher than some time later) that occurred at the site. Pile capacities determined from dynamic formulas are routinely calculated from initial driving observations. Therefore, the time dependent decrease in pile capacity would not likely have been detected if only dynamic formulas had been used for pile driving control on this project.

The case histories above illustrate that different methods often result in a range of predicted capacities at a given site. The magnitude of pile capacity changes with time. Both hammer performance characteristics and soil behavior can be different from those than typically assumed. The three case histories presented illustrate that pile capacity evaluations with modern dynamic methods handle these variations better than traditional dynamic formulas.

REFERENCES

- American Association of State Highway and Transportation Officials [AASHTO], (1994). Standard Specifications for Highway Bridges. Division 2, AASHTO Highway Subcommittee on Bridges and Structures, Washington, D.C.
- Chellis R.D. (1961). Pile Foundations. Second Edition, McGraw-Hill Book Company, New York, 21-23.
- Fragasny, R.J., Higgins, J.D. and Argo, D.E. (1988). Comparison of Methods for Estimating Pile Capacity. Report No. WA-RD 163.1, Washington State Department of Transportation, 62.
- Peck, R.B. (1942). Discussion: Pile Driving Formulas. Proceedings of the American Society of Civil Engineers, Vol. 68, No. 2, 905-909.
- Rausche, F., Thendean, G., Abou-matar, H., Likins, G.E. and Goble, G.G. (1996). Determination of Pile Driveability and Capacity from Penetration Tests. Final Report, U.S. Department of Transportation, Federal Highway Administration Research Contract DTFH61-91-C-00047.
- Sowers, G.F. (1979). Introductory Soil Mechanics and Foundations. Fourth Edition, Macmillan Publishing Co., Inc., New York, 531-533.

STUDENT EXERCISE #9 - GATES FORMULA ULTIMATE CAPACITY

Use the Gates formula described in Section 16.3 to calculate the ultimate pile capacity of a 356 mm O.D. pipe pile driven with an ICE 42-S single acting diesel hammer to the driving resistances given in the table below. The field observed hammer strokes and corresponding manufacturer's rated energy are also included in the table. The Gates formula is presented below:

$$R_u = [7 \sqrt{E_r} \log (10 N_b)] - 550$$

Where: R_u = ultimate pile capacity (kN).
 E_r = manufacturer's rated energy at field stroke (joules).
 N_b = number of hammer blows for 25 mm penetration.

Group Number	Pile Driving Resistance (blows / 250 mm)	Field Observed Stroke (m)	Manufacturer's Rated Energy (joules)	Gates Ultimate Pile Capacity (kN)
1	3	1.67	30,377	
2	7	2.43	44,202	
3	18	2.88	52,387	
4	37	3.10	56,389	
5	53	3.13	56,935	
6	72	3.02	54,934	
7	87	3.04	55,298	
8	107	3.04	55,298	
9	133	3.05	55,480	
10	168	3.05	55,480	

STUDENT EXERCISE #10 - GATES FORMULA DRIVING CRITERION

The Gates formula is to be used for construction control on a new bridge project. The piles have a design load of 620 kN and are to be driven through 5 meters of scourable soils that were calculated to provide 90 kN of resistance at the time of driving. A Kobe K 25 single acting diesel hammer will be used to drive the piles. First determine the required ultimate pile capacity. Then use the Gates formula provided below and described in Section 16.3 to calculate the required driving resistance for the ultimate pile capacity at the hammer strokes shown in the table below.

$$N_{qm} = 10(10^x)$$

$$x = [(R_u + 550)/(7 \sqrt{E_r})] - 1$$

Where: N_{qm} = number of hammer blows for 250 mm penetration.
 R_u = ultimate pile capacity (kN).
 E_r = manufacturer's rated energy at field stroke (joules).

Group Number	Field Observed Stroke (m)	Manufacturer's Rated Energy (joules)	Exponent (x)	Required Driving Resistance (blows / 250 mm)
1	1.50	36,870		
2	1.65	40,458		
3	1.80	44,136		
4	1.95	47,814		
5	2.10	51,492		
6	2.25	55,170		
7	2.40	58,848		
8	2.55	62,526		
9	2.70	66,204		
10	2.85	69,882		

17. DYNAMIC ANALYSIS BY WAVE EQUATION

17.1 INTRODUCTION

As discussed in previous chapters, dynamic formulas, together with observed driving resistances, do not yield acceptably accurate predictions of actual pile capacities. Moreover, they do not provide information on stresses in the piles during driving. The so-called wave equation analysis of pile driving has eliminated many shortcomings associated with dynamic formulas by realistically simulating the hammer impacts and pile penetration process. For most engineers, the term wave equation refers to a partial differential equation. However, for the foundation specialist, it means a complete approach to the mathematical representation of a system consisting of hammer, cushions, helmet, pile and soil, and an associated computer program for the convenient calculation of the motions and forces in this system after ram impact.

The approach was developed by E.A.L. Smith (1960), and after the rationality of the approach had been recognized, several researchers developed a number of computer programs. For example, the Texas Department of Highways supported research at the Texas Transportation Institute (TTI) in an attempt to reduce concrete pile damage using a realistic analysis method. FHWA sponsored the development of both the TTI program (Hirsch *et al.* 1976) and the WEAP program (Goble and Rausche, 1976). FHWA supported the WEAP development to obtain analysis results backed by measurements taken on construction piles during installation for a variety of hammer models. The WEAP program was updated several times under FHWA sponsorship, the last time (Goble and Rausche, 1986) when the WEAP86 program was released. Later, additional options, improved data files, refined mathematical representations and modernized user conveniences were added to this program on a proprietary basis, and the program is now known as GRLWEAP (Goble Rausche Likins and Associates, Inc., 1996). GRLWEAP has been accepted for use on public projects by a variety of agencies (*e.g.* AASHTO, 1992, US Army Corps of Engineers, 1993), State Departments of Transportation, and the FHWA for routine analyses. However, this should not be construed as a promotion or endorsement.

The wave equation approach has been subjected to a great number of checks and correlation studies. Studies on the performance of WEAP, the most widely accepted program, produced publications demonstrating the program's performance and utility (e.g. Blendy 1979, Soares *et al.* 1984).

This chapter will explain what a wave equation analysis is, how it works, and what problems it can solve. Example problems, highlighting program applications, will be demonstrated. Also, basic program usage and application of program results will be presented.

17.2 WAVE PROPAGATION

Input preparation for wave equation analyses is often very simple, requiring only very basic driving system and pile parameters in addition to a few standard soil properties. Thus, a wave equation program can be run without much specialized knowledge. However, interpretation of calculated results is facilitated, and errors in result application may be avoided, by a knowledge of the mechanics of stress wave propagation.

In the first moment, when a pile is struck by a hammer, it is only compressed at the ram-pile interface. This compressed zone, or force pulse, as shown in Figure 17.1, expands into the pile toward the pile toe at a constant wave speed, C , which depends on the pile's elastic modulus and mass density (or specific weight). When the force pulse reaches the embedded portion of the pile, its amplitude is reduced by the action of static and dynamic soil resistance forces. Depending on the magnitude of the soil resistances along the pile shaft and at the pile toe, the force pulse will generate either a tensile or a compressive force pulse which travels back to the pile head. Both incident and reflected force pulses will cause a pile toe motion and produce a permanent pile set if their combined energy and force are sufficient to overcome the static and dynamic resistance effects of the soil.

17.3 WAVE EQUATION METHODOLOGY

In a wave equation analysis, the hammer, helmet, and pile are modeled by a series of segments each consisting of a concentrated mass and a weightless spring. The hammer and pile segments are approximately one meter in length. Shorter segments

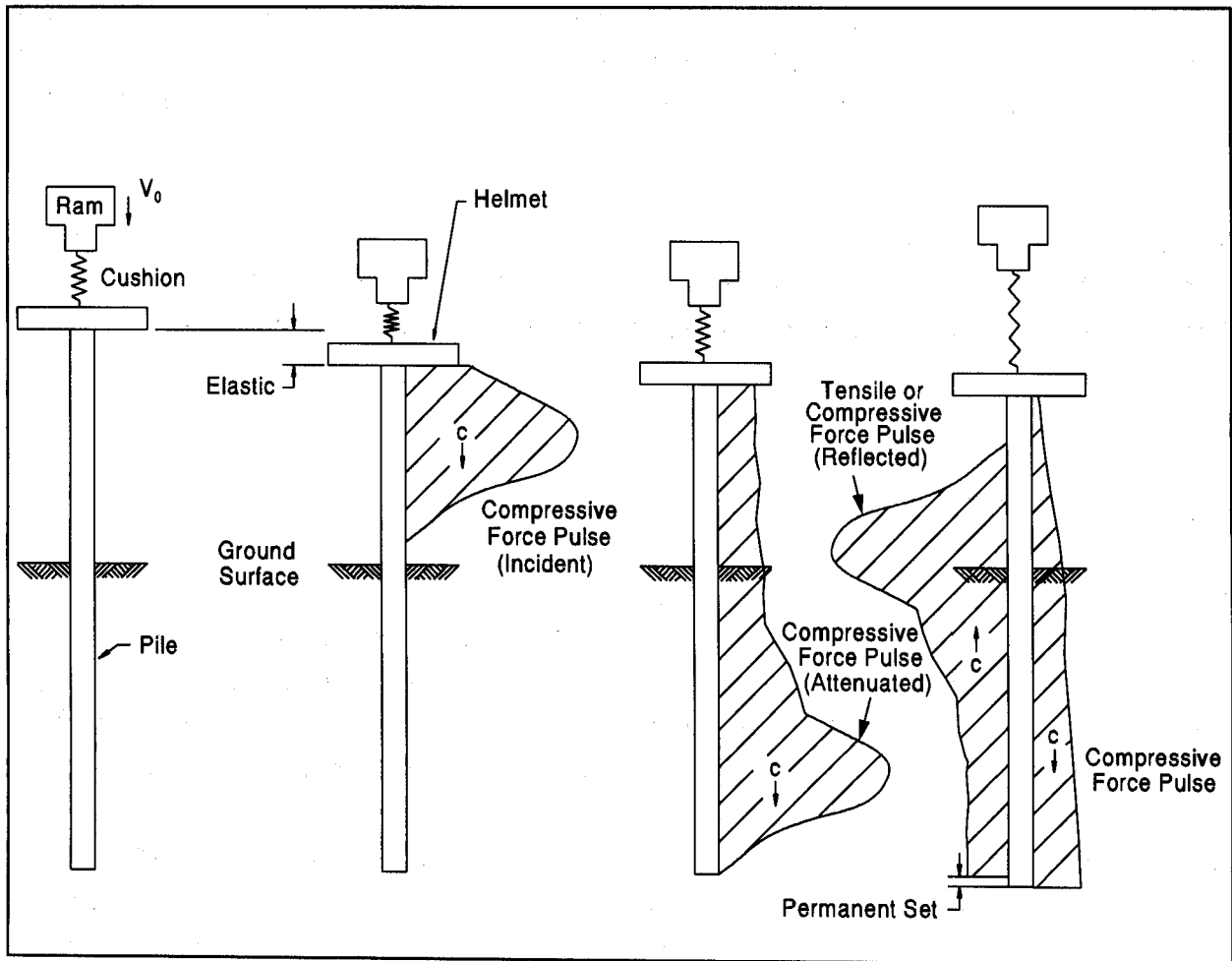


Figure 17.1 Wave Propagation in a Pile (adapted from Cheney and Chassie, 1993)

often improve the accuracy of the numerical solution at the expense of longer computer times. Spring stiffnesses are calculated from the cross sectional area and modulus of elasticity of the corresponding pile section. Hammer and pile cushions are represented by additional springs whose stiffnesses are calculated from area, modulus of elasticity, and thickness of the cushion materials. In addition, coefficients of restitution (COR) are usually specified to model energy losses in cushion materials, and in all segments which can separate from their neighboring segments by a certain slack distance. The COR is equal to one for a perfectly elastic collision which preserves all energy and is equal to zero for a perfectly plastic condition which loses all deformation energy. Partially elastic collisions are modeled with an intermediate COR value.

The soil resistance along the embedded portion of the pile and at the pile toe is represented by both static and dynamic components. Therefore, both a static and a dynamic soil resistance force acts on every embedded pile segment. The static soil resistance forces are modeled by elasto-plastic springs and the dynamic soil resistance by linear viscous dashpots. The displacement at which the soil changes from elastic to plastic behavior is referred to as the soil "quake". In the Smith damping model, the dynamic soil resistance is proportional to a damping factor times the pile velocity times the assigned static soil resistance. A schematic of the wave equation hammer-pile-soil model is presented in Figure 17.2.

As the analysis commences, a calculated or assumed ultimate capacity, R_{ut} , from user specified values is distributed according to user input among the elasto-plastic springs along the shaft and toe. Similarly, user specified damping factors are assigned to shaft and toe to represent the dynamic soil resistance. The analysis then proceeds by calculating a ram velocity using the input hammer efficiency and stroke. The ram movement causes displacements of helmet and pile head springs, and therefore compressions (or extensions) and related forces acting at the top and bottom of the segments. Furthermore, the movement of a pile segment causes soil resistance forces. A summation of all forces acting on a segment, divided by its mass, yields the acceleration of the segment. The product of acceleration and time step summed over time is the segment velocity. The velocity multiplied by the time step yields a change of segment displacement which then results in new spring forces. These forces divided by the pile cross sectional area at the corresponding section equal the stress at that point.

Similar calculations are made for each segment until the accelerations, velocities and displacements of all segments have been calculated during the time step. The analysis then repeats for the next time step using the updated motion of the segments from the previous time step. From this process, the accelerations, velocities, displacements, forces, and stresses of each segment are computed over time. Additional time steps are analyzed until the pile toe begins to rebound.

The permanent set (mm) of the pile toe is calculated by subtracting a weighted average of the shaft and toe quakes from the maximum pile toe displacement. The inverse of the permanent set is the driving resistance (blow count) in blows per meter that corresponds to the input ultimate capacity. By performing wave equation analyses over a wide range of ultimate capacities, a curve or "bearing graph" can be plotted which relates ultimate capacity to driving resistance.

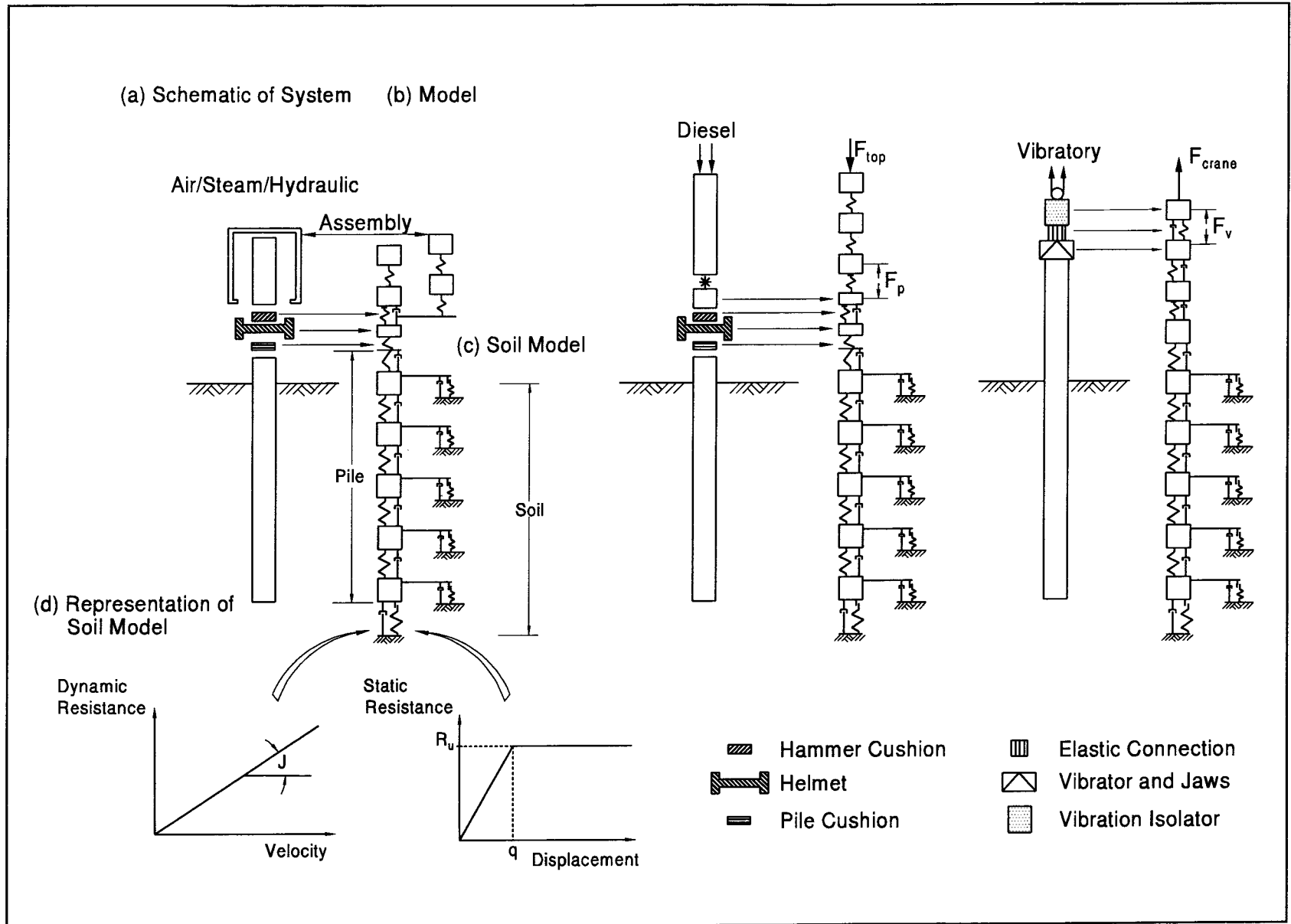


Figure 17.2 Typical Wave Equation Model

A wave equation bearing graph is substantially different from a similar graph generated from a dynamic formula. The wave equation bearing graph is associated with a single driving system, hammer stroke, pile type, soil profile, and a particular pile length. If any one of the above items is changed, the bearing graph will also change. Furthermore, wave equation bearing graphs also include the maxima of calculated compression and tension stresses.

In addition to the bearing graph, GRLWEAP provides options for two alternative results, the constant capacity analysis, or "inspector's chart", and the driveability analysis. The inspector's chart establishes a relationship between hammer energy or stroke and driving resistance for one particular, user specified, ultimate capacity value. Associated stress maxima are also included in the chart, enabling the user to select a practical hammer energy or stroke range both for reasonable driving resistances and driving stress control. This analysis option is described in greater detail in Section 17.5.2.

The driveability analysis calculates driving resistances and stresses from user input shaft and toe resistance values at up to 100 user selected pile penetrations. The calculated results can then be plotted together with the capacity values versus pile penetration. The resulting plot would depict those pile penetrations where refusal might be expected or where dangerously high driving stress levels could develop. In addition, a crude estimate of pure driving time (not counting interruptions) is provided by this analysis option. The driveability option is described in greater detail in Section 17.5.5.

17.4 WAVE EQUATION APPLICATIONS

A bearing graph provides the wave equation analyst with two types of information:

1. It establishes a relationship between ultimate capacity and driving resistance. From the user's input data on the shaft and toe bearing resistances, the analysis estimates the permanent set (mm/blow) under one hammer blow. Specifying up to ten ultimate capacity values yields a relationship between ultimate capacity and driving resistance (or blow count) in blows per meter.
2. The analysis also relates driving stresses in the pile to pile driving resistance.

The user usually develops a bearing graph or an inspector's chart for different pile lengths and uses these graphs in the field, with the observed driving resistance, to determine when the pile has been driven sufficiently for the required bearing capacity.

In the design stage, the foundation engineer should select typical pile types and driving equipment known to be locally available. Then by performing the wave equation analysis with various equipment and pile size combinations, it becomes possible to rationally:

1. Design the pile section for driveability to the required depth and/or capacity.

For example, scour considerations or consolidation of lower soft layers may make it necessary to drive a pile through hard layers whose driving resistance exceeds the resistance expected at final penetration. A thin walled pipe pile may have been initially chosen during design. However when this section is checked for driveability, the wave equation analysis may indicate that even the largest hammers will not be able to drive the pipe pile to the required depth because it is too flexible (its impedance is too low). Therefore, a wall thickness greater than necessary to carry the design load, has to be chosen for driveability considerations. (Switching to an H-pile or predrilling may be other alternatives).

2. Aid in the selection of pile material properties to be specified based on probable driving stresses in reaching penetration and/or capacity requirements.

Suppose that, in the above example, it would be possible to drive the thinner walled pile to the desired depth, but with excessive driving stresses. More cushioning or a reduced hammer energy would lower the stresses but would result in a refusal driving resistance. Choosing a high strength steel grade could solve this problem. For concrete piles, higher concrete strength and/or higher prestress levels may provide acceptable solutions.

3. Support the decision for a new penetration depth, design load, and/or different number of piles.

In the above example, after it has been determined that the pile section or its material strength had to be increased to satisfy pile penetration requirements, it may have become feasible to increase the design load of each pile and to reduce the total number of piles. Obviously, these considerations would require revisiting geotechnical and/or structural considerations.

Once the project has reached the construction stage, additional wave equation analyses should be performed on the actual driving equipment by:

1. Construction engineers - for hammer approval and cushion design.

Once the pile type, material, and pile penetration requirements have been selected by the foundation designer, the hammer size and hammer type may have a decisive influence on driving stresses. For example, a hammer with adjustable stroke or fuel pump setting may have the ability to drive a concrete pile through a hard layer while allowing for reduced stroke heights and tension stress control when penetrating soft soil layers.

Cushions are often chosen to reduce driving stresses. However, softer cushions absorb and dissipate greater amounts of energy thereby increasing the driving resistance. Since it is both safer (reducing fatigue effects) and more economical to limit the number of blows applied to a pile, softer cushions cannot always be chosen to maintain acceptable driving stresses. Also, experience has shown that changes of hammer cushion material are relatively ineffective for limiting driving stresses.

Hammer size, energy setting, and cushion materials should always be chosen such that the maximum expected driving resistance is less than 120 blows per 0.25 meter or 480 blows/m (exceptions are end-of-driving blow counts of pure toe bearing piles). The final driving resistance should also be greater than 30 blows per 0.25 meter (120 blows/m) for a reasonably accurate driving criterion (the lower the blow count the greater the possibility of inaccurate blow count measurements).

2. Contractors - to select an economical combination of driving equipment to minimize installation cost.

While the construction engineer is interested in the safest installation method, contractors would like to optimize driving time for cost considerations. Fast hitting, light weight, simple and rugged hammers which have a high blow rate are obviously preferred. The wave equation analysis can be used to roughly estimate the anticipated number of hammer blows and the time of driving. This information is particularly useful for a relative evaluation of the economy of driving systems.

Additional considerations might include the cost of pile cushions which are usually discarded after a pile has been installed. Thus, thick plywood pile cushions may be expensive.

Near refusal driving resistances are particularly time-consuming and since it is known that stiffer piles drive faster with lower risk of damage, the contractor may even choose to upgrade the wall thickness of a pipe pile or the section of an H-pile for improved overall economy.

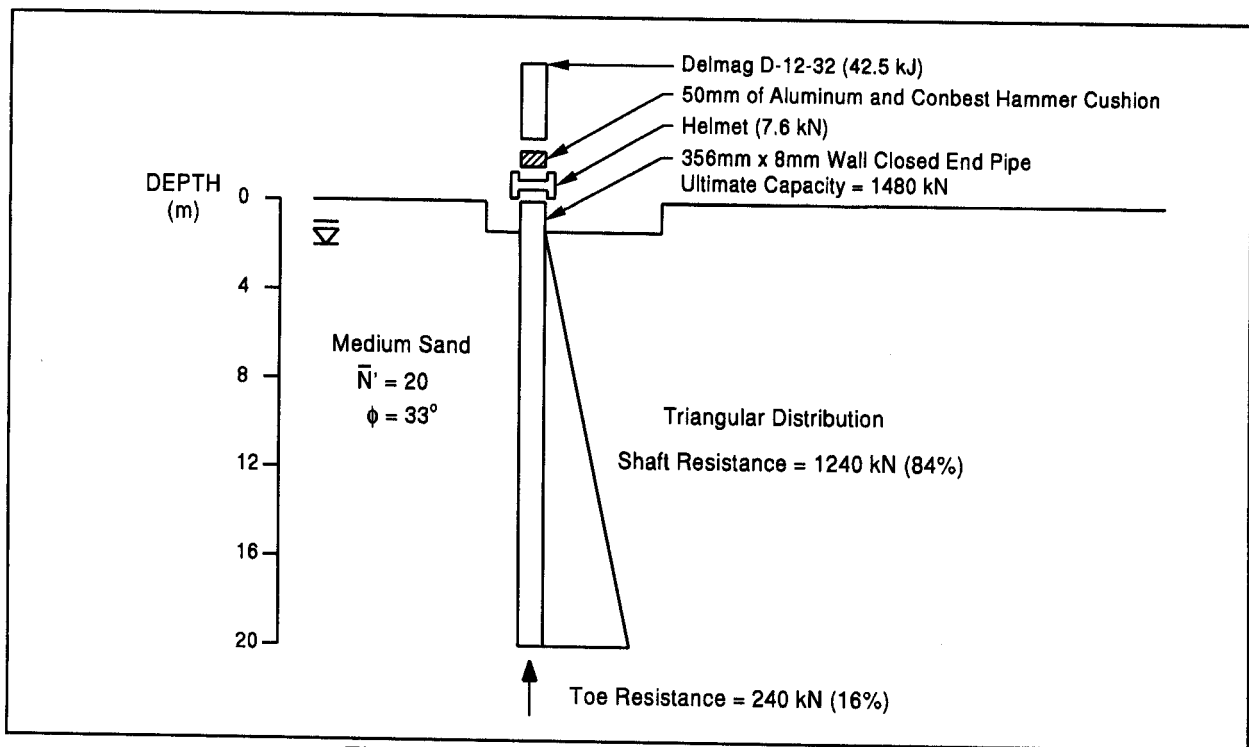
17.5 WAVE EQUATION EXAMPLES

This section presents several examples that illustrate the application of the wave equation analysis for the solution of design and construction problems. The factor of safety applied to the design load in the following examples is 2. This assumes that a static pile load test was performed on each project. As noted in Chapter 15, a factor of safety of 2.5 to 2.75 should be applied to the design load in wave equation analyses if static load testing or dynamic testing is not included in the project. The ultimate capacity in a wave equation analysis should consist of the factor of safety, times the design load, plus the sum of the ultimate resistances from any overlying layers unsuitable for long term support.

Note: The figures illustrating the following examples were generated from the proprietary program GRLWEAP. These figures are not intended as endorsements of Goble Rausche Likins and Associates, Inc. (GRL), its products or services.

17.5.1 Example 1 - General Bearing Graph

A primary application of a wave equation analysis is to develop a bearing graph relating the ultimate pile capacity to the pile driving resistance. For a desired ultimate pile capacity, the required driving resistance can be easily found from this graph. Consider the soil profile in Figure 17.3. In this example, a 356 mm by 8 mm wall, closed end pipe pile (yield strength 241 MPa) is to be driven into a deep deposit of medium sands. A static analysis performed using the SPILE program indicates that an ultimate pile capacity of 1480 kN can be obtained for the proposed pile type at a penetration depth



of 19 meters. The static analysis also indicates that the ultimate capacity is distributed as 84% shaft resistance and 16% toe bearing resistance with the shaft resistance being distributed triangularly along the pile shaft.

The contractor selected a Delmag D-12-32 single acting diesel hammer for driving the pipe piles. The contractor's hammer submittal indicates that the hammer cushion will consist of 25 mm of aluminum and 25 mm of Conbest with a cross sectional area of 1464 cm². A helmet weight of 7.6 kN is reported.

Based on this information, a wave equation analysis can be performed. The ultimate pile capacity of 1480 kN is input along with selected additional ultimate capacities. The wave equation analysis calculates the net set of the pile toe for each input ultimate capacity. The inverse of the set is the driving resistance for that ultimate capacity expressed in blows per meter (blows/m). By plotting the calculated driving resistances versus the corresponding ultimate capacities, a bearing graph is developed. The results of such a calculation are shown in Figure 17.4 for the 356 mm closed end pipe pile.

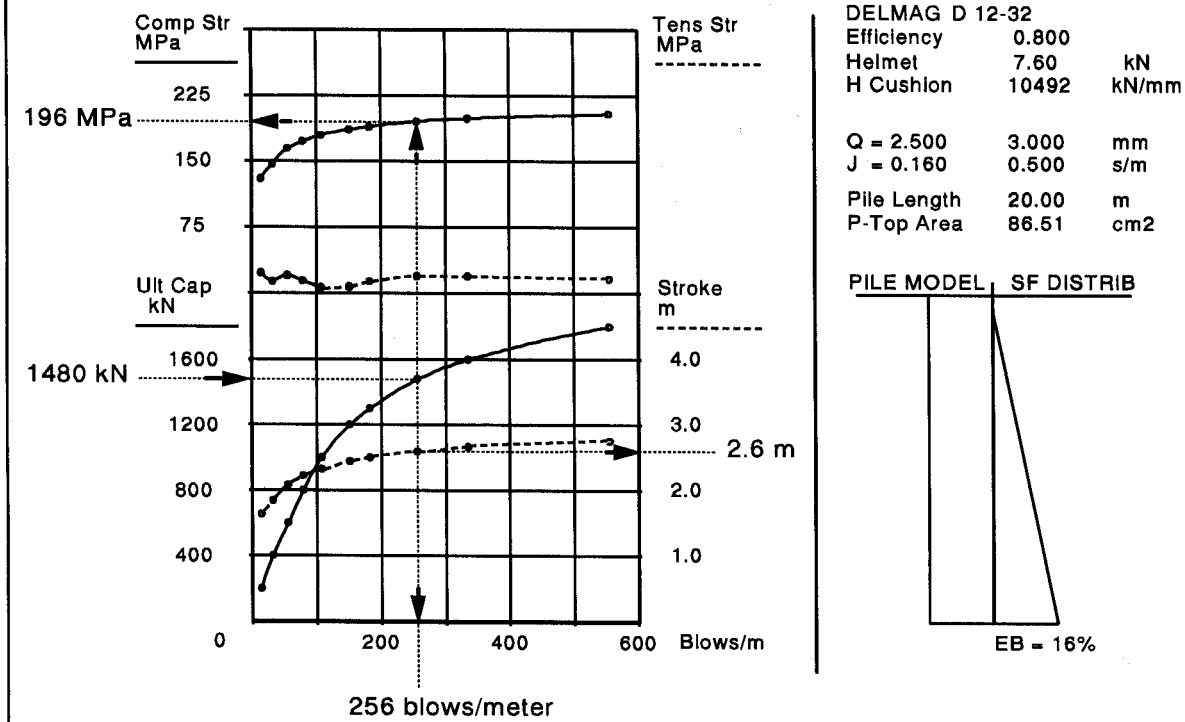


Figure 17.4 Example 1 Typical Bearing Graph

In the bottom half of Figure 17.4, the ultimate pile capacity versus driving resistance in blows/m is represented by the solid line. This graph shows that for an ultimate pile capacity of 1480 kN a blow count of 256 blows/m is required. (This requirement is really equivalent to a criterion of 64 blows per 0.25 meter penetration, or approximately 40 mm for 10 blows). As a driving criterion, this is a reasonable blow count requirement being neither excessively high which would demand extreme driving efforts nor very low and therefore inaccurate. Also in the bottom half of the graph, the corresponding hammer stroke versus driving resistance is represented by the dashed line. This curve is important for a check on hammer performance when the driving criterion is applied. In this case, the driving resistance of 256 blows/m for the 1480 kN capacity is based upon a hammer stroke of 2.6 meters. Should field observations indicate significantly (say more than 10% difference) higher or lower strokes, then a lower or higher blow count would be satisfactory (needed) for the same capacity. Hammer stroke information is

therefore essential for field evaluation and control of the pile installation process. For significantly differing hammer field performance, new wave equation analyses would be necessary with a modified maximum combustion pressure or a fixed input stroke.

In the upper half of Figure 17.4, maximum compression and tension driving stresses are also plotted as a function of driving resistance. Of primary interest for a steel pile is the compression driving stress which is represented by the solid line. This curve shows that at the driving resistance of 256 blows/m associated with the required ultimate pile capacity, the maximum compression stress calculated in the pile is 196 MPa which is less than 90% of yield strength of steel ($0.9 (241) = 217$ MPa), and therefore acceptable. Note, however, that any non-axial stress components (such as from bending) are not included in the wave equation results and would be additional.

Though the analysis was conducted for an estimated penetration of 19 m, the required driving resistance may be reached at a shallower depth, or additional penetration may be required. The static analysis only serves as an initial estimate of the required penetration depth. The actual driving behavior and construction monitoring will confirm whether or not the static calculation was adequate. If the actual driving behavior is significantly different from the analyzed situation (say the driving resistance is already reached at 15 m penetration) then an additional analysis should be performed to better match the field observations. However, in general, the bearing graph is relatively insensitive to changes in penetration unless there is a significant change in the soil profile. Higher driving resistances from penetrating embankment fills or scour susceptible material, *etc.*, would also need to be considered in this assessment.

17.5.2 Example 2 - Constant Capacity / Variable Stroke Option

The hammer-pile-soil information used in Example 1 will be reused for a constant capacity (or Inspector's chart) analysis in Example 2. In this example, the driving resistance required for the 1480 kN ultimate capacity is evaluated at hammer strokes other than the predicted 2.6 meter stroke. This information will be helpful for field personnel in determining when pile driving can be terminated if the field observed hammer stroke varies from the hammer stroke predicted by the wave equation.

In the constant capacity/variable stroke option, a single ultimate capacity (usually the required ultimate capacity) is chosen and the hammer stroke is varied from minimum to maximum values. The necessary driving resistance at each hammer stroke is then calculated for the input ultimate capacity. The lower half of Figure 17.5 presents these results for an ultimate pile capacity of 1480 kN. When the point of intersection of the observed stroke and driving resistance plots below the curve, the ultimate pile capacity has not been obtained. Any combination of stroke and driving resistance plotting above the curve indicates that the required ultimate pile capacity has been reached. Hence this analysis option is useful for field control by inspection personnel.

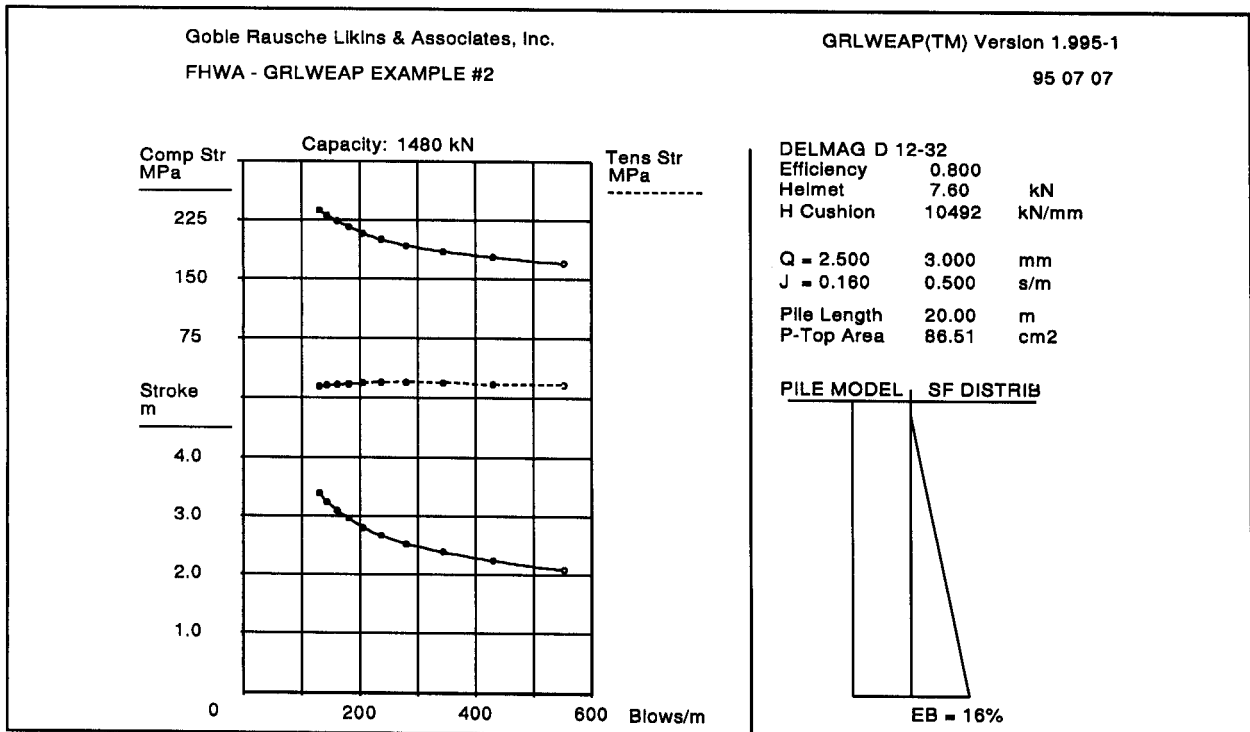


Figure 17.5 Example 2 Constant Capacity Analysis

17.5.3 Example 3 - Tension and Compression Stress Control

Example 3 illustrates the use of the wave equation for the control of tension stresses in concrete piles. The North Abutment of the Peach Freeway design problem presented in Chapter 13 will be used for this example problem. For the North Abutment, static calculations performed using the Nordlund method indicated that a 356 mm square prestressed concrete pile driven through 4 m of loose silty fine sand, 7 m of medium dense silty fine sand, and 0.5 m into a dense sand and gravel deposit could develop an ultimate pile capacity of 1807 kN (which is slightly more than the 1780 kN required). The static analysis also indicates that the ultimate capacity is distributed as 48% shaft resistance and 52% toe resistance, with the shaft resistance being distributed triangularly along the pile shaft. The soil profile for this problem is presented in Figure 17.6.

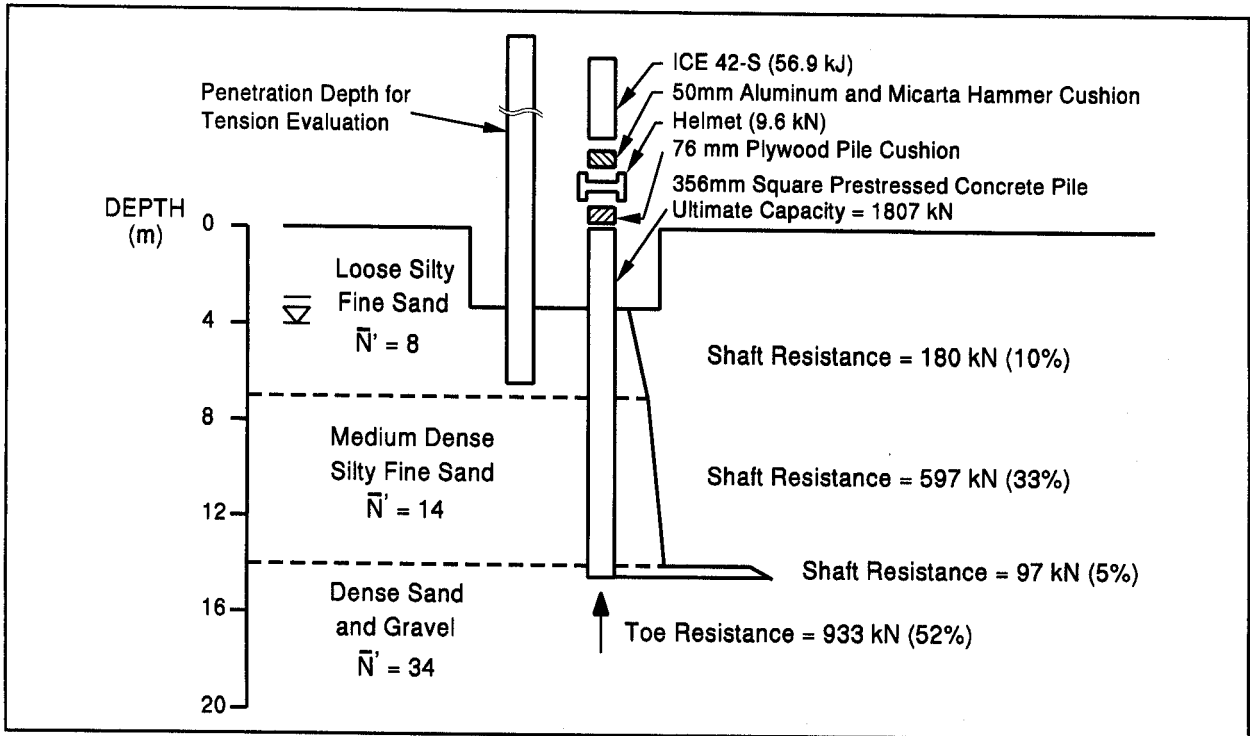


Figure 17.6 Example 3 Problem Profile

The contractor selected an ICE 42-S single acting diesel hammer for driving the prestressed concrete piles. The contractor's hammer submittal indicates that the hammer cushion will consist of 25 mm of aluminum and 25 mm of Micarta with a cross sectional area of 2568 cm². A helmet weight of 9.6 kN is reported. The proposed pile cushion is 76 mm of plywood. The pile will have a concrete compression strength of 37.9 MPa and an effective prestress after losses of 5.2 MPa. Using the AASHTO driving

stress recommendations from Chapter 11, this results in a maximum recommended compression stress of 27.0 MPa and a maximum tension driving stress of 6.7 MPa.

One of the main concerns with concrete piles is the possibility of developing high tension stresses during easy driving conditions when the soil provides little or no toe resistance. Therefore, the wave equation should be used to evaluate the contractor's proposed driving system during both low and high resistance conditions.

First, it is necessary to evaluate tension stresses during easy driving. The weight of the pile and driving system is anticipated to be on the order of 100 kN. Hence, the pile penetration depth for the wave equation analysis should be selected below the depth to which the pile will likely penetrate or "run" under the weight of the pile and driving system. At a depth of 3.5 m, the pile is still within the loose silty fine sand stratum and tension driving stresses are anticipated to be near their peak. At this depth, a pile capacity of 357 kN was calculated from a static analysis.

The contractor has submitted a plywood pile cushion design comprised of four 19 mm sheets with a total thickness of 76 mm. The pile cushion stiffness will significantly affect the tension driving stresses. Therefore it is necessary to check whether or not the contractor's proposed pile cushion thickness is sufficient to maintain tension stress levels within specified limits. In the first analysis, the 76 mm pile cushion is anticipated to compress to about 80% of its initial thickness early in the driving process. Therefore, a pile cushion thickness of 61 mm will be used in the analysis instead of 76 mm to evaluate tension stresses during easy driving. The elastic modulus of the plywood at the start of driving is estimated to be 207 MPa.

Based on this information, the wave equation analysis indicates a maximum tension stress of 6.9 MPa at 6 m below the pile head. The magnitude of the tension stress exceeds the allowable driving stress limitation of 6.7 MPa. Thus, the pile cushion thickness should be increased, and another wave equation analysis should be performed. In the second analysis, eight sheets of 19 mm thick plywood with a total thickness of 152 mm are used for the pile cushion material. It is also assumed that this cushion thickness will compress to about 80% of its initial thickness or to 122 mm early in the driving process. The result of the second wave equation analysis indicates that the maximum tension stress reduces to 2.6 MPa for the thicker pile cushion, which is within specification limits. A comparison of the driving stresses for these two wave equation analyses along with standard bearing graphs is presented in Figure 17.7.

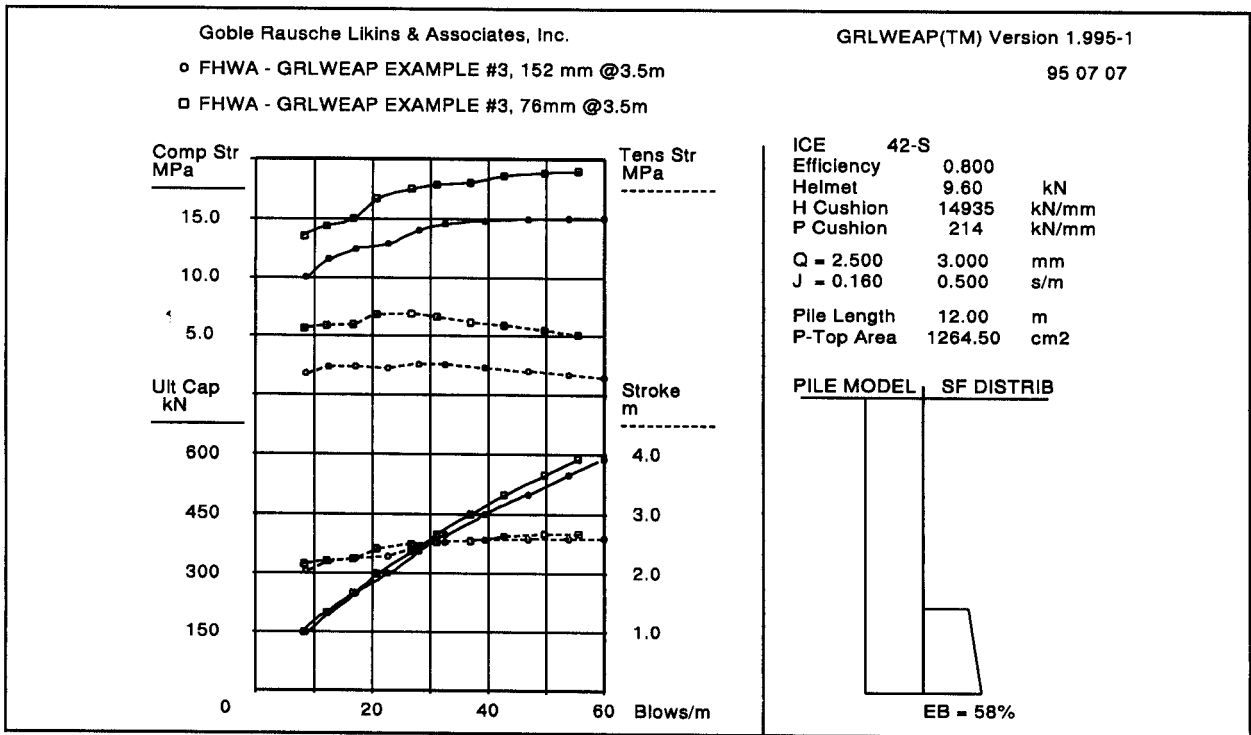


Figure 17.7 Example 3 Bearing Graph Comparison of Two Pile Cushion Thickness

Next, the driving stresses and driving resistance at final driving for the required 1780 kN ultimate pile capacity should be checked. In this analysis, it is assumed that the additional hammer blows required to achieve the final pile penetration depth have resulted in additional compression of the pile cushion material to 75% of its original height, or to a thickness of 114 mm. The additional hammer blows have also resulted in an assumed increase in the modulus of elasticity of the pile cushion material from 207 MPa to 414 MPa. Hence, these assumptions result in the pile cushion stiffness at final driving being approximately 2.7 times stiffer than during early driving.

The analysis indicates a final driving resistance of 236 blows per meter for a 1780 kN ultimate capacity which should result in efficient driving time. Figure 17.8 shows that the maximum compression stresses of 23.3 MPa at final driving are below the allowable limit of 27.0 MPa. Therefore, the thicker pile cushion (152 mm) is recommended for control of both tension stresses during easy driving and compression stresses at final driving.

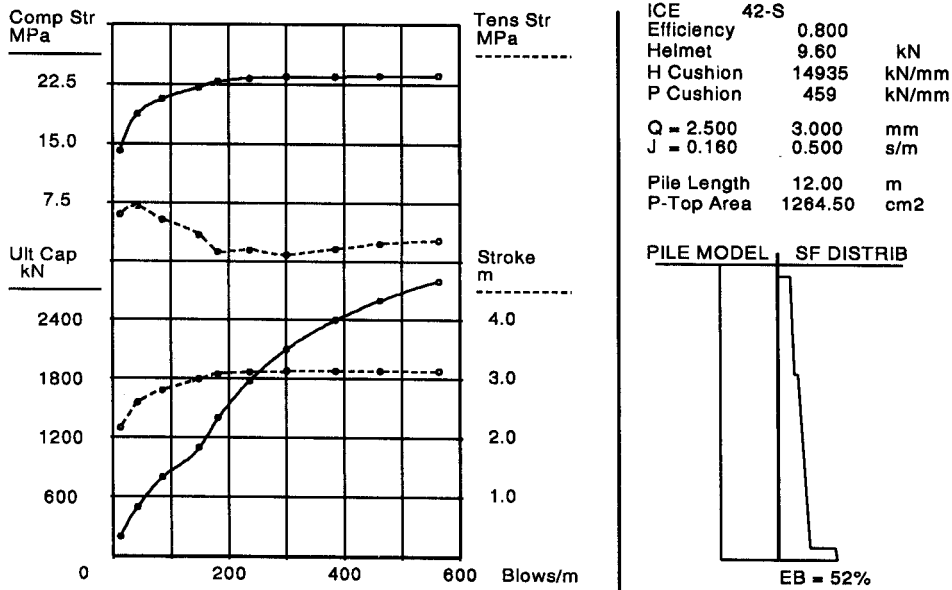


Figure 17.8 Example 3 Bearing Graph for End of Driving Condition

17.5.4 Example 4 - Use of Soil Setup

Consider the soil profile in Figure 17.9. In this example, a 305 mm square prestressed concrete pile is to be driven into a thick deposit of stiff clay. The stiff clay deposit has an average shear strength of 70 kPa. Based on field vane shear tests, it is estimated that the remolded shear strength at the time of driving will be 52.5 kPa, resulting in an expected soil setup factor of 1.33. A static analysis performed using the SPILE program indicates that an ultimate pile capacity of 1340 kN after setup can be obtained for the proposed pile type at a penetration depth of 15 meters. The static analysis also indicates that the ultimate capacity is distributed as 92% shaft resistance and 8% toe bearing resistance, with the shaft resistance being distributed uniformly along the pile shaft.

A Vulcan 08 single acting air hammer was selected by the contractor for driving the prestressed concrete piles. The contractor's hammer submittal indicates that the hammer cushion will consist of 216 mm of Hamortex with a cross sectional area of 958 cm². The pile cushion will consist of eight 19 mm sheets of plywood. It is anticipated

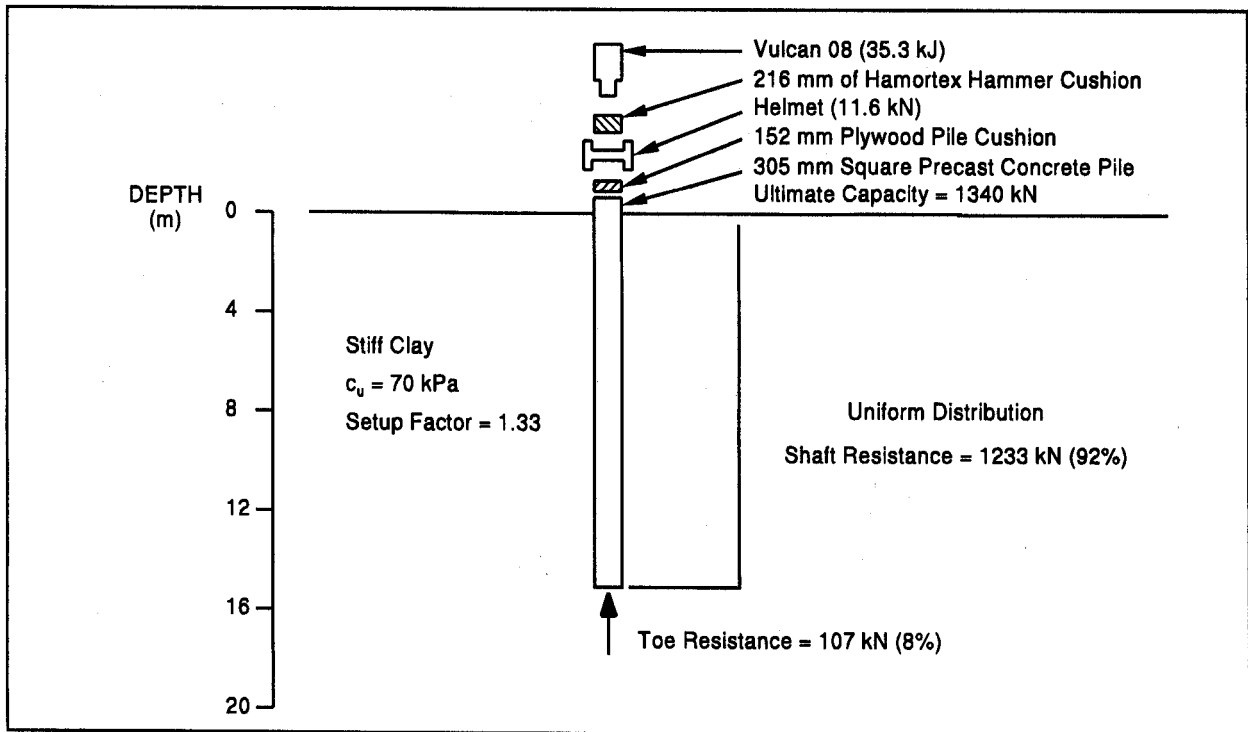


Figure 17.9 Example 4 Problem Profile

that the pile cushion will compress and stiffen during driving similar to that described in Example 3. The contractor's submittal indicates that the helmet weighs 11.6 kN.

Based upon the reported soil type and setup behavior, a 33% increase in pile capacity with time is expected at this site. Therefore, piles could be driven to a capacity of 1005 kN instead of the ultimate capacity of 1340 kN with remaining 335 kN of capacity expected from soil setup. As noted in Section 17.5 of this chapter, a static load test will be performed on the project to confirm the expected pile capacity.

The wave equation results presented in Figure 17.10 indicate a final driving resistance of 138 blows/m could be used as the driving criteria for a 1005 kN capacity. This is significantly less than the 259 blows/m required for an ultimate pile capacity of 1340 kN. Hence, significant pile length may be saved by driving the piles to the lower 1005 kN capacity instead of the required 1340 kN ultimate pile capacity, subject to confirmation of the anticipated soil setup.

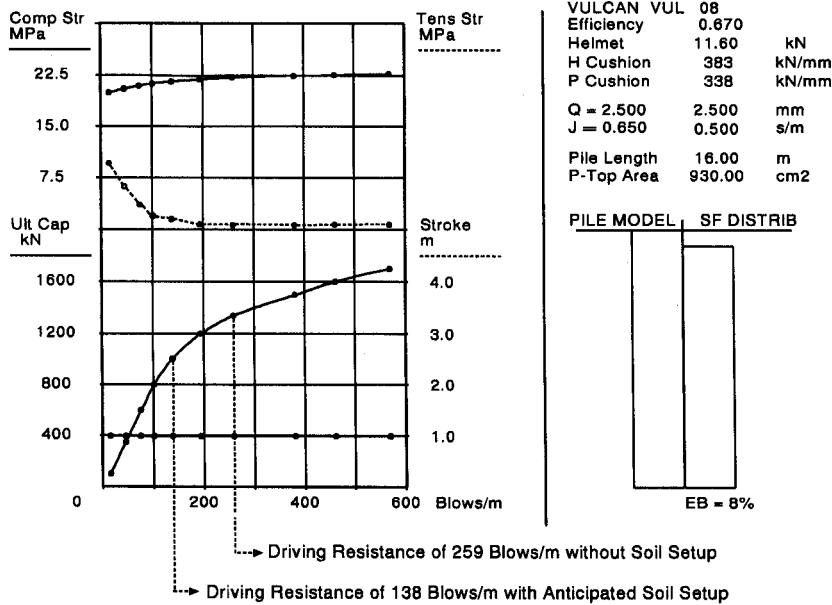


Figure 17.10 Example 4 Using of Bearing Graph with Soil Setup

17.5.5 Example 5 - Driveability Studies

The effect of scour and seismic design considerations on pile foundations often result in increased pile penetration requirements. Therefore, the ability of a given pile to be driven to the depth required by static analysis should be evaluated in a design stage wave equation driveability study, as presented in this example.

Figure 17.11 illustrates the installation conditions at interior Pier 2 of the Peach Freeway design problem from Chapter 13. A cofferdam will be required for pier construction. The interior of the cofferdam will be excavated 5 meters below original grade prior to pile installation. The extremely dense sand and gravel layer was estimated to have a soil friction angle, ϕ , of 43° . This ϕ angle was used in the static calculations of toe resistance. However a limiting ϕ angle of 36° , for hard angular gravel, was used for shaft resistance calculations in this layer as discussed in Section 9.5.

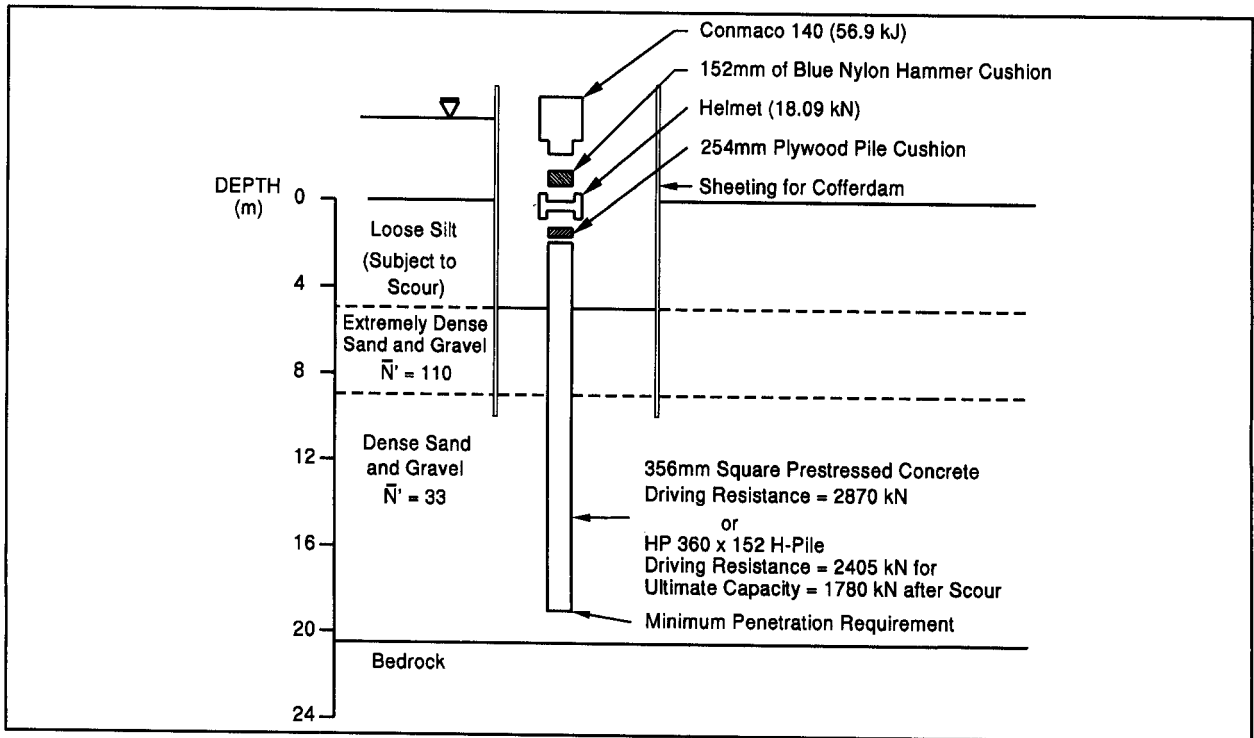


Figure 17.11 Example 5 Problem Profile

During construction, the silt soils will be removed inside the cofferdam area. However, the weight from the silt soils outside the cofferdam will still be present at the time of construction. Therefore, the soil resistance to pile driving should be calculated including the overburden pressure from these materials. However, the 5 meters of loose silt may be completely eroded by channel degradation scour according to hydraulic experts. Thus, for long term pile capacity, static calculations should ignore the effective weight of the silt layer. For the pile installation condition however, the silt layer would be present. Therefore a higher soil resistance than required to meet the static load requirements must be anticipated during pile installation. The soil resistance calculations for the driving conditions should therefore include the effective weight of the silt layer.

Initial static analyses indicate a 356 mm square prestressed concrete pile would develop the ultimate capacity of 1780 kN, primarily through toe bearing, at a depth of 3 meters below the cofferdam excavation level. However, when the reduction in the effective overburden pressure from removal of the silt layer from scour is considered, the piles would have an ultimate capacity of only 924 kN at the 3 meter depth. Additional static capacity calculations were performed at multiple pile penetration depths to determine

the depth where a 1780 kN ultimate capacity pile could be obtained. These calculations indicated a 1780 kN ultimate capacity pile could again be obtained through shaft and toe resistance at a depth of 10 meters below cofferdam excavation level. However, once the overburden pressure reduction from channel degradation scour is considered, an ultimate pile capacity of only 1321 kN would be obtained at this depth. To obtain the desired 1780 kN ultimate pile capacity after scour, static calculations indicate a penetration depth of 14 meters below the cofferdam excavation level will be required, and the pile will need to be driven against a soil resistance of 2300 kN to reach this penetration depth.

The static pile capacity calculations versus depth were then input into a wave equation driveability study. Since this study is conducted in the design stage, a locally available single acting air hammer driving system was assumed as a typical driving system that might be used during construction. The driveability analysis indicated that the 356 mm concrete pile would encounter a driving resistance of 255 blows/m in the extremely dense sand and gravel deposit. While this is a relatively high value, the driving resistances decreased considerably after penetrating through this upper stratum and it could be concluded that the 356 mm concrete pile could be driven to the 14 meter penetration depth required.

This would be an erroneous conclusion. The static analyses would likely provide an adequate assessment of soil resistance for the first pile driven. However, an increase in the ϕ angle from group densification could significantly affect the resistance to driving of additional displacement piles, particularly within the added confinement from the cofferdam. The dense deposits are also likely to develop negative pore pressures during shear, resulting in a temporary increase in soil resistance to driving. If it is assumed that these factors cause a 33% increase in both shaft and toe resistances during driving of subsequent piles, a second driveability analysis would indicate that the piles practically refuse at a penetration depth of 3.5 meters with a driving resistance of 582 blows/m. A soil resistance of 2870 kN must also be overcome during driving to reach the 14 m penetration depth. Maximum compression driving stresses approach 31 MPa so a larger hammer would not appear to be a viable option. If displacement piles are used, predrilling or jetting would be required to advance the piles through the upper stratum. A low displacement pile would be a more attractive foundation solution.

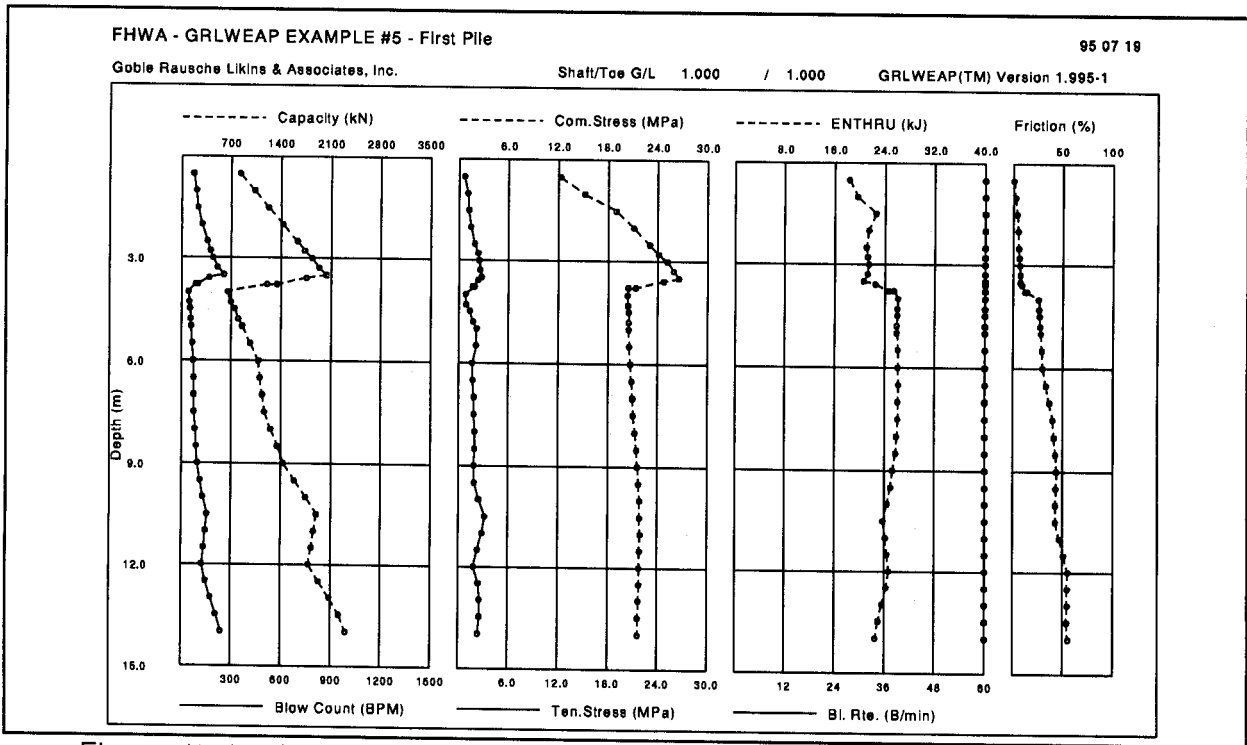


Figure 17.12 Example 5 Driveability Results for First 356 mm Concrete Pile

The wave equation driveability results for the first and later 356 mm concrete piles driven in the above soil profile are presented in Figures 17.12 and 17.13, respectively. Wave equation driveability results for a low displacement HP 360 x 152 H-pile are shown in Figure 17.14. Note that the penetration depths in these figures correspond to the depth below cofferdam excavation level. The maximum driving resistance calculated for the H-pile to penetrate the extremely dense sand and gravel stratum is only 94 blows/m. Compression driving stresses do not exceed 218 MPa and are therefore within the recommended limits for H-piles given in Chapter 11. Based on the driveability study results, the low displacement H-pile would be a preferable foundation design. The results also indicate the H-pile could be driven to bedrock, and therefore likely for a higher ultimate pile capacity.

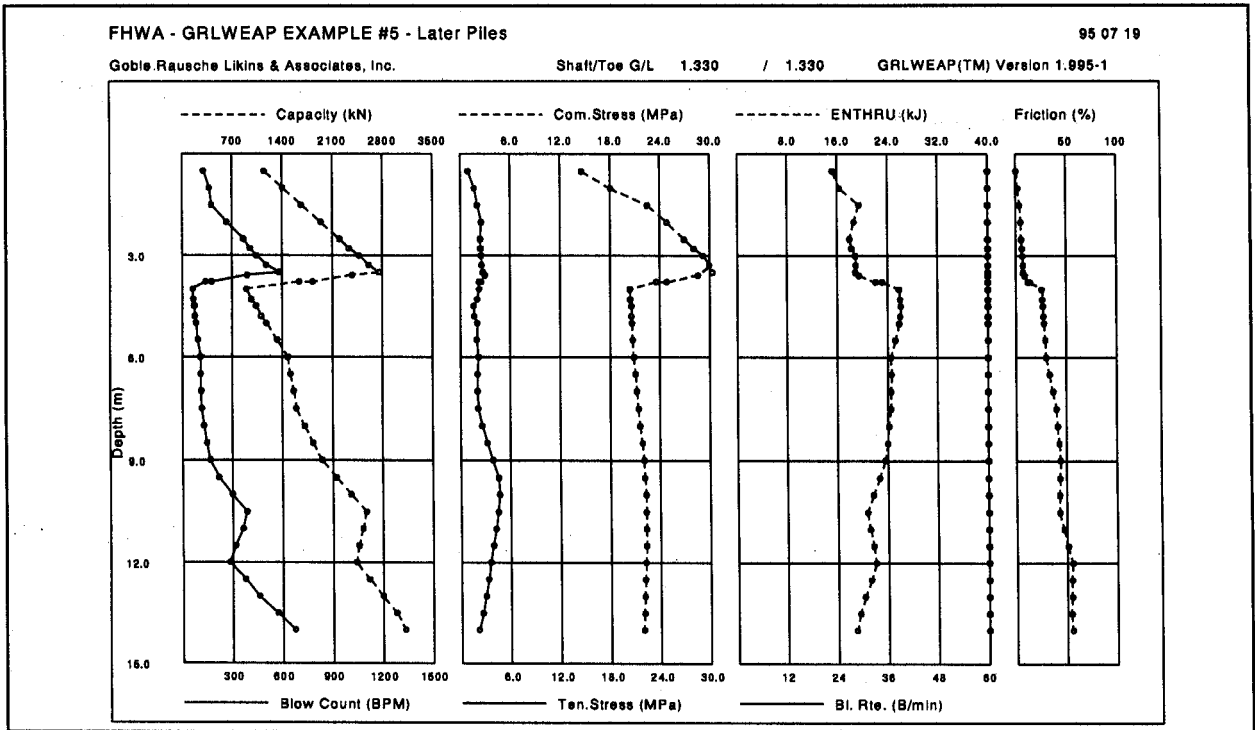


Figure 17.13 Example 5 Driveability Results for Later 356 mm Concrete Piles with Densification

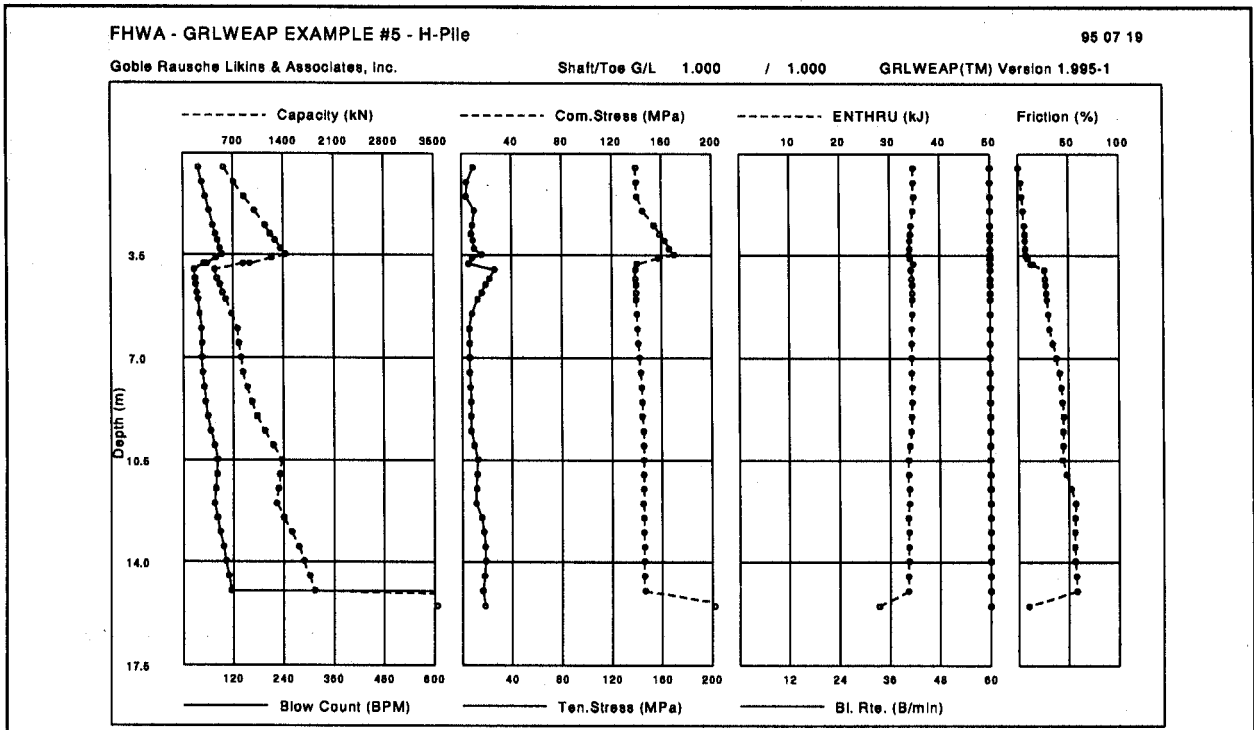


Figure 17.14 Example 5 Driveability Results for H-Pile

17.5.6 Example 6 - Driving System Characteristics

Example 6 presents a wave equation comparison of two hammers having the same potential energy. Both Engineering News and Gates dynamic formulas consider only the potential energy of the driving system. The driving resistance required for a specific capacity by either of these formulas would be the same as long as two hammers had the same potential energy. The wave equation predicted driving resistances for the two hammers in the same pile-soil condition is, however, quite different.

In this example problem, a 356 mm by 9.5 mm wall closed end pipe pile is to be driven to an ultimate pile capacity of 1800 kN. The pile has a furnished length of 20 meters and an embedded length of 16 meters. A static analysis indicates that the soil resistance distribution will be 30% shaft resistance and 70% toe resistance. The shaft resistance will be distributed triangularly along the embedded portion of the pile shaft. Experience has shown that the materials near the pile toe are highly elastic and therefore have a larger (7.5 mm) than normal (3.0 mm) toe quake. The example problem's soil profile is presented in Figure 17.15.

The contractor is considering using either a Vulcan 014 or an ICE 42-S to drive the piles. Both hammers have a rated energy of about 57 kJ. For the Vulcan 014 hammer, the rated energy is based upon a 62.3 kN ram and a 0.91 m stroke whereas the ICE 42-S hammer is rated based upon a 18.2 kN ram and a 3.13 m stroke. The helmet weights for the Vulcan 014 and ICE 42-S are 7.45 and 9.12 kN, respectively. The contractor indicates that for the Vulcan 014, the hammer cushion will consist of 152 mm of Nycast with an elastic modulus of 1428 MPa, and a cross sectional area of 1508 cm². For the ICE 42-S, the hammer cushion will consist of 51 mm Blue Nylon, which has an area of 2568 cm², and an elastic modulus of 1257 MPa.

Wave equation results for the two hammers are plotted on the same bearing graph in Figure 17.16. For the pile and soil condition analyzed, the Vulcan 014 (Hy Ram) requires a driving resistance of 275 blows/m for an 1800 kN ultimate pile capacity whereas the ICE 42-S (Lt Ram) requires a driving resistance of 533 blows/m. Hence, even though both hammers have the same potential energy, the required driving resistance for an 1800 kN ultimate pile capacity is quite different. The Vulcan 014 requires a lower driving resistance because the duration of the hammer blow is longer and is more efficient in advancing the pile in this particular example of a highly elastic soil.

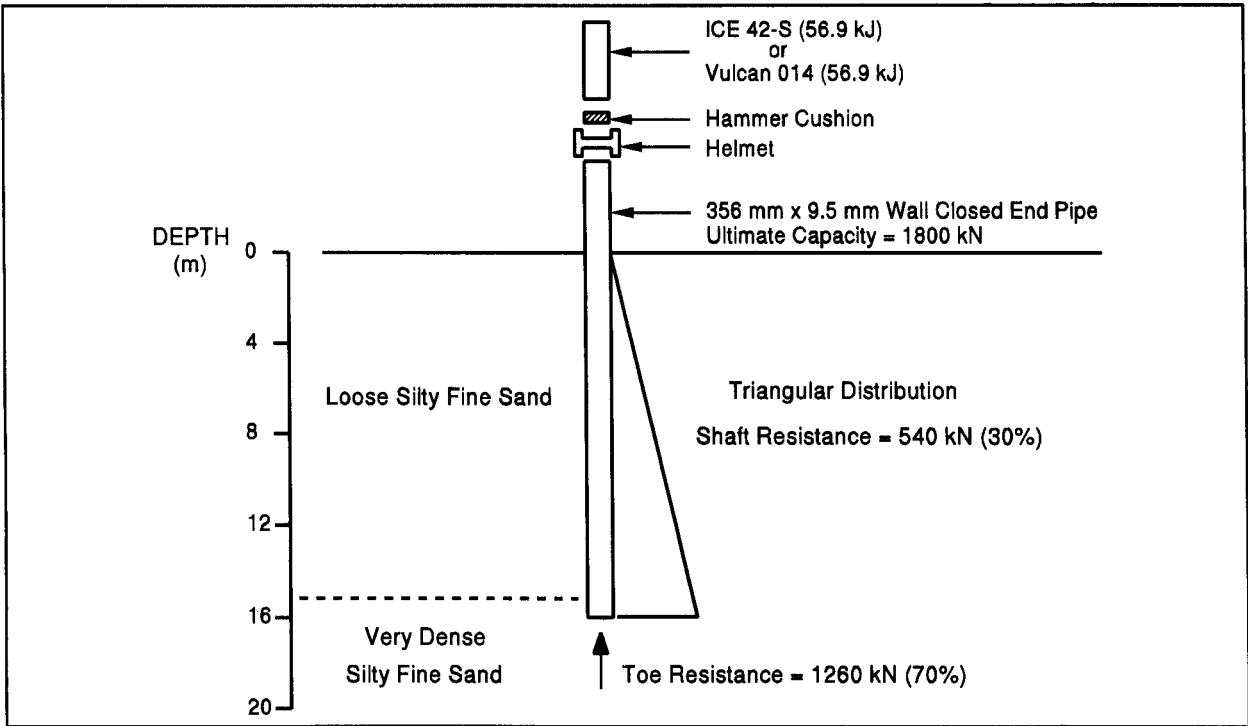


Figure 17.15 Example 6 Problem Profile

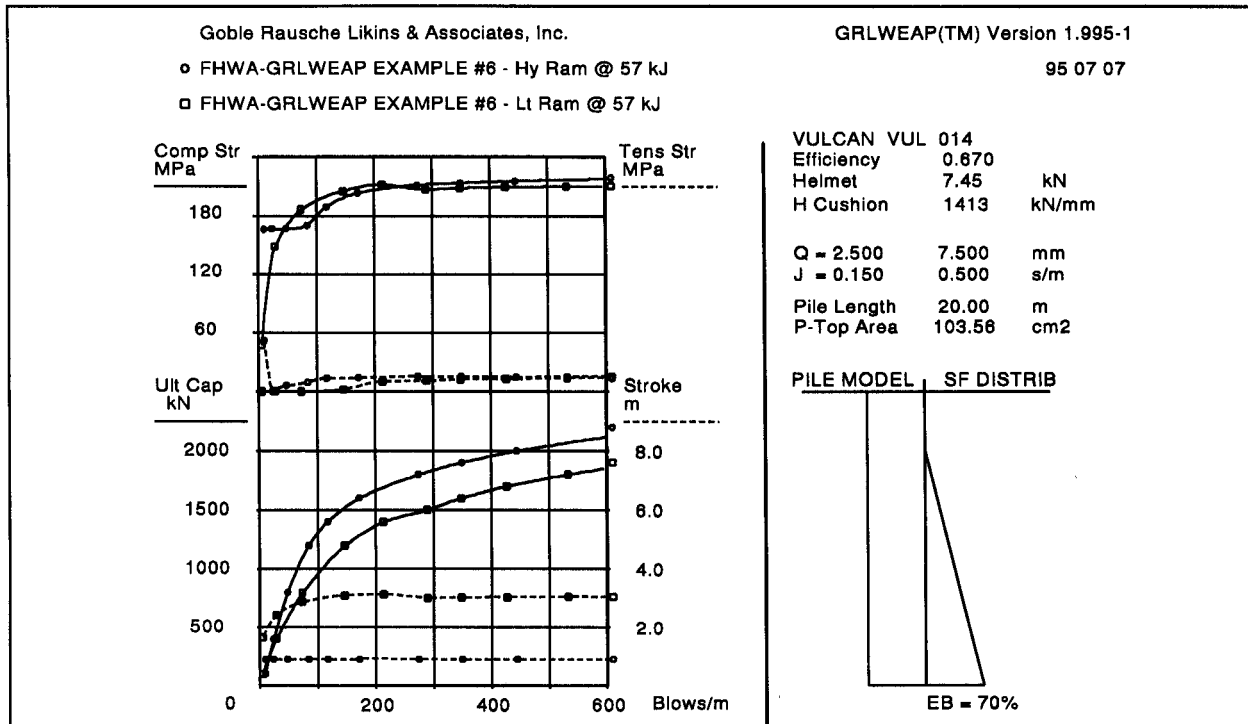


Figure 17.16 Example 6 Bearing Graph Comparison of Two Hammers with Equivalent Potential Energy

This example illustrates the dynamic complexities of hammer-pile-soil interaction. Clearly the potential energy alone, which is all that is considered in dynamic formulas, is not an adequate assessment of pile driveability.

17.5.7 Example 7 - Assessment of Pile Damage

Another pile driving construction problem is pile damage. It is frequently assumed that steel H-piles can be driven through boulders and fill materials containing numerous obstructions. Investigations reveal this is not true. H-piles without commercially manufactured pile toe reinforcement are one of the most easily damaged pile types. The damage occurs because of the ease with which flanges can be curled, rolled and torn. Pile damage has detrimental effects on both driving resistance and ultimate capacity.

This example will illustrate how the wave equation was used to obtain insight into a construction problem involving pile damage. The project conditions are shown in Figure 17.17. The HP 310 x 79 H-piles were 10.5 meters in length with a design load of 845 kN and an ultimate pile capacity of 1690 kN. The soil profile consisted of 4.5 to 5.0 m of miscellaneous fill, including some bricks and concrete. Below the fill was 4.5 m of silty clay that increased in strength with depth. The clay overlaid bedrock which was encountered at a depth of about 10 m.

The contractor selected an MKT DE-40 single acting diesel hammer with a rated energy of 43.4 kJ to drive the piles. Using the Engineering News formula specified in the contract documents, the required driving resistance was 590 blows/m for this hammer. Figure 17.18 presents the wave equation results. These results indicate that the maximum compression stress at a driving resistance of 590 blows/m was 285 MPa, which is well in excess of the 248 MPa yield stress of the pile material. The wave equation results indicate this maximum compression stress is located at the pile toe. In addition, the pile capacity at that driving resistance is well in excess of the 1690 kN required ultimate capacity. The wave equation results clearly indicate the Engineering News formula driving criteria resulted in significant overdriving of the piles at very high driving stress levels.

In accordance with the contract requirement, several load tests were conducted. In all cases the piles failed to carry the 1690 kN ultimate capacity, in spite of the fact that several of the piles were driven to a dynamic resistance exceeding 800 blows/m with no indication of damage at the pile head. As a result of the high driving resistances to

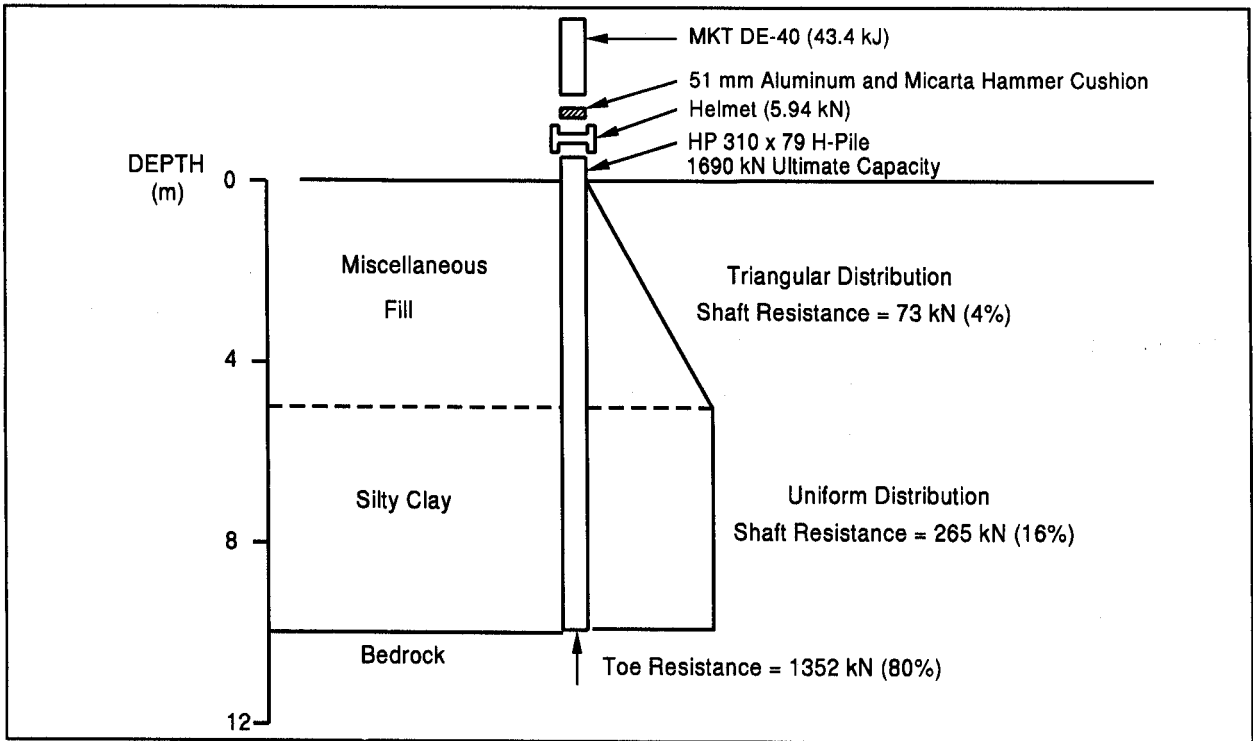


Figure 17.17 Example 7 Problem Profile

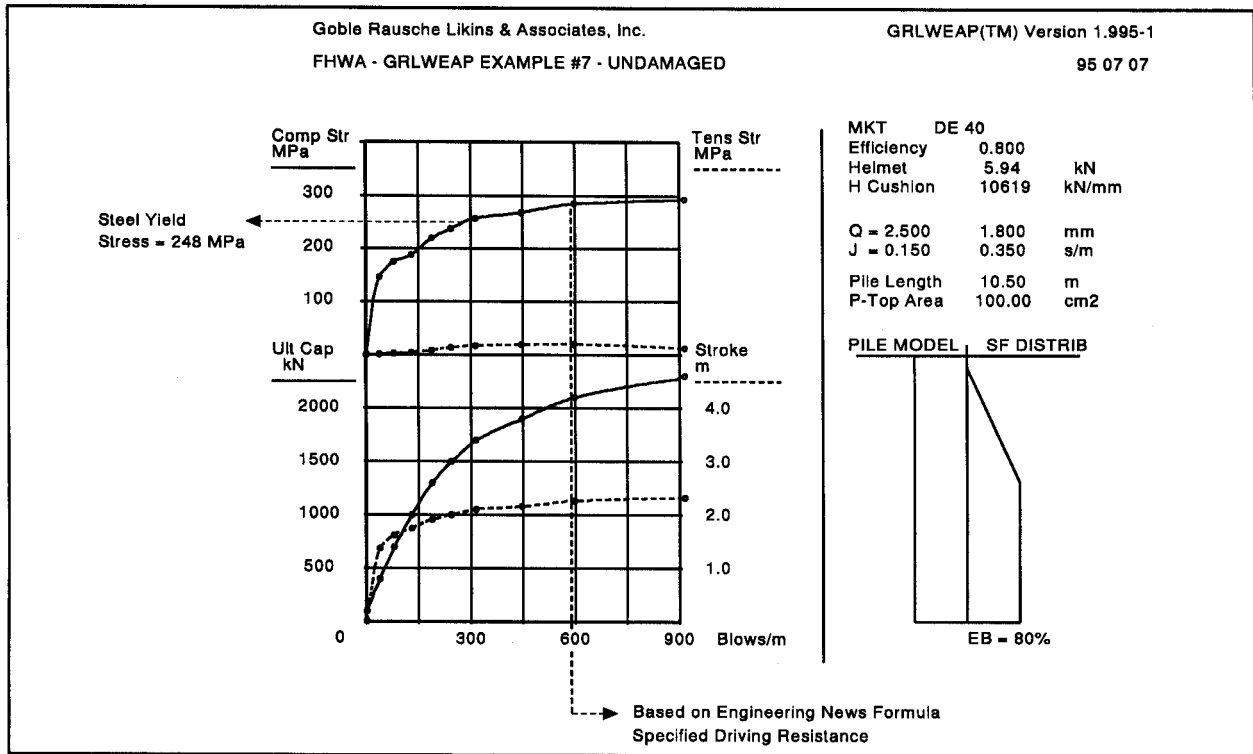


Figure 17.18 Example 7 Wave Equation Bearing Graph for Proposed Driving System

which several piles were driven, it was apparent that additional driving would not result in satisfactory pile performance. Consequently, the contractor was requested to pull several of the piles to check for possible damage. Upon extraction, it was noted that the piles were severely damaged. The flanges were separated and rolled up from the web. The damage occurred as the unprotected piles were driven through the miscellaneous rubble fill.

The effect of the damage on pile driveability can be evaluated with a wave equation analysis. Records indicate piles driven as hard as 800 blows/m did not support the 1690 kN ultimate capacity. Hence, this provides a reference point on the wave equation bearing graph on the driveability of a damaged pile. The bearing graph for the damaged pile was determined by adjusting the stiffness of the lower pile segment until the results agreed with the driving resistance and capacity observations. The resulting toe segment stiffness was roughly only 10% of that of an undamaged pile.

Figure 17.19 presents wave equation results for both an undamaged pile and a damaged pile. The results indicate that the ultimate load of 1690 kN could not be obtained for the damaged pile, regardless of the magnitude of the driving resistance. Essentially, the damaged pile section "cushioned" the hammer blow and attenuated the hammer energy. Once damaged, the soil resistance at the pile toe could not be overcome and, therefore the pile would not advance. This illustrates that driving stresses can also limit the driveability of a pile to the required ultimate capacity.

The pile damage potential on this project could have been greatly reduced if a wave equation had been performed during the design stage or had been specified for construction control. The wave equation bearing graph in Figure 17.18 illustrates that the ultimate capacity of 1690 kN could be obtained by the contractor's driving system at a driving resistance slightly greater than 300 blows/m. The compression driving stress at this driving resistance is slightly above the steel yield strength of 248 MPa. Hence the potential damage problem would have been clearly apparent at the time of the contractor's hammer submittal. Additional wave equation analyses of the contractor's driving system could have been performed to determine if driving stress levels could be reduced to acceptable levels by using reduced fuel settings and shorter hammer strokes. If driving stresses could not be controlled in this manner, approval of the proposed driving system should not have been obtained, and alternate hammers should have been evaluated.

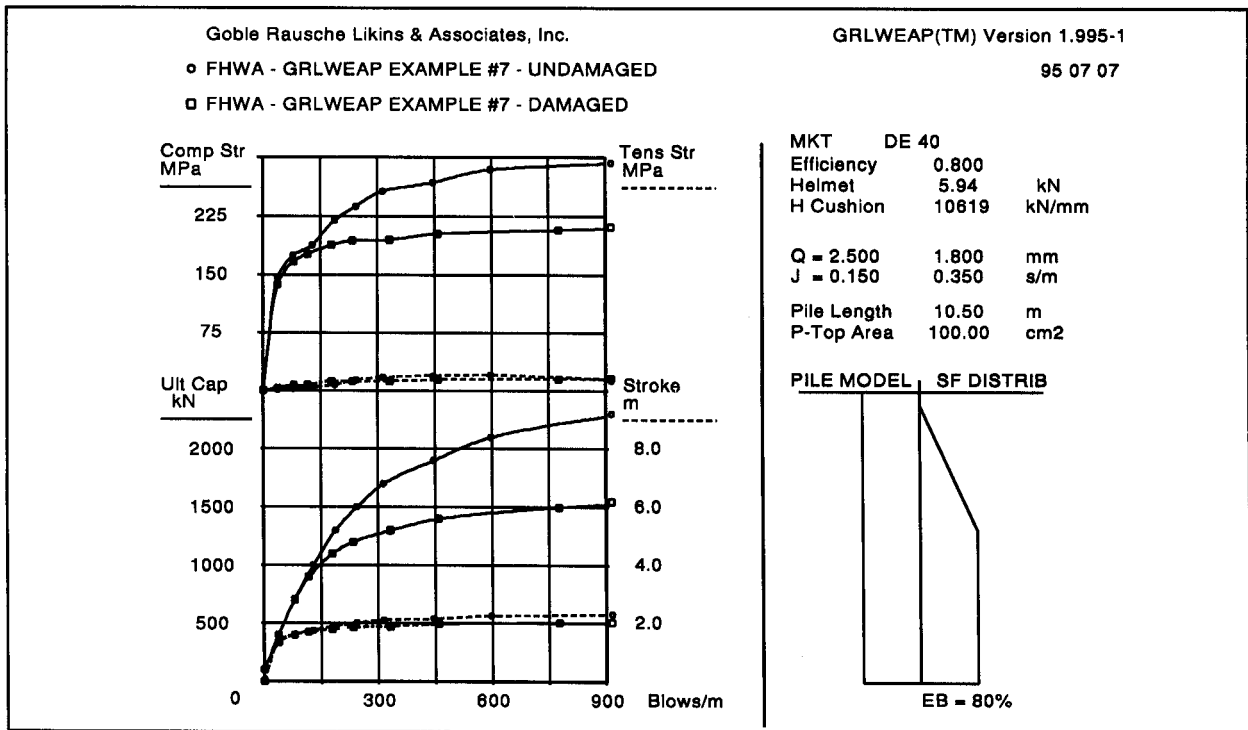


Figure 17.19 Example 7 Comparison of Wave Equation Bearing Graphs for Damaged and Undamaged Piles

17.5.8 Example 8 - Selection of Wall Thickness

This wave equation example demonstrates the evaluation of the required wall thickness for a pipe pile. Consider the soil and problem profile presented in Figure 17.20. Based upon static analyses and structural loading conditions, a 324 mm outside diameter closed end pipe pile with a design load of 665 kN is selected as the pile foundation type. Static analysis indicates the overlying unsuitable layers provide 140 kN of resistance. Hence the required ultimate pile capacity is 1470 kN. The calculated embedded pile length for this ultimate capacity is 14 m.

Since this is a design stage issue, the actual hammer and driving system configuration is unknown. Therefore, a typical hammer size and driving system configuration must be assumed with consideration of typical, locally available equipment as well as the calculated soil resistance at the time of driving. These factors led to the selection of a Berminghammer B-225 single acting diesel hammer with a rated energy of 39.7 kJ.

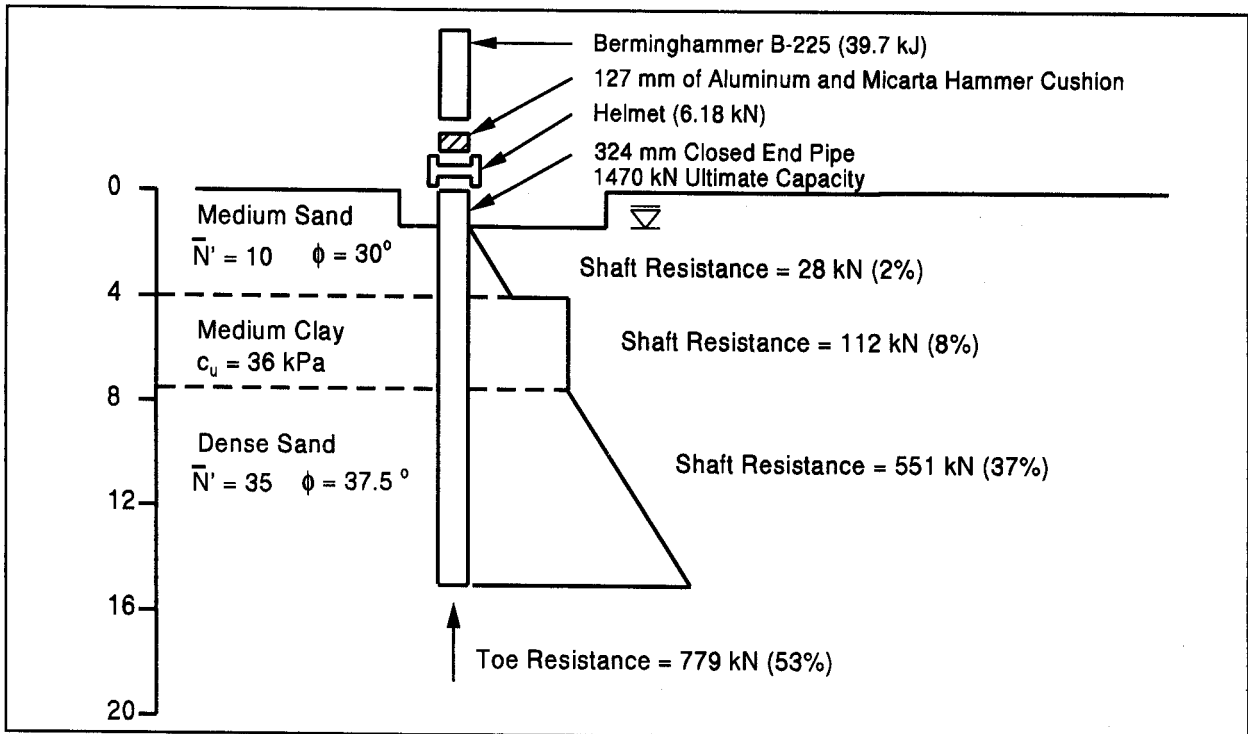


Figure 17.20 Example 8 Problem Profile

Wave equation analyses were performed for a 324 mm outside diameter pipe pile with wall thicknesses of 6.3, 7.1, 7.9 and 9.5 mm. Figures 17.21 and 17.22 present the results of these analyses. For the 6.3 mm wall thickness, the wave equation results indicate that a driving resistance of 615 blows/m will be required for the ultimate capacity of 1470 kN and that compression driving stresses approach 256 MPa. While this compression driving stress level is acceptable for Grade 3 pipe with a yield strength of 310 MPa, the 6.3 mm wall thickness pipe does not have suitable driveability for the project conditions. (As per Chapter 12, suitable driveability is a driving resistance between 30 and 120 blows per 0.25 meter or 120 and 480 blows/m.)

Wave equation results for the 7.1 mm wall thickness indicate that a driving resistance of 487 blows/m will be encountered for the ultimate capacity of 1470 kN and that compression driving stresses approach 225 MPa. While the driving stresses are again within acceptable limits for Grade 3 pipe, the driving resistance is still considered high and exceeds the 120 to 480 blow/m acceptance criteria. Differences between actual and assumed soil parameters (resistance distribution, quake, and damping) could easily increase the required driving resistance in the field and turn the high driving resistance into a refusal driving situation.

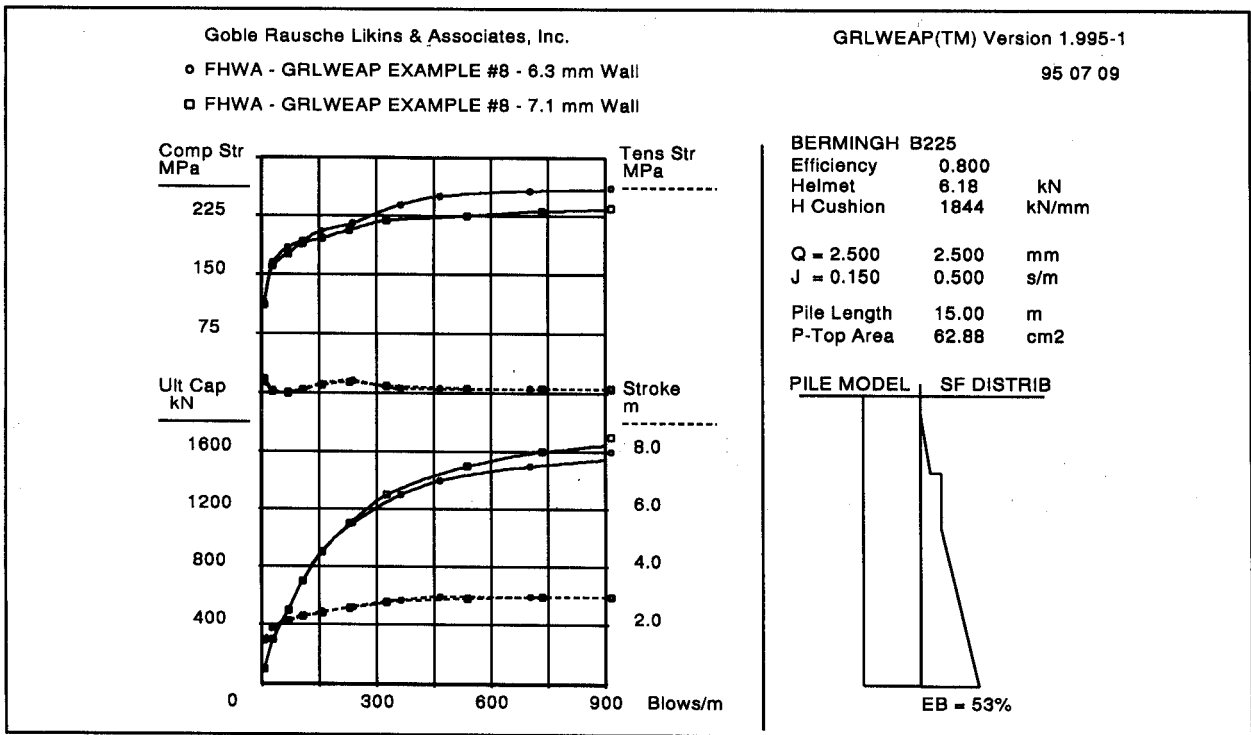


Figure 17.21 Example Bearing Graphs for 6.3 and 7.1 mm Wall Pipe Piles

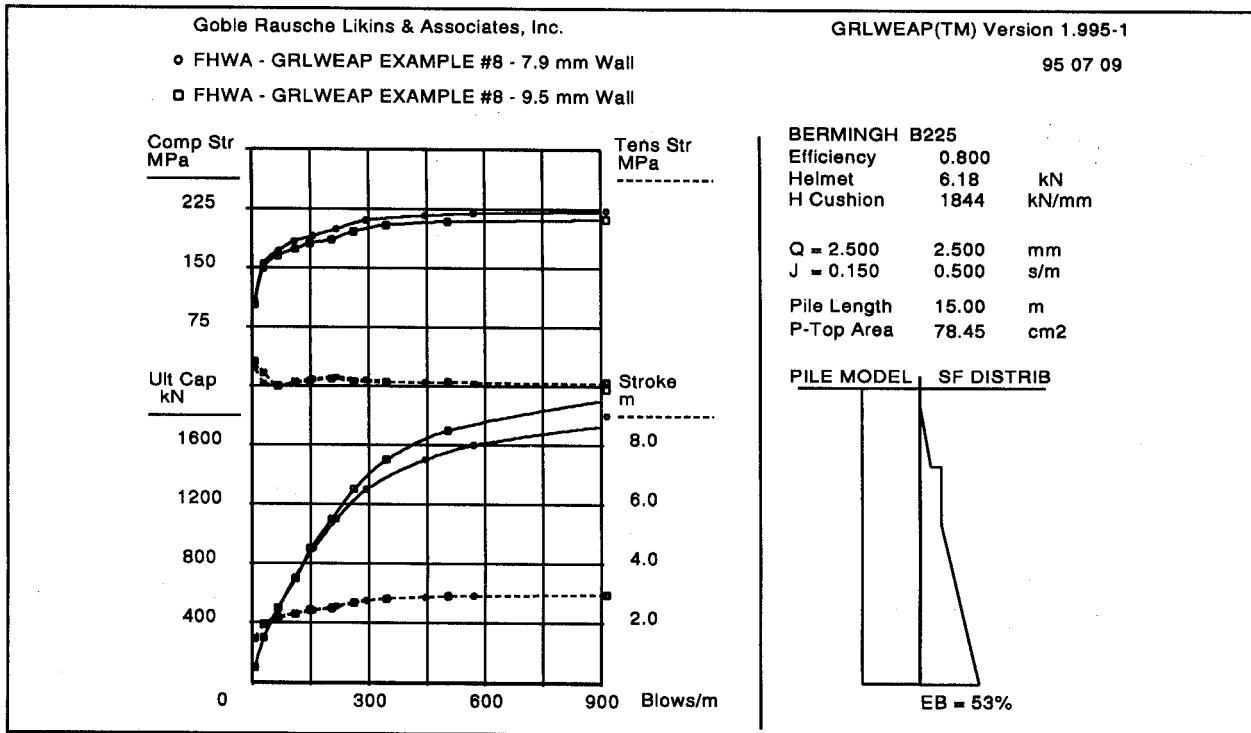


Figure 17.22 Example 8 Bearing Graph for 7.9 and 9.5 mm Wall Pipe Piles

For the 7.9 mm wall thickness, wave equation results indicate that a driving resistance of 412 blows/m is required for the ultimate capacity of 1470 kN and that compression driving stresses approach 217 MPa. Both the driving resistance and driving stresses are now within acceptable limits. Therefore, the 7.9 mm wall thickness pipe has the suitable driveability for the required capacity and is considered an acceptable foundation design. The 9.3 mm wall thickness pipe has even greater driveability and could also be chosen for reason of time savings during installation or other design considerations.

17.5.9 Example 9 - Evaluation of Vibratory Driving

This example will illustrate the use of a wave equation analysis for evaluating vibratory hammer installation of the sheet piles required for cofferdam construction in Example 5. The sheet piles of Example 5 have to be installed using a vibratory hammer. The contractor has an ICE 815 hammer available and intends to drive pairs of PZ27 sheet piles whose combined cross sectional area is 154 cm². These are Z-section sheets, each with a width of 460 mm, a depth of 300 mm, and a thickness of 10 mm. At the time of sheet pile installation, the soil within the cofferdam is not excavated and the piles are therefore driven from mudline to an estimated depth of 10 m. The sheet pile length is 15 m.

An evaluation of the static soil resistance by the effective stress method has been demonstrated earlier. For the non-excavated condition, first a 5 m thick layer of soft silt has to be penetrated by the sheet piles, followed by the extremely dense sand and the dense sand and gravel layers. The corresponding calculated soil resistance and the associated dynamic soil parameters are shown in Figure 17.23(a). Note that soil damping has been set to twice the normal values to model, in a very approximate manner, the effects of lock friction.

Depth m	Skin Frictn kPa	End Bearing kN	Skin Quake mm	Toe Quake mm	Skin Damping s/m	Toe Damping s/m
0.00	.00	.00	2.500	2.500	1.300	1.000
5.00	7.70	8.00	2.500	2.500	1.300	1.000
5.00	10.70	27.00	2.500	2.500	.330	1.000
9.00	29.90	77.00	2.500	2.500	.330	1.000
9.00	27.70	77.00	2.500	2.500	.300	1.000
15.00	50.70	140.00	2.500	2.500	.330	1.000

Figure 17.23(a) Example 9 Soil Resistance Information for Vibratory Sheet Pile Driving

Analyses are performed for pile penetration depths between 4 and 10 m at 1 m increments. For the driveability analysis, the statically calculated resistance values are directly used without any gain or loss factors. This might be in contrast to common experience which indicates that a large percentage of a soil's shaft resistance is lost due to soil vibration when driving with a vibratory hammer. The analysis therefore presents a worst case situation and would be particularly interesting to the contractor.

Figure 17.23(b) lists the hammer model, which consists of two masses and an elastomer connection modeled by a spring with 140 kN/mm spring stiffness. The product of the listed eccentric weight and the eccentric radius equals the hammer's rated moment. As per input, the frequency has been chosen at 16 Hz (960 RPM) even though the hammer is capable of running at 26 Hz. Also, an efficiency value of 0.8 and a start-up time of 0.1 second have been entered. In reality, the start-up time is probably much longer, as it includes the elapsed time between turning the hammer on and reaching full frequency in the hammer. However, for all except the first penetration analyzed, the start-up time is really non-existent as the hammer is run continuously. Furthermore, the start-up time has no significant effect on the results and is primarily important for reaching a numerically satisfactory solution. Finally, a 25 kN line pull (an upward directed crane force) has been entered to keep the hammer/pile system stable. This line pull effectively reduces the dead weight of the hammer-pile system, which plays a major role in advancing the pile. Probably, during harder driving, the operator will let the line slacken which will allow for a significant increase of the speed of pile penetration. Of course, the crane operator will not be able to maintain an exact line pull force and additional analyses should be run to check the effect of this force on the sheet pile penetration.

Vibratory ICE 815, 2 PZ 27 Sheet Piles					
Hammer Model of: 815			Made by: ICE		
No.	Weight kN	Stiffn kN/mm	CoR	C-Slk mm	Dampg kN/m/s
1	35.600				
2	41.720	140.0	1.000	3.0480	1425.6
Top Weight	(kN)	35.60	Bottom Weight + Clamp (kN)		41.72
Connect. Stiffness	(kN/mm)	140.00	Connect. Dashpot (kN/m/s)		1425.6
Eccenter Radius	(m)	.112	Eccenter Weight (kN)		4.450
Line Pull	(kN)	25.00	Actual Target Freq. (1/s)		16.00
Efficiency		.8000	Rated Power (kW)		375.0
Start-Up Time	(s)	.1000			

Figure 17.23(b) Example 9 Vibratory Hammer Model and Hammer Options

Figure 17.23(c) summarizes pile and soil model. For the first analyzed depth of 4 m, the static capacity of 12.1 kN is very small. This capacity was obtained after subtracting the weight of the sheet pile section extending above grade from the statically calculated pile capacity. Considering the hammer weight of nearly 80 kN minus line pull of 25 kN, the sheet pile will penetrate very rapidly at this depth as indicated in the final result table in Figure 17.23(d). After the pile penetrates into the sand layer, the required penetration time will increase, eventually reaching 46 seconds for 1 m at a penetration of 10 m. The calculated total time of penetration is 1.4 minutes, and although this result is subject to many uncertainties, it can be concluded that the hammer is easily capable of driving the sheet pile pairs to the design depth.

Depth 1 at 4.0 m; Dead Load 12.1 kN; Shaft/Toe G/L: 1.000/ 1.000

PILE PROFILE:

L b Top	Area	E-Mod	Spec Wt	Circumf	Strength	Wave Sp	EA/c
m	cm ²	MPa	kN/m ³	m	MPa	m/s	kN/m/s
.00	153.6	210000.	78.50	3.150	248.00	5123.	629.45
15.00	153.6	210000.	78.50	3.150	248.00	5123.	629.45

Wave Travel Time - 2L/c - = 5.856 ms

Pile and Soil Model for Rut = 33.2 kN

No.	Weight	Stiffn	C-Slk	T-Slk	CoR	Soil-S	Soil-D	Quake	LbTop	Circumf	Area
	kN	kN/mm	mm	mm		kN	s/m	mm	m	m	cm ²
1	1.205	3225.	3.000	.000	.85	.0	.000	2.50	1.00	3.2	153.6
2	1.205	3225.	.000	.000	1.00	.0	.000	2.50	2.00	3.2	153.6
3	1.205	3225.	.000	.000	1.00	.0	.000	2.50	3.00	3.2	153.6
12	1.205	3225.	.000	.000	1.00	1.8	1.300	2.50	12.00	3.2	153.6
13	1.205	3225.	.000	.000	1.00	5.3	1.300	2.50	13.00	3.2	153.6
14	1.205	3225.	.000	.000	1.00	8.9	1.300	2.50	14.00	3.2	153.6
15	1.205	3225.	.000	.000	1.00	12.5	1.300	2.50	15.00	3.2	153.6
Toe						4.7	1.000	2.50			

PILE, SOIL, ANALYSIS OPTIONS:

Uniform/Non-Uniform/2-Pile	0	Pile Segment Generation	Automatic
No. of Slacks/Splices	0	Pile Damping (%)	1
Soil Damping Option	Smith	Pile Damping Fact. (kN/m/s)	12.589
Soil Resistance Distr. No.	0	Soil Damping Exponent	1.000
Max No Analysis Iterations	0	Time Increment/Critical	160
Residual Stress Analysis	0	Output Option	25
Output Segment Generation	Automatic	Output Time Interval	10
Analysis Time-Input (ms)	0		

Figure 17.23(c) Example 9 Pile and Soil Model and Options

SUMMARY OVER DEPTHS

Depth	G/L at Shaft and Toe: 1.000 1.000							
	Rut	Frictn	End Bg	PenTime	max Str	min Str	Power	
m	kN	kN	kN	s/m	MPa	MPa	kW	
4.0	33.2	28.5	4.7	1.3	11.403	-5.946	44.5	
5.0	57.8	51.1	6.7	3.7	13.216	-4.822	22.0	
6.0	131.8	95.0	36.8	6.8	18.043	-6.560	30.5	
7.0	201.8	151.9	49.9	9.2	22.229	-12.856	44.9	
8.0	287.1	224.1	62.9	13.4	27.848	-21.055	64.9	
9.0	387.4	311.6	75.8	24.3	35.571	-29.803	88.9	
10.0	492.4	405.7	86.7	46.0	44.184	-37.742	110.2	

Total Driving Time 1.40 minutes

Driving time for continuously running hammer; any waiting times not included

Figure 17.23(d) Example 9 Final Summary Table

17.6 ANALYSIS DECISIONS FOR WAVE EQUATION PROBLEMS

17.6.1 Selecting the Proper Approach

Even though the wave equation analysis is an invaluable tool for the pile design process, it should not be confused with a static geotechnical analysis. The wave equation does not determine the capacity of a pile based on soil boring data. The wave equation calculates a driving resistance for an assumed ultimate capacity, or conversely, it assigns an estimated ultimate capacity to a pile based on a field observed driving resistance. It is one thing to perform a wave equation bearing graph for a certain capacity and a totally different matter to actually realize that capacity at a certain depth. The greatest disappointments happen when pile lengths required during construction vary significantly from those computed during design. To avoid such disappointments, it is absolutely imperative that a static analysis, as described in Chapter 9, precede the wave equation analysis. The static analysis will yield an approximate pile penetration for a desired capacity or a capacity for a certain depth. The static analysis can also generate a plot of estimated pile capacity as a function of depth. It is important that the static analysis evaluates the soil resistance in the driving situation (e.g. remolded soil strengths, before excavation, before scour, before fill placement, etc.).

After the static analysis has been completed, a wave equation analysis can be performed leading either to a bearing graph or to driving resistances and stresses versus depth (driveability). Sometimes both analyses are performed. The bearing graph analysis is only valid within the proximity of the analyzed soil profile depending on the variability of the soil properties. The driveability analysis calculates driving resistances and stresses for a number of penetration depths, and therefore provides a more complete result. However, there is a very basic difference between these two approaches. The bearing graph approach allows the engineer to assess pile capacity given a driving resistance at a certain depth. The driveability analysis points out certain problems that might occur during driving. If the pile actually drives differently from the wave equation predictions, then a reanalysis with different soil resistance parameters would be needed to match the observed behavior.

Even though an accurate static analysis and a wave equation analysis have been performed with realistic soil parameters, the experienced foundation engineer would not be surprised if the driving resistance during pile installation were to differ substantially from the predicted one. Most likely the observed driving resistance would be lower than

calculated. As an example, suppose that a 500 kN pile had to be driven into a clay. With a factor of safety of 2.5, the required ultimate capacity would be 1250 kN. The static soil analysis indicates that the pile has to be 25 m long for this ultimate capacity. There would be negligible toe resistance, and based upon remolded soil strength parameters, the soil may exhibit only 50% of its long term strength during driving. It is therefore only necessary to drive the pile to a capacity of 625 kN, which should be achieved at the 25 m depth. The expected end of installation driving resistance would then correspond to 625 kN. In a restrrike test, say 7 days after installation, the 1250 kN capacity would be expected, and therefore a much higher driving resistance would be encountered than observed at the end of driving.

The above discussion points out one major reason for differences between analysis and reality. However, as with all mathematical simulations of complex situations, agreement of wave equation results with actual pile performance depends on the realism of the method itself, and on the accuracy of the model parameters. The accuracy of the wave equation analysis will be poor when either soil model or soil parameters inaccurately reflect the actual soil behavior, and when the driving system parameters do not represent the state of maintenance of hammer or cushions. The pile behavior is satisfactorily represented by the wave equation approach in the majority of cases. A review of potential wave equation error sources follows.

17.6.2 Hammer Data Input, External Combustion Hammers

The most important input quantity is the hammer efficiency. It is defined as that portion of the potential ram energy that is available in the form of kinetic ram energy immediately preceding the time of impact. Many sources of energy loss are usually lumped into this one number. If the hammer efficiency is set too high, then an optimistically low driving resistance would be predicted. This in turn could lead to overpredictions of ultimate pile capacity. If the efficiency is set very low, for conservative pile capacity assessments, then the stresses may be underpredicted, leading to possible pile failures during installation.

Hammer efficiency should be reduced for battered pile driving. The efficiency reduction depends on the hammer type and batter angle. For hammers with internal ram energy measurements, no reductions are required. Modern hydraulic hammers often allow for a continuously adjustable ram kinetic energy which is measured and displayed on the control panel. In this case the hammer efficiency does not have to cover friction losses

of the descending ram, but only losses that occur during the impact (e.g. due to improper ram-pile alignment) and it may therefore be relatively high (say 0.95). For such hammers, the wave equation analysis can select the proper energy level for control of driving stresses and economical driving resistances by trying various energy (stroke) values which are lower than the rated value.

Similarly, a number of air/steam hammers can be fitted with equipment that allows for variable strokes. The wave equation analysis can then help to find that driving resistance at which the stroke can be safely increased to maximum. It is important, however, to realize that the reduced stroke is often exceeded, and that the maximum stroke not fully reached. Corresponding increases and decreases of efficiency for the low and high stroke may therefore be necessary.

17.6.3 Hammer Data Input, Diesel Hammers

The diesel hammer stroke increases when the soil resistance, and therefore driving resistance, increases. GRLWEAP simulates this behavior by trying a down stroke, and when the calculated up stroke is different, repeats the analysis with that new value for the down stroke. The accuracy of the resulting stroke is therefore dependent on the realism of the complete hammer-pile-soil model and should therefore be checked in the field by comparison with the actual stroke. The consequences of an inaccurate stroke could be varied. For example, an optimistic assumption of combustion pressure could lead to high stroke predictions and therefore to non-conservative predictions of ultimate pile capacity while stress estimates would be conservatively high (which may lead to a hammer rejection).

Stroke and energy transferred into the pile appear to be closely related, and large differences (say more than 10%) between stroke predictions and observations should be explained. Unfortunately, higher strokes do not always mean higher transferred energy values. When a hammer preignites, probably because of poor maintenance, then the gases combusting before impact slow the speed of the descending ram and cushion its impact. As a result, only a small part of the ram energy is transferred to the pile. A larger part of the ram energy remains in the hammer producing a high stroke. If, in this case, the combustion pressure would be calculated by matching the computed with the observed stroke under the assumption of a normally performing hammer, then the calculated transferred energy would be much higher than the measured one and calculated blow counts would be non-conservatively low. It is therefore recommended

that hammer problems are corrected as soon as possible on the construction site. If this is not possible then several diesel stroke or pressure options should be tried when matching analysis with field observation and the most conservative results should be selected. Section 17.7.1.1 discusses the available diesel hammer stroke options in greater detail.

GRLWEAP's hammer data file contains reduced combustion pressures for those hammers which have stepwise adjustable fuel pumps. Note that decreasing combustion pressures may be associated with program input fuel pump settings that have increasing numbers. For example, Delmag hammers' fuel pump settings 4 (maximum), 3, 2, and 1 (minimum) correspond to GRLWEAP hammer setting inputs 1 (or 0) 2, 3, and 4.

17.6.4 Cushion Input

Cushions are subjected to destructive stresses during their service and therefore continuously change properties. Pile cushions experience a particularly pronounced increase in their stiffness because they are generally made of soft wood with its grain perpendicular to the load. Typically, the effectiveness of wood cushions in transferring energy increases until they start to burn. Then they quickly deteriorate; this happens after approximately 1500 blows. To be conservative, the harder cushion (increased elastic modulus, reduced thickness) should be used for driving stress evaluations and the less effective cushion (lower stiffness, lower coefficient of restitution) should be analyzed for pile capacity calculations. If accurate values are not known, parameter changes of 25% from nominal might be tried. Wood chips as a hammer cushion are totally unpredictable and therefore should not be allowed. This is particularly true when the wave equation is used for construction control.

In recent years, uncushioned hammers have been used with increasing frequency. For the wave equation analysis, since there is no cushion spring, the stiffness of the spring between hammer and helmet is derived from either ram or impact block (diesels). This stiffness is very high, much higher than the stiffnesses of most other components within the system, and for numerical reasons, may lead to inaccurate stress predictions. Analyses with different numbers of pile segments would show the sensitivity of the numerical solution. In general, the greater the number of pile segments, the more accurate the stress calculation.

17.6.5 Soil Parameter Selection

The greatest errors in ultimate capacity predictions are usually observed when the soil resistance has been improperly considered. A very common error is the confusion of design loads with the wave equation's ultimate capacity. Note that the wave equation capacity always must be divided by a factor of safety to yield the allowable design load. Factors of safety suggested by FHWA and AASHTO were discussed in Chapter 15.

Since the soil is disturbed at the end of driving, it often has a lower capacity at that time (occasionally also a higher one) than at a later time. For this reason, a restrike test should be conducted to assess the ultimate pile capacity after time dependent soil strength changes have occurred. However, restrike testing is not always easy. The hammer is often not warmed up and only slowly starts to deliver the expected energy while at the same time the bearing capacity of the soil deteriorates. Depending on the sensitivity of the soil, the driving resistance may be taken from the first 75 mm of pile penetration even though this may be conservative for some sensitive soils. For construction control, rather than restrike testing many piles, it is more reasonable to develop a site specific setup factor in a preconstruction test program. As long as the hammer is powerful enough to move the pile during restrike and mobilize the soil resistance, restrike tests with dynamic measurements are an excellent tool to calculate setup factors. For the production pile installation criterion, the required end of driving capacity is then the required ultimate capacity divided by the setup factor. Using the wave equation analysis and the reduced end of driving capacity, the required end of driving blow count is then calculated.

Although the proper consideration of static resistance at the time of driving or restriking is of major importance for accurate results, dynamic soil resistance parameters sometimes play an equally important role. Damping factors have been observed to vary with waiting times after driving. Thus, damping factors higher than recommended in the GRLWEAP Manual (say twice as high) may have to be chosen for analyses modeling restrike situations. Studies on this subject are still continuing. In any event, damping factors are not a constant for a given soil type. For soft soils, they may be much higher than recommended and on hard rock they may be much lower. Choosing a low damping factor may produce non-conservative capacity predictions.

Shaft quakes are usually satisfactory as recommended at 2.5 mm. However, larger toe quakes than the typically recommended pile diameter divided by 120 may have to be

chosen, particularly when the soil is rather sensitive to dynamic effects. Only dynamic measurements can reveal a more accurate magnitude of soil quakes. However, short of such measurements, conservative assumptions sometimes have to be made to protect against unforeseen problems. Fortunately, toe quakes have a relatively insignificant effect on the wave equation results of piles having most of their resistance acting along the shaft. For end bearing piles however, particularly displacement piles, large toe quakes often develop during driving in saturated soils causing the toe resistance to build up only very slowly during the hammer blow. Thus, at the first instant of stress wave arrival at the pile toe, little resistance exists and tension stresses can develop. In the case of concrete piles, the tension stresses can produce pile damage. At the same time, large toe quakes dissipate an unusually large amount of energy and therefore cause high blow counts. Thus, more cushioning or lower hammer strokes may not be a possible alternative for stress reductions. Instead, in extreme cases, hammers with heavier rams and lower strokes had to be chosen to reduce the detrimental effects of large toe quakes (see also Example 6 in Section 17.5.6).

Stress predictions, particularly tension stresses, are also sensitive to the input of the resistance distribution and to the percentage of toe resistance. If the soil resistance distribution is based on a static analysis, then chances are that the shaft resistance is set too high because of the loss of shaft resistance during driving. It is therefore recommended that driveability analyses be performed with shaft resistances reduced by estimated setup factors which will adjust the statically calculated capacity to the conditions occurring during driving.

Residual stress wave equation analyses are superior to normal analyses in basic concept and probably also in results. Unfortunately, not enough correlation work has been performed to empirically determine dynamic soil constants (quakes and dampings) that should be used with residual stress analyses. Another reason for its slow acceptance is the slower analysis performance. However, for long slender piles with significant shaft resistance components, residual stress analyses should be performed (maybe in addition to standard analyses) to assess potentially damaging stress conditions and the possibility of ultimate capacities which could be much higher than indicated by the standard wave equation analysis. Note that residual stress analyses may not be meaningful to represent early restrike situations where energies increase from blow to blow while, in sensitive soils, capacities successively decrease. The residual stress analysis assumes that hammer energy and pile capacity are constant under several hammer blows.

17.6.6 Comparison With Dynamic Measurements

Often the first impression is that wave equation predicted stresses and capacity values agree quite well with results from field dynamic measurements described in Chapter 18. However, there are additional observations and measurements that should be compared, such as stroke, bounce chamber pressure, and transferred energy. Often transferred energy values are somewhat lower than calculated, and adjustment of hammer efficiency alone may improve energy agreement but produce problems with driving stress and capacity agreement. Thus instead of adjusting hammer efficiency, the coefficients of restitution may have to be lowered. Sometimes matching of measured values can be very frustrating and difficult, and the task should be done with reason. Matching stresses and transferred energies within 10% of the observed or measured quantities may be accurate enough. **The wave equation maximum stresses in the final summary table can be anywhere along the length of the pile and may therefore not occur at the same location where the field measured maxima occur. When comparing GRLWEAP and field measurement results, it is therefore important to check the driving stresses in the extreme tables for the pile segment that corresponds to the measurement location.**

In summary, the following procedure is suggested for matching wave equation predictions with field measurements:

- a. All adjustments are done until the quantities to be matched agree within 10%. It is to be realized that CAPWAP and GRLWEAP work with different models and input quantities and therefore cannot agree perfectly.
- b. Perform wave equation modeling as accurately as possible for the system which measurements were taken. Use observed stroke, CAPWAP bearing capacity and associated soil parameters, and cushion properties as per standard recommended values.
- c. For matching of transferred energy, vary hammer efficiency by increasing it to at most 0.95 and decreasing it to no less than 50% of the standard recommended hammer efficiency for that hammer type. If efficiency changes are insufficient to produce agreement between wave equation calculation and field measurement results to within 10%, adjust cushion coefficients of restitution. The cushion coefficients of restitution should not be increased to values above 0.98 nor decreased to values less than 50% of the standard recommended coefficient of restitution for that cushion material.

- d. For matching the measured force, adjust cushion stiffness (pile cushion if present otherwise hammer cushion). This process may then require readjusting hammer efficiency and coefficient of restitution for energy match as per step c. Additional iterations through steps c and d should be made until transferred energy and force are within 10%.
- e. Compare blow counts. Change the shaft and toe damping and the toe quake simultaneously and proportionately to achieve agreement between measured and computed blow counts.

17.7 WAVE EQUATION INPUT PARAMETERS

As described in the previous sections, the input for a wave equation analysis consists of information about the soil, pile, hammer, cushions, helmet, splices, and any other devices which participate in the transfer of energy from hammer to soil. This input information is usually gathered from contract plans, the contractor's completed Pile and Driving Equipment Data Form (Figure 17.24), soil boring, and a static pile capacity analysis. Helpful information can also be found in the tables of the GRLWEAP Users Manual (1996) which, at least in part, is included in the "Help" display of GRLWEAP's input section. These tables are correct only for ideal situations, but may yield valuable data before a specific driving system has been identified. In general, contractors tend to assemble equipment from a variety of sources, not all of them of a standard type. It is therefore important to check and confirm what equipment the contractor has actually included in the driving system on the job.

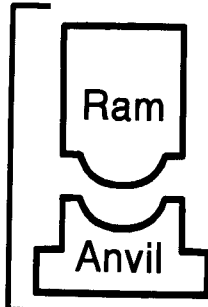
The following sections explain the most important input quantities for the data input process in the GRLWEAP program. For a more detailed explanation of input quantities, reference is made to the program's Users Manual.

For a simple bearing graph analysis, only three of the fourteen possible GRLWEAP data input pages must be used. These three pages are shown in Figures 17.25 through Figure 17.27. A cursor can be moved from one variable to another. For the variable activated by the cursor, a short help is given at the bottom of the input page. Additional help is available if an "H" is displayed at the lower right hand corner (see Input Page 1 and Input Page 2 in Figures 17.25 and 17.26). The following input descriptions summarize what type of input is requested without describing in detail the full implications of choosing certain options.

Contract No.: _____ Structure Name and/or No.: _____
 Project: _____
 County: _____ Pile Driving Contractor or Subcontractor: _____

 _____ (Piles driven by)

Hammer Components



Hammer

Manufacturer: _____ Model No.: _____
 Hammer Type: _____ Serial No.: _____
 Manufacturers Maximum Rated Energy: _____ (Joules)
 Stroke at Maximum Rated Energy: _____ (meters)
 Range in Operating Energy: _____ to _____ (Joules)
 Range in Operating Stroke: _____ to _____ (meters)
 Ram Weight: _____ (kg)
 Modifications: _____



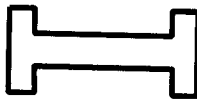
Striker Plate

Weight: _____ (N) Diameter: _____ (mm)
 Thickness: _____ (mm)



Hammer Cushion

Material #1 Material #2
 (for Composite Cushion)
 Name: _____ Name: _____
 Area: _____ (cm²) Area: _____ (cm²)
 Thickness/Plate: _____ (mm) Thickness/Plate: _____ (mm)
 No. of Plates: _____ No. of Plates: _____
 Total Thickness of Hammer Cushion: _____



Helmet (Drive Head)

Weight: _____ (kN)



Pile Cushion

Material: _____
 Area: _____ (cm²) Thickness/Sheet: _____ (mm)
 No. of Sheets: _____
 Total Thickness of Pile Cushion: _____ (mm)



Pile

Pile Type: _____
 Wall Thickness: _____ (mm) Taper: _____
 Cross Sectional Area: _____ (cm²) Weight/Meter: _____
 Ordered Length: _____ (m)
 Design Load: _____ (kN)
 Ultimate Pile Capacity: _____ (kN)

Description of Splice: _____

Driving Shoe/Closure Plate Description: _____

Submitted By: _____ Date: _____
 Telephone No.: _____ Fax No.: _____

Figure 17.24 Pile and Driving Equipment Data Form

17.7.1 GRLWEAP Input - Page 1

The first page requires title input (important for problem identification), important hammer options, pile and soil resistance input, and hammer cushion and helmet information.

```
Title:
Page: 1
SI Units

HAMMER INPUT AND ANALYSIS OPTIONS
  Hammer Stroke Fuel
  ID Number Option Setting

PILE INPUT AND ANALYSIS OPTIONS
  Number of Number of Non-uniform Pile
  Pile Segments Splices Pile Option Damping

SHAFT RESISTANCE INPUT AND DRIVEABILITY ANALYSIS OPTION
  % Shaft Shaft Resistance
  Resistance Distribution

HELMET AND HAMMER CUSHION INFORMATION
  Helmet
  Weight Area ElasMod Thickness Hammer Cushion
  .00 .00 .0 .000 .800 RoundOut Stiffness
  3.0000 .0

[ H E L P _____ Units ]
  Hammer Identification Number [H]
```

Figure 17.25 Input Page 1: Title, Options, Hammer Cushion

17.7.1.1 Hammer Input and Analysis Options

Hammer ID Number - GRLWEAP contains a hammer data file with approximately 500 different hammer models. The user only has to pick a number from the hammer listing given in the Help section of the program. Note that the hammer data in the file assumes that the hammer has been well maintained and not been significantly modified.

Stroke Option - For any diesel hammer, the stroke is a function of pile size and soil resistance. The stroke option lets the user decide whether a fixed stroke (option 1 or -1) is to be analyzed or whether the program should calculate the diesel hammer stroke (option 0). Also, an entry 2, or -2 will produce the so-called inspectors chart for a fixed ultimate capacity and an automatically varied stroke.

The positive stroke options 1 and 2 simply analyze one hammer blow and ignore whether or not the calculated rebound stroke matches the analyzed down stroke. The negative options -1 and -2 will repeat the analyses with adjusted combustion pressures until the upward stroke matches the analyzed downward stroke. Thus, if a high stroke (relative to the soil resistance) has to be analyzed then, at first, the calculated upward stroke will be small compared to the down stroke. Increasing the combustion pressure in the analysis provides the hammer model the energy necessary to maintain a high stroke in the presence of a low soil resistance. As pointed out in Section 17.6.3, analyzing a hammer with a high combustion pressure, even though the high stroke was the result of preignition, may lead to high calculated transferred energies and therefore non-conservative capacity predictions. On the other hand, if the observed hammer stroke is relatively low and if friction (which should be modeled with a lower hammer efficiency) has been eliminated as a reason for the low stroke, then a reduced combustion pressure is a very reasonable analysis option.

Fuel Setting - A number of diesel hammers have stepwise adjustable fuel pumps which allow for the injection of measured, variable amounts of fuel into the combustion chamber. This option allows the user the choice of such a hammer setting. For hammers with continuously variable fuel pumps, the program's reduced fuel settings do not correspond to a specific fuel setting that can be selected in the field but rather an arbitrary value between the hammer's maximum and minimum available settings.

17.7.1.2 Pile Input and Analysis Options

Number of Pile Segments - Usually the number of pile segments is left to the program to calculate. The user may choose a larger or smaller value to make the analysis more accurate or faster, respectively.

Number of Splices - Some piles are spliced with devices that allow for some slippage during extension or compression. A welded splice does not allow for slippage and therefore is modeled like a uniform pile section and not counted as splice.

Non-uniform Pile Option - Simply enter 0, 1, or 2 for specifying a uniform pile, a non-uniform pile, or two parallel piles (for example, a mandrel driven pile), respectively.

Pile Damping Option - Depending on the pile material, this option is entered as 1, 3, or 5 for steel, concrete or timber, respectively, and corresponds to a percentage of pile structural damping.

17.7.1.3 Shaft Resistance Input and Driveability Analysis Options

% Shaft Resistance - This very important option has two functions. If set to zero it generates a driveability analysis. Otherwise it causes a bearing graph, or inspector's chart, to be produced and represents the percentage of ultimate resistance acting along the pile shaft.

Shaft Resistance Distribution - After the percentage of shaft resistance and, therefore, the total shaft resistance has been determined for an ultimate capacity value, this shaft resistance must be distributed along the embedded portion of the pile. Often a triangular or a rectangular distribution is sufficiently accurate and can be selected here with a simple number input. Alternatively, the user may input a more complex distribution on another input page.

17.7.1.4 Helmet and Hammer Cushion Information

As pointed out earlier, the following information may either be retrieved from the User's Manual, the program's help section or the contractor's completed Pile and Driving Equipment Data Form (Figure 17.24). Since contractors seldom use standard equipment on construction sites, the latter is the preferable data source.

Helmet Weight should be the combined weight of the helmet, hammer cushion, striker plate, inserts, and all other components located between hammer and pile (kN).

Area of the hammer cushion perpendicular to the load (cm²).

ElasMod is the elastic modulus of the hammer cushion material (MPa).

Thickness of the hammer cushion. For sandwiched cushions, this is the thickness of the entire cushion stack and the striker plate is not included (mm).

C.O.R. is the Coefficient of Restitution of the hammer cushion material.

RoundOut (compressive slack) deformation of the hammer cushion (mm). This quantity is a small distance of cushion compression over which the stiffness of the hammer cushion is thought to increase from 0 to its nominal value. Usually the user leaves this quantity at the preprogrammed default value.

Stiffness of the hammer cushion (kN/m). Use of this input will override previous inputs for area, elastic modulus and thickness.

17.7.2 GRLWEAP Input - Page 2

Title:							Page: 2
PILE CUSHION INFORMATION							SI Units
Area	Elastic Modulus	Thickness	Coeff. of Restitution	Round Out	Stiffness		
.00	.0	.000	.500	3.0000	.0		
PILE INFORMATION							
Total Length	X-Sectn Area	Elastic Modulus	Specific Weight	Circumference	Strength/Yield	Coeff. of Restitutn	Round Out
.00	.00	210000.0	78.500	.000	.000	.8500	3.0000
HAMMER OVERRIDE VALUES							
Stroke	Effcy	Pressure	Reaction Weight	ComDelay Ign Vol	Comb Exp Coeff	Stroke Conv Crit	Unused
.00	.000	.0	.000	.000	.00	.00	.00
SOIL PARAMETERS							
Quake		Damping		Toe No. 2		Depth	
Skin	Toe	Skin	Toe	Quake	Damping	Fraction	Depth
2.500	2.500	.000	.000	.000	.000	.000	.00
HELP							Units
Area of the Pile Cushion							cm ² H

Figure 17.26 Input Page 2: Pile Cushion, Pile, Hammer Modifications, Soil

17.7.2.1 Pile Cushion Information

When a pile cushion is used, usually for concrete piles, input is required for the pile cushion area, elastic modulus, thickness, coefficient of restitution, round out, and stiffness, as previously described for the hammer cushion.

17.7.2.2 Pile Information

Total Length is the total pile length in the leads (m). For example if plans require a 15 m long pile but the contractor is driving 18 m long piles, then the analysis length should be 18 m. If pile sections are spliced together to form a long pile then an analysis before and after splicing may be of interest. In that case, "Total Length" may be the length of the short first section before splicing or the combined length after splicing.

X-Sectn Area is the pile cross sectional area at the pile head (cm²).

Elastic Modulus is the elastic modulus of the pile material at the pile head (MPa).

Specific Weight is the weight per unit volume of the pile material at the pile head (kN/m^3).

Circumference of pile head for the calculation of capacity from unit shaft resistance for driveability analyses (m).

Strength/Yield used for piles with more than one material for an evaluation of the critical but not necessarily the maximum stresses (MPa). For example, in a concrete pile with a steel H-pile tip, the program uses the strength/yield information to include the critical concrete stresses rather than the much higher but possibly non-critical steel stresses in the final table.

Coeff. of Restitutn of the pile head - helmet interface. The manual provides experience values.

Round Out (compressive slack) deformation of the pile head - helmet interface (mm). Again the program provides experience values for standard cases.

For piles with non-uniform cross sections, additional information would also be needed.

17.7.2.3 Hammer Override Values

Hammer overrides allows one or more values of the hammer data file to be changed for a particular analysis. The most commonly used overrides are discussed below.

Stroke (m) and **Effcy** (efficiency) are probably the most important hammer override values. Under certain circumstances the user may want to analyze a stroke which is different from the rated stroke or from the automatically calculated one. For hammers with read-out of energy (this is sometimes available in modern hydraulic hammers), stroke should be entered as a proportionally reduced value when energy is not at the maximum rated value. The user should also seriously consider whether or not the data file efficiency (which is the same for all hammer makes of the same type) should be adjusted to reflect actual field conditions.

Pressure (kPa) is important for diesel hammers when calculated and observed hammer stroke differ. A new pressure value may then be tried for better agreement.

Reaction Weight, ComDel Ign Vol, Delay, Comb Exp. Coeff, and Stroke Conv Crit are quantities associated with specific diesel hammer functions and are not routinely input unless an unusual hammer performance has to be modeled (e.g., the combustion delay - ComDel Ign Vol - is the quantity that allows for modeling of preignition in diesel hammers with liquid fuel injection).

17.7.2.4 Soil Parameters

Both the Users Manual and the program's Help section provide tables with very basic suggestions for the dynamic soil resistance parameters.

Quake Skin is the soil quake along the pile shaft usually chosen as 2.5 mm.

Quake Toe is the soil quake at the pile toe. Often chosen as $b/120$ (mm) where b is the effective pile diameter or width of the pile toe.

Damping Skin is the soil damping constant along the shaft. A Smith shaft damping constant of 0.65 s/m is commonly chosen for cohesive soils and 0.16 s/m for non-cohesive soils. Although several damping models are available in most wave equation programs, the Smith approach is generally preferred.

Damping Toe is the soil damping constant at the toe. Most commonly, Smith toe damping constants of 0.50 s/m are chosen regardless of soil type.

Toe No. 2 input quantities are reserved for those situations when piles have more than one pile toe interface, as for an H-pile section cast into a concrete pile. Then end bearing acts both against the concrete bottom and the steel toe. Toe No. 2 would be the concrete bottom in this example.

17.7.3 GRLWEAP Input - Page 3

17.7.3.1 Ultimate Capacities

For bearing graphs, up to 10 ultimate resistance values (kN) may be analyzed in one analysis. For the inspector's graph, only one capacity value will be analyzed with varying strokes.

```
Title:
Page: 3
SI Units
ULTIMATE CAPACITIES
Give up to 10 Capacities
.0 .0 .0 .0 .0 .0 .0 .0 .0 .0
HELP
Bearing Capacity for 1st analysis Units
kN
```

Figure 17.27 Input Page 3: Ultimate Capacities

For a simple bearing graph, these three input pages complete the required program input. When more complex problems are analyzed, additional input pages are required. For a discussion of more complex problems, the interested reader should consult the GRLWEAP Manual (1996).

17.8 GRLWEAP OUTPUT

The printed GRLWEAP output begins with a listing of file names used for input and a listing of the input file. There follows a disclaimer statement which points out some of the uncertainties associated with wave equation analyses. The user is urged to check that the correct data file was used and consider the disclaimer when drawing conclusions from analysis results.

The first page of output, shown in Figure 17.28, lists the hammer and drive system components used in the analysis. Hence hammer model, hammer stroke and efficiency, helmet weight, as well as hammer and pile cushion properties including thickness, area, elastic modulus and coefficient of restitution, are but a few of the input details printed on this page of output.

		Hammer Model of: D 12		Made by: DELMAG	
No.	Weight	Stiffn	CoR	C-Strk	Dampg
	kN	kN/mm		mm	kN/m/s
1	4.079				
2	4.079	15989.4	1.000	3.0480	
3	4.079	15989.4	1.000	3.0480	
Imp Block	3.604	9924.2	.900	3.0400	
Helmet	9.560	6950.0	.800	3.0480	81.3
HAMMER OPTIONS:					
Hammer File ID No.		3	Hammer Type		1
Stroke Option		0	Stroke Convergence Crit.		.020
Fuel Pump Setting		1	Hammer Damping		2
HAMMER DATA:					
Ram Weight	(kN)	12.24	Ram Length	(mm)	2652.01
Maximum Stroke	(m)	2.62	Actual Stroke	(m)	1.63
			Efficiency		.800
Maximum Pressure	(kPa)	9711.70	Actual Pressure	(kPa)	9711.70
Compression Exponent		1.350	Expansion Exponent		1.250
Ram Diameter	(cm)	299.97	Minimum Stroke	(m)	1.63
Combustion Delay	(s)	.00200	Ignition Duration	(s)	.00200
The Hammer Data Includes Estimated (NON-MEASURED) Quantities					
HAMMER CUSHION			PILE CUSHION		
Cross Sect. Area	(cm ²)	1829.03	Cross Sect. Area	(cm ²)	.00
Elastic-Modulus	(MPa)	1930.3	Elastic-Modulus	(MPa)	.0
Thickness	(mm)	50.80	Thickness	(mm)	.00
Stiffness	(kN/mm)	6950.0	Stiffness	(kN/mm)	.0

Figure 17.28 Hammer Model, Driving System and Hammer Option Output

The second page of output, presented in Figure 17.29, summarizes the pile and soil model used in the analysis. A brief summary of the pile profile is provided at the top of the page, and includes the pile length, area, modulus of elasticity, specific weight, circumference, material strength, wave speed, and pile impedance. A detailed summary of the pile and soil model follows beneath the pile profile. The detailed pile model includes the number of pile segments, their weight and stiffness, any compression (C-Slk) or tension (T-Slk) slacks with associated coefficient of restitution (CoR). The listing also shows segment bottom depth (LbTop), and the averages of both segment circumference and cross sectional area.

PILE PROFILE:											
L b Top	Area	E-Mod	Spec Wt	Circumf	Strength	Wave Sp	EA/c				
m	cm ²	MPa	kN/m ³	m	MPa	m/s	kN/m/s				
.00	100.0	209820.	78.80	1.000	1.00	5111.	410.54				
12.20	100.0	209820.	78.80	1.000	1.00	5111.	410.54				
Wave Travel Time - 2L/c - = 4.774 ms											
Pile and Soil Model for Rut = 250.0 kN											
No.	Weight	Stiffn	C-Slk	T-Slk	CoR	Soil-S	Soil-D	Quake	LbTop	Circmf	Area
	kN	kN/mm	mm	mm		kN	s/m	mm	m	m	cm ²
1	1.202	1376.	3.048	.000	.80	.4	.164	2.54	1.52	1.0	100.0
2	1.202	1376.	.000	.000	1.00	1.2	.164	2.54	3.05	1.0	100.0
3	1.202	1376.	.000	.000	1.00	2.0	.164	2.54	4.57	1.0	100.0
4	1.202	1376.	.000	.000	1.00	2.7	.164	2.54	6.10	1.0	100.0
5	1.202	1376.	.000	.000	1.00	3.5	.164	2.54	7.63	1.0	100.0
6	1.202	1376.	.000	.000	1.00	4.3	.164	2.54	9.15	1.0	100.0
7	1.202	1376.	.000	.000	1.00	5.1	.164	2.54	10.67	1.0	100.0
8	1.202	1376.	.000	.000	1.00	5.9	.164	2.54	12.20	1.0	100.0
Toe						225.0	.492	2.54			
PILE, SOIL, ANALYSIS OPTIONS:											
Uniform/Non-Uniform/2-Pile	0	Pile Segment Generation	Automatic								
No. of Slacks/Splices	0	Pile Damping (%)	1								
% Skin Friction	10	Pile Damping Fact. (kN/m/s)	8.211								
Soil Damping Option	Smith	% End Bearing	90								
Soil Resistance Distr. No.	1	Soil Damping Exponent	1.000								
Max No Analysis Iterations	0	Time Increment/Critical	160								
Residual Stress Analysis	0	Output Option	10								
Output Segment Generation	Automatic	Output Time Interval	1								
Analysis Time-Input (ms)	0										

Figure 17.29 Pile, Soil Model and Analysis Options

The soil model summarized includes the soil static soil resistance distribution (Soil-S), the soil damping parameters (Soil-D) along the shaft and at the pile toe as well as the soil quakes along the shaft and at the pile toe. Additional pile and soil modeling options, including the percent shaft and toe resistance, are summarized below the detailed model.

A review of the "printed output" can be accomplished on the computer screen before printing. This review is extremely important as it can point out inadvertent omissions or erroneous input data. The reviewer should carefully check ram weight, stroke, efficiency, cushion stiffness, pile masses, stiffnesses, soil parameters, etc. Furthermore, any error messages or warnings issued by the program should be checked for relevance to the results.

Rut (kN)	B1 Ct (bpm)	Stroke down	(m) up	min Str (MPa)	i,t	max Str (MPa)	i,t	ENTHRU (kJ)	B1 Rt (b/min)
250.0	32.2	1.41	1.39	-1.18	(6, 46)	113.18	(5, 3)	14.5	55.3
500.0	76.6	1.63	1.64	-3.18	(5, 32)	131.10	(4, 3)	12.9	51.0
750.0	124.5	1.81	1.80	-5.68	(5, 26)	148.15	(8, 4)	12.8	48.6
1250.0	272.2	2.12	2.11	-16.46	(5, 16)	200.98	(8, 4)	13.8	44.9
1500.0	422.9	2.28	2.27	-24.81	(5, 16)	221.10	(8, 4)	14.5	43.4
1750.0	763.6	2.42	2.42	-29.52	(5, 15)	237.24	(8, 4)	15.1	42.1
2000.0	1829.8	2.55	2.56	-33.53	(5, 15)	251.59	(1, 7)	15.7	41.0

Figure 17.31 GRLWEAP Final Summary for Bearing Graph Analyses

17.9 PLOTTING OF GRLWEAP RESULTS

The summary table results are usually presented in the form of a bearing graph relating the ultimate capacity to driving resistance. Compression and tension stresses versus driving resistance are also plotted. A typical GRLWEAP bearing graph was presented in Figure 17.4 as part of Example 1.

The wave equation bearing graph should be provided to the resident construction engineer, pile inspector, and the contractor.

17.10 SUGGESTIONS FOR PROBLEM SOLVING

Table 17-1 summarizes some of the field problems that can be solved through use of wave equation analysis. Field problems may arise due to soil, hammer, driving system, and pile conditions which are not as anticipated. Of course all possibilities cannot be treated in this summary. Sometimes, there are also difficulties in performing a wave equation analysis. Some of these cases are listed in Table 17-2. Further information may also be found in the program manual.

TABLE 17-1 SUGGESTED USE OF THE WAVE EQUATION TO SOLVE FIELD PROBLEMS

Problem	Solution
Concrete pile spalling or slabbing near pile head.	Perform wave equation analysis; find pile head stress for observed blow count and compare with allowable stresses. If high calculated stress add pile cushioning. If low calculated stress investigate pile quality, hammer performance, hammer-pile alignment.
Concrete piles develop complete horizontal cracks	Perform wave equation analysis; check tension stresses along pile (extrema tables) for observed blow counts. If

Concrete piles develop complete horizontal cracks in hard driving.	high calculated tension stresses- add cushioning or reduce stroke. If low calculated tension stresses check hammer performance and/or perform measurements.
Concrete piles develop complete horizontal cracks in hard driving.	Perform wave equation analysis; check tension stresses along pile (extrema table). If high calculated tension stresses consider heavier ram. If low calculated tension stresses take measurements and determine quakes which are probably higher than anticipated.
Concrete piles develop partial horizontal cracks in easy driving.	Check hammer-pile alignment since bending may be the problem. If alignment appears to be normal, tension and bending combined may be too high; solution as for complete cracks.

TABLE 17-1 SUGGESTED USE OF THE WAVE EQUATION TO SOLVE FIELD PROBLEMS (CONTINUED)

Problem	Solution
Steel pile head deforms, timber pile top mushrooms.	Check helmet size/shape; check steel strength; check evenness of pile head, banding of timber pile head. If okay perform wave equation and determine pile head stress. If calculated stress is high, reduce hammer energy (stroke) for low blow counts; for high blow counts different hammer or pile type may be required.
Unexpectedly low blow counts during pile driving.	Investigate soil borings; if soil borings do not indicate soft layers, pile may be damaged below grade. Perform wave equation and investigate both tensile stresses along pile and compressive stresses at toe. If calculated stresses are acceptable, investigate possibility of obstructions / uneven toe contact on hard layer or other reasons for pile toe damage.
Higher blow count than expected.	Review wave equation analysis and check that all parameters were reasonably considered. Check hammer and driving system. If no obvious defects are found in driving system, field measurements should be taken. Problem could be preignition, preadmission, low hammer efficiency, soft cushion, large quakes, high damping, greater soil strengths, or temporarily increased soil resistance with later relaxation (perform restrike tests to check).
Lower blow count than expected.	Probably soil resistance is lower than anticipated. Perform wave equation and assess soil resistance. Perform restrike testing (soil resistance may have been lost during driving), establish setup factor and drive to lower capacity. Hammer performance may also be better than anticipated, check by measurement.

TABLE 17-1 SUGGESTED USE OF THE WAVE EQUATION TO SOLVE FIELD PROBLEMS (CONTINUED)

Problem	Solution
<p>Diesel hammer stroke (bounce chamber pressure) higher than calculated.</p>	<p>The field observed stroke exceeds the wave equation calculated stroke by more than 10%. Compare calculated and observed blow counts. If observed are higher, soil resistance is probably higher than anticipated. If blow counts are comparable, reanalyze with higher combustion pressure to match observed stroke <u>and</u> assure that preignition is not a problem, e.g., by measurements.</p>
<p>Diesel hammer stroke (bounce chamber pressure) lower than calculated.</p>	<p>The field observed stroke is less than 90% of the stroke calculated by the wave equation. Check that ram friction is not a problem (ram surface should have well lubricated appearance). Compare calculated and observed blow count. If observed one is lower, soil resistance is probably lower than anticipated. If blow counts are comparable, reanalyze with lower combustion pressure to match observed hammer stroke.</p>

TABLE 17-2 WAVE EQUATION ANALYSIS PROBLEMS

Problem	Solution
Cannot find hammer in data file.	See if there is a hammer of same type, similar ram weight and energy rating and modify its data.
Cannot find an acceptable hammer to drive pile within driving stress and driving resistance limits.	<p>Both calculated stresses and blow counts are too high. Increase pile impedance or material strength or redesign for lower capacities.</p> <p>Alternatively, check whether soil has potential for setup. If soil is fine grained or known to exhibit setup gains after driving then end of driving capacity may be chosen lower than required. Capacity should be confirmed by restrrike testing or static load testing.</p>
Diesel hammer analysis with low or zero transferred energies.	Probably soil resistance too low for hammer to run. Try higher capacities.
Unknown hammer energy setting.	Perform analyses until cushion thickness/hammer energy setting combination is found that yields acceptable stresses with minimum cushion thickness. Specify that this thickness be used in the field and its effectiveness verified by measurements.
Cannot find a suggested set of driving system data.	Contact contractor, equipment manufacturer, or use data for similar systems.
Unknown pile cushion thickness.	Perform analyses until cushion thickness/hammer energy setting combination is found that yields acceptable stresses with minimum cushion thickness. Specify that this thickness be used in the field and its effectiveness verified by measurements.
Calculated pile cushion thickness is uneconomical.	In order to limit stresses, an unusually thick pile cushion was needed for pile protection. Try to analyze with reduced energy settings. For tension stress problems, energy settings often can be increased after pile reaches sufficient soil resistance.

TABLE 17-2 WAVE EQUATION ANALYSIS PROBLEMS (CONTINUED)

Problem	Solution
Calculated driving times unrealistically high or low.	The calculation of driving times is very sensitive, particularly at high blow counts. Use extreme caution when using these results for cost estimation. Also, no interruption times are included and the estimate is only applicable to non-refusal driving.
Wave equation calculated energy and/or forces difficult to match with field measurements.	In general, it is often difficult to make all measured quantities agree with their calculated equivalents. A 10% agreement should be sufficient. Parameters to be varied include hammer efficiency, coefficients of restitution, hammer and/or pile cushion stiffnesses.

REFERENCES

- AASHTO, American Association of State Highway and Transportation Officials, (1992). Interim Specifications, Bridges, 1993 and 1994. Standard Specifications for Highway Bridges, ISBN 1-56051-014-5, 444 North Capitol Street, N.W., Suite 249, Washington, D.C. 20001.
- Blendy, M.M. (1979). Rational Approach to Pile Foundations. Symposium on Deep Foundations, ASCE National Convention.
- Cheney, R.S. and Chassie, R.G. (1993). Soils and Foundations Workshop Manual. Second Edition, Report No. HI-88-009, U.S. Department of Transportation, Federal Highway Administration, Office of Engineering, Washington, D.C., 353-362.
- Goble, G.G. and Rausche, F. (1976). Wave Equation Analysis of Pile Driving - WEAP Program, U.S. Department of Transportation, Federal Highway Administration, Office of Research and Development, Washington, D.C., Volumes I-IV.
- Goble, G.G. and Rausche, F. (1986). Wave Equation Analysis of Pile Driving - WEAP86 Program, U.S. Department of Transportation, Federal Highway Administration, Implementation Division, McLean, Volumes I-IV.
- Goble, Rausche, Likins and Associates, Inc. (1996). GRLWEAP Users Manual. 4535 Emery Industrial Parkway, Cleveland, OH 44128.
- Hirsch, T.J., Carr, L. and Lowery, L.L. (1976). Pile Driving Analysis. TTI Program, U.S. Department of Transportation, Federal Highway Administration, Offices of Research and Development, IP-76-13, Washington, D.C., Volumes I-IV.
- Soares, M., de Mello, J. and de Matos, S. (1984). Pile Driveability Studies, Pile Driving Measurements. Proceedings of the Second International Conference on the Application of Stress-Wave Theory to Piles, Stockholm, 64-71.

Smith, E.A.L. (1960). Pile Driving Analysis by the Wave Equation. American Society of Civil Engineers, Journal of the Soil Mechanics and Foundations Division, 86(4), 35-61.

U.S. Army Corps of Engineers, Department of the Army (1993) Engineering Manual EM 1110-2-2906, reprinted by American Society of Civil Engineers in Design of Pile Foundations, 345 East 47th Street, New York, NY 10017-2398.

STUDENT EXERCISE #11 - WAVE EQUATION HAMMER APPROVAL

A contractor owns two hammers that he may use on a bridge construction project but is unsure which hammer will actually be available for the project. Therefore, he has submitted Pile Driving and Equipment Data forms for both hammers to the engineer for approval. The pile foundation design requires 25 meter long, 356 mm diameter, closed end pipe piles to be driven for an ultimate pile capacity of 2670 kN. The pipe piles have a wall thickness of 12.7 mm and are to comply with ASTM A-252, Grade 3 steel. Therefore, the piles have a minimum yield strength of 310 MPa.

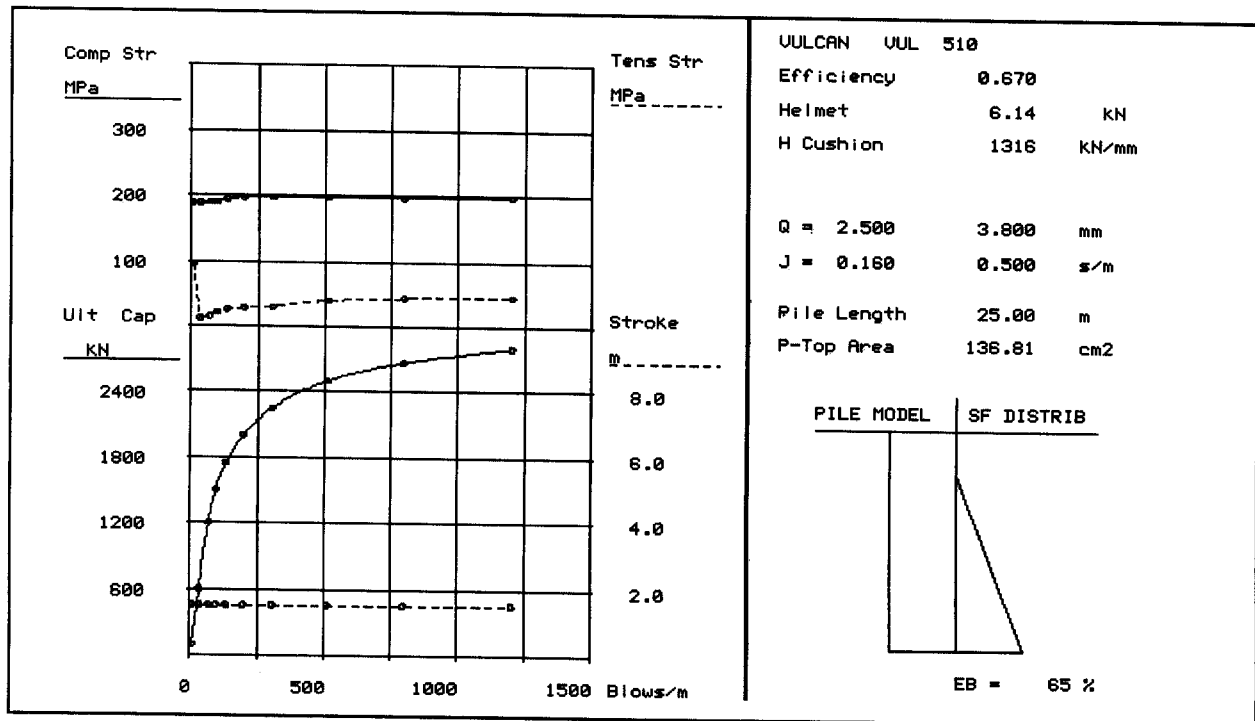
The first driving system consists of a Vulcan 510 single acting air hammer with a manufacturer's rated hammer energy of 67.8 kJ. The Vulcan 510 hammer will have an aluminum and micarta hammer cushion. The second driving system consists of an IHC S-70 double acting hydraulic hammer which has a manufacturer's rated energy of 70.0 kJ. The contractor proposes to operate this hammer at an equivalent stroke of 1.9 meters or roughly 92% of the maximum energy. The IHC hammer does not utilize a hammer cushion. The results of the wave equation analyses for the two proposed driving systems are attached.

Based on the submitted hammer information and wave equation results, should both, or either of these hammers be approved?

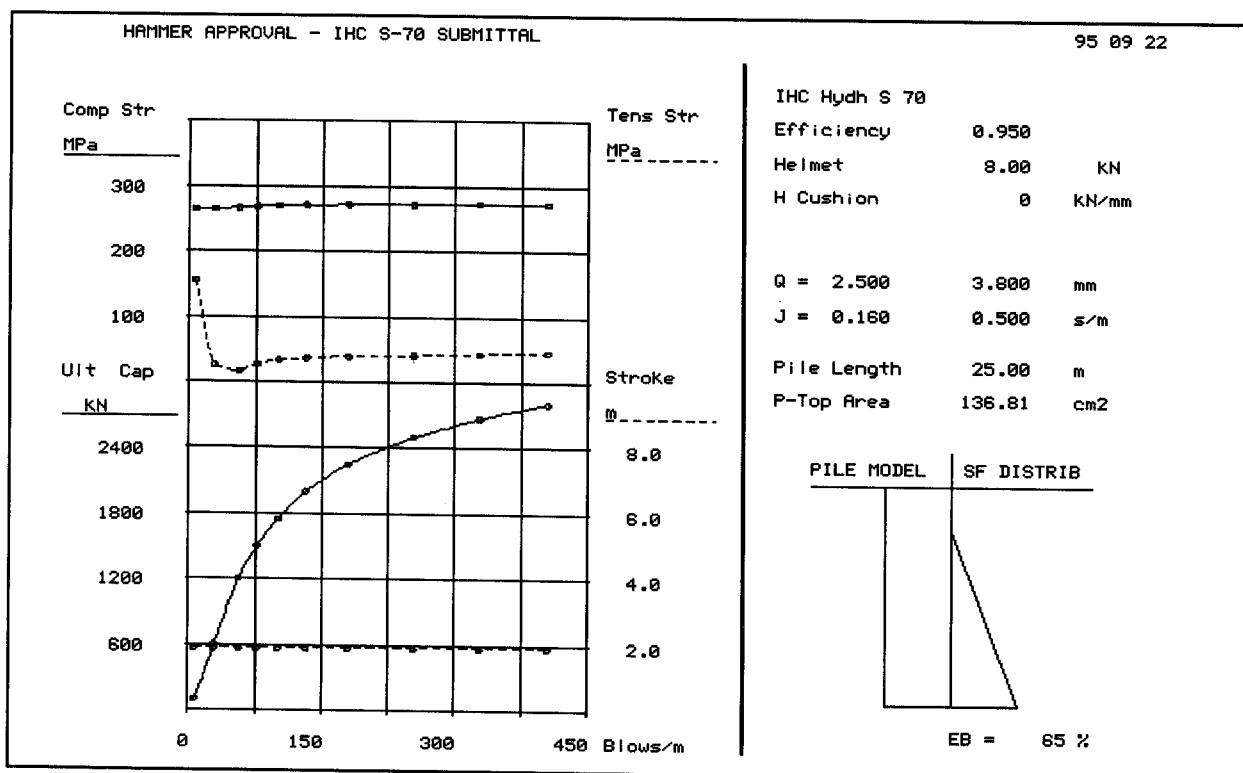
Note: Recommended driving resistances for hammer approval are presented on Page 12-12.

Recommended driving stress limits for steel pipe piles are presented on Page 11-5.

Rut (kN)	Bl Ct (bpm)	Stroke(eq.) (m)	min Str (MPa)	i,t	max Str (MPa)	i,t	ENTHRU (kJ)
100.0	7.5	1.52	-94.84	(5, 12)	188.83	(7, 4)	38.1
600.0	33.1	1.52	-12.54	(12, 47)	189.12	(8, 5)	41.9
1200.0	67.8	1.52	-15.71	(12, 33)	189.70	(9, 5)	41.5
1500.0	95.8	1.52	-21.81	(13, 31)	190.04	(8, 5)	40.6
1750.0	134.5	1.52	-25.95	(15, 45)	193.46	(25, 8)	39.9
2000.0	199.3	1.52	-28.52	(14, 30)	197.31	(25, 8)	39.7
2250.0	306.7	1.52	-30.44	(10, 41)	198.28	(25, 8)	39.7
2500.0	511.9	1.52	-40.46	(11, 40)	197.83	(25, 8)	39.6
2670.0	796.8	1.52	-44.19	(11, 40)	197.03	(25, 8)	39.6
2800.0	1202.6	1.52	-46.29	(11, 39)	198.47	(2, 13)	39.6



Rut (kN)	Bl Ct (bpm)	Stroke(eq.) (m)	min Str (MPa)	i,t	max Str (MPa)	i,t	ENTHRU (kJ)
100.0	6.5	1.90	-155.26	(6, 11)	265.77	(3, 3)	51.1
600.0	29.2	1.90	-25.68	(6, 47)	265.77	(3, 3)	55.0
1200.0	56.7	1.90	-17.12	(13, 32)	267.25	(4, 3)	54.9
1500.0	77.1	1.90	-27.35	(13, 29)	269.03	(7, 3)	54.0
1750.0	100.8	1.90	-33.58	(13, 28)	270.15	(7, 3)	53.5
2000.0	132.1	1.90	-37.35	(14, 28)	271.23	(7, 3)	53.2
2250.0	179.7	1.90	-39.84	(14, 28)	271.79	(7, 3)	53.2
2500.0	253.7	1.90	-41.38	(14, 27)	272.41	(8, 4)	53.1
2670.0	328.1	1.90	-43.87	(14, 26)	273.02	(7, 3)	53.1
2800.0	405.1	1.90	-46.17	(14, 26)	273.23	(7, 3)	53.1



STUDENT EXERCISE #12 - WAVE EQUATION INSPECTORS CHART

A contractor has chosen a Kobe K-35 for foundation installation of HP 360 x 174 H-piles. The H-piles are to be driven to a limestone bedrock for an ultimate pile capacity of 3250 kN. The H-piles are to be A-36 steel.

For hammer approval, a standard wave equation bearing graph analysis was performed. The results from this analysis are the next page and indicate that both the driving resistance (Chapter 12) and driving stresses (Chapter 11) are within specification limits for the ultimate capacity of 3250 kN. The standard bearing graph indicates a driving resistance of 255 blows per meter at a hammer stroke of 2.40 m should result in the required ultimate pile capacity.

A constant capacity wave equation analysis or inspectors chart was then performed to assist field personnel in the determining the required driving resistance at other field observed hammer strokes. The results of this constant capacity analysis for Pier 2 piles is presented on page 17-69. The analysis results have been furnished to the inspector in expanded form as presented on page 17-70 and should be used to answer the following questions.

1. Pile #1 has a field observed hammer stroke is 2.20 m and a driving resistance of 275 blows/m. Does this pile have the required ultimate capacity?

Any additional action required by the inspector?

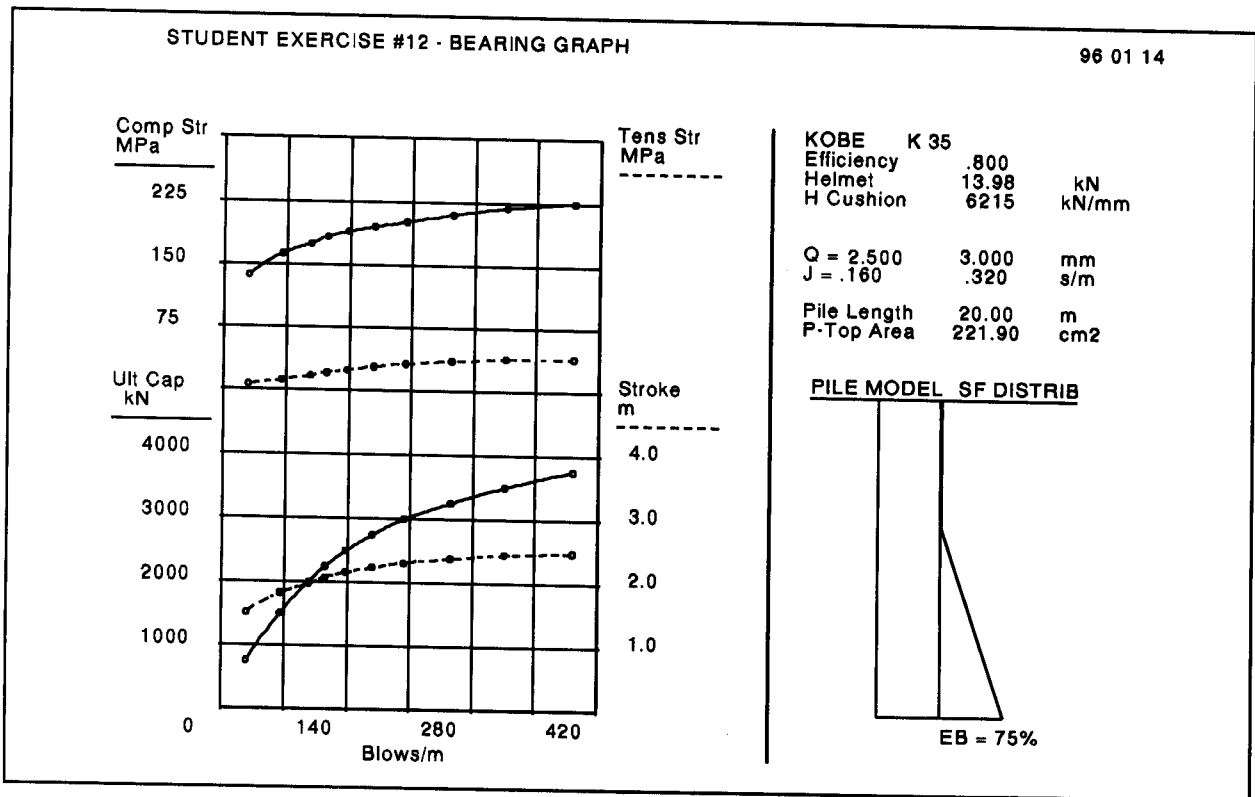
2. Pile #2 has a field observed hammer stroke of 2.85 m and a driving resistance of 195 blows/m. Does this pile have the required ultimate capacity?

Any additional action required by the inspector?

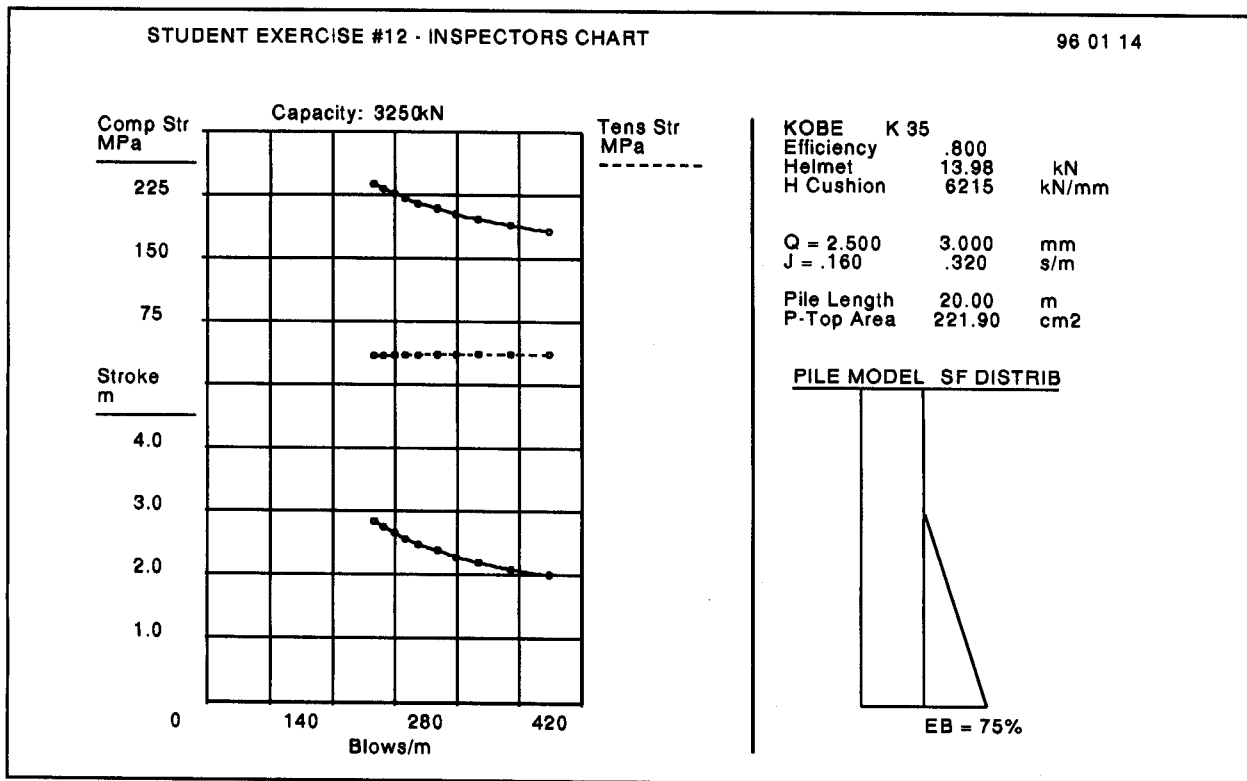
STUDENT EXERCISE #12 - BEARING GRAPH
 Goble Rausche Likins & Associates, Inc.

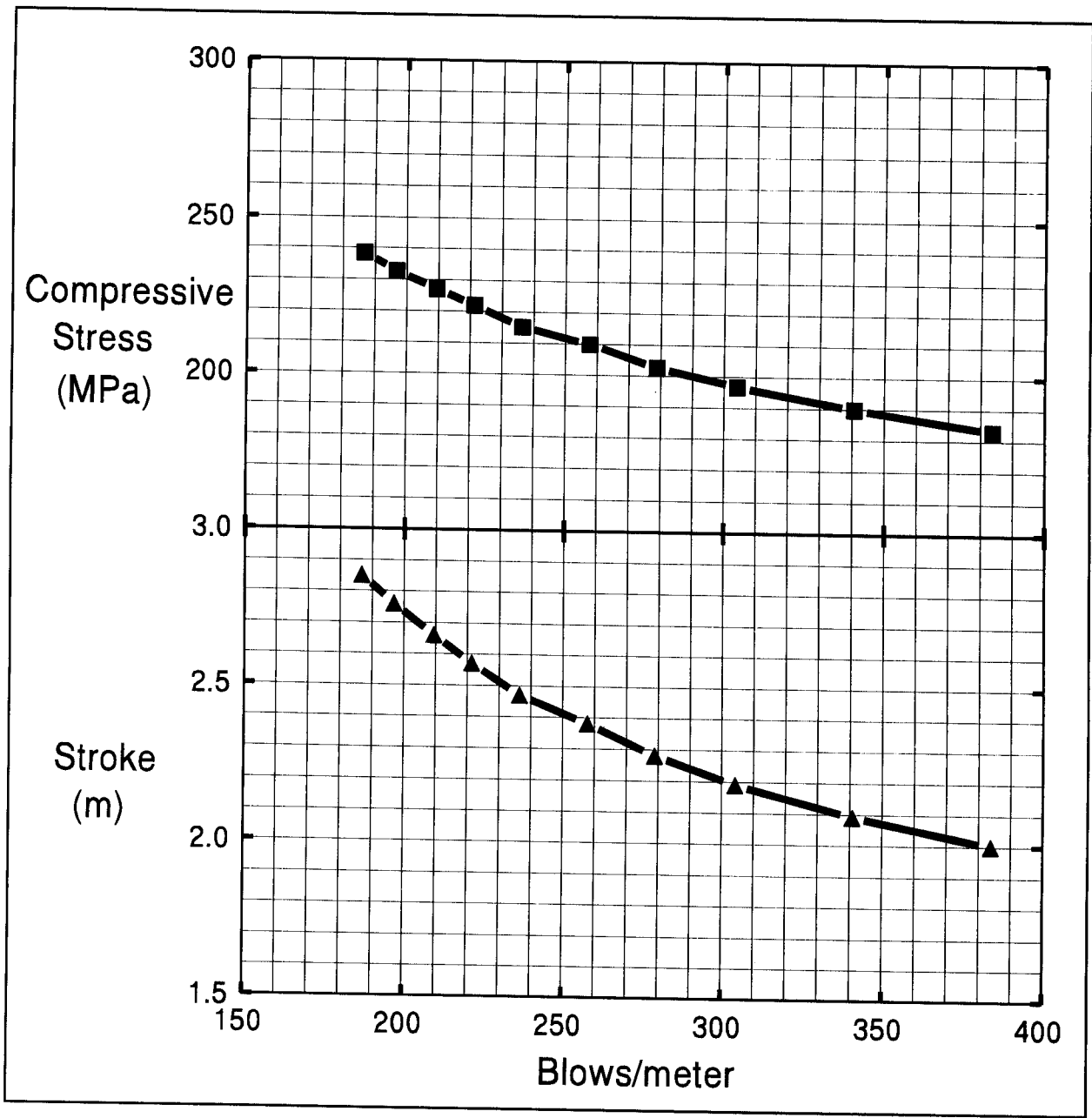
96/01/14
 GRLWEAP(TM) Version 1.995-1

Rut (kN)	Bl Ct (bpm)	Stroke down	(m) up	min Str (MPa)	i,t	max Str (MPa)	i,t	ENTHRU (kJ)	Bl Rt (b/min)
750.0	27.5	1.52	1.54	-7.39	(9, 46)	137.40	(4, 3)	44.7	52.7
1500.0	65.2	1.82	1.83	-12.30	(10, 30)	163.13	(10, 4)	41.7	48.2
2000.0	96.8	1.97	1.99	-17.55	(11, 27)	175.50	(10, 4)	41.9	46.2
2250.0	114.8	2.08	2.07	-21.69	(12, 26)	183.43	(10, 4)	43.2	45.2
2500.0	138.5	2.16	2.16	-24.44	(12, 24)	189.75	(11, 4)	44.1	44.3
2750.0	167.9	2.24	2.24	-28.96	(11, 23)	195.82	(11, 4)	45.1	43.6
3000.0	203.5	2.32	2.32	-32.91	(11, 23)	201.83	(10, 4)	46.2	42.8
3250.0	255.1	2.39	2.40	-36.08	(11, 22)	210.55	(20, 6)	47.0	42.2
3500.0	315.8	2.46	2.46	-39.09	(11, 22)	219.45	(20, 6)	48.2	41.6
3750.0	392.0	2.49	2.51	-40.49	(10, 22)	225.05	(20, 6)	48.9	41.3



Rut (kN)	Bl Ct (bpm)	Stroke down	(m) up	min Str (MPa)	i,t	max Str (MPa)	i,t	ENTHRU (kJ)	Bl Rt (b/min)
3250.0	383.7	2.00	2.40	-37.17	(11, 22)	182.91	(20, 6)	39.2	44.0
3250.0	340.7	2.09	2.40	-36.94	(11, 22)	189.80	(20, 6)	41.1	43.5
3250.0	304.2	2.19	2.39	-36.76	(11, 22)	196.77	(20, 6)	43.1	43.1
3250.0	278.9	2.28	2.39	-36.44	(11, 22)	202.57	(20, 6)	45.0	42.6
3250.0	257.7	2.38	2.39	-36.13	(11, 22)	209.78	(20, 6)	46.8	42.2
3250.0	236.4	2.47	2.39	-35.92	(11, 22)	215.22	(20, 6)	48.8	41.8
3250.0	221.3	2.57	2.39	-35.61	(11, 22)	221.89	(20, 6)	50.6	41.4
3250.0	209.4	2.66	2.40	-35.26	(11, 22)	227.07	(20, 6)	52.3	41.0
3250.0	196.8	2.76	2.40	-35.01	(11, 23)	232.65	(20, 6)	54.2	40.7
3250.0	186.6	2.85	2.40	-34.69	(11, 23)	238.40	(20, 6)	56.0	40.3





18. DYNAMIC PILE TESTING AND ANALYSIS

Dynamic test methods use measurements of strain and acceleration taken near the pile head as a pile is driven or restruck with a pile driving hammer. These dynamic measurements can be used to evaluate the performance of the pile driving system, calculate pile installation stresses, determine pile integrity, and estimate static pile capacity.

Dynamic test results can be further evaluated using signal matching techniques to determine the relative soil resistance distribution on the pile, as well as representative dynamic soil properties for use in wave equation analyses. This chapter provides a brief discussion of the equipment and methods of analysis associated with dynamic measurements.

18.1 BACKGROUND

Work on the development of the dynamic pile testing techniques that have become known as the Case Method started with a Master thesis project at Case Institute of Technology. This work was done by Eiber (1958) at the suggestion and under the direction of Professor H.R. Nara. In this first project, a laboratory study was performed in which a rod was driven into dry sand. The Ohio Department of Transportation (ODOT) and the Federal Highway Administration subsequently funded a project with HPR funds at Case Institute of Technology beginning in 1964. This project was directed by Professors R.H. Scanlan and G.G. Goble. At the end of the first two year phase, Professor Scanlan moved to Princeton University. The research work at Case Institute of Technology under the direction of Professor Goble continued to be funded by ODOT and FHWA, as well as several other public and private organizations until 1976.

Four principal directions were explored during the 12 year period that the funded research project was active. There was a continuous effort to develop improved transducers for the measurement of force and acceleration during pile driving. Field equipment for recording and data processing was also continually improved. Model piles were driven and tested both statically and dynamically at sites in Ohio. Full scale piles driven and statically tested by ODOT, and later other DOT's, were also tested dynamically to obtain capacity correlations. Finally, analysis method improvements were

developed, including both field solutions (Case Method) and a rigorous numerical modeling technique (CAPWAP program). Additional information on the research project and its results may be found in Goble and Rausche (1970), Rausche *et al.* (1972) and Goble *et al.* (1975).

ODOT began to apply the results of this research to their construction projects in about 1968. Commercial use of the methods began in 1972 when the Pile Driving Analyzer and CAPWAP became practical for use in routine field testing by a trained engineer. There have been continual improvements in the hardware and software since 1972, making the equipment more reliable and easier to use. Further implementation of dynamic testing methods resulted from FHWA Demonstration Project 66, in which additional correlation data was collected, and the method benefits were demonstrated on real projects throughout the US. Other dynamic testing and analysis systems have subsequently been developed, primarily in Europe, such as the FPDS equipment and its associated signal matching technique, TNOWAVE, Reiding *et al.* (1988). However, based on the current state of practice in the United States, this manual will focus on the Pile Driving Analyzer and CAPWAP because of specific advantages relating to the comparatively extensive correlation database with static tests.

18.2 APPLICATIONS FOR DYNAMIC TESTING METHODS

Cheney and Chassie (1993) note that dynamic testing costs much less and requires less time than static pile load testing. They also note that important information can be obtained regarding the behavior of the pile driving hammer and pile-soil systems that is not available from a static pile load test. Consequently, dynamic testing has many applications. Some of these applications are discussed below.

18.2.1 Static Pile Capacity

- a. Evaluation of static pile capacity at the time of testing. The soil setup or relaxation potential can be assessed by restriking several piles and comparing restrike capacities with end-of-initial driving capacities.
- b. Assessments of static pile capacity versus pile penetration depth can be obtained by testing from the start to the end of driving. This can be helpful in profiling the depth to the bearing strata and thus the required pile lengths.

- c. CAPWAP analysis can provide refined estimates of static capacity, assessment of soil resistance distribution, and soil quake and damping parameters for wave equation input.

18.2.2 Hammer and Driving System Performance

- a. Calculation of energy transferred to the pile for comparison with the manufacturer's rated energy and wave equation predictions which indicate hammer and drive system performance. Energy transfer can also be used to determine effects of changes in hammer cushion or pile cushion materials on pile driving resistance.
- b. Determination of drive system performance under different operating pressures, strokes or batters, or changes in hammer maintenance by comparative testing of hammers or of a single hammer over an extended period of use.
- c. Identification of hammer performance problems, such as preignition problems with diesel hammers or preadmission in air/steam hammers.
- d. Determination of whether soil behavior or hammer performance is responsible for changes in observed driving resistances.

18.2.3 Driving Stresses and Pile Integrity

- a. Calculation of compression and tension driving stresses. In cases with driving stress problems, this information can be helpful when evaluating adjustments to pile installation procedures. Calculated stresses can also be compared to specified driving stress limits.
- b. Determination of the extent and location of pile structural damage, Rausche and Goble (1979). Thus, costly extraction may not be necessary to confirm or quantify damage suspected from driving records.
- c. CAPWAP analysis for stress distribution throughout pile.

18.3 DYNAMIC TESTING EQUIPMENT

A typical dynamic testing system consists of a minimum of two strain transducers and two accelerometers bolted to diametrically opposite sides of the pile to monitor strain and acceleration and account for nonuniform hammer impacts and pile bending. The reusable strain transducers and accelerometers are generally attached two to three diameters below the pile head. Almost any driven pile type (concrete, steel pipe, H, Monotube, timber, etc.) can be tested with the pile preparation for each pile type slightly varying.

Figures 18.1 and 18.2 illustrate the typical pile preparation procedures required for dynamic testing. In Figure 18.1, a prestressed concrete pile is being prepared for gage attachment by drilling and then installing concrete anchors. In Figure 18.2, the concrete pile to be tested during driving has been positioned in the leads for driving. A member of the pile crew climbs the leads and then bolts the gages to the pile at this time. Piles to be tested during restrike can be instrumented at any convenient location and the climbing of the leads is usually not necessary. Pile preparation and gage attachment typically requires 10 to 20 minutes per pile tested. After the gages are attached, the driving or restrike process continues following usual procedures. Most restrike tests are only 20 blows or less.

A close up view of a strain transducer and an accelerometer bolted to a steel pipe pile is shown in Figure 18-3. The individual cables from each gage are combined into a single main cable which in turn relays the signals from each hammer blow to the data acquisition system on the ground. The data acquisition system, such as the Pile Driving Analyzer shown in Figure 18-4, conditions and converts the strain and acceleration signals to force and velocity records versus time. The force is computed from the measured strain, ϵ , times the product of the pile elastic modulus, E , and cross sectional area, A , or: $F(t) = EA\epsilon(t)$. The velocity is obtained by integrating the measured acceleration, record, a , or: $V(t) = \int a(t) dt$.

Older dynamic testing systems required multiple components for processing, recording, and display of dynamic test signals. In newer dynamic testing systems, these components have been combined into one PC computer based system. During driving, the Pile Driving Analyzer performs integrations and all other required computations to analyze the dynamic records for transferred energy, driving stresses, structural integrity, and pile capacity. Numerical results for each blow for up to nine dynamic quantities are



Figure 18.1 Pile Preparation for Dynamic Testing



Figure 18.2 Pile Positioned for Driving and Gage Attachment

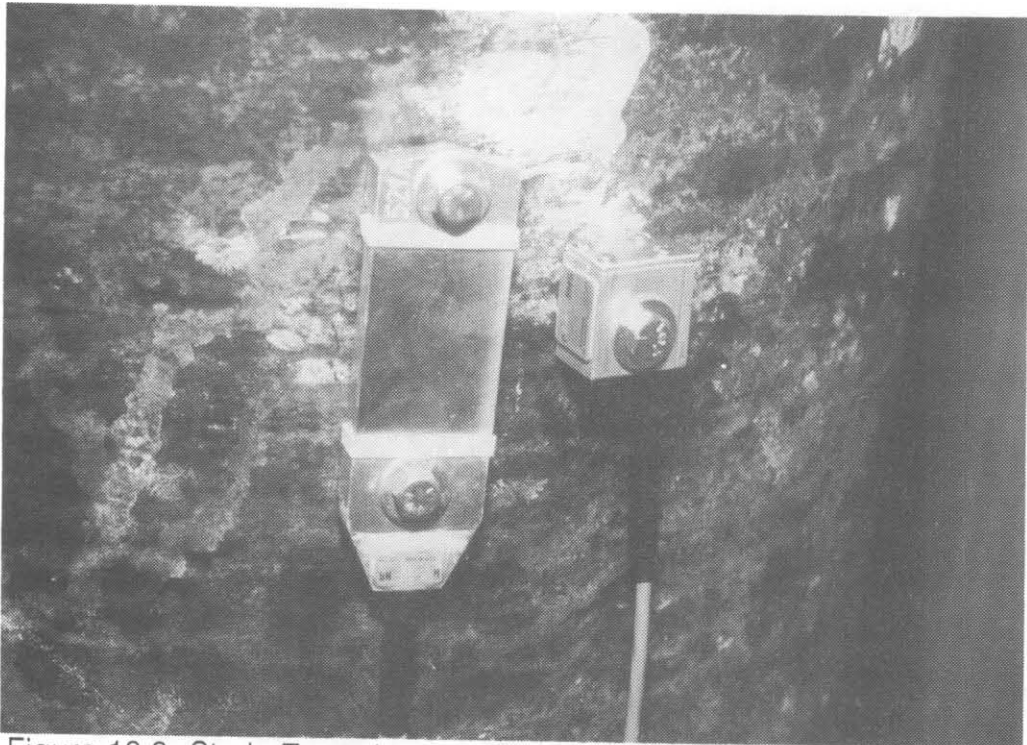


Figure 18.3 Strain Transducer and Accelerometer Bolted to Pipe Pile

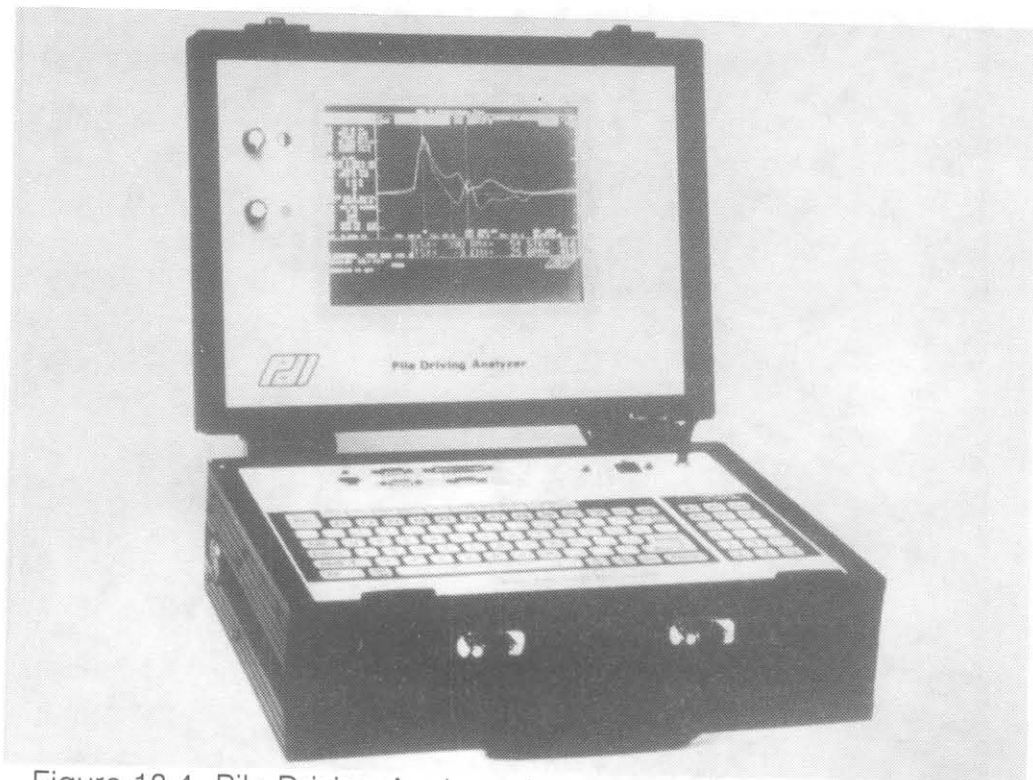


Figure 18.4 Pile Driving Analyzer (courtesy of Pile Dynamics, Inc.)

electronically stored in a file which can be later used to produce graphical and numeric summary outputs. In this system, force and velocity records are also viewed on a graphic LCD computer screen during pile driving to evaluate data quality, soil resistance distribution, and pile integrity. Complete force and velocity versus time records from each gage are also digitally stored for later reprocessing and data analysis by CAPWAP.

Data quality is automatically evaluated by the Pile Driving Analyzer and if any problem is detected, then a warning is given to the test engineer. Other precautionary advice is also displayed to assist the engineer in collecting data. The capabilities discussed in the remainder of this chapter are those included in these newer systems.

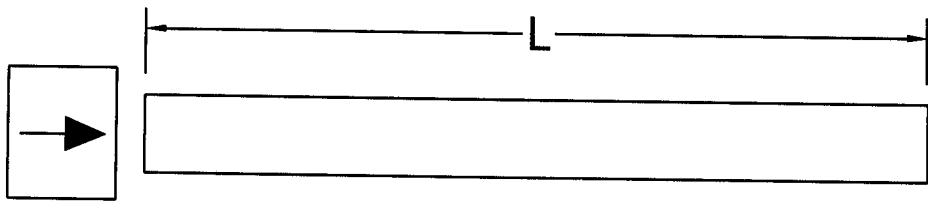
Additional information on the equipment requirements for dynamic testing are detailed in ASTM D-4945, Standard Test Method for High Strain Dynamic Testing of Piles and in AASHTO T-298-33, Standard Method of Test for High Strain Dynamic Testing of Piles.

18.4 BASIC WAVE MECHANICS

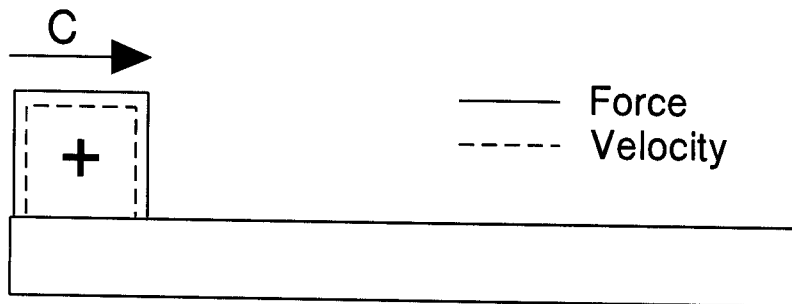
This section is intended to summarize wave mechanics principles applicable to pile driving. Through this general overview, an understanding of how dynamic testing functions and how test results can be qualitatively interpreted can be obtained.

When a uniform elastic rod of cross sectional area, A , elastic modulus, E , and wave speed, C , is struck by a mass, then a force, F , is generated at the impact surface of the rod. This force compresses the adjacent part of the rod. Since the adjacent material is compressed, it also experiences an acceleration and attains a particle velocity, V . As long as there are no resistance effects on the uniform rod, the force in the rod will be equal to the particle velocity times the rod impedance, EA/C .

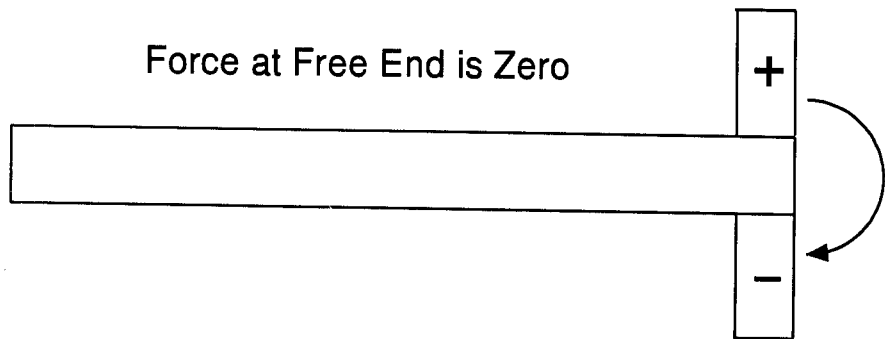
Figure 18.5(a) illustrates a uniform rod of length, L , with no resistance effects, that is struck at one end by a mass. Force and velocity (particle velocity) waves will be created in the rod, as shown in Figure 18.5(b). These waves will then travel down the rod at the material wave speed, C . At time L/C , the waves will arrive at the end of the rod, as shown in Figures 18.5(c) and 18.5(d). Since there are no resistance effects acting on the rod, a free end condition exists, and a tensile wave reflection occurs, which doubles the pile velocity at the free end and the net force becomes zero. The wave then travels up the rod with force of the same magnitude as the initial input, except in tension, and the velocity of the same magnitude and same sign.



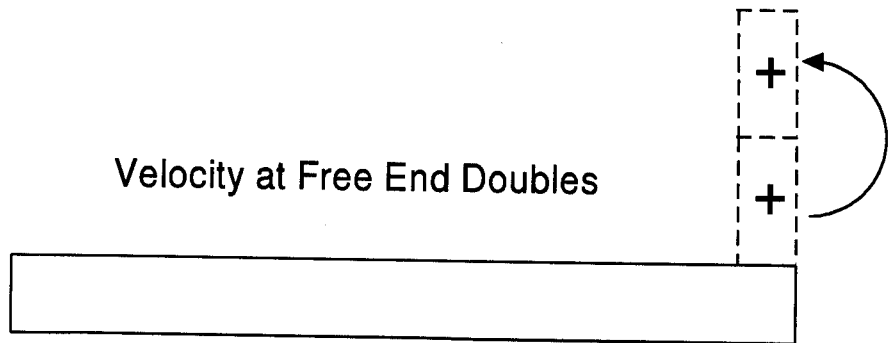
(a)



(b)



(c)



(d)

Figure 18.5 Free End Wave Mechanics

Consider now that the rod is a pile with no resistance effects, and that force and velocity measurements are made near the pile head. Typical force and velocity measurements versus time for this "free end" condition are presented in Figure 18.6. The toe response in the records occurs at time $2L/C$. This is the time required for the waves to travel to the pile toe and back to the measurement location, divided by the wave speed. Since there are no resistance effects acting on the pile shaft, the force and velocity records are equal until the reflection from the free end condition arrives at the measurement location. At time $2L/C$, the force wave goes to zero and the velocity wave doubles in magnitude. Note the repetitive pattern in the records at $2L/C$ intervals generated as the waves continue to travel down and up the pile. This illustration is typical of an easy driving situation where the pile "runs" under the hammer blow.

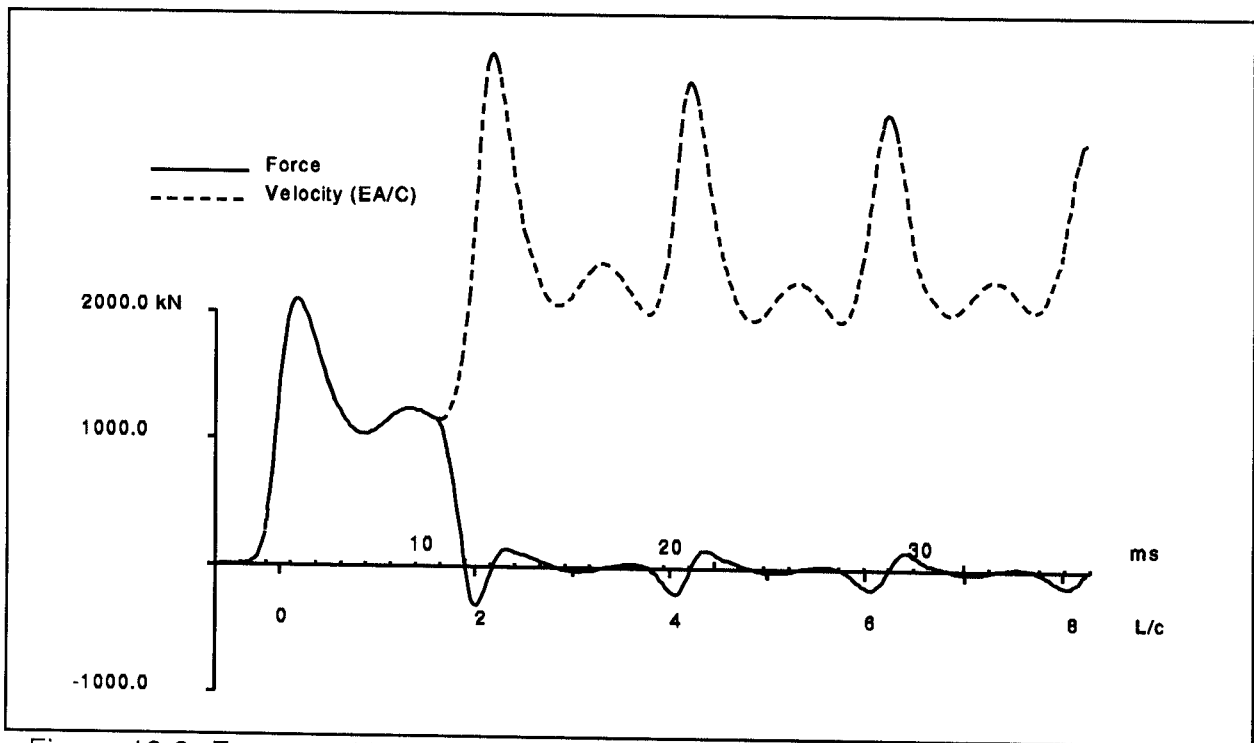
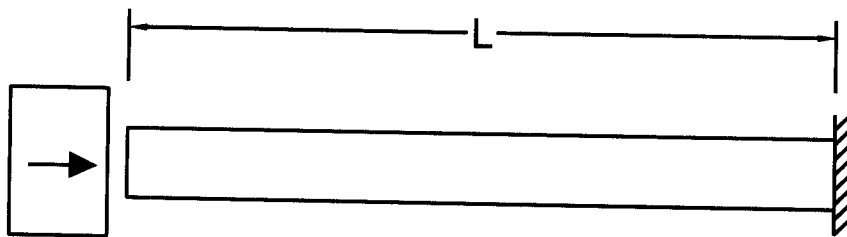
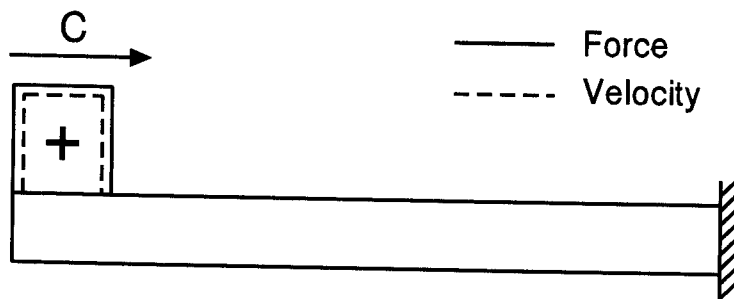


Figure 18.6 Force and Velocity Measurements versus Time for Free End Condition

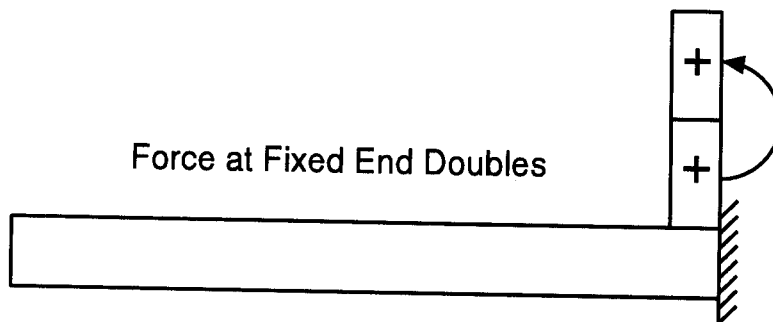
Figure 18.7(a) illustrates a uniform rod of length, L , that is struck by a mass. Again there are no resistance effects along the rod length, but the pile end is fixed, *i.e.*, it is prevented by some mechanism from moving in such a manner that the particle velocity must be zero at that point. The mass impact will impart force and velocity waves in the rod as shown in Figure 18.7(b). These waves will again travel down the rod at the



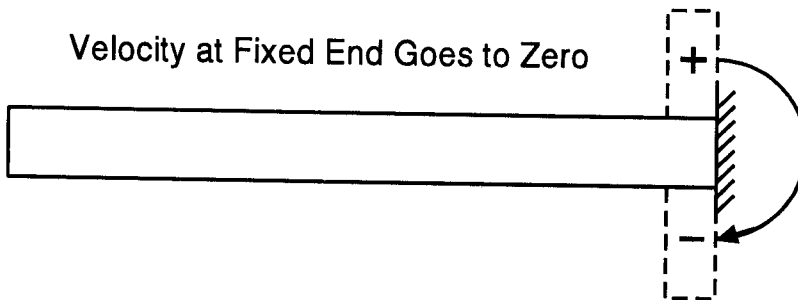
(a)



(b)



(c)



(d)

Figure 18.7 Fixed End Wave Mechanics

material wave speed, C . At time L/C , the waves will arrive at the end of the rod as shown in Figures 18.7(c) and 18.7(d). There the fixed end condition will cause a compression wave reflection and therefore the force at the fixed end doubles in magnitude and the pile velocity becomes zero. A compression wave then travels up the rod.

Consider now that the rod is a pile with a fixed end condition and that force and velocity measurements are again made near the pile head. The force and velocity measurements versus time for this condition are presented in Figure 18.8. Since there are no resistance effects acting on the pile shaft, the force and velocity records are equal until the reflection from the fixed end condition arrives at the measurement location. At time $2L/C$, the force wave increases in magnitude and the velocity wave goes to zero. This illustration is typical of a hard driving situation where the pile is driven to rock.

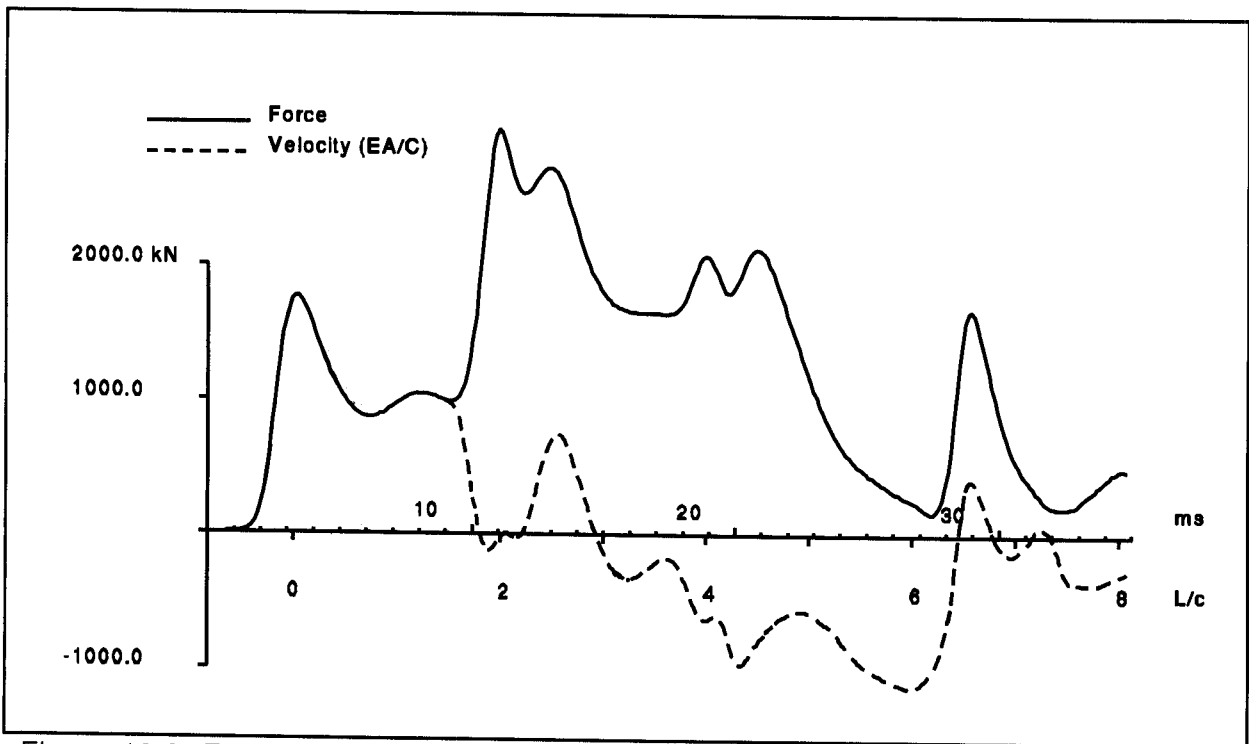


Figure 18.8 Force and Velocity Measurements versus Time for Fixed End Condition

As discussed above, the force and velocity records versus time are equal or proportional at impact and remain proportional thereafter until affected by soil resistance or cross sectional changes. Reflections from either effect will arrive at the measurement location

at time $2X/C$ where X is the distance to the soil resistance or cross section change. Both soil resistance effects and cross sectional increases will cause an increase in the force record and a proportional decrease in the velocity record. Conversely, cross sectional reductions, such as those caused by pile damage, will cause a decrease in the force record and an increase in the velocity record.

The concept of soil resistance effects on force and velocity records can be further understood by reviewing the theoretical soil resistance example presented in Figure 18.9. In this case, the soil resistance on a pile consists only of a small resistance located at a depth, A , below the measurement location, and a larger soil resistance at depth B . No other resistance effects act on the pile, so a free end condition is present at the pile toe. The force and velocity records versus time for this example will be proportional until time $2A/C$, when the reflection from the small soil resistance effect arrives at the measurement location. This soil resistance reflection will then cause a small increase in the force record and a small decrease in the velocity record.

No additional soil resistance effects act on the pile between times $2A/C$ and $2B/C$. Therefore, the force and velocity records will remain parallel over this time interval with no additional separation. At time $2B/C$, the reflection from the large soil resistance effect will arrive at the measurement location. This large soil resistance reflection will then cause a large increase in the force record and a large decrease in the velocity record. No additional soil resistance effects act on the pile between times $2B/C$ and $2L/C$. Therefore, the force and velocity records will again remain parallel over this time interval with no additional separation between the records.

At time $2L/C$, the reflection from the pile toe will arrive at the measurement location. Since no resistance is present at the pile toe, a free end condition exists and a tensile wave will be reflected. Hence, an increase in the velocity record and a decrease in the force record will occur.

These basic interpretation concepts of force and velocity records versus time can be used to qualitatively evaluate the soil resistance effects on a pile. In Figure 18.10(a), minimal separation occurs between the force and velocity records between time 0, or the time of impact, and time $2L/C$. In addition, a large increase in the velocity record and corresponding decrease in the force record occurs at time $2L/C$. Hence, this record indicates minimal shaft and toe resistance on the pile.

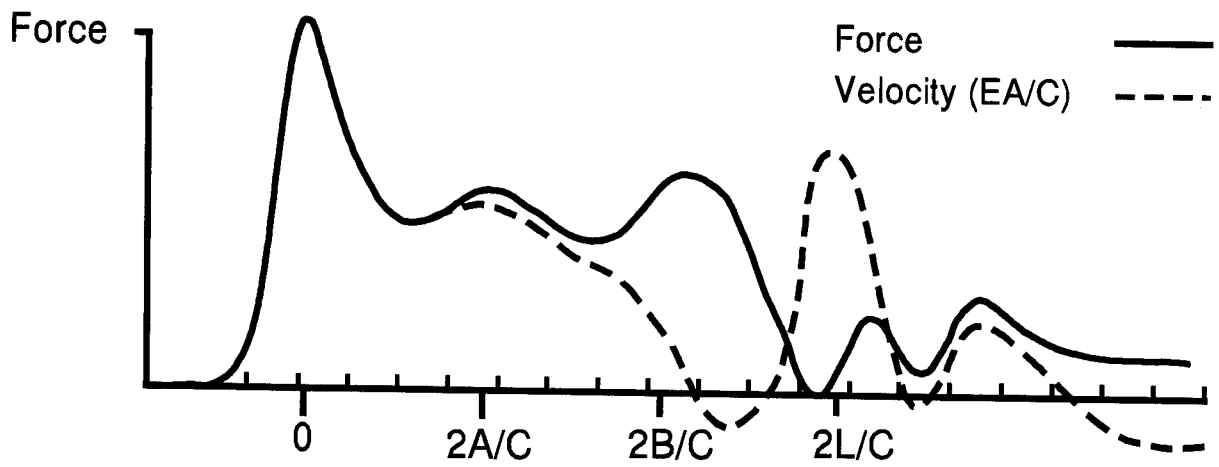
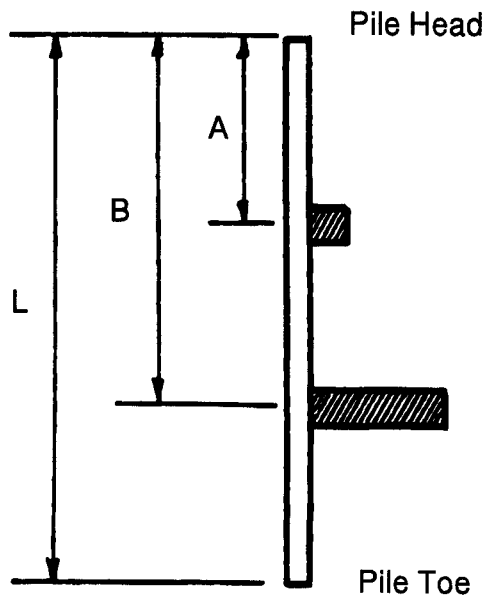
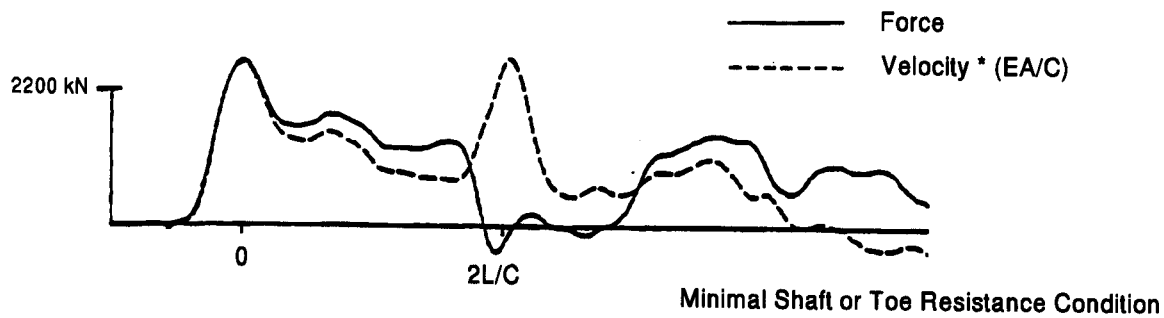
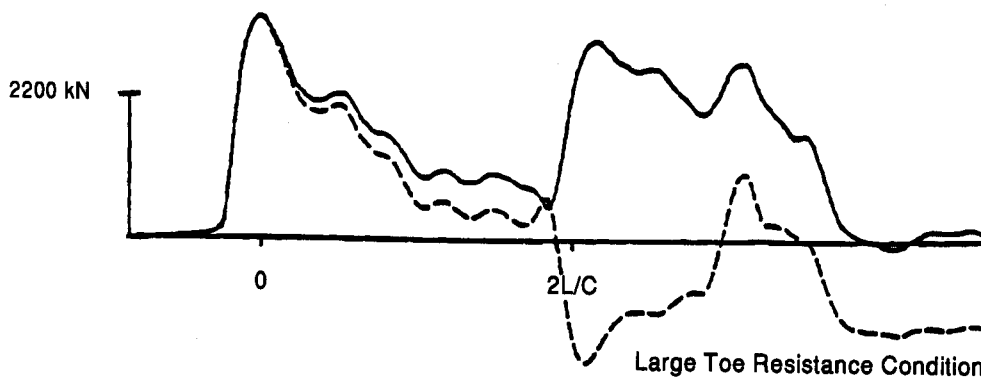


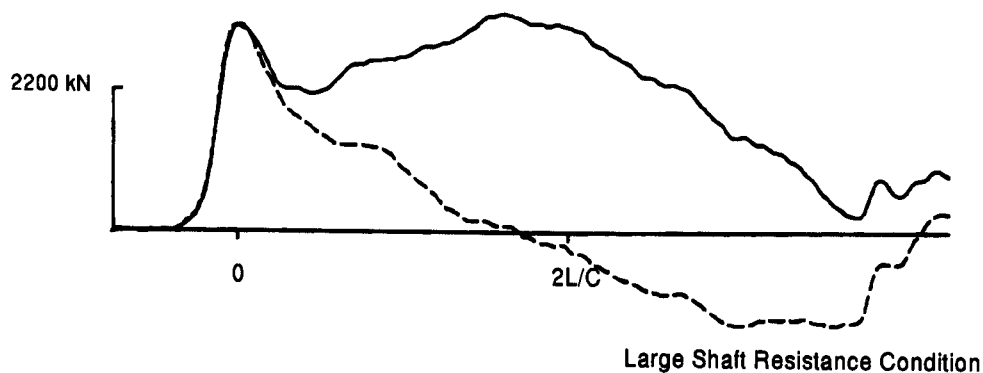
Figure 18.9 Soil Resistance Effects on Force and Velocity Records (after Hannigan, 1990)



(a)



(b)



(c)

Figure 18.10 Typical Force and Velocity Records for Various Soil Resistance Conditions (after Hannigan, 1990)

In Figure 18.10(b), minimal separation again occurs between the force and velocity records between time 0 and time $2L/C$. However in this example, a large increase in the force record and corresponding decrease in the velocity record occurs at time $2L/C$. Therefore, this force and velocity record indicates minimal shaft and a large toe resistance on the pile.

In Figure 18.10(c), a large separation between the force and velocity records occurs between time 0 and time $2L/C$. This force and velocity record indicates a large shaft resistance on the pile.

18.5 DYNAMIC TESTING METHODOLOGY

As introduced in Section 18.1, two methods have developed for analyzing dynamic measurement data, the Case Method and CAPWAP. In the field, the Pile Driving Analyzer uses the Case Method equations for estimates of static pile capacity, calculation of driving stresses and pile integrity, as well as computation of transferred hammer energy. The CAPWAP analysis method is a more rigorous numerical analysis procedure that uses dynamic records of force and velocity along with wave equation type pile and soil modeling to calculate static pile capacity, the relative soil resistance distribution, and dynamic soil properties of quake and damping. Static pile capacity evaluation from these two methods will be described in greater detail in subsequent sections. For additional details of the dynamic analysis procedures, references are provided at the end of this chapter.

18.5.1 Case Method Capacity

Research conducted at Case Western Reserve University in Cleveland, Ohio, resulted in a method which uses electronic measurements taken during pile driving to predict static pile capacity. Assuming the pile is linearly elastic and has constant cross section, the total static and dynamic resistance on a pile during driving, RTL , can be expressed using the following equation, which was derived from a closed form solution to the one dimensional wave propagation theory:

$$RTL = 1/2[F(t_1) + F(t_2)] + 1/2[V(t_1) - V(t_2)] EA/C$$

Where: F = Force measured at gage location.
V = Velocity measured at gage location.
t₁ = Time of initial impact.
t₂ = Time of reflection of initial impact from pile toe (t₁ + 2L/C).
E = Pile modulus of elasticity.
C = Wave speed of pile material.
A = Pile area at gage location.
L = Pile length below gage location.

To obtain the static pile capacity, the dynamic resistance (damping) must be subtracted from the above equation. Goble *et al.* (1975) found that the dynamic resistance component could be approximated as a linear function of a damping factor times the pile toe velocity, and that the pile toe velocity could be estimated from dynamic measurements at the pile head. This led to the standard Case Method capacity equation, RSP, expressed below:

$$RSP = RTL - J[V(t_1) EA/C + F(t_1) - RTL]$$

Where: J = Dimensionless damping factor based on soil type near the pile toe.

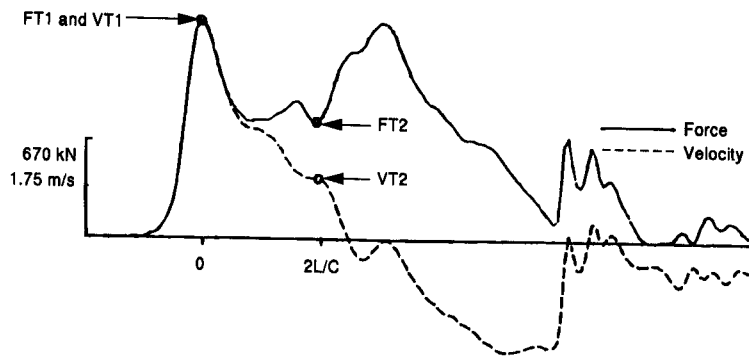
Typical damping factors versus soil type at the pile toe were determined by finding the range in the Case damping factor, J, for a soil type that provided a correlation of the RSP static capacity within 20% of the static load test failure load, determined using the Davisson (1972) offset limit method. The original range in Case damping factor versus soil type from this correlation study, Goble *et al.* (1975), as well as typical ranges in Case damping factor for the RSP equation based on subsequent experience, Pile Dynamics, Inc. (1996), are presented in Table 18-1. While use of these values with the RSP equation may provide good initial capacity estimates, site specific damping correlations should be developed based upon static load test results or CAPWAP analysis. It should also be noted that Case damping is a non-dimensional damping factor and is not the same as the Smith damping discussed in Chapter 17 for wave equation analysis.

TABLE 18-1 SUMMARY OF CASE DAMPING FACTORS FOR RSP EQUATION		
Soil Type at Pile Toe	Original Case Damping Correlation Range Goble <i>et al.</i> (1975)	Updated Case Damping Ranges Pile Dynamics (1996)
Clean Sand	0.05 to 0.20	0.10 to 0.15
Silty Sand, Sand Silt	0.15 to 0.30	0.15 to 0.25
Silt	0.20 to 0.45	0.25 to 0.40
Silty Clay, Clayey Silt	0.40 to 0.70	0.40 to 0.70
Clay	0.60 to 1.10	0.70 or higher

The RSP or standard Case Method equation is best used to evaluate the capacity of low displacement piles, and piles with large shaft resistances. For piles with large toe resistances and for displacement piles driven in soils with large toe quakes, the toe resistance is often delayed in time. This condition can be identified from the force and velocity records. In these instances, the standard Case Method equation may indicate a relatively low pile capacity and the maximum Case Method equation, RMX, should be used. The maximum Case Method equation searches for the t_1 time in the force and velocity records which results in the maximum capacity. An example of this technique is presented in Figure 18.11. When using the maximum Case Method equation, experience has shown that the Case damping factor should be at least 0.4, and on the order of 0.2 higher than that used for the standard Case Method capacity equation, RSP.

The RMX and RSP Case Method equations are the two most commonly used solutions for field evaluation of pile capacity. Additional automatic Case Method solutions are available that do not require selection of a Case damping factor. These automatic methods, referred to as RAU and RA2, search for the time when the pile toe velocity is zero and hence damping is minimal. The RAU method may be applicable for piles with minimal shaft resistance and the RA2 method may be applicable to piles with toe resistance plus moderate shaft resistance. It is recommended that these automatic methods be used as supplemental indicators of pile capacity where appropriate with the more traditional standard or maximum Case Method equations primarily used to evaluate pile capacity.

STANDARD CASE METHOD, RSP



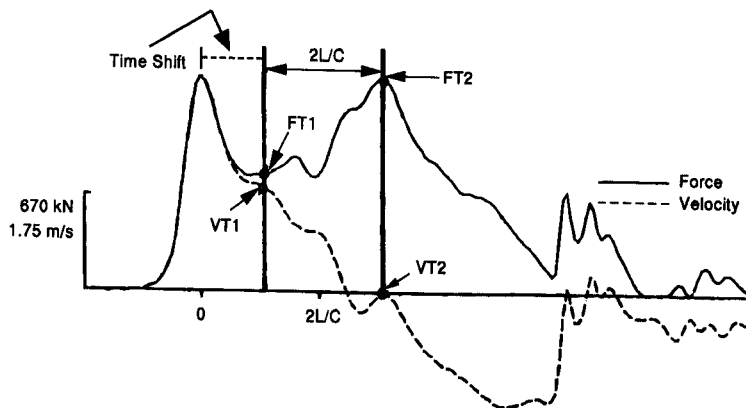
TOTAL RESISTANCE

$$\begin{aligned} \text{RTL} &= 1/2 (\text{FT1} + \text{FT2}) + 1/2 (\text{VT1} - \text{VT2}) (\text{EA/C}) \\ &= 1/2 (1486 + 819) + 1/2 (3.93 - 1.07) 381 \\ &= 1153 + 545 = 1698 \text{ kN.} \end{aligned}$$

STATIC RESISTANCE

$$\begin{aligned} \text{RSP} &= \text{RTL} - J[\text{VT1} (\text{EA/C}) + \text{FT1} - \text{RTL}] \\ &= 1698 - 0.4 [3.93 (381) + 1486 - 1698] \\ &= 1698 - 514 = 1184 \text{ kN.} \end{aligned}$$

MAXIMUM CASE METHOD, RMX



TOTAL RESISTANCE

$$\begin{aligned} \text{RTL} &= 1/2 (\text{FT1} + \text{FT2}) + 1/2 (\text{VT1} - \text{VT2}) (\text{EA/C}) \\ &= 1/2 (819 + 1486) + 1/2 (1.92 - 0.0) 381 \\ &= 1153 + 366 = 1519 \text{ kN.} \end{aligned}$$

STATIC RESISTANCE

$$\begin{aligned} \text{RMX} &= \text{RTL} - J[\text{VT1} (\text{EA/C}) + \text{FT1} - \text{RTL}] \\ &= 1519 - 0.7 [1.92 (381) + 819 - 1519] \\ &= 1519 - 22 = 1497 \text{ kN.} \end{aligned}$$

Figure 18.11 Standard, RSP and Maximum, RMX, Case Method Capacity Estimates

18.5.2 Energy Transfer

The energy transferred to the pile head can be computed from the strain and acceleration measurements. As described in Section 18.3, the acceleration signal is integrated to obtain velocity and the strain measurement is converted to force. Transferred energy is equal to the work done which can be computed from the integral of the force and velocity records over time as given below:

$$E_p(t) = \int_0^t F(t)V(t) dt$$

Where: E_p = The energy at the gage location expressed as a function of time.
 F = The force at the gage location expressed as a function of time.
 V = The velocity at the gage location expressed as a function of time.

This procedure is illustrated in Figure 18.12. The maximum energy transferred to the pile head corresponds to the maximum value of $E_p(t)$ and can be used to evaluate the performance of the hammer and driving system as described in Section 18.7.

18.5.3 Driving Stresses and Integrity

The Pile Driving Analyzer calculates the compression stress at the gage location using the measured strain and pile modulus of elasticity. However, the maximum compression stress in the pile may be greater than the compression stress calculated at the gage location, such as in the case of a pile driven through soft soils to rock. In these cases CAPWAP or wave equation analysis may be used to evaluate the maximum compression stress in the pile. Computed tension stresses are based upon the superposition of the upward and downward traveling force waves calculated by the Pile Driving Analyzer.

The basic concepts of wave mechanics were presented in Section 18.4. Convergence between the force and velocity records prior to the toe response at time $2L/C$ indicates an impedance (EA/C) reduction in the pile. For uniform cross section piles an impedance reduction is therefore pile damage. The degree of convergence between the force and velocity records is termed BTA, which can be used to evaluate pile damage following the guidelines presented in Rausche and Goble, (1979). These guidelines are provided in Table 18-2. Piles with BTA values below 80% correspond to damaged or broken piles.

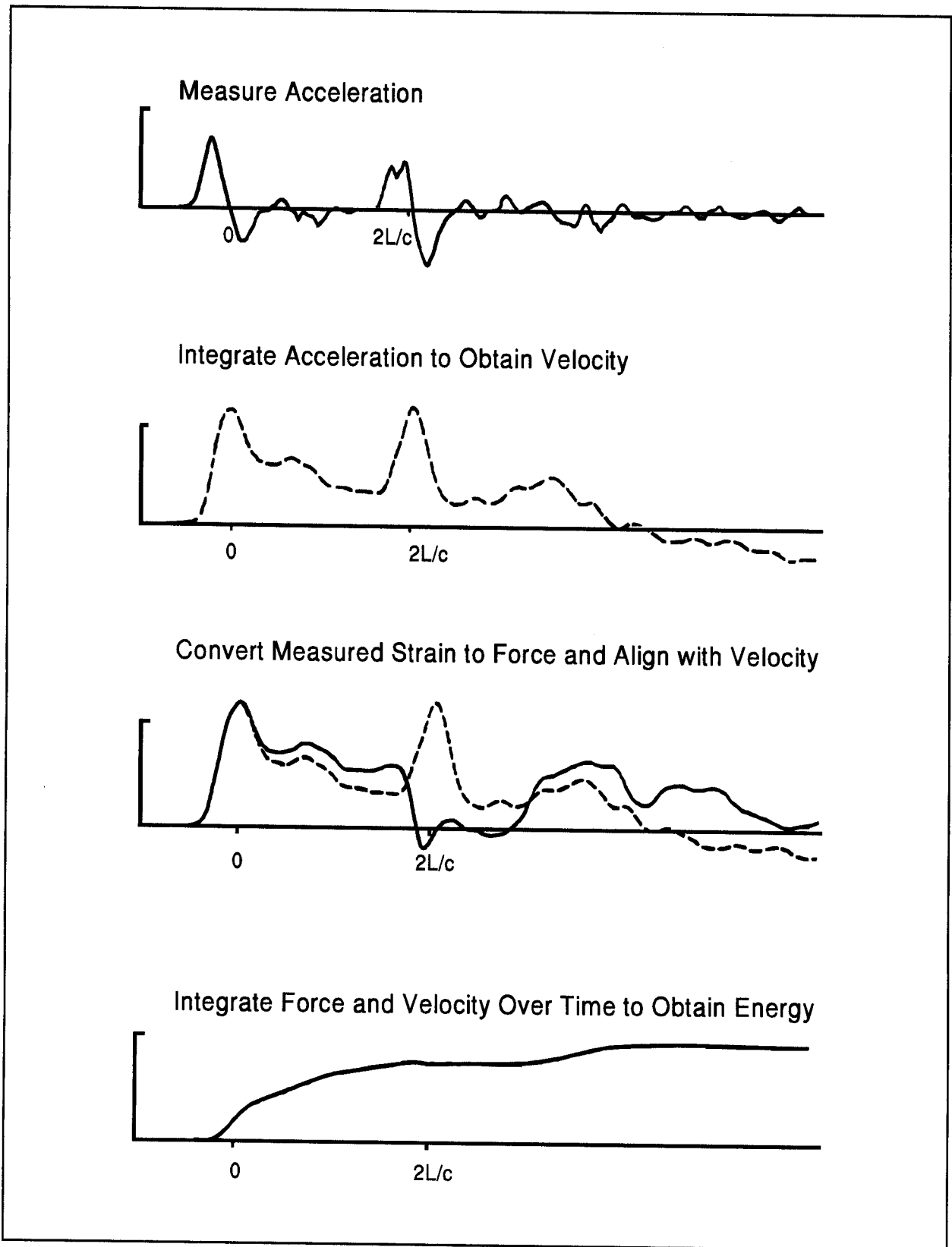


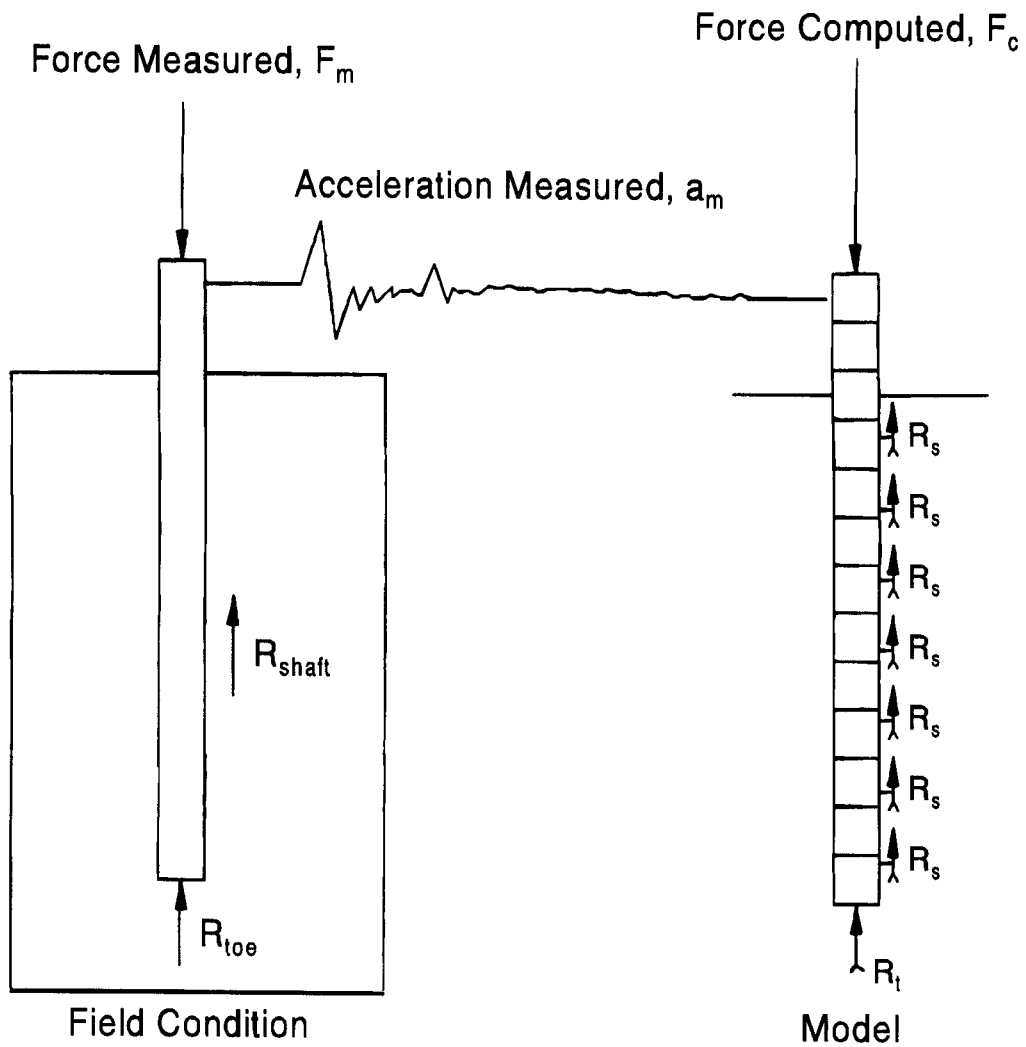
Figure 18.12 Energy Transfer Computation (after Hannigan, 1990)

TABLE 18-2 PILE DAMAGE GUIDELINES (Rausche and Goble, 1979)	
BTA	Severity of Damage
1.0	Undamaged
0.8 - 1.0	Slightly Damaged
0.6 - 0.8	Damaged
Below 0.6	Broken

18.5.4 The CAPWAP Method (Case Pile Wave Analysis Program)

CAPWAP is a computer program for a more rigorous evaluation of static pile capacity, the relative soil resistance distribution, and soil quake and damping characteristics. A CAPWAP analysis is performed on an individual hammer blow that is usually selected from the end of driving or beginning of restrike. As such, a CAPWAP analysis refines the Case Method dynamic test results at a particular penetration depth or time. CAPWAP uses wave equation type pile and soil models; the Pile Driving Analyzer measured force and velocity records are used as the head boundary condition, replacing the hammer model.

In the CAPWAP method depicted in Figure 18.13, the pile is modeled by a series of continuous pile segments and the soil resistance modeled by elasto-plastic springs (static resistance) and dashpots (dynamic resistance). The force and acceleration data from the Pile Driving Analyzer are used to quantify pile force and pile motion, which are two of the three unknowns. The remaining unknown is the boundary conditions, which are defined by the soil model. First, reasonable estimates of the soil resistance distribution and quake and damping parameters are made. Then, the measured acceleration is used to set the pile model in motion. The program then computes the equilibrium pile head force, which can be compared to the Pile Driving Analyzer determined force. Initially, the computed and measured pile head forces will not agree with each other. Adjustments are made to the soil model assumptions and the calculation process repeated.



- | | |
|------------|----------------------------|
| 1. Measure | F_m, a_m |
| 2. Compute | $F_c = F_c(a_m, R_s, R_t)$ |
| 3. Compare | $F_m \leftrightarrow F_c$ |
| 4. Correct | R_s, R_t |
| 5. Iterate | (go to 2) |

Figure 18.13 Schematic of CAPWAP Analysis Method

In the CAPWAP matching process, the ability to match the measured and computed waves at various times is controlled by different factors. Figure 18.14 illustrates the factors that most influence match quality in a particular zone. The assumed shaft resistance distribution has the dominant influence on match quality beginning with the rise of the record at time t_r before impact and continuing for a time duration of $2L/C$ thereafter. This is identified as Zone 1 in Figure 18.14.

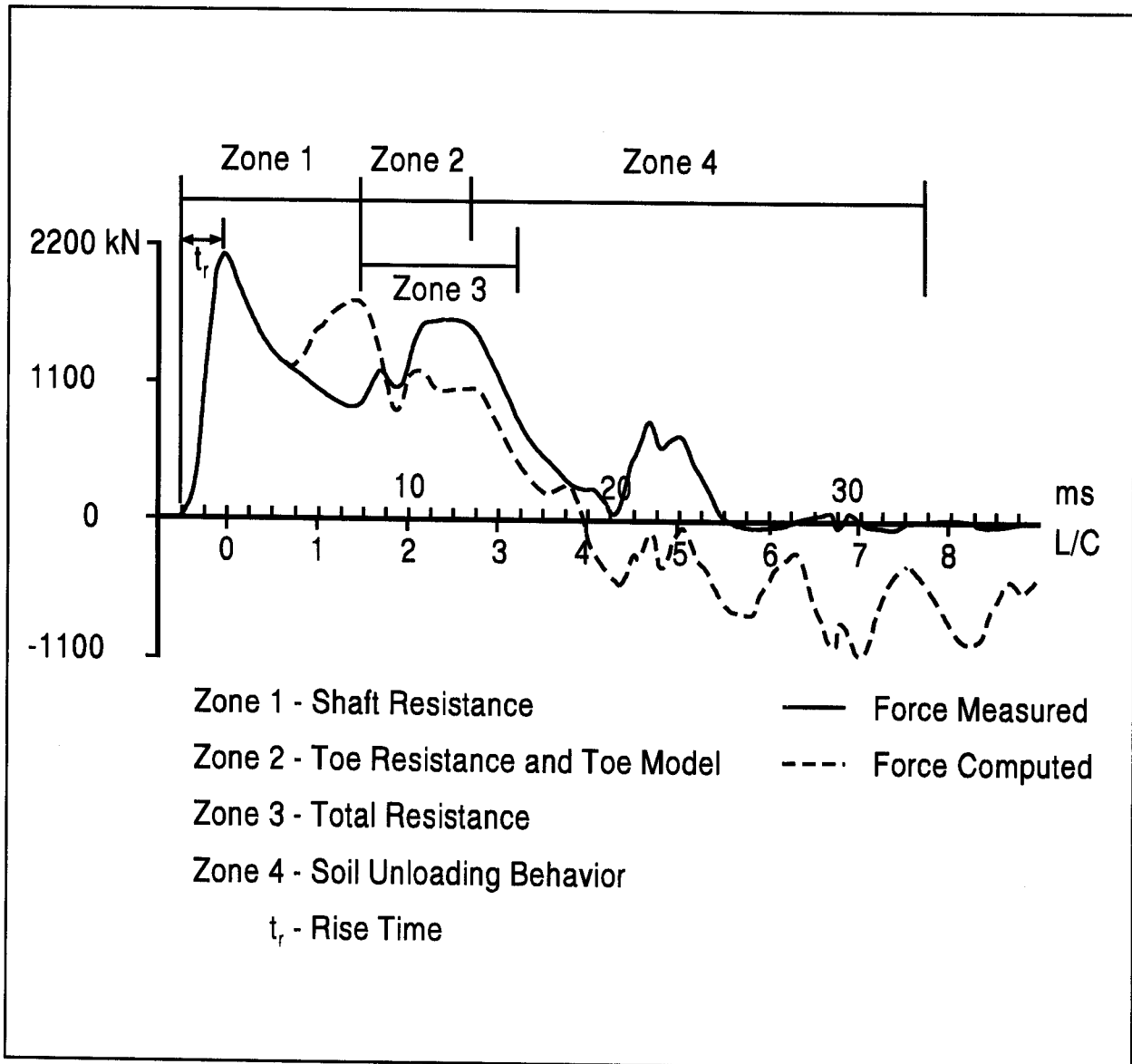


Figure 18.14 Factors Most Influencing CAPWAP Force Wave Matching (after Hannigan, 1990)

In Zone 2, the toe resistance and toe model (toe damping, toe quake and toe gap) most influence the wave match. Zone 2 begins where Zone 1 ends and continues for a time duration equal to the rise time, t_r , plus 3 ms. During Zone 3, which begins where Zone 1 ends and continues for a time duration of the rise time t_r , plus 5 ms, the overall capacity controls the match quality. A good wave match in Zone 3 is essential for accurate capacity assessments. Zone 4 begins at the end of Zone 2 and continues for a duration of about 20 ms. The unloading behavior of the soil most influences match quality in this zone.

With each analysis, the program evaluates the match quality by summing the absolute values of the relative differences between the measured and computed waves. The program computes a match quality number for each analysis that is the sum of the individual match quality numbers for each of these four zones. An illustration of the CAPWAP iteration process is presented in Figure 18.15.

Through this trial and error iteration adjustment process to the soil model as illustrated in Figure 18.13, the soil model is refined until no further agreement can be obtained between the measured and computed pile head forces. The resulting soil model is then considered the best estimate of the static pile capacity, the soil resistance distribution, and the soil quake and damping characteristics. An example of the final CAPWAP result summary is presented in 18.16. A summary of the stress distribution throughout the pile is also obtained as illustrated in Figure 18.17. Lastly, CAPWAP includes a simulated static load-set graph based on the CAPWAP calculated static resistance parameters and the elastic compression characteristics of the pile.

CAPWAP is a proprietary computer program of Goble, Rausche, Likins and Associates, Inc. and the program software is available from the developer. Alternatively, analysis of dynamic test data can be obtained from the developer or other consulting engineers who have acquired program licenses.

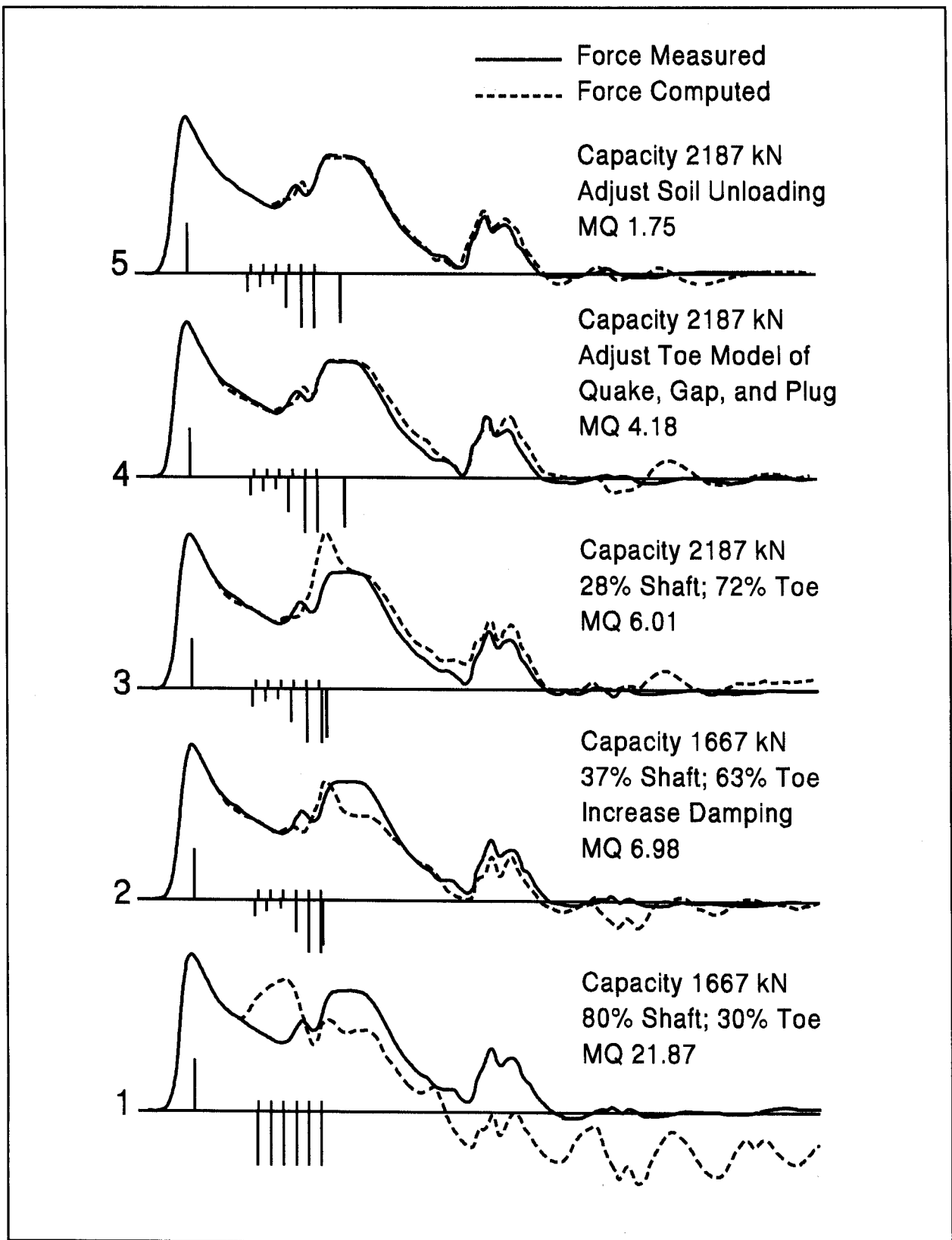


Figure 18.15 CAPWAP Iteration Matching Process (after Hannigan, 1990)

Goble Rausche Likins & Associates, Inc.

09-Nov-95

PEACH FREEWAY BRIDGE

Pile: PIER-2L Blow: 528

Collected: 01-Oct-92

CAPWAP(R) Ver. 1.994-1

CAPWAP FINAL RESULTS

Total CAPWAP Capacity: 2187.0; along Shaft 612.1; at Toe 1575.0 kN

=====

Soil Sgmnt No.	Depth Below Gages m	Depth Below Grade m	Ru kN	Force in Pile at Ru kN	Sum of Ru kN	Unit Resist. w. Respect to Depth kN/m	Resist. Area kN/m2	Smith Damping Factor s/m	Quake mm
				2187.0					
1	10.2	2.3	44.0	2143.0	44.0	21.58	15.20	.550	2.300
2	12.2	4.3	28.0	2115.0	72.0	13.71	9.65	.550	2.300
3	14.3	6.4	21.0	2094.0	93.0	10.29	7.25	.550	2.300
4	16.3	8.4	119.0	1975.0	212.0	58.35	41.09	.550	2.300
5	18.4	10.5	202.0	1773.0	414.0	99.03	69.74	.550	2.300
6	20.4	12.5	198.0	1575.0	612.1	97.08	68.36	.550	2.300

Average Skin Values 102.0 48.96 35.21 .550 2.300
 Toe 1575.0 17499.63 .290 3.600

Soil Model Parameters/Extensions Skin Toe
 Case Damping Factor .488 .662

Figure 18.16 CAPWAP Final Results Table

Goble Rausche Likins & Associates, Inc.

09-Nov-95

PEACH FREEWAY BRIDGE

Pile: PIER-2L Blow: 528

Collected: 01-Oct-92

CAPWAP(R) Ver. 1.994-1

EXTREMA TABLE

Pile Sgmnt No.	Depth Below Gages m	max. Force kN	min. Force kN	max. Comp. Stress kN/cm2	max. Tension Stress kN/cm2	max. Trnsfd. Energy kN- m	max. Veloc. m/s	max. Displ. cm
1	1.0	3174.0	-72.5	18.848	-.430	32.31	4.4	1.737
2	2.0	3195.0	.0	18.973	.000	31.13	4.3	1.680
4	4.1	3214.2	.0	19.086	.000	29.83	4.3	1.560
6	6.1	3235.5	.0	19.213	.000	28.49	4.2	1.440
8	8.2	3273.7	.0	19.440	.000	27.20	4.2	1.320
10	10.2	3342.5	-60.9	19.848	-.362	25.92	4.1	1.200
12	12.2	3257.1	-83.6	19.342	-.497	23.56	4.0	1.080
14	14.3	3252.0	-140.1	19.311	-.832	21.75	3.9	.960
16	16.3	3379.0	-126.5	20.065	-.751	20.15	3.6	.850
18	18.4	3182.0	-49.7	18.895	-.295	17.11	3.4	.730
19	19.4	2718.8	.0	16.145	.000	14.02	3.3	.680
20	20.4	3005.1	.0	17.845	.000	11.97	3.0	.640
Absolute	16.3			20.065		(T=	24.7 ms)	
	14.3				-.832	(T=	41.2 ms)	

Figure 18.17 CAPWAP Stress Distribution Profile

18.6 USAGE OF DYNAMIC TESTING METHODS

Dynamic testing is specified in many ways, depending upon the information desired or purpose of the testing. For example, a number of test piles driven at preselected locations may be specified. In this application, the test piles are usually driven in advance of, or at the start of, production driving so that the information obtained can be used to establish driving criteria and/or pile order lengths for each substructure unit. Alternatively, or in addition to a test pile program, testing of production piles on a regular interval may be specified. Production pile testing is usually performed for quality assurance checks on hammer performance, driving stress compliance, pile integrity, and ultimate capacity. Lastly, dynamic testing can be used on projects where it was not specified to troubleshoot problems that arise during construction.

The number of piles that should be dynamically tested on the project depends upon the project size, variability of the subsurface conditions, the availability of static load test information, and the reasons for performing the dynamic tests. A higher percentage of piles should be tested, for example, where there are difficult subsurface conditions with an increased risk of pile damage, or where time dependent soil strength changes are being relied upon for a significant portion of the ultimate pile capacity.

On small projects, a minimum of two dynamic tests is recommended. On larger projects and small projects with anticipated installation difficulties or significant time dependent capacity issues, a greater number of piles should be tested. Dynamically testing one or two piles per substructure location is not unusual in these situations. Regardless of the project size, specifications should allow the engineer to adjust the number and locations of dynamically tested piles based on design or construction issues that arise.

Restrike dynamic tests should be performed whenever pile capacity is being evaluated by dynamic test methods. Restrikes are commonly specified 24 hours after initial driving. However, in fine grained soils, longer time periods are generally required for the full time dependent capacity changes to occur. Therefore, longer restrike times should be specified in these soil conditions whenever possible. On small projects, long restrike durations can present significant construction sequencing problems. Even so, at least one longer term restrike should be performed in these cases. The longer term restrike should be specified 2 to 6 days after the initial 24 hour restrike, depending upon the soil type. A warmed up hammer (from driving or restriking a non-test pile) should be used whenever restrike tests are performed.

When dynamic testing is performed by a consultant, the requirements for CAPWAP analyses should be specifically addressed in the dynamic testing specification. On larger projects, CAPWAP analyses are typically performed on 20 to 40% of the dynamic test data obtained from both initial driving and restrrike dynamic tests. This percentage typically increases on smaller projects with only a few test piles, or on projects with highly variable subsurface conditions.

It is often contractually convenient to specify that the general contractor retain the services of the dynamic testing firm. However, this can create potential problems since the contractor is then responsible for the agency's quality assurance program. Some agencies have contracted directly with the dynamic testing firm to avoid this potential conflict and many large public owners have purchased the equipment and perform the tests with their own staff.

18.7 PRESENTATION AND INTERPRETATION OF DYNAMIC TESTING RESULTS

The results of dynamic pile tests should be summarized in a formal report that is sent to both the construction engineer and foundation designer. The construction engineer should understand the information available from the dynamic testing and its role in the project construction. As discussed in Chapter 9, numerous factors are considered in a pile foundation design. Therefore, the foundation designer should interpret the dynamic test results since many other factors; (downdrag, scour, uplift, lateral loading, settlement, etc.) may be involved in the overall design and construction requirements.

Construction personnel are often presented with dynamic testing results with minimal guidance on how to interpret or use the information. Therefore, it may be helpful to both construction personnel and foundation designers to familiarize themselves with the typical screen display and information available during a dynamic test. Figure 18.18 presents a typical Pile Driving Analyzer display for a 356 mm square prestressed concrete pile driven with a diesel hammer having a maximum rated energy of 89.6 kJ.

The main Pile Driving Analyzer input quantities are displayed in the upper left corner of the screen and include the pile length below gages, LE; the pile cross sectional area at the gages, AR; the pile elastic modulus, EM; the unit weight of the pile material, SP; the pile wave speed, WS; as well as the Case damping factor, JC. The lower left corner includes input quantities for display scales and transducer calibrations and is generally of little interest except to the test engineer. Construction personnel reviewing field

results should, however, note the units indicator, UN, in this area of the screen. The force units are noted to be in "kN * 10" or kilonewtons times 10. This means any forces (but not stresses), capacity, or energy results displayed in the numerical results area must be multiplied by 10.

The screen is dominated by the graphical display of force (solid line) and velocity (dashed line) records versus time. This display will change for each hammer blow. The first vertical line represents time t_1 in the Case Method calculations and corresponds to the time of impact as the waves pass the gage location near the pile head. The second vertical line represents time t_2 in the Case Method calculations and corresponds to the time when the input waves have traveled to the pile toe and returned to the gage location or time $2L/C$.

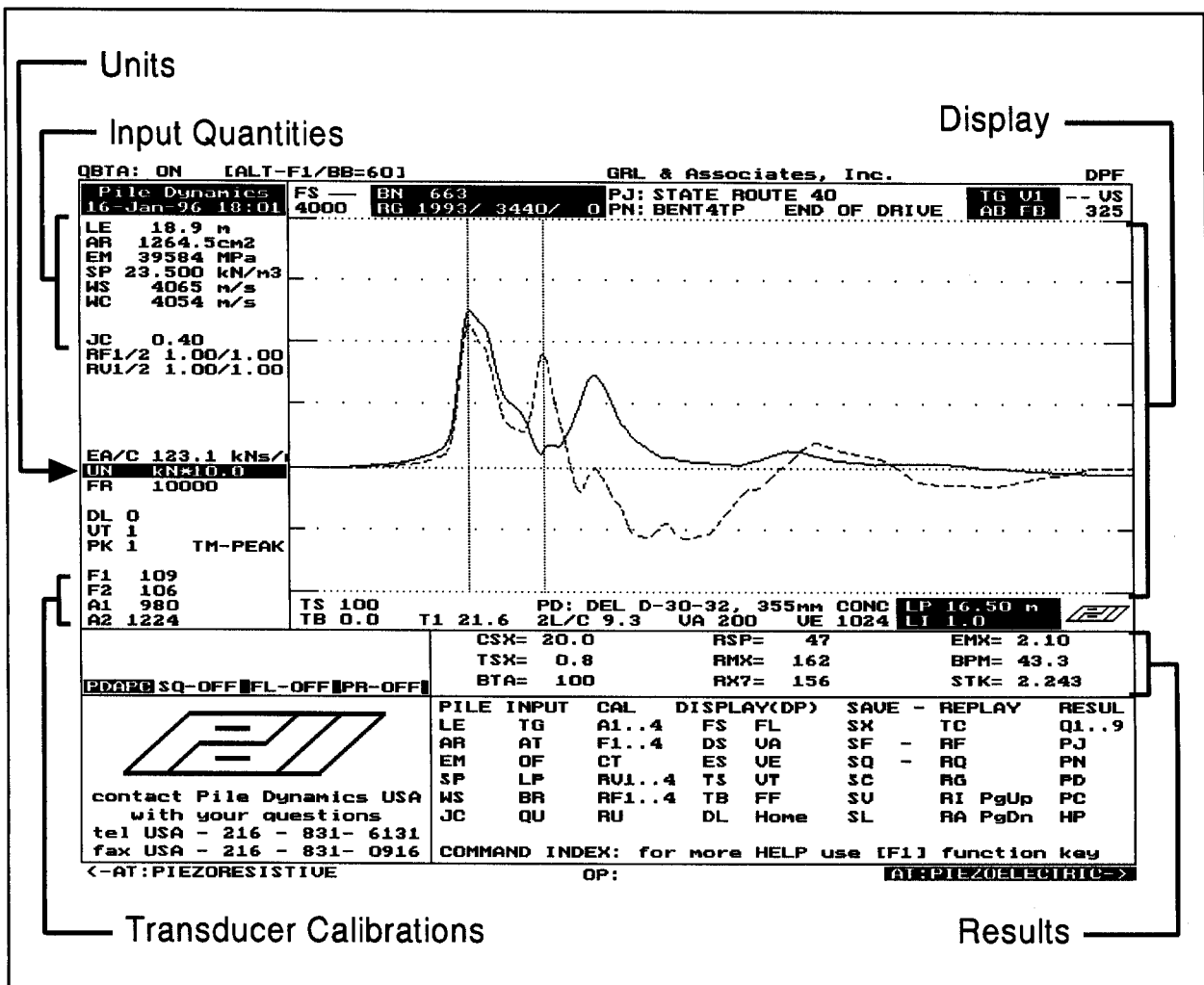


Figure 18.18 Typical Dynamic Test System Screen Display

An experienced test engineer can visually interpret these signals for data quality, soil resistance distribution and pile integrity. As discussed earlier, soil resistance forces cause a relative increase in the force wave and a corresponding relative decrease in the velocity wave. Therefore on a pile with a uniform cross section, the separation between the force and velocity records between times t_1 and t_2 indicates the shaft resistance. The magnitude of separation is also indicative of the magnitude of the soil resistance at that depth. Toe resistance is indicated by the separation between these records near and after time t_2 .

The Pile Driving Analyzer searches for convergence between the force and velocity records beginning at the time of the sharp rise in the records prior to time t_1 and continuing for a time interval of $2L/C$ thereafter. If convergence between the force and velocity records occurs prior to the rise in the velocity record preceding time t_2 , a cross sectional reduction or pile damage is indicated. The degree of convergence between the force and velocity records is expressed by the BTA integrity value as a percentage of the approximate reduced cross sectional area.

Numerical results from Case Method computations are identified by three letter codes displayed below the graphical records. In the example given in Figure 18.18, the first column of results provides information on the driving stresses and pile integrity. The compression stress at the pile head, CSX, is 20.0 MPa and the calculated tension stress, TSX, is 0.8 MPa. These calculated stress levels are below the recommended driving stress limits for a prestressed concrete pile given in Chapter 11. Pile integrity, BTA, is calculated as 100%, indicating that no damage is present.

The middle column of results includes computations for the standard Case Method capacity, RSP, and maximum Case Method capacity, RMX, both calculated with the input Case damping factor, JC, of 0.4. These results are 470 and 1620 kN respectively, when adjusted by the units multiplier. As noted earlier, a damping factor at least 0.2 higher is usually used with the maximum Case Method as compared to the standard Case Method. Therefore, the capacity using the RMX equation with a damping factor of 0.7 labeled RX7 was calculated and indicated a capacity of 1560 kN. From the force and velocity records in the example, the experienced test engineer would note that the resistance is delayed in time, based upon the separation between the force and velocity records occurring after time t_2 . Therefore, the maximum Case Method equation should be used for capacity evaluation, and from the capacity results noted above, a Case Method capacity of 1560 kN would be chosen.

The final column of numerical results includes the transferred hammer energy, EMX, which is 21 kJ; the hammer operating speed in blows per minute, BPM, which is 43.3; and the calculated hammer stroke for the single acting diesel hammer of 2.24 meters.

Depending upon the hammer-pile combination, average transferred energies as a percentage of the rated energy range from about 25% for a diesel hammer on a concrete pile to 50% for an air hammer on a steel pile, Rausche *et al.* (1985a). Hence, the transferred energy of 21 kJ is 23% of the rated energy and is therefore slightly below average. The performance of a hammer and driving system can be evaluated from a driving system's rated transfer efficiency, which is defined as the energy transferred to the pile head divided by the manufacturer's rated hammer energy. Figure 18.19 presents transfer efficiencies for selected hammer and pile type combinations expressed as a percentile. In this graph, the average transfer efficiency for a given hammer-pile combination can be found by noting where that graph intersects the 50 percentile. Histograms of the transfer efficiencies for each of these hammer and pile types are also presented in Figure 18.20. The histograms may be useful in assessing drive system performance as they provided the distribution and standard deviation of drive system performance for a given hammer-pile combination at the end of drive condition.

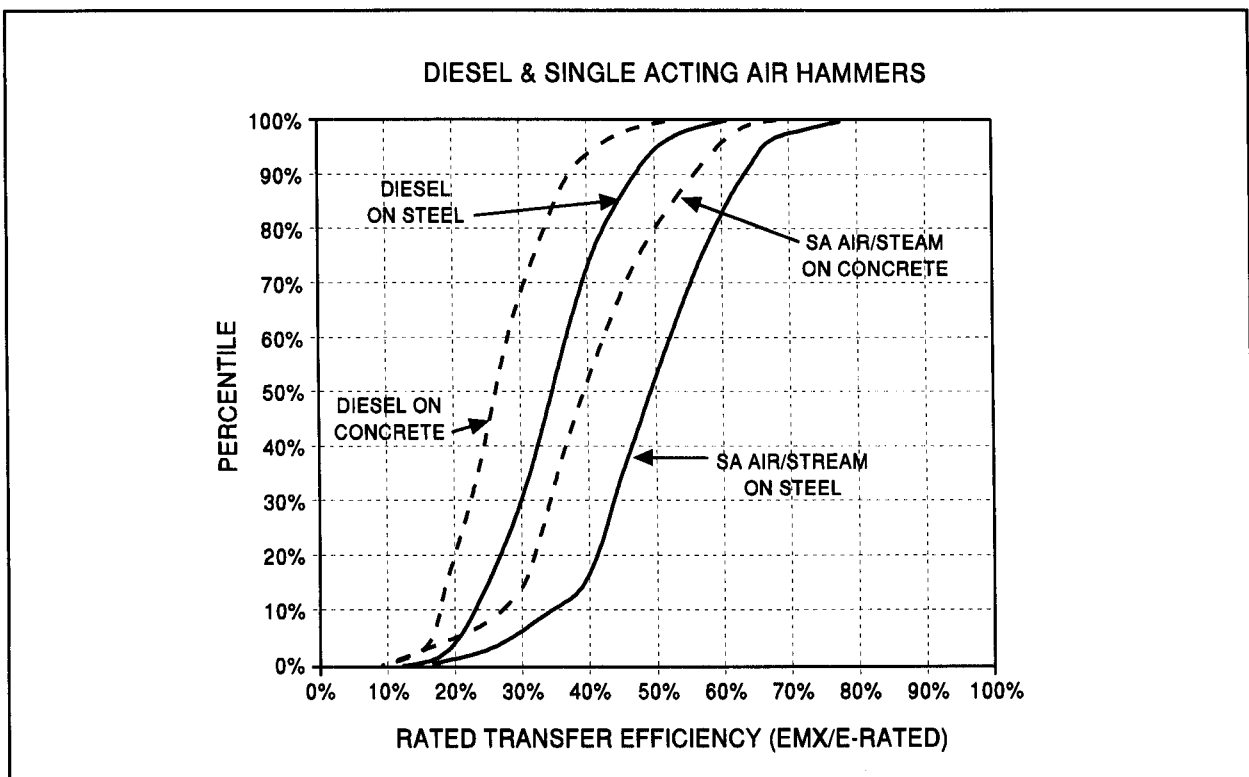
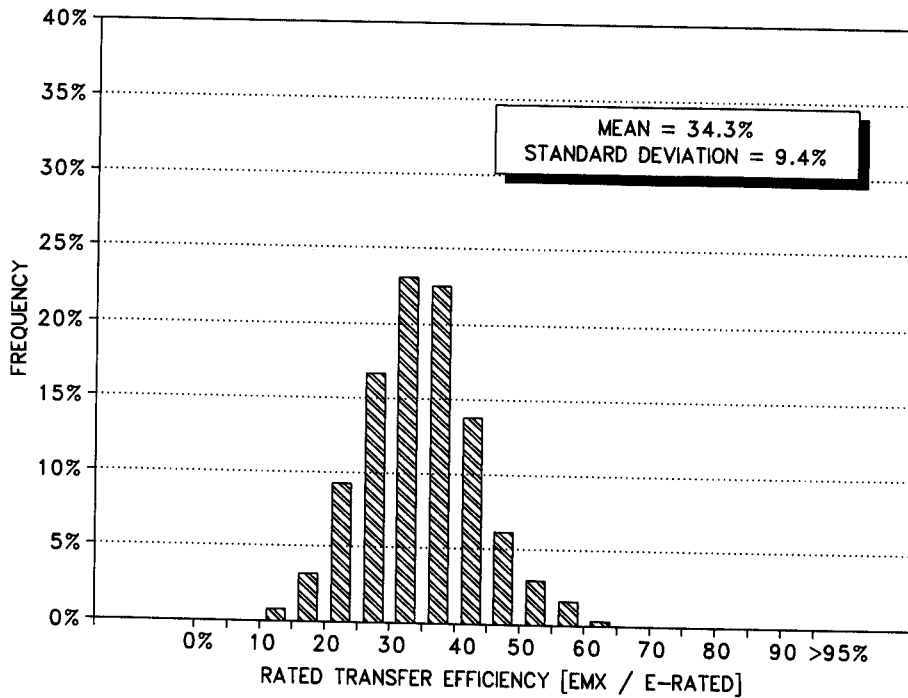
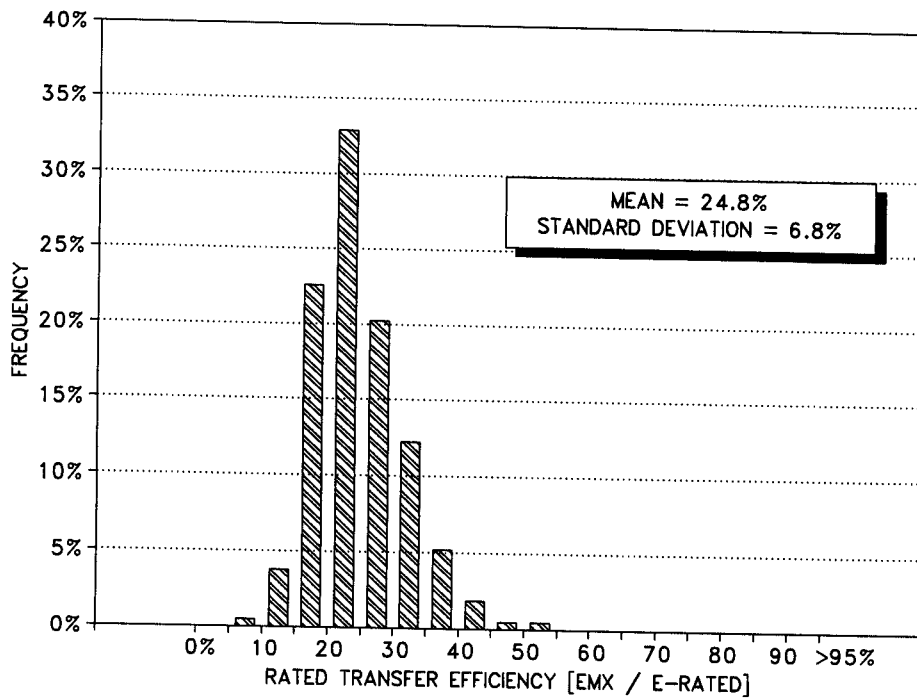


Figure 18.19 Transfer Efficiencies for Select Hammer and Pile Combinations

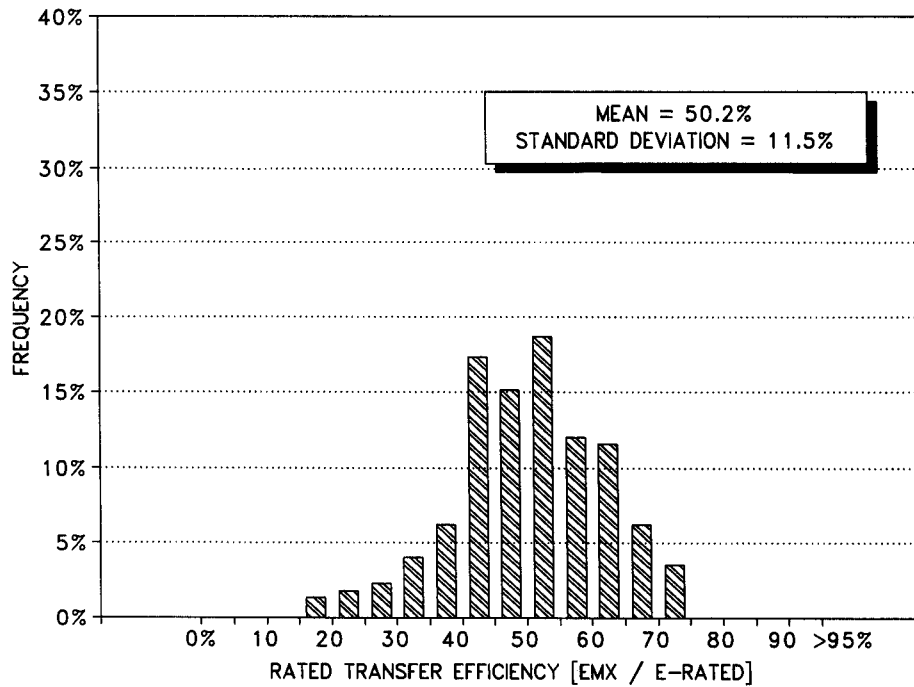


Diesel on Steel

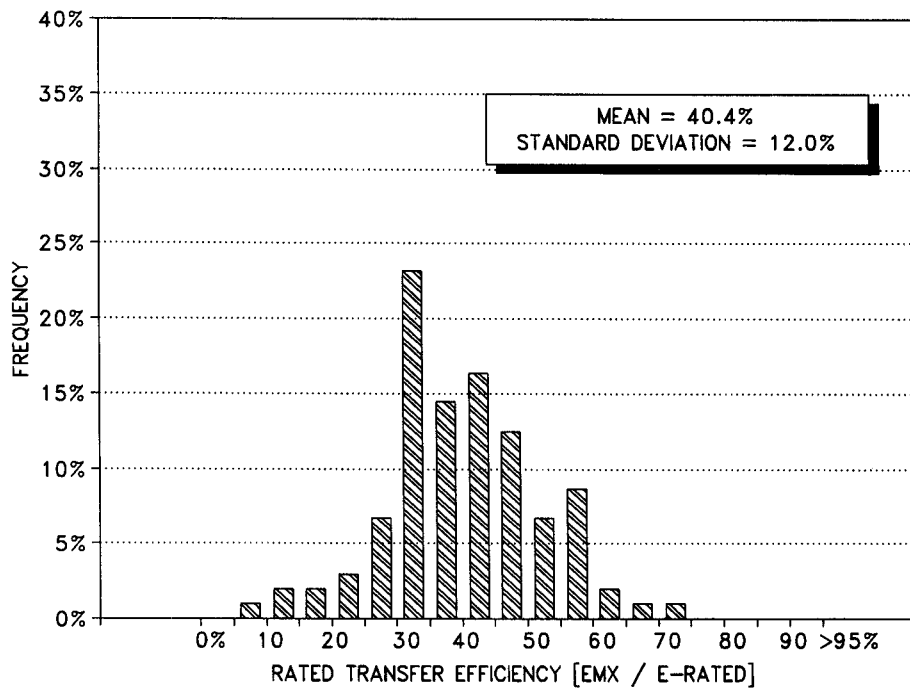


Diesel on Concrete/Timber

Figure 18.20(a) Histograms of Transfer Efficiency for Diesel Hammers



SA Air/Steam on Steel



SA Air/Steam on Concrete/Timber

Figure 18.20(b) Histograms of Transfer Efficiency for Single Acting Air/Steam Hammers

In the field, construction personnel should check that the calculated driving stresses, CSX and TSX, are maintained within specification limits. Drive system performance indicated by the transferred energy, EMX, should be within a reasonable range of that predicted by wave equation analysis or recorded on previous tests at the site. If significant variations in energy are noted, the reasons for the discrepancy should be evaluated. The recorded hammer speed should be compared to the manufacturer's specifications. Capacity estimates should be compared with the required ultimate pile capacity. In soils with time dependent changes in capacity, this comparison should be based on restrrike tests and not end-of-initial driving results.

A force and velocity record for a 406 mm x 13 mm wall closed end pipe pile is presented in Figure 18.21. As can be seen from the input properties, the pipe pile is 29.1 meters long below gages. A visual interpretation of the signal would indicate the pile has developed moderate shaft resistance over the lower portion of the pile with the majority of the pile capacity due to toe resistance. Note that an intermediate vertical line labeled D has also appeared between the two vertical lines corresponding to the pile head, t_1 , and pile toe, t_2 . Convergence between the force and velocity records before time $2L/C$, as noted by the D line, indicates a pile impedance reduction or damage. A warning box has also appeared on the screen asking the test engineer if damage is occurring. For the example shown, damage was occurring at a depth of 14.9 meters below gages due to a welding problem at the pile splice.

In Figure 18.22, a force and velocity record for a HP 360 x 132 H-pile is presented. This record is typical of a pile driven to rock. Note the strong separation in the force and velocity records at time $2L/C$ (second vertical line). The compression stress at the gage location, CSX, is 211 MPa. This is within the recommended driving stress limit of 223 MPa for A-36 steel given in Chapter 11. The Pile Driving Analyzer can also compute an estimate of the compression stress at the pile toe, CSB. This quantity may be helpful in driving stress control for piles to rock. For the record shown, CSB is calculated to be 232 MPa which is above the recommended driving stress limit. Therefore, a slight reduction in hammer stroke at final driving may be necessary. The CSB quantity is an approximate value. A better assessment of the compression stresses at the pile toe could be gained from CAPWAP or wave equation analyses.

Additional insight into the pile and soil behavior during driving can be obtained by comparing the dynamic test numerical results versus pile penetration depth and corresponding driving resistance. Dynamic testing systems typically assign a sequential

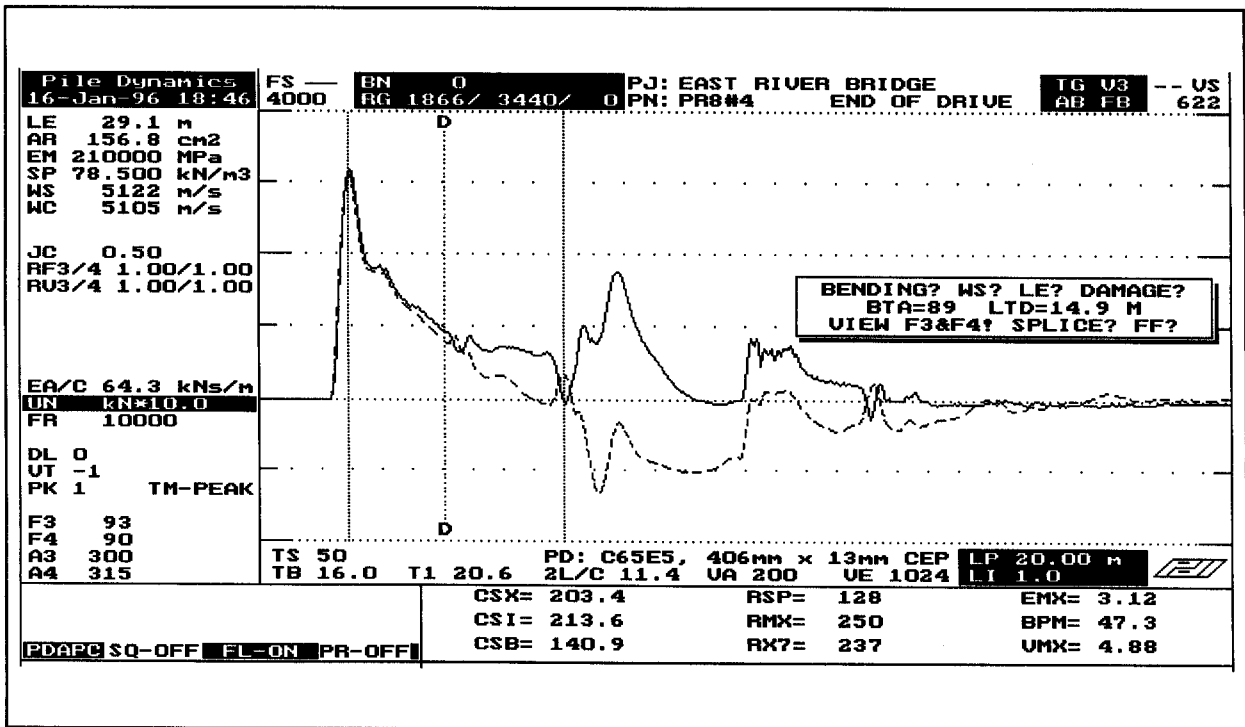


Figure 18.21 Force and Velocity Record for Damaged Pile

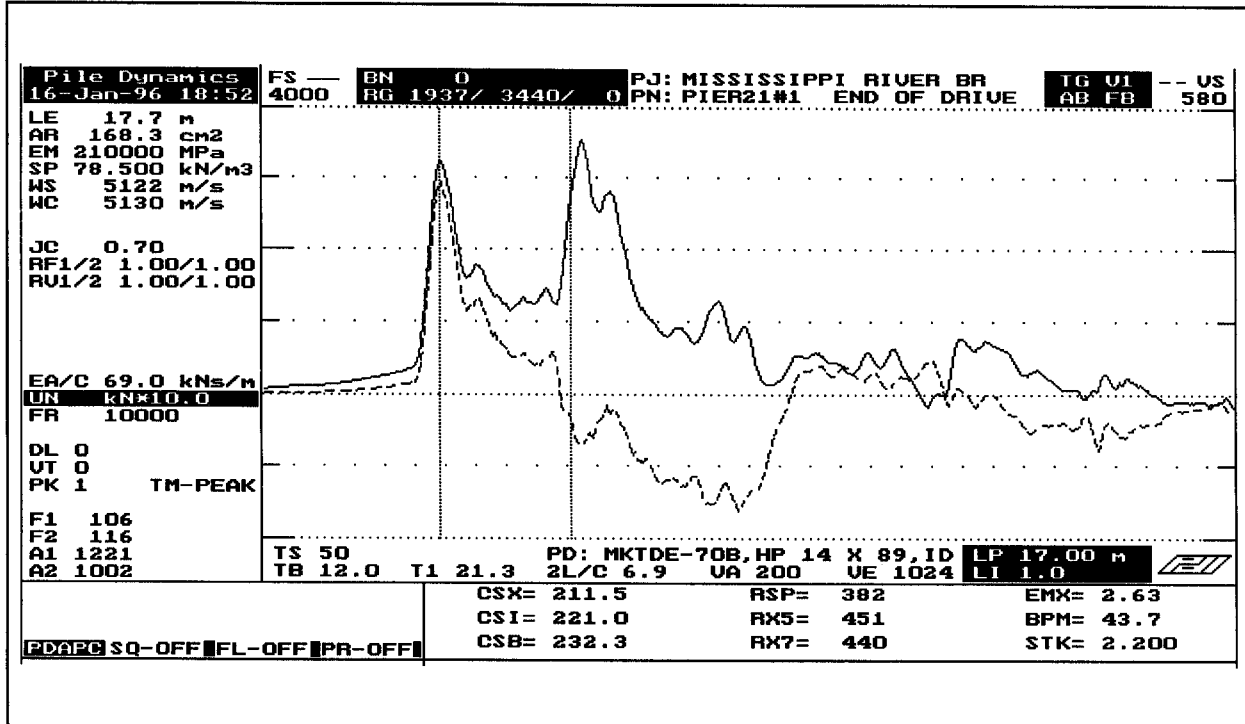


Figure 18.22 Force and Velocity Record for H-pile to Rock

blow number to each hammer blow. By comparing the pile driving records with these blow numbers, numerical and graphical summaries of the dynamic testing results versus pile penetration depth and driving resistance can be prepared. An example of a numerical summary of the dynamic testing results versus depth for a 610 mm octagonal concrete pile is presented in Table 18-3 with accompanying graphical results presented in Figure 18.23. These results can then easily be compared to project requirements by construction personnel.

TABLE 18-3 TYPICAL TABULAR PRESENTATION OF DYNAMIC TESTING RESULTS VERSUS DEPTH

Proj: PDAPLOT EXAMPLE		Increment = (depth)		Pg1					
File: PRESTRESSED CONCRETE		FileName = FGCTP5.MDF							
Desc: DIESEL HAMMER		BL# 2 to 1349		31-Oct-94					
CSX: Max Measured C-Stress		RMX: Capacity - RMX							
TSX: Max Computed T-Stress		BPM: Blows Per Minute							
EMX: Max Transferred Energy		STK: Stroke (O.E.Diesels)							
BL#	depth	TYPE	#Bls	CSX	TSX	EMX	RMX	BPM	STK
end	bl/m	m		MPa	MPa	kN-m	kN	bl/min	m
11	18	8.00	AVG 6	8.48	2.05	18.85	285	56.1	1.439
34	23	9.00	AVG 9	12.04	2.92	27.03	584	49.6	1.696
64	30	10.00	AVG 23	14.67	3.63	27.40	1107	47.6	1.845
92	28	11.00	AVG 12	15.25	3.43	27.98	1210	47.5	1.846
123	31	12.00	AVG 15	15.62	4.08	28.03	1059	47.6	1.843
166	43	13.00	AVG 14	15.93	5.33	30.79	577	48.1	1.801
199	33	14.00	AVG 11	17.29	3.92	30.55	1143	47.1	1.882
225	26	15.00	AVG 8	17.62	4.96	33.44	875	47.5	1.850
245	20	16.00	AVG 7	18.29	6.23	33.91	586	47.4	1.857
266	21	17.00	AVG 6	18.03	6.47	33.83	340	48.1	1.802
289	23	18.00	AVG 8	18.09	6.65	35.90	284	48.0	1.808
322	33	19.00	AVG 16	18.25	6.14	36.47	529	47.1	1.880
370	48	20.00	AVG 24	20.80	5.75	39.59	1104	45.9	1.989
409	39	21.00	AVG 20	25.14	7.97	45.27	1137	45.3	2.045
453	44	22.00	AVG 22	26.33	7.91	45.81	1124	45.5	2.026
493	40	23.00	AVG 20	26.31	8.10	46.87	1003	45.6	2.014
568	75	24.00	AVG 30	15.65	1.52	33.30	1040	47.3	1.863
609	41	25.00	AVG 13	16.63	3.56	34.01	931	47.8	1.824
641	32	26.00	AVG 15	17.01	4.48	32.45	893	48.3	1.780
668	27	27.00	AVG 14	18.19	5.50	33.36	857	48.2	1.793
696	28	28.00	AVG 14	19.54	6.30	36.02	864	47.5	1.847
730	34	29.00	AVG 16	19.88	6.67	35.87	816	48.2	1.794
759	29	30.00	AVG 14	20.50	6.51	39.53	870	47.1	1.876
785	26	31.00	AVG 13	23.97	8.49	44.45	868	46.9	1.896
820	35	32.00	AVG 18	25.61	9.52	45.19	761	47.2	1.868
857	37	33.00	AVG 18	27.16	9.16	48.37	861	46.4	1.939
893	36	34.00	AVG 18	28.13	8.13	51.74	1056	45.8	1.994
933	40	35.00	AVG 20	27.48	9.15	49.39	868	46.5	1.933
971	38	36.00	AVG 19	26.64	9.04	45.58	767	47.3	1.867
1012	41	37.00	AVG 41	25.49	7.91	38.45	899	48.9	1.739
1050	38	38.00	AVG 38	24.55	9.00	36.31	796	49.4	1.699
1078	28	39.00	AVG 14	24.27	9.75	36.11	671	49.5	1.692
1106	28	40.00	AVG 10	22.62	8.52	35.04	596	49.6	1.689
1199	93	41.00	AVG 49	15.60	1.67	28.10	948	49.4	1.703
1235	144	41.25	AVG 18	17.01	0.60	31.84	1672	47.6	1.839
1275	160	41.50	AVG 18	16.88	1.16	30.38	2072	47.7	1.835
1329	216	41.75	AVG 26	19.70	1.50	40.17	2434	44.7	2.115
1349	200	41.85	AVG 9	33.30	6.11	67.31	2623	41.5	2.451

GRL & ASSOC, INC. 31-Oct-94
 PDAPLOT EXAMPLE, PRESTRESSED CONCRETE, DIESEL HAMMER

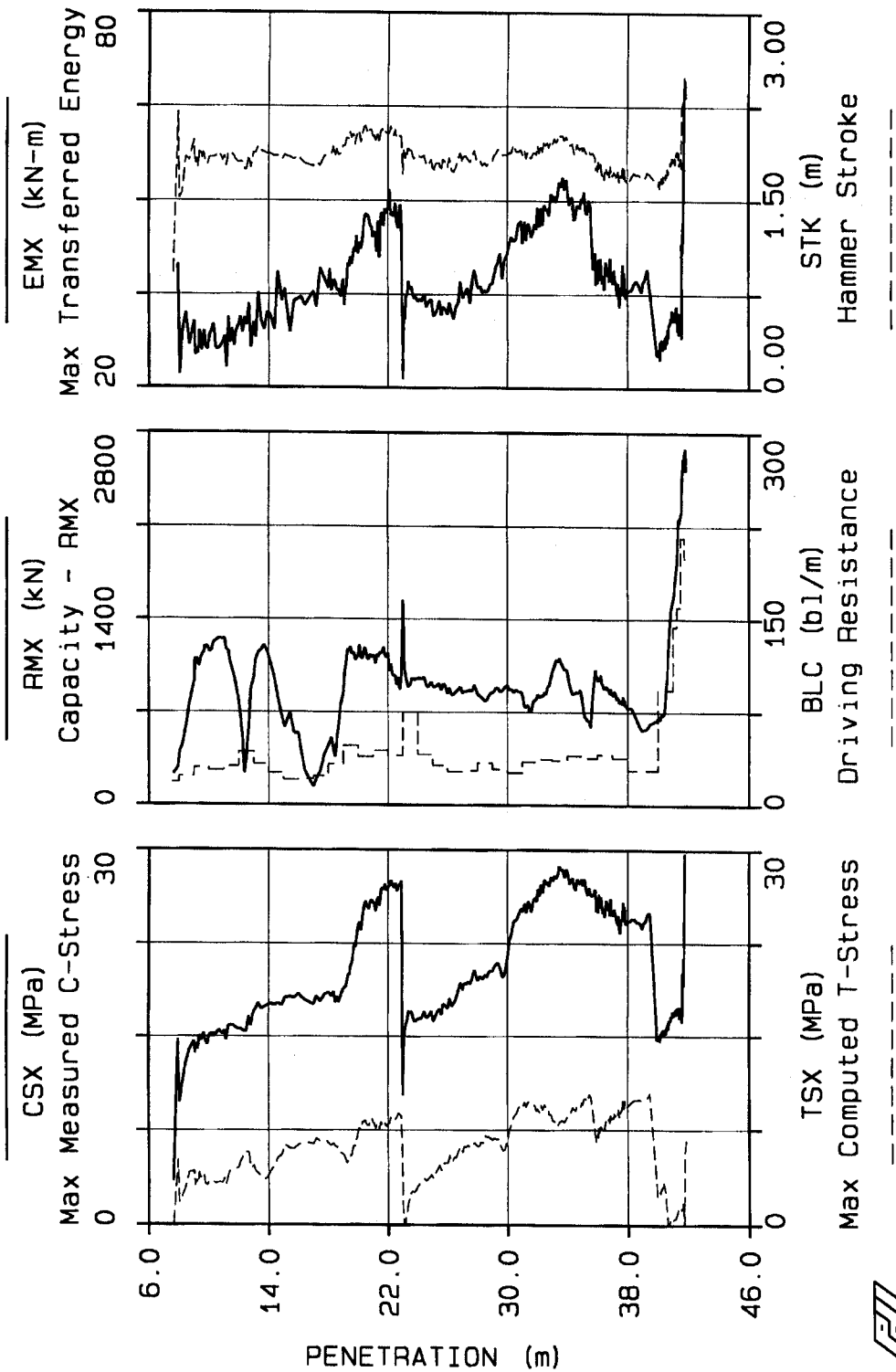


Figure 18.23 Typical Graphical Presentation of Dynamic Testing Results versus Depth

18.8 ADVANTAGES

Dynamic tests provide information on the complete pile installation process. Test results can be used to estimate pile capacity, to check hammer and drive system performance, to monitor driving stresses, and to assess pile structural integrity.

Many piles can be tested during initial driving or during restrike in one day. This makes dynamic testing an economical and quick testing method. Results are generally available immediately after each hammer blow.

On large projects, dynamic testing can be used to supplement static pile load tests or reduce the overall number of static tests to be performed. Since dynamic tests are more economical than static tests, additional coverage can also be obtained across a project at reduced costs. On small projects where static load tests may be difficult to justify economically, dynamic tests offer a viable construction control method.

Dynamic tests can provide information on pile capacity versus depth, capacity variations between locations, and capacity variations with time after installation through restrike tests. This information can be helpful in augmenting the foundation design, when available from design stage test pile programs, or in optimizing pile lengths when used early in construction test programs.

When used as a construction monitoring and quality control tool, dynamic testing can assist in early detection of pile installation problems such as poor hammer performance or high driving stresses. Test results can then facilitate the evaluation and solution of these installation problems.

On projects where dynamic testing was not specified and unexpected or erratic driving behavior or pile damage problems develop, dynamic testing offers a quick and economical method of troubleshooting.

Results from dynamic testing and analysis can be used for driving criteria development including wave equation input parameter selection and refinement of wave equation results as described in Section 17.6.6.

18.9 DISADVANTAGES

Dynamic testing to determine the ultimate static pile capacity requires that the driving system mobilize all the soil resistance acting on the pile. Shaft resistance can generally be mobilized at a fraction of the movement required to mobilize the toe resistance. However, when driving resistances approach 100 blows per quarter meter, the full soil resistance is difficult to mobilize at and near the pile toe. In these circumstances, dynamic test capacities tend to produce lower bound capacity estimates unless a larger hammer or higher stroke can be used to increase the pile net penetration per blow.

Dynamic testing estimates of static pile capacity indicate the capacity at the time of testing. Since increases and decreases in the pile capacity with time typically occur due to soil setup/relaxation, restrike tests after an appropriate waiting period are usually required for a better indication of long term pile capacity. This may require an additional move of the pile driving rig for restrike testing.

Larger diameter open ended pipe piles or H-piles which do not bear on rock may behave differently under dynamic and static loading conditions. This is particularly true if a soil plug does not form during driving. In these cases, limited toe bearing resistance develops during the dynamic test. However, under slower static loading conditions, these open section piles may develop a soil plug and therefore a higher pile capacity under static loading conditions. Interpretation of test results by experienced personnel is important in these situations.

18.10 CASE HISTORY

The following case history illustrates how dynamic pile testing and analysis was used on a small single span bridge constructed in a remote area. The subsurface exploration for the project found a 30 m deposit of moderately clean, medium dense to dense sands with SPT N values ranging from 17 to 50. Based upon these conditions, the foundation report recommended 324 mm O.D. closed end pipe piles be used for the bridge abutment foundations. The pipe piles had an estimated length of 12 m for an ultimate pile capacity of 1450 kN. The foundation report recommended wave equation analysis be used for construction control. Dynamic testing of one test pile at each abutment was also specified with the test pile information to be used by the engineer to provide the contractor pile order lengths.

The Case Method was used to evaluate pile capacity versus penetration depth during the test pile driving. More rigorous CAPWAP analyses were also performed on the dynamic test data to check the Case Method results at selected pile penetration depths. During initial driving at Abutment 1, the 324 mm pipe pile drove beyond the estimated pile penetration depth without developing the required ultimate capacity. The pile was driven to a depth of 23 m and had an end of drive ultimate capacity of 1044 kN. A restrike dynamic test performed one day after initial driving indicated the pile capacity increased slightly to 1089 kN.

While the test pile information from Abutment 1 was being evaluated, three additional test piles were driven at Abutment 2. First, dynamic testing of a 406 mm O.D. closed end pipe pile was performed to determine if a larger diameter pipe pile could develop the required ultimate pile capacity and, if so what pile penetration depth was necessary. The 406 mm was driven to a depth of 27 m and had an end of drive ultimate capacity of 989 kN. A one day restrike test on this pile indicated an ultimate capacity of 1245 kN. The 406 mm pile was driven deeper following the restrike test to a final penetration depth of 34 m. With the additional driving, the end of redrive ultimate capacity decreased to 1067 kN.

Approximately two weeks later, a 324 mm O.D. closed end pipe pile and a 356 mm diameter Monotube pile with a 7.6 m tapered lower section were driven at Abutment 2. The 324 mm pipe pile was driven to a penetration depth of 29 m with an end of drive ultimate capacity of 778 kN. The Monotube pile was driven to a depth of 13 m and had an end of drive ultimate capacity of 845 kN. One day restrike tests on both piles indicated a slight increase in ultimate capacity to 800 kN and 911 kN, respectively. During this same site visit, a 16 day restrike test was performed on the 406 mm pipe pile. The long term restrike ultimate capacity for the 406 mm pipe pile was 1778 kN.

The dynamic testing results from both abutments indicated that the desired ultimate pile capacity could not be obtained at or near the estimated pile penetration depth with the 324 mm pipe piles. However, two foundation solutions were indicated by the dynamic testing results. If a reduced ultimate capacity were chosen, the test results indicated a Monotube pile driven to a significantly shorter penetration depth could develop about the same ultimate pile capacity as could be developed by the 324 mm pipe piles. Alternatively, if the original ultimate pile capacity was desired, 406 mm pipe piles could be driven on the order of 28 m below grade.

Although not originally planned, two static load tests were performed to confirm the ultimate pile capacities that could be developed at the site. The 324 mm pipe and the 356 mm Monotube piles at Abutment 2 were selected for testing. The static load test results indicated the 324 mm pipe pile with a pile penetration depth of 29 m had an ultimate capacity of 1022 kN and the Monotube pile with a pile penetration depth of 13 m had an ultimate capacity of 978 kN. The dynamic test restrike capacities were in good agreement with these static load tests results particularly when the additional time between the dynamic restrike tests and static load tests is considered.

Based on the required pile lengths and capacities determined from the dynamic and static load testing, a cost evaluation of the foundation alternatives was performed. The cost analysis indicated that the Monotube piles would be the most economical pile foundation type. This case study illustrates how the routine application of dynamic testing on a small project helped facilitate the solution to an unexpected foundation problem.

18.11 LOW STRAIN INTEGRITY TESTING METHODS

The previous sections of the chapter described high strain dynamic testing methods and their applications. This section will discuss low strain integrity testing methods which can be used on driven pile foundations. These low strain methods may be used to evaluate pile length or integrity of piles with a high impedance (EA/C), such as solid concrete piles or concrete filled pipe piles. Additional details on low strain methods including equipment requirements and analysis of measurements may be found in ASTM D-5882 Standard Test Method for Low Strain Integrity Testing of Piles. Low strain integrity methods are not applicable to steel H-piles or unconcreted pipe piles.

18.11.1 Pulse Echo Method

Pulse echo pile testing consists of applying a low strain impact to the head of a pile, and monitoring the resulting pile head response. A small hand-held hammer (0.5 to 4 kg) is employed to deliver a clean impact to the pile head. An accelerometer, temporarily attached to the pile head, records pile head response as the generated low strain stress wave propagates down the pile length. Any changes in pile impedance (determined by the cross sectional area, the elastic modulus of the pile material and the stress wave speed of the pile material) along the pile shaft will generate a partial reflection of the downward travelling stress wave, thus identifying pile damage. At the pile toe a significant change in impedance would also occur, therefore allowing determination of pile length. The accelerometer records the magnitude and arrival time of the reflected waves. For undamaged piles, if a toe reflection is apparent, then it is possible to reasonably estimate an unknown pile length based upon an assumed wave speed.

The returning analog signals are captured and digitized by a portable high accuracy analog to digital data acquisition system. A display panel presents the record of one or more (averaged) blows for review and interpretation. Typically, the acceleration versus time data is integrated to a velocity versus time record to facilitate record evaluation.

This test method can also be used in cases where the pile length is known but the pile integrity is in question. In this application, a clearly indicated toe signal, together with a fairly steady velocity trace between the impact time and toe reflection, are signs of a sound pile. Strong velocity reflections before the expected toe signal are the result of changes in pile cross section and indicate pile damage.

Pulse echo integrity records of velocity versus time are presented in Figures 18.24 and 18.25 for two 305 mm square prestressed concrete piles. These records were obtained after a slope failure occurred during construction and the integrity of the driven piles was questioned. Figure 18.24 shows an amplified record for an undamaged 16.3 m long pile. Note the record drops below the origin at a depth 5 m which corresponds to soil resistance effects. A clear toe signal is apparent in the record at a depth of 16.3 m.

In Figure 18.25, an amplified pulse echo record on a nearby pile is presented. This pile has a clear indication of damage due to the slope movements based on the positive velocity reflection starting at a depth of 4 m.

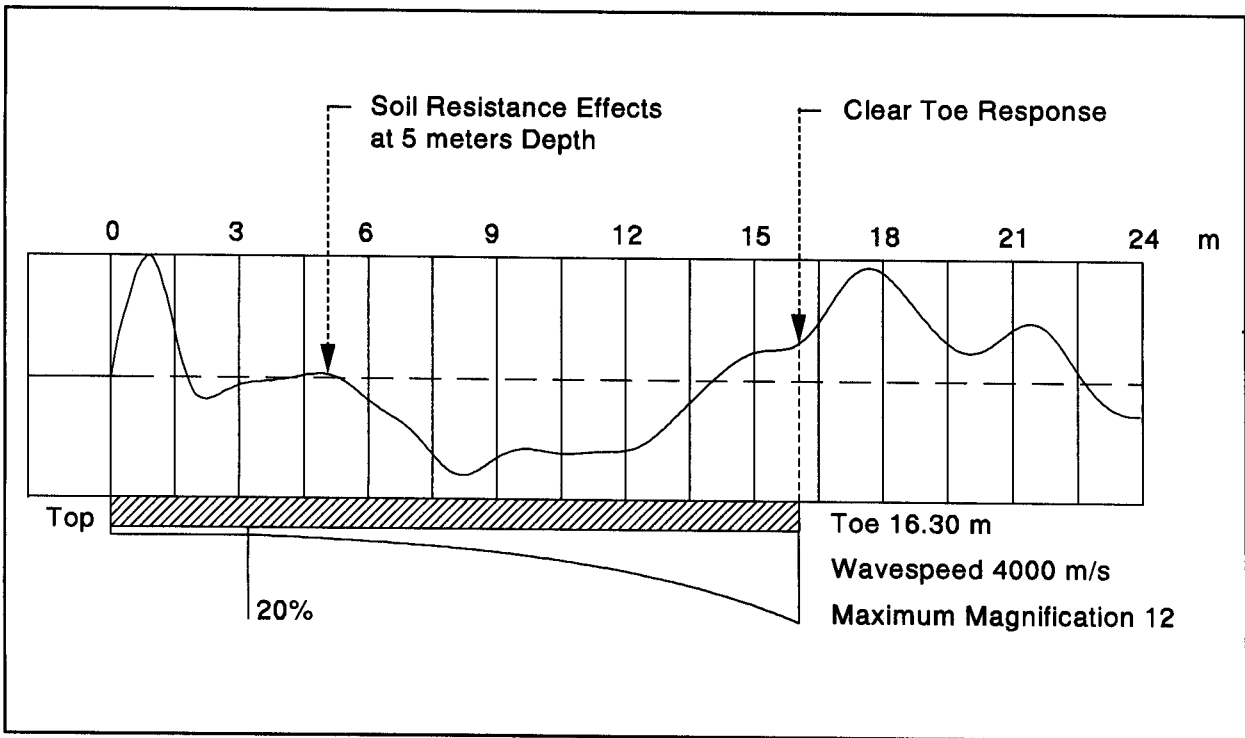


Figure 18.24 Pulse Echo Velocity versus Time Record for Undamaged Pile

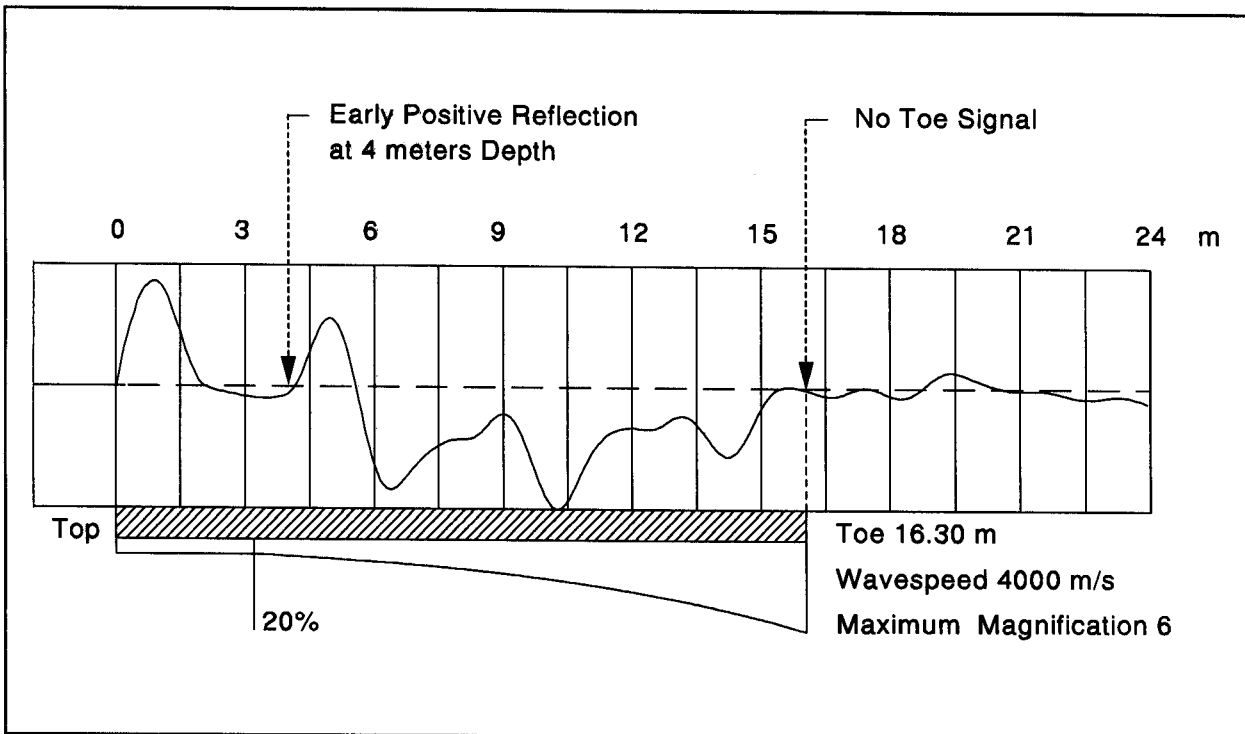


Figure 18.25 Pulse Echo Velocity versus Time Record for Damaged Pile

18.11.2 Transient Response Method (TRM)

In the TRM method, both the pile head response and the impact force are measured. A simple hand held hammer can adequately produce the frequency components necessary to test both well constructed and defective piles with TRM. The standard TRM plot of the ratio of the frequency velocity spectrum to force spectrum is called "mobility", and is an indication of the pile's velocity response to a particular excitation force at a certain frequency. Figure 18.26 depicts a typical response curve for a TRM test.

A mobility peak occurs at a frequency indicative of the time when the velocity changes due to a reflection from the pile toe or an intermediate impedance reduction or defect. Mobility peaks occurring at regular intervals are indicative of a dominant frequency Δf . The corresponding length to the pile toe or to a major defect at which the change in frequency occurs is calculated from:

$$L = C / 2 \Delta f$$

Where: C = Wave speed.
L = Pile length.
 Δf = Change in frequency.

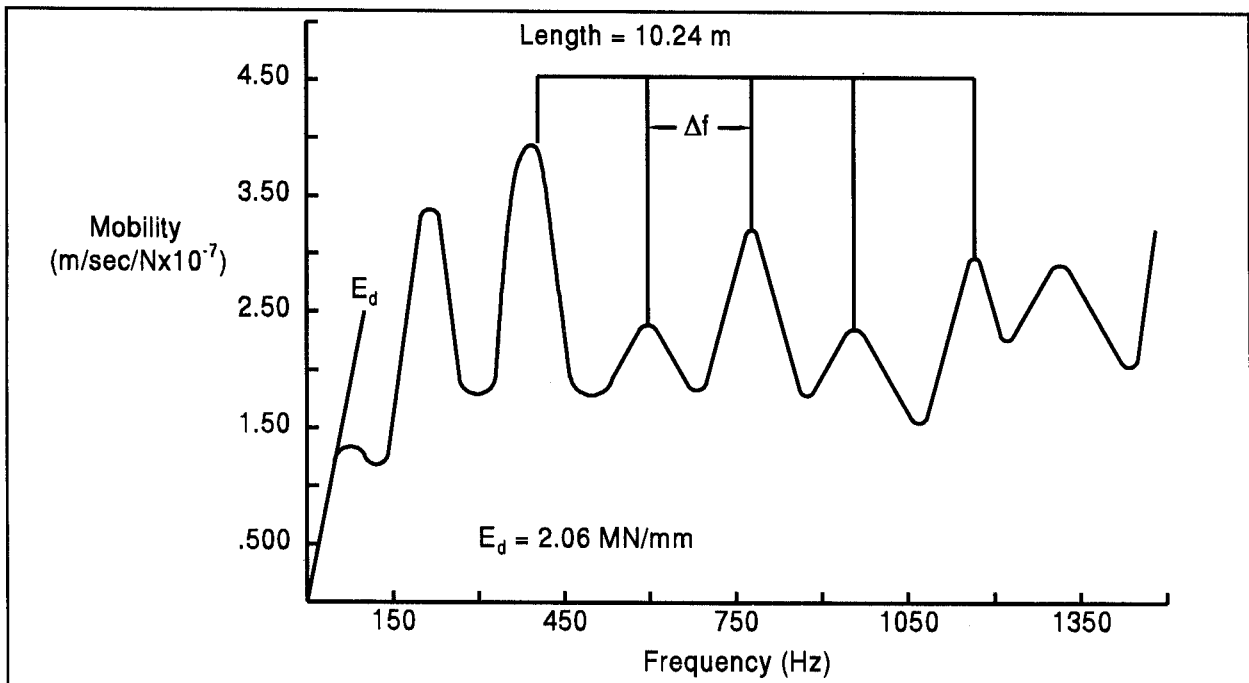


Figure 18.26 Typical Response Curve from a TRM Test

In practice, low frequency (*i.e.* near static) values are divided by the associated mobility yielding a so-called dynamic stiffness, E_d . This quantity increases with decreasing pile toe response. A low pile toe response is often the result of high soil resistance. A low pile toe resistance may also be caused by highly variable pile properties of internal pile damping, and is therefore only indirectly related to pile capacity. However, E_d is calculated, since it does provide a quantitative result for the evaluation of pile quality. Generally, higher stiffness values (for piles on the same site and of comparable length) indicate piles of higher strength (structural and soil) while lower stiffnesses indicate piles with potential defects or lower soil strength.

18.11.3 Low Strain Applications to Unknown Foundations

Design or construction records on many older bridges are not available. In some cases, the foundation supporting these structures is unknown and therefore the performance of these structures under extreme events such as scour is uncertain. A recent NCHRP research effort by Olson (1996) on the application of non-destructive testing methods to the evaluation of unknown foundations found the pulse echo and transient response methods fair to excellent in their ability to identify the depth of exposed piles and poor to good in their ability to determine the depth of footing or pile cap. These techniques are most applicable when the bridge is supported on a columnar substructure rather than a pier or abutment. Access to the bridge substructure is also generally required for implementation of these techniques. FHWA Geotechnical Guideline No. 16 (1998), provides a summary of this NCHRP study.

18.11.4 Limitations and Conclusions of Low Strain Methods

The low strain methods can typically be used for integrity or length assessments of pile foundations where the length to diameter ratio does not exceed about 30. For piles with severe cracks or manufactured mechanical joints, the stress wave will generally not be transmitted below the gap. Therefore, the pile integrity or length below this gap cannot be evaluated. Records from piles with multiple or varying (*i.e.* tapered piles) cross sectional areas can also be difficult to interpret. For piles of low impedance (H-piles and unfilled pipe piles) low strain methods are generally not suitable. When used for pile length determinations, the length information obtained from a toe signal (or a governing frequency) is only as accurate as the wave speed value assumed in the processing of the records. Wave speed variations of approximately 10% are not uncommon. Some defects can also have secondary and tertiary wave reflections. For example, if an

impedance reduction occurs in the middle of the pile, then what may appear to be the pile toe response may actually be a secondary reflection of the mid-pile defect.

The additional force measurement obtained during TRM testing provides supplemental information of cross sectional changes near the pile head, *i.e.* within the distance corresponding to the impact signal. The minor additional expense of the force measurements is therefore worthwhile whenever questions arise as to the integrity of upper (1.5 m) pile portion.

Using low strain methods, many piles can be tested for integrity in a typical day. Therefore, low strain methods are a relatively economical test method and can provide valuable information when used in the proper application such as illustrated in the case study discussed in Section 18.11.1. Low strain testing has been used to assist in evaluating integrity questions on high impedance piles due to construction equipment or vessel impact, pulling on out of position piles, and storm damage.

REFERENCES

- American Association of State Highway and Transportation Offices (AASHTO). Standard Method of Test for High Strain Dynamic Testing of Piles, AASHTO Designation T-298-33.
- American Society for Testing and Materials, ASTM (1994). Annual Book of Standards, ASTM D-4945, Standard Test Method for High-Strain Dynamic Testing of Piles.
- American Society for Testing and Materials, ASTM (1996). Annual Book of Standards, ASTM D-5882, Standard Test Method for Low-Strain Dynamic Testing of Piles.
- Cheney, R.S. and Chassie, R.G. (1993). Soils and Foundations Workshop Manual. Second Edition, Publication No. FHWA HI-88-009, Federal Highway Administration, National Highway Institute, Washington, D.C., 353-362.
- Davisson, M.T. (1972). High Capacity Piles. Proceedings of the Soil Mechanics Lecture Series on Innovations in Foundation Construction, American Society of Civil Engineers, ASCE, Illinois Section, 81-112.
- Eiber, R.J. (1958). A Preliminary Laboratory Investigation of the Prediction of Static Pile Resistances in Sand. Master's Thesis, Department of Civil Engineering, Case Institute of Technology, Cleveland, OH.
- Federal Highway Administration (1998). Geotechnical Guideline No. 16, Geotechnical Engineering Notebook, U.S. Department of Transportation, Washington D.C., 69.
- Goble, G.G., Likins, G.E. and Rausche, F. (1975). Bearing Capacity of Piles from Dynamic Measurements. Final Report, Department of Civil Engineering, Case Western Reserve University, Cleveland, OH.
- Goble, G.G. and Rausche, F. (1970). Pile Load Test by Impact Driving. Highway Research Record, Highway Research Board, No. 333, Washington, DC.

- Goble, G.G., Rausche, F. and Likins, G.E. (1980). The Analysis of Pile Driving - A State-of-the-Art. Proceedings of the 1st International Seminar on the Application of Stress-Wave Theory on Piles, Stockholm, H. Bredenberg, Editor, A.A. Balkema Publishers, 131-161.
- Hannigan, P.J. (1990). Dynamic Monitoring and Analysis of Pile Foundation Installations. Deep Foundations Institute Short Course Text, First Edition, 69.
- Olson, L.D. (1996). Non-Destructive Testing of Unknown Subsurface Bridge Foundations - Results of NCHRP Project 21-5, National Cooperative Highway Research Program, Transportation Research Board, Washington, D.C., 42.
- Pile Dynamics, Inc. (1996). Pile Driving Analyzer Manual; Model PAK, Cleveland, OH.
- Rausche, F., Goble, G.G. and Likins, G.E. (1985b). Dynamic Determination of Pile Capacity. American Society of Civil Engineers, ASCE, Journal of the Geotechnical Engineering Division, Vol 111, No. 3, 367-383.
- Rausche, F. and Goble, G.G. (1979). Determination of Pile Damage by Top Measurements. Behavior of Deep Foundations. American Society for Testing and Materials, ASTM STP 670, R. Lundgren, Editor, 500-506.
- Rausche, F., Likins, G.E., Goble, G.G. and Miner, R. (1985a). The Performance of Pile Driving Systems. Main Report, U.S. Department of Transportation, Federal Highway Administration, Office of Research and Development, Washington, D.C., Volumes I-IV.
- Rausche, F., Moses, F., and Goble, G.G. (1972). Soil Resistance Predictions from Pile Dynamics. Journal of the Soil Mechanics and Foundations Division, ASCE, Vol. 98, No. SM9.
- Reiding, F.J., Middendorp, P., Schoenmaker, R.P., Middendorp, F.M. and Bielefeld, M.W. (1988). FPDS-2, A New Generation of Foundation Diagnostic Equipment, Proceeding of the 3rd International Conference on the Application of Stress Wave Theory to Piles, Ottawa, B.H. Fellenius, Editor, BiTech Publishers, 123-134.

19. STATIC PILE LOAD TESTING

Static load testing of piles is the most accurate method of determining load capacity. Depending upon the size of the project, static load tests may be performed either during the design stage or construction stage. Conventional load test types include the axial compression, axial tension and lateral load tests.

The purpose of this chapter is to provide an overview of static testing and its importance as well as to describe the basic test methods and interpretation techniques. For additional details on pile load testing, reference should be made to FHWA publication FHWA-SA-91-042, "Static Testing of Deep Foundation" by Kyfor *et al.* (1992) as well as the other publications listed at the end of this chapter.

19.1 REASONS FOR LOAD TESTING

1. Load tests are performed to develop information for use in the design and/or construction of a pile foundation.
2. Load tests are performed to confirm the suitability of the pile-soil system to support the pile design load with an appropriate factor of safety.

19.2 PREREQUISITES FOR LOAD TESTING

In order to adequately plan and implement a static load testing program, the following information should be obtained or developed.

1. A detailed subsurface exploration program at the test location. A load test is not a substitute for a subsurface exploration program.
2. Well defined subsurface stratigraphy including engineering properties of soil materials and identification of groundwater conditions.
3. Static pile capacity analyses to select pile type(s) and length(s) as well as to select appropriate location(s) for load test(s).

19.3 DEVELOPING A LOAD TEST PROGRAM

The goal of a load test program should be clearly established. A significantly different level of effort and instrumentation is required if the goal of the load test program is to confirm the ultimate pile capacity or if detailed load-transfer information is desired for design. The following items should be considered during the test program planning so that the program provides the desired information.

1. The capacity of the loading apparatus (reaction system and jack) should be specified so that the pile(s) may be loaded to plunging failure. A loading apparatus designed to load a pile to only twice the design load is usually insufficient to obtain plunging failure. Hence, the true factor of safety on the design load cannot be determined, and the full benefit from performing the static test is not realized.
2. Specifications should require use of a load cell and spherical bearing plate as well as dial gages with sufficient travel to allow accurate measurements of load and movement at the pile head. (Where possible, deformation measurements should also be made at the pile toe and at intermediate points to allow for an evaluation of shaft and toe bearing resistance).
3. The load test program should be supervised by a person experienced in this field of work.
4. A test pile installation record should be maintained with installation details appropriately noted. Too often, only the hammer model and driving resistance are recorded on a test pile log. Additional items such as hammer stroke (particularly at final driving), fuel setting, accurately determined final set, installation aids used and depths such as predrilling, driving times, stops for splicing, *etc.*, should be recorded.
5. Use of dynamic monitoring equipment on the load test pile is recommended for estimates of pile capacity at the time of driving, evaluation of drive system performance, calculation of driving stresses, and subsequent refinement of soil parameters for wave equation analysis.

19.4 ADVANTAGES OF STATIC LOAD TESTING

The advantages of performing static load tests are summarized below.

1. A static load test allows a more rational design. Confirmation of pile-soil capacity through static load testing is considerably more reliable than capacity estimates from static capacity analyses and dynamic formulas.
2. An improved knowledge of pile-soil behavior is obtained that may allow a reduction in pile lengths or an increase in the pile design load, either of which may result in potential savings in foundation costs.
3. With the improved knowledge of pile-soil behavior, a lower factor of safety may be used on the pile design load. A factor of safety of 2.0 is generally applied to design loads confirmed by load tests as compared to a factor of safety of 3.5 used on design loads in the Gates dynamic formula. Hence, a cost savings potential again exists.
4. The ultimate pile capacity determined from load testing allows confirmation that the design load may be adequately supported at the planned pile penetration depth.

Engineers are sometimes hesitant to recommend a static load test because of cost concerns or potential time delays in design or construction. While the cost of performing a static load test should be weighed against the anticipated benefits, cost alone should not be the determining factor. Cost benefits resulting from static load testing in both the design and construction stage were noted in the case studies presented in Chapter 2.

Delays to a project in the design or construction stage usually occur when the decision to perform static load tests is added late in the project. During a design stage program, delays can be minimized by determining early in the project whether a static load test program should be performed. In the construction stage, delays can be minimized by clearly specifying the number and locations of static load test to be performed as well as the time necessary for the engineer to review the results. In addition, the specifications should state that the static test must be performed prior to ordering pile lengths or commencing production driving. In this way, the test results are available to the design and construction engineer early in the project so that the maximum benefits can be obtained. At the same time the contractor is also aware of the test requirements and analysis duration and can schedule the project accordingly.

19.5 WHEN TO LOAD TEST

The following criteria from FHWA-SA-91-042 by Kyfor *et al.* (1992) summarizes the various conditions when pile load testing can be effectively utilized:

1. When the potential for substantial cost savings is readily apparent. This is often the case on large projects either involving friction piles (to prove that lengths can be reduced) or end bearing piles (to prove that the design load can be increased).
2. When a safe design load is in doubt due to limitations of an engineer's experience base or due to unusual site or project conditions.
3. When subsurface conditions vary considerably across the project, but can be delineated into zones of similar conditions. Static tests can then be performed in representative areas to delineate foundation variation.
4. When a significantly higher design load is contemplated relative to typical design loads and practice.
5. When time dependent changes in pile capacity are anticipated as a result of soil setup or relaxation.
6. When using precast concrete friction piles, it is important to determine pile cast lengths so that time consuming and costly splices can be avoided during construction.
7. When new, unproven pile types and/or installation procedures are utilized.
8. When existing piles will be reused to support a new structure with heavier design loads.
9. When a reliable assessment of pile uplift capacity or lateral behavior is important.
10. When, during construction, the estimated ultimate capacity using dynamic formulas or dynamic analysis methods differs from the estimated capacity at that depth determined by static analysis. For example, H-piles that "run" when driven into loose to medium dense sands and gravels.

Experience has also shown that load tests will typically confirm that pile lengths can be reduced at least 15 percent versus the lengths that would be required by the Engineering News formula on projects where piles are supported predominantly by shaft resistance. This 15 percent pile length reduction was used to establish the following rule of thumb formula to compute the total estimated pile length which the project must have to make the load test cost effective based purely on material savings alone.

$$\text{Total estimate pile length in meters on project} \geq \frac{\text{cost of load test}}{(0.15) (\text{cost/meter of pile})}$$

19.6 EFFECTIVE USE OF LOAD TESTS

19.6.1 Design Stage

The best information for design of a pile foundation is provided by the results of a load testing program conducted during the design phase. The number of static tests, types of piles to be tested, method of driving and test load requirements should be selected by the geotechnical and structural engineers responsible for design. A cooperative effort between the two is necessary. The following are the advantages of load testing during the design stage.

- a. Allows load testing of several different pile types and lengths resulting in the design selection of the most economical pile foundation.
- b. Confirm driveability to minimum penetration requirements and suitability of foundation capacity at estimated pile penetration depths.
- c. Establishes preliminary driving criteria for production piles.
- d. Pile driving information released to bidders should reduce their bid "contingency."
- e. Reduces potential for claims related to pile driving problems.
- f. Allows the results of load test program to be reflected in the final design and specifications.

19.6.2 Construction Stage

Load testing at the start of construction may be the only practical time for testing on smaller projects that can not justify the cost of a design stage program. Construction stage static tests are invaluable to confirm that the design loads are appropriate and that the pile installation procedure is satisfactory. Driving of test piles and load testing is frequently done to determine the pile order length at the beginning of construction. These results refine the estimated pile lengths shown on the plans and establish minimum pile penetration requirements.

19.7 COMPRESSION LOAD TESTS

Piles are most often tested in compression, but they can also be tested in tension or for lateral load capacity. Figure 19.1 illustrates the basic mechanism of performing a compression pile load test. This mechanism normally includes the following steps:

1. The pile is loaded incrementally from the pile head using some predetermined loading sequence, or it can be loaded at a continuous, constant rate.
2. Measurements of load, time, and movement at the pile head and at various points along the pile shaft are recorded during the test.
3. A load movement curve is plotted.
4. The failure load and the movement at the failure load are determined by one of the several methods of interpretation.
5. The movement is usually measured only at the pile head. However, the pile can be instrumented to determine movement anywhere along the pile. Telltales (solid rods protected by tubes) shown in Figure 19.1 or strain gages may be used to obtain this information.

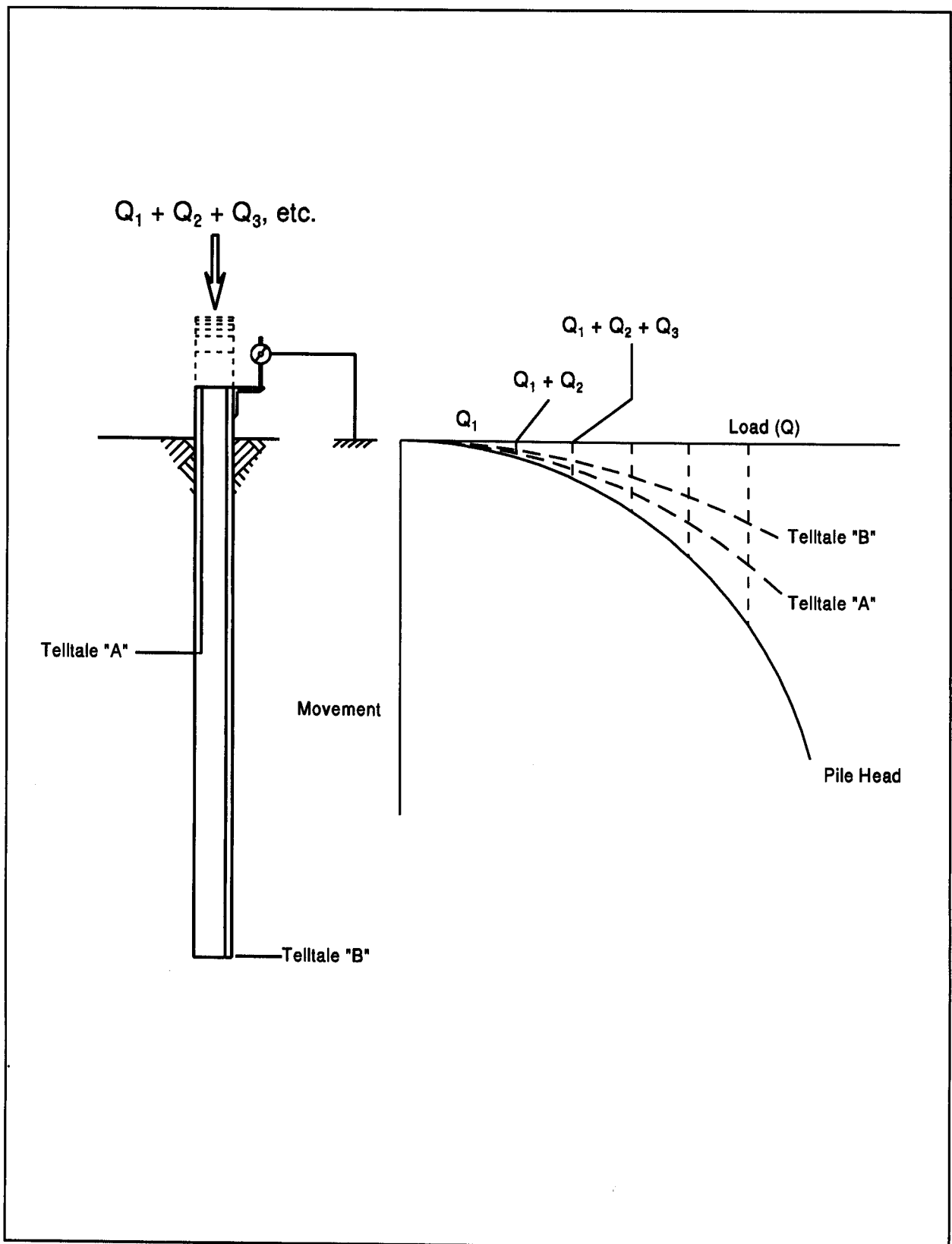


Figure 19.1 Basic Mechanism of a Pile Load Test

19.7.1 Compression Test Equipment

ASTM D-1143 recommends several alternative systems for (1) applying compressive load to the pile, and (2) measuring movements. Most often, compressive loads are applied by hydraulically jacking against a beam that is anchored by piles or ground anchors, or by jacking against a weighted platform. The primary means of measuring the load applied to the pile should be with a calibrated load cell. The jack load should also be recorded from a calibrated pressure gage. To minimize eccentricities in the applied load, a spherical bearing plate should be included in the load application arrangement.

Axial pile head movements are usually measured by dial gages or LVDT's that measure movement between the pile head and an independently supported reference beam. ASTM requires the dial gages or LVDT's have a minimum of 50 mm of travel and a precision of at least 0.25 mm. It is preferable to have gages with a minimum travel of 75 mm (particularly for long piles with large elastic deformations under load) and with a precision of 0.025 mm. A minimum of two dial gages or LVDT's mounted equidistant from the center of the pile and diametrically opposite should be used. Two backup systems consisting of a scale, mirror, and wire system should be provided with a scale precision of 0.25 mm. The backup systems should also be mounted on diametrically opposite pile faces. Both the reference beams and backup wire systems are to be independently supported with a clear distance of not less than 2.5 m between supports and the test pile. A remote backup system consisting of a survey level should also be used in case reference beams or wire systems are disturbed during the test.

ASTM specifies that the clear distance between a test pile and reaction piles be at least 5 times the maximum diameter of the reaction pile or test pile (whichever has the greater diameter if not the same pile type) but not less than 2 meters. If a weighted platform is used, ASTM requires the clear distance between cribbing supporting the weighted platform and the test pile exceed 1.5 meters.

A schematic of a typical compression load test setup is presented in Figure 19.2. A photograph of a typical compression load test arrangement using reaction piles is presented in Figure 19.3 and a weighted platform arrangement is shown in Figure 19.4. Additional details on load application as well as pile head load and movement measurements may be found in ASTM D-1143 as well as in FHWA-SA-91-042 by Kyfor *et al.* (1992).

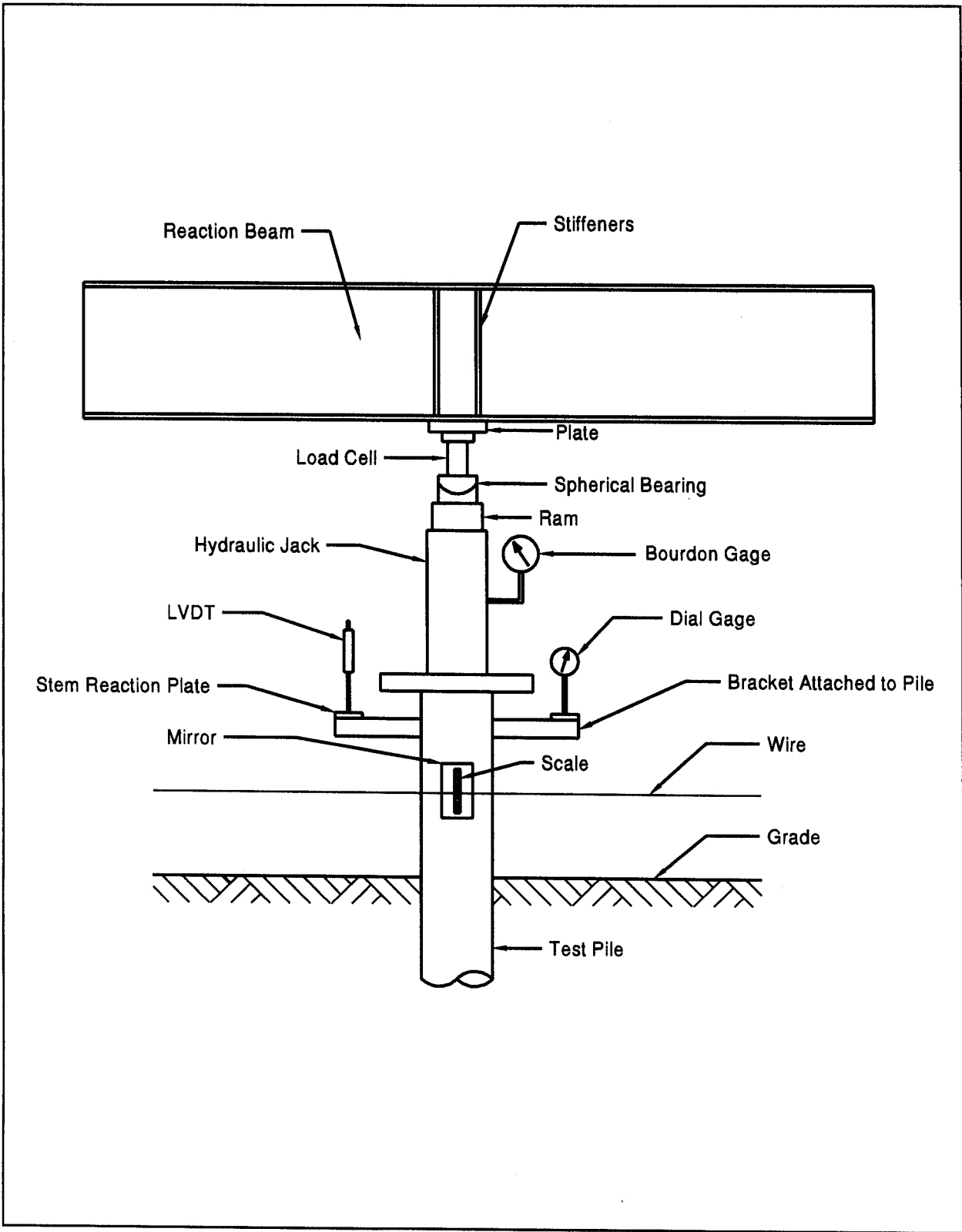


Figure 19.2 Typical Arrangement for Applying Load in an Axial Compressive Test (Kyfor et al. 1992)

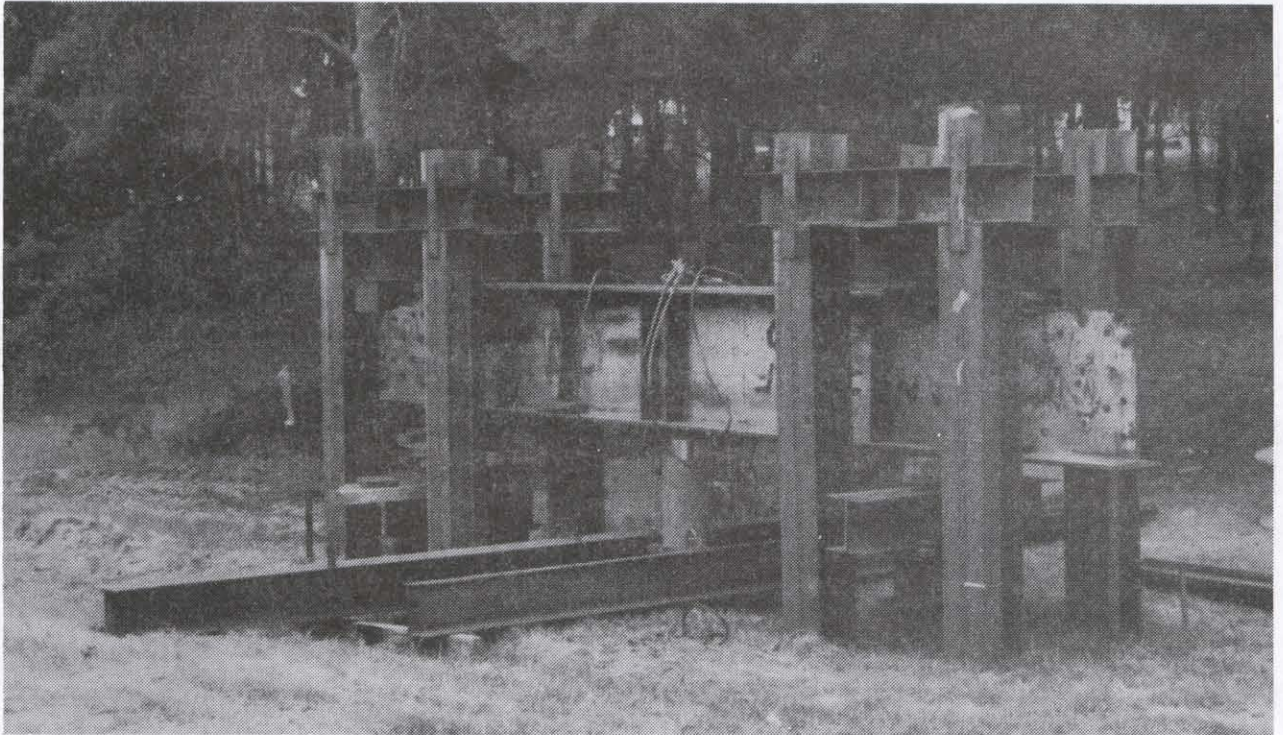


Figure 19.3 Typical Compression Load Test Arrangement with Reaction Piles

19.7.2 Recommended Compression Test Loading Method

It is extremely important that standardized load testing procedures are followed. Several loading procedures are detailed in ASTM D-1143, Standard Test Method for Piles Under Static Axial Compressive Load. The quick load test method is recommended. This method replaces traditional methods where each load increment was held for extended periods of time. The quick test method requires that load be applied in increments of 10 to 15% of the pile design load with a constant time interval of 2½ minutes or as otherwise specified between load increments. Readings of time, load, and gross movement are to be recorded immediately before and after the addition of each load increment. This procedure is to continue until continuous jacking is required to maintain the test load or the capacity of the loading apparatus is reached, whichever occurs first. Upon reaching and holding the maximum load for 5 minutes, the pile is unloaded in four equal load decrements which are each held for 5 minutes. Readings of time, load, and gross movement are once again recorded immediately after, 2½ minutes after, and 5 minutes after each load reduction, including the zero load.



Figure 19.4 Typical Compression Load Test Arrangement using a Weighted Platform

19.7.3 Presentation and Interpretation of Compression Test Results

The results of load tests should be presented in a report conforming to the requirements of ASTM D-1143. A load-movement curve similar to the one shown in Figure 19.5 should be plotted for interpretation of test results.

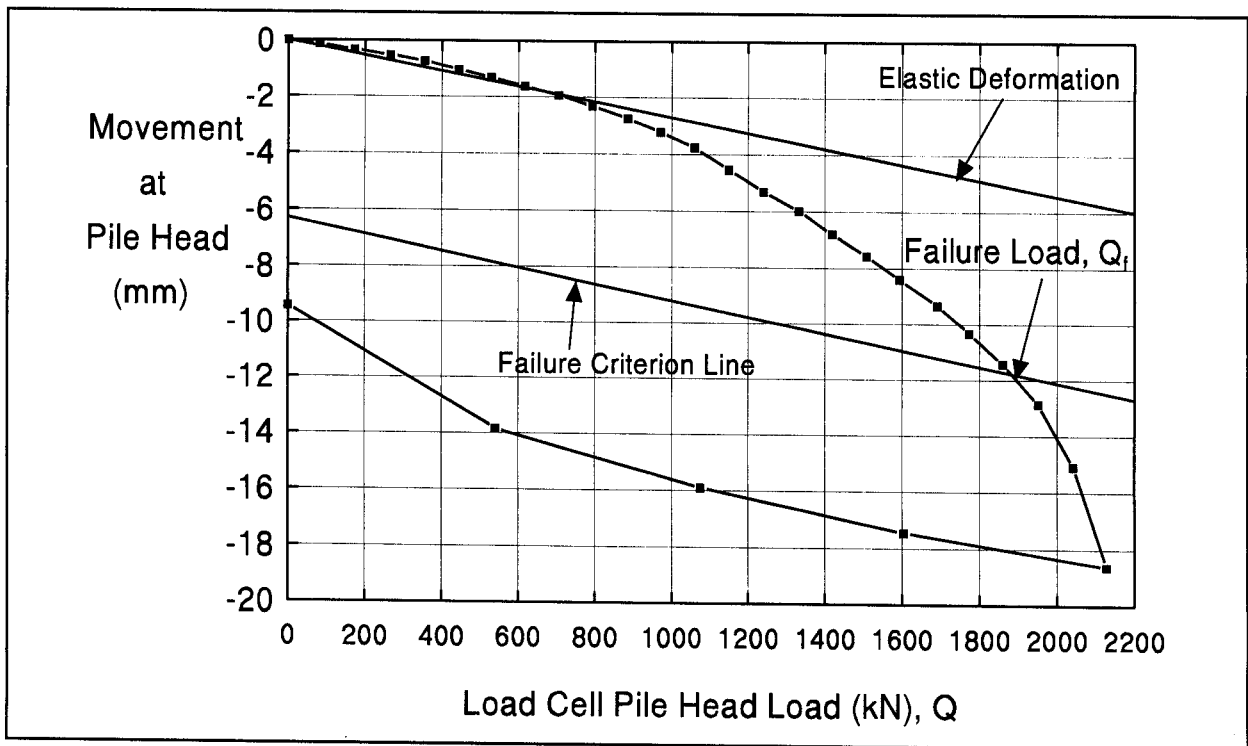


Figure 19.5 Presentation of Typical Static Pile Load-Movement Results

The literature abounds with different methods of defining the failure load from static load tests. Methods of interpretation based on maximum allowable gross movements, which do not take into account the elastic deformation of the pile shaft, are not recommended. These methods overestimate the allowable capacities of short piles and underestimate the allowable capacities of long piles. The methods which account for elastic deformation and are based on failure criterion provide a better understanding of pile performance and provide more accurate results.

AASHTO (1992) and FHWA SA-91-042, Kyfor *et al.* (1992) recommend compression test results be evaluated using an offset limit method as proposed by Davisson (1972). This method is described in the following section and is applicable for load tests in which the increment of load is held for not more than 1 hour.

19.7.4 Plotting the Load-Movement Curve

Figure 19.5 shows the load-movement curve from a pile load test. To facilitate the interpretation of the test results, the scales for the loads and movements are selected so that the line representing the elastic deformation Δ of the pile is inclined at an angle of about 20° from the load axis. The elastic deformation Δ is computed from:

$$\Delta = \frac{QL}{AE}$$

Where: Δ = Elastic deformation in mm.
Q = Test load in kN.
L = Pile length in mm.
A = Cross sectional area of the pile in m^2 .
E = Modulus of elasticity of the pile material in kPa.

19.7.5 Determination of the Ultimate Load

The ultimate or failure load Q_f of a pile is that load which produces a movement of the pile head equal to:

$$s_f = \Delta + (4.0 + 0.008b)$$

Where: b = Pile diameter in mm.

A failure criterion line parallel to the elastic deformation line is plotted as shown in Figure 19.5. The point at which the observed load-movement curve intersects the failure criterion is by definition the failure load. If the load-movement curve does not intersect the failure criterion line, the pile has an ultimate capacity in excess of the maximum applied test load.

For large diameter piles (diameter greater than 610 mm), additional pile toe movement is necessary to develop the toe resistance. Therefore for large diameter piles, FHWA SA-91-042, Kyfor *et al.* (1992) recommends the failure load be determined from:

$$s_f = \Delta + \frac{b}{30}$$

19.7.6 Determination of the Allowable Load

The allowable design load is usually determined by dividing the ultimate load, Q_u , by a suitable factor of safety. A factor of safety of 2.0 is recommended in AASHTO code (1992) and is often used. However, larger factors of safety may be appropriate under the following conditions:

- a. Where soil conditions are highly variable.
- b. Where a limited number of load tests are specified.
- c. For friction piles in clay, where group settlement may control the allowable load.
- d. Where the total movement that can be tolerated by the structure is exceeded.
- e. For piles installed by means other than impact driving, such as vibratory driving or jetting.

19.7.7 Load Transfer Evaluations

Kyfor *et al.* (1992) provides a method for evaluation of the soil resistance distribution from telltales embedded in a load test pile. The average load in the pile, Q_{avg} , between two measuring points can be determined as follows:

$$Q_{avg} = A E \frac{R_1 - R_2}{\Delta L}$$

Where:

- ΔL = Length of pile between two measuring points under no load condition.
- A = Cross sectional area of the pile.
- E = Modulus of elasticity of the pile.
- R_1 = Deflection readings at upper of two measuring points.
- R_2 = Deflection readings at lower of two measuring points.

If the R_1 and R_2 readings correspond to the pile head and the pile toe respectively, then an estimate of the shaft and toe resistances may be computed. For a pile with an assumed constant soil resistance distribution (uniform), Fellenius (1990) states that an estimate of the toe resistance, R_t , can be computed from the applied pile head load, Q_h . The applied pile head load, Q_h , is chosen as close to the failure load as possible.

$$R_t = 2Q_{avg} - Q_h$$

For a pile with an assumed linearly increasing soil resistance distribution (triangular), the estimated toe resistance may be calculated using:

$$R_t = 3Q_{avg} - 2Q_h$$

The estimated shaft resistance can then be calculated from the applied pile head load minus the toe resistance.

During driving, residual loads can be locked into a pile that does not completely rebound after a hammer blow (*i.e.* return to a condition of zero stress along its entire length). This is particularly true for flexible piles, piles with large frictional resistances, and piles with large toe quakes. Load transfer evaluations using telltale measurements described above assume that no residual loads are locked in the pile during driving. Therefore, the load distribution calculated from the above equations would not include residual loads. If measuring points R_1 and R_2 correspond to the pile head and pile toe of a pile that has locked-in residual loads, the calculated average pile load would also include the residual loads. This would result in a lower toe resistance being calculated than actually exists as depicted in Figure 19.6. Additional details on telltale load transfer evaluation, including residual load considerations, may be found in Fellenius (1990).

When detailed load transfer data is desired, telltale measurements alone are insufficient, since residual loads can not be directly accounted for. Dunnycliff (1988) suggests that weldable vibrating wire strain gages be used on steel piles and sister bars with vibrating wire strain gages be embedded in concrete piles for detailed load transfer evaluations. A geotechnical instrumentation specialist should be used to select the appropriate instrumentation to withstand pile handling and installation, to determine the redundancy required in the instrumentation system, to determine the appropriate data acquisition system, and to reduce and report the data acquired from the instrumentation program.

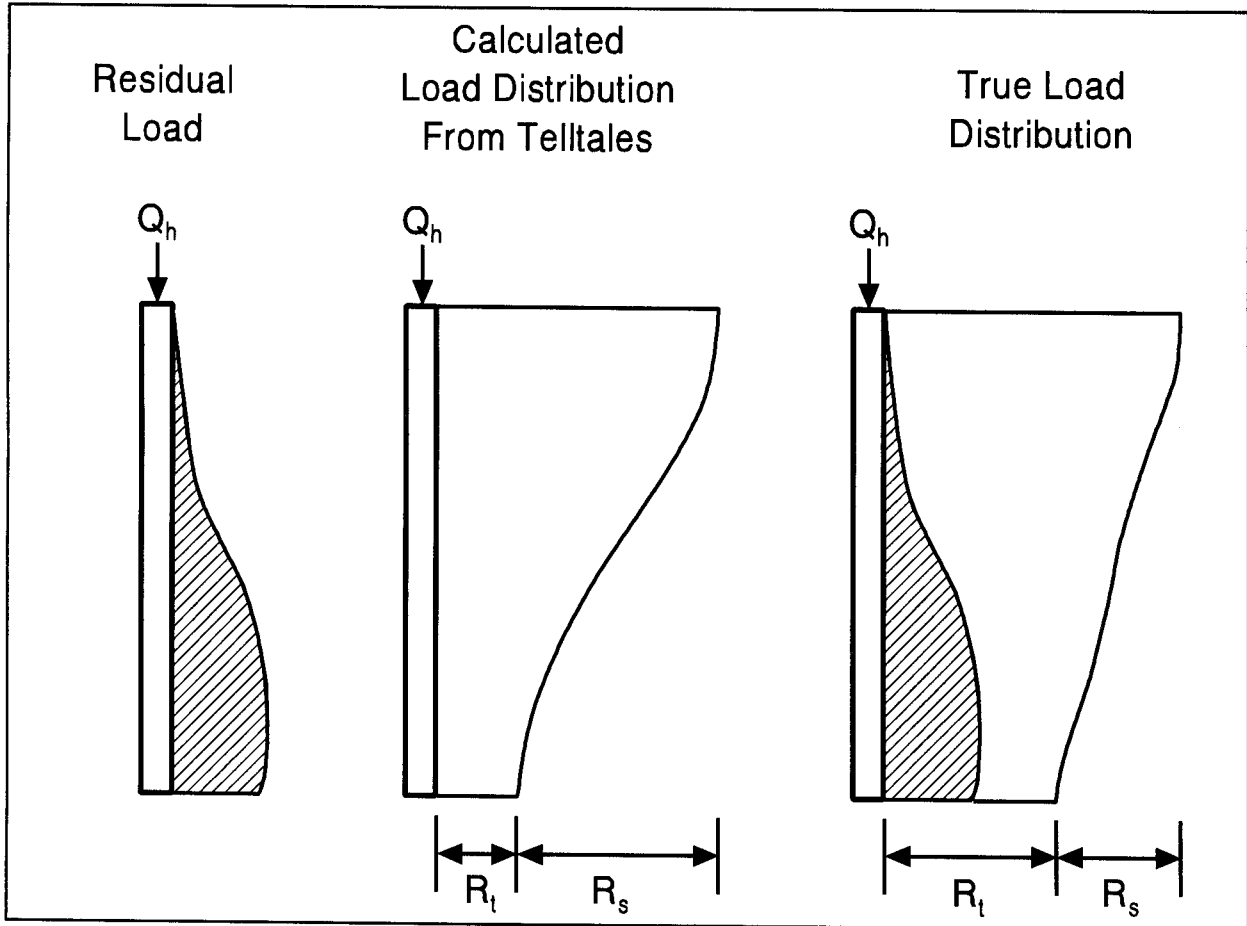


Figure 19.6 Example of Residual Load Effects on Load Transfer Evaluation

19.7.8 Limitations of Compression Load Tests

Compression load tests can provide a wealth of information for design and construction of pile foundations and are the most accurate method of determining pile capacity. However, static load test results cannot be used to account for long-term settlement, downdrag from consolidating and settling soils, or to adequately represent pile group action. Other shortcomings of static load tests include test cost, the time required to setup and complete a test, and the minimal information obtained on driving stresses or extent of pile damage (if any). Static load test results can also be misleading on projects with highly variable soil conditions.

19.8 TENSILE LOAD TESTS

Tensile load tests are performed to determine axial tensile (uplift) load capacities of piles. The uplift capacity of piles is important for pile groups subjected to large overturning moments. Hence, the importance of determining pile uplift capacity has greatly increased in recent years, particularly with regard to seismic design issues. The basic mechanics of the test are similar to compression load testing, except the pile is loaded in tension.

19.8.1 Tension Test Equipment

ASTM D-3689 describes The Standard Method of Testing Individual Piles Under Static Axial Tensile Load by the American Society of Testing Materials. Several alternative systems for (1) applying tensile load to the pile, and (2) measuring movements are provided in this standard. Most often, tensile loads are applied by centering a hydraulic jack on top of a test beam(s) and jacking against a reaction frame connected to the pile to be tested. The test beam in turn is supported by piles or cribbing. When a high degree of accuracy is required, the primary means of measuring the load applied to the pile should be from a calibrated load cell with the jack load recorded from a calibrated pressure gage as backup. A spherical bearing plate should be included in the load application arrangement.

Axial pile head movements are usually measured by dial gages or LVDT's that measure movement between the pile head and an independently supported reference beam. For tensile load testing, ASTM requires a longer travel length and higher precision for movement measuring devices than in a compression load test. For tensile testing, ASTM requires that the dial gages or LVDT's have a minimum of 75 mm of travel and a precision of at least 0.025 mm. A minimum of two dial gages or LVDT's mounted equidistant from the center of the pile and diametrically opposite should be used. Two backup systems consisting of a scale, mirror, and wire system should also be provided with a scale precision of 0.25 mm. The backup systems should be mounted on diametrically opposite pile faces and be independently supported systems. Additional details on load application, and pile head load and movement measurements may be found in ASTM D-3689. A photograph of a typical tension load test arrangement is presented in Figure 19.7.

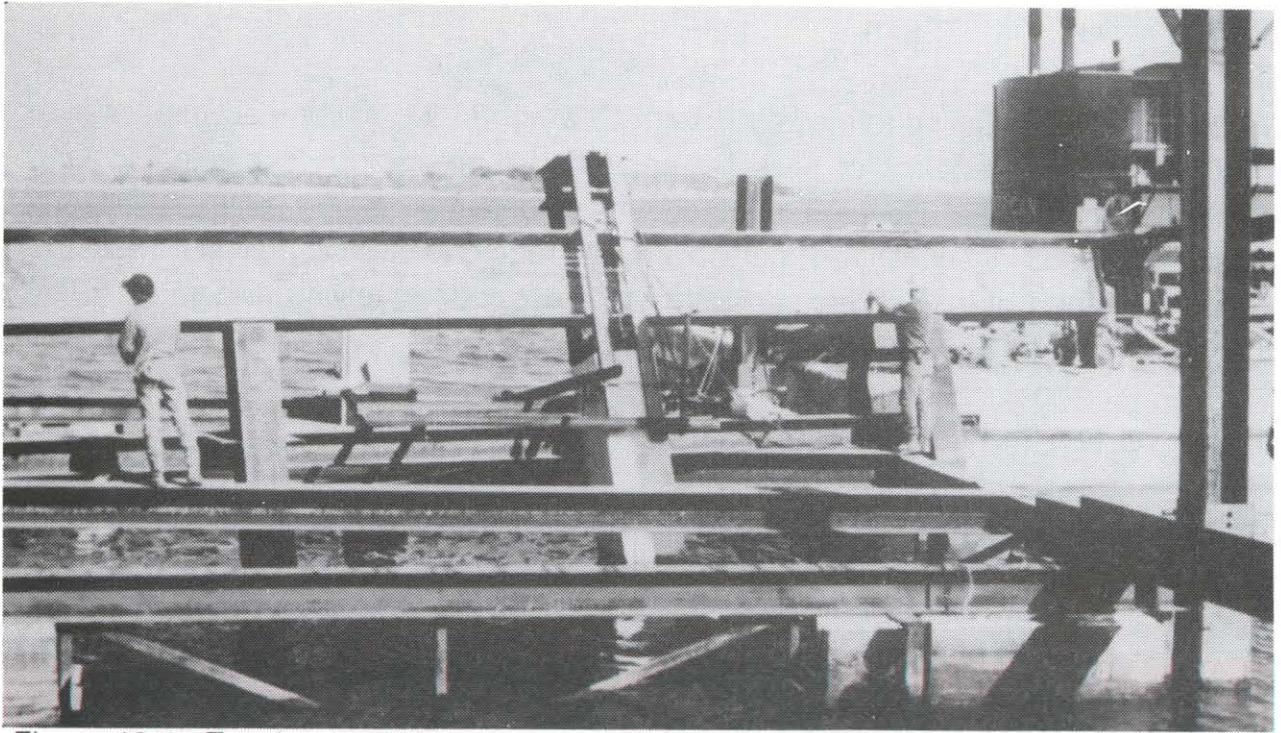


Figure 19.7 Tension Load Test Arrangement on Batter Pile (courtesy of Florida DOT)

19.8.2 Tension Test Loading Methods

Several loading procedures are detailed in ASTM D-3689. The quick loading procedure is recommended. This procedure requires that load be applied in increments of 10 to 15% of the pile design load with a constant time interval of 2½ minutes, or as otherwise specified between load increments. Readings of time, load, and gross movement are to be recorded immediately before and after the addition of each load increment. This procedure is to continue until continuous jacking is required to maintain the test load, or the capacity of the loading apparatus is reached, whichever occurs first. Upon reaching and holding the maximum load for 5 minutes, the pile is unloaded in four equal load decrements which are each held for 5 minutes. Readings of time, load, and gross movement are once again recorded immediately after, 2½ minutes after, and 5 minutes after each load reduction including the zero load. Additional optional loading procedures are detailed in ASTM D-3689.

It is generally desirable to test a pile in tensile loading to failure, particularly during a design stage test program. If construction stage tensile tests are performed on production piles, the piles should be re-driven to the original pile toe elevation and the previous driving resistance upon completion of the testing.

19.8.3 Presentation and Interpretation of Tension Test Results

The results of tensile load tests should be presented in a report conforming to the requirements of ASTM D-3689. A load-movement curve similar to the one shown in Figure 19.8 should be plotted for interpretation of tensile load test results.

A widely accepted method for determining the ultimate pile capacity in uplift loading has not been published. Fuller (1983) reported that acceptance criteria for uplift tests have included a limit on the gross or net upward movement of the pile head, the slope of the load movement curve, or an offset limit method that accounts for the elastic lengthening of the pile plus an offset.

Due to the increased importance of tensile load testing, it is recommended that the elastic lengthening of the pile plus an offset limit be used for interpretation of test results. For tensile loading, the suggested offset is 4.0 mm. The load at which the load movement curve intersects the elastic lengthening plus 4.0 mm is then defined as the tensile failure load. The uplift design load may be chosen between $\frac{1}{2}$ to $\frac{2}{3}$ of this failure load.

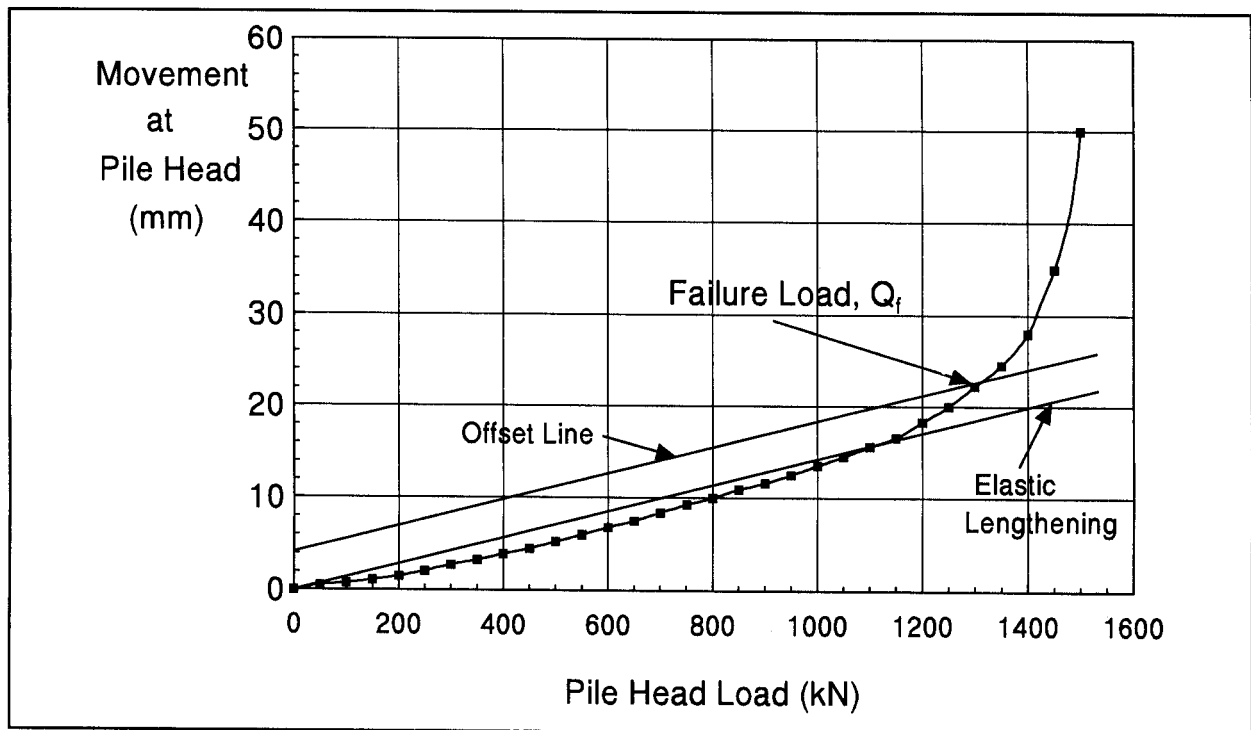


Figure 19.8 Typical Tension Load Test Load-Movement Curve

19.9 LATERAL LOAD TESTS

Lateral load tests are performed on projects where piles are subjected to significant lateral loads. The importance of determining pile response to lateral loading has greatly increased in recent years, particularly with regard to special design events such as seismic and vessel impact. This need has also increased due to the greater use of noise walls and large overhead signs. The primary purpose of lateral load testing is to determine the p-y curves to be used in the design or to verify the appropriateness of the p-y curves on which the design is based.

19.9.1 Lateral Load Test Equipment

ASTM D-3966 describes The Standard Method of Testing Piles Under Lateral Load by the American Society of Testing Materials. Several alternative systems for (1) applying the lateral load to the pile, and (2) measuring movements are provided in this standard. Most often, lateral loads are applied by a hydraulic jack acting against a reaction system (piles, deadman, or weighted platform), or by a hydraulic jack acting between two piles. The primary means of measuring the load applied to the pile(s) should be from a calibrated load cell with the jack load recorded from a calibrated pressure gage as backup. ASTM requires a spherical bearing plate(s) be included in the load application arrangement unless the load is applied by pulling.

Lateral pile head movements are usually measured by dial gages or LVDT's that measure movement between the pile head and an independently supported reference beam mounted perpendicular to the direction of movement. For lateral load testing, ASTM requires the dial gages or LVDT's have a minimum of 75 mm of travel and a precision of at least 0.25 mm. For tests on a single pile, one dial gage or LVDT is mounted on the side of the test pile opposite the point of load application. A backup system consisting of a scale, mirror, and wire system should be provided with a scale precision of 0.25 mm. The backup system is mounted on the top center of the test pile or on a bracket mounted along the line of load application.

It is strongly recommended that lateral deflection measurements versus depth also be obtained during a lateral load test. This can be accomplished by installing an inclinometer casing on or in the test pile to a depth of 10 to 20 pile diameters and recording inclinometer readings immediately after application or removal of a load increment held for a duration of 30 minutes or longer. Kyfor *et al.* (1992) noted that

lateral load tests in which only the lateral deflection of the pile head is measured are seldom justifiable. Additional details on load application, and pile head load and movement measurements may be found in ASTM D-3966 and FHWA-SA-91-042. A photograph of a typical lateral load test arrangement is presented in Figure 19.9.

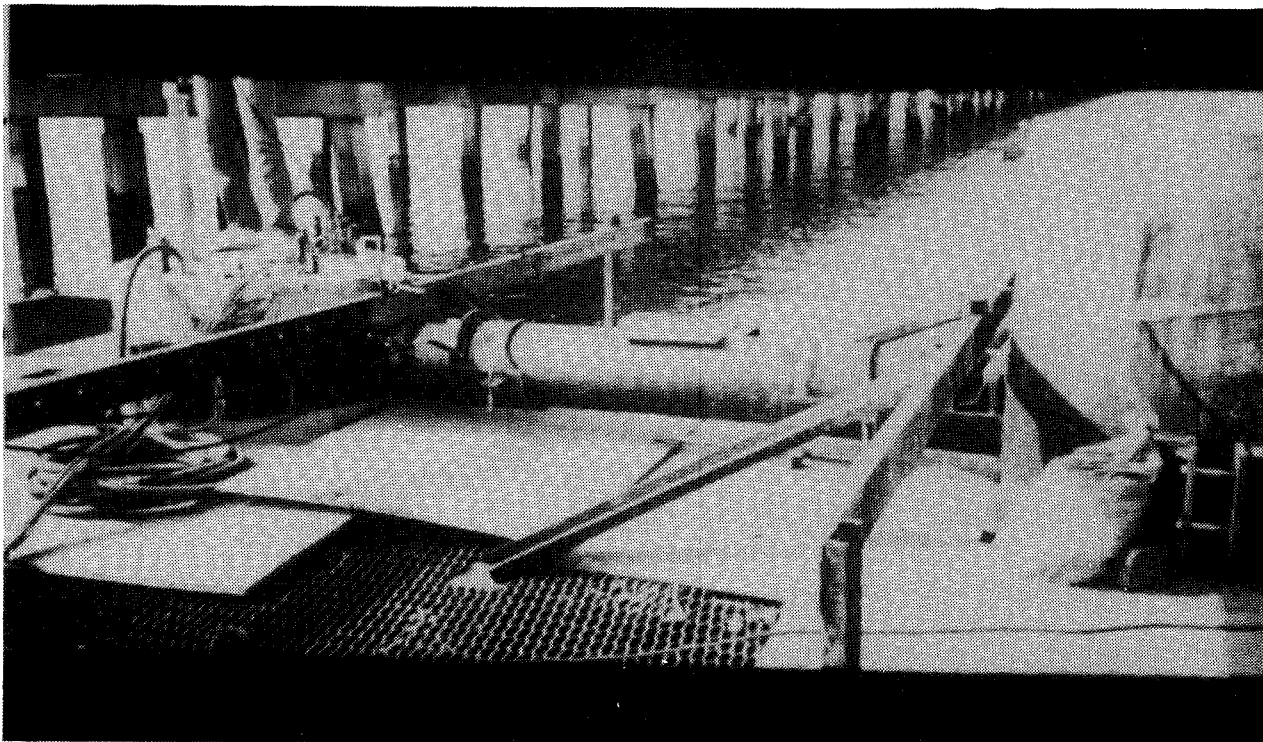


Figure 19.9 Typical Lateral Load Test Arrangement (courtesy of Florida DOT)

19.9.2 Lateral Test Loading Methods

Several loading procedures are detailed in ASTM D-3966. The standard loading procedure requires that the total test load be 200% of the proposed lateral design load. Variable load increments are applied with the magnitude of load increment decreasing with applied load. The load duration is also variable, increasing from 10 minutes early in the test to 60 minutes at the maximum load. Upon completing the maximum test load, the pile is unloaded in four load decrements equal to 25% of the maximum load with 1 hour between load decrements.

A modified lateral loading schedule was proposed by Kyfor *et al.* in FHWA-SA-91-042. The recommended loading increment is 12.5% of the total test load with each load increment held for 30 minutes. Upon reaching and holding the maximum load for 60

minutes, the pile is unloaded and held for 30 minutes at 75, 50, 25 and 5% of the test load.

Readings of time, load, and gross movement are recorded immediately after each change in load. Additional readings are taken at 1, 2, 4, 8, 15 and 30 minutes. This procedure is followed during both the loading and unloading cycle.

19.9.3 Presentation and Interpretation of Lateral Test Results

The results of lateral load tests should be presented in a report conforming to the requirements of ASTM D-3966. The interpretation and analysis of lateral load test results is much more complicated than those for compression and tensile load testing. Figure 19.10 presents a typical lateral load test pile head load-movement curve. A lateral deflection versus depth curve similar to the one shown in Figure 19.11 should also be plotted for interpretation of lateral load test results that include lateral deflection measurements versus depth. The measured lateral load test results should then be plotted and compared with the calculated result as indicated in Figure 19.11.

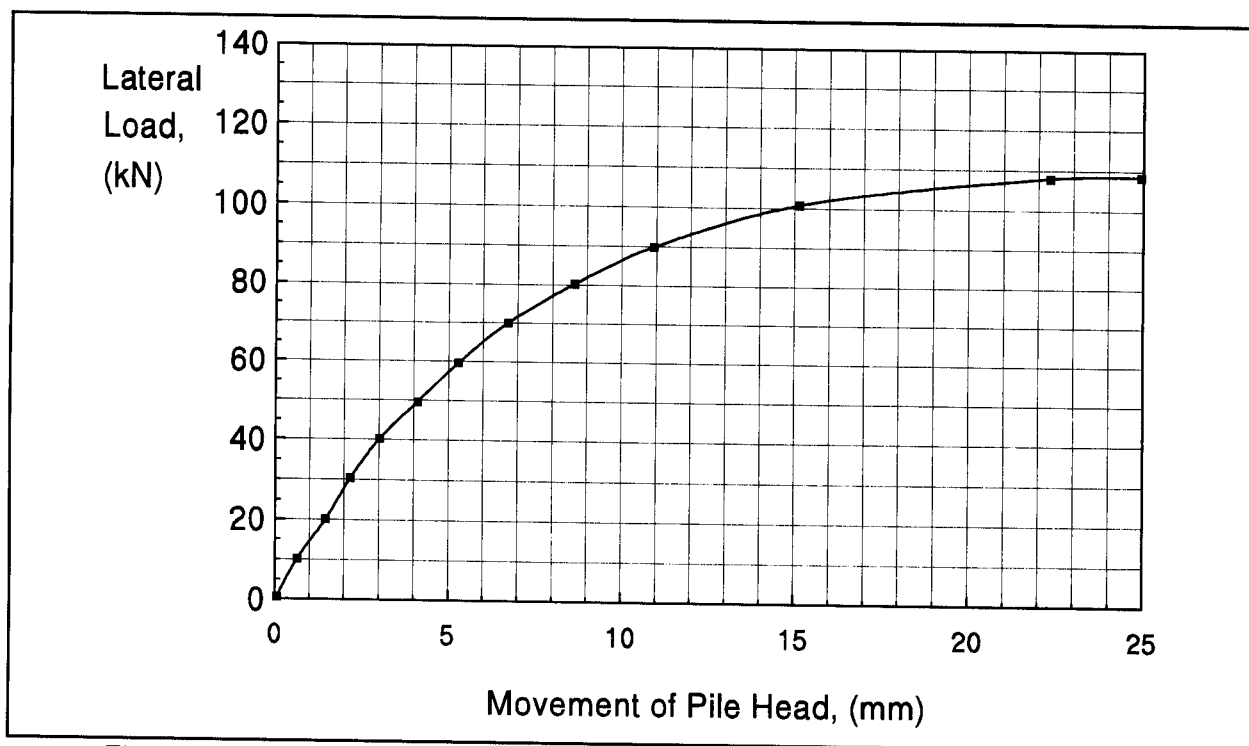


Figure 19.10 Typical Lateral Load Test Pile Head Load-Deflection Curve

Based upon the comparison of measured and predicted results, the p-y curves to be used for design (design stage tests), or the validity of the p-y curves on which the design was based (construction stage tests) can be determined.

Refer to FHWA-IP-84-11, Handbook on Design of Piles and Drilled Shafts Under Lateral Load by Reese (1984) as well as FHWA-SA-91-042, Static Testing of Deep Foundation by Kyfor *et al.* (1992) for additional information on methods of analysis and interpretation of lateral load test results.

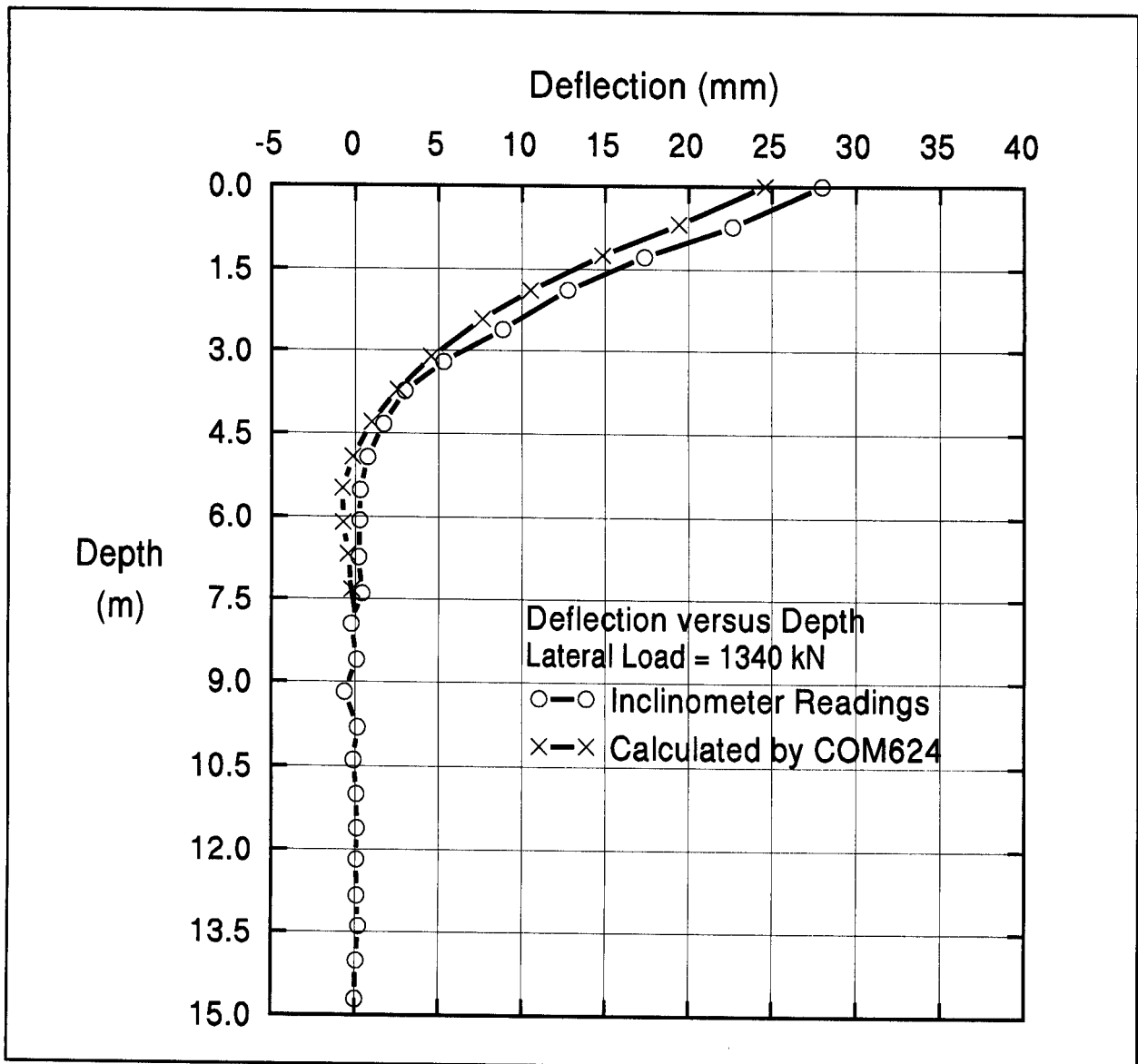


Figure 19.11 Comparison of Measured and COM624P Predicted Load-Deflection Behavior versus Depth (after Kyfor *et al.* 1992).

REFERENCES

- American Association of State Highway and Transportation Officials [AASHTO], (1992). Standard Specifications for Highway Bridges. Division 2, Washington, D.C.
- American Society for Testing and Materials, ASTM (1994). Annual Book of Standards, ASTM D-1143, Standard Test Method for Piles Under Static Axial Compressive Load.
- American Society for Testing and Materials, ASTM (1994). Annual Book of Standards, ASTM D-3936, The Standard Method of Testing Individual Piles Under Static Axial Tensile Load.
- American Society for Testing and Materials, ASTM (1994). Annual Book of Standards, ASTM D-3936, The Standard Method of Testing Piles Under Lateral Load.
- Cheney, R.S. and Chassie, R.G. (1993). Soils and Foundations Workshop Manual. Second Edition, Publication No. FHWA HI-88-009, Federal Highway Administration, National Highway Institute, Washington, D.C., 353-362.
- Crowther, C.L. (1988). Load Testing of Deep Foundations: the Planning, Design, and Conduct of Pile Load Tests. John Wiley & Sons, New York, 233.
- Davisson, M.T. (1972). High Capacity Piles, Proceedings, Soil Mechanics Lecture Series on Innovations in Foundation Construction. American Society of Civil Engineers, ASCE, Illinois Section, Chicago, 81-112.
- Dunnicliff, J. (1988). Geotechnical Instrumentation for Monitoring Field Performance. John Wiley & Sons, New York, 467-479.
- Fellenius, B.H. (1990). Guidelines for the Interpretation of the Static Loading Test. Deep Foundations Institute Short Course Text, First Edition, 44.
- Fuller, F.M. (1983). Engineering of Pile Installations. McGraw-Hill, New York, 286.

Kyfor, Z.G., Schnore, A.S., Carlo, T.A. and Bailey, P.F. (1992). Static Testing of Deep Foundations. Report No. FHWA-SA-91-042, U.S. Department of Transportation, Federal Highway Administration, Office of Technology Applications, Washington, D.C., 174.

Reese, L.C. (1984). Handbook on Design of Piles and Drilled Shafts Under Lateral Load. Report No. FHWA-IP-84-11, U.S. Department of Transportation, Federal Highway Administration, Office of Implementation, McLean, 386.

STUDENT EXERCISE #13 - DETERMINATION OF LOAD TEST FAILURE LOAD

An axial compression static load test has been performed and the results must be interpreted to determine if the pile has an ultimate capacity in excess of the required ultimate capacity. The load - movement curve from the static load on a 356 mm square prestressed concrete pile is presented on the following page. The pile has a cross sectional area, A , of 0.127 m^2 and a length, L , of 24 m. The concrete compression strength, f'_c is 34.5 MPa. The pile has a required ultimate pile capacity of 2200 kN.

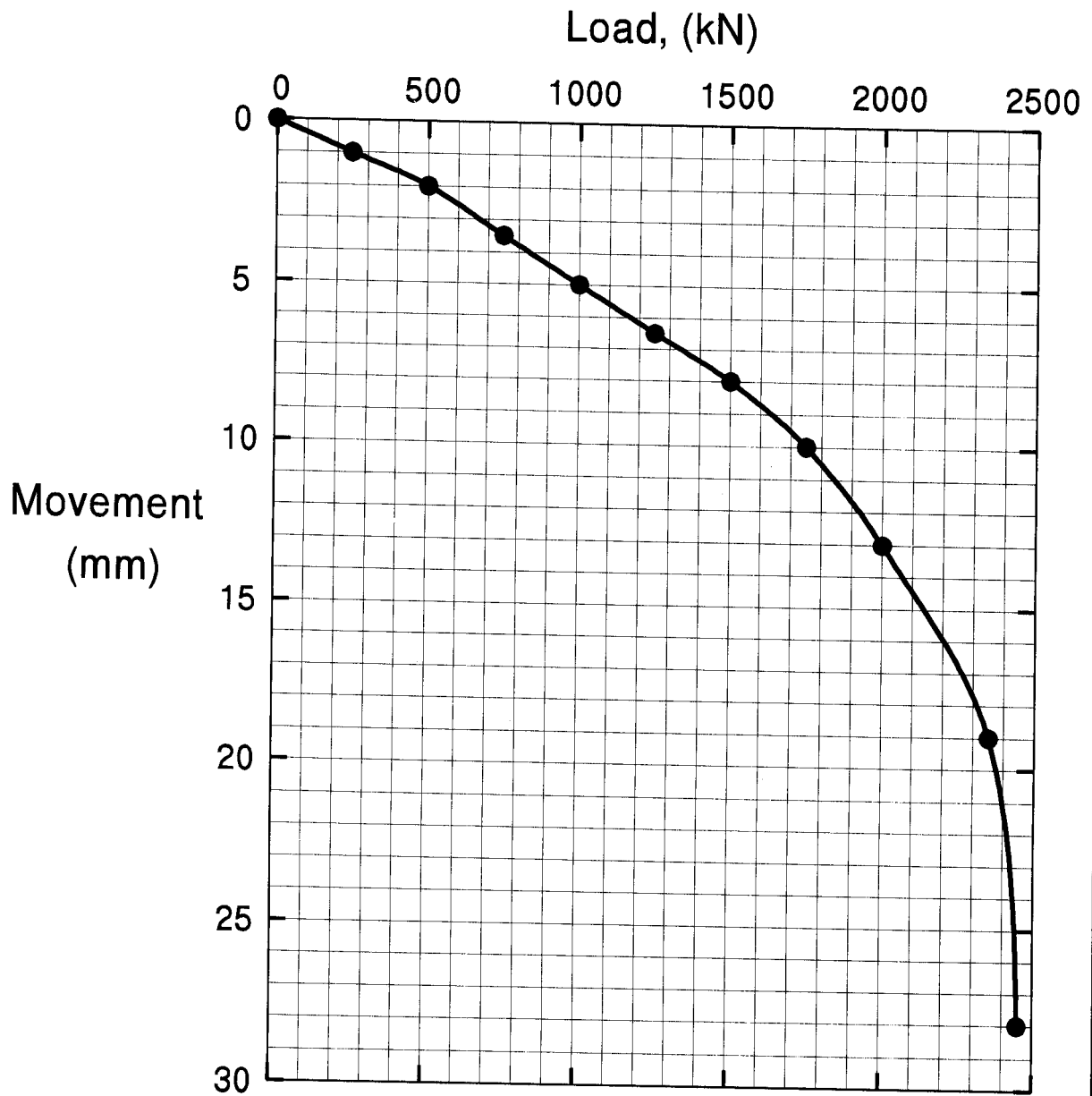
Recommended Procedure:

First determine, the elastic modulus, E , of the pile from the concrete compressive strength using $E = 4700 \sqrt{f'_c}$ where f'_c must be in MPa.

Next, calculate and plot the elastic deformation line using zero and any other load. However, for consistency between solutions and ease in plotting, calculate the elastic deformation using a load of 2500 kN from $\Delta = QL / AE$. Make sure the units for the terms in this equation are as required in the equation description provided in Section 19.7.4.

Then calculate the failure criterion line for the 356 mm pile from $s_f = \Delta + (4.0 + 0.008b)$ as described in Section 19.7.5. Remember at zero load, the failure criterion line will start at a movement equal to $(4.0 + 0.008b)$ and at 2500 kN, the failure criterion line will be equal to a movement of $s_f = \Delta + (4.0 + 0.008b)$.

Last, plot the failure criterion line on the load-movement curve and determine whether the failure load is greater than the required ultimate pile capacity of 2200 kN.



20. THE OSTERBERG CELL METHOD

Another recent development for evaluation of driven pile capacity is the Osterberg Cell test or O-cell test. This device provides a simple, efficient and economical method of performing a static test on a deep foundation. The O-cell is a sacrificial jack which is generally attached to the toe of a driven pile before driving.

The Osterberg Cell test can be easily applied to driven, displacement piles such as closed end pipe piles and prestressed concrete piles. The O-cell cannot be employed with H-piles, sheet piles or timber piles. Closed end pipe piles and concrete piles require cell installation prior to driving, and thus additional prior planning is needed. For open end pipe piles and mandrel driven piles, the cell may be installed after driving is complete.

Testing a driven pile with an O-cell eliminates the need for a reaction system and can provide significant cost and time savings. The Osterberg Cell has many applications and provides the engineer with a new, cost effective tool and added versatility for the static testing of driven piles. The Osterberg Cell Method is not standardized by AASHTO or ASTM and is nationally licensed to a single source. Additional information on the Osterberg Cell may be found in FHWA publication FHWA-SA-94-035 by Osterberg (1995).

20.1 OSTERBERG CELL BACKGROUND

Dr. Jorj Osterberg, Professor Emeritus at Northwestern University, developed and patented the test which now carries his name. The device was first used in an experimental drilled shaft in 1984. Following this successful prototype test, the O-cell evolved from a bellows type expansion cell to the current design, which is very similar to the piston type jack commonly used for conventional tests. However, the piston of the O-cell extends downward instead of upward.

The first O-cell test on a driven pile occurred in 1987. In this initial driven pile application, a 457 mm diameter O-cell was welded to the toe of an 457 mm diameter, closed end, steel pipe pile. In 1994, the first O-cell tests were performed on 457 mm square, prestressed concrete piles. For these piles, the O-cell was cast into the pile toe.

Figure 20.1 presents a schematic of the difference between a conventional static load test and an O-cell test. A conventional static test loads the pile in compression from the pile head using an overhead reaction system or dead load. The combination of shaft and toe resistances resist the applied pile head load. The shaft and toe resistances can be separated by analysis of strain gage or telltale measurements.

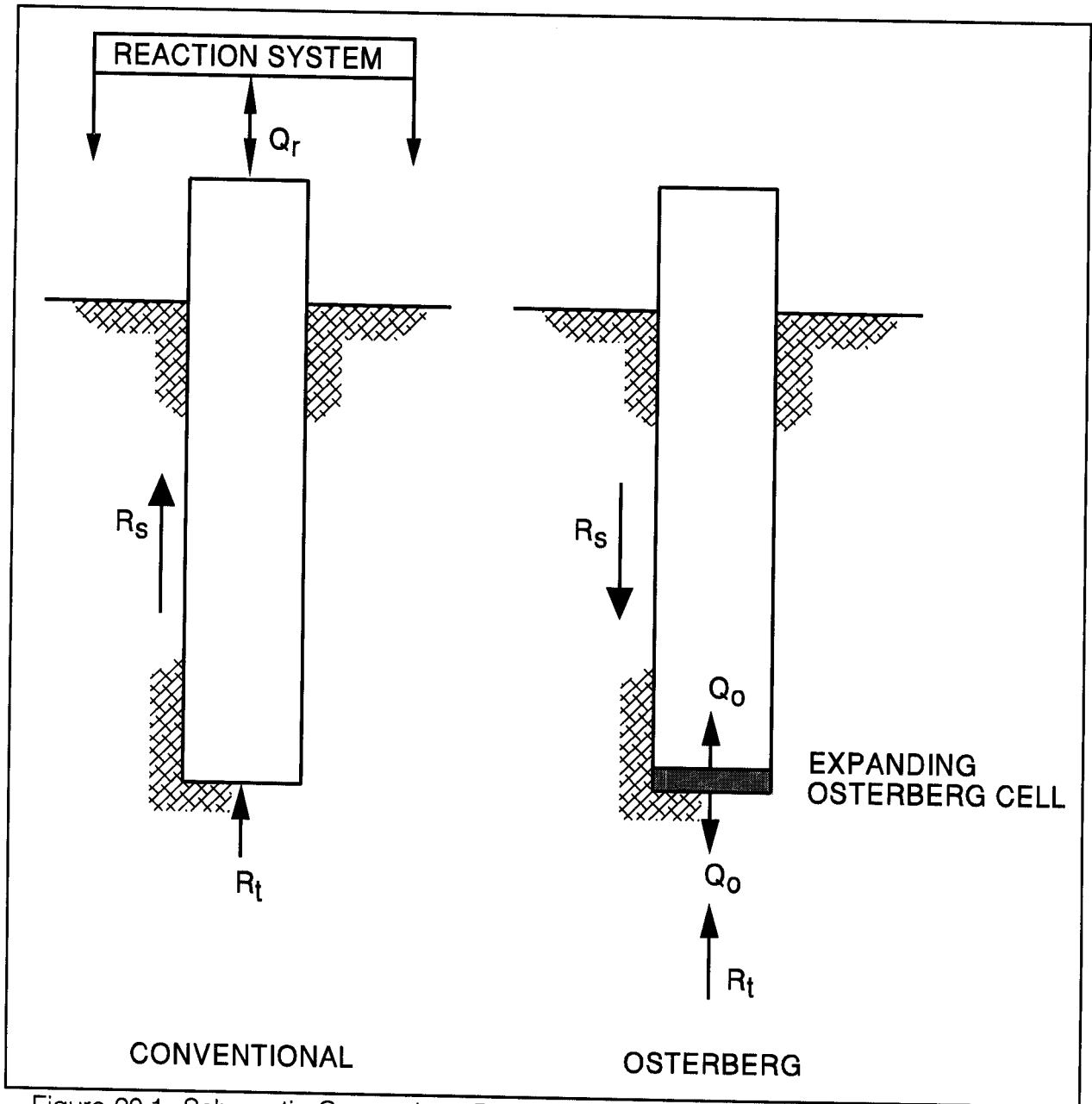


Figure 20.1 Schematic Comparison Between Osterberg Cell and Conventional Tests

In an O-cell test, the pile is also loaded in compression, but the load is applied at the pile toe. As the cell expands, the toe resistance provides reaction for the shaft resistance, and vice versa. The test is complete when either the ultimate shaft or toe resistance is reached, or the cell reaches its capacity.

An O-cell test automatically separates the toe and shaft resistance components. When one of the components fails at an O-cell load, Q_o , the conventional pile head load, Q_r , required to fail both the shaft resistance and toe resistance would have to exceed $2Q_o$. Thus, an O-cell test load placed at the pile toe is always twice as effective as the same load placed at the pile head.

20.2 TEST EQUIPMENT

The O-cell in its current design is capable of developing an internal pressure of 69 MPa. Typical cell capacities for driven piles of up to 8000 kN have been used. The cell consists of a piston and cylinder coupled to high strength pipe that extends inside the pile to the ground surface. The total allowable expansion of a standard O-cell is about 150 mm with greater expansion possible by special order. Figure 20.2 shows a typical cross section of a concrete pile and the setup for an O-cell test.

Tests performed using the O-cell usually follow the quick loading method described in ASTM D-1143, Standard Test Method for Piles Under Static Axial Compressive Load. However, other methods are not precluded. Instrumentation used to measure load and movement is similar to that used for conventional load tests. The O-cell is designed so that driving forces are transmitted through the cell without damage to the cell or the pile. An O-cell ready for placement in a 457 mm prestressed concrete pile is shown in Figure 20.3. After this pile was cast, the only visible parts of the O-cell were the bottom plates.

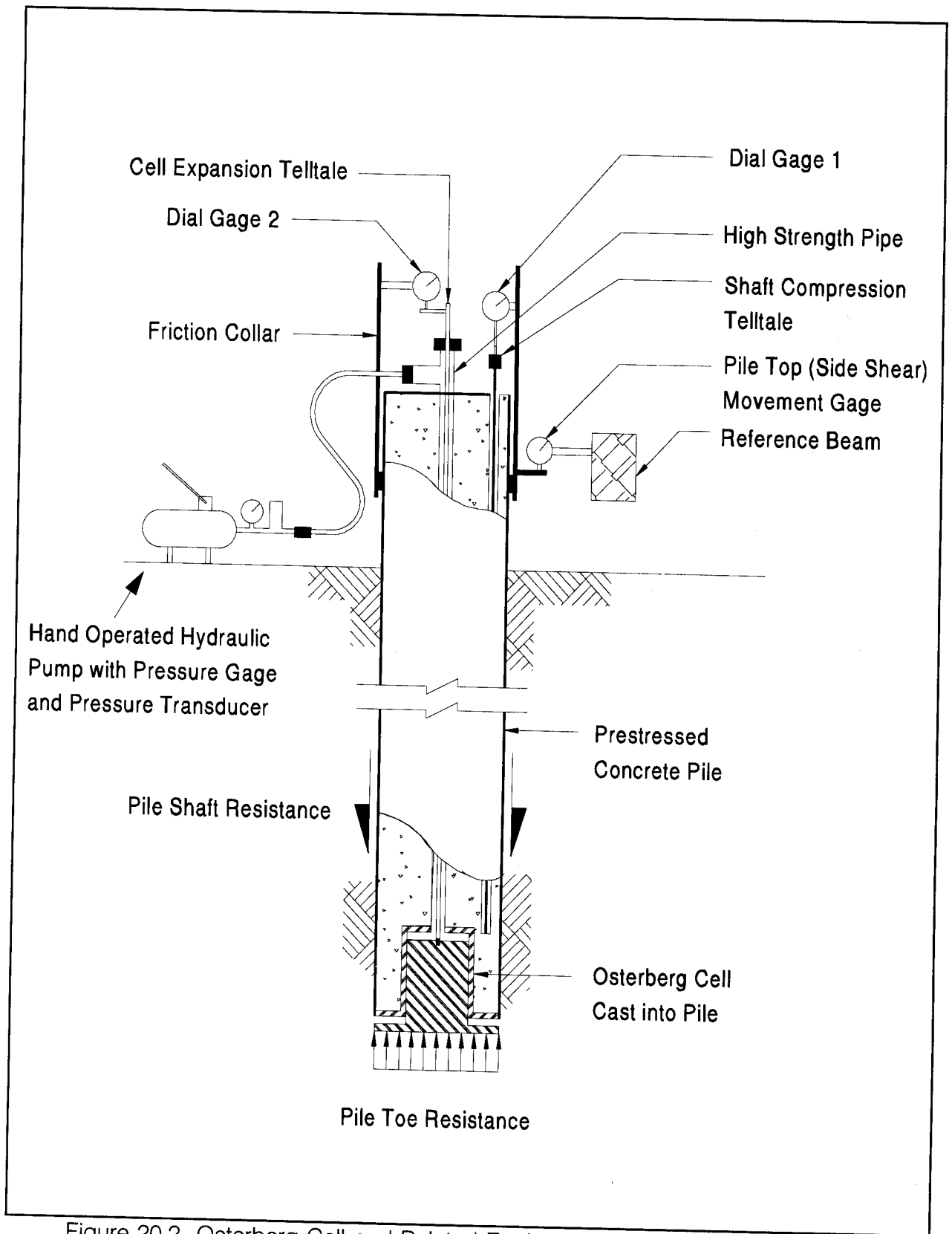


Figure 20.2 Osterberg Cell and Related Equipment Used for Static Pile Tests

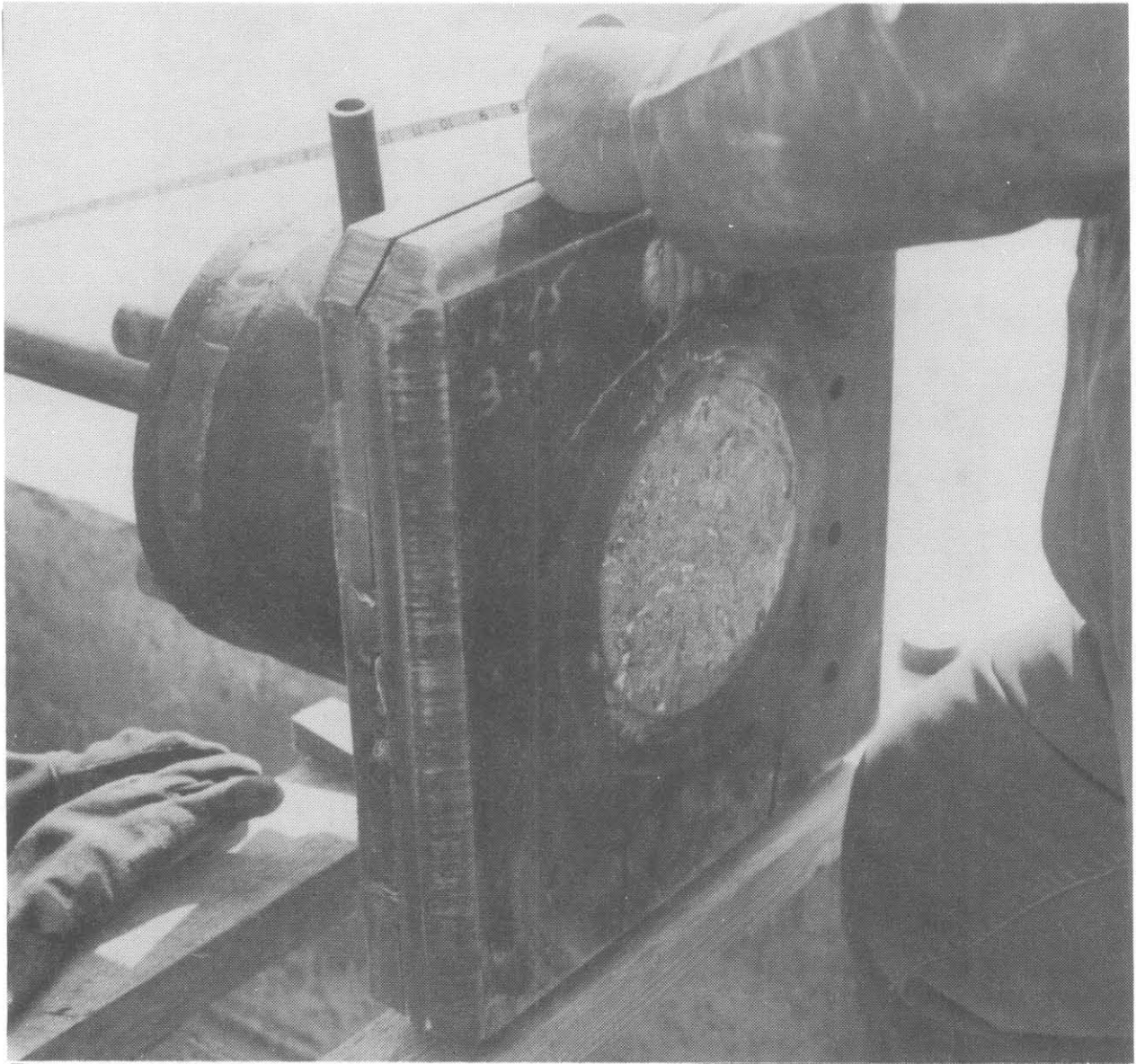


Figure 20.3 Osterberg Cell Ready for Placement in Concrete Pile Form (courtesy of Loadtest, Inc.)

After the pile is driven, a hand pump or small automatic pump (electric or air driven) is connected to a central pipe which provides a pressure conduit to the O-cell. The load applied by an O-cell is calibrated versus hydraulic pressure before installation and the pressure applied to the cell is measured using a Bourdon gage or pressure transducer. The O-cell seals typically limit internal friction to less than 2% of the applied load. In Figure 20.4, both a vibrating wire piezometer and a test gage are being used to measure the cell pressure, which is applied with a hand pump.

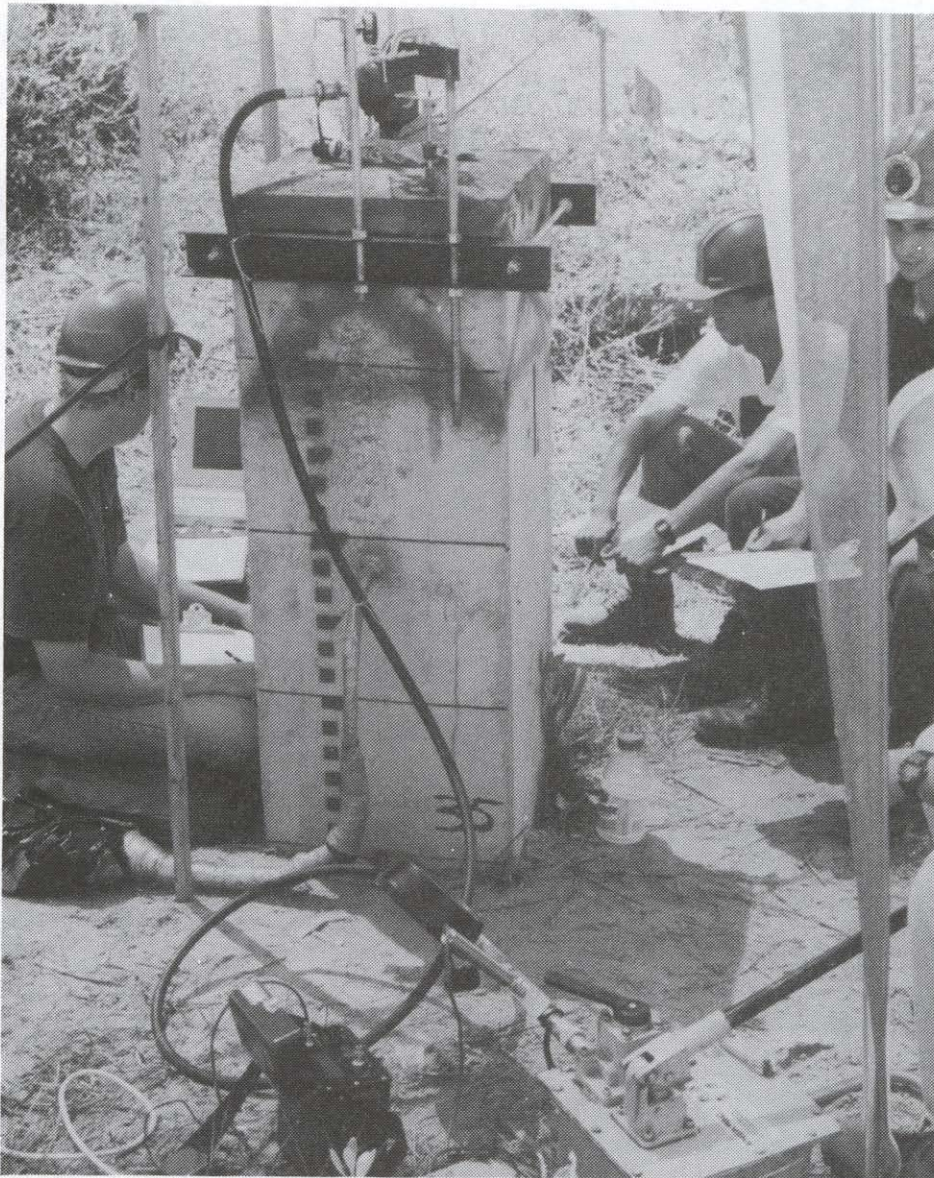


Figure 20.4 Osterberg Test in Progress on a 457 mm Concrete Pile (courtesy of Loadtest, Inc.)

For closed end pipe piles the cell must be installed before driving the pile but the pressure pipe and connection tee may be installed afterwards. The cell and pipe are normally installed in concrete piles during construction of the pile and the pipe tee is welded on after driving. For open ended pipe piles and mandrel driven piles, the cell and pipe assembly may be placed as a combined unit after the pile is driven and then concreted in place.

Movements during an O-cell test are typically measured using mechanical or electronic gages. The cell expansion (less any pile compression) is directly indicated by a steel telltale

which extends to the bottom of the cell. This telltale is placed in the central pressure pipe and exits through an O-ring seal on the connection tee. Other telltales, indicating compression of the pile, are usually installed in pairs. They help with estimating the shaft resistance distribution and calculations for movement. The upward movement of the pile, which is resisted by the downward shaft resistance, is measured by gages mounted to a reference beam and checked by an independent measurement such as a survey level.

When an O-cell test is performed on a production pile it will usually be necessary to grout the O-cell after completing the test. This is accomplished by unscrewing the cell expansion telltale illustrated in Figure 20.2 from the O-cell and inserting a grout pipe in its place. The grout pipe is gradually removed as the grout flows out of the pipe under gravity flow. A fitting can also be attached to the top of the high strength pipe and the grout pipe connected directly to the grout pump in cases where it is desirable to place the grout under pressure to partially mobilize the pile toe resistance. However, to avoid soil creep, the grout pressure should be maintained below the maximum pressure applied in the O-cell test.

20.3 INTERPRETATION OF TEST RESULTS

The Osterberg Cell loads the test pile in compression similar to a conventional static load test. Data from an Osterberg test is therefore analyzed much the same as conventional static test data. The only significant difference is that the O-cell provides two load-movement curves, one for shaft resistance and one for toe resistance. The failure load for each component may be determined from these curves using a failure criteria similar to that recommended for conventional load tests. To determine the shaft resistance capacity, the buoyant weight of the pile should be subtracted from the upward O-cell load, and the elastic deformation of the pile shaft should be included. Analysis for the toe resistance should not include the elastic pile deformation since the load is applied directly at the pile toe.

The engineer may further utilize the component curves to construct an equivalent pile head load-movement curve and investigate the overall pile capacity. Construction of the equivalent pile head load-movement curve begins by determining the shaft resistance at an arbitrary movement point on the shaft resistance-movement curve. If the pile is assumed rigid, the pile head and toe move together and have the same movement at this load. By adding the shaft resistance to the mobilized toe resistance at the chosen movement, a single point on the equivalent pile head load-movement curve is determined. Additional points may then be calculated to develop the curve up to the maximum movement (or maximum extrapolated movement) of the component that did not fail. Points beyond the

maximum movement of the non-failing component may also be obtained by conservatively assuming that at greater movements it remains constant at the maximum applied load. Example results using this method are included with the case history data below.

As noted by Osterberg (1994), the above construction makes three basic assumptions:

1. The shaft resistance load-movement curve resulting from the upward movement of the top of the O-cell is the same as developed by the downward pile head movement of a conventional compression load test.
2. The toe resistance load-movement curve resulting from the downward movement of the bottom of the O-cell is the same as developed by the downward pile toe movement of a conventional load test.
3. The compression of the pile is considered negligible, *i.e.* a rigid pile.

The first of these assumptions highlights a significant difference between the O-cell test and a conventional compression load test, namely the change in direction of the mobilized shaft resistance from downward to upward. Researchers at the University of Florida have investigated the effect of this direction reversal using the finite element method. Their results indicate that the O-cell produces slightly lower shaft resistance than a conventional load test, but that in general the effect is small and may be ignored. A few full scale field tests tend to confirm these findings. Note that the shaft resistance direction in an O-cell test matches that in a conventional tension or uplift test.

Lower confining stresses due to the gap induced around the expanding cell may also cause the O-cell to measure a slightly lower toe resistance, but this effect is conservative and also seems negligible. The compression of the pile is normally a second order effect and the assumption of a rigid pile causes a negligible error. In general, the above assumptions seem to produce conservative and reasonable results.

20.4 APPLICATIONS

Although its use is not feasible for all pile types, the O-cell test has many potential applications with common driven piles. Its versatility also provides additional options. A partial list of applications follows:

1. Displacement Piles: The O-cell may be installed prior to driving solid concrete piles and closed end pipe piles.
2. Mandrel Driven Piles: Mandrel driven piles can be tested by grouting the O-cell into the pile toe after removing the mandrel.
3. Open Ended Pipe Piles: The O-cell may be installed in open ended pipe piles and voided concrete piles by removing the soil plug after driving.
4. Batter Piles: Conventional static load tests to evaluate the axial capacity of batter piles can be very difficult to perform. For applicable pile types in these situations, the O-cell test offers an alternate test method that is easier to perform.
5. Testing Over Water or at Constricted Sites: Because the O-cell test requires no overhead reaction, the surface test setup is minimized. Tests over water require only a work platform. Sites with poor access, limited headroom or confined work area are ideal applications for an O-cell test.
6. Proof Tests: Because of the simplicity and usually lower cost of O-cell tests compared to conventional static load tests, several piles can be economically proof tested as a check of pile capacity.
7. Repetitive Tests: Multiple static tests on the same pile may be performed with the O-cell to investigate the effect of time on pile capacity. Use of the O-cell minimizes the mobilization required for each static test.
8. Exploratory Testing: With the proper design, it is possible to use the O-cell to test the same pile at different pile penetration depths. After each test, the pile is driven deeper and retested. This method also develops the shaft resistance distribution incrementally.

20.5 ADVANTAGES

Osterberg (1994) and Schmertmann (1993) summarized a number of potential advantages, vs. conventional testing that may be realized by using the Osterberg Cell. These include:

1. Economy: The O-cell test is usually less expensive to perform than a conventional static test despite sacrificing the cell. Savings are realized through reduced setup time and capital outlay, less heavy equipment, fewer structural connections and less test design effort. O-cell tests are typically $\frac{1}{3}$ - $\frac{2}{3}$ the cost of conventional tests. The relative economy improves as the required maximum test load increases.
2. Static Creep and Setup Effects: Because the O-cell test is static, and the test load can be held for any desired length of time (typically 5 minute increments), data about the creep behavior of the shaft and toe resistances can be obtained. Creep limits may be obtained which are similar to those from pressuremeter tests described in ASTM D4719 (ASTM,1993). Soil setup effects can also be conveniently measured at any time after driving.
3. Improved Safety: Because there is no overhead load, failure of the load system creates a minimal safety hazard.
4. Reduced Work Area: The work area required to perform an O-cell test is much smaller, both overhead and laterally, than the area required for a conventional load system.
5. High Load Capacity: Very high capacity loading is possible for large piles or whole groups of piles. Drilled shafts have been tested to over 53,400 kN equivalent conventional test load.
6. Shaft/Toe Resistance Determination: The O-cell test clearly separates the shaft and toe resistance components.
7. Multiple Tests: The O-cell provides a convenient method to obtain additional tests on the same pile, at multiple toe elevations and/or after elapsed time at the same toe elevation.

20.6 DISADVANTAGES

The O-cell has some disadvantages or limitations compared to conventional tests as discussed below:

1. Not Suitable for Certain Types of Piles: The O-cell cannot be used to test H-piles. Installation of an O-cell on a timber pile would be difficult. Installation in open end pipe piles is feasible, but requires internal pile cleanout after driving for cell placement and subsequent concrete or grout placement above the installed cell. In tapered piles, the equivalent shaft resistance of a tapered pile loaded in compression will not be developed since the effects of the taper will be lost when loaded upward from the pile toe in an O-cell test.
2. Need for Planning: With closed end and solid displacement piles, the O-cell must be installed prior to driving. For these pile types, an O-cell test cannot be chosen after installation.
3. Limited Capacity: An O-cell test reaches the ultimate load in only one of the two resistance components. The pile capacity demonstrated by the O-cell test is limited to two times the failed component. Also, once installed, the cell capacity cannot be increased if inadequate. To use the cell efficiently, the engineer should first analyze the expected shaft and toe resistances, and then attempt to balance the two or ensure a failure in the preferred component.
4. Equivalent Pile Head Load-Movement Curve: Although the equivalent static load-movement curve can be constructed from O-cell test data, it is not a direct measurement and may be too conservative.

20.7 CASE HISTORIES

To date, only closed end pipe piles and prestressed concrete driven piles have been tested using the O-cell. Case studies for both pile types are presented below.

In 1987, a 457 mm diameter steel pipe pile with an O-cell of the same diameter welded to the pile toe was driven at the Pines River Bridge in Saugus, MA. As shown in Figure 20.5, this pile was driven through soft clay and a layer of glacial till, then founded in weathered Argillite rock at a depth of 36 m below the ground surface. It was driven to practical refusal

with a Delmag D 36-13 diesel hammer with a rated energy 112.7 kJ. The final driving resistance was 10 blows for the last 13 mm.

As indicated by the shaft and toe resistance load-movement curves shown in Figure 20.6, the Pines River pile failed in shaft resistance at a cell load of 1910 kN. The small upward movement evident during the initial portion of the test is due to pressure effects on the central pipe and has little effect on the capacity results. After subtracting the pile weight to get shaft resistance, the minimum ultimate capacity of this pile was estimated as 3740 kN. An equivalent pile head load-movement curve constructed from the test data is included in Figure 20.7. The maximum toe resistance of 1910 kN was used at movements greater than 1.0 mm. For reference, the numbered pile head load-movement points were calculated at movements corresponding to the numbered points on the shaft resistance curve. Thompson *et al.* (1989) provides additional details on this case history.

O-cell tests can also be useful for special investigations. For example, O-cells were recently cast into four 457 mm square, prestressed concrete piles which were then driven and tested as part of a research project by the University of Florida (UF). This research project is investigating long term shaft resistance changes. The O-cell is being used in this application to perform repeated tests over a period of at least two years after the piles are driven. To allow the prestressed pile manufacturer to cast ordinary production piles along with the research piles, the O-cell used for the UF research is designed to fit within the standard prestressed cable pattern. The strands were then pulled through holes drilled in the load plates of the cell. These cells have a 229 mm diameter piston and a maximum stroke of 152 mm. They provide a capacity of 2700 kN at a pressure of 69 MPa. To prevent damage during driving extra lateral reinforcement was added at the pile toe. Longitudinal reinforcement was also added above the O-cell to insure good load transfer during testing and driving. Otherwise, the research piles followed a standard Florida DOT design and were cast as part of a full production bed of piles.

The pile driven at Aucilla River is 22 m long and has been tested four times over a 2 month period. Its shaft resistance has increased 64% over this time period to 1490 kN, and indications are that it will continue to increase in capacity with additional time. As shown in Figure 20.8, this pile was driven to bearing on limerock at 16 blows for the final 25 mm using a Fairchild 32 air hammer with a rated energy of 43.4 kJ. Figures 20.9 and 20.10 show the component and equivalent pile head load-movement curves for the most recent test. The maximum toe resistance of 1560 kN was used at deflections greater than 2.3 mm. Repeated tests have influenced the toe resistance, which now shows some disturbance effects in the early loads. Otherwise this test is representative of the research results.

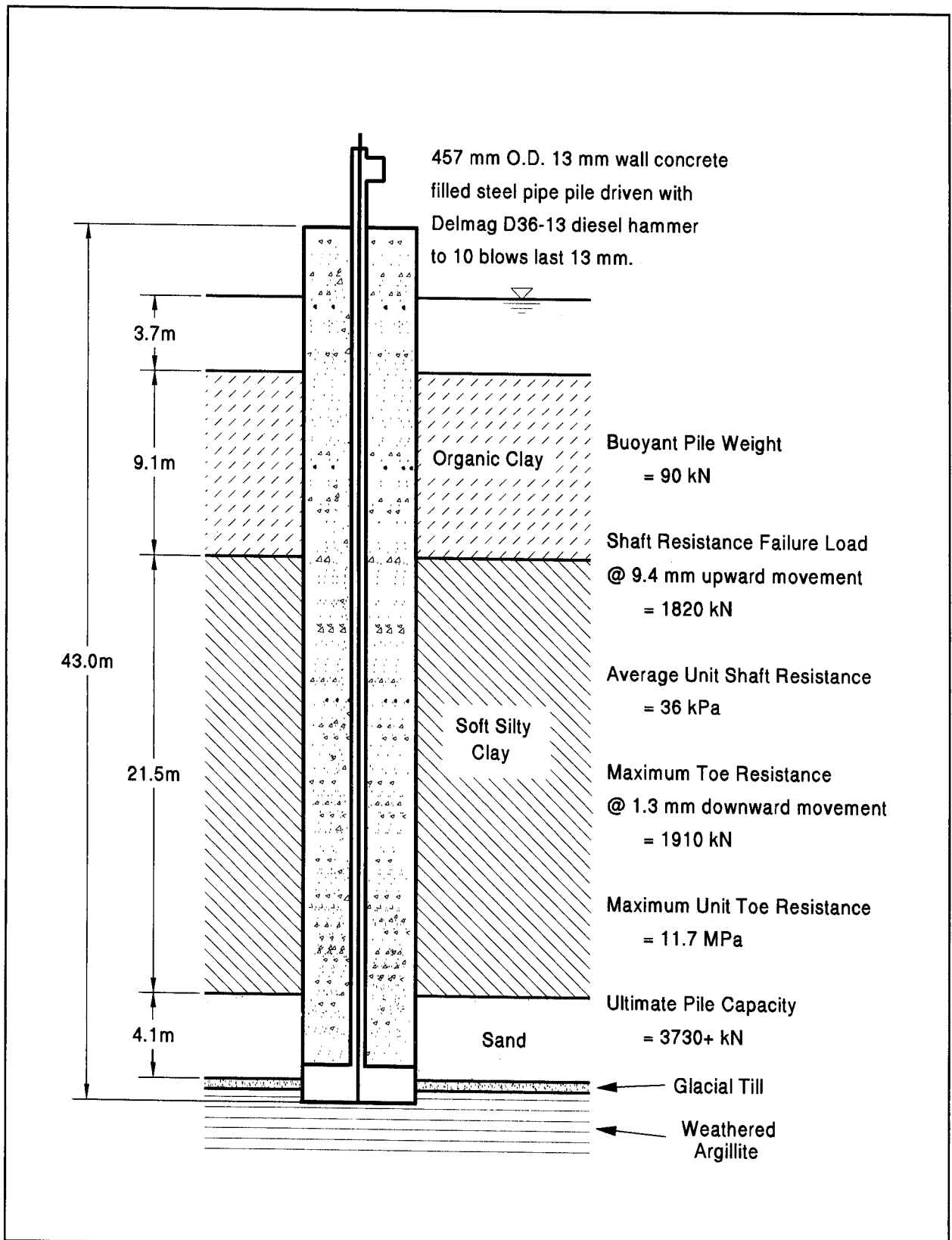


Figure 20.5 Summary of Subsurface Profile and Test Results at Pines River Bridge, MA

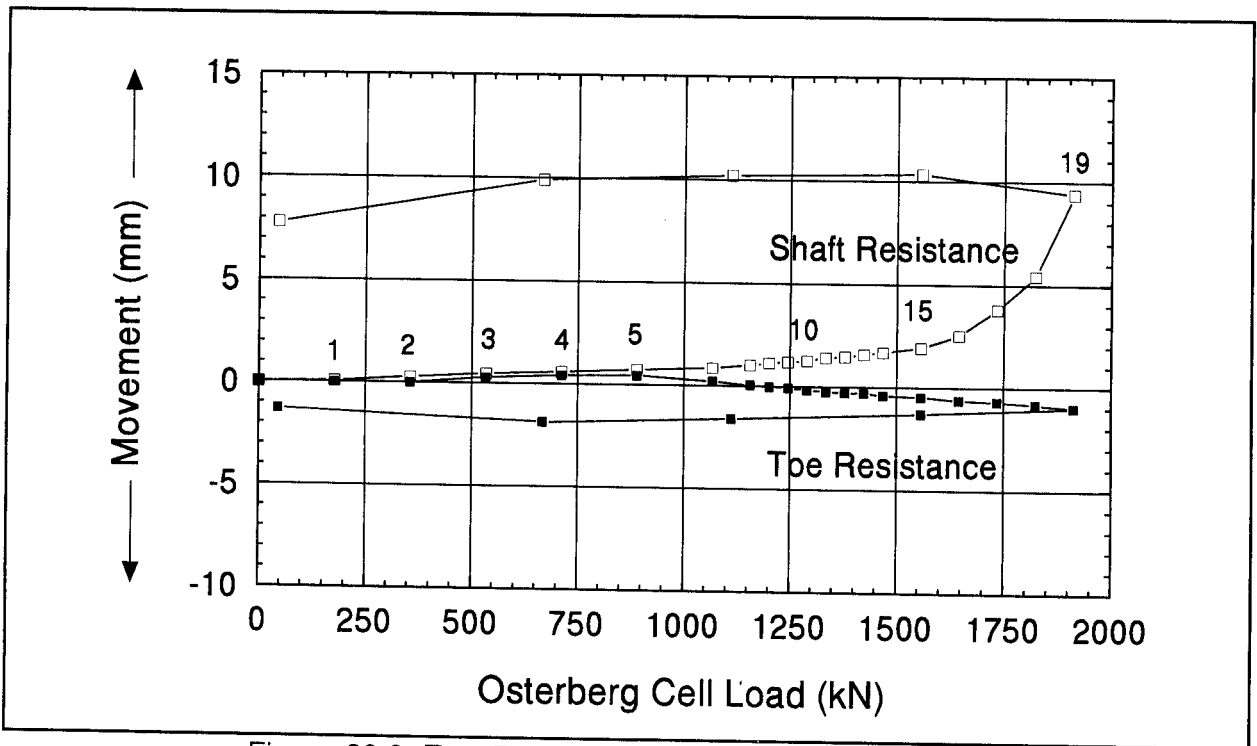


Figure 20.6 Test Results from Pines River Bridge, MA

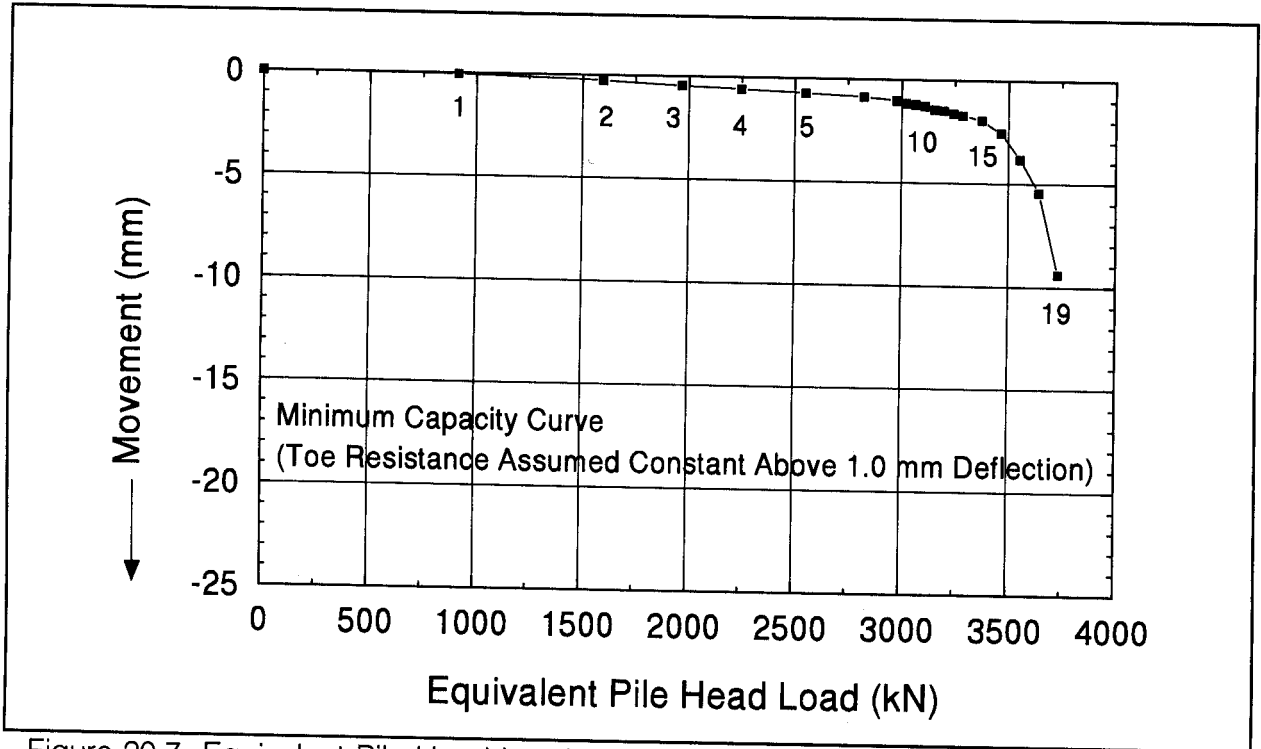


Figure 20.7 Equivalent Pile Head Load-Movement Curve from Pines River Bridge, MA

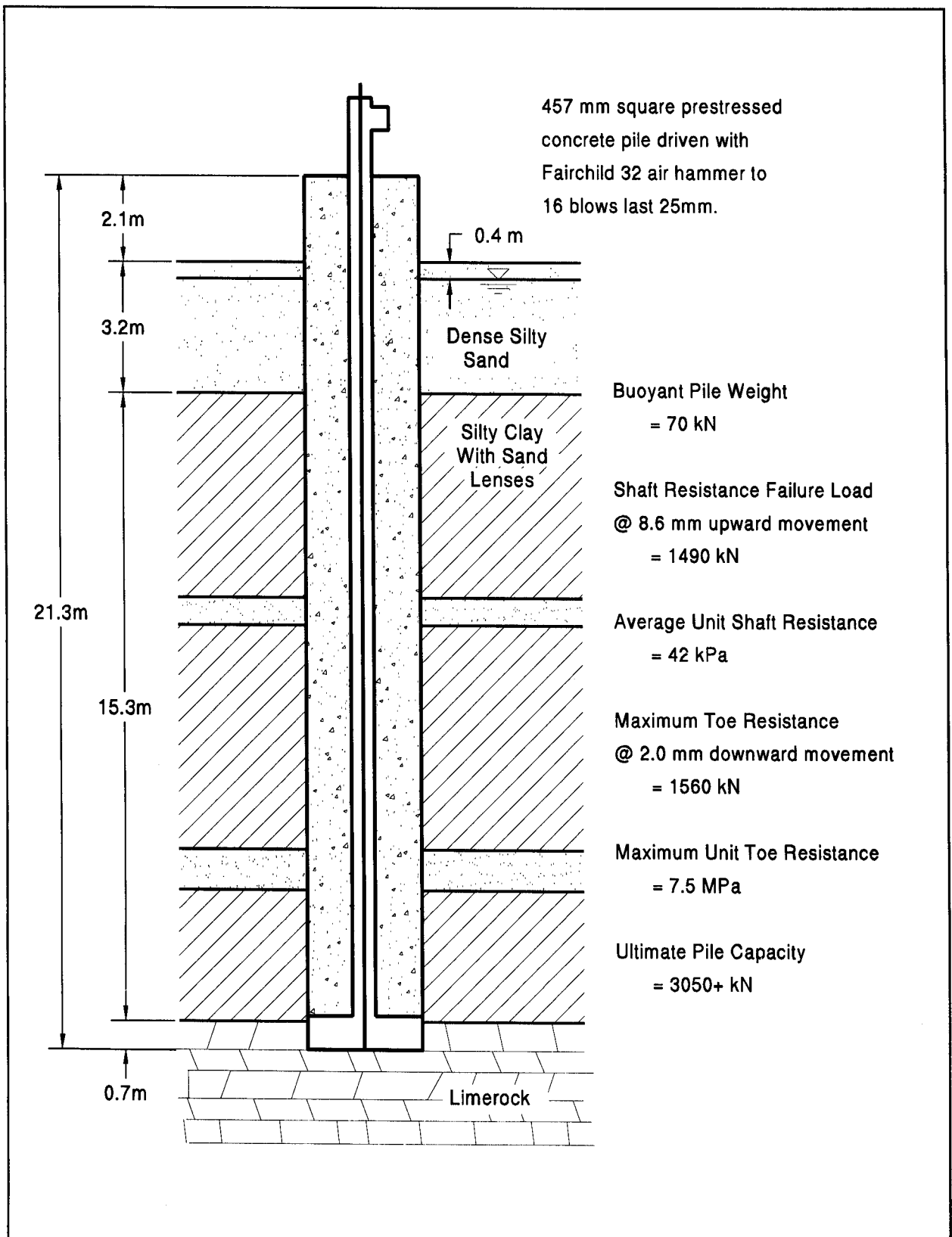


Figure 20.8 Summary of Subsurface Profile and Test Results at Aucilla River Bridge, FL

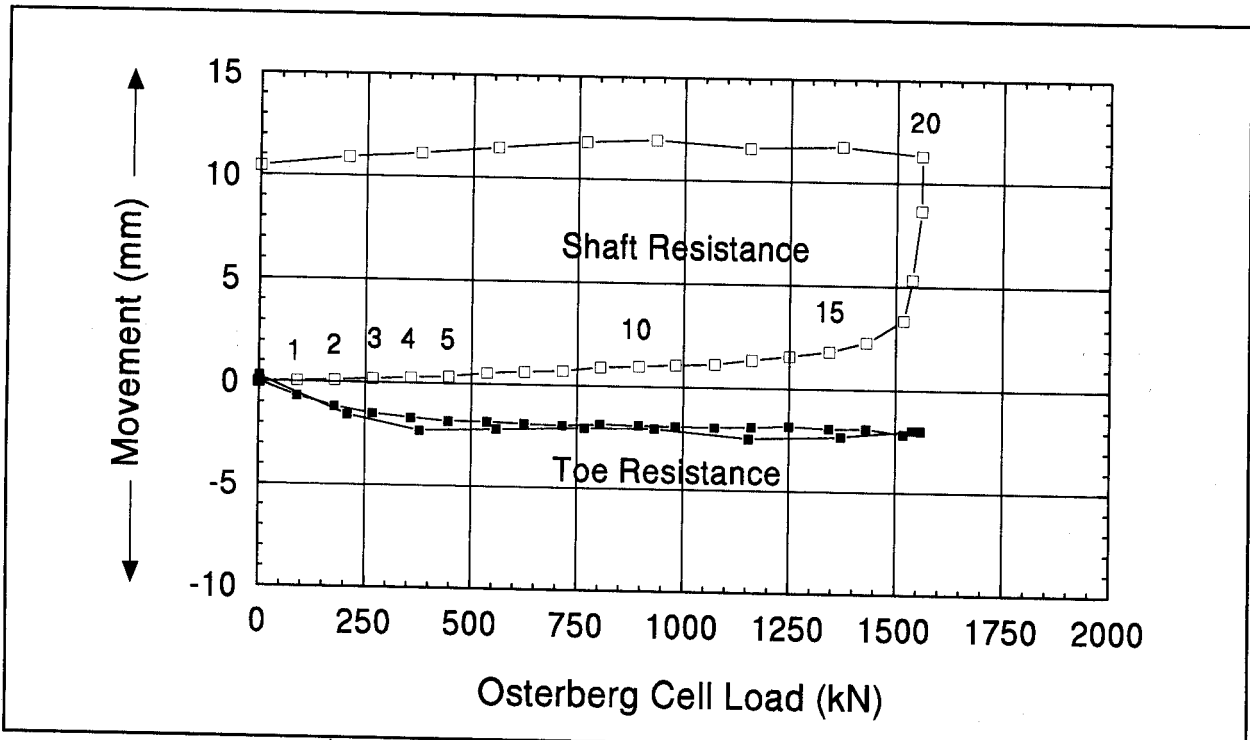


Figure 20.9 Test Results from Aucilla River Bridge, FL

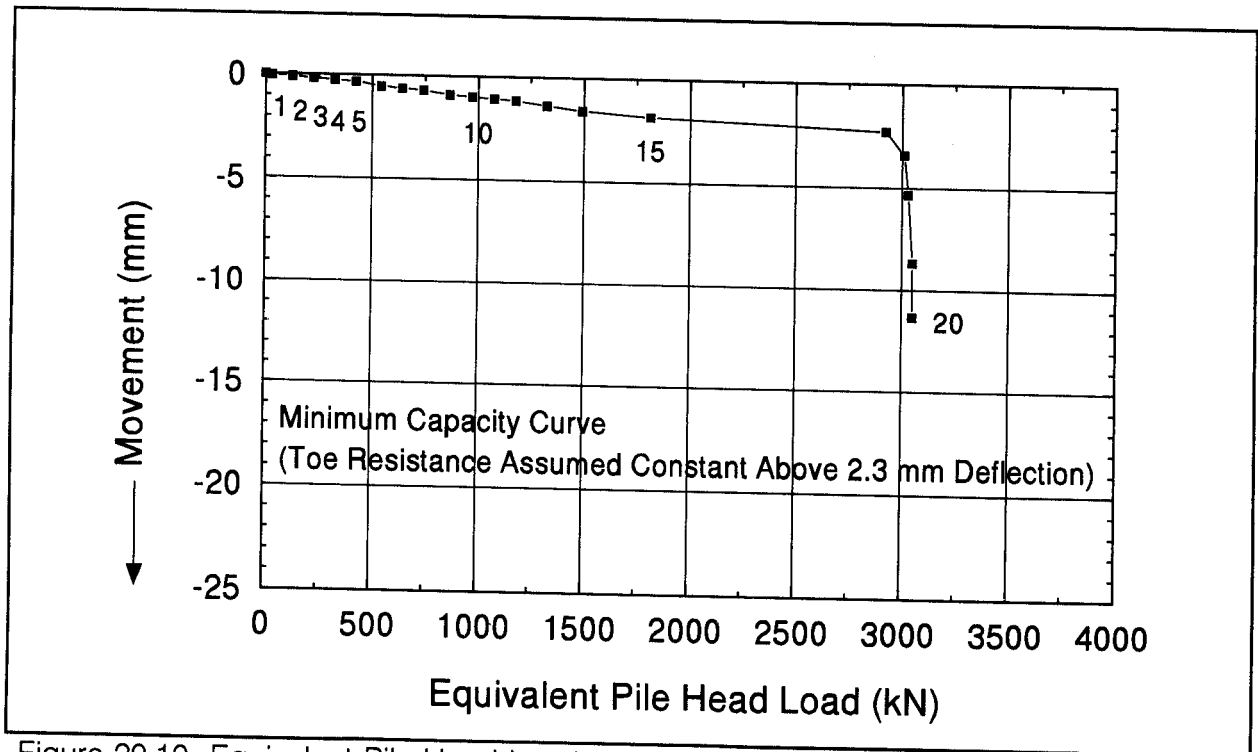


Figure 20.10 Equivalent Pile Head Load-Movement Curve from Aucilla River Bridge, FL

REFERENCES

- American Society for Testing and Materials [ASTM], (1994). Annual Book of Standards. ASTM D-1143, Standard Test Method for Piles Under Axial Compressive Load, Vol. 4.08, Philadelphia, PA.
- Goodwin, J.W. (1993). Bi-Directional Load Testing of Shafts to 6000 tons. Design and Performance of Deep Foundations: Piles and Piers in Soil and Soft Rock, ASCE, NY, NY, 204-217.
- Osterberg, J.O. (1984). A New Simplified Method for Load Testing Drilled Shafts. Foundation Drilling, ADSC, Dallas, TX, Vol. 23, No. 6, 9-11.
- Osterberg, J.O. (1994). Recent Advances in Load Testing Driven Piles and Drilled Shafts using the Osterberg Load Cell Method. Geotechnical Lecture Series, Geotechnical Division of the Illinois Section, ASCE, Chicago, IL.
- Osterberg, J.O. (1995). The Osterberg Cell for Load Testing Drilled Shafts and Driven Piles. Report No. FHWA-SA-94-035, U.S. Department of Transportation, Federal Highway Administration, Office of Technology Applications, Washington, D.C., 92.
- Schmertmann, J.H. (1993). The Bottom-up, Osterberg Cell Method for Static Testing of Shafts and Piles. Progress in Geotechnical Engineering Practice Proceedings, Hershey PA, Central Pennsylvania ASCE, Harrisburg, PA, 7.
- Thompson, D.E., Erikson, C.M. and Smith, J.E. (1989). Load Testing of Deep Foundations Using the Osterberg Cell. Proceedings of the 14th Annual Members Conference, Deep Foundations Institute, Sparta, NJ, 31-44.

21. THE STATNAMIC METHOD

A recent testing development for evaluation of driven pile capacity is the Statnamic testing method, Bermingham and Janes, (1989). The Statnamic test method uses solid fuel burned within a pressure chamber to rapidly accelerate upward the reaction mass positioned on the pile head. As the gas pressure increases, an upward force is exerted on the reaction mass, while an equal and opposite force pushes downward on the pile. Loading increases to a maximum and then unloads by a venting of the gas pressure. Built-in instrumentation (load cell, accelerometer, and laser sensor) measures load, acceleration and displacement. The Statnamic test method is not standardized by AASHTO or ASTM and is a proprietary method.

21.1 STATNAMIC BACKGROUND

The principles of Statnamic can be described by Newton's Laws of Motion:

1. A body will continue in a state of rest or uniform motion unless compelled to change by an external force.
2. A body subjected to an external force accelerates in the direction of the external force and the acceleration is proportional to the force magnitude ($F = ma$).
3. For every action there is an opposite and equal reaction ($F_{12} = -F_{21}$).

In the Statnamic test, a reaction mass is placed on top of the pile to be tested. The ignition and burning of the solid fuel creates a gas pressure force, F , that causes the reaction mass, m , to be propelled upward so that the acceleration amounts to about 20 g's ($F=ma$). An equivalent downward force is applied to the foundation element, ($F_{12} = -F_{21}$). The Statnamic concept is illustrated in Figure 21.1.

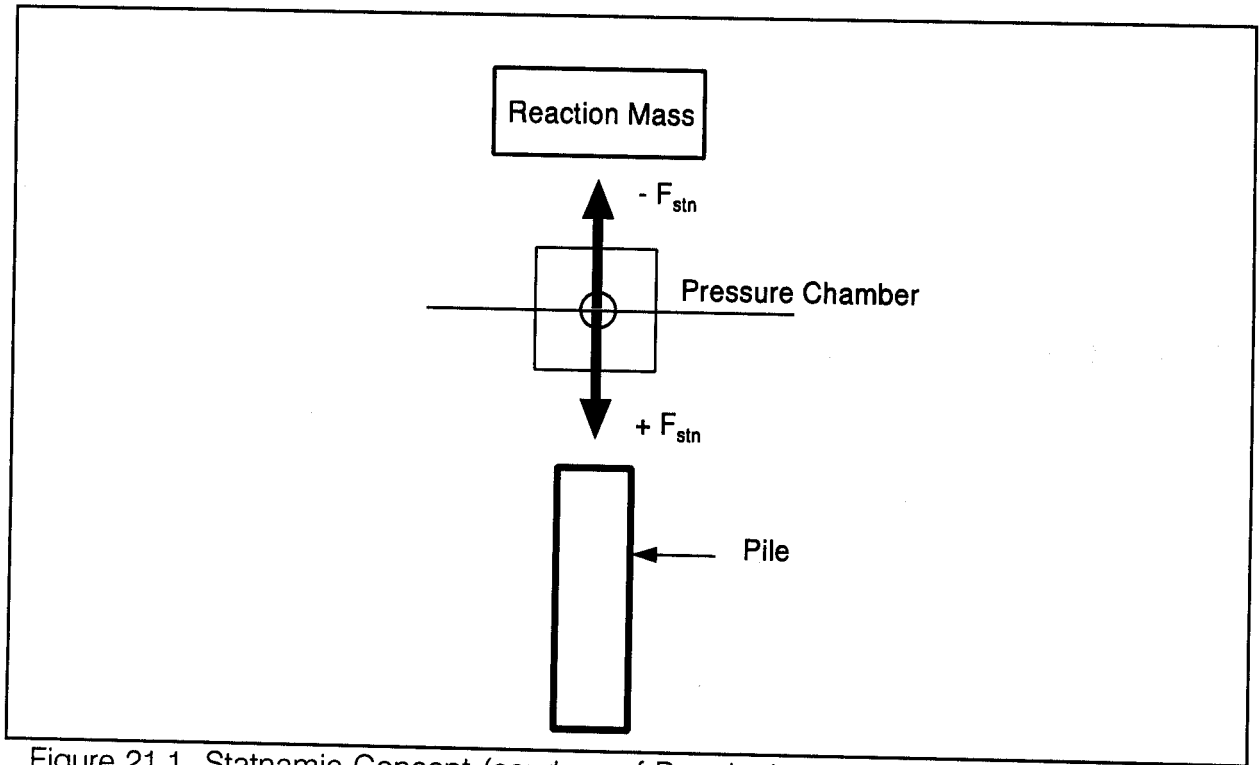


Figure 21.1 Statnamic Concept (courtesy of Berminghammer Foundation Equipment)

21.2 TEST EQUIPMENT

Development began in 1988 with a Statnamic device capable of a 100 kN test load. From 1988 through 1992, the test load capability was incrementally increased to 16,000 kN. In 1994, a 30,000 kN testing device was introduced.

The components of the Statnamic test equipment are shown in Figure 21.2 and a test in progress is shown in Figure 21.3. The base plate is attached to the pile head. The load cell, accelerometer, photo voltaic laser sensor, and piston base are positioned on top of the base plate. Next, the launching cylinder is placed on top of the piston base, thus enclosing the pressure chamber and propellant material. The reaction mass is then stacked on the launching cylinder and a retention structure is placed around the reaction mass. Finally, a sand or gravel backfill is placed in the annulus between the reaction mass and corrugated retention structure. After propellant ignition and reaction mass launch, the granular backfill slumps into the remaining void to cushion the reaction mass fall. Last, a remote laser reference source is positioned about 20 meters from the test apparatus.

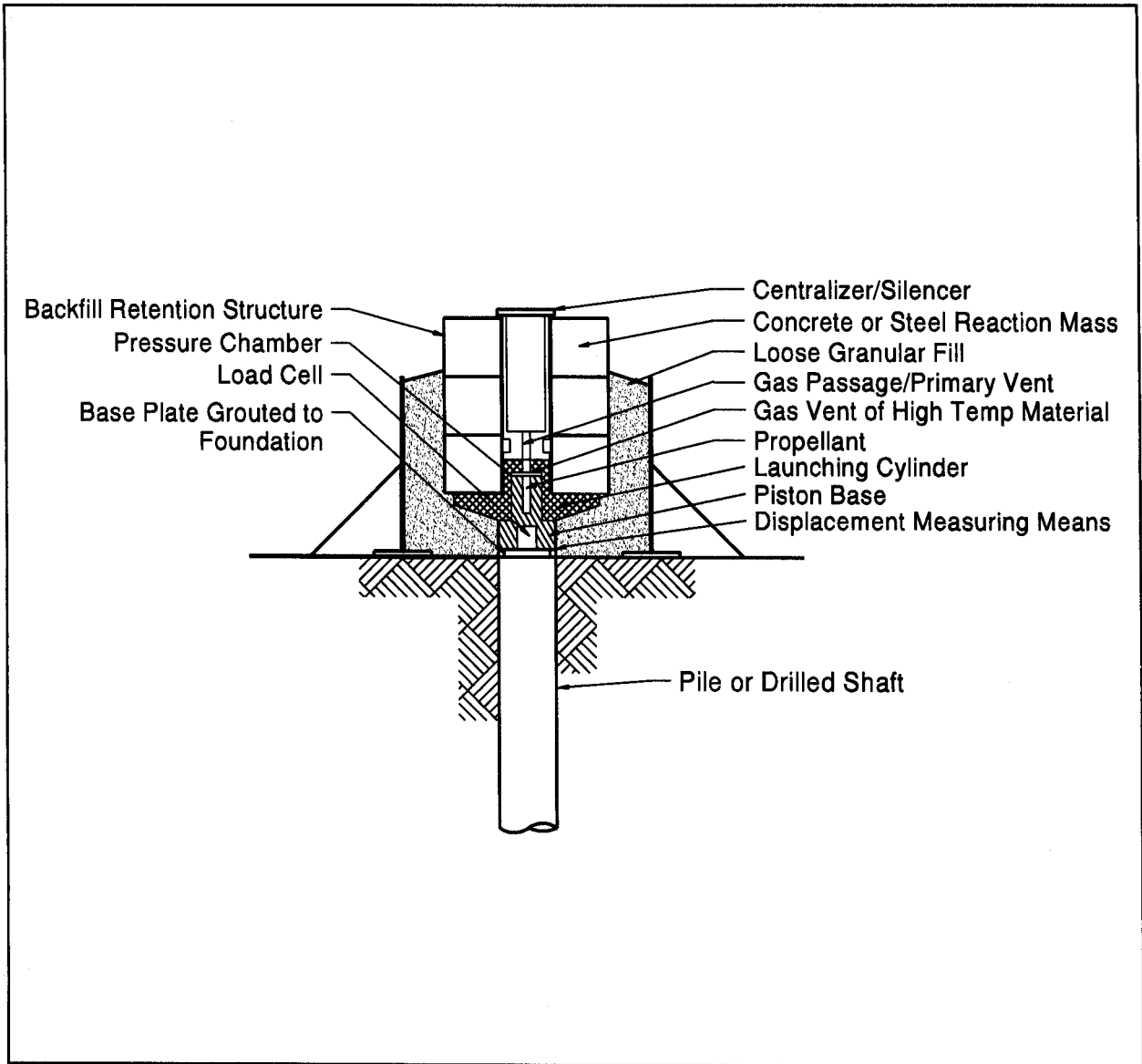


Figure 21.2 Schematic of Statnamic Loading System (after Bermingham and Janes, 1989)

The magnitude and duration of the applied load and the loading rate are controlled by the selection of piston and cylinder size, the fuel mass, the fuel type, the reaction mass, and the gas venting technique. The force applied to the pile is measured by the load cell. The acceleration of the pile head is monitored by the accelerometer and is integrated once to obtain pile head velocity and again to obtain displacement. Pile displacement relative to the reference laser source is measured with the photo voltaic laser sensor. Load and displacement data from the load cell and photo voltaic cell are

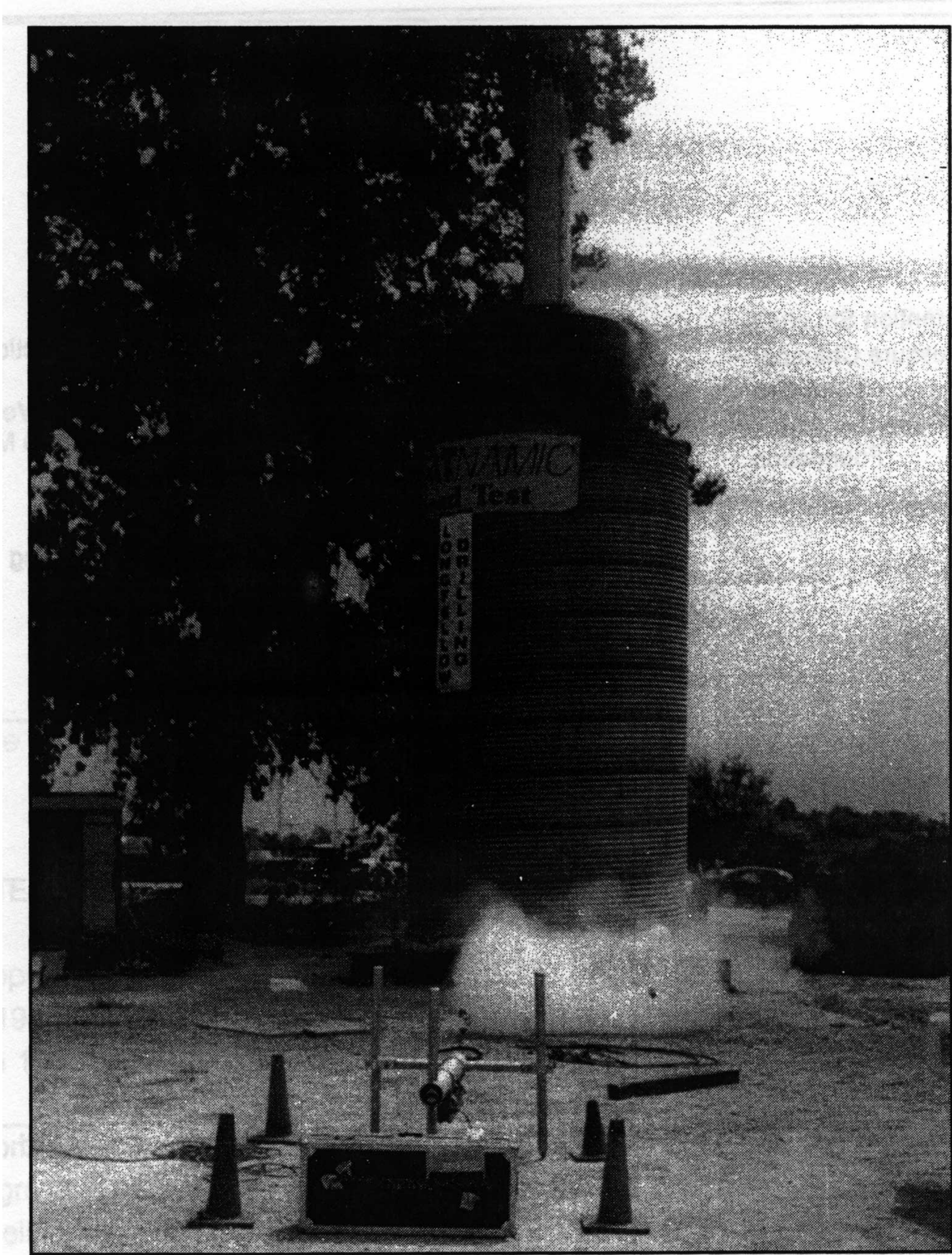


Figure 21.3 Statnamic Test in Progress

recorded, digitized, and displayed immediately in the field. Typical raw signals of the load and displacement records are given in Figure 21.4. These signals can then be converted into a raw load - displacement curve as given in Figure 21.5, which requires interpretation to derive the static pile capacity.

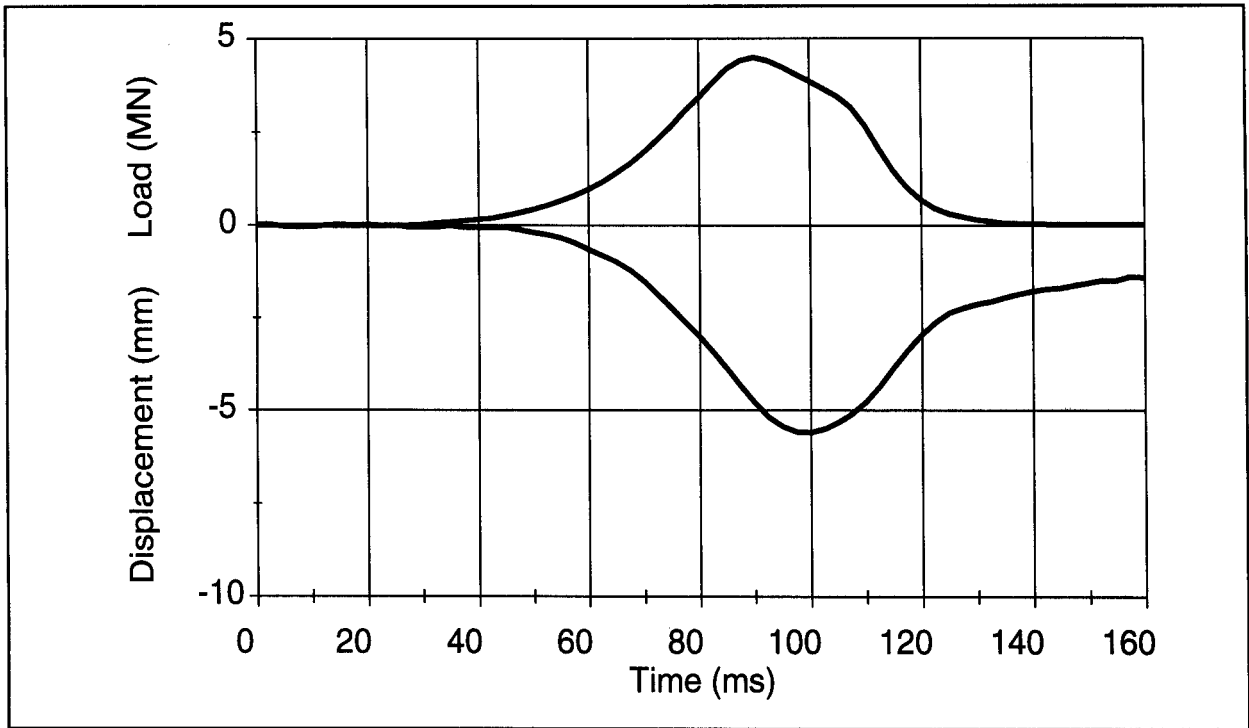


Figure 21.4 Measured Static Signals (courtesy of Berminghammer Foundation Equipment)

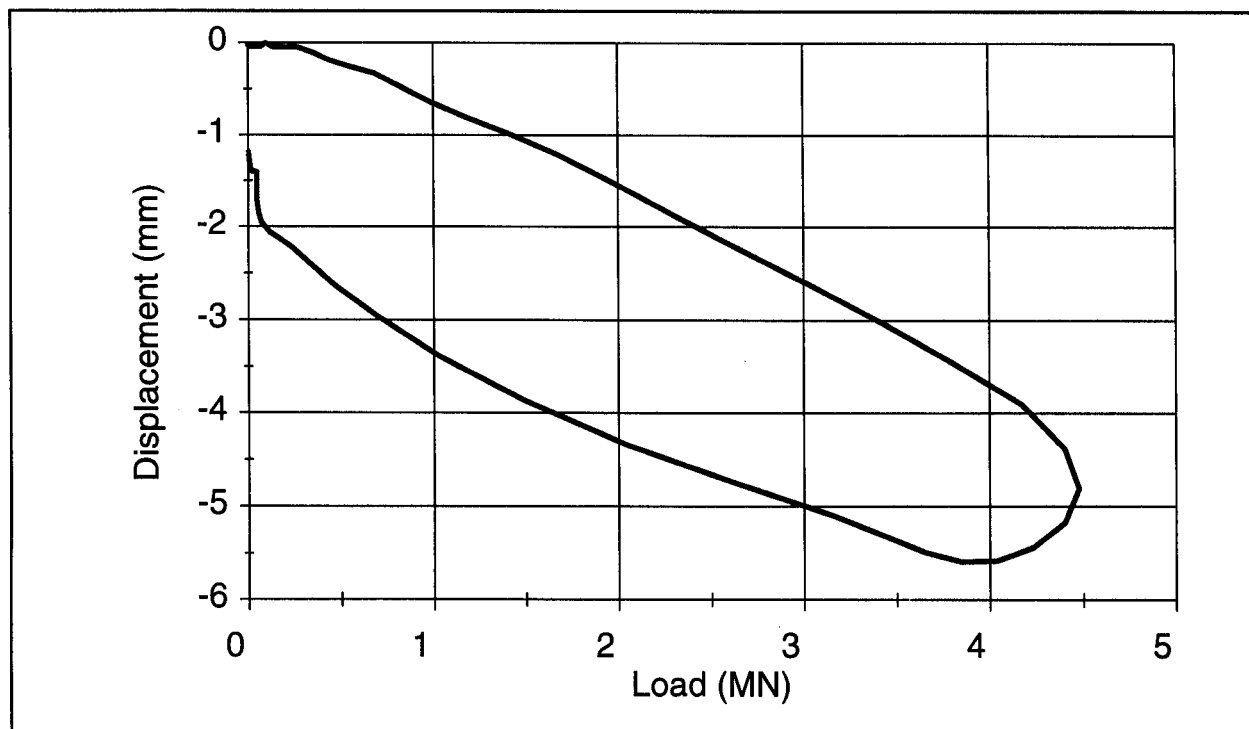


Figure 21.5 Load versus Displacement (courtesy of Berminghammer Foundation Equipment)

21.3 TEST INTERPRETATION

Initial correlations of Statnamic tests with static load tests for toe bearing piles founded in till and rock showed good agreement without adjustment of the Statnamic load - displacement results, Janes *et al.* (1991). However, later tests found that Statnamic can overpredict the ultimate pile capacity in some soils due to the dynamic loading effects. Middendorp *et al.* (1992) proposed an analysis procedure to adjust the raw Statnamic load - displacement results for dynamic loading rate effects, which is described below.

Because the duration of loading in a Statnamic test is about 100 ms, all elements of the pile move in the same direction and with almost the same velocity. According to the developers, this allows the pile to be treated as a rigid body undergoing translation. However, analytical studies by Brown (1995) have shown that this rigid body assumption can result in overpredictions of capacity and is not appropriate for long slender shafts or piles. The forces acting on the pile during a Statnamic test include the Statnamic induced load, F_{stn} , the pile inertia force, F_a , and the soil resistance forces which include the static soil resistance, F_u , the dynamic soil resistance, F_v , and the resistance from pore water pressure, F_p . A free body diagram of the forces acting on a pile during a Statnamic test is presented in Figure 21.6. The soil resistance forces shown in the free body diagram are distributed along the pile shaft as well as at the pile toe.

In mathematical terms, the force equilibrium on the pile may be described as follows:

$$F_{\text{stn}}(t) = F_a(t) + F_u(t) + F_v(t) + F_p(t)$$

This equation may be rewritten in terms of static soil resistance as follows:

$$F_u(t) = F_{\text{stn}}(t) - F_a(t) - F_v(t) - F_p(t)$$

A simplifying assumption is made that the pore water pressure resistance, F_p , can be treated as part of the damping resistance, F_v . This simplifies the above equation to:

$$F_u(t) = F_{\text{stn}}(t) - F_a(t) - F_v(t)$$

Consider the Statnamic load - displacement data presented in Figure 21.7, representative of a Statnamic load causing high dynamic loading effects. The Statnamic load - displacement data can be separated into five stages. Stage 1 includes the

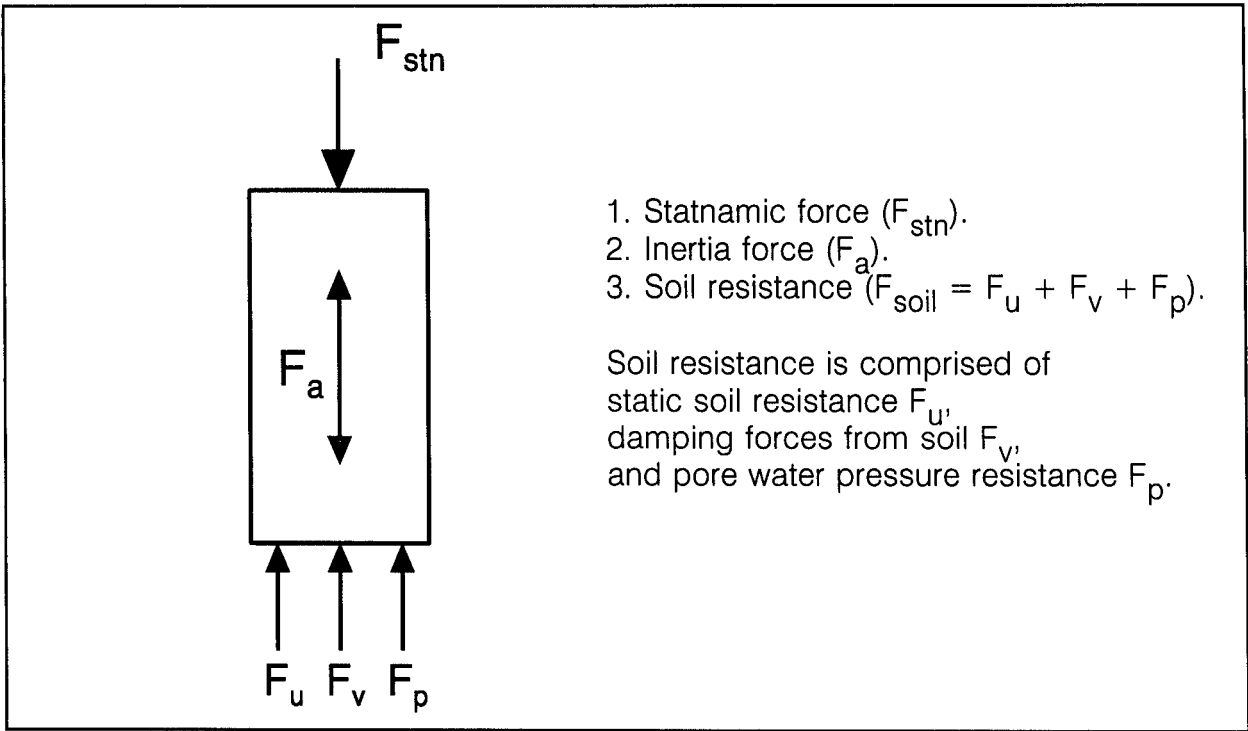


Figure 21.6 Free Body Diagram of Pile Forces in a Statnamic Test (after Middendorp *et al.* 1992)

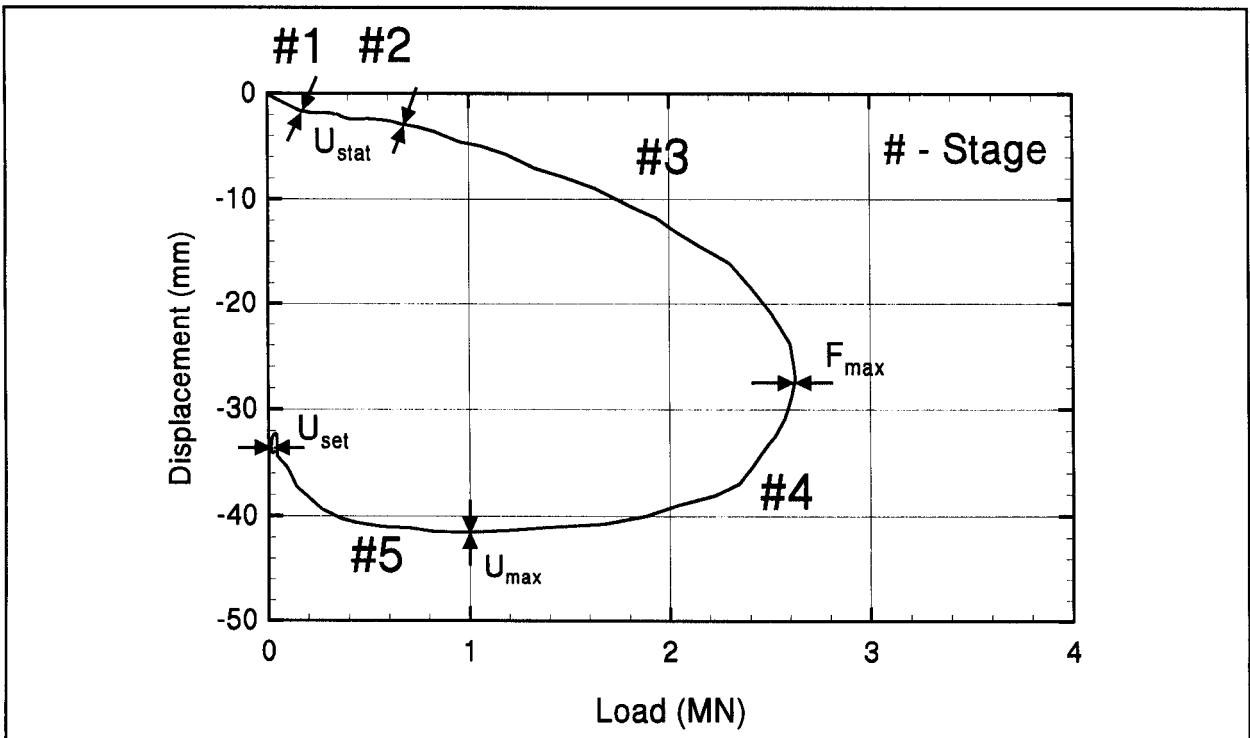


Figure 21.7 Five Stages of a Statnamic Test (after Middendorp *et al.* 1992)

assembling of the Statnamic piston and reaction mass and thus is a static loading phase. The reaction mass is launched and Stage 2 therefore provides the initial loading of the dynamic event. The soil resistance is treated as linearly elastic. Pile acceleration and velocity are small, resulting in low inertia and damping forces on the pile.

Stage 3 is the basic load application portion of the cycle with fuel burning and pressure in the combustion chamber. In Stage 3, significant nonlinear soil behavior occurs as the pile and soil experience high acceleration and velocity. Thus the highest inertia and damping forces are generated in this stage. The maximum Statnamic applied load is reached at the end of Stage 3.

In Stage 4 pressure in the combustion chamber is allowed to vent. Pile downward velocity and displacement continue but decrease throughout Stage 4. While the maximum Statnamic load is reached at the end of Stage 3, the maximum displacement occurs at the end of Stage 4. This is often due to the pile inertia force or significant dynamic resistance forces, $F_v(t)$ but may also occur in soils with strain softening (the residual soil resistance is significantly lower than the peak resistance). Since the pile velocity is zero at the point of maximum displacement, t_{umax} , the viscous damping, $F_v(t)$, on the pile is also zero at the end of Stage 4 and the static pile capacity may be expressed only at that time as:

$$F_u(t_{umax}) = F_{stn}(t_{umax}) - F_a(t_{umax})$$

In Stage 5, the soil rebounds from the loading event and to achieve final equilibrium the pile unloads and rebounds as load and movement cease. The displacement at the end of Stage 5 is the permanent displacement or set experienced under the test event.

The data processing system records the applied Statnamic load and pile head acceleration and displacement throughout the test. The ultimate static soil resistance, F_u , can then be calculated from the Statnamic load at the point of maximum displacement, $F_{stn}(t_{umax})$, minus the pile inertia force. This ultimate static soil resistance yields one point on the derived static load - displacement curve and may occur at a large displacement. If a limiting movement criterion such as described in Section 19.7.5 is used for load test interpretation, the ultimate pile capacity may be less than this ultimate static soil resistance.

To obtain the remaining points on the derived static load - displacement curve, the damping resistance, F_v , at other load - displacement points must be determined. Assuming all damping is viscous (e.g., linear), then the damping resistance force can be expressed in terms of a damping constant, C_4 , times the pile velocity at the corresponding time $v(t)$. The pile velocity is obtained by differentiating the measured pile head displacement.

If the maximum applied Statnamic load is greater than the ultimate pile capacity, then the soil resistance at the beginning of Stage 4 through the point of maximum displacement at the end of Stage 4 will be a constant and will be equal to $F_u(t_{max})$, assuming the soil is perfectly plastic and does not exhibit strain hardening. The damping constant, C_4 , may be calculated from the maximum Statnamic load at the beginning of Stage 4, t_4 . This may be expressed as:

$$C_4 = [F_{stn}(t_4) - F_u(t_{u_{max}}) - ma(t_4)] / v(t_4)$$

Assuming the damping constant, C_4 , is constant throughout the Statnamic loading event, the derived static load may be calculated at any point in time from:

$$F_u(t) = F_{stn}(t) - ma(t) - C_4v(t)$$

The derived Statnamic load - displacement curve is then constructed using the above equation and corresponding pile head displacement. An example of the derived load-displacement curve illustrating how the dynamic rate effects are subtracted from the new Statnamic results is presented in Figure 21.8.

21.4 APPLICATIONS

Statnamic tests for evaluation of static pile capacity have been performed on steel, concrete and timber piles. Individual piles or pile groups with a combined static and dynamic resistance less than 30,000 kN can be tested. Axial compressive capacity tests have been conducted on both vertical and battered piles. The test method has been used on land and over water.

Recently, the feasibility of using the Statnamic method to conduct lateral load test has begun to be explored, Berminghammer (1994). However, significant research work

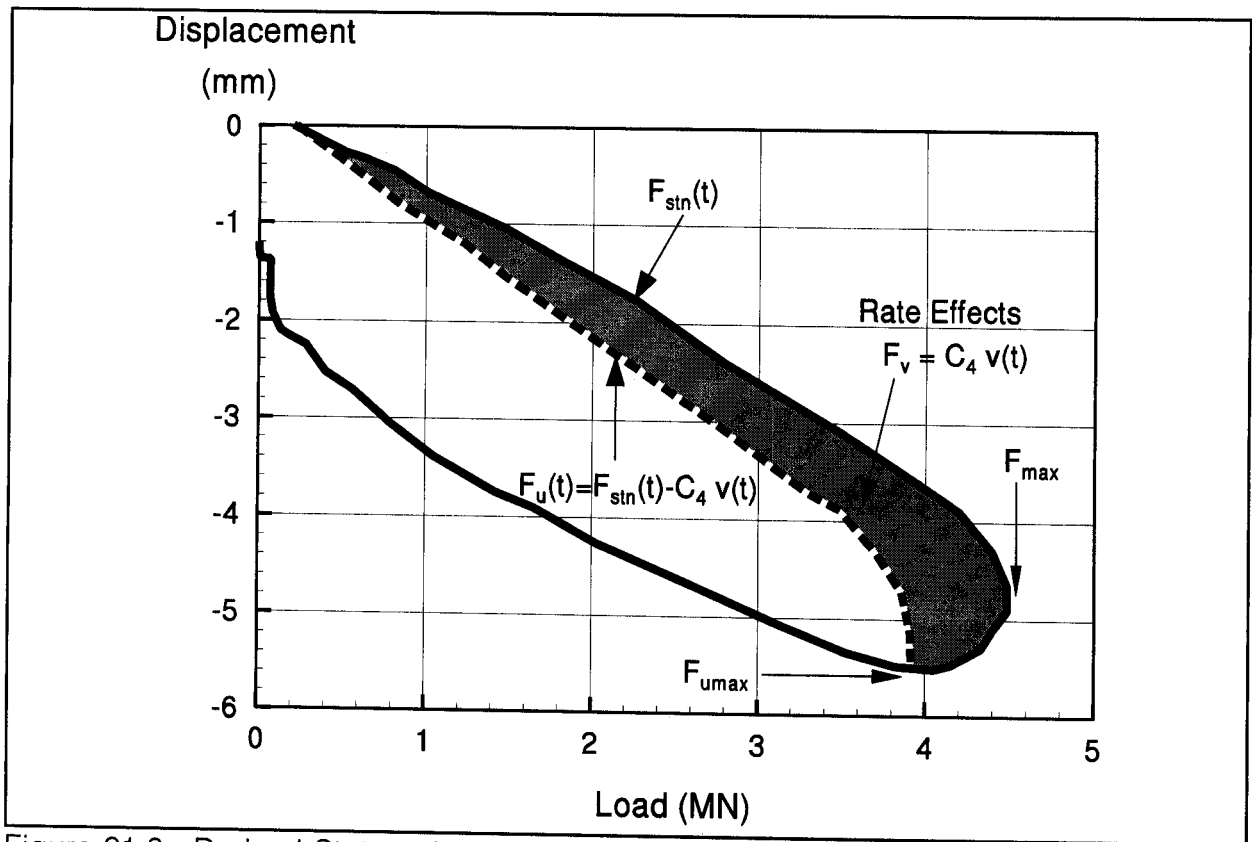


Figure 21.8 Derived Statnamic Load-Displacement Curve With Rate Effects (courtesy of Berminghammer Foundation Equipment)

remains to be done for this potential application. In September 1995, the FHWA granted partial funding to the Alabama DOT to conduct a series of lateral Statnamic tests to simulate vessel impact loading to further study this application. The Statnamic test for lateral load application is also being studied in the current NCHRP research project 24-09, Static and Dynamic Lateral Loading of Pile Groups. A lateral Statnamic test on a nine pile group is shown in Figure 21.9. The maximum lateral load applied to date in a Statnamic test is 7320 kN. However, this is not a limit of the Statnamic test device but rather of the pile group response.

21.5 CASE HISTORIES

Statnamic test results for two cases are presented with comparisons to static load test results. The first case involves an 18.6 meter long HP 310 x 110 H-pile driven through gravelly clay and into sandstone in Pittsburgh, Pennsylvania. As indicated in the results

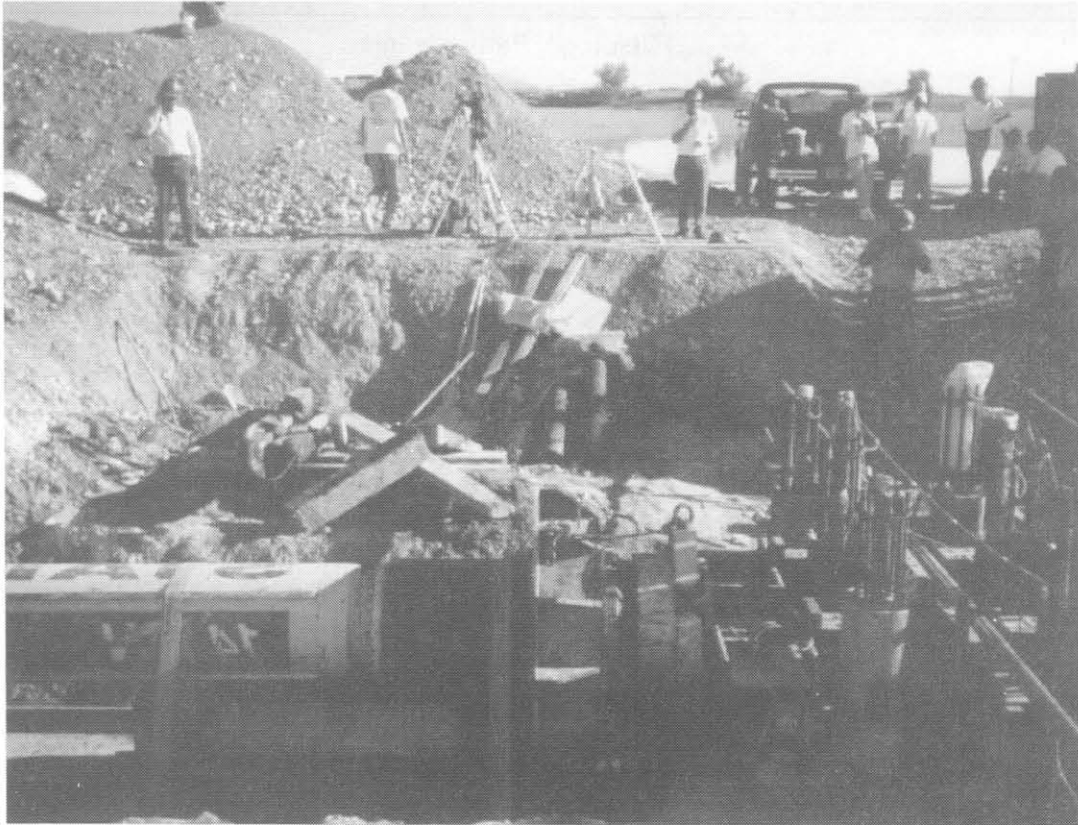


Figure 21.9 Lateral Static Test on Nine Pile Group (courtesy of Utah State University)

shown in Figure 21.10 the dynamic resistance appears low and the agreement between the maximum Statnamic load, the Statnamic unloading point, and the static load test maximum capacity appears to be good. It should be noted that the Statnamic and static test results are from piles nearby, but not the same piles. Unfortunately, neither the static test nor the Statnamic test loaded the pile to a traditional failure load based on the measured displacements and loads, and therefore the ultimate static load is not determined from either test method. Hence, this case is more of a comparison in load deflection behavior than a correlation case of ultimate pile capacity from the two test methods.

The second study presents a correlation case in which the soils have a significant dynamic resistance. This case was for the I-280 test program in San Francisco, California and involved a 406 mm diameter, 32.2 meter long, closed-ended pipe pile in very soft bay mud. Test results presented in Figure 21.11 illustrate that the maximum Statnamic load is 3.3 MN or 2.5 times greater than the maximum static load test

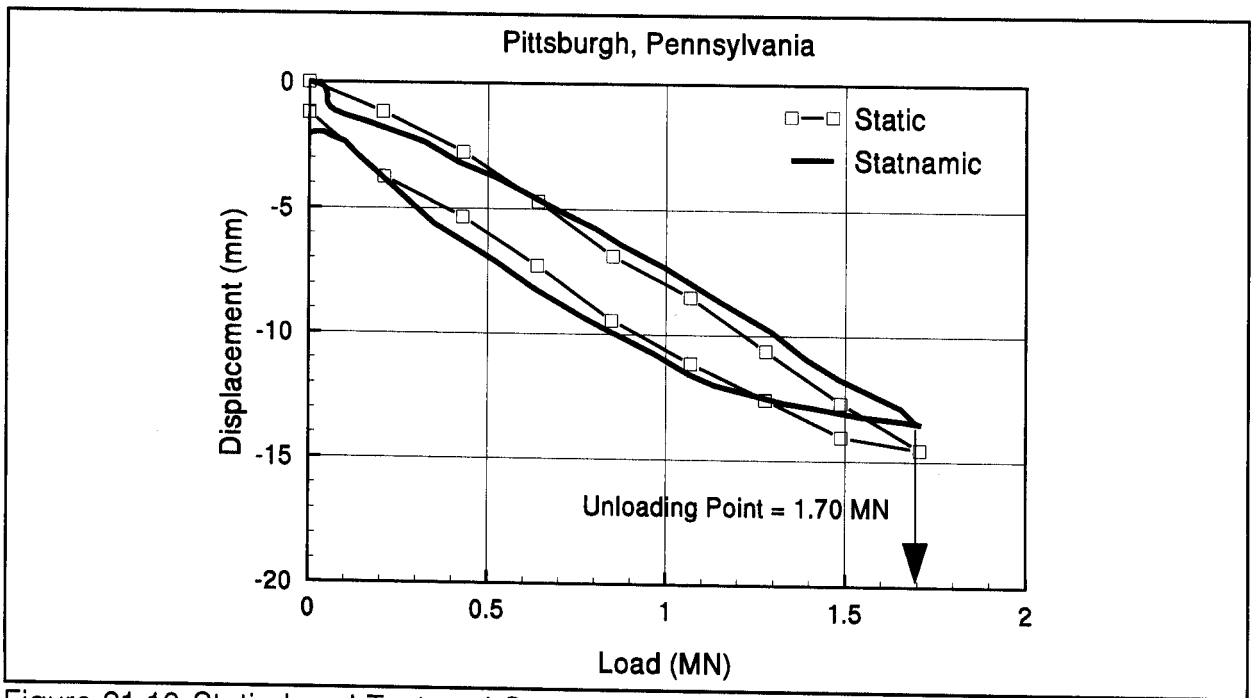


Figure 21.10 Static Load Test and Statnamic Comparison from Pittsburgh Site (courtesy of Berminghammer Foundation Equipment)

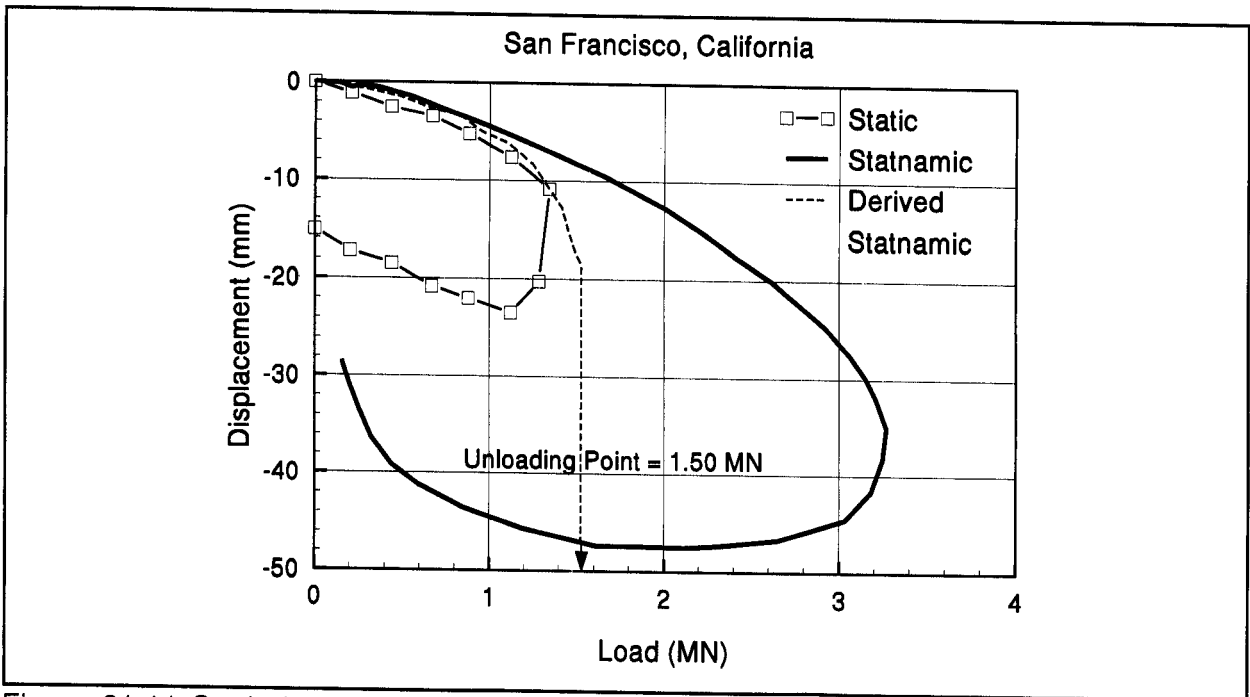


Figure 21.11 Static Load Test and Statnamic Comparison from San Francisco Site (courtesy of Berminghammer Foundation Equipment)

capacity of 1.3 MN. The maximum displacement occurs at a load of 2.1 MN or 1.6 times greater than the maximum static load capacity. The Statnamic capacity determined using the unloading point method is 1.5 MN or 1.15 times the reported ultimate static pile capacity. Additional information on this test may be found in Berkovitz and Hahn (1995).

21.6 ADVANTAGES

Advantages of Statnamic testing include lower cost, shorter test time, and mobility. Depending upon the magnitude of load, the site location, and labor costs, the cost of a Statnamic test is on the order of one quarter to one half the cost of an equivalent capacity static load test. Savings may increase for higher pile capacities or for multiple tests performed.

Once Statnamic is mobilized to a site, one or two tests can typically be performed in one day. The design of a segmental reaction mass allows assembly with relatively small hoisting equipment. In addition, since the reaction mass is typically 5 to 10 percent of the applied load, movement around a site for multiple tests is easier than for a static test using dead weight. Recent equipment advances include a hydraulic catch mechanism to replace the gravel retention structure. This mechanism, shown in Figure 21.12, permits a higher number of tests to be conducted per day.

Applied pile head load and displacement are measured by load cell and photo voltaic laser. The laser eliminates problems with measuring displacement from required reference beams during a static test, although the laser source can be sensitive to ground vibrations. The load, acceleration, and displacement readings are digitized 4000 samples per second.

The Statnamic method is a simple concept governed by Newtonian principles.

21.7 DISADVANTAGES

Some of the disadvantages of Statnamic testing may be attributed to its recent and continuing development. Correlations with conventional static tests are still being obtained and refinement of the analysis procedure is expected to continue. Both Janes

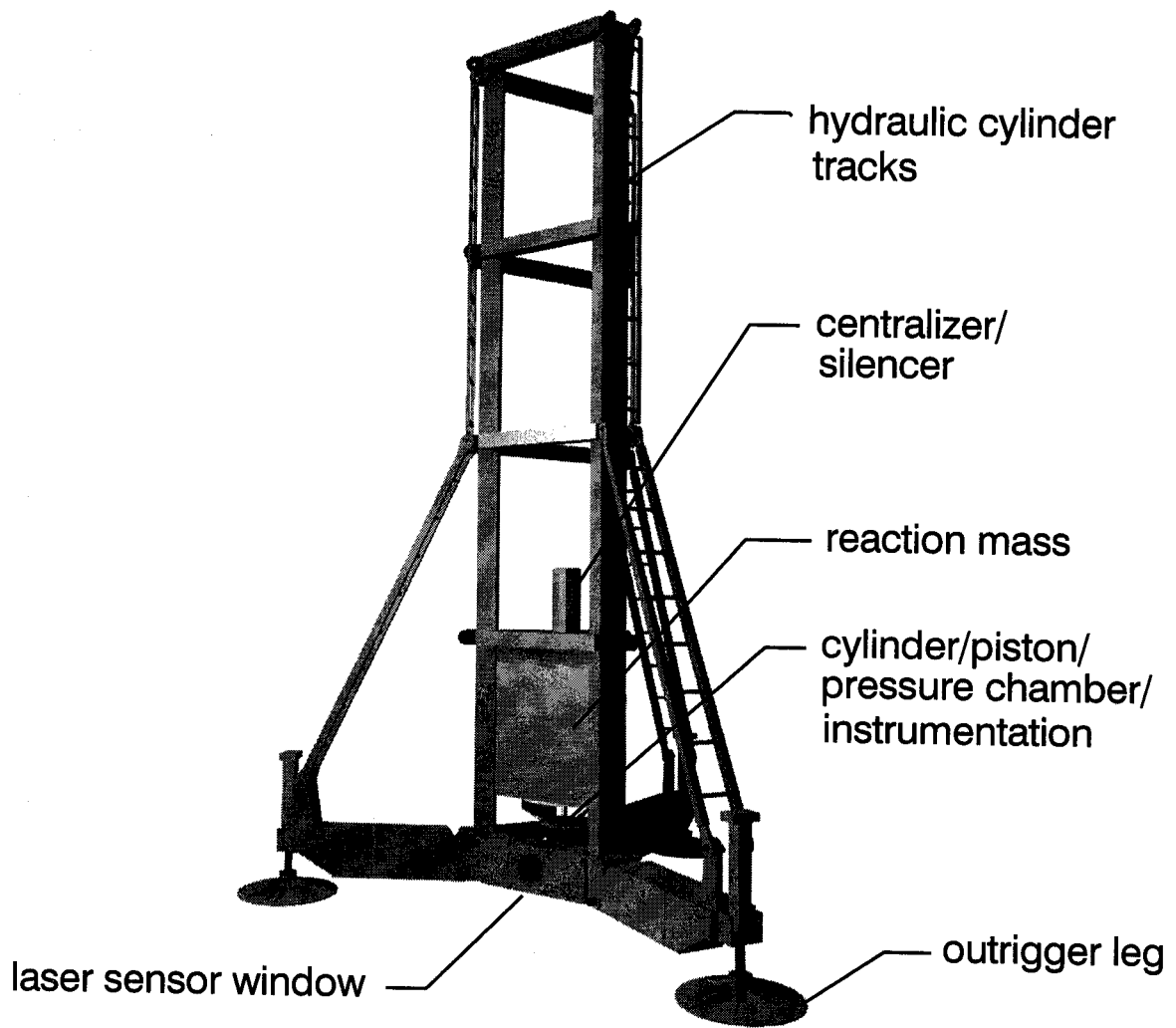


Figure 21.12 Statnamic Hydraulic Catch Mechanism (courtesy of Berminghammer Foundation Equipment)

et al (1994) and Brown (1995) have recommended additional Statnamic - static load testing correlations be obtained to enhance the data base and to improve interpretive procedures. In addition, the interpretation method is sufficiently complicated that it is difficult to independently check the proprietary result. The instrumentation is also complex and lacks the redundant checks available in conventional static or dynamic testing to verify the calibration accuracy.

Middendorp *et al.* (1992) noted that the 100 ms duration of loading is short enough that Statnamic is still a dynamic test. Hence, adjustment of the raw field results for dynamic phenomena is required. When proposing the current analysis method, Middendorp *et al.* (1992), suggested that the unloading point method allows direct calculation of the maximum static soil resistance when pore pressures play a minor role. He further concluded that a method to determine the pore pressure effect and make a correction for it in a Statnamic test has to be developed.

A subsequent Statnamic test reported by Matsumoto *et al.* (1994), instrumented with pore pressure transducers, measured Statnamic induced pore pressures near the pile toe on the order of 0.4 MPa for a pile founded in mudstone. This resulted in a reduction of the Statnamic unloading point capacity by about 4%.

To assure that the ultimate pile capacity has been achieved, a significant permanent pile set at the conclusion of a Statnamic test must be achieved. This often requires the applied Statnamic force to be larger than the combined ultimate static and dynamic soil resistances. If the Statnamic test does not cause soil failure and a significant permanent set, then an overprediction of static capacity may occur (Janes 1994). For example, if the Statnamic test in Figure 21.11 had only been loaded to 2.5 MN, a Statnamic load-displacement curve similar to the Statnamic result shown in Figure 21.8 would likely be obtained. This type of load-displacement result in this soil condition would make determination and subtraction of the dynamic rate effects difficult and increase the probability of static capacity overprediction. Additional discussion of Statnamic - load test correlations may be found in Brown (1994), Brown (1995) and Goble *et al.* (1995).

A summary of FHWA recent experience with Statnamic testing may be found in Berkovitz and Hahn (1995). Until the Statnamic interpretation procedures have been modified to fully account for inertia, damping and pore pressure effects, the FHWA recommends the Statnamic test be accompanied by a correlating static test.

REFERENCES

- Berkovitz, B.C., and Hahn, M. (1995). A Review of Statnamic Experiences for Transportation Applications. FHWA Regions 4 and 6 Design and Field Engineers Conference, 17.
- Bermingham, P. and Janes, M. (1989). An Innovative Approach to Load Testing of High Capacity Piles. Proceedings of the International Conference on Piling and Deep Foundations, Volume 1, J.B Burland and J.M. Mitchell Editors, A.A. Balkema Publishers, Rotterdam, 409-413.
- Bermingham Corporation, Ltd. (1994). Statnamic Newsletter, Volume 2, Number 1.
- Brown, D.A. (1994). Evaluation of Static Capacity of Deep Foundations from Statnamic Testing. ASTM, Geotechnical Testing Journal, GTJODJ, Vol. 17, No. 4, 403-414.
- Brown, D.A. (1995). Closure - Evaluation of Static Capacity of Deep Foundations from Statnamic Testing. ASTM, Geotechnical Testing Journal, GTJODJ, Vol. 18, No. 4, 495-498.
- Goble, G.G., Rausche, F. and Likins, G. (1995). Discussion of Evaluation of Static Capacity of Deep Foundations from Statnamic Testing. ASTM, Geotechnical Testing Journal, GTJODJ, Vol. 18, No. 4, 493-495.
- Janes, M., Sy, A. and Campanella, R.G. (1994). A Comparison of Statnamic and Static Load Tests on Steel Pipe Piles in the Fraser Delta. Deep Foundations. Proceedings of the 8th Annual Vancouver Geotechnical Society Symposium, Vancouver, 1-17.
- Janes, M., Bermingham, P. and Horvath, B. (1991). Pile Load Test Results Using the Statnamic Method. Proceedings of the 4th International Conference on Piling and Deep Foundations, Vol. 1, Deep Foundations Institute, Editor, A.A Balkema Publishers, Rotterdam, 481-489.
- Janes, M. (1995). Statnamic Load Testing of Bridge Pier Foundations in North America. Proceedings of the 31st First Symposium on Engineering Geology and Geotechnical Engineers, Utah State University, Logan, Utah.

Matsumoto, T., Tsuzuki, M. and Michi, Y. (1994). Comparative Study of Static Loading Test and Statnamic On a Steel Pipe Pile Driven in Soft Rock. Proceedings of the 5th International Conference and Exhibition on Piling and Deep Foundations, Deep Foundations Institute, Bruges, 5.3.1-5.3.7.

Middendorp, P., Bermingham, P. and Kuiper, B. (1992). Statnamic Load Testing of Foundation Piles. Proceedings of the 4th International Conference on the Application of Stress-Wave Theory to Piles, A.A. Balkema Publishers, Rotterdam, 581-588.

22. PILE DRIVING EQUIPMENT

The task of successfully installing piles involves selecting the most cost-effective equipment to drive each pile to its specified depth without damage in the least amount of time. The pile driving system is also used as a measuring instrument to evaluate driving resistance. Therefore, the challenge to both the engineer and the pile contractor becomes one of knowing, or learning about, the most suitable equipment for a given set of site conditions, and then confirming that the driving system is operating properly.

Figures 22.1 and 22.2 show the components of a typical driving system. The crane, leads, hammer and helmet are the primary components of any driving system. Followers and equipment for jetting, predrilling, and spudding, may be permitted under certain circumstances for successful pile driving. This chapter presents a basic description of each component of a driving system. For additional guidance, readers are referred to pile driving equipment manufacturer's and suppliers.

22.1 LEADS

The function of a set of leads is to maintain alignment of the hammer-pile system so that a truly concentric blow is delivered to the pile for each impact. Figures 22.1 through 22.4 show several lead systems used for pile driving. Figure 22.5 shows various lead types. The box lead is the most versatile lead and its use allows all the configurations shown in Figures 22.1 through 22.4.

Swinging leads, illustrated in Figure 22.1, are widely used because of their simplicity, lightness and low cost. The most common arrangement is shown in Figure 22.1(b) where the lead and hammer are held by separate crane lines. The leads can also be hung from the boom with hanger straps as illustrated in Figure 22.1(a) with the hammer held by a crane line. Swinging leads are free to rotate sufficiently to align the hammer and the head of the pile without precise alignment of the crane with the pile head. Because the weight of the leads is low, this type of lead generally permits the largest crane operating radius, providing more site coverage from one crane position.

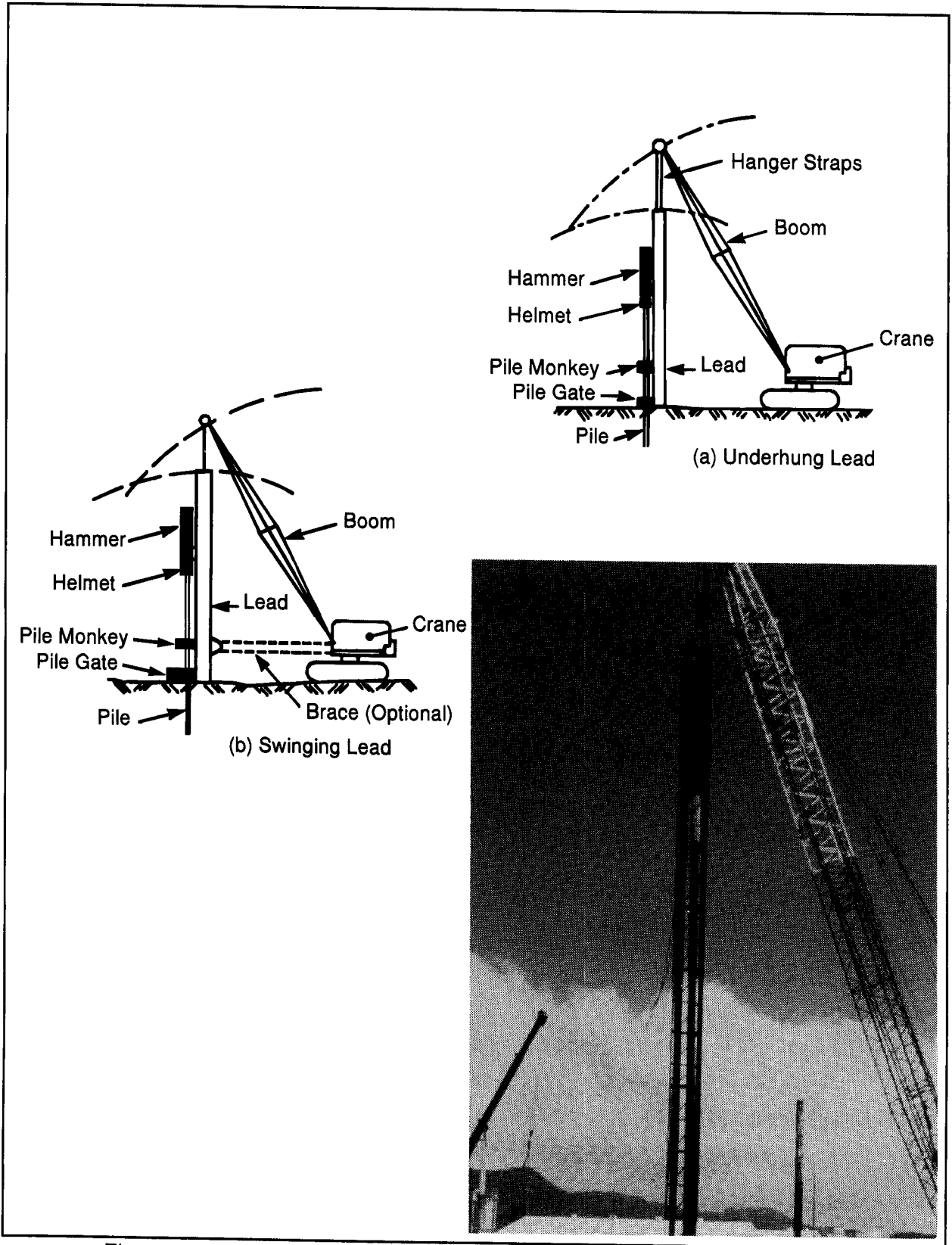
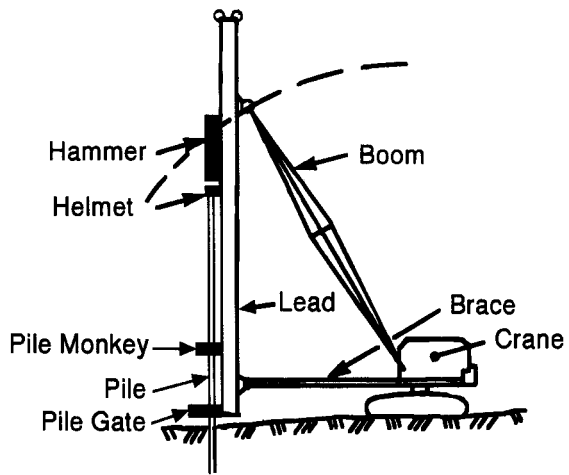
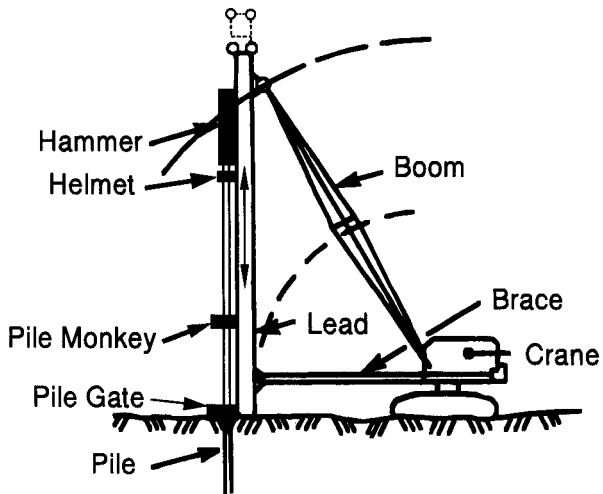


Figure 22.1 Swinging Lead Systems (after D.F.I. Publication, 1981)



(a) Fixed or Extended with Brace



(b) Semifixed or Vertical Travel with Brace

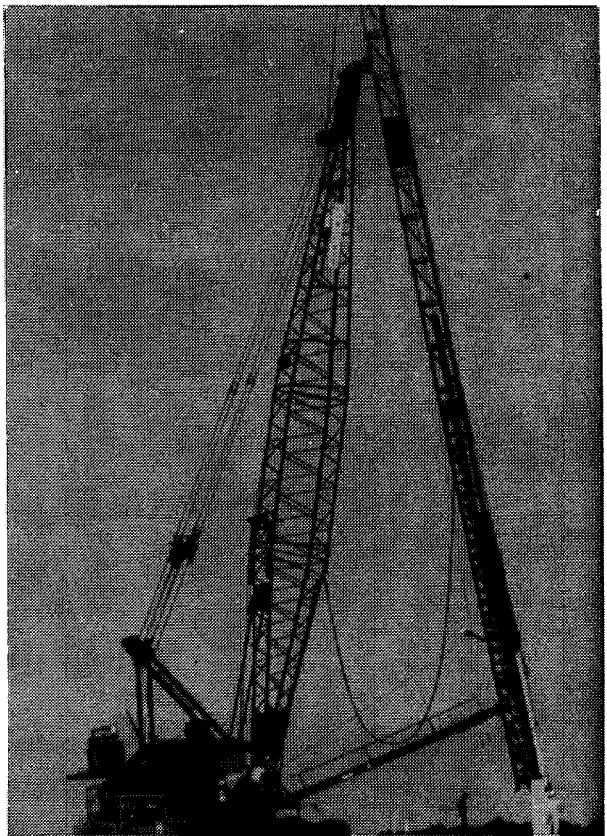
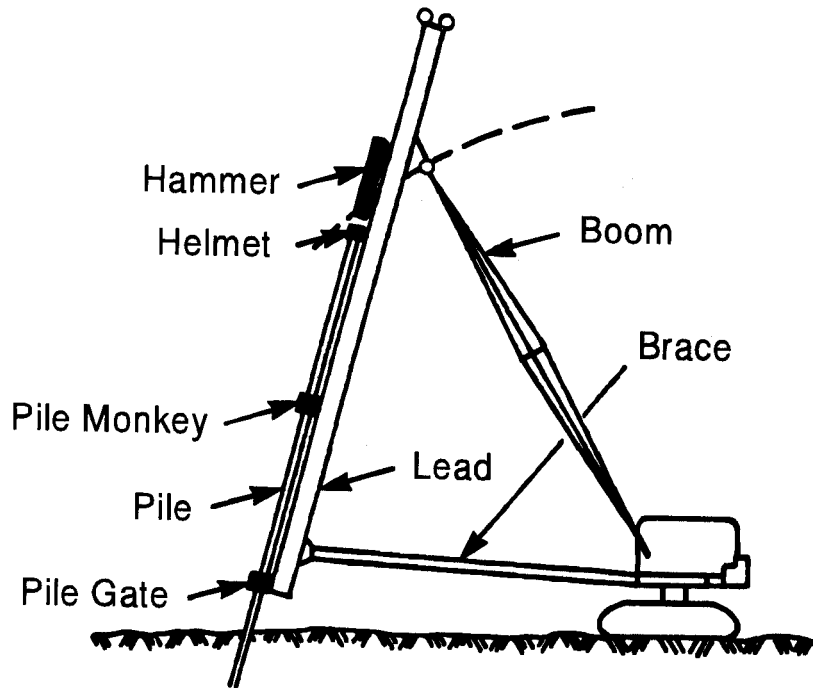
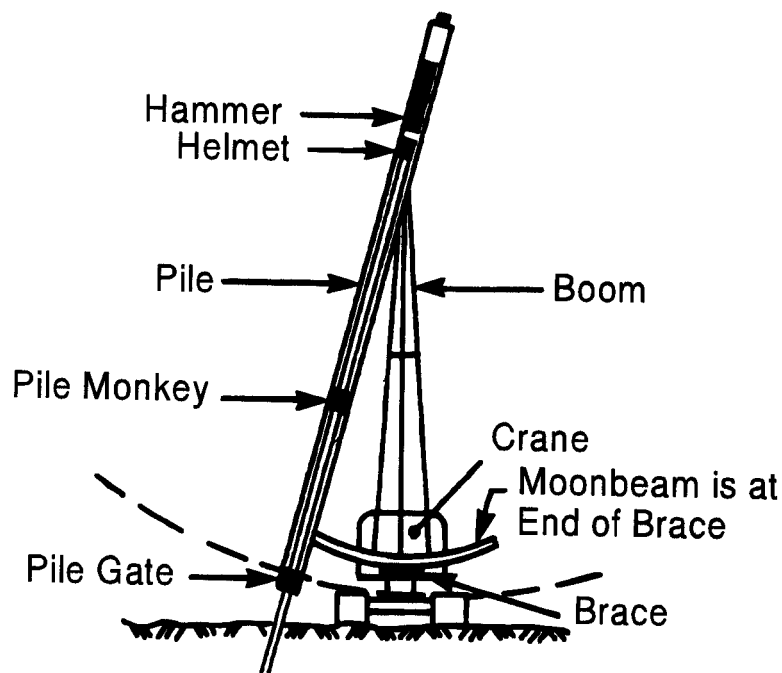


Figure 22.2 Fixed Lead Systems (after D.F.I. Publication, 1981)

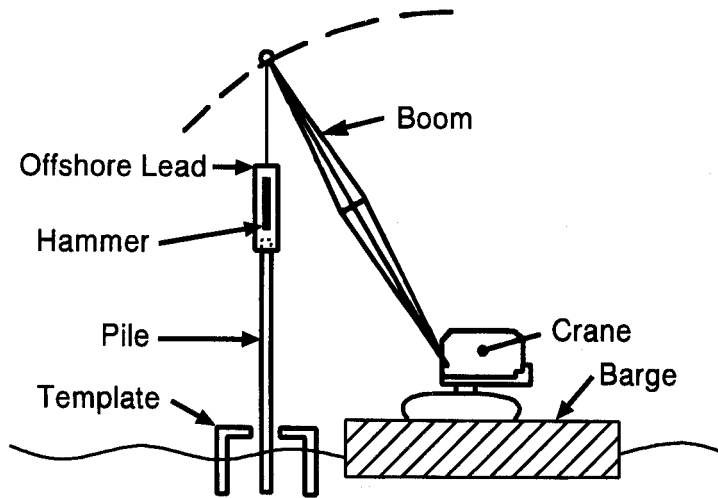


(a) Fore (Positive) Batter



(b) Side Batter by Moonbeam

Figure 22.3 Lead Configurations for Batter Piles (after D.F.I. Publication, 1981)



(a) Fixed or Extended with Brace

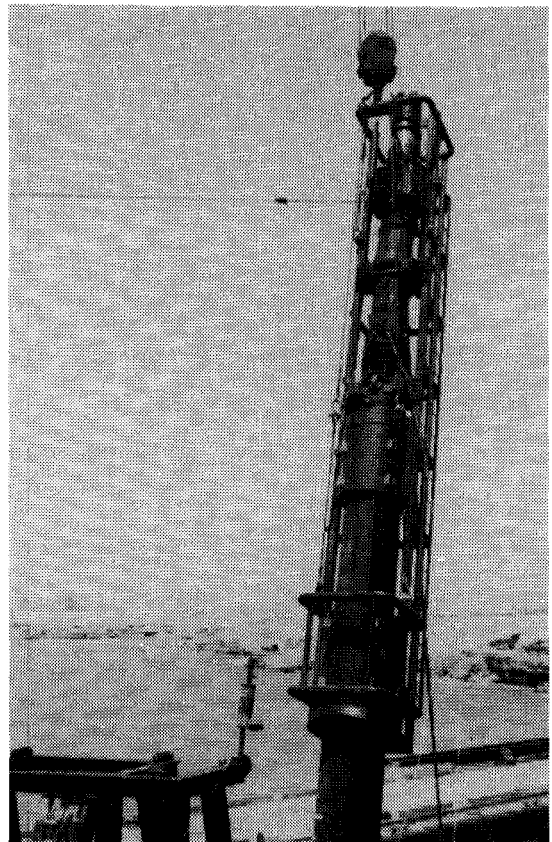


Figure 22.4 Typical Offshore Lead Configuration

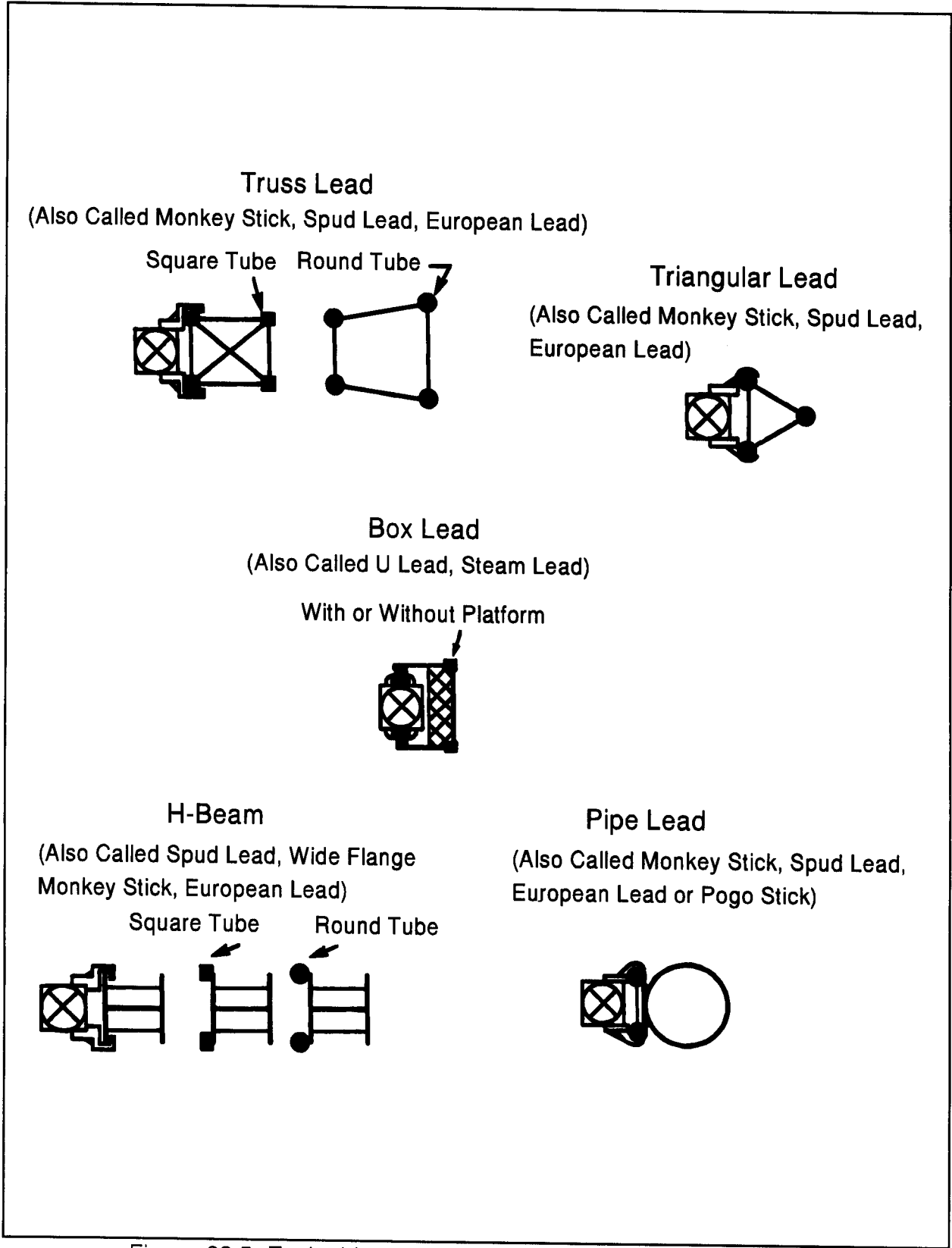


Figure 22.5 Typical Lead Types (after D.F.I. Publication, 1981)

Standard fixed leads shown in Figure 22.2 are slung from the boom point with a brace running from the bottom of the leads to the crane cab frame. A schematic of a typical fixed lead system is depicted in Figure 22.2(a). A variation of a fixed lead system is a semi-fixed or vertical travel lead as shown in Figure 22.2(b). The semi-fixed lead allows vertical lead movement at the lead connection points to the boom and brace which the standard fixed lead system does not. Figure 22.3(a) illustrates that a fixed lead is limited to plumb piles or batter piles in line with the leads and crane boom. To drive side batter piles, a moonbeam must be attached at the end of the brace as depicted in Figure 22.3(b). A fixed lead attempts to hold the pile in true alignment while driving but may require more set up time.

Offshore leads shown in Figure 22.4 are similar to swinging leads in that they are free to rotate sufficiently to align the hammer and head of the pile without precise alignment of the crane with the pile head. They generally consist of a short lead section of sufficient length to hold the hammer and axially align the hammer with the pile head. Offshore leads are used with a template that holds the pile in place.

Pile driving specifications have historically penalized or prohibited swinging leads. This general attitude is not justified based on currently available equipment. In fact, there are many cases where swinging leads are more desirable than fixed leads. For example, swinging leads are preferable for pile installation in excavations or over water. The function of a lead is to hold the pile in good alignment with the driving system in order to prevent damage, and to hold the pile in its proper position for driving. If a swinging lead is long enough so that the bottom is firmly embedded in the ground, and if the bottom of the lead is equipped with a gate, then bottom alignment of the pile will be maintained. In this situation, if the pile begins to move out of position during driving, it must move the bottom of the lead with it. Swinging leads should be of sufficient length so that the free line between the boom tip and the top of the leads is short, thus holding the top of the lead in good alignment. When batter piles are driven, pile alignment is more difficult to set with swinging leads. This problem is accentuated for diesel hammers since the hammer starting operation will tend to pull the pile out of line.

Regardless of lead type chosen, the pile must be kept in good alignment with the hammer to avoid eccentric impacts which could cause local stress concentrations and pile damage. The hammer and helmet, centered in the leads and on the pile head, keep the pile head in alignment. A pile gate at the bottom of the leads should be used to keep the lower portion of the pile centered in the leads.

22.2 TEMPLATES

Templates are required to hold piles in proper position and alignment when an offshore type or swinging lead system is used over water. The top of the template should be located within 1.5 m of the pile cutoff elevation or the water elevation, whichever is lower. The preferred elevation of the template is at or below the pile cutoff elevation so that final driving can occur without stopping for template removal. A photograph of a typical template is presented in Figure 22.6.

When positioning templates that include batter piles, it must be remembered that the correct template position of batter piles will vary depending upon the template elevation relative to the pile cutoff elevation. For example, consider a template located 1.5 meters above pile cutoff elevation. If the plan pile locations at cutoff are used at the template elevation, a 1H:4V batter pile would be 375 mm out of location at the pile cutoff elevation. This problem is illustrated in Figure 22.7. Template construction should also allow the pile to pass freely through the template without binding. Templates with rollers are preferable, particularly for batter piles.

22.3 HELMETS

Figure 22.8 shows the components of a typical helmet (also called a drive cap) and the nomenclature used for these components. The helmet configuration and size used depends upon the lead type, pile type and the type of hammer used for driving. Details on the proper helmet for a particular hammer can be obtained from hammer manufacturers, suppliers and contractors. To avoid the transmission of torsion or bending forces, the helmet should fit loosely, but not so loosely as to prevent the proper alignment of hammer and pile. Helmets should be approximately 2 to 5 mm larger than the pile diameter. Proper hammer-pile alignment is particularly critical for precast concrete piles. Figure 22.9 shows a helmet for a steel H-pile.

Most hammers use a hammer cushion between the hammer and the helmet to relieve the impact shock, thus protecting the pile hammer. However, some hammer models exist that do not require a hammer cushion, or utilize a direct drive option where the hammer cushion is replaced by a steel striker plate. Ineffective hammer cushions in hammers requiring a cushion can cause damage to hammer striking parts, anvil, helmet or pile. All cushion materials become compressed and stiffen as additional hammer impacts are applied. Therefore, hammer cushions eventually become ineffective, or may

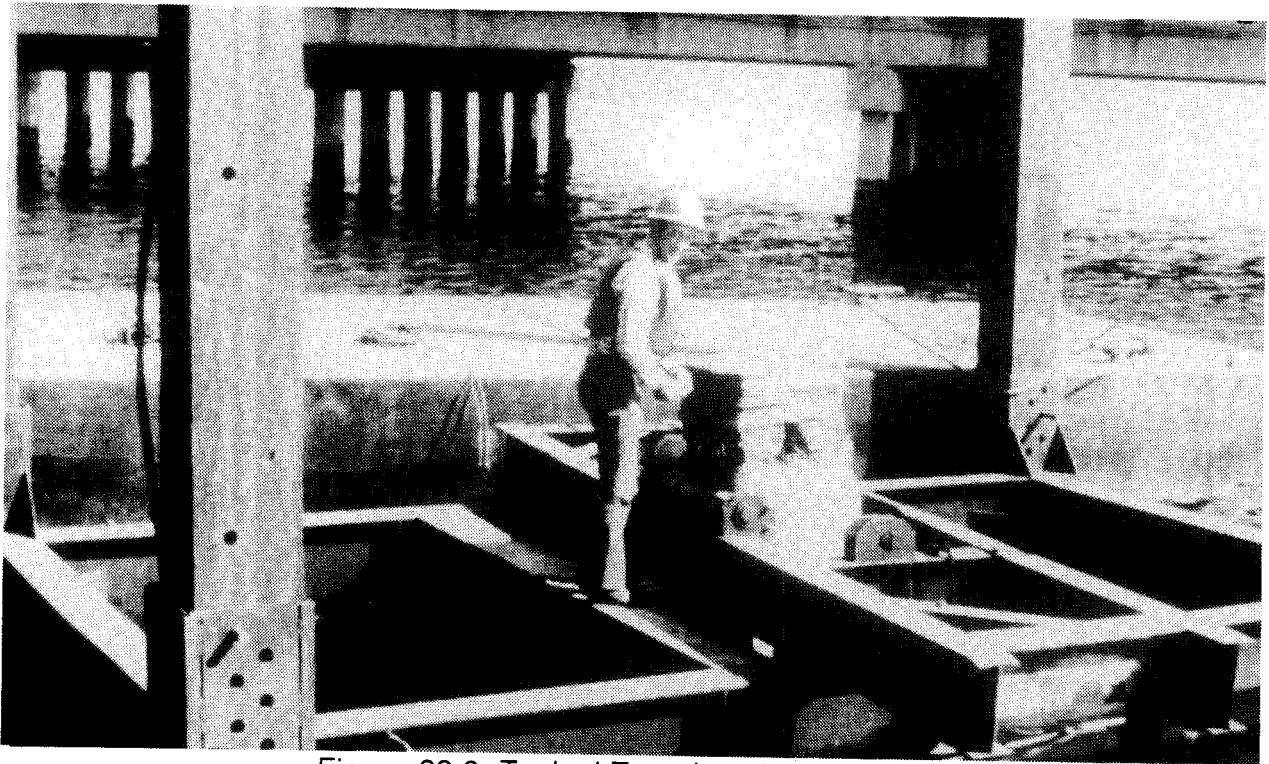


Figure 22.6 Typical Template Arrangement

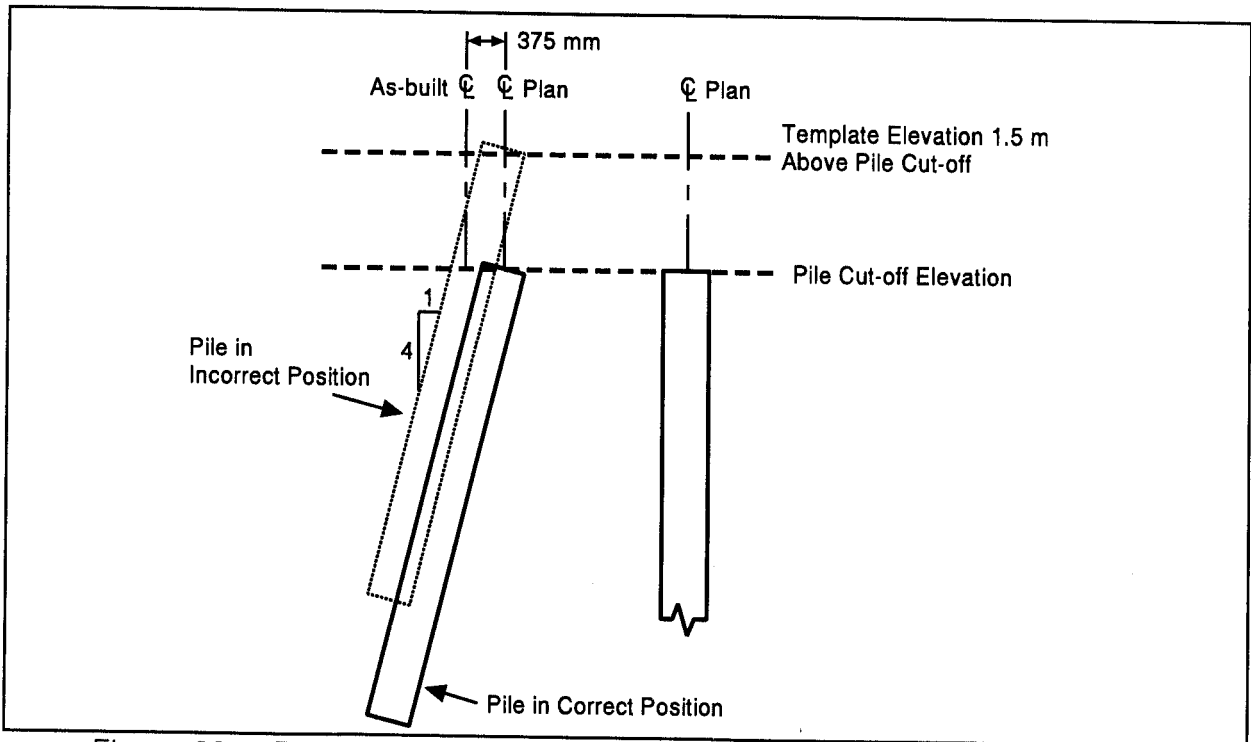


Figure 22.7 Template Elevation Effects on Batter Piles (after Passe 1994)

result in significant reduction in transferred energy or increased bending stress. Hammer cushion materials are usually proprietary man-made materials such as micarta, nylon, urethane or other polymers. In the past, a commonly used hammer cushion was made of hardwood (one piece), approximately 150 mm thick, with the wood grain parallel to the pile axis. This type of cushioning has the disadvantage of quickly becoming crushed and burned as well as having variable elastic properties during driving. With the widespread availability of manufactured hammer cushion materials, hardwood hammer cushions are no longer recommended.

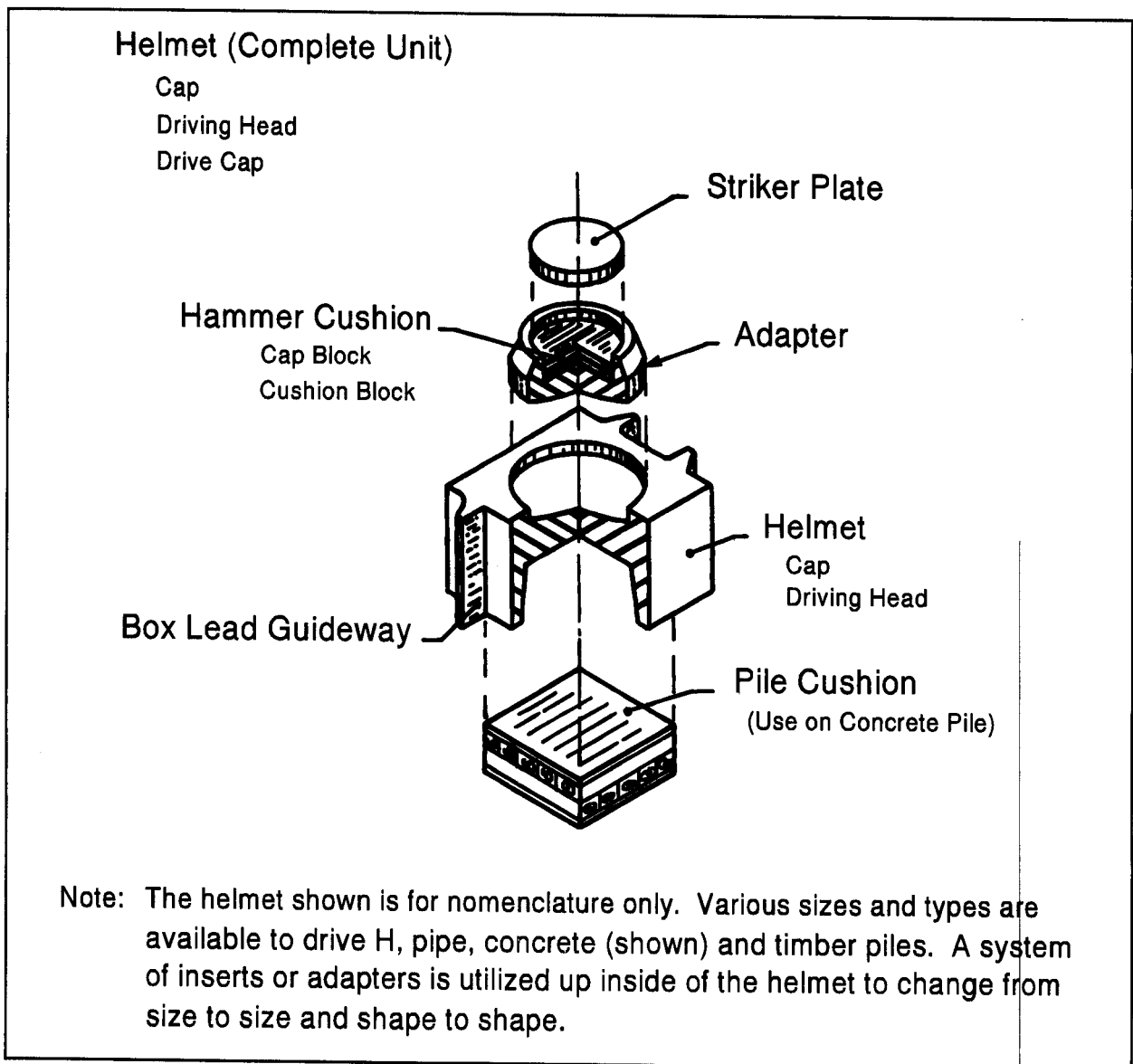


Figure 22.8 Helmet Components (after D.F.I. Publication, 1981)

The proprietary man-made hammer cushion materials have better energy transmission characteristics than a hardwood block, maintain more nearly constant elastic properties, and have a relatively long life. Their use results in more consistent transmission of hammer energy to the pile and more uniform driving. Since laminated cushioning materials have a long life, up to 200 hours of pile driving for some materials, it is often sufficient to inspect the cushion material only once before the driving operation begins for smaller projects. Periodic inspections of hammer cushion wear and thickness should be performed on larger projects. Many hammers require a specific cushion thickness for proper hammer timing. In these hammers, improper cushion thickness will result in poor hammer performance. Some man-made hammer cushions are laminated, such as aluminum and micarta, for example. The aluminum is used to transfer the heat generated during impact out of the cushion, thus prolonging its useful life. Hammer cushions consisting of small pieces of wood, coils or chunks of wire rope, or other highly elastic material should not be permitted. Cushion materials containing asbestos are not acceptable because of health hazards.



Figure 22.9 Helmet on H-pile

22.4 PILE CUSHIONS

To avoid damage to the head of a concrete pile as a result of direct impact from the helmet, a pile cushion should be placed between the helmet and the pile head. Typical pile cushions are made of compressible material such as plywood, hardwood, plywood and hardwood composites or other man made materials. Wood pile cushions should have a minimum thickness of 100 mm. Pile cushions should be checked periodically for damage and replaced before excessive compression or charring takes place. After replacing a cushion during driving, the blow count from the first 100 blows should not be used for pile acceptance as the cushion is still rapidly absorbing energy. The blow count will only be reliable after 100 blows of full energy application. The total number of blows which can be applied to a wood cushion is generally between 1000 and 2000. For wood pile cushions, it is recommended that a new, dry cushion be used for each pile. Old or water soaked cushions do not have good energy transfer, and will often deteriorate quickly. A photograph of a typical plywood pile cushion is presented in Figure 22.10.

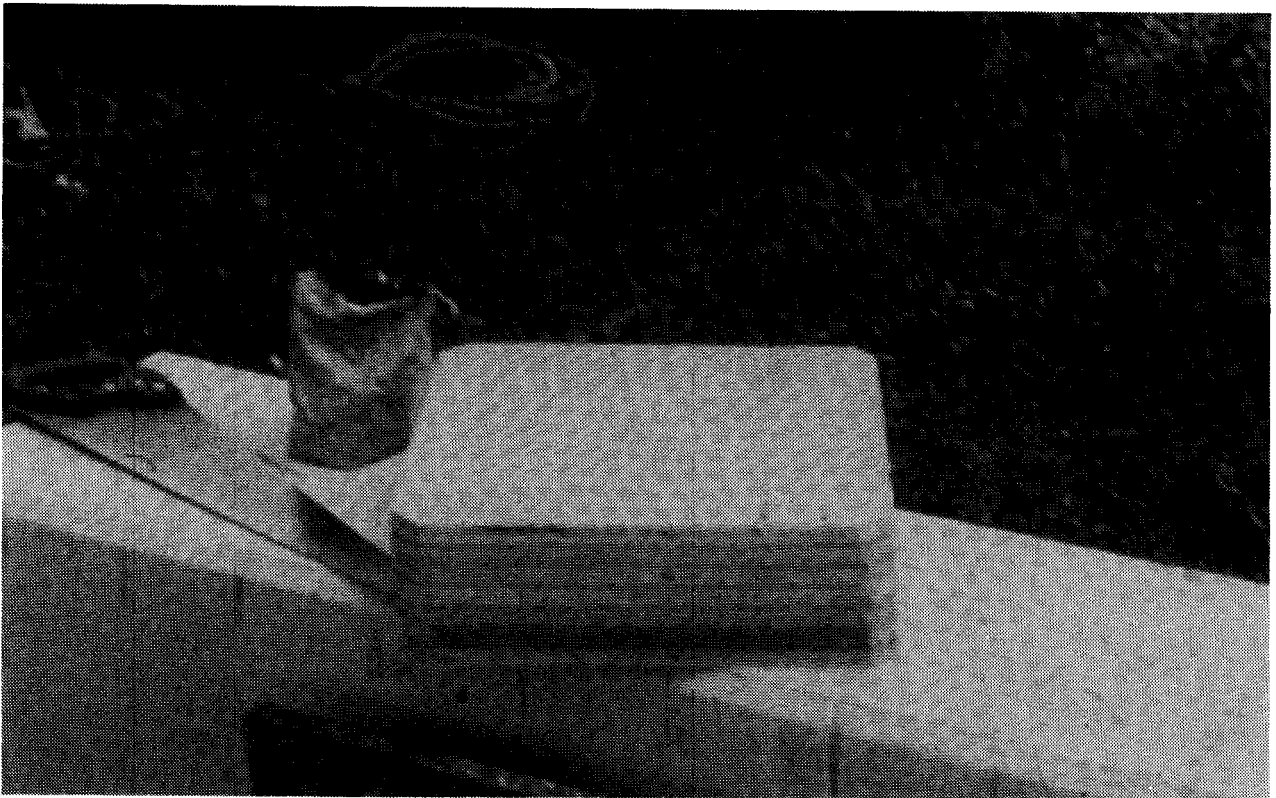


Figure 22.10 Plywood Pile Cushion

22.5 HAMMERS

Pile hammers can be categorized in two main types: impact hammers and vibratory hammers. There are numerous types of impact hammers having variations in the types of power source, configurations, and rated energies. Figure 22.11 shows a classification of hammers based on motivation and configuration factors. Table 22-1 presents characteristics and uses of several types of hammers. A discussion of various types of hammers follows in this chapter. Additional detailed descriptions of the operation of each hammer type and inspection guides are given in Chapter 24 of this manual, in Rausche *et al.* (1986), and in the Deep Foundation Institute Pile Inspector's Guide to Hammers (1995). Appendix D includes information on a majority of the currently available pile hammers.

22.5.1 Hammer Energy Concepts

Before the advent of computers and the availability of the wave equation to evaluate pile driving, driving criteria for a certain pile capacity was evaluated by concepts of work or energy. Work is done when the hammer forces the pile into the ground a certain distance. The hammer energy was equated with the work required, defined as the pile resistance times the final set. This simple idea led engineers to calculate energy ratings for pile hammers and resulted in numerous dynamic formulas which ranged from very simple to very complex. Dynamic formulas have since been widely discredited and replaced by the more accurate wave equation analysis. However, the energy rating legacy for pile hammers remains.

The energy rating of hammers operating by gravity principles only (drop, single acting air/steam or hydraulic hammers) was assigned based on their potential energy at full stroke (ram weight times stroke, h). Although single acting (open end) diesel hammers could also be rated this way, some manufacturers have used other principles for energy rating. Historically, these hammers have usually been rated by the manufacturer's rating, while the actual observed stroke was often ignored in using the dynamic formula. In current practice, the stroke is often measured electronically from the blow rate, which is an improvement over past practice. In the case of all double acting hammers (air/steam, hydraulic, or diesel), the net effect of the downward pressure on the ram during the downstroke is to increase the equivalent stroke and reduce time required per blow cycle. The equivalent stroke is defined as the stroke of the equivalent single acting hammer yielding the same impact velocity. The manufacturers generally calculate the potential energy equivalent for double acting hammers.

PILE HAMMERS

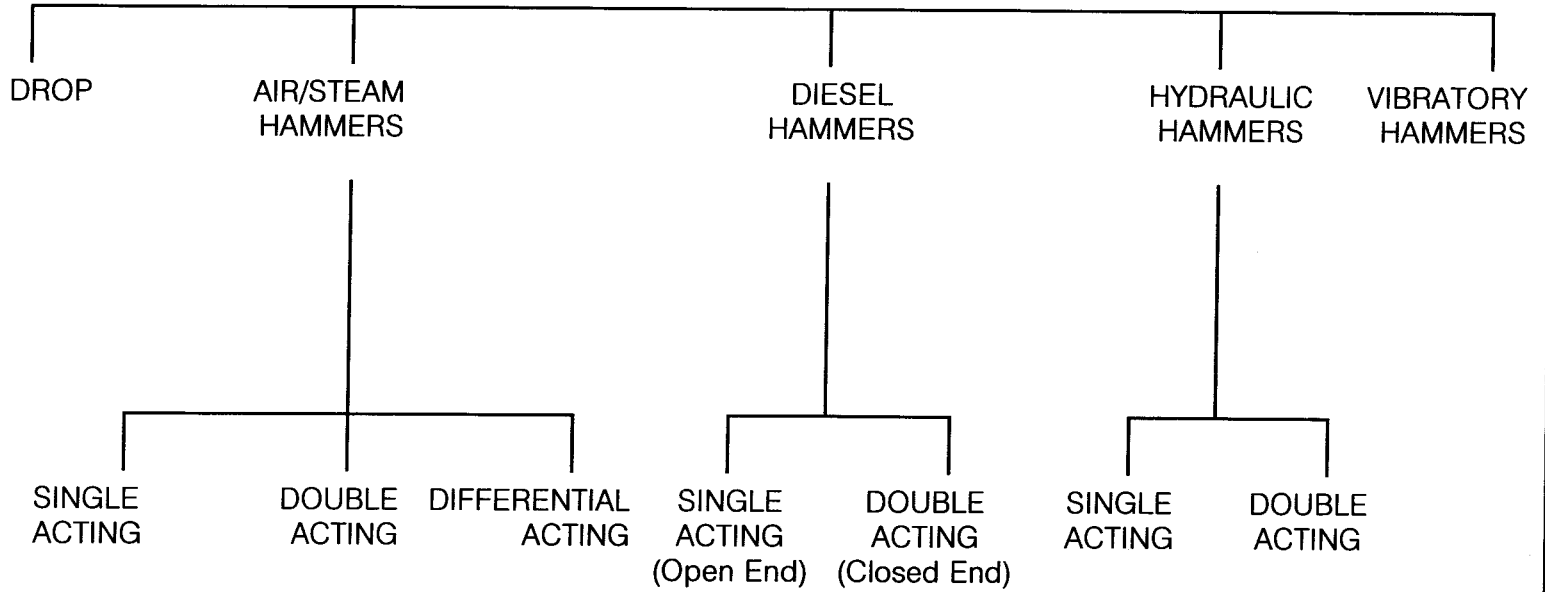


Figure 22.11 Pile Hammer Classification

TABLE 22-1 TYPICAL PILE HAMMER CHARACTERISTICS AND USES

Hammer Type	Drop	Steam or Air			Diesel		Hydraulic		Vibratory
		Single Acting	Double Acting	Differential	Single Acting (open end)	Double Acting (closed end)	Single Acting	Double Acting	
Rated energy range (kJ)	9 to 81	9 to 2440	5 to 225	20 to 68	5 to 380	11 to 88	35-2932	35-2984	----
Impact velocity (m/sec)	7 to 10	2.5 to 5	4.5 to 6	4 to 4.5	*	**	*	**	----
Blows/minute	4 to 8	35 to 60	95 to 300	98 to 303	40 to 60	80 to 105	30 to 50	40 to 90	750 to 2,000 pulses/minute
Energy (per blow)	Ram weight x height of fall.	Ram weight x ram stroke.	(Ram weight + effective piston head area x effective fluid pressure) x stroke.		Ram weight x stroke.	(Ram weight + chamber pressure) x stroke.	Ram weight x stroke.	(Ram weight + effective piston head area x effective fluid pressure) x stroke.	----
Lifting power	Provided by hoisting engine or a crane.	Steam or air.	Steam or air.		Provided by the explosion of injected diesel fluid.		Hydraulic	Hydraulic	Electricity or hydraulic power.
Maintenance	Simple	More complex than for drop hammer.	More complex than for single acting.		More complex than most air impact hammers.		More complex than other impact hammers.	More complex than other impact hammers.	Highest maintenance cost.
Hammer suitability for types of piles	All types except concrete piles.	Versatile for any pile, particularly large concrete and steel pipe.	Timber, steel H and pipe piles.		All types of piles.		All types of piles.	All types of piles.	Steel H and pipe end bearing piles. Very effective in granular soils.
Major advantages	Lowest initial cost equipment.	Relatively simple and moderate cost.	Fully enclosed and permit underwater operation. More productive than single acting. Generate lower dynamic forces. Differential hammer uses less volume of air or steam than double acting and has lower impact velocity.		Carry their own fuel from which power is internally generated. Stroke is a function of pile resistance.		Fully variable energy can be delivered.	Energy is variable over a wide range. Can be used for underwater driving.	Can be used for pulling or driving. Fastest operating installation tool.
Major disadvantages	Very high dynamic forces and danger of pile damage. Lowest pile productivity.	Need air compressor or steam plant. Heavy compared with most diesel hammers.	Costs more than single acting. Need air compressor or steam plant. Heavy compared to diesel hammer.		Pollutes air with exhaust. High cost hammer. Low blows per minute at higher strokes for single acting.		High initial cost.	High initial cost.	High investment and maintenance. Not recommend for friction pile installations.
Remarks	Becoming obsolete.	----	Ram accelerates downward under pressure.		Stroke variable in single acting diesel hammer. Becoming very popular.		New hammer type and may require additional field inspection and/or testing.	New hammer type and may require additional field inspection and/or testing.	----

* Depends on stroke
 ** Depends on chamber pressure

Ideally, the impact velocity, v_i , could be directly computed using basic laws of physics from the equivalent maximum stroke

$$v_i = \sqrt{2gh}$$

Where: g = Acceleration due to gravity, m/s^2 .
 h = Hammer stroke, m .

The kinetic energy could be computed from the equation

$$K.E. = \frac{1}{2} m v_i^2$$

Where: m = Ram mass.

If there were no losses, the kinetic energy would equal the potential energy. In reality however, energy losses occur due to a variety of factors (friction, residual air pressures, preadmission, gas compression in the diesel combustion cylinder, preignition, etc.) which result in the kinetic energy being less than the potential energy. It is the inspector's task to minimize these losses when and where possible, or to at least identify and try to correct situations where losses are excessive. Some hammers, such as modern hydraulic hammers, measure the velocity near impact and hence can calculate the actual kinetic energy available.

Further losses occur in the transmission of energy to the pile. The hammer cushion, helmet, and pile cushion all have kinetic energy and store some strain energy. The pile head also has inelastic collision losses. The hammer transfers its energy to the pile with time. The energy delivered to the pile can be calculated from the work done as the integral of the product of force and velocity with time and is referred to as the transferred energy or ENTHRU.

The pile length, stiffness and capacity influence the energy delivered to the pile. The actual stroke (or potential energy) of diesel hammers depends on the pile resistance and the net transferred energy is also a variable. The stroke of single acting air/steam hammers is also somewhat dependent upon the pile capacity and rebound. The stroke of all double acting hammers is even more dependent on pile capacity due to lift-off considerations. Actually the transferred energy increases only when both the force and velocity are positive (compression forces; downward velocity). As resistance increases and/or the pile becomes shorter, the rebound or upward velocity occurs earlier and the pile then transfers energy back to the driving system. In fact, the energy returning to the hammer may occur before all the energy has been transferred into the pile.

22.6 DROP HAMMERS

The most rudimentary pile hammer still in use today is the drop hammer as shown in Figure 22.12. These hammers consist of a hoisting engine having a friction clutch, a hoist line, and a drop weight. The hammer stroke is widely variable and often not very precisely controlled. The hammer is operated by engaging the hoist clutch to raise the drop weight or ram. The hoist clutch is then disengaged, allowing the drop weight to fall as the hoist line pays out. The fall may not be very efficient since the ram attached by cable to the hoist must also overcome the rotational inertia of the hoist. Ideally, the crane operator engages the clutch immediately after impact to prevent excessive cable spooling. If the operator prematurely engages the clutch, or it is partially engaged during spooling, then the fall efficiency and hence impact energy is further reduced.

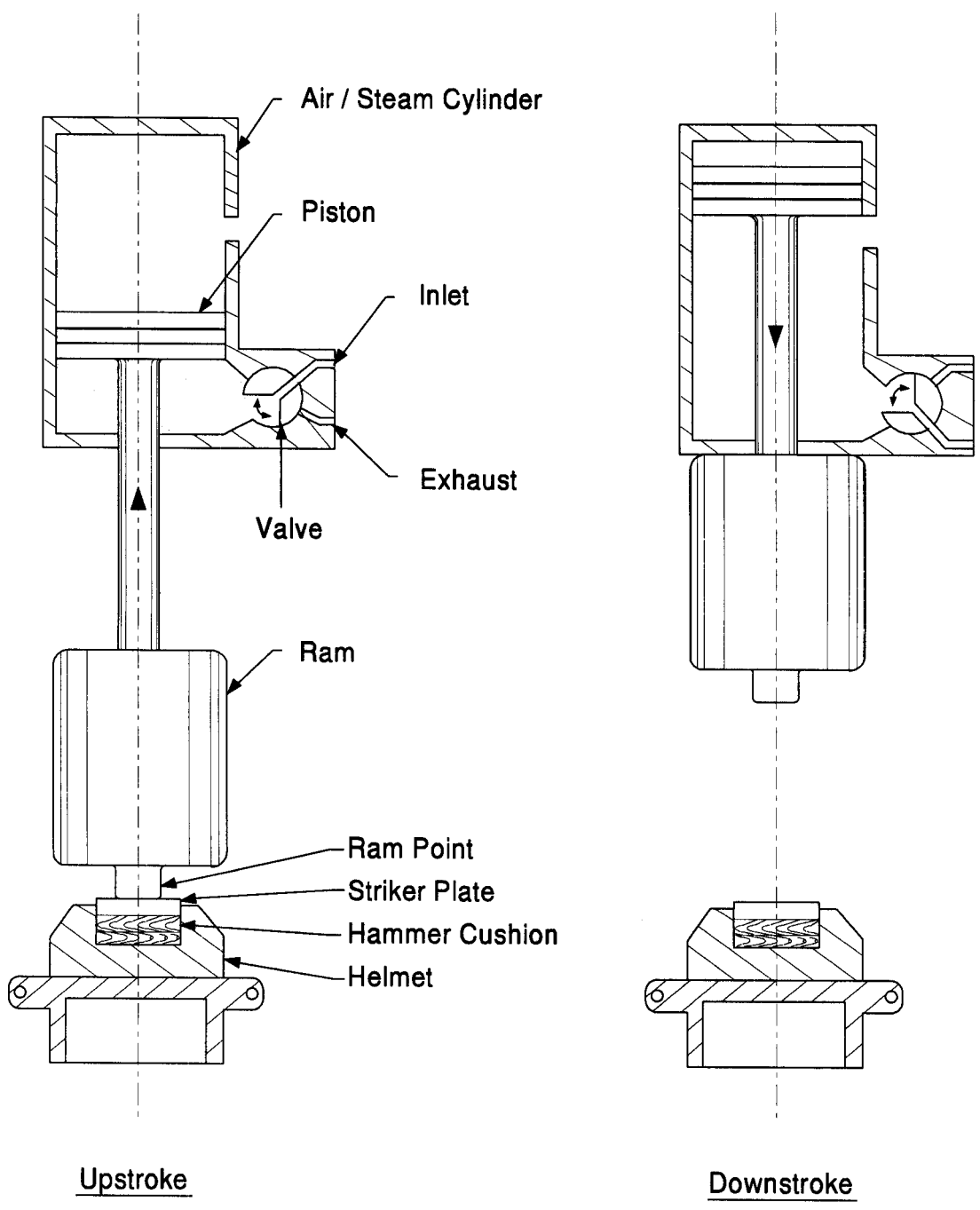
The hammer operating speed (blows per minute) depends upon the skill of the operator and the height of fall being used, but is generally very slow. One of the greatest risks in using a drop hammer is overstressing and damaging the pile. Pile stresses are generally increased with an increase in the impact velocity (hammer stroke) of the striking weight. Therefore, the maximum stroke should be limited to those strokes where pile damage is not expected to occur. In general, drop hammers are not as efficient as other impact hammers but are inexpensive and simple to operate and maintain. Current use of these hammers is generally limited to sheet pile installations where pile capacity is not an issue. Because of the uncertainties described above, drop hammers are not recommended for foundation piles.



Figure 22.12 Typical Drop Hammer

22.7 SINGLE ACTING AIR/STEAM HAMMERS

Single acting air/steam hammers are essentially gravity, or drop hammers, for which the hoist line has been replaced by a pressurized medium, being either steam or air. While originally developed for steam power, most of these hammers today operate on compressed air. To lift the ram weight with motive pressure, a simple one-cylinder steam engine principle is used. The ram consists of a compact block with a so-called ram point attached at its base. The ram point strikes against a striker plate as illustrated in Figure 22.13. A photograph of a typical single acting air/steam hammer is presented in Figure 22.14.



Single Acting Air / Steam Hammer

Figure 22.13 Schematic of Single Acting Air/Steam Hammer

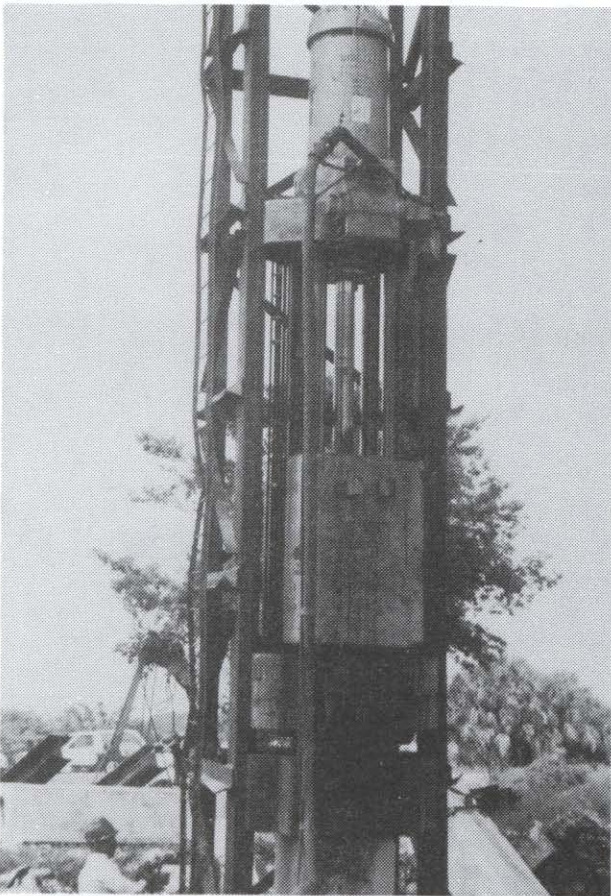


Figure 22.14 Single Acting Air Hammer

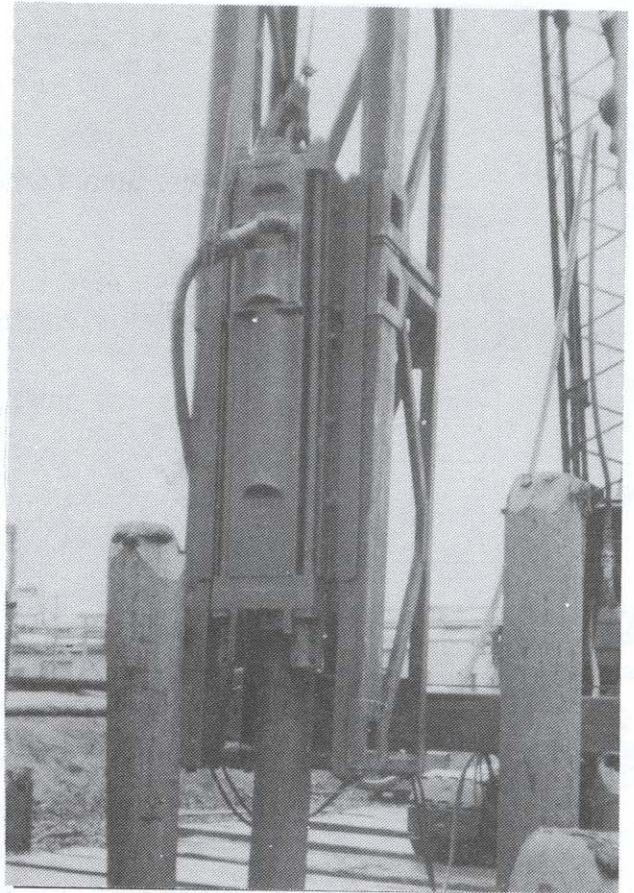


Figure 22.15 Double Acting Air Hammer

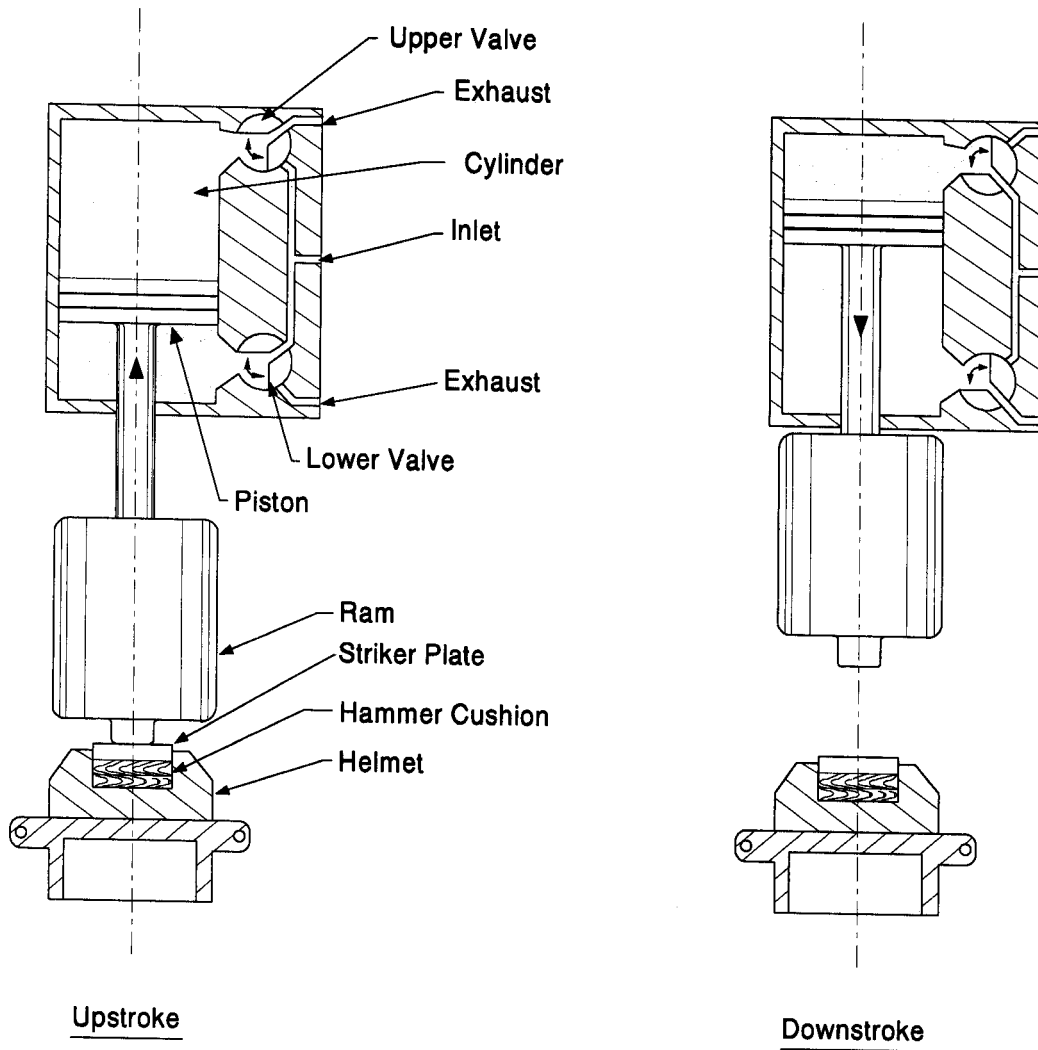
During the upstroke cycle, the ram is raised by externally produced air or steam pressure acting against a piston housed in the hammer cylinder. The piston in turn is connected to the ram by a rod. Once the ram is raised a certain distance, a valve is activated and the pressure in the chamber is released. At that time, the ram has some remaining upward velocity that depends upon the pile rebound, inlet air pressure, and volume of air within the hammer cylinder. Against the action of gravity and friction, the ram then "coasts" up to the maximum height (stroke). The maximum stroke, and hence hammer potential energy, is therefore not constant and depends upon the pressure and volume of air or steam supplied, as well as the amount of pile rebound due to pile resistance effects. During the downstroke cycle, the ram falls by gravity (less friction) to impact the striker plate and hammer cushion. Just before impact, the pressure valve is activated and pressure again enters the cylinder. This occurs approximately 50 mm before impact, but depends on having the correct hammer cushion thickness. If the hammer cushion height is too low, then the pressure is introduced too early, reducing the impact energy of the ram. This is referred to as "preadmission".

The dynamic forces exerted on a pile by a single acting air/steam hammer are of the same short-time duration as those exerted by a drop hammer. Because operating strokes are generally shorter, the accelerations generated by single acting air/steam hammers do not reach the magnitude of drop hammers. Some hammers may be equipped with two nominal strokes, one full stroke and another of lesser height. The hammer operator can switch between the two to better match the driving conditions and limit driving resistance or control tension driving stresses as needed. The maximum stroke of single acting air/steam hammers generally ranges from 0.9 to 1.5 meters. The weights of single acting air/steam hammer rams are usually considerably higher than drop hammer weights. Single acting air/steam hammers have the advantages of moderate cost and relatively simple operation and maintenance. They are versatile for many pile types, particularly large concrete and steel pipe piles.

22.8 DOUBLE ACTING AIR/STEAM HAMMERS

A photograph of an enclosed double acting air hammer is presented in Figure 22.15 and the working principle of a double acting hammer is illustrated in Figure 22.16. The ram of a double acting hammer is raised by pressurized steam or air during the upstroke. As the ram nears the maximum up stroke, the lower air valve opens, allowing the lower cylinder chamber to release the pressurized air. Once the ram reaches full stroke, the upper valve changes to admit pressurized steam or air to the upper cylinder. Gravity and the upper cylinder pressure accelerate the ram through its downward fall. As with the single acting hammer, the stroke is again not constant, due to variable lift pressure and volume as well as differing pile rebound. During hard driving with high pile rebound, the pressure may need to be reduced to prevent lift-off, with the hammer actually lifting up away from the pile. Since the maximum stroke is limited and the same lifting pressure is applied during downstroke, a pressure reduction may cause the kinetic energy at impact to be reduced during these hard driving situations. Just before impact, the valve positions are reversed and the cycle repeats.

The correct cushion thickness is extremely important for the proper operation of the hammer. If the hammer timing is off significantly, it is possible for the hammer to run with the ram moving properly, but with little or no impact force delivered to the pile. The kinetic energy of the ram at impact depends on the ram weight and stroke as well as the motive pressure effects. The overall result is that a properly operating double acting hammer with its shorter stroke delivers comparable impact energy per blow at up to about two times the blow rate of a single acting hammer of the same ram weight.



Double Acting Air / Steam Hammer

Figure 22.16 Schematic of Double Acting Air/Steam Hammer

Some double acting air/steam hammers are fully enclosed and can be operated underwater such as the one shown in Figure 22.15. They may be more productive than single acting hammers, but are more dependent upon the air pressure. Experience has shown that on average, they are slightly less efficient than equivalently rated single acting hammers. Double acting hammers generally cost more than single acting hammers and require additional maintenance. Similar to single acting air/steam hammers, they require an air compressor or a steam plant. However, double acting air/steam hammers consume more air and require greater air pressures than equivalent single acting hammers.

22.9 DIFFERENTIAL ACTING AIR/STEAM HAMMERS

A differential acting air/steam hammer is another type of double acting hammer with relatively short stroke and fast blow rates. The working principle of a differential hammer is illustrated in Figure 22.17. Operation is achieved by pressure acting on two different diameter pistons connected to the ram. At the start of the cycle, the single valve is positioned so that the upper chamber is open to atmospheric pressure only and the lower chamber is pressurized with the motive fluid. The pressure between the two pistons has a net upward effect due to the differing areas, thus raising the ram. The ram has an upward velocity when the valve position changes and applies air pressure into the upper chamber, causing the net force to change to the downward direction. Thus air pressure along with gravity and friction slows the ram, and after attaining the maximum stroke of the cycle, assists gravity during the downstroke to speed the ram.

As with the double acting hammers, the kinetic energy at impact may need to be reduced during hard driving since the pressure, which assists gravity during downstroke, must be reduced to prevent hammer lift-off. As with the other air/steam hammers, when the ram attains its maximum kinetic energy just before impact, the valve position is reversed and the cycle begins again. Therefore, the hammer cushion must be of the proper thickness to prevent preadmission which could cause reduced transferred energy. Very high air pressures between 820 and 970 kPa at the hammer inlet are required for proper operation. However, most air compressors only produce pressures of about 820 to 900 kPa at the compressor. As with the double acting hammer, the efficiency of a differential hammer is somewhat lower than the equivalent single acting air/steam hammer. The heavier ram of the differential acting hammer is lifted and driven downward with a lower volume of air or steam than is used by a double acting hammer.

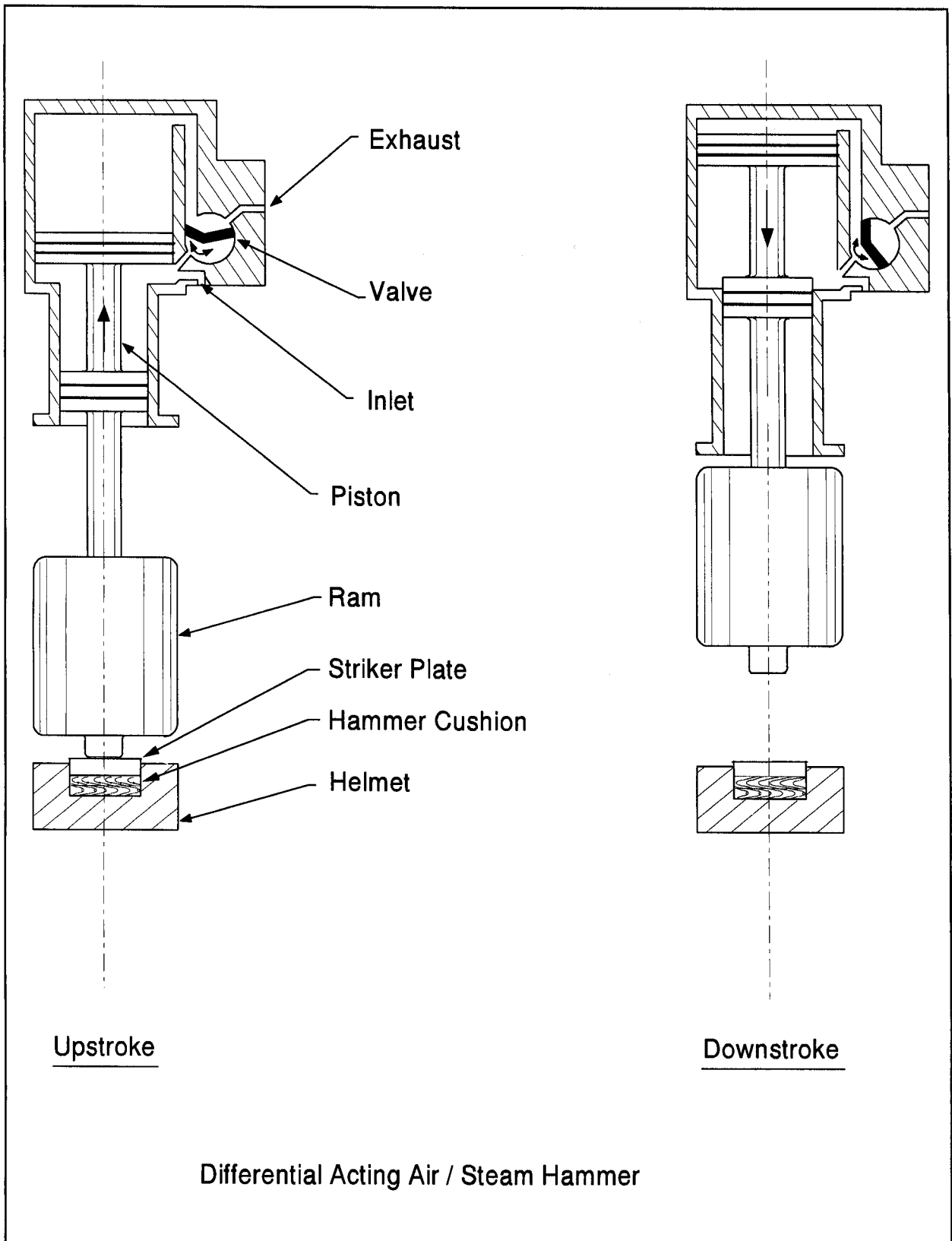
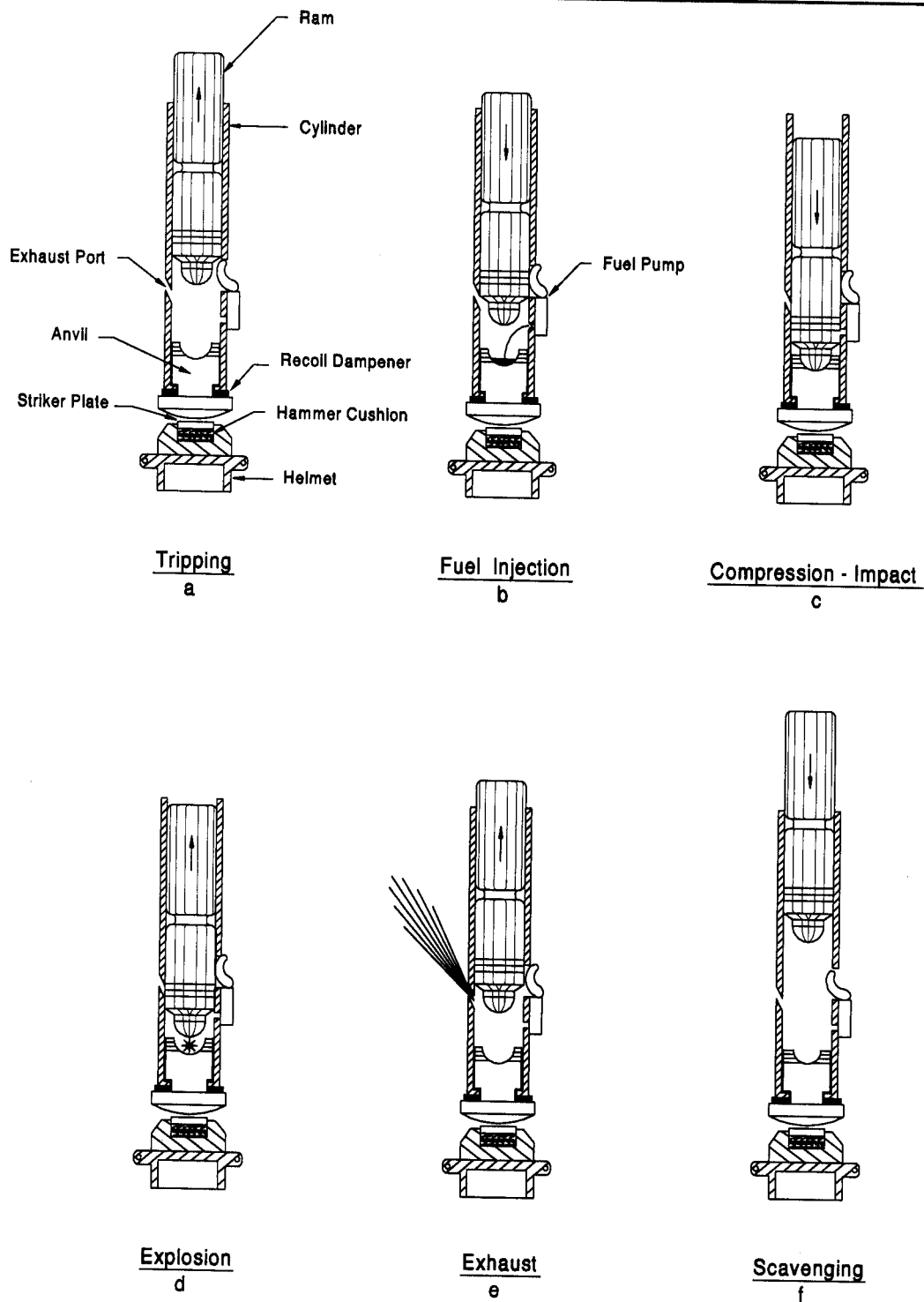


Figure 22.17 Schematic of Differential Air/Steam Hammer

22.10 SINGLE ACTING (OPEN END) DIESEL HAMMER

The basic distinction between all diesel hammers and all air/steam hammers is that, whereas air/steam hammers are one-cylinder engines requiring motive power from an external source, diesel hammers carry their own fuel from which they generate power internally. Figure 22.18 shows the working principle of a single acting diesel hammer. The initial power to lift the ram must be furnished by a hoist line or other source to lift the ram upward on a trip block. After the trip mechanism is released, the ram guided by the outer hammer cylinder falls under gravity. As the ram falls, diesel fuel is injected into the cylinder below the air/exhaust ports. Once the ram passes the air/exhaust ports the diesel fuel is compressed and heats the entrapped air. As the ram impacts the anvil the fuel explodes, increasing the gas pressure. In some hammers the fuel is injected in liquid form as shown in Figure 22.18(b), while in other hammers the fuel is atomized and injected later in the cycle and just prior to impact. In either case, the combination of ram impact and fuel explosion drives the pile downward, and the gas pressure and pile rebound propels the ram upward in the cylinder. On the upstroke, the ram passes the air ports and the spent gases are exhausted. Since the ram has a velocity at that time, the ram continues upward against gravity, and fresh air is pulled into the cylinder. The cycle then repeats until the fuel input is interrupted.

There is no consensus by the various hammer manufacturers on how a single acting diesel hammer should be rated. Many manufacturers use the maximum potential energy computed simply from maximum stroke times the ram weight. The actual hammer stroke achieved is a function of fuel charge, condition of piston rings containing the compressed gases, recoil dampener thickness, driving resistance, and pile length and stiffness. Therefore, the hammer stroke cannot be controlled. A set of conditions will generate a certain stroke which can only be adjusted within a certain range by the fuel charge. It may not be possible to achieve the manufacturer's maximum rated stroke under normal conditions. In normal conditions, part of the available potential energy is used to compress the gases as the ram proceeds downward after passing the air ports. The gases ignite when they attain a certain combination of pressure and temperature. Under continued operation, when the hammer's temperature increases due to the burning of the gases, the hammer fuel may ignite prematurely. This condition, called "preignition", reduces the effectiveness of the hammer, as the pressure increases dramatically before impact, causing the ram to do more work compressing the gases and leaving less energy available to be transferred into the pile.



Single Acting Diesel Hammer

Figure 22.18 Schematic of Single Acting Diesel Hammer

When driving resistance is very low, the upward ram stroke may be insufficient to scavenge (or suction) the air into the cylinder and the hammer may not continue to operate. Thus, the ram must be manually lifted repeatedly until resistance increases. The stroke can be reduced for most hammers by reducing the amount of fuel injected. Some hammers have stepped fuel settings while others have continuously variable throttles. Other hammers use pressure to maintain fuel flow by connecting a hand operated fuel pump to the hammer, which is operated at the ground. By adjusting the fuel pump pressure, hammer strokes may be reduced. Using the hammer on reduced fuel can be useful for limiting driving stresses. For single acting diesel hammers, the stroke is also a function of pile resistance, which also helps in limiting driving stresses. This feature is very useful in controlling tensile stresses in concrete piles during easy driving conditions. The actual stroke can and should be monitored. The stroke of a single acting diesel hammer can be calculated from the following formula:

$$h = [4400/[bpm^2]] - 0.09$$

Where: h = Hammer stroke in meters.
bpm = Blows per minute.

Diesel hammers may be expensive and their maintenance more complex. Concerns over air pollution from the hammer exhaust have also arisen, causing some areas to require a switch to kerosene fuel. However, it should be noted that diesel hammers burn far less fuel to operate than the air compressor required for an air/steam hammer. Diesel hammers are also considerably lighter than air/steam hammers with similar energy ratings, allowing a larger crane operating radius and/or a lighter crane to be used. A photograph of a typical single acting diesel hammer is shown in Figure 22.19.

22.11 DOUBLE ACTING (CLOSED END) DIESEL HAMMER

The double acting diesel hammer works very much in principle like the single acting diesel hammer. The main change consists of a closed cylinder top. When the ram moves upward, air is being compressed at the top of the ram in the so called "bounce chamber" which causes a shorter stroke and therefore a higher blow rate. A photograph of a typical double acting diesel hammer is provided in Figure 22.20.

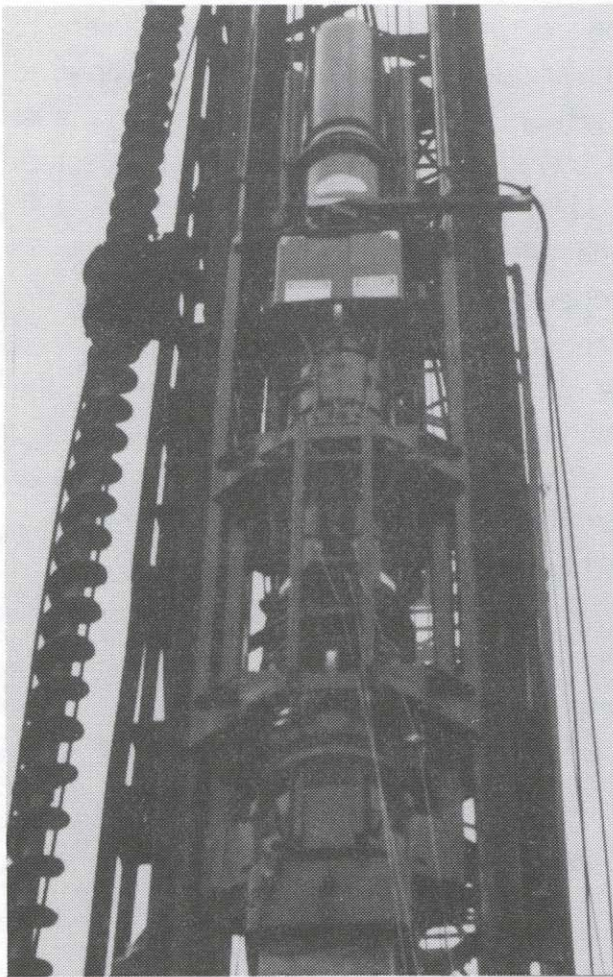
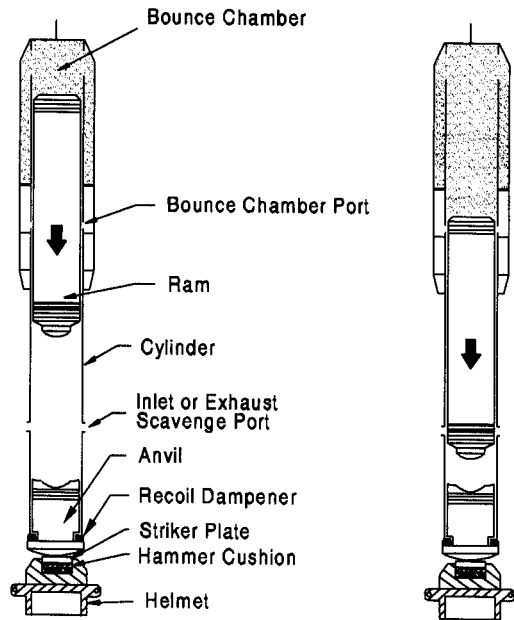


Figure 22.19 Single Acting Diesel Hammer
(courtesy of Pileco)



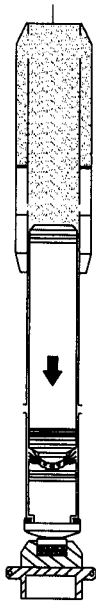
Figure 22.20 Double Acting Diesel Hammer

The bounce chamber has ports so that atmospheric pressure exists as long as the ram top is below these ports, as shown in Figure 22.21. Operationally, as the ram passes the bounce chamber port and moves toward the cylinder top, it creates a pressure which effectively reduces the stroke and stores energy, which in turn will be used on the downstroke. Like the single acting hammer, the actual stroke depends on fuel charge, pile length and stiffness, soil resistance, and condition of piston rings. As the stroke increases, the chamber pressure also increases until the total upward force is in balance with the weight of the cylinder itself. Further compression beyond this maximum stroke is not possible, and if the ram still has an upward velocity, uplift of the hammer will result. This uplift should be avoided as it can lead both to an unstable driving condition and to hammer damage. For this reason, the fuel amount, and hence maximum

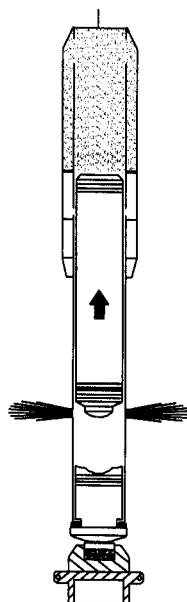


Tripping
a

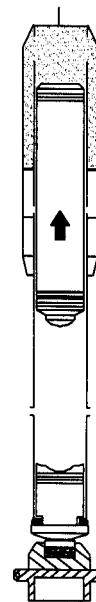
Compression
b



Combustion - Impact
c



Exhaust
d



Scavenging
e

Double Acting Diesel Hammer

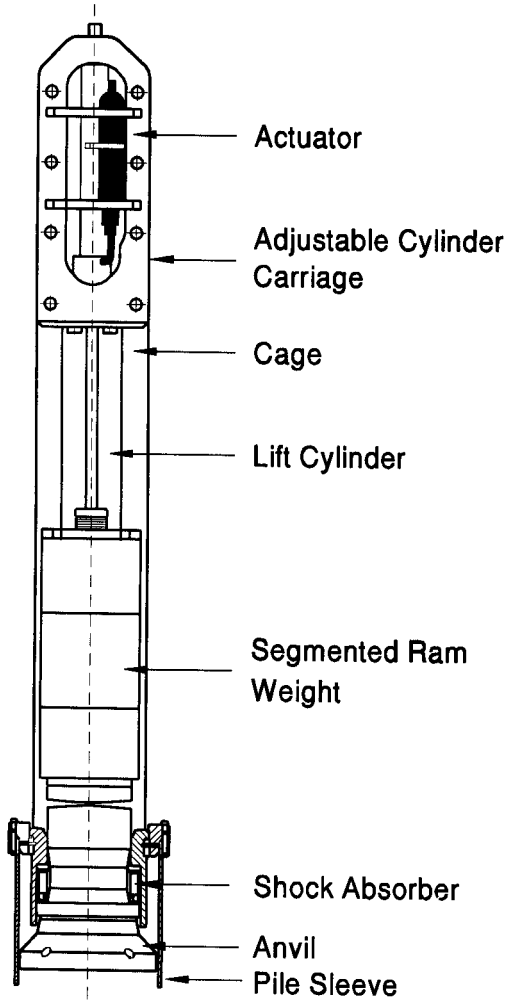
Figure 22.21 Schematic of Double Acting Diesel Hammer

combustion chamber pressure, has to be reduced so that there is only a very slight lift-off or none at all. Most of these hammers have hand held fuel pumps connected by rubber hose to control the fuel flow. Hammer strokes, and therefore hammer energy, may be increased or decreased by the fuel pump pressure.

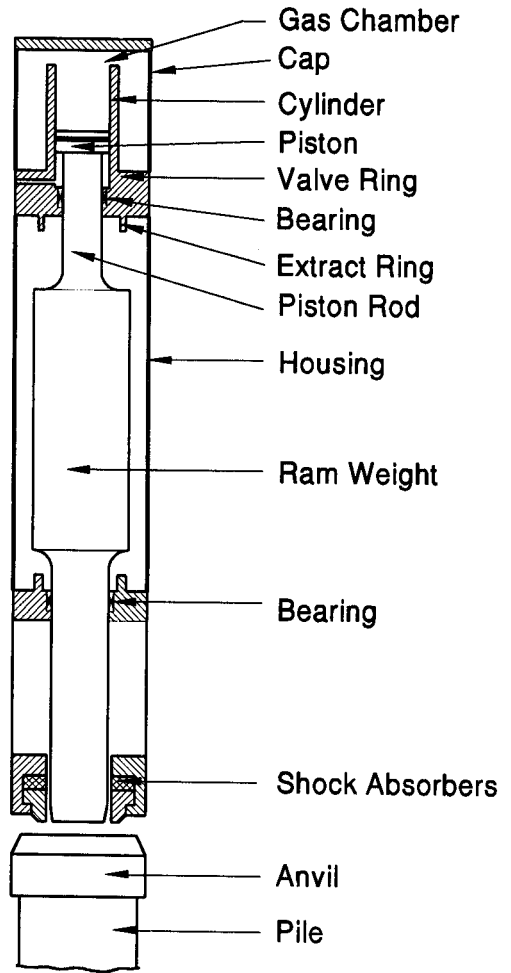
To determine the energy provided by the hammer, the peak bounce chamber pressure in the hammer is read from a bounce chamber pressure gage. The hammer manufacturer should supply a chart which correlates the bounce chamber pressure gage reading as a function of hose length with the energy provided by the hammer.

22.12 HYDRAULIC HAMMERS

There are many different types of hydraulic hammers. However, all hydraulic hammers use an external hydraulic power source to lift the ram, as illustrated in Figure 22.22. The ram drop may be due to gravity only, or may be hydraulically assisted. They can be perhaps thought of as a modern, although more complicated, version of air/steam hammers in that the ram weights and maximum strokes are similar in sizes and the ram is lifted by an external power source. The simplest version lifts the ram with hydraulic cylinders which then retract quickly, fully releasing the ram, which then falls under gravity. The ram impacts the striker plate and hammer cushion located in the helmet. The hydraulic cylinder then lifts the ram again and the cycle is repeated. Other models employ hydraulic accumulators during the downstroke to store a volume of hydraulic fluid used to speed up the ram lifting operation after impact. Similar to air/steam hammers, hydraulic hammers are also made in both single and double acting versions. The above models with hydraulic accumulators often have a relatively small double acting component. Other more complicated models have nitrogen charged accumulator systems, which store significant energy allowing a shortened stroke and increased blow rate. Photographs of single acting and double acting hydraulic hammers are provided in Figures 22.23 and 22.24, respectively.



Single Acting
a



Nitrogen Assisted Double Acting
b

Figure 22.22 Schematics of Single and Double Acting Hydraulic Hammers



Figure 22.23
Single Acting Hydraulic Hammer

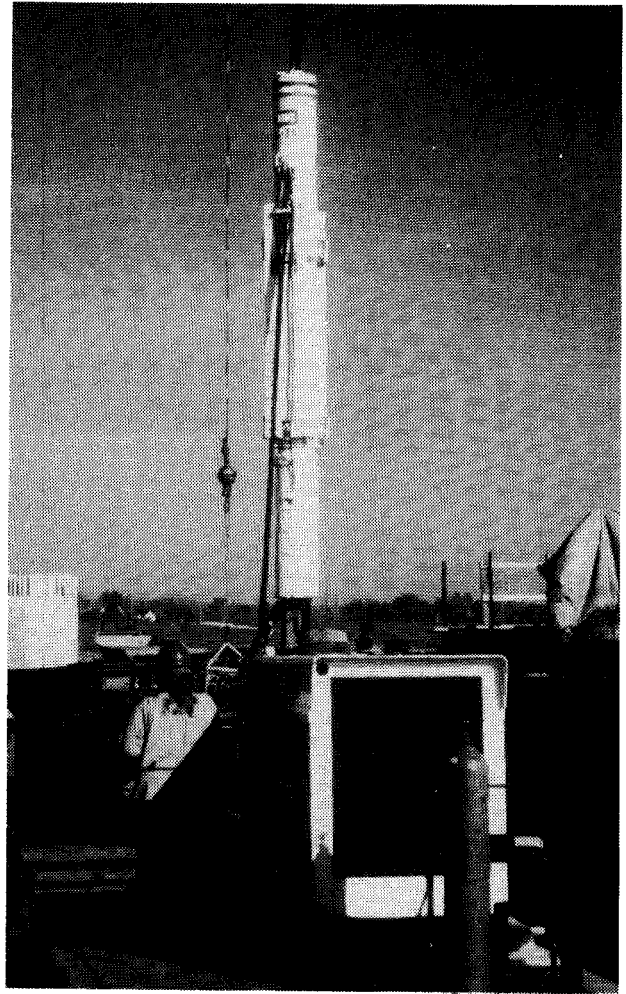


Figure 22.24
Double Acting Hydraulic Hammer

All hydraulic hammers allow the ram stroke to be continuously variable and controlled to adapt to the driving conditions. Very short strokes for easy driving may be used to prevent pile run or to minimize tension stresses in concrete piles. Higher strokes are available for hard driving conditions. On many hydraulic hammers, the stroke can be visually estimated. However, most hydraulic hammers include a built-in monitoring system which determines the ram velocity just before impact. The ram velocity can be converted to kinetic energy or equivalent stroke. Because of the variability of stroke, this hammer monitor should be required as part of the hammer system. The monitor results should be observed during pile driving with appropriate hammer performance notes recorded on the driving log.

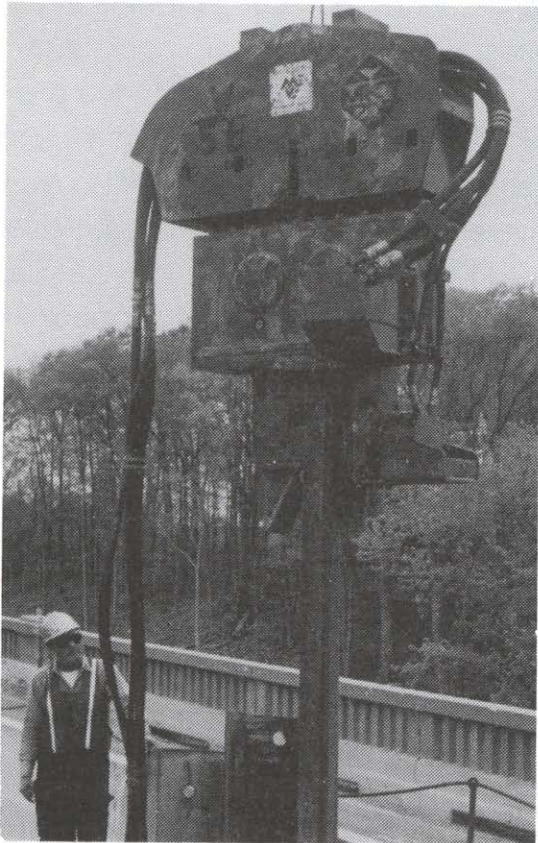
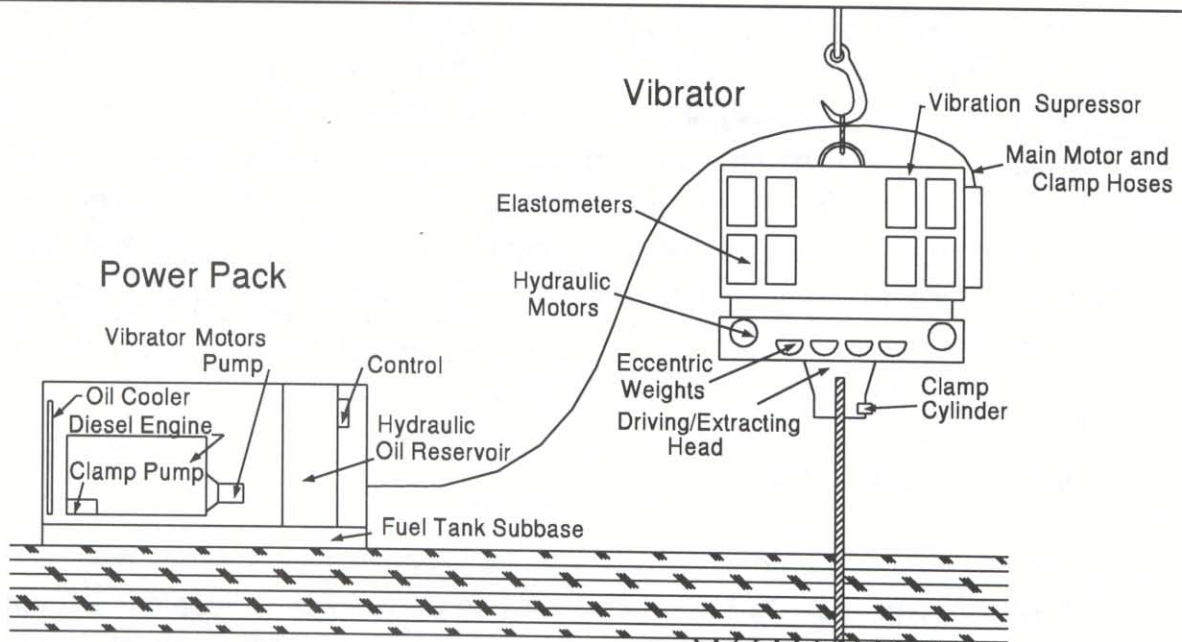
Some hydraulic hammers can be equipped with extra noise abatement panels. A significant advantage of some hydraulic hammers is that they are fully enclosed and can operate underwater. This allows piles to be driven without using a follower or extra length pile. Some hydraulic hammers do not have hammer cushions and thus generate steel to steel impacts with high hammer efficiencies. Therefore, hydraulic hammers are often not used at their full energy potential. Hydraulic hammers require a dedicated hydraulic power pack, and can be more complex to operate and maintain compared to other hammers.

22.13 VIBRATORY HAMMERS

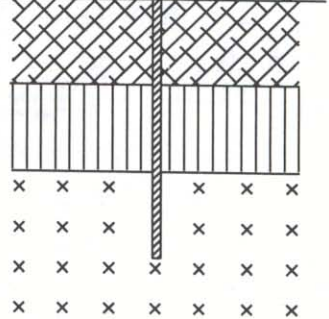
Vibratory hammers use paired counter-rotating eccentric weights to impart a sinusoidal vibrating axial force to the pile (the horizontal components of the paired eccentors cancel). A schematic of a vibratory hammer is presented in Figure 22.25(a) and a photograph is included in Figure 22.25(b). Most common hammers operate at about 1000 Hz. These hammers are rigidly connected by hydraulic clamps to the pile head and may be used for either pile installation or extraction. These hammers typically do not require leads, although templates are often required for sheet pile cells. Vibratory hammers are not rated by impact energy delivered per blow, but instead are classified by energy developed per second and/or by the driving force they deliver to the pile. The power source to operate a vibratory hammer is usually a hydraulic power pack.

Vibratory hammers are commonly used for driving/extracting sheet piles and can also be used for installing non-displacement H-piles and open end pipe piles. However, it is often difficult to install closed end pipes and other displacement piles due to difficulty in displacing the soil laterally at the toe. Vibratory hammers should not be used for precast concrete piles because of possible pile damage due to tensile and bending stress considerations. Vibratory hammers are most effective in granular soils, particularly if submerged. They also may work in silty or softer clays, but most experience suggests they are less effective in stiff to hard clays.

Some wave equation analysis programs can simulate vibratory driving. Dynamic measurements have also been made on vibratory hammer installed piles. However, a reliable technique for estimating pile capacity during vibratory hammer installation has not yet been developed. Hence, if a vibratory hammer is used for installation, a confirmation test of pile capacity by some method is still necessary.



(b)
 (courtesy of Mississippi Valley Equipment)



(a)

Figure 22.25 Vibratory Hammer

22.14 HAMMER SIZE SELECTION

It is important that the contractor and the engineer choose the proper hammer for efficient use on a given project. A hammer which is too small may not be able to drive the pile to the required capacity, or may require an excessive number of blows. On the other hand, a hammer which is too large may damage the pile. The use of empirical dynamic pile formulas to select a hammer energy should be discontinued because this approach incorrectly assumes these formulas result in the desired pile capacities. Results from these formulas become progressively worse as the complexity of the hammers increase.

A wave equation analysis, which considers the hammer cushion-pile-soil system, is the recommended method to determine the optimum hammer size. For preliminary equipment evaluation, Table 22-2 provides approximate minimum hammer energy sizes for ranges of ultimate pile capacities. This is a generalization of equipment size requirements that should be modified based on pile type, pile loads, pile lengths, and local soil conditions. In some cases, such as short piles to rock, a smaller hammer than indicated may be more suitable to control driving stresses. This generalized table should not be used in a specification. Guidance on developing a minimum energy table for use in a specification is provided in Chapter 12.

Ultimate Pile Capacity (kN)	Minimum Manufacturers Rated Hammer Energy (Joules)
800 and under	16,500
800 to 1350	28,500
1351 to 1850	39,000
1851 to 2400	51,000
2401 to 2650	57,000

22.15 FOLLOWERS

A follower is a structural member interposed between the pile hammer and the pile, to transmit hammer blows to the pile head when the pile head is below the reach of the hammer. This occurs when the pile head is below the bottom of leads. Followers are sometimes used for driving piles below the deck of existing bridges, for driving piles underwater, or for driving the pile head below grade.

Maintaining pile alignment, particularly for batter piles, is a problem when a follower is used while driving below the bottom of the leads. The use of a follower is accompanied by a loss of effective energy delivered to the pile due to compression of the follower and losses in the connection. This loss of effective energy delivered to the pile affects the necessary driving resistance for the ultimate pile capacity. These losses can be estimated by an extensive and thorough wave equation analysis, or field evaluated by dynamic measurements. A properly designed follower should have about the same stiffness (per unit length) as the equivalent length of pile to be driven. Followers with significantly less stiffness should be avoided. Followers often require considerable maintenance. In view of the difficulties that can be associated with followers, their use should be avoided when possible. For piles to be driven underwater, one alternative is to use a hammer suitable for underwater driving. A photograph of a follower used to drive steel H-piles underwater is presented in Figure 22.26.

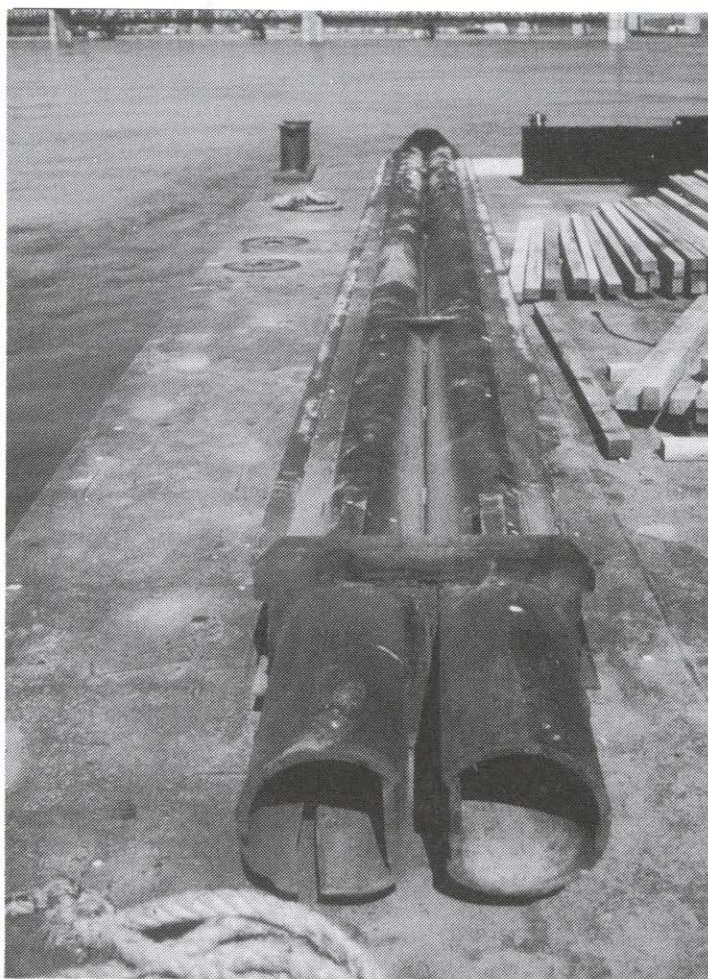


Figure 22.26 Follower used for Driving H-piles

22.16 JETTING

Jetting is the use of water or air to facilitate pile penetration by displacing the soil. In some cases, a high pressure air jet may be used in combination with water. Jets may be used to create a pilot hole prior to or simultaneously with pile placement. Jetting pipes may be located either inside or outside the pile. Jetting is usually most effective in loose to medium dense granular soils.

Jetting is not recommended for friction piles because the frictional resistance is reduced by jetting. Jetting should also be avoided if the piles are designed to provide substantial lateral resistance. For end bearing piles, the final required resistance must be obtained by driving (without jetting). Backfilling should be required if the jetted hole remains open after the pile installation. A separate pay item for jetting should be included in the contract documents when jetting is anticipated. Alternatives to jetting include predrilling and spudding.

The use of jetting has been greatly reduced due to environmental restrictions. Hence, jetting is rarely used unless containment of the jetted materials can be provided. Photographs of a dual jet system mounted on a concrete pile and a jet/punch system are presented in Figures 22.27 and 22.28, respectively.

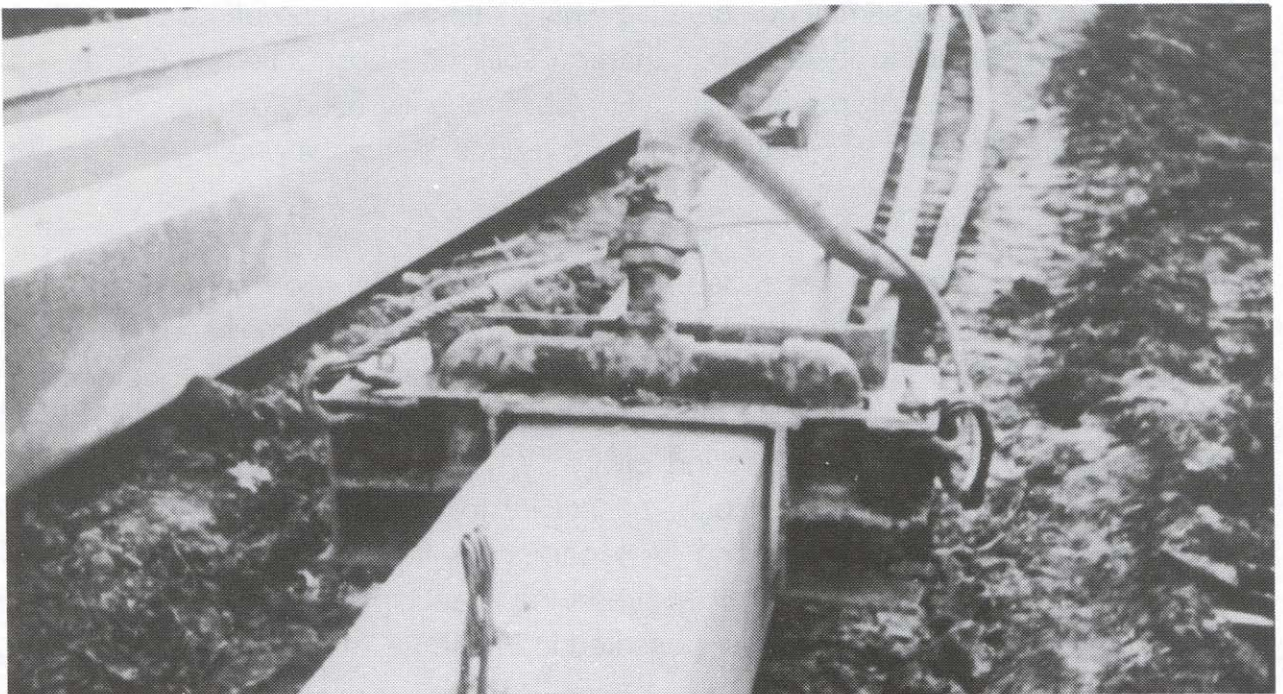


Figure 22.27 Dual Jet System Mounted on a Concrete Pile (courtesy of Florida DOT)

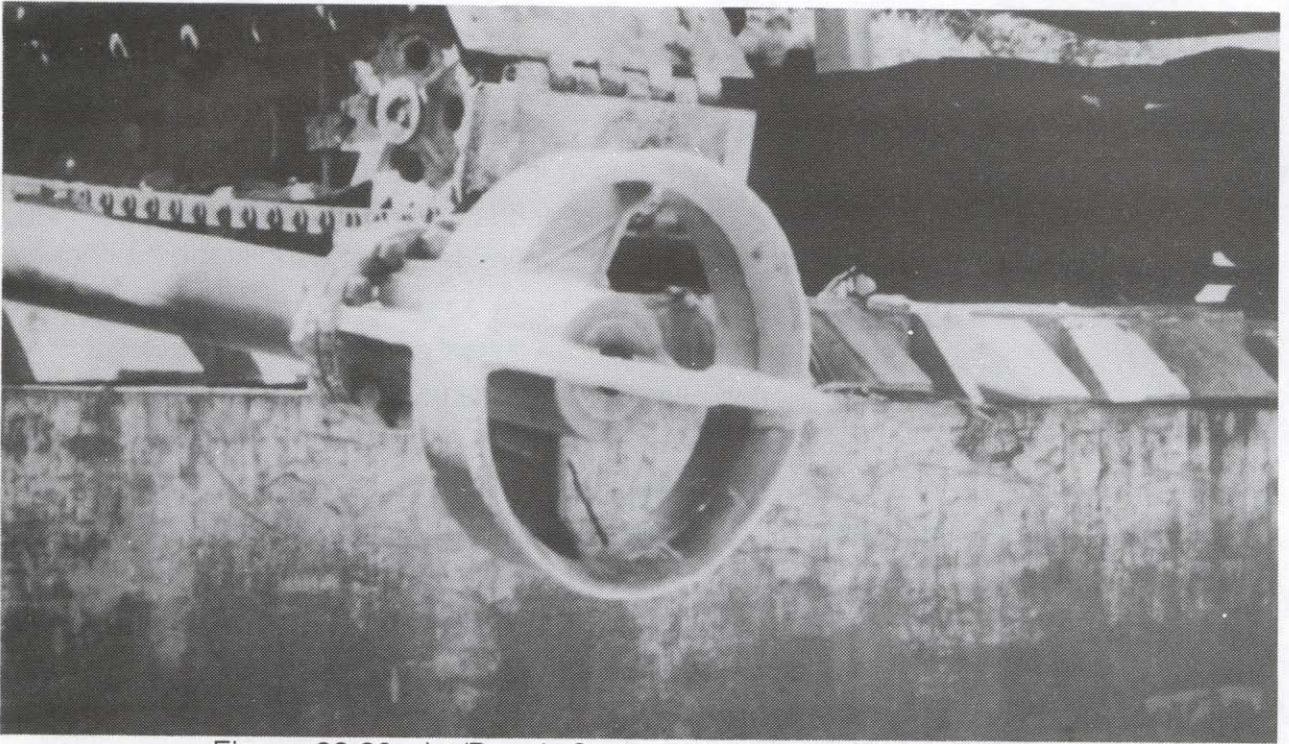


Figure 22.28 Jet/Punch System (courtesy of Florida DOT)

22.17 PREDRILLING

Soil augers or drills may sometimes be used where jetting is inappropriate. Predrilling is sometimes necessary to install a pile through soils with obstructions, such as old timbers, boulders, and riprap. Predrilling is also frequently used for pile placement through soil embankments and may be helpful to reduce pile heave when displacement piles are driven at close spacings.

The predrilled hole diameter depends upon the size and shape of the pile, and soil conditions. The hole should be large enough to permit driving but small enough so the pile will be supported against lateral movement. Under most conditions, the predrilled hole diameter should be 100 mm less than the diagonal of square or steel-H piling, and 25 mm less than the diameter of round piling. Where piles must penetrate into or through very hard material, it is usually necessary to use a diameter equal to the diagonal width or diameter of the piling. A separate pay item for predrilling should be included in the contract documents when predrilling is anticipated. A photograph of a solid flight auger predrilling system is presented in Figure 22.29.

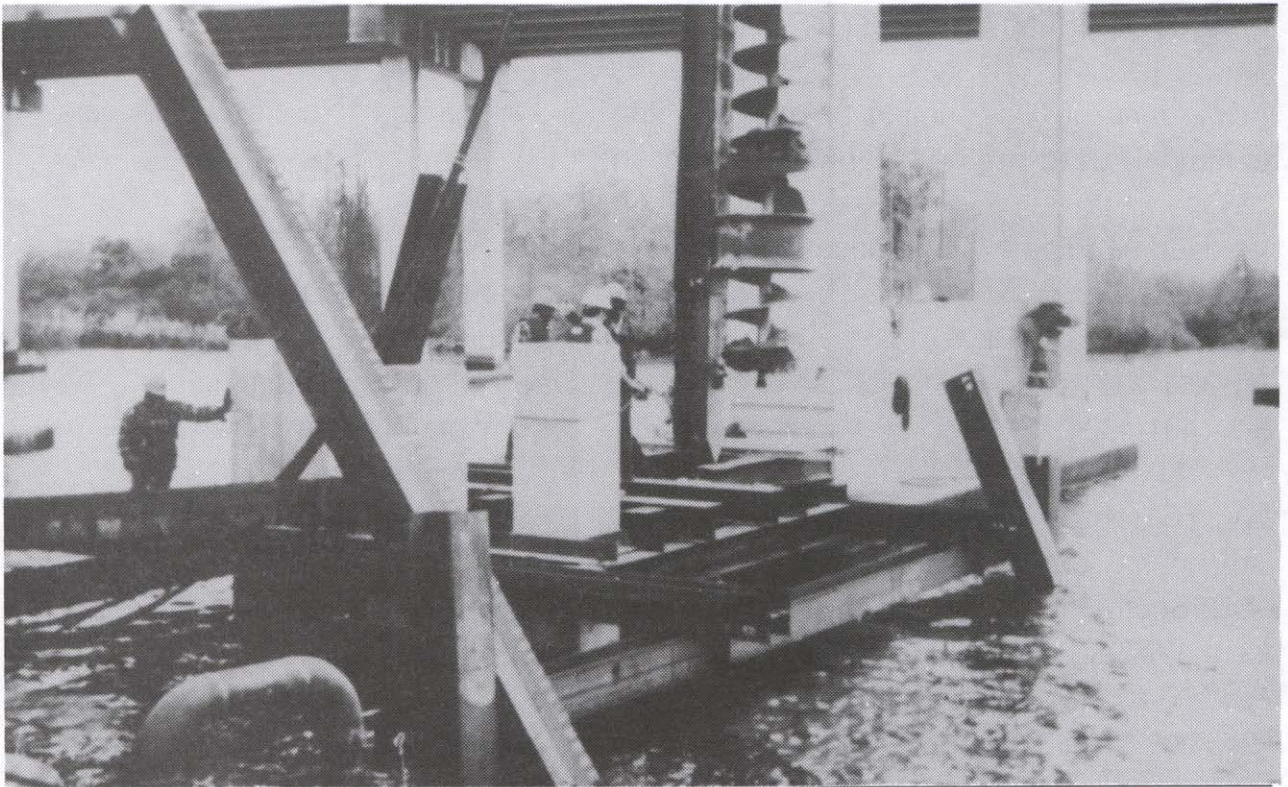


Figure 22.29 Solid Flight Auger Predrilling System (courtesy of Florida DOT)

22.18 SPUDDING

Spudding is the act of opening a hole through dense material by driving or dropping a short and strong member and then removing it. The contractor may resort to spudding in lieu of jetting or predrilling when the upper soils consist of miscellaneous fill and debris. A potential difficulty of spudding is that a spud may not be able to be pulled when driven too deep. However, an advantage of spudding is that soil cuttings and groundwater are not brought to the ground surface, which could then require disposal due to environmental concerns.

22.19 REPRESENTATIVE LIST OF U.S.A. HAMMER MANUFACTURERS AND SUPPLIERS

At the time of final printing this manual, the following manufacturers or suppliers of commonly used pile hammers were identified:

American Equipment & Fabricating Corp. 100 Water St. East Providence, RI 02914 Ph: 401-438-2626 Fax: 401-438-0764	Supplier: Berminghammer Diesel Hammers Dawson Hydraulic Hammers Dawson Vibratory Hammers H&M Vibratory Hammers Vulcan Air Hammers
---	--

American Piledriving Equipment, Inc. 7032 South 196th Kent, WA 98032 Ph: 206-872-1041 or 800-248-8498 Fax: 206-872-8710	Manufacturer: APE Hydraulic Hammers APE Vibratory Hammers
---	---

Berminghammer Foundation Equipment Wellington Street Marine Terminal Hamilton, Ontario L8L 4Z9 Ph: 905-528-0425 or 800-668-9432 Fax: 905-528-6187	Manufacturer: Berminghammer Diesel Hammers
---	---

Continental Machine Co., Inc. 1602 Engineers Road Belle Chasse, LA 70037 Ph: 504-394-7330 or 800-259-7330 Fax: 504-393-8715	Manufacturer: Conmaco Air Hammers Supplier: HPSI Hydraulic Hammers HPSI Vibratory Hammers MKT Diesel Hammers MKT Vibratory Hammers PTC Vibratory Hammers
---	---

Drive-Con, Inc.
8225 Washington Blvd.
Jessup, MD 20794
Ph: 410-799-8963 or 800-255-8963
Fax: 410-799-5264

Supplier:
ICE Diesel Hammers
ICE Hydraulic Hammers
ICE Vibratory Hammers
MKT Air Hammers

Equipment Corporation of America
P.O. Box 306
Coraopolis, PA 15108-0306
Ph: 412-264-4480
Fax: 412-264-1158

Supplier:
Delmag Diesel Hammers
HPSI Hydraulic Hammers
HPSI Vibratory Hammers
MKT Air Hammers
Tunkers Vibratory Hammers
Vulcan Air Hammers

L. B. Foster
415 Holiday Drive
Pittsburgh, PA 15220
Ph: 412-928-5625
Fax: 412-928-7891

Supplier:
IHC Hydraulic Hammers

Foundation Equipment Corporation
P.O. Box 566
270 S. Tuscarosa
Dover, OH 44622
Ph: 330-364-7521
Fax: 330-364-7524

Supplier:
FEC Diesel Hammers

Gardella Equipment Corporation
111 Harbor Avenue
Norwalk, CT 06850
Ph: 203-855-8160
Fax: 203-853-0342

Supplier:
Junttan Hydraulic Hammers

Geoquip, Inc.
1201 Cavalier Blvd.
Chesapeake, VA 23323
Ph: 757-485-2500
Fax: 757-485-5631

Supplier:
Delmag Diesel Hammers
HPSI Hydraulic Hammers
HPSI Vibratory Hammers
Menck Hydraulic Hammers
Vulcan Air Hammers
Vulcan Vibratory Hammers

Hammer and Steel, Inc.
11912 Missouri Bottom Road
St. Louis, MO 63042
Ph: 314-895-4600
Fax: 314-895-4070

Supplier:
Dawson Hydraulic Hammers
Delmag Diesel Hammers
HPSI Hydraulic Hammers
HPSI Vibratory Hammers

Hercules Machinery
Mid-America-Foundation Supply, Inc.
P.O. Box 5198
3101 New Haven Avenue
Fort Wayne, IN 46803
Ph: 219-424-0405 or 800-348-1890
Fax: 219-422-2040

Supplier:
H&M Vibratory Hammers
HPSI Hydraulic Hammers
HPSI Vibratory Hammers
ICE/Linkbelt Diesel Hammers
ICE Hydraulic Hammers
ICE Vibratory Hammers
Vulcan Air Hammers
Vulcan Vibratory Hammers

Hercules Machinery Corporation
8 Bryant Court
Sterling, VA 20166
Ph: 800-223-8427
Fax: 703-435-4530

Supplier:
APE Vibratory Hammers
Berminghammer Diesel Hammers
ICE/Linkbelt Diesel Hammers
Kobe Diesel Hammers
MKT Air Hammers

Hydraulic Power Systems, Inc.
1203 Ozark
North Kansas City, MO 64116
Ph: 816-221-4774
Fax: 816-221-4591

Manufacturer:
HPSI Hydraulic Hammers
HPSI Vibratory Hammers

International Construction Equipment, Inc.
301 Warehouse Drive
Matthews, NC 28105
Ph: 704-821-8200 or 800-438-9281
Fax: 704-821-6448

Supplier:
ICE Diesel Hammers
ICE Hydraulic Hammers
ICE Vibratory Hammers

Midwest Vibro Inc.
3715-28th Street S.W.
P.O. Box 224
Grandville, MI 49468-0224
Ph: 616-532-7670
Fax: 616-532-8505

Supplier:
H&M Vibratory Hammers
Dawson Vibratory Hammers
(Dawson for Michigan only)

MKT Manufacturing, Inc.
1198 Pershall Road
St. Louis, MO 63137
Ph: 314-869-8600
Fax: 314-869-6862

Manufacturer:
MKT Air Hammers
MKT Diesel Hammers
MKT Vibratory Hammers

New England Construction Products, Inc.
P.O. Box 1124
Taunton, MA 02780
Ph: 508-821-4450
Fax: 508-821-4438

Supplier:
Conmaco Air Hammers
Delmag Diesel Hammers
HPSI Hydraulic Hammers
HPSI Vibratory Hammers
Menck Hydraulic Hammers

Pacific American Commercial Company
7400 Second Avenue South
P.O. Box 3742
Seattle, WA 98124
Ph: 206-762-3550 or 800-678-6379
Fax: 206-763-4232

Supplier:
BSP Hydraulic Hammers
Delmag Diesel Hammers
HPSI Hydraulic Hammers
HPSI Vibratory Hammers
MKT Air Hammers
MKT Diesel Hammers
MKT Vibratory Hammers
Tunkers Vibratory Hammers
Vulcan Air Hammers
Vulcan Vibratory Hammers

Pile Equipment, Inc.
1058 Roland Avenue
Green Cove Springs, FL 32043
Ph: 800-367-9416
Fax: 904-284-2588

Supplier:
Delmag Diesel Hammers
HPSI Hydarulic Hammers
HPSI Vibratory Hammers
Menck Hydraulic Hammers
Vulcan Air Hammers
Vulcan Vibratory Hammers

Pileco, Inc.
P.O. Box 16099
Houston, TX 77222
Ph: 713-691-3000
Fax: 713-691-0089

Supplier:
Delmag Diesel Hammers
Menck Hydraulic Hammers
Tunkers Vibratory Hammers

Seaboard Steel Corporation
P.O. Box 3408
Sarasota, FL 34230
Ph: 941-355-9773 or 800-533-2736
Fax: 941-351-7064

Supplier:
MKT Air Hammers
MKT Diesel Hammers
MKT Vibratory Hammers

Uddcomb Equipment A B
U. S. Representative - Sullivan Services
P.O. Box 385
San Andreas, CA 95249
Ph: 209-286-1290
Fax: 209-286-1290

Supplier:
Uddcomb Hydraulic Hammers

Vulcan Iron Works
P.O. Box 5402
2909 Riverside Dr.
Chattanooga, TN 37406
Ph: 423-698-1581
Fax: 423-698-1587

Supplier:
Vulcan Air Hammers
Vulcan Diesel Hammers
Vulcan Vibratory Hammers

REFERENCES

- Associated Pile and Fitting Corporation. Design and Installation of Driven Pile Foundations.
- Chellis, R.D. (1961). Pile Foundations. McGraw-Hill Book Company.
- Compton, G.R. (1977). Piletalk Panel on Hammers and Equipment, APF Piletalk Seminar, San Francisco.
- Davisson, M.T. (1975). Pile Load Capacity. Design, Construction and Performance of Deep Foundations, ASCE and University of California, Berkeley.
- Davisson, M.T. (1980). Pile Hammer Selection. Presentation at the APF Piletalk Seminar in Carlsbad, California.
- Deep Foundations Institute (1981). A Pile Inspector's Guide to Hammers, First Edition, Deep Foundations Institute.
- Deep Foundations Institute (1995). A Pile Inspector's Guide to Hammers. Second Edition, Deep Foundations Institute.
- Fuller, F.M. (1983). Engineering of Pile Installations. McGraw-Hill Book Company.
- Goble, G.G. and Rausche F. (1981). WEAP Program, Vol. I Background. Implementation Package Prepared for the Federal Highway Administration.
- Passe, Paul D. (1994). Pile Driving Inspector's Manual. State of Florida Department of Transportation.
- Rausche, F., Likins, G.E., Goble, G.G. and Hussein, M. (1986). The Performance of Pile Driving Systems. Inspection Report, FHWA/RD-86/160, U.S. Department of Transportation, Federal Highway Administration, Office of Research and Development, Washington, D.C., 92.

STUDENT EXERCISE #14 - EQUIPMENT SUBMITTAL REVIEW

Project specifications require the contractor to use a pile driving hammer having a minimum rated energy of 20.0 kJ to install the 20 m long, 305 mm square, prestressed concrete piles on this project. The piles have a required ultimate pile capacity of 1200 kN. Soil conditions consist of 15 m of soft clay over 20 meters of medium dense to dense sands. Static analyses indicate the piles should develop the required ultimate capacity at a penetration depth of 19 m. The Gates dynamic formula will be used for construction control.

The following pages contain the contractor's submittal package on this project. Based on the submittal, the final driving resistance required by the Gates formula is 56 blows per 0.25 m for the 1200 kN ultimate capacity. Review the submittal information and decide if the submittal should be approved. Do you have any questions or concerns ?

- STEP 1 Check if hammer meets minimum energy requirements.
- STEP 2 Determine line pressure loss in air hose between compressor and hammer by entering hose detail table on page 22-49 at compressor air delivery of 28 m³/min. (Note, this table indicates the line loss in 15.2 m of hose.)
- STEP 3 Check if the pressure at the hammer meets manufacturer's requirements.
- STEP 4 Determine the rated energy based on the pressure at the hammer using the following manufacturer's formula for a differential hammer:

$$E_r = (W + A_{np} (p_h)) h$$

- Where:
- E_r = rated energy (kJ).
 - W = ram weight (kN).
 - A_{np} = net area of piston (m²).
 - p_h = pressure at hammer (kPa).
 - h = hammer stroke (m).

Equipment Submittal

- Hammer: Vulcan 50-C differential acting air hammer.
Rated energy = 20.5 kJ at 0.39 m stroke.
(additional hammer details on page 22-49)
- Hammer Cushion: 152 mm of Aluminum and Micarta.
Hammer Cushion Area = 641 cm².
- Helmet: 4.6 kN
- Pile Cushion: 100 mm of Plywood.
Pile Cushion Area = 930 cm².
- Air Compressor: Model 1000
Rated Delivery: 28.3 m³ / min.
Rated Pressure: 827 kPa.
- Hose: 61 m of 51 mm I.D. (additional details on page 22-49).
- Pile: 20 m long, 305 mm square precast, prestressed concrete
Compressive Strength: 40 MPa.
Effective Prestress after losses: 6 MPa.

Equipment Submittal

Hammer Details:

Ram Weight: 22.25 kN
 Normal Stroke: 0.39 m
 Rated Operating Pressure at Hammer: 827 kPa
 Air Consumption: 24.9 m³ / min
 Required Air Compressor Size: 25.5 m³ / min
 Net Area of Piston: 0.036 m²

Hose Details:

Hose		Pressure Loss in Hose (kPa)						
Inside Dia. (mm)	Length (m)	Air Delivery (m ³ / min)	Line Pressure (kPa)					
			414	552	690	827	1034	1378
51	15.2	16.8	13.1	-----	-----	-----	-----	-----
		22.4	22.1	17.2	14.5	-----	-----	-----
		28.0	34.5	26.9	22.1	18.6	12.2	11.7
		33.6	48.3	37.9	31.0	26.2	21.4	16.5
		39.2	64.1	51.0	42.1	35.9	29.0	22.1
		44.8	-----	66.2	54.5	46.2	37.9	29.0
		50.4	-----	83.4	69.3	57.9	47.6	36.5
56.0	-----	-----	84.1	71.7	58.6	44.8		

23. ACCESSORIES FOR PILE INSTALLATION

Pile accessories are sometimes used for pile toe protection and for splicing. Accessories available for driven piles can make installation easier and faster. They can also reduce the possibility of pile damage and help provide a more dependable permanent support for any structure. Heavier loading on piles, pile installation in sloping rock surfaces or into soils with obstructions, and longer pile length, are project situations where the use of pile shoes and splice accessories are often cost effective and sometimes necessary for a successful installation. However, pile accessories may add significant cost to the project and should not be used unless specifically needed. Pile toe attachments and splices for timber, steel, concrete and composite piles are discussed in this chapter. A list of the manufacturers and suppliers of pile accessories is provided at the end of this chapter.

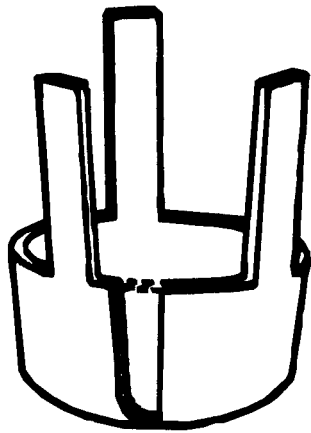
During driving and in service, pile toe attachments and splices should develop the required strength in compression, bending, tension, shear, and torsion at the point of the toe attachment or splice. The current AASHTO Bridge Specifications require that a splice must provide the full strength of a pile. Some of the manufactured splices do not satisfy this AASHTO requirement.

23.1 TIMBER PILES

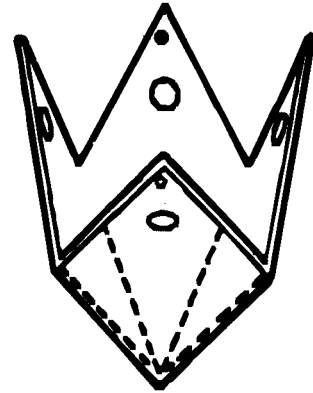
The potential problems associated with driving timber piles are splitting and brooming of the pile toe and pile head, splitting or bowing of the pile body, and breaking of the pile during driving. Protective attachments at the pile toe and at the pile head can minimize these problems.

23.1.1 Pile Toe Attachments

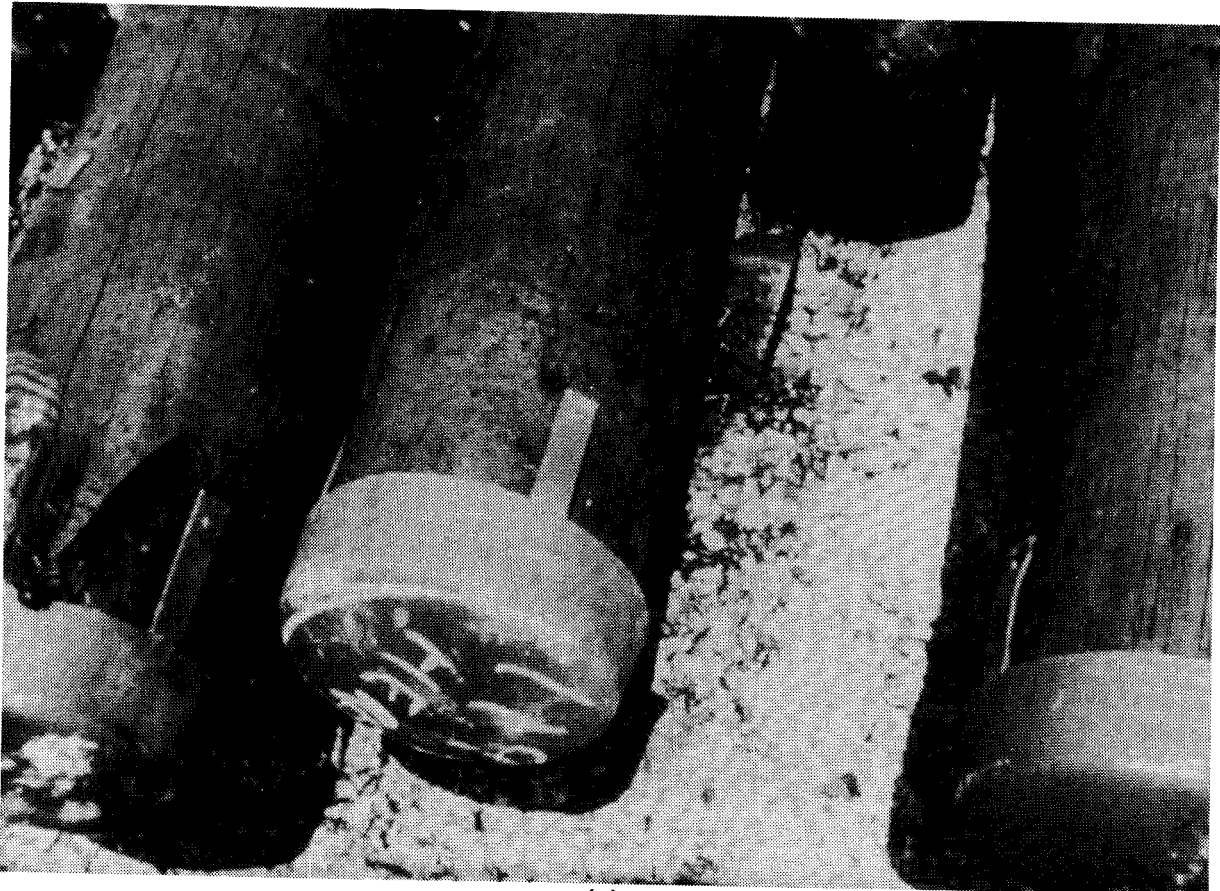
A timber pile toe can be protected by a metal boot or a point. The trend toward heavier hammers and heavier design loading may result in greater risk of damage for timber piles if obstructions are encountered. The pile toe attachment shown in Figure 23.1(a) and (c) covers the entire pile toe without the need for trimming. Figure 23.1(b) shows another type of pile toe protection attachment, which requires trimming of the pile toe.



(a)



(b)



(c)

Figure 23.1 Timber Pile Toe Attachments

23.1.2 Attachment at Pile Head

The American Wood Preservers Institute (AWPI) recommends banding timber piles with heavy metal strapping at the pile head prior to driving to prevent splitting. A photograph of a banded timber pile head is shown in Figure 23.2

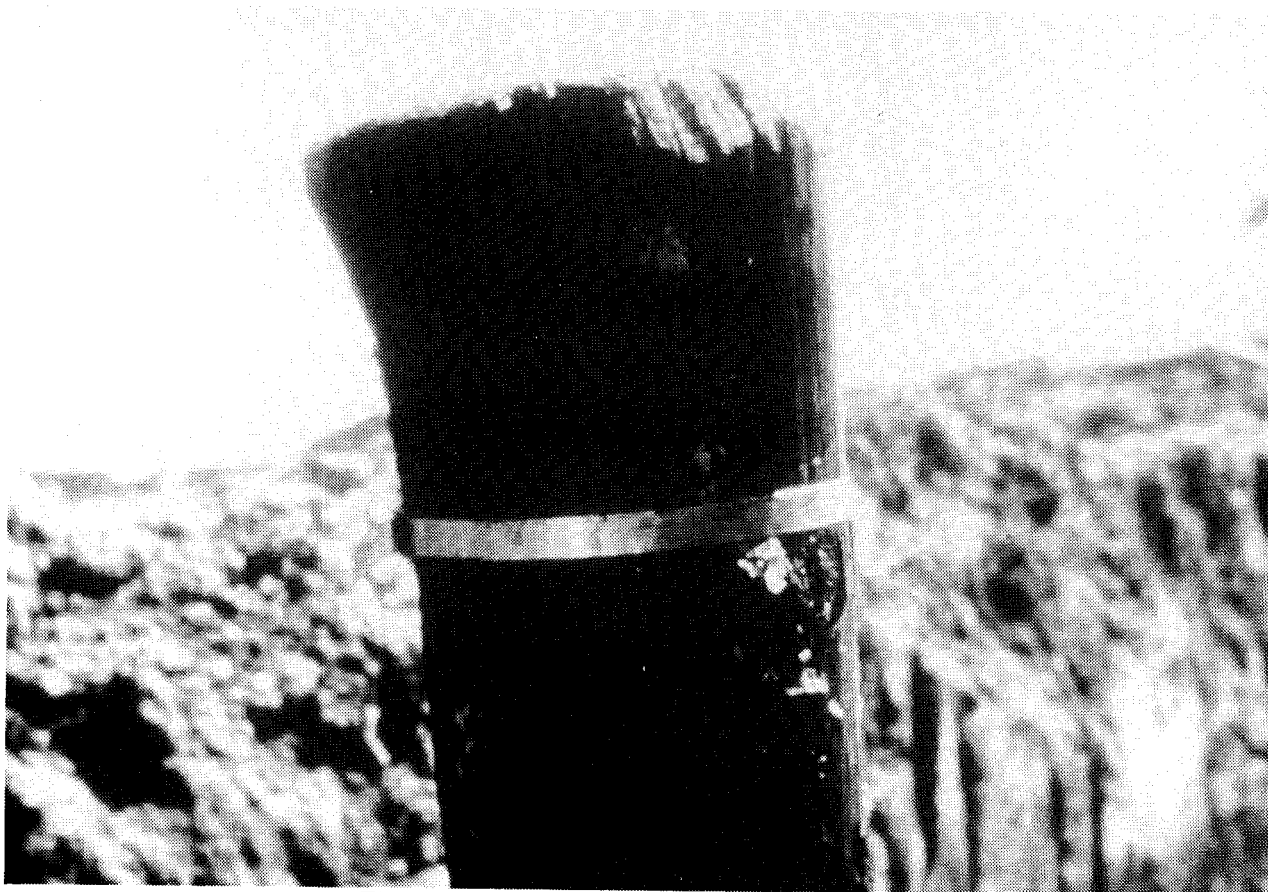


Figure 23.2 Banded Timber Pile Head

23.1.3 Splices

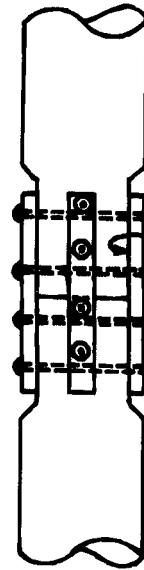
Timber pile splices are undesirable. It is virtually impossible to develop the full bending strength of the piling through simple splices such as those shown in Figure 23.3(a through c). In order to develop full bending strength, a detail similar to that shown in Figure 23.3(d) is required.



Both Ends Sawed
for Good Bearing

Metal Sleeve
(Trim Pile for
Tight Fit in Sleeve.
Drive Spikes
Through Sleeve
to Hold in Place
if Necessary)

(a)

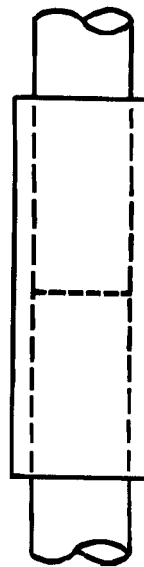


Trim for
Bearing

(b)



(c)



Concrete
Cover

(d)

Figure 23.3 Splices for Timber Piles

23.2 STEEL H-PILES

23.2.1 Pile Toe Attachments

Steel H-piles are generally easy to install due to the non-displacement character of the pile. Problems arise when driving H-piles through man-made fills, very dense gravel or deposits containing boulders. If left unprotected under these conditions, the pile toe may deform to an unacceptable extent and separation of the flanges and web may occur (Figure 23.4). Pile toe attachments can help prevent these problems. Such attachments are also desirable for H-piles driven to rock, particularly on sloping rock surfaces.

Pile toe reinforcement consisting of steel plates welded to the flanges and web are not recommended because the reinforcement provides neither protection nor increased strength at the critical area of the flange-to-web connection. Several manufactured driving shoes are available, as shown in Figure 23.5(a through d). These shoes are attached to the H-piles with fillet welds along the outside of each flange. Pile shoes fabricated from cast steel (ASTM A 27) are recommended because of their strength and durability.

Prefabricated H-pile shoes come in various shapes and sizes. Manufacturers also recommend different shapes for various applications. It is recommended that for a given set of subsurface conditions, pile shoes from different manufacturers should be considered as equivalent if they are manufactured from similar materials and by similar fabrication techniques. Minor variations in configuration should be given minimum importance, except in specific subsurface conditions where a certain shape would give a definite advantage.

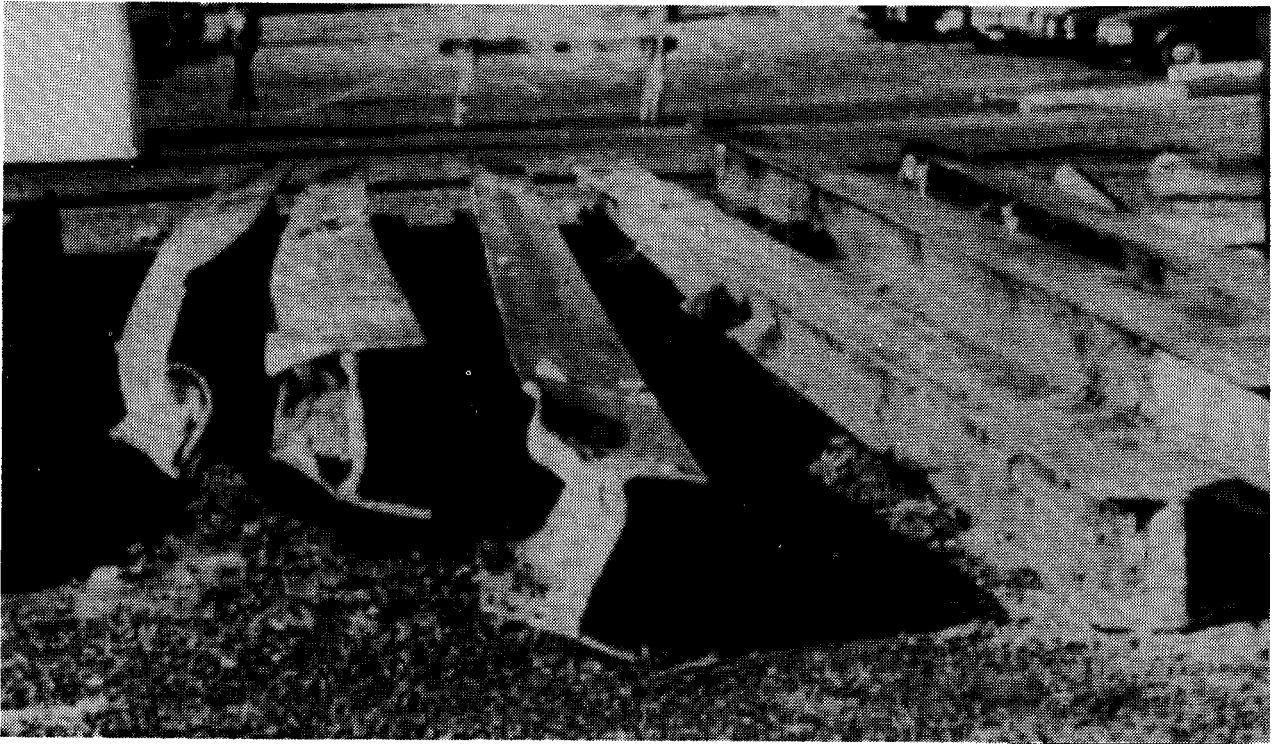


Figure 23.4 Damaged H-piles without Pile Toe Protection

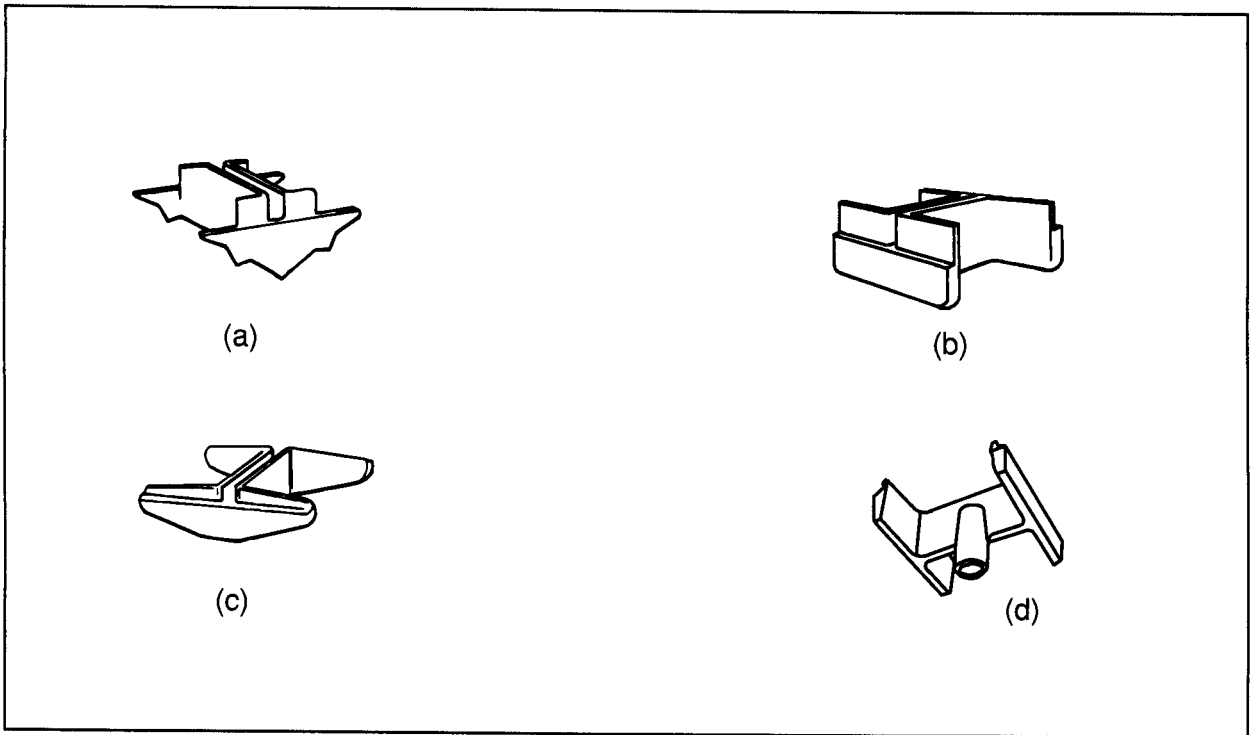


Figure 23.5 Driving Shoes for Protection of H-pile Toes

23.2.2 Splices

H-pile splices are routinely made by full penetration groove welding along the web and both flanges, or with manufactured splicers such as the ones shown in Figures 23.6(a) and 23.6(b). For the manufactured splicer shown, a notch is cut into the web of the driven section of pile and the splicer is slipped over the pile. Short welds are then made to the flanges near the corners of the splicer. The top section must have the flanges chamfered to achieve effective welding. Typically the section of pile to be added is positioned and held while welds across flanges are made. H-pile splicers are fabricated from ASTM A 36 steel. These splicers have been tested in the laboratory and the results have shown they provide full strength in bending as required by the AASHTO Bridge Specifications.

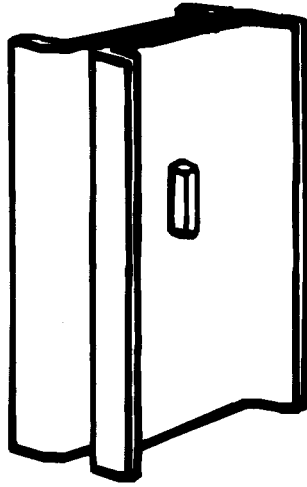
23.3 ACCESSORIES FOR STEEL PIPE PILES

23.3.1 Pile Toe Attachments

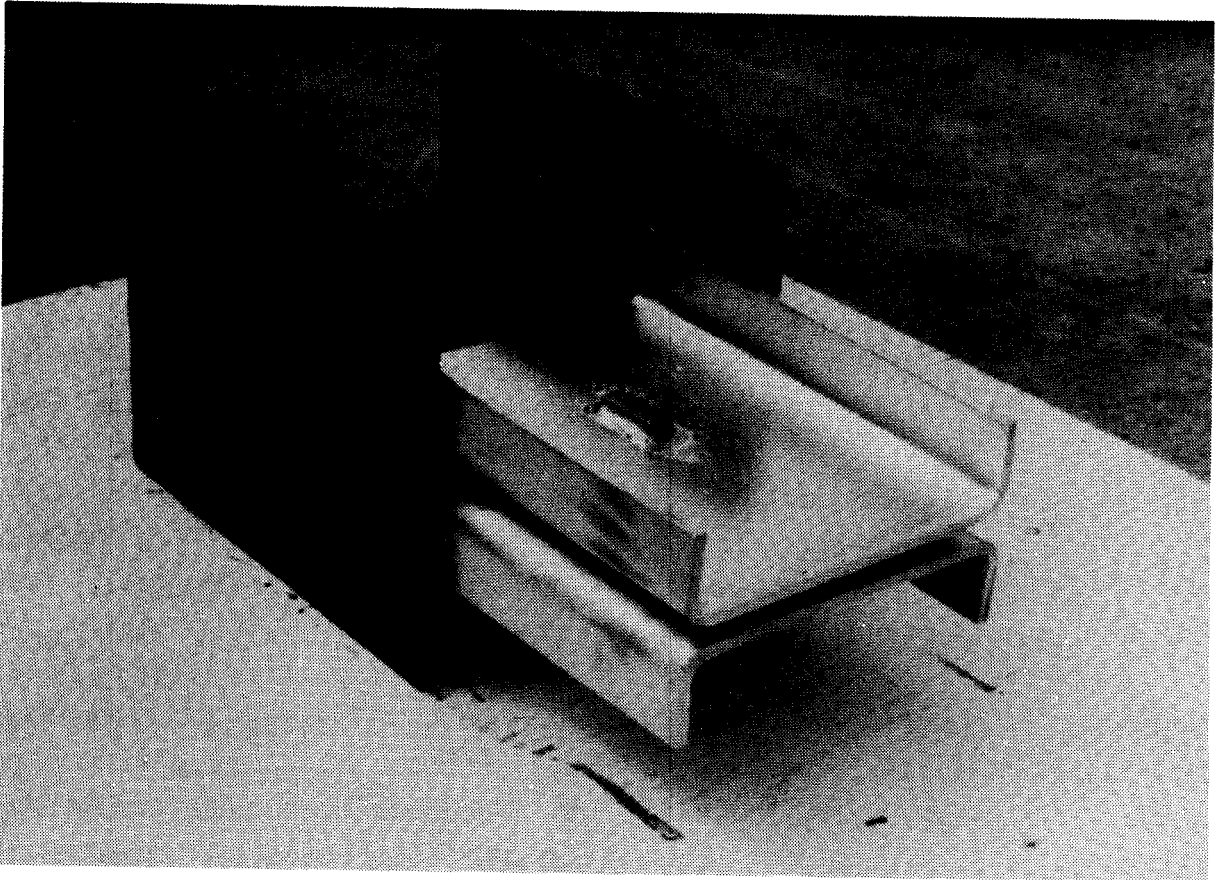
Problems during installation of closed end pipe piles arise when driving through materials containing obstructions. In this case, piles may deflect and deviate from their design alignment to an unacceptable extent. In case of driving open end pipe piles through or into very dense materials, the toe of the pile may be deformed. Pile toe attachments on closed end and open end piles are used to reduce the possibilities of damage and excessive deflection.

When pipe piles are installed with a closed end, a 12 to 25 mm thick flat plate is usually used as a form of toe protection. Conical toe attachments as shown in Figures 23.7(a) and 23.7(b) are also available as end-closures for pipe piles, although they generally cost more than flat plate type protection.

Generally, conical attachments have sixty degree configurations and are available with either an inside flange connection as shown in Figure 23.7(b) or outside flange connection as illustrated in Figure 23.7(a). The outside flange attachment can be driven with a press fit, so welding is not required. This additional benefit can save time and money.

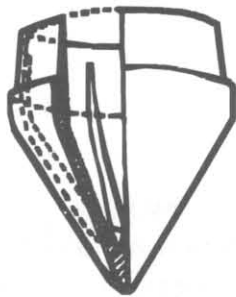


(a)

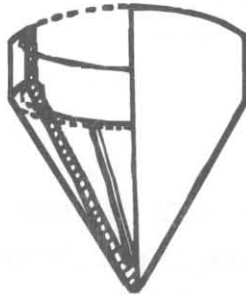


(b)

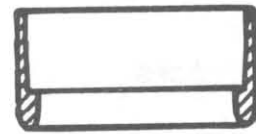
Figure 23.6 Typical H-pile Splicer



(a)



(b)



(c)



(d)

Figure 23.7 Pile Toe Attachments for Pipe Piles

When installing open end piles in dense gravel or to rock, the use of cutting shoes will help protect the piles and may make it possible to use thinner wall pipe. Cutting shoes are made from cast steel with a ridge for pile shoe bearing, as shown in Figure 23.7(c and d). Cutting shoes are welded to piles.

23.3.2 Splices

Full penetration groove welds or fillet welds as shown in Figure 23.8 are commonly used for splicing pipe piles. Pipe piles can also be spliced with manufactured splicers similar to the one shown in Figure 23.9. This splicer is fabricated from ASTM A 36 steel and is designed with a taper for a drive fit without welding so no advance preparation is required. Unless the drive fit or friction splicer is fillet welded to the pile, the splice will not provide full strength in bending.

23.4 PRECAST CONCRETE PILES

23.4.1 Pile Toe Attachments

The toe of precast concrete piles may be crushed in compression under hard driving. For hard driving conditions, or for end bearing on rock, special steel toe attachments can be used. Cast iron or steel shoes as depicted in Figure 23.10(a), or "Oslo Point" shown in Figure 23.10(b), are also used for toe protection. The characteristics of the Oslo Point are such that it can be chiseled into any type of rock to ensure proper seating. All toe attachments to precast concrete piles must be attached during casting of the piles and not in the field.

Another common type of toe attachment to increase concrete pile penetration depths in hard materials is a structural H sectional embedded in the pile, as shown in Figure 23.11. The H section extension is most often used to obtain additional penetration when uplift and scour are a concern. The H section should be proportionately sized to the concrete section to prevent overstressing and must be embedded sufficiently far for proper bonding and to develop bending strength. The H section should be protected by a H-pile toe attachment as discussed previously.

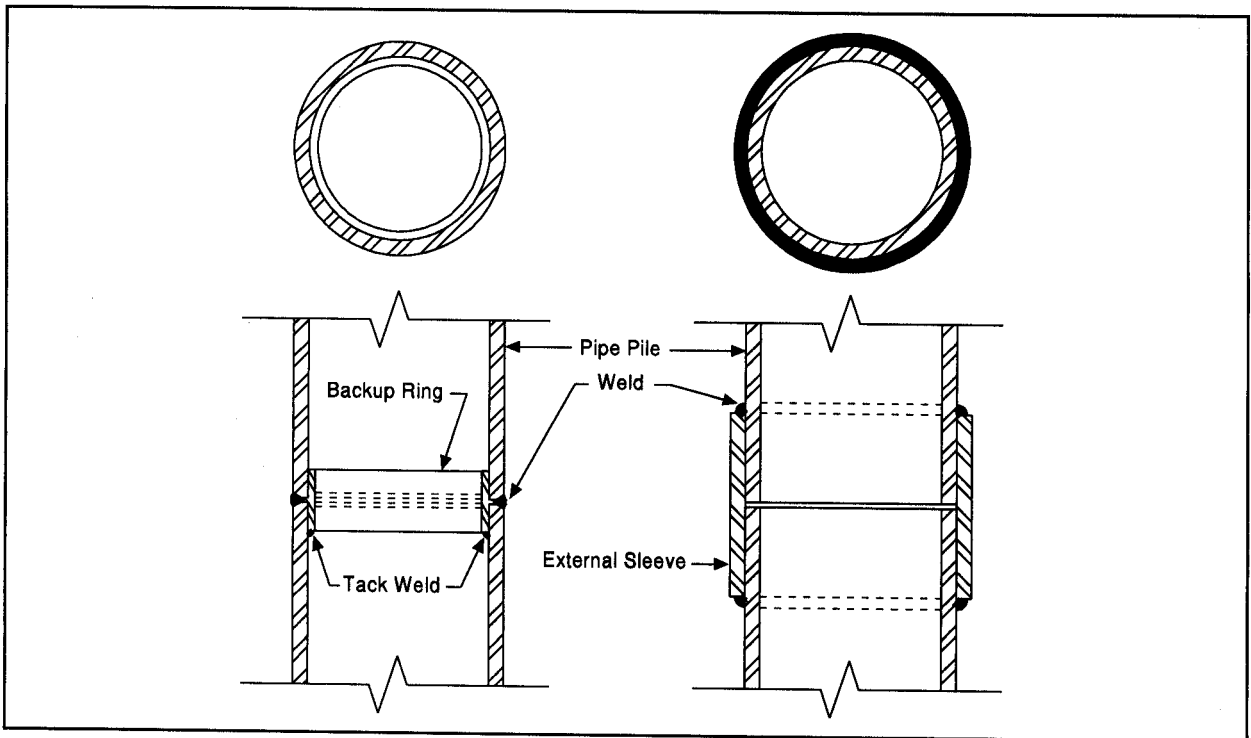


Figure 23.8 Splices for Pipe Piles

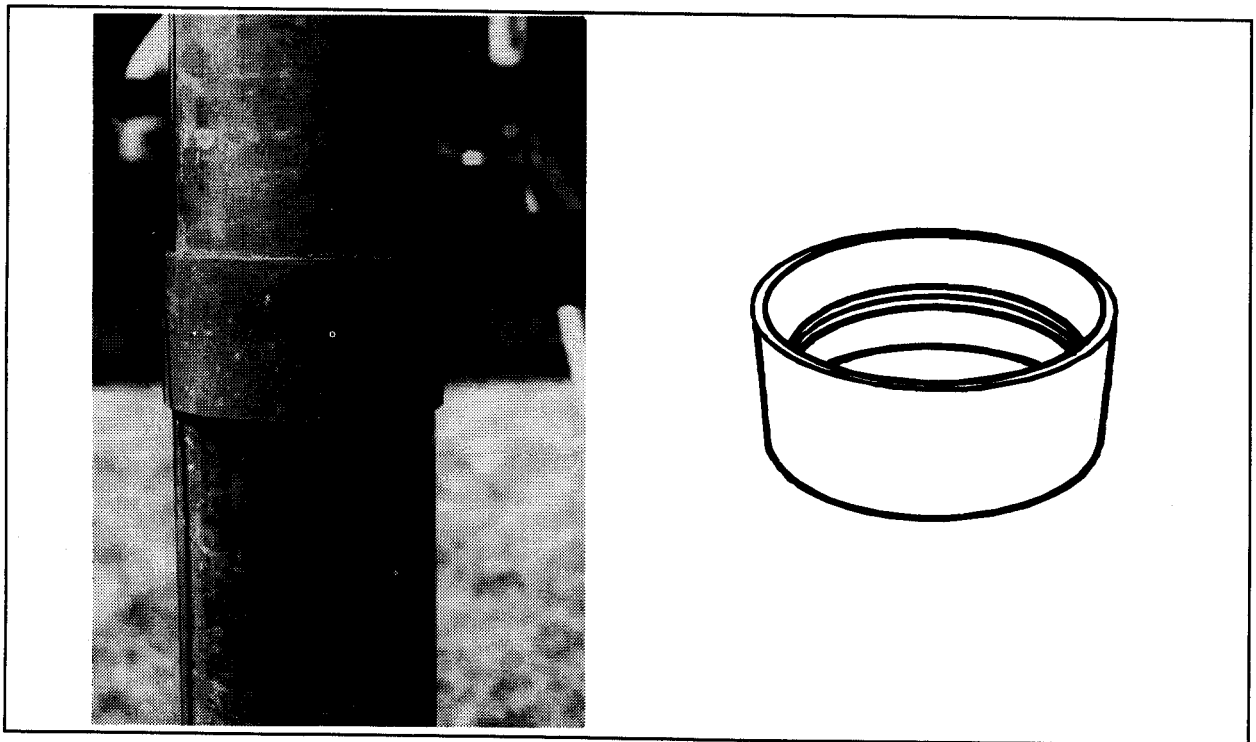


Figure 23.9 Splicer for Pipe Pile

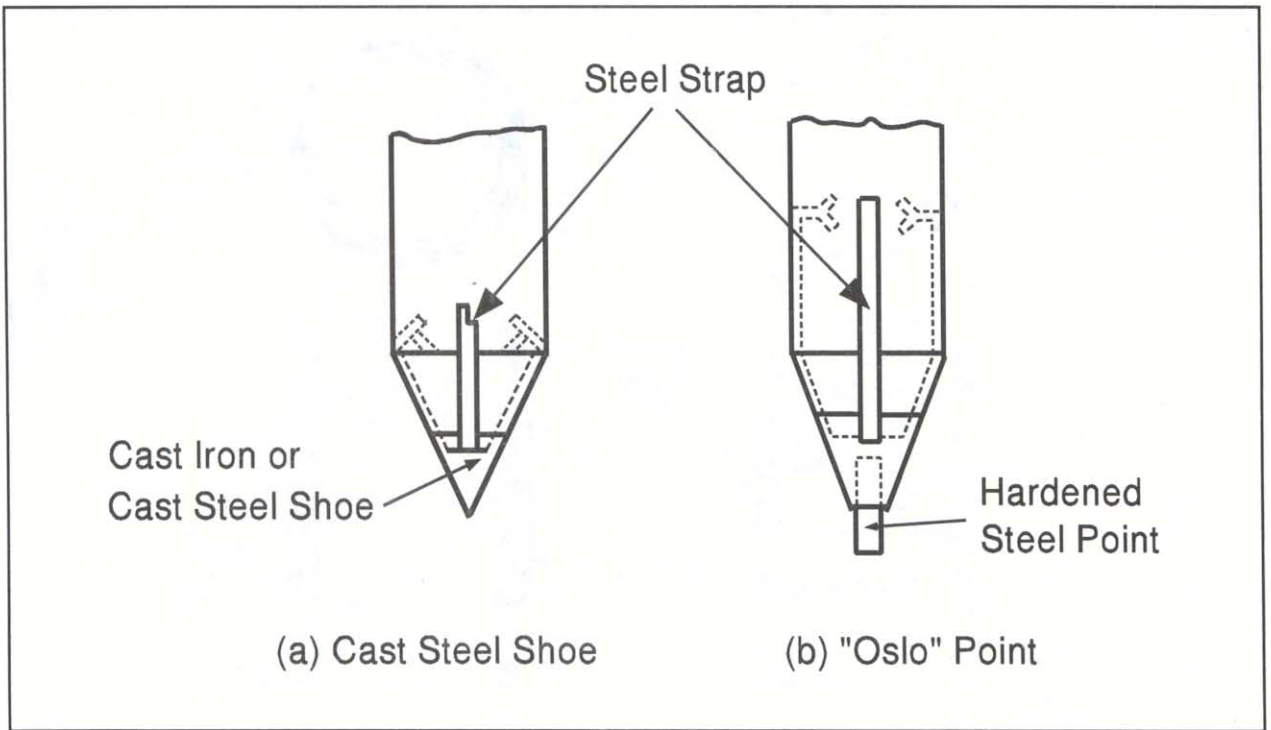


Figure 23.10 Pile Toe Attachments for Precast Concrete Piles

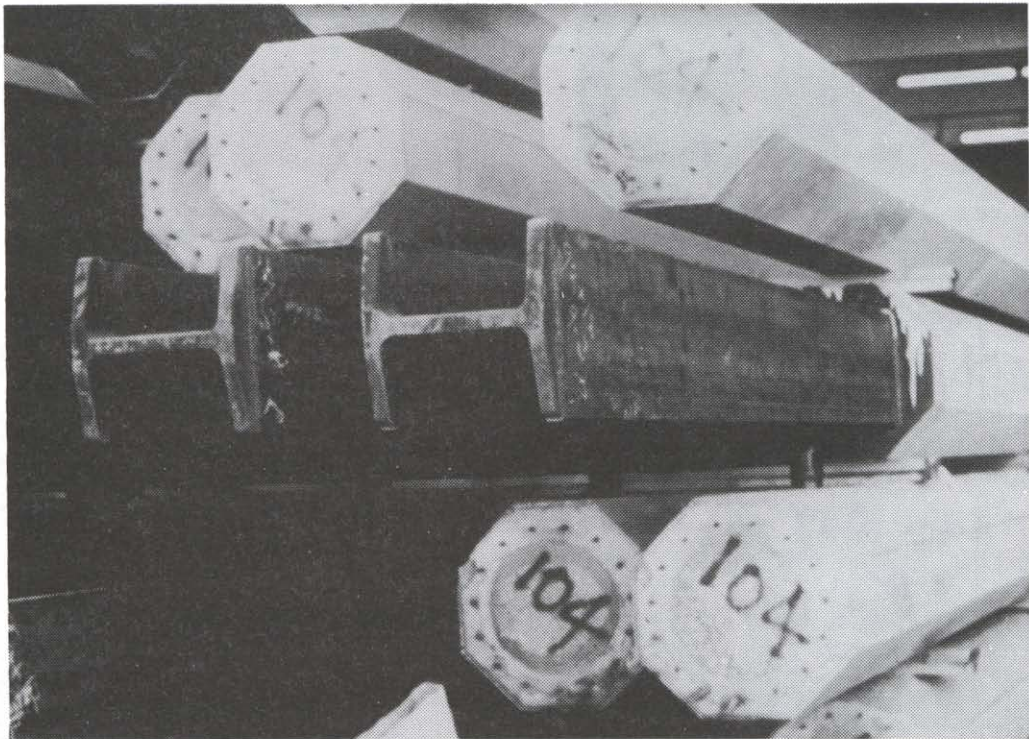


Figure 23.11 Steel H-pile Tip for Precast Concrete Pile

23.4.2 Splices

Most concrete piles driven in the United States are prestressed to minimize potential problems associated with handling and tension stresses during driving. However, the ends of prestressed concrete piles are not effectively prestressed due to development length, and thus special precautions must be taken when splicing prestressed concrete piles.

Table 23-1 from Bruce and Hebert (1974) shows a summary of splices for precast concrete piles. While this information is 20 years old, it still adequately summarizes the state of concrete pile splices. The table also provides guidelines concerning the compressive, tensile and flexural strength of the splice mechanisms. However, the actual performance of this and other splices should be evaluated on a project by project basis.

Whenever possible, concrete piles should be ordered with sufficient length to avoid splicing. However, if splicing is required, the splices available can be divided into four types: Dowel, Welded, Mechanical, and Sleeve. An overview of these splice types is given in Figure 23.12.

The generic epoxy dowel splice shown in Figure 23.13 can be used on prestressed and conventionally reinforced concrete piles. The bottom pile section to be spliced has holes which receive the dowels. These holes may be cast into the pile when splicing is planned, or drilled in the field when splicing is needed, but was unexpected. The bottom section is driven with no special consideration and the top section is cast with the dowel bars in the end of the pile. When spliced together in the field, the top section with the protruding dowels is guided and set in position and a thin sheet metal form is placed around the splice. Epoxy is then poured, filling the holes of the bottom section and the small space between the piles. The form can be removed after 15 minutes and driving resumed after curing of the epoxy. Dowel splices may be time consuming but are comparatively inexpensive. These splices have been proven reliable if dowel bars are of sufficient length and strength, and if proper application of the epoxy is provided. The number, length, and location of the dowel holes, as well as the dowel bar size, must be designed.

TABLE 23-1 SUMMARY OF PRECAST CONCRETE PILE SPLICES*

Name of Splice	Type	Origin	Approximate Size Range (mm)	Approximate Field Time minutes	Strength		
					Percent Compressive	Percent Tensile	Percent Flexural Cracking
Marrier	Mechanical	Canada	254-330	30	100	100	100
Herkules	Mechanical	Sweden	254-508	20	100	100	100
ABB	Mechanical	Sweden	254-305	20	100	100	100
NCS	Welded	Japan	305-1195	60	100	100	100
Tokyu	Welded	Japan	305-1195	60	100	100	100
Raymond cyl.	Welded	USA	914-1372	90	100	100	100
Bolognesi-Mor.	Welded	Argentina	Varied	60	100	55	100
Japanese bolted	Bolted	Japan	Varied	30	100	90	90
Brunsplice	Connect-ring	USA	305-355	20	100	20	50
Anderson	Sleeve	USA	Varied	20	100	0	100
Fuentes	Weld-sleeve	Puerto Rico	254-305	30	100	100	100
Hamilton form	Sleeve	USA	Varied	90	100	75	100
Cement dowel	Dowel	USA	Varied	45	100	40	65
Macalloy	Post-tension	England	Varied	120	100	100	100
Mouton	Combination	USA	254-355	20	100	40	100
Raymond wedge	Welded wedge	USA	Varied	40	100	100	100
Pile coupler	Connect-ring	USA	305-1372	20	100	100	100
Nilsson	Mechanical	Sweden	Varied	20	100	100	100
Wennstrom	Wedge	Sweden	Varied	20	100	100	100
Pogonowski	Mechanical	USA	Varied	20	100	100	100

* (after Bruce and Herbert, 1974)

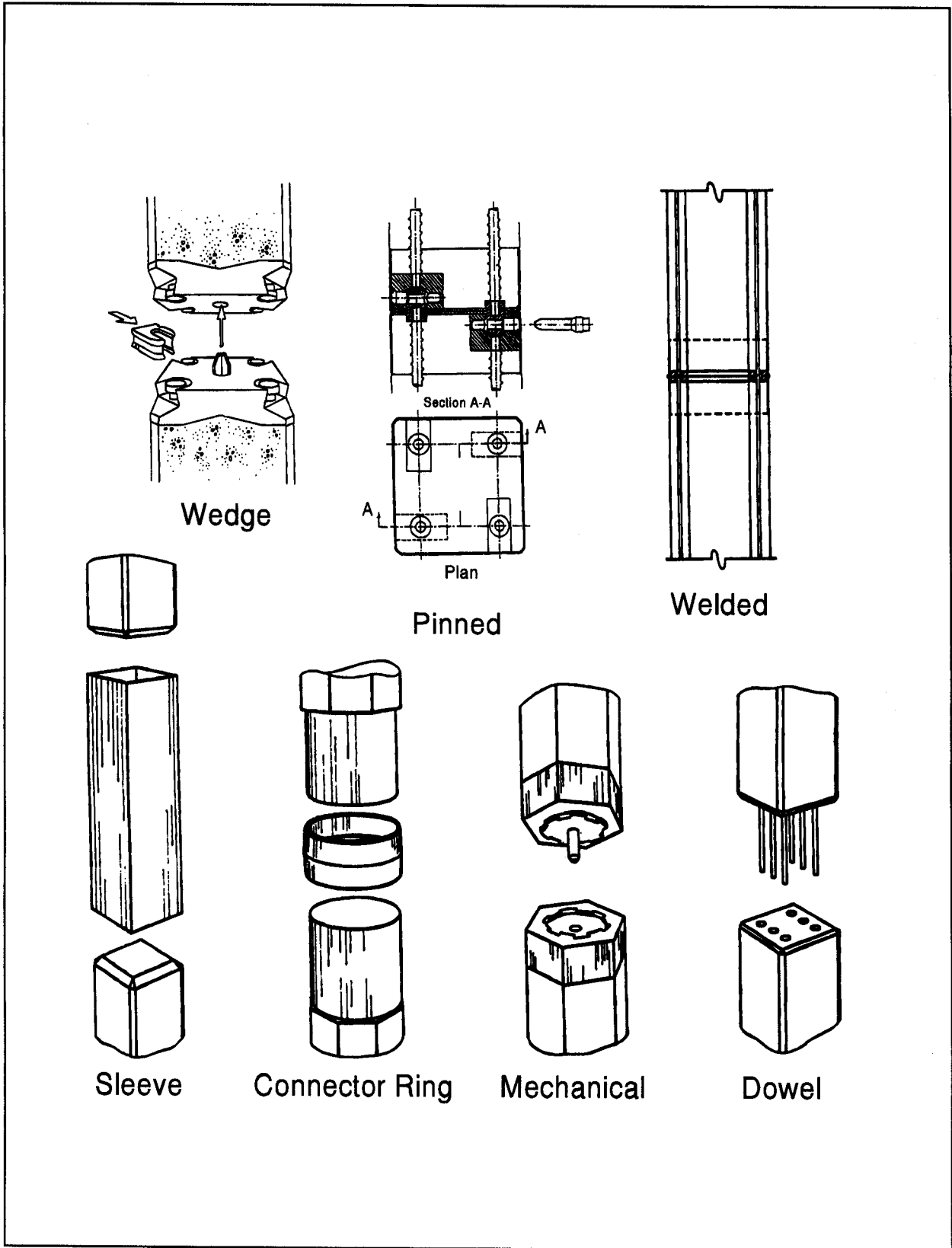


Figure 23.12 Commonly used Prestressed Concrete Pile Splices (after PCI, 1993)

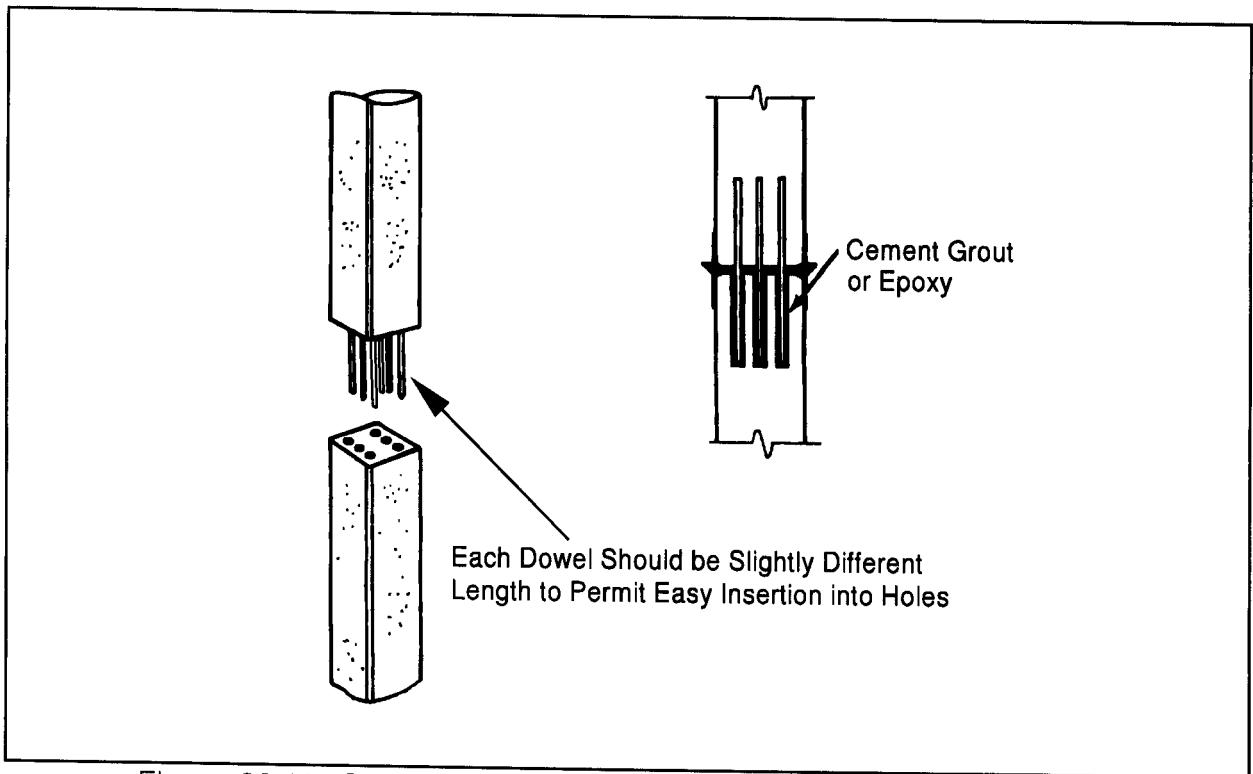


Figure 23.13 Cement-Dowel Splice (after Bruce and Herbert, 1974)

Welded splices require steel fittings be cast at the end of the sections to be spliced. The two sections are then welded around the entire perimeter. Most mechanical splices, such as the Herkules, Harddrive, Sure Lock, ABB, and Dyn-A-Splice, among others, are made of steel castings and are available for square, octagonal, hexagonal, and/or round sectional shapes. They can be used either for reinforced or prestressed concrete piles and are cast into the pile at the time of manufacture. The Herkules splice requires mating both male and female castings, while most other mechanical splices are gender neutral. All mechanical splices are then locked by inserting wedges, pins, keys, or other mechanical connections after aligning the sections. Although mechanical splices can be expensive, they do save considerable time and they have been designed to properly account for all loading conditions, including tension.

Sleeve type concrete splices can also be rapidly applied and are very effective in reducing tension driving stresses, but they cannot be used where static uplift loading will be required. The sleeve must have sufficient length and strength if lateral or bending loads are anticipated. The shorter connector ring design has limited tensile and flexural strength and is generally not recommended.

If a specific splice is specified based on previous experience, then an option for substituting some other concrete splice should not be allowed unless the substitute splicer is field tested. The alternative splice should be required to have equivalent compressive, tensile, and flexural strength to the originally specified splice. The substitute splicer can be tested by driving a number of spliced test piles and observing the performance.

23.5 A LIST OF MANUFACTURERS AND SUPPLIERS OF PILE ACCESSORIES

1. A-Joint Corporation (concrete splices)
P.O. Box 317
Voorhees, NJ 08043
Ph: 609-767-0609; Fax: 609-767-7458
2. National Ventures, Inc., Division of Agra Industries Ltd. (concrete splices)
198 Union Boulevard, Suite 200
Lakewood, CO 80238
Ph: 303-989-2800; Fax: 303-989-0667
3. Associated Pile and Fitting Corporation (shoes and splices)
P.O. Box 1048
Clifton, NJ 07014-1048
Ph: 800-526-9047, 201-773-8400; Fax: 201-773-8442
4. Dougherty Foundation Products (shoes and splicers)
P.O. Box 688
Franklin Lakes, NJ 07417
Ph: 201-337-5748; Fax: 201-337-9022
5. International Construction Equipment, Inc. (ICE)
301 Warehouse Drive
Matthews, NC 28105
Ph: 800-438-9281; Fax: 704-821-6448

6. International Pipe Products
P.O. Box 546
Ambridge, PA 15003
Ph: 412-266-8110; Fax: 412-266-4766

7. Mid-America Foundation Supply, Inc. (shoes)
P.O. Box 5198
Fort Wayne, IN 46895
Ph: 800-348-1890, 219-422-8767; Fax: 219-422-2040

8. Versabite Foundations Accessories (shoes and splices)
19600 S.W. Cipole Road
Tualatin, OR 97062
Ph: 800-678-8772; Fax: 503-692-5939

REFERENCES

- American Wood Preserves Institute (1981). Splicing Treated Timber Piling. AWPI Technical Guidelines for Pressure Treated Wood, 2.
- American Wood Preservers Institute (1981). Specification for Strapping Timber Piling, PH.
- Bruce, R.N. and Hebert, D.C. (1974). Splicing of Precast Prestressed Concrete Piles, Parts I and II, PCI Journal, Volume 19, No. 5 and 6, September-October and November-December, 1974.
- Dougherty, J.J. (1978). Accessories for Pile Installation. Presentation made at the ASCE Metropolitan Section Seminar on Pile Driving and Installation.
- PCI (1993). Precast/Prestressed Concrete Institute Journal. Volume 38, No. 2, March-April, 1993.

24. INSPECTION OF PILE INSTALLATION

Knowledgeable supervision and inspection play a very important role in the proper installation of pile foundations. The present trend in pile foundation design and construction is to use larger piles with higher load capacities, installed by larger equipment to achieve cost savings, made possible by advances in the state-of-the-art of design and construction methods. The inspection of these higher capacity pile installations becomes critical because of less redundancy (fewer piles required), and the smaller tolerances and factors of safety.

Inspection is only as good as the knowledge, experience and qualifications of the inspector. The inspector must understand the operation of the hammer and its accessories, the pile behavior, the soil conditions, and how these three components interact. Most pile installation problems are avoidable if a competent inspector uses systematic inspection procedures coupled with good communication and cooperation with the contractor. The inspector must be more than just a "blow counter". The inspector is the "eyes and ears" for the engineer and the owner. Timely observations, suggestions, reporting, and correction advice can ultimately assure the success of the project. **The earlier a problem or unusual condition is detected and reported by the inspector, the earlier a solution or correction in procedures can be applied, and hence a potentially negative situation can be limited to a manageable size.** If the same problem is left unattended, the number of piles affected increases, as do the cost of remediation and the potential for claims or project delays. Thus, early detection and reporting of any problem may be critical to keep the project on schedule and within budget.

An outline of inspection procedures and maintenance of pile driving records is provided in this chapter. Procedures and record keeping methods should be refined periodically as more experience is gathered by those responsible for construction operations.

24.1 ITEMS TO BE INSPECTED

There are several items to be checked by the inspector on every pile foundation project for test piles and/or production piles. Test piles may be driven for establishing order lengths or for load testing. Each of these items can be grouped under one of the following areas:

1. Review of the foundation design report, project plans and specifications prior to the arrival at the project site.
2. Inspection of piles prior to installation.
3. Inspection of pile driving equipment both before and during operation.
4. Inspection of test or indicator piles.
5. Inspection during production pile driving and maintenance of driving records.

A flow chart identifying the key components of the pile inspection process is presented in Figure 24.1.

24.2 REVIEW OF PROJECT PLANS AND SPECIFICATIONS

The first task of an inspector is to thoroughly review the project plans and specifications as they pertain to pile foundations. All equipment and procedures specified, including any indicator or test program of static and/or dynamic testing, should be clearly understood. If questions arise, clarification should be obtained from the originator of the specifications. The preliminary driving criteria should be known, as well as methods for using the test program results to adjust this criteria to site specific hammer performance and soil conditions. At this stage, the pile inspector should also determine the responsibility of his/her organization and should have answers to the following questions:

1. Is the inspector on the project in an observational capacity reporting to the foundation designer?, or

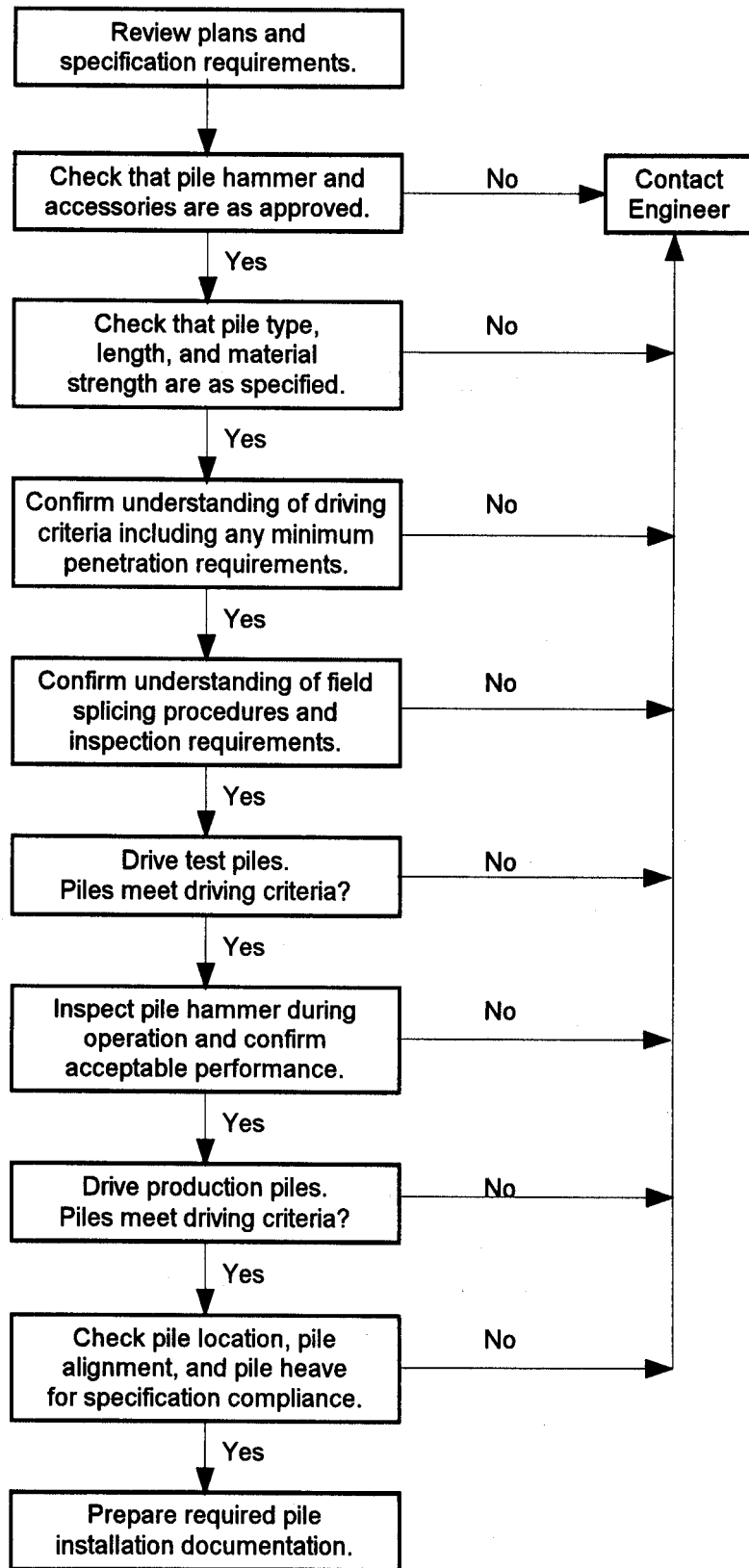


Figure 24.1 Pile Inspection Flow Chart

2. Does his/her organization have the direct responsibility to make decisions during driving of the test pile(s) and/or the production piles?

The inspector should also know:

1. Whom to contact if something goes wrong, and/or where to seek advice.
2. Whom to send copies of driving records and daily inspection reports.
3. What is required in the report during driving and at the completion of the project.

24.3 INSPECTOR'S TOOLS

The following check list, modified from Williams Earth Science (1995) summarizes the tools a pile inspector should have readily available to perform their job.

Approved Job Information

- Project Plans and Specifications with Revisions
- Special Provisions
- Pile Installation Plan
- Driving Criteria
- Casting/Ordered Lengths
- Approved Splice Detail

Daily Essentials

- Hard Hat
- Boots
- Ear Protection
- Pen/Pencil (and spare)
- Scale
- Measuring Tape
- Builder's Square
- Level
- Watch
- Calculator
- Camera

Indexed Notebook of Driven Piles

- Test Pile Program
- Production
- Construction Daily

Blank Forms

- Pile Driving Log
- Daily Inspection Reports
- Personal Diary

References

- State Standard Specifications
- Design and Construction of Driven Pile Foundations (Vol. II)
- Performance of Pile Driving Systems Inspectors Manual (FHWA/RD-86/160)

24.4 INSPECTION OF PILES PRIOR TO AND DURING INSTALLATION

The inspection check list will be different for each type of pile, but some items will be the same. A certificate of compliance for the piles is generally required by the

specifications. The inspector should obtain this certificate from the contractor and compare the specification requirements with the information provided on the certificate. The following sections contain specific guidance for each major pile type.

24.4.1 Timber Piles

Physical details for round timber piles are sometimes referred to in the ASTM pile specification, ASTM D25. Regardless of the referenced specifications, the following items should be checked for compliance:

- a. The timber should be of the specified species.
- b. The piles should have the specified minimum length, and have the correct pile toe and butt sizes. The pile butt must be cut squarely with the pile axis.
- c. The twist of spiral grain and the number and distribution of knots should be acceptable.
- d. The piles should be acceptably straight.
- e. The piles must be pressure treated as specified.
- f. The pile butts and/or toe may require banding as detailed in Chapter 23.
- g. Steel shoes which may be specified must be properly attached. Details are provided in Chapter 23.
- h. Pile splices, if allowed by plans and specifications, must meet the project requirements.

24.4.2 Precast Concrete Piles

On many projects, inspection and supervision of casting operations for precast concrete piles is provided by the State transportation department. Frequently, in lieu of this inspection, a certificate of compliance is required from the contractor. The following checklist provides items to be inspected at the casting yard (when applicable):

- a. Geometry and other characteristics of the forms.
- b. Dimensions, quantity, and quality of spiral reinforcing and prestressing steel strands, including a certificate indicating that the prestressing steel meets specifications.
- c. If the pile is to have mechanical or welded splices, or embedded toe protection, the splice or toe protection connection details including number, size and lengths of dowel bars should be checked for compliance with the approved details and for the required alignment tolerance. They should be cast within tolerance of the true axial alignment.
- d. Quality of the concrete (mix, slump, strength, etc.) and curing conditions.
- e. Prestressing forces and procedures, including time of release of tension, which is related to concrete strength at time of transfer.
- f. Handling and storage procedures, including minimum curing time for concrete strength before removal of piles from forms.

The following is a list of items for prestressed concrete piles to be inspected at the construction site:

- a. The piles should be of the specified length and section. Many specifications require a minimum waiting period after casting before driving is allowed. Alternatively, the inspector must be assured that a minimum concrete strength has been obtained. If the piles are to be spliced on the site, the splices should meet the specified requirements (type, alignment, etc.).
- b. There should be no evidence that any pile has been damaged during shipping to the site, or during unloading of piles at the site. Lifting hooks are generally cast into the piling at pick-up points. Piles should be unloaded by properly sized and tensioned slings attached to each lifting hook. Piles should be inspected for cracks or spalling.

- c. The piles should be stored properly. When piles are being placed in storage, they should be stored above ground on adequate blocking in a manner which keeps them straight and prevents undue bending stresses.
- d. The contractor should lift the piles into the leads properly and safely. Cables looped around the pile are satisfactory for lifting. Chain slings should never be permitted. Cables should be of sufficient strength and be in good condition. Frayed cables are unacceptable and should be replaced. For shorter piles, a single pick-up point may be acceptable. The pick-up point locations should be as specified by the casting yard. For longer piles, two or more pick-up points at designated locations may be required.
- e. The pile should be free to twist and move laterally in the helmet.
- f. Piles should have no noticeable cracks when placed in leads or during installation. Spalling of the concrete at the top or near splices should not be evident.

24.4.3 Steel H-Piles

The following should be inspected at the construction site:

- a. The piles should be of the specified steel grade, length, or section/weight.
- b. Pile shoes, if required for pile toe protection, should be as specified. Pile shoe details are provided in Chapter 23.
- c. Splices should be either proprietary splices or full penetration groove welds as specified. The top and bottom pile sections should be in good alignment before splicing. Pile splice details are discussed in Chapter 23.
- d. Pile shoe attachments and splices must be welded properly.
- e. The piles being driven must be oriented with flanges in the correct direction as shown on the plans. Because the lateral resistance to bending of H-piles is considerably more in the direction perpendicular to flanges, the correct orientation of H-piles is very important.

- f. There should be no observable pile damage, including deformations at the pile head.

24.4.4 Steel Pipe Piles

The following should be inspected at the construction site:

- a. The piles should be of specified steel grade, length, or minimum section/weight (wall thickness) and either seamless or spiral welded as specified.
- b. Piles should be driven either open-ended or closed-ended. Closed-ended pipe piles should have bottom closure plates or conical points of the correct size (diameter and thickness) and be welded on properly, as specified. Open end pipe piles should have cutting shoes that are welded on properly.
- c. The top and bottom pile sections should be in good alignment before splicing. Splices or full penetration groove welds should be installed as specified. Pile splice details are discussed in Chapter 23.
- d. There should be no observable pile damage, including deformations at the pile head. After installation, closed-end pipes should be visually inspected for damage or water prior to filling with concrete.

24.5 INSPECTION OF DRIVING EQUIPMENT

A typical driving system consists of crane, leads, hammer, hammer cushion, helmet, and in the case of concrete piles, a pile cushion. As discussed in Chapter 22, each component of the drive system has a specific function and plays an important role in the pile installation. The project plans and specifications may specify or restrict certain items of driving equipment. The inspector must check the contractor's driving equipment and obtain necessary information to determine conformity with the plans and specifications prior to the commencement of installation operations.

The following checklist will be useful in the inspection of driving equipment before driving:

1. The pile driving hammer should be the specified type/size.

Usually the specifications require certain hammer types and/or specify minimum and/or maximum energy ratings. A listing of hammer energy ratings is provided in Appendix D. The inspector should make sure for single acting air/steam or hydraulic hammers that the contractor uses the proper size external power source and that, for adjustable stroke hammers, the stroke necessary for the required energy be obtained. For double acting or differential air/steam or hydraulic hammers, the contractor must again obtain the proper size external power source and the operating pressure and volume must meet the hammer manufacturer's specification. For open end diesel hammers, the inspector should obtain a chart for determining stroke from visual observation, or alternatively have available a device for electronically estimating the stroke from the blow rate. For closed end diesel hammers, the contractor should supply the inspector with a calibration certificate for the bounce chamber pressure gauge and a chart which correlates the bounce chamber pressure with the energy developed by the hammer. The bounce chamber pressure gauge should be provided by the contractor.

2. The hammer cushion being used should be checked to confirm it is of the approved material type, size and thickness.

The main function of the hammer cushion is to protect the hammer itself from fatigue and high frequency accelerations which would result from steel to steel impact with the helmet and/or pile. The hammer cushion should have the proper material and same shape/area to snugly fit inside the helmet (drive cap). If the cushion diameter is too small, the cushion will break or badly deform during hammer blows and become ineffective. The hammer cushion must not be excessively deformed or compressed. Some air/steam hammers rely upon a certain total thickness (of cushion plus striker plate) for proper valve timing. Hammers with incorrect hammer cushion thickness may not operate, or will have improper kinetic energy at impact. Since it is difficult to inspect this item once the driving operation begins, it should be checked before the contractor starts pile driving on a project as well as periodically during production driving on larger projects. A photograph of a hammer cushion check is presented in Figure 24.2.

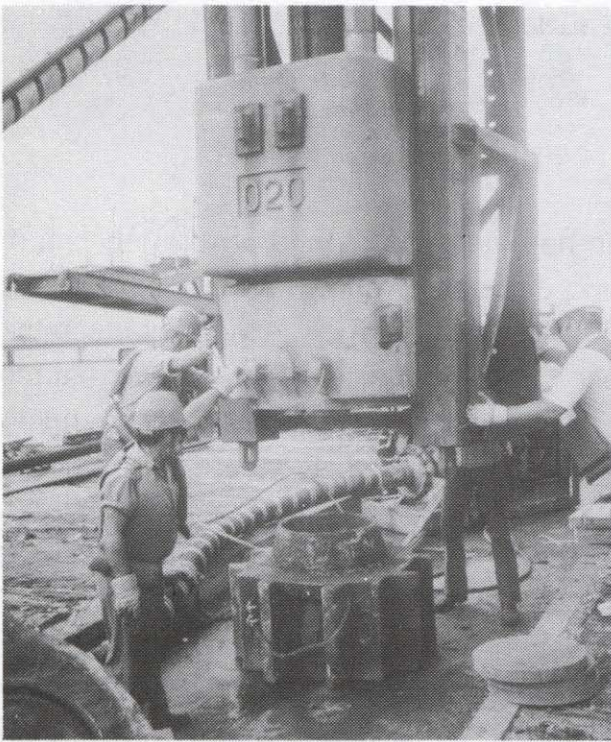


Figure 24.2 Hammer Cushion Check



Figure 24.3 Damaged Hammer Cushion

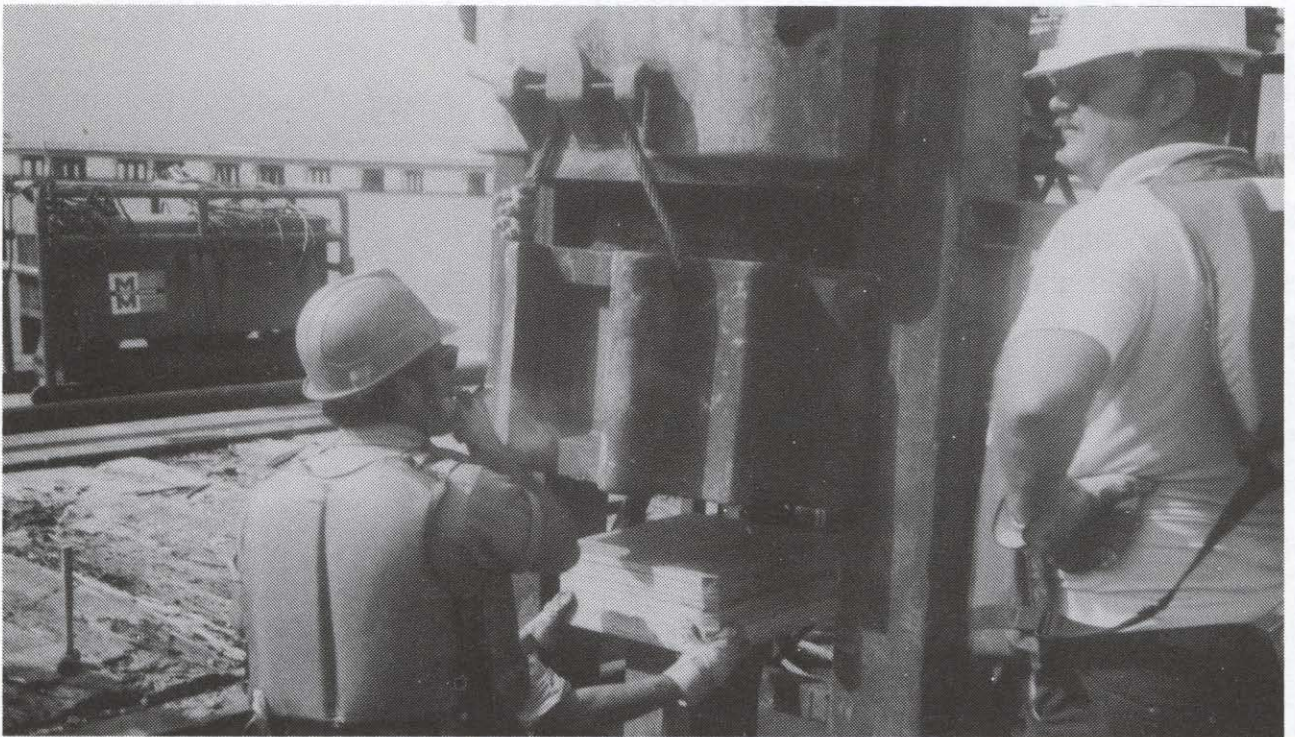


Figure 24.4 Pile Cushion Replacement

The hammer cushion material disks are shown in the lower right corner of the photograph. A damaged hammer cushion detected by a hammer cushion check is shown in Figure 24.3.

3. The helmet (drive cap) should properly fit the pile.

The purpose of the helmet is to hold the pile head in alignment and transfer the impact concentrically from the hammer to the pile. The helmet also houses the hammer cushion, and must accommodate the pile cushion thickness for concrete piles. The helmet should fit loosely to avoid transmission of torsion or bending forces, but not so loosely as to prevent the proper alignment of hammer and pile. Helmets should ideally be of roughly similar size to the pile diameter. Although generally discouraged, spacers may be used to adapt an oversize helmet, provided the pile will still be held concentrically with the hammer. A properly fitting helmet is important for all pile types, but is particularly critical for precast concrete piles. A poorly fitting helmet often results in pile head damage. Check and record the helmet weight for conformance to wave equation analysis or for future wave equation analysis. Larger weights will reduce the energy transfer to the pile.

4. The pile cushion should be of correct type material and thickness for concrete piles.

The purpose of the pile cushion is to reduce high compression stresses, to evenly distribute the applied forces to protect the concrete pile head from damage, and to reduce the tension stresses in easy driving. Pile cushions for concrete piles should have the required thickness determined from a wave equation analysis but not less than 100 mm. A new plywood, hardwood, or composite wood pile cushion, which is not water soaked, should be used for every pile. The cushion material should be checked periodically for damage and replaced before excessive compression (more than half the original thickness), burning, or charring occurs. Wood cushions may take only about 1,000 to 2,000 blows before they deteriorate. During hard driving, more than one cushion may be necessary for a single pile. Longer piles or piles driven with larger hammers may require thicker pile cushions. A photograph of a pile cushion being replaced is presented in Figure 24.4.

5. Predrilling, jetting or spudding equipment, if specified or permitted, should be available for use and meet the requirements. The depth of predrilling, jetting or spudding should be very carefully controlled so that it does not exceed the

allowable limits. Predrilling, jetting, or spudding below the allowed depths will generally result in a reduced pile capacity, and the pile acceptance may become questionable. Additional details on predrilling, jetting, and spudding are presented in Chapter 22.

6. The lead system being used must conform to the requirements, if any, in the specifications. Lead system details are presented in Chapter 22.

The leads perform the very important function of holding the hammer and pile in good alignment with each other. Poor alignment reduces energy transfer as some energy is then imparted into horizontal motion. Poor alignment also generally results in higher bending stresses and higher local contact stresses which can cause pile damage. This is particularly important at end of driving when driving resistance is highest and driving stresses are generally increased. Sometimes the specifications do not allow certain lead systems or may require a certain type system. A pile gate at the lead bottom which properly centers the pile should be required, as it helps maintain good alignment.

Note: On most projects, a wave equation analysis is used to determine preliminary driving criteria for design and/or construction control. The contractor is usually required to provide a pile and driving equipment data form similar to Figure 17.3 and obtain prior approval from the State transportation agency. Even if wave equation analysis is not required, this form should be included in the project files so a wave equation analysis could be performed in the future. This form can also function as a check list for the inspector to compare the proposed equipment with the actual equipment on-site.

24.6 INSPECTION OF DRIVING EQUIPMENT DURING INSTALLATION

The main purpose of inspection is to assure that piles are installed so that they meet the driving criteria and the pile remains undamaged. The driving criteria is often defined as a minimum driving resistance as measured by the blow count in blows per 0.25 meter. The driving criteria is to assure that piles have the desired capacity. However, the driving resistance is also dependent upon the performance of the pile driving hammer. The driving resistance will generally be lower when the hammer imparts higher energy and force to the pile, and the driving resistance will be higher if the hammer imparts lower energy and force to the pile. High driving resistances can be due either to soil

resistance or to a poorly performing hammer. Thus, for the inspector to assure that the minimum driving criteria has been met and therefore the capacity is adequate, the inspector must evaluate if the hammer is performing properly.

Each hammer has its own operating characteristics; the inspector should not blindly assume that the hammer on the project is in good working condition. In fact, two different types of hammers with identical energy rating will not drive the same pile in the same soil with the same driving resistance. In fact, two supposedly identical hammers (same make and model) may not have similar driving capability due to several factors including differing friction losses, valve timing, air supply hose type-length-condition, fuel type and intake amount, and other maintenance status items. The inspector should become familiar with the proper operation of the hammer(s) used on site. The inspector may wish to contact the hammer manufacturer or supplier who generally will welcome the opportunity to supply further information. The inspector should review the operating characteristics for the hammer which are included in Chapter 22. The following checklists briefly summarize key hammer inspection issues.

24.6.1 Drop Hammers

- a. Determine/confirm the ram weight. Ram weight can be calculated from the ram volume and steel density of 78.5 kN/m^3 if necessary.
- b. The leads should have sufficient tolerance and/or the guides greased to allow the ram to fall without obstruction or binding.
- c. Make sure the desired stroke is maintained. Low strokes will reduce energy. Excessively high strokes increase pile stresses and could cause pile damage.
- d. Make sure the helmet stays properly seated on the pile and that the hammer and pile maintain alignment during operation.
- e. Make sure the hammer hoist line is spooling out freely during the drop and at impact. If the hoist line drags, less energy will be delivered. If the crane operator catches the ram too early, not only is less energy delivered, but energy is transmitted into the hoist line, crane boom, and hoist, which could cause maintenance and/or safety problems.

24.6.2 Single Acting Air/Steam Hammers

- a. Determine/confirm the ram weight. Ram weight can be calculated from the ram volume and steel density of 78.5 kN/m^3 if necessary. Check for and record any identifying labels as to hammer make, model and serial number.
- b. Check the air or steam supply and confirm it is of adequate capacity to provide the required pressure and flow volume. Also check the number, length, diameter, and condition of the air/steam hoses. Manufacturers provide guidelines for proper compressors and supply hoses. Air should be blown through the hose before attaching it to the hammer. The motive fluid lubricator should occasionally be filled with the appropriate lubricant as specified by the manufacturer. During operation, check that the pressure at the compressor or boiler is equal to the rated pressure plus hose losses. The pressure should not vary significantly during driving. The photograph of an air compressor display panel in Figure 24.5 illustrates the discharge pressure dial that should be checked.
- c. Visually inspect the slide bar and its cams for excessive wear. Some hammers can be equipped with a slide bar with dual set of cams to offer two different strokes. The stroke can be changed with a valve, usually operated from the ground. Measure the stroke being attained and confirm it meets specification.
- d. Check that the columns or ram guides, piston rod, and slide bar are well greased.
- e. For most air/steam hammers, the total thickness of hammer cushion and striker plate must match the hammer manufacturer's recommendation and the hammer cushion cavity in the helmet for proper valve timing and hammer operation. This thickness must be maintained and should be checked before placing the helmet into the leads, and thereafter by comparison of cam to valve position and/or gap between ram and hammer base when the ram is at rest on the pile top.
- f. Make sure the helmet stays properly seated on the pile and that the hammer and pile maintain alignment during operation.
- g. The ram and column keys used to fasten together hammer components should all be tight.

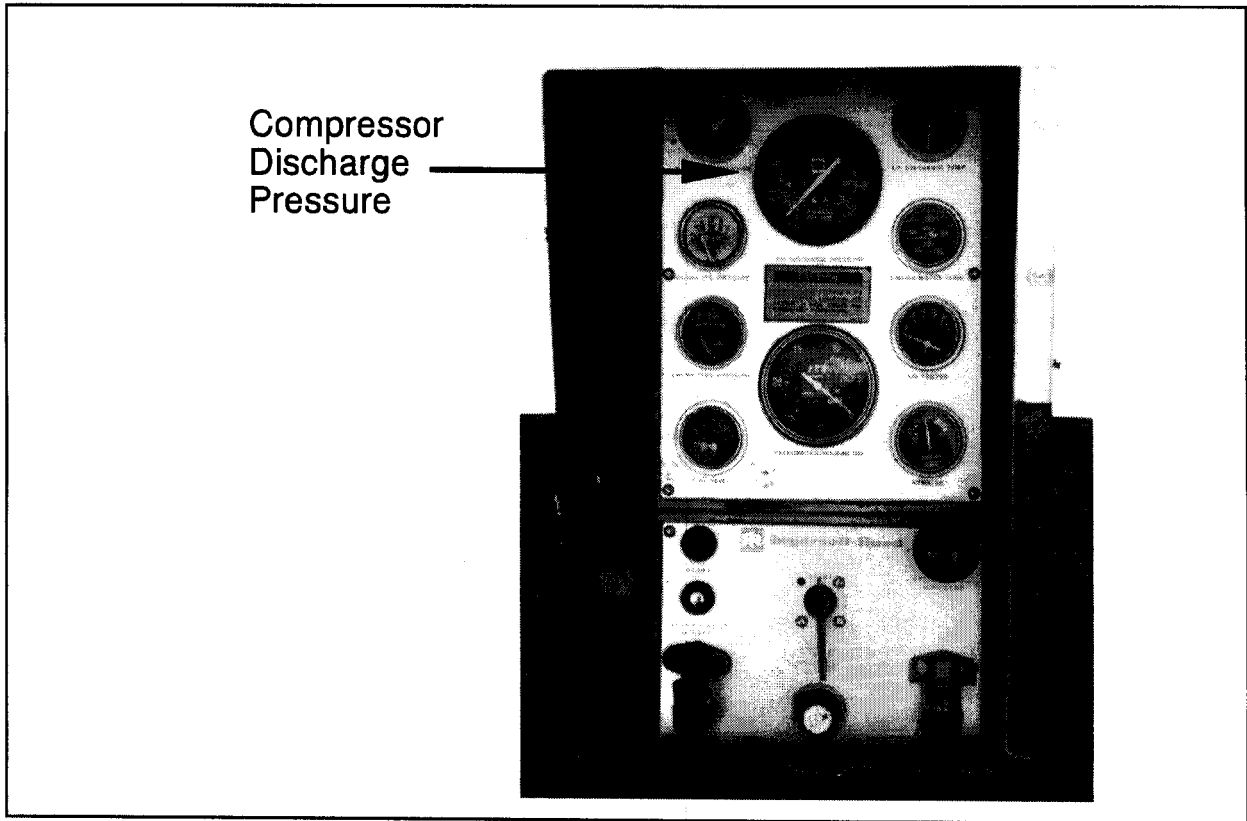


Figure 24.5 Air Compressor Display Panel

- h. The hammer hoist line should always be slack, with the hammer's weight fully carried by the pile. Excessive tension in the hammer hoist line is a safety hazard and will reduce energy to the pile. Leads should always be used.
- i. Compare the observed hammer speed in blows per minute near end of driving with the manufacturer's specifications. Blows per minute can be timed with a stopwatch or a saximeter. Slower operating rates may imply a short stroke (from inadequate pressure or volume, restricted or undersized hose, or inadequate lubrication) or improper valve timing (possibly from incorrect cushion thickness or worn parts). Erratic hammer operation, such as skipping blows, can result from improper cushion thickness, poor lubrication, foreign material in a valve, faulty valve/cam system, or loose hammer fasteners or keys.
- j. As the driving resistance increases, the ram stroke may also increase, causing it to strike the upper hammer assembly and lifting the hammer ("racking") from the pile. If this behavior is detected, the air pressure flow should be reduced

gradually until racking stops. The flow should not be overly restricted so that the stroke is reduced.

- k. Some manufacturers void their warranty if the hammer is consistently operated above 100 blows per 250 mm of penetration beyond short periods such as required when toe bearing piles are driven to rock. Therefore, in prolonged hard driving situations, it may be more desirable to use a larger hammer or stiffer pile section.
- l. Common problems and problem indicators for air/steam hammers are summarized in Table 24-1.

TABLE 24-1 COMMON PROBLEMS AND PROBLEM INDICATORS FOR AIR/STEAM HAMMERS (from Williams Earth Sciences, 1995)	
Common Problems	Indicators
Air trip mechanism on hammer malfunctioning.	Erratic operation rates or air valve sticking open or close.
Cushion stack height not correct (affects timing of trip mechanism air valve).	Erratic operation rates.
Compressor not supplying correct pressure and volume of air to hammer.	Blows per minute rate is varying either faster or slower than the manufacturer specified.
Air supply line kinked or tangled in leads, boom or other.	Visually evident.
Moisture in air ices up hammer.	Ice crystals exiting exhaust ports of hammer.
Lack of lubricant in air supply lines.	Erratic operation rates.
Packing around air chest worn, allowing air blow by.	Ram raises slowly - blows per minute rate slower than manufacturer specifications - air leaking around piston shaft and air chest.
Nylon slide bar worn.	Visually evident.
Ram columns not sufficiently greased.	Visually evident.

An inspection form for single and differential acting air/steam hammers is provided in Figure 24.6. The primary feature of this form is the three column area in the middle of the form. The left column illustrates the key objects of the driving system. The middle column contains the manufacturer's requirements for key objects and the right column is used to record the observed condition of those objects. This format allows the inspector to quickly identify potential problems and an immediate correction may be possible. The hammer inspection form is intended to be used periodically during the course of the project as a complement to the pile driving log.

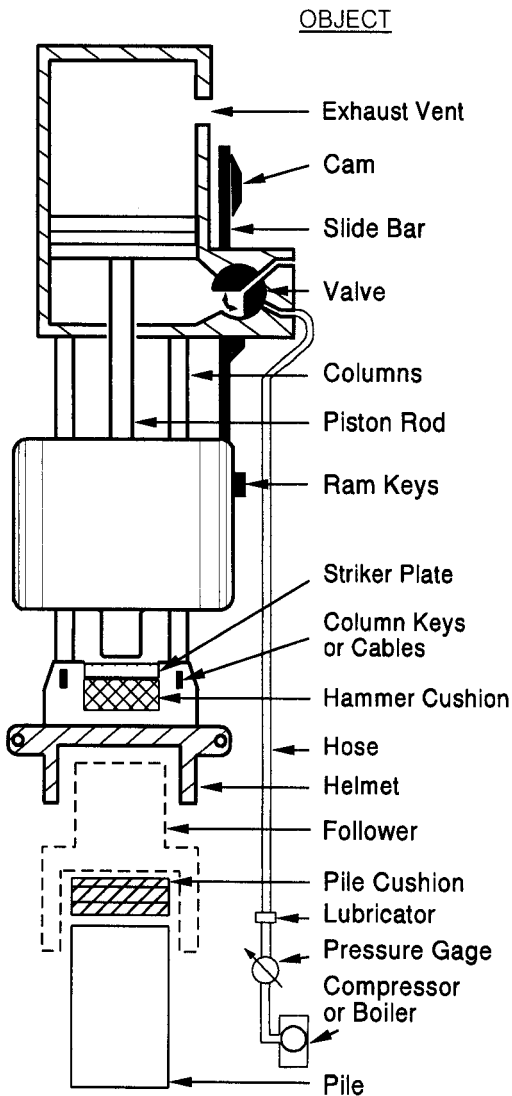
The bottom portion of the hammer inspection form contains an area where observations at final driving should be recorded. This information may be particularly interesting to an engineer who has performed a wave equation analysis as the actual situation can then be compared to the analyzed one. Therefore, it is recommended that a copy of the completed hammer inspection form be provided to appropriate design and construction personnel.

24.6.3 Double Acting or Differential Air/Steam Hammers

- a. Determine/confirm the ram weight. Ram weight can be calculated from the ram volume and steel density of 78.5 kN/m^3 if necessary. Check for and record any identifying labels as to hammer make, model and serial number.
- b. Check the air or steam supply and confirm it is of adequate capacity to provide the required pressure and flow volume. This is extremely important since approximately half the rated energy comes from the pressure on the ram during the downstroke. Check also the number, length, diameter, and condition of the air/steam hoses. Manufacturers provide guidelines for proper compressors and supply hoses. Air should be blown through the hose before attaching it to the hammer. The motive fluid lubricator should occasionally be filled with the appropriate lubricant as specified by the manufacturer. During operation, check that the pressure at the compressor or boiler is equal to the rated pressure plus hose losses. The pressure should not vary significantly during driving. Record the pressure at the beginning of driving.

Project/Pile: _____
 Date: _____
 Conditions: _____

Hammer Name: _____
 Serial No: _____



OBJECT

REQUIREMENTS

OBSERVATIONS

REQUIREMENTS	OBSERVATIONS
Slide Bars / Cams Greased? Tight?	Yes / No
Columns Greased?	Yes / No
Ram Keys Tight?	Yes / No
Column Keys or Cables Tight?	Yes / No
Striker Plate	t = _____ D = _____
Hammer Cushion	t = _____ D = _____ Material _____ How long in use? _____
Helmet	Type or Weight? _____
Follower	Yes / No; Type _____
Pile Cushion	Material _____ t = _____ Size _____ How long in use? _____
Pile	Material _____ Length _____ Size _____ Batter _____
Hose	I.D. Size _____ Length _____ Leaks? _____ Obstructions? _____
Lubricator Filled?	Yes / No
Pressure at Hammer _____ kPa	Measured _____ kPa at _____ meters from Hammer
Fluctuating during Driving?	Yes / No; How much? _____ kPa
Check Compressor and Boiler?	Size _____ m ³ /min Make _____

MANUFACTURER'S HAMMER DATA

Ram Weight _____
 Max. Stroke _____
 Rated Energy _____
 Blows/min in Hard Driving _____

ATTACHED SAXIMETER PRINTOUT

OBSERVATION WHEN BEARING IS CONFIRMED

Full Ram Stroke Yes/No, _____ %
 Blows/min; Blows/m _____
 High Pile Rebound; Pile Whipping Yes/No; Yes/No
 Pile-Hammer Alignment Front/Back _____ Sides _____
 Crane Size and Make _____
 Lead Type _____
 Hammer Lead Guides Lubricated Yes/No
 Piston Rod Lubricated _____
 Exhaust Description: Freezing? Condensing?
 Lubricant Apparent? _____

Figure 24.6 Inspection Form for Single and Differential Acting Air/Steam Hammers

- c. Visually inspect the slide bar and its cams for excessive wear. Measure the stroke being attained and confirm that it meets specification.
- d. Check that the columns or ram guides, piston rod, and slide bar are well greased.
- e. For most air/steam hammers, the total thickness of hammer cushion and striker plate must match the hammer manufacturer's recommendation and the hammer cushion cavity in the helmet for proper valve timing and hammer operation. This thickness must be maintained, and can be checked before assembly of the helmet into the leads, and thereafter by comparison of cam to valve position and/or gap between ram and hammer base when the ram is at rest on the pile.
- f. Make sure the helmet stays properly seated on the pile and that the hammer and pile maintain alignment during operation.
- g. The ram and column keys used to fasten together hammer components should all be tight.
- h. The hammer hoist line should always be slack with the hammer's weight and be fully carried by the pile. Excessive tension in the hammer hoist line is a safety hazard and will reduce energy to the pile. Leads should always be used.
- i. Compare the observed hammer speed in blows per minute near end of driving with the manufacturer's specifications. Blows per minute can be timed with a stopwatch or a saximeter. Slower operating rates may imply a short stroke (from inadequate pressure or volume, restricted or undersized hose, or inadequate lubrication) or improper valve timing (possibly from incorrect cushion thickness or worn parts). Erratic hammer operation, such as skipping blows, can result from improper cushion thickness, poor lubrication, foreign material in a valve, faulty valve/cam system, or loose hammer fasteners or keys.
- j. As the driving resistance increases, the ram stroke may also increase, causing it to strike the upper hammer assembly and lifting the hammer (racking) from the pile. If this behavior is detected, the pressure flow should be reduced gradually until racking stops. This will result in a reduction in energy since the pressure also acts during the downstroke, thereby contributing to the rated energy.

Record the final pressure. The flow should not be overly restricted so that the stroke is also reduced, causing a further reduction in energy. For optimum performance, the pressure flow should be kept as full as possible so that the hammer lift-off is imminent.

- k. Some manufacturers void their warranty if the hammer is consistently operated above 100 blows per 250 mm of penetration beyond short periods such as required when toe bearing piles are driven to rock. Therefore, in prolonged hard driving situations, it may be more desirable to use a larger hammer or stiffer pile section.
- l. Record the final pressure and compare with manufacturer's energy rating at this pressure.
- m. Common problems and problem indicators for air/steam hammers are summarized in Table 24-1.

An inspection form for enclosed double acting air/steam hammers is provided in Figure 24.7. The primary feature of this form is the three column area in the middle of the form. The left column identifies key objects of the driving system. The middle column contains the manufacturer's requirements for key objects and the right column is used to record the observed condition of those objects. This format allows the inspector to quickly identify potential problems and an immediate correction may be possible. The hammer inspection form is intended to be used periodically during the course of a project as a complement to the pile driving log.

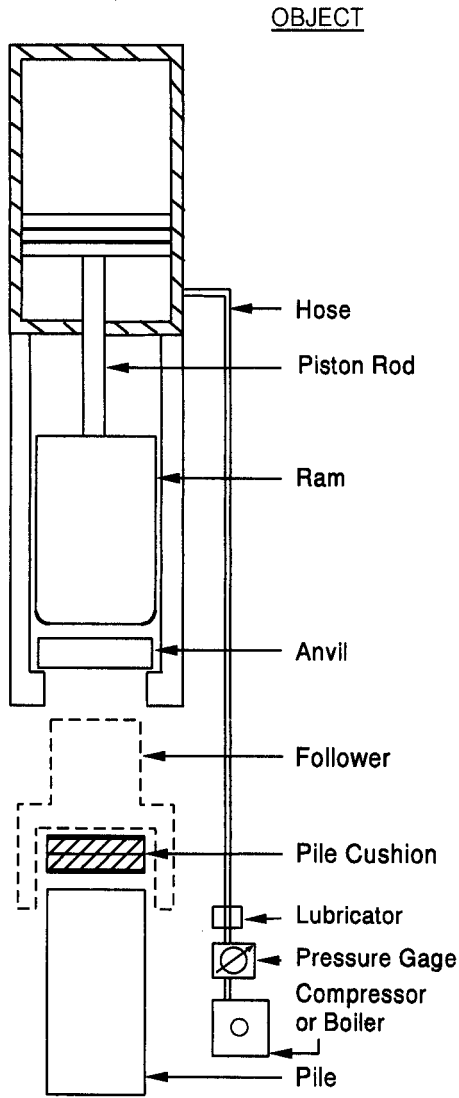
The bottom portion of the hammer inspection form contains an area where observations at final driving should be recorded. This information may be particularly interesting to an engineer who has performed a wave equation analysis as the actual situation can then be compared to the analyzed one. Therefore, it is recommended that a copy of the completed hammer inspection form be provided to appropriate design and construction personnel.

24.6.4 Single Acting Diesel Hammers

- a. Determine/confirm that the hammer is the correct make and model. Check for and record any identifying labels as to hammer make, model and serial number.

Project/Pile: _____
 Date: _____
 Conditions: _____

Hammer Name: _____
 Serial No: _____



OBJECT

REQUIREMENTS

OBSERVATIONS

Follower	Yes / No; Type _____
Pile Cushion	Material _____ t = _____ Size _____ How long in use? _____
Pile	Material _____ Length _____ Size _____ Batter _____
Hose Size?	I.D. Size _____ Length _____ Leaks? _____ Obstructions? _____
Lubricator Filled?	Yes / No
Pressure at Hammer _____ kPa	Measured _____ kPa at _____ meters from Hammer
Fluctuating during Driving?	Yes / No; How much? _____
Check Compressor and Boiler?	Size _____ m ³ / min Make _____

MANUFACTURER'S HAMMER DATA

Ram Weight _____
 Max. Stroke _____
 Rated Energy _____
 Blows/min in Hard Driving _____

ATTACHED SAXIMETER PRINTOUT

OBSERVATION WHEN BEARING IS CONFIRMED

Full Ram Stroke Yes/No, _____ %
 Blows/min; Blows/m _____
 High Pile Rebound; Pile Whipping Yes/No; Yes/No
 Pile-Hammer Alignment Front/Back _____ Sides _____
 Crane Size and Make _____
 Lead Type _____
 Hammer Lead Guides Lubricated Yes/No
 Piston Rod Lubricated _____
 Exhaust Description: Freezing? _____ Condensing? _____
 Lubricant Apparent? _____

Figure 24.7 Inspection Form for Enclosed Double Acting Air/Steam Hammers

- b. Make sure all exhaust ports are open with all plugs removed.
- c. Inspect the recoil dampener for condition and thickness. If excessively worn or improper thickness (consult manufacturer) it should be replaced. If the recoil dampener is too thin, the stroke will be reduced. If it is too thick, or if cylinder does not rest on dampener between blows, the ram could blow out the hammer top and become a safety hazard.
- d. Check that lubrication of all grease nipples is regularly made. Most manufacturers recommend the impact block be greased every half hour of operation.
- e. As the ram is visible between blows, check the ram for signs of uniform lubrication and ram rotation. Poor lubrication will increase friction and reduce energy to the pile.
- f. Determine the hammer stroke, especially at end of driving or beginning of restrike. A "jump stick" attached to the cylinder is a safety hazard and should not be used. The stroke can be determined by a saximeter which measures the time between blows and then calculates the stroke. The hammer stroke can also be calculated from this formula if the number of blows per minute (bpm) is manually recorded.

$$h \text{ [meters]} = [4400/[\text{bpm}^2]] - 0.09$$

The calculated stroke may require correction for batter or inclined piles. The inspector should always observe the ram rings and visually estimate the stroke using the manufacturer's chart.

- g. As the driving resistance increases, the stroke should also increase. At the end of driving, if the ram fails to achieve the correct stroke (part of the driving criteria from a wave equation analysis), the cause could be lack of fuel. Most hammers have adjustable fuel pumps. Some have distinct fuel settings as shown in Figure 24.8, others are continuously variable as shown in Figure 24.9, and some use a pressure pump as shown in Figure 24.10. Make sure the pump is on the correct fuel setting or pressure necessary to develop the required stroke. The fuel and fuel line should be free of dirt or other contaminants. A clogged or defective fuel injector will also reduce the stroke and should be replaced if needed.



Figure 24.8 Fixed Four Step Fuel Pump on Delmag Hammer



Figure 24.9 Variable Fuel Pump on FEC Hammer

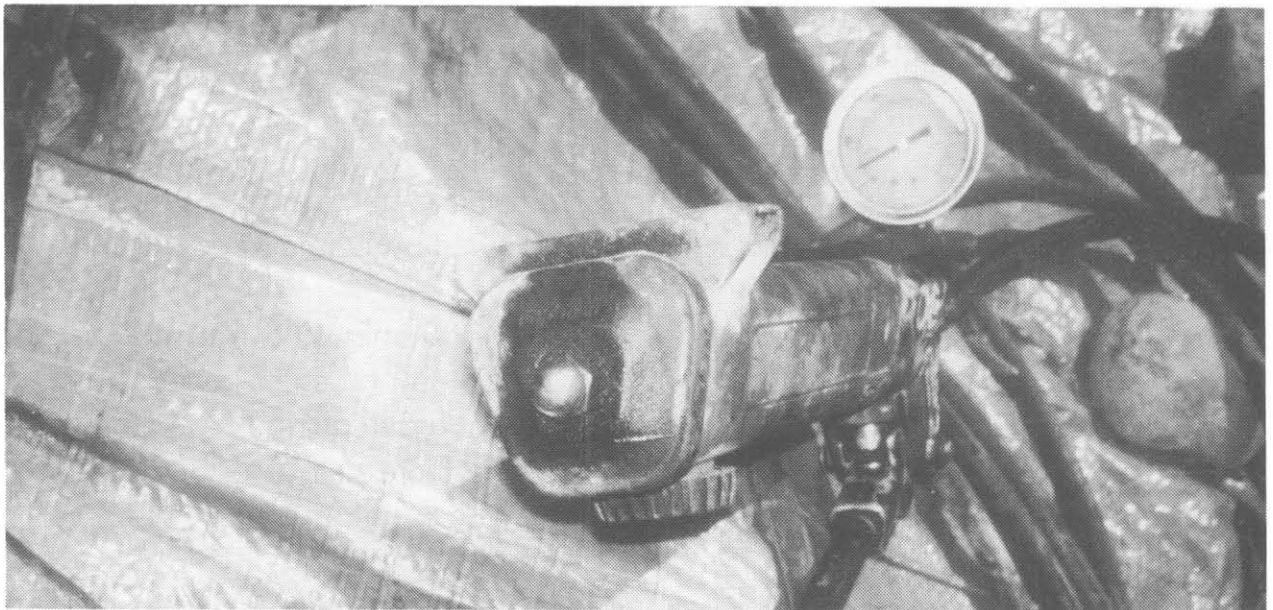


Figure 24.10 Adjustable Pressure Pump for Fuel Setting on ICE Hammer

- h. Low strokes could be due to poor compression caused by worn or defective piston or anvil rings. Check compression by raising the ram, and with the fuel turned off, allowing the ram to fall. The ram should bounce several times if the piston and anvil rings are satisfactory.
- i. Watch for signs of preignition. When a hammer preignites, the fuel burns before impact, requiring extra energy to compress gas and leaving less energy to transfer to the pile. In long sustained periods of driving, or if the wrong fuel with a low flash point is used, the hammer could overheat and preignite. When preignition occurs, less energy is transferred and the driving resistance rises, giving a false indication of high pile capacity. If piles driven with a cold hammer drive deeper or with less hammer blows, or if the driving resistances decrease after short breaks, preignition could be the cause and should be investigated. Dynamic testing is the preferable method to check for preignition.
- j. For some diesel hammers, the total thickness of hammer cushion and striker plate must match the hammer manufacturer's recommendation and the hammer cushion cavity in the helmet for proper fuel injection and hammer operation. This total thickness must be maintained.
- k. Make sure the helmet stays properly seated on the pile and that the hammer and pile maintain alignment during operation.
- l. The hammer hoist line should always be slack, with the hammer's weight fully carried by the pile. Excessive tension in the hammer hoist line is a safety hazard and will reduce energy to the pile. Leads should always be used.
- m. Some manufacturers void their warranty if the hammer is consistently operated above 100 blows per 250 mm of penetration beyond short periods, such as those required when toe bearing piles are driven to rock. Therefore, in prolonged hard driving situations, it may be more desirable to use a larger hammer or stiffer pile section.
- n. Common problems and problem indicators for single acting diesel hammers are presented in Table 24.2.

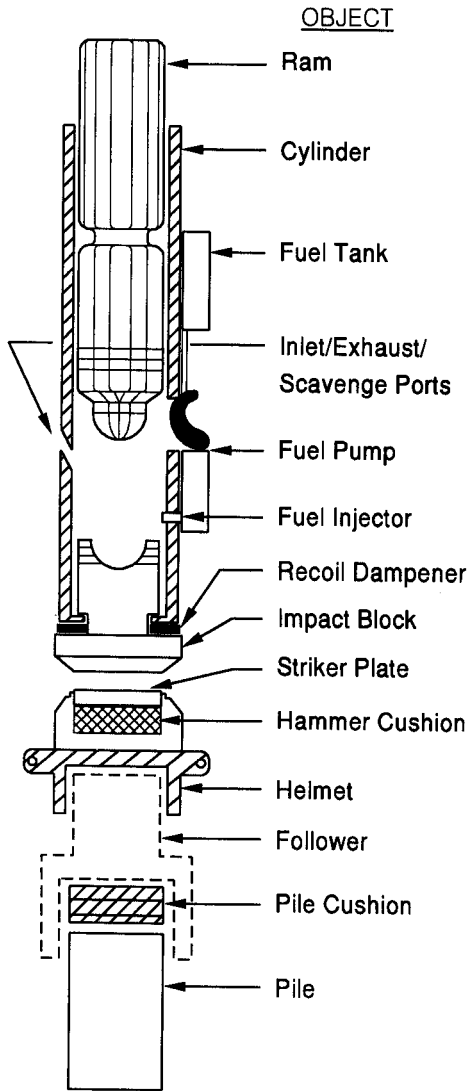
TABLE 24-2 COMMON PROBLEMS AND PROBLEM INDICATORS FOR SINGLE ACTING DIESEL HAMMERS (from Williams Earth Sciences, 1995)	
Common Problems	Indicators
Water in fuel.	Hollow sound, white smoke.
Fuel lines clogged.	No smoke or little gray smoke.
Fuel pump malfunctioning.	Inconsistent ram strokes, little gray smoke or black smoke.
Fuel injectors malfunctioning.	Inconsistent ram strokes, little gray smoke or black smoke.
Oil low.	Blows per minute rate is lower than specified.
Oil pump malfunctioning.	Blows per minute rate is lower than specified.
Water in combustion chamber.	Hollow sound, white smoke.
Piston rings worn.	Low strokes.
Tripping device broken.	Pawl or pin used to lift piston does not engage piston. Pawl engages but does not lift piston.
Over heating.	Paint and oil on cooling fins start to burn/ sound changes.

An inspection form for single acting diesel hammers is provided in Figure 24.11. The primary feature of this form is the three column area in the middle of the form. The left column identifies key objects of the driving system, the middle column contains the manufacturer's requirements for that object and the right column is used to record the observed condition of that object. This format allows the inspector to quickly identify potential problems and an immediate correction may be possible. The hammer inspection form is intended to be used periodically during the course of a project as a complement to the pile driving log.

The bottom portion of the hammer inspection form contains an area where observations at final driving should be recorded. This information may be particularly interesting to an engineer who has performed a wave equation analysis as the actual situation can then be compared to the analyzed one. Therefore, it is recommended that a copy of the completed hammer inspection form be provided to appropriate design and construction personnel.

Project/Pile: _____
 Date: _____
 Conditions: _____

Hammer Name: _____
 Serial No: _____



OBJECT

REQUIREMENTS

OBSERVATIONS

Ram Lubricated?	Yes / No
Fuel Tank Filled with Type II Diesel?	Yes / No
Exhaust Ports Open?	Yes / No
Fuel Pump	Hammer Setting _____
Recoil Dampener Undamaged?	Yes / No
Impact Block Lubricated?	Yes / No
Striker Plate	t = _____ D = _____
Hammer Cushion	t = _____ D = _____ Material _____ How long in use? _____
Helmet	Type or Weight? _____
Follower	Yes / No; Type _____
Pile Cushion	Material _____ t = _____ Size _____ How long in use? _____
Pile	Material _____ Length _____ Size _____ Batter _____

MANUFACTURER'S HAMMER DATA

Ram Weight _____

Hammer Setting	Rated Energy kJ	Rated Stroke m
min.		
max.		

ATTACHED SAXIMETER PRINTOUT

OBSERVATION WHEN BEARING IS CONFIRMED

Excessive Cylinder Rebound	Yes/No
High Pile Rebound	Yes/No
Pile Whipping	Yes/No
Pile-Hammer Alignment	Front/Back ___ Sides ___
Crane Size and Make	_____
Lead Type	_____
Hammer Lead Guides Lubricated	Yes/No
Color of Smoke	_____
Steel to Steel Impact Sound	_____

Figure 24.11 Inspection Form for Single Acting Diesel Hammers

24.6.5 Double Acting Diesel Hammers

- a. Determine/confirm that the hammer is the correct make and model. Check for and record any identifying labels as to hammer make, model and serial number.
- b. Make sure all exhaust ports are open with all plugs removed.
- c. Inspect the recoil dampener for condition and thickness. If excessively worn or of improper thickness (consult manufacturer), it should be replaced. If it is too thin, the stroke will be reduced. If it is too thick or if cylinder does not rest on dampener between blows, the ram will cause hammer lift-off.
- d. Check that lubrication of all grease nipples is regularly made. Most manufacturers recommend the impact block be greased every half hour of operation.
- e. After the hammer is stopped, check the ram for signs of lubrication by looking into the exhaust port or trip slot. Poor lubrication increases friction, thus reducing energy to the pile.
- f. Always measure the bounce chamber pressure, especially at end of driving or restrike. This indirectly measures the equivalent stroke or energy. All double acting diesels have a gauge. On most hammers an external gauge is connected by a hose to the bounce chamber. A photograph of a typical external bounce chamber pressure gauge is presented in Figure 24.12. The manufacturer should supply a chart relating the bounce chamber pressure for a specific hose size/length to the rated energy. The inspector should compare measured bounce chamber pressure with the manufacturer's chart to estimate the energy. The bounce chamber pressure measured may require correction for batter or inclined piles.
- g. As the driving resistance increases, the stroke and bounce chamber pressure should also increase. At the end of driving, if the ram fails to achieve the correct stroke or bounce chamber pressure (part of the driving criteria from a wave equation analysis), the cause could be lack of fuel. All these hammers have continuously variable fuel pumps. Check that the fuel pump is on the correct fuel setting. The fuel should be free of dirt or other contaminants. A clogged or defective fuel injector reduces the stroke.



Figure 24.12 Typical External Bounce Chamber Pressure Gauge

- h. In hard driving, high strokes cause high bounce chamber pressures. If the cylinder weight cannot balance the bounce chamber pressure, the hammer will lift-off of the pile, and the operator must reduce the fuel to prevent this unstable racking behavior. Ideally it is set and maintained so that lift-off is imminent. The bounce chamber pressure gauge reading should correspond to the hammer's maximum bounce chamber pressure for the hose length used when lift-off is imminent. If not, then the bounce chamber pressure gauge is out of calibration and should be replaced, or the bounce chamber pressure tank needs to be drained.
- i. Low strokes indicated by a low bounce chamber pressure could be due to poor compression caused by worn or defective piston or anvil rings. Check compression with the fuel turned off by allowing the ram to fall. The ram should bounce several times if the piston and anvil rings are satisfactory.
- j. Watch for preignition. When a hammer preignites, the fuel burns before impact requiring extra energy to compress the gas and reducing energy transferred to the pile. When preignition occurs, the pile driving resistance increases giving

a false indication of high pile capacity. In long sustained periods of driving or if low flash point fuel is used, the hammer could overheat and preignite. If piles driven with a cold hammer drive deeper or with fewer hammer blows, or if the driving resistance decreases after short breaks, investigate for preignition, preferably with dynamic testing.

- k. For some diesel hammers, the total thickness of the hammer cushion and striker plate must match the manufacturer's recommendation for proper fuel injection timing and hammer operation. This total thickness must be maintained.
- l. Make sure the helmet stays properly seated on the pile and that the hammer and pile maintain alignment during operation.
- m. The hammer hoist line should always be slack, with the hammer's weight fully carried by the pile. Excessive tension in the hammer hoist line is a safety hazard and will reduce energy to the pile. Leads should always be used.
- n. Some manufacturers void their warranty if the hammer is consistently operated above 100 blows per 250 mm of penetration beyond short periods such as those required when toe bearing piles are driven to rock. Therefore, in prolonged hard driving situations, it may be more desirable to use a larger hammer or stiffer pile section.
- o. Common problems and problem indicators for double acting diesel hammers are presented in Table 24.3.

An inspection form for double acting diesel hammers is provided in Figure 24.13. The primary feature of this form is the three column area in the middle of the form. The left column identifies key objects of the driving system, the middle column contains the manufacturer's requirements for that object and the right column is used to record the observed condition of that object. This format allows the inspector to quickly identify potential problems and an immediate correction may be possible. The hammer inspection form is intended to be used periodically during the course of a project as a complement to the pile driving log.

TABLE 24-3 COMMON PROBLEMS AND PROBLEM INDICATORS FOR DOUBLE ACTING DIESEL HAMMERS (from Williams Earth Sciences, 1995)	
Common Problems	Indicators
Water in fuel.	Hollow sound, white smoke.
Fuel lines clogged.	No smoke or little gray smoke.
Fuel pump malfunctioning.	Inconsistent ram strokes, little gray smoke or black smoke.
Fuel injectors malfunctioning.	Inconsistent ram strokes, little gray smoke or black smoke.
Oil low.	Blows per minute rate is lower than specified.
Oil pump malfunctioning.	Blows per minute rate is lower than specified.
Build-up of oil in bounce chamber.	Not visible from exterior.
Water in combustion chamber.	Hollow sound, white smoke.
Piston rings worn.	Low strokes.
Tripping device broken.	Pawl or pin used to lift piston does not engage piston. Pawl engages but does not lift piston.
Over heating.	Paint and oil on cooling fins start to burn/ sound changes.

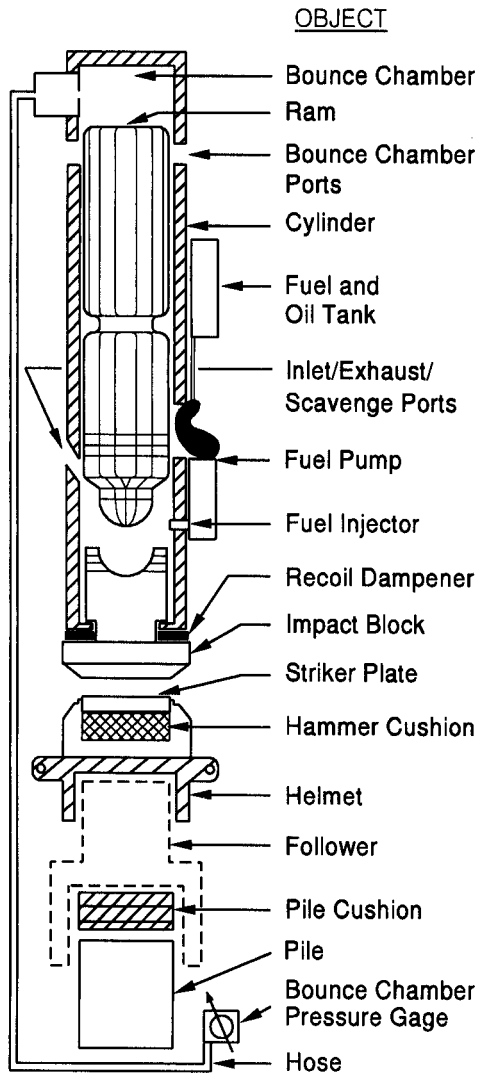
The bottom portion of the hammer inspection form contains an area where observations at final driving should be recorded. This information may be particularly interesting to an engineer who has performed a wave equation analysis as the actual situation can then be compared to the analyzed one. Therefore, it is recommended that a copy of the completed hammer inspection form be provided to appropriate design and construction personnel.

24.6.6 Hydraulic Hammers

- a. Determine/confirm the ram weight. If necessary, the ram weight can be calculated from the ram volume and steel density of 78.5 kN/m^3 , although some rams may be hollow or filled with lead. There may also be identifying labels as to hammer make, model, and serial number which should be recorded.

Project/Pile: _____
 Date: _____
 Conditions: _____

Hammer Name: _____
 Serial No: _____



OBJECT

REQUIREMENTS

OBSERVATIONS

Ram Lubricated?	Yes / No
Fuel Tank Filled with Type II Diesel?	Yes / No
Exhaust Ports Open?	Yes / No
Fuel Pump	Hammer Setting _____
Recoil Dampener Undamaged?	Yes / No
Impact Block Lubricated?	Yes / No
Striker Plate	t = _____ D = _____
Hammer Cushion	t = _____ D = _____ Material _____ How long in use? _____
Helmet	Type or Weight? _____
Follower	Yes / No; Type _____
Pile Cushion	Material _____ t = _____ Size _____ How long in use? _____
Pile	Material _____ Length _____ Size _____ Batter _____
Bounce Chamber Hose	Length _____

MANUFACTURER'S HAMMER DATA

Ram Weight _____
 Max. Stroke _____

Bounce Chamber Pressure (kPa)	Rated Energy (kJ)

ATTACHED SAXIMETER PRINTOUT

OBSERVATION WHEN BEARING IS CONFIRMED

Bounce Chamber Pressure	Time or Depth _____
Cylinder Lift-off	Yes/No
Excessive Cylinder Rebound	Yes/No
High Pile Rebound	Yes/No
Pile Whipping	Yes/No
Pile-Hammer Alignment	Front/Back _____ Sides _____
Crane Size and Make	_____
Lead Type	_____
Hammer Lead Guides Lubricated	Yes/No
Color of Smoke	_____
Steel to Steel Impact Sound	_____

Figure 24.13 Inspection Form for Double Acting Diesel Hammers

- b. Check the power supply and confirm it has adequate capacity to provide the required pressure and flow volume. Also, check the number, length, diameter, and condition of the hoses (no leaks in hoses or connections). Manufacturers provide guidelines for power supplies and supply hoses. Hoses bent to a radius less than recommended could adversely affect hammer operation or cause hose failure.
- c. Hydraulic hammers must be kept clean and free from dirt and water. Check the hydraulic filter for blocked elements. Most units have a built in warning or diagnostic system.
- d. Check that the hydraulic power supply is operating at the correct speed and pressure. Check and record the pre-charge pressures or accumulators for double acting hammers. Allow the hammer to warm up before operation, and do not turn off power pack immediately after driving.
- e. Most hydraulic hammers have built in sensors to determine the ram velocity just prior to impact. This result may be converted to kinetic energy or equivalent stroke. The inspector should verify that the correct ram weight is entered in the hammer's "computer". **This monitored velocity, stroke, or energy result should be constantly monitored and recorded. Some hammers have, or can be equipped with, a printout device to record that particular hammer's performance information with pile penetration depth and/or pile driving resistance.** This is the most important hammer check that the inspector can and should make for these hammers. A photograph of a hydraulic hammer readout panel is presented in Figure 24.14.
- f. For hydraulic hammers with observable rams, measure the stroke being attained and confirm that it meets specification. For hammers with enclosed rams, it is impossible to observe the ram and estimate the stroke.
- g. Check that the ram guides and piston rod are well greased.
- h. Where applicable, the total thickness of hammer cushion and striker plate must be maintained to match the manufacturer's recommendation for proper valve timing and hammer operation.

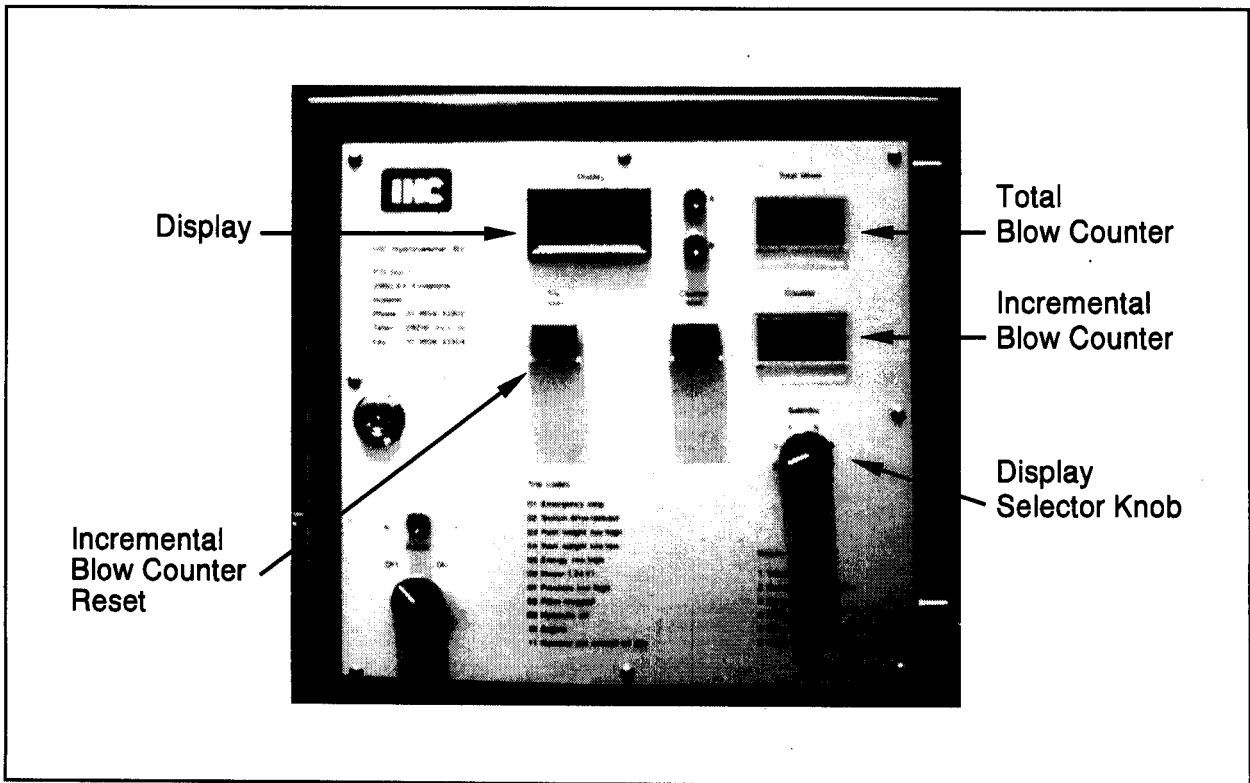


Figure 24.14 IHC Hydraulic Hammer Readout Panel (courtesy of L.B. Foster Co.)

- i. Make sure the helmet stays properly seated on the pile and that the hammer and pile maintain alignment during operation.
- j. The hammer hoist line should always be slack, with the hammer's weight fully carried by the pile. Excessive tension in the hammer hoist line is a safety hazard and will reduce energy to the pile. Leads should always be used.
- k. Compare the observed hammer speed in blows per minute from near end of driving with the manufacturer's specifications. Blows per minute can be timed with a stopwatch or a saximeter. Slower operating rates at full stroke may imply excessive friction, or incorrect hydraulic power supply.
- l. As the driving resistance increases, the ram stroke may also increase, causing the ram to strike the upper hammer assembly and lifting the hammer from the pile (racking). If this behavior is detected, the pressure flow should be reduced gradually until racking stops. Many of these hammers have sensors, and if they

detect this condition, the hammer will automatically shut down. The flow should not be overly restricted so that the correct stroke is maintained.

- m. Some manufacturers void their warranty if the hammer is consistently operated above 100 blows per 250 mm of penetration beyond short periods such as those required when toe bearing piles are driven to rock. Therefore, in prolonged hard driving situations, it may be more desirable to use a larger hammer or stiffer pile section.
- n. Common problems and problem indicators for hydraulic hammers are summarized in Table 24-4.

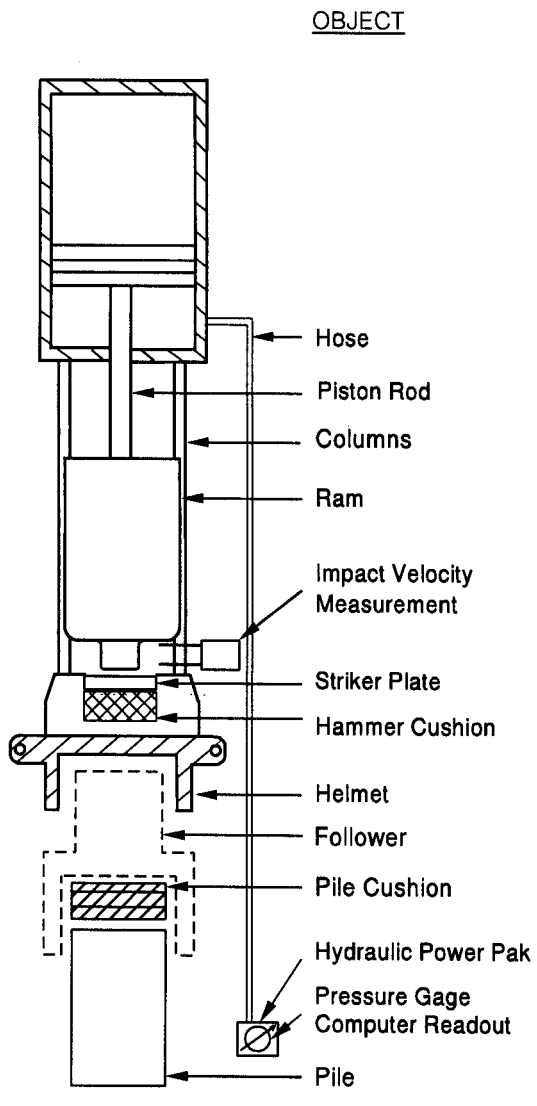
TABLE 24-4 COMMON PROBLEMS AND PROBLEM INDICATORS FOR HYDRAULIC HAMMERS (from Williams Earth Sciences, 1995)	
Common Problems	Indicators
Hoses getting caught in leads.	Visually evident.
Fittings leaking.	Hydraulic fluid dripping.
Electrical connections.	Erratic performance.
Sensors.	Erratic performance.

An inspection form for hydraulic hammers is provided in Figure 24.15. The primary feature of this form is the three column area in the middle of the form. The left column identifies key objects of the driving system, the middle column contains the manufacturer's requirements for that object, and the right column is used to record the observed condition of that object. The hammer inspection form is intended to be used periodically during the course of a project as a complement to the pile driving log.

The bottom portion of the hammer inspection form contains an area where observations at final driving should be recorded. This information may be particularly interesting to an engineer who has performed a wave equation analysis as the actual situation can then be compared to the analyzed one. Therefore, it is recommended that a copy of the completed hammer inspection form be provided to appropriate design and construction personnel.

Project/Pile: _____
 Date: _____
 Conditions: _____

Hammer Name: _____
 Serial No: _____



REQUIREMENTS	OBSERVATIONS
Ram Visible?	Yes / No _____
Observed Ram Stroke	_____ m
Ram Downward Pressure Provided ?	Yes / No _____
Hydraulic Pressure, Rated	_____ kPa
Hydraulic Pressure, Actual	_____ kPa
Impact Velocity Measurement ?	Yes / No _____
If Without Velocity Measurement Then ?	Free Fall? _____
Observed Fall Height	_____ m
Pressure under ram during fall	_____
Preadmission Possible?	_____
Striker Plate	t = _____ D = _____
Hammer Cushion	t = _____ D = _____
Material	_____
How long in use?	_____
Helmet	Type or Weight? _____
Follower	Yes / No; Type _____
Pile Cushion	Material _____
t = _____ Size _____	
How long in use?	_____
Hydraulic Power Pack	Make _____
Model	_____
Pressure Gage ?	Yes / No Reading _____
Computer Readout ?	Yes / No Reading _____
Pile	Material _____
Length _____ Size _____	
Batter	_____

MANUFACTURER'S HAMMER DATA

Ram Weight _____
 Max. Stroke _____
 Min. Stroke _____
 Max. Energy _____
 Min. Energy _____

ATTACH SAXIMETER PRINTOUT

OBSERVATION WHEN BEARING IS COMPLETED

Hammer Uplifting Yes/No _____
 Reduced Pressure Yes/No _____
 Blows/Minute _____
 Blow/meter _____
 High Pile Rebound Yes/No _____
 Pile Whipping Yes/No _____
 Pile-Hammer Alignment Front/Back _____ Sides _____
 Crane Size and Make _____
 Lead Type _____
 Lead Guides Lubricated Yes/No _____

Figure 24.15 Inspection Form for Hydraulic Hammers

24.6.7 Vibratory Hammers

- a. Confirm that the hammer make and model meets specifications. There may also be identifying labels as to hammer make, model and serial number which should be recorded.
- b. Check the power supply to confirm adequate capacity to provide the required pressure and flow volume. Check also the number, length, diameter, and condition of the hoses (no leaks in hoses or connections). Manufacturers provide guidelines for proper power supplies and supply hoses. Hoses bent to a smaller radius than recommended could affect hammer operation or cause hose failure.
- c. Vibratory hammers must be kept clean, free from dirt and water. Check the hydraulic filter for blocked elements. Most units have a built in warning or diagnostic system.
- d. Check and record that the hydraulic power supply is operating at the correct speed and pressure. Allow the hammer to warm up before operation, and do not turn off the power pack immediately after driving.
- e. Record, if available, the vibrating frequency.
- f. Make sure the hydraulic clamps for attachment to the pile are in good working order and effective.
- g. The hammer hoist line should always be slack enough to allow penetration with the hammer's weight primarily carried by the pile. Excessive tension in the hammer hoist line will retard penetration. If used for extraction, the hoist line should be tight at all times. Leads are rarely used.

24.7 INSPECTION OF TEST OR INDICATOR PILES

Most specifications call for preconstruction verification of the foundation design through the testing of some selected piles. The size of the foundation and relative costs of testing often dictate the type and amount, if any, of confirmation testing. The inspector may be responsible for coordinating the test pile program with the contractor, other state personnel, and/or outside testing agencies.

Small foundations with few piles may be designed conservatively with high safety factors and oversized pile length and no further tests are required. All piles are then production piles and the entire pile foundation is usually installed in one or two days.

The piles, hammers, and other observations are recorded by the inspector and information appropriately passed on or filed. Inspection should be thorough as it is the only assurance of a good foundation. If any problems are observed, such as very low blow counts, refusal driving above scour depths, or excessive pile lengths, the problems and all pertinent observations must be reported quickly so that immediate corrective action can be taken.

On most projects, some additional verification is specified. Smaller projects may have only a single static test (Chapter 19) on one pile at a specific depth, or there may be a few dynamic test piles (Chapter 18). The dynamic tests may include either testing during driving to assess hammer performance and driving stresses, or testing during restrrike to assess capacity, or both. The static or dynamic tests should be performed by state department of transportation personnel having appropriate knowledge of test procedures, or engineering consultants. Generally, tests are done on some of the first piles driven to verify or adjust the driving criteria which will then be used for subsequent production piles. This further verification provides rational basis for changes to the driving criteria, if necessary, which should be applied to subsequent production pile driving.

On larger projects, multiple test piles distributed across the site are often required to verify or adjust the driving criteria. The goal is to determine a driving criteria which will lead to a safe, but economical, foundation. Such tests could be primarily done at one time at the beginning of the construction. For example, so-called indicator piles are driven in selected locations across the project site to establish order lengths for concrete piles. Such selected piles are generally statically and/or dynamically tested. Alternatively, testing could be performed as the construction progresses with some test(s) establishing the driving criteria for piles in close proximity to the test pile(s), followed by production pile driving, and then repeating the process in stages across the site.

The test piles are often the most critical part of the foundation installation. The procedures and driving criteria established during this phase will be applied to all subsequent production piles. The largest savings are often found at this time. For example, test results may determine that the design pile length results in a greater pile capacity than required and that the piles could be made substantially shorter.

Alternatively, problems with the test piles are usually followed by the same problems with production piles. Since problems are in themselves costly, and if left unresolved may eventually escalate, determination of the best solution as quickly as possible should be accomplished. It is the inspector's responsibility to be observant and communicate significant observations precisely and in a timely manner to the state design and testing teams.

The answers to the following questions should be known before driving test piles. Usually the inspector has the responsibility and the decision making authority regarding these items, although advice from various agency personnel and/or outside consultants may be necessary or desirable.

1. Who determines test pile locations?
2. Who determines the test pile driving criteria?
3. Who stops the driving when the driving criteria is met?
4. Who decides at what depth to stop the indicator/test piles?
5. Who checks cutoff elevations?
6. Who checks for heave?
7. Who determines if static test and/or dynamic test results indicate an acceptable test pile?
8. Who determines if additional tests are required?
9. Who determines if modifications to procedures or equipment are required?
10. Who has authority to allow production pile installation? When is this approval to proceed to production granted?
11. Who produces what documentation?

24.8 INSPECTION OF PRODUCTION PILES

During the production pile driving operations, the inspector's function is to apply the knowledge gained from the test program to each and every production pile. Quality assurance measures for the pile quality and splices; hammer operation and cushion replacement; overall evaluation of pile integrity; procedures for completing the piles (e.g. filling pipe piles with concrete); and unusual or unexpected occurrences need to be addressed. Complete documentation for each and every pile must be obtained, and then passed on to the appropriate destination in a timely manner.

The following items should be checked frequently (e.g. for each production pile):

1. Does the pile meet specifications of type, size, length, and strength?
2. Is the pile installed in the correct location, within acceptable tolerances, and with the correct orientation?
3. Are splices, if applicable, made to specification?
4. Is pile toe protection required and properly attached?
5. Is the pile acceptably plumb?
6. Is the hammer working correctly?
7. Is the hammer cushion the correct type and thickness?
8. Is the pile cushion the correct type and thickness? Is it being replaced regularly?
9. Did the pile meet the driving criteria as expected?
10. Did the pile have unusual driving conditions and therefore potential problems?
11. Is there any indication of pile heave?
12. Is the pile cutoff at the correct elevation?

13. Is there any visual damage?
14. If appropriate, has the pipe pile been visually inspected prior to concrete filling? Has it been filled with the specified strength concrete? Were concrete samples taken?
15. Are piles which are to be filled with concrete, such as open ended pipes and prestressed concrete piles with center voids, being cleaned properly after driving is completed?
16. If there is any question about pile integrity, has the issue been resolved? Is the pile acceptable, or does it need remediation or replacement?
17. Is the documentation for this pile complete, including driving log? Has it been submitted on a timely basis to the appropriate authority?

Many of the above questions are self explanatory and need no further explanation. Every previous section of this chapter has material which will relate to inspection of production piles and offer the detailed answers to other questions raised above. Although the inspector has now had the experience of test pile installation, a few additional details and concerns are perhaps appropriate.

Counting the number of hammer blows per minute and comparing it to the manufacturer's specification will provide a good indication of whether or not the hammer is working properly. The stroke of the hammer for most single and double acting air/steam hammers can be observed. Check the stroke of a single acting diesel hammer with a saximeter or by computation from the blows per minute. Check the bounce chamber pressure for double acting diesel hammers. Most hydraulic hammers have built-in energy monitors, and this information should be recorded for each pile. The hammer inspection form presented earlier in this chapter should be completed for the hammer type being used.

A hammer cushion of manufactured material usually lasts for many hours of pile driving, (as much as 200 hours for some manufactured materials) so it is usually sufficient to check before the pile driving begins and periodically thereafter. Pile cushions (usually made of plywood) need frequent changing because of excessive compression or charring and have a typical life of about 1000 to 2000 hammer blows. Pile cushions

should preferably be replaced as soon as they compress to one half of the original thickness, or if they begin to burn. No changes to the pile cushion thickness should be permitted near final driving. The required driving resistance for pile acceptance should only be allowed after the first 100 blows after cushion replacement.

Inspection of splices is important for pile integrity. Poorly made splices are a potential source of problems and possible pile damage during driving. In some cases damage may be detected from the blow count records. Dynamic pile testing can be useful in questionable cases.

Pile driving stresses should be kept within specified limits. If dynamic monitoring equipment was used during test pile driving, the developed driving criteria should keep driving stresses within specified limits. If periodic dynamic tests are made, a check that the driving stresses are within the specified limits can be provided. Adjustments of the ram stroke for all hammer types may be necessary to avoid pile damage. For concrete piles, cushion thicknesses or driving procedures may need adjustment to control tension and compression stresses. If dynamic testing is not used, a wave equation analysis is essential to evaluate the anticipated driving stresses.

Driving of piles at high driving resistances, above 120 blows per 250 mm, should be avoided by matching the driving system with the pile type, length and subsurface conditions. This should have been accomplished in the design phase by performing wave equation analysis. However, conditions can change across the project due to site variability.

All piles should be checked for damage after driving is completed. The driving records for all pile types can be compared with adjacent piles for unusual records or vastly different penetrations. Piles suspected of damage (including timber, H, and solid concrete piles) could be tested to confirm integrity and/or determine extent and location of damage using the pile driving analyzer, or for concrete piles, low strain integrity testing methods. These methods are discussed in Chapter 18. Alternatively, the pile could be replaced or repaired, if possible.

Check for water leakage for closed end pipe piles before placing concrete. The concrete mix should have a high slump and small aggregate. A pipe pile can be easily checked for damage and sweep by lowering a light source inside the pile.

The driving sequence of piles in a pier or bent can be important. The driving sequence can affect the way piles drive as well as the influence the new construction has on adjacent structures. This is especially true for displacement piles. For non-displacement piles the driving sequence is generally not as critical.

The driving sequence of displacement pile groups should be from the center of the group outward or from one side to the other side. The preferred driving sequence of the displacement pile group shown in Figure 24.16 would be (a) by the pile number shown, (sequence 1), (b) by driving each row starting in the center and working outward (sequence 2), or (c) by driving each row starting on one side of the group and working to the other side (sequence 3).

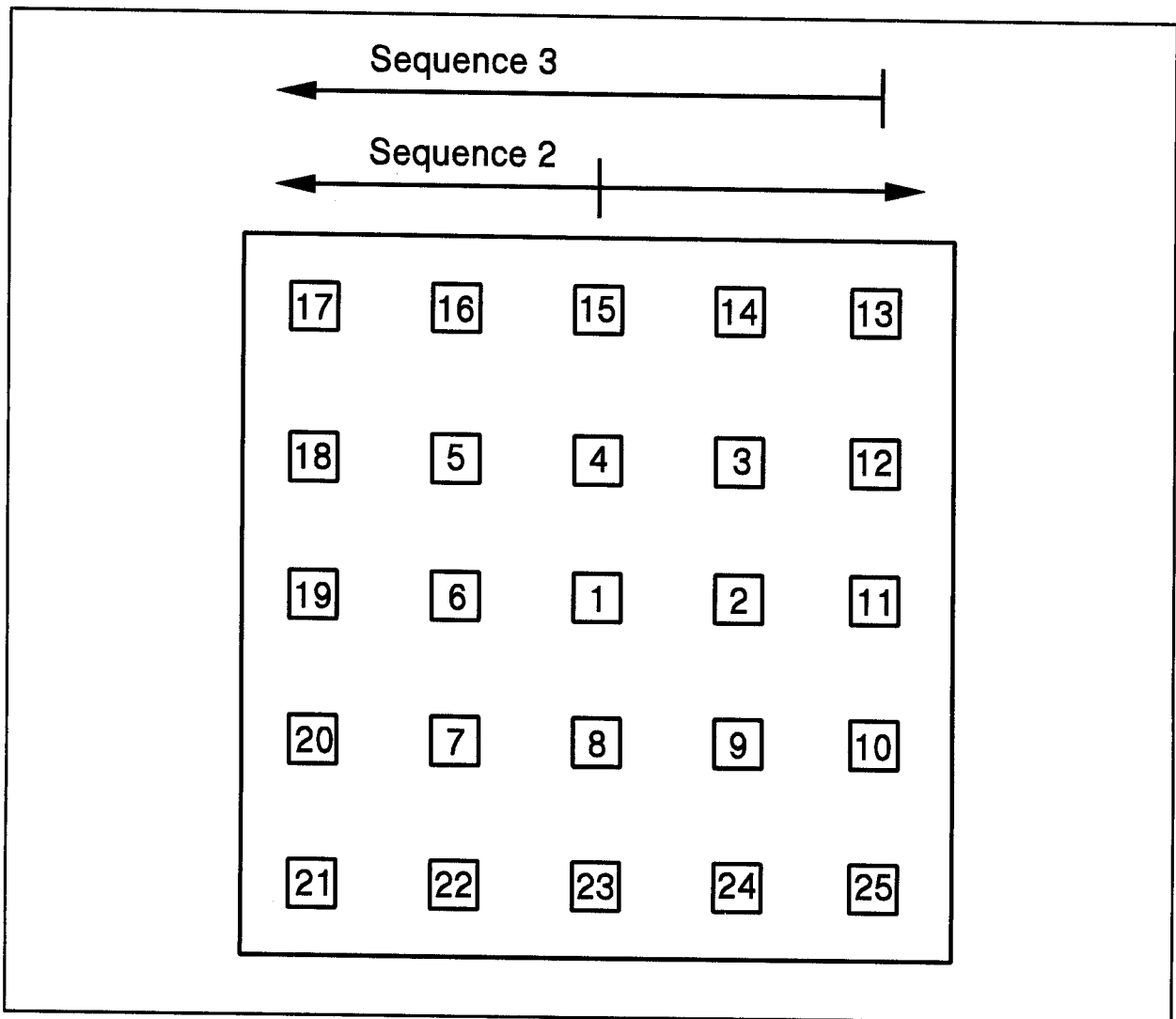


Figure 24.16 Driving Sequence of Displacement Pile Groups (after Passe, 1994)

Pile groups should not be driven from the outside to the center (the reverse of sequences 1 or 2). If groups are driven in that order, displaced soils becomes trapped and compacted in the center of the pile group. This can cause problems with driving the piles in the center of the group.

When driving close to an existing structure, it is generally preferable to drive the piles nearest the existing structure first and work away. For example, if a structure was located on the right side of the pile group shown in Figure 24.16, the piles should be driven by sequence 3. This reduces the amount of soil displaced toward the existing structure. The displacement of soil toward an existing structure has caused problems before. It can be especially critical next to a bascule bridge where, very small movements can prevent the locking mechanism from locking.

On some projects, vibration measurements may be required to ascertain if pile driving induced vibrations are within acceptable and/or specified maximum levels. Woods (1997) noted that vibration damage is relatively uncommon at a distance of one pile length away from driving. However, damage from vibration induced settlement of loose, clean sands can be a problem up to 400 m away from driving. To document existing conditions of nearby structures, a preconstruction survey of structures within 120 m of pile driving activities is often performed prior to the start of construction. The preconstruction survey generally consists of photographing or videotaping existing damage, as well as affixing crack gages to existing cracks in some cases. Woods also noted that damage to freshly placed concrete from pile driving vibrations may not be a risk but further research on the setting and curing of concrete may be warranted.

A cold hammer should not be used when restriking piles after a setup period. Twenty hammer blows are usually sufficient to warm up most hammers. Also be sure to record the restrike driving resistance for each 25 mm during the first 250 mm of restrike.

A summary of common pile installation problems and possible solutions is presented in Table 24-5.

TABLE 24-5 COMMON PILE INSTALLATION PROBLEMS & POSSIBLE SOLUTIONS

Problem	Possible Solutions
<p>Piles encountering refusal driving resistance (blow count) above minimum pile penetration requirements.</p>	<p>Have wave equation analysis performed and check that pile has sufficient driveability and that the driving system is matched to the pile. If the pile and driving system are suitably matched, check driving system operation for compliance with manufacturer's guidelines. If no obvious problems are found, dynamic measurements should be made to determine if the problem is driving system or soil behavior related. Driving system problems could include preignition, preadmission, low hammer efficiency, or soft cushion. Soil problems could include greater soil strength than anticipated, temporarily increased soil resistance with later relaxation (requires restrike to check), large soil quakes, or high soil damping.</p>
<p>Piles driving significantly deeper than estimated pile penetration depths.</p>	<p>Soil resistance at the time of driving probably is lower than anticipated or driving system performance is better than anticipated. Have wave equation analysis performed to assess ultimate pile capacity based on the blow count at the time of driving. Perform restrike tests after an appropriate waiting period to evaluate soil strength changes with time. If the ultimate capacity based on restrike blow count is still low, check drive system performance and restrike capacity with dynamic measurements. If drive system performance is as assumed and restrike capacity low, the soil conditions are weaker than anticipated. Foundation piles will probably need to be driven deeper than originally estimated or additional piles will be required to support the load. Contact the structural engineer/designer for recommended change.</p>

TABLE 24-5 COMMON PILE INSTALLATION PROBLEMS & POSSIBLE SOLUTIONS
(CONTINUED)

Problem	Possible Solutions
Abrupt change or decrease in driving resistance (blow count) for bearing piles.	If borings do not indicate weathered profile above bedrock/bearing layer then pile toe damage is likely. Have wave equation analysis performed and evaluate pile toe stress. If calculated toe stress is high and blow counts are low, a reduced hammer energy (stroke) and higher blow count could be used to achieve capacity with a lower toe stress. If calculated toe stress is high at high blow counts, a different hammer or pile section may be required. For piles that allow internal inspection, reflect light to the pile toe and tape the length inside the pile for indications of toe damage. For piles that cannot be internally inspected, dynamic measurements could be made to evaluate problem or pile extraction could be considered for confirmation of a damage problem.
Driving resistance (blow count) significantly lower than expected during driving.	Review soil borings. If soil borings do not indicate soft layers, pile may be damaged below grade. Have wave equation analysis performed and investigate both tensile stresses along pile and compressive stresses at toe. If calculated stresses are within allowable limits, investigate possibility of obstructions / uneven toe contact on hard layer or other reasons for pile toe damage. If pile was spliced, re-evaluate splice detail and field splicing procedures for possible splice failure.
Vertical (heave) or lateral movement of previously installed piles when driving new piles.	Pile movements likely due to soil displacement from adjacent pile driving. Contact geotechnical engineer for recommended action. Possible solutions include redriving of installed piles, change in sequence of pile installation, or predrilling of pile locations to reduce ground movements. Lateral pile movements could also result from adjacent slope failure in applicable conditions.

TABLE 24-5 COMMON PILE INSTALLATION PROBLEMS & POSSIBLE SOLUTIONS
(CONTINUED)

Problem	Possible Solutions
Piles driving out of alignment tolerance.	Piles may be moving out of alignment tolerance due to hammer-pile alignment control or due to soil conditions. If due to poor hammer-pile alignment control, a pile gate, template or fixed lead system may improve the ability to maintain alignment tolerance. Soil conditions such as near surface obstructions (see subsequent section) or steeply sloping bedrock having minimal overburden material (pile point detail is important) may prevent tolerances from being met even with good alignment control. In these cases, survey the as-built condition and contact the structural engineer for recommended action.
Piles driving out of location tolerance.	Piles may be moving out of location tolerance due to hammer-pile alignment control or due to soil conditions. If due to poor hammer-pile alignment control, a pile gate, template or fixed lead system may improve the ability to maintain location tolerance. Soil conditions such as near surface obstructions (see subsequent section) or steeply sloping bedrock having minimal overburden material (pile point detail is important) may prevent tolerances from being met even with good alignment control. In these cases, survey the as-built condition and contact the structural engineer for recommended action.
Piles encountering shallow obstructions.	If obstructions are within 3 m of working grade, obstruction excavation and removal is probably feasible. If obstructions are at deeper depth, are below the water table, or the soil is contaminated, excavation may not be feasible. Spudding or predrilling of pile locations may provide a solution with method selection based on the type of obstructions and soil conditions.

TABLE 24-5 COMMON PILE INSTALLATION PROBLEMS & POSSIBLE SOLUTIONS
(CONTINUED)

Problem	Possible Solutions
Piles encountering obstructions at depth.	If deep obstructions are encountered that prevent reaching the desired pile penetration depth, contact the structural engineer/designer for remedial design. Ultimate capacity of piles hitting obstructions should be reduced based upon pile damage potential and soil matrix support characteristics. Additional foundation piles may be necessary.
Concrete piles develop complete horizontal cracks in easy driving.	Have wave equation analysis performed and check tension stresses along pile (extrema tables) for the observed blow counts. If the calculated tension stresses are high, add cushioning or reduce stroke. If calculated tension stresses are low, check hammer performance and/or perform dynamic measurements.
Concrete piles develop complete horizontal cracks in hard driving.	Have wave equation analysis performed and check tension stresses along pile (extrema table). If the calculated tension stresses are high, consider a hammer with a heavier ram. If the calculated tension stresses are low, perform dynamic measurements and evaluate soil quakes which are probably higher than anticipated.
Concrete piles develop partial horizontal cracks in easy driving.	Check hammer-pile alignment since bending may be causing the problem. If the alignment appears to be normal, tension and bending combined may be too high. The possible solution is as above with complete cracks.
Concrete pile spalling or slabbing near pile head.	Have wave equation analysis performed. Determine the pile head stress at the observed blow count and compare predicted stress with allowable material stress. If the calculated stress is high, increase the pile cushioning. If the calculated stress is low, investigate pile quality, hammer performance, and hammer-pile alignment.

TABLE 24-5 COMMON PILE INSTALLATION PROBLEMS & POSSIBLE SOLUTIONS (CONTINUED)	
Problem	Possible Solutions
Steel pile head deforms.	Check helmet size/shape, steel yield strength, and evenness of the pile head. If all seem acceptable, have wave equation analysis performed and determine the pile head stress. If the calculated stress is high and blow counts are low, use reduced hammer energy (stroke) and higher blow count to achieve capacity. If the calculated stress is high at high blow counts, a different hammer or pile type may be required. Ultimate capacity determination should not be made using blow counts obtained when driving with a deformed pile head.
Timber pile head mushrooms	Check helmet size/shape, the evenness of the pile head, and banding of the timber pile head. If all seem acceptable, have wave equation analysis performed and determine the pile head stress. If the calculated stress is high and blow counts are low, use reduced hammer energy (stroke) and higher blow count to achieve capacity. Ultimate capacity determination should not be made using blow counts obtained when driving with a mushroomed pile head.

24.9 DRIVING RECORDS AND REPORTS

Pile driving records vary with the organization performing the inspection service. A typical pile driving record is presented in Figure 24.17. The following is a list of items that appear on most pile driving records:

1. Project identification number.
2. Project name and location.
3. Structure identification number.

PILE DRIVING LOG

STATE PROJECT NO.: _____ DATE: _____

JOB LOCATION: _____

PILE TYPE: _____ LENGTH: _____ BENT/PIER NO.: _____ PILE NO.: _____

HAMMER: _____ ENERGY/BLOW: _____ OPERATING RATE: _____ HELMET WEIGHT: _____

REF. ELEV.: _____ PILE TOE ELEV.: _____ PILE CUTOFF ELEV.: _____

PILE CUSHION THICKNESS AND MATERIAL: _____

WEATHER: _____ TEMP.: _____ START TIME: _____ STOP TIME: _____

METERS	BLOWS	STROKE / PRESSURE	REMARKS	METERS	BLOWS	STROKE / PRESSURE	REMARKS
0 - 0.25				8.00 - 8.25			
0.25 - 0.50				8.25 - 8.50			
0.50 - 0.75				8.50 - 8.75			
0.75 - 1.00				8.75 - 9.00			
1.00 - 1.25				9.00 - 9.25			
1.25 - 1.50				9.25 - 9.50			
1.50 - 1.75				9.50 - 9.75			
1.75 - 2.00				9.75 - 10.00			
2.00 - 2.25				10.00 - 10.25			
2.25 - 2.50				10.25 - 10.50			
2.50 - 2.75				10.50 - 10.75			
2.75 - 3.00				10.75 - 11.00			
3.00 - 3.25				11.00 - 11.25			
3.25 - 3.50				11.25 - 11.50			
3.50 - 3.75				11.50 - 11.75			
3.75 - 4.00				11.75 - 12.00			
4.00 - 4.25				12.00 - 12.25			
4.25 - 4.50				12.25 - 12.50			
4.50 - 4.75				12.50 - 12.75			
4.75 - 5.00				12.75 - 13.00			
5.00 - 5.25				13.00 - 13.25			
5.25 - 5.50				13.25 - 13.50			
5.50 - 5.75				13.50 - 13.75			
5.75 - 6.00				13.75 - 14.00			
6.00 - 6.25				14.00 - 14.25			
6.25 - 6.50				14.25 - 14.50			
6.50 - 6.75				14.50 - 14.75			
6.75 - 7.00				14.75 - 15.00			
7.00 - 7.25				15.00 - 15.25			
7.25 - 7.50				15.25 - 15.50			
7.50 - 7.75				15.50 - 15.75			
7.75 - 8.00				15.75 - 16.00			

PILE INFORMATION: _____ MANUFACTURED BY: _____

WORK ORDER NO.: _____ DATE CAST: _____

MANUFACTURER'S PILE NO.: _____ PILE HEAD CONDITIONS: _____

PILE TOE ATTACHMENTS: _____ SIGNATURE: _____

Figure 24.17 Pile Driving Log

4. Date and time of driving (start, stop, and interruptions).
5. Name of the contractor.
6. Hammer make, model, ram weight, energy rating. The actual stroke and operating speed should also be recorded whenever it is changed.
7. Hammer cushion description, size and thickness, and helmet weight.
8. Pile cushion description, size and thickness, depth where changed.
9. Pile location, type, size and length.
10. Pile number or designation matching pile layout plans.
11. Pile ground surface, cut off, and final penetration elevations and embedded length.
12. Driving resistance data in blows per 0.25 meter with the final 0.25 meter normally recorded in blows per 25 mm.
13. Graphical presentation of driving data (optional).
14. Cut-off length, length in ground and order length.
15. Comments or unusual observations, including reasons for all interruptions.
16. Signature and title of the inspector.

The importance of maintaining detailed pile driving records can not be overemphasized. The driving records form a basis for payment and for making engineering decisions regarding the adequacy of the foundation to support the design loads. Great importance is given to driving records in litigations involving claims. Sloppy, inaccurate, or incomplete records encourage claims and result in higher cost foundations. The better the pile driving is documented, the lower the cost of the foundation will probably be and the more likely it will be completed on schedule.

In addition to the driving records, the inspector should be required to prepare a daily inspection report. The daily inspection report should include information on equipment working at the site, description of construction work accomplished, and the progress of work. Figure 24.18 shows an example of a daily inspection report.

DAILY INSPECTION REPORT

Project No.: _____

Date: _____

Project: _____

Weather Conditions: _____

Contractor: _____

Contractor's Personnel Present: _____

Equipment Working: _____

Description of Work Accomplished: _____

Special Persons Visiting Job: _____

Test Performed: _____

Special Comments: _____

Figure 24.18 Daily Inspection Report

REFERENCES

- Associated Pile and Fitting Corporation. Design and Installation of Driven Pile Foundations.
- Canadian Geotechnical Society (1978). Canadian Foundation Engineering Manual. Part 3, Deep Foundations.
- Deep Foundations Institute (1981). Glossary of Foundation Terms.
- Deep Foundations Institute (1995). A Pile Inspector's Guide to Hammers, Second Edition Deep Foundations Institute.
- Fuller, F.M. (1983). Engineering of Pile Installations. McGraw-Hill Book Company.
- Passe, Paul D. (1994). Pile Driving Inspector's Manual. State of Florida Department of Transportation.
- Rausche, F., Likins, G.E., Goble, G.G., Hussien, M. (1986). The Performance of Pile Driving Systems; Inspector's Manual.
- Williams Earth Sciences (1995). Inspector's Qualification Program for Pile Driving Inspection Manual. State of Florida Department of Transportation.
- Woods, R.D. (1997). Dynamic Effects of Pile Installations on Adjacent Structures. NCHRP Synthesis 253, National Cooperative Highway Research Program, Transportation Research Board, Washington, D.C.

STUDENT EXERCISE #15 - HAMMER INSPECTION

You are inspecting the pile driving operations on two bridge projects. On the first project, Bridge #1, the contractor is using a single acting diesel hammer. The driving criteria with this hammer has been established as follows:

Minimum Toe Elevation: EL 96.5 m
Minimum Driving Resistance: 80 blows / 250 mm at a 3.0 m stroke.

The driving record for the first pile driven is attached. The hammer operating speed was timed at 40 blows per minute at final driving. Has this pile met the driving criteria ?

STEP 1. Calculate the stroke hammer stroke based on the recorded hammer operating speed using the formula on page 24-22.

STEP 2. Determine the pile toe elevation.

STEP 3. Based on hammer stroke, driving resistance and pile toe elevation, determine if the pile has met the driving criteria.

On the second project, Bridge #2, the contractor is using a double acting diesel hammer. The bounce chamber - equivalent energy correlation for the hammer as provided by the contractor in the equipment submittal is attached. The driving criteria on the second project has been established as follows:

Minimum Toe Elevation:	EL 80
Minimum Driving Resistance:	60 blows / 250 mm at a bounce chamber pressure of 180 kPa. (Based on 15.2 m of hose.)

The driving record for the first production pile driven on this project is attached. The hose between the bounce chamber pressure is 24.4 m long. Has this pile met the driving criteria?

STEP 1. Determine equivalent hammer energy based on the bounce chamber pressure on the driving log.

STEP 2. Compare observed equivalent hammer energy with required energy.

STEP 3. Based on observed hammer energy, driving resistance and pile toe elevation, determine if the pile has met the driving criteria.

PILE DRIVING LOG

STATE PROJECT NO.: Bridge #1 DATE: 5-29-98

JOB LOCATION: Bogalusa

PILE TYPE: 457 mm PCC LENGTH: 15 m BENT/PIER NO.: 1 PILE NO.: 1

HAMMER: D-30-32 ENERGY/BLOW: 99.9 kJ OPERATING RATE: 36-52 BPM HELMET WEIGHT: 14.5 kN

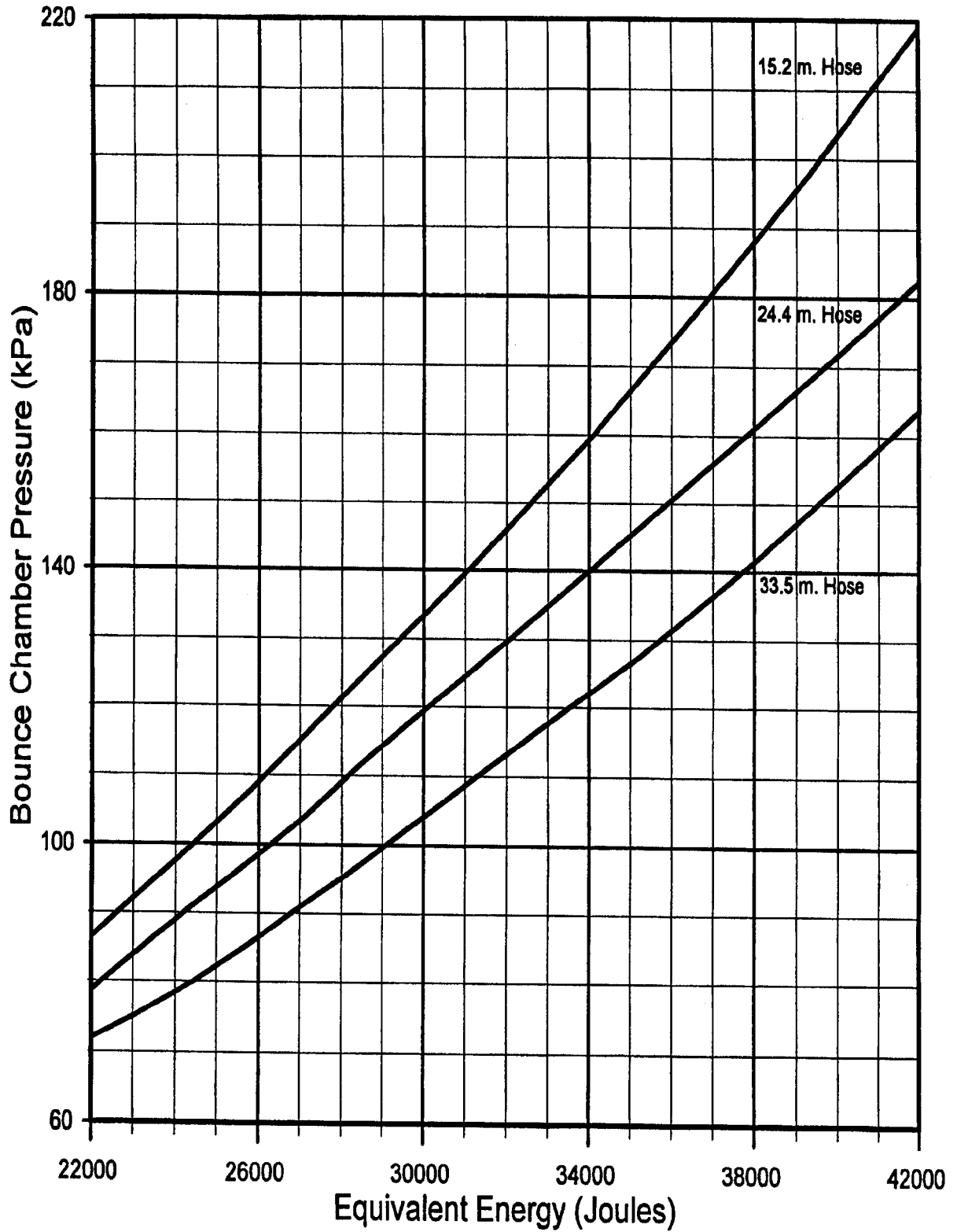
REF. ELEV.: 109.5 m PILE TOE ELEV.: _____ PILE CUTOFF ELEV.: 108.3 m

PILE CUSHION THICKNESS AND MATERIAL: 190 mm of plywood

WEATHER: sunny TEMP.: 80° START TIME: 8:23 am STOP TIME: 8:58 am

METERS	BLOWS	STROKE / PRESSURE	REMARKS	METERS	BLOWS	STROKE / PRESSURE	REMARKS
0 - 0.25	W.O.P			8.00 - 8.25	25		
0.25 - 0.50	W.O.P			8.25 - 8.50	21	51 BPM	
0.50 - 0.75	W.O.P			8.50 - 8.75	23		
0.75 - 1.00	W.O.P			8.75 - 9.00	26		
1.00 - 1.25	W.O.P			9.00 - 9.25	22	51 BPM	
1.25 - 1.50	W.O.P			9.25 - 9.50	21		
1.50 - 1.75	W.O.H			9.50 - 9.75	23		
1.75 - 2.00	W.O.H			9.75 - 10.00	24	51 BPM	
2.00 - 2.25	W.O.H			10.00 - 10.25	22		
2.25 - 2.50	5		Fuel #2	10.25 - 10.50	26		
2.50 - 2.75	6	52 BPM		10.50 - 10.75	30	44 BPM	
2.75 - 3.00	8			10.75 - 11.00	34		
3.00 - 3.25	10			11.00 - 11.25	40		
3.25 - 3.50	12			11.25 - 11.50	51	43 BPM	
3.50 - 3.75	17	50 BPM		11.50 - 11.75	38	42 BPM	Fuel #4
3.75 - 4.00	22			11.75 - 12.00	41		
4.00 - 4.25	30	49 BPM		12.00 - 12.25	42	42 BPM	
4.25 - 4.50	21	47 BPM	Fuel #3	12.25 - 12.50	53		
4.50 - 4.75	24			12.50 - 12.75	58	41 BPM	
4.75 - 5.00	27			12.75 - 13.00	65		
5.00 - 5.25	29			13.00 - 13.25	77	40 BPM	
5.25 - 5.50	31	45 BPM		13.25 - 13.50	80	40 BPM	
5.50 - 5.75	32			13.50 - 13.75			
5.75 - 6.00	32			13.75 - 14.00			
6.00 - 6.25	35	45 BPM		14.00 - 14.25			
6.25 - 6.50	31			14.25 - 14.50			
6.50 - 6.75	25			14.50 - 14.75			
6.75 - 7.00	21	47 BPM		14.75 - 15.00			
7.00 - 7.25	18			15.00 - 15.25			
7.25 - 7.50	20			15.25 - 15.50			
7.50 - 7.75	19	51 BPM		15.50 - 15.75			
7.75 - 8.00	22			15.75 - 16.00			

Bounce Chamber Pressure vs. Equivalent Energy



PILE DRIVING LOG

STATE PROJECT NO.: Bridge #2 DATE: 5-29-98

JOB LOCATION: Hoboken

PILE TYPE: 324 mm CEP LENGTH: 15.5 m BENT/PIER NO.: 4 PILE NO.: 1

HAMMER: LB 520 ENERGY/BLOW: 35.7 kJ OPERATING RATE: 80-84 BPM HELMET WEIGHT: 8.9 KN

REF. ELEV.: 91.25 PILE TOE ELEV.: _____ PILE CUTOFF ELEV.: 94.1 m

PILE CUSHION THICKNESS AND MATERIAL: none

WEATHER: cloudy TEMP.: 75° START TIME: 10:52 STOP TIME: 11:09

METERS	BLOWS	STROKE / PRESSURE	REMARKS	METERS	BLOWS	STROKE / PRESSURE	REMARKS
0 - 0.25	W.O.H.		24.4 m hose	8.00 - 8.25	38		
0.25 - 0.50	W.O.H.			8.25 - 8.50	37	BCP 160	
0.50 - 0.75	W.O.H.			8.50 - 8.75	39		
0.75 - 1.00	W.O.H.			8.75 - 9.00	41		
1.00 - 1.25	3			9.00 - 9.25	40		
1.25 - 1.50	5			9.25 - 9.50	39	BCP 160	
1.50 - 1.75	6			9.50 - 9.75	42		
1.75 - 2.00	5			9.75 - 10.00	41		
2.00 - 2.25	6			10.00 - 10.25	44	BCP 160	
2.25 - 2.50	4	BCP 110		10.25 - 10.50	50		
2.50 - 2.75	5			10.50 - 10.75	51		
2.75 - 3.00	6			10.75 - 11.00	53	BCP 165	
3.00 - 3.25	8	BCP 115		11.00 - 11.25	51		min pen
3.25 - 3.50	10			11.25 - 11.50	54		
3.50 - 3.75	12			11.50 - 11.75	55	BCP 170	
3.75 - 4.00	20	BCP 125		11.75 - 12.00	57		
4.00 - 4.25	22			12.00 - 12.25	58	BCP 170	
4.25 - 4.50	21			12.25 - 12.50	60		
4.50 - 4.75	20			12.50 - 12.75	65	BCP 175	
4.75 - 5.00	23	BCP 135		12.75 - 13.00			
5.00 - 5.25	21			13.00 - 13.25			
5.25 - 5.50	25			13.25 - 13.50			
5.50 - 5.75	28	BCP 150		13.50 - 13.75			
5.75 - 6.00	30			13.75 - 14.00			
6.00 - 6.25	33			14.00 - 14.25			
6.25 - 6.50	32	BCP 155		14.25 - 14.50			
6.50 - 6.75	33			14.50 - 14.75			
6.75 - 7.00	35			14.75 - 15.00			
7.00 - 7.25	33	BCP 155		15.00 - 15.25			
7.25 - 7.50	37			15.25 - 15.50			
7.50 - 7.75	36			15.50 - 15.75			
7.75 - 8.00	33	BCP 155		15.75 - 16.00			

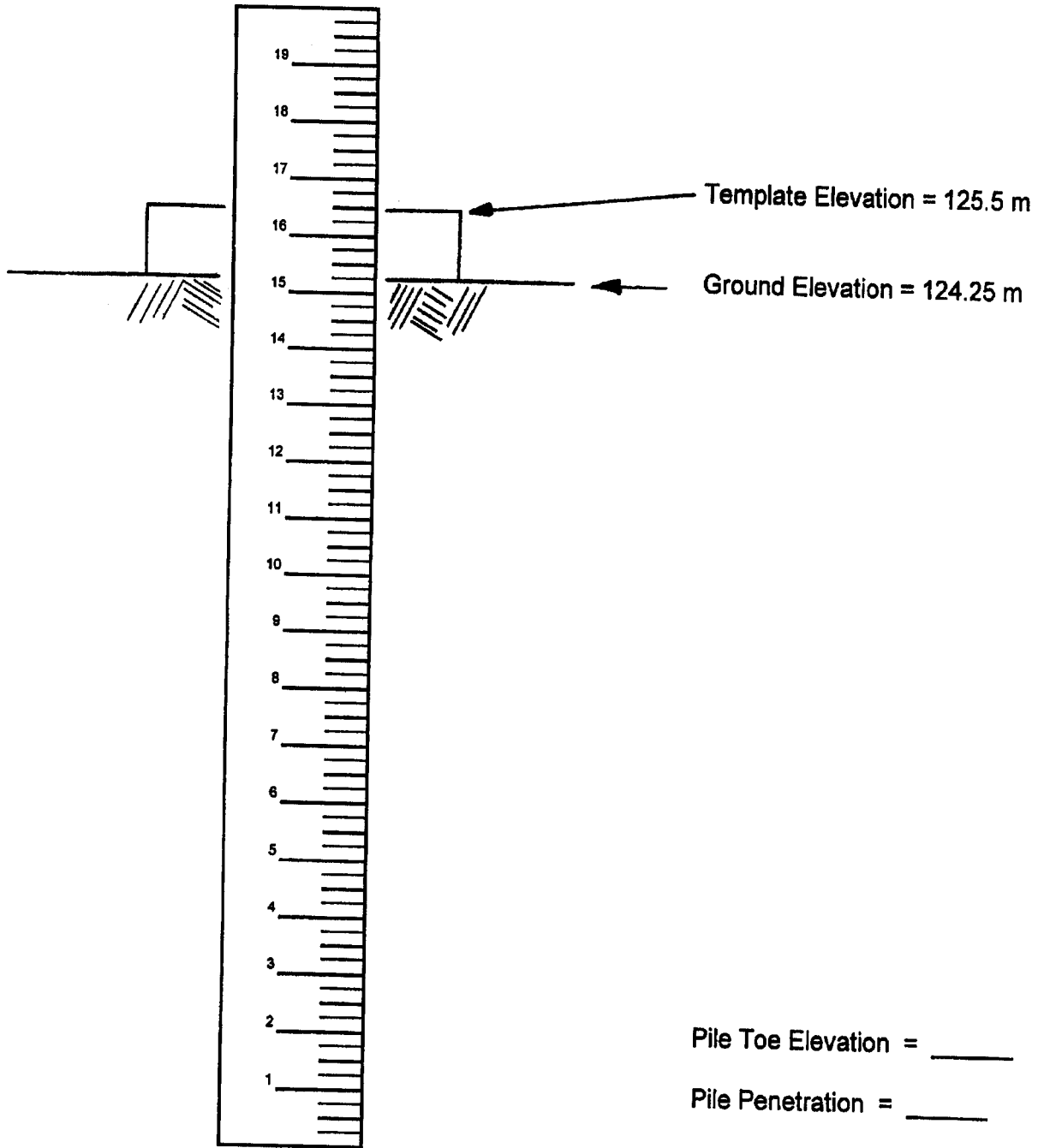
STUDENT EXERCISE #16 - DETERMINING PILE TOE ELEVATIONS

Pile driving criteria often include obtaining a specified driving resistance in conjunction with a pile penetration requirement or pile toe elevation. For many land based driving situations determination of the pile toe elevation is a relatively straightforward task. For batter pile driving and pile installations over water, determination of the pile toe elevation can be more problematic.

The following pages contain pile installation illustrations where the reference elevation is given and the pile penetration shown. For each example, calculate the final pile toe elevation and pile penetration depth.

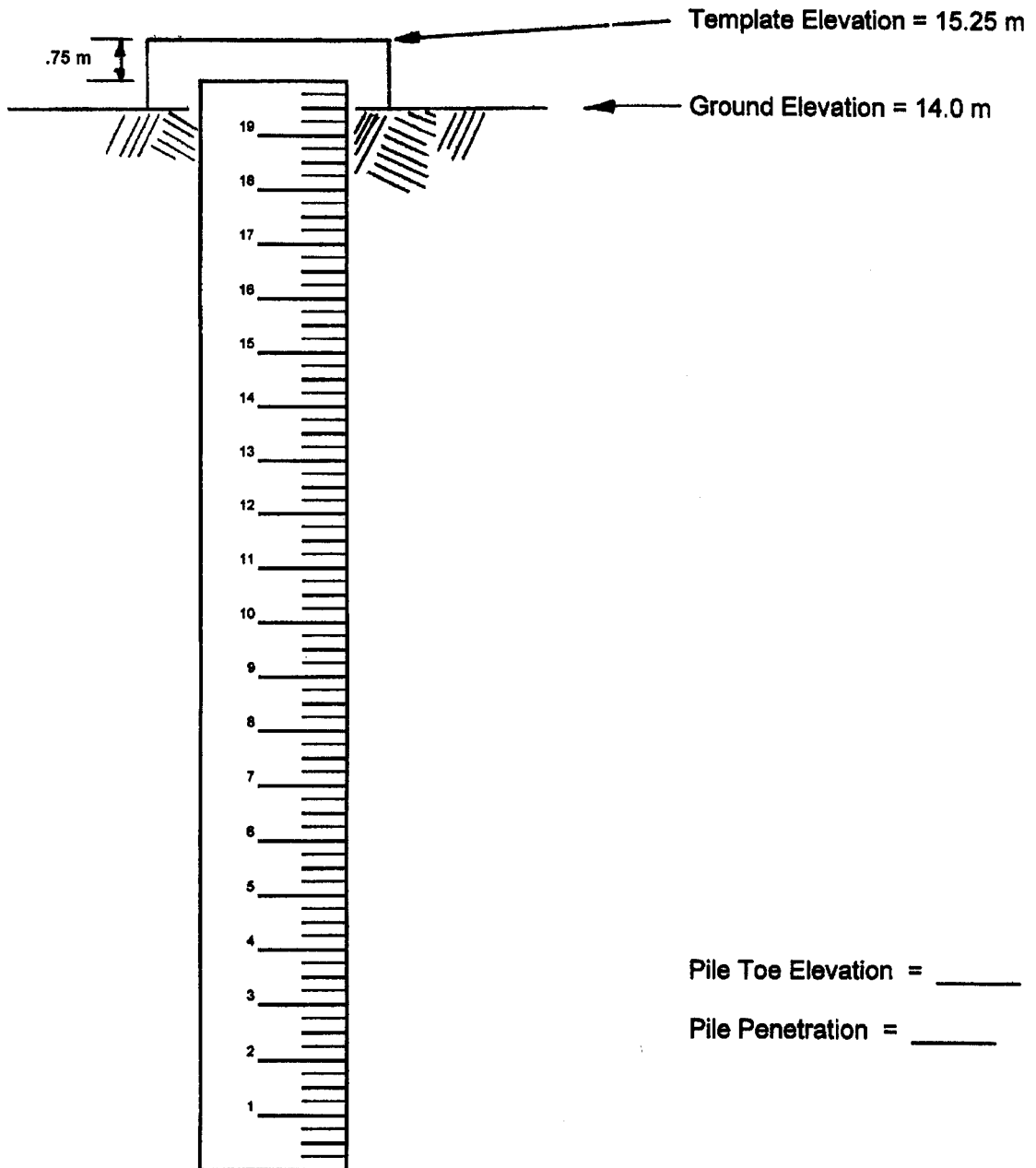
STUDENT EXERCISE 16a - DETERMINING PILE TOE ELEVATIONS

Land Pile Installation



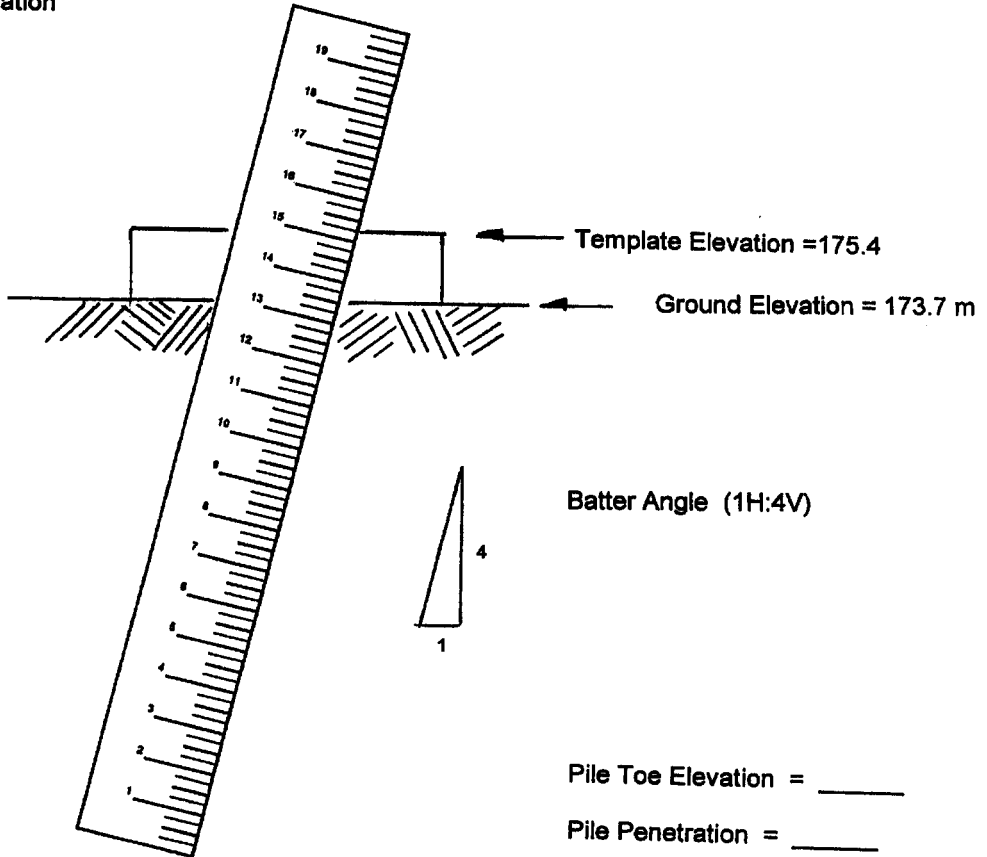
STUDENT EXERCISE #16b - DETERMINING PILE TOE ELEVATIONS

Land Pile Installation



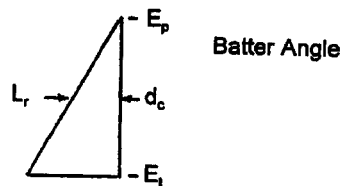
STUDENT EXERCISE #16c - DETERMINING PILE TOE ELEVATIONS

Batter Pile Installation



Calculating Pile Toe Elevation of Batter Piles

Batter Angle	Correction Factor. (B_c)
1H : 12V	.997
1.5H : 12V	.992
2H : 12V (1H : 6V)	.986
3H : 12V (1H : 4V)	.971
4H : 12V (1H : 3V)	.949
5H : 12V	.923



Definitions

- L_r = Pile Length Below Reference Point (m)
- E_p = Reference Point Elevation (m)
- d_c = Corrected Pile Depth (m)
- E_t = Pile Toe Elevation

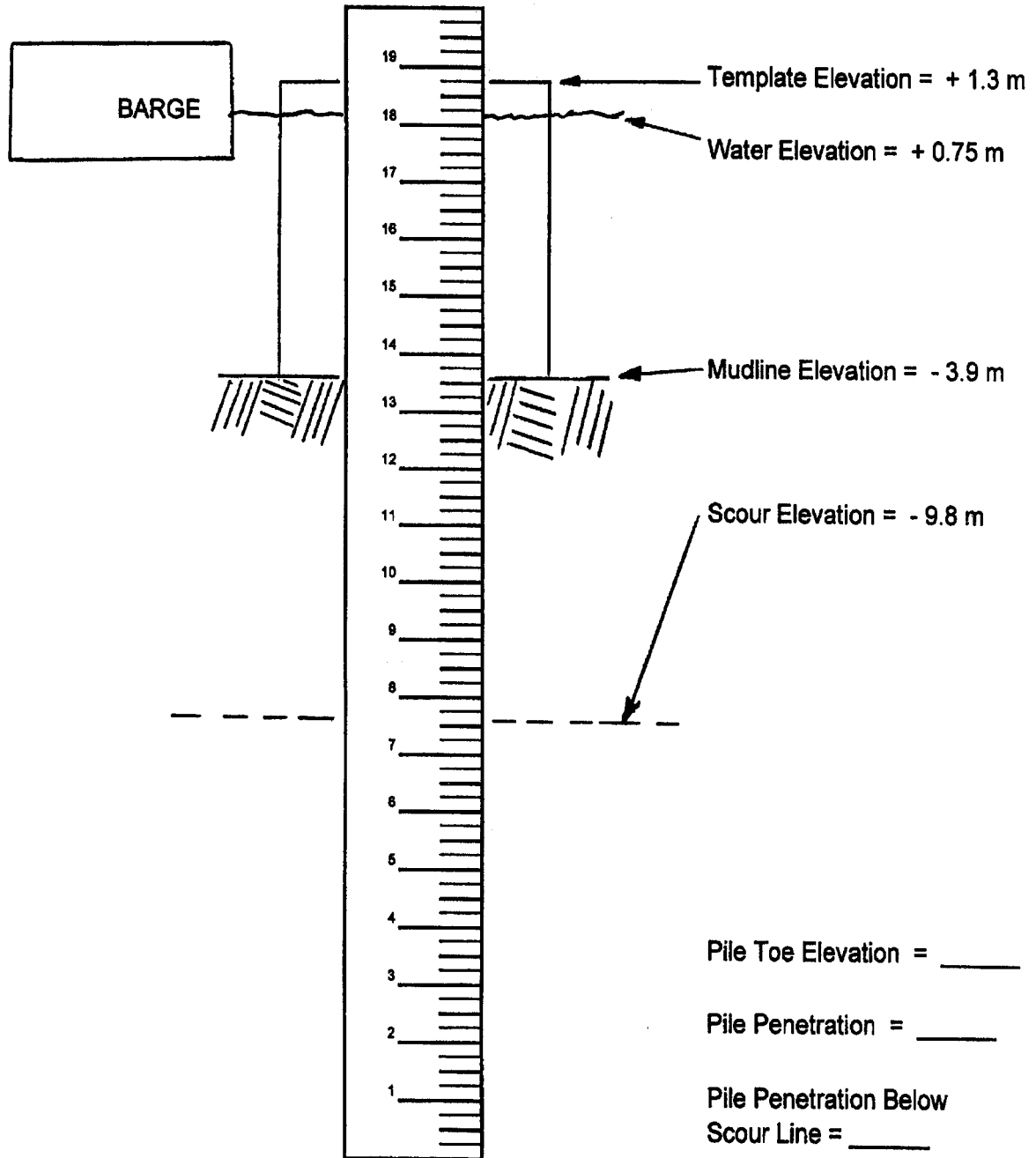
Formulas

$$d_c = (L_r)(B_c)$$

$$E_t = E_p - d_c$$

STUDENT EXERCISE #16d - DETERMINING PILE TOE ELEVATIONS

Pile Installation over Water



APPENDIX A

List of FHWA Pile Foundation Design and Construction References

- Briaud, J-L. (1989). The Pressuremeter Test for Highway Applications. Report No. FHWA IP-89-008, U.S. Department of Transportation, Federal Highway Administration, Office of Implementation, McLean, 156.
- Briaud, J-L. and Miran, J. (1991). The Cone Penetrometer Test. Report No. FHWA-SA-91-043, U.S. Department of Transportation, Federal Highway Administration, Office of Technology Applications, Washington, D.C., 161.
- Briaud, J-L. and Miran, J. (1992). The Flat Dilatometer Test. Report No. FHWA-SA-91-44, U.S. Department of Transportation, Federal Highway Administration, Office of Technology Applications, Washington, D.C., 102.
- Briaud, J-L., Tucker, L., Lytton, R.L. and Coyle, H.M. (1985). Behavior of Piles and Pile Groups in Cohesionless Soils. Report No. FHWA/RD-83/038, U.S. Department of Transportation, Federal Highway Administration, Office of Research - Materials Division, Washington, D.C., 233.
- Cheney, R.S. and Chassie, R.G. (1993). Soils and Foundations Workshop Manual. Second Edition, Report No. HI-88-009, U.S. Department of Transportation, Federal Highway Administration, Office of Engineering, Washington, D.C., 395.
- Goble, G.G., and Rausche, F. (1986). Wave Equation Analysis of Pile Driving - WEAP86 Program. U.S. Department of Transportation, Federal Highway Administration, Implementation Division, McLean, Volumes I-IV.
- Kyfor, Z.G., Schnore, A.S., Carlo, T.A. and Bailey, P.F. (1992). Static Testing of Deep Foundations. Report No. FHWA-SA-91-042, U.S. Department of Transportation, Federal Highway Administration, Office of Technology Applications, Washington, D.C., 174.

- Lam, I.P. and Martin, G.R. (1986). Seismic Design of Highway Bridge Foundations. Volume II - Design Procedures and Guidelines, Report No. FHWA/RD-86/102, U.S. Department of Transportation, Federal Highway Administration, Office of Engineering and Highway Operations, McLean, 181.
- Mathias, D. and Cribbs, M. (1998). DRIVEN 1.0: A Microsoft Windows™ Based Program for Determining Ultimate Vertical Static Pile Capacity. Report No. FHWA-SA-98-074, U.S. Department of Transportation, Federal Highway Administration, Office of Technology Applications, Washington D.C. 112.
- Osterberg, J.O. (1995). The Osterberg Cell for Load Testing Drilled Shafts and Driven Piles. Report No. FHWA-SA-94-035, U.S. Department of Transportation, Federal Highway Administration, Office of Technology Applications, Washington, D.C., 92.
- Rausche, F., Likins, G.E., Goble, G.G. and Miner, R. (1985). The Performance of Pile Driving Systems. Main Report, U.S. Department of Transportation, Federal Highway Administration, Office of Research and Development, Washington, D.C., Volumes I-IV.
- Reese, L.C. (1984). Handbook on Design of Piles and Drilled Shafts Under Lateral Load. Report No. FHWA-IP-84 11, U.S. Department of Transportation, Federal Highway Administration, Office of Implementation, McLean, 386.
- Urzua, A. (1992). SPILE A Microcomputer Program for Determining Ultimate Vertical Static Pile Capacity. Users Manual, Report No. FHWA-SA-92-044, U.S. Department of Transportation, Federal Highway Administration, Office of Engineering and Office of Technology Applications, Washington, D.C., 58.
- Wang, S-T, and Reese, L.C. (1993). COM624P - Laterally Loaded Pile Analysis Program for the Microcomputer, Version 2.0. Report No. FHWA-SA-91-048, U.S. Department of Transportation, Federal Highway Administration, Office of Technology Applications, Washington, D.C., 504.

APPENDIX B

List of ASTM Pile Design and Testing Specifications

DESIGN

Standard Specification for Welded and Seamless Steel Pipe Piles.
ASTM Designation: A 252

Standard Specification for Round Timber Piles.
ASTM Designation: D 25

Standard Method for Establishing Design Stresses for Round Timber Piles.
ASTM Designation: D 2899

Standard Methods for Establishing Clear Wood Strength Values.
ASTM Designation: D 2555

TESTING

Standard Method for Testing Piles under Axial Compressive Load.
ASTM Designation: D 1143

Standard Method for Testing Individual Piles under Static Axial Tensile Load.
ASTM Designation: D 3689

Standard Method for Testing Piles under Lateral Load.
ASTM Designation: D 3966

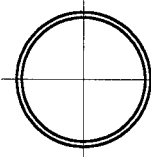
Standard Test Method for High Strain Dynamic Testing of Piles.
ASTM Designation: D 4945

Standard Test Method for Low Strain Dynamic Testing of Piles.
ASTM Designation: D 5882

APPENDIX C

Information and Data on Various Pile Types

	Page
Dimensions and Properties of Pipe Piles	C-3
Data for Steel Monotube Piles	C-17
Typical Prestressed Concrete Pile Sections	C-19
Dimensions and Properties of H-Piles	C-21
Sample Specification for Bitumen Coating on Concrete Piles	C-23
Sample Specification for Bitumen Coating on Steel Piles	C-25



PIPE PILES

Approximate Pile Dimensions and Design Properties

Designation and Outside Diameter	Wall Thickness	Area A	Weight per Meter	Section Properties			Area of Exterior Surface	Inside Cross Sectional Area	Inside Volume	External Collapse Index
				I	S	r				
mm	mm	mm ²	N	mm ⁴ x 10 ⁶	mm ³ x 10 ³	mm	m ² /m	mm ²	m ³ /m	*
PP203	3.58	2,245	173	11.197	110.12	70.61	0.64	30,193	0.0301	266
	4.17	2,607	200	12.903	127.00	70.36	0.64	29,806	0.0298	422
	4.37	2,729	210	13.486	132.74	70.36	0.64	29,677	0.0296	487
	4.55	2,839	218	13.985	137.82	70.36	0.64	29,613	0.0296	548
	4.78	2,974	229	14.651	144.21	70.10	0.64	29,484	0.0293	621
	5.56	3,452	266	16.857	165.51	69.85	0.64	28,968	0.0291	874
PP219	2.77	1,884	145	10.989	100.45	76.45	0.69	35,806	0.0359	97
	3.18	2,155	166	12.570	114.55	76.45	0.69	35,548	0.0356	147
	3.58	2,426	187	14.069	128.47	76.20	0.69	35,290	0.0354	212
	3.96	2,678	206	15.484	141.42	75.95	0.69	35,032	0.0351	288
	4.17	2,813	216	16.233	148.30	75.95	0.69	34,903	0.0349	335
	4.37	2,949	227	16.982	155.02	75.95	0.69	34,774	0.0349	388
	4.55	3,065	236	17.648	160.92	75.95	0.69	34,645	0.0346	438
	4.78	3,213	247	18.481	168.79	75.69	0.69	34,452	0.0344	508
	5.16	3,465	266	19.813	180.26	75.69	0.69	34,258	0.0341	623
	5.56	3,729	287	21.269	195.01	75.44	0.69	33,935	0.0339	744
	6.35	4,245	326	24.017	219.59	75.18	0.69	33,419	0.0334	979
	7.04	4,684	360	26.389	240.89	74.93	0.69	33,032	0.0331	1,180
	7.92	5,258	404	29.344	267.11	74.68	0.69	32,452	0.0324	1,500
	8.18	5,420	417	30.177	275.30	74.68	0.69	32,258	0.0324	1,600
	8.74	5,775	444	31.967	291.69	74.42	0.69	31,935	0.0319	1,820
	9.53	6,271	482	34.506	314.63	74.17	0.69	31,419	0.0314	2,120
	10.31	6,775	520	36.920	337.57	73.91	0.69	30,903	0.0309	2,420
	11.13	7,291	559	39.417	358.88	73.66	0.69	30,452	0.0304	2,740
12.70	8,259	633	44.121	401.48	73.15	0.69	29,484	0.0293	3,340	

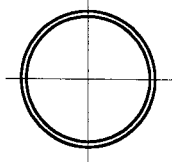
Pile design data converted to SI units from US units published in 1985 version of this manual.

Note: Designer must confirm section properties and local availability of selected pile section.

Material Specifications - ASTM A252

Example of suggested method of designation: PP219 x 2.77

* The External Collapse Index is a non-dimensional function of the diameter to wall thickness ratio and is for general guidance only. The higher the number, the greater is the resistance to collapse.



PIPE PILES

Approximate Pile Dimensions and Design Properties

Designation and Outside Diameter	Wall Thickness	Area A	Weight per Meter	Section Properties			Area of Exterior Surface	Inside Cross Sectional Area	Inside Volume	External Collapse Index
				I	S	r				
mm	mm	mm ²	N	mm ⁴ x 10 ⁶	mm ³ x 10 ³	mm	m ² /m	mm ²	m ³ /m	*
PP254	2.77	2,187	168	17.232	135.68	88.90	0.80	48,516	0.0484	62
	3.05	2,400	185	18.939	148.96	88.65	0.80	48,258	0.0482	83
	3.40	2,678	206	21.020	165.51	88.65	0.80	48,000	0.0479	116
	3.58	2,820	217	22.102	173.70	88.65	0.80	47,871	0.0479	135
	3.81	2,994	230	23.434	185.17	88.39	0.80	47,677	0.0477	163
	4.17	3,271	251	25.515	201.56	88.39	0.80	47,419	0.0474	214
	4.37	3,426	263	26.680	209.75	88.39	0.80	47,226	0.0472	247
	4.55	3,562	274	27.721	217.95	88.14	0.80	47,097	0.0472	279
	4.78	3,742	287	29.053	229.42	88.14	0.80	46,903	0.0469	324
	5.16	4,033	310	31.217	245.81	87.88	0.80	46,645	0.0467	409
	5.56	4,342	334	33.507	263.83	87.88	0.80	46,322	0.0464	515
	6.35	4,942	380	37.919	298.24	87.63	0.80	45,742	0.0457	719
PP273	2.77	2,349	181	21.478	157.32	95.50	0.86	56,193	0.0562	50
	3.05	2,587	199	23.559	172.06	95.50	0.86	56,000	0.0559	67
	3.18	2,690	207	24.516	180.26	95.50	0.86	55,871	0.0559	76
	3.40	2,884	222	26.223	191.73	95.25	0.86	55,677	0.0557	93
	3.58	3,032	233	27.513	201.56	95.25	0.86	55,548	0.0554	109
	3.81	3,226	248	29.219	214.67	95.25	0.86	55,355	0.0554	131
	3.96	3,349	258	30.343	222.86	95.25	0.86	55,226	0.0552	148
	4.17	3,516	271	31.800	232.70	95.00	0.86	55,032	0.0549	172
	4.37	3,691	284	33.299	244.17	95.00	0.86	54,839	0.0549	199
	4.55	3,832	295	34.589	254.00	95.00	0.86	54,710	0.0547	224
	4.78	4,026	310	36.212	265.47	94.74	0.86	54,516	0.0544	260
	5.16	4,342	334	38.959	285.13	94.74	0.86	54,193	0.0542	328
5.56	4,679	359	41.623	306.44	94.49	0.86	53,871	0.0539	414	

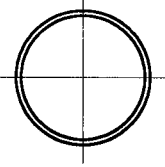
Pile design data converted to SI units from US units published in 1985 version of this manual.

Note: Designer must confirm section properties and local availability of selected pile section.

Material Specifications - ASTM A252

Example of suggested method of designation: PP219 x 2.77

* The External Collapse Index is a non-dimensional function of the diameter to wall thickness ratio and is for general guidance only. The higher the number, the greater is the resistance to collapse.



PIPE PILES

Approximate Pile Dimensions and Design Properties

Designation and Outside Diameter	Wall Thickness	Area A	Weight per Meter	Section Properties			Area of Exterior Surface	Inside Cross Sectional Area	Inside Volume	External Collapse Index
				I	S	r				
mm	mm	mm ²	N	mm ⁴ x 10 ⁶	mm ³ x 10 ³	mm	m ² /m	mm ²	m ³ /m	*
PP273 (cont'd)	5.84	4,904	377	43.704	321.19	94.49	0.86	53,677	0.0537	480
	6.35	5,323	409	47.450	347.41	94.23	0.86	53,226	0.0532	605
	7.09	5,923	455	52.445	383.46	93.98	0.86	52,645	0.0527	781
	7.80	6,517	500	57.024	419.51	93.73	0.86	52,064	0.0522	951
	8.74	7,226	558	63.267	465.39	93.47	0.86	51,290	0.0514	1,180
	9.27	7,678	591	67.013	489.97	93.22	0.86	50,903	0.0509	1,320
	11.13	9,162	704	78.668	576.82	92.71	0.86	49,419	0.0494	1,890
	12.70	10,389	799	88.241	645.65	92.20	0.86	48,193	0.0482	2,380
PP305	3.40	3,226	248	36.587	240.89	106.68	0.96	69,677	0.0697	67
	3.58	3,387	261	38.460	252.36	106.43	0.96	69,677	0.0695	78
	3.81	3,600	277	40.791	267.11	106.43	0.96	69,677	0.0695	94
	4.17	3,936	303	44.537	291.69	106.43	0.96	69,032	0.0690	123
	4.37	4,123	317	46.618	304.80	106.17	0.96	69,032	0.0687	142
	4.55	4,291	330	48.283	317.91	106.17	0.96	68,387	0.0687	161
	4.78	4,503	346	50.780	332.66	106.17	0.96	68,387	0.0685	186
	5.16	4,852	373	54.526	357.24	105.92	0.96	68,387	0.0682	235
	5.56	5,233	402	58.689	383.46	105.92	0.96	67,742	0.0677	296
	5.84	5,484	422	61.186	403.12	105.66	0.96	67,742	0.0675	344
	6.35	5,955	458	66.181	435.90	105.66	0.96	67,097	0.0670	443
	7.14	6,646	513	74.089	485.06	105.16	0.96	66,451	0.0662	616
	7.92	7,420	568	81.581	534.22	104.90	0.96	65,806	0.0655	784
PP324	2.77	2,794	215	36.004	222.86	113.54	1.02	79,355	0.0795	30
	3.18	3,200	246	41.124	254.00	113.28	1.02	79,355	0.0793	45
	3.40	3,426	264	44.121	272.03	113.28	1.02	78,710	0.0790	56
	3.58	3,607	277	46.202	285.13	113.28	1.02	78,710	0.0788	65
	3.81	3,832	295	49.115	303.16	113.29	1.02	78,710	0.0785	78
	3.96	3,981	306	50.780	314.63	113.03	1.02	78,710	0.0785	88
	4.17	4,181	322	53.278	329.38	113.03	1.02	78,064	0.0783	103

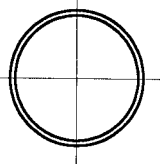
Pile design data converted to SI units from US units published in 1985 version of this manual.

Note: Designer must confirm section properties and local availability of selected pile section.

Material Specifications - ASTM A252

Example of suggested method of designation: PP219 x 2.77

* The External Collapse Index is a non-dimensional function of the diameter to wall thickness ratio and is for general guidance only. The higher the number, the greater is the resistance to collapse.



PIPE PILES

Approximate Pile Dimensions and Design Properties

Designation and Outside Diameter	Wall Thickness	Area A	Weight per Meter	Section Properties			Area of Exterior Surface	Inside Cross Sectional Area	Inside Volume	External Collapse Index
				I	S	r				
mm	mm	mm ²	N	mm ⁴ x 10 ⁶	mm ³ x 10 ³	mm	m ² /m	mm ²	m ³ /m	*
PP324 (cont'd)	4.37	4,387	337	55.775	345.77	113.03	1.02	78,064	0.0780	118
	4.55	4,562	351	58.272	358.88	113.03	1.02	78,064	0.0778	134
	4.78	4,787	368	60.770	376.90	112.78	1.02	77,419	0.0775	155
	5.16	5,162	397	65.765	404.76	112.78	1.02	77,419	0.0773	196
	5.56	5,562	428	70.343	435.90	112.52	1.02	76,774	0.0768	246
	5.84	5,839	449	73.673	455.56	112.52	1.02	76,774	0.0765	286
	6.35	6,336	487	79.916	493.25	112.27	1.02	76,129	0.0760	368
	7.14	7,097	546	89.074	550.61	112.01	1.02	75,484	0.0753	526
	7.92	7,871	605	98.231	606.32	111.76	1.02	74,193	0.0745	684
	8.38	8,323	639	103.225	639.10	111.51	1.02	74,193	0.0740	776
	8.74	8,646	665	107.388	663.68	111.51	1.02	73,548	0.0737	848
	9.53	9,420	723	116.129	717.75	111.25	1.02	72,903	0.0730	1,010
	10.31	10,131	781	124.869	771.83	111.00	1.02	72,258	0.0722	1,170
	11.13	10,905	840	133.610	825.91	110.74	1.02	71,613	0.0715	1,350
12.70	12,389	955	150.676	929.15	109.98	1.02	69,677	0.0700	1,760	
PP356	3.40	3,768	290	58.272	327.74	124.47	1.12	95,484	0.0956	42
	3.58	3,962	305	61.186	345.77	124.47	1.12	95,484	0.0953	49
	3.81	4,213	324	65.348	367.07	124.46	1.12	94,839	0.0951	59
	3.96	4,374	337	67.846	380.18	124.21	1.12	94,839	0.0948	66
	4.17	4,600	354	71.176	399.84	124.21	1.12	94,839	0.0948	77
	4.37	4,820	371	74.505	417.87	124.21	1.12	94,193	0.0946	89
	4.55	5,013	386	77.419	434.26	124.21	1.12	94,193	0.0943	101
	4.78	5,265	405	81.165	455.56	123.95	1.12	94,193	0.0941	117
	5.16	5,678	436	86.992	489.97	123.95	1.12	93,548	0.0936	147
	5.33	5,871	451	89.906	506.36	123.95	1.12	93,548	0.0936	163
	5.56	6,116	470	93.652	527.66	123.70	1.12	92,903	0.0933	815
	5.84	6,420	494	98.231	552.24	123.70	1.12	92,903	0.0928	215
	6.35	6,968	536	106.139	598.13	123.44	1.12	92,258	0.0923	277

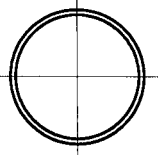
Pile design data converted to SI units from US units published in 1985 version of this manual.

Note: Designer must confirm section properties and local availability of selected pile section.

Material Specifications - ASTM A252

Example of suggested method of designation: PP219 x 2.77

* The External Collapse Index is a non-dimensional function of the diameter to wall thickness ratio and is for general guidance only. The higher the number, the greater is the resistance to collapse.



PIPE PILES

Approximate Pile Dimensions and Design Properties

Designation and Outside Diameter	Wall Thickness	Area A	Weight per Meter	Section Properties			Area of Exterior Surface	Inside Cross Sectional Area	Inside Volume	External Collapse Index
				I	S	r				
mm	mm	mm ²	N	mm ⁴ x 10 ⁶	mm ³ x 10 ³	mm	m ² /m	mm ²	m ³ /m	*
PP356 (cont'd)	7.14	7,807	601	118.626	666.95	123.19	1.12	91,613	0.0916	395
	7.92	8,646	666	130.697	735.78	122.94	1.12	90,968	0.0906	542
	8.74	9,549	732	143.184	806.24	122.68	1.12	89,677	0.0898	691
	9.53	10,389	796	155.254	873.43	122.43	1.12	89,032	0.0890	835
	11.13	12,065	926	178.563	1,006.17	121.92	1.12	87,097	0.0873	1,130
	11.91	12,839	989	190.218	1,070.08	121.67	1.12	86,451	0.0865	1,280
	12.70	13,678	1,052	201.456	1,132.35	121.41	1.12	85,806	0.0855	1,460
PP406	3.40	4,310	331	87.409	430.98	142.49	1.28	125,161	1.2542	28
	3.58	4,529	348	91.987	452.28	142.49	1.28	125,161	0.1252	33
	3.81	4,820	371	97.814	480.14	142.24	1.28	125,161	0.1249	39
	3.96	5,007	385	101.560	499.81	142.24	1.28	124,516	0.1247	44
	4.17	5,265	405	106.555	524.39	142.24	1.28	124,516	0.1244	52
	4.37	5,516	424	111.550	548.97	142.24	1.28	124,516	0.1242	60
	4.55	5,742	441	115.712	570.27	141.99	1.28	123,871	0.1239	67
	4.78	6,026	463	121.540	598.13	141.99	1.28	123,871	0.1237	78
	5.16	6,517	500	130.697	644.01	141.99	1.28	123,226	0.1232	98
	5.56	7,033	539	140.686	693.17	141.73	1.28	122,580	0.1227	124
	5.84	7,355	565	147.346	725.95	141.73	1.28	122,580	0.1224	144
	6.35	8,000	614	159.833	786.58	141.48	1.28	121,935	0.1217	185
	7.14	8,968	688	178.563	878.35	141.22	1.28	120,645	0.1207	264
	7.92	9,936	763	196.877	970.11	140.97	1.28	120,000	0.1199	362
	8.74	10,905	839	216.024	1,061.88	140.72	1.28	118,709	0.1189	487
	9.53	11,873	913	233.922	1,152.01	140.46	1.28	118,064	0.1179	617
	11.13	13,807	1,062	270.134	1,328.99	139.70	1.28	116,129	0.1159	874
11.91	14,775	1,135	287.616	1,414.20	139.45	1.28	114,838	0.1149	1,000	
12.70	15,679	1,208	304.681	1,499.42	139.19	1.28	114,193	0.1141	1,130	

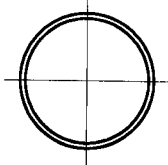
Pile design data converted to SI units from US units published in 1985 version of this manual.

Note: Designer must confirm section properties and local availability of selected pile section.

Material Specifications - ASTM A252

Example of suggested method of designation: PP219 x 2.77

* The External Collapse Index is a non-dimensional function of the diameter to wall thickness ratio and is for general guidance only. The higher the number, the greater is the resistance to collapse.



PIPE PILES

Approximate Pile Dimensions and Design Properties

Designation and Outside Diameter	Wall Thickness	Area A	Weight per Meter	Section Properties			Area of Exterior Surface	Inside Cross Sectional Area	Inside Volume	External Collapse Index
				I	S	r				
mm	mm	mm ²	N	mm ⁴ x 10 ⁶	mm ³ x 10 ³	mm	m ² /m	mm ²	m ³ /m	*
PP457	3.58	5,104	392	131.113	573.55	160.27	1.44	159,355	0.1590	23
	4.37	6,213	478	159.417	696.45	160.02	1.44	158,064	0.1580	42
	4.78	6,775	522	173.569	760.36	160.02	1.44	157,419	0.1573	55
	5.16	7,291	563	186.888	817.71	159.77	1.44	156,774	0.1568	69
	5.56	7,871	607	201.456	879.99	159.77	1.44	156,129	0.1563	87
	5.84	8,259	637	211.029	922.59	159.51	1.44	156,129	0.1558	101
	6.35	8,968	692	228.511	999.61	159.51	1.44	155,484	0.1553	129
	7.14	10,065	776	255.566	1,117.60	159.26	1.44	154,193	0.1540	184
	7.92	11,163	860	282.205	1,235.58	158.75	1.44	152,903	0.1530	253
	8.74	12,323	947	309.676	1,353.57	158.50	1.44	151,613	0.1518	341
	9.53	13,420	1,030	335.899	1,468.28	158.24	1.44	150,967	0.1508	443
	10.31	14,452	1,113	361.705	1,581.35	157.99	1.44	149,677	0.1498	559
	11.13	15,615	1,199	387.928	1,704.25	157.73	1.44	148,387	0.1485	675
11.91	16,646	1,281	413.318	1,802.58	157.48	1.44	147,742	0.1475	788	
12.70	17,743	1,364	437.043	1,917.29	157.23	1.44	146,451	0.1465	900	
PP508	3.58	5,678	436	180.644	711.20	178.31	1.60	196,774	0.1969	17
	4.37	6,904	531	219.354	863.60	178.05	1.60	195,483	0.1957	30
	4.78	7,549	581	238.917	940.62	177.80	1.60	194,838	0.1952	40
	5.16	8,130	626	257.647	1,014.36	177.80	1.60	194,838	0.1947	50
	5.56	8,775	675	277.210	1,091.38	177.55	1.60	194,193	0.1939	63
	6.35	10,002	769	314.671	1,238.86	177.29	1.60	192,903	0.1926	94
	7.14	11,226	864	352.132	1,386.35	177.04	1.60	191,613	0.1914	134
	7.92	12,452	957	389.176	1,532.19	176.78	1.60	190,322	0.1901	184
	8.74	13,678	1,054	428.718	1,687.87	176.53	1.60	189,032	0.1889	247

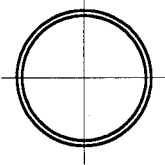
Pile design data converted to SI units from US units published in 1985 version of this manual.

Note: Designer must confirm section properties and local availability of selected pile section.

Material Specifications - ASTM A252

Example of suggested method of designation: PP219 x 2.77

* The External Collapse Index is a non-dimensional function of the diameter to wall thickness ratio and is for general guidance only. The higher the number, the greater is the resistance to collapse.



PIPE PILES

Approximate Pile Dimensions and Design Properties

Designation and Outside Diameter	Wall Thickness	Area A	Weight per Meter	Section Properties			Area of Exterior Surface	Inside Cross Sectional Area	Inside Volume	External Collapse Index
				I	S	r				
mm	mm	mm ²	N	mm ⁴ x 10 ⁶	mm ³ x 10 ³	mm	m ² /m	mm ²	m ³ /m	*
PP508 (cont'd)	9.53	14,904	1,147	462.017	1,818.96	176.28	1.60	187,742	0.1879	321
	10.31	16,130	1,240	499.478	1,966.45	176.02	1.60	186,451	0.1866	409
	11.13	17,357	1,335	536.939	2,113.93	175.77	1.60	185,161	0.1854	515
	11.91	18,583	1,428	570.237	2,245.03	175.51	1.60	183,871	0.1841	618
	12.70	19,743	1,520	607.698	2,392.51	175.26	1.60	183,225	0.1829	719
PP559	4.37	7,613	585	292.611	1,047.13	196.09	1.76	237,419	0.2375	23
	4.78	8,323	639	318.833	1,142.18	195.83	1.76	236,774	0.2370	30
	5.56	9,678	743	370.030	1,324.07	195.58	1.76	235,483	0.2355	47
	6.35	11,034	847	420.394	1,504.33	195.33	1.76	234,193	0.2343	70
	7.14	12,389	951	470.342	1,687.87	195.07	1.76	232,903	0.2328	100
	7.92	13,744	1,055	520.289	1,868.13	194.82	1.76	231,612	0.2315	138
	8.74	15,099	1,161	570.237	2,048.38	194.56	1.76	230,322	0.2303	185
	9.53	16,454	1,264	620.185	2,212.25	194.31	1.76	229,032	0.2288	241
	10.31	17,743	1,366	670.133	2,392.51	194.06	1.76	227,741	0.2275	306
	11.13	19,162	1,472	715.918	2,572.77	193.55	1.76	225,806	0.2260	386
	11.91	20,454	1,574	765.866	2,736.64	193.29	1.76	224,516	0.2248	475
	12.70	21,809	1,675	811.651	2,900.51	193.04	1.76	223,225	0.2235	571
PP610	4.37	8,323	639	380.436	1,248.69	213.87	1.91	283,870	0.2834	18
	4.78	9,097	698	414.983	1,361.77	213.87	1.91	282,580	0.2834	23
	5.56	10,582	812	482.828	1,579.71	213.61	1.91	281,290	0.2809	36
	6.35	12,065	925	549.425	1,802.58	213.36	1.91	279,999	0.2809	54
	7.14	13,486	1,039	611.860	2,015.61	213.11	1.91	278,064	0.2784	77
	7.92	14,970	1,152	678.457	2,228.64	212.85	1.91	276,774	0.2759	106
	8.74	16,517	1,268	745.054	2,441.67	212.34	1.91	275,483	0.2759	142
	9.53	17,937	1,381	807.489	2,654.70	212.09	1.91	274,193	0.2734	185

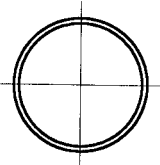
Pile design data converted to SI units from US units published in 1985 version of this manual.

Note: Designer must confirm section properties and local availability of selected pile section.

Material Specifications - ASTM A252

Example of suggested method of designation: PP219 x 2.77

* The External Collapse Index is a non-dimensional function of the diameter to wall thickness ratio and is for general guidance only. The higher the number, the greater is the resistance to collapse.



PIPE PILES

Approximate Pile Dimensions and Design Properties

Designation and Outside Diameter	Wall Thickness	Area A	Weight per Meter	Section Properties			Area of Exterior Surface	Inside Cross Sectional Area	Inside Volume	External Collapse Index
				I	S	r				
mm	mm	mm ²	N	mm ⁴ x 10 ⁶	mm ³ x 10 ³	mm	m ² /m	mm ²	m ³ /m	*
PP610 (cont'd)	10.31	19,421	1,493	869.924	2,867.74	211.84	1.91	272,258	0.2734	235
	11.13	20,904	1,608	936.521	3,080.77	211.58	1.91	270,967	0.2709	296
	11.91	22,388	1,720	998.955	3,277.41	211.33	1.91	269,677	0.2684	364
	12.70	23,809	1,831	1,061.390	3,474.06	211.07	1.91	267,741	0.2684	443
PP660	6.35	13,033	1,003	699.269	2,113.93	231.14	2.08	329,677	0.3286	43
	7.14	14,646	1,126	782.515	2,359.74	230.89	2.08	327,741	0.3286	61
	7.92	16,259	1,249	865.761	2,621.93	230.63	2.08	326,451	0.3261	83
	8.74	17,872	1,376	949.008	2,884.12	230.38	2.08	324,515	0.3236	112
	9.53	19,485	1,498	1,032.254	3,129.93	230.12	2.08	323,225	0.3236	145
	10.31	21,034	1,620	1,111.338	3,375.74	229.87	2.08	321,290	0.3211	184
	11.13	22,711	1,745	1,194.584	3,621.54	229.62	2.08	319,999	0.3211	232
	11.91	24,260	1,866	1,277.830	3,867.35	229.36	2.08	318,064	0.3186	286
	12.70	25,873	1,987	1,356.914	4,113.15	229.11	2.08	316,774	0.3161	347
	14.27	28,969	2,228	1,510.920	4,588.38	228.60	2.08	313,548	0.3135	495
	15.88	32,132	2,472	1,669.088	5,063.60	227.84	2.08	310,322	0.3110	656
	17.48	35,292	2,714	1,823.094	5,522.44	227.33	2.08	307,096	0.3060	814
	19.05	38,389	2,951	1,977.099	5,981.28	226.82	2.08	303,870	0.3035	970
PP711	6.35	14,065	1,081	874.086	2,458.06	249.17	2.23	383,225	0.3838	34
	7.14	15,807	1,214	978.144	2,753.03	248.92	2.23	381,290	0.3813	48
	7.92	17,486	1,346	1,082.202	3,047.99	248.67	2.23	379,999	0.3788	66
	8.74	19,291	1,483	1,190.422	3,342.96	248.41	2.23	378,064	0.3788	89
	9.53	20,969	1,615	1,294.480	3,637.93	248.16	2.23	376,128	0.3763	116
	10.31	22,711	1,746	1,394.375	3,916.51	247.90	2.23	374,838	0.3737	147
	11.13	24,453	1,881	1,498.433	4,211.48	247.65	2.23	372,902	0.3737	185
11.91	26,195	2,012	1,598.329	4,506.44	247.40	2.23	370,967	0.3712	228	

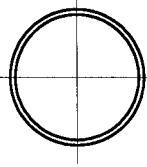
Pile design data converted to SI units from US units published in 1985 version of this manual.

Note: Designer must confirm section properties and local availability of selected pile section.

Material Specifications - ASTM A252

Example of suggested method of designation: PP219 x 2.77

* The External Collapse Index is a non-dimensional function of the diameter to wall thickness ratio and is for general guidance only. The higher the number, the greater is the resistance to collapse.



PIPE PILES

Approximate Pile Dimensions and Design Properties

Designation and Outside Diameter	Wall Thickness	Area A	Weight per Meter	Section Properties			Area of Exterior Surface	Inside Cross Sectional Area	Inside Volume	External Collapse Index
				I	S	r				
mm	mm	mm ²	N	mm ⁴ x 10 ⁶	mm ³ x 10 ³	mm	m ² /m	mm ²	m ³ /m	*
PP711 (cont'd)	12.70	27,874	2,143	1,698.224	4,785.02	246.89	2.23	369,677	0.3687	277
	14.27	31,229	2,403	1,898.015	5,342.18	246.38	2.23	365,806	0.3587	395
	15.88	34,713	2,667	2,097.806	5,899.34	245.87	2.23	362,580	0.3612	544
	17.48	38,068	2,929	2,293.435	6,440.12	245.36	2.23	359,354	0.3587	691
	19.05	41,423	3,185	2,480.739	6,980.89	244.86	2.23	356,128	0.3562	835
PP762	6.35	15,099	1,159	1,078.039	2,818.58	266.70	2.39	440,644	0.4415	28
	7.14	16,904	1,302	1,207.071	3,162.70	266.70	2.39	439,354	0.4390	39
	7.92	18,775	1,444	1,336.103	3,506.83	266.70	2.39	437,418	0.4365	54
	8.74	20,646	1,590	1,465.135	3,850.96	266.70	2.39	435,483	0.4365	72
	9.53	22,517	1,731	1,594.166	4,178.70	266.70	2.39	433,548	0.4340	94
	10.31	24,324	1,873	1,719.036	4,522.83	266.70	2.39	431,612	0.4314	120
	11.13	26,261	2,018	1,848.068	4,850.57	266.70	2.39	429,677	0.4289	150
	11.91	28,066	2,159	1,972.937	5,178.31	264.16	2.39	427,741	0.4289	185
	12.70	29,874	2,299	2,097.806	5,506.05	264.16	2.39	426,451	0.4264	225
	14.27	33,550	2,578	2,343.383	6,145.15	264.16	2.39	422,580	0.4214	321
	15.88	37,228	2,861	2,588.959	6,800.63	264.16	2.39	418,709	0.4189	443
	17.48	40,907	3,143	2,834.536	7,439.73	264.16	2.39	415,483	0.4164	584
	19.05	44,454	3,419	3,071.788	8,062.44	261.62	2.39	411,612	0.4114	719
PP813	6.35	16,065	1,237	1,306.967	3,211.86	284.48	2.55	502,580	0.5017	23
	7.14	18,067	1,389	1,465.135	3,605.15	284.488	2.55	500,644	0.5017	32
	7.92	20,067	1,541	1,623.303	3,998.44	284.48	2.55	498,709	0.4992	44
	8.74	22,067	1,697	1,785.633	4,391.73	284.48	2.55	496,773	0.4967	60
	9.53	24,067	1,848	1,939.638	4,768.64	284.48	2.55	494,838	0.4942	77
	10.31	26,002	1,999	2,093.644	5,145.54	284.48	2.55	492,902	0.4916	98
	11.13	28,003	2,155	2,251.812	5,538.83	284.48	2.55	490,967	0.4916	124
	11.91	30,003	2,305	2,401.655	5,915.73	281.94	2.55	489,031	0.4891	152

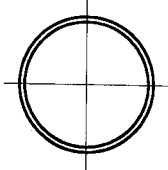
Pile design data converted to SI units from US units published in 1985 version of this manual.

Note: Designer must confirm section properties and local availability of selected pile section.

Material Specifications - ASTM A252

Example of suggested method of designation: PP219 x 2.77

* The External Collapse Index is a non-dimensional function of the diameter to wall thickness ratio and is for general guidance only. The higher the number, the greater is the resistance to collapse.



PIPE PILES

Approximate Pile Dimensions and Design Properties

Designation and Outside Diameter	Wall Thickness	Area A	Weight per Meter	Section Properties			Area of Exterior Surface	Inside Cross Sectional Area	Inside Volume	External Collapse Index
				I	S	r				
mm	mm	mm ²	N	mm ⁴ x 10 ⁶	mm ³ x 10 ³	mm	m ² /m	mm ²	m ³ /m	*
PP813 (cont'd)	12.70	31,937	2,455	2,555.661	6,292.63	281.94	2.55	487,096	0.4866	185
	14.27	35,810	2,754	2,855.348	7,030.05	281.94	2.55	483,225	0.4841	264
	15.88	39,744	3,056	3,155.034	7,767.47	281.94	2.55	479,354	0.4791	364
	17.48	43,680	3,358	3,454.721	8,504.89	281.94	2.55	475,483	0.4741	487
	19.05	47,488	3,653	3,741.921	9,209.53	281.94	2.55	471,612	0.4716	617
PP864	6.35	17,099	1,315	1,569.192	3,637.93	302.26	2.71	568,386	0.5694	19
	7.14	19,228	1,477	1,760.659	4,080.38	302.26	2.71	566,450	0.5669	27
	7.92	21,293	1,638	1,947.963	4,522.83	302.26	2.71	564,515	0.5644	37
	8.74	23,485	1,804	2,143.592	4,965.28	302.26	2.71	562,580	0.5619	50
	9.53	25,551	1,965	2,330.896	5,391.34	302.26	2.71	559,999	0.5594	64
	10.31	27,615	2,126	2,518.200	5,833.79	302.26	2.71	558,063	0.5569	82
	11.13	29,808	2,291	2,705.504	6,276.25	302.26	2.71	556,128	0.5569	103
	11.91	31,873	2,451	2,888.646	6,702.31	302.26	2.71	554,192	0.5544	127
	12.70	33,938	2,611	3,071.788	7,111.99	299.72	2.71	551,612	0.5518	154
	14.27	38,068	2,929	3,433.909	7,964.11	299.72	2.71	547,741	0.5468	219
	15.88	42,262	3,251	3,800.193	8,799.85	299.72	2.71	543,225	0.5443	303
	17.48	46,454	3,572	4,158.152	9,635.59	299.72	2.71	539,354	0.5393	405
	19.05	50,519	3,887	4,495.299	10,438.56	299.72	2.71	535,483	0.5343	527
	22.23	58,779	4,517	5,202.893	12,044.49	297.18	2.71	527,096	0.5268	767
25.40	67,102	5,143	5,868.863	13,617.65	297.18	2.71	518,709	0.5192	1,010	
PP914	6.35	18,130	1,393	1,868.879	4,080.38	320.04	2.87	638,708	0.6396	16
	7.14	20,325	1,564	2,093.644	4,571.99	320.04	2.87	636,128	0.6371	23
	7.92	22,582	1,735	2,318.409	5,063.60	320.04	2.87	634,192	0.6346	31
	8.74	24,840	1,912	2,547.336	5,571.60	320.04	2.87	631,612	0.6321	42

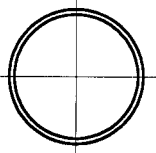
Pile design data converted to SI units from US units published in 1985 version of this manual.

Note: Designer must confirm section properties and local availability of selected pile section.

Material Specifications - ASTM A252

Example of suggested method of designation: PP219 x 2.77

* The External Collapse Index is a non-dimensional function of the diameter to wall thickness ratio and is for general guidance only. The higher the number, the greater is the resistance to collapse.



PIPE PILES

Approximate Pile Dimensions and Design Properties

Designation and Outside Diameter	Wall Thickness	Area A	Weight per Meter	Section Properties			Area of Exterior Surface	Inside Cross Sectional Area	Inside Volume	External Collapse Index
				I	S	r				
mm	mm	mm ²	N	mm ⁴ x 10 ⁶	mm ³ x 10 ³	mm	m ² /m	mm ²	m ³ /m	*
PP914 (cont'd)	9.53	27,098	2,082	2,772.101	6,063.21	320.04	2.87	629,676	0.6296	54
	10.31	29,292	2,252	2,992.704	6,538.44	320.04	2.87	627,096	0.6271	69
	11.13	31,550	2,428	3,221.631	7,046.44	320.04	2.87	625,160	0.6246	87
	11.91	33,808	2,597	3,438.072	7,521.66	320.04	2.87	623,225	0.6221	107
	12.70	36,002	2,766	3,658.674	7,996.89	320.04	2.87	620,644	0.6221	129
	14.27	40,390	3,104	4,087.393	8,947.34	317.50	2.87	616,128	0.6171	184
	15.88	44,841	3,446	4,536.923	9,897.79	317.50	2.87	611,612	0.6120	254
	17.48	49,230	3,786	4,953.154	10,831.85	317.50	2.87	607,741	0.6070	341
	19.05	53,616	4,120	5,369.385	11,749.52	317.50	2.87	603,225	0.6020	443
	22.23	62,326	4,790	6,201.848	13,568.49	314.96	2.87	594,192	0.5945	674
	25.40	70,972	5,455	7,034.311	15,338.29	314.96	2.87	585,805	0.5870	900
31.75	87,747	6,770	8,574.367	18,845.12	312.42	2.87	568,386	0.5694	1,380	
PP965	6.35	19,099	1,471	2,197.702	4,555.60	337.82	3.03	709,676	0.7124	14
	7.14	21,485	1,652	2,464.090	5,112.76	337.82	3.03	709,676	0.7099	19
	7.92	23,809	1,833	2,730.478	5,653.54	337.82	3.03	709,676	0.7074	26
	8.74	26,261	2,019	3,001.029	6,227.08	337.82	3.03	703,224	0.7049	35
	9.53	28,582	2,199	3,263.254	6,767.86	337.82	3.03	703,224	0.7023	46
	10.31	30,971	2,379	3,525.480	7,308.63	337.82	3.03	703,224	0.6998	59
	11.13	33,358	2,564	3,796.031	7,865.79	337.82	3.03	696,773	0.6973	74
	11.91	35,680	2,743	4,054.094	8,406.56	337.82	3.03	696,773	0.6973	90
	12.70	38,002	2,922	4,328.807	8,930.95	337.82	3.03	696,773	0.6923	110
	14.27	42,649	3,279	4,828.285	9,996.11	335.28	3.03	690,321	0.6898	156
	15.88	47,359	3,641	5,327.762	11,061.27	335.28	3.03	683,870	0.6848	216
17.48	52,003	4,001	5,827.240	12,110.04	335.28	3.03	677,418	0.6798	289	

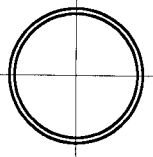
Pile design data converted to SI units from US units published in 1985 version of this manual.

Note: Designer must confirm section properties and local availability of selected pile section.

Material Specifications - ASTM A252

Example of suggested method of designation: PP219 x 2.77

* The External Collapse Index is a non-dimensional function of the diameter to wall thickness ratio and is for general guidance only. The higher the number, the greater is the resistance to collapse.



PIPE PILES

Approximate Pile Dimensions and Design Properties

Designation and Outside Diameter	Wall Thickness	Area A	Weight per Meter	Section Properties			Area of Exterior Surface	Inside Cross Sectional Area	Inside Volume	External Collapse Index
				I	S	r				
mm	mm	mm ²	N	mm ⁴ x 10 ⁶	mm ³ x 10 ³	mm	m ² /m	mm ²	m ³ /m	*
PP965 (cont'd)	19.05	56,649	4,354	6,326.718	13,142.43	335.28	3.03	677,418	0.6748	376
	22.23	65,810	5,063	7,325.673	15,174.42	332.74	3.03	664,515	0.6647	590
	25.40	74,843	5,767	8,283.005	17,206.42	332.74	3.03	658,063	0.6572	805
	31.75	92,909	7,160	10,156.047	20,975.44	330.20	3.03	638,708	0.6396	1,230
	38.10	110,974	8,533	11,945.842	24,744.47	327.66	3.03	620,644	0.6221	1,780
PP1016	7.92	25,098	1,930	3,188.333	6,276.25	355.60	3.20	787,095	0.7851	23
	8.74	27,679	2,126	3,508.831	6,898.95	355.60	3.20	780,644	0.7826	30
	9.53	30,131	2,316	3,812.680	7,505.28	355.60	3.20	780,644	0.7801	39
	10.31	32,583	2,505	4,120.691	8,111.60	355.60	3.20	780,644	0.7776	50
	11.13	35,099	2,701	4,453.676	8,734.31	355.60	3.20	774,192	0.7751	63
	11.91	37,551	2,890	4,745.038	9,324.24	355.60	3.20	774,192	0.7726	77
	12.70	40,002	3,078	5,036.400	9,914.17	355.60	3.20	767,740	0.7701	94
	14.27	44,906	3,454	5,619.124	11,094.04	353.06	3.20	767,740	0.7651	134
	15.88	49,874	3,836	6,243.471	12,273.91	353.06	3.20	761,289	0.7600	185
	17.48	54,842	4,215	6,826.195	13,453.78	353.06	3.20	754,837	0.7550	247
	19.05	59,681	4,588	7,408.919	14,600.87	353.06	3.20	748,386	0.7500	321
	22.23	69,682	5,336	8,574.367	16,878.68	350.52	3.20	741,934	0.7425	514
	25.40	79,360	6,078	9,698.192	19,172.86	350.52	3.20	729,031	0.7324	719
	31.75	98,070	7,549	11,904.219	23,433.50	347.98	3.20	709,676	0.7124	1,130
	38.10	116,781	9,001	14,026.999	27,530.27	345.44	3.20	696,773	0.6923	1,620
44.45	135,492	10,433	16,024.910	31,627.03	342.90	3.20	677,418	0.6748	2,140	
PP1067	7.92	26,389	2,027	3,696.135	6,931.73	373.38	3.35	864,514	0.8679	20
	8.74	29,034	2,233	4,066.581	7,619.98	373.38	3.35	864,514	0.8654	26
	9.53	31,615	2,433	4,412.053	8,291.85	373.38	3.35	864,514	0.8629	34
	10.31	34,260	2,632	4,786.661	8,947.34	373.38	3.35	864,514	0.8604	43

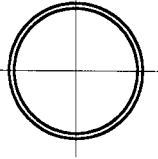
Pile design data converted to SI units from US units published in 1985 version of this manual.

Note: Designer must confirm section properties and local availability of selected pile section.

Material Specifications - ASTM A252

Example of suggested method of designation: PP219 x 2.77

* The External Collapse Index is a non-dimensional function of the diameter to wall thickness ratio and is for general guidance only. The higher the number, the greater is the resistance to collapse.



PIPE PILES

Approximate Pile Dimensions and Design Properties

Designation and Outside Diameter	Wall Thickness	Area A	Weight per Meter	Section Properties			Area of Exterior Surface	Inside Cross Sectional Area	Inside Volume	External Collapse Index
				I	S	r				
mm	mm	mm ²	N	mm ⁴ x 10 ⁶	mm ³ x 10 ³	mm	m ² /m	mm ²	m ³ /m	*
PP1067 (cont'd)	11.13	36,905	2,837	5,161.270	9,635.59	373.38	3.35	858,063	0.8579	54
	11.91	39,486	3,036	5,494.255	10,291.08	373.38	3.35	851,611	0.8554	67
	12.70	42,067	3,234	5,827.240	10,946.56	373.38	3.35	851,611	0.8528	81
	14.27	47,229	3,630	6,534.833	12,257.52	373.38	3.35	845,160	0.8478	116
	15.88	52,390	4,030	7,242.427	13,568.49	370.84	3.35	838,708	0.8403	159
	17.48	57,616	4,430	7,950.020	14,863.07	370.84	3.35	838,708	0.8353	213
	19.05	62,713	4,822	8,615.991	16,141.26	370.84	3.35	832,256	0.8303	277
	22.23	72,908	5,608	9,947.931	18,681.25	368.30	3.35	819,353	0.8202	443
	25.40	83,231	6,390	11,279.872	21,139.31	368.30	3.35	812,902	0.8102	641
	31.75	103,232	7,939	13,818.883	25,891.56	365.76	3.35	793,547	0.7901	1,030
	38.10	123,233	9,468	16,316.272	30,643.81	363.22	3.35	767,740	0.7701	1,460
	44.45	142,589	10,978	18,688.791	35,068.32	360.68	3.35	748,386	0.7500	1,970
50.80	161,945	12,468	20,978.064	39,328.95	360.68	3.35	729,031	0.7324	2,470	
PP1118	8.74	30,453	2,341	4,661.792	8,373.79	391.16	3.51	948,385	0.9507	23
	9.53	33,163	2,550	5,078.023	9,111.21	391.16	3.51	948,385	0.9482	30
	10.31	35,873	2,759	5,494.255	9,832.24	391.16	3.51	941,934	0.9457	38
	11.13	38,647	2,974	5,910.486	10,586.04	391.16	3.51	941,934	0.9432	47
	11.91	41,357	3,182	6,326.718	11,323.46	391.16	3.51	941,934	0.9406	58
	12.70	44,067	3,390	6,742.949	12,044.49	391.16	3.51	935,482	0.9381	70
	15.88	54,971	4,225	8,324.629	14,928.62	388.62	3.51	929,030	0.9256	138
	19.05	65,810	5,056	9,906.308	17,698.03	388.62	3.51	916,127	0.9156	241
	22.23	76,779	5,881	11,487.987	20,483.83	388.62	3.51	903,224	0.9055	384
	25.40	87,102	6,702	12,986.420	23,269.63	386.08	3.51	896,772	0.8930	571

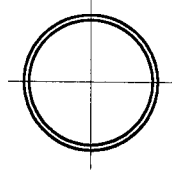
Pile design data converted to SI units from US units published in 1985 version of this manual.

Note: Designer must confirm section properties and local availability of selected pile section.

Material Specifications - ASTM A252

Example of suggested method of designation: PP219 x 2.77

* The External Collapse Index is a non-dimensional function of the diameter to wall thickness ratio and is for general guidance only. The higher the number, the greater is the resistance to collapse.



PIPE PILES

Approximate Pile Dimensions and Design Properties

Designation and Outside Diameter	Wall Thickness	Area A	Weight per Meter	Section Properties			Area of Exterior Surface	Inside Cross Sectional Area	Inside Volume	External Collapse Index
				I	S	r				
mm	mm	mm ²	N	mm ⁴ x 10 ⁶	mm ³ x 10 ³	mm	m ² /m	mm ²	m ³ /m	*
PP1118 (cont'd)	31.75	108,394	8,328	15,983.287	28,513.49	383.54	3.51	870,966	0.8729	941
	38.10	129,040	9,936	18,855.284	33,757.35	381.00	3.51	851,611	0.8528	1,300
	44.45	149,686	11,524	21,602.411	38,673.47	381.00	3.51	832,256	0.8303	1,810
	50.80	170,333	13,092	24,266.292	43,425.72	378.46	3.51	812,902	0.8102	2,290
	57.15	190,334	14,641	26,846.927	48,014.10	375.92	3.51	793,547	0.7901	2,770
PP1219	8.74	33,228	2,555	6,076.979	9,979.72	426.72	3.84	1,135,482	1.1338	18
	9.53	36,196	2,784	6,618.080	10,864.62	426.72	3.84	1,129,030	1.1313	23
	10.31	39,164	3,012	7,159.181	11,733.14	426.72	3.84	1,129,030	1.1288	29
	11.13	42,196	3,247	7,700.281	12,634.43	426.72	3.84	1,122,578	1.1263	36
	11.91	45,164	3,474	8,241.382	13,502.94	426.72	3.84	1,122,578	1.1212	45
	12.70	48,132	3,702	8,740.860	14,371.46	426.72	3.84	1,116,127	1.1187	54
	15.88	60,004	4,615	10,863.640	17,861.90	426.72	3.84	1,109,675	1.1087	106
	19.05	71,617	5,523	12,944.797	21,139.31	424.18	3.84	1,096,772	1.0962	185
	22.23	83,876	6,427	14,984.331	24,580.60	424.18	3.84	1,083,869	1.0836	295
	25.40	95,490	7,325	16,982.242	27,858.01	421.64	3.84	1,070,966	1.0711	443
	31.75	118,717	9,108	20,894.818	34,248.96	419.10	3.84	1,051,611	1.0485	787
	38.10	141,299	10,871	24,682.524	40,476.05	416.56	3.84	1,025,804	1.0259	1,130
	44.45	163,881	12,614	28,345.360	46,539.26	416.56	3.84	1,006,450	1.0034	1,530
	50.80	186,463	14,339	31,883.327	52,274.73	414.02	3.84	980,643	0.9808	1,970
	57.15	208,400	16,043	35,296.425	57,846.34	411.48	3.84	961,288	0.9582	2,410
63.50	230,336	17,729	38,626.276	63,254.07	408.94	3.84	935,482	0.9381	2,850	

Pile design data converted to SI units from US units published in 1985 version of this manual.

Note: Designer must confirm section properties and local availability of selected pile section.

Material Specifications - ASTM A252

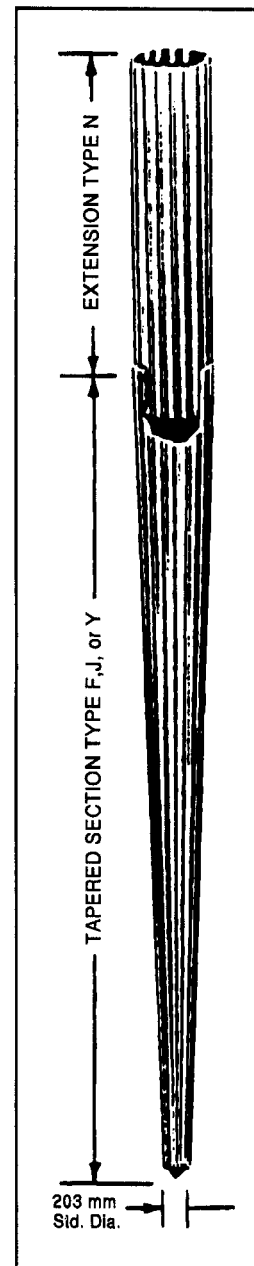
Example of suggested method of designation: PP219 x 2.77

* The External Collapse Index is a non-dimensional function of the diameter to wall thickness ratio and is for general guidance only. The higher the number, the greater is the resistance to collapse.

MONOTUBE PILES

Standard Monotube Weights and Volumes

TYPE	SIZE POINT DIAMETER x BUTT DIAMETER x LENGTH	Weight (N) per m				EST. CONC. VOL. m ³
		9 GA.	7 GA.	5 GA.	3 GA.	
F Taper 3.6 mm per Meter	216 mm x 305 mm x 7.62 m	248	292	350	409	0.329
	203 mm x 305 mm x 9.14 m	233	292	336	394	0.420
	216 mm x 356 mm x 12.19 m	277	321	379	452	0.726
	203 mm x 406 mm x 18.29 m	292	350	409	482	1.284
	203 mm x 457 mm x 22.86 m	-	379	452	511	1.979
J Taper 6.4 mm per Meter	203 mm x 305 mm x 5.18 m	248	292	336	394	0.244
	203 mm x 356 mm x 7.62 m	263	321	379	438	0.443
	203 mm x 406 mm x 10.06 m	292	350	409	467	0.726
	203 mm x 457 mm x 12.19 m	-	379	438	511	1.047
Y Taper 10.2 mm per Meter	203 mm x 305 mm x 3.05 m	248	292	350	409	0.138
	203 mm x 356 mm x 4.57 m	277	321	379	438	0.260
	203 mm x 406 mm x 6.10 m	292	350	409	482	0.428
	203 mm x 457 mm x 7.62 m	-	379	452	511	0.657



Extensions (Overall Length 0.305 m Greater than indicated)

TYPE	DIAMETER + LENGTH	9 GA.	7 GA.	5 GA.	3 GA.	m ³ /m
N 12	305 mm x 305 mm x 6.10 / 12.19 m	292	350	409	482	0.065
N 14	356 mm x 356 mm x 6.10 m / 12.19 m	350	423	496	598	0.088
N 16	406 mm x 406 mm x 6.10 m / 12.19 m	409	482	569	671	0.113
N 18	457 mm x 457 mm x 6.10 m / 12.19 m	-	555	642	759	0.145

Note: Designer must confirm section properties of selected pile section.

Pile design data converted to SI units from US units published in Monotube Pile Corporation Catalog 592.

MONOTUBE PILES

Physical Properties

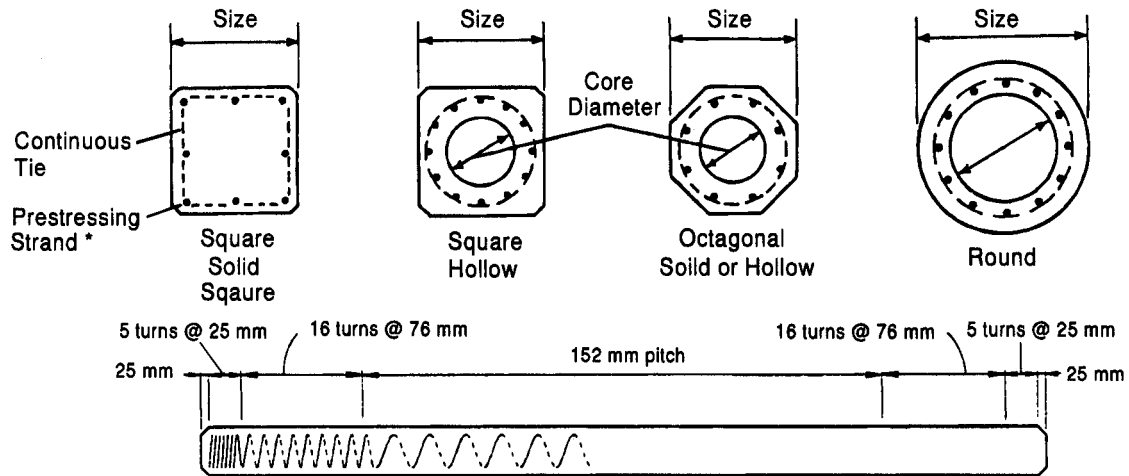
STEEL THICKNESS	POINTS		BUTTS OF PILE SECTIONS							
	203 mm	216 mm	305 mm				356 mm			
	A mm ²	A mm ²	A mm ²	I mm ⁴ x 10 ⁶	S mm ³ x 10 ³	r mm	A mm ²	I mm ⁴ x 10 ⁶	S mm ³ x 10 ³	r mm
9 GAUGE 3.797 mm	2,342	2,535	3,748	42.456	267.109	106	4,355	66.181	360.515	123
7 GAUGE 4.554 mm	2,839	3,077	4,497	50.780	319.548	106	5,252	80.749	437.535	124
5 GAUGE 5.314 mm	3,348	3,619	5,277	60.354	376.902	107	6,129	94.485	507.999	124
3 GAUGE 6.073 mm	3,787	4,245	5,781	61.602	396.567	103	6,839	99.479	550.605	121
CONCRETE AREA mm ²	27,290	30,518	65,161				87,742			

STEEL THICKNESS	POINTS		BUTTS OF PILE SECTIONS							
	203 mm	216 mm	406 mm				457 mm			
	A mm ²	A mm ²	A mm ²	I mm ⁴ x 10 ⁶	S mm ³ x 10 ³	r mm	A mm ²	I mm ⁴ x 10 ⁶	S mm ³ x 10 ³	r mm
9 GAUGE 3.797 mm	2,342	2,535	4,929	96.566	463.754	140	-	-	-	-
7 GAUGE 4.554 mm	2,839	3,077	5,923	115.712	555.521	140	6,710	168.157	712.837	158
5 GAUGE 5.314 mm	3,348	3,619	6,968	136.940	555.521	140	7,871	198.959	839.018	159
3 GAUGE 6.073 mm	3,787	4,245	7,742	144.849	706.282	137	8,774	209.781	907.843	155
CONCRETE AREA mm ²	27,290	30,518	113,548				144,516			

Note: Designer must confirm section properties of selected pile section.

Pile design data converted to SI units from US units published in Monotube Pile Corporation Catalog 592.

PRECAST/PRESTRESSED CONCRETE PILES



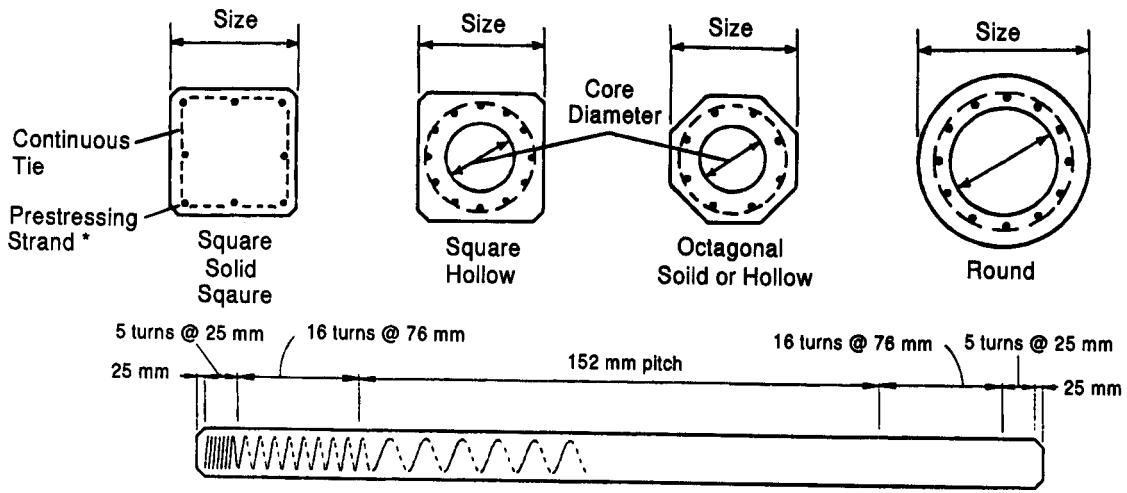
* Strand pattern may be circular or square

Size mm	Section Properties						
	Core Diameter mm	Area mm ²	Weight N/m	Moment of Inertia mm ⁴ x 10 ⁶	Section Modulus mm ³ x 10 ³	Radius of Gyration mm	Perimeter m
Square Piles							
254	Solid	64,516	1,518	346.721	2,736.640	73.4	1.015
305	Solid	92,903	2,189	719.248	4,719.474	87.9	1.219
356	Solid	126,451	2,977	1,332.357	7,488.888	102.6	1.423
406	Solid	165,161	3,896	2,273.040	11,192.365	117.3	1.625
457	Solid	209,032	4,932	3,641.193	15,928.226	132.1	1.829
508	Solid	258,064	6,085	5,549.614	21,843.956	146.6	2.033
508	279 mm	196,774	4,641	5,250.759	20,680.475	163.3	2.033
610	Solid	371,612	8,756	11,507.966	37,755.795	176.0	2.438
610	305 mm	298,709	7,034	11,084.243	36,362.895	192.5	2.438
610	356 mm	272,258	6,406	10,722.954	35,183.026	198.4	2.438
610	381 mm	257,419	6,056	10,473.631	34,363.673	201.7	2.438
762	457 mm	416,773	9,807	25,950.781	68,121.025	249.4	3.048
914	457 mm	672,257	15,834	56,114.240	122,739.109	289.1	3.658

Note: Designer must confirm section properties for a selected pile. Form dimensions may vary with producers, with corresponding variations in section properties.

Data converted to SI units from US unit properties in PCI (1993), Precast/Prestressed Concrete Institute Journal, Volume 38, No. 2, March-April, 1993.

PRECAST/PRESTRESSED CONCRETE PILES



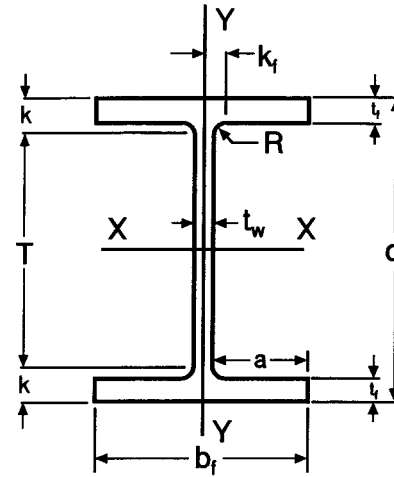
* Strand pattern may be circular or square

Size mm	Section Properties						
	Core Diameter mm	Area mm ²	Weight N/m	Moment of Inertia mm ⁴ x 10 ⁶	Section Modulus mm ³ x 10 ³	Radius of Gyration mm	Perimeter m
Octagonal Piles							
254	Solid	53,548	1,240	231.008	1,818.964	65.8	0.841
305	Solid	76,774	1,824	472.006	3,097.155	78.5	1.009
356	Solid	104,516	2,466	876.167	4,932.506	91.4	1.180
406	Solid	136,774	3,210	1,495.103	7,357.792	104.6	1.347
457	Solid	172,903	4,086	2,374.600	10,471.334	117.1	1.515
508	Solid	213,548	5,035	3,650.350	14,371.455	130.8	1.682
508	279 mm	152,258	3,575	3,350.663	13,191.587	148.3	1.682
559	Solid	258,709	6,129	5,343.163	19,123.704	143.8	1.853
559	330 mm	172,903	4,086	4,761.688	17,042.547	165.9	1.853
610	Solid	307,741	7,224	7,567.087	24,826.402	156.7	2.021
610	381 mm	193,548	4,597	6,533.168	21,434.280	183.6	2.021
Round Piles							
914	660 mm	314,193	7,399	24,976.799	54,634.471	281.9	2.874
1,067	813 mm	374,838	8,829	42,153.005	79,034.810	335.3	3.353
1,219	965 mm	435,483	10,259	65,856.969	108,023.526	388.9	3.831
1,372	1118 mm	496,773	11,704	97,137.176	141,633.394	442.2	4.310
1,676	1372 mm	729,676	17,191	213,954.191	255,261.296	541.5	5.267

Note: Designer must confirm section properties for a selected pile. Form dimensions may vary with producers, with corresponding variations in section properties.

Data converted to SI units from US unit properties in PCI (1993), Precast/Prestressed Concrete Institute Journal, Volume 38, No. 2, March-April, 1993.

H-PILES



C-21

Section Designation	Area A	Depth d	Web Thickness t_w	Flange		Distance				Fillet Radius R	Elastic Properties					
				Width b_f	Thickness t_f	T	k	k_f	a		X-X			Y-Y		
											I	S	r	I	S	r
mm x kg/m	mm ²	mm	mm	mm	mm	mm	mm	mm	mm	mm	mm ⁴ x 10 ⁶	mm ³ x 10 ³	mm	mm ⁴ x 10 ⁶	mm ³ x 10 ³	mm
HP360 x 174	22,200	361	20.4	378	20	277	42	30.2	179	20	511	2,830	152	183	968	91
HP360 x 152	19,400	356	17.9	376	18	277	40	29.0	179	20	442	2,480	151	158	840	90
HP360 x 132	16,900	351	15.6	373	16	277	37	27.8	179	20	378	2,150	150	135	724	89
HP360 x 108	13,800	346	12.8	370	13	277	34	26.4	179	20	306	1,770	148	108	584	88
HP310 x 125	15,800	312	17.4	312	17	244	34	23.7	147	15	270	1,730	131	88	565	75
HP310 x 110	14,000	308	15.4	310	15	244	32	22.7	147	15	236	1,530	130	77	497	74
HP310 x 93	11,800	303	13.1	308	13	244	30	21.6	148	15	196	1,290	129	64	414	74
HP310 x 79	9,970	299	11.0	306	11	244	28	20.5	148	15	162	1,080	127	53	343	73
HP250 x 85	10,800	254	14.4	260	14	196	29	20.2	123	13	123	969	107	42	325	63
HP250 x 62	7,980	246	10.5	256	11	96	25	18.3	123	13	88	711	105	30	234	61
HP200 x 53	6,810	204	11.3	207	11	158	23	15.7	98	10	50	487	86	17	161	50

Note: Designer must confirm section properties for a selected pile.

Data obtained from FHWA Geotechnical Metrication Guidelines (1995) FHWA-SA-95-035.

BITUMEN COATING FOR CONCRETE PILES

(This is a generic specification that should be modified to meet the specific needs of a given project.)

Description. This work shall consist of furnishing and applying bituminous coating and primer to prestressed concrete pile surfaces as required in the plans and as specified herein.

Materials

- A. Bituminous Coating. Bituminous coating shall be an asphalt type bitumen conforming to ASTM D946, with a minimum penetration grade 50 at the time of pile driving. Bituminous coating shall be applied uniformly over an asphalt primer. Grade 40-50 or lower grades shall not be used.
- B. Primer. Primer shall conform to the requirements of ASTM D41.

Construction Requirements. All surfaces to be coated with bitumen shall be dry and thoroughly cleaned of dust and loose materials. No primer or bitumen shall be applied in wet weather, nor when the temperature is below 18 degrees Celsius.

The primer shall be applied to the surfaces and allowed to completely dry before the bituminous coating is applied. Primer shall be applied uniformly at the quantity of one liter per 2.43 square meters.

Bitumen shall be applied uniformly at a temperature of not less than 149 degrees Celsius, nor more than 177 degrees Celsius, and shall be applied either by mopping, brushing, or spraying at the project site. All holes or depressions in the concrete surface shall be completely filled with bitumen. The bituminous coating shall be applied to a minimum dry thickness of 3.2 mm, but in no case shall the quantity of application be less than 3.29 liters per square meters.

Bitumen coated piles shall be stored before driving and protected from sunlight and heat. Pile coatings shall not be exposed to damage during storage, hauling or handling. The Contractor shall take appropriate measures to preserve and maintain the bitumen coating. At the time of pile driving, the bitumen coating shall have a minimum dry thickness of 3.2 mm and a minimum penetration value of 50. If necessary, the Contractor shall recoat the piles, at his expense, to comply with these requirements.

Method of Measurement. Bitumen coating will be measured by the square meter of coating in place on concrete pile surfaces. No separate payment will be made for primer.

Basis of Payment. The accepted quantities of bitumen coating will be paid for at the contract unit price per square meter, which price shall be full compensation for furnishing all labor, materials, tools, equipment, and incidentals, and for doing all the work involved in applying the bituminous coating and primer, as shown in the plans, and as specified in these specifications, and as directed by the Engineer.

Payment will be made under:

<u>Pay Item</u>	<u>Pay Unit</u>
Bitumen Coating	Square Meters.

BITUMEN COATING FOR STEEL PILES

(This is a generic specification that should be modified to meet the specific needs of a given project.)

Description. This work shall consist of furnishing and applying bituminous coating and primer to steel pile surfaces as required in the plans and as specified herein.

Materials

- A. Bituminous Coating. Canal Liner Bitumen (ASTM D-2521) shall be used for the bitumen coating and shall have a softening point of 88 to 93 degrees Celsius, a penetration of 56 to 61 at 25 degrees Celsius, and a ductility at 25 degrees Celsius, in excess of 35.0 mm.
- B. Primer. Primer shall conform to the requirements of AASHTO M116.

Construction Requirements. All surfaces to be coated with bitumen shall be dry and thoroughly cleaned of dust and loose materials. No primer or bitumen shall be applied in wet weather, nor when the temperature is below 18 degrees Celsius.

Application of the prime coat shall be with a brush or other approved means and in a manner to thoroughly coat the surface of the piling with a continuous film of primer. The purpose of the primer is to provide a suitable bond of the bitumen coating to the pile. The primer shall set thoroughly before the bitumen coating is applied.

The bitumen should be heated to 149 degrees Celsius, and applied at a temperature between 93 and 149 degrees Celsius, by one or more mop coats, or other approved means, to apply an average coating depth of 9.5 mm. Whitewashing of the coating may be required, as deemed necessary by the engineer, to prevent running and sagging of the asphalt coating prior to driving, during hot weather.

Bitumen coated piles shall be stored immediately after the coating is applied for protection from sunlight and heat. Pile coatings shall not be exposed to damage or contamination during storage, hauling, or handling. Once the bitumen coating has been applied, the contractor will not be allowed to drag the piles on the ground or to use cable wraps around the pile during handling. Pad eyes, or other suitable devices, shall be attached to the pile to be used for lifting and handling. If necessary, the contractor shall recoat the piles, at his expense to comply with these requirements.

A nominal length of pile shall be left uncoated where field splices will be required. After completing the field splice, the splice area shall be brush or map coated with at least one coat of bitumen.

Method of Measurement. Bitumen coating will be measured by the linear meter of coating in place on the pile surfaces. No separate payment will be made for primer or coating of the splice areas.

Basis of Payment. The accepted quantities of bitumen coating will be paid for at the contract unit price per linear meter, which price shall be full compensation for furnishing all labor, materials, tools, equipment, and incidentals, and for doing all the work involved in applying the bituminous coating and primer, as shown in the plans, and as specified in these specifications, and as directed by the Engineer.

Payment will be made under:

<u>Pay Item</u>	<u>Pay-Unit</u>
Bitumen Coating	Meter.

APPENDIX D

Pile Hammer Information

	Page
TABLE D-1 DIESEL HAMMER LISTING (sorted by Maximum Energy)	D-3
TABLE D-2 EXTERNAL COMBUSTION HAMMER LISTING (sorted by Maximum Energy)	D-7
TABLE D-3 COMPLETE HAMMER LISTING (sorted by GRLWEAP ID Numbers)	D-13

Note: GRLWEAP hammer ID numbers correspond to those contained in Version 1.996-2 of the GRLWEAP program.

TABLE D-1 DIESEL HAMMER LISTING
(sorted by Maximum Energy)

GRLWEAP ID	Hammer Mfgr	Hammer Name E	Max. Energy kN-m	Ram Weight kN	Eq. Max. Stroke m	Hammer Type T
81	LINKBELT	LB 180	10.98	7.70	1.43	CED
120	ICE	180	11.03	7.70	1.43	CED
1	DELMAG	D 5	11.16	4.89	2.28	OED
36	DELMAG	D 6-32	14.24	5.88	2.42	OED
82	LINKBELT	LB 312	20.37	17.18	1.19	CED
146	MKT	DE 10	20.75	7.57	2.74	OED
147	MKT	DE 20	21.70	8.90	2.44	OED
2	DELMAG	D 8-22	23.87	7.83	3.05	OED
402	BERMINGH	B200	24.41	8.90	2.74	OED
83	LINKBELT	LB 440	24.69	17.80	1.39	CED
122	ICE	440	25.17	17.80	1.41	CED
141	MKT 20	DE333020	27.13	8.90	3.05	OED
151	MKT	DA 35B	28.48	12.46	2.29	CED
148	MKT	DE 30	30.38	12.46	2.44	OED
41	FEC	FEC 1200	30.51	12.24	2.49	OED
127	ICE	30-S	30.52	13.35	2.29	OED
401	BERMINGH	B23	31.18	12.46	2.50	CED
414	BERMINGH	B23 5	31.18	12.46	2.50	CED
121	ICE	422	31.36	17.80	1.76	CED
3	DELMAG	D 12	32.00	12.24	2.62	OED
149	MKT	DA35B SA	32.28	12.46	2.59	OED
150	MKT	DE 30B	32.28	12.46	2.59	OED
61	MITSUB.	M 14	34.24	13.22	2.59	OED
350	HERA	1250	34.38	12.50	2.75	OED
101	KOBE	K 13	34.49	12.77	2.70	OED
84	LINKBELT	LB 520	35.69	22.56	1.58	CED
42	FEC	FEC 1500	36.75	14.68	2.50	OED
201	VULCANI	VUL V12	36.77	12.26	3.00	OED
142	MKT 30	DE333020	37.98	12.46	3.05	OED
62	MITSUB.	MH 15	38.16	14.73	2.59	OED
4	DELMAG	D 15	38.40	14.68	2.62	OED
403	BERMINGH	B225	39.67	13.35	2.97	OED
123	ICE	520	41.19	22.56	1.83	CED
351	HERA	1500	41.25	15.00	2.75	OED
152	MKT	DA 45	41.67	17.80	2.34	CED
37	DELMAG	D 12-32	42.50	12.55	3.39	OED
153	MKT	DE 40	43.40	17.80	2.44	OED
143	MKT 33	DE333020	44.76	14.68	3.05	OED
415	BERMINGH	B250 5	48.02	13.35	3.60	OED
161	MKT	DA 55B	51.81	22.25	2.33	CED
202	VULCAN	VUL V18	52.97	17.66	3.00	OED

**TABLE D-1 DIESEL HAMMER LISTING
(sorted by Maximum Energy)**

GRLWEAP ID	Hammer Mfgr	Hammer Name E	Max. Energy kN-m	Ram Weight kN	Eq. Max. Stroke m	Hammer Type T
5	DELMAG	D 16-32	53.23	15.66	3.40	OED
128	ICE	40-S	54.25	17.80	3.05	OED
144	MKT 40	DE333020	54.25	17.80	3.05	OED
160	MKT	DA55B SA	54.25	22.25	2.44	OED
404	BERMINGH	B300	54.68	16.69	3.28	OED
410	BERMINGH	B300 M	54.68	16.69	3.28	OED
6	DELMAG	D 22	55.08	21.85	2.52	OED
124	ICE	640	55.10	26.70	2.06	CED
129	ICE	42-S	56.97	18.19	3.13	OED
38	DELMAG	D 19-32	57.51	17.80	3.23	OED
159	MKT	DE 50B	57.65	22.25	2.59	OED
63	MITSUB.	M 23	58.34	22.52	2.59	OED
412	BERMINGH	B400 4.8	58.59	21.36	2.74	OED
413	BERMINGH	B400 5.0	61.04	22.25	2.74	OED
103	KOBE	K22-Est	61.51	21.58	2.85	OED
64	MITSUB.	MH 25	63.53	24.52	2.59	OED
416	BERMINGH	B350 5	64.02	17.80	3.60	OED
7	DELMAG	D 22-02	65.78	21.58	3.05	OED
8	DELMAG	D 22-13	65.78	21.58	3.05	OED
43	FEC	FEC 2500	67.81	24.47	2.77	OED
163	MKT 50	DE70/50B	67.82	22.25	3.05	OED
352	HERA	2500	68.75	25.00	2.75	OED
9	DELMAG	D 22-23	69.53	21.58	3.22	OED
104	KOBE	K 25	69.88	24.52	2.85	OED
125	ICE	660	70.03	33.69	2.08	CED
85	LINKBELT	LB 660	70.03	33.69	2.08	CED
405	BERMINGH	B400	72.90	22.25	3.28	OED
411	BERMINGH	B400 M	72.90	22.25	3.28	OED
44	FEC	FEC 2800	75.95	27.41	2.77	OED
353	HERA	2800	77.00	28.00	2.75	OED
203	VULCAN	VUL V25	78.51	24.53	3.20	OED
417	BERMINGH	B400 5	80.03	22.25	3.60	OED
162	MKT	DE 70B	80.70	31.15	2.59	OED
11	DELMAG	D 30	80.84	29.37	2.75	OED
10	DELMAG	D 25-32	83.40	24.52	3.40	OED
65	MITSUB.	M 33	83.70	32.31	2.59	OED
45	FEC	FEC 3000	85.49	29.37	2.91	OED
66	MITSUB.	MH 35	89.00	34.35	2.59	OED
12	DELMAG	D 30-02	89.52	29.37	3.05	OED
13	DELMAG	D 30-13	89.52	29.37	3.05	OED
131	ICE	70-S	94.95	31.15	3.05	OED

TABLE D-1 DIESEL HAMMER LISTING
(sorted by Maximum Energy)

GRLWEAP ID	Hammer Mfgr	Hammer Name E	Max. Energy kN-m	Ram Weight kN	Eq. Max. Stroke m	Hammer Type T
164	MKT 70	DE70/50B	94.95	31.15	3.05	OED
354	HERA	3500	96.25	35.00	2.75	OED
107	KOBE	K 35	97.90	34.35	2.85	OED
126	ICE	1070	98.47	44.50	2.21	OED
130	ICE	60-S	98.93	31.15	3.18	OED
46	FEC	FEC 3400	99.02	33.29	2.97	OED
14	DELMAG	D 30-23	99.90	29.37	3.40	OED
15	DELMAG	D 30-32	99.90	29.37	3.40	OED
418	BERMINGH	B450 5	105.63	29.37	3.60	OED
67	MITSUB.	M 43	109.06	42.10	2.59	OED
16	DELMAG	D 36	113.69	35.29	3.22	OED
17	DELMAG	D 36-02	113.69	35.29	3.22	OED
18	DELMAG	D 36-13	113.69	35.29	3.22	OED
68	MITSUB.	MH 45	115.87	44.72	2.59	OED
421	BERMINGH	B550 C	119.36	48.95	2.44	OED
19	DELMAG	D 36-23	120.04	35.29	3.40	OED
20	DELMAG	D 36-32	120.04	35.29	3.40	OED
133	ICE	90-S	122.07	40.05	3.05	OED
21	DELMAG	D 44	122.67	42.27	2.90	OED
419	BERMINGH	B500 5	124.84	34.71	3.60	OED
110	KOBE	K 45	125.81	44.14	2.85	OED
24	DELMAG	D 46-13	130.93	45.12	2.90	OED
132	ICE	80-S	134.77	35.60	3.79	OED
136	ICE	200-S	135.64	89.00	1.52	OED
355	HERA	5000	137.50	50.00	2.75	OED
420	BERMINGH	B550 5	144.05	40.05	3.60	OED
22	DELMAG	D 46	145.37	45.12	3.22	OED
23	DELMAG	D 46-02	145.37	45.12	3.22	OED
25	DELMAG	D 46-23	145.37	45.12	3.22	OED
165	MKT 110	DE110150	149.20	48.95	3.05	OED
26	DELMAG	D 46-32	153.49	45.12	3.40	OED
356	HERA	5700	156.75	57.00	2.75	OED
134	ICE	100-S	162.76	44.50	3.66	OED
27	DELMAG	D 55	168.91	52.78	3.20	OED
357	HERA	6200	170.50	62.00	2.75	OED
112	KOBE	KB 60	176.58	58.87	3.00	OED
70	MITSUB.	MH 72B	183.31	70.75	2.59	OED
135	ICE	120-S	202.15	53.40	3.79	OED
71	MITSUB.	MH 80B	202.91	78.32	2.59	OED
166	MKT 150	DE110150	203.45	66.75	3.05	OED
358	HERA	7500	206.25	75.00	2.75	OED

TABLE D-1 DIESEL HAMMER LISTING
(sorted by Maximum Energy)

GRLWEAP ID	Hammer Mfgr	Hammer Name E	Max. Energy kN-m	Ram Weight kN	Eq. Max. Stroke m	Hammer Type T
28	DELMAG	D 62-02	206.77	60.79	3.40	OED
29	DELMAG	D 62-12	206.77	60.79	3.40	OED
30	DELMAG	D 62-22	206.77	60.79	3.40	OED
113	KOBE	KB 80	235.43	78.50	3.00	OED
359	HERA	8800	242.00	88.00	2.75	OED
31	DELMAG	D 80-12	252.61	78.41	3.22	OED
32	DELMAG	D 80-23	266.71	78.41	3.40	OED
33	DELMAG	D100-13	333.47	98.03	3.40	OED

TABLE D-2 EXTERNAL COMBUSTION HAMMER LISTING
(sorted by Maximum Energy)

GRLWEAP ID	Hammer Mfgr	Hammer Name	Max. Energy kN-m	Ram Weight kN	Eq. Max. Stroke m	Hammer Type
301	MKT	No. 5	1.36	.89	1.52	ECH
302	MKT	No. 6	3.39	1.78	1.90	ECH
303	MKT	No. 7	5.63	3.56	1.58	ECH
205	VULCAN	VUL 02	9.85	13.35	.74	ECH
220	VULCAN	VUL 30C	9.85	13.35	.74	ECH
521	DAWSON	HPH 1200	11.73	10.20	1.15	ECH
304	MKT	9B3	11.87	7.12	1.67	ECH
305	MKT	10B3	17.78	13.35	1.33	ECH
306	MKT	C5-Air	19.26	22.25	.87	ECH
171	CONMACO	C 50	20.35	22.25	.91	ECH
204	VULCAN	VUL 01	20.35	22.25	.91	ECH
251	RAYMOND	R 1	20.35	22.25	.91	ECH
221	VULCAN	VUL 50C	20.48	22.25	.92	ECH
307	MKT	C5-Steam	21.97	22.25	.99	ECH
308	MKT	S-5	22.04	22.25	.99	ECH
522	DAWSON	HPH 2400	23.49	18.64	1.26	ECH
541	BANUT	3 Tonnes	23.53	29.41	.80	ECH
309	MKT	11B3	25.97	22.25	1.17	ECH
222	VULCAN	VUL 65C	26.01	28.92	.90	ECH
172	CONMACO	C 65	26.45	28.92	.91	ECH
206	VULCAN	VUL 06	26.45	28.92	.91	ECH
252	RAYMOND	R 1S	26.45	28.92	.91	ECH
253	RAYMOND	R 65C	26.45	28.92	.91	ECH
254	RAYMOND	R 65CH	26.45	28.92	.91	ECH
223	VULCAN	VUL 65CA	26.54	28.92	.92	ECH
311	MKT	C826 Air	28.75	35.60	.81	ECH
341	IHC Hydh	SC 30	30.02	16.20	1.85	ECH
542	BANUT	4 Tonnes	31.39	39.25	.80	ECH
255	RAYMOND	R 0	33.06	33.38	.99	ECH
310	MKT	C826 Stm	33.10	35.60	.93	ECH
224	VULCAN	VUL 80C	33.20	35.60	.93	ECH
256	RAYMOND	R 80C	33.20	35.60	.93	ECH
257	RAYMOND	R 80CH	33.20	35.60	.93	ECH
449	MENCK	MHF3-3	33.59	31.39	1.07	ECH
515	UDDCOMB	H3H	33.75	29.37	1.15	ECH
173	CONMACO	C 550	33.91	22.25	1.52	ECH
235	VULCAN	VUL 505	33.91	22.25	1.52	ECH
320	IHC Hydh	S 35	35.01	32.35	1.08	ECH
225	VULCAN	VUL 85C	35.25	37.91	.93	ECH
175	CONMACO	C 80	35.27	35.60	.99	ECH
207	VULCAN	VUL 08	35.27	35.60	.99	ECH

TABLE D-2 EXTERNAL COMBUSTION HAMMER LISTING
(sorted by Maximum Energy)

GRLWEAP ID	Hammer Mfgr	Hammer Name	Max. Energy kN-m	Ram Weight kN	Eq. Max. Stroke m	Hammer Type
312	MKT	S-8	35.27	35.60	.99	ECH
381	BSP	HH 3	35.29	29.42	1.20	ECH
481	JUNTTAN	HHK 3	36.01	29.46	1.22	ECH
543	BANUT	5 Tonnes	39.22	49.04	.80	ECH
342	IHC Hydh	SC 40	39.98	24.52	1.63	ECH
321	IHC Hydh	S 40	41.18	24.52	1.68	ECH
313	MKT	MS-350	41.78	34.35	1.22	ECH
450	MENCK	MHF3-4	41.99	39.24	1.07	ECH
174	CONMACO	C 565	44.08	28.92	1.52	ECH
176	CONMACO	C 100	44.08	44.50	.99	ECH
208	VULCAN	VUL 010	44.08	44.50	.99	ECH
236	VULCAN	VUL 506	44.08	28.92	1.52	ECH
258	RAYMOND	R 2/0	44.08	44.50	.99	ECH
314	MKT	S 10	44.08	44.50	.99	ECH
506	HPSI	650	44.08	28.92	1.52	ECH
372	FAIRCHLD	F-32	44.15	48.28	.91	ECH
226	VULCAN	VUL 100C	44.62	44.50	1.00	ECH
516	UDDCOMB	H4H	45.00	39.16	1.15	ECH
544	BANUT	6 Tonnes	47.09	58.87	.80	ECH
482	JUNTTAN	HHK 4	47.97	39.25	1.22	ECH
227	VULCAN	VUL 140C	48.80	62.30	.78	ECH
177	CONMACO	C 115	50.69	51.17	.99	ECH
315	MKT	S 14	50.89	62.30	.82	ECH
551	ICE	110-SH	51.16	51.17	1.00	ECH
552	ICE	115-SH	51.47	51.17	1.01	ECH
441	MENCK	MHF5-5	52.48	49.05	1.07	ECH
451	MENCK	MHF3-5	52.48	49.05	1.07	ECH
209	VULCAN	VUL 012	52.90	53.40	.99	ECH
178	CONMACO	C 80E5	54.25	35.60	1.52	ECH
237	VULCAN	VUL 508	54.25	35.60	1.52	ECH
545	BANUT	7 Tonnes	54.92	68.66	.80	ECH
259	RAYMOND	R 3/0	55.10	55.62	.99	ECH
517	UDDCOMB	H5H	56.25	48.95	1.15	ECH
182	CONMACO	C 140	56.97	62.30	.91	ECH
210	VULCAN	VUL 014	56.97	62.30	.91	ECH
382	BSP	HH 5	58.83	49.04	1.20	ECH
316	MKT	MS 500	59.68	48.95	1.22	ECH
501	HPSI	110	59.68	48.95	1.22	ECH
489	JUNTTAN	HHK 5A	59.79	49.04	1.22	ECH
483	JUNTTAN	HHK 5	59.99	49.08	1.22	ECH
343	IHC Hydh	SC 60	60.00	34.35	1.75	ECH

TABLE D-2 EXTERNAL COMBUSTION HAMMER LISTING
(sorted by Maximum Energy)

GRLWEAP ID	Hammer Mfgr	Hammer Name	Max. Energy kN-m	Ram Weight kN	Eq. Max. Stroke m	Hammer Type
322	IHC Hydh	S 60	60.04	58.86	1.02	ECH
371	FAIRCHLD	F-45	61.04	66.75	.91	ECH
282	MENCK	MRBS 500	61.13	49.04	1.25	ECH
442	MENCK	MHF5-6	62.98	58.86	1.07	ECH
452	MENCK	MHF3-6	62.98	58.86	1.07	ECH
183	CONMACO	C 160	66.12	72.31	.91	ECH
211	VULCAN	VUL 016	66.12	72.31	.91	ECH
260	RAYMOND	R 150C	66.12	66.75	.99	ECH
261	RAYMOND	R 4/0	66.12	66.75	.99	ECH
271	MENCK	MH 68	66.70	34.35	1.94	ECH
518	UDDCOMB	H6H	67.50	58.74	1.15	ECH
179	CONMACO	C 100E5	67.82	44.50	1.52	ECH
507	HPSI	1000	67.82	44.50	1.52	ECH
238	VULCAN	VUL 510	67.82	44.50	1.52	ECH
228	VULCAN	VUL 200C	68.09	89.00	.77	ECH
323	IHC Hydh	S 70	70.05	34.35	2.04	ECH
191	CONMACO	C 160 **	70.23	76.81	.91	ECH
484	JUNTTAN	HHK 6	71.96	58.87	1.22	ECH
443	MENCK	MHF5-7	73.48	68.67	1.07	ECH
453	MENCK	MHF3-7	73.48	68.67	1.07	ECH
262	RAYMOND	R 5/0	77.14	77.88	.99	ECH
180	CONMACO	C 115E5	77.99	51.17	1.52	ECH
344	IHC Hydh	SC 80	79.89	50.02	1.60	ECH
184	CONMACO	C 200	81.38	89.00	.91	ECH
212	VULCAN	VUL 020	81.38	89.00	.91	ECH
231	VULCAN	VUL 320	81.38	89.00	.91	ECH
239	VULCAN	VUL 512	81.38	53.40	1.52	ECH
317	MKT	S 20	81.38	89.00	.91	ECH
502	HPSI	150	81.38	66.75	1.22	ECH
383	BSP	HH 7	82.44	68.65	1.20	ECH
503	HPSI	154	83.55	68.53	1.22	ECH
490	JUNTTAN	HHK 7A	83.71	68.66	1.22	ECH
444	MENCK	MHF5-8	83.97	78.48	1.07	ECH
485	JUNTTAN	HHK 7	83.98	68.71	1.22	ECH
181	CONMACO	C 125E5	84.77	55.62	1.52	ECH
553	ICE	160-SH	86.81	71.20	1.22	ECH
324	IHC Hydh	S 90	90.01	44.14	2.04	ECH
283	MENCK	MRBS 750	91.92	73.56	1.25	ECH
519	UDDCOMB	H8H	94.06	78.32	1.20	ECH
272	MENCK	MH 96	94.17	49.04	1.92	ECH
384	BSP	HH 8	94.27	78.50	1.20	ECH

TABLE D-2 EXTERNAL COMBUSTION HAMMER LISTING
(sorted by Maximum Energy)

GRLWEAP ID	Hammer Mfgr	Hammer Name	Max. Energy kN-m	Ram Weight kN	Eq. Max. Stroke m	Hammer Type
445	MENCK	MHF5-9	94.47	88.29	1.07	ECH
263	RAYMOND	R 30X	101.73	133.50	.76	ECH
446	MENCK	MHF5-10	104.97	98.10	1.07	ECH
345	IHC Hydh	SC 110	105.01	67.68	1.55	ECH
385	BSP	HH 9	106.03	88.29	1.20	ECH
491	JUNTTAN	HHK 9A	107.64	88.29	1.22	ECH
504	HPSI	200	108.51	89.00	1.22	ECH
264	RAYMOND	R 8/0	110.2	111.25	.99	ECH
508	HPSI	1605	112.58	73.87	1.52	ECH
447	MENCK	MHF5-11	115.46	107.91	1.07	ECH
520	UDDCOMB	H10H	117.84	98.12	1.20	ECH
486	JUNTTAN	HHK 10	119.93	98.12	1.22	ECH
185	CONMACO	C 300	122.07	133.50	.91	ECH
213	VULCAN	VUL 030	122.07	133.50	.91	ECH
232	VULCAN	VUL 330	122.07	133.50	.91	ECH
270	9K DROP	9K DROP	122.07	40.05	3.05	ECH
505	HPSI	225	122.07	100.12	1.22	ECH
448	MENCK	MHF5-12	125.96	117.72	1.07	ECH
284	MENCK	MRBS 800	126.53	84.37	1.50	ECH
285	MENCK	MRBS 850	126.53	84.37	1.50	ECH
509	HPSI	2005	128.99	84.64	1.52	ECH
386	BSP	HH 11	129.59	107.91	1.20	ECH
186	CONMACO	C 5200	135.64	89.00	1.52	ECH
240	VULCAN	VUL 520	135.64	89.00	1.52	ECH
265	RAYMOND	R 40X	135.64	178.00	.76	ECH
346	IHC Hydh	SC 150	140.12	107.91	1.30	ECH
273	MENCK	MH 145	142.15	73.56	1.93	ECH
487	JUNTTAN	HHK 12	143.92	117.75	1.22	ECH
229	VULCAN	VUL 400C	154.08	178.00	.87	ECH
454	MENCK	MHF10-15	157.39	147.12	1.07	ECH
214	VULCAN	VUL 040	162.76	178.00	.91	ECH
233	VULCAN	VUL 340	162.76	178.00	.91	ECH
387	BSP	HH 14	164.92	137.33	1.20	ECH
286	MENCK	MRBS1100	167.42	107.91	1.55	ECH
488	JUNTTAN	HHK 14	167.90	137.37	1.22	ECH
287	MENCK	MRBS1502	183.90	147.16	1.25	ECH
388	BSP	HH 16	188.35	156.96	1.20	ECH
274	MENCK	MH 195	191.41	98.12	1.95	ECH
325	IHC Hydh	S 200	199.63	97.90	2.04	ECH
461	MENCK	MHUT 200	199.90	117.75	1.70	ECH
187	CONMACO	C 5300	203.45	133.50	1.52	ECH

TABLE D-2 EXTERNAL COMBUSTION HAMMER LISTING
(sorted by Maximum Energy)

GRLWEAP ID	Hammer Mfgr	Hammer Name	Max. Energy kN-m	Ram Weight kN	Eq. Max. Stroke m	Hammer Type
241	VULCAN	VUL 530	203.45	133.50	1.52	ECH
266	RAYMOND	R 60X	203.45	267.00	.76	ECH
347	IHC Hydh	SC 200	204.81	134.39	1.52	ECH
455	MENCK	MHF10-20	209.81	196.11	1.07	ECH
510	HPSI	3005	209.32	137.35	1.52	ECH
275	MENCK	MHU 220	215.76	111.83	1.93	ECH
389	BSP	HH 20	235.44	196.20	1.20	ECH
390	BSP	HH 20S	235.44	196.20	1.20	ECH
511	HPSI	3505	239.16	156.93	1.52	ECH
348	IHC Hydh	SC 250	240.04	174.62	1.37	ECH
230	VULCAN	VUL 600C	243.01	267.00	.91	ECH
215	VULCAN	VUL 060	244.14	267.00	.91	ECH
234	VULCAN	VUL 360	244.14	267.00	.91	ECH
326	IHC Hydh	S 250	250.44	122.82	2.04	ECH
288	MENCK	MRBS1800	257.46	171.68	1.50	ECH
242	VULCAN	VUL 540	271.27	182.01	1.49	ECH
327	IHC Hydh	S 280	280.11	132.61	2.11	ECH
188	CONMACO	C 5450	305.18	200.25	1.52	ECH
290	MENCK	MRBS2502	306.47	245.24	1.25	ECH
291	MENCK	MRBS2504	306.47	245.24	1.25	ECH
391	BSP	HA 30	353.16	294.30	1.20	ECH
289	MENCK	MRBS2500	355.52	284.49	1.25	ECH
276	MENCK	MHU 400	392.74	225.66	1.74	ECH
328	IHC Hydh	S 400	399.58	197.13	2.03	ECH
462	MENCK	MHUT 400	400.29	234.51	1.71	ECH
243	VULCAN	VUL 560	406.91	278.13	1.46	ECH
245	VULCAN	VUL 3100	406.91	445.00	.91	ECH
292	MENCK	MRBS3000	441.30	294.28	1.50	ECH
392	BSP	HA 40	470.88	392.40	1.20	ECH
189	CONMACO	C 5700	474.73	311.50	1.52	ECH
329	IHC Hydh	S 500	499.54	246.08	2.03	ECH
463	MENCK	MHUT 500	499.89	264.95	1.89	ECH
277	MENCK	MHU 600	588.17	343.36	1.71	ECH
294	MENCK	MRBS4600	676.74	451.27	1.50	ECH
246	VULCAN	VUL 5100	678.18	445.00	1.52	ECH
190	CONMACO	C 6850	691.74	378.25	1.83	ECH
293	MENCK	MRBS3900	696.28	386.53	1.80	ECH
464	MENCK	MHUT700U	700.06	413.09	1.69	ECH
295	MENCK	MRBS5000	735.60	490.52	1.50	ECH
330	IHC Hydh	S 800	800.05	363.00	2.20	ECH
465	MENCK	MHUT700A	839.83	413.09	2.03	ECH

TABLE D-2 EXTERNAL COMBUSTION HAMMER LISTING
(sorted by Maximum Energy)

GRLWEAP ID	Hammer Mfgr	Hammer Name	Max. Energy kN-m	Ram Weight kN	Eq. Max. Stroke m	Hammer Type
297	MENCK	MRBS7000	856.41	685.30	1.25	ECH
466	MENCK	MHUT1000	999.52	588.73	1.70	ECH
331	IHC Hydh	S 1000	999.99	451.26	2.22	ECH
278	MENCK	MHU 1000	1000.58	565.02	1.77	ECH
247	VULCAN	VUL 5150	1017.27	667.50	1.52	ECH
296	MENCK	MRBS6000	1029.79	588.60	1.75	ECH
298	MENCK	MRBS8000	1176.97	784.85	1.50	ECH
299	MENCK	MRBS8800	1294.69	863.34	1.50	ECH
332	IHC Hydh	S 1600	1597.52	694.20	2.30	ECH
279	MENCK	MHU 1700	1666.80	922.17	1.81	ECH
280	MENCK	MHU 2100	2099.09	1138.31	1.84	ECH
300	MENCK	MBS12500	2145.53	1226.33	1.75	ECH
333	IHC Hydh	S 2300	2298.99	1008.37	2.28	ECH
248	VULCAN	VUL 6300	2441.45	1335.00	1.83	ECH
281	MENCK	MHU 3000	2945.54	1618.73	1.82	ECH
334	IHC Hydh	S 3000	2997.72	1477.40	2.03	ECH

TABLE D-3 COMPLETE HAMMER LISTING
(sorted by GRLWEAP ID Numbers)

GRLWEAP ID	Hammer Mfgr	Hammer Name	Max. Energy kN-m	Ram Weight kN	Eq. Max. Stroke m	Hammer Type
1	DELMAG	D 5	11.16	4.89	2.28	OED
2	DELMAG	D 8-22	23.87	7.83	3.05	OED
3	DELMAG	D 12	32.00	12.24	2.62	OED
4	DELMAG	D 15	38.40	14.68	2.62	OED
5	DELMAG	D 16-32	53.23	15.66	3.40	OED
6	DELMAG	D 22	55.08	21.85	2.52	OED
7	DELMAG	D 22-02	65.78	21.58	3.05	OED
8	DELMAG	D 22-13	65.78	21.58	3.05	OED
9	DELMAG	D 22-23	69.53	21.58	3.22	OED
10	DELMAG	D 25-32	83.40	24.52	3.40	OED
11	DELMAG	D 30	80.84	29.37	2.75	OED
12	DELMAG	D 30-02	89.52	29.37	3.05	OED
13	DELMAG	D 30-13	89.52	29.37	3.05	OED
14	DELMAG	D 30-23	99.90	29.37	3.40	OED
15	DELMAG	D 30-32	99.90	29.37	3.40	OED
16	DELMAG	D 36	113.69	35.29	3.22	OED
17	DELMAG	D 36-02	113.69	35.29	3.22	OED
18	DELMAG	D 36-13	113.69	35.29	3.22	OED
19	DELMAG	D 36-23	120.04	35.29	3.40	OED
20	DELMAG	D 36-32	120.04	35.29	3.40	OED
21	DELMAG	D 44	122.67	42.27	2.90	OED
22	DELMAG	D 46	145.37	45.12	3.22	OED
23	DELMAG	D 46-02	145.37	45.12	3.22	OED
24	DELMAG	D 46-13	130.93	45.12	2.90	OED
25	DELMAG	D 46-23	145.37	45.12	3.22	OED
26	DELMAG	D 46-32	153.49	45.12	3.40	OED
27	DELMAG	D 55	168.91	52.78	3.20	OED
28	DELMAG	D 62-02	206.77	60.79	3.40	OED
29	DELMAG	D 62-12	206.77	60.79	3.40	OED
30	DELMAG	D 62-22	206.77	60.79	3.40	OED
31	DELMAG	D 80-12	252.61	78.41	3.22	OED
32	DELMAG	D 80-23	266.71	78.41	3.40	OED
33	DELMAG	D100-13	333.47	98.03	3.40	OED
36	DELMAG	D 6-32	14.24	5.88	2.42	OED
37	DELMAG	D 12-32	42.50	12.55	3.39	OED
38	DELMAG	D 19-32	57.51	17.80	3.23	OED
41	FEC	FEC 1200	30.51	12.24	2.49	OED
42	FEC	FEC 1500	36.75	14.68	2.50	OED
43	FEC	FEC 2500	67.81	24.47	2.77	OED
44	FEC	FEC 2800	75.95	27.41	2.77	OED
45	FEC	FEC 3000	85.49	29.37	2.91	OED

TABLE D-3 COMPLETE HAMMER LISTING
(sorted by GRLWEAP ID Numbers)

GRLWEAP ID	Hammer Mfgr	Hammer Name	Max. Energy kN-m	Ram Weight kN	Eq. Max. Stroke m	Hammer Type
46	FEC	FEC 3400	99.02	33.29	2.97	OED
61	MITSUB.	M 14	34.24	13.22	2.59	OED
62	MITSUB.	MH 15	38.16	14.73	2.59	OED
63	MITSUB.	M 23	58.34	22.52	2.59	OED
64	MITSUB.	MH 25	63.53	24.52	2.59	OED
65	MITSUB.	M 33	83.70	32.31	2.59	OED
66	MITSUB.	MH 35	89.00	34.35	2.59	OED
67	MITSUB.	M 43	109.06	42.10	2.59	OED
68	MITSUB.	MH 45	115.87	44.72	2.59	OED
70	MITSUB.	MH 72B	183.31	70.75	2.59	OED
71	MITSUB.	MH 80B	202.91	78.32	2.59	OED
81	LINKBELT	LB 180	10.98	7.70	1.43	CED
82	LINKBELT	LB 312	20.37	17.18	1.19	CED
83	LINKBELT	LB 440	24.69	17.80	1.39	CED
84	LINKBELT	LB 520	35.69	22.56	1.58	CED
85	LINKBELT	LB 660	70.03	33.69	2.08	CED
101	KOBE	K 13	34.49	12.77	2.70	OED
103	KOBE	K22-Est	61.51	21.58	2.85	OED
104	KOBE	K 25	69.88	24.52	2.85	OED
107	KOBE	K 35	97.90	34.35	2.85	OED
110	KOBE	K 45	125.81	44.14	2.85	OED
112	KOBE	KB 60	176.58	58.87	3.00	OED
113	KOBE	KB 80	235.43	78.50	3.00	OED
120	ICE	180	11.03	7.70	1.43	CED
121	ICE	422	31.36	17.80	1.76	CED
122	ICE	440	25.17	17.80	1.41	CED
123	ICE	520	41.19	22.56	1.83	CED
124	ICE	640	55.10	26.70	2.06	CED
125	ICE	660	70.03	33.69	2.08	CED
126	ICE	1070	98.47	44.50	2.21	CED
127	ICE	30-S	30.52	13.35	2.29	OED
128	ICE	40-S	54.25	17.80	3.05	OED
129	ICE	42-S	56.97	18.19	3.13	OED
130	ICE	60-S	98.93	31.15	3.18	OED
131	ICE	70-S	94.95	31.15	3.05	OED
132	ICE	80-S	134.77	35.60	3.79	OED
133	ICE	90-S	122.07	40.05	3.05	OED
134	ICE	100-S	162.76	44.50	3.66	OED
135	ICE	120-S	202.15	53.40	3.79	OED
136	ICE	200-S	135.64	89.00	1.52	OED
141	MKT 20	DE333020	27.13	8.90	3.05	OED

TABLE D-3 COMPLETE HAMMER LISTING
(sorted by GRLWEAP ID Numbers)

GRLWEAP ID	Hammer Mfgr	Hammer Name	Max. Energy kN-m	Ram Weight kN	Eq. Max. Stroke m	Hammer Type
142	MKT 30	DE333020	37.98	12.46	3.05	OED
143	MKT 33	DE333020	44.76	14.68	3.05	OED
144	MKT 40	DE333020	54.25	17.80	3.05	OED
146	MKT	DE10	20.75	7.57	2.74	OED
147	MKT	DE 20	21.70	8.90	2.44	OED
148	MKT	DE 30	30.38	12.46	2.44	OED
149	MKT	DA35B SA	32.28	12.46	2.59	OED
150	MKT	DE 30B	32.28	12.46	2.59	OED
151	MKT	DA 35B	28.48	12.46	2.29	CED
152	MKT	DA 45	41.67	17.80	2.34	CED
153	MKT	DE 40	43.40	17.80	2.44	OED
159	MKT	DE 50B	57.65	22.25	2.59	OED
160	MKT	DA55B SA	54.25	22.25	2.44	OED
161	MKT	DA 55B	51.81	22.25	2.33	CED
162	MKT	DE 70B	80.70	31.15	2.59	OED
163	MKT 50	DE70/50B	67.82	22.25	3.05	OED
164	MKT 70	DE70/50B	94.95	31.15	3.05	OED
165	MKT110	DE110150	149.20	48.95	3.05	OED
166	MKT150	DE110150	203.45	66.75	3.05	OED
171	CONMACO	C 50	20.35	22.25	.91	ECH
172	CONMACO	C 65	26.45	28.92	.91	ECH
173	CONMACO	C 550	33.91	22.25	1.52	ECH
174	CONMACO	C 565	44.08	28.92	1.52	ECH
175	CONMACO	C 80	35.27	35.60	.99	ECH
176	CONMACO	C 100	44.08	44.50	.99	ECH
177	CONMACO	C 115	50.69	51.17	.99	ECH
178	CONMACO	C 80E5	54.25	35.60	1.52	ECH
179	CONMACO	C 100E5	67.82	44.50	1.52	ECH
180	CONMACO	C 115E5	77.99	51.17	1.52	ECH
181	CONMACO	C 125E5	84.77	55.62	1.52	ECH
182	CONMACO	C 140	56.97	62.30	.91	ECH
183	CONMACO	C 160	66.12	72.31	.91	ECH
184	CONMACO	C 200	81.38	89.00	.91	ECH
185	CONMACO	C 300	122.07	133.50	.91	ECH
186	CONMACO	C 5200	135.64	89.00	1.52	ECH
187	CONMACO	C 5300	203.45	133.50	1.52	ECH
188	CONMACO	C 5450	305.18	200.25	1.52	ECH
189	CONMACO	C 5700	474.73	311.50	1.52	ECH
190	CONMACO	C 6850	691.74	378.25	1.83	ECH
191	CONMACO	C 160 **	70.23	76.81	.91	ECH
201	VULCAN	VUL V15	36.77	12.26	3.00	OED

TABLE D-3 COMPLETE HAMMER LISTING
(sorted by GRLWEAP ID Numbers)

GRLWEAP ID	Hammer Mfgr	Hammer Name	Max. Energy kN-m	Ram Weight kN	Eq. Max. Stroke m	Hammer Type
202	VULCAN	VUL V18	52.97	17.66	3.00	OED
203	VULCAN	VUL V25	78.51	24.53	3.20	OED
204	VULCAN	VUL 01	20.35	22.25	.91	ECH
205	VULCAN	VUL 02	9.85	13.35	.74	ECH
206	VULCAN	VUL 06	26.45	28.92	.91	ECH
207	VULCAN	VUL 08	35.27	35.60	.99	ECH
208	VULCAN	VUL010	44.08	44.50	.99	ECH
209	VULCAN	VUL012	52.90	53.40	.99	ECH
210	VULCAN	VUL014	56.97	62.30	.91	ECH
211	VULCAN	VUL016	66.12	72.31	.91	ECH
212	VULCAN	VUL020	81.38	89.00	.91	ECH
213	VULCAN	VUL030	122.07	133.50	.91	ECH
214	VULCAN	VUL040	162.76	178.00	.91	ECH
215	VULCAN	VUL060	244.14	267.00	.91	ECH
220	VULCAN	VUL30C	9.85	13.35	.74	ECH
221	VULCAN	VUL50C	20.48	22.25	.92	ECH
222	VULCAN	VUL65C	26.01	28.92	.90	ECH
223	VULCAN	VUL 65CA	26.54	28.92	.92	ECH
224	VULCAN	VUL80C	33.20	35.60	.93	ECH
225	VULCAN	VUL85C	35.25	37.91	.93	ECH
226	VULCAN	VUL 100C	44.62	44.50	1.00	ECH
227	VULCAN	VUL 140C	48.80	62.30	.78	ECH
228	VULCAN	VUL 200C	68.09	89.00	.77	ECH
229	VULCAN	VUL 400C	154.08	178.00	.87	ECH
230	VULCAN	VUL 600C	243.01	267.00	.91	ECH
231	VULCAN	VUL320	81.38	89.00	.91	ECH
232	VULCAN	VUL330	122.07	133.50	.91	ECH
233	VULCAN	VUL340	162.76	178.00	.91	ECH
234	VULCAN	VUL360	244.14	267.00	.91	ECH
235	VULCAN	VUL505	33.91	22.25	1.52	ECH
236	VULCAN	VUL506	44.08	28.92	1.52	ECH
237	VULCAN	VUL508	54.25	35.60	1.52	ECH
238	VULCAN	VUL510	67.82	44.50	1.52	ECH
239	VULCAN	VUL512	81.38	53.40	1.52	ECH
240	VULCAN	VUL520	135.64	89.00	1.52	ECH
241	VULCAN	VUL530	203.45	133.50	1.52	ECH
242	VULCAN	VUL540	271.27	182.01	1.49	ECH
243	VULCAN	VUL560	406.91	278.13	1.46	ECH
245	VULCAN	VUL 3100	406.91	445.00	.91	ECH
246	VULCAN	VUL 5100	678.18	445.00	1.52	ECH
247	VULCAN	VUL 5150	1017.27	667.50	1.52	ECH

TABLE D-3 COMPLETE HAMMER LISTING
(sorted by GRLWEAP ID Numbers)

GRLWEAP ID	Hammer Mfgr	Hammer Name	Max. Energy kN-m	Ram Weight kN	Eq. Max. Stroke m	Hammer Type
248	VULCAN	VUL 6300	2441.45	1335.00	1.83	ECH
251	RAYMOND	R 1	20.35	22.25	.91	ECH
252	RAYMOND	R 1S	26.45	28.92	.91	ECH
253	RAYMOND	R 65C	26.45	28.92	.91	ECH
254	RAYMOND	R 65CH	26.45	28.92	.91	ECH
255	RAYMOND	R 0	33.06	33.38	.99	ECH
256	RAYMOND	R 80C	33.20	35.60	.93	ECH
257	RAYMOND	R 80CH	33.20	35.60	.93	ECH
258	RAYMOND	R 2/0	44.08	44.50	.99	ECH
259	RAYMOND	R 3/0	55.10	55.62	.99	ECH
260	RAYMOND	R 150C	66.12	66.75	.99	ECH
261	RAYMOND	R 4/0	66.12	66.75	.99	ECH
262	RAYMOND	R 5/0	77.14	77.88	.99	ECH
263	RAYMOND	R 30X	101.73	133.50	.76	ECH
264	RAYMOND	R 8/0	110.20	111.25	.99	ECH
265	RAYMOND	R 40X	135.64	178.00	.76	ECH
266	RAYMOND	R 60X	203.45	267.00	.76	ECH
270	9K DROP	9K DROP	122.07	40.05	3.05	ECH
271	MENCK	MH 68	66.70	34.35	1.94	ECH
272	MENCK	MH 96	94.17	49.04	1.92	ECH
273	MENCK	MH 145	142.15	73.56	1.93	ECH
274	MENCK	MH 195	191.41	98.12	1.95	ECH
275	MENCK	MHU 220	215.76	111.83	1.93	ECH
276	MENCK	MHU 400	392.74	225.66	1.74	ECH
277	MENCK	MHU 600	588.17	343.36	1.71	ECH
278	MENCK	MHU 1000	1000.58	565.02	1.77	ECH
279	MENCK	MHU 1700	1666.80	922.17	1.81	ECH
280	MENCK	MHU 2100	2099.09	1138.31	1.84	ECH
281	MENCK	MHU 3000	2945.54	1618.73	1.82	ECH
282	MENCK	MRBS 500	61.13	49.04	1.25	ECH
283	MENCK	MRBS 750	91.92	73.56	1.25	ECH
284	MENCK	MRBS 800	126.53	84.37	1.50	ECH
285	MENCK	MRBS 850	126.53	84.37	1.50	ECH
286	MENCK	MRBS1100	167.42	107.91	1.55	ECH
287	MENCK	MRBS1502	183.90	147.16	1.25	ECH
288	MENCK	MRBS1800	257.46	171.68	1.50	ECH
289	MENCK	MRBS2500	355.52	284.49	1.25	ECH
290	MENCK	MRBS2502	306.47	245.24	1.25	ECH
291	MENCK	MRBS2504	306.47	245.24	1.25	ECH
292	MENCK	MRBS3000	441.30	294.28	1.50	ECH
293	MENCK	MRBS3900	696.28	386.53	1.80	ECH

TABLE D-3 COMPLETE HAMMER LISTING
(sorted by GRLWEAP ID Numbers)

GRLWEAP ID	Hammer Mfgr	Hammer Name	Max. Energy kN-m	Ram Weight kN	Eq. Max. Stroke m	Hammer Type
294	MENCK	MRBS4600	676.74	451.27	1.50	ECH
295	MENCK	MRBS5000	735.60	490.52	1.50	ECH
296	MENCK	MRBS6000	1029.79	588.60	1.75	ECH
297	MENCK	MRBS7000	856.41	685.30	1.25	ECH
298	MENCK	MRBS8000	1176.97	784.85	1.50	ECH
299	MENCK	MRBS8800	1294.69	863.34	1.50	ECH
300	MENCK	MBS12500	2145.53	1226.33	1.75	ECH
301	MKT	No. 5	1.36	.89	1.52	ECH
302	MKT	No. 6	3.39	1.78	1.90	ECH
303	MKT	No. 7	5.63	3.56	1.58	ECH
304	MKT	9B3	11.87	7.12	1.67	ECH
305	MKT	10B3	17.78	13.35	1.33	ECH
306	MKT	C5-Air	19.26	22.25	.87	ECH
307	MKT	C5-Steam	21.97	22.25	.99	ECH
308	MKT	S-5	22.04	22.25	.99	ECH
309	MKT	11B3	25.97	22.25	1.17	ECH
310	MKT	C826 Strm	33.10	35.60	.93	ECH
311	MKT	C826 Air	28.75	35.60	.81	ECH
312	MKT	S-8	35.27	35.60	.99	ECH
313	MKT	MS-350	41.78	34.35	1.22	ECH
314	MKT	S 10	44.08	44.50	.99	ECH
315	MKT	S 14	50.89	62.30	.82	ECH
316	MKT	MS 500	59.68	48.95	1.22	ECH
317	MKT	S 20	81.38	89.00	.91	ECH
320	IHC Hyd	S 35	35.01	32.35	1.08	ECH
321	IHC Hyd	S 40	41.18	24.52	1.68	ECH
322	IHC Hyd	S 60	60.04	58.86	1.02	ECH
323	IHC Hyd	S 70	70.05	34.35	2.04	ECH
324	IHC Hyd	S 90	90.01	44.14	2.04	ECH
325	IHC Hyd	S 200	199.63	97.90	2.04	ECH
326	IHC Hyd	S 250	250.44	122.82	2.04	ECH
327	IHC Hyd	S 280	280.11	132.61	2.11	ECH
328	IHC Hyd	S 400	399.58	197.13	2.03	ECH
329	IHC Hyd	S 500	499.54	246.08	2.03	ECH
330	IHC Hyd	S 800	800.05	363.00	2.20	ECH
331	IHC Hyd	S 1000	999.99	451.26	2.22	ECH
332	IHC Hyd	S 1600	1597.52	694.20	2.30	ECH
333	IHC Hyd	S 2300	2298.99	1008.37	2.28	ECH
334	IHC Hyd	S 3000	2997.72	1477.40	2.03	ECH
341	IHC Hyd	SC 30	30.02	16.20	1.85	ECH
342	IHC Hyd	SC 40	39.98	24.52	1.63	ECH

TABLE D-3 COMPLETE HAMMER LISTING
(sorted by GRLWEAP ID Numbers)

GRLWEAP ID	Hammer Mfgr	Hammer Name	Max. Energy kN-m	Ram Weight kN	Eq. Max. Stroke m	Hammer Type
343	IHC Hydh	SC 60	60.00	34.35	1.75	ECH
344	IHC Hydh	SC 80	79.89	50.02	1.60	ECH
345	IHC Hydh	SC 110	105.01	67.68	1.55	ECH
346	IHC Hydh	SC 150	140.12	107.91	1.30	ECH
347	IHC Hydh	SC 200	204.81	134.39	1.52	ECH
348	IHC Hydh	SC 250	240.04	174.62	1.37	ECH
350	HERA	1250	34.38	12.50	2.75	OED
351	HERA	1500	41.25	15.00	2.75	OED
352	HERA	2500	68.75	25.00	2.75	OED
353	HERA	2800	77.00	28.00	2.75	OED
354	HERA	3500	96.25	35.00	2.75	OED
355	HERA	5000	137.50	50.00	2.75	OED
356	HERA	5700	156.75	57.00	2.75	OED
357	HERA	6200	170.50	62.00	2.75	OED
358	HERA	7500	206.25	75.00	2.75	OED
359	HERA	8800	242.00	88.00	2.75	OED
371	FAIRCHLD	F-45	61.04	66.75	.91	ECH
372	FAIRCHLD	F-32	44.15	48.28	.91	ECH
381	BSP	HH 3	35.29	29.42	1.20	ECH
382	BSP	HH 5	58.83	49.04	1.20	ECH
383	BSP	HH 7	82.44	68.65	1.20	ECH
384	BSP	HH 8	94.27	78.50	1.20	ECH
385	BSP	HH 9	106.03	88.29	1.20	ECH
386	BSP	HH 11	129.59	107.91	1.20	ECH
387	BSP	HH 14	164.92	137.33	1.20	ECH
388	BSP	HH 16	188.35	156.96	1.20	ECH
389	BSP	HH 20	235.44	196.20	1.20	ECH
390	BSP	HH 20S	235.44	196.20	1.20	ECH
391	BSP	HA 30	353.16	294.30	1.20	ECH
392	BSP	HA 40	470.88	392.40	1.20	ECH
401	BERMINGH	B23	31.18	12.46	2.50	CED
402	BERMINGH	B200	24.41	8.90	2.74	OED
403	BERMINGH	B225	39.67	13.35	2.97	OED
404	BERMINGH	B300	54.68	16.69	3.28	OED
405	BERMINGH	B400	72.90	22.25	3.28	OED
410	BERMINGH	B300 M	54.68	16.69	3.28	OED
411	BERMINGH	B400 M	72.90	22.25	3.28	OED
412	BERMINGH	B400 4.8	58.59	21.36	2.74	OED
413	BERMINGH	B400 5.0	61.04	22.25	2.74	OED
414	BERMINGH	B23 5	31.18	12.46	2.50	CED
415	BERMINGH	B250 5	48.02	13.35	3.60	OED

TABLE D-3 COMPLETE HAMMER LISTING
(sorted by GRLWEAP ID Numbers)

GRLWEAP ID	Hammer Mfgr	Hammer Name	Max. Energy kN-m	Ram Weight kN	Eq. Max. Stroke m	Hammer Type
416	BERMINGH	B350 5	64.02	17.80	3.60	OED
417	BERMINGH	B400 5	80.03	22.25	3.60	OED
418	BERMINGH	B450 5	105.63	29.37	3.60	OED
419	BERMINGH	B500 5	124.84	34.71	3.60	OED
420	BERMINGH	B550 5	144.05	40.05	3.60	OED
421	BERMINGH	B550 C	119.36	48.95	2.44	OED
441	MENCK	MHF5-5	52.48	49.05	1.07	ECH
442	MENCK	MHF5-6	62.98	58.86	1.07	ECH
443	MENCK	MHF5-7	73.48	68.67	1.07	ECH
444	MENCK	MHF5-8	83.97	78.48	1.07	ECH
445	MENCK	MHF5-9	94.47	88.29	1.07	ECH
446	MENCK	MHF5-10	104.97	98.10	1.07	ECH
447	MENCK	MHF5-11	115.46	107.91	1.07	ECH
448	MENCK	MHF5-12	125.96	117.72	1.07	ECH
449	MENCK	MHF3-3	33.59	31.39	1.07	ECH
450	MENCK	MHF3-4	41.99	39.24	1.07	ECH
451	MENCK	MHF3-5	52.48	49.05	1.07	ECH
452	MENCK	MHF3-6	62.98	58.86	1.07	ECH
453	MENCK	MHF3-7	73.48	68.67	1.07	ECH
454	MENCK	MHF10-15	157.39	147.12	1.07	ECH
455	MENCK	MHF10-20	209.81	196.11	1.07	ECH
461	MENCK	MHUT 200	199.90	117.75	1.70	ECH
462	MENCK	MHUT 400	400.29	234.51	1.71	ECH
463	MENCK	MHUT 500	499.89	264.95	1.89	ECH
464	MENCK	MHUT700U	700.06	413.09	1.69	ECH
465	MENCK	MHUT700A	839.83	413.09	2.03	ECH
466	MENCK	MHUT1000	999.52	588.73	1.70	ECH
481	JUNTTAN	HHK 3	36.01	29.46	1.22	ECH
482	JUNTTAN	HHK 4	47.97	39.25	1.22	ECH
483	JUNTTAN	HHK 5	59.99	49.08	1.22	ECH
484	JUNTTAN	HHK 6	71.96	58.87	1.22	ECH
485	JUNTTAN	HHK 7	83.98	68.71	1.22	ECH
486	JUNTTAN	HHK 10	119.93	98.12	1.22	ECH
487	JUNTTAN	HHK 12	143.92	117.75	1.22	ECH
488	JUNTTAN	HHK 14	167.90	137.37	1.22	ECH
489	JUNTTAN	HHK 5A	59.79	49.04	1.22	ECH
490	JUNTTAN	HHK 7A	83.71	68.66	1.22	ECH
491	JUNTTAN	HHK 9A	107.64	88.29	1.22	ECH
501	HPSI	110	59.68	48.95	1.22	ECH
502	HPSI	150	81.38	66.75	1.22	ECH
503	HPSI	154	83.55	68.53	1.22	ECH

TABLE D-3 COMPLETE HAMMER LISTING
(sorted by GRLWEAP ID Numbers)

GRLWEAP ID	Hammer Mfgr	Hammer Name	Max. Energy kN-m	Ram Weight kN	Eq. Max. Stroke m	Hammer Type
504	HPSI	200	108.51	89.00	1.22	ECH
505	HPSI	225	122.07	100.12	1.22	ECH
506	HPSI	650	44.08	28.92	1.52	ECH
507	HPSI	1000	67.82	44.50	1.52	ECH
508	HPSI	1605	112.58	73.87	1.52	ECH
509	HPSI	2005	128.99	84.64	1.52	ECH
510	HPSI	3005	209.32	137.35	1.52	ECH
511	HPSI	3505	239.16	156.93	1.52	ECH
515	UDDCOMB	H3H	33.75	29.37	1.15	ECH
516	UDDCOMB	H4H	45.00	39.16	1.15	ECH
517	UDDCOMB	H5H	56.25	48.95	1.15	ECH
518	UDDCOMB	H6H	67.50	58.74	1.15	ECH
519	UDDCOMB	H8H	94.06	78.32	1.20	ECH
520	UDDCOMB	H10H	117.84	98.12	1.20	ECH
521	DAWSON	HPH 1200	11.73	10.20	1.15	ECH
522	DAWSON	HPH 2400	23.49	18.64	1.26	ECH
541	BANUT	3 Tonnes	23.53	29.41	.80	ECH
542	BANUT	4 Tonnes	31.39	39.25	.80	ECH
543	BANUT	5 Tonnes	39.22	49.04	.80	ECH
544	BANUT	6 Tonnes	47.09	58.87	.80	ECH
545	BANUT	7 Tonnes	54.92	68.66	.80	ECH
551	ICE	110-SH	51.16	51.17	1.00	ECH
552	ICE	115-SH	51.47	51.17	1.01	ECH
553	ICE	160-SH	86.81	71.20	1.22	ECH
701	ICE	1412	27.13	4.45	6.10	VIB
702	ICE	815	36.21	4.45	8.14	VIB
703	ICE	812	32.59	4.01	8.14	VIB
704	ICE	416	18.11	2.23	8.14	VIB

APPENDIX E

Student Exercise - Solutions

	Page
STUDENT EXERCISE #9 SOLUTION - GATES FORMULA ULTIMATE CAPACITY	E-3
STUDENT EXERCISE #10 SOLUTION - GATES FORMULA DRIVING CRITERION	E-5
STUDENT EXERCISE #11 SOLUTION - WAVE EQUATION HAMMER APPROVAL	E-7
STUDENT EXERCISE #12 SOLUTION - WAVE EQUATION INSPECTORS CHART	E-11
STUDENT EXERCISE #13 SOLUTION - DETERMINATION OF LOAD TEST FAILURE LOAD	E-15
STUDENT EXERCISE #14 SOLUTION - EQUIPMENT SUBMITTAL REVIEW	E-17
STUDENT EXERCISE #15 SOLUTION - HAMMER INSPECTION	E-21
STUDENT EXERCISE #16 SOLUTION - DETERMINING PILE TOE ELEVATIONS	E- 27

STUDENT EXERCISE #9 SOLUTION - GATES FORMULA ULTIMATE CAPACITY

Use the Gates formula described in Section 16.3 to calculate the ultimate pile capacity of a 356 mm O.D. pipe pile driven with an ICE 42-S single acting diesel hammer to the driving resistances given in the table below. The field observed hammer strokes and corresponding manufacturer's rated energy are also included in the table. The Gates formula is presented below:

$$R_u = [7 \sqrt{E_r} \log (10 N_b)] - 550$$

Where: R_u = ultimate pile capacity (kN).
 E_r = manufacturer's rated energy at field stroke (joules).
 N_b = number of hammer blows for 25 mm penetration.

For 168 blows / 250 mm at a 3.05 m stroke the solution is as follows:

$$R_u = [7 \sqrt{55480} \log (10 (16.8))] - 550$$

$$R_u = [7 (235.5) \log (168)] - 550 = 3119 \text{ kN}$$

The table on the following page provides the problem solutions at other driving resistances and field observed strokes.

Group Number	Pile Driving Resistance (blows / 250 mm)	Field Observed Stroke (m)	Manufacturer's Rated Energy (joules)	Gates Ultimate Pile Capacity (kN)
1	3	1.67	30,377	32
2	7	2.43	44,202	693
3	18	2.88	52,387	1461
4	37	3.10	56,389	2057
5	53	3.13	56,935	2330
6	72	3.02	54,934	2497
7	87	3.04	55,298	2643
8	107	3.04	55,298	2791
9	133	3.05	55,480	2952
10	168	3.05	55,480	3119

STUDENT EXERCISE #10 SOLUTION - GATES FORMULA DRIVING CRITERION

The Gates formula is to be used for construction control on a new bridge project. The piles have a design load of 620 kN and are to be driven through 5 meters of scourable soils that were calculated to provide 90 kN of resistance at the time of driving. A Kobe K 25 single acting diesel hammer will be used to drive the piles. First determine the required ultimate pile capacity. Then use the Gates formula provided below and described in Section 16.3 to calculate the required driving resistance for the ultimate pile capacity at the hammer strokes shown in the table below.

STEP 1 Calculate the required ultimate pile capacity:

$$\begin{aligned} R_u &= (\text{design load})(\text{factor of safety}) + \text{scour resistance} \\ &= (620 \text{ kN})(3.5) + 90 \text{ kN} = 2260 \text{ kN}. \end{aligned}$$

STEP 2 Calculate x: (Solution provided for a stroke of 2.85 m, $E_r = 69882$ joules)

$$\begin{aligned} x &= [(R_u + 550)/(7 \sqrt{E_r})] - 1 \\ x &= [(2260 + 550)/(7 \sqrt{69882})] - 1 \\ x &= [(2810) / (7)(264.3)] - 1 = 0.518 \end{aligned}$$

STEP 3 Calculate N_{qm} :

$$\begin{aligned} N_{qm} &= 10(10^x) = 10(10^{0.518}) = 10(3.29) \\ &= 33 \text{ blows} / 250 \text{ mm} \end{aligned}$$

Where: N_{qm} = Number of hammer blows for 250 mm penetration.
 R_u = Ultimate pile capacity (kN).
 E_r = Manufacturer's rated energy at field stroke (joules).

Solutions for other field observed hammer strokes and corresponding rated hammer energies are provided in table on following page.

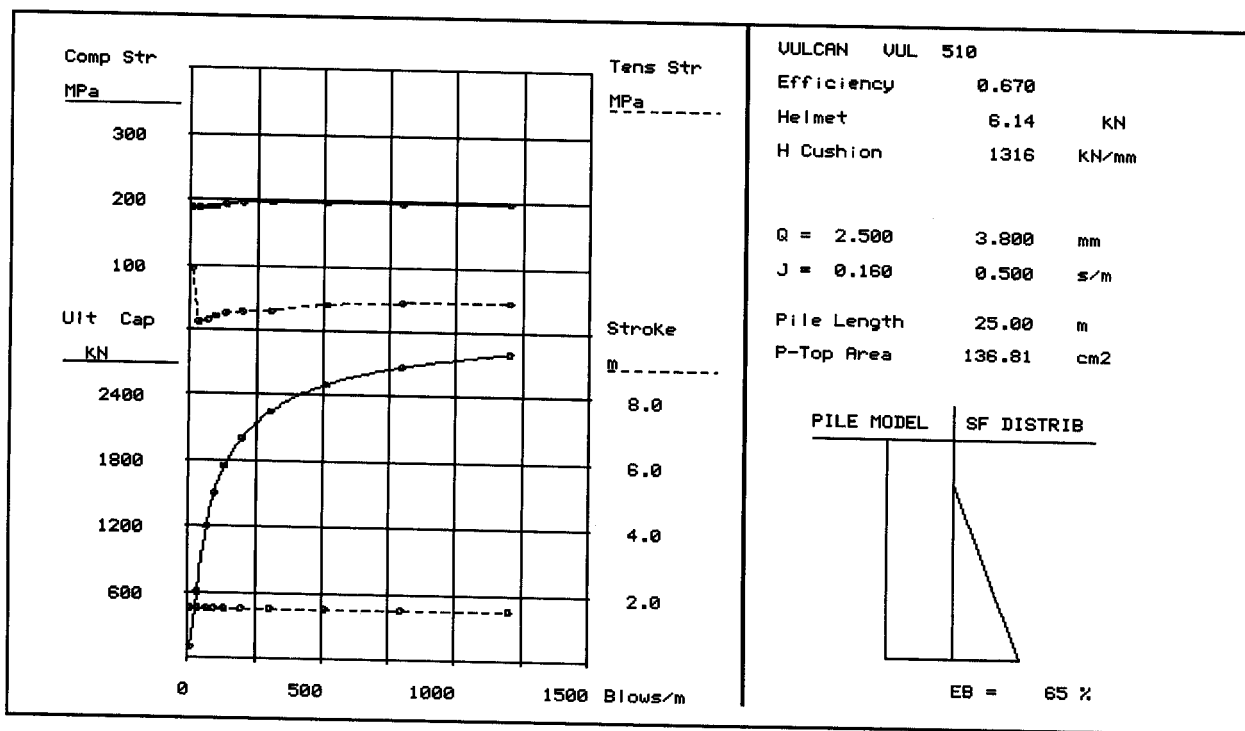
Group Number	Field Observed Stroke (m)	Manufacturer's Rated Energy (joules)	Exponent (x)	Required Driving Resistance (blows / 250 mm)
1	1.50	36,870	1.091	123
2	1.65	40,458	0.996	99
3	1.80	44,136	0.911	81
4	1.95	47,814	0.836	69
5	2.10	51,492	0.769	59
6	2.25	55,170	0.709	51
7	2.40	58,848	0.655	45
8	2.55	62,526	0.605	40
9	2.70	66,204	0.561	36
10	2.85	69,882	0.518	33

STUDENT EXERCISE #11 SOLUTION - WAVE EQUATION HAMMER APPROVAL

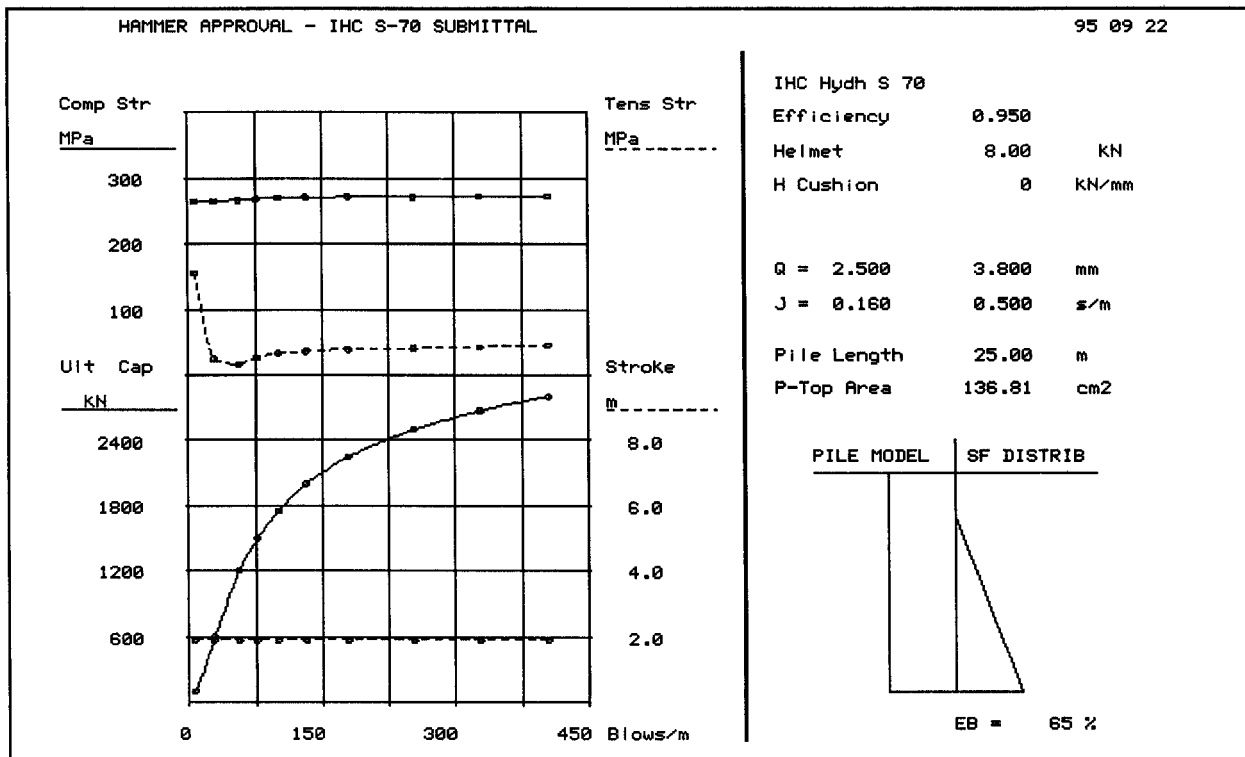
The wave equation results for the Vulcan 510 driving system indicate that a driving resistance of 797 blows per meter is required for the ultimate pile capacity. Maximum compression driving stresses are 197 MPa. Based on these results, the compression driving stresses are below the maximum allowable of 279 MPa for Grade 3 steel but the driving resistance is greater than the recommended ranged of 120 to 480 blows per meter. Therefore, this hammer should not be approved.

The wave equation results for the IHC S-70 driving system indicate that a driving resistance of 328 blows per meter is required for the ultimate pile capacity. Maximum compression driving stresses are 273 MPa. Based on these results, the driving stresses are high, but within acceptable limits, and the driving resistance is within the recommended ranged of 120 to 480 blows per meter. The IHC hammer equivalent stroke could be slightly reduced, if necessary, to further decrease compression driving stress levels. This would increase the driving resistance but since the driving resistance is well below the maximum value this should not be a problem. An additional wave equation analysis should be performed if a reduced equivalent stroke will be used. Based on the above analysis, the IHC S-70 hammer should be approved.

Rut (kN)	Bl Ct (bpm)	Stroke(eq.) (m)	min Str (MPa)	i,t	max Str (MPa)	i,t	ENTHRU (kJ)
100.0	7.5	1.52	-94.84	(5, 12)	188.83	(7, 4)	38.1
600.0	33.1	1.52	-12.54	(12, 47)	189.12	(8, 5)	41.9
1200.0	67.8	1.52	-15.71	(12, 33)	189.70	(9, 5)	41.5
1500.0	95.8	1.52	-21.81	(13, 31)	190.04	(8, 5)	40.6
1750.0	134.5	1.52	-25.95	(15, 45)	193.46	(25, 8)	39.9
2000.0	199.3	1.52	-28.52	(14, 30)	197.31	(25, 8)	39.7
2250.0	306.7	1.52	-30.44	(10, 41)	198.28	(25, 8)	39.7
2500.0	511.9	1.52	-40.46	(11, 40)	197.83	(25, 8)	39.6
2670.0	796.8	1.52	-44.19	(11, 40)	197.03	(25, 8)	39.6
2800.0	1202.6	1.52	-46.29	(11, 39)	198.47	(2, 13)	39.6



Rut (kN)	Bl Ct (bpm)	Stroke(eq.) (m)	min Str (MPa)	i,t	max Str (MPa)	i,t	ENTHRU (kJ)
100.0	6.5	1.90	-155.26	(6, 11)	265.77	(3, 3)	51.1
600.0	29.2	1.90	-25.68	(6, 47)	265.77	(3, 3)	55.0
1200.0	56.7	1.90	-17.12	(13, 32)	267.25	(4, 3)	54.9
1500.0	77.1	1.90	-27.35	(13, 29)	269.03	(7, 3)	54.0
1750.0	100.8	1.90	-33.58	(13, 28)	270.15	(7, 3)	53.5
2000.0	132.1	1.90	-37.35	(14, 28)	271.23	(7, 3)	53.2
2250.0	179.7	1.90	-39.84	(14, 28)	271.79	(7, 3)	53.2
2500.0	253.7	1.90	-41.38	(14, 27)	272.41	(8, 4)	53.1
2670.0	328.1	1.90	-43.87	(14, 26)	273.02	(7, 3)	53.1
2800.0	405.1	1.90	-46.17	(14, 26)	273.23	(7, 3)	53.1



STUDENT EXERCISE #12 SOLUTION - WAVE EQUATION INSPECTORS CHART

A contractor has chosen a Kobe K-35 for foundation installation of HP 360x174 H-piles. The H-piles are to be driven to a limestone bedrock for an ultimate pile capacity of 3250 kN. The H-piles are to be A-36 steel.

For hammer approval, a standard wave equation bearing graph analysis was performed. The results from this analysis are the next page and indicate that both the driving resistance (Chapter 12) and driving stresses (Chapter 11) are within specification limits for the ultimate capacity of 3250 kN. The standard bearing graph indicates a driving resistance of 255 blows per meter at a hammer stroke of 2.40 m should result in the required ultimate pile capacity.

A constant capacity wave equation analysis or inspectors chart was then performed to assist field personnel in the determining the required driving resistance at other field observed hammer strokes. The results of this constant capacity analysis for Pier 2 piles is presented on page 17-69. The analysis results have been furnished to the inspector in expanded form as presented on page 17-70 and should be used to answer the following questions.

1. Pile #1 has a field observed hammer stroke is 2.20 m and a driving resistance of 275 blows/m. Does this pile have the required ultimate capacity?

No, at 2.2 m stroke a driving resistance of 304 blows/m is required for 3,250 kN.

Any additional action required by the inspector?

Yes, drive pile further.

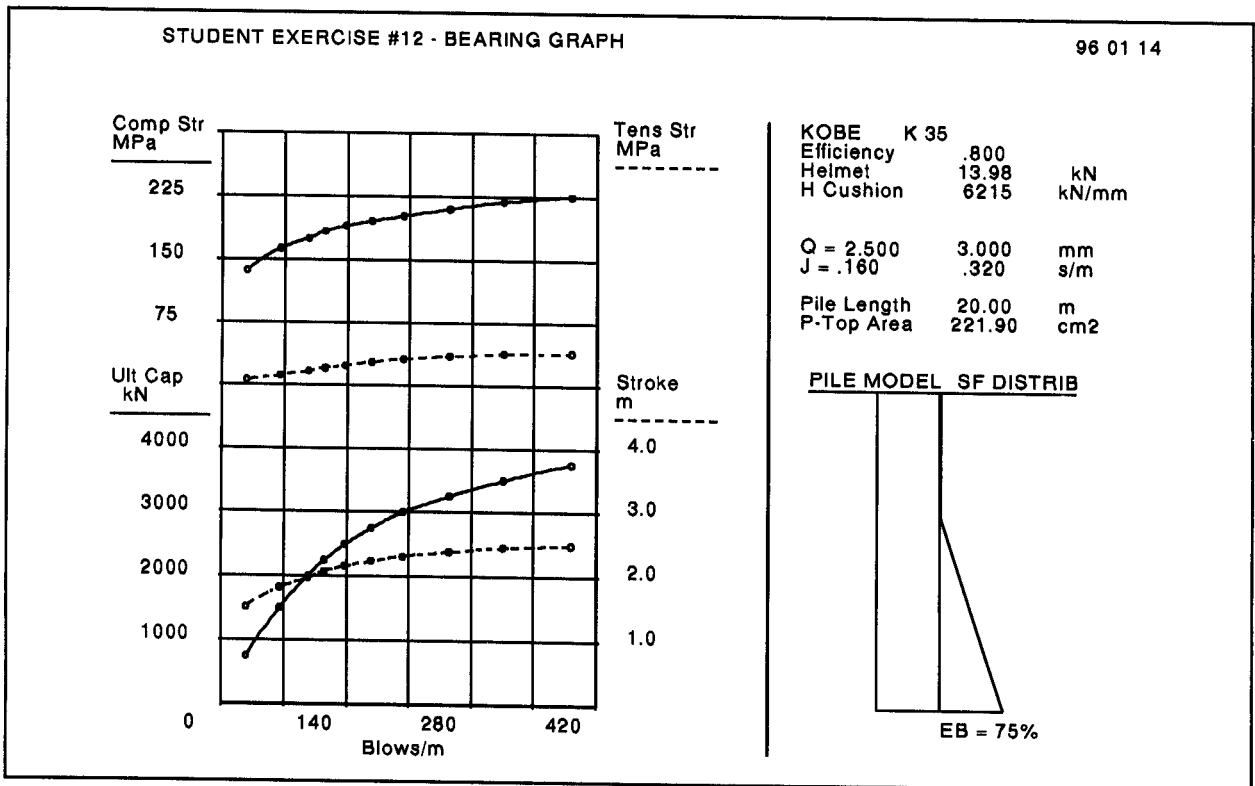
2. Pile #2 has a field observed hammer stroke of 2.85 m and a driving resistance of 195 blows/m. Does this pile have the required ultimate capacity?

Yes.

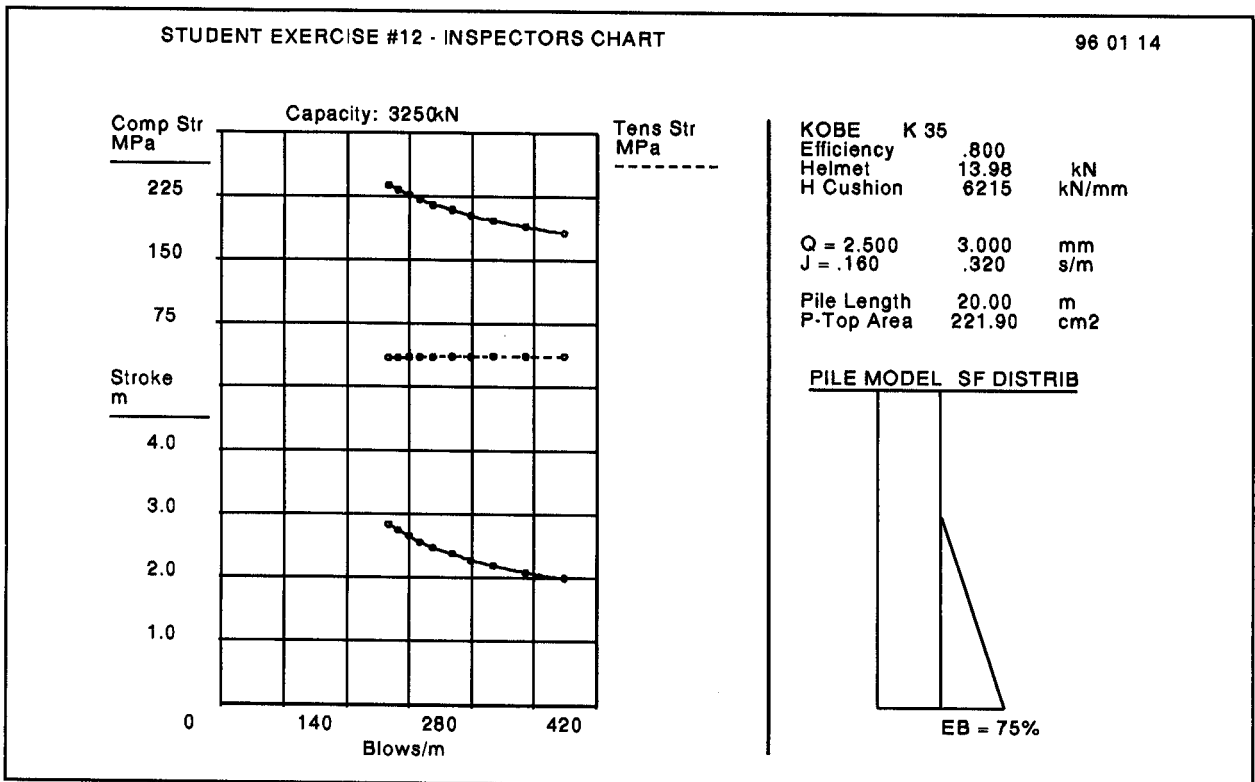
Any additional action required by the inspector?

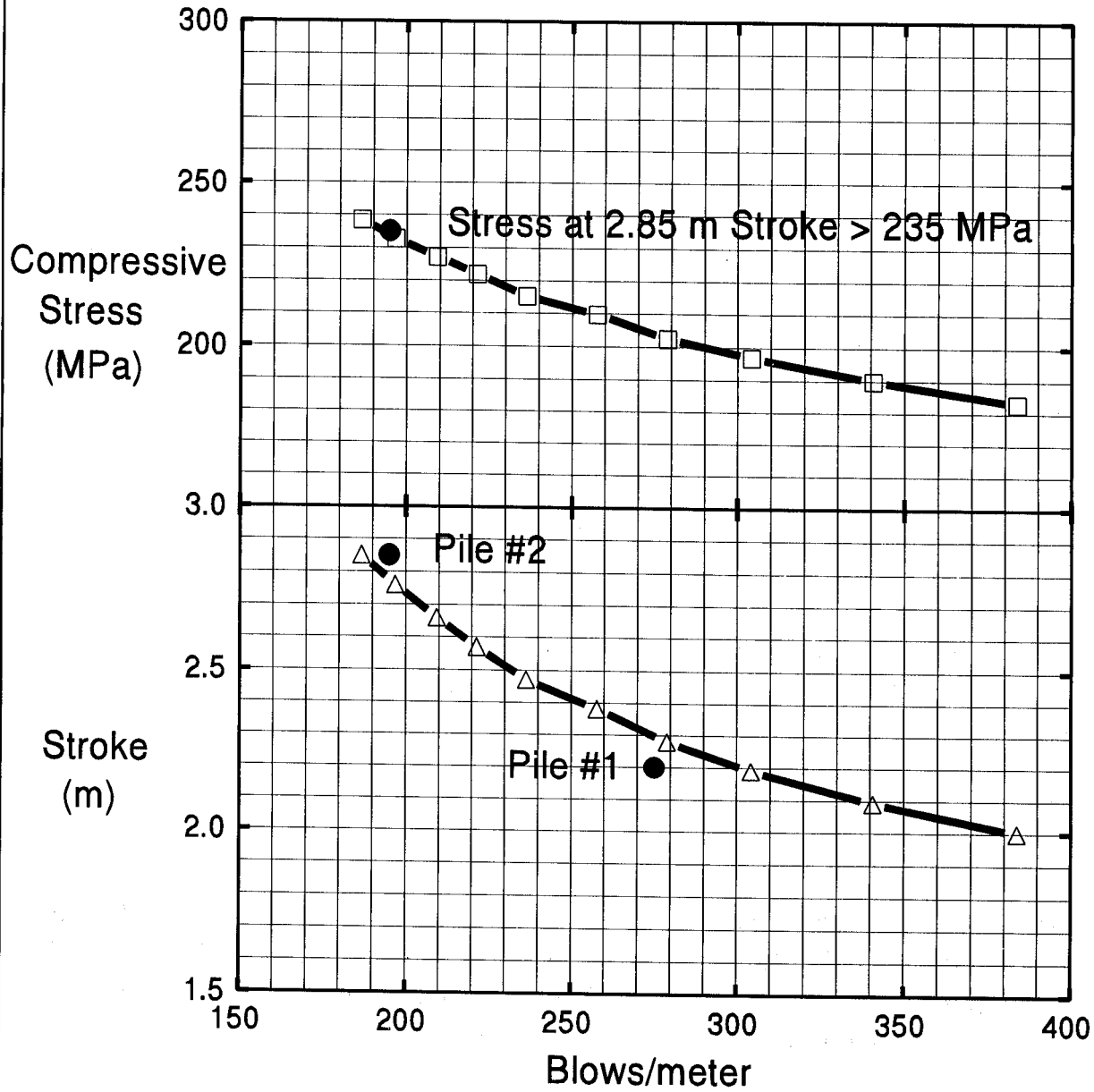
Yes, driving stress are greater than 235 MPa which are too high since they are greater than 223 MPa ($0.90 f_y$). Drive piles with a reduced hammer stroke.

Rut (kN)	Bl Ct (bpm)	Stroke down	(m) min up	Str (MPa)	i,t	max Str (MPa)	i,t	ENTHRU (kJ)	Bl Rt (b/min)
750.0	27.5	1.52	1.54	-7.39	(9, 46)	137.40	(4, 3)	44.7	52.7
1500.0	65.2	1.82	1.83	-12.30	(10, 30)	163.13	(10, 4)	41.7	48.2
2000.0	96.8	1.97	1.99	-17.55	(11, 27)	175.50	(10, 4)	41.9	46.2
2250.0	114.8	2.08	2.07	-21.69	(12, 26)	183.43	(10, 4)	43.2	45.2
2500.0	138.5	2.16	2.16	-24.44	(12, 24)	189.75	(11, 4)	44.1	44.3
2750.0	167.9	2.24	2.24	-28.96	(11, 23)	195.82	(11, 4)	45.1	43.6
3000.0	203.5	2.32	2.32	-32.91	(11, 23)	201.83	(10, 4)	46.2	42.8
3250.0	255.1	2.39	2.40	-36.08	(11, 22)	210.55	(20, 6)	47.0	42.2
3500.0	315.8	2.46	2.46	-39.09	(11, 22)	219.45	(20, 6)	48.2	41.6
3750.0	392.0	2.49	2.51	-40.49	(10, 22)	225.05	(20, 6)	48.9	41.3



Rut (kN)	Bl Ct (bpm)	Stroke down	(m) up	min Str (MPa)	i,t	max Str (MPa)	i,t	ENTHRU (kJ)	Bl Rt (b/min)
3250.0	383.7	2.00	2.40	-37.17	(11, 22)	182.91	(20, 6)	39.2	44.0
3250.0	340.7	2.09	2.40	-36.94	(11, 22)	189.80	(20, 6)	41.1	43.5
3250.0	304.2	2.19	2.39	-36.76	(11, 22)	196.77	(20, 6)	43.1	43.1
3250.0	278.9	2.28	2.39	-36.44	(11, 22)	202.57	(20, 6)	45.0	42.6
3250.0	257.7	2.38	2.39	-36.13	(11, 22)	209.78	(20, 6)	46.8	42.2
3250.0	236.4	2.47	2.39	-35.92	(11, 22)	215.22	(20, 6)	48.8	41.8
3250.0	221.3	2.57	2.39	-35.61	(11, 22)	221.89	(20, 6)	50.6	41.4
3250.0	209.4	2.66	2.40	-35.26	(11, 22)	227.07	(20, 6)	52.3	41.0
3250.0	196.8	2.76	2.40	-35.01	(11, 23)	232.65	(20, 6)	54.2	40.7
3250.0	186.6	2.85	2.40	-34.69	(11, 23)	238.40	(20, 6)	56.0	40.3





STUDENT EXERCISE #13 SOLUTION - DETERMINATION OF LOAD TEST FAILURE LOAD

An axial compression static load test has been performed and the results must be interpreted to determine if the pile has an ultimate capacity in excess of the required ultimate capacity. The load - movement curve from the static load on a 356 mm square prestressed concrete pile is presented on the following page. The pile has a cross sectional area, A_c , of 0.127 m² and a length, L , of 24 m. The concrete compressive strength, f'_c , is 34.5 MPa. The pile has a required ultimate pile capacity of 2200 kN.

Recommended Procedure:

First determine the elastic modulus, E , of the pile from the concrete compressive strength using $E = 4700 \sqrt{f'_c}$ where f'_c must be in MPa.

$$E = 4700 \sqrt{34.5} = 27606 \text{ MPa}$$

Next, calculate and plot the elastic deformation line using zero and any other load. However, for consistency between solutions and ease in plotting, calculate the elastic deformation using a load of 2500 kN from $\Delta = QL / AE$. Make sure the units for the terms in this equation are as required in the equation description provided in Section 19.7.4.

$$\Delta = QL / AE = [2500 \text{ kN} (24 \text{ m})(1000 \text{ mm} / \text{m})] / [0.127 \text{ m}^2 (27606000 \text{ kPa})] = 17.1 \text{ mm}$$

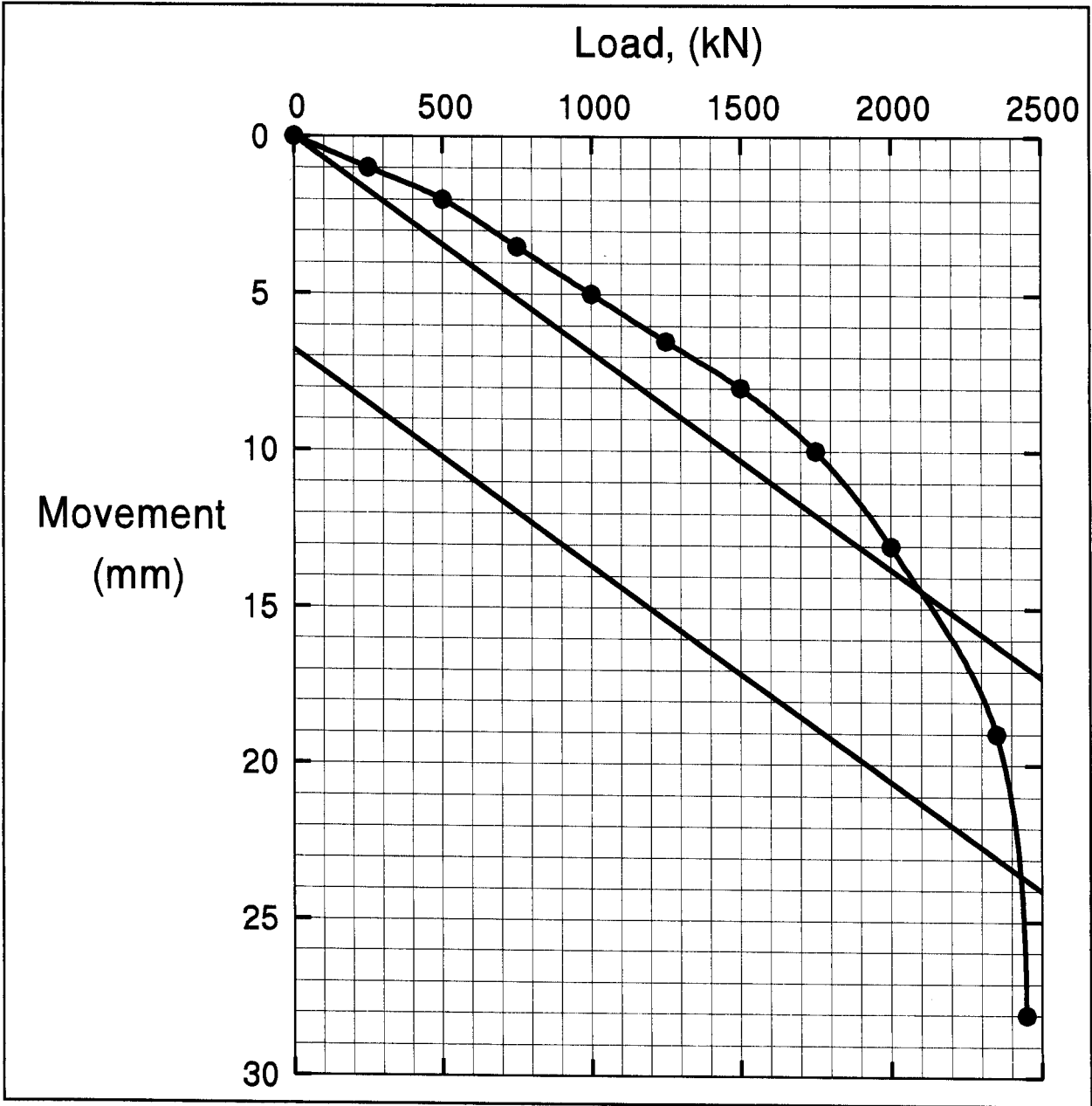
Then calculate the failure criterion line for the 356 mm pile from $s_f = \Delta + (4.0 + 0.008b)$ as described in Section 19.7.5. Remember at zero load, the failure criterion line will start at a movement equal to $(4.0 + 0.008b)$ and at 2500 kN, the failure criterion line will be equal to a movement of $s_f = \Delta + (4.0 + 0.008b)$.

$$\text{At } 0 \text{ kN, } s_f = (4.0 \text{ mm} + 0.008b) = 6.8 \text{ mm}$$

$$\text{At } 2500 \text{ kN, } s_f = \Delta + (4.0 \text{ mm} + 0.008b) = 17.2 + (4.0 \text{ mm} + 0.008(356)) = 23.9 \text{ mm}$$

Last, plot the failure criterion line on the load-movement curve and determine whether the failure load is greater than the required ultimate pile capacity of 2200 kN.

Based on the attached plot, the failure load is 2425 kN which is greater than the required ultimate capacity of 2200 kN.



STUDENT EXERCISE #14 SOLUTION - EQUIPMENT SUBMITTAL REVIEW

Project specifications require the contractor to use a pile driving hammer having a minimum rated energy of 20.0 kJ to install the 20 m long, 305 mm square, prestressed concrete piles on this project. The piles have a required ultimate pile capacity of 1200 kN. Soil conditions consist of 15 m of soft clay over 20 meters of medium dense to dense sands. Static analyses indicate the piles should develop the required ultimate capacity at a penetration depth of 19 m. The Gates dynamic formula will be used for construction control.

The following pages contain the contractor's submittal package on this project. Based on the submittal, the final driving resistance required by the Gates formula is 56 blows per 0.25 m for the 1200 kN ultimate capacity. Review the submittal information and decide if the submittal should be approved. Do you have any questions or concerns ?

STEP 1 Check if hammer meets minimum energy requirements.

Yes, the rated energy of 20.5 kJ for the Vulcan 50-C is greater than the 20.0 kJ required.

STEP 2 Determine line pressure loss in air hose between compressor and hammer by entering hose detail table on page E-20 at compressor air delivery of 28 m³/min. (Note, this table indicates the line loss in 15.2 m of hose.)

At 28 m³ / min and a line pressure of 827 kPa the expected pressure loss in the hose is 18.6 kPa per 15.2 m. Therefore for 61 m of hose, the pressure loss is (61m / 15.2 m)(18.6 kPa) or 74.6 kPa. The actual pressure at the hammer is then 827 kPa - 74.6 kPa or 752.3 kPa.

STEP 3 Check if the pressure at the hammer meets manufacturer's requirements.

No, the required pressure at the hammer is 827 kPa in order to develop the full rated energy.

STEP 4 Determine the rated energy based on the pressure at the hammer using the following manufacturer's formula for a differential hammer:

$$E_r = [W + A_{np} (p_h)]h$$

Based on the pressure at the hammer, the rated energy is:

$$\begin{aligned} E_r &= [22.25 \text{ kN} + 0.036 \text{ m}^2 (752.3 \text{ kPa})] 0.39 \text{ m} \\ &= [22.25 \text{ kN} + 27.08 \text{ kN}] 0.39 \text{ m} = 19.2 \text{ kJ} \end{aligned}$$

Note: At this rated energy, the Gates formula would require 64 blows / 0.25 m for the 1200 kN ultimate pile capacity. In addition more than half the rated energy is due to the pressure at the hammer.

Equipment Submittal

- Hammer: Vulcan 50-C differential acting air hammer.
Rated energy = 20.5 kJ at 0.39 m stroke.
(additional hammer details on page 22-49)
- Hammer Cushion: 152 mm of Aluminum and Micarta.
Hammer Cushion Area = 641 cm².
- Helmet: 4.6 kN
- Pile Cushion: 100 mm of Plywood.
Pile Cushion Area = 930 cm².
- Air Compressor: Model 1000
Rated Delivery: 28.3 m³ / min.
Rated Pressure: 827 kPa.
- Hose: 61 m of 51 mm I.D. (additional details on page 22-49).
- Pile: 20 m long, 305 mm square precast, prestressed concrete
Compressive Strength: 40 MPa.
Effective Prestress after losses: 6 MPa.

Equipment Submittal

Hammer Details:

Ram Weight: 22.25 kN
 Normal Stroke: 0.39 m
 Rated Operating Pressure at Hammer: 827 kPa
 Air Consumption: 24.9 m³ / min
 Required Air Compressor Size: 25.5 m³ / min
 Net Area of Piston: 0.036 m²

Hose Details:

Hose		Pressure Loss in Hose (kPa)						
Inside Dia. (mm)	Length (m)	Air Delivery (m ³ / min)	Line Pressure (kPa)					
			414	552	690	827	1034	
51	15.2	16.8	13.1	-----	-----	-----	-----	-----
		22.4	22.1	17.2	14.5	-----	-----	-----
		28.0	34.5	26.9	22.1	18.6	12.2	11.7
		33.6	48.3	37.9	31.0	26.2	21.4	16.5
		39.2	64.1	51.0	42.1	35.9	29.0	22.1
		44.8	-----	66.2	54.5	46.2	37.9	29.0
		50.4	-----	83.4	69.3	57.9	47.6	36.5
		56.0	-----	-----	84.1	71.7	58.6	44.8

STUDENT EXERCISE #15 SOLUTION - HAMMER INSPECTION

You are inspecting the pile driving operations on two bridge projects. On the first project, Bridge #1, the contractor is using a single acting diesel hammer. The driving criteria with this hammer has been established as follows:

Minimum Toe Elevation: EL 96.5 m
Minimum Driving Resistance: 80 blows / 250 mm at a 3.0 m stroke.

The driving record for the first pile driven is attached. The hammer operating speed was timed at 40 blows per minute at final driving. Has this pile met the driving criteria ?

STEP 1. Calculate the hammer stroke based on the recorded hammer operating speed using the formula on page 24-22.

$$\begin{aligned}\text{Stroke, h} &= [4400/\{\text{BPM}^2\}] - 0.09 \\ &= [4400/\{40^2\}] - 0.09 = 2.66 \text{ m}\end{aligned}$$

STEP 2. Determine the pile toe elevation.

$$\begin{aligned}\text{Toe elevation} &= \text{reference elevation} - \text{pile penetration depth} \\ &= 109.5 - 13.5 = 96.0 \text{ m}\end{aligned}$$

STEP 3. Based on hammer stroke, driving resistance and pile toe elevation, determine if the pile has met the driving criteria.

The pile has met the required driving resistance and toe elevation. However, the stroke is less than required. Therefore, the pile has not met the driving criteria, so continue driving.

PILE DRIVING LOG

STATE PROJECT NO.: Bridge #1 DATE: 5-29-98

JOB LOCATION: Bogalusa

PILE TYPE: 457 mm PCC LENGTH: 15 m BENT/PIER NO.: 1 PILE NO.: 1

HAMMER: D-30-32 ENERGY/BLOW: 99.9 kJ OPERATING RATE: 36-52 BPM HELMET WEIGHT: 14.5 kN

REF. ELEV.: 109.5 m PILE TOE ELEV.: _____ PILE CUTOFF ELEV.: 108.3 m

PILE CUSHION THICKNESS AND MATERIAL: 190 mm of plywood

WEATHER: sunny TEMP.: 80° START TIME: 8:23 am STOP TIME: 8:58 am

METERS	BLOWS	STROKE / PRESSURE	REMARKS	METERS	BLOWS	STROKE / PRESSURE	REMARKS
0 - 0.25	W.O.P			8.00 - 8.25	25		
0.25 - 0.50	W.O.P			8.25 - 8.50	21	51 BPM	
0.50 - 0.75	W.O.P			8.50 - 8.75	23		
0.75 - 1.00	W.O.P			8.75 - 9.00	26		
1.00 - 1.25	W.O.P			9.00 - 9.25	22	51 BPM	
1.25 - 1.50	W.O.P			9.25 - 9.50	21		
1.50 - 1.75	W.O.H			9.50 - 9.75	23		
1.75 - 2.00	W.O.H			9.75 - 10.00	24	51 BPM	
2.00 - 2.25	W.O.H			10.00 - 10.25	22		
2.25 - 2.50	5		Fuel #2	10.25 - 10.50	26		
2.50 - 2.75	6	52 BPM		10.50 - 10.75	30	44 BPM	
2.75 - 3.00	8			10.75 - 11.00	34		
3.00 - 3.25	10			11.00 - 11.25	40		
3.25 - 3.50	12			11.25 - 11.50	51	43 BPM	
3.50 - 3.75	17	50 BPM		11.50 - 11.75	38	42 BPM	Fuel #4
3.75 - 4.00	22			11.75 - 12.00	41		
4.00 - 4.25	30	49 BPM		12.00 - 12.25	42	42 BPM	
4.25 - 4.50	21	47 BPM	Fuel #3	12.25 - 12.50	53		
4.50 - 4.75	24			12.50 - 12.75	58	41 BPM	
4.75 - 5.00	27			12.75 - 13.00	65		
5.00 - 5.25	29			13.00 - 13.25	77	40 BPM	
5.25 - 5.50	31	45 BPM		13.25 - 13.50	80	40 BPM	
5.50 - 5.75	32			13.50 - 13.75			
5.75 - 6.00	32			13.75 - 14.00			
6.00 - 6.25	35	45 BPM		14.00 - 14.25			
6.25 - 6.50	31			14.25 - 14.50			
6.50 - 6.75	25			14.50 - 14.75			
6.75 - 7.00	21	47 BPM		14.75 - 15.00			
7.00 - 7.25	18			15.00 - 15.25			
7.25 - 7.50	20			15.25 - 15.50			
7.50 - 7.75	19	51 BPM		15.50 - 15.75			
7.75 - 8.00	22			15.75 - 16.00			

On the second project, Bridge #2, the contractor is using a double acting diesel hammer. The bounce chamber - equivalent energy correlation for the hammer as provided by the contractor in the equipment submittal is attached. The driving criteria on the second project has been established as follows:

Minimum Toe Elevation: EL 80
Minimum Driving Resistance: 60 blows / 250 mm at a bounce chamber pressure of 180 kPa. (Based on 15.2 m of hose)

The driving record for the first production pile driven on this project is attached. The hose between the bounce chamber pressure is 24.4 m long. Has this pile met the driving criteria?

STEP 1. Determine the equivalent hammer energy based on the bounce chamber pressure on the driving log.

At a bounce chamber pressure of 175 kPa and a hose length of 24.4 m, the equivalent hammer energy is 40,500 joules.

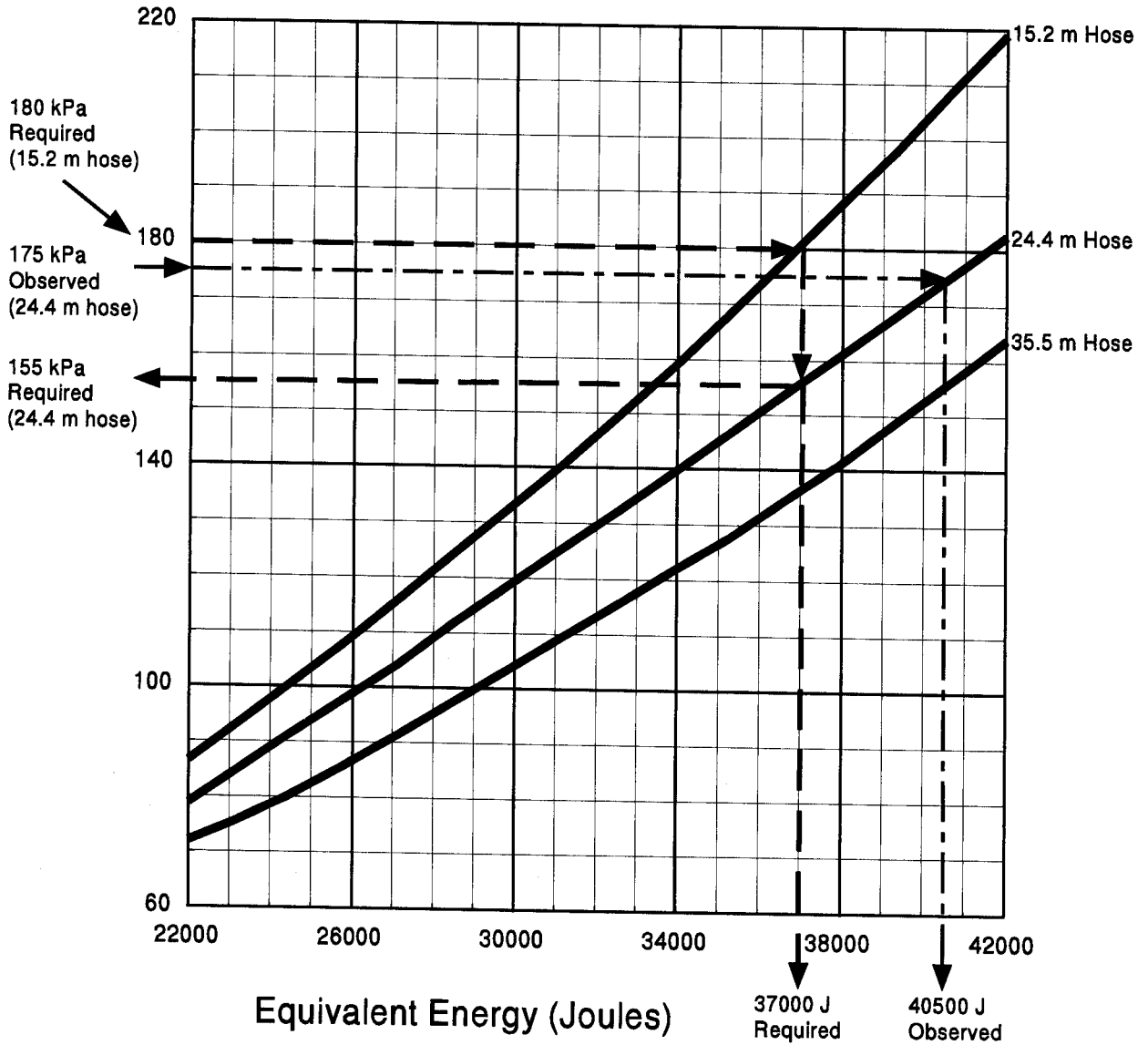
STEP 2. Compare observed equivalent hammer energy with required energy.

The driving criteria required a bounce chamber pressure of 180 kPa with a 15.2 m hose. Hence, an equivalent hammer energy of 37,000 joules was needed with the 60 blows / 250 mm driving criteria.

STEP 3. Based on observed hammer energy, driving resistance and pile toe elevation, determine if the pile has met the driving criteria.

The hammer is delivering 40,500 joules and only 37,000 joules are required. For the 24.4 m hose length used, a bounce chamber pressure of only 155 kPa is needed for 37,000 joules. The minimum pile toe elevation of 80 was exceeded at a penetration depth of 11.25 m. The required final driving resistance of 65 blows / 250 mm also exceeds the required driving resistance of 60 blows / 250 mm. Therefore, this pile has more than met the driving criteria and has actually been overdriven.

Bounce Chamber Pressure, (kPa)



PILE DRIVING LOG

STATE PROJECT NO.: Bridge #2 DATE: 5-29-98

JOB LOCATION: Hoboken

PILE TYPE: 324 mm CEP LENGTH: 15.5 m BENT/PIER NO.: 4 PILE NO.: 1

HAMMER: LB 520 ENERGY/BLOW: 35.7 kJ OPERATING RATE: 80-84 BPM HELMET WEIGHT: 8.9 kN

REF. ELEV.: 91.25 PILE TOE ELEV.: _____ PILE CUTOFF ELEV.: 94.1 m

PILE CUSHION THICKNESS AND MATERIAL: none

WEATHER: cloudy TEMP.: 75° START TIME: 10:52 STOP TIME: 11:09

METERS	BLOWS	STROKE / PRESSURE	REMARKS	METERS	BLOWS	STROKE / PRESSURE	REMARKS
0 - 0.25	W.O.H.		24.4 m hose	8.00 - 8.25	38		
0.25 - 0.50	W.O.H.			8.25 - 8.50	37	BCP 160	
0.50 - 0.75	W.O.H.			8.50 - 8.75	39		
0.75 - 1.00	W.O.H.			8.75 - 9.00	41		
1.00 - 1.25	3			9.00 - 9.25	40		
1.25 - 1.50	5			9.25 - 9.50	39	BCP 160	
1.50 - 1.75	6			9.50 - 9.75	42		
1.75 - 2.00	5			9.75 - 10.00	41		
2.00 - 2.25	6			10.00 - 10.25	44	BCP 160	
2.25 - 2.50	4	BCP 110		10.25 - 10.50	50		
2.50 - 2.75	5			10.50 - 10.75	51		
2.75 - 3.00	6			10.75 - 11.00	53	BCP 165	
3.00 - 3.25	8	BCP 115		11.00 - 11.25	51		min pen
3.25 - 3.50	10			11.25 - 11.50	54		
3.50 - 3.75	12			11.50 - 11.75	55	BCP 170	
3.75 - 4.00	20	BCP 125		11.75 - 12.00	57		
4.00 - 4.25	22			12.00 - 12.25	58	BCP 170	
4.25 - 4.50	21			12.25 - 12.50	60		
4.50 - 4.75	20			12.50 - 12.75	65	BCP 175	
4.75 - 5.00	23	BCP 135		12.75 - 13.00			
5.00 - 5.25	21			13.00 - 13.25			
5.25 - 5.50	25			13.25 - 13.50			
5.50 - 5.75	28	BCP 150		13.50 - 13.75			
5.75 - 6.00	30			13.75 - 14.00			
6.00 - 6.25	33			14.00 - 14.25			
6.25 - 6.50	32	BCP 155		14.25 - 14.50			
6.50 - 6.75	33			14.50 - 14.75			
6.75 - 7.00	35			14.75 - 15.00			
7.00 - 7.25	33	BCP 155		15.00 - 15.25			
7.25 - 7.50	37			15.25 - 15.50			
7.50 - 7.75	36			15.50 - 15.75			
7.75 - 8.00	33	BCP 155		15.75 - 16.00			

STUDENT EXERCISE #16 SOLUTION - DETERMINING PILE TOE ELEVATIONS

Pile driving criteria often include obtaining a specified driving resistance in conjunction with a pile penetration requirements or pile toe elevation. For many land based driving situations determination of the pile toe elevation is a relatively straightforward task. For batter pile driving and pile installations over water, determination of the pile toe elevation can be more problematic.

The following pages contain pile installation illustrations where the reference elevation is given and the pile penetration shown. For each example calculate the final pile toe elevation and pile penetration depth.

$$\begin{aligned} 16a. \quad \text{pile toe elevation} &= \text{template elevation} - \text{length below reference} \\ &= 125.5 - 16.5 \text{ m} = 109.0 \end{aligned}$$

$$\begin{aligned} \text{pile penetration} &= \text{ground elevation} - \text{pile toe elevation} \\ &= 124.25 - 109.0 = 15.25 \text{ m} \end{aligned}$$

$$\begin{aligned} 16b. \quad \text{pile toe elevation} &= \text{template elevation} - \text{length below reference} \\ &= 15.25 - 20.75 \text{ m} = -5.5 \end{aligned}$$

$$\begin{aligned} \text{pile penetration} &= \text{ground elevation} - \text{pile toe elevation} \\ &= 14.0 - (-5.5) = 19.5 \text{ m} \end{aligned}$$

$$\begin{aligned} 16c. \quad \text{corrected pile length} &= \text{length below template (correction factor for 1H:4V)} \\ &= 15.25 (0.971) = 14.81 \text{ m} \end{aligned}$$

$$\begin{aligned} \text{pile toe elevation} &= \text{template elevation} - \text{length below reference} \\ &= 175.40 - 14.81 \text{ m} = 160.59 \end{aligned}$$

$$\begin{aligned} \text{pile penetration} &= (\text{ground elevation} - \text{pile toe elevation}) \\ &\quad / (\text{correction factor for 1H:4V}) \\ &= (173.70 - 160.59) / (.971) = 13.50 \text{ m} \end{aligned}$$

16d. pile toe elevation

$$\begin{aligned} &= 13.11 / (.971) = 13.5 \text{ m} \\ &= \text{template elevation} - \text{length below reference} \\ &= +1.3 - 18.75 \text{ m} = -17.45 \end{aligned}$$

pile penetration

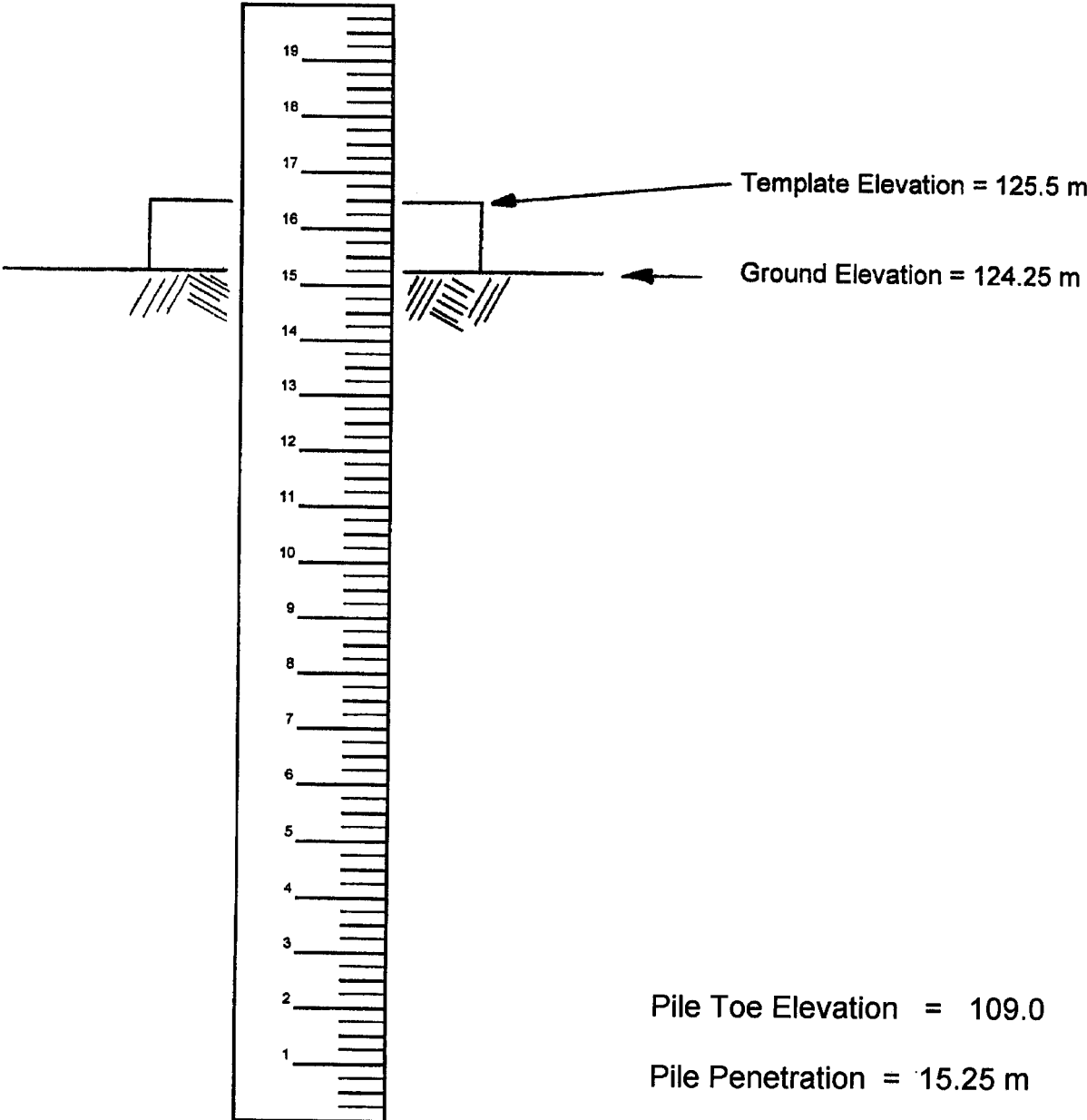
$$\begin{aligned} &= \text{mudline elevation} - \text{pile toe elevation} \\ &= -3.9 - (-17.45) = 13.55 \text{ m} \end{aligned}$$

penetration below scour

$$\begin{aligned} &= \text{scour elevation} - \text{pile toe elevation} \\ &= -9.8 - (-17.45) = 7.65 \text{ m} \end{aligned}$$

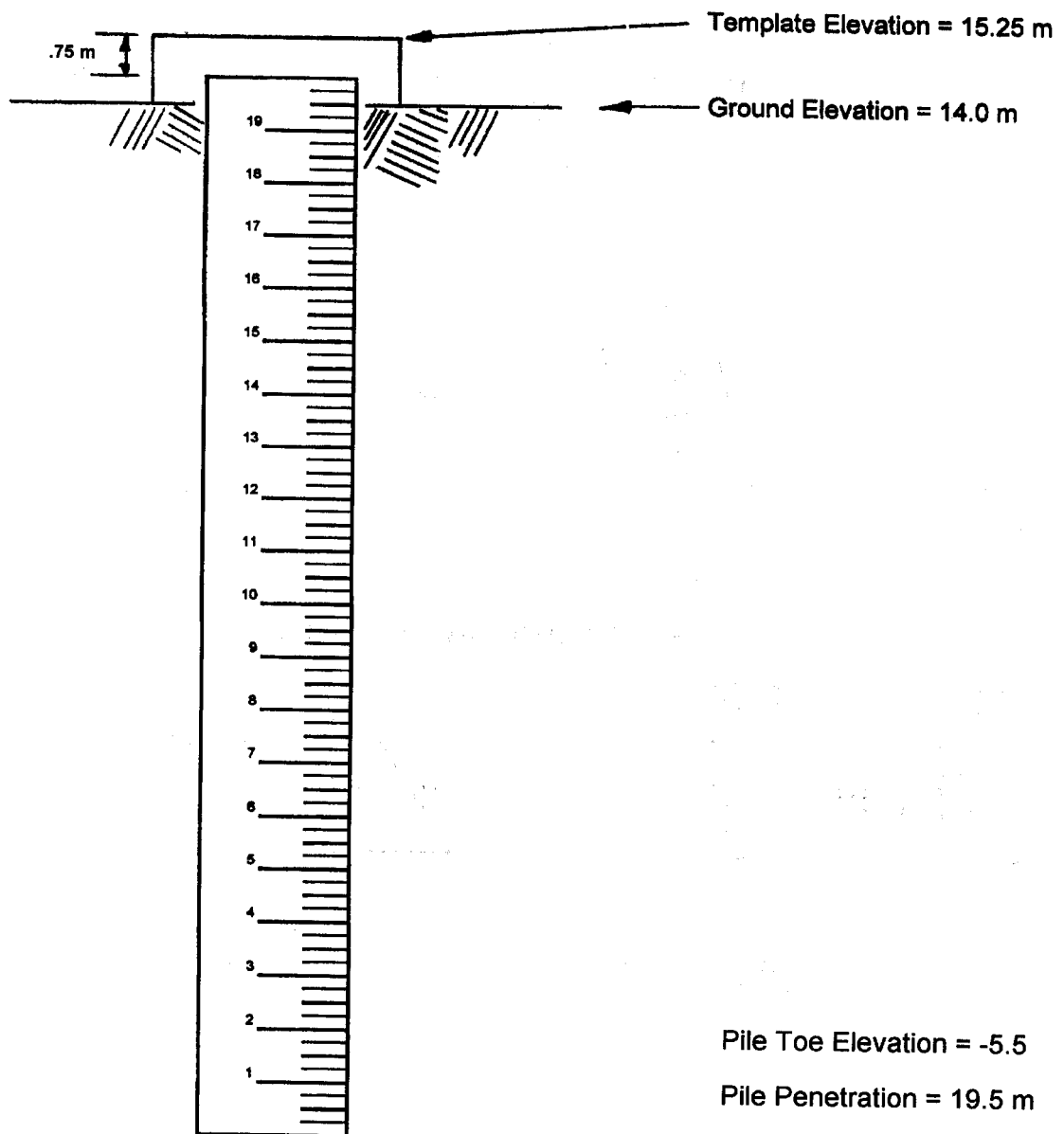
STUDENT EXERCISE 16a - DETERMINING PILE TOE ELEVATIONS

Land Pile Installation



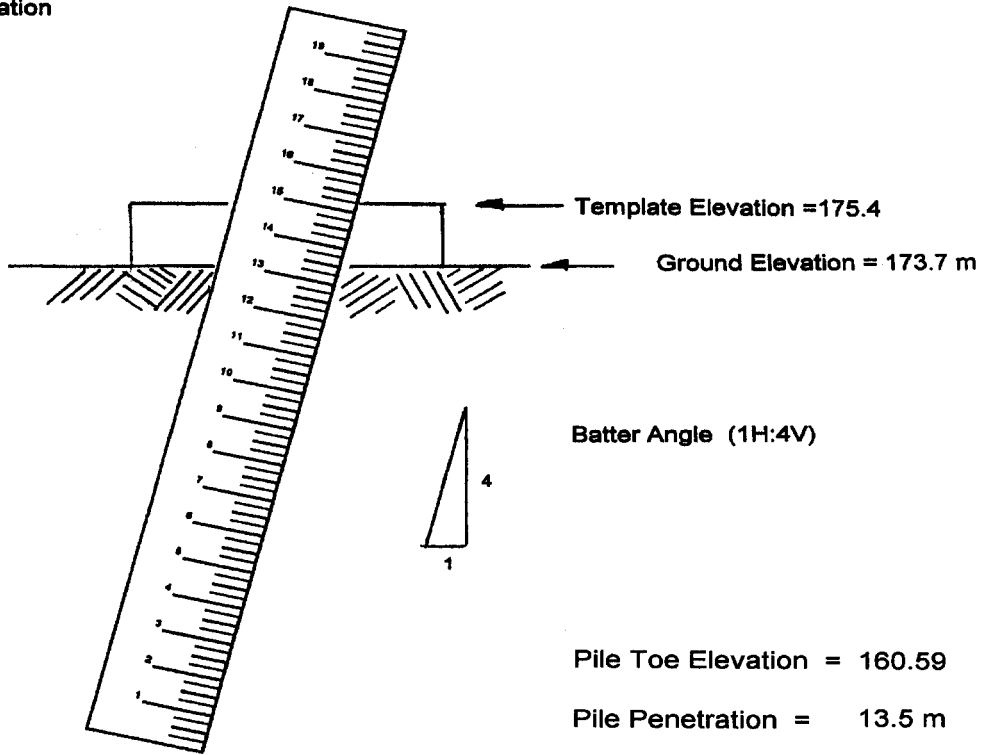
STUDENT EXERCISE #16b - DETERMINING PILE TOE ELEVATIONS

Land Pile Installation



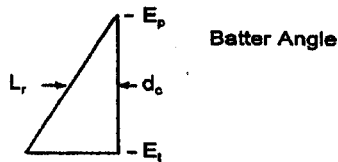
STUDENT EXERCISE #16c - DETERMINING PILE TOE ELEVATIONS

Batter Pile Installation



Calculating Pile Toe Elevation of Batter Piles

Batter Angle	Correction Factor, (B_c)
1H : 12V	.997
1.5H : 12V	.992
2H : 12V (1H : 6V)	.986
3H : 12V (1H : 4V)	.971
4H : 12V (1H : 3V)	.949
5H : 12V	.923



Definitions

- L_r = Pile Length Below Reference Point (m)
- E_p = Reference Point Elevation (m)
- d_c = Corrected Pile Depth (m)
- E_t = Pile Toe Elevation

Formulas

$$d_c = (L_r)(B_c)$$

$$E_t = E_p - d_c$$

STUDENT EXERCISE #16d - DETERMINING PILE TOE ELEVATIONS

Pile Installation over Water

